International Indian Ocean Expedition

Collected reprints IV

Published upon the recommendation
of the Scientific Committee on Oceanic Research (SCOR)
and the
Intergovernmental Oceanographic Commission (IOC)

Unesco

UNESCO ARCHIVES

International Indian Ocean Expedition. Collected reprints IV

Copyright in each paper reprinted in this
collected edition remains in the possession
of each author and publisher, from whom
permission to reproduce has been obtained.

Collected edition published in 1967 by the
United Nations
Educational, Scientific and Cultural Organization,
Place de Fontenoy, Paris 7e
Printed by Les Presses Saint-Augustin, Bruges.

NS.66/D.37/4A
Printed in Belgium

Preface

The fourth volume of collected reprints of the International Indian Ocean Expedition comprises reprints received by Unesco during the second half of 1966. The papers presented in the volume are roughly grouped into five major parts :

I. Marine biology;
II. Marine chemistry;
III. Physical oceanography;
IV. Marine geology and geophysics;
V. Papers presented by title or an abstract only.

As was indicated previously, this classification is only a very approximate one which is accepted here simply for convenience of presentation. Some papers of biological importance are included in Part III, "Physical oceanography" since they treat environmental processes, although with application to biological ones. Everyone knows also how difficult it is to separate a chemical description of the environment from a physical one.

It is planned, therefore, to complete eventually the series of volumes of collected reprints with an index volume which will contain both the name and the subject indexes.

The fifth volume of the series will be compiled by the middle of 1967.

Collected reprints of the IIOE

List of reprints

Part I. Marine biology

Part I Marine biology

COMMONWEALTH OF AUSTRALIA

Commonwealth Scientific and Industrial Research Organization

Division of Fisheries and Oceanography

REPORT 28

CHECK-LIST OF DINOFLAGELLATES RECORDED FROM THE INDIAN OCEAN

By E. J. F. Wood

Marine Biological Laboratory
Cronulla, Sydney
1963

CHECK-LIST OF DINOFLAGELLATES RECORDED FROM THE INDIAN OCEAN

By E.J.F. Wood

INTRODUCTION

Because of the international interest in the Indian Ocean as an object of study by oceanographers from various countries of the world, it seemed opportune to scan previous work which has been carried out in the region. Phytoplankton studies have been considerable, and because many of the papers are not easy of access, a check-list of previous records from the Indian Ocean region has been prepared. It is hoped that this check-list will prove useful to phytoplanktologists working on dinoflagellates collected from the Indian Ocean region during the SCOR-UNESCO project in the Indian Ocean (1959-1965).

Genus AMPHIDINIUM

Amphidinium extensum Wulff, 1916

Matzenauer, 1933; Indian Ocean

A. globosum Schroeder, 1911

Matzenauer, 1933; Indian Ocean

A. turbo Kofoid, 1922

Matzenauer, 1933; Indian Ocean

Genus AMPHISOLENIA

Amphisolenia bidentata Schroeder, 1900

Ostenfeld and Schmidt, 1901; Red Sea, Gulf of Aden
Schroeder, 1906; Red Sea, G. of Aden, Arabian Sea, Indian Ocean to Sumatra
Karsten, 1907; East African Coast, Indian Ocean
Ostenfeld, 1915; Boeton Strait
Matzenauer, 1933; Indian Ocean
Subrahmanyan, 1958; Arabian Sea
Wood, 1962; Indian Ocean, Java Seas, Timor Sea, Arafura Sea

When citing this report abbreviate as follows:
C.S.I.R.O. Aust. Div. Fish. Oceanogr. Rep. No. 28

Amphisolenia bifurcata Murray and Whitting, 1899

Karsten, 1907; Indian Ocean

A. brevicauda Kofoid, 1907

Wood, 1962; Indian Ocean

A. claviceps Kofoid, 1907

Wood, 1962; Indian Ocean

A. elongata Kofoid and Skogsberg, 1928

Subrahmanyan, 1958; Arabian Sea

A. globifera Stein, 1883

Cleve, 1901; Malaya
Cleve, 1903; Red Sea, Arabian Sea
Wood, 1962; Indian Ocean

A. inflata Murray and Whitting, 1899

Cleve, 1903; Arabian Sea
Schroeder, 1906; G. of Aden, Indian Ocean to Sumatra

A. lemmermanni Kofoid, 1907

Matzenauer, 1933; Indian Ocean
Wood, 1962; Indian Ocean

A. palaeotheroides Kofoid, 1907

Wood, 1962; Indian Ocean

A. palmata Stein, 1883

Cleve, 1900, 1901; Red Sea, Arabian Sea, Indian Ocean
Cleve, 1903; Red Sea, Arabian Sea, G. of Aden
Schroeder, 1906; G. of Aden, Arabian Sea
Karsten, 1907; Indian Ocean

A. rectangulata Kofoid, 1907

Wood, 1962; Indian Ocean

Amphisolenia schauinslandi Lemmermann, 1899

Ostenfeld and Schmidt, 1901; G. of Aden
Schroeder, 1906; Indian Ocean
Matzenauer, 1933; G. of Aden, Indian Ocean
Ballantine, 1961; Zanzibar
Wood, 1962; Indian Ocean

A. schroederi Kofoid, 1907

Wood, 1962; Indian Ocean

A. thrinax Schütt, 1895

Ostenfeld and Schmidt, 1901; Arabian Sea
Cleve, 1901; Arabian Sea
Schroeder, 1906; Arabian Sea, Indian Ocean
Matzenauer, 1933; Indian Ocean
Wood, 1962; Indian Ocean

Genus BLEPHAROCYSTA

Blepharocysta paulseni Schiller, 1937

Wood, 1962; Indian Ocean

B. splendor maris Ehrenberg, 1873

Ostenfeld and Schmidt, 1901; G. of Aden
Schroeder, 1906; Red Sea, G. of Aden
Wood, 1962; Indian Ocean

Genus CENTRODINIUM

Centrodinium eminens Bohm, 1933

Wood, 1962; Indian Ocean(N.E.)

C. intermedium Pavillard, 1930

Wood, 1962; Indian Ocean (N.E.)

Genus CERATIUM

Ceratium arcticum (Ehr.) Cleve, 1901 .

Wood, 1961; Indian Ocean

C. arietinum Cleve, 1900b; South Indian Ocean

Cleve, 1901; Arabian Sea, Indian Ocean
Schroeder, 1906; Indian Ocean
Karsten, 1907; Indian Ocean
Matzenauer, 1933; Indian Ocean
Steemann Nielsen, 1939; Indian Ocean
Wood, 1954; Cape Inscription, Western Australia

C. axiale Kofoid, 1907

Steemann Nielsen, 1939; Indian Ocean
Wood, 1954; West of King I.

C. azoricum Cleve, 1900b; South Indian Ocean

Cleve, 1901, 1903; Indian Ocean, Arabian Sea
Schroeder, 1906; Red Sea, Arabian Sea, Colombo-Sumatra
Karsten, 1907; Indian Ocean
Czapek, 1909; Indian Ocean
Steemann Nielsen, 1939; Indian Ocean
Wood, 1954; south and west coasts of Australia, Indian Ocean

C. belone Cleve, 1900

Cleve, 1901; Indian Ocean
Schroeder, 1906; Red Sea, G. of Aden, Arabian Sea
Karsten, 1907; Indian Ocean
Steemann Nielsen, 1939; Indian Ocean
Wood, 1962; Indian Ocean

C. bigelowi Kofoid, 1907

Steemann Nielsen, 1939; Indian Ocean
Wood, 1962; Indian Ocean

C. brachyceros Daday, 1907; tropical lakes of Africa and Asia

Schroeder, 1914; East Africa

Ceratium breve (Ostenfeld and Schmidt) Schroeder, 1906

Ostenfeld and Schmidt, 1901 (as C. tripos v. breve); Red and Arabian Seas
Schroeder, 1906; Arabian Sea
Karsten, 1907 (as C. tripos azoricum); Indian Ocean
Ostenfeld, 1915; Boeton Strait
Steemann Nielsen, 1939; Indian Ocean
Subrahmanyan, 1958; Arabian Sea
Wood, 1962; eastern Indian Ocean
Ballantine, 1961; Zanzibar

C. bucephalum (Cleve) Cleve, 1901

Cleve, 1901, 1903 (as C. heterocamptum Jörg.); Arabian Sea, south Indian Ocean
Ostenfeld and Schmidt, 1901 (as C. heterocamptum); G. of Aden
Schroeder, 1906; Arabian Sea
Subrahmanyan, 1958; Arabian Sea
Wood, 1962; Indian Ocean

C. buceros Zacharias, 1905

v. tenue (Ost. and Schmidt) Jörg., 1911

Ostenfeld and Schmidt, 1901 (as C. tenue n. sp.); Red Sea
Steemann Nielsen, 1939 (as C. tenue); Indian Ocean
Wood, 1954; west and south Australia: 1960; Indian Ocean
Subrahmanyan, 1958; Arabian Sea

v. molle (Kofoid) Jorgensen, 1911

Schroeder, 1906 (as C. undulatum); Indian Ocean
Karsten, 1907 (as C. tripos inversum, and C. tripos buceros) Indian Ocean
Steemann Nielsen, 1939 (as C. molle); Indian Ocean
Wood, 1954; C. Inscription to C. Leeuwin: 1962; Indian Ocean

C. candelabrum (Ehr.) Stein, 1883

Ostenfeld and Schmidt, 1901; Red Sea, G. of Aden
Cleve, 1901, 1903; Red Sea, G. of Aden, Arabian Sea, Indian Ocean, Malaya
Schroeder, 1906; Red Sea, G. of Aden, Arabian Sea, Indian Ocean, Singapore, Sunda Sea
Ostenfeld, 1915; Boeton Str.
Steemann Nielsen, 1939; Indian Ocean
Subrahmanyan, 1958; Arabian Sea
Ballantine, 1961; Zanzibar

Ceratium candelabrum (contd)

f. depressum Pouchet, 1883

Karsten, 1907; south Indian Ocean
Steemann Nielsen, 1939; Indian Ocean
Wood, 1954; southern Australia, Bass Strait to Albany: 1962; Indian Ocean
Subrahmanyan, 1958; Arabian Sea

C. carriense Gourret, 1883 (and vars.)

Cleve, 1900, 1901, 1903 (as C. volans); Red Sea, G. of Aden, Arabian Sea, Malaya
Ostenfeld and Schmidt, 1901 (as C. volans, C. patentissimum); Red Sea
Schroeder, 1906 (as C. ceylonicum, n. sp., C. elegans, C. patentissimum); Fremantle Harbour, G. of Aden, Indian Ocean
Karsten, 1907 (as C. tripos volans, etc.); Indian Ocean
Steemann Nielsen, 1939; Indian Ocean
Wood, 1955; west and south coasts of Australia: 1962; Indian Ocean
Subrahmanyan, 1958; Arabian Sea

C. cephalotum (Lemm.) Jörg., 1911

Schroeder, 1906 (as C. gravidum v. hydrocephala); Ceylon to Sumatra
Karsten, 1907; Indian Ocean
Steemann Nielsen, 1939; Indian Ocean
Wood, 1962; Indian Ocean

C. concilians Jörg., 1920

Karsten, 1909; Indian Ocean
Steemann Nielsen 1939; Indian Ocean
Wood, 1954, 1962; west of Bass Str., Indian Ocean

C. contortum (Gourret) Cleve, 1900a; Arabian Sea, Red Sea, Indian Ocean
Ostenfeld and Schmidt, 1901; Red Sea, G. of Aden
Cleve, 1901, 1903; Red Sea, G. of Aden, Arabian Sea, Indian Ocean
Schroeder, 1906 (as C. subcontortum); Arabian Sea, Fremantle, Indian Ocean, Singapore
Karsten, 1907; Indian Ocean
Czapek, 1909 (as C. arcuatum f. contortum); Indian Ocean
Steemann Nielsen, 1939; Indian Ocean
Wood, 1962; Indian Ocean

Ceratium contrarium (Gourret) Pav., 1905

Cleve, 1900a, 1901 (as C. flagelliferum); Red Sea, Indian Ocean, Malaya
Schroeder, 1906; Indian Ocean east of Colombo
Karsten, 1907 (as C. tripos flagelliferum v. undulata); Indian Ocean
Ostenfeld, 1915 (as C. inflexum); Boeton Str.
Steemann Nielsen, 1939; Indian Ocean
Wood, 1954 (as C. trichoceros v. contrarium): 1962; Indian Ocean

C. curvicorne v. Daday, 1888

Cleve, 1901, 1903; Red Sea, G. of Aden, Arabian Sea

C. declinatum Karsten, 1907 (and as C. tripos heterocamptum); Indian Ocean
Steemann Nielsen, 1939; Indian Ocean
Subrahmanyan, 1958; Arabian Sea
Wood, 1962; Indian Ocean

C. deflexum (Kofoid) Jörgensen, 1911

Schroeder, 1906 (as C. recurvatum); east of Ceylon
Ostenfeld, 1915; Boeton Str.
Steemann Nielsen, 1939; Indian Ocean
Wood, 1962; Indian Ocean

C. dens Ostenfeld and Schmidt, 1901; Red Sea, Arabian Sea

Cleve, 1903; Red Sea, Arabian Sea
Schroeder, 1906; Red Sea, G. of Aden, Indian Ocean
Karsten, 1907; Indian Ocean
Ostenfeld, 1915; Boeton Str.
Steemann Nielsen, 1939; Indian Ocean
Subrahmanyan, 1958; Arabian Sea
Wood, 1962; Indian Ocean

C. digitatum Schütt, 1895

Karsten, 1907; Indian Ocean
Steemann Nielsen, 1939; Indian Ocean
Wood, 1962; Indian Ocean

Ceratium euarcuatum Jörg., 1920

Schroeder, 1906 (as C. inflexum (Gour.) Schr.); Indian Ocean
Karsten, 1907; Indian Ocean
Steemann Nielsen, 1939; Indian Ocean
Wood, 1962; Indian Ocean

C. extensum (Gourret) Cleve, 1901

Cleve, 1901, 1903; Red Sea, Arabian Sea, Malaya
Ostenfeld and Schmidt, 1901 (as C. fusus v. extensa); Red Sea, G. of Aden
Schroeder, 1906; Arabian Sea, G. of Aden, Singapore, Sunda Sea
Ostenfeld, 1915; Boeton Str.
Steemann Nielsen, 1939; Indian Ocean
Wood, 1954, 1962; west of Bass Str., Indian Ocean, west of Australia

f. strictum

Ostenfeld 1915; Boeton Str.
Wood, 1954, 1962; Indian Ocean

C. falcatiforme Jörg. 1920

Karsten, 1907; Indian Ocean
Steemann Nielsen, 1939; Indian Ocean
Wood, 1954, 1962; Indian Ocean

C. falcatum (Kofoid) Jörg., 1920

Cleve, 1900a (as C. pennatum); Arabian Sea, Indian Ocean, Red Sea
Karsten, 1907 (as C. pennatum f. falcatum); Indian Ocean
Steemann Nielsen, 1939; Indian Ocean
Wood, 1954; 1962; west of Bass Str., Indian Ocean
Ballantine, 1961; Zanzibar

C. filicorne Steemann Nielsen, 1934

Steemann Nielsen, 1939; Indian Ocean

C. furca (Ehr.) Clap. and Lach.

Schroeder, 1906; Red Sea, G. of Aden east to Sunda Sea

Ceratium furca (contd)

v. eugrammum (Ehr.) Jörg., 1911

Steemann Nielsen, 1939; Indian Ocean
Subrahmanyan, 1958; Arabian Sea
Wood, 1954; Swan R. to Kangaroo I.
Ballantine, 1961; Zanzibar

v. berghi (Jörg.) Schiller, 1911

Ostenfeld and Schmidt, 1901; Red Sea, G. of Aden
Cleve, 1901, 1903; Red Sea, G. of Aden, Arabian Sea, Malaya
Schroeder, 1906; N.E. Indian Ocean
Czapek, 1909; Indian Ocean
Ostenfeld, 1915; Boeton Str.
Steemann Nielsen, 1939; Indian Ocean
Wood, 1954; 1962; Bass Strait, Southern and Indian Oceans

C. fusus (Ehr.) Dujardin, 1841

Cleve, 1900 a,b, 1901; Indian Ocean, Red Sea
Ostenfeld and Schmidt, 1901; Red Sea, G. of Aden
Schroeder, 1906; Red Sea, G. of Aden, Arabian Sea, N.E. Indian Ocean
Karsten, 1907; Indian Ocean
Czapek, 1909; Indian Ocean
Ostenfeld, 1915; Boeton Str.
Steemann Nielsen, 1939; Indian Ocean
Wood, 1954; south and west coasts of Australia: 1962; Indian Ocean
Subrahmanyan, 1954; Arabian Sea
Ballantine, 1961; Zanzibar

C. gallicum Kofoid, 1907

Schroeder, 1906 (as C. hundhauseni); Indian Ocean
Karsten, 1907 (as C. tripos macroceros v. tenuissima); Indian Ocean
Ostenfeld, 1915; Boeton Str.
Wood, 1954, 1962; south and west coasts of Australia, Indian Ocean
Subrahmanyan, 1958 (as C. macroceros v. gallicum); Arabian Sea

C. geniculatum (Lemm.) Cleve, 1901

Karsten, 1907; Indian Ocean
Steemann Nielsen, 1939; Indian Ocean
Wood, 1962; Indian Ocean

Ceratium gibberum Gourret, 1883

Ostenfeld and Schmidt, 1901 (as C. curvicorne Daday)
Cleve; Red Sea
Cleve, 1901, 1903; Red Sea, G. of Aden, Arabian Sea
Schroeder, 1906; Indian Ocean, Fremantle Harbour
Karsten, 1907; Indian Ocean
Ostenfeld, 1915; Boeton Str.
Steemann Nielsen, 1939; Indian Ocean
Subrahmanyan, 1958; Arabian Sea
Wood, 1962; Indian Ocean

C. gravidum Gourret, 1883

Ostenfeld and Schmidt, 1901; G. of Aden, Red Sea
Cleve, 1901, 1903; Red Sea, Arabian Sea, Indian Ocean
Schroeder, 1906; Red Sea, G. of Aden, Arabian Sea,
Indian Ocean
Karsten, 1907; Indian Ocean
Steemann Nielsen, 1939; Indian Ocean
Wood, 1954; west of Bass Strait. 1962; Indian Ocean

C. hexacanthum Gourret, 1883

Ostenfeld and Schmidt, 1901; Red Sea, G. of Aden
Cleve, 1901, 1903 (as C. reticulatum (Pouchet));
Red Sea, Arabian Sea, Indian Ocean, Malaya
Schroeder, 1906 (as C. reticulatum); Indian Ocean
Karsten, 1907; Indian Ocean
Ostenfeld, 1915 (as C. reticulatum); Boeton Str.
Steemann Nielsen, 1939; Indian Ocean
Wood, 1954, 1962; Indian Ocean to Bass Str.

C. hirundinella (O.F.M.) Bergh, 1882

West, 1907; Victoria Nyanza
Ostenfeld, 1909, Tanganyika
Woloszynska, 1912; Java
Schroeder, 1914; East Africa
Wood, 1954; Swan River, West Australia

C. horridum Gran, 1902

Subrahmanyan, 1958; Arabian Sea
Wood, 1962; Indian Ocean

C. humile Jörg., 1911

Steemann Nielsen, 1939; Indian Ocean
Subrahmanyan, 1958; Arabian Sea
Wood, 1962; Indian Ocean

Ceratium incisum (Karsten) Jörg. 1911

Schroeder, 1906; Red Sea
Karsten, 1907; Indian Ocean
Steemann Nielsen, 1939; Indian Ocean
Wood, 1962; Indian Ocean

C. inflatum (Kofoid) Jörg. 1911

Schroeder, 1906; N.E. Indian Ocean
Steemann Nielsen, 1939; Indian Ocean
Subrahmanyan, 1958; Arabian Sea
Wood, 1962; Indian Ocean

C. karsteni Pav., 1907

Ostenfeld and Schmidt, 1901 (as C. tripos v. arcuata); Red Sea, G. of Aden
Cleve, 1901, 1903 (as C. arcuatum Gourret); Red Sea, G. of Aden, Arabian Sea
Schroeder, 1906 (as C. arcuatum); Red Sea, G. of Aden, Arabian Sea, Indian Ocean
Karsten, 1907 (as C. tripos schranki); Indian Ocean
Czapek, 1909 (as C. arcuatum); Indian Ocean
Steemann Nielsen, 1939; Indian Ocean
Wood, 1954, 1962; Indian Ocean
Subrahmanyan, 1958; Arabian Sea
Ballantine, 1961; Zanzibar

C. kofoidi Jörg., 1911

Karsten, 1907; Indian Ocean
Steemann Nielsen, 1939; Indian Ocean
Wood, 1962; Indian Ocean

C. limulus Gourret, 1883

Ostenfeld and Schmidt, 1901; Arabian Sea
Cleve, 1901, 1903; Red Sea, Malaya
Schroeder, 1906; Arabian Sea
Karsten, 1907; Indian Ocean
Steemann Nielsen, 1939; Indian Ocean
Wood, 1954, 1962; Southern and Indian Oceans

C. lineatum (Ehr.) Cleve, 1899

Cleve 1900a,b (probably in part = C. pentagonum); South Indian Ocean, Red Sea, Arabian Sea, Malaya

Ceratium lineatum (contd)

Schroeder, 1906 (= C. pentagonum); Red Sea, G. of Aden, Arabian Sea
Wood, 1954, 1960; Subantarctic Convergence, central Indian Ocean

C. longinum Karsten, 1906

Schiller, 1937; Indian Ocean

C. longipes (Bailey) Gran, 1902

Subrahmanyan, 1958; Arabian Sea

C. longirostrum Gourret, 1883

Ostenfeld, 1915; Boeton Str.
Steemann Nielsen, 1939; Indian Ocean
Subrahmanyan, 1958; Arabian Sea
Wood, 1962; Indian Ocean

C. longissimum (Schroeder) Kofoid, 1907

Steemann Nielsen, 1939; Indian Ocean

C. lunula Schimper, 1900

Karsten, 1907; Indian Ocean
Czapek, 1909; Indian Ocean
Steemann Nielsen, 1939; Indian Ocean
Wood, 1954, 1962; Southern and Indian Oceans
Subrahmanyan, 1958; Arabian Sea

C. macroceros (Ehr.) Cleve, 1900

Ostenfeld and Schmidt, 1901 (as C. macroceras); Red Sea, G. of Aden
Cleve, 1901, 1903; Red Sea, G. of Aden, Arabian Sea, Indian Ocean, Malaya
Schroeder, 1906; Red Sea, G. of Aden, Arabian Sea, Singapore, Fremantle
Karsten, 1907; Indian Ocean
Czapek, 1909; Indian Ocean
Steemann Nielsen, 1939; Indian Ocean
Subrahmanyan, 1958; Arabian Sea
Wood, 1962; Indian Ocean
Ballantine, 1961; Zanzibar

Ceratium massiliense (Gourret) Jörg., 1911

Schroeder, 1906 (as C. aequatoriale); Singapore, Red Sea, G. of Aden
Karsten, 1907 (as C. tripos longipes v. cristata, C. tripos flagelliferum v. crassa etc.); Indian Ocean
Ostenfeld, 1915; Boeton Str.
Steemann Nielsen, 1939; Indian Ocean
Subrahmanyan, 1958; Arabian Sea
Wood, 1962; Indian Ocean

v. macroceroides (Karst.) Jörg. 1911

Wood, 1954; Great Australian Bight, coastal waters of west Australia south of Shark Bay (characteristic): 1962; Indian Ocean
Subrahmanyan, 1958; Arabian Sea

C. minutum Jörg., 1920

Schroeder, 1906; Fremantle
Wood, 1954, 1962; central and S.E. Indian Ocean, south-west coast of Australia

C. okamurai Schroeder, 1906; Indian Ocean, Arabian Sea

C. paradoxides Cleve, 1900

Schroeder, 1906; Arabian Sea
Steemann Nielsen, 1939; Indian Ocean

C. pavillardi Jörg., 1911

Steemann Nielsen, 1939; Indian Ocean
Wood, 1954, 1962; Southern and Indian Oceans

C. pentagonum Gourret, 1883

Cleve, 1900a (as C. lineatum v. robusta Cl.); south Indian Ocean
Ostenfeld and Schmidt, 1901 (as C. lineatum and v. robusta); Red Sea, G. of Aden
Cleve, 1903 (as C. lineatum v. longiseta Ost. and Sch.); Red Sea, Arabian Sea
Schroeder, 1906; Indian Ocean
Karsten, 1907; Indian Ocean
Steemann Nielsen, 1939 (as C. subrobustum); Indian Ocean
Wood, 1954, 1962; Heard I., Antarctic, Southern and Indian Oceans
Ballantine, 1961 (f. tenera); Zanzibar

Ceratium platycorne v. Daday, 1888

Cleve, 1903; Arabian Sea
Karsten, 1907; Indian Ocean
Steemann Nielsen, 1939; Indian Ocean
Wood, 1954; west of Bass Str.

C. porrectum Karsten, 1907; Seychelles

Wood, 1962; Indian Ocean

C. praelongum (Lemm.) Kofoid, 1907

Ostenfeld and Schmidt, 1901 (as C. gravidum v. praelongum); Red Sea, Arabian Sea
Steemann Nielsen, 1939; Indian Ocean
Wood, 1962; Indian Ocean

C. pulchellum Schroeder, 1906; Arabian Sea

Karsten, 1907; Indian Ocean
Czapek, 1909; Indian Ocean
Wood, 1962; Indian Ocean (including C. eupulchellum)

v. semipulchellum Jörg. 1920

Steemann Nielsen, 1939 (as C. semipulchellum); Indian Ocean
Subrahmanyan, 1958; Arabian Sea
Wood, 1962; Indian Ocean
Ballantine, 1961; Zanzibar

v. eupulchellum Jörg. 1920

Steemann Nielsen, 1939 (as C. pulchellum); Indian Ocean
Wood, 1962; Indian Ocean

C. ranipes Cleve, 1900, 1903; Arabian Sea, Malaya

Schroeder, 1906; G. of Aden
Karsten, 1907; Indian Ocean
Steemann Nielsen, 1939; Indian Ocean
Wood, 1954; S.W. Australia: 1962; Indian Ocean

C. reflexum Cleve 1900

Ostenfeld and Schmidt, 1901; Red Sea, G. of Aden
Cleve, 1903; Red Sea
Schroeder, 1906; N.E. Indian Ocean
Karsten, 1907; Indian Ocean
Steemann Nielsen, 1939; Indian Ocean
Wood, 1962; Indian Ocean

Ceratium schmidti Jörg., 1911

Ostenfeld, 1915; Boeton Str.
Bohm, 1931; Indian Ocean
Steemann Nielsen, 1939; Indian Ocean
Subrahmanyan, 1958; Arabian Sea
Wood, 1962; Indian Ocean

C. scapiforme Kofoid, 1907 (probably = C. falcatum Jörg.)

Steemann Nielsen, 1939; Indian Ocean

C. schroeteri Schroeder, 1906; Arabian Sea

Wood, 1962; Indian Ocean

C. setaceum Jörg., 1911

Ostenfeld and Schmidt, 1901 (as C. lineatum v. longiseta); Red Sea, G. of Aden
Schroeder, 1906; east Indian Ocean
Steemann Nielsen, 1939; Indian Ocean
Subrahmanyan, 1958; Arabian Sea
Wood, 1962; Indian Ocean

C. symmetricum Pav., 1905

Karsten, 1907; Indian Ocean
Steemann Nielsen, 1939; Indian Ocean
Wood, 1954, 1962; Port Fairy to Albany, Indian Ocean

C. teres Kofoid, 1907

Steemann Nielsen, 1939; Indian Ocean
Wood, 1954, 1962; Southern Ocean, Indian Ocean
Subrahmanyan, 1958; Arabian Sea

C. trichoceros (Ehr.) Kofoid, 1907

Cleve, 1900a, 1903 (as C. flagelliferum); Indian Ocean, Red Sea, Arabian Sea
Ostenfeld and Schmidt, 1901 (as C. flagelliferum); Red Sea
Schroeder, 1906 (as C. flagelliferum); Red Sea to Singapore
Karsten, 1907 (as C. tripos flagelliferum); Indian Ocean
Steemann Nielsen, 1939; Indian Ocean
Wood, 1954, 1962; Southern and Indian Oceans
Subrahmanyan, 1958; Arabian Sea
Ballantine, 1961; Zanzibar

Ceratium tripos (O.F. Müller) Nitzsch, 1817

Schroeder, 1906; Arabian Sea
Karsten, 1907; Indian Ocean
Czapek, 1909; Indian Ocean
Steemann Nielsen, 1939; Indian Ocean
Subrahmanyan, 1958; Arabian Sea
Wood, 1954, 1962; Indian Ocean

C. vultur Cleve, 1900a; Red Sea, Indian Ocean

Cleve, 1900b, 1903 (as C. robustum Ost. and Sch.); Red Sea, Arabian Sea, Malaya
Ostenfeld and Schmidt, 1901 (as C. robustum); Red Sea
Schroeder, 1906; Red Sea, Arabian Sea, G. of Aden, Indian Ocean
Karsten, 1907 (as C. tripos robustum); Indian Ocean
Ostenfeld, 1915; Boeton Str.
Steemann Nielsen, 1939; Indian Ocean
Wood, 1962; Indian Ocean

v. sumatranum (Karst.); Steemann Nielsen, 1934

Ostenfeld and Schmidt (as C. vultur); Red Sea
Schroeder, 1906; Indian Ocean
Karsten, 1907 (as C. tripos vultur and v. sumatranum); Indian Ocean
Ostenfeld, 1915 (as C. sumatranum); Boeton Str.
Steemann Nielsen, 1939; Indian Ocean
Wood, 1954; Southern and Indian Oceans
Subrahmanyan, 1958; Arabian Sea
Ballantine, 1961; Zanzibar

Genus CERATOCORYS

Ceratocorys armata (Schütt) Kofoid, 1910

Ostenfeld and Schmidt, 1901; Red Sea, G. of Aden
Schroeder, 1906 (as Goniaulax fimbriatum); Indian Ocean
Matzenauer, 1933; Indian Ocean
Wood, 1962; Indian Ocean

C. bipes (Cleve) Kofoid, 1910

Cleve, 1903 (as Goniodoma bipes); Red Sea, Arabian Sea
Karsten, 1907 (as C. asymmetrica); Indian Ocean
Wood, 1962; Indian Ocean

Ceratocorys gouretti Paulsen, 1930

Ostenfeld and Schmidt, 1901 (as C. jourdani); Red Sea, G. of Aden
Matzenauer, 1933 (as C. jourdani); Indian Ocean
Wood, 1954; west of Bass Str.: 1962, Indian Ocean

C. hirsuta Matzenauer, 1933; Indian Ocean

C. horrida Stein, 1883

Ostenfeld and Schmidt, 1901; Red Sea, G. of Aden
Cleve, 1901, 1903; Red Sea, G. of Aden, Malaya, Indian Ocean
Schroeder, 1906; Red Sea, G. of Aden, Arabian Sea, Indian Ocean
Karsten, 1907 (as v. africana); Indian Ocean
Ostenfeld, 1915; Boeton Str.
Matzenauer, 1933; Indian Ocean
Wood, 1954, 1962; Southern and Indian Oceans
Subrahmanyan, 1958; Arabian Sea
Ballantine, 1961; Zanzibar

Genus CITHARISTES

Citharistes apsteini Schütt, 1895

Wood, 1962; Indian Ocean

Genus CLADOPYXIS

Cladopyxis brachiolata Stein, 1883

Ostenfeld and Schmidt, 1901; G. of Aden
Cleve, 1901; Indian Ocean
Schroeder, 1906; G. of Aden, Indian Ocean

Genus CONGRUENTIDIUM

Congruentidium compressum Abe, 1927

Matzenauer, 1933; Indian Ocean

Genus DESMOCAPSA

Desmocapsa sp

Subrahmanyan, 1958; Arabian Sea

Genus DINOPHYSIS

Dinophysis acuminata Clap. and Lach., 1859

Wood, 1954; Swan River, W. Australia
Subrahmanyan, 1958; Arabian Sea

D. acuta Ehr., 1839

Wood, 1954; south-west coast of Australia

D. arctica Mereschowsky, 1879

Wood, 1954; Heard I., Antarctic

D. antarctica Balech, 1957; Adelie Land

D. caudata Saville Kent, 1881

Cleve, 1900a, 1901; South Indian Ocean, Arabian Sea, Indian Ocean
Ostenfeld and Schmidt, 1901 (as D. homunculus); Arabian Sea
Schroeder, 1906 (and as D. homunculus); Arabian Sea
Karsten, 1907; Indian Ocean
Czapek, 1909 (as D. homunculus); Indian Ocean
Matzenauer, 1933; Indian Ocean
Wood, 1954; west and south coasts of Australia: 1962; Indian Ocean
Subrahmanyan, 1958; Arabian Sea
Ballantine, 1961; Zanzibar

D. diegensis Kofoid, 1907

Ostenfeld, 1915; Boeton Str.

D. exigua Kofoid and Skogsberg, 1928

Wood, 1962; Indian Ocean

Dinophysis fortii Pav., 1923

Matzenauer, 1933; Indian Ocean
Wood, 1954, 1962; southern Tasmania, Southern Ocean, Indian Ocean

D. hastata Stein, 1883

Ostenfeld and Schmidt, 1901; G. of Aden, Red Sea
Cleve, 1901, 1903; Red Sea, Arabian Sea, G. of Aden, Indian Ocean
Karsten, 1907; Indian Ocean
Matzenauer, 1933; Indian Ocean
Wood, 1962; Indian Ocean

D. hyalina Wood, 1962; Indian Ocean

D. miles Cleve, 1900a; Red Sea

Ostenfeld and Schmidt, 1901 (and as D. michaelis); Red Sea
Cleve, 1901, 1903; Red Sea, Arabian Sea, Malaya
Lemmermann, 1901; East Indies
Schroeder, 1906; Red Sea, Arabian Sea, G. of Aden, Indian Ocean, Singapore
Czapek, 1909; Indian Ocean
Ostenfeld, 1915; Boeton Str.
Matzenauer, 1933; Indian Ocean
Subrahmanyan, 1958; Arabian Sea
Wood, 1962; Java Seas, northern Australia
Ballantine, 1961; Zanzibar

D. nias Karsten, 1907; Indian Ocean

D. ovum Schütt, 1895

Ostenfeld and Schmidt, 1901; Aden
Karsten, 1907; Indian Ocean
Wood, 1954; Swan R., Antarctic: 1962, Indian Ocean
Subrahmanyan, 1958; Arabian Sea

D. parva Schiller, 1929

Wood, 1962; Indian Ocean

D. punctata Jörg., 1923

Matzenauer, 1933; Indian Ocean

D. rotundata Karsten, 1907 = Phalacroma rotundatum q.v.

Dinophysis sacculus Stein, 1883

Wood, 1954; Tasmania, Albany, W. Australia

D. schroederi Pav., 1909

Wood, 1962; Indian Ocean

D. schuetti Mur. and Whit., 1899

Cleve, 1901; Indian Ocean
Karsten, 1907; Indian Ocean
Wood, 1962; Indian Ocean

D. sphaerica Stein (em. Kof. and Skogs., 1928)

Cleve, 1900a, 1900b, 1903 (as D. vanhoffeni); South Indian Ocean, Red Sea
Ostenfeld and Schmidt, 1901; Red Sea, G. of Aden
Matzenauer, 1933; Indian Ocean
Wood, 1954; Swan R., Antarctic: 1962; Indian Ocean

D. tripos Gourret, 1883

Ostenfeld and Schmidt, 1901 (as D. homunculus v. tripos); Red Sea
Cleve, 1903; Red Sea, G. of Aden, Arabian Sea
Ostenfeld, 1915 (as D. pedunculata); Boeton Str.
Wood, 1954; South Australia

D. truncata Cleve, 1900b; South Africa, South Indian Ocean

Wood, 1954; Subantarctic, Tasmania

D. tuberculata Mangin, 1912

Wood, 1954; Antarctic
Balech, 1958; Adelie Land

D. uracantha Stein, 1883

Ostenfeld and Schmidt, 1901; G. of Aden
Cleve, 1903; Red Sea
Schroeder, 1906; Indian Ocean
Karsten, 1907; Indian Ocean
Matzenauer, 1933; Indian Ocean
Wood, 1962; Indian Ocean

Genus DIPLOPSALIS

Diplopsalis lenticula Bergh 1882

Cleve, 1900a, 1900b, 1901, 1903; South Indian Ocean, Red Sea, G. of Aden, Arabian Sea, Malaya, Indian Ocean
Ostenfeld and Schmidt, 1901; Red Sea, G. of Aden
Schroeder, 1906; Red Sea, G. of Aden, Indian Ocean, Arabian Sea
Karsten, 1907; Indian Ocean
Czapek, 1909; Indian Ocean
Ostenfeld, 1915 (as Peridinium asymmetricum); Boeton Str.
Wood, 1954, 1962; Antarctic, northern Australia, Indian Ocean
Ballantine, 1961 (as Peridiniopsis asymmetrica); Zanzibar

D. minor Paulsen 1907

Matzenauer, 1933 (as Peridinium asymmetricum); Indian Ocean
Subrahmanyan, 1958 (as Glenodinium lenticula v. asymmetrica); Arabian Sea
Wood, 1954, 1962; Antarctic, Indian Ocean
Balech, 1958 (as Diplopeltopsis); Adelie Land

D. pilula Ostenfeld, 1908

Subrahmanyan, 1958 (as Glenodinium); Arabian Sea

D. orbicularis (Paulsen) Lebour, 1922

Matzenauer, 1933; Indian Ocean
Wood, 1954; Antarctic, northern Australia

D. rotundata Lebour, 1922

Wood, 1954; Swan R., Antarctic

D. saecularis Mur. and Whit., 1899

Ostenfeld and Schmidt, 1901; Red Sea, G. of Aden
Schroeder, 1906; Red Sea, G. of Aden, Arabian Sea

Genus EXUVIAELLA

Exuviaella baltica Lohmann, 1908

Wood, 1962; Indian Ocean

UNESCO ARCHIVES

Exuviaella compressa (Bailey) Ost., 1903

Cleve, 1900b, 1901, 1903; Red Sea, G. of Aden, Indian Ocean, Malaya
Ostenfeld and Schmidt, 1901; Red Sea, G. of Aden
Schroeder, 1906; Red Sea, G. of Aden, Fremantle Harbour, Indian Ocean
Matzenauer, 1933; Indian Ocean
Wood, 1954; Fremantle Harbour: 1962; Indian Ocean
Subrahmanyan, 1958; Arabian Sea

E. lenticulata Matzenauer, 1933; Indian Ocean

E. marina Cienkowski, 1881

Wood, 1962; Indian Ocean

E. mediterranea Schiller, 1928

Wood, 1962; Indian Ocean

E. oblonga Schiller, 1928

Matzenauer, 1933; Red Sea, G. of Aden

Genus GLENODINIOPSIS

Glenodiniopsis pretiosa Lindemann, 1931; Sumatra

Genus GLENODINIUM

Glenodinium cinctum Ehr. (dubious form)

West, 1909; Yan Yean reservoir, Victoria

G. elpatiewskyi (Ost.) Lemm. 1910

Lemm., 1910; Malaya: 1931 (as Peridinium); Indonesia

G. lindemanni Lefevre, 1932; Madagascar

G. penardi Lemm., 1900

Schroeder, 1914 (as Peridinium); East Africa

Glenodinium penardiforme (Lind.) Schiller, 1937

Lindemann, 1931 (as Peridinium); Indonesia

G. pulvisculus (Ehr.) Stein, 1883

West, 1907; Tanganyika

G. pygmaeum (Lind.) Schiller, 1937

Lindemann, 1931 (as Peridinium); Indonesia

G. quadridens Stein 1883

West, 1907 (as Peridiniopsis cunningtoni); Tanganyika

Woloszynska, 1912 (as P. treubi Wol. and P. wildmanni Wol.) Java
Schroeder, 1914 (as Peridiniopsis cunningtoni); Tanganyika
Lindemann, 1931 (as Peridinium and as P. wildemanni); Indonesia
Lefevre, 1932; Asia

G. viguieri (Lefevre) Schiller, 1937; Madagascar

Genus GONIAULAX

Goniaulax alaskensis Kofoid, 1911

Wood, 1954, 1962; Antarctic, Indian Ocean

G. apiculata (Penard) Entz, 1904

Wood, 1962; Indian Ocean

G. birostris Stein, 1883

Karsten, 1907; Indian Ocean
Matzenauer, 1933; Indian Ocean
Wood, 1954, 1962; off Port Fairy, Indian Ocean
Ballantine, 1961; Zanzibar

G. conjuncta Wood, 1954

Ballantine, 1961; Zanzibar

Goniaulax diegensis Kofoid, 1911

Wood, 1954, 1962; Swan R., west New Guinea, Indian Ocean
Subrahmanyan, 1958; Arabian Sea

G. digitale (Pouchet) Kofoid, 1911

Wood, 1954, 1962; Swan R., Indian Ocean

G. fragilis (Schütt) Kofoid, 1911

Wood, 1962; Indian Ocean

G. glyptorhynchus Mur. and Whit., 1899

Wood, 1962; Indian Ocean

G. highleyi Mur. and Whit., 1899

Cleve, 1901; Indian Ocean

G. hyalina Ostenfeld and Schmidt, 1901; G. of Aden

Matzenauer, 1933; Indian Ocean
Wood, 1962; Indian Ocean

G. jolliffei Mur. and Whit. 1899

Schroeder, 1906; Red Sea (probably does not = Ceratocorys gouretti as Schiller, 1937, suggests)

G. kofoidi Pavillard, 1909

Wood, 1954; south of Port Fairy: 1962; Indian Ocean

G. longispina Lebour, 1925

Matzenauer, 1933; Indian Ocean

G. milneri (Mur. and Whit.) Kof., 1911

Wood, 1962; Indian Ocean

G. minima Matzenauer, 1933; Indian Ocean

Wood, 1954; Indian Ocean, south-west of Albany: 1962; Indian Ocean

Goniaulax monacantha Pavillard, 1916

Wood, 1962; Indian Ocean

G. orientalis Lindemann, 1924

Matzenauer, 1933; Indian Ocean

G. ovalis Schiller, 1937

Matzenauer, 1933 (as C. ovata); Indian Ocean

G. pacifica Kofoid, 1907

Karsten, 1907 (as Steiniella cornuta); Indian Ocean
Wood, 1954; Southern Ocean, Port Fairy: 1962, Indian Ocean

G. polyedra Stein, 1883

Matzenauer, 1933; Indian Ocean
Wood, 1962; Indian Ocean

G. polygramma Stein, 1883

Ostenfeld and Schmidt, 1901; Red Sea, G. of Aden
Cleve, 1901, 1903; Red Sea, Arabian Sea, Indian Ocean
Matzenauer, 1933; Indian Ocean
Ostenfeld, 1915; Boeton Str.
Wood, 1954; south of Port Fairy: 1962; Indian Ocean
Ballantine, 1961; Zanzibar

G. scrippsae Kofoid, 1911

Wood, 1954, 1962; Swan R., Indian Ocean
Subrahmanyan, 1958; Arabian Sea

G. sphaeriodea Kofoid, 1911

Matzenauer, 1933; Indian Ocean

G. spinifera (Clap. and Lach.) Diesing, 1866

Schroeder, 1906 (as Ceratocorys); Indian Ocean
Karsten, 1907; Indian Ocean
Matzenauer, 1933; Indian Ocean
Wood, 1954; Antarctic Convergence: 1962; Indian Ocean
Ballantine, 1961; Zanzibar

Goniaulax turbynei Mur. and Whit., 1899

Schroeder, 1906; Indian Ocean
Matzenauer, 1933; Indian Ocean
Wood, 1954, 1962; Swan R., Indian Ocean

Genus GONIODOMA

Goniodoma polyedricum (Pouchet) Jörg., 1899

Cleve, 1900b, 1901, 1903 (as G. acuminatum); Red Sea, Malaya, Indian Ocean
Ostenfeld and Schmidt, 1901 (as G. acuminatum); Red Sea, G. of Aden
Schroeder, 1906; Red Sea, G. of Aden
Matzenauer, 1933; Indian Ocean
Wood, 1962; Indian Ocean
Ballantine, 1961; Zanzibar

G. sphaericum Mur. and Whit., 1899

Ostenfeld and Schmidt, 1899; G. of Aden, Red Sea
Matzenauer, 1933; Indian Ocean
Wood, 1954; west of Bass Str.

Genus GYMNASTER

Gymnaster pentasterias Schütt, 1895

Cleve, 1900, 1901; south Indian Ocean

Genus GYMNODINIUM

Gymnodinium bogoriense Klebs., 1912; Java

G. chuckwani Ballantine, 1961; Zanzibar

G. diploconus Schütt, 1895

Balech, 1958; Adelie Land

G. fusus Schütt, 1895

Karsten, 1907; Indian Ocean

Gymnodinium galaeiforme Matzenauer, 1933; Red Sea

Wood, 1962; Indian Ocean

G. gelbum Kofoid, 1931

Subrahmanyan, 1958; Arabian Sea

G. marinum Saville Kent, 1882

Subrahmanyan, 1958; Arabian Sea
Wood, 1962; Indian Ocean

G. mirabile Penard, 1891

Subrahmanyan, 1958; Arabian Sea

G. simplex (Lohmann) Kofoid and Swezy, 1921

Wood, 1962; Indian Ocean

G. splendens Lebour, 1925

Subrahmanyan, 1958; Arabian Sea

G. uberrimum (Allmann) Kofoid and Swezy, 1921

Subrahmanyan, 1958; Arabian Sea

G. variable Herdman, 1924

Subrahmanyan, 1958; Arabian Sea

Genus GYRODINIUM

Gyrodinium aureum Conrad, 1926

Subrahmanyan, 1958; Arabian Sea

G. citrinum Kofoid, 1931

Subrahmanyan, 1958; Arabian Sea

G. fusiforme Kofoid and Swezy, 1921

Subrahmanyan, 1958; Arabian Sea

Gyrodinium lingulifera Lebour, 1925

Subrahmanyan, 1958; Arabian Sea

G. obtusum (Schütt) Kofoid and Swezy, 1921

Subrahmanyan, 1958; Arabian Sea

G. pepo (Schütt) Kofoid and Swezy, 1921

Subrahmanyan, 1958; Arabian Sea

G. pingue (Schütt) Kofoid and Swezy, 1921

Subrahmanyan, 1958; Arabian Sea

G. spirale (Bergh) Kofoid and Swezy, 1921

Subrahmanyan, 1958; Arabian Sea

Genus HAPLODINIUM

Haplodinium antjoliense Klebs, 1912; Java

Haplodinium spp. Subrahmanyan, 1958; Arabian Sea

Genus HEMIDINIUM

Hemidinium nasutum Stein, 1883

Wood, 1954; Swan R.

Genus HETERODINIUM

Heterodinium assymetricum Kofoid and Adamson, 1933

Wood, 1954; Southern Ocean west of Bass Str.

H. australe Wood, 1962; Indian Ocean

H. blackmani (Mur. and Whit.) Kofoid, 1906

Schroeder, 1906; N.E. Indian Ocean
Karsten, 1907; Indian Ocean

Heterodinium dispar Kofoid and Adamson, 1933

Wood, 1962; Indian Ocean

H. doma (Mur. and Whit.) Kofoid, 1906

Wood, 1954, 1962; Southern Ocean west of Bass Str., Indian Ocean

H. rigdeni Kofoid, 1906

Karsten, 1907; Indian Ocean
Wood, 1962; Indian Ocean

H. scripps Kofoid, 1906

Wood, 1954; Southern Ocean west of Bass Str.: 1962; Indian Ocean

Genus HISTIONEIS

Histioneis caminus Bohm in Schiller, 1933; Indian Ocean

H. cerasus Bohm in Schiller, 1933; Indian Ocean
Wood, 1962; Indian Ocean

H. costata Kofoid and Michener, 1911

Wood, 1962; Indian Ocean

H. dolon Mur. and Whit., 1899

Karsten, 1907; Indian Ocean
Wood, 1962; Indian Ocean

H. elongata Kofoid and Michener, 1911

Schiller, 1933; Indian Ocean
Wood, 1962; Indian Ocean

H. fragilis Bohm in Schiller, 1933; Indian Ocean

H. gubernans Schütt, 1895

Schütt, 1896; Indian Ocean

H. helenae Mur. and Whit, 1899

Wood, 1962; Indian Ocean

Histioneis hyalina Kofoid and Michener, 1911

Schiller, 1933; Indian Ocean
Wood, 1962; Indian Ocean

H. inclinata Kofoid and Michener, 1911

Wood, 1962; Indian Ocean

H. longicollis Kofoid, 1907

Wood, 1962; Indian Ocean

H. milneri Mur. and Whit., 1899

Wood, 1962; Indian Ocean

H. mitchellana Mur. and Whit., 1899

Schroeder, 1906; Indian Ocean

H. panaria Kofoid and Skogsberg, 1928

Wood, 1962; Indian Ocean

H. pietschmanni Bohm in Schiller, 1933; Indian Ocean

H. remora Stein, 1883

Cleve, 1901; Arabian Sea, Indian Ocean
Wood, 1962; Indian Ocean

H. schilleri Bohm in Schiller, 1933; Indian Ocean

H. tubifera Bohm in Schiller, 1933; Indian Ocean

Wood, 1962; Indian Ocean

H. variabilis Schiller, 1933

Wood, 1962; Indian Ocean

Genus LISSODINIUM

Lissodinium schilleri Matzenauer, 1933; Indian Ocean

Genus MASSARTIA

Massartia glauca (Lebour) Schiller, 1933

Subrahmanyan, 1958; Arabian Sea

Genus MELANODINIUM

Melanodinium nigricans Schiller, 1937

Wood, 1962; Indian Ocean

Genus NOCTILUCA

Noctiluca miliaris Suriray, 1816

Prasad, 1958; Indian Ocean, coast of India
Subrahmanyan, 1958; Arabian Sea

Genus ORNITHOCERCUS

Ornithocercus cristatus Matzenauer, 1933; Indian Ocean

O. geniculatus Dangeard, 1927

Wood, 1962; Indian Ocean

O. heteroporus Kofoid, 1907

Matzenauer, 1933; Indian Ocean

O. magnificus Stein, 1883

Cleve, 1900a, 1901, 1903 (as Histioneis magnifica);
Red Sea, Arabian Sea, Indian Ocean, Malaya
Ostenfeld and Schmidt, 1901; Red Sea, G. of Aden
Schroeder, 1906; Red Sea, G. of Aden, Arabian Sea,
Indian Ocean, Fremantle Harbour
Karsten, 1907; Indian Ocean
Ostenfeld, 1915; Boeton Str.
Matzenauer, 1933; Indian Ocean
Wood, 1954, 1962; Southern and Indian Oceans
Subrahmanyan, 1958; Arabian Sea
Ballantine, 1961; Zanzibar

Ornithocercus quadratus Schütt, 1900

Ostenfeld and Schmidt, 1901; Red Sea, G. of Aden
Cleve, 1903; Red Sea, Arabian Sea
Schroeder, 1906; Arabian Sea, Indian Ocean
Karsten, 1907; Indian Ocean
Matzenauer, 1933; Indian Ocean
Wood, 1954, 1962; Southern and Indian Oceans

O. splendidus Schütt, 1895

Schroeder, 1906; N.E. Indian Ocean
Karsten, 1907; Indian Ocean
Matzenauer, 1933; Indian Ocean
Wood, 1962; Indian Ocean

O. steini Schütt, 1895

Ostenfeld, 1915; Boeton Str.
Matzenauer, 1933; Indian Ocean
Wood, 1962; Indian Ocean

O. thurni (Schmidt) Kof. and Skogsb., 1928

Matzenauer, 1933; Indian Ocean
Wood, 1962; Indian Ocean
Ballantine, 1961; Zanzibar

Genus OXYRRHIS

Oxyrrhis marina Dujardin 1841

Subrahmanyan, 1958; Arabian Sea

Genus OXYTOXUM

Oxytoxum caudatum Schiller, 1937

Wood, 1962; Indian Ocean

O. challengeroides Kofoid, 1907

Wood, 1962; Indian Ocean

Oxytoxum compressum Kofoid, 1907

Wood, 1962; Indian Ocean

O. constrictum Stein, 1883

Ostenfeld and Schmidt, 1901; Red Sea
Cleve, 1903; Arabian Sea
Schroeder, 1906; Arabian Sea
Wood, 1962; Indian Ocean

O. coronatum Schiller, 1937

Wood, 1962; Indian Ocean

O. curvatum Kofoid, 1911

Wood, 1962; Indian Ocean

O. diploconus Stein, 1883

Cleve, 1903; Arabian Sea
Karsten, 1907; Indian Ocean
Wood, 1962; Indian Ocean

O. elegans Pavillard, 1910

Matzenauer, 1933; Indian Ocean
Wood, 1962; Indian Ocean

O. gladiolus Stein 1883

Ostenfeld and Schmidt, 1901; Red Sea
Schroeder, 1906; Arabian Sea, Indian Ocean

O. milneri Mur. and Whit., 1899

Ostenfeld and Schmidt, 1901; Red Sea, G. of Aden
Schroeder, 1906; N.E. Indian Ocean
Karsten, 1907; Indian Ocean
Wood, 1962; Indian Ocean

O. mitra (Stein) Schroeder, 1906; Arabian Sea

Wood, 1962; Indian Ocean

O. parvum Schiller, 1937

Wood, 1962; Indian Ocean

Oxytoxum reticulatum (Stein) Schütt, 1896

Wood, 1962; Indian Ocean

O. sceptrum Stein, 1883

Cleve, 1901; Arabian Sea, Indian Ocean
Schroeder, 1906; Arabian Sea
Wood, 1962; Indian Ocean

O. scolopax Stein, 1883

Cleve, 1900a,b, 1901; south Indian Ocean, Arabian Sea, Red Sea
Ostenfeld and Schmidt, 1901; Red Sea, G. of Aden
Schroeder, 1906; Arabian Sea, G. of Aden, Indian Ocean, Fremantle
Karsten, 1907; Indian Ocean
Wood, 1962; Indian Ocean

O. sphaeroideum Stein, 1883

Cleve, 1900b; Indian Ocean
Ostenfeld and Schmidt, 1901; Red Sea
Wood, 1962; Indian Ocean

O. subulatum Kofoid, 1907

Wood, 1962; Indian Ocean

O. tessellatum Stein, 1883

Cleve, 1901, 1903; Red Sea, Arabian Sea
Ostenfeld and Schmidt, 1901; Red Sea; G. of Aden
Schroeder, 1906; Arabian Sea
Matzenauer, 1933; Indian Ocean
Wood, 1962; Indian Ocean

O. turbo Kofoid, 1907

Wood, 1962; Indian Ocean

O. variabile Schiller, 1937

Wood, 1962; Indian Ocean

Genus PACHYDINIUM

Pachydinium indicum Matzenauer, 1933; Indian Ocean

Genus PARAHISTIONEIS

Parahistioneis acuta Bohm in Schiller, 1933; Indian Ocean

P. crateriformis (Stein) Kofoid, 1907

Cleve, 1901 (as Histioneis); Red Sea, G. of Aden
Ostenfeld and Schmidt, 1901 (as Histioneis), Red Sea, G. of Aden

P. rotundata Kofoid and Michener, 1911

Subrahmanyan, 1958; Arabian Sea

Genus PERIDINIUM

Peridinium abei Paulsen, 1930

Matzenauer, 1933 (as P. biconicum Abe); Indian Ocean
Wood, 1954; Swan R.

P. achromaticum Levander, 1902

Matzenauer, 1933; Indian Ocean

P. adeliense Balech 1958; Adelie Land

P. adense Matzenauer, 1933; G. of Aden

P. affine Balech, 1958; Adelie Land (= P. pallidum)

P. africanoides Dangeard, 1927 (= P. steini)

Matzenauer, 1933; Indian Ocean

P. africanum Lemm., 1907; Madagascar, Malaya

West, 1907; Tanganyika
Schroeder, 1914; East Africa
Lindemann, 1931 (as P. ornamentosum); Java

Peridinium amplum Matzenauer, 1933; Indian Ocean

P. ampulliforme Wood, 1954; Swan R.

P. antarcticum Schimper 1907 (= P. depressum)

Balech, 1958; Adelie Land

P. applanatum Mangin, 1914

Balech, 1958; Adelie Land

P. archiovatum Balech, 1957

Balech, 1958; Adelie Land

P. avellana (Meunier) Lebour, 1925

Wood, 1954, 1962; Antarctic, Indian Ocean

P. baliense Lindemann, 1931; Malaya, Bali

P. berolinense Lemm., 1910

West, 1907; Tanganyika (doubtful)

P. biconicum Dangeard, 1927

Matzenauer, 1933; Indian Ocean

P. brachypus Schiller, 1937; Sumatra

P. breve Paulsen, 1907

Matzenauer, 1933; Indian Ocean
Wood, 1954; Antarctic, Heard I.

P. brevipes Paulsen, 1908

Wood, 1954; Antarctic, Heard I.

P. brochi Kofoid and Swezy, 1921

Subrahmanyan, 1958; Arabian Sea
Wood, 1962; Indian Ocean

f. inflatum Okamura, 1912

Matzenauer, 1933; Indian Ocean
Subrahmanyan, 1958; Arabian Sea

Peridinium bulla Meunier, 1910

Subrahmanyan, 1958; Arabian Sea

P. centenniale (Play) Lefevre, 1932

Lindemann, 1931; Indonesia
Lefevre, 1932; Malaya

P. cerasus Paulsen, 1907

Matzenauer, 1933; Indian Ocean
Wood, 1962; Indian Ocean

P. charcoti Balech, 1958; Adelie Land

P. cinctum (O.F.M.) Ehr., 1838; Asia

Woloszynska, 1912; Java
Schiller, 1914 (as P. westi); East Africa
Lindemann, 1931; East Indies

v. tuberosum Meunier, 1919; Madagascar

P. claudicans Paulsen, 1907

Karsten, 1907; Indian Ocean
Matzenauer, 1933; Indian Ocean
Wood, 1954; Southern Ocean, Swan R.: 1962; Indian Ocean
Subrahmanyan, 1958; Arabian Sea

P. colombense Matzenauer, 1933; Colombo Harbour

P. conicum (Gran) Ostenfeld and Schmidt, 1901; Red Sea, G. of Aden

Ostenfeld, 1915; Boeton Str.
Matzenauer, 1933; Indian Ocean
Wood, 1954; Southern Ocean, Heard I.
Subrahmanyan, 1958; Arabian Sea

f. concava Matzenauer, 1933; Indian Ocean
f. guardafuiana Matz., 1933; Indian Ocean

P. conicoides Paulsen, 1905

Wood, 1954; Albany, Antarctic, Heard I
Subrahmanyan, 1958; Arabian Sea

P. crassipes Kofoid, 1907

Karsten, 1907; Indian Ocean
Ostenfeld, 1915; Boeton Str.

Peridinium crassipes (contd)

Matzenauer, 1933 (as f. asymmetrica); Indian Ocean
Wood, 1954; west coast of Australia, Heard I., Antarctic
1962; Indian Ocean
Subrahmanyan, 1958; Arabian Sea

P. curtipes Jörgensen, 1913

Karsten, 1907; Indian Ocean
Matzenauer, 1933 (and as f. asymmetrica); Indian Ocean
Wood, 1954; Antarctic, Heard I.

P. curtum Balech, 1958; Adelie Land

P. curvipes Ostenfeld, 1906

Wood, 1954; Antarctic

P. decipiens Jörgensen, 1899

Matzenauer, 1933; Indian Ocean
Wood, 1954; Antarctic

P. depressum Bailey, 1855

Karsten, 1907; Indian Ocean
Ostenfeld, 1915; Boeton Str.
Matzenauer, 1933 (and f. antarctica); Indian Ocean
Wood, 1954, 1962; Antarctic, Heard I., Indian and
Southern Oceans
Subrahmanyan, 1958; Arabian Sea
Ballentine, 1961; Zanzibar

P. diabolus Cleve, 1900a ; Red Sea

Cleve, 1900b, 1901, 1903; South Indian Ocean, G. of Aden,
Arabian Sea, Indian Ocean, Malaya
Ostenfeld and Schmidt, 1901; G. of Aden
Schroeder, 1906; east Indian Ocean
Karsten, 1907 (as P. longipes); Indian Ocean
Matzenauer, 1933; Indian Ocean
Wood, 1954, 1962; Antarctic, Heard I., Indian Ocean

P. divergens Ehr., 1840

Cleve, 1900a, 1903; Red Sea, Arabian Sea, Indian Ocean
Ostenfeld and Schmidt, 1901; Red Sea, G. of Aden
Schroeder, 1906; G. of Aden to Malaya, Fremantle
Karsten, 1907; Indian Ocean

Peridinium divergens (contd)

Ostenfeld, 1915; Boeton Str.
Matzenauer, 1933 (as P. acutipes); Indian Ocean
Wood, 1954, 1962; Albany, South Australia, Indian Ocean
Subrahmanyan, 1958; Arabian Sea

P. elegans Cleve, 1900a; Red Sea

Cleve, 1901, 1903; Red Sea, G. of Aden, Arabian Sea, Malaya
Ostenfeld and Schmidt, 1901; Red Sea, G. of Aden
Schroeder, 1906; Red Sea to Malaya
Matzenauer, 1933 (and f. granulata); Indian Ocean
Wood, 1962; Indian Ocean

P. excentricum Paulsen, 1907

Matzenauer, 1933; Malacca Str.
Subrahmanyan, 1958; Arabian Sea
Wood, 1962; Indian Ocean

P. fatulipes Kofoid, 1907

Matzenauer, 1933 (and as P. tumidum Okam.); Indian Ocean
Wood, 1962; Indian Ocean

P. gatunense

v. madagascarense Lefevre, 1927; Madagascar

P. gibbosum Matzenauer, 1933; Indian Ocean

P. globulus Stein, 1883

Cleve, 1900a, 1901, 1903; Red Sea, G. of Aden to Malaya
Ostenfeld and Schmidt, 1901; Red Sea, G. of Aden
Schroeder, 1906; Red Sea to Malaya, Fremantle
Karsten, 1907; Indian Ocean
Matzenauer, 1933 (and as P. sphaeroides); Indian Ocean
Wood, 1954, 1962; Port Fairy to Fremantle Harbour, Indian Ocean
Subrahmanyan, 1958; Arabian Sea

P. grande Kofoid, 1907

Karsten, 1907; Indian Ocean
Czapek, 1909; Indian Ocean

Peridinium grande (contd)

Ostenfeld, 1915; Boeton Str.
Matzenauer, 1933; Indian Ocean
Wood, 1954, 1962; Great Australian Bight, Indian Ocean
Subrahmanyan, 1954; Arabian Sea

P. grani Ostenfeld, 1906

Matzenauer, 1933; Indian Ocean
Subrahmanyan, 1958; Arabian Sea
Wood, 1954, 1962; Heard I., Indian Ocean

P. gutwinskyi Woloszynska 1912; Java, Madagascar

Lindemann, 1931; Indonesia

P. heteracanthum Dangeard, 1927

Matzenauer, 1933; Indian Ocean

P. heteroconicum Matzenauer, 1933; Indian Ocean

P. hirobis Abé, 1927

Wood, 1962; Indian Ocean

P. humile Schiller, 1937

Matzenauer, 1933 (as P. decipiens); Indian Ocean
Subrahmanyan, 1958; Arabian Sea

P. hyalinum Meunier, 1910

Subrahmanyan, 1958; Arabian Sea

P. inconspicuum Lindemann, 1931; Malaya

Woloszynska, 1912, 1932 (as P. parvulum and P. steinmanni); Malaya

P. keyense Nygaard, 1926; Malaya

P. leonis Pavillard, 1916

Matzenauer, 1933; Indian Ocean
Subrahmanyan, 1958; Arabian Sea
Wood, 1962; Indian Ocean

Peridinium levanderi Abé, 1927

Matzenauer, 1933; Indian Ocean

P. marchicum Lemm. 1906

Woloszynska, 1912; Java

P. marielebourae Paulsen, 1930

Schiller, 1937; Indian Ocean

P. mediochre Balech, 1958; Adelie Land

P. minutum Kofoid, 1907

Subrahmanyan, 1958; Arabian Sea

P. mite Pavillard, 1916

Karsten, 1907; Indian Ocean
Matzenauer, 1933; Indian Ocean
Wood, 1954; Antarctic, Heard I.

P. monacanthum Brock, 1910

Wood, 1962; Indian Ocean

P. murrayi Kofoid, 1907

Matzenauer, 1933; Indian Ocean
Wood, 1954, 1962; Albany, Indian Ocean
Subrahmanyan, 1958; Arabian Sea

P. nipponicum Abé, 1927

Matzenauer, 1933; Indian Ocean
Wood, 1962; Indian Ocean

P. nux Schiller, 1937; Indian Ocean

P. obesum Matzenauer, 1933 (cf. P. heteracanthum); Indian Ocean

P. oblongum (Aurivillius) Cleve, 1900

Ostenfeld, 1915; Boeton Str.
Matzenauer, 1933; Indian Ocean
Wood, 1954, 1962; Albany, Heard I., Indian Ocean

Peridinium obovatum Wood, 1954; Antarctic

P. obtusum Karsten, 1906

Subrahmanyan, 1958 (? = P. marielebourae); Arabian Sea

P. oceanicum Vanhöffen, 1897

Cleve, 1900a,b, 1901, 1903; Red Sea, G. of Aden to Malaya, south Indian Ocean
Ostenfeld and Schmidt, 1901; Red Sea, G. of Aden
Schroeder, 1906; Arabian Sea, G. of Aden, Red Sea
Karsten, 1907; Indian Ocean
Ostenfeld, 1915; Boeton Str.
Matzenauer, 1933; Indian Ocean
Wood, 1954; Victoria to Albany, Indian Ocean: 1962; Indian Ocean
Subrahmanyan, 1958; Arabian Sea
Ballantine, 1961; Zanzibar

P. okamurai Abé, 1927

Wood, 1962; Indian Ocean

P. orientale Matzenauer, 1933; Indian Ocean

P. ovatum (Pouchet) Schütt, 1895

Matzenauer, 1933; Indian Ocean
Wood, 1954; Heard I.
Subrahmanyan, 1958 (as P. globulus v. ovatum); Arabian Sea

P. oviforme Dangeard, 1937

Matzenauer, 1933; Indian Ocean

P. pallidum Ostenfeld, 1899

Balech, 1958 (as P. affine); Adelie Land
Wood, 1962; Indian Ocean

P. parvicollum Balech, 1957

Balech, 1958; Adelie Land

P. pedunculatum Schütt, 1895

Cleve, 1900a,b, 1901; Indian Ocean, Malaya
Ostenfeld and Schmidt, 1901; Red Sea, G. of Aden

Peridinium pedunculatum (contd)

Schroeder, 1906; Red Sea to Singapore, Fremantle
Matzenauer, 1933 (as P. pellucidum); Indian Ocean
Wood, 1954, 1962; Albany, Indian Ocean
Subrahmanyan, 1958; Arabian Sea

P. pellucidum (Bergh) Schütt, 1883

Cleve, 1900b; south Indian Ocean
Ostenfeld and Schmidt, 1901; Red Sea, G. of Aden
Ostenfeld, 1915; Boeton Str.
Matzenauer, 1933; Indian Ocean
Wood, 1954: 1962; Indian Ocean

P. pentagonum Gran, 1902

Karsten, 1907; Indian Ocean
Ostenfeld, 1915; Boeton Str.
Matzenauer, 1933; Indian Ocean
Wood, 1954; Victoria, Swan R., North Australia:
1962; Indian Ocean
Subrahmanyan, 1958; Arabian Sea

v. latissima Kofoid, 1907

Ostenfeld, 1915; Boeton Str.
Matzenauer, 1933; Indian Ocean
Wood, 1954; Swan R.
Ballantine, 1961; Zanzibar

P. perrieri Faure Fremiet, 1909; Indian Ocean

P. persicum Schiller, 1937

Bohm, 1931 (as P. schilleri); Persian Gulf

P. pietschmanni Bohm, 1931; Persian Gulf

P. pyriforme Paulsen, 1904

Ostenfeld, 1915; Boeton Str
Wood, 1954; Heard I.

P. playfairi Lindemann, 1931; Malaya, Bali

P. pseudoantarcticum Balech, 1937

Peridinium punctulatum Paulsen, 1908

Matzenauer, 1933; Indian Ocean
Wood, 1954; Israelite Bay, Albany, Heard I.
Ballantine, 1961; Zanzibar

P. pyriforme Paulsen, 1907

Matzenauer, 1933; Indian Ocean
Wood, 1954; Heard I., Antarctic, Indian Ocean
Balech, 1958; Adelie Land

P. quadratum Matzenauer, 1933; Indian Ocean

P. quarnerense Schroeder, 1910; Indian Ocean

Ostenfeld, 1915; Boeton Str.
Matzenauer, 1933 (as P. subpyriforme Dang.); Indian Ocean
Wood, 1954; Swan R., Northern Australia
Subrahmanyan, 1958 (as P. globulus v. quarnerense);
Arabian Sea

P. raciborskii Woloszynska, 1912, Java

P. remotum Karsten 1907; Indian Ocean

Matzenauer, 1933; Indian Ocean

P. retiferum Matzenauer, 1933; Indian Ocean

P. rosaceum Balech, 1957

Balech, 1958; Adelie Land

P. roseum Paulsen, 1929

Wood, 1954, 1962; Swan R., Indian Ocean

P. sanguineum Carter, 1858

Saville Kent, 1880; Bombay

P. sinaicum Matzenauer, 1933; Red Sea

Subrahmanyan, 1958; Arabian Sea

P. solidicorne Mangin, 1926

Matzenauer, 1933; Indian Ocean
Wood, 1962; Indian Ocean

Peridinium somma Matzenauer, 1933; Indian Ocean

P. sp? Subrahmanyan, 1958; Arabian Sea

P. sphaericum Okamura, 1912

Matzenauer, 1933 (v. gracilis as P. sphaeroidea Abè); Indian Ocean
Ballantine, 1961; Zanzibar

P. steini Jörgensen, 1899

Cleve, 1900a,b, 1901, 1903; Red Sea to Malaya, south Indian Ocean
Ostenfeld and Schmidt, 1901; Red Sea, G. of Aden
Schroeder, 1906; Red Sea to Singapore
Karsten, 1907; Indian Ocean
Ostenfeld, 1915; Boeton Str.
Matzenauer, 1933; Indian Ocean
Wood, 1954, 1962; Fremantle, Geraldton, Indian Ocean, Antarctic convergence
Subrahmanyan, 1958; Arabian Sea
Ballantine, 1961; Zanzibar

P. subinerme Paulsen, 1904

Matzenauer, 1933 (as P. asymmetrica); Indian Ocean
Wood, 1954, 1962; Victoria, Albany, Antarctic convergence, Indian Ocean
Subrahmanyan, 1958; Arabian Sea

P. tenuissimum Kofoid, 1907

Karsten, 1907; Indian Ocean
Matzenauer, 1933; Indian Ocean
Wood, 1962; Indian Ocean

P. thorianum Paulsen, 1905

Matzenauer, 1933; Indian Ocean
Subrahmanyan, 1958; Arabian Sea
Wood, 1962; Indian Ocean

P. treubi Woloszynska (v. Glenodinium quadridens Stein)

Peridinium tristylum Stein, 1883

Ostenfeld and Schmidt, 1901; Red Sea, G. of Aden
Matzenauer, 1933; Indian Ocean

f. ovata Schroeder, 1906; Indian Ocean, Fremantle Harbour

P. trochoideum (Stein) Lemm., 1910

Subrahmanyan, 1958 (as Glenodinium); Arabian Sea

P. turbinatum Mangin, 1926

Wood, 1954; Heard I., Antarctic
Balech, 1958; Adelie Land (= P. inaequale Peters)

P. umbonatum Stein, 1883

Woloszynska, 1912; Java
Lindemann, 1931 (as P. ambiguum, Glenodinium guildfordense, and G. geminum); Java

P. variegatum Peters, 1928

Wood, 1954, 1962; Antarctic, Indian Ocean
Balech, 1958, Adelie Land

P. ventricum Abé, 1927

Wood, 1962; Indian Ocean

P. venustum Matzenauer, 1933; Indian Ocean

Subrahmanyan, 1958; Arabian Sea
Ballantine, 1961; Zanzibar

P. volzi Lemm., 1905; Madagascar, Africa

West, 1909; Yan Yean, Victoria
Lindemann, 1931; Indonesia

v. botanicum Lindemann, 1909; Malaya

f. sinuatum (Lindemann) Lefevre, 1932
Lindemann, 1931 (as P. sinuatum); Malaya

P. wildemani Woloszynska, 1912 (v. Glenodinium quadridens Stein)

Peridinium willei Huitfeld-Kaas, 1900

Lindemann, 1931; Indonesia

Genus PHALACROMA

Phalacroma acutum (Schütt) Pav., 1916

Matzenauer, 1933; Indian Ocean
Wood, 1962; Indian Ocean

P. argus Stein, 1883

Ostenfeld and Schmidt, 1901; Red Sea, G. of Aden
Cleve, 1901; Arabian Sea, Indian Ocean
Schroeder, 1906; Red Sea, Arabian Sea
Matzenauer, 1933; Indian Ocean
Wood, 1954; west of Bass Str.

P. circumsutum Karsten, 1907; Indian Ocean

Matzenauer, 1933; Indian Ocean
Ballantine, 1961; Zanzibar

P. cuneus Schütt, 1895

Cleve, 1901, 1903; Arabian Sea, Indian Ocean
Ostenfeld and Schmidt, 1901; G. of Aden
Schroeder, 1906 (as P. blackmani); Arabian Sea, Fremantle, Indian Ocean
Karsten, 1907; Indian Ocean
Matzenauer, 1933; Indian Ocean
Wood, 1962; Indian Ocean

P. dolichopterygium Mur. and Whit., 1899

Cleve, 1901; Indian Ocean
Matzenauer, 1933; Indian Ocean
Subrahmanyan, 1958; Arabian Sea

P. doryphorum Stein, 1883

Cleve, 1900, 1903; Red Sea, Arabian Sea, Indian Ocean
Ostenfeld and Schmidt, 1901; Red Sea, G. of Aden
Schroeder, 1906; G. of Aden, Arabian Sea, Indian Ocean
Wood, 1962; Indian Ocean

Phalacroma favus Kof. and Mich., 1911

Matzenauer, 1933; Indian Ocean
Wood, 1962; Indian Ocean

P. hindmarchi Mur. and Whit., 1899

Wood, 1962; Indian Ocean

P. irregulare Lebour, 1926

Wood, 1954; south coast of Australia

P. jourdani Gourret, 1883

Cleve, 1901, 1903; Red Sea, G. of Aden, Arabian Sea, Indian Ocean

P. latevelatum Kof. and Skogsb., 1928

Matzenauer, 1933; Indian Ocean

P. lens Kof. and Skogs., 1928

Wood, 1954; Swan R.

P. mawsoni Wood, 1954; Antarctic convergence

P. mitra Schütt, 1895

Ostenfeld and Schmidt, 1901; Red Sea, G. of Aden
Schroeder, 1906; Arabian Sea, east Indian Ocean
Wood, 1962; Indian Ocean

P. operculatum Stein, 1883

Cleve, 1901, 1903; Red Sea, G. of Aden, Arabian Sea, Indian Ocean
Schroeder, 1906; Arabian Sea, N.E. Indian Ocean
Karsten, 1907; Indian Ocean
Wood, 1962; Indian Ocean

P. ovum Schütt, 1895

Wood, 1954, 1962; Swan R., Indian Ocean

Phalacroma parvulum (Schütt) Jörgensen, 1923

Ostenfeld and Schmidt, 1901 (as P. porodictyum v. parvulum); G. of Aden
Matzenauer, 1933; Indian Ocean
Wood, 1962; Indian Ocean

P. porodictyum Stein, 1883

Ostenfeld and Schmidt, 1901; Red Sea, G. of Aden
Schroeder, 1906 (as P. porodictum); Arabian Sea
Ostenfeld, 1915; Boeton Str.
Matzenauer, 1933; Indian Ocean

P. porosum (Kof. and Mich.) Kof. and Skogs., 1928

Wood, 1954; Antarctic

P. pulchellum Lebour, 1925

Wood, 1954; Antarctic convergence south of C. Leeuwin

P. rapa Stein, 1883

Cleve, 1901, 1903; Arabian Sea, Indian Ocean
Ostenfeld and Schmidt, 1901; G. of Aden
Matzenauer, 1933; Indian Ocean, Red Sea
Wood, 1962; Indian Ocean

P. rotundatum (Clap. and Lach.) Kof. and Mich., 1911

Karsten, 1907 (as Dinophysis rotundatum); Indian Ocean
Matzenauer, 1933; G. of Aden, Indian Ocean
Subrahmanyan, 1958; Arabian Sea

P. rudgei Mur. and Whit., 1899

Schroeder, 1906; Indian Ocean
Wood, 1962; Indian Ocean

P. striatum Kofoid, 1907

Wood, 1962; Indian Ocean

P. vastum Schroeder, 1906; G. of Aden, Arabian Sea

Genus PODOLAMPAS

Podolampas bipes Stein, 1883

Cleve, 1901, 1903; Red Sea, G. of Aden, Arabian Sea, Indian Ocean, Malaya
Ostenfeld and Schmidt, 1901; Red Sea, G. of Aden
Schroeder, 1906; Red Sea, Arabian Sea, Indian Ocean
Ostenfeld, 1915; Boeton Str.
Matzenauer, 1933; Indian Ocean
Subrahmanyan, 1958; Arabian Sea
Wood, 1962; Indian Ocean
Ballantine, 1961; Zanzibar

f. reticulata (Kofoid) Schiller, 1937

Matzenauer, 1933 (as P. reticulata Kof.), Indian Ocean
Wood, 1962; Indian Ocean

P. elegans Schütt, 1895

Schroeder, 1906; Red Sea, G. of Aden, Arabian Sea
Matzenauer, 1933; Indian Ocean
Wood, 1962; Indian Ocean

P. palmipes Stein, 1883

Cleve, 1900a, 1903; Red Sea, G. of Aden, Arabian Sea
Ostenfeld and Schmidt, 1901; Red Sea, G. of Aden
Schroeder, 1906; Red Sea to Sunda Sea
Matzenauer, 1933; Indian Ocean
Subrahmanyan, 1958; Arabian Sea
Wood, 1962; Indian Ocean

P. spinifer Okamurai 1912

Wood, 1962; Indian Ocean

Genus POLYKRIKOS

Polykrikos schwartzi Butschli, 1873

Subrahmanyan, 1958; Arabian Sea

Genus PRONOCTILUCA

Pronoctiluca pelagria Fabre-Domergue, 1889

Wood, 1962; Indian Ocean

P. spinifera (Lohmann) Schiller, 1933

Wood, 1962; Indian Ocean

Genus PROROCENTRUM

Prorocentrum arcuatum Issel, 1928

Matzenauer, 1933 (as P. gibbosum Schiller); Indian Ocean
Wood, 1962; Indian Ocean

P. dentatum Stein, 1883

Wood, 1954, 1962; Swan R., Indian Ocean

P. maximum Schiller, 1931

Matzenauer, 1933; Indian Ocean

P. gracile Schütt, 1895

Ostenfeld and Schmidt, 1901; Red Sea
Schroeder, 1906; Arabian Sea, Indian Ocean

P. micans Ehr., 1833

Ostenfeld and Schmidt, 1901; Red Sea, G. of Aden
Cleve, 1903; Arabian Sea
Schroeder, 1906; G. of Aden, Red Sea, Arabian Sea
Ostenfeld, 1915; Boeton Str.
Matzenauer, 1933; Indian Ocean
Wood, 1954, 1962; Swan R., Indian Ocean
Subrahmanyan, 1958; Arabian Sea

P. minimum Schiller, 1933

Wood, 1962; Indian Ocean

P. rostratum Stein, 1883

Wood, 1962; Indian Ocean

Prorocentrum scutellum Schroeder, 1901; India

P. sigmoides Bohm, 1931

Subrahmanyan, 1958; Arabian Sea

P. spinulosum Karsten, 1907; Indian Ocean

Genus PROTOCERATIUM

Protoceratium areolatum Kofoid, 1907

Matzenauer, 1933; Indian Ocean
Wood, 1962; Indian Ocean

P. reticulatum (Clap. and Lach.) Butschli, 1885

Ostenfeld and Schmidt, 1901; Red Sea, G. of Aden
Matzenauer, 1933; Indian Ocean

Genus PTYCHODISCUS

Ptychodiscus carinatus Kofoid, 1907

Matzenauer, 1933; Indian Ocean

P. inflatus Pavillard, 1916

Matzenauer, 1933; Indian Ocean

Genus PSEUDOPHALACROMA

Pseudophalacroma nasutum (Stein) Jörg., 1923

Karsten, 1907; Indian Ocean
Matzenauer, 1933; Indian Ocean

Genus PYROCYSTIS

Pyrocystis elegans Pav., 1931

Matzenauer, 1933; Indian Ocean
Wood, 1962; Indian Ocean

Pyrocystis ellipsoides (Hackel) Lemm., 1890

Matzenauer, 1933; Indian Ocean

P. fusiformis Murray, 1885

Ostenfeld and Schmidt, 1901; Red Sea, G. of Aden
Cleve, 1901; Indian Ocean, Malaya
Karsten, 1907; Indian Ocean
Matzenauer, 1933; Indian Ocean
Subrahmanyan, 1958; Arabian Sea
Wood, 1962; Indian Ocean

P. hamulus Cleve, 1900

Cleve, 1901, 1903; Indian Ocean, Malaya, Red Sea
Ostenfeld and Schmidt, 1901; G. of Aden
Schroeder, 1906; Indian Ocean
Karsten, 1907; Indian Ocean
Matzenauer, 1933; Indian Ocean
Wood, 1962; Indian Ocean

f. semicircularis Kofoid, 1907

Matzenauer, 1933; Indian Ocean
Wood, 1962; Indian Ocean

P. lanceolata Schroeder, 1900

Karsten, 1907; Indian Ocean
Matzenauer, 1933; Indian Ocean

P. lunula Schütt, 1896

Ostenfeld and Schmidt, 1901; Red Sea, G. of Aden
Cleve, 1901; Arabian Sea, Indian Ocean
Schroeder, 1906; Indian Ocean
Karsten, 1907; Indian Ocean
Wood, 1962; Indian Ocean

P. micans Schroeder, 1906; Red Sea

P. minima Matzenauer, 1933; Indian Ocean

P. obtusa Pav., 1931

Matzenauer, 1933; Indian Ocean

Pyrocystis pseudonoctiluca W. Thompson, 1876

Cleve, 1900a,b, 1901, 1903; Red Sea, G. of Aden, Arabian Sea, Malaya, Indian Ocean
Ostenfeld and Schmidt, 1901; Red Sea, G. of Aden
Karsten, 1907; Indian Ocean
Matzenauer, 1933; Indian Ocean
Wood, 1954, 1962; Indian and Southern Oceans
Subrahmanyan, 1958; Arabian Sea

P. rhomboides Matzenauer, 1933; Indian Ocean

P. robusta Kofoid, 1907

Matzenauer, 1933; Indian Ocean
Karsten, 1907; Indian Ocean
Wood, 1962, Indian Ocean
Ballantine, 1961; Zanzibar

Genus PYRODINIUM

Pyrodinium schilleri (Matz.) Schiller, 1937

Matzenauer, 1933 (as Goniaulax); Red Sea, Persian Gulf

Genus PYROPHACUS

Pyrophacus horologicum Stein, 1883

Cleve, 1900a,b, 1901, 1903; Red Sea, Indian Ocean, Malaya
Ostenfeld and Schmidt, 1901; Red Sea, G. of Aden
Schroeder, 1906; Red Sea to Sunda Sea
Ostenfeld, 1915; Boeton Str.
Matzenauer, 1933; Indian Ocean
Wood, 1954, 1962; Bass Strait to Indian Ocean
Subrahmanyan, 1958 (and v. steini); Arabian Sea
Ballantine, 1961; Zanzibar

Genus SPHAERODINIUM

Sphaerodinium javanicum Woloszynska, 1930; Java

S. spp. Subrahmanyan, 1958; Arabian Sea

Genus SPIRAULAX

Spiraulax jolliffei (Mur. and Whit.) Kofoid, 1911

Cleve, 1903 (as Goniaulax); Red Sea, Arabian Sea
Schroeder, 1906 (as Goniaulax); Indian Ocean
Matzenauer, 1933; Indian Ocean
Wood, 1962; Indian Ocean

1305

BIBLIOGRAPHY

This bibliography contains the papers consulted in preparing the check-list, and does not include species references which are available elsewhere.

BALECH, E. (1957).- Dinoflagelles et tintinnides de la terre Adelie (Secteur francaise Antarctique). Vie et Milieu 8: 382-408.

BALECH, E. (1958).- Plancton de la compana Antarctica Argentina. Physis 21: 75-108.

BALLANTINE, Dorothy (1961).- Gymnodinium chuckwanii n. sp. and other marine dinoflagellates collected in the vicinity of Zanzibar. J. Protozool. 8: 217-228.

BOHM, A. (1931).- Zur Verbreitung einige Peridinium. Arch. Protistenk. 75: 498.

CLEVE, P.T. (1900a).- Plankton from the Red Sea. Ofv. Kongl. Sv. Vet-Akad Forh. 57(9).

CLEVE, P.T. (1900b).- Plankton from the South Atlantic and South Indian Oceans Ofv. Kongl. Sv. Vet-Akad Forh. 57(9).

CLEVE, P.T. (1901).- Plankton from the Indian Ocean and the Malay Archipelago. Ofv. Kongl. Sv. Vet-Akad Forh. 35(5)

CLEVE, P.T. (1903).- Report on plankton collected by Mr Thorild Wulff during a voyage to and from Bombay. Ark. Zool. 1: 329-391.

C.S.I.R.O. Aust. (1962).- Oceanic observations in the Indian Ocean in 1959. H.M.A.S. Diamantina Cruises Dm1/59, Dm2/59. C.S.I.R.O. Aust. Oceanogr. Cruise Rep. 1.

C.S.I.R.O. Aust. (1962).- Oceanic observations in the Indian Ocean in 1960. H.M.A.S. Diamantina Cruise Dm1/60. C.S.I.R.O. Aust. Oceanogr. Cruise Rep. 2.

C.S.I.R.O. Aust. (1962).- Oceanic observations in the Indian Ocean in 1960. H.M.A.S. Diamantina Cruise Dm2/60. C.S.I.R.O. Aust. Oceanogr. Cruise Rep. 3 (in press).

CZAPEK, F. (1909).- Zur Kenntnis der Phytoplanktons im Indischen Ozean.
Sitz. Akad. Wiss. Wien. 118: 231-239.

KARSTEN, G. (1907).- Das Indische Phytoplankton.
Wiss. Erg. Deutsch. Tiefsee Exp. VALDIVIA. 2: 221-348.

LEMMERMANN, E. (1899).- Ergebnis einer Reise nach dem Pacific Planktonalgen.
Abh. Naturw. Ver. Bremen 16: 298-313.

LEMMERMANN, E. (1910).- Klasse Peridiniales. Algen in Kryptogamenflora der Mark Brandenberg und angrenzender Gebiete. 3: 563-712.

LINDEMANN, E. (1931).- Die Peridineen der Deutsch Limnol. Sunda Exp. nach Sumatra, Java u. Bali
Arch. Hydrobiol. Suppl. Bd 8. 691.

MATZENAUER, G. (1933).- Die Dinoflagellaten des Indischen Ozeans.
Bot. Arch. 35: 437-510

OSTENFELD, C.H. (1915).- A list of phytoplankton from the Boeton Strait.
Dansk Bot. Ark. 2(4): 1-18.

OSTENFELD, C.H. and SCHMIDT, J. (1901).- Plankton fra det Röde Hav og Adenbugten.
Vidensk. Medd. Naturh. Foren. Kjöbenhavn: No. 141.

SCHILLER, J. (1933/1937).- Dinoflagellatae (Peridineae). In Rabenhorsts Kryptogamen-flora. 10(3): 1-580.

SCHROEDER, B. (1906).- Beiträge zur Kenntnis der Phytoplanktons warmer meere.
Vierteljahr naturf. Ges. Zurich. 51: 319-377.

SCHROEDER, B. (1914).- Zellpflanzen Ostafrikas.
Hedwigia 55: 183-208.

STEEMANN-NIELSEN, E. (1939).- De Ceratien des Indisches Ozeans und ser Ostasiatischen Gewässer.
Dana Rept. 17: 1-33.

SUBRAHMANYAN, R. (1958).- Phytoplankton organisms of the Arabian Sea off the west coast of India.
J. Ind. Bot Soc. 37: 435-441

WEST, G.S. (1907).- Report on freshwater algae of the Third Tanganyika Expedition conducted by Dr W.A. Cunnington.
J. Linn. Soc. (Bot.) 38: 81-197.

WEST, G.S. (1909).- The algae of Yan Yean reservoir.
J. Linn. Soc. (Bot.) 39: 1-88.

WOLOSZYNSKA, J. (1912).- Das Phytoplankton einiger javanischer Seen. Beruch. Sawa-Plankton.
Bull. Int. Acad. Sci. Cracovie (B): 649-704.

WOLOSZYNSKA, J. (1930).- Beitrag zur Kenntnis des Phytoplanktons tropischen Seen.
Arch. Hydrobiol. 5(1-2): 159-169.

WOOD, E.J.F. (1954).- Dinoflagellates in the Australian region.
Aust. J. Mar. Freshw. Res. 5: 171-351.

WOOD, E.J.F. (1962).- Phytoplankton in Report of H.M.A.S. Diamantina Cruises Dm1/59, Dm2/59.
See C.S.I.R.O. Aust. (1962).

WOOD, E.J.F. (1962).- Phytoplankton in Report of H.M.A.S. Diamantina Cruise Dm1/60.
See C.S.I.R.O. Aust. (1962).

WOOD, E.J.F. (1962).- Phytoplankton in Report of H.M.A.S. Diamantina Cruise Dm2/60.
See C.S.I.R.O. Aust. (1962).

Reprinted from *Bull. fish. res. Stn., Ceylon*, vol. 16, no. 1, 1963, p. 9-24.

Studies on the Seasonal Cycle of Sea Surface Temperatures, Salinities and Phytoplankton in Puttalam Lagoon, Dutch Bay and Portugal Bay along the West Coast of Ceylon

M. DURAIRATNAM
Department of Fisheries, Colombo 3, Ceylon

Introduction

A study of the sea surface temperatures, salinities and phytoplankton was carried out at Puttalam lagoon, which is the largest lagoon in Ceylon and in the adjacent bays, Dutch Bay and Portugal Bay, for one year from June, 1960 to May, 1961. Lagoon fishing is carried out throughout the year, but most of the fishing is done during the South West Monsoon, as the sea outside is too rough for small vallams, theppams and orus to go out fishing. Surface temperatures and salinities for the Bay of Bengal have been reported by Sewell (1925), Das (1954) and Jayaraman (1954). They have made detailed studies for specific nearshore locations along the Indian coasts. La Fond (1954, 1957) had shown the relation of these data to the water masses and circulation. La Fond (1958) had also described the seasonal cycle of sea surface temperatures and salinities along the East Coast of India. Studies on the plankton of the inshore waters off Mandapam were made by Prasad (1954, 1956). Studies on plankton were also made by Chacko (1950), Ganapathi and Murthy (1953 and 1955), Ganapathy and Rao (1953), and Menon (1945).

However, no work on marine plankton had been described for Ceylon waters. It was thought worthwhile to study the seasonal cycle of sea surface temperatures, salinities and phytoplankton and their effect on fisheries production in these areas, as phytoplankton forms the food of zooplankton and the food of fishes directly or indirectly.

Material and Methods

Surface plankton hauls were made with Kitahara's surface plankton net with an over all length of 120 cms. and diameter of 30 cms. The mesh is in conformity with the International Standard No. 13 and with the Japanese standard XX 13. Plankton hauls were made once a month from the departmental motor launches the " Seer ", " Kelawalla ", and " Halmessa ". The speed of the boat was kept constant during the tow which was confined to 15 minutes. The plankton collected was transferred into clean bottles and preserved in 4% formalin. Temperature readings of surface water were made on the dates of collection. Salinities were obtained by determining chlorinity by Knudsen's method and reading salinity values directly from Knudsen's table. Quantitative estimations were made by counting under a binocular microscope the plankton contained in 1 c.c. samples. Different symbols were used to denote the comparative abundance of the differant diatoms, dinoflagellates and Cyanophyceae.

Sea surface temperature

The mean monthly surface temperatures at Puttalam lagoon vary from 27.6° C to 30.8° C. The peak temperatures were in April, May and June and the lowest found were in November, December

and January. The temperature range is 3.2° C. There is a gradual fall in temperature from April to September and from October to January. The lowering of the temperature from April to September is probably due to the high winds during the South-West Monsoon which causes turbulence, which results in the mixing of the surface water and subsurface cold water. The lowering of temperature from October to December can be attributed to the general cooling of the atmosphere and the onset of the North-East winds as reported by Ganapathi and Venkata Rama Sarma (1958). The surface temperatures at Dutch Bay and Portugal Bay reveal the same pattern as in Puttalam lagoon, although the temperatures are relatively lower. This is because Puttalam lagoon is further away from the sea and is rather shallow compared to Dutch Bay and Portugal Bay.

TABLE I

MONTHLY SURFACE TEMPERATURE AND SALINITY AT FOUR LOCATIONS ON PUTTALAM LAGOON FROM JUNE, 1960 TO MAY, 1961

	Puttalam Lagoon		*Dutch Bay*		*Portugal Bay towards Pallugaturai*		*Portugal Bay towards Kovil Munai*	
	Temp. (°C)	*Sal.* (‰)	*Temp.* (°C)	*Sal.* (‰)	*Temp.* (°C)	*Sal.* (‰)	*Temp.* (°C)	*Sal.* (‰)
January	27·6	20·4	27·0	21·3	27·1	30·0	27·1	30·5
February	28·0	24·7	27·5	25·2	27·6	30·5	27·6	30·8
March	29·2	24·5	28·8	29·1	28·8	30·2	28·6	30·1
April	30·8	22·8	30·4	29·6	30·4	30·5	30·6	31·4
May	30·6	29·9	30·2	20·0	30·3	32·0	30·4	31·9
June	30·0	30·4	28·9	30·8	29·0	31·8	29·2	35·6
July	28·8	33·8	28·2	35·0	29·4	33·2	29·2	34·3
August	28·6	35·3	28·0	34·5	28·2	32·2	28·3	32·1
September	28·2	33·8	27·6	33·4	27·7	33·1	27·7	32·2
October	28·4	36·4	27·8	34·8	27·8	35·4	27·9	35·6
November	28·0	20·0	27·4	18·5	27·5	28·2	27·6	29·4
December	27·8	20·2	27·2	20·4	27·2	31·4	27·2	31·5

Salinity

The highest salinities at Puttalam lagoon are from May to October ranging from 29.9‰ in May to 36.4‰ in October. The salinities vary from 20‰ in November to 22.8‰ in April. This shows that during the South-West Monsoon the salinity is high and low during the North-East Monsoon. Probably the salinities are relatively high from May to October due to the high evaporation that takes place during these months, as the lagoon is rather shallow not exceeding two fathoms in the deepest area and 1-2 feet in the shallowest area, and to the prevalence of high winds during the S.-W. Monsoon. Further, higher salinity waters are brought into the lagoon from the Central Indian Ocean and southern part of the Arabian Sea as the current is from South to North (Sewell 1925–32). There is a close resemblance between the temperature and salinity of waters at Mandapam described by La Fond (1958) and in the bays of the west coast of Ceylon. During the North-East Monsoon the current is reversed, i.e., from North to South (Sewell 1925–32), as a result, the salinity values are low from November to April, namely 20‰ to 24.7‰. At Dutch Bay the salinity range was similar to Puttalam lagoon except that the salinities in March and April were higher which coincides with the high temperatures reached during these months. The salinities at Portugal Bay towards Kovil Munai and Pallugaturai are comparatively higher than at Puttalam Lagoon or Dutch Bay as Portugal Bay is closer to the sea. Although there is an increase in the salinities in Portugal Bay from April to October during the South-West Monsoon the increase is not as high as in Puttalam lagoon.

Fig. 1

MONTHLY SURFACE TEMPERATURE AND SALINITY AT FOUR LOCATIONS ON PUTTALAM LAGOON FROM JUNE 1960 TO MAY 1961.

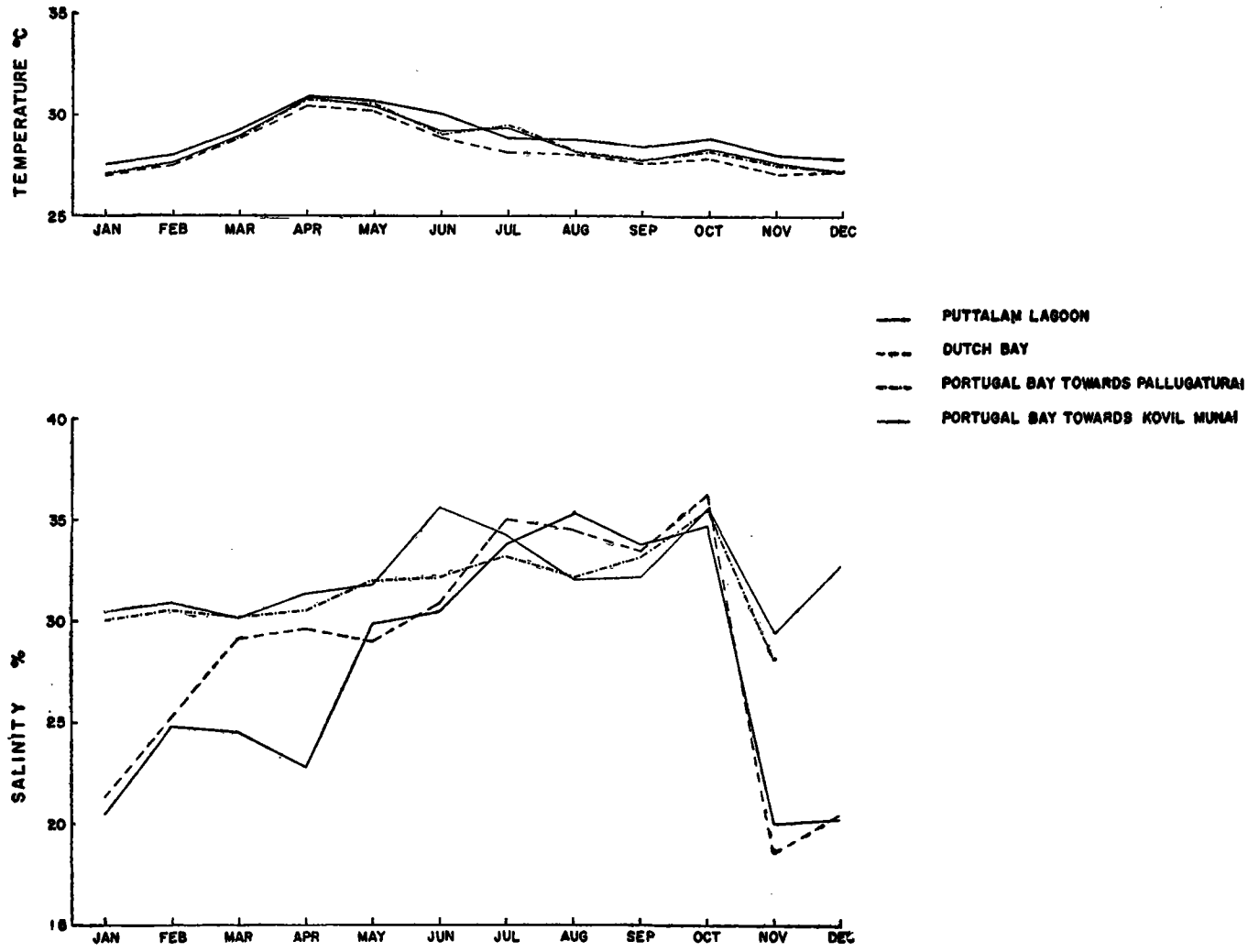

Plankton

There were sudden fluctuations in the distribution of phytoplankton but no definite conclusions can be drawn due to the short period of observation. The distribution of phytoplankton including Dinophyceae and Cyanophyceae is shown in tables 2, 3, 4 and 5. There are more than one phytoplankton maximum in a year. At Puttalam lagoon blooms of *Thalassiosira subtilis* occurred in November, *Rhizosolenia alata* in February, *Rhizosolenia imblricata* in March and May, *Chaetoceros lascinosus* in February, *Thallassionema nitzschioides* and *Thallassiothrix Frauenfeldii* in May. At Dutch Bay blooms of *Coscinodiscus gigas* occurred in June, *Sceletonema costatum* in August, *Bacteriastrum varians* in July, *Chaetoceros diversus* in October, *Rhizosolenia imbricata* in February, *Rhizosolenia alata* in March, *Biddulphia mobilensis* in May, *Thallassiothrix frauenfeldii* July to September, *Rhaphoneis discoides* in September, *Asterionella japonica* May and in October, *Thallassionema nitzschioides* in April and May. Blooms at Portugal Bay towards Kovil Munai were identical with those of Dutch Bay. Blooms at Portugal Bay towards Pallugaturai were mostly identical, but blooms of *Chaetoceros pervianus* occurred in October, and *Thalassiosira subtilis* in November.

In all the 4 regions the bulk of phytoplankton occurred from May to September during the South-West Monsoon and is the cumulative effect of several species. For example the bulk of phytoplankton in May was composed of *Thalassiosira decipens, Thalassiosira subtilis, Coscinodiscus gigas, Rhizosolenia imbricata, Rhizosolenia alata, Rhizosolenia styliformis, Bacteriastrum varians, Chaetoceros lorenzianus, Chaetoceros pervianus, Biddulphia sinensis, Biddulphia pulchella, Rhaphoneis discoides, Thallasionema nitzschoides, Thallassiothrix longissima, Thallassiothrix frauenfeldii* and *Gyrosigma balticum*. There were two outburts of diatoms in June and in October. The June outburst consisted of several species, the dominant ones being *Sceletonema costatum, Coscinodiscus gigas, Rhizosolenia styliformis, Rhizosolenia alata, Biddulphia sinensis, Thallassionema nitzschioides, Thallassiothrix frauenfeldii* and *Asterionella japonica*. The October outburst consisted of several species of *Chaetoceros, Chaetoceros lorenzianus, Chaetoceros pervianus, Chaetoceros lascinosus, Chaetoceros diversus, Thallassiothrix frauenfeldii, Asterionella japonica, Rhizosolenia imbricata, Rhizosolenia alata and Rhizosolenia styliformis*.

Sudden outbursts of a single species were common especially *Thallassiothrix frauenfeldii, Chaetoceros* species and *Rhizosolenia* species. The distribution of diatoms at Puttalam lagoon is different from the other three localities. The relative abundance of plankton was small and the number of species of diatoms much less. This may be attributed to the fact that it is further away from the sea and lacks nutrient salts. In the other three areas the rivers Kal Aru and Pomparippu Aru empty and bring in nutrient salts.

Four species of Dinophyceae were found in these areas and their relative abundance is shown in the tables 2-5.

Trichodesmium erythraeum a blue green algae belonging to the Cyanophyceae was found in plenty in January, February, March and November. Devanesan (1942) states that *Trichodesmium* found off Krusadai in abundance forms a favourite item in the food of the Indian sprat (*Sardinella gibbosa*) and the mullet (*Mugil waigiensis*). During the year June, 1960 to May, 1961 the months in which sprats were caught in large quantities were January, February, March and November. This seems to correspond with the relative abundance of *Trichodesmium erythraeum* during these months.

From the fisheries statistics available for this period the best fishing months were from May to September which corresponded to the peak months for phytoplankton. But no conclusions can be derived as there is more intensive fishing during these months of the S.-W. Monsoon in these protected regions due to the sea being too rough for distant fishing.

Fig. 2

MAP OF PUTTALAM LAGOON, DUTCH BAY, AND PORTUGAL BAY, SHOWING LOCATIONS WHERE PLANKTON WAS COLLECTED.

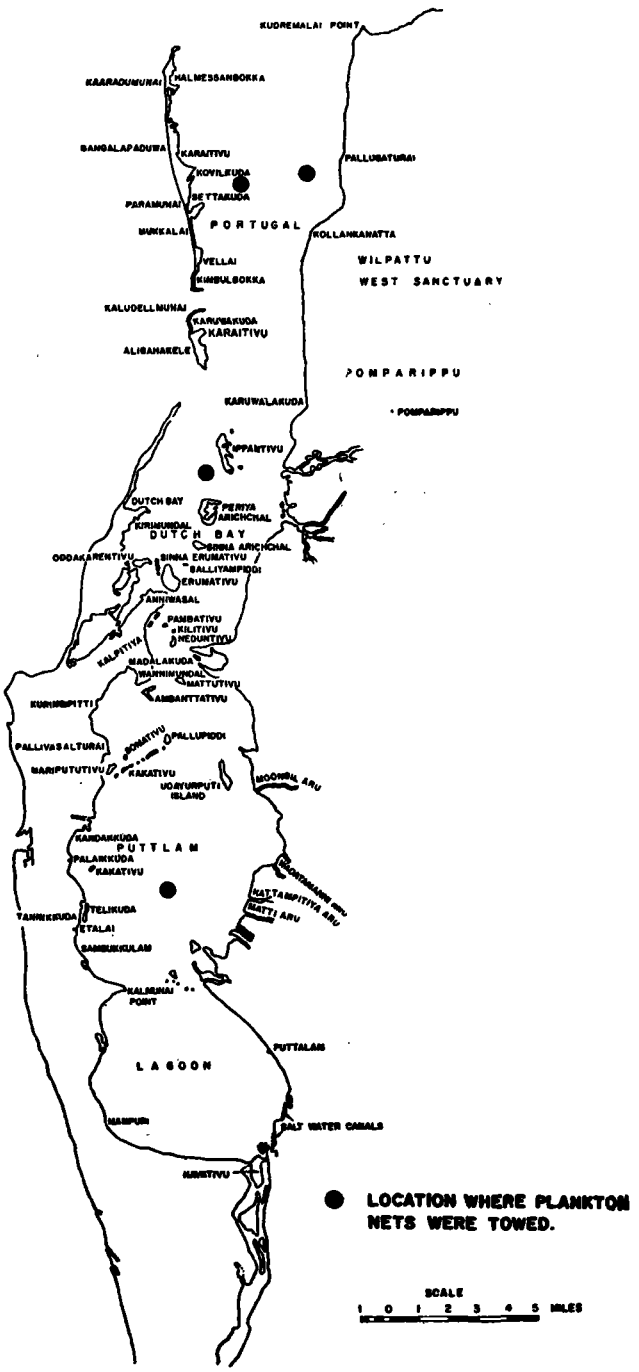

TABLE II

PHYTOPLANKTON CALENDAR, PUTTLAM LAGOON, JUNE, 1960 TO MAY, 1961

	Species	1960							1961				
		June	*July*	*Aug.*	*Sept.*	*Oct.*	*Nov.*	*Dec.*	*Jan.*	*Feb.*	*March*	*April*	*May*
1.	Melosira sulcata (Ehrenberg) Kuetzing	R	—	—	F	F	—	—	—	—	F	R	R
2.	Stephanopyxis palmeriana (Greville) Grunow	—	—	—	—	—	—	—	—	—	R	—	—
3.	Sceletonema costatum (Greville) Cleve	—	—	—	—	—	—	C	—	—	—	—	—
4.	Thalassiosira coramandeliana Subr.	—	—	—	—	F	—	—	—	—	—	—	—
5.	Thalassiosira decipiens (Grunow) Jorgenson	—	—	—	—	—	P	—	R	—	—	R	R
6.	Thalassiosira subtilis (Ostenfeld) Gran	C	—	—	C	C	B	F	C	—	—	—	—
7.	Coscinodiscus gigas Ehrenberg	C	C	C	—	—	—	—	—	—	—	R	R
8.	Coscinodiscus marginatus Ehrenberg	C	C	C	C	F	P	—	—	F	R	F	F
9.	Planktoniella sol (Wallich) Schutt	R	R	—	—	R	—	R	R	—	—	—	—
10.	Aulacodiscus orbiculatus Subr.	—	—	—	R	R	—	—	R	—	—	R	R
11.	Corethron inerme Karsten	—	—	—	—	—	—	—	—	—	—	—	R
12.	Schroederella delicatula (Peragallo) Pavillard	—	—	R	—	—	—	—	—	—	—	—	R
13.	Leptocylindricus danicus Cleve	—	—	—	R	—	—	—	—	—	—	—	—
14.	Leptocylindricus minimus Gran	—	—	—	—	—	—	—	—	R	—	—	—
15.	Guinardia flaccida (Castracane) Peragallo	—	—	—	—	—	—	—	R	—	—	—	R
16.	Rhizosolenia cylindrus Cleve	R	R	R	—	—	—	—	—	—	—	R	R
17.	Rhizosolenia styliformis Brightwell	R	R	—	—	—	R	—	—	—	R	—	C
18.	Rhizosolenia setigera Brightwell	R	—	—	—	—	R	—	—	—	R	R	—
19.	Rhizosolenia crassipiana Schroeder	—	—	R	R	—	—	—	—	—	—	—	R
20.	Rhizosolenia alata Brightwell	R	R	C	C	C	—	C	F	B	R	R	C
21.	Rhizosolenia imbricata Brightwell	—	P	P	—	—	—	C	R	—	B	—	B
22.	Bacteriastrum varians Lauder	R	R	—	F	—	—	R	R	—	—	—	R
23.	Chaetoceros lorenzianus Grunow	—	R	—	—	—	R	—	—	R	—	—	R
24.	Chaetoceros pervianus Brightwell	—	—	P	—	F	—	R	R	—	—	R	—
25.	Chaetoceros lascinosus Schutt	—	—	P	R	R	—	R	R	B	R	—	—
26.	Chaetoceros didymus Ehrenberg	—	R	P	—	—	—	R	R	—	—	C	—
27.	Chaetoceros diversus Cleve	—	—	—	—	—	R	—	R	C	R	—	—
28.	Eucampia cornuta (Cleve) Grunow	—	—	—	—	—	—	C	—	—	—	—	—
29.	Eucampia zoodiacus Ehrenberg	—	—	—	—	—	—	—	—	R	R	—	—
30.	Ditylum brightwellii (West) Grunow	C	R	—	—	—	—	—	—	—	—	—	R
31.	Triceratium favus Ehrenberg	C	C	C	C	C	—	R	R	R	R	F	—
32.	Triceratium dubium Brightwell	—	—	R	—	—	—	—	—	—	—	—	—
33.	Triceratium alternans Bailey	P	F	F	—	—	—	—	—	—	—	—	—
34.	Biddulphia pulchella Gray	F	F	—	C	C	C	—	—	R	R	F	—
35.	Biddulphia sinensis Greville	—	—	R	C	C	—	—	—	—	R	—	—
36.	Biddulphia mobilen is Bailey	R	F	R	R	—	—	R	R	—	—	—	—
37.	Rhabdonema mirificum W. Smith	—	—	R	R	F	—	C	R	—	—	—	—

38.	Rhabdonema arcuatum Kuetzing	R	..	R	..	—	..	R	..	F	..	—	..	—	..	—	..	—	..	—	..	—	..	—	..	—
39.	Hemidiscus hardmannianus (Greville) Mann	R	..	R	..	—	..	R	..	—	..	—	..	—	..	—	..	—	..	R	..	—	..	—	..	—
40.	Licmorpha abbreviata Agardh	—	..	—	..	C	..	—	..	C	..	—	..	—	..	—	..	—	..	—	..	R	..	—	..	—
41.	Licomorpha littoralis Misra	—	..	—	..	—	..	—	..	—	..	R	..	—	..	—	..	C	..	—	..	F	..	R	..	—
42.	Climacosphenia moniligera Ehrenberg	C	..	—	..	—	..	—	..	—	..	—	..	—	..	—	..	—	..	—	..	F	..	R	..	—
43.	Climacosphenia elongata Bailey	C	..	—	..	—	..	—	..	—	..	—	..	—	..	—	..	—	..	—	..	R	..	—	..	—
44.	Fragilaria oceanica Cleve	—	..	—	..	—	..	—	..	—	..	—	..	—	..	—	..	—	..	—	..	—	..	R	..	—
45.	Rhaphoneis discoides Subrahmanyan	—	..	R	..	C	..	C	..	R	..	—	..	—	..	—	..	—	..	R	..	C	..	—	..	—
46.	Synedra closterioides Grunow	—	..	—	..	—	..	—	..	—	..	—	..	—	..	—	..	—	..	—	..	—	..	—	..	—
47.	Synedra formosa Hantzsch	—	..	—	..	—	..	R	..	—	..	R	..	—	..	—	..	—	..	—	..	—	..	—	..	—
48.	Thallassionema nitzschioides Grunow	—	..	—	..	C	..	—	..	F	..	—	..	—	..	—	..	—	..	—	..	R	..	B	..	—
49.	Thallassiothrix longissima Cleve and Grunow	F	..	—	..	—	..	—	..	—	..	—	..	R	..	R	..	R	..	—	..	R	..	R	..	—
50.	Thallassiothrix frauenfeldii Grunow	C	..	—	..	C	..	C	..	C	..	—	..	—	..	—	..	—	..	F	..	C	..	B	..	—
51.	Asterionella japonica Cleve	—	..	—	..	—	..	—	..	B	..	P	..	P	..	C	..	—	..	R	..	R	..	—	..	—
52.	Gyrosigma balticum (Ehrenberg) Rabenhorst	F	..	F	..	—	..	—	..	—	..	—	..	—	..	—	..	—	..	—	..	—	..	—	..	—
53.	Pleurosigma elongatum W. Smith	C	..	—	..	—	..	C	..	C	..	—	..	—	..	—	..	R	..	—	..	—	..	R	..	—
54.	Pleurosigma normanii Ralfs	—	..	—	..	—	..	R	..	R	..	—	..	R	..	R	..	—	..	—	..	—	..	—	..	—
55.	Pleurosigma angulatum (Quekett) W. Smith	—	..	—	..	—	..	—	..	—	..	R	..	—	..	—	..	—	..	—	..	—	..	—	..	—
56.	Pleurosigma aestuarii Brébisson	C	..	—	..	C	..	—	..	C	..	—	..	—	..	—	..	—	..	—	..	R	..	R	..	—
57.	Pleurosigma carinatum Donkin	—	..	—	..	—	..	R	..	—	..	R	..	—	..	—	..	R	..	F	..	—	..	—	..	—
58.	Diploneis weissflogii (A. Schmidt) Cleve	—	..	—	..	—	..	—	..	R	..	—	..	—	..	—	..	—	..	R	..	—	..	R	..	—
59.	Diploneis robustus Subr.	—	..	—	..	—	..	R	..	R	..	—	..	—	..	—	..	—	..	—	..	—	..	—	..	—
60.	Navicula hennedyii W. Smith	—	..	—	..	—	..	R	..	R	..	—	..	—	..	—	..	—	..	—	..	—	..	—	..	—
61.	Navicula longa (Gregory) Ralfs.	—	..	—	..	—	..	F	..	—	..	—	..	—	..	—	..	—	..	—	..	—	..	—	..	—
62.	Pinnularia directa Smith	R	..	—	..	—	..	—	..	—	..	—	..	—	..	—	..	—	..	—	..	—	..	—	..	—
63.	Trachyneis aspera Ehrenberg	—	..	—	..	—	..	—	..	—	..	R	..	—	..	—	..	—	..	—	..	R	..	R	..	—
64.	Cymbella marina Castracane	—	..	—	..	R	..	—	..	—	..	—	..	—	..	—	..	—	..	—	..	—	..	—	..	—
65.	Bacillaria paradoxa Gmelin	—	..	—	..	—	..	C	..	C	..	C	..	R	..	R	..	—	..	R	..	R	..	R	..	—
66.	Amphora salina Smith	—	..	—	..	R	..	—	..	R	..	—	..	R	..	R	..	—	..	—	..	—	..	—	..	—
67.	Nitzschia closterium (Ehrenberg) W. Smith	C	..	—	..	—	..	C	..	—	..	—	..	—	..	—	..	—	..	—	..	R	..	—	..	—
68.	Nitzschia longissima (Brébisson) Ralfs.	C	..	—	..	—	..	P	..	F	..	—	..	R	..	F	..	C	..	—	..	F	..	—	..	—
69.	Nitzschia seriata Cleve	R	..	R	..	—	..	—	..	R	..	—	..	—	..	—	..	C	..	R	..	R	..	R	..	—
70.	Nitzschia sigma (Kuetzing) Smith	R	..	—	..	—	..	R	..	—	..	—	..	F	..	F	..	—	..	—	..	—	..	—	..	—
	Dinophyceae																								
71.	Ceratium trichoceros Kofoid	—	..	—	..	R	..	R	..	—	..	—	..	—	..	—	..	—	..	—	..	—	..	—	..	R
72.	Ceratium massiliense Gourret	—	..	R	..	R	..	—	..	—	..	—	..	—	..	—	..	—	..	—	..	R	..	R	..	—
73.	Ceratium tripos Nitzsch	R	..	R	..	R	..	—	..	—	..	R	..	—	..	—	..	—	..	—	..	—	..	—	..	—
74.	Peridineum sp.	R	..	R	..	—	..	R	..	R	..	—	..	—	..	—	..	—	..	—	..	—	..	R	..	—

TABLE II—(*contd.*)

PHYTOPLANKTON CALENDAR, PUTTALAM LAGOON, JUNE, 1960 TO MAY, 1961

Species	1960 June	July	Aug.	Sept.	Oct.	Nov.	Dec.	1961 Jan.	Feb.	March	April	May
Cyanophyceae												
75. Trichodesmium erythraeum Ehrenberg	P	C	C	R	—	P	—	P	P	C	C	C

* R = Rare 1—10 individuals per C.C.
F = Few 11—25 do.
C = Common 26—75 do.
P = Plenty 76—200 do.
B = Bloom = more than 200 do.

TABLE III

PHYTOPLANKTON CALENDAR, DUTCH BAY, JUNE, 1960 TO MAY, 1961

Species	1960 June	July	Aug.	Sept.	Oct.	Nov.	Dec.	1961 Jan.	Feb.	March	April	May
1. Melosira sulcata (Ehrenberg) Kuetzing	R	R	R	R	—	—	—	—	F	F	F	R
2. Stephanopyxis palmeriana (Greville)	R	R	R	—	—	R	—	—	—	F	F	R
3. Sceletonema costatum (Greville) Cleve	P	P	B	F	P	P	P	—	R	R	—	—
4. Thalassiosira coramandeliana Subr.	R	R	—	—	—	—	—	—	—	—	R	R
5. Thalassiosira decipiens (Grunow) Jorgenson	F	F	R	C	C	C	—	—	R	R	R	C
6. Thalassiosira subtilis (Ostenfeld) Gran	C	R	—	C	—	B	—	R	C	—	R	C
7. Coscinodiscus gigas Ehrenberg	B	B	P	C	C	C	C	F	F	R	C	C
8. Coscinodiscus marginatus Ehrenberg	C	P	P	C	R	F	F	C	C	—	—	R
9. Planktoniella sol (Wallich) Schutt.	R	R	R	R	C	R	F	F	F	C	C	C
10. Aulacodiscus orbiculatus Subr.	—	—	—	—	C	—	—	R	R	—	R	—
11. Corethron inerme Karsten	—	—	—	—	—	R	R	—	—	—	—	R
12. Schroederella delicatula (Peragallo) Pavillard	—	—	R	—	—	—	—	—	—	—	—	R
13. Leptocylindricus danicus Cleve	C	R	—	—	—	—	—	R	—	—	R	R
14. Leptocylindricus minimus Gran	C	R	—	—	—	—	—	—	C	—	—	R
15. Guinardia flaccida (Castracane) Peragallo	—	R	—	—	—	—	—	—	R	F	—	—
16. Rhizosolenia cylindrus Cleve	C	R	R	R	—	—	—	—	—	—	R	R
17. Rhizosolenia styliformis Brightwell	R	R	C	R	—	—	R	C	—	R	R	R
18. Rhizosolenia setigera Brightwell	C	F	C	C	P	F	F	C	R	R	R	R
19. Rhizosolenia crassipiana Schroeder	C	F	—	—	C	C	C	F	R	R	F	F
20. Rhizosolenia alata Brightwell	P	F	—	—	P	C	C	F	R	R	F	F
21. Rhizosolenia imbricata Brightwell	R	P	P	R	P	C	C	C	R	B	—	C

22. Bacteriastrum varians Lauder ..	C	B	P	—	R	R	R	P	P	C	R	P
23. Chaetoceros lorenzianus Grunow ..	R	R	—	—	P	—	—	—	—	—	P	P
24. Chaetoceros pervianus Brightwell ..	—	C	C	P	P	C	C	—	—	—	C	P
25. Chaetoceros lascinosus Schutt ..	C	C	C	C	C	—	—	—	—	—	R	P
26. Chaetoceros didymus Ehrenberg ..	C	—	—	C	C	C	—	—	—	—	F	—
27. Chaetoceros diversus Cleve ..	—	—	—	F	P	—	—	—	—	—	—	—
28. Eucampia cornuta (Cleve) Grunow	—	R	—	R	R	—	—	—	—	—	R	—
29. Eucampia zoodiacus Ehrenberg ..	—	R	—	R	—	—	—	—	—	—	—	R
30. Ditylum brightwellii (West) Grunow	P	C	C	—	—	—	—	—	—	R	R	—
31. Triceratium favus Ehrenberg ..	C	R	F	P	F	R	R	—	F	R	R	R
32. Triceratium dubium Brightwell ..	R	R	—	—	—	—	—	—	—	R	—	R
33. Triceratium alternans Bailey ..	C	C	C	—	—	—	—	—	—	—	R	—
34. Biddulphia pulchella Gray ..	C	C	—	—	C	—	—	—	—	C	—	—
35. Biddulphia sinensis Greville ..	P	R	R	R	R	R	R	R	R	—	R	P
36. Biddulphia mobilensis Bailey ..	P	P	C	C	C	P	R	R	C	R	F	B
37. Rhabdonema mirificum W. Smith ..	F	C	—	—	—	—	—	—	—	—	R	R
38. Rhabdonema arcuatum Kuetz ..	R	—	—	—	—	—	—	—	—	—	—	R
39. Hemidiscus hardmannianus (Greville) Mann	—	—	—	—	R	R	—	—	—	R	R	R
40. Licmorpha abbreviata Agardh ..	R	F	F	—	—	—	—	—	—	—	—	—
41. Licmorpha littoralis Misra ..	R	F	—	R	R	—	—	—	—	—	—	—
42. Climacosphenia moniligera Ehrenberg	R	—	—	R	R	—	—	—	—	—	F	—
43. Climacosphenia elongata Bailey ..	—	—	F	—	—	—	—	—	—	—	—	R
44. Fragilaria oceanica Cleve ..	—	—	R	R	R	R	—	—	—	—	R	R
45. Rhaphoneis discoides Subrahmanyan	P	C	C	C	C	R	R	—	—	—	C	C
46. Synedra closterioides Grunow ..	R	R	—	—	R	R	—	—	—	—	R	R
47. Synedra formosa Hantzsch ..	R	R	—	—	—	—	—	—	—	—	R	—
48. Thallassionema nitzschioides Grunow	P	C	R	P	C	C	C	C	R	P	P	B
49. Thallassiothrix longissima Cleve and Grunow	F	R	R	C	C	—	—	—	C	C	—	C
50. Thallassiothrix frauenfeldii Grunow	P	B	B	B	P	P	P	C	R	C	C	B
51. Asterionella japonica Cleve ..	P	C	—	—	B	R	—	—	—	—	—	B
52. Gyrosigma balticum (Ehrenberg) Rabenhorst	F	—	—	—	C	—	—	—	C	C	C	C
53. Pleurosigma elongatum W. Smith	C	F	—	—	R	C	—	—	—	C	F	F
54. Pleurosigma normanii Ralfs ..	—	R	R	F	R	R	R	R	F	C	F	F
55. Pleurosigma angulatum (Quekett) W. Smith	—	R	R	R	F	C	R	R	—	F	F	F
56. Pleurosigma aestuarii Brébisson ..	R	R	R	R	R	—	—	—	—	R	R	F
57. Pleurosigma carinatum Donkin ..	R	C	—	R	R	—	—	—	—	F	R	R
58. Diploneis weissflogii (A. Schmidt) Cleve	—	—	R	R	—	—	—	—	—	—	—	—
59. Diploneis robustus Subr. ..	—	—	—	R	R	—	—	—	—	—	—	—
60. Navicula hennedyii W. Smith ..	—	—	R	R	R	—	—	—	—	—	—	—
61. Navicula longa (Gregory) Ralfs ..	R	R	—	R	R	R	—	—	—	R	R	R
62. Pinnularia directa Smith ..	—	—	—	R	R	—	—	—	—	—	—	—
63. Trachyneis aspera Ehrenberg ..	—	—	—	—	—	—	R	R	R	—	—	R
64. Cymbella marina Castracane ..	—	—	—	R	R	—	—	—	R	—	—	R
65. Bacillaria paradoxa Gmelin ..	R	—	—	—	R	R	R	R	—	R	—	—

TABLE III—(*contd.*)

HYTOPLANKTON CALENDAR DUTCH BAY JUNE 1960 TO MAY 1961

	Species	1960 June	July	Aug.	Sept.	Oct.	Nov.	Dec.	1961 Jan.	Feb.	March	April	May
66.	Amphora salina Smith	R	—	—	—	R	R	R	R	—	R	—	—
67.	Nitzschia closterium (Ehrenberg) W. Smith	R	R	F	—	C	—	—	R	—	—	R	—
68.	Nitzschia longissima (Brébisson) Ralfs	R	R	R	R	R	F	F	F	—	R	R	R
69.	Nitzschia seriata Cleve	C	R	—	—	R	—	—	—	R	—	—	—
70.	Nitzschia sigma (Kuetzing) Smith	R	R	R	R	R	F	F	F	R	R	R	R
	Dinophyceae												
71.	Ceratium trichoceros Kofoid	R	R	R	R	R	R	—	—	—	R	R	R
72.	Ceratium massiliense Gourret	R	R	R	R	—	—	—	R	—	R	R	R
73.	Ceratium tripos Nitzsch	R	R	F	R	R	R	—	—	—	—	—	—
74.	Peridineum sp.	R	R	—	R	R	—	—	—	—	—	—	R
	Cyanophyceae												
75.	Trichodesmium erythraeum Ehrenberg	P	C	C	C	—	P	—	P	P	C	C	C

TABLE IV

PHYTOPLANKTON CALENDAR PORTUGAL BAY TOWARDS KOVIL MUNAI JUNE, 1960 TO MAY 1961

	Species	1960 June	July	Aug.	Sept.	Oct.	Nov.	Dec.	1961 Jan.	Feb.	March	April	May
1.	Melosira sulcata (Ehrenberg) Kuetzing	C	R	R	R	C	—	R	—	R	R	F	F
2.	Stephanopyxis palmeriana (Greville) Grunow	F	F	R	R	—	—	—	—	R	R	F	F
3.	Sceletonema costatum (Greville) Cleve	P	P	B	C	P	P	P	—	—	—	F	R
4.	Thalassiosira coramandeliana Subr.	R	R	R	C	C	F	—	—	—	R	C	C
5.	Thalassiosira decipiens (Grunow) Jorgenson	F	F	F	C	C	F	—	—	—	R	F	C
6.	Thalassiosira subtilis (Ostenfeld) Gran	C	C	R	C	R	B	—	F	C	—	C	C
7.	Coscinodiscus gigas Ehrenberg	B	B	C	C	C	C	R	R	R	R	R	C
8.	Coscinodiscus marginatus Ehrenberg	C	C	C	F	C	F	C	R	F	C	R	R
9.	Planktoniella sol (Wallich) Schutt	R	R	R	C	F	—	—	F	F	F	F	F
10.	Aulacodiscus orbiculatus Subr.	—	—	—	—	C	C	—	R	R	—	R	R
11.	Corethron inerme Karsten	—	—	—	R	R	R	—	—	—	—	—	—
12.	Schroederella delicatula (Peragallo) Pavillard	—	—	—	—	—	—	R	—	—	—	—	—

13.	Leptocylindricus danicus Cleve	R	R	—	—	—	·	—	R	—	—	R	R
14.	Leptocylindricus minimus Gran	F	—	—	—	R	—	R	—	C	R	—	—
15.	Guinardia flaccida (Castracane) Peragallo	—	—	R	—	—	—	—	—	R	—	—	—
16.	Rhizosolenia cylindrus Cleve	C	R	F	R	—	—	—	R	—	R	R	R
17.	Rhizosolenia cylindrus Cleve	C	R	F	R	—	—	—	R	—	R	R	R
18.	Rhizosolenia setigera Brightwell	C	R	R	F	C	R	R	C	C	R	R	R
19.	Rhizosolenia crassipiana Schroeder	C	R	—	—	C	F	C	R	R	R	R	R
20.	Rhizosolenia alata Brightwell	P	C	F	P	C	C	C	C	—	R	F	C
21.	Rhizosolenia imbricata Brightwell	C	P	P	P	C	C	C	F	R	B	C	C
22.	Bacteriastrum varians Lauder	F	B	P	—	R	R	—	C	B	R	R	C
23.	Chaetoceros lorenzianus Grunow	R	C	R	—	R	—	—	—	—	—	P	C
24.	Chaetoceros pervianus Brightwell	—	R	C	—	P	C	R	—	—	—	C	C
25.	Chaetoceros lascinosus Schutt	C	C	F	P	P	—	—	—	R	—	R	R
26.	Chaetoceros didymus Ehrenberg	R	R	—	—	R	C	R	R	—	—	R	—
27.	Chaetoceros diversus Cleve	R	—	R	—	P	—	—	—	—	—	—	—
28.	Eucampia cornuta (Cleve) Grunow	—	R	—	—	R	R	—	—	—	—	R	R
29.	Eucampia zoodiacus Ehrenberg	R	—	R	—	—	—	—	—	—	—	—	—
30.	Ditylum brightwellii (West) Grunow	P	C	C	—	—	—	—	R	—	—	R	R
31.	Triceratium favus Ehrenberg	C	C	F	C	R	C	R	—	—	R	R	R
32.	Triceratium dubium Brightwell	R	R	—	—	—	—	—	—	—	—	—	—
33.	Triceratium alternans Bailey	C	F	R	—	—	R	—	—	R	R	R	—
34.	Biddulphia pulchella Gray	C	F	F	F	P	R	—	—	—	—	R	R
35.	Biddulphia sinensis Greville	P	C	R	C	R	R	R	F	R	—	R	C
36.	Biddulphia mobilensis Bailey	P	P	C	C	C	P	R	R	F	F	F	B
37.	Rhabdonema mirificum W. Smith	F	F	—	—	—	—	—	—	R	—	R	R
38.	Rhabdonema arcuatum Kuetzing	R	—	—	—	—	R	—	—	—	—	—	R
39.	Hemidiscus hardmannianus (Greville) Mann.	R	—	—	—	R	—	—	—	—	F	F	F
40.	Licmorpha abbreviata Agardh	R	—	R	—	R	—	—	—	—	—	—	—
41.	Licmorpha littoralis Misra	R	—	—	—	F	—	—	—	R	R	—	—
42.	Climacosphenia moniligera Ehrenberg	R	R	—	R	R	—	—	—	—	—	R	—
43.	Climacosphenia elongata Bailey	—	—	—	R	R	—	—	—	—	—	—	—
44.	Fragilaria oceanica Cleve	—	—	—	F	—	—	—	—	—	—	—	R
45.	Rhaphoneis discoides Subrahmanyan	—	—	—	P	F	—	—	—	—	—	—	—
46.	Synedra closterioides Grunow	C	C	C	P	C	R	—	—	—	R	R	—
47.	Synedra formosa Hantzsch	R	R	—	R	—	—	—	—	—	—	R	—
48.	Thallassionema nitzschioides Grunow	P	C	F	P	P	C	C	R	R	P	B	B
49.	Thallassiothrix longissima Cleve and Grunow	C	C	F	F	F	—	—	—	F	F	F	C
50.	Thallassiothrix Frauenfeldii Grunow	P	B	B	B	P	P	C	C	C	F	F	B
51.	Asterionella japonica Cleve	P	C	—	—	—	F	—	—	—	—	C	B
52.	Gyrosigma balticum (Ehrenberg) Rabenhorst	F	R	—	—	R	—	—	—	—	F	C	C
53.	Pleurosigma elongatum W. Smith	C	C	—	C	C	C	—	—	—	C	C	F
54.	Pleurosigma normanii Ralfs	—	—	R	R	F	—	—	R	—	F	F	R
55.	Pleurosigma angulatum Quekett) W. Smith	—	—	R	L	R	F	—	R	—	R	F	R

TABLE IV—(*contd.*)

PHYTOPLANKTON CALENDAR PORTUGAL BAY TOWARDS KOVIL MUNAI JUNE, 1960 TO MAY 1961

Species	1960 June	July	Aug.	Sept.	Oct.	Nov.	Dec.	1961 Jan.	Feb.	March	April	May
56. Pleurosigma aestuarii Brébisson	R	R	R	F	C	—	—	—	R	R	R	F
57. Pleurosigma carinatum Donkin	R	C	R	F	R	—	—	—	—	R	R	R
58. Diploneis weissflogii (A. Schmidt) Cleve	—	—	R	—	—	—	—	—	—	—	—	—
59. Diploneis robustus Subr.	—	—	R	—	R	—	—	—	—	—	—	—
60. Navicula hennedyii W. Smith	—	—	R	R	R	—	—	—	—	—	—	—
61. Navicula longa (Gregory) Ralfs	R	R	R	R	R	—	—	—	—	R	R	—
62. Pinnularia directa Smith	—	—	R	R	—	—	—	—	—	—	—	—
63. Trachyneis aspera Ehrenberg	—	—	—	—	—	—	R	R	—	—	—	R
64. Cymbella marina Castracane	—	—	—	R	R	—	—	—	R	—	—	—
65. Bacillaria paradoxa Gmelin	R	—	—	F	R	R	R	—	—	—	R	—
66. Amphora salina Smith	R	R	—	R	R	R	—	—	—	R	—	—
67. Nitzschia closterium (Ehrenberg) W. Smith	R	R	R	F	F	—	—	R	—	—	—	R
68. Nitzschia longissima (Brébisson) Ralfs	R	R	F	F	R	R	R	F	—	R	R	R
69. Nitzschia seriata Cleve	C	C	—	—	F	—	—	—	R	—	—	
70. Nitzschia sigma (Kuetzing) Smith	—	—	—	R	R	R	R	—	—	R	R	—
Dinophyceae												
71. Ceratium trichoceros Kofoid	R	R	R	R	R	R	—	—	R	R	—	R
72. Ceratium massiliense Gourret	R	R	R	R	—	—	—	—	R	—	R	R
73. Ceratium tripos Nitzsch	R	R	F	F	R	R	R	R	—	R	R	R
74. Peridineum species	R	R	—	—	R	—	—	—	—	—	—	R
Cyanophyceae												
75. Trichodesmium erythraeum Ehrenberg	C	C	F	C	—	P	—	F	P	P	C	C

TABLE V

PHYTOPLANKTON CALENDAR PORTUGAL BAY TOWARDS PALLUGATURAI JUNE 1960 TO MAY 1961

Species	1960 June	July	Aug.	Sept.	Oct.	Nov.	Dec.	1961 Jan.	Feb.	March	April	May
1. Melosira sulcata (Ehrenberg)	F	F	C	C	C	—	R	—	R	R	F	R
2. Stephanophyxis Palmeriana (Greville) Grunow	R	F	R	F	R	—	—	—	R	R	R	F
3. Sceletonema costatum (Greville) Cleve	P	P	B	P	P	C	C	—	—	—	R	R
4. Thalassiosira coramandeliana Subr.	F	R	R	F	F	F	—	—	—	R	F	C

5. Thalassiosira decipiens (Grunow) Jorgenson	F	F	R	C	C	R	—	—	—	F	C	F
6. Thalassiosira subtilis (Ostenfeld) Gran	C	C	C	C	C	C	—	R	C	—	C	C
7. Coscinodiscus gigas Ehrenberg	B	B	C	C	C	R	R	R	F	F	F	C
8. Coscinodiscus marginatus Ehrenberg	P	P	C	C	C	R	C	R	R	C	F	R
9. Planktoniella sol (Wallich) Schutt	R	R	R	F	F	—	—	R	R	F	R	F
10. Aulacodiscus orbiculatus Subr.	—	—	—	C	C	—	R	R	—	R	R	R
11. Corethron inerme Karsten	—	—	—	R	R	—	—	—	—	—	—	—
12. Schroederella delicatula (Peragallo) Pavillard	—	R	—	R	R	—	—	—	—	—	—	—
13. Leptocylindricus danicus Cleve	R	R	R	—	—	—	—	—	—	—	—	R
14. Leptocylindricus minimus Gran	F	—	—	R	—	R	—	F	F	R	—	—
15. Guinardia flaccida (Castracane) Peragallo	—	—	R	R	—	—	—	—	—	R	R	—
16. Rhizosolenia cylindrus Cleve	C	F	F	F	—	—	—	—	—	R	—	—
17. Rhizosolenia styliformis Brightwell	P	F	C	F	R	—	F	C	—	—	R	C
18. Rhizosolenis setigera Brightwell	C	R	R	R	F	F	R	R	F	F	R	R
19. Rhizosolenia crassipiana Schroeder	F	R	—	—	C	F	F	—	—	R	R	R
20. Rhizosolenia alata Brightwell	P	C	F	C	R	C	C	R	R	B	R	C
21. Rhizosolenia imbricata Brightwell	R	C	P	C	P	C	F	R	B	R	C	C
22. Bacteriastrum varians Lauder	R	B	P	—	R	R	—	R	R	—	R	R
23. Chaetoceros lorenzianus Grunow	R	C	C	C	P	—	—	—	—	—	C	C
24. Chaetoceros pervianus Brightwell	—	R	F	—	B	C	R	—	—	—	C	C
25. Chaetoceros lascinosus Schutt	F	R	F	P	B	—	—	—	—	R	R	R
26. Chaetoceros didymus Ehrenberg	R	R	—	—	R	R	R	R	—	—	R	R
27. Chaetoceros diversus Cleve	R	R	R	—	B	—	—	—	—	—	—	—
28. Eucampia cornuta	—	R	—	—	R	R	—	—	—	—	R	R
29. Eucampia zoodiacus Ehrenberg	R	—	R	—	—	—	—	—	—	—	—	—
30. Ditylum brightwellii (West) Grunow	P	C	C	C	—	—	—	R	—	—	R	R
31. Triceratium favus Ehrenberg	C	C	C	P	F	F	R	—	—	R	R	R
32. Triceratium dubium Brightwell	R	R	—	—	—	—	—	—	—	—	—	—
33. Triceratium alternans Bailey	F	C	R	R	—	R	—	—	R	R	—	—
34. Biddulphia pulchella Gray	C	C	F	F	C	R	—	—	—	—	R	—
35. Biddulphia sinensis Greville	P	C	R	P	R	R	R	R	R	R	R	R
36. Biddulphia mobilensis Bailey	P	C	C	C	C	P	R	R	R	R	C	B
37. Rhabdonema mirificum W. Smith	R	R	—	R	—	—	—	—	—	R	R	R
38. Rhabdonema arcuatum Kuetzing	F	R	—	—	—	R	—	—	—	—	R	R
39. Hemidiscus hardmannianus (Greville) Mann	F	R	—	—	R	R	—	—	—	R	F	F
40. Licmorpha abbreviata Agardh	R	R	R	—	R	—	—	—	—	—	—	R
41. Licmorpha littoralis Misra	R	—	—	—	R	—	—	—	—	—	R	—
42. Climacosphenia moniligera Ehrenberg	R	—	R	—	—	—	—	—	—	—	R	R
43. Climacosphenia elongata Bailey	—	R	—	R	R	—	—	—	—	—	—	—
44. Fragilaria oceanica Cleve	—	—	R	R	—	—	—	—	—	—	—	R
45. Rhaphoneis discoides Subrahmanyan	C	C	C	B	—	—	—	—	—	R	R	—
46. Synedra closterioides Grunow	C	R	C	P	C	R	—	—	—	R	R	R

TABLE V—(*contd.*)

PHYTOPLANKTON CALENDAR PORTUGAL BAY TOWARDS PALLUGATURAI JUNE, 1960 TO MAY 1961.

	Species	1960							1961				
		June	*July*	*Aug.*	*Sept.*	*Oct.*	*Nov.*	*Dec.*	*Jan.*	*Feb.*	*March*	*April*	*May*
47.	Synedra formosa Hantzsch	—	C	R	R	R	—	—	—	—	—	R	R
48.	Thallassionema nitzschioides Grunow	P	C	F	P	P	C	C	R	R	P	B	B
49.	Thallassiothrix longissima Cleve and Grunow	C	C	F	F	F	—	—	—	R	C	C	C
50.	Thallassiothrix frauenfeldii Grunow	P	B	B	B	P	P	C	C	C	F	C	B
51.	Asterionella japonica Cleve	P	P	—	C	B	—	—	—	—	—	C	B
52.	Gyrosigma balticum (Ehrenberg) Rabenhorst.	F	F	—	—	R	—	—	—	F	C	C	C
53.	Pleurosigma elongatum W. Smith	F	C	C	C	C	C	—	—	—	C	C	C
54.	Pleurosigma normarii Ralfs	—	—	R	R	R	—	—	R	R	R	R	R
55.	Pleurosigma angulatum (Quekett) W. Smith	R	—	—	R	R	R	—	R	—	R	F	R
56.	Pleurosigma aestuarii Brébisson	R	R	R	R	C	—	—	—	R	R	F	F
57.	Pleurosigma carinatum Donkin	R	R	F	F	F	—	—	—	—	R	R	R
58.	Diploneis weissflogii (A. Schmidt) Cleve	—	—	R	R	—	—	—	—	—	—	—	—
59.	Diploneis robustus Subr.	—	—	R	F	R	—	—	—	—	—	—	—
60.	Navicula hennedyii W. Smith	—	—	R	R	R	—	—	—	—	—	—	—
61.	Navicula longa (Gregory) Ralfs.	F	R	R	R	F	F	—	—	—	—	F	R
62.	Pinnularia directa Smith	—	—	R	R	—	—	—	—	—	—	—	—
63.	Trachyneis aspera Ehrenberg	—	—	—	—	—	—	R	R	—	—	—	R
64.	Cymbella marina Castracane	—	—	R	R	—	—	—	—	R	—	—	—
65.	Bacillaria paradoxa Gmelin	C	R	—	F	F	R	R	—	—	—	R	—
66.	Amphora salina Smith	R	—	—	R	R	—	—	—	—	R	—	—
67.	Nitzschia closterium (Ehrenberg) W. Smith	F	R	R	R	F	—	—	R	—	—	—	R
68.	Nitzschia longissima (Brébisson.) Ralfs	F	R	F	C	R	R	R	R	—	R	R	R
69.	Nitzschia seriata Cleve	F	C	—	—	R	—	—	—	R	—	—	—
70.	Nitzschia sigma (Kuetzing) Smith	—	R	—	R	R	R	R	—	—	R	R	R
	Dinophyceae												
71.	Ceratium trichoceros Kofoid	R	R	R	R	R	—	—	R	R	—	—	R
72.	Ceratium massiliense Gourret	R	R	—	R	R	—	—	—	R	—	R	R
73.	Ceratium tripos Nitzsch	R	R	—	—	F	R	—	—	—	—	—	—
74.	Peridineum species	R	R	R	—	R	—	—	—	—	—	—	—
	Cyanophyceae												
75.	Trichodesmium erythraeum Ehrenberg	C	C	C	C	—	P	—	P	P	C	C	C

Summary

The monthly average temperatures at Puttalam Lagoon, Dutch Bay, Portugal Bay towards Kovilmunai and Portugal Bay towards Pallugaturai showed a distinct annual cycle. The peak was in April and values gradually fell till September. There was a further gradual fall in temperature from October to January. The highest tempertures in all four stations were in April.

The highest salinities in all the stations were from May to October i.e., during the South-West Monsoon. The salinities at Dutch Bay and Portugal Bay were high in March and April corresponding to the highest temperatures reached during these months.

Two maxima have been observed in phytoplankton production. A primary maximum in May-June and a secondary maximum in October. The primary and secondary maxima are due to the influx of nutrient laden waters from the rivers Kal Aru and Pomparippu Aru.

The phytoplankton producing blooms were *Rhizosolenia alata. Rhizosolenia imbricata, Chaetoceros lascinosus, Chaetoceros pervianus, Chaetoceros diversus, Coscinodiscus gigas, Thallasionema nitzschioides, Thalassiosira subtilis, Thallassiothrix frauenfeldii, Asterionella japonica, Sceletonema costatum, Bacteriastrum varians* and *Biddulphia sinensis.*

Sudden outbursts of a single species were common. These diatoms were species of *Chaetoceros* and *Rhizosolenia*, and *Thallassiothrix frauenfeldii.*

Wide fluctuations have been observed in the distribution of phytoplankton but no definite conclusions can be drawn as the period of observation was only one year.

Acknowledgments

I wish to express my sincere thanks to Mr. K. J. M. S. Grero, Laboratory Assistant, for accompanying me in all the field trips and assisting me in the counting of phytoplankton and determining the salinities.

References

BAINBRIDGE, R., 1953. Studies on the interrelationships of zooplankton and phytoplankton. *Jour. Mar. Biol. Ass.*, U. K. 32, 385-447.

CHACKO, P. I., 1950. Marine plankton from waters around the Krusadai Island. *Proc. Ind. Acad. Sci.* 31, p. 162-74.

CHIDAMBARAM, K. and MUKUNDANUNNY, M. 1944. Notes on the swarming of the planktonic algae *Trichodesmium erythraeum* in the Pamban are a and its effect on the fauna. *Current* Science, 13, p. 263.

DAS, P. K., 1954. *Ind. Jour. Met. and Geophy., 5.*

GANAPATHY, P. N. and RAO, C. G., 1953. Observation on the seasonal variations in the phytoplankton production of the Indian coast with special reference to Waltair Coast. *Indian Science Congress* Part III, p. 184.

GANAPATHY, P. N. and MURTHY, V. S. R., 1953. Salinity and temperature variations of the surface waters off the Visakhapatnam coast. *Memoirs in Oceanography, Andhra University* Waltair, 49 (i), 125-142.

——— 1955. Preliminary observations on the hydrography and inshore plankton in the Bay of Bengal, off Visakhapatnam coast. *Indian Journal of Fisheries* Vol. 2, pp. 84-95.

GONZALVES, E. A., 1947. Variations in the seasonal composition of the phytoplankton of Bombay Harbour. *Current Science* 16, 304-05.

JEYARAMAN, R., 1951. Observations on the chemistry of the waters of the Bay of Bengal off Madras City during 1948-49. *Proc. Ind. Acad. Sci.* 38, 92-99.

——— 1957. Salinity and temperature variations in the surface waters of the Arabian sea off the Bombay and Saurashtra coasts. *Proc. Ind. Acad.* Vol. XLV, 151-164.

LA FOND, E. C., 1954. Seasonal cycle of surface temperatures and salinities along the East Coast of India. *Andhra University Memoirs in Oceanography* 52, Vol. II, 12-21.

MENON, M. A. S. 1945. Observations on the seasonal distribution of the plankton of Trivandram Coast. *Proc. Ind. Acad. Sci.*, 22, Sec. B, 31-62.

PRASAD, R. R., 1954. The characteristics of marine plankton at an inshore station in the Gulf of Mannar near Mandapam, *Indian Journal of Fisheries* I, 1-36.

——— 1956. Further studies on the plankton of the inshore waters off Mandapam, *Indian Journal of Fisheries* 3, 1-42.

PRASAD, R. R. and RAMACHANDRAN NAIR, 1960. Observations on the distribution and occurrence of diatoms in the inshore waters of the Gulf of Mannar and Palk Bay, *Indian Journal of Fisheries*, Vol. 7, 49-68.

RAMACHANDRAN NAIR, P. V., 1959. The marine plankton diatoms of Trivandram coast, *Bull Res. Inst. Univ. Kerala* ser. C, 1-63.

SEWELL, R. B., S, 1937. Oceans round India. From " an outline of the Field Sciences of India " *Ind. Sci. Congr. Assn.* 17-41.

——— 1955. A study of the Sea Coast of Southern Arabia, *Proc. Linn. Soc. Lond.* (Session 1952-53) Part II.

SUBRAMANYAN, R., 1946. A systematic account of the marine plankton diatoms of the Madras Coast, *Proc. Ind. Acad. Sci.* Vol. XXIV, 85-197.

——— 1958. Ecological studies of the marine phytoplankton of the West Coast of India. *Mem. Ind. Bot. Soc.*, 1. 145-151.

——— 1959. Studies on the phytoplankton of the West Coast of India. *Proc. Ind. Acad. Sci.* 50B, 113-187.

Reprinted from J. oceanogr. Soc. Japan, vol. 19, no. 4, 1964, p. 22-28.

Primary Production in the Antarctic Ocean*

Yatsuka SAIJO** and Takuji KAWASHIMA***

Abstract: Studies on primary production were made in the Antarctic Ocean, between 40°W and 100°E, during December 1961 to February 1962. At ten stations, chlorophyll-a and photosynthetic rate were determined for sample waters from surface as well as the depth of Secchi disk reading, and at other 35 stations only chlorophyll-a in surface water was determined. At most of the stations the chlorophyll-a contents were very low (*i.e.* 0.02 to 0.22 mg/m^3) except at a few stations where higher values, (*i.e.* 0.3–0.6 g/m^3) were obtained. The photosynthetic rates determined by ^{14}C technique under the optimum light ranged from 0.06 to 0.80 mg C/m^3/hr, and the mean value of photosynthesis per unit amount of chlorophyll was 1.22 mg C/mg chl./hr. The daily primary production beneath a unit surface, calculated from the above results and light data were ranged from 0.01 to 0.15 g C/m^2/day. After consideration about the high concentration of nutrients in the sample waters and rather plenty incident radiation during this period, it was concluded that such low values of primary production in the Antarctic Ocean might be caused by the near freezing water temperature and deep mixing layer in that area.

1. Introduction

In the study of primary production in the sea, the Antarctic Ocean might be one of the most interesting field because of its characteristic environmental conditions, such as long day- or night-time, low water temperature and high concentration of inorganic nutrients. Valuable observations have been reported on the species and quantitative distribution of plankton in this ocean, however, only a few results have yet appeared in the available publications concerning the phytoplankton production by recently developed ^{14}C and chlorophyll techniques.

During the Antarctic summer of 1958–59, BURKHOLDER and SIEBURTH (1961) made the studies on chlorophyll-a content in waters along the western coast of the Antarctic Peninsula on the Argentine Hydrographic ship "Chiriguano" and icebreaker "San Martin." In January-March 1959, DYSON (IGY Oceanography Report, No. 4, 1961) made the measurements on primary production by ^{14}C technique and plant pigment determination in the area between 110° and 160° E until 66°39' S on board Australian ship "Magga Dan." But studied area by these researches are quite limited and insufficient to know the general feature of primary production in that ocean.

From December 1961 to February 1962, during the cruise of "Umitaka-maru" (the trainning and research ship of Tokyo University of Fisheries) one of the authors, KAWASHIMA had an opportunity to collect the samples for primary production in the Antarctic Ocean while his work on chemical analysis of sea water. The measurement of ^{14}C activity and chlorophyll-a analysis on filtered samples were made at senior author's laboratory.

2. Area studied and method

The studied area was between 40°W and 100°E, mainly the region so-called Atlantic-Indian Antarctic basin which covers about one third of the sea surrounding Antarctica. At ten stations, the sample waters were collected with a plastic Van Dorn sampler from surface and the depth of Secchi disk reading. For measuring chlorophyll-a content, normally five liter samples from each depth were filtered with Membrane No. 1 filters, then treated with steam for about 30 seconds and kept in a desiccator at dark place. Having been brought

* Received Oct. 4, 1963

** Water Research Laboratory, Faculty of Science, Nagoya University

*** Institute of Chemistry, Faculty of Science, Nagoya University

to the laboratory chlorophyll-a determinations were made on these samples according to the method of RICHARDS and THOMPSON (1952). For measuring photosynthetic rate of phytoplankton, sample water from each depth was dispensed into two transparent and one darkened bottles, and 5 μc Na_2 $^{14}CO_3$ solution was added into each bottle. All six bottles were then placed in a incubator (ICHIMURA and SAIJO, 1959) during 4 hours cooled with running surface water, and illuminated with two circular fluorescent lamps which provide a light intensity of about 10,000 lux. These bottles were removed after 4 hours, filtered, and then G.M. counting were made at the home laboratory.

At the other 35 stations, only chlorophyll-a was determined on the surface waters. The solar radiation was recorded every day with Robitzsch pyrheliometer equipped on the upper bridge. Third officer KOTAKE was in charge of this work.

3. Chlorophyll

The results of chlorophyll-a determination were presented in Tables 1 and 2, and horizontal distribution of chlorophyll-a was illustrated in Fig. 1. In the same figure, some of the chlorophyll-a data obtained by DYSON were added as a reference. As seen from these data, the chlorophyll-a content of pelagic waters in the Antarctic Ocean is generally low including a few exceptions.

In the area from southwestern Australia to the subtropical convergence (St. 56–63), chlorophyll-a content were about 0.1 mg/m^3 except St. 61 (0.29 mg/m^3), whereas at two stations (St. 64 and 66) between subtropical and antarctic convergence, maximum values in this cruise, 0.72 anb 0.64 mg/m^3 were obtained. Beyond the antarctic convergence, in the antarctic region, the chlorophyll-a contents were ranged from 0.02 to 0.22 mg/m^3, except some stations in the area between 30°E and 20°W, off Queen Maud Land, where the chlorophyll-a contents were 0.3–0.6 mg/m^3. At St. 164 which situates on the antarctic convergence, a rather high value 0.30 mg/m^3 was obtained.

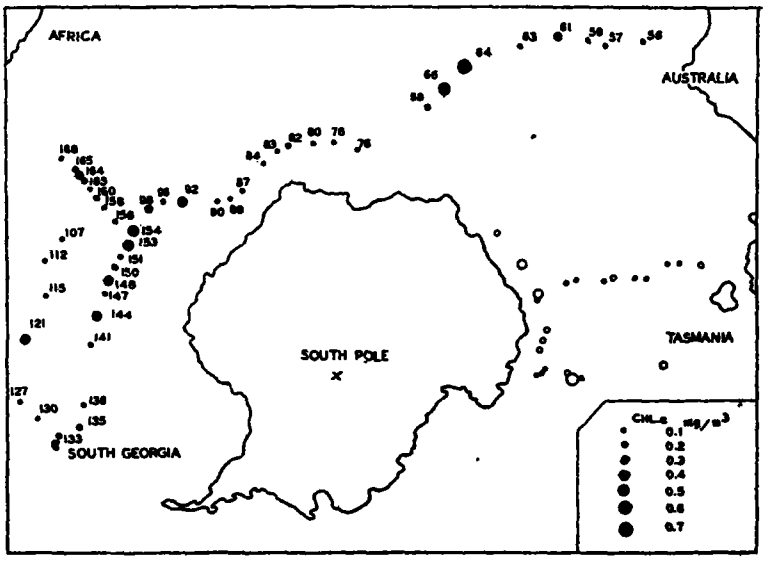

Fig. 1. Distribution of the chlorophyll-a content in surface waters in the Antarctic Ocean. The figures show the station numbers. The close circles represent the values obtained by the authors, and the open circles are values obtained by DYSON.

Table 1. Chlorophyll-a, and temperature of surface waters.

St.	Lat.	Long.	Date	Time	Water temperature °C	Secchi disk m	Chlorophyll-a mg/m³
56	37-°59.'0S	106°-44.'2 E	5, Dec. 1961	1140	15.3	11	0.09
57	39-35.2	104-32.2	6,	0200	12.8	19	0.08
59	42-09.7	100-49.8	7.	0210	12.0	17	0.12
61	44-47.2	97-06.3	8,	0230	10.5	13	0.29
63	47-30.8	93-11.2	9,	0240	7.6	16	0.13
64	49-55.7	90-00.0	10,	0255	4.7	12	0.72
66	52-52.6	87-43.9	11,	0300	4.1	10	0.64
76	63-09.0	72-09.0	16,	0410	−0.7	12	0.05
78	62-28.0	66-07.5	17,	0440	−1.3	26	0.07
80	62-01.0	60-47.5	18,	0500	−1.2	24	0.04
83	62-30.4	52-23.0	19,	1520	−0.4	15	0.14
84	63-15.4	48-34.5	20,	0550	−0.2	16	0.11
87	64-49.0	38-52.3	21,	1615	−0.6	23	0.05
88	65-02.3	34-47.5	22,	1640	−1.2	23	0.06
92	61-18.8	33-55.6	25,	0700	−0.8	20	0.36
107	52-35.5	3-57.8W	31,	1940	0.4	23	0.07
112	52-29.0	2-58.8	2, Jan. 1962	0800	1.4	—	0.05
115	52-16.8	7-25.5	3,	0820	0.7	18	0.10
127	50-51.9	26-58.7	7,	0940	4.2	10	0.07
130	52-41.9	31-02.0	8,	1140	1.8	26	0.02
133	54-25.2	35-02.7	9,	1035	2.2	20	0.18
135	56-20.7	33-06.0	15,	1010	1.8	18	0.22
138	58-47.1	20-26.0	16,	1010	−1.1	20	0.06
141	58-51.5	15-33.0	18,	1030	0.1	16	0.09
147	59-30.0	4-17.0	20,	0840	−1.1	12	0.14
150	59-30.5	3-05.0 E	21,	0750	−0.3	12	0.17
151	59-34.7	5-45.5	21,	1750	−0.1	9	0.13
153	59-41.7	9-46.1	22,	0750	0.0	—	0.50
156	57-13.9	12-30.4	23,	0720	−0.1	18	0.06
158	54-45.3	12-57.0	24,	0720	0.4	20	0.05
159	54-00.3	13-18.9	24,	1220	0.5	—	0.08
160	53-20.8	13-48.0	24,	1620	0.4	—	0.18
164	50-14.5	15-10.5	25,	1240	3.7	—	0.30
165	49-54.8	15-11.2	25,	1440	4.2	—	0.16
168	47-03.4	15-49.5	26,	0730	5.3	—	0.13

It is interesting to compare these values with those of DYSON shown in Fig. 1. As seen from this figure, both data coincide well. Namely, most of Dyson's results ranged from 0.1 to 0.2 mg/m³ and at only four stations higher values 0.31, 0,33, 0.44 and 0.76 mg/m³ were obtained. ICHIMURA and FUKUSHIMA (unpublished) also found similar chlorophyll-a values on the samples collected on board "Soya" in arctic summer 1960 to 1961 in the

Table 2. Chlorophyll-a, photosynthetic rate of waters and primary production.

St.	Lat.	Long.	Depth m	Date	Time	Water temperature °C	Chl. a mg/m³	Photosynthetic rate		Primary production gC/m²/day
								mg C/m³/hr	mg C/mg chl./hr	
68	56°-17′. 8 S	86°-25′. 2 E	0	12, Dec. 1961	0310	0. 25	0. 15	0. 12	0. 81	0. 03
			15			—	0. 10	0. 14	1. 38	
82	62 -02 . 9	54 -48 . 0	0	19, Dec.	0520	−0. 6	0. 19	0. 17	0. 66	0. 07
			20			−0. 8	0, 16	0. 08	0. 48	
90	64 -05 . 5	31 -54 . 0	0	23, Dec.	0655	−1. 4	0. 13	0. 15	1. 14	0. 03
			14			−1. 5	0. 12	0. 13	1. 05	
96	60 -01 . 8	22 -19 . 0	0	27, Dec.	0610	−1. 5	0. 05	0. 10	2. 04	0. 02
			22			−1. 4	0. 05	0. 06	1. 20	
98	58 -33 . 2	18 -47 . 0	0	28, Dec.	0630	−1. 1	0. 27	0. 34	1. 26	0. 14
			13			−1. 2	0. 35	0. 26	0. 75	
121	50 -56 . 1	16 -29 . 9W	0	5, Jan. 1962	0900	4. 0	0. 41	0. 56	1. 38	0. 14
			16			4. 0	0. 22	0. 41	1. 89	
144	59 -25 . 7	9 -11 . 5	0	19, Jan.	0900	−1. 0	0. 41	0. 57	1. 38	0. 09
			12			−1. 0	0. 40	0. 40	1. 00	
148	59 -30 . 0	1 -06 . 8	0	20, Jan.	1820	−0. 8	0. 41	0. 63	1. 53	0. 14
			10			−0. 9	0. 51	0. 80	1. 56	
154	59 -10 . 2	12 -26 . 1 E	0	22, Jan.	1730	−0. 1	0. 48	0. 53	1. 11	0. 17
			10			−0. 1	0. 66	0. 63	0. 96	
163	50 -39 . 4	15 -08 . 6	0	25, Jan.	0720	2. 8	—	0. 43	—	0. 11
			15			2. 9	0. 25	0. 42	1. 64	

area off the Prince Harald Coast.

According to the results obtained by BURKHOLDER and SIEBURTH, in northeastern Bransfield Strait, the chlorophyll-a contents were ranged from 0.3 to 0.5 mg/m³, whereas in the Gerlache Strait the values were in the range of 10 to 25 mg/m³. The highest values of chlorophyll-a contents in the Gerlache Strait are comparable to those found in some eutrophic coastal waters in Japan at the time of phytoplankton blooming.

Summerizing the data described above, it can be said that the chlorophyll-a contents in the antarctic offshore water are commonly very low, *i. e.* smaller than 0.2 mg/m³, even in antarctic summer, and only in some restricted areas rather high values, 0.3 to 0.6 mg/m³ will be observed. When comparing these values with those obtained in the Northwestern Pacific, the former low values are comparable to chlorophyll-a contents in the Kuroshio area, on the other hand, the latter high values are same order with the data obtained in the Oyashio area.

Concerning the stratification of the chlorophyll-a contents, no marked differences were observed between the surface and the depth of Secchi disk reading (10~25 m). DYSON found also that there was almost no difference between the surface and 25 m depth water. Therefore, the stratification of chrolophyll-a contents might be obscure in offshore area except some restricted regions where distinct stagnation of the water can be found. On this problem discussions will be repeated later on in relation to the hydrographic condition in the Antarctic Ocean.

4. Photosynthetic rate

The photosynthetic rates determined by ^{14}C technique were presented in Table 2. As seen from this table, at the 4 stations the obtained values were ranged from 0.06 to 0.17 mg C/m³/hr, whereas at the other 6 stations from 0.26 to 0.80 mg C/m³/hr. Through all ten stations, no clear difference was found between the surface water and the water from the depth of Secchi disk reading. These values are

also fairly in accordance with those obtained by DYSON which were commonly in the range between 0.2–0.6mg C/m³/hr except a few stations where high values, maximum 1.45mg C/m³/hr, were observed. If our results are compared with those of Pacific water in the area off Japan, these values are substantially same with the data obtained in the Kuroshio area and considerably lower than the values in the Oyashio area.

When we consider the photosynthetic rate per unit amount of chlorophyll-a, these values correspond to 0.48 to 2.04 mg C/mg chl. hr and the mean value is 1.22 mg C/mg chl. hr. These values are almost same as the value 1.5mg C/mg chl./hr which was adopted by SAIJO and ICHIMURA (1960) as mean value of photosynthetic rate in Kuroshio area for calculating the daily production, however, they are considerably lower than the value 3.7mg C/mg chl./hr employed by RYTHER and YENTSCH (1957) for similar calculation in the area of Long Island Sound.

From these results of photosynthetic rate and chlorophyll-a determination, daily production beneath a square meter of sea surface was estimated by using the data of incident radiation and Secchi disk reading. The process of calculation is substantially same as that described by RYTHER and YENTSCH (1957), but the light-photosynthesis curve was constructed from the data obtained by SAIJO in the Oyashio area off Japan in summer 1961, and as photosynthetic rate under the optimum light the mean value described above, 1.22mg C/mg chl./hr was adopted. As the incident radiation value the data recorded by Robitzsch pyrheliometer fixed on deck was employed, and the extinction coefficient of sea water was estimated from Secchi disk reading by using the relationship

$$k=1.7/\text{Secchi disk}$$

by POOLE and ATKINS (1929). The chlorophyll-a contents were assumed to be uniform within euphotic layers and mean value for each station was employed as basis for calculation. The daily primary production calculated from these data are given in Table 2. The production value obtained were ranged from 0.01 to 0.15 C/m²/day. These results are almost same value with those obtained by SAIJO and ICHIMURA (1960) in summer in the Kuroshio area off midcoast of Japan, one of the typical low productive area in the Pacific.

5. Discussion

From these results it may be surmised that the standing crop of phytoplankton, which indicated by chlorophyll-a content, as well as primary production are very low in the antarctic offshore water even in antarctic summer, though much higher amount of phytoplankton can be observed in some restricted areas.

This fact seems incompatible with well known high concentration of inorganic nutrients in the antarctic water. The results of PO_4-P and SiO_2-Si determination of water for the stations, where production was studied, were summarized in Table 3. Although this data does not include

Table 3. Phosphate and silicate of waters.

Station	Depth m	PO_4-P μg atom/l	SiO_2-Si μg atom/l
82	0	1.69	32
	18	1.66	32
90	0	1.69	36
	20	1.69	35
96	0	1.55	39
	25	1.51	38
98	0	1.46	37
	10	1.48	37
144	0	1.40	43
	10	1.40	43
148	0	1.31	37
	10	1.31	35
154	0	1.39	40
	10	1.37	40
163	0	1.31	4
	19	1.26	4

the values on nitrogen compounds, it is clear that the nutrients concentrations are very high even in surface water. During the cruise of "Soya" (Japanese Antarctic Expedition ship) in the antarctic water off the Prince Harald Coast, similar high values of nutrients were observed in which the amount of NO_3-N were 20 μg atom/l or so. Therefore, it can be said that in the antarctic offshore water the nutrients

condition will not usually become a limiting factor for phytoplankton production.

As a next step to analyse the factors regulating the primary production, it will be necessary to consider about the solar radiation in the Antarctic Ocean. Kimball's table (1928) on the distribution of incident radiation shows that the average amount of radiation from sun and sky at the location 60°S, 45°W is in the range from 0.204 to 0.221 g cal/cm^2/min from November to January, these values are approximately same as those obtained at the location 30°N, 67–77°W or 128–130°E in March or September. If fact the solar radiation data, recorded on "Umitaka-maru" during this cruise, gave considerably high amount of radiation. The maximum radiation was 65 g cal/cm^2/hr, which corresponds to about 70.000 lux as the intensity of illumination. The length of daytime was also very long in comparison with that of the region in temperate latitude. These results show clearly the fact that at water surface the incident radiation is sufficient for photosynthetic activity of phytoplankton in the Antarctic Ocean during a summer period.

It is well known fact that the photosynthetic rate of phytoplankton generally decreases with the lowering of water temperature. SAIJO and SAKAMOTO (unpublished) found in some Japanese lakes in winter that the rate of photosynthesis per unit amount of chlorophyll-a are consistently low near the freezing temperature regardless of their nutrient concentration. This phenomena may be one of the important reason for low photosynthetic rate and low primary production in the antarctic water where high nutrient contents were observed It will be necessary to consider the problem of vertical stability of the water as an another reason for the low primary production in that area. In high latitudes, the average plant cell does not receive sufficient light to grow when the depth of mixed layer is deeper than that of euphotic layer and the phytoplankton production remains at low level. This phenomena was discussed precisely by SVERDRUP (1953) and others as the problem of so-called critical depth.

During the previous cruise of "Umitaka-maru" in the Antarctic Ocean from December 1956 to January 1957, the immense phytoplankton bloom was found only in the area where marked change of σt in a vertical direction was observed. In this cruise there was no such clear relation between the phytoplankton standing crop and vertical difference of σt. However, it is quite probable that the vertical mixing takes place easily even to the much deeper layer than the depth of euphotic layer because the surface water temperatures were near the freezing point and the vertical differences of σt were generally very small in the area studied.

From the results presented here, it can be concluded that the chlorophyll-a a content and primary production in the Antarctic offshore water is generally very low in spite of its high concentration of nutrients. As the reasons of these low values two facts were considered. The one is low photosynthetic rate of phytoplankton caused by near freezing water temperature, and the other is the insufficience of submarine light for growing of phytoplankton as a result of the low stability of the waters in the upper layer.

Acknowledgements

The cooperation given by the late Prof. T. KUMAGORI, Captain K. OZAWA, his officers and crew, is gratefully acknowledged. Our heartfelt appreciation is extended to Dr. M. ISHINO of the Tokyo University of Fisheries, for his kind permission to use data from his physical and chemical observations. We owe much to Miss. J. BANNO and Mr. K. OGIYAMA for their assistance on radiation counting and pigment analysis.

References

BURKHOLDDR, P. R. and J. M. SIEBURTH (1961): Phytoplankton and chlorophyll in Gerlache and Bransfield Straits of Antarctica. Limnol, Oceanogr., **6**, 45–52.

ICHIMURA, S. and Y. SAIJO (1959): Chlorophyll content and primary production of the Kuroshio off the southern midcoast of Japan. Bot. Mag. Tokyo, **72**, 193–202.

IGY World Data Center A, Oceanography (1961): Production measurements in the world ocean,

part II. IGY Oceanography Report, No. 4, 517-519.

KIMBALL, H. H. (1928): Amount of solar radiation that reaches the surface of the earth on the land and on the sea, and the method by which it is measured. Mon Weath. Rev., **56**, 393-398.

POOLE, H.H. and W.G.R. ATKINS (1929): Photoelectric measurements of submarine illumination throughout the year. Jour. Mar. Biol. Assoc. U.K., **16**, 279-324.

RICHARDS, F.A. and T.G. THOMPSON (1952): The estimation and characterization of plankton population by pigment analysis. II. A spectrophotometric method for the estimation of plankton pigments. Jour. Mar. Res., **11**, 156.

RYTHER, J.H. and C.S. YENTSCH (1957): The estimation of photoplankton production in the ocean from chlorophyll and light data. Limnol. Oceanogr., **2**, 281-286.

SAIJO, Y. and S. ICHIMURA (1960): Primary production in the northwestern Pacific Ocean. Jour. Oceanogr. Soc. Jap., **16**, 139-145.

SVERDRUP, H.U. (1953): On conditions for the vernal blooming of phytoplankton. Jour. Cons. Int. Explor. Mer, **18**, 287-295.

Reprinted from J. oceanogr. Soc. Japan, vol. 19, no. 4, 1964, p. 19-21.

Size Distribution of Photosynthesizing Phytoplankton in the Indian Ocean*

Yatsuka SAIJO**

Abstract: The size distribution of photosynthesizing phytoplankton was estimated at 7 stations in the Indian Ocean for the waters at the surface as well as at 50m depth. Four light bottles filled with the same sample water were incubated under light source after adding ^{14}C solution, and then filtered through XX13 net, Millipore HA, AA, SM filter respectively. The photosynthetic activities of each fraction were evaluated from the results of counting for each filter. The activity of organisms retained by net is only a small part of total activity whereas the phytoplankton with the size between 0.8 and 110μ play the most part of the activity. The smallest size fraction with the size smaller than 0.8μ has a considerable activity for the surface water, but is almost negligible for the water from 50m depth.

1. Introduction

The significant role of nano- or microplankton in primary production in the ocean has been pointed out by HOLMES (1958) in his study in the Tropical Eastern Pacific. He attempted to estimate the size range of photosynthesizing phytoplankton in surface waters by using ^{14}C technique, and found that the bulk of carbon fixating organisms passes through fine nylon or silk net, and moreover, only about one-half of them retained by AA Millipore filter with pore size 0.8μ. YENTSCH and RYTHER (1959) compared the chlorophyll, photosynthesis and cell numbers in the net- and nanoplankton in the waters of Vineyard Sound. They found also that the net portion comprises a small percentage of the total population and exhibits marked seasonal trends, whereas the nanoplankton does not show any marked difference. In the North Pacific Ocean and Bering Sea, KAWAMURA (1961) determined the difference of photosynthetic activity between net filtered and unfiltered water also by ^{14}C technique. In a fresh water lake, RODHE *et al.* (1960) carried out similar experiments throughout a year, and their results show the importance of small size plankton in primary production in the lake.

For the purpose of accumulating further knowledge in this field, the author attempted to determine the size distribution of phytoplankton according to their photosynthetic rate during the Indian Ocean Expedition from November 1962 to January 1963 on board "Umitaka-maru".

2. Method and stations

The experiments were made at 7 stations in

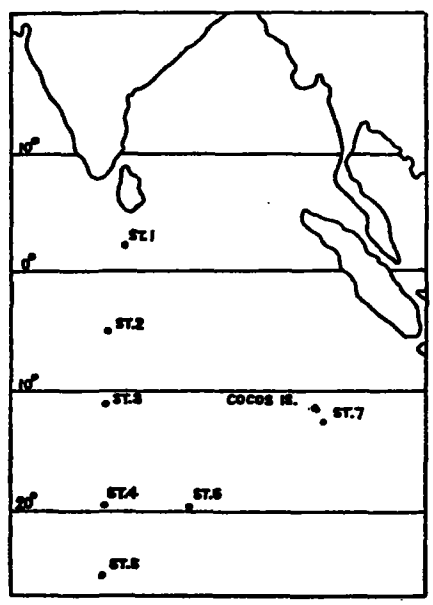

Fig. 1. Location of the sampling stations in the Indian Ocean.

* Received Oct. 4, 1963

** Water Research Laboratory, Faculty of Science, Nagoya University

the Eastern Indian Ocean as illustrated in Fig. 1. The method employed is similar to that of HOLMES. The sample waters were taken from surface and 50m depth with plastic Van Dorn type sampler. Each sample water was poured into four 250m*l* transparent bottles. After adding 1m*l* $Na_2{}^{14}CO^3$ (10μc) in each bottle, all light bottles were incubated for four hours under 15,000 lux illumination at surface water temperature. Then, each of four bottles from the same sample water was filtered through Millipore HA, AA, SM filter and XX13 net respectively. The pore size of these filters is 0.45, 0.8, 5.0 and 110μ. The radioactivity of the precipitate caught on each filter was determined. The counting value of each size fraction was shown as the percentage, assuming that the total counting for HA filter is 100%.

3. Results and discussion

Table 1 shows that the activity of netplankton, which retained by XX13 net, represents 0~12% of total activity. These values are comparable to those obtained by HOLMES also in tropical waters, or by YENTSCH and RYTHER in temperate waters but considerably lower than the values observed by KAWAMURA in the North Pacific or Bering Sea. KAWAMURA found the values from 16.1 to 56.0%. The method employed by KAWAMURA is a little different from that of HOLMES and the author's. KAWAMURA filtered the sample waters with XX13 net before the incubation, whereas HOLMES and the author filtered the sample waters with a similar size net after the incubation. However, it seems that such big difference between the results was not caused by the slight difference in technique employed, but instead by geographical variation of plankton species relating to the environmental conditions.

On the other hand, about one-half or more of total activity was retained by SM Millipore filter. The fractions of this size correspond to the so-called nanoplankton, and their average activity was 48% in surface and 73% in 50m depth water. Mean value of the activity of microplankton retained by AA and HA filters was 49% in surface water and 22% in 50m depth water respectively. Therefore, in surface water the activity of microplankton seems to be comparable to that of nanoplankton, whereas in 50m depth water the former is far smaller than the latter.

Table 1. Size distribution of photosynthesizing phytoplankton in the Indian Ocean.

	Station	Depth	Millipore filter			Net	Total
			HA 0.45~0.8μ	AA 0.8~5μ	SM 5~110μ	XX 13<110μ	
1	3°-22.'5 N, 79°-07.'6 E	0 m	15%	36%	46%	3%	100%
2	4 -58. 9 S, 78 -03. 4 E	0	37	36	27	0	100
		50	0	28	70	2	100
3	10 -55. 5 S, 78 -07. 0 E	0	25	26	49	0	100
		50	0	40	60	0	100
4	19 -54. 1 S, 78 -01. 0 E	0	5	41	48	6	100
		50	0	5	85	10	100
5	24 -58. 7 S, 77 -59. 6 E	0	33	3	52	12	100
		50	0	25	71	4	100
6	19 -50. 2 S, 86 -11. 9 E	0	2	35	63	0	100
		50	0	11	78	11	100
7	12 -44. 3 S, 97 -20. 0 E	0	16	47	37	0	100
		50	10	16	74	0	100
	Mean value	0	19	30	48	3	100
		50	2	20	73	5	100

It is interesting that at five out of seven stations in surface waters the activity of organisms passed through AA filter plays 15 to 37% of total activity. For same fraction, HOLMES obtained the value 44.5, 8.4 and 51.9% in the surface waters. He was in doubt to attribute all of high values to the carbon fixating activity of bacteria, and he attempted to explain it by protoplasmatic frangments released from fragile cells which ruptured on the filters surface. In the present study such phenomena also might be one of the reasons of high activity of small size fraction. But for final explanation further precise studies including the dark bottle experiments for each fraction and simultaneous microscopic inspection on board will be necessary.

It can be concluded that in the Indian Ocean, the significance of netplankton in photosynthetic activity is generally very small, on the other hand the phytoplankton with the size between 0.8 and 90μ play the most part of the activity. The smallest size fraction retained by HA filter also has considerable activity for surface waters, but almost negligible for 50m depth waters. From these fact it may be said that the size of photosynthesizing phytoplankton in tropical water is smaller at the surface and larger in 50m depth. This tendency coincides with many results of microscopic study on the geographical distribution of plankton in the ocean. GESSNER (1960) described that the smaller phytoplankton in a fresh water lake have higher photosynthetic activity by unit amount than that of bigger organisms. Similar phenomena might be observed in the ocean in future studies in this field. Including such problem, the studies on size distribution of phytoplankton will give important basis for the explanation of primary production in the oceans.

References

GESSNER, F. (1959): Hydrobotanik, II Stoffhaushalt, Berlin, 619-621.

HOLMES, R. W. (1658): Size fractionation of photosynthesizing phytoplankton. Special Scientific Report-Fisheries, No. 279, 69-71.

KAWAMURA, T. (1960): The "Oshoro Maru" cruise 46 to the Bering Sea and North Pacific in June-August 1960, 11. Data on phytoplankton photosynthetic activity. Data Rec. Oceanogr. Obs. Exp. Fish. Hokkaido Univ. No. 5, 142-165

RODHE, W., R.A. VOLLENWEIDER and A. NAUWERCK (1960): The primary production and standing crop of phytoplankton. Perspective in marine biology. California, 299-322.

YENTSCH, C. S. and J. H. RYTHER (1959): Relative significance of the net phytoplankton and nanoplankton in the waters of Vineyard Sound. Jour. Cons. Int. Explor. Mer, 24, (2), 231-238.

Reprinted from *La terre et la vie*, no. 2, 1964, p. 215-220.

PREMIERES DONNEES SUR LES BIOMASSES DE L'HERBIER A *MACROCYSTIS PYRIFERA* DE LA BAIE DU MORBIHAN (ARCHIPEL KERGUELEN)

par Paul GRUA,
Station Biologique de Roscoff (Finistère)

Au cours d'un programme d'étude de biotopes marins infralittoraux, des plongées avec scaphandres autonomes se sont déroulées dans la Baie du Morbihan, dans l'archipel Kerguelen, du 23 décembre 1962 au 5 février 1963 ; un peu plus tôt, du 17 au 19 décembre, quelques plongées avaient eu lieu à l'Ile de la Possession dans l'Archipel de Crozet. Plus de cinquante heures ont été passées ainsi dans l'eau, entre la surface et 15 mètres de profondeur, au cours de 54 plongées (Grua, 1963). La Baie du Morbihan est une vaste étendue abritée de 25 kilomètres sur 18, semée d'îles et de fjords dans sa moitié Ouest, et communiquant vers l'Est avec le large par la Passe Royale de 13 kilomètres de largeur. La transparence des eaux intérieures de la Baie est moindre que celle des rivages extérieurs. Des indications écologiques sont données dans Borojevic et Grua ; il paraît inutile de les reprendre ici.

Les limites supérieures et inférieures de fixation des *Macrocystis* varient suivant les lieux. Le facteur essentiel responsable de la distribution verticale a paru être l'éclairement du fond, lié à la transparence des eaux. Dans les stations visitées, ces limites sont à 1 m. et 12 m. sous la surface en eaux peu transparentes, tandis que dans les eaux plus claires ces limites sont déplacées vers la profondeur : à l'extérieur de la Passe (Ile Buchanan), le peuplement s'établit à 8 m. et descend bien au-dessous de 15 m. (Grua, 1964).

La détermination de l'étendue des herbiers ne peut être encore qu'imprécise. En appliquant les résultats des observations relatives à la distribution verticale en fonc-

tion de la transparence des eaux, il est possible de faire une évaluation de la répartition des *Macrocystis* dans la Baie. Il y a lieu de considérer séparément les parties Est et Ouest de celle-ci. La première, entourée de côtes basses ou rarement élevées, offre des fonds peu inclinés le long de rivages sans découpures. Dans la partie Ouest, les côtes très développées sont principalement rocheuses et plongent rapidement sous la surface. La présence des *Macrocystis* est porté sur les cartes avec quelque validité dans le secteur Nord-Est de la Baie, aux abords de Port aux Français (carte 6087). Les herbiers existent cependant en dehors de cette zone, mais la mention en est faite de façon très incomplète sur la carte générale (5748) figurant la partie Ouest. En comparant nos observations personnelles, faites à diverses stations, en plongée et en surface, et en tenant compte de la surface de l'herbier représenté dans la partie Est, un chiffre de l'ordre de 45 kilomètres carrés paraît une valeur admissible pour l'ensemble des herbiers de la Baie.

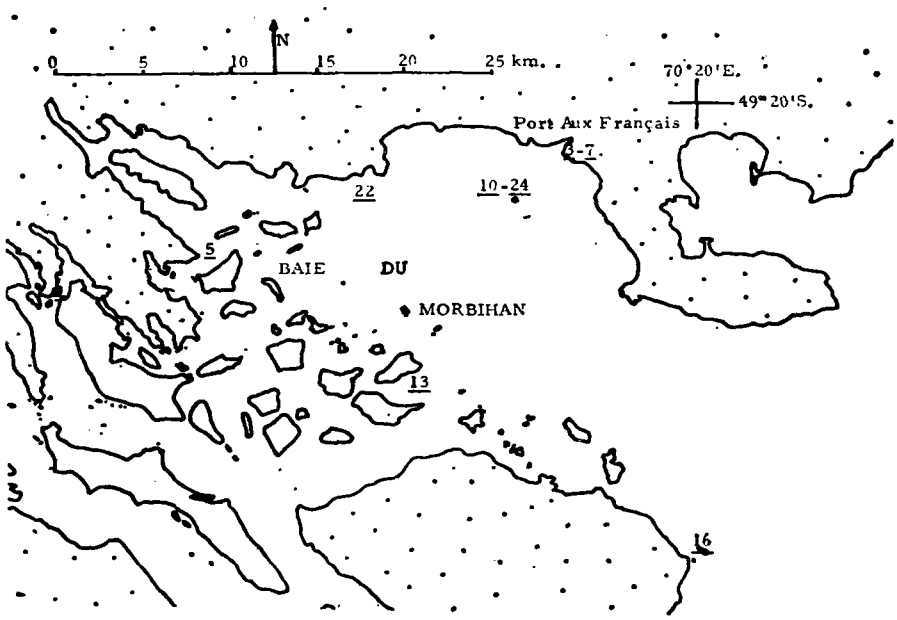

Figure 1. — Carte schématique de la Baie du Morbihan, avec indication de l'emplacement des stations d'observation mentionnées dans le texte.

Pour permettre une estimation de la biomasse de ces algues, un procédé pratique prend pour référence le poids moyen du mètre linéaire de stipe, de préférence à de laborieuses récoltes à grande échelle suivies de pesées difficiles. Le nombre de mètres linéaires est tiré du dénom-

brement des stipes au mètre carré, multiplié par la longueur moyenne de ces stipes. Le poids moyen du mètre linéaire a été déterminé d'après un pied détaché en totalité, en coupant ses haptères au ras du substrat, au milieu d'un herbier représentatif au Cap Kidder ; ce pied a été pesé au retour au port. Le « poids du mètre linéaire de stipe » fait intervenir le poids frais global du pied, avec ses haptères et ses lames, que l'on a rapporté conventionnellement au mètre de stipe. Ce poids pris comme unité de calcul est de 190 grammes. Le tableau 1 montre les variations du nombre de stipes au m² de substrat et celles de la longueur des stipes en différentes stations.

TABLEAU 1

Localité	N° de la stat.	Nombre de stipes au m²	Longueur moyenne (m.) de la végétation au milieu du peuplement	Mètres linéaires de stipes au m²	Poids au m² arrondis au kg
— Eaux propres :					
Ile Buchanan .	16	20	25	500	95
— Eaux moyennement transparentes :					
Cap Kidder ..	22	60	11	660	125
Ilot Channer .	24	60	14	840	160
— Eaux peu claires :					
Ile Mussel	5	90	8	720	137
Pointe des Cormorans	3-7	290	11	3190	606

La valeur relevée à la Pointe des Cormorans est très nettement supérieure aux autres. La cause en est la proximité de Port aux Français dont les égoûts enrichissent les eaux en matières nutritives. L'Ile Buchanan, quant à elle, demeure en dehors du domaine propre de la Baie dont les eaux sont moins claires que celles du large. Ces brèves remarques nous conduisent à écarter les deux valeurs extrêmes du tableau pour prendre un chiffre de l'ordre de 140 kg comme moyenne du poids de *Macrocystis* au mètre carré d'herbier dans la Baie. La masse des *Macrocystis*, en prenant pour termes du calcul le chiffre précédent et une surface d'herbier de 45 km², s'établit donc à 6,3 millions de tonnes pour la Baie.

La sous-strate des herbiers est un espace où l'éclairrement est réduit. La masse de végétation y est faible. Au point de vue zoologique, les groupes les plus importants pondéralement sont par ordre décroissant les moules, les éponges, les astéries, les tuniciers, les holothuries, les annélides, les ophiures. Les biomasses qui ont été relevées présentaient des valeurs diverses, en ce qui concerne leur poids total et les proportions relatives des parties animales et végétales. Les chiffres suivants donnent une idée de l'abondance des Invertébrés benthiques se pressant sur le substrat ou en épibioses multiples pour former une couche vivante dépassant parfois 10 centimètres d'épaisseur.

Nos quelques prélèvements, réalisés chaque fois sur des surfaces de 4 à 6 décimètres carrés, ne peuvent guère donner qu'un ordre de grandeur. Sur la base des dix valeurs de biomasse obtenues dans différentes conditions dans le cadre de l'herbier, il paraît cependant possible d'adopter comme moyenne au décimètre carré un chiffre de l'ordre de 300 à 400 grammes (poids frais). Comme cela a été fait pour la masse d'ensemble des *Macrocystis* réparties dans la Baie, il est alors intéressant de tenter une estimation de la biomasse de la sous-strate de l'herbier. Il faut pour cela considérer la surface réelle du fond rocheux, avec son relief irrégulier, de laquelle doit être retranchée la surface occupée par les haptères des *Macrocystis*. Si le calcul est fait sur ces bases, la masse totale de la sous-strate atteint ainsi 2,8 millions de tonnes dans l'aire couverte par l'herbier.

TABLEAU 2

Localité	N° de station	Profondeur en mètres	Inclinaison du substrat	Proportion relative d'organismes		Poids total en g/dm²
				animaux %	végétaux %	
Cap Kidder	22.a	7	Horizontal	11	89	56
Ile Buchanan	16.b	15	Horizontal	20	80	192
	16.a	15	Vertical	80	20	127
Ile du Chat	13.a	15	Vertical	90	10	360
Pointe des Cormorans	7.a	5	Vertical	90	10	1200
Ilot Channer	10.a	7	Oblique	90	10	1500

Envisagée après les formes sessiles ou sédentaires, la faune benthique mobile n'est représentée que par de très rares poissons. Alors que les fonds constitués de sédiments nourrissent une masse peu importante de poissons, l'herbier de *Macrocystis* peut sembler à priori le milieu propice à une concentration d'individus nombreux. Or, ce n'est pas du tout le cas. Durant une trentaine d'heures passées dans des zones à *Macrocystis*, une dizaine de poissons seulement ont été vus, appartenant aux genres *Chaenichthys* et *Notothenia*.

Les Vertébrés rencontrés dans la zone superficielle de l'herbier étaient des cormorans *Phalacrocorax verrucosus*, des manchots *Aptenodytes patagonica* et *Pygoscelis papua*, et, à petite distance de côtes basses, des éléphants de mer *Mirounga leonina*. Dans une zone à *Macrocystis* clairsemées sur un fond de 12 m. a été remarqué à l'Ile du Chat, un *Hydrurga leptonyx* (Léopard de mer), inhabituel à cette période de l'année, dont le comportement à notre égard a été circonspect — quoique investigateur au cours des trois quarts d'heure que dura notre confrontation. A l'Ile de la Possession (Crozet), au-dessus de fonds comparables, une troupe de quatre *Orcinus orca* a longé le rivage de la Baie du Navire alors que l'un de nous venait de reprendre pied sur le radeau. Ces Vertébrés à respiration aérienne ne sont que des hôtes occasionnels des secteurs où croissent les *Macrocystis* et leur présence constatée est mentionnée pour mémoire ici. L'évaluation de leur biomasse est hors de propos, et serait d'ailleurs illusoire du fait des déplacements au long cours qui poussent nombre d'entre eux à abandonner temporairement les lieux.

CONCLUSION. — Les estimations de biomasses que nous avons tentées dans l'herbier de *Macrocystis pyrifera* de la Baie du Morbihan (Archipel des Kerguelen), étage bionomique défini comme un milieu précis, n'ont pu être accompagnées du calcul de l'erreur pouvant entacher les valeurs indiquées. Dans une étude plus large, la question abordée brièvement ici sera traitée de façon critique. Cependant les chiffres obtenus indiquent que les masses vivantes, animales et végétales, y atteignent des valeurs dépassant largement ce que l'on peut rencontrer dans les mers boréales tempérées pour lesquelles des estimations analogues ont été faites.

BIBLIOGRAPHIE

BOROJEVIC, R. et GRUA, P. — Eponges calcaires de KERGUELEN, systématique et écologie. *Arch. Zool. Exp. Gén.* (sous presse).

GRUA, P. (1963). — Etude de biotopes marins infralittoraux, KERGUELEN 1962-63. *T.A.A.F., 23-24 : 69-73.*

— (1964). — Sur la structure des peuplements de *Macrocystis pyrifera* (L.) C. Ag. observés en plongée à Kerguelen et Crozet. *C. R. Acad. Sc. Paris, 259 : 1541-1543.*

Service Hydrographique de la Marine, PARIS.

Carte 5748. — Iles de KERGUELEN, 3e *Ed., 1961.*

Carte 6087. — Baie du Morbihan. Partie Est. 3e *Ed., 1961.*

L'herbier de *Macrocystis* tel qu'il apparaît au plongeur : ci-dessus, en eau claire, 15 m de profondeur, exposé au large, Ile Buchanan. Ci-dessous, herbier en état décadent, à 7 m de profondeur, Ilot Channer.

Sous-strate très riche dans un peuplement très dense de *Macrocystis*, à 5 m de profondeur, à la Pointe des Cormorans. Au centre, des actinies dans un banc de moules caractéristique de l'étage infralittoral et, à la périphérie, des Rhodophyceae et des Serpulidae.

Cette photographie, comme celles de la planche précédente, a été faite par l'auteur. Cliché P. Grua, CNRS.

Reprinted from *Biologie antarctique*, Paris, 1964, p. 279-282.

PLONGÉES AUX ILES SAINT-PAUL ET NOUVELLE AMSTERDAM

PLONGÉES EN EAUX FROIDES

P. GRUA

Station Biologique de Roscoff, Finistère, France

The possibilities of research using diving techniques, and the precautions required, at these two French southern islands are examined. Local conditions of topography and hydrography and potential dangers are reviewed from the point of view of an underwater biologist and in the particular context of diving. Emphasis is placed on the importance, in unfamiliar waters, of knowing one's personal capacities, which depend on good physical and psychological condition as well as equipment. Work in cold water, although often less efficient, is nevertheless quite feasible with the equipment available and some practical advice is given on this subject.

Les plongées sous-marines présentent d'incontestables avantages par rapport aux méthodes conventionnelles d'investigation. Les dragages ont en effet l'inconvénient de détériorer et la faune et la flore sédentaires, de provoquer la fuite de la faune mobile, de mélanger les peuplements biologiques, sans même pouvoir permettre l'exploration des zones anfractueuses.

Tous ces inconvénients sont évités par les plongées qui donnent en outre au biologiste la possibilité d'observer et de photographier directement les communautés biologiques et leur étagement.

Toutefois les plongées ne sont pas sans présenter quelques inconvénients. La basse température de l'eau et le dépaysement provoquent une inhibition appréciable des facultés mentales. Aussi le plongeur doit-il avant de s'introduire dans l'eau, être assuré que son matériel est parfaitement au point. Ceci étant, son sentiment de sécurité et de confiance en lui-même sera d'autant moins altéré, s'il se trouve brusquement placé devant une situation imprévue.

A la faveur des plongées faites aux Iles Saint-Paul et Nouvelle Amsterdam au cours de l'été 1958-1959 (Grua, 1963*a*), dans les premiers mètres de la surface, nous préciserons ce que sont les conditions du travail sous-marin dans ces régions. Nous terminerons cette brève note par quelques indications sur le matériel qu'il convient d'utiliser en eaux très froides (Grua, 1963*b*).

La côte et les fonds

Les côtes de ces deux îles sont en général formées de falaises abruptes, à l'exception du rivage nord-est de la Nouvelle Amsterdam et de l'ouverture du cratère à Saint-Paul. En conséquence, une embarcation à moteur, transportant le plongeur et son matériel, s'avère indispensable. On peut, par ce moyen, s'approcher sans difficulté de la plupart des rivages, à l'exception toutefois des côtes ouest des deux îles, battues par une houle quasi-permanente.

Les fonds proches de la côte sont formés d'éboulis rocheux parsemés çà et là de petites étendues de sable. Au pied des falaises on peut trouver, à certains endroits, quelques grottes.

Les algues géantes, *Macrocystis pyrifera*, allant de 10 à 30 m de profondeur jusqu'à la surface, sont fréquentes, particulièrement sur les côtes orientées à l'Est. Au cours d'une récente campagne de plongées aux Iles de Kerguelen (1962-63) nous avons pu pénétrer sous leur couvert sans trop de difficulté.

Comme on le sait, l'Ile Saint-Paul est d'origine volcanique et les eaux de son cratère communiquent avec celles du large par un étroit goulet, dont le fond est un seuil rocheux où la barre est très fréquente. On peut atteindre aisément la zone des galets qui entoure le goulet et un plongeur équipé peut, avec quelques difficultés faire le tour du cratère. Cette île étant inhabitée en permanence il est nécessaire d'y établir au préalable un campement.

La mer et le vent

L'amplitude maximum des marées est de l'ordre de 1,80 m. Les courants, dont l'intensité et la direction sont très variables, sont assez fréquents à proximité de la côte. Le plongeur en scaphandre autonome doit donc en tenir compte pour éviter tout essoufflement superflu. Mais ces courants peuvent aussi provoquer la dérive de l'embarcation; pour assurer efficacement la sécurité du plongeur, cette dernière doit donc toujours être maintenue à l'endroit où les bulles d'air viennent crever à la surface. Une corde d'appel reliant le plongeur au bateau, n'est toutefois pas souhaitable en raison de la présence des bancs de *Macrocystis* et du relief accidenté du fond.

La température des eaux de surface varie entre 12,7° en septembre et 17,4°C en février à la Nouvelle Amsterdam et entre 12,3° et 16,8°C respectivement à l'Ile Saint-Paul (Météorologie Nationale, comm. pers.). A trente mètres de profondeur en janvier 1959, l'eau de l'Ile Saint-Paul était voisine de 14° celle de la Nouvelle Amsterdam de 18°C.

En hiver les tempêtes sont fréquentes et compliquent ou interdisent même totalement tout travail sous-marin. La période d'été est nettement plus favorable, mais il faut toujours se souvenir que le vent peut se lever, en toute saison, en deux ou trois heures. Toute embarcation évoluant sans secours éventuel doit donc tenir compte de ce laps de temps, notamment quand elle se trouve face à une côte hostile.

La transparence des eaux, plus agréable que nécessaire, procure néanmoins un sentiment subjectif de sécurité. Ces petites îles sont entourées par des eaux du large toujours propres et renouvelées. Ce n'est pas le cas pour le cratère de l'Ile Saint-Paul; la relative turbidité de ses eaux est due à la présence de nombreuses sources sous-marines d'eau chaude et de gaz qui sont libérées dans un milieu relativement confiné.

Aspects généraux de sécurité

Les délais de transport vers un moyen de secours pouvant être assez longs, les plongées doivent être effectuées avec d'autant plus de prudence. En effet, les incidents physiologiques ou les blessures prennent dans ces régions une importance plus grande que sur les côtes bien équipées de nos régions habitées. Si la station de la Nouvelle Amsterdam héberge en permanence un médecin susceptible d'intervenir, il n'y a rien par contre à l'Ile Saint-Paul.

Certains animaux représentent des dangers directs pour l'homme immergé, tandis que d'autres peuvent simplement effrayer. Ce sont *Orca gladiator*, *Isurus glaucus*, *Carcharodon* sp., *Squalus fernandinus*, *Thyrsites atun*, *Polyprion americanus*, *Mirounga leonina*, *Arctocephalus australis*.

Un plongeur même expérimenté doit donc se garder de dépasser 10 mètres de profondeur; au-delà il est indispensable qu'il soit accompagné. Mais dans tous les cas un veilleur doit se tenir à proximité, que ce soit sur la côte ou dans l'embarcation, prêt à intervenir.

Les conditions de travail en eaux froides

Les eaux de l'Océan Antarctique, limitées au Nord par la ligne de convergence, ont une température de surface variant selon les lieux et la saison entre — 2° et + 4° C, tandis que les températures moyennes de l'air restent voisines de 0° C pendant l'été.

Les glaces dérivantes ou fixées, la présence de banquettes côtières, les vents violents et subits peuvent sérieusement gêner les plongées. Ces dernières sont d'autant plus efficaces que le plongeur est mieux protégé du froid ambiant. Ceci implique donc le choix de vêtements isothermiques particulièrement adaptés au genre de travail à effectuer. Une épaisseur de dix millimètres de néoprène

mousse obtenue de préférence par la superposition de deux combinaisons bien ajustées, isole de façon pratique et confortable le plongeur évoluant entre la surface et une quinzaine de mètres de profondeur. Le vêtement étanche, avec les doublures nécessaires, quoique d'un emploi plus délicat, peut être préféré au-dessous de ce niveau pour les travaux statiques; ce vêtement une fois gonflé procure d'ailleurs un meilleur isolement au froid. Une nouvelle combinaison en feuille de latex mince non doublée de tissu, d'une grande résistance aux accrocs, semble une heureuse innovation. Elle peut recouvrir la combinaison en néoprène et son élasticité diminue les inconvénients du placage en plongée. Ces enveloppes protectrices étant relativement épaisses il faut donc augmenter le lestage et le répartir de préférence sur les divers sanglages plutôt que d'utiliser une lourde ceinture.

L'étanchéité au niveau des poignets et du cou n'est pas encore résolue de façon satisfaisante. Un vêtement trop serré à ce niveau peut provoquer en effet des constrictions gênant la circulation sanguine, dont les effets sont rapidement ressentis en eaux très froides.

La préhension manuelle doit rester précise pour les manipulations diverses et l'isolement avec des gants de néoprène est le meilleur compromis. On peut limiter le refroidissement périphérique par l'emploi d'un révulsif provoquant une vaso-dilatation superficielle. Il est bon de consommer une préparation polyvitaminée aidant à conserver une bonne forme physique.

Pour éviter au plongeur de respirer un air trop froid, il est préférable que les scaphandres soient tiédis à l'avance, et isolés dans une enveloppe de néoprène. Le détendeur à deux étages, avec valve située contre la bouche et tube unique, est également préférable.

Mentionnons accessoirement la récente sortie sur le marché du « Calypso-Phot », appareil photographique complet de format 24 × 36 étanche et de manipulation facile.

Références

Fane, F. D. 1959. Skin diving in polar waters. *Polar Rec.*, **9** : 433-5.

Grua, P. 1963*a*. Plongées biologiques sous-marines aux îles St-Paul et Nouvelle Amsterdam. *C.N.F.R.A.*, Paris, **4** : 37-49.

Grua, P. 1963*b*. Lutte contre le froid et adaptation rapide aux conditions de plongée dans des eaux froides. Kerguelen 1962-63. In *Third Intern. Biometeor. Congr.*, Pau (*sous presse*).

Neushul, M. 1961. Diving in Antarctic Waters. *Polar Rec.*, **10** : 353-8.

Reprinted from *Biologie antarctique*, Paris, 1964, p. 471-480.

LE CYCLE SEXUEL ET L'ÉVOLUTION DES SOIES OVIGÈRES DES FEMELLES DE *JASUS PAULENSIS* (PALINURIDAE)

P. GRUA

Station Biologique, Roscoff, Finistère, France

The southern crayfish live in two separate populations around Iles Saint-Paul and Nouvelle Amsterdam.

The annual sexual cycle, determined for the population of Nouvelle Amsterdam, is related to water temperature : egg-laying occurs in May and June and hatching takes place in August and September. At both islands, the ovigerous setae then become very variable in size, being damaged by the female taking off the empty egg-shells. The setae are renewed during the southern summer.

This phenomenon is being studied by an original biometric method involving size ratios, the validity of which is discussed. Pilosity becomes complete again about March, owing to a moult distinct from the pre-breeding one. The populations at the two islands, and the various size-classes, differ in their detailed pattern.

La biologie des langoustes australes, vivant autour des îles Saint-Paul et Nouvelle Amsterdam, n'est connue que de façon très fragmentaire. Après une campagne d'été en 1958-59 à bord du navire langoustier congélateur SAPMER, une première étude a contribué à la connaissance de l'écologie de cette espèce. L'objet de cette communication est de préciser le cycle annuel de *J. paulensis* Heller ; lors de la recherche de la taille de maturité précisée récemment (Grua, 1963), un phénomène estival particulier intéressant les soies ovigères a été étudié au moyen d'une méthode biométrique qui, à notre connaissance tout au moins, n'avait jamais été utilisée auparavant (1).

LE CYCLE SEXUEL

La figure 1 exprime, par période de quinze jours, la proportion de femelles portant des œufs extérieurs fixés aux pléopodes par rapport au nombre total des

(1) Nous retiendrons avec L. B. Holthuis le nom de *J. paulensis* Heller 1862 pour la langouste australe française. Holthuis a en effet rejeté dernièrement *J. lalandii* Lamk., H. M. Edw 1837, employé jusqu'à maintenant par assimilation avec les langoustes du Cap.

femelles capturées. Ces captures systématiques ont été faites au casier, de juin 1959 à septembre 1960, à la cale de débarquement de la Nouvelle Amsterdam, par le Docteur Aubert qui a bien voulu suivre les indications de l'auteur. Les casiers ont été immergés dans une seule station proche du rivage à quelques mètres de profondeur.

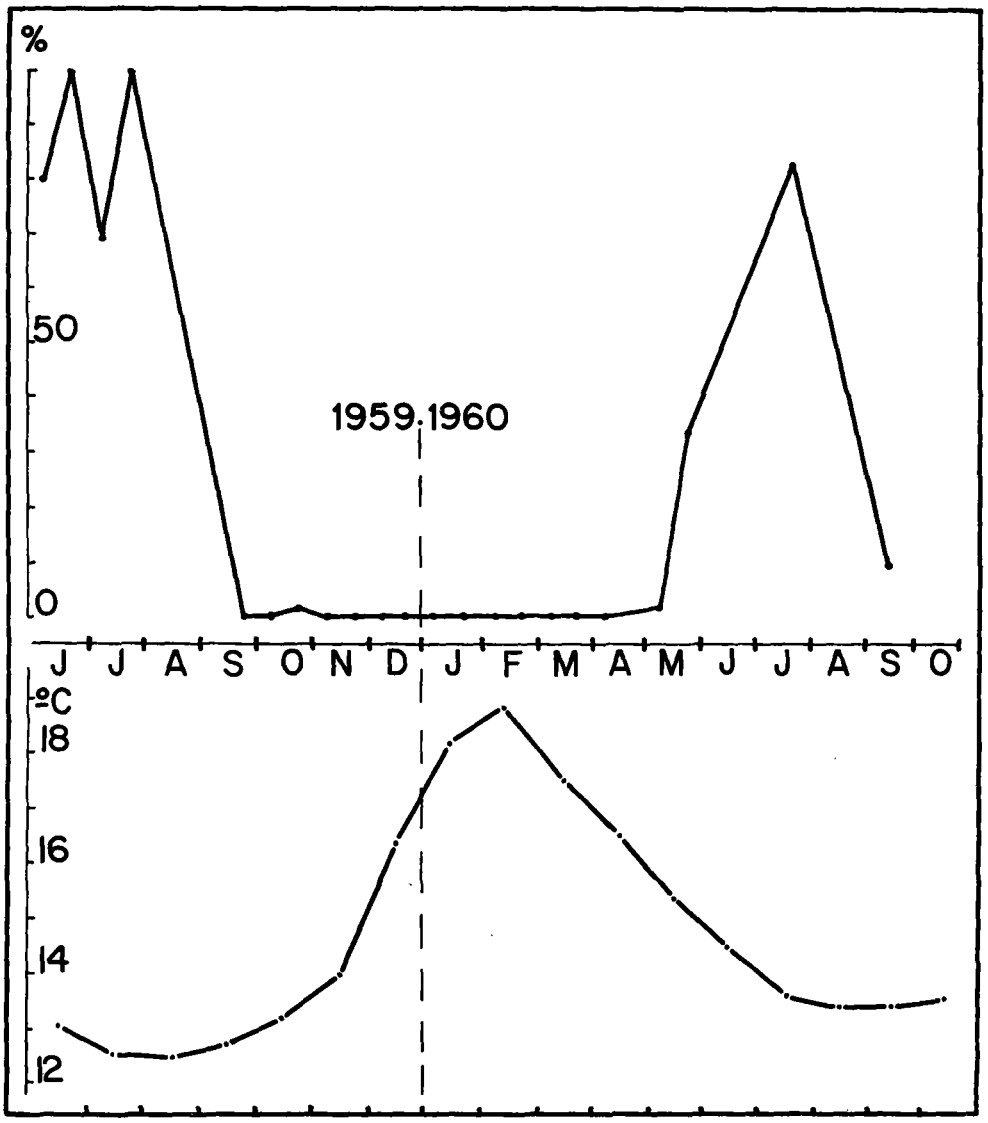

FIG. 1. — *Nouvelle Amsterdam.* a) *Pourcentage du nombre de femelles œuvées, par rapport au nombre total de femelles capturées chaque quinzaine, en fonction du temps.* b) *Températures moyennes mensuelles en* 1959-60.

Ces résultats ne rendent sans doute pas compte exactement du phénomène tel qu'il se produit dans l'ensemble des populations exploitées ; ces précisions sont cependant intéressantes car ce sont les seules dont nous disposons. Notons enfin que la température de l'eau a été relevée systématiquement au même endroit en 1959-60.

Nous avons pu déduire de ces observations que la ponte de l'année 1960 avait commencé à la fin du mois d'avril ou au début de mai, dans une eau dont la température atteignait 16°C environ. L'éclosion se produit dans la deuxième moitié de l'hiver, étalée sensiblement sur deux mois, tandis que la température de l'eau recommence à s'élever. A la fin du mois de septembre, les températures de l'eau étaient voisines de 13°C et les femelles ne portaient plus d'œufs extérieurs. Les femelles sont donc dépourvues d'œufs pendant sept à neuf mois, le milieu de cette période se situant au mois de janvier, un mois environ avant que la température moyenne de l'eau atteigne sa valeur la plus élevée. La fréquence maximum du nombre des femelles œuvées a été observée vers le milieu de juillet, quelques semaines avant que l'eau atteigne sa température minimum.

Les soies ovigères en été

Au cours de la campagne d'été 1958-1959 à bord du navire Sapmer nous avons étudié la longueur et la densité de la pilosité de 1 720 langoustes femelles. Quand les femelles ne portent pas d'œufs extérieurs (après l'éclosion des larves à la fin de l'hiver) leurs soies sont de longueurs très inégales, selon que la taille des individus est plus ou moins grande, mais il existe aussi des différences entre deux spécimens de même taille. Les pléopodes paraissent partiellement épilés, et les soies sont irrégulièrement écourtées. La proportion de femelles aux soies écourtées diminue pendant le déroulement de l'été austral. Cette épilation est probablement imputable aux femelles elles-mêmes qui détachent les coques d'œufs vides fixées aux soies par la sécrétion cémentaire avec la petite pince terminale de leur cinquième paire de péréiopodes. Cette toilette des pléopodes paraît responsable de l'amputation de très nombreuses soies.

Méthode utilisée

Pour rendre compte des divers états des soies, nous avons utilisé le rapport existant entre leur longueur et la largeur de l'article sétigère de l'endopodite, ce qui nous a permis d'indexer la pilosité individuelle à la taille de l'animal. En effet une mesure millimétrique aurait pu donner le même chiffre pour deux états de pilosité de signification différente. L'établissement de ces notations a été rendue possible du fait de la grande largeur de l'article sétigère de *Jasus* (Boas, 1880 ; Holthuis, 1946).

Nous avons classé les soies en quatre catégories en fonction de quatre valeurs type du rapport précédent.

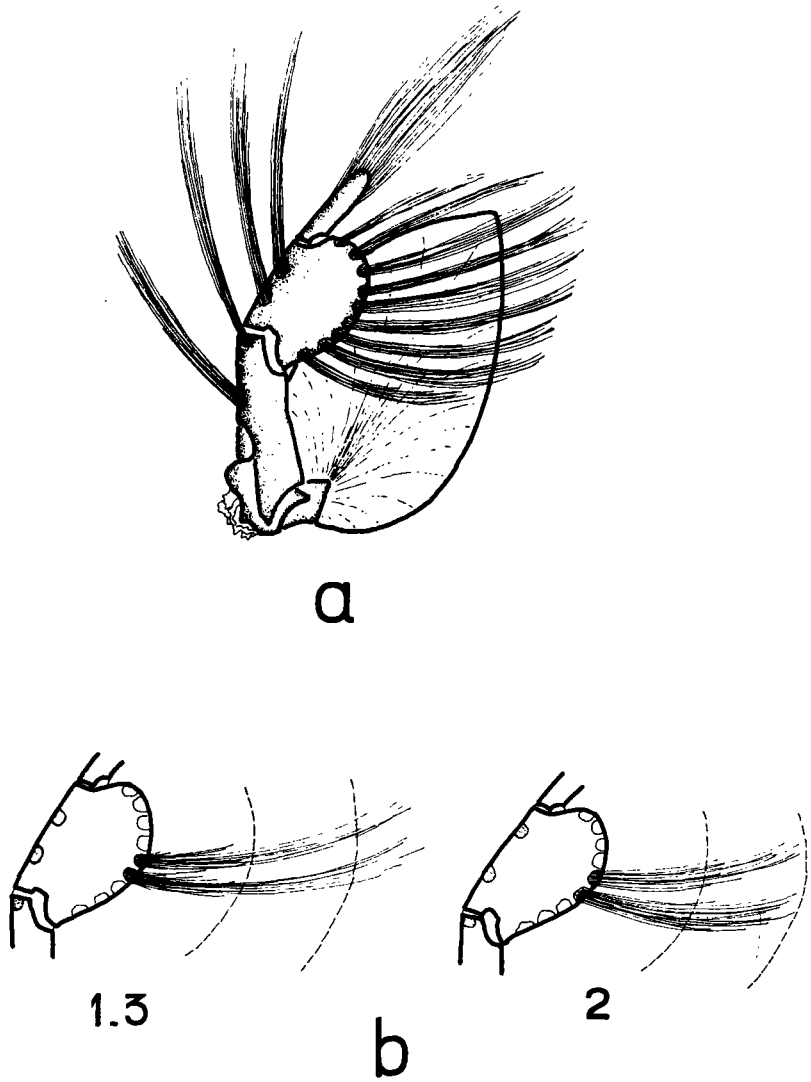

FIG. 2. — *Pléopodes et soies ovigères de* Jasus paulensis. a) *Pilosité complète.* b) *deux exemples d'épilation avec la notation correspondante utilisée pour en rendre compte.*

Rapport 0. — aucune soie,
— 1. — soie de longueur inférieure à la largeur de la palette sétigère,
— 2. — soie de longueur comprise entre une et deux largeurs de palette,
— 3. — soie de longueur supérieure à deux largeurs de palette.

Il est exceptionnel que des soies atteignent trois largeurs de palette.

Il faut remarquer par ailleurs qu'il existe souvent sur un même pléopode, des soies de longueurs diverses. Dans un tel cas, nous avons relevé les valeurs extrêmes, celles des soies longues et celle des soies courtes. Dans nos calculs nous avons utilisé soit ces valeurs extrêmes, soit leur moyenne arithmétique. Remarquons aussi que sur un même animal l'ensemble des pléopodes présente très sensiblement le même aspect d'épilation ; par conséquent la notation appliquée à chacun d'entre eux rend compte de l'état de tous les pléopodes.

De plus nous avons rangé l'ensemble des sujets étudiés en deux catégories fonction de la richesse et de la densité de l'ensemble de la pilosité : la catégorie I, qui correspond à une pilosité moyenne ou réduite, comprend la majorité des individus. La catégorie II, où les franges de soies sont très fournies, n'est guère observée que chez des sujets de grande taille.

La combinaison réciproque de ces deux notations a été appliquée à toutes les langoustes, sans aucune difficulté. On pourrait faire des réserves sur ce mode de chiffrage soumis à un élément subjectif d'appréciation, mais nous avons pu constater que la variabilité de la longueur et de la densité des soies entre individus de même taille est très largement supérieure à la latitude d'estimation.

Chaque mensuration de pilosité a été prise en même temps que la longueur totale de l'animal (de l'extrémité de l'épine supra-orbitaire à l'extrémité du telson).

L'ensemble des animaux étudiés a permis d'établir deux mille deux cents notations de pilosité. Les chiffres obtenus rendent compte de la grande diversité présentée par les soies, que ce soit en fonction des tailles ou en fonction de la date des captures ; aussi a-t-il été nécessaire de les classer en plusieurs groupes. Les moyennes obtenues statistiquement donnent des courbes continues à évolution progressive. Par contre, à l'échelon individuel, chaque langouste étant soumise aux brusques étapes de croissance, l'évolution de ses soies ne peut être continue.

Mise en évidence du phénomène

Discussion

Avant toute interprétation il faut être certain que la codification adoptée et le rapport caractérisant les soies sont justifiées. En d'autres termes, il s'agit de savoir si les variations de ce rapport dépendent effectivement de l'inégalité de longueurs de soies.

Définissons donc les variables entrant dans les graphiques. Elles se composent sous la forme suivante :

$$\frac{y}{x} = \frac{\dfrac{\text{longueur de soie}}{\text{largeur de l'article sétigère}}}{\text{longueur totale de la femelle}}$$

Soient deux états pileux correspondant à deux sujets dont la capture est séparée par un long intervalle de temps. En ordonnée sont représentées les valeurs décimales obtenues par les moyennes arithmétiques définissant la pilosité.

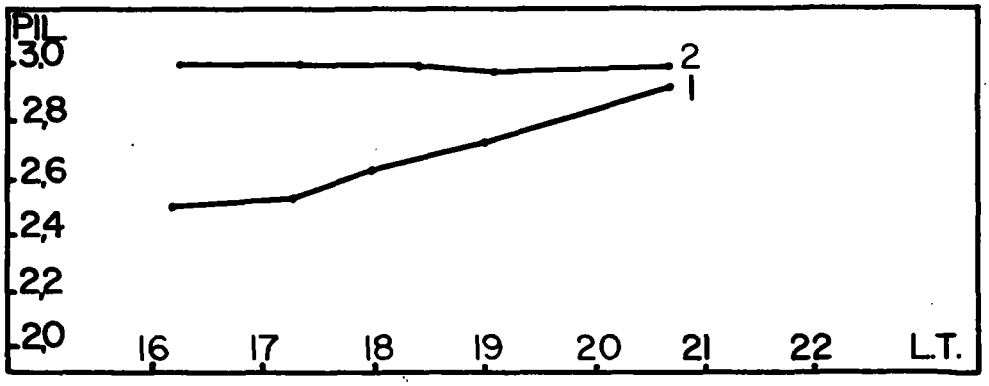

FIG. 3. — *Aspects de la pilosité ovigère des femelles au milieu et à la fin de son renouvellement à la Nouvelle Amsterdam.* a) 17 *et* 19 *janvier*, 127 *femelles* ; b) 2 et 4 *mars* 1959, 113 *femelles.*

La courbe 1 de la figure 3 est assimilable à une droite inclinée de forme $y = ax + b$, de pente a positive. Pour des valeurs de x croissantes, y croît également.

Quatre cas sont alors possibles pour y :

I. L'article sétigère s'accroît moins vite que les soies.
II. L'article reste de taille constante et les soies grandissent.
III. L'article décroît et les soies restent de même taille.
IV. L'article décroît plus vite que ne diminuent les soies.

Comme l'on sait que l'article sétigère s'accroît en même temps que la taille de l'animal augmente, on en déduit que seul le premier cas est possible et l'on conclut donc à une augmentation de la longueur absolue des soies.

La courbe 2 de la figure 3, également assimilable à une droite de formule $y = ax + b$, a un coefficient angulaire a égal à zéro. Pour toute valeur de x, y est égal à la constante b ; y étant constant, la longueur des soies et la largeur de l'article sétigère varient de façon directement proportionnelle. Donc pour des tailles successives croissantes, la longueur absolue des soies augmente.

De la courbe 1 à la courbe 2, le passage dans le temps, d'une valeur de y à une autre plus élevée, peut être défini en prenant une valeur constante de x. Pour une taille donnée de langouste x, l'article sétigère conserve une même dimension, c'est le cas II. Donc l'accroissement de y est lié à un allongement absolu des soies.

La discrimination précédente basée sur la longueur totale de l'animal et la largeur de l'article sétigère nous permet de conclure que le rapport caractérisant la dimension des soies varie dans le même sens que les soies, jusqu'au rapport 3 qui est une valeur-limite constante.

Résultats

La figure 4 représente l'évolution des soies dans le temps. Les résultats concernant les spécimens des deux îles ont été juxtaposés chronologiquement. En nous référant à la taille de maturité, plus petite à la Nouvelle Amsterdam qu'à Saint-Paul, nous avons pu séparer les langoustes de chaque île en trois groupes homologues deux à deux.

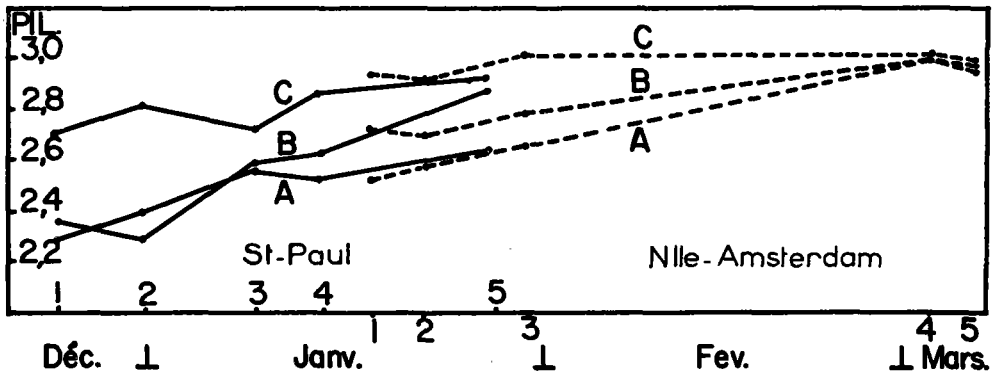

Fig. 4. — *Iles Saint-Paul et Nouvelle Amsterdam. Evolution chronologique de la pilosité en fonction de trois groupes de tailles* : A - *petites*; B - *moyennes*; C - *grandes.*

Les courbes obtenues ont une pente générale ascendante, malgré quelques inflexions dues à des captures effectuées dans des conditions topographiques et météorologiques différentes (Grua, 1960). Tous les groupes de taille subissent un allongement progressif des soies et les courbes tendent toutes vers la pilosité 3. Les langoustes de grande taille y accèdent avant celles dont la taille est moyenne, elles-mêmes plus avancées que les petites. La précocité relative des grands individus a déjà été remarquée par Bradstock (1950) chez *Jasus lalandii*, et par George (1957) chez *Palinurus longipes*. Cela nous incite à penser que les richesses en soies, différentes selon les tailles, sont dues également à un décalage du cycle sexuel aux îles australes françaises, avec une éclosion comparativement plus tardive des œufs chez les individus de taille inférieure.

L'association des courbes nous permet de faire la synthèse du rythme de renouvellement des soies dans son ensemble : le début est lent, suivi d'une phase intermédiaire d'accroissement rapide, avec un ralentissement terminal au voisinage de l'état pileux complet. Ce schéma est à rapprocher de la courbe sigmoïde représentant le processus des croissances limitées.

Une représentation complémentaire du phénomène est donnée dans la figure 5.

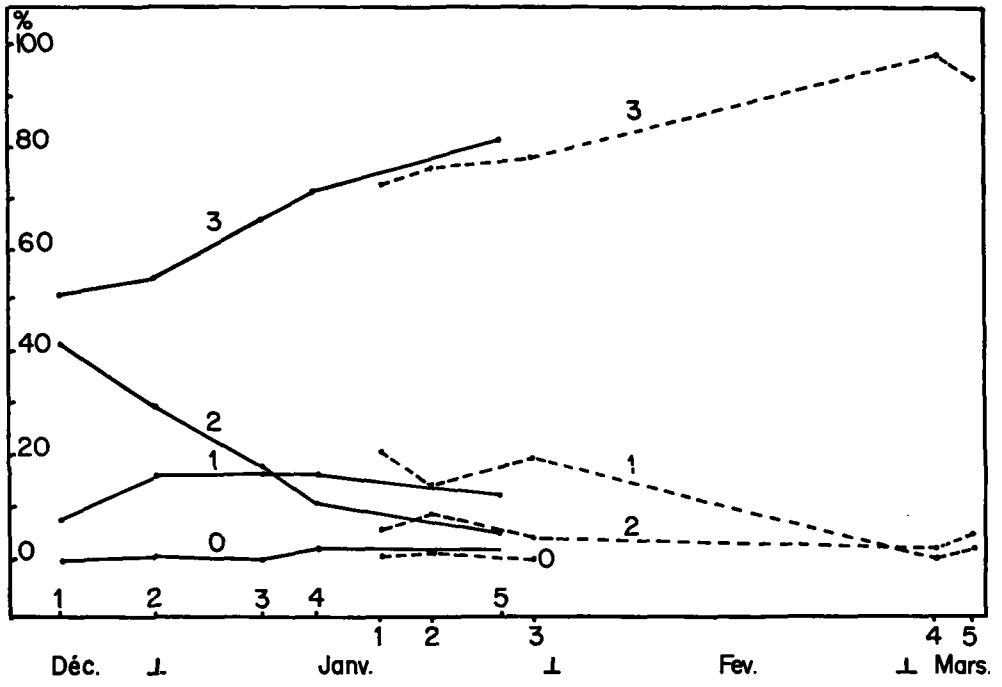

FIG. 5. — *Iles Saint-Paul et Nouvelle Amsterdam. Evolution chronologique du pourcentage de femelles présentant la même pilosité : pourcentage du nombre de femelles de même pilosité par rapport au nombre total des femelles capturées, à chaque période de l'été.*

Les langoustes dont la pilosité est du groupe 0, sont très rarement capturées par le bateau ; ce sont pour la plupart des immatures dont il ne sera pas question dans cette discussion. Le fléchissement observé à la cinquième période, à la Nouvelle Amsterdam, ne correspond pas au début d'une évolution ultérieure, mais à une cause mineure tenant simplement aux conditions de pêche.

A ce stade, deux faits évidents s'imposent : d'une part la réduction du pourcentage des individus de pilosité 2 et 1, qui diminue jusqu'à devenir nul ; d'autre part, l'augmentation relative du pourcentage des individus du stade 3 : l'état 3 incorpore peu à peu toutes les femelles qui y parviennent successivement.

Nous devons nous rappeler ici que le milieu de la période où les femelles ne portent pas d'œufs extérieurs se situe en janvier. Nous ne disposons d'aucun relevé concernant le début de cette période, mais il est très vraisemblable de supposer que le renouvellement des soies a débuté sensiblement avant la fin de décembre.

Les individus à pilosité très fournie 3-II, sont plus fréquents à l'Ile Saint-Paul qu'à la Nouvelle Amsterdam ; nous savons en effet que les grosses langoustes, celles dont les soies sont les plus riches, sont plus nombreuses dans la première des deux îles.

L'hypothèse retenue pour expliquer l'allongement des soies est celle de la mue. D'ailleurs, l'examen des pléopodes épilés montre des soies tronquées, alors que les soies complètes ont une extrémité effilée. Les soies écourtées sont donc remplacées par d'autres, lors de l'exuviation, selon le processus décrit par Drach (1939).

La courbe 3 de la figure 5 est une courbe cumulative. Cette courbe est l'expression additive de la courbe normale de distribution de Gauss. La distribution des date de la mue, responsable du renouvellement des soies, doit être comme la distribution des dates de ponte et d'éclosion dans le cycle sexuel. Le renouvellement des soies correspond donc naturellement, sous sa forme sigmoïde, à la sommation du nombre des mues dans la population.

Avant de conclure, un rapprochement doit être fait.
La richesse des soies d'un animal donné, c'est-à-dire, la longueur absolue de ses soies et leur abondance, est en relation directe avec sa taille. L'on sait par ailleurs depuis Herrick (1895) que la relation entre la fertilité et la taille chez les crustacés est donnée par la formule : $E \times KL^3$. Si d'une part la fertilité est proportionnelle à la taille de la femelle, et si d'autre part la pilosité est liée à cette même taille, la pilosité, autrement dit la capacité à porter les œufs produits, est en rapport avec la fertilité.

Conclusion

L'ensemble des résultats acquis nous permet d'établir le schéma du déroulement du cycle annuel et celui de l'évolution des soies. La femelle immature accède à la maturité qui s'établit à la taille moyenne de 172-173 mm à Saint-Paul et de 167-168 mm à la Nouvelle Amsterdam ; elle acquiert, à ce stade, des soies ovigères. Dès lors son cycle sexuel se déroule comme suit : fécondation puis ponte en mai et juin, incubation des œufs, éclosion des larves en août et septembre (à la Nouvelle Amsterdam), nettoyage actif des pléopodes pour les débarrasser des coques d'œufs vides avec amputation partielle des soies ovigères, mue estivale pouvant intervenir au cours d'une période de 4 à 5 mois, s'achevant en mars et responsable du renouvellement des soies, enfin mue précédant immédiatement la fécondation. Les grosses femelles sont généralement plus précoces que les petites.

Les soies redevenues complètes, de longueur supérieure à deux largeurs de la palette sétigère de l'endopodite, sont plus longues chez les gros individus que chez les petits. La longueur et la densité de la pilosité des pléopodes est en rapport avec la fertilité des femelles.

Références

Boas, J.E.V. 1880. Studier over decapodernes slaegtskasforhold. *Vidensk. Selsk. Skr.*, **1-2** : 23-210.

Bradstock, C.A. 1950. A study on the marine spiny crayfish *Jasus lalandii* (Milne-Edwards), including accounts of autonomy and autospasy. *Zool. Publ. Victoria Univ. Coll.*, **7** : 1-36.

Drach, P. 1939. Mue et cycle d'intermue chez les Crustacés Décapodes. *Ann. Inst. Océanogr. Monaco*, **19** : 103-391.

George, R.W. 1957. Continuous crayfishing tests: Pelsart group, Houtman Abrolhos, Western Australia. (*Palinurus longipes.*). *C.S.I.R.O., Austral., J. Mar. Freshw. Res.*, **8** : 476-490.

Grua, P. 1960. Les langoustes australes *Jasus lalandii*. Biologie, milieu, exploitation commerciale. *T.A.A.F.*, n° 10 : 15-40.

Grua, P. 1963. Maturité, cycle sexuel, soies ovigères des langoustes australes femelles, *Jasus paulensis*, Heller 1863. Etude statistique. *C.N.F.R.A.*, n° 4 : 1-35.

Heller, C. 1861-1862. Vorlaüfiger Bericht über die während der Weltumsegelegung der K. Fregatte Novara gesammelten Crustaceen. *Verhandl. Zool. Bot. Ges.*, **11** : 495-498 ; 12 : 519-528.

Herrick, F.H. 1895. The american Lobster : a study of its habits and development. *Bull. U.S. Fish. Commission*, **15** : 1-52.

Holthuis, L.B. 1946. The Decapoda Macrura of the Snellius Expedition. *Temminckia*, **7** : 1-178.

Holthuis, L.B. 1963. Preliminary descriptions of some new species of Palinuridea (Crustacea, Decapoda, Macrura, Reptantia). *Koninkl. Nederl. Akad. Wetenschappen, Proc.*, Ser. C. **66** : 54-60.

Reprinted from C.R. Acad. Sc. Paris, vol. 259, groupe II, 1964, p. 1541-1543.

OCÉANOGRAPHIE BIOLOGIQUE. — *Sur la structure des peuplements de* Macrocystis pyrifera *(L.) C. Ag. observés en plongée à Kerguelen et Crozet.* Note (*) de M. **Paul Grua**, présentée par M. Roger Heim.

La pénétration en scaphandre autonome dans l'épaisseur de ces herbiers a rendu possibles des précisions écologiques reliées à la transparence des eaux, concernant la configuration verticale, la densité et les limites bathymétriques de la végétation. Des constatations sur la faune sont rapportées.

Les observations ont porté, entre 0 et 15 m d'immersion, sur l'étage infralittoral de terres situées au voisinage de la convergence antarctique dont la localisation semble être à quelques degrés tout au plus au Sud des îles étudiées (1). Après quelques plongées à l'île de la Possession, dans l'archipel de Crozet, les autres se sont déroulées à Kerguelen, dans la baie du Morbihan, vaste espace intérieur s'ouvrant sur une large passe en direction de l'Est. Les eaux fréquentées, au long des rivages côtiers ou autour d'îlots, étaient de transparences diverses; les valeurs relevées au disque de Secchi s'établissaient en moyenne entre 4 et 15 m. La température fraîche (2) de ces eaux varie, pour la couche superficielle, entre les moyennes mensuelles de 2 et 8,5°C, selon les lieux et les saisons.

Les pieds de *Macrocystis*, individualisables par leur bloc de haptères, ne sont pas contigus et laissent entre eux des espaces variables de l'ordre de 0,5 à 1 m. Dans la partie centrale de l'herbier, les stipes issus de chaque pied sont souvent nombreux, de quelques dizaines à plusieurs centaines, s'élevant verticalement en un faisceau serré et plus ou moins tressé sur lui-même. Dans le cas des pieds dont le nombre de stipes est limité à quelques unités, l'espacement entre eux peut être inférieur aux valeurs indiquées ci-dessus. La fixation des haptères, constituant parfois des masses volumineuses, s'effectue sur des faces subhorizontales, le plus souvent surélevées. Les faces horizontales des creux et les faces verticales ne sont pas colonisées, à moins d'être occupées par l'extension des haptères voisins. Le substrat n'est pas nécessairement de la roche en place, la végétation étant possible sur des blocs dont la stabilité est suffisante pour résister à la turbulence des eaux. En eaux calmes, on peut observer comme base des galets isolés, entourés parfois de sédiment, ou des galets rapprochés recouverts par la croissance progressive des haptères. Dans les zones favorables à une végétation puissante, celle-ci subsiste sur des roches pesantes ou fixes.

Dans les eaux peu transparentes, rencontrées le plus souvent, la limite supérieure d'implantation apparaît à 2 ou 3 m de profondeur. Cette fixation peut se faire plus près de la surface, exceptionnellement jusqu'à la ceinture de *Durvillea antarctica* (Cham.) Hariot, soit à la frange inférieure de l'étage littoral. Batham (3), qui a relevé la présence de *Macrocystis* à un niveau homologue dans les stations abritées de Nouvelle-Zélande, explique le fait par la faible turbulence locale, élément directement accessible à

un observateur de surface. Cette relation ne paraît pas généralisable, car elle porte sur un cas particulier de la limite supérieure du peuplement. L'éclairement reçu par le fond se révèle par contre un facteur limitatif essentiel de la distribution verticale (4). Le peuplement disparaît progressivement en s'espaçant aux environs de 12 m de profondeur. Entre ces limites, la végétation est dense, soit que l'espace compris entre les pieds soit réduit, soit que de nombreux pieds comptent une grande quantité de stipes serrés les uns contre les autres, formant alors des sortes de colonnes atteignant 30 cm de diamètre. Des pieds peu prolifiques se répartissent autour de ces fûts, mais cependant ils n'empêchent pas totalement la circulation entre eux. Dans la couche d'eau, d'une épaisseur voisine de 1 m compté au-dessous de la surface, la végétation forme une masse considérable de stipes et de lames dont certaines, enchevêtrées, s'étendent parallèlement à la surface au lieu de pendre obliquement vers le fond. Cela constitue un écran dense que des rais de lumière traversent difficilement par endroit. Il en résulte un espace ombragé au-dessous. Lorsque le couvert est très épais, les stipes ne portent que peu de lames dans leur portion inférieure. Par ailleurs, les lames sont ondulées, rappelant l'aspect des frondes de *Laminaria saccharina*, et cela d'autant plus que les eaux sont plus turbides.

Si l'on considère des eaux plus transparentes, soumises à l'influence du large, la limite supérieure de fixation des pieds a été constatée à 8 m de profondeur. Sur un fond de 15 m, le peuplement se manifeste en pleine puissance et se poursuit au-delà vers la profondeur. Il est connu que les *Macrocystis* se fixent sur des fonds plus importants, et les nombres de 30 ou 40 m sont couramment avancés; nous verrons plus loin ce qu'il faut penser des limites bathymétriques. A la différence de ce qui a été remarqué en eaux peu claires, l'impression générale ressentie dans le corps du peuplement est celle donnée par une forêt plus claire, plus pénétrable à la lumière, et dont le faîte, en surface, reste lâche. La végétation est moins serrée du fait que les pieds peuvent être moins rapprochés et que, d'autre part et surtout, le nombre des stipes issus de chacun d'eux se limite le plus souvent à quelques unités.

Tous les intermédiaires ont été rencontrés, entre les cas schématiques ci-dessus, depuis l'aspect d'une futaie portant sa frondaison au niveau supérieur, ne comptant que des troncs volumineux quoique peu élevés, jusqu'à celui d'un champ de cannes à sucre démesurées, aux pieds peu serrés et au feuillage prospère, en passant par le bois taillis aux plants d'importance inégale et où tous les individus, bien verticaux, atteindraient cependant la couche de surface. Dans les cas extrêmes qui ont été observés, une estimation a donné les valeurs approchées suivantes, par mètre carré de fond situé dans le milieu d'herbiers bien établis : 500 m linéaires de stipes en eaux claires et jusqu'à 3 000 m linéaires de stipes en eaux enrichies de matières organiques (5). Parfois ont été rencontrées des

clairières à peuplement détérioré, avec des pieds dont les stipes restants, après avoir perdu la majorité des lames et des flotteurs pendaient en guirlandes festonnantes entre la surface et le fond. Sur le substrat ne subsistaient par place que les blocs de haptères morts enlacés de stipes affaissés.

Les limites des peuplements imposent les remarques suivantes. Au voisinage de la limite extérieure des bancs, au-dessus des fonds dont le faible éclairement est encore favorable à l'espèce, le peuplement se poursuit en profondeur tandis que la hauteur de la végétation diminue. Le sommet des plants s'éloigne progressivement de la surface, les pieds s'espacent, et, pour chacun d'eux, décroît le nombre de stipes. On ne peut, en conséquence, déterminer l'étendue de l'herbier à *Macrocystis* par l'observation des contours de celui-ci à la surface. D'ailleurs, sous l'effet de courants qui inclinent les stipes, les limites visibles des bancs se rétrécissent. A la limite opposée, du côté des éclairements importants, le peuplement typique ne présente pas un éclaircissement symétrique : la bordure supérieure s'érige en une lisière précise, surgissant du fond jusqu'à la surface.

Un fait inattendu est la rareté de la faune mobile dans cet herbier. Durant une trentaine d'heures passées dans des zones à *Macrocystis*, outre des incursions de manchots *Aptenodytes patagonica* Miller, *Pygoscelis papua* (Forster), et de cormorans *Phalacrocorax verrucosus* Cabanis, une dizaine de poissons ont été vus, encore n'était-ce que sur les marges des bancs. Le nombre généralement faible de poissons vivant dans la Baie n'est peut-être pas étranger à cette pauvreté constatée dans l'herbier; celui-ci n'est pas le milieu d'élection favorable qu'on a pu supposer. Les *Macrocystis* exercent-elles une influence à laquelle seraient sensibles certains vertébrés ? Des extraits analysés de *M. pyrifera* californiennes se sont révélés toxiques pour les souris ([6]). Des invertébrés peuvent se nourrir de cette algue ([7]) tandis que sous leur couvert d'autres viennent chercher abri ([8]) et que des formes sessiles s'y développent en masses considérables. Des mesures de biomasse animale ont donné des valeurs s'élevant jusqu'à 1,5 kg/dm^2; les espèces constituantes, actuellement à l'étude, sont surtout constituées par des synascidies, des moules et des éponges.

Une collection de photographies en couleurs a été faite dans les herbiers.

(*) Séance du 17 août 1964.
([1]) R. Delépine, *C.N.F.R.A.*, 3, 1963, p. 25.
([2]) P. Grua, *Third Intern. Biometeor. Congr.*, Pau, 1963, Pergamon Press, Oxford (sous presse).
([3]) E. J. Batham, *Trans. Roy. Soc. New Zealand*, 84, 1956, p. 447.
([4]) P. Drach, *C. R. Soc. Biogéogr.*, 227, 1949, p. 46.
([5]) Le mètre linéaire utilisé comme unité est le produit du nombre de stipes comptés à 1 m au-dessus du fond, par la longueur moyenne de la végétation au lieu considéré.
([6]) R. C. Habekost, M. F. Ian et W. H. Bruce, *J. Washington Acad. Sc.*, 45, 1955, p. 101.
([7]) W. J. North, *Nature*, 190, 1961, p. 1214.
([8]) P. Grua, *T. A. A. F.*, 10, 1960, p. 15.

(*Station Biologique de Roscoff, Finistère.*)

Reprinted from *Bull. Soc. Phycol. de France*, no. 10, 1964, p. 14.

La végétation infra-littorale de la Baie du Morbihan (Kerguelen)

par R. DELÉPINE et P. GRUA

Dans le cadre de l'étude de la flore algale des îles australes, l'un de nous avait déjà eu l'occasion de présenter ici même des photographies en couleurs sur l'étagement de la végétation littorale. Lors d'une mission d'été en 1962-1963, P. GRUA a réalisé des photographies sous-marines au cours de plongées en scaphandre autonome, pour une étude des peuplements infra-littoraux jamais entreprise ainsi. Il a pu préciser certains points écologiques de cet étage qu'il expose ici au sujet de la végétation. Par ailleurs, des problèmes systématiques sont signalés ; les photographies suivantes illustrent ces points.

Le caractère fondamental de la végétation de l'étage littoral est la ceinture de *Durvillea antarctica*, qui indique la limite inférieure de l'étage médio-littoral. Les photos sous-marines laissent suggérer qu'une deuxième espèce (*D. caepaestipes*) est peut-être présente à Kerguelen et se situerait au sommet de l'étage infra-littoral. L'absence de données certaines sur la base de fixation nécessite d'autres investigations.

Un échantillonnage de la végétation infra-littorale est ensuite montré : Delesseriacées, *Iridaea, Ulva, Acrosiphonia* et diverses *Desmarestia* de caractères écologiques différents. Une espèce de ces dernières peut former une strate caractéristique d'eaux calmes, notamment sous les *Macrocystis* dans des zones où celles-ci sont peu denses.

Les plongées ont permis de retrouver en place, dans l'herbier de *Macrocystis* à 15 mètres de profondeur, à l'Ilot Buchanan, une espèce de *Lessonia* qui n'y avait été localisée que par quelques fragments l'année précédente. Une autre localisation a été découverte à l'Ile du Chat à la même profondeur.

Enfin, la végétation caractéristique de cet étage infra-littoral est formée par *Macrocystis pyrifera*, dont les folioles portées par les grandes lanières flottent à la surface de l'eau, formant ainsi d'immenses herbiers dans la Baie du Morbihan (Kerguelen). Ces herbiers dessinent souvent une ceinture très nette à quelque 10 ou 20 m de l'aplomb des côtes, correspondant à des thalles fixés au substrat à des profondeurs variant de quelques mètres à 25 m environ.

En outre, des prises de vue en 16 mm ont été effectuées ; ce film sur l'écologie infralittorale à Kerguelen, est en préparation.

• Laboratoire de Biologie végétale marine, Paris.
• Station Biologique, Roscoff.

Reprinted from Zoologischer Anzeiger, Bd. 175, Heft 4-6, 1965, S. 371-377.

Aus dem Instituto Oceanografico Cumaná, Venezuela

Ptychodera flava (Enteropneusta) von Tanikely, Madagaskar

Ergebnisse der Österreichischen Indo-Westpazifik-Expedition 1959/60

Teil X

Von

ERNST KIRSTEUER[1]

Mit 4 Abbildungen

(Eingegangen am 5. November 1964)

Das vorliegende Material wurde im Verlaufe der von der „Österreichischen Indo-Westpazifik-Expedition 1959/60" durchgeführten faunistisch-ökologischen Untersuchungen an madagassischen Korallenriffen gesammelt und beschränkt sich auf eine Art, *Ptychodera flava* Eschscholtz 1825. Es ist dies nicht nur die am längsten bekannte und oftmals in der Literatur erscheinende Enteropneusten-Species, sondern nach den gemachten Erfahrungen auch der im Bereich des Indischen Ozeans (und pazifischen Raumes) weitest verbreitete Vertreter der Gruppe (Abb. 1). Wenn nun dieser an sich wohlbekannten Art noch eine weitere Studie gewidmet ist, so möge dies damit begründet sein, daß es sich zum einen um einen für die marine Fauna Madagaskars neuen Repräsentanten handelt, zum anderen aber eine Art zur Rede steht, die nach bisherigen Mitteilungen eine große Vielfalt an anatomisch-morphologischen Abweichungen aufweisen kann, welche ihren Niederschlag in der Beschreibung von nicht weniger als 15 Varietäten fand (PUNNETT [1903] meldet allein sieben Varietäten der Art von den Malediven und Lakkadiven, RAO [1963] fünf weitere von der Insel Krusadai und deren näherer Umgebung) und vereinzelt auch zur Darstellung neuer Arten führten, die erst durch die eingehenden Arbeiten von TREWAVAS (1931) und HORST (1939) als mit *Ptychodera flava* identisch erkannt wurden.

Die Nachricht über einen tiergeographisch neuen Fund sollte demnach einer Wiedergabe der anatomischen Organisationsverhältnisse nicht entbehren. Für letzteres stehen 14 in Bouin fixierte, vollständige und gut erhaltene Individuen zur Verfügung, welche auf der Madagaskar im NW unmittelbar vorgelagerten Insel Tanikely (48°14'9'0, 13°28'9'S) gesammelt wurden. Die Tiere befanden sich unter Steinen an der Oberfläche eines Grobsandbodens in einem durchschnittlich 20 cm tiefen Fluttümpel an der Ostseite der Insel.

Ptychodera flava ESCHSCHOLTZ 1825
Clamydothorax ceylonensis NARAYANARAO 1934
C. krusadiensis ders. 1934
Ptychodera flava HORST 1940

[1] Dr. Ernst Kirsteuer, Museum of Natural History, Department of Living Invertebrates, CENTRAL PARK WEST at 79 St. NEW YORK, N.Y.

P. f. Rao 1952
P. f. ders. 1954
P. f. ders. 1962
(weitere, ältere Literatur siehe bei Horst 1939)

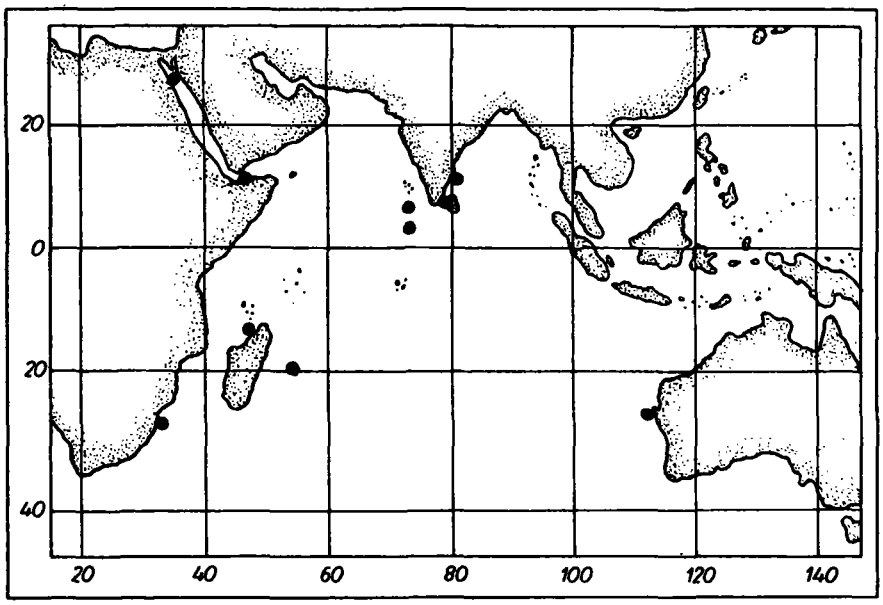

Abb. 1. Übersichtskarte mit den Fundorten von *Ptychodera flava* im Bereich des Indischen Ozeans

Habitus

In der Färbung zeigen die madagassischen Exemplare der Art eine weitgehende Übereinstimmung mit der von Willey (1897) gegebenen Beschreibung. Allerdings ist die Grundfarbe etwas heller, nämlich weißgelb, und intensives Gelb tritt nur an der Eichelspitze und am Vorderrand des Kragens sowie dorsomedian entlang des Rückennervenstranges auf. Die Genitalflügel haben einen schwachen grauen Anflug, offensichtlich durch das Durchschimmern der Gonaden bedingt. Die Lebersäckchen sind größtenteils dunkelbraun, mit fortschreitendem Kleinerwerden der Säckchen gegen das caudale Ende der Leberregion zu wird aber das Braun mehr und mehr von einem gelben Farbton verdrängt. In der Abdominalregion kann der Darm je nach Füllungszustand stellenweise oder durchlaufend grau durchscheinen.

Die lebenden Tiere maßen 40 bis 55 mm in der Länge. Bei einem 50 mm langen Exemplar (Abb. 2) war die Eichel annähernd 5.7 mm lang und 4,5 mm im Durchmesser. In ihrer Form veränderlich, zeigte sie jedoch immer und bei allen beobachteten Tieren einige in der Längsrichtung verlaufende Einbuchtungen, die sich bei der Fixierung noch verstärkten (Abb. 3, a). Der Kragen mit seiner typischen Einengung in der Mitte und der Ringfurche in der Nähe seines Hinterendes hatte eine Länge von 5.5 mm und kam an Dicke der Eichel gleich.

Anschließend an den Kragen und mit diesem verwachsen erstreckten sich über rund 9 mm die ventrolateral vom Körper abgehenden Genitalflügel, welche an ihrer äußeren Oberfläche durch seichte und unregelmäßige Ringkerben etwas gewellt sind. Sie reichen caudal über die 6 mm lange Kiemenregion hinaus und in die etwa 12 mm lange Leberregion hinein. Die größte Breite des Körpers liegt mit ungefähr 5,5 mm in der mittleren Genitalregion. Die Lebersäckchen sind relativ schwach entwickelt und weisen wie bei *Ptychodera flava* var. *saxicola* und *P. f.* var. *gracilis* (PUNNETT 1903) keine Lappenbildungen auf. In der Abdominalregion treten mehr oder minder regelmäßig angeordnete Ringwülste auf, welche dorso- und ventromedian unterbrochen sind. Die oben angeführten Maße zeigen, daß sich die madagassische Form in den Körperproportionen den gleich großen Individuen in dem von TREWAVAS (1931, p. 42) beschriebenen australischen Material stark nähert.

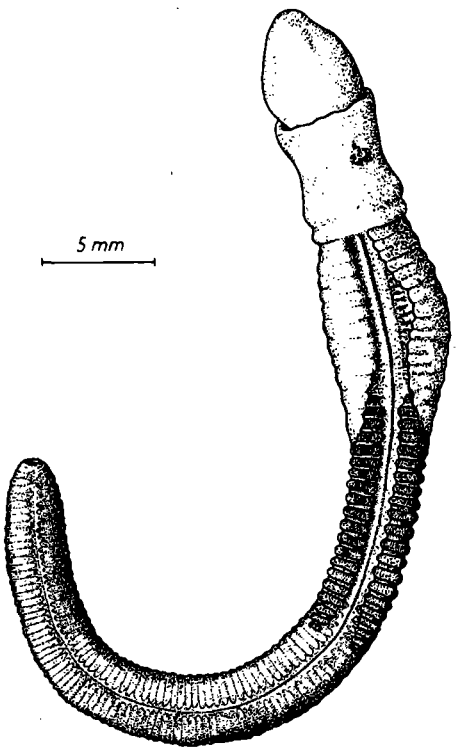

Abb. 2. *Ptychodera flava* von Tanikely. Habitus von dorsal (nach einem lebenden Tier gezeichnet)

Anatomie

Das Epithel der Eichel erreicht durchschnittlich 1/7 der Muskularisdicke und wird von einer kräftigen Nervenschicht unterlagert. Im Bereiche der anschließenden Basalmembran sind an den Querschnitten mehrere Längsgefäße zu beobachten. Wie üblich ist die Ringmuskulatur zart entwickelt und die den Hauptteil der Muskularis stellenden Längsfasern in radiären Bündeln angeordnet (Abb. 3. a). Die inneren Enden der letzteren liegen größtenteils dicht bei-

sammen und in Verbindung mit locker verteilten zirkulären Bindegewebsfibrillen wird damit eine deutliche Begrenzung des Eichelcoeloms geschaffen. Das ventrale Septum reicht weit caudal und obliteriert erst kurz vor dem Hinterende des ventral am Eichelhals auftretenden traubigen Organs, welches im vorliegenden Fall sehr einfach gestaltet ist, anfänglich zwei Lappen zeigt und caudal in einen ungegliederten Sack ausläuft (Abb. 3, b). Von den beiden dorsalen

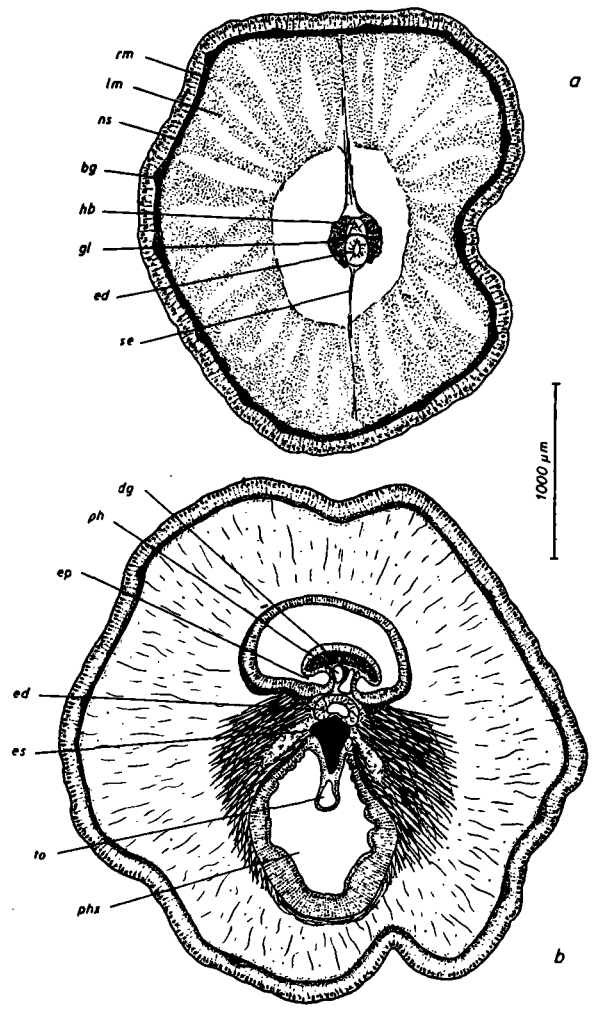

Abb. 3. *Ptychodera flava*. a) Querschnitt durch die Eichel. b) Querschnitt durch die vordere Kragenregion (Erklärung der Abkürzungen s. S. 5)

Coelomtaschen steht die rechte über einen Porus mit der rechten Eichelpforte in Kommunikation, während die Verbindung der linken Tasche zur linken Pforte unterbrochen ist. Die Pforten sind symmetrisch angeordnet und gleich groß (Abb. 3, b). Die verschiedenen innerhalb der Art auftretenden Kombinationsmöglichkeiten von durchlaufenden Coelomporen und Eichelpforten sind bei Willey (1899), Spengel (1903, 1904) und Horst (1930, 1939) ausführlich

behandelt und können an dieser Stelle übergangen werden. Die Herzblase endet terminal ein Stück hinter der Eicheldarmspitze. Die den beiden Organen größtenteils lateral aufliegenden Glomerulushälften vereinigen sich dorsal im vorderen Herzblasenbereich und umhüllen vollständig das Vorderende des Eicheldarms. Letzterer besitzt ein durchgehendes und relativ weit terminal reichendes zentrales Lumen von stark wechselndem Durchmesser, welches in der vorderen Eicheldarmhälfte stellenweise nur einen engen vertikalen Schlitz darstellt. Der größte Durchmesser des Kanals als auch des Eicheldarmes selbst ist an jener Stelle zu beobachten, wo die durch Zusammenfließen der beiden lateroventralen Blindsäcke gebildete ventromediane kurze Tasche mit dem Hauptlumen in Verbindung tritt. Hinsichtlich des Eichelskeletts ist nur zu vermerken, daß der Kiel anfänglich trotz des kleinen traubigen Organs ventral eingebuchtet ist, und zwar so weit als das erwähnte Organ zweilappig in Erscheinung tritt, in der Fortsetzung nach caudal aber dann ventral zugespitzt und im Querschnitt keilförmig ist (Abb. 3, b).

In der Kragenregion zeigt die Epidermis annähernd gleiche Dicke wie an der Eichel. Unterschiedlich ist nur die abwechselnde Folge von Zonen mit weniger Drüsen und solchen wo diese dicht angelagert sind, wobei insgesamt, und wie bisher immer bei *P. flava* beobachtet, fünf Zonen zu unterscheiden sind. Eine äußere Ringmuskulatur fehlt, und eine dünne Längsmuskellage legt sich von innen her der Basalmembran direkt an. Die den Pharynx umschließende Muskulatur ist gut ausgebildet. Das Kragenmark mit seinem durchgehenden Zentralkanal ist zu Beginn im Querschnitt nierenförmig, gegen die Kragenmitte wird es rund, und nur der Kanal behält seine ursprüngliche Querschnittsform, und im caudalen Drittel des Längsverlaufes tritt wieder eine ventrale Einbuchtung des Neurochords auf, und der Kanal zeigt hier einen elliptischen Querschnitt. Bei der vorliegenden Form entsendet das Kragenmark nur eine Dorsalwurzel, deren Kanal auf den proximalen Abschnitt beschränkt ist. Sie liegt etwas links außerhalb der Mediansagittalen und zieht terminal ansteigend zur Epidermis, in die sie eindringt. Die Epidermis zeigt aber an dieser Stelle keine Invagination, wie sie etwa TREWAVAS (1931) bei australischen Individuen der Art vorgefunden hat. Das dorsale Kragenseptum fängt erst etwas hinter der Dorsalwurzel an und erstreckt sich bis an das caudale Kragenende, wobei es im hinteren Teil stark gefaltet ist. Die überwiegend von Längsmuskelfasern durchsetzten Perihaemalräume liegen dem Kragenmark lateral und ventral auf und schließen sich mit ihren medianen Wänden, soweit es das Rückengefäß zuläßt, dicht zusammen. Das ventrale Kragenseptum beginnt ein wenig früher als das dorsale, ist aber unvollständig und reicht nicht bis an die ventrale Kragenwand heran. Besonders am Anfang, d. h. unmittelbar hinter dem Kragenringgefäß ist es sehr kurz und stellt nur eine das Ventralgefäß haltende Falte dar. Die Kragenpforten sind von dorsal her tief eingefaltet und münden in die ersten Kiementaschen.

Die Kiemenregion ist vergleichsweise kurz. Von den beiden durch einen kräftigen Grenzwulst getrennten Darmabschnitten dieses Gebietes ist der Kiemendarm der mit dem größeren Volumen, selbst wenn man berücksichtigt, daß

der nutritive Darm durch Kontraktion etwas eingeengt wurde, wie dies die Faltung seiner Wand anzeigt (Abb. 4, a). Gegen das caudale Ende des Kiemendarms zu steigen die Grenzwülste mit zunehmendem Kürzerwerden der Kiemenspalten mehr und mehr dorsal auf, um letztlich das Darmdach der Postbranchialregion zu bilden. Es entspricht dies vollkommen der von TREWAVAS

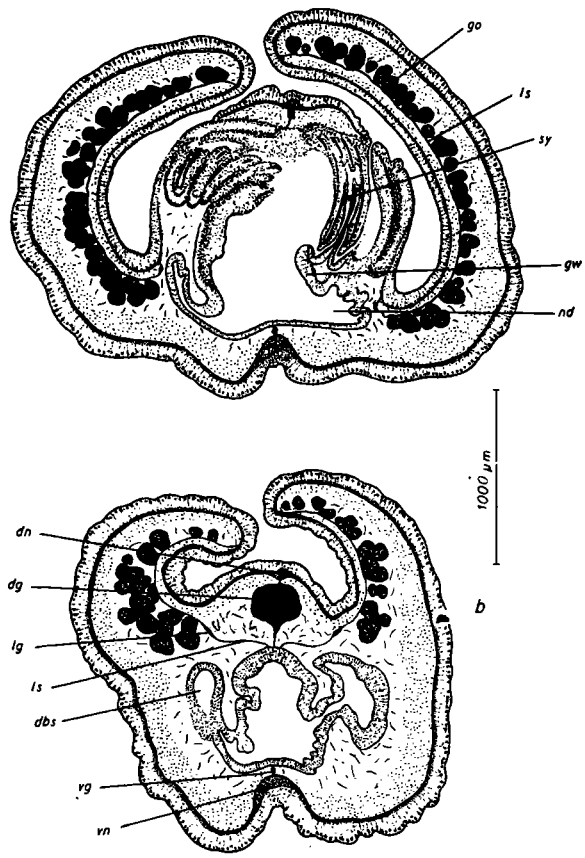

Abb. 4. *Ptychodera flava*. a) Querschnitt durch die Kiemenregion. b) Querschnitt durch die Postbranchialregion im Bereich der Darmblindsäcke (Erklärung der Abkürzungen s. S. 5)

(1931) gegebenen Beschreibung. Die Zahl der vorliegend zu findenden Synaptikel liegt mit maximal sechs Stück an der unteren Grenze des bisher bei *P. flava* Registrierten.

Über die ganze Länge des Kiemengebietes liegt der Abgang der Genitalflügel vom Körper tief ventrolateral (Abb. 4, a), verschiebt sich aber postbranchial rasch dorsal, so daß die caudal auslaufenden Enden der Flügel dorsolateral angeheftet sind (Abb. 4, b). Die Gonaden haben vorliegend noch nicht ihre vollständige Reife erreicht. Sie befinden sich ventral von den die Genitalflügel bis zur Spitze durchziehenden Lateralsepten, es sind jedoch keine Gonoporen ausgebildet. Proximal setzen die Lateralsepten in dem von Kiemenkorb und Genitalflügel begrenzten Winkel an, hinter der Kiemenregion in der Mitte der dor-

salen Darmwand und in der caudalen Genitalregion dorsolateral am Darm. Die in der Postbranchialregion auftretenden lateralen Darmblindsäcke (Abb. 4, b), die durch ihre dorsale Verlötung mit der Darmwand zwei in das Darmlumen caudal hineinreichende Coelomblindsäcke bilden, entsprechen in Form- und Lageverhältnissen ganz der von TREWAVAS (1931, Fig. 2, p. 44) gegebenen Darstellung. Die bei dem zur Diskussion stehenden Material in diesem Abschnitt stellenweise zu beobachtende enorme Erweiterung des dorsalen Gefäßstammes (Abb. 4, b) ist vermutlich kontraktionsbedingt. Die terminal ungefähr gleichzeitig mit der Leberregion beginnenden beiden dorsolateralen Wimperstreifen des Darmes sind verhältnismäßig seicht, die sie medianwärts abdeckende Epithelleiste ist schmal, und es sind keine sehr ausgeprägten, mit den Lebersäckchen alternierenden Vertiefungen der Wimperstreifen gegeben. Was das Pygochord betrifft, so liegen die gleichen Verhältnisse vor wie sie WILLEY (1899, p. 243) beschrieben hat.

Erklärung der Abkürzungen

bg	Blutgefäß	*lm*	Längsmuskulatur
dbs	Darmblindsack	*ls*	Lateralseptum
dg	Dorsalgefäß	*nd*	nutritiver Darm
dn	Dorsalnerv	*ns*	Nervenschicht
ed	Eicheldarm	*ph*	Perihaemalraum
ep	Eichelpforte	*phr*	Pharynx
es	Eichelskelett	*rm*	Ringmuskulatur
gl	Glomerulus	*se*	Eichelseptum
go	Gonaden	*sy*	Synaptikel
gw	Grenzwulst	*to*	traubiges Organ
hb	Herzblase	*vg*	Ventralgefäß
lg	Latralgefäß	*vn*	Ventralnerv

Schrifttum

HORST, C. J. VAN DER: Observations on some Enteropneusta. Papers from Dr. Th. Mortensen's Pacific Expedition 1914—16. Vidensk. Medd. fra Dansk naturh. Foren. 87 (1930) 135—200.

— Hemichordata. In Bronns Klassen und Ordnungen des Tierreichs 4 (1939).

— The Enteropneusta from Inyack Island, Delagoa Bay. Ann. S. Afric. Mus. 32 (1940) 293—380.

NARAYANARAO, C.: Enteropneusta of the Krusadai Island. Curr. Sci. 3 (1934).

PUNNETT, R. C.: The Enteropneusta. In Fauna and Geography of the Maldive and Laccadive Archipelagoes. 2 (1903) 631—680.

RAO, K. P.: Significance of variation in *Ptychodera flava*. Evolution 6 (1952) 342—343.

— Bionomics of *Ptychodera flava* Eschscholtz. J. Madras Univ. 24 (1954).

— Enteropneusta from the east coast of India, with a note on the probable course of distribution of *Ptychodera flava*. Proc. Indian Ac. Sci. 55 (1962) 224—232.

SPENGEL, J. W.: Neue Beiträge zur Kenntnis der Enteropneusten. I. *Ptychodera flava* Eschsch. von Laysan. Zool. Jb. Anat. 18 (1903) 271—326.

— Neue Beiträge zur Kenntnis der Enteropneusten. II. *Ptychodera flava* von Funafuti (Ellice-Gruppe). Zool. Jb. Syst. 20 (1904) 1—18.

TREWAVAS, E.: Enteropneusta. Great Barrier Reef Expedition 1928—29. Sci. Rep. 4 (1931) 39—67.

WILLEY, A.: On *Ptychodera flava* Eschscholtz. Quart. J. Micr. Sci. 40 (1897) 165—183.

— Enteropneusta from the South Pacific, with notes on West Indian Species. Willey, A. Zoological Results, Part 3 (1899) 223—334.

Reprinted from *Boll. Mus. Ist. Biol. Univ. Genova*, vol. XXXIII, 1964-65, no. 199, p. 33-38.

N. DELLA CROCE - L.B. HOLTHUIS *

Istituto di Zoologia della Università di Genova

* Rijksmuseum van Natuurlijke Historie, Leiden

Swarming of *Charybdis (Goniohellenus) edwardsi* Leene & Buitendijk in the Indian Ocean (Crustacea Decapoda, Portunidae)

Swimming crabs of the family Portunidae as a rule are bottom dwelling animals. An exception is the only known species of the genus *Polybius*, *P. henslowi* Leach, which has been observed in large groups (often in hundreds or thousands of specimens) on the surface of the sea at considerable distances from the shore (Clark, 1909, p. 287; Balss, 1955, pp. 1318-1319; Della Croce, 1961, pp. 5-13, where older records are cited).

The pelagic occurrence of this species evidently is a periodic phenomenon; schools appear rather suddendly and disappear equally abruptly. Whether this occurrence is connected with the reproductive cycle, or is caused by the temporary presence of food in the upper layers of the sea (*Polybius* often attacks sardines voraciously and is considered a severe pest by sardine fishermen), is still an open question.

So far as is known to us, this swarming habit has not been observed in other Portunidae. It seems therefore of interest to report here on the observations of such swarms of the Portunid *Charybdis* (*Goniohellenus*) *edwardsi* Leene & Buitendijk, 1949 made in the Indian Ocean during cruise no. 8 of the R./V. « Anton Bruun » of the National Science Foundation, held under the auspices of the U.S. Biological Program for the International Indian Ocean Expedition.

UNESCO

During this expedition swimming crabs were spotted in surface waters on three consecutive days and at three different stations:

Date	Sta.	Lat.	Long.	Temper.	Salinity
1 November 1964	416	09° 45′ S	- 43° 39′ E	25,91°C	35,108°/oo
2 November 1964	417	07° 03′ S	- 42° 34′ E	26,54°C	35,308°/oo
3 November 1964	418	05° 14′ S	- 41° 40′ E	26,30°C	35,393°/oo

The stations were located in the open sea at a distance of not less than 120 miles from the nearest land (in the case of Sta. 416 the nearest land were the Comore Islands, and in that of Sta. 418 the East African coast). The area covered by these stations exceeds 240 miles in length from South to North, and we may therefore assume that the area occupied by these swimming crabs was very extensive. The crabs appeared on 1 November after sunset, between 0700 and 0800 p.m. and were very abundant. Fourteen males and 26 females (none ovigerous) were collected. The size range of the measured males varied from 51 to 65 mm carapace breadth, and that of the females from 48 to 61 mm. On 2 November the crabs appeared again in the evening, but were not so numerous as the day before, while only few specimens were observed, again after sunset, on 3 November.

Examination of the crabs showed them to belong to the species *Charybdis* (*Goniohellenus*) *edwardsi* Leene & Buitendijk, 1949, a species, the correct status of which was only recently ascertained. It was described and figured as early as 1861 by A. Milne Edwards (1861, p. 380, pl. 34, fig. 4) and identified by him as *Goniosoma truncatum* (Fabricius, 1798) (= *Charybdis truncata* (Fabr.)), but Leene & Buitendijk (1949, p. 296, figs. 3, 4 c) showed that A. Milne Edwards's material was different from Fabricius's species and represented an unnamed form for which they proposed the new name *Charybdis edwardsi*. The descriptions and figures provided by A. Milne Edwards and by Leene & Buitendijk agree very well with our specimen, so that we are fully convinced of their identity. Leene & Buitendijk described and figured a male specimen from Malabar, west coast of India, which is now selected to be the lectotype of the species. A. Milne Edwards's material came also from the Malabar coast of India and furthermore from Port Natal (= Durban, Natal, South Africa).

Barnard (1950, p. 818) suggested that the present species should be identical with *Gonioneptunus smithii* (MacLeay, 1838). He based this conclusion on a photograph of the type specimen of *Charybdis smithii* Mac Leay and on information provided on this type specimen by Mr. Melbourne Ward, who was of the opinion that MacLeay's species is identical

Charybdis (*Goniohellenus*) *edwardsi* Leene & Buitendijk, 1949. Female from the R./V. « A. Bruun ». Station 416.

with *Goniosoma truncatum* A. Milne Edwards non Fabr. In our opinion this identification seems rather unlikely, since the type of *Charybdis smithii* is described by Barnard (1950, p. 163) as having « very faint fine granular transverse lines, with patches of granules on cardiac and inner branchial regions », while in our specimens, as well as in the type of *Charybdis edwardsi* the carapace « is absolutely smooth » (Leene & Buitendijk, 1949, p. 296). Though Barnard (1950) in his description of *Gonioneptunus smithii* did not mention the position of the antennule, the fact that he placed the species in the genus *Gonioneptunus* shows that the antennule is not excluded from the orbit. In *Charybdis edwardsi*, however,

the antennule is definitely excluded from the orbit, as is shown by our specimens and clearly indicated by Leene & Buitendijk. It is interesting to note that Leene (1938, p. 16) mentioned that, again at the suggestion of Mr. Melbourne Ward, who had examined MacLeay's type, she considered *Charybdis smithii* MacLeay to be a synonym of *Charybdis* (*Gonioneptunus*) *bimaculata* (Miers), which in our opinion indeed seems far more likely. It is not clear why Leene (1938, p. 126) did not include a reference to *C. smithii* MacLeay, 1836, in her synonymy of *C. bimaculata* (Miers, 1886), and why she did not substitute the former name for the latter, as it has distinct priority.

It is of interest that the smooth and highly polished (though minutely shagreened) carapace of *Charybdis edwardsi* is one of the conspicuous and most characteristic features of this species, which it has in common with *Polybius henslowi* Leach.

So far nothing was known about the biology of *Charybdis edwardsi*. The present observations of its pelagic occurrence in the open ocean, and the fact that it forms swarms, therefore are of special interest.

We may state that the only certain locality, from where the present species has been reported before, is Malabar on the west coast of India. The present records to some degree do extend the known range of the species, which remains restricted to the western Indian Ocean. *C. edwardsi* may possibly also occurs in Natal. It would be interesting to know whether A. Milne Edwards's Durban specimen actually is identical (*) with the present species or that it perhaps belongs to *Gonioneptunus smithii* (MacLeay), so that Ward indeed was correct in identifying MacLeay's type with (part of) A. Milne Edwards's *G. truncatum*. Only the examination of the Durban specimen can solve this problem, while new records from that area would prove a more wide pattern of distribution of the species.

ADDENDUM

We received through the kindness of Dr. Isabella Gordon, British Museum (Natural History), London, the following extract from an entry in the log book of M.V. « Herefordshire » made on a voyage from Colombo towards Aden:

(*) The figure of *Goniosoma truncatum* by A. Milne Edwards (1861) is based on a specimen « des mers de l'Inde », thus evidently on the Malabar specimen mentioned in his text. This figured specimen is unmistakably *Charybdis edwardsi*.

« 21st October, 1963, between 0345 and 0400 G.M.T. in 10° 43′ N, 59° 26′ E. During this time observed a great number of crabs (approximately 1 crab every 15 feet for 4 miles and stretching either side of ship's course as far as could be seen by binoculars) floating on surface. The crabs were dark reddish brown in colour, average size about 5 inches long and 2½ inches wide, they appeared to be lying still until disturbed by bow wave, when they were observed to paddle their legs. Sea temperature 83°, sea smooth, no swell, calm, fine and clear ».

This phenomenon shows a remarkable resemblance to that observed during the cruise of the R./V. « Anton Bruun ». The colour of the animals checks well with that of *Charybdis edwardsi*, while the measurements could pertain to the animal with extended legs, the given width then should be the actual length and viceversa. Unfortunately no specimens were taken by the « Herefordshire », and therefore the identity of the species must remain uncertain. It is interesting to note that this observation resembles those made at the « Anton Bruun » in that it is made (1) in the extreme western part of the Indian Ocean, (2) in the autumn and (3) at night.

LITERATURE

BALSS H., 1955 - *Decapoda*. 10. Lieferung. In: *H.G. Bronn, Klassen und Ordnungen des Tierreichs*. Vol. 5, sect. 1, pt. 7, 10, 1285-1367.

BARNARD K.H., 1950 - Descriptive catalogue of South African Decapod Crustacea. *Ann. S. Afr. Mus.*, 38, 1-837.

CLARK J., 1909 - Notes on Cornish Crustacea. *Zoologist*, S. 4, 13, 281-308.

DELLA CROCE N., 1961 - Considerazioni su *Polybius henslowi* Leach (*Crustacea Brachyura*). *Boll. Mus. Ist. Biol. Univ. Genova*, 31, 5-13.

LEENE J.E., 1938 - Brachygnatha: Portunidae. The Decapoda Brachyura of the Siboga Expedition. *VII. Siboga Exped. Mon.*, 39 (C 3), 1-156.

LEENE J.E., BUITENDIJK A.M., 1949 - Note on *Charybdis ihlei* nov. spec., *Charybdis beauforti* nov. spec., and *Charybdis edwardsi* nom. nov., from the collection of the British Museum (Natural History), London. *Bijdr. Dierk. Amsterdam*, 28, 291-298.

MILNE EDWARDS A., 1861 - Études zoologiques sur les Crustacés récents de la famille des Portuniens. *Arch. Mus. Hist. nat. Paris*, 10, 309-428.

RIASSUNTO

Gli A.A. riportano alcune osservazioni biologiche e sistematiche su *Charybdis edwardsi* raccolto nel corso della crociera n. 8 del R./V. « A. Bruun » in occasione della Spedizione Internazionale nell'Oceano Indiano.

SUMMARY

The A.A. report some biological and systematic observations on *Charybdis edwardsi* collected on cruise no. 8 of the R./V. « A. Bruun » during the International Indian Ocean Expedition.

Reprinted from J. oceanogr. Soc. Japan, vol. 20, no. 6, 1965, p. 10-17.

Further Studies on the Size Distribution of Photosynthesizing Phytoplankton in the Indian Ocean*

Yatsuka SAIJO** and Kaoru TAKESUE***

Abstract: The measurement of the size distribution of photosynthesizing phytoplankton was repeated at 8 stations in the Indian Ocean and one station in the South China Sea. The sample waters were taken from 0, 25 and 75 m depth. After incubating by ^{14}C tank technique, the sample waters were filtered through XX17 net, Millipore HA, AA and SM filter respectively, and the precipitates were counted by windowless G.M. counter. The chlorophyll-a contents of each fraction were also determined after the filtration through the same filters with ^{14}C technique.

Concerning the photosynthetic activity, the results obtained in this cruise were essentially same to those determined in the last cruise. Namely, the photosynthetic activity caught by XX17 net (90 μ pore size) takes only a small part of the total activity and increases with depth, whereas the phytoplankton with the size between 0.8 and 90 μ play the most part of the activity. The smallest size fraction with the size smaller than 0.8 μ has a considerable activity for the surface water, but it decreases with depth.

Though there were no marked differences among the rates of dark fixation of carbon for each fraction of same sample water, the highest rate of dark fixation was generally found in the smallest size. The size fractionation of the chlorophll-a content seems to give a similar inclination with that of photosynthesis. But the details were obscure because of the difficulties of measuring the extreme low concentration of pigments in the tropical water.

The photosynthetic activity by unit amount of chlorophyll-a was the highest in the fraction retained by AA filters, whereas it was the lowest in XX17 net retained samples. The low photosynthetic rates were also found in most of the samples taken from 75 m depth.

1. Introduction

In a previous paper the senior author (SAIJO 1964) reported on the size distribution of photosynthesizing phytoplankton which was measured during the Indian Ocean Expedition from November 1 62 through January 1963. It was found that the activity of organisms retained by XX13 net is only a small part of total activity, whereas the organisms with the size between 0.8 and 110 μ play the essential part of the activity. The smallest size fraction with the size smaller than 0.8 μ has a considerable activity for the surface water, but is negligible for the water from 50 m depth. In the previous study, however some important questions were still remained unanswered, one of which was the relation between the size of each fraction and the rate of dark fixation in tropical waters. It has often observed that the rates of dark fixation in tropical waters are sometimes considerably higher than those obtained in high latitude waters, probably due to the vigorous uptake of carbon by the bacteria in tropical waters. Therefore, the measurement of dark fixation at each fraction will give some explanation for this problem.

Another question was the relation between the size of fraction and the rate of photosynthesis by unit amount of chlorophyll-a. GESSNER (1959) pointed out the fact that the phytoplankton of smaller size give higher photosynthetic activity than the lager phytoplankton in his study of the fresh water lakes. This fact seems to be probable in the tropical waters where the smaller size plankton are dominant.

To have more precise knowledge on these

* Received Sept. 18, 1964

** Water Research Laboratory, Nagoya University
*** Shimonoseki, University of Fisheries

problems the experiments were repeated by the junior author on board "Koyo-maru", the training and research ship of the Shimonoseki, University of Fisheries, during the second cruise of the Indian Ocean Expedition from November 1963 through January 1964.

2. Area studied and method

The experiments were made at 8 stations in the Eastern Indian Ocean and one station in the South China Sea as illustrated in Fig. 1.

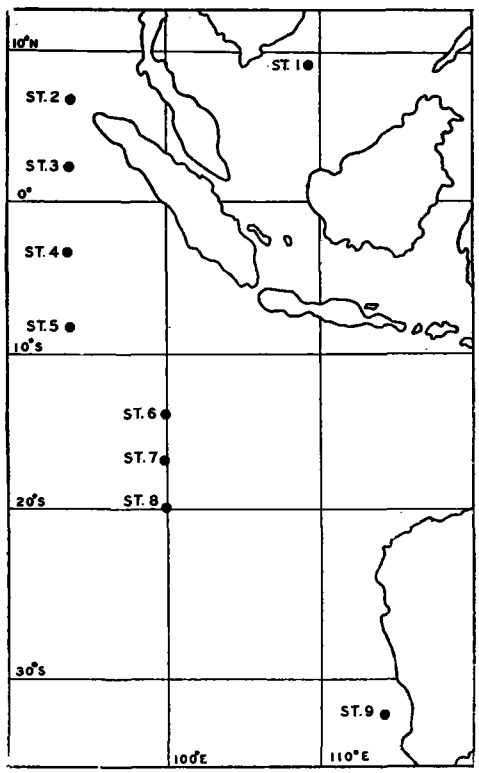

Fig. 1. Location of the sampling stations.

The sample waters were collected with a Van Dorn type twin sampler (12*l* capacity) from the surface, 25 m and 75 m depth at each station. About 50*l* waters were taken from each depth and mixed thoroughly in a big plastic bucket A part of each sample water was poured into four transparent and four darkened bottles of 250 m*l* capacity respectively. After adding 1 m*l* of $Na_2{}^{14}CO_3$ solution (10 μc radioactivity/m*l*) in each bottle, all transparent bottles were incubated in a water tank which was illuminated by six 30W reflecter type fluorescent lamps and kept at surface water temperature by running water. In this tank the bottles received the light intensity of about 15 000 lux. The darkened bottles were immersed in the water of bucket and also kept at same water temperature with the illuminated bottles. After 4 hours incubation, each of four bottles from the same sample water was filtered through Millipore HA, AA, SM type filters and XX17 net (24 mm diameter). The pore size of these filters is 0.45, 0.8, 5.0 and 90 μ respectively. The radioactivity of the precipitate caught on each filter was determined with windowless GM counter.

On the other hand, 40*l* of sample water was filtered through XX17 net of 47 mm diameter, and then the each of 8~8*l* of the filtrate was filtered through Millipore HA, AA and SM type filters (47 mm diameter) separately. The filters were treated by steam about 30 seconds, and kept in a dessicator in the refrigerator. The chlorophyll-a content of the precipitates on each filters was determined by using the RICHARDS and THOMPSON (1952) technique with some modification. The most important point of the modification is the treatment of filtered samples by 10KC sonic oscillation for 5 to 10 min. at the first stage of the extraction by aceton.

3. Results and discussion

(1) Photosynthetic activity

The raw data of GM counting for each size fraction of the samples were summerized in Table 1. The absolute values of photosynthesis were illustrated in Figure 2 as diagram and the relative ratio of the photosynthesis of each size fraction was shown in Table 2, assuming the photosynthetic activity on HA filter is 100%.

As seen from these data, the ratio of photosynthetic activity of each fraction is fairly constant at almost all the stations, even though the absolute value of the total photosynthesis differs considerably from one station to another. Namely, the fraction between 5 and 90 μ was the largest and ranged from 55 to 72% (in the previous study, it was 48~73%) of the total photosynthetic activity and this fraction increas-

Table 1. Raw data of GM counting (c.p.m.). Upper value shows the ^{14}C uptake in light bottle and under value shows that of in dark bottle.

Station	Date	Depth m	Millipore filter			Net XX17 >90 μ
			HA >0.45 μ	AA >0.8 μ	SM >5 μ	
1 9-00′N 109-22′E	Oct. 18 '63	0	161	143	97	5
			15	14	13	0
		25	461	413	310	21
			68	50	17	0
		75	365	339	275	43
			19	16	13	0
2 6-30′N 93-59′E	Oct. 24	0	688	618	393	30
			69	62	36	0
		25	678	614	506	46
			54	34	19	0
		75	451	415	326	44
			50	18	15	0
3 2-00′N 94-00′E	Oct. 27	0	369	329	210	20
			23	20	10	0
		25	359	331	261	25
			17	16	11	0
		75	101	99	89	5
			14	12	10	0
4 3-30′S 94-00′E	Dec. 1	0	333	299	240	13
			13	13	11	0
		25	481	433	305	33
			117	100	61	0
		75	147	141	108	9
			96	90	60	0
5 8-30′S 94-00′E	Dec. 18	0	130	99	76	4
			15	11	5	0
		25	171	155	115	13
			14	13	9	0
		75	259	250	214	14
			21	18	7	2
6 14-00′S 100-00′E	Jan. 4 '64	0	228	199	115	6
			31	27	21	0
		25	283	256	190	5
			34	22	14	0
		75	288	280	230	16
			32	29	15	0
7 17-00′S 100-00′E	Jan. 6	0	122	113	81	3
			33	33	20	0
		25	245	223	161	5
			50	44	31	0
		75	231	125	94	14
			34	31	12	0
8 20-00′S 100-00′E	Jan. 8	0	238	203	134	3
			33	27	17	0
		25	227	207	168	50
			41	33	33	3
		75	209	195	159	32
			42	32	18	5
9 31-56′S 111-40′E	Jan. 19	0	311	260	163	10
			18	15	12	0
		25	282	268	212	3
			21	19	16	0
		75	177	165	132	16
			17	17	16	0

Table 2. Relative rate of photosynthesis of each size fraction.

Station	Depth m	Millipore filter			Net XX17 90 μ	Total
		HA 0.45–0.8 μ	AA 0.8–5 μ	SM 5–90 μ		
1	0	11.4%	31.2%	53.8%	3.6%	100%
	25	7.4	17.9	69.1	5.6	
	75	6.8	18.1	63.0	12.1	
2	0	10.3	32.1	52.8	4.8	100
	25	7.1	15.1	70.9	6.9	
	75	1.1	21.4	66.6	10.9	
3	0	10.9	31.4	52.0	5.7	100
	25	7.8	18.9	65.8	6.5	
	75	1.5	9.3	84.1	5.1	
4	0	10.3	18.2	67.5	4.0	100
	25	8.5	25.1	58.2	8.2	
	75	1.1	6.5	75.1	17.3	
5	0	22.3	15.1	59.3	3.2	100
	25	9.0	22.9	60.0	8.1	
	75	2.5	10.9	81.7	4.9	
6	0	12.8	39.6	44.7	3.4	100
	25	6.0	23.1	68.9	2.0	
	75	1.9	14.1	77.7	6.3	
7	0	9.9	20.7	61.0	3.4	100
	25	8.5	24.8	64.2	2.5	
	75	3.0	12.3	70.5	14.2	
8	0	14.0	28.8	55.6	1.6	100
	25	6.5	21.0	48.1	24.4	
	75	3.0	12.5	68.7	15.8	
9	0	16.2	32.2	48.3	3.3	100
	25	5.0	20.2	73.8	1.0	
	75	7.4	20.0	62.7	9.9	
Average	0	13.2	27.8	55.2	3.8	100
	25	7.4	21.0	64.3	7.3	100
	75	3.2	13.9	72.2	10.7	100

ed obviously with depth. The fraction between 0.8~5.0 μ was 14~28% (in the previous study, 20~30%) of the total activity, and this fraction decreased with depth. Furthermore, the fraction smaller than 0.8 μ was ranged from 3 to 1% (in the previous s udy, 2~19%) of the total activity, and decreased remarkably with depth. The activity of the fraction which was retained by XX17 net and has the size of larger than 90 μ represented only 4 to 11% (in the previous study, 3~5%) of the total activity, and showed marked increase with depth. As understood from these results, the general features of the photosynthetic rate of the each fraction in this cruise coincide surprisingly well with those obtained during the previous cruise, in spite of the difference of studied areas. Furthermore these results are also comparable to those obtained by HOLMES (1958) in the Equatorial Pacific or by YENTSCH and RYTHER (1959) in the Sargasso Sea. On the other hand, considerably high activities in larger size fraction were found by KAWAMURA (1960) in the North Pacific or Bering Sea and by HOLMES and ANDERSON (1963) in Friday Harbor or East Sound.

(2) Fixation of the carbon in dark place

The ratio of the carbon fixation in dark bottle to that of light bottle obtained for each fraction of sample water was summerized in Table 3. As seen from this table, the rate of dark fixation of the carbon was generally ranged from several percent to 20 percent or more of that of light fixation. These values are considerably high compared with those obtained in temperate or high latitude areas, where the rate of dark fixation is usually two or three percent in surface

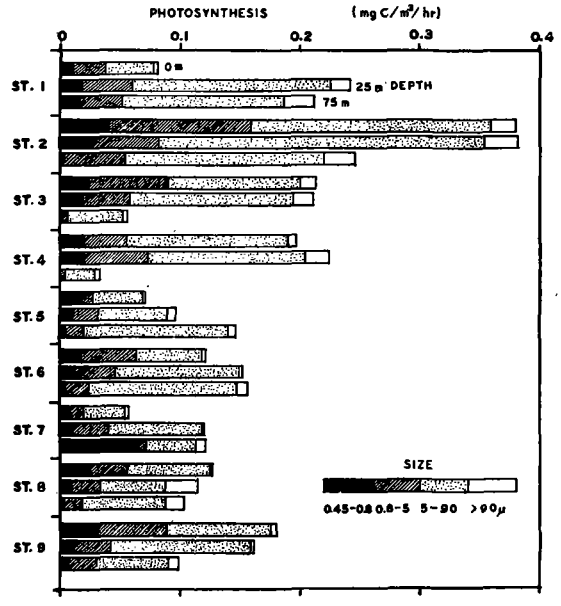

Fig. 2. The photosynthesis of each size fraction.

Table 3. The ratio of the carbon uptake in dark bottle to light bottle for each size fraction.

Station	Depth m	Millipore filter HA 0.45-0.8μ	AA 0.8-5μ	SM 5-90μ	Net XX17 90μ
1	0	9.6%	10.0%	13.7%	0%
	25	14.8	12.1	5.6	0
	75	5.3	4.8	4.8	0
2	0	10.0	10.0	9.2	0
	25	7.9	5.5	3.8	0
	75	11.1	4.3	4.7	0
3	0	6.2	6.1	4.6	0
	25	4.7	4.7	4.1	0
	75	13.6	12.6	11.7	0
4	0	4.0	4.2	4.6	0
	25	24.0	23.2	19.9	0
	75	65.0	64.0	56.0	0
5	0	11.9	10.8	6.6	0
	25	8.4	8.1	7.6	0
	75	8.1	7.1	3.4	0
6	0	13.6	13.4	18.0	0
	25	12.2	8.6	7.3	0
	75	11.1	10.4	6.5	0
7	0	27.3	28.0	24.4	0
	25	20.4	19.7	19.4	0
	75	14.7	24.9	12.8	0
8	0	14.0	13.2	12.9	0
	25	18.1	16.1	19.0	6.8
	75	20.0	16.5	11.0	16.4
9	0	5.8	5.8	7.5	0
	25	7.4	6.9	7.5	0
	75	9.7	10.2	12.5	0

layers as stated by STEEMANN NIELSEN (1960). Such high dark values in tropical waters have been reported in some papers, and believed to be caused by the vigorous bacterial activity in the water of high temerature or by the low photosynthetic activity of the algae due to the deficit of the nutrients.

On the other hand, in our results, the relation between the rate of dark fixation and the size of fraction was not so obvious. However, when we compare the rates of dark fixation for each fraction within a certain sample water, it can be recognized that in most cases the highest rate of dark fixation is obtained in the smallest size fractions except a few stations. This tendency might be came from the activity of bacteria which supposed to be most abundant in the smallest size fraction, but it can be said that even in the Indian Ocean, the influence of the bacterial activity to the size distribution of dark fixation was not so conspicuous as we expected. HOLMES and ANDERSON (1963) could not find any indication that dark uptake by bacteria or other heterotrophic organisms can account the greater amount of activity

Table 4. The chlorophyll-a (mg/m³) content of each fraction which was retained by the different pore size filters.

Station	Depth m	Millipore filter HA >0.45μ	AA >0.8μ	SM >5μ	Net XX17 >90μ
1	0	0.12	0.094	0.073	0.014
	25	0.12	0.076	0.070	0.009
	75	0.25	0.29	0.31	0.014
2	0	0.40	0.13	0.086	0.036
	25	0.13	0.14	0.099	0.014
	75	0.12	0.36	0.27	0.011
3	0	0.073	0.085	0.052	0.005
	25	0.075	0.062	0.059	0.007
	75	0.34	0.28	0.23	0.013
4	0	0.086	0.084	0.047	0.009
	25	0.070	0.077	0.078	0.009
	75	0.27	0.22	0.19	0.077
5	0	0.076	0.062	0.053	0.021
	25	0.085	0.054	0.053	0.009
	75	0.25	0.24	0.025	0.009
6	0	0.069	0.042	0.050	0.009
	25	0.077	0.048	0.039	0.004
	75	0.13	0.096	0.078	0.008
9	0	0.078	0.055	0.038	0.005
	25	0.083	0.090	0.057	0.007
	75	0.089	0.091	0.046	0.005

Table 5. The relative amount of the chlorophyll-a for each fraction which was retained by the different pore size filters, assuming the amount of HA filtered fraction is 100%.

Station	Depth m	Millipore filter HA >0.45μ	AA >0.8μ	SM >5μ	Net XX17 >90μ
1	0	100%	81.8%	63.5%	12.2%
	25		61.8	57.0	7.3
	75		113.5	122.0	5.5
2	0	100	32.0	21.4	9.0
	25		105.2	76.8	8.5
	75		304.0*	226.0*	9.3
3	0	100	106.0	71.3	6.9
	25		82.8	78.8	9.3
	75		83.0	67.1	3.9
4	0	100	97.8	54.7	10.4
	25		110.0	111.2	12.9
	75		81.3	70.2	28.4
5	0	100	81.6	70.0	27.7
	25		63.5	62.4	11.2
	75		99.5	10.2	3.7
6	0	100	61.0	72.5	13.0
	25		62.4	50.7	5.2
	75		73.1	59.5	6.1
9	0	100	71.0	48.8	6.4
	25		109.0	58.6	5.8
	75		102.0	51.5	5.6
Average	0	100	75.9	57.5	12.2
	25	100	85.0	70.8	8.6
	75	100	92.1	63.4	8.9

* Omitted from the average.

retained by the finer porosity filters.

(3) Chlorophyll-a

The results of the chlorophll-a determination were given in Table 4. The total amount of chlorophyll-a which was retained by the different pore size filters were given in Table 5 as the relative value, assuming the amount of HA filtered fraction is 100%. At some samples in these tables the retention by coarser filters exceeded the retention by finer ones as seen at the St. 1, 100 m, St. 2, 25 and 75 m etc., even though there was no such a discrepancy in the results of ^{14}C determination. Such phenomena might be resulted from the difficulties of measuring the very few amount of chlorophyll in the tropical waters. Then, it was impossible to calculate accurately the ratio of each size fraction for all of the samples, though some of which were illustrated as diagram in Fig. 2.

However, these data show that, on the average, the fraction of 5~90μ size takes the largest part of the chlorophyll content in the samples and the value increased with depth. This tendency seems to be similar with that of photosynthetic activity. Also, the fraction, which has larger size than the 90μ, represented the part of smaller than 10%. Other relations were obscure because of the insufficience of the accuracy of the determination.

(4) Photosynthetic activity by unit amount of chlorophyll-a

From the ecological view point, it is interesting to know the relation between the size of phytoplankton and their photosynthetic activity by unit amount of chlorophyll. The rates of photosynthesis by unit amount of chlorophyll at each fraction were given in Table 6. In this table the ratios were calculated from the value of photosynthesis and chlorophyll-a content, not on each size fraction but as the total

Table 6. The rate of photosynthesis by unit amount of chlorophyll-a (mg C/mg Chl.-a/hr.) for each fractions which retained by the different pore size filter.

Station	Depth m	Millipore filter HA >0.45μ	AA >0.8μ	SM >5μ	Net XX17 >90μ
1	0	0.8	0.8	0.7	0.2
	25	2.0	2.9	2.7	1.5
	75	0.8	0.7	0.5	1.9
2	0	0.9	2.7	2.5	0.5
	25	3.0	2.6	3.0	2.0
	75	2.0	0.7	0.7	2.4
3	0	2.9	2.2	2.4	2.4
	25	2.8	3.1	2.6	2.2
	75	0.2	0.2	0.2	0.2
4	0	2.3	2.1	3.0	0.9
	25	3.2	2.7	1.9	2.2
	75	0.1	0.1	0.2	0.7
5	0	0.9	0.9	0.8	0.1
	25	1.1	1.6	1.4	0.9
	75	0.6	0.6	5.1*	0.8
6	0	1.8	2.5	1.1	0.4
	25	2.0	3.0	2.8	0.8
	75	1.2	1.6	1.7	1.2
9	0	2.2	2.7	2.5	1.2
	25	1.9	1.7	2.1	0.3
	75	1.1	1.0	1.5	1.9
Average	0	1.7	2.0	1.9	0.8
	25	2.3	2.5	2.3	1.4
	75	0.9	0.7	0.8	1.3

* Omitted from the average.

amount retained on each pore size filters, *i.e.*, the each value shows the total amount of the part which is larger than the pore size of the filters employed, because of the insufficience of the accuracy of the chlorophyll-a determination in these samples.

Even though detailed discussions are impossible on each value, following facts can be recognized as the tendency of this table.

1) The photosynthetic activity by unit amount of chlorophyll was very low for the fraction of phytoplankton which were retained by XX17 net (90μ pore size). But it is improbable fact that all of the phytoplankton retained by XX17 net are composed of larger size phytoplankton which has low photosynthetic activity, and it seems more plausible that most part of this fraction was formed by the floccuration of phytoplankton which nearly lost their activity. This phenomena might be more conspicuous at the samples taken from deeper layer. In fact, the XX17 fraction from 75m depth showed the lowest activity except St. 6.

2) In general, the photosynthetic activity of the samples from the surface and 25m depth gave rather high values of 2~3mg C/mg chl./hr. except the fraction retained by XX17 net. The highest values were obtained in AA fraction, especially at 25m depth. The somewhat smaller values in HA fraction might be caused by the fact that some part of this fraction were composed of protoplasmic fragments released from fragile cells which ruptured on the filter surface, as stated by HOLMES (1959).

From these results it can be said that as the tendency the phytoplankton of smaller size have higher photosynthetic activity than those of larger fractions, even though the difference is not so much. Here, it is noteworthy that these comparisons were made not among the values at each size fraction but among the total values retained on each pore size filter. Therefore, real differences of photosynthetic rate among each size fraction might be considrably higher than those given in this table.

These results coincide fairly well with those obtained by GESSNER (1959) in a fresh water lake. In some japanese lakes SAKAMOTO and SAIJO (unpublished) also found similar tendency in the relation between the size of fraction and the photosynthetic rate by unit amount of chlorophyll, *i.e.*, the higher photosynthetic rates were found in smaller size fraction.

4. Conclusion

From the results described above, it can be concluded as follows:

(1) The general features of the photosynthetic rate of the each size fraction in this cruise coincide very well with those obtained during the previous cruise. Namely, the activity of the organisms retained by XX17 net represents only small part of the total activity, on the other hand, the organisms having the size between 5 and 90μ play the largest part (55~72%) of the activity. The activity of the organisms in larger fractions increased with depth, whereas that of the smaller fractions shown inverse relation to the depth.

(2) Though there were no marked difference of the rate of dark fixation among the organisms in each fraction from the same sample, at most of the stations, the highest rate of dark fixation was found in the smallest size fraction.

(3) The size fraction of the chlorophyll-a content seems to give a similar inclination with that of photosynthesis, though it was not so clear as the case of photosynthesis, probably due to the difficulties of determinating such a low concentration of pigments in the tropical waters.

(4) The photosynthetic activity by unit amount of chlorophyll-a was the highest in the fraction which was retained by AA filter (0.8μ pore size), while the value was the lowest in XX17 net filtered samples. The low photosynthetic activity was also found in most of the 75m sample waters.

Now, it can be expected that the studies on the size distribution of phytoplankton will give an important basis for the explanation of the geographical and seasonal variation of primary production in the oceans. From this view point, we should begin our future studies from the accumlation of the data in this direction, because our present knowledge concerned is quite limited to the resticted space and time.

Acknowledgements

The cooperation given by Captain G. SAKURAI of "Koyo-maru", his officers and crew, is greatefully acknowledged.

References

GESSNER, F. (1959): Hydrobotanik, II Stoffhaushalt, Berlin, 619–621.

HOLMES, R. W. (1958): Size fractionation of photosynthesizing phytoplankton. Special Scientific Report-Fisheries, No. 279, 69–71.

HOLMES, R. W. and C. G. ANDERSON (1963): Size fractionation of ^{14}C-labelled natural phytoplankton communities. Symposium on marine microbiology, Charles C. Thomas Pub., Springfield.

KAWAMURA, T. (1960): The "Oshoro Maru" Cruise 46 to the Bering Sea and North Pacific in June-August 1960, 11. Data Rec. Oceanogr. Obs. Exp. Fish. Hokkaido Univ., No. 5, 142–165.

SAIJO, Y. (1964): Size distribution of photosynthesizing phytoplankton in the Indian Ocean. Jour. Oceanogr. Soc. Japan, **19**, 187–189.

STEEMANN NIELSEN, E. (1960): Dark fixation of CO_2 and measurements of organic productivity. With remarks on chemo-synthesis. Physiological Plantarum, **13**, 348–357.

YENTSCH, C. S. and J. H. RYTHER (1959): Relative significance of the net phytoplankton and nanoplankton in the waters of Vineyard Sound. Jour. Cons. Int. Explor. Mer, **24** (2), 231–238.

Reprinted from *Bull. fish. res. Stn., Ceylon*, vol. 17, no. 2, 1964, p. 159-168.

Some Planktonic Diatoms from the Indian Ocean

By

M. Durairatnam

(*Fisheries Research Station, Colombo 3, Ceylon*)

Introduction

Collections of phytoplankton were made by me at various stations between latitude 5°S and 25°S and longitude 78° E and 101° E (Fig. 1) from December 1962 to January 1963 during a cruise of the research vessel " Umitaka Maru " belonging to the Tokyo University of Fisheries. This vessel was engaged in work in connection with the I. I. O. E. The collections made by me from these stations were examined at the Fisheries Research Station, Colombo, for the various diatoms present and the findings are reported in this paper.

Some Stations covered by Umitaka Maru in connection with I.I.O.E.

29.12.62	Station 11	Latitude 4°–57′.2″S	Longitude 78°–49′.6″E
30.12.62	Station 12	Latitude 7°.05′.0″S	Longitude 78°–04′.0″E
31.12.62	Station 13	Latitude 8°–52′.4″S	Longitude 78°–03′.0″E
2. 1.63	Station 15	Latitude 12°–55′.9″S	Longitude 78°–02′.2″E
3. 1.63	Station 16	Latitude 15°–10′.6″S	Longitude 78°–03′.8″E

Some Stations where experimental tuna fishing was carried out from the Umitaka Maru

13. 1.62	Station 1	Latitude 12°–46′S	Longitude 97°–19′E
15. 1.63	Station 2	Latitude 10°–10′.8″S	Longitude 98°–41″E
16. 1.63	Station 3	Latitude 8°–15′.2″S	Longitude 100°–04′.6″E

Stations covered in connection with the International Indian Ocean Expedition will be referred to as I. I. O. E; Stations covered for experimental tuna fishing will be referred to as T. G.

Material and Method

Horizontal hauls were made at Stations 11–16 with the following nets :—

(1) Pocket high-speed sampler, 4·5 cm. dia., 30 cm. long metal cylinder, 2 cm. dia. mouth opening with Japanese standard net No. XX 13.
(2) Marutoku net, 45 cm. diameter mouth ring, 90 cm. long with Japanese standard net No. XX 13.

Vertical hauls were made at Stations 1–3 with a Hart closing net, 25 cm. dia. mouth ring, 30 cm. diameter trunk ring ; Japanese standard net No. XX 13.

The plankton collected was poured into a plankton concentration net and transferred into glass bottles, preserved in 10% formalin and examined in the laboratory.

Bacillariophyceae

Order : Centrales
Sub-order : Discoideae
Family : Coscinodisceae
Genus : *Melosira* Agardh

Melosira sulcata (Ehrenberg) Kuetzing

Cupp 1943, p. 40, fig. 2, *Orthosira marina* Smith 1856, p. 59, pl. 53, fig. 338, *Paralia sulcata* (Ehrenberg) Gran 1908, p. 14, fig. 5, Lebour 1930, p. 28, fig. 9.

Cells were found in long chains. Cells disc shaped thick walled 20–28 μ in diameter. Valves concave, areolate and punctate. Margin of valve with double rows of cells. Chromatophores numerous and disc shaped.

Station : T. G. 1, 2, 3.

Geographic distribution : Arctic Ocean, Indian Ocean, Atlantic and Pacific coasts of America, West Coast of France, Northern seas, Mediterranean Sea, Java Sea, Skaggerak.

Sub-family Sceletonemineae

Genus *Skeletonema* Greville

Skeletonema costatum (Greville) Cleve

Cleve 1878, p. 18, Lebour 1930, p. 311, fig. 149, Cupp 1943, p. 43, fig. 6.

Melosira costata Greville 1866, p. 77, pl. 8, figs. 3–6.

These were found in long straight chains, cells lens-shaped or cylindrical with rounded ends. Cells separated from each other by a long space and connected by straight marginal spines. Chromatophores two, plate like, sometimes dissected. Diameter of cells 12–18 μ. Auxospores were observed.

Station : T.G. 1, 2, 3.

Geographic distribution : Generally neritic and widely distributed, Indian Ocean, English coasts, Baltic Sea, Arctic Sea, and Java Sea.

Genus *Thalassiosira* Cleve

Thalassiosira decipiens (Grunow) Jorgenson

Hustedt 1864, p. 322, fig. 158. Cupp. 1943, p. 48, fig. 10.

Coscinodiscus decipiens Grunow 1899, p. 532, pl. 34, fig. 905.

Cells disc-shaped, united in loose chains with long spaces between cells. Valves with minute spines along the border ; diameter 18 μ. Areolae in the valves larger in the centre than towards the periphery. Chromatophores small and numerous.

Station : T. G. 1, 2, 3.

Geographic distribution : Europe, Indian Ocean, Mediteranean Sea, Aral Sea, Caspian Sea.

Sub-family Coscinodiscineae

Genus *Coscinodiscus* Ehrenberg

Conscinodiscus lineatus Grunow

Cupp. 1943, p. 53, fig. 15.

Cells disc-shaped 34–36 μ in diameter. Valve surface areolated. Areolae arranged in straight lines, those at the centre larger than those at the periphery. Valve margin radially striated, striae 12 in 10 μ ; marginal spinulae strong.

Station T.G. 1, 2.

Geographic distribution : Europe, Indian Ocean, Pacific coast of America, Campechi Bay, Florida, Vera Cruz, Java.

Coscinodiscus centralis Ehrenberg

Lebour 1930, p. 39, fig. 16 a–b, 17b, 18b., Cupp. 1943, p. 60, fig. 24.

Disc-shaped cells of 162 μ diameter. Valves with distinct rosette at the centre. Areolae 4 in 10 μ near centre, 4–5 midway to margin and 5–6 near the margin. Valve margin radially striated, 6–8 striae in 10 μ.

Station : I. I. O. E. 15.

Geographic distribution : North Atlantic Ocean, Mediterranean Sea, Gulf of California, Florida, Algeria.

Coscinodiscus marginatus Ehrenberg

De Toni, 1891–94, p. 1241, Allen and Cupp. 1935, p. 115, fig. 7, Cupp. 1943, 55, fig. 19; plate 1, fig. 3.

Cells with flat valves, diameter 35–128 μ. Valves with areolae 3 in 10 μ at centre becoming smaller towards margin, 5 in 10 μ. Central rosette absent. Border of valve striated.

Station : T. G. 2, 3.

Geographic distribution : Sumatra, Indian Ocean, Singapore, Antarctic, Ceylon, Arabian Sea and in all oceans.

Genus *Planktoniella* Schutt

Planktoniella sol (Wallich) Schutt

Lebour 1930, p. 50, pl. 1, fig. 5, Cupp. 1943, p. 63.

Coscinodiscus sol Wallich, 1860, p. 38, figs. 1–2.

Cells disc-shaped ; diameter of central disc 45 μ with wing 120 μ.

Valve surface areolated ; areolae 5–7 in 10 μ at the centre of valve, 7-8 in the middle and 8–9 in the margin, wing like expansions present on cell margin.

Station : T. G. 1, 2, 3.

Geographic distribution : Widely distributed, common in sub-tropical and tropical seas. Red Sea, Gulf of Aden, Arabian Sea, Indian Ocean, Antarctic, Arafura Sea. In Europe only in the Mediterranean region.

Genus *Asteromphalus* Ehrenberg

Asteromphalus wyvillei Castracane

Castracane 1876, p. 134, Pl. 5, fig. 6.

Cells round ; diameter 72 μ, with numerous small disc-shaped chromotophores. Segments wedge-shaped, areolated.

Station : T. G. 1, 2, 3.

Geographic distribution : Indian Ocean.

Asteromphalus flabellatus (Brebisson) Greville

Greville, 1859, p. 160, pl. 7, figs. 4, 5, 1891–94, De Toni, p. 1414.

Cells convex, valves sub-elliptical ; long axis 55–60 μ, short axis 40–52 μ. Compartments finely reticulated. Median ray straight or slightly curved. Border segments areolated.

Station : T. G. 1, 2, 3.

Geographic distribution : Mediterranean Sea, Campeche Bay, Java Sea, Peruvian guano, North Sea, Indian Ocean.

Genus *Gossleriella* Schutt

Gossleriella tropica Schutt

Schutt 1893, p. 20 ; Subrahmanyan 1946, p. 107, fig. 86.

Cells disciform, valves orbicular, diameter 180 to 190 μ. Valve border with a ring of hairs of equal length but of unequal thickness. Chromatophores numerous and disc-shaped.

Station : I. I. O. E. 11; T. G. 1, 2, 3.

Geographic distribution : Mediterranean Sea, Indian Ocean.

Genus *Actinocyclus* Ehrenberg

Actinocyclus ehrenbergii Ralfs

Pritchard 1861, p. 834 ; De Toni 1891–94, p. 1177 ; Lebour 1930, p. 53 ; Subrahmanyan 1946 p. 109, figs. 82–92 and 96, *Eupodiscus crassus* Smith 1853, p. 24, Pl. IV, fig. 41.

Cells disc-shaped, slightly convex 54 μ in diameter. Valve circular, pseudo-nodule very large, sub-marginal. Central area with scattered areolae. Valve magin finely striated.

Station : T. G. 1, 2, 3.

Geographic distribution : Atlantic and Pacific Coasts of America, North Sea, Norwegian and Danish Seas, Gulf of Finland Gulf of Bothnia, Baltic, Skaggerak, Aral and Caspian Seas, Black Sea, North Atlantic, Mediterranean, Peruvian guano.

Sub-order : Solenoideae

Family : Solenieae

Sub-family : Lauderiineae

Genus : *Corethron* Castracane

Corethron hystrix Hensen

Hustedt 1930, p. 547, fig. 311 ; Cupp. 1943, p. 70. *Corethron criophylum* Castracane 1886, p. 85, pl. 21, figs. 12, 14 and 15 ; Lebour 1930, p. 80, fig. 24.

Cells with cylindrical mantle and valves arched hemispherically. Diameter 52 μ. Valve margin with a crown of slender spines. Spines of both valves pointed in the same direction. Chromatophores numerous, small and disc-shaped.

Station : T. G. 1, 3.

Geographic distribution : Atlantic Ocean, Java Sea, Vancouver, California.

Sub-family Rhizosoleniinae

Genera : *Rhizosolenia* Ehrenberg

Rhizosolenia setigera Brightwell

Brightwell 1858, p. 95, pl. 5, fig. 7, De Toni, 1891–94, p. 827, Lebour 1930, p. 98, fig. 70, Hustedt 1930, p. 588, fig. 336, Cupp. 1943, p. 88, fig. 40.

Cells cylindrical, diameter 38 μ, length 512 μ, valves conical, slightly oblique. Apical process hollow for some distance and ending in a long spine. Chromatophores numerous, small and ellipsoidal.

Station : T. G. 1, 2.

Geographic distribution : California, Vancouver, Java Sea, European Seas, Bay of Fundy.

Rhizosolenia robusta Norman

Norman 1861, p. 866, pl. 8, fig. 42, Lebour 1930, p. 94, fig. 68, Cupp. 1943, p. 83, fig. 46.

Cells cylindrical, valves convex or conical curved, 52-258 μ in diameter cells crescent-shaped or S-shaped. Intercalary bands robust, collar shaped. Cell wall thin, membrane delicately punctuated, puncta in three lines self crossing system. Numerous chromatophores lying along the wall.

Station : T. G. 2.

Geographic distribution : European Seas, Pacific Coast of America.

Rhizosolenia alata Brightwell

Brightwell 1858, p. 96, pl. 5, fig. 8, Lebour 1930, p. 88, fig. 60 ; Allen and Cupp 1935, p. 131, fig. 43 ; Cupp 1943, p. 90, fig. 52A.

Cells rod shaped, cylindrical, 7–24 μ in diameter and 658–980 μ in length. Valves conical ending in tube-like or curved oblique process. Depression at the base of tube into which the apical process of adjoining cell fits. Intercalary bands scalelike rhombic in two dorsiventral rows. Cell wall thin and finely striated. Chromatophores small and numerous.

Station : I. I. O. E. 11, 12, 13, 16.

Geographic distribution : Java Sea, Indian Ocean, Red Sea, Gulf of Aden, Arabia, Malaya, Antarctic, Madras, Boston Strait, America.

Rhizosolenia alata Brightwell forma *gracillima* (Cleve) Grunow

Allen and Cupp 1935, p. 131, fig. 44 ; Cupp 1943, p. 92, fig. 52B ; Subrahmanyan 1946, p. 121

Cells rod-shaped, straight 4–7 μ in diameter.

Station : T. G. 1, 2.

Geographic distribution : Coastal form found in most, usually northern, seas.

Rhizosolenia alata Brightwell forma *indica* (Peragallo) Ostenfeld

Allen and Cupp 1935, p. 131, fig. 45 ; Cupp 1943, p. 93.

Cells much broader than the type 15–110 μ. Calyptrae suddenly attenuated due to the greater diameter of cell. Process very strikingly curved. Cell wall finely punctuated, puncta in quincunx.. rows short and irregular.

Station : T. G. 1, 2, 3.

Geographic distribution : In all warm seas, California.

Rhizosolenia styliformis Brightwell

Brightwell 1858, p. 95, Pl. 5, fig. 5d ; De Toni, 1891–94, p. 826 ; Hustedt 1930, p. 584, fig 335 ; Cupp. 1943, p. 87, fig. 46.

Cells cylindrical, diameter 54 μ and length 484 μ, valves obliquely pointed. Apical process long and hollow. Wing not distinct. Intercalary bands scale like in two rows, punctuate. Chromatophores round, small, and numerous.

Station : I. I. O. E. 12, 13, 16 ; T. G. 2, 3.

Geographic distribution : European seas, Vancouver, California, West Indies, Antarctic, coast of Barbardos, Java Sea.

Sub-order : Biddulphioideae
Family : Chaetocereae

Chaetoceros pervianus Brightwell

1856, p. 107, pl. 7, figs. 16–18 ; Allen and Cupp 1935, p. 137, fig. 57, Cupp 1943, p. 113.

Cells usually single, sometimes forming short chains 15–35 μ broad. Valves dissimilar, the upper rounded, the lower flat. Both with well developed valve mantles. Setae of upper valve originate near the centre, turn sharply and runs backwards in wide outwardly convex curves. Setae of lower valve originate near the margin, curve outwards and run parallel to the pervalvar axis. Setae strong, four sided, 3–5 μ thick with strong spines ; striated 19–25 in 10 μ. Chromatophores numerous, small and disc-shaped, present in setae as well.

Station : I. I. O. E. 16 ; T. G. 2, 3.

Geographic distribution : Atlantic and Pacific Oceans, Java Sea, Peruvian guano, Mediterranean Sea, widely distributed in warmer seas.

Chaetoceros didymus var. *protuberans* (Lauder) Gran and Yendo

Allen and Cupp 1935, p. 139, fig. 62 ; Cupp 1943, p. 121 ; *Chaetoceros protuberans* Lauder, 1864, pl. 8, fig. 11.

Cells forming straight chains 15–36 μ wide with concave surface and with semicircular knob in the middle. Setae arising from the corners of the adjacent cells crossing at the base or further out. Terminal setae mostly thicker than others and strongly divergent. Chromatophores two in each cell pressed against the valve with a pyrenoid located in the protuberance.

Station : T. G. 2, 3.

Geographic distribution : Mediterranean, warmer seas, California, Arctic and Atlantic Oceans Peruvian guano, Europe.

Chaetoceros affinis Lauder

Lauder 1864, p. 78, pl. 8, fig. 5, Lebour 1930, p. 135, fig. 99 ; Allen and Cupp 1935, p. 140, fig. 66 ; Cupp 1943, p. 125.

Chains straight, 6–25 μ wide, apertures lanceolate and constricted in the middle. Cells oblong in broad girdle view. Setae delicate, terminal setae strongly divergent with spirally arranged spines; chromatophores one in each cell lying on broad side of girdle with single pyrenoid.

Station : T. G. 1, 2, 3.

Geographic distribution : Common in all seas.

Chaetoceros diversus Cleve

Cleve 1873, p. 9, pl. 11, fig. 12; Allen and Cupp 1935, p. 142, fig. 71 ; Cupp 1943, p. 132, fig. 87.

Short straight chains 10–12 μ broad. Valves flat or slightly raised at the centre. Apical axis 5–12 μ long. Apertures very small. Setae arise from 4 corners of cell. Setae thick, tubular and spinous, more or less curved or straight turning towards chain ends. Terminal setae thin and hair-like. Chromatophores are in each cell on girdle side.

Station : T. G. 1, 2, 3.

Geographic distribution : Tropical and sub-tropical, North Sea, Mediterranean.

Chaetoceros coarctatus Lauder

Lauder 1864, p. 79, pl. 8, fig. 8 ; Lebour 1930, p. 119, Allen and Cupp 1935, p. 135, fig. 52 ; Cupp 1943, p. 107, fig. 62.

Cells cylindrical, elliptical in valve view. Apical axis 30–48 μ. in length. Cells united to form chains robust in appearance. Mantle with clear ring like furrow. Valve surface flat. Posterior

terminal setae shorter than others, strongly curved and heavily spined. Anterior terminal setae less robust, curved backwards and sparsely spined. Inner setae resembling the anterior ones. Chromatophores numerous and disc-shaped.

Station : I. I. O. E. No. 15.

Geographic distribution : Tropical and sub-tropical seas, Mediterranean Sea.

Family Biddulphieae
Sub-family Eucampineae
Genus *Eucampia* Ehrenberg
Eucampia zodiacus Ehrenberg

Ehrenberg 1840, p. 71, pl. 4. fig. 8. ; Lebour 1930, p. 187, fig. 147 ; Allen and Cupp, 1935, p. 143 ; Cupp 1943, p. 145, fig. 103.

Eucampia britannica, W. Smith 1856, p. 25, pl. 71, fig. 378 ; *Eucampia groenlandica*, Cleve 1896, p. 10, pl. 2, fig. 10.

Cells flattened, linear united in chains by two blunt processes. Chains spirally curved. Valves in surface view elliptical. Apical axis 20–60 μ. Apertures of variable size. Punctae 16–20 in 10 μ. Chromatophores numerous, small and highly refractive.

Station : T. G. 1, 2, 3.

Geographic distribution : North Sea, Skaggerak, Baltic Sea, English Channel, Mediterranean, North Atlantic, California, Europe, Belgian Coast.

Genus *Climacodium* Grunow
Climacodium frauenfeldianum Grunow

Grunow 1867, p. 102, pl. 1a, fig. 24 ; De Toni 1891–94, p. 986 ; Lebour 1930, p. 189, fig. 149a Allen and Cupp, 1935, p. 144, fig. 76 ; Cupp 1943, p. 147, fig. 10J.

Cells flat, forming ribbon-like chains. Length of apical axis 70–158 μ, pervalvar axis 12–20 μ. In valve view cells are linear-elliptical. Apertures large, oblong or almost at right angles and wider than the cell in pervalvar direction.

Station : I. I. O. E. 11, 13 ; T. G. 1, 3.

Geographic distribution : Mediterranean, Red Sea, California, Central America.

Order : Pennales
Sub-order : Araphidineae
Family : Fragilarioideae
Sub-family : Fragilarieae, Fragilariinae

Genus *Fragilariae* Lyngbye
Fragilaria oceanica Cleve

Cleve 1873, p. 22, pl. 4, fig. 25 ; Lebour 1930, p. 193, fig. 153.

Fragilaria arctica Grunow, Cleve and Grunow, p. 110, pl. 7, fig. 124.

Cells in girdle view rectangular, forming compact ribbon-like chains ; valves lanceolate or elliptical, with rounded ends 12–30 μ in length and 7–8 μ broad. Pseudoraphi, narrow and linear.

Station : T. G. 1.

Geographic distribution : Norway, Denmark, Russia, Davis Strait, England and Gulf of Maine.

Genus *Synedra*

Synedra formosa Hantzsch

Hustedt 1931–32, p. 233, fig. 720 ; Subrahmanyan 1946, p. 167, figs. 342, 343 and 348.

Ardissonia formosa (Hantzsch), De Toni 1891–94, p. 675.

Valves linear with rounded ends, 135–300 μ long, 18–21 μ broad. Cell wall porous, valves with three longitudinal ribs. Outer membrane areolate punctate. Double series of areolae lie between two ribs.

Station : T. G. 1.

Geographic distribution : Honduras, Vera Cruz, East Indian Archipelago, Europe.

Genus *Thallassiothrix* Cleve and Grunow

Thallassiothrix longissima Cleve and Grunow

Cleve and Grunow 1880, p. 108 ; De Toni 1891–94, p. 672 ; Lebour 1930, p. 199, fig. 159 ; Cupp 1943, p. 184, fig. 134.

Cells four sided, long and threadlike often more or less curved. Valves narrow and linear, ends slightly narrowed more in one end than the other. Length 0·5 to 4 mm. width 2·5–6 μ. Delicate spines present in the corner of the valves, more towards the centre than towards the ends or absent.

Station : I. I. O. E. 12, 13, 15 ; T. G. 1, 2, 3.

Geographic distribution : North Atlantic, Arctic Sea, Scotland, Belgium, Russia, Sweden, Norway, Germany, California and Antarctic, Denmark, Mediterranean.

Genus *Pleurosigma* W. Smith

Pleurosigma angulatum (Quekett) W. Smith

var *strigosa* (W. Smith) Van Heurck

Van Heurck 1899, p. 251, pl. 6, fig. 261 ; De Toni 1891–94, p. 233, Allen and Cupp 1935, p. 158, fig. 108 ; *Pleurosigma* " *strigosum* " W. Smith, p. 7, pl. 1, fig. 6.

Valves lanceolate, slightly sigmoid, 110 μ long and 15 μ broad, raphe sigmoid, excentric at the ends. Oblique and transverse striae equidistant, 18–22 in 10 μ.

Station : T. G. 1.

Geographic distribution : England, Sicily, Italy, Finmark, Adriatic Sea, Mediterranean Baltic.

Nitzschia longissima (Brebisson) Ralfs

De Toni 1891–94, p. 547 ; Allen and Cupp 1935, p. 163, fig. 121, Allen and Cupp 1935, p. 163, fig. 121 ; Cupp 1943, p. 200, fig. 154.

Nitzschia birostrata W. Smith 1853, p. 42, pl. 14, fig. 119 ; *Ceratoneis longissima* (Brébisson) Ralfs, 1861, p. 783 ; *Nitzschiella longissima* (Brébisson) Rabenhorst, 1864, p. 164.

Cells 95–565 μ long and 3–6 μ broad ; valves linear, lanceolate ; ends elongated into hair-like horns. Keel punctae, 8–14 in 10 μ. Chromatophores, two in the centre.

Station : T. G. 1, 2, 3.

Geographic distribution : England, Denmark, France, Virgin Islands, New Jersey, Pacific Coast of America, Java Sea.

Nitzschia closterium (Ehrenberg) W. Smith

W. Smith 1853, p. 42, pl. 15 ; Lebour 1930, p. 212, fig. 176 ; Allen and Cupp 1935, p.163, fig. 122 ; Cupp 1943, p. 200, fig. 153.

Ceratoneis closterium Ralfs 1861, p. 783, pl. 12, fig. 59 ; *Nitzschiella closterium* (Ehrenberg) Rabenhorst 1864, p. 163.

Cells single, valves spindle-shaped or lanceolate in the middle, ends hair-like, slightly bent. Two Chromatophores placed in the centre. Valves 25–150 μ in length, 3–7 μ broad.

Station : T. G. 1, 2, 3.

Geographic distribution : England, Scotland, Davis Strait, Norway, Sweden, Denmark, California, Java Sea.

Nitzschia seriata Cleve

Cleve 1883, p. 478, pl. 38, fig. 75 ; De Toni 1891–94, p. 501 ; Lebour 1930, p. 213, fig. 178 ; Allen and Cupp 1935, p. 164, fig. 124 ; Cupp 1943, p. 201, fig. 155.

Cells spindle shaped, ends pointed or slightly rounded, united into stiff hair-like chains by the overlapping points of the cells. Length of valves 60–135 μ, width 3–5·8 μ. Striae 13–19 in 10 μ. Chromatophores 2 on each side of the central nucleus.

Station : T. G. 1, 2, 3.

Geographic distribution : Davis Strait, England, Scotland, Holland, Belgium, Germany, Sweden, Denmark, Atlantic and Pacific Coasts of America, Antarctic and Java Sea.

Navicula hennedyii W. Smith

W. Smith 1856, p. 93 ; De Toni 1891–94, p. 103 ; Cleve 1894, p. 57 ; Subrahmanyan, p. 181, fig. 402.

Valves elliptical, 38–62 μ long, 21–36 μ wide. Lateral areas, narrow, linear, lanceolate or broad semilanceolate with parallel inner margins. Striae 12–15 in 10 μ.

Station : I. I. O. E. 16.

Geographic distribution : England, Belgium, Italy, Greenland, Spitzbergen, Finmark, Lusitania, Adriatic, North America, Ceylon.

Sub-family : Amphiproroideae

Genus *Amphiprora* Ehrenberg

Amphiprora gigantea Grunow, var. *sulcata* (O'meara) Cleve

Cleve 1894, p. 18 ; Allen and Cupp 1935, p. 160, fig. 113 ; Cupp 1943, p. 198, fig. 151.

Amphiprora sulcata O'meara 1871, p. 22, pl. 3, fig. 3.

Cells strongly constricted, keel with hyaline margin broader towards the ends. Junction line curved like a bow. Cells 62–122 μ long. Striae of the valve curved and divergent from the central nodule. Striae in connecting zone 20–24 in 10 μ.

Station : T. G. 1, 2, 3.

Geographic distribution : Java Sea, California.

Acknowledgments

I wish to thank Dr. Sekine, President of the Tokyo University of Fisheries, and the Japanese Government for granting me permission to join the research boat " Umitaka Maru " to enable me

to make collections on the cruise between Colombo and Singapore. I am also grateful to Professor Hiroshi Nino of the Tokyo University of Fisheries, expedition leader, and to the Captain of the boat for making my trip comfortable and granting me all facilities to work.

My sincere thanks are due to Dr. Sigeru Motoda, Professor of Planktology, Hokkaido University, for loaning me his plankton nets and helping me in my collection of phytoplankton.

References

ALLEN, W. E. and CUPP, E. E. 1935. Plankton diatoms of Java seas, *Ann. D. Jard. Buitenzord,*, 44 (2), pp. 101–174.

CHACKO, P. I. 1950. Marine plankton from waters around Krusadai Island. *Proc. Ind. Ac. Sci*, Vol. 31, pp. 162–174

CUPP, E. E. 1943. Marine plankton diatoms of the West Coast of North America, *Bull. Scripps Inst. Oceanogr.* Vol. 5. No. 1, pp. 1–238

DE TONI, J. B. 1891–94. Sylloge Algarum, Vol. 2, pts. 1, 2 & 3.

DURAIRATNAM, M. 1964. Vertical Distribution of Phytoplankton in an area near Cocos-Keeling Islands, Indian Ocean. *Information Bulletin on Planktology in Japan, No. 11, pp. 1–6.*

LEBOUR, M. V. 1930. The planktonic diatoms of the Northern seas. Ray Society Publications.

RAMACHANDRAN NAIR, P. V. 1959. The marine planktonic diatoms of the Trivandrum Coast. *Bull. Res. Inst. Univ. Kerala* Ser. C., Vol. VII, No. 1.

SMITH, W. 1853–56. A synopsis of the British Diatomaceae, Vols. 1 and 2.

SUBRAHMANYAN, R. 1946. Marine plankton diatoms of Madras Coast. *Proc. Ind. Acad Sci.* Vol. 24, B. 4 pp. 85–197.

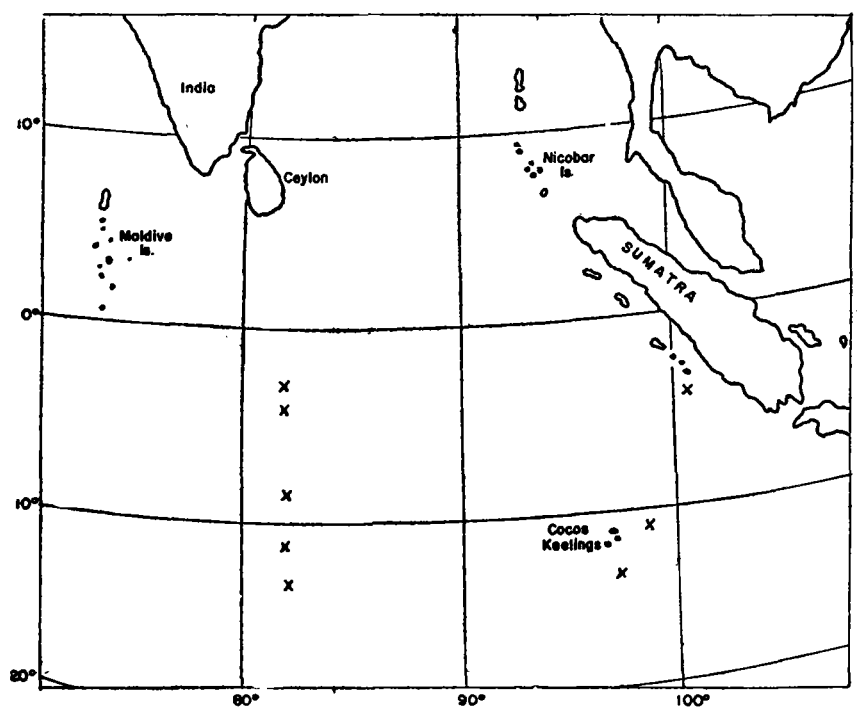

Fig. 1. Collecting Stations marked X.

Reprinted from *Annual reports for 1965 of the American Malacological Union*, p. 6-8.

COELENTERATE-ASSOCIATED PROSOBRANCH GASTROPODS.[1] Robert Robertson, Academy of Natural Sciences of Philadelphia, Pennsylvania.

(Abstract)

Nematocysts presumably protect coelenterates from most animals which might otherwise feed on them. Nevertheless, there are animals in various groups which feed in whole or in part on the soft, nematocyst-bearing, living tissues. Many associates of hydroids, sea anemones, and corals feed on their hosts.

Among the prosobranch gastropods, 21 genera in seven families are now known that include such associates:

ARCHITECTONICIDAE [= "Solariidae"] (*Heliacus* [= "*Torinia*"] with the zoanthids *Palythoa* and *Zoanthus*).

EPITONIIDAE [= "Scalidae"] (*Alexania* [= "*Habea*"], *Epitonium*, *Opalia*, and *Amaea* with sea anemones, zoanthids, and stony corals).

JANTHINIDAE (*Janthina* with pleustonic siphonophores and sea anemones on *Sargassum*; *Recluzia* with *Minyas*, a pleustonic sea anemone).

[1] The field work in the Indian Ocean was supported by the National Science Foundation as a part of the U.S. Program in Biology, International Indian Ocean Expedition.

LAMELLARIIDAE (*Velutina plicatilis* with hydroids in Europe).

OVULIDAE [= "Amphiperatidae"] (*Simnia*, *Primovula*, *Neosimnia*, *Cyphoma*, *Calpurnus*, and *Ovula* with gorgonians, soft corals, and rarely hydroids; *Pedicularia* with hydrocorals and doubtfully stony corals).

CORALLIOPHILIDAE [= "Magilidae" & "Rapidae"] (*Coralliophila*, *Quoyula*, *Leptoconchus* and *Magilus* with stony corals, zoanthids, and gorgonians; *Rapa* with soft corals).

COLUMBELLIDAE (*Nitidella nitida* with the sea anemone *Stoichactis helianthus* in the West Indies).

Most of these prosobranchs are known to feed on the living tissues of their hosts, but none are as specialized for this habit as are the aeolid nudibranchs. In the Architectonicidae, only *Heliacus* spp. are known coelenterate-(zoanthid-) associates; nothing is yet known about the food and possible associations in other genera in the family. Lamellariidae other than *Velutina plicatilis* are mostly tunicate-associates. In the Columbellidae, *Nitidella nitida* is exceptional; whether it feeds on its anemone host is unknown; other columbellids are nonspecialized carnivores or even herbivores (Marcus, 1962). Associations with coelenterates involving feeding are so prevalent in the other four families (Epitoniidae, Janthinidae, Ovulidae, and Coralliophilidae) that the habit may virtually be characteristic of each entire group. However, *Janthina* is so voracious that it will swallow noncoelenterate foods—there even is cannibalism (Bayer, 1963)—and the larger epitoniids commonly forage for smaller coelenterates. Epitoniids have a cuticularized esophageal lining which may prevent injury from nematocysts. Coralliophilids have no radula or jaws; seemingly, penetration of coral tissues is aided by salivary secretions, and the muscular proboscis functions as an ingesting pump (J. Ward, 1965). Otherwise, there are few obvious anatomical specializations.

In 1964, I spent from January to May in the Indian Ocean, where I made general collections of marine mollusks and observed prosobranchs associated with coelenterates in three areas: near Central Marine Fisheries Research Institute, Mandapam Camp (coast of Gulf of Mannar), S.E. India; Beruwala and Galle, S.W. Ceylon; Maldive Islands.

Locality	Prosobranch	Coelenterate host
S.E. India	*Alexania* sp.	*Anthopleura* sp. [a sea anemone]
" " "	*Epitonium* 3 spp.	" " " " "
S.W. Ceylon	*Calpurnus verrucosus* (Linn.)	soft corals
" " "	*Calpurnus lacteus* (Lamarck)	" "
Ceylon and Maldives	*Coralliophila* cf. *C. sugimotonis* Kuroda, 1930–31	*Palythoa* sp. [a zoanthid]
" " "	*Epitonium* sp.	" " " "
Maldives	*Heliacus trochoides* (Deshayes)	*Palythoa tuberculata* (Esper)
"	*Epitonium* sp.	*Fungia* [a stony coral]
"	*Amaea* sp.	*Tubastraea aurea* (Quoy & Gaimard) [a stony coral]

The *Epitonium* with *Palythoa* in Ceylon and the Maldives is the first epitoniid to be found with a zoanthid. The shell and body of the Maldivian *Amaea* was bright orange in life, and its coral host was similarly colored.

Much remains to be learned about coelenterate-associated prosobranchs; for example: their taxonomy and zoogeography, their specificity and their methods of feeding without injury from nematocysts. Architectonicid, ovulid, and coralliophilid larvae occur in tropical plankton far from shallow-water benthic sources, so there are also interesting problems in larval ecology—especially the location of and settlement on appropriate hosts.

Reprinted from Océanographie, vol. III, no. 2, 1965, p. 51-63.

SIPUNCULIDS OF MADAGASCAR

by

Edward B. CUTLER *

RESUME

Cet article est un compte-rendu sur les Sipunculides dans la région de Nosy-Bé, Madagascar. Ils ont été réunis par l'auteur pendant sa participation à l'Expédition Internationale dans l'Océan Indien, du 24 juin au 10 septembre 1964. Neuf espèces y sont enregistrées : *Sipunculus indicus, S. robustus, Siphonosoma cumanense, S. australe, Phascolosoma nigrescens, P. scolops, P. dentigerum, Aspidosiphon corallicola* et *Cleosiphon aspergillum*. Aucune de ces espèces n'est nouvelle pour la science, mais cinq d'entre elles sont nouvelles pour cette région, faisant un total de 13 espèces maintenant connues à Madagascar. Une discussion quant à leur habitat préféré et leurs relations commensales est présentée en supplément à une brève discussion relative à chaque espèce. Une clé illustrée des 13 espèces connues est également jointe.

ABSTRACT

This paper is a report of the sipunculids in the region of Nosy Be, Madagascar. They were collected by the author during his participation in the International Indian Ocean Expedition from 24 June to 10 September 1964. There are nine species recorded : *Sipunculus indicus, S. robustus, Siphonosoma cumanense, S. australe, Phascolosoma nigrescens, P. scolops, P. dentigerum, Aspidosiphon corallicola*, and *Cleosiphon aspergillum*. None of these are new to science but five are new to this country, making a total of thirteen species now known from Madagascar. A discussion of their habitat preference and commensal relationships is presented in addition to a brief discussion of each species. An illustrated key to the thirteen known species is also included.

INTRODUCTION

The information presented in this paper is based on collections I made as a participant in the U.S. Program in Biology of the International Indian Ocean Expedition. Most of the specimens were collected in the vicinity of Nosy Bé, Madagascar, between 24 June 1964 and 24 July 1964. A few specimens were collected at Tuléar, Madagascar, during a stopover of the R/V «Anton Bruun» from 8-10 August 1964.

The sipunculid fauna has been described from surrounding areas (Figure 1): Mauritius (**Wesenberg-Lund** 1959), Zanzibar (**Lanchester** 1905; **Stephens & Robertson** 1952), Mozambique (**Kalk** 1958, 1962), South Africa (**Stephens** 1942; **Wesenberg-Lund** 1963), and Australia (**Edmonds** 1955, 1956). In **Herubel** (1908) six species are listed from Madagascar. **Hammerstein** (1915) added two more to this list, each represented by only one specimen and one of these (*Dendrostomum signifer*) was in poor condition. In the material I collected were nine species, none new

* Zoology Department University of Rhode Island Kingston, Rhode Island U.S.A.

to science but five previously unreported from Madagascar. The collection has been deposited in the U.S. National Museum, Washington, D.C.

LIST OF MADAGASCAR SIPUNCULIDS

Sipunculus indicus - He, pp
Sipunculus robustus - pp
Siphonosoma cumanense - He, pp
Siphonosoma australe - pp
Phascolosoma nigrescens - He, Ha, pp
Phascolosoma scolops - He, Ha, pp
Phascolosoma dentigerum - pp
Phascolosoma asser - He
Phascolosoma lobostomum - Ha
Dendrostomum signifer - Ha
Aspidosiphon truncatus - He, Ha
Aspidosiphon corallicola - pp
Cleosiphon aspergillum - pp

He - Herubel (1908)
Ha - Hammerstein (1915)
pp - the present paper

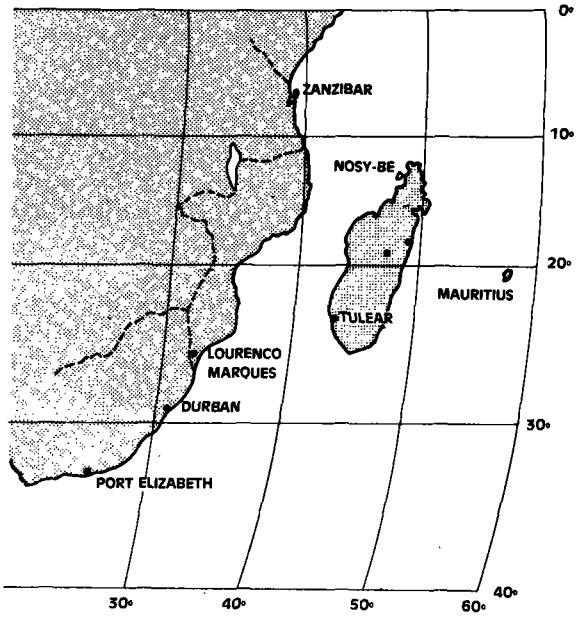

Fig. 1 - The southwestern Indian Ocean showing localities where sipunculids have been collected.

THE AREAS AND STATIONS

The island of Nosy Bé lies off the northwestern coast of Madagascar at 13° 20' S and 48° 15' E (Figure 1). Located on the southeastern corner of the island is the Centre de l'Océanographie et des Pêches which is operated by the Office de la Recherche Scientifique et Technique Outre-Mer. This served as the headquarters for the American IIOE program on Madagascar.

The climate is tropical with a warm rainy season from October to April and a cool dry season from May to September. The total average rainfall is 2244 mm with a maximum recorded in January of 462 mm and a minimum of 37 mm in July. The air temperature ranges from 34.8°C in November to 15.0°C in June. The surface water temperature ranges from 25.2°C in August-September to 31.3°C in January-February and the salinity from 35.57 ‰ in August-October to 29.05 ‰ in January. The average tide differential is 2.2 m but may increase to 4.4 m at spring tides (Centre records). There is a wide variety of habitats within easy reach of the Centre ranging from coral islands through sand and mud flats to mangrove swamps.

Tulear is about 900 miles south of Nosy Be just north of the Tropic of Capricorn at 23° 20' S and 43° 40' E. Along the shore is a broad muddy sand flat and off shore lies a large fringing reef which is partially exposed at low tide. As time and equipment were limited these collections were not extensive.

The stations where collections were made are described in Appendix I and shown in Figure 2.

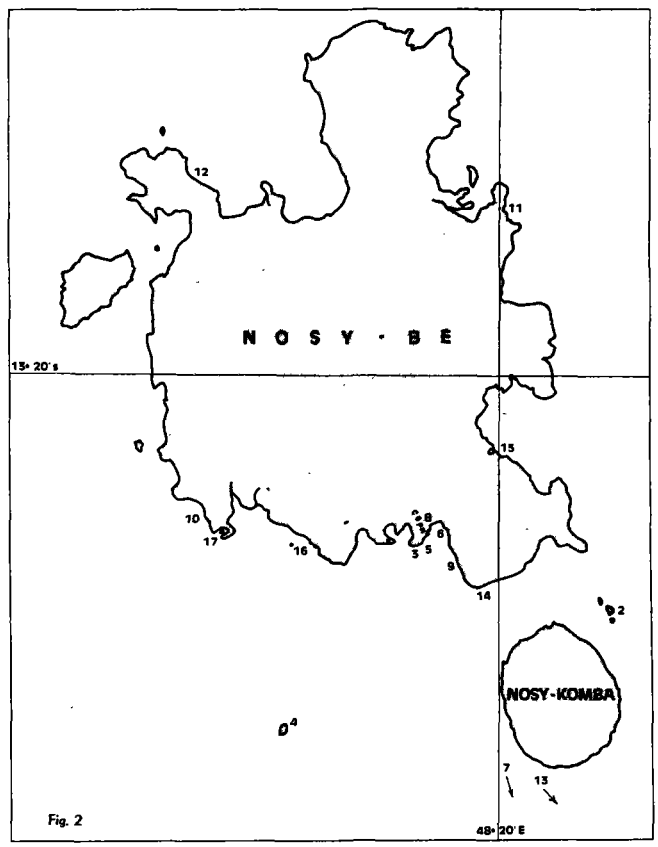

Fig. 2 - Map of Nosy Be, Madagascar, showing stations where collections for this study were made. (For the descriptions of the stations see Appendix I).

ECOLOGICAL RELATIONSHIPS

A clear-cut pattern of habitat preference emerged from this study. From the information summarized in Table 1 and Appendix 1, I was able to make the following observations.

Most of the coral formations (Stations 10, 14, 16, 17 and 20) were inhabited by a complex of four species. The most numerous and cosmopolitan was *Phascolosoma nigrescens*. The

other *Phascolosoma (P. dentigerum* and *P. scolops)* were found here as well as *Cleosiphon asperigillum*. Most of the *Cleosiphon* were found in *Millipora*. The *Phascolosoma* spp. were also found in the peculiar rock-like clay (hardened, indurated, muddy sand) at Station 5. The fact that one mass of material about 25 cm in diameter yielded sixteen specimens indicates the unusually high density in this material. A few specimens were found under rocks in tide pools in this same area (Station 3). Only *P. nigrescens* was found in the coral from the two small islands (Stations 2 and 4). Possibly more extensive collecting would have produced other forms.

This information leads to the conclusion that these four species prefer a hard, rock-like environment where they can live in holes and cracks, either of their own construction or abandoned works of other organisms. Additional evidence was supplied by the following experiment: Two *P. nigrescens* from Station 5 were placed in an aquarium containing two inches of sand with a piece of *Tubipora* at one end. One worm worked its way into the *Tubipora* and the second (which was at the other end, 5 or 6 inches away) buried itself in the sand. When checked six hours later, both individuals were located in the *Tubipora*. In addition to the four sipunculids mentioned there were numerous polychaetes, crustaceans, pelecypods *(Rocellaria* and *Lithophaga),* ophiuroids, holothurians, and tunicates present at these stations.

A unique commensal relationship, which appears to be obligatory, exists between the *Aspidosiphon corallicola* and two genera of solitary coral. A bivalve mollusc is sometimes a third member of this complex. This association has been previously reported by **Bovier** (1894), **Bourne** (1906), **Sluiter** (1902), and **Stephens** and **Robertson** (1952). In this instance the corals were *Heteropsammia* (cf) *geminale* and *Heterocyanthus* (cf) *rouseanus,* the former being more numerous. On the trunk of two of the worms within *Heteropsammia* there were several small white bivalves. After conferring with Dr. **W.J. Clench,** Museum of Comparative Zoology, Harvard University, it was decided they were members of the genus *Jousseaumiella* and probably *J. heteropsammia* (familly Montacutidae).

The question of how this relationship comes into being has been discussed at length but no experimentation has been done nor has an indisputable answer been given. The most reasonable idea seems to be **Sluiter**'s (1902) suggestion that the young worm inhabits an empty gastropod shell which is then covered by the coral, the shell being subsequently absorbed or dissolved. The relationship seems to be beneficial to both the worm (provides protection) and the coral (keeps it upright and provides locomotion to more desireable habitats).

A third type of habitat was preferred by the two species of *Sipunculus (S. indicus* and *S. robustus).* They were found at widely separated points but at both stations (12 and 13b) there was a very low tide and clean, white, apparently well oxygenated, coarse sand. There was no apparent mixing of these two populations.

The two members of *Siphonosoma* were also segregated from one another, but a different substrate preference was apparent. All of the *S. cumanense* came from a rather homogenous, muddy sand (Stations 6, 11, 13, 15, 19). The *S. australe* were found in a more heterogenous substrate, mostly firm, muddy sand but also containing larger particles such as pebbles, mangrove roots, etc. (Stations 8, 9). It would have been illustrative had I made a transect between Stations 6 and 8 to see if there was a distinct separation or how much overlap of species occurred at the border area.

These *Siphonosoma* stations all differed from the *Sipunculus* stations in that the former were exposed with almost every low tide. This information about these two genera *(Siphonosoma* and *Sipunculus)* is interesting because of the physiological implications. Without doing any laboratory experiments one could predict that the *Siphonosoma* are much more tolerant with regard to at least three parameters: temperature, salinity, and oxygen (Figure 3).

Fig. 3 -
Hypothetical relative tolerance limits
for *Sipunculus* (——) and *Siphonosoma* (• • •)

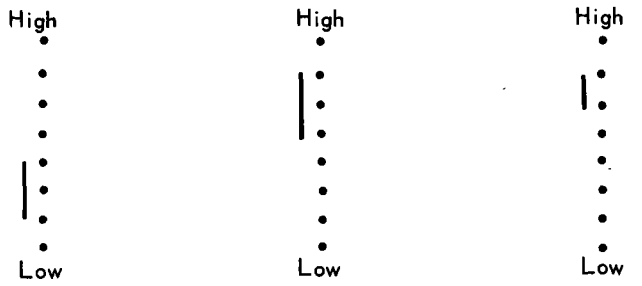

This also has interesting evolutionary-phylogenetic implications if it is true that *Siphonosoma* does have more of a capacity to acclimate (as reflected by wider tolerance limits). The evolutionary significance of the capacity to acclimate is based on the assumption that genetic adaptation is selection acting upon genetic variation. Therefore, genetic adaptation is a primary mechanism of evolution (**Kinne** 1963), i.e. the more capacity to acclimate, the more genetic adaptation which is, in a sense, evolution. As yet, within the sipunculids, no attempt has been made to establish any taxa between genus and phylum. The foregoing ideas may be helpful when such an attempt is made.

Habitats which consistantly yielded no specimens were those areas composed of soft, fine, silty mud. This probably was a very unstable situation and not suitable for worm burrows of any sort.

I. Coral, rock, hard clay
Phascolosoma scolops, P nigrescens, P dentigerum and *Cleosiphon aspergillum*
II. Within base of solitary corals
Aspidosiphon corallicola
III. Clean, white, coarse sand; exposed rarely
Sipunculus indicus and *S. robustus*
IV. Homogenous, muddy sand; exposed regularly
Siphonosoma cumanense
V. Firm, muddy sand with pebbles, stones, roots, etc.
Siphonosoma australe

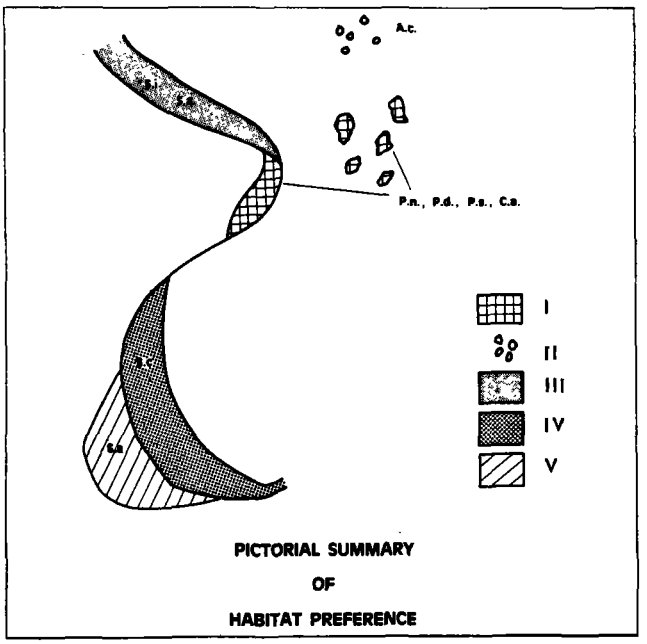

Fig. 4 - Diagramatic, pictoral summary of habitat preference

DISCUSSION OF SPECIES

Sipunculus indicus PETERS, 1850

8 specimens. Length ranged from 165-510 mm; diameter 7-11 mm; color, white.

These animals were very abundant at this station but apparently quite restricted. There are many interesting similarities between the situation here and that reported on Zanzibar by **Stephen** and **Robertson** (1952). When we arrived at Antsakoabe, there was a fisherman collecting the animals for bait by inserting a square, straight stick, which was «burred» on the end, into the burrow and exerting just the proper amount of pressure so that as the animal retracted the introvert it pulled the stick down inside immobilizing itself. The native then dug down in the sand next to the worm with his hand, loosened the sand around the worm, got a firm grasp and pulled it out more or less intact. Even though it looked easy I was unable to obtain any in this manner, finally gave up, and purchased some from the fisherman.

Sipunculus robustus KEFERSTEIN, 1865

1 specimen. Size 185 mm × 13 mm; color, grey.

This individual was found moving along the surface of the sand. As the tide was very low and the sun was hot that day, its micro-habitat might have become intolerable causing it to move to a better location. Although Dr. **Humes** had seen them there on previous occasions, I was unable to locate any more. When found, it was covered with a layer of sand and mucus. After returning to the laboratory it was placed in an aquarium but was not very active. It did produce, however, copius amounts of mucus, much of it apparently coming from the posterior bulb. This species closely resembles *S. angasi* Baird, but lacks the tufted organs near the rectum.

Siphonosoma cumanense (KEFERSTEIN, 1866)

54 specimens. Length ranged from 35-245 mm (average 120 mm); color, pinkish when alive, dirty white to pale yellow preserved.

These individuals are common and fit published descriptions quite well. **Edmonds** (1955) uses the terms «skin bodies» and «**papillae**» as synonyms to describle the multicellular epidermal glands present in this form. **Gerould** (1913) uses «epidermal organs». It should be pointed out that these are quite different from the papillae in the *Phascolosoma* which protrude as well-defined «warts» or «knobs» that remain after the underlying muscle layers are stripped off. In *Siphonosoma*, however, when the muscle layer is removed there is left only a thin piece of skin with holes which were the pores of the glands. The glands themselves remain attached to the muscle layer. As the term papillae suggests well-developed protuberances, it could be misleading to a person to look for them on the smooth-skinned *Siphonosoma*. Therefore, in this species I suggest that the term multicellular epidermal glands be used rather than papillae, skin bodies, or epidermal organs.

An interesting example of autotomy occurred when one individual, damaged while being dug out, pinched off the posterior damaged quarter of the trunk within 24 hours after it was collected. This portion contained part of the digestive tract but no other organs. I have been unable to find any previous record of this for the sipunculids.

Siphonosoma australe (KEFERSTEIN, 1865)

17 specimens. Length ranged from 45-210 mm (average 105 mm); color, yellow (straw) to dark brown; 50-20 rows of hooks.

One noteworthy feature of this group is the variability of color. Some were a uniform dark brown, others mottled, some uniform yellow with a darker introvert, and one, small, damaged specimen had an almost white trunk but retained the brown introvert. On examination this color proved to be a transient, superficial layer, probably due to the animals' environment. This color can be rubbed off exposing an irridescent bluish-grey color similar to *Siphonosoma cumanense*. Attached by byssal threads to the posterior end of one specimen was a small bivalve which looked very similar to the *Jousseaumielle* found on the *Aspidosiphon* (page 5).

Phascolosoma nigrescens KEFERSTEIN sensu STEPHEN

44 specimens. Because of the varied states of contraction the size measurements are not very meaningful. The approximate range is from 25-120mm, most between 40-80mm in length. The color varied from dark to very pale brown; most with, but some without, the alternating dark and light cross bands on the introvert. In a few the skin was very loose and easily removed.

This species is common in this region of the world and has been reported by several authors. There does exist, however, a good deal of variation in the descriptions, and the distinction between *P. nigrescens* and *P. puntarenae* is not always clear. Many structures such as the hooks, papillae, segmental organs, etc. are quite variable and it may be that these two species are the same (**Edmonds** 1956, page 289; **Wesenberg-Lund** 1963, page 129 and table 1; **Fisher** 1952, page 430). **Wesenberg-Lund's** (1963) description of *P. nigrescens* is particularly confusing for several reasons and seems to more closely agree with other descriptions of *P. puntarenae* (e.g. caecum and contractile vessel villi). The material I have is *P. nigrescens* based on Dr. **Stephen's** criteria, **Selenka's** (1883) figure 130, and comparison to specimens of both species from the United States National Museum as identified by **W.K. Fisher.**

One characteristic which is sometimes reported is the hook dimensions. On the assumption that this might be important I measured the height and width of 152 hooks from thirteen *P. nigrescens* and fifteen hooks from the one *P. puntarenae* (Figure 5 and Appendix 3). At first it looked as though there was a positive correlation between body size and hook size, but as I measured more hooks, the correlation was not always consistent. It is difficult to say anything more than: as the hook size of *P. nigrescens* is variable it should not be used as a taxonomic character. In most of the specimens, which are between 40 and 80mm long, the width of the hook (at the base) is between 70 and 80 μ.

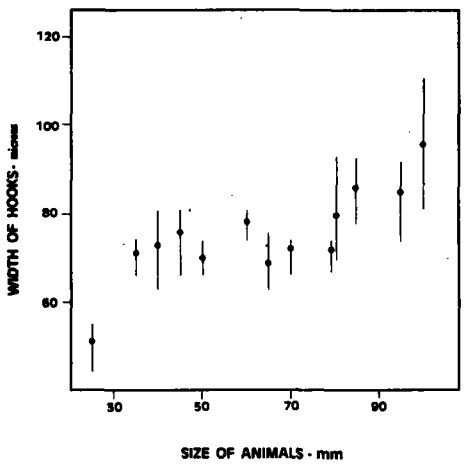

Fig. 5 - The hook size of *Phascolosoma nigrescens*

These two forms, *P. nigrescens* and *P. puntarenae* are a good example of a situation where analysis of specimens from around the world should be carried out. Either a better distinction between the two should be made or the two should be combined as one species.

Phascolosoma scolops (SELENKA and DE MAN, 1883)

These two specimens (60 and 15 mm respectively) represent another common Indo-Pacific form. It is perhaps noteworthy that only two were found. On the Zanzibar-Mozambique-South Africa coast they generally comprise a large percentage of the total. They have not been reported, however, from Mauritius. This apparent decrease in frequency with distance from

the continent may be significant. This species, together with *P. agassizi*, *P. japonicum* and others form another complex of *Phascolosoma* with very similar hooks and the internal anatomy exhibiting only minor differences. This species differs from *P. agassizi* by the absence of a rectal caecum. The nature of the papillae platelets separates it from *P. japonicum*.

Phascolosoma dentigerum (SELENKA and DE MAN, 1883)

20 specimens. The trunks ranged in length from 20-52 mm. The expanded introverts were all at least half as long and some as long as the body. The largest individual was 77 mm overall. Most of these individuals had a very pale body with the tall, conical, preanal papillae oriented posteriorly and the introvert showing the reddish-brown bands or blotches which characterize this species.

Aspidosiphon corallicola SLUITER, 1902

11 specimens. I am indebted to Dr. **M. Pichon** for pointing these out to me in the bases of the solitary corals. The anal shields fit **Stephen's** (1952) description very well. They are dark red-brown and composed of longitudinal furrows next to the anus changing to rounded granules anteriorly. The caudal shield is not deep red-brown, however, but a rather pale tan becoming somewhat darker towards the center. The secondary tooth on the hook is quite variable in size but usually present.

Cleosiphon aspergillum (QUATREFAGES 1865)

15 specimens. Most of these were an ivory color but a few were a rather dark brown. These are unique animals with their white, compound, acorn-like cap or knob at the anterior end of the trunk through which the introvert protrudes. The hooks differ slightly from **Edmonds** (1956, Figure 21) in that the secondary tooth is even more strongly developed as in **Selenka** (1883) Figure 216. The size of the trunk ranged from 30-75 mm. The average was 48 mm. These were very difficult to obtain intact as they were most abundant in very hard *Millipora*.

KEY TO THE KNOWN SPECIES OF SIPUNCULIDS OF MADAGASCAR

1 a. Horny or calcareous shields absent from both ends of the trunk 2
1 b. Above shields present at one or both ends of trunk 10
2 a. Longitudinal muscles gathered into a number of bands 3
2 b. Longitudinal muscles form a continuous sheath 12
3 a. Skin divided into numerous rectangles or squares (Figure 6-1). 4
3 b. Skin not divided into rectangles or squares 5
4 a. 24-30 strong longitudinal muscle bands . . . . . *Sipunculus robustus*
4 b. 41-43 weak longitudinal muscle bands . . . . . *Sipunculus indicus*
5 a. Skin papillae complex; made up of numerous platelets (Figure 6-2 & 3) 6
5 b. Protruding and complex skin papillae absent 9
6 a. Hooks present on introvert. 7
6 b. Introvert without hooks . . . . . *Phasyolosoma asser*
7 a. Clear streak of hook merged with basal, triangular clear space (Figure 6-4) . . . . . *Phascolosoma nigrescens*
7 b. Clear streak of hook separate from triangular clear space (Figure 6-5 & 6). 8
8 a. Introvert with reddish bands and tall, conical, preanal papillae oriented somewhat posteriorly (Figure 6-7). . . . . *Phascolosoma dentigerum*
8 b. Papillae smaller and not as above . . . . . *Phascolosoma scolops*
9 a. Introvert with hooks . . . . . *Siphonosoma australe*
9 b. Introvert lacking hooks . . . . . *Siphonosoma cumanense*
10 a. A white pineapple-like cap at the anterior end of trunk (Figure 6-8) . . . . . *Cleosiphon asperigillum*
10 b. Corrugated shields at both ends of trunk. The caudal shield is pale with radiating grooves 11
11 a. Grooves of anal shield run from ventral edge to margin . . . . . *Aspidosiphon truncatus*

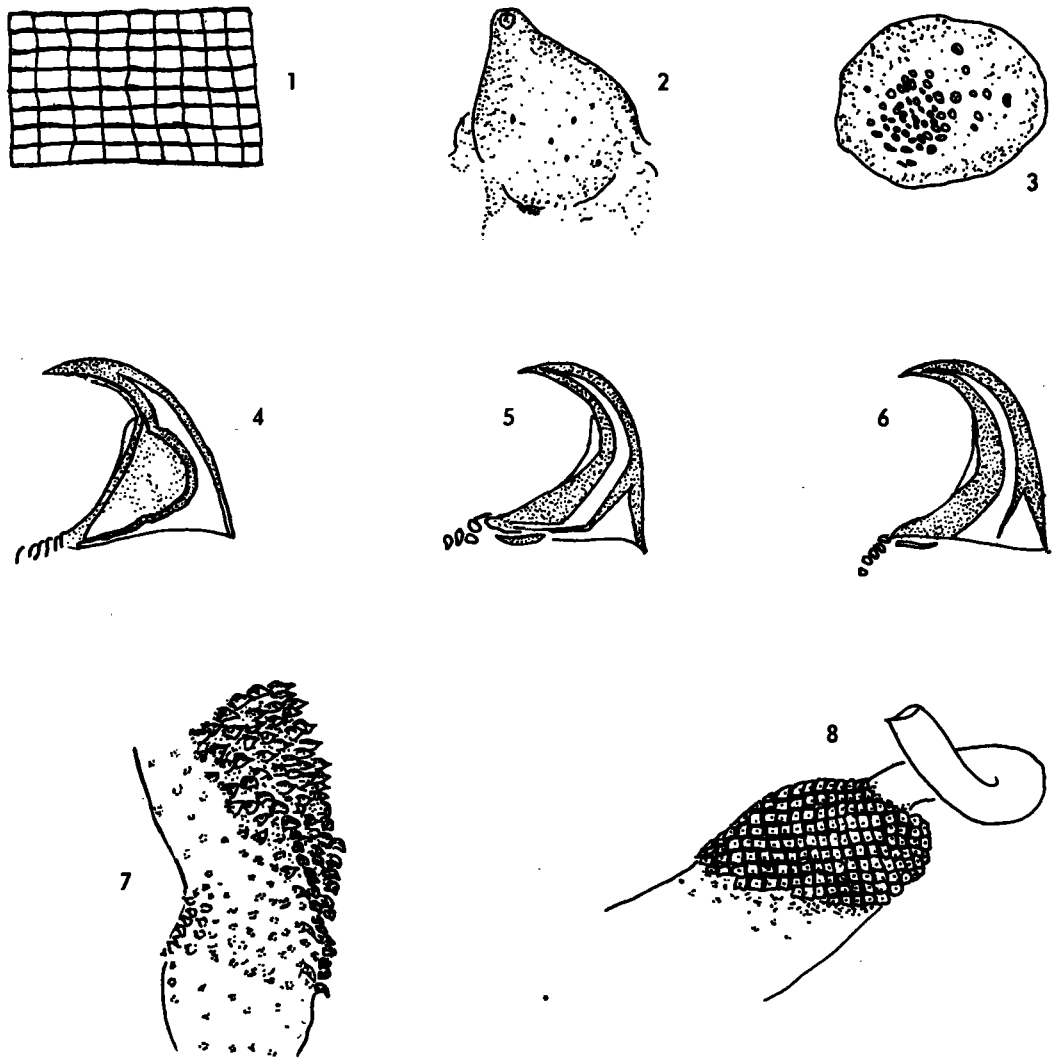

1. Generalized appearance of body surface in *Sipunculus*
2-3. Two views of a complex *Phascolosoma* papillae covered with numerous small platelets.
4. Hook of *Phascolosoma nigrescens*; clear streak merged with triangular clear space.
5-6. *Phascolosoma* hook with separate triangular clear space (*P. scolops* and *P. dentigerum*).
7. Base of introvert of *Phascolosoma dentigerum* showing tall, conical, pre-anal papillae.
8. Anterior end of *Cleosiphon aspergillum* showing complex "cap".
9. Anal shield of *Aspidosiphon corallicola*.

Fig. 6 - Morphological features to assist in identifying the known sipunculids of Madagascar.

11 b. Anal shield with two distinct areas; longitudinal grooves posteriorly, granules near introvert (Figure 6-9) . . . . . *Aspidosiphon corallicola*

12 a. Tentacles dendritic . . . . . *Themiste signifer* (formerly *Dendrostomum*)

12 b. Tentacles filiform or digitiform; complicated hooks present . . . . . *Fisherana lobostomum* (formerly *Phascolosoma*)

ACKNOWLEDGMENTS

The author is especially indebted to the following: Dr. **A.C. Stephen,** Royal Scottish Museum, Edinburgh, for several kinds of assistance; the personnel at the COPN, particularly the director and Dr. **M. Pichon** for their cooperation and facilities; Dr. **A.G. Humes,** Boston University, American liason officer at Nosy Be, for his suggestions and help in collecting; the National Science Foundation for financial support; and Dr. **D.J. Zinn,** University of Rhode Island, for assistance in preparing the manuscript.

BIBLIOGRAPHY

BOURNE, G.C.- 1906. On *Jousseaumia* in Report on the pearl oyster fisheries of the Gulf of Manaar (Ceylon), edited by W.A. Herdman. The Royal Soc. London. Part 5 : 243-266, 3 pls.

1907. Note to correct the name *Jousseaumia*. Proc. Malacological Soc. London. 7 : 260.

BOVIER. 1894. Un nouveau cas de commensalisme : association d'Aspidosiphon avec des polypiers madreporaires et un Mollusque bivalve. C.R. Acad. Sc. Paris CXIX : 95.

EDMONDS, S.J.- 1955. Australian Sipunculoidea, I. The genera *Sipunculus, Xenosiphon,* and *Siphonosoma.* Austral. J. Mar. and Freshwater Res. 6: 82-97, 1 pl., 9 textfigs.

1956. Australian Sipunculoidea, II. The genera *Phascolosoma Dendrostomum, Golfingia, Aspidosiphon,* and *Cleosiphon.* Austral. J. Mar. and Freshwater Res. 7: 281-315, 3 pls., 21 textfigs.

1961. On *Sipunculus aeneus* Baird (Sipunculoidea). Ann. and Mag. Nat. Hist. Ser. 13; 4: 217.

FISHER, W.K.- 1952. The Sipunculid worms of California and Baja California. Proc. U. S. Nat. Mus. 192 : 371-450, 22 pls.

GEROULD, J.H.- 1913. The sipunculids of the eastern coast of North America. Proc. U. S. Nat. Mus. 44 : 373-437, 5 pls., 16 figs.

GRUBE, E. and OERSTED, A.S.- 1859. Annulata Oerstediana. Vid. Medd. naturh. Foren. Kjobenhavn for 1858.

HAMMERSTEIN, O.- 1915. Gephyreen von Madagascar, gesammelt von W. Kaudern 1911-1912. Arkiv for Zool. 9 (10): 1-3, 1 fig.

HERUBEL, M.A.- 1908. Recherches sur les sipunculides. Mem. Soc. Zool. France. 1907. 20 : 107-418, pls. 5-10.

KALK, M.- 1958. The intertidal fauna of rocks at Inhaca Island, Mozambique. Ann. Natal Mus. 14 : 189.

KEFERSTEIN, W.- 1865. Beitrage zur anatomischen und systematischen Kenntnis der Sipunculoiden. Zeitschr. f. wiss. Zool. 15: 404-445.

KINNE, O.- 1963. The effects of temperature and salinity on marine and brackish water animals. I. Temperature. In Oceanography and Marine Biology, Vol. 1. H. Barnes, editor.

LANCHESTER, W.E.- 1905. The marine fauna of Zanzibar and British East Africa from collections made by C. Crossland in the years 1901 and 1902. Gephyrea. Proc. Zool. Soc. London. L: 28-35, pl. 1.

MACNAE, W. and KALK, M.- 1962. The fauna and flora of sand flats at Inhaca Island, Mozambique. J. Animal Ecol. 31 (1): 93-128.

SELENKA, E., DEMAN, I.G., and BULOW, C.- 1883. Die Sipunculiden, eine systematische Monographie. Semper, Reisen im Archipel. d. Philippinen II. 4: 1-131, 14 pls.

SLUITER, C.Ph.- 1902. Die Sipunculiden und Echiuriden. Siboga-Expedition XXV : 1-53.

STEPHEN, A.C.- 1942. Notes on the Intertidal Sipunculids of Cape Province and Natal. Ann. Natal Mus. 10: 245-256, 1 pl.

- and ROBERTSON, I.D.- 1952. A preliminary report on the Echiuridae and Sipunculidae of Zanzibar. Proc. Royal Soc. Edinburgh. Sect. B 64: 426-444, 1 chart, 1 pl.

WESENBERG-LUND, E.- 1959. Sipunculoidea and Echiuroidea from Mauritius. Vid. Medd. Dsk. Naturhist. Foren. 121: 55-73, 6 figs.

1963. South African sipunculids and echiuroids from coastal waters. Vid. Medd. Dsk. Naturhist. Foren. 125: 101-146.

TABLE I

DISTRIBUTION OF SIPUNCULID SPECIES AT EACH STATION

SPECIES	STATIONS																		Total no. of each sp.
	2	3	4	5	6	7	8	9	10	11	12	13	14	15	16	17	19	20	
Sipunculus indicus											8								8
Sipunculus robustus												b1							1
Siphonosoma cumanense					7					14		a12		3			18		54
Siphonosoma australe							16	1											17
Phascolosoma nigrescens	4	5	3	20					1				5		3	2		1	44
Phascolosoma scolops				1									1						2
Phascolosoma dentigerum				1					2				9		4	4			20
Aspidosiphon corallicola						11													11
Cleosiphon aspergillum													5		4	2		4	15
Total no. of individuals at each station	4	5	3	22	7	11	16	1	3	14	8	12 &1	20	3	11	8	18	5	172

APPENDIX I

Station List

2. Nosy Ambariobe; 25 June 1964; 2.3 m tide; coral masses.
3. Shore south of laboratory; 25 June 1964; tide pools under rocks.
4. Nosy Tanikely; 26 June 1964; 2.3 m tide; coral, dead and living.
5. Shore south of laboratory; 28 June 1964 and 21 July 1964; hardened, muddy sand (indurated) appeared like rock but with the consistency of hard clay.
6. Ambanoro Bay; 30 June 1964, 1 & 9 July 1964; 3.1 m, 3.5 m, 1.3 m tides; north end of bay; muddy sand flats with some rocks.
7. Southwest of Nosy Komba; 13° 30' S 48° 20' E; 2 July 1964; dredged in 20 m; bottom - sand, shell fragments, and solitary corals.
8. A Kirintsa, mangrove at north end of Ambanoro Bay; 5 & 19 July 1964; firm sandy mud, stones, and roots.
9. Ampasindava, east side of Ambanoro Bay; 6 July 1964; mostly rocks, few sandy patches with underlying pebbles and stones.

10. Ambatoloaka; 8 July 1964; 1.9 m tide; coral, sandstone.
11. Antafianambitry; 10 July 1964; 0.9 m tide; collected by R. Maddocks; extensive black, muddy sandflats.
12. Antsakoabe; 12 July 1964; 0.9 m tide; clean, white, coarse, well-oxygenated sand.
13. Ankifi, east of coffee factory; 11 & 14 July 1964;
    13a. sand with «grasses» and some organic material;
    13b. clean, barren sand.
14. Lokobe Point; 13, 16 & 17 July 1964; 1.4 m, 4.0m, 4.7 m tides; coral.
15. Ambatozavavy; 16 July 1964; coarse, muddy sand.
16. Ilot Ambariotsimaramara; 20 July 1964; coral heads.
17. Crater Lake; flooded extinct volcanic crater with one side somewhat open to sea; 22 July 1964; 3.4 m tide; coral.
19. Tulear; 8 & 9 August 1964; sandy mud flats south of pier.
20. Tulear; 10 August 1964; coral reef.

APPENDIX II

Methods and Materials

The collecting methods were of two general types: (1) digging and sifting sand and/or mud; and (2) snorkeling in the coral areas, breaking off large pieces of coral, and subsequently fragmenting these with a hammer to obtain the enclosed organisms.

Several types of relaxing agents were tried, but menthol crystals generally gave the best results. Other substances tried less successfully were propylene phenoxetol, MgCl, and slow addition of ethanol. All the specimens were preserved in 70 per cent ethanol, but the larger ones were first injected with formalin to prevent deterioration of the internal structures.

APPENDIX III

Data on *Phascolosoma nigrescens* Hook Size

Animal	Size (in mm)	Number of Hooks measured	Average height (in microns)	Average width at base (in microns)
s-12	25	12	48	51
t-1	35	12	74	73
s-13	40	14	66	73
USNM-1	45	5	72	76
s-124	50	9	74	70
s-15	60	9	74	79
s-9	65	10	71	69
s-157	70	10	67	72
s-165	80	10	62	72
s-5	80	23	68	80
s-150	85	16	87	86
s-8	95	10	84	85
s-1	100	12	92	96

Reprinted from *Océanographie*, vol. III, no. 2, 1965, p. 79-113.

NEW SPECIES OF THE GENUS *ANTHESSIUS* (COPEPODA, CYCLOPOIDA) ASSOCIATED WITH MOLLUSKS IN MADAGASCAR

ARTHUR G. HUMES *

and

JU-SHEY HO *

Four species of *Anthessius* are already known from Madagascar, all of them from pelecypods at Nosy Bé. They comprise *Anthessius pinnae* Humes, 1959, from *Pinna muricata* L., and three other species from *Tridacna* whose descriptions are currently in press (Humes and Stock).

This report deals with three new species of *Anthessius*, two from opisthobranchs and one from a pelecypod. These were collected at Nosy Bé by the first author during 1963-64 as part of the work of the U.S. Program in Biology of the International Indian Ocean Expedition.

The study of the material has been aided by a grant from the National Science Foundation of the United States.

The authors wish to thank Dr. William J. **Clench** of the Museum of Comparative Zoology, Harvard University, for the identification of the pelecypod and Mrs. J. **Nijssen-Meyer** of the Zoological Museum, University of Amsterdam, for the determinations of the opisthobranchs. It is a pleasure also to express appreciation for the help received from the staff of the Centre d'Océanographie et des Pêches at Nosy Bé during the year and a half when the first author was resident there.

ANTHESSIUS DOLABELLAE n. sp. Figs. 1-34

Type materials. 17 females, 42 males, and 17 copepodids washed from 29 tectibranchs, *Dolabella scapula* (Martijn), under rocks in 0.5 m at Tany Kely, near Nosy Bé, Madagascar. Collected by AGH on March 29, 1964. Holotype female, allotype, and 40 paratypes (10 females and 30 males) deposited in the United States National Museum, Washington, and the remaining paratypes in the collection of A.G. **Humes.**

Other specimens (all from *Dolabella scapula*). 2 females, 2 males, and 5 copepodids from 4 hosts, under intertidal rocks at Ambariotelo, between Nosy Bé and Nosy Komba, August 9, 1960; 1 male and 1 copepodid from 1 host, under intertidal rock at Nosy N'Tangam, near Nosy Bé, October 5, 1960; 1 male from 4 hosts, on an intertidal flat on the west side of Nosy Faly, near Nosy Bé, October 21, 1960; 3 copepodids from 2 hosts, under intertidal rocks at Nosy N'Tangam, March 17, 1964; 1 female and 1 male, from 2 hosts, under dead coral in 1 m, Pte. Ambarionaomby, Nosy Komba, September 11, 1964; and 1 female from 2 hosts, under rocks in 0.5 m, Tany Kely, September 23, 1964.

* Department of Biology, Boston University, Massachusetts. U.S.A.

Female. The body (fig. 1) resembles that of other species in the genus. The length (not including the setae on the caudal rami) is 1.67 mm (1.58-1.76 mm) and the greatest width, just in front of the segment bearing leg 1, is 0.78 mm (0.73-0.85 mm), based on 7 specimens. The prosome is rather broad, not unusually inflated, the ratio of length to width being 1.3 : 1. The segment of leg 1 is separated from the head dorsally and laterally by a furrow. The epimeral areas of the metasomal segments are rounded.

The segment of leg 5 (figs. 2 and 3) has a swelling on its midlateral margins and is widest posteriorly. The fifth legs arise slightly dorsally. The segment measures 221 × 226 μ in its greatest dimensions, and the width at the lateral swellings is 198 μ. The genital segment (fig. 4) is somewhat wider than long, measuring 169 × 192 μ. On its lateral margins there are slight identations at the beginning of the posterior third. These indentations are posterior to the areas of attachment of the egg sacs (fig. 5), which are dorsal in position and show two small unequal spines 20 μ and 11 μ in length respectively. The three postgenital segments are 64, 55 and 69 μ in length from anterior to posterior. The anal segment bears ventrally on each posterior outer margin a row of minute spinules.

The caudal ramus (fig. 6) is moderately elongate, 70 × 45 μ (the length taken along its outer margin), the ratio of the length to the greatest width being about 1.55 : 1. On the outer basal margin there is a small hyaline setule (hair ?). The outer lateral seta is inserted dorsally slightly beyond the midregion of the ramus. It measures 234 μ in length and is naked. The pedicellate dorsal seta, 62 μ long, bears a few lateral hairs. The outer subterminal seta, 146 μ, bears hairs along its inner margin. The inner terminal seta, 258 μ, bears prominent lateral hairs. The two long terminal setae, 582 and 874 μ in length respectively, bear lateral hairs ; the basal portion of these two setae proximal to the «joint» is finely punctate, and the two setae are inserted somewhat dorsally on the ramus between two flaps, the ventral one of which bears a marginal row of minute spinules. There are refractile points on the dorsal and ventral surfaces of the ramus as indicated in figs. 4 and 6.

The dorsal surface of the prosome bears scattered refractile points and hairs. The dorsal and ventral surfaces of the urosome bear refractile points as shown in the figures. The ratio of the length of the prosome to that of the urosome is about 1.9 : 1.

The egg sacs (fig. 1) reach a little beyond the setae on the caudal rami. Each sac measures about 1187 × 336 μ (in one female) and contains many small eggs 65 μ in diameter.

The rostral region (fig. 7) is not strongly delimited ventrally, and bears refractile points as shown in the figure.

The seven segments of the first antenna (fig. 8) have the following lengths (measured along their posterior non-setiferous margins) : 21 (65 μ along the anterior margin), 164, 39, 127, 94, 36, and 42 μ respectively. The first segment bears 4 setae; the second a basal group of 7 setae and a distal group of 9 setae (the distalmost one bearing hairs along its posterior margin) ; the third 5 setae; the fourth a basal haired seta and 2 distal setae; the fifth 2 centrally located haired setae and 2 terminal setae plus 1 aesthete; the sixth 2 setae and 1 aesthete ; and the seventh 7 setae and 1 aesthete. The formula thus is 4, 16 (7 + 9), 5, 3, 4 + 1 aesthete, 2 + 1 aesthete, and 7 + 1 aesthete. Except for those specified, all the setae are naked. The dorsal surface of the first antenna bears a few refractile points as indicated in the figure. The sixth segment has a sclerotized groove on its ventral surface in which the aesthete of the fifth segment may fit closely.

The second antenna (fig. 9) is apparently 4-segmented and relatively slender. Its entire length, including the claws, is about 390 μ and its width 56 μ. Each of the first two segments bears a small naked seta. The third segment bears 4 small, slender setae, three of them in a row (one of these with an interruption in the sclerotization suggesting a claw) and the fourth adjacent but separate from the row. The fourth segment is short and rather poorly delimited from the third ; it bears one inner seta, 2 unequal outer setae, and 4 claws, one of which is more sclerotized and unguiform than the others. A row of minute spinules occurs on the proximal outer area of this segment.

The labrum (fig. 7) bears lateral groups of long slender setules ; its posterior edge is

bifurcated, each lobe having a short distal marginal row of minute spinules. The ventral surface of the labrum bears refractile points and hairs as shown in the figure.

The mandible (fig. 10) has the usual apical lash, at whose base there are two inner ornamented articulated tooth-like spines and an outer long setiform element, on whose inner basal area there are two hyaline lamellate lobes. The paragnath (fig. 11) is probably represented by a small sclerotized lobe seen in ventral view under the inner edge of the lobe of the labrum at the level of the mandibles and first maxillae. The first maxilla (fig. 12) consists of a single flattened segment with a bilobed margin and bearing a smooth slender seta, a prominent spine, four small hyaline spinules, and a crescentic row of still smaller spinules. The smaller of the two lobes shows a distinct marginal notch. The second maxilla (fig. 13) is 2-segmented. The distal segment has five teeth on the distal median margin (the second and third large, the first and fourth small, and the distalmost intermediate in size), a hyaline spine on the posterior surface, and on the proximal median surface a small protuberance (fig. 14) armed with small spinules and with an adjacent row of minute spinules. The maxilliped (fig. 15) appears to be 3-segmented, with distally a minute spiniform process and a hyaline spine (?), in addition to rows of minute spinules as shown in the figure.

The area between the maxillipeds and the first pair of legs is not produced ventrally. A transverse line extends between the bases of the maxillipeds (fig. 16).

The rami of legs 1-4 (figs. 17, 18, 20 and 21) are 3-segmented, with the spine and setal formula as follows:

P1	protopod	0:1	1:0	exp	1:0	1:1	III,I,4
				end	0:1	0:1	I,5
P2	protopod	0:1	1:0	exp	1:0	1:1	III,I,5
				end	0:1	0:2	III,3
P3	protopod	0:1	1:0	exp	1:0	1:1	III,I,5
				end	0:1	0:2	IV,2
P4	protopod	0:1	1:0	exp	1:0	1:1	II,I,5
				end	0:1	0:2	IV,1

All four coxae bear a feathered inner seta, but the seta on the fourth coxa is much smaller (26 μ in length) than the others. The basis of each leg bears an outer seta, a row of hairs on the rounded inner margin, and between the rami (except on leg 4) a row of spinules. The basis of leg 1 has an additional row of spinules adjacent to the row of hairs. The detailed ornamentation of the rami may be seen in the figures. The distal end of the endopod in legs 2-4 shows a bifurcated spinous process, illustrated for leg 2 in fig. 19. The last segment of the endopod of leg 4 is 96 μ in length, the inner seta 78 μ, and the four spines from inner to outer 95, 62, 55, and 44 μ.

Leg 5 (fig. 22) has a free segment measuring 130 $\times$ 46 μ in greatest dimensions, being about 2.8 times longer than wide. The three fringed spines are of nearly equal length (57, 52, and 61 μ from proximal to distal) and the slender naked seta is 91 μ long. Rows of spinules occur ventrally on the segment near the insertions of the spines. The seta arising from the body near the insertion of the free segment is 60 μ long and naked.

Leg 6 is probably represented by the two spines near the attachment of the egg sacs (see fig. 5).

The color in life in transmitted light is translucent to light tan, with the eye red, the intestine brown, and the egg sacs gray.

Male. The body (fig. 23) is similar in form to that of the female, but the prosome is relatively less broadened, the ratio of length to width being 1.44:1. The length (not including the setae on the caudal rami) is 1.13 mm (1.01-1.25 mm) and the greatest width 0.51 mm (0.45-0.57 mm), based on 10 specimens. The segment of leg 5 (fig. 24) is more bell-shaped than in the female and lacks the midlateral swellings. The genital segment is subrectangular and only slightly swollen, measuring 122 μ in length by 138 μ in width. The four postanal segments are 56, 49, 38, and 49 μ in length respectively, the third being the shortest.

The caudal ramus (fig. 25) resembles that of the female but is smaller, 44 × 39 μ, and relatively shorter, the ratio being 1.13:1.

The surface ornamentation of the prosome and urosome resembles that of the female. The ratio of prosome to urosome is about 1.6:1.

The rostral area is like that of the female. The first antenna resembles that of the female, but three more setae are added on the second segment (fig. 26), so that the formula becomes 4, 19 (9 + 10), 5, 3, 4 + 1 aesthete, 2 + 1 aesthete, and 7 + 1 aesthete.

The second antenna resembles that of the female, but the seta on the first segment is large (88 μ in length) and spiniform (fig. 27) with a row of hairs along the inner margin.

The labrum, mandible, paragnath, and first maxilla resemble those in the female. The second maxilla (fig. 28) shows sexual dimorphism in having a distinct outer gibbosity on the first segment. There are only four teeth on the distal segment, the first small tooth being absent in the specimens dissected.

The maxilliped (fig. 29) is 4-segmented, assuming that part of the claw represents the fourth segment. The first segment bears a distal group of long spinules. The second segment bears on its posterior and inner surface a longitudinal row of minute spinules, a seta, and two dense patches of spines; and on its anterior and dorsal surface a seta and a row of slender spinules. A hyaline lamella protrudes like a crest along the ventral margin of the segment, and the dorsal margin of the segment shows two processes. The third segment is relatively very short and bears a spiniform seta 40 μ long and an adjacent smaller spiniform process. The claw (fig. 30) is 216 μ in length (measured along its greatest axis and not along the curvature), is rather strongly recurved, and bears a hyaline fringe along part of its concave margin, distal to which there is a row of hairs. Near the base of the claw on the anterodorsal surface there is a small setule.

The ventral area between the maxillipeds and the first pair of legs (fig. 31) is not produced, and shows a sclerotized area joining the bases of the maxillipeds.

Legs 1-4 resemble those of the female, except for the last segment of the endopod of leg 1 (fig. 32) where the outermost of the five setae is transformed to a spine, the formula for that segment being I,I,4.

Leg 5 resembles that of the female.

Leg 6 (fig. 33) is represented by a posterolateral flap on the ventral surface of the genital segment; it bears a spiniform seta 44 μ in length and a slender and somewhat shorter seta 27 μ long.

The spermatophore (fig. 34), seen only inside the body of the male, is elongate, 159 × 57 μ (not including the neck of 6 μ).

The color in life is similar to that of the female.

(The specific name *dolabellae* is derived from *Dolabella*, the generic name of the host.)

REMARKS : This species differs from all known species of *Anthessius* which also have the formula II,I,5 on the third segment of the exopod of leg 4. In the female of *A. navanacis* (**Wilson**, 1935) the free segment of leg 5 is relatively shorter (1.8:1), the caudal ramus is of different proportions (2.5.1), and the genital segment appears to be relatively shorter and wider. In the male the second segment of the maxilliped apparently lacks the two processes and the lamella seen in *A. dolabellae*. (Part of the information for this comparison is taken from III g, 1960.)

In the female of *A. varidens* **Stock, Humes & Gooding**, 1963, the genital segment is of a different form, the egg sacs are relatively shorter, and the two hyaline lamellae between the apical elements of the mandible are absent. The male is somewhat larger, and the two spines on the last segment of the endopod of leg 1 are peculiarly modified. The male also lacks the two processes and the lamella on the second segment of the maxilliped.

In the female of *A. proximus* **Stock, Humes & Gooding**, 1963, the spinules ornamenting leg 5 are inconspicuous and occur only at the bases of the spines. In the male the two spines on the last segment of the endopod of leg 1 are modified as in *A. varidens*.

In *A. sensitivus* **Stock, Humes & Gooding,** 1963, the female is smaller (the male is unknown), and the first antenna bears numerous aesthetes.

In *A. nortoni* **Illg,** 1960, the female has a more elongate caudal ramus (3:1), and the accessory ornamentation with spinules on leg 5 is less conspicuous. In the male there is slight sexual dimorphism in the proximal outer spine on the third segment of the endopod of leg 3, and the second segment of the maxilliped lacks the two processes and the lamella.

In the male of *A. investigatoris* **Sewell,** 1949 (the female is unknown), the free segment of leg 5 is clavate, and, as illustrated in Sewell's fig. 18 A, is longer than the genital segment. The caudal ramus is about 1.5 times longer than wide, being somewhat longer than in *A. dolabellae*.

In *A. dilatatus* (**Sars,** 1918) the female is somewhat smaller (the male is unknown). The caudal rami are more elongate (longer than the anal segment), the second antenna appears to be shorter and more robust and has three terminal claws, and the free segment of leg 5 has almost parallel sides rather than being as in *A. dolabellae*.

In *A. leptostylis* (**Sars,** 1916) the female is larger, and the caudal rami are very elongate.

In *A. pinnae* **Humes,** 1959, the female is somewhat smaller, the caudal rami are more elongate (much longer than the anal segment), the egg sacs reach only to the midpoint of the caudal rami, the free segment of leg 5 is only 1.7 times longer than wide and rather ovoid, and of the terminal claws on the second antenna two are strong and two are very weakly developed and setiform. (The distal armature of the second antenna of *A. pinnae* has been verified by us in freshly dissected paratypic material. The armature is seen to be similar to that in other species, namely, four delicate setae on the third segment and three stronger setae and four more or less claw-like elements on the fourth segment.) The male is also smaller, has prominent aesthetes on the first antenna, and shows a modified spine on the last segment of the endopod of leg 1.

In *A. saecularis* **Stock,** 1964, the caudal ramus is more elongate (3.5 times longer than wide, and 1.5 times longer than the anal segment), on the free segment of leg 5 in the female the lengths of the three spines and the details of the spinular ornamentation are somewhat different, and the second segment of the maxilliped in the male lacks the two processes and the lamella seen in *A. dolabellae*.

Other detailed differences may be found between these 10 species and *A. dolabellae*, but the comparisons made serve to indicate some of the major dissimilarities. *A. dolabellae* seems to be unique in the form of the second segment of the maxilliped in the male, with its two processes and its lamella.

ANTHESSIUS STYLOCHEILI n. sp. Figs 35-62

Type material. 24 females, 21 males, and 5 copepodids washed from 58 tectibranchs, *Stylocheilus longicauda* (**Quoy & Gaimard**), exposed on intertidal sand on the eastern side of Ankify, on the mainland of Madagascar opposite Nosy Komba. Collected by AGH on October 4, 1963. Holotype female, allotype, and 30 paratypes (16 females and 14 males) deposited in the United States National Museum, Washington, and the remaining paratypes in the collection of A.G. **Humes**.

Other specimens (all from *Stylocheilus longicauda* in the same locality as the types). 16 females, 4 males, and 3 copepodids from 150 hosts, November 2, 1963; 11 females and 9 males from 53 hosts, August 8, 1964; and 11 females and 8 males from 400 small hosts, September 9, 1964.

Female. The body (fig. 35) is similar to that in the preceding species but is a little less broadened. The length (excluding the setae on the caudal rami) is 1.82 mm (1.60-2.04 mm), and the greatest width is 0.73 mm (0.61-0.85 mm), based on 10 specimens. The prosome is moderately broad, the ratio of length to width being 1.4:1. The segment of leg 1 is separated from the head by a dorsal transverse furrow. The rounded epimeral area of the segments of legs 2 and 3 slightly overlap posteriorly the succeeding segments. The tergum of the segment of leg 4 is not indented posteriorly as in the preceding species.

The segment of leg 5 (figs. 35 and 36) is inserted under the tergum of the last prosomal segment; here the segment has nearly parallel sides. The segment expands laterally behind this point. Its dorsal posterior margin slightly overlaps the genital segment. On the ventral surface of the segment there are two crescentic lines. Between the segment of leg 5 and the genital segment there is seen ventrally a short intersegmental sclerite. The genital segment is wider than long, 205 × 300 μ. It is widest at its middle, where it is abruptly idented and constricted posteriorly. The areas of attachment of the egg sacs (fig. 37) are dorsal in position just in front of the indentation, and have two small setae 13 μ and 9 μ in length. The three postgenital segments are 117, 78 and 161 μ in length from anterior to posterior. The anal segment bears on each outer posterior ventral margin a short row of minute spinules.

The caudal ramus (fig. 38) is elongate, about equal in length to the anal segment; its greatest length is 180 μ, its length along the inner margin 156 μ, and its greatest width 61 μ, the ratio of length to width being about 2.8:1. The arrangement of the setae is similar to that in the preceding species. The naked outer lateral seta, 55 μ in length, is inserted somewhat dorsally about halfway on the outer margin. The short naked pedicellate dorsal seta is 30 μ long. The naked outer terminal seta is 66 μ; the inner terminal seta is 108 μ in length and bears lateral hairs. The two long median terminal setae, 140 and 247 μ in length respectively, are less attenuated than usual and naked. The ramus is inserted dorsally on the anal segment. The terminal setae are inserted somewhat dorsally and the distal ventral margin of the ramus bears a row of minute spinules. There are refractile points and hairs on the dorsal and ventral surfaces of the ramus as indicated in figs. 36 and 38.

The dorsal surface of the prosome and the dorsal and ventral surfaces of the urosome bear scattered refractile points and hairs. The ratio of the length of the prosome to that of the urosome is about 1.3:1.

The egg sacs extend to the end of the setae on the caudal rami. Each sac (fig. 39) is about 896 × 325 μ (in one female) and contains many small eggs 57 μ in diameter.

The rostral area is similar to that of *A. dolabellae*.

The seven segments of the first antenna (fig. 40) have the following lengths (measured along their posterior non-setiferous margins): 24 (65 μ along the anterior margin), 162, 31, 81, 73, 20, and 21 μ respectively. The formula for the armature is the same as in the preceding species. The setae are relatively shorter than in *A. dolabellae* and all are naked.

The second antenna resembles that of the preceding species, except that the second segment is less slender.

The labrum resembles that of *A. dolabellae*, but the fine ornamentation of the two lobes is rather different (fig. 41), with minute marginal spinules and a submarginal row of larger hyaline spinules.

The mandible (fig. 42) resembles that of *A. dolabellae*, but the hyaline lobes at the inner basal area of the setiform element are of a different form. The paragnaths are probably represented by two small sclerotized lobes (fig. 43) between the insertions of the first maxillae. The first maxilla is like that of the preceding species. The second maxilla (fig. 44) resembles in general form that of *A. dolabellae*, but the distal segment usually has six teeth, as in the specimen illustrated. (The second maxilla on the opposite side of the same individual had seven teeth as in fig. 45.) In other females there may be five teeth (fig. 46). The maxilliped resembles that of *A. dolabellae*.

The area between the maxillipeds and the first pair of legs (fig. 47) is produced ventrally in a balloon-like swelling, which in lateral view of the animal is rather prominent. A transverse line connects the bases of the maxillipeds.

The segmentation of the legs and the form of the intercoxal plates are in major respects similar to the preceding species. The spine and setal formula is also similar except that for the exopod of leg 4 the arrangement is I,0; I,1; III,I,5. Leg 1 (fig. 48) shows only minor differences from that of *A. dolabellae*. The last segment of the endopod of leg 2 (fig. 49) shows a distal bifurcation (present also in leg 3). The exopod of leg 4, with three outer spines on the last segment (instead of two as in *A. dolabellae*), is illustrated in fig. 50.

Leg 5 (fig. 51) has a free segment measuring 117 μ (the length along the inner margin) $\times$ 41 μ (the greatest width), the ratio being about 3:1. The three spines, each with smooth lateral lamellae, are nearly equal in length (39, 36, and 42 μ from proximal to distal) and the slender naked seta is 36 μ long. There are rows of spinules ventrally near the insertions of the spines, but these rows tend to be shorter than in the preceding species. The seta arising from the body near the insertion of the free segment is relatively short, only 28 μ in length.

Leg 6 is probably represented by the two setae near the attachment of the egg sacs (see fig. 37).

The color in life in transmitted light is pale amber, nearly translucent, with the eye red, the egg sacs opaque gray. A few females had a slight pink color.

Male. The body (fig. 52) has a general form similar to that of the female. The ratio of the length of the prosome to its width is about 1.5:1. The length (without the setae on the caudal rami) is 1.70 mm (1.57-1.83 mm) and the greatest width 0.63 mm (0.58-0.68 mm), based on 10 specimens. The segment of leg 5 (figs. 52 and 53) is not inserted under the tergum of the last prosomal segment as it is in the female. The genital segment is about as long as wide (177 $\times$ 172 μ), with its sides very slightly swollen. The four postgenital segments are 99, 104, 72, and 130 μ in length respectively, the third being the shortest.

The caudal ramus (fig. 53) resembles that of the female, but is somewhat longer and narrower, being a little longer than the anal segment. There is some variation in its length; in one male the ramus was 156 $\times$ 44 μ (ratio of 3.54:1) and in another 143 $\times$ 41 μ (ratio of 3.49:1), in both cases the length being measured along the inner margin.

The surface ornamentation of the prosome and urosome is much like that of the female. The ratio of prosome to urosome is 1.28:1.

The rostral area resembles that of the female.

The first antenna (fig. 54) resembles that of the female except for the addition of four long aesthetes (three on segment 2 and one on segment 4), so that the formula becomes 4, 16 (7 + 2 aesthetes and 9 + 1 aesthete), 5, 3 + 1 aesthete, 4 + 1 aesthete, 2 + 1 aesthete, and 7 + 1 aesthete.

The second antenna resembles that of the female, but the seta on the first segment (fig. 55) is spiniform (44 μ in length) with a row of hairs along its inner margin.

The labrum, mandible, and paragnath are like those in the female. The first maxilla also resembles that in the female except that the seta seems to be a little shorter than the spine. The second maxilla (fig. 56) has a distinct outer gibbosity on the first segment as in the male of *A. dolabellae*. There are five teeth (three large and two small) on the distal segment; the hyaline spine on that segment has a finely dentate lamella along the distal margin (fig. 57).

The maxilliped (fig. 58) has 4 segments, assuming part of the claw to represent the fourth segment. There is a pronounced, rather angular projection on the mid-inner margin of the first segment. The second segment is rather slender (lacking the ventral lamella and the irregularities of the dorsal margin seen in the preceding species), and the row of slender spinules on its anterior and dorsal surfaces is short. The seta on the third segment is rather long and slender (68 μ in length). The arcuate claw is 242 μ in length (measured along its greatest axis and not along its curvature). Otherwise the armature and ornamentation is similar to that in the preceding species.

The ventral area between the maxillipeds and the first pair of legs (fig. 59) is less produced than in the female. In preserved specimens the concave surfaces of the claws of the maxillipeds often rest against the anterior part of the swollen area. A sclerotized line joins the bases of the maxillipeds as in the female.

Legs 1-4 resemble those of the female, except for the last segment of the endopod of leg 1 (fig. 60), where the outermost of the five setae is transformed to a spine as in the preceding species. The formula for that segment is 1,1,4.

Leg 5 (fig. 61) is relatively longer and more slender than in the female, measuring 130 $\times$ 31 μ in greatest dimensions, with a ratio of about 4.2:1.

Leg 6 (fig. 62) consists of a posterolateral flap on the ventral surface of the genital segment. This is extended posterolaterally into a subconical projection bearing a distal seta 48 μ in length and a more proximal, smaller, and less sclerotized seta 21 μ long.

Spermatophores were not observed.

The color in life is similar to that in the female.

(The specific name *stylocheili* is derived from *Stylocheilus*, the generic name of the host.)

REMARKS : *A. stylocheili* belongs to the group of species of *Anthessius* which have the formula III,I,5 on the third segment of the exopod of leg 4. It thus should be compared with each of the 17 species in this group. From these *A. stylocheili* may be distinguished on the basis of a combination of three characters: the relatively short apical setae on the caudal ramus (only about 1.4 times longer than the ramus), the abruptly indented genital segment in the female, and the angular projection on the inner margin of the first segment of the maxilliped in the male.

In addition, *A. fitchi* **Illg,** 1960, has a very different body form, is much larger, the caudal rami in the female are elongate and about 2 times the length of the anal segment, and the free segment of leg 5 is 2 times longer than wide and of a different form.

Each of the three species of *Anthessius* from *Tridacna* at Nosy Bé (**Humes & Stock,** in press) have a marked lateral indentation of the cephalosome near the level of the maxillipeds.

A. lighti **Illg,** 1960, and *A. hawaiiensis* (**Wilson,** 1921) are much larger.

In *A. brevifurca* **Sewell,** 1949, the caudal rami in the female are short, but little longer than wide, and less than the length of the anal segment (the male is unknown).

In *A. arenicola* (**Brady,** 1872) and *A. teissieri* **Bocquet & Stock,** 1958, the first antenna has six segments, and the anal segment has two ventral rows of spines *(arenicola)* or spinules *(teissieri)*.

In *A. minor* **Stock,** 1959, the female is much smaller in size, and there are two ventral rows of spines on the anal segment.

A. solecurti **Della Valle,** 1880 (based on **Stock,** 1959) is larger; the female shows two rows of spinules on the ventral surface of the anal segment, and the caudal rami are 3.5-4 times longer than wide.

A. ovalipes **Stock, Humes & Gooding,** 1963, is larger; the free segment of leg 5 is elliptical or oval in outline, less than two times as long as wide.

A. concinnus (**A. Scott,** 1909) is larger, has a more rounded prosome (in dorsal view), and leg 5 is of a somewhat different outline.

In *A. pleurobrancheae* **Della Valle,** 1880, the female is much larger, and the genital segment is more elongate. The distal end of the second maxilla has more than 10 teeth.

A. pectinis **Tanaka,** 1961, is much larger; the caudal rami are very elongate (in the female 12 times longer than wide).

A. groenlandicus (**Hansen,** 1923) has in the female a shorter genital segment, of quite different form than in *A. stylocheili*.

A. brevicauda (**Leigh-Sharpe,** 1934) has in the female a very short caudal ramus and the fifth leg is irregularly elliptical, nearly 1.5 times longer than wide.

ANTHESSIUS DISTENSUS **n sp.** Figs. 63-88

Type material. 24 females, 44 males, and 11 copepodids from the mantle cavity of 19 pelecypods, *Pteria macroptera* Lamarck, attached to coral in 6 m, east of Pte. Ambarionaomby, Nosy Komba, near Nosy Bé, Madagascar. Collected by AGH on September 21, 1964. Holotype female, allotype, and 50 paratypes (15 females and 35 males) deposited in the United States National Museum, Washington, and the remaining paratypes in the collection of A.G. **Humes**.

Other specimens (all from *Pteria macroptera*). 1 male from 1 host, in 2 m, west of Ambariotelo, between Nosy Bé and Nosy Komba, August 24, 1960; 2 females and 3 males from 1 host, in

20 m, Tany Kely, December 20, 1963; 13 females, 3 males, and 3 copepodids from 3 hosts, in 4-10 m, off Ampombilava, Nosy Bé, December 21, 1963; 4 females, 13 males, and 13 copepodids from 1 host, in 10 m, Pte. Lokobe, Nosy Bé, December 27, 1963; 9 females and 3 males from 4 hosts, in 7 m, Ambariotelo, August 18, 1964; 3 females and 1 male from 2 hosts, in 3 m, east of Pte. Ambarionaomby, Nosy Komba, September 18, 1964; and 1 female and 4 males from 3 hosts, Ambariobe, between Nosy Bé and Nosy Komba, September 19, 1964.

Female. The body (fig. 63) has a form somewhat different from either of the two preceding species. The length (not including the setae on the caudal rami) is 1.52 mm (1.26-1.77 mm) and the greatest width is 0.67 mm (0.55-0.79 mm), based on 10 specimens. The prosome in dorsal view is elongate rather than suboval, the ratio of length of width being 1.6:1. The segment bearing leg 1 is set off from the head by a dorsal transverse furrow. The epimeral areas of the segments bearing legs 2 and 3 are rather acute posteriorly.

The segment of leg 5 (figs. 64 and 65) is inserted slightly under the tergum of the last prosomal segment. The sides of the segment are somewhat swollen in the anterior half (the width here being 244 μ) but nearly parallel in the posterior half (203 μ). The length of the segment is 155 μ. In ventral view there is a lightly sclerotized line between the bases of the fifth legs. Between the segment of leg 5 and the genital segment a narrow intersegmental sclerite may be seen on the ventral surface. The genital segment is longer than wide, 231 $\times$ 203 μ. It is widest in its posterior half, at the level of the areas of attachment of the egg sacs. Behind this area the segment is indented laterally and the sides are nearly parallel (the width here being 138 μ). The egg sacs are attached dorsally, and each area of attachment (fig. 66) shows two setae, one 29 μ in length and bent, the other 7 μ, hyaline, and rather obscure. The three postgenital segments are 65, 49, and 60 μ in length from anterior to posterior (the last segment being measured along its outer margin rather than in the midline where the length is 75 μ). Ventrally the posterior margins of the genital segment and the first two postgenital segments bear a row of hyaline spinules; the anal segment bears a row of smaller spinules near the insertion of each caudal ramus. Dorsally these margins are unornamented.

The caudal ramus (fig. 67) is nearly quadrate, about half as long as the anal segment. Its greatest length (to the tip of the terminal flap) is 37 μ, and its width is 36 μ. Its length along the outer margin is 27 μ, and along the inner margin 23 μ. The ratio of the greatest length to the width is about 1:1. The setae are arranged as in the preceding species. The outer lateral seta, inserted somewhat dorsally, is 75 μ in length; the pedicellate dorsal seta 52 μ; the outer terminal seta 114 μ; the inner terminal seta 146 μ; and the two long median terminal setae 336 and 550 μ respectively. All the setae are naked except for the innermost terminal one which bears slender spinules along the inner edge. The ramus is inserted on the anal segment between slight dorsal and ventral flaps. The terminal setae are inserted dorsally above a terminal ventral triangular flap which bears a submarginal row of spinules. There are refractile points and hairs on the dorsal and ventral surfaces of the ramus as shown in figs. 64 and 67.

The dorsal surface of the prosome and the dorsal and ventral surfaces of the urosome bear scattered refractile points and hairs. The ratio of the length of the prosome to that of the urosome is about 2.25:1.

The elongate egg sacs extend far beyond the end of the setae on the caudal rami. Each sac (fig. 63) is about 1175 $\times$ 225 μ (in one female) and contains many small eggs 75 μ in diameter.

The rostral area (fig. 68) resembles in general aspects that in *A. dolabellae* and *A. stylocheili*.

The seven segments of the first antenna (fig. 69) have the following lengths (measured along their posterior non-setiferous margins): 18 (55 μ along the anterior margin), 146, 35, 61, 47, 22, and 21 μ respectively. The formula for the armature is the same as in the two preceding species. All the setae are naked. The pattern of sclerotization between the second and third segments (fig. 70) suggests another incomplete segment.

The second antenna (figs. 71 and 72) has the same armature as in the two preceding

species. The second segment shows a few rugosities on its postero-inner surface and terminates distally on its antero-inner surface in a small sclerotized process. On the third segment, in addition to the four hyaline setae (the outermost more blunt than the others), there are two rows of spinules as shown in fig. 71. Of the four terminal claws, two are strongly formed, one is short and weak, and the other is long and rather slender.

The two lobes of the labrum (fig. 73) are different from those in either of the two preceding species. Each lobe is rather acute instead of being rounded and bears two smaller hyaline lobes on the median margin.

The mandible (fig. 74) is in general similar to that of *A. dolabellae* and *A. stylocheili*, but the two tooth-like inner spines at the base of the apical lash are more slender and have long spinules rather than denticles, and the hyaline lobes adjacent to the base of the lash resemble those of *A. stylocheili* more closely than those of *A. dolabellae*. The paragnaths are probably represented by two small lobes seen in ventral view under the tips of the lobes of the labrum (see fig. 73, indicated in dashed lines). The first maxilla (fig. 75) has the same general armature and ornamentation as in the two preceding species, but the small inner lobe has no notch and its two hyaline processes are unequal in size. The second maxilla (fig. 76) differs considerably from that in *A. dolabellae* and *A. stylocheili*. The second segment bears on its proximal outer margin a small hyaline process (seta ?) preceded by a minute prominence, and has on its posterior surface two very unequal setae, one long, spiniform, and armed with spinules along one side, the other short (only about 1/4 the length of the first), slender, and naked. The segment is extended distally to form a long blade with a row of 13-14 spines along the outer edge. The maxilliped (fig. 77) is highly modified. Its segmentation is obscure, though there is a suggestion of division into four segments. The area of the second segment is outwardly swollen, so that the appendage in posteroventral view appears to be greatly inflated. The only ornamentation, aside from a few refractile points, consists of a terminal hyaline process (seta ?) 6 μ long and an adjacent small spiniform projection.

The area between the maxillipeds and the first pair of legs (fig. 78) is slightly swollen ventrally, but less so than in *A. stylocheili*. A transverse line connects the bases of the maxillipeds.

The segmentation of legs 1-4 (figs. 79, 80, 81, and 82) is like that in the two preceding species, but the last two segments of the endopods are noticeably longer and slenderer. The spine and setal formula is like that of *A. stylocheili*. On the basis of all four legs the spinules near the insertion of the endopod are unusually prominent, and there is a minute hyaline setule (?) near the outer end of the row of hairs on the rounded inner margin. The last segment of the endopod of leg 4 is 70 μ in length, the outer seta 100 μ, and the four spines from inner to outer 76, 26, 27, and 24 μ.

Leg 5 (fig. 83) has a short free segment measuring 64 $\times$ 48 μ in greatest dimensions, the ratio being about 1.33:1. This segment is attached ventrally on the body. The three prominent fringed spines are of about equal length (33 μ); their narrow hyaline fringes are dentate along the edge, with the tips of the fringes projecting near the extremities of the spines so as to produce a trifid appearance. The naked seta is 56 μ in length. The segment is ornamented with a row of strong spinules along the inner margin and other similar spinules submarginally on the dorsal outer area. The seta arising from the body near the insertion of the free segment is about 80 μ long and naked.

Leg 6 is probably represented by the two setae near the attachment of the egg sacs (see fig. 66).

The color in life in transmitted light is translucent to light tan, with the eye red, the ovary dark gray, and the egg sacs gray.

Male. The body (fig. 84) resembles that of the female, though the cephalosome is somewhat more rounded. The length (not counting the setae on the caudal rami) is 0.91 mm (0.84-0.98 mm) and the greatest width is 0.42 mm (0.37-0.47 mm), based on 10 specimens. The ratio of the length of the prosome to its width is about 1.5:1. The segment bearing leg 5 (fig. 85) is

shaped differently from that in the female, being narrowed anteriorly (109 μ wide) and expanded posteriorly (164 μ wide); its length is 78 μ. The genital segment is wider than long (86 $\times$ 143 μ), being slightly swollen in front of the sixth legs. The four postgenital segments are 47, 40, 30, and 39 μ in length from anterior to posterior (the last segment being measured along its outer margin rather than in the midline where its length is 43 μ). The posterior ventral margin of the genital segment is unornamented, but those margins of the postgenital segments have rows of hyaline spinules as in the female. Dorsally such spinules are absent.

The caudal ramus, its greatest dimensions being 30 $\times$ 29 μ, is much like that of the female.

The surface ornamentation of the prosome and urosome is similar to that in the female. The ratio of the length of the prosome to that of the urosome is about 2.4:1.

The rostral area, first antenna, second antenna, labrum, mandible, paragnath, first maxilla, and second maxilla resemble those of the female.

The maxilliped (fig. 86) has 4 segments, assuming part of the claw to represent the fourth segment. The first segment is rather elongate and bears a distal group of long spinules. The slender second segment shows rugosities or folds in the sclerotization of its outer margin and the row of minute spinules seen in the two preceding species is here apparently absent. The seta on the third segment is 47 μ in length. The gently arcuate claw is 200 μ long (measured along its greatest axis and not along its curvature). Otherwise the armature and ornamentation is similar to that in *A. dolabellae* and *A. stylocheili*.

The ventral area between the maxillipeds and the first pair of legs (fig. 87) is not much produced. The line between the bases of the maxillipeds is somewhat better sclerotized than in the female.

Legs 1-4 resemble those of the female, except that, as in *A. dolabellae* and *A. stylocheili*, the outermost of the five setae on the last segment of the endopod of leg 1 is transformed to a spine, thus creating the formula of I,I,4 for that segment.

Leg 5 resembles that of the female.

Leg 6 (fig. 88) consists of a posterolateral flap on the ventral surface of the genital segment. This flap is slightly produced posterolaterally where it bears a spiniform process and a distal seta 33 μ in length, with nearby another seta 43 μ long.

Spermatophores were not observed.

Several pairs of males and females in amplexus were seen. In these the claws of the maxillipeds were placed around the lateroventral areas of the segment of leg 5, and the surfaces of the second segments of the maxillipeds (those bearing the patches of spinules) were pressed against the dorsolateral areas of this segment.

The color in life resembles that of the female.

(The specific name *distensus*, from Latin, *distendere*, to stretch out, to become swollen, alludes to the tumid form of the maxilliped in the female.)

REMARKS : *A. distensus* belongs to the group of species of *Anthessius* having the formula III,I,5 on the third segment of the exopod of leg 4. It may be distinguished from most of the species of this group by the swollen nature of the maxilliped in the female. In the following species the maxilliped is of the usual elongate and rather slender type: *A. pleurobrancheae* **Della Valle**, 1880, *A. concinnus* (**A. Scott**, 1909), *A. solecurti* **Della Valle**, 1880, *A. arenicola* (**Brady**, 1872), *A. hawaiiensis* (**Wilson**, 1921), *A. brevifurca* **Sewell**, 1949, *A. teissieri* **Bocquet & Stock**, 1958, *A. minor* **Stock**, 1959, *A. fitchi* **Illg**, 1960, *A. lighti* **Illg**, 1960, *A. ovalipes* **Stock, Humes & Gooding**, 1963, and the three species of *Anthessius* from *Tridacna* at Nosy Bé (**Humes & Stock**, in press). In *A. brevicauda* (**Leigh-Sharpe**, 1934) the maxillipeds in the female were described by **Leigh-Sharpe** as having enormous bases, but Stock's (1964) redescription based on paratypic material shows the maxilliped to be of the usual more or less slender form. In *A. groenlandicus* (**Hansen**, 1923) the form of the maxilliped in the female is not

described of figured, but this species has a much more elongate caudal ramus and fewer teeth on the end of the second maxilla than in *A. distensus*.

In only one species of this group does the maxilliped of the female approach the swollen condition seen in *A. distensus*. In the large *A. pectinis* **Tanaka**, 1961, the second segment articulates with the following segment almost at a right angle, and the whole appendage is less tumid than in the species from Madagascar. The caudal rami of this Japanese species are very long (12 times longer than wide).

REMARKS ON THE GENUS *ANTHESSIUS*

The genus *Anthessius* is a rather large, fairly homogeneous group. Its species are often recognized on the basis of rather subtle differences. During the last five years (starting with 1960) the fairly complete descriptions of fifteen new species have been published. This equals the number of all previously described species since 1880 when **Della Valle** erected the genus.

Twenty-four species of *Anthessius* are known to be associated with mollusks, either with gastropods (12 species) or with pelecypods (12 species). The remaining six species have been recovered from weed-washings, plankton, or dredged material, but is seems likely that they too may actually be associated with mollusks.

Among the species known from mollusks there seem to be no obvious morphological characters which might serve to distinguish those from gastropods from those from pelecypods. Although the genus may readily be divided into two groups on the basis of the formula of the last segment of the exopod of leg 4 (for example, in the key provided by **Stock, Humes & Gooding**, 1963), this division does not reflect host preferences. Thus, of those with the formula II,I,5, two are known from pelecypods, four from tectibranchs, and two from other gastropods, and of those with III,I,5 ten are known from pelecypods, three from nudibranchs, two from tectibranchs, and one from another gastropod. Other characters, such as the dentition of the second maxilla and the form of the caudal ramus, do not appear to be correlated with host preferences. The three species from *Tridacna* soon to be described by **Humes** and **Stock** (in press) show, however, a surprisingly similar facies, especially in the form of the lateral areas of the cephalosome.

REFERENCES

BOCQUET, C. and STOCK, J.H.- 1958, Copépodes parasites d'invertébrés des côtes de la Manche. III. Sur deux espèces, jusqu'ici confondues, du genre *Anthessius*; description d'*Anthessius teissieri*, n. sp. Arch. Zool. exp. gén., 95 (2) : 99-112.

BRADY, G.S.- 1872, Contributions to the study of the Entomostraca. VII. A list of the non-parasitic marine Copepoda of the north-east coast of England. Ann. Mag. Nat. Hist., (4) 10:1-17.

DELLA VALLE, A.- 1880, Sui Coriceidi parassiti, e sull'anatomia del gen. *Lichomolgus*. Atti R. Acad. Lincei 1879-1880, (3) 5: 107-124.

HANSEN, H.J.- 1923, Crustacea Copepoda. II. Copepoda parasita and hemiparasita. Danish Ingolf-Exped., 3:1-92.

HUMES, A.G.- 1959, Copépodes parasites de mollusques à Madagascar. Mém. Inst. Sci. Madagascar, 1958, sér. F, 2:285-342.

HUMES, A.G. and STOCK, J.H.- (in press). Three new species of *Anthessius* (Copepoda, Cyclopoida, Myicolidae) associated with *Tridacna* from the Red Sea and Madagascar.

ILLG, P.L.- 1960, Marine copepods of the genus *Anthessius* from the northeastern Pacific Ocean. Pacific Science, 14 (4):337-372.

LEIGH-SHARPE, W.H.- 1934, The Copepoda of the Siboga Expedition. II. Commensal and parasitic Copepoda. Siboga Exped. 29 b, pp. 1-40.

SARS, G.O.- 1916, Liste systématique des Cyclopoidés, Harpacticoidés et Monstrilloidés recueillis pendant les campagnes de S.A.S. le Prince Albert de Monaco avec descriptions et figures des espèces nouvelles. Bull. Inst. Océan. Monaco, n° 233, pp. 1-15.

SARS, G.O.- 1918, An account of the Crustacea of Norway with short descriptions and figures of all the species. Vol. 6, Copepoda, Cyclopoida, parts 13 and 14, *Lichomolgidae* (concluded), *Oncaeidae, Corycaeidae, Ergasilidae, Clausiidae, Eunicicolidae*, Supplement, pp. 173-225. Bergen Museum, Bergen.

SCOTT, A.- 1909, The Copepoda of the Siboga Expedition. I. Free-swimming, littoral and semi-parasitic Copepoda. Siboga Exped. 29 a, pp. 1-323.

SEWELL, R.B.S.- 1949, The littoral and semi-parasitic Cyclopoida, the Monstrilloida and Notodelphyoida. John Murray Exped. 1933-34, Sci. Repts., 9 (2):17-199.

STOCK, J.H.- 1959, Copepoda associated with Neapolitan Mollusca. Pubbl. Staz. Zool. Napoli, 31:43-58.

STOCK, J.H.- 1964, Sur deux espèces d'*Anthessius* (Copepoda) des Indes Orientales. Zoologische Mededelingen, vol. 39, Festbundel H. Boschma, pp. 111-124.

STOCK, J.H, HUMES, A.G. and GOODING, R.U.- 1963, Copepoda associated with West Indian invertebrates. III. The genus *Anthessius* (Cyclopoida, Myicolidae). Studies on the Fauna of Curaçao and other Caribbean Islands, 17 (73):1-37.

TANAKA, O.- 1961, On copepods associated with marine pelecypods in Kyushu. Jour. Fac. Agric. Kyushu Univ., 11 (3):249-278.

WILSON, C.B.- 1921, New species and a new genus of parasitic copepods. Proc. U.S. Nat. Mus., 59 (2354):1-17.

WILSON, C.B.- 1935, Parasitic copepods from the Pacific Coast. Amer. Midl. Nat., 16 (5):776-797.

*

* *

EXPLANATION OF THE FIGURES

All the figures have been drawn with the aid of a camera lucida. The letter after the explanation of each figure refers to the scale at which the figure was drawn.

PLANCHES

Fig. 1-7 - *Anthessius dolabellae* n. sp., female

1 - Body, dorsal (A)
2 - Segment of leg 5, dorsal (B)
3 - Segment of leg 5, ventral (B)
4 - Genital and postgenital segments, ventral (C)
5 - Area of attachment of egg sac, dorsal (D)
6 - Caudal ramus, dorsal (D)
7 - Rostral area and labrum, ventral (B)

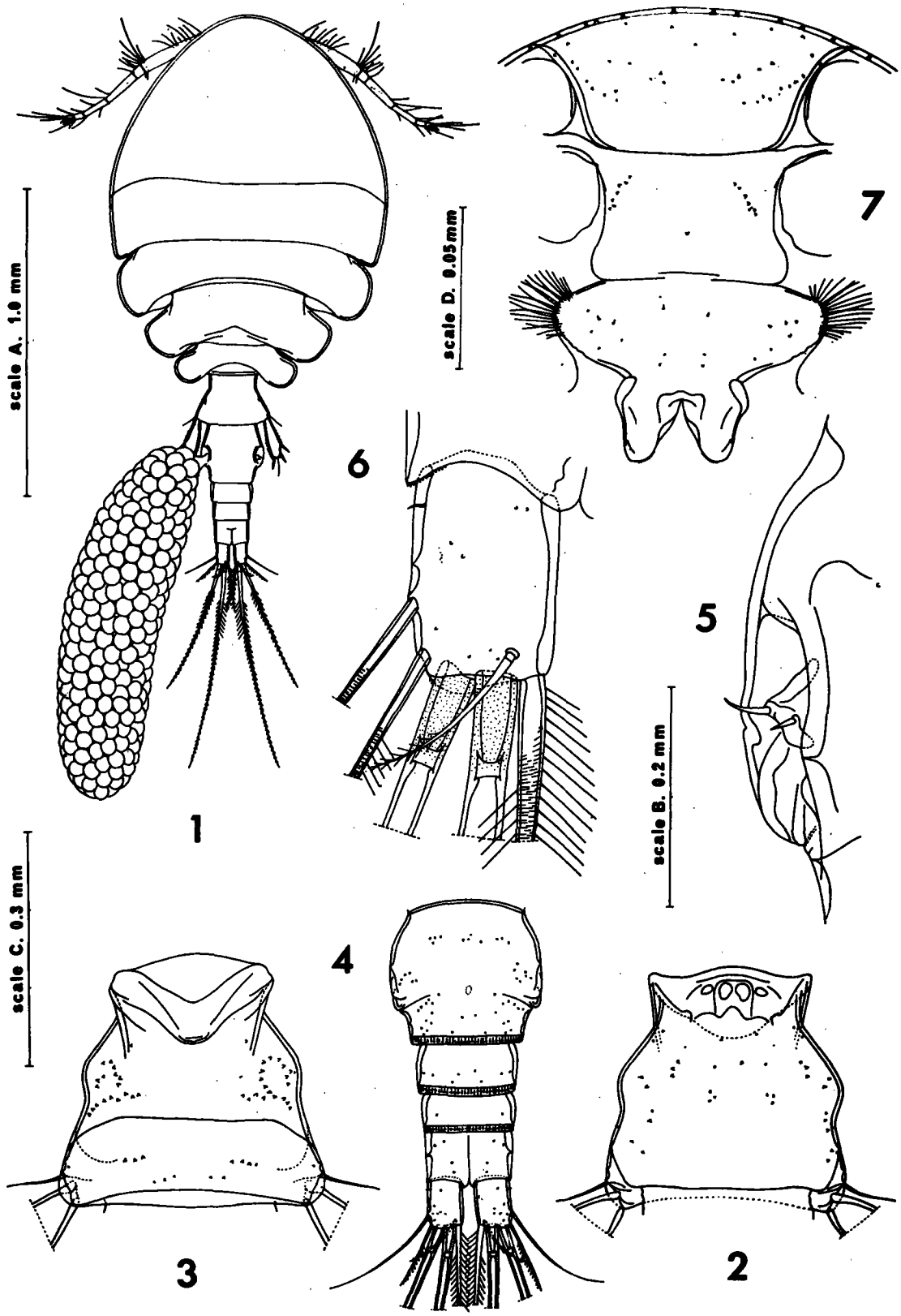
scale A. 1.0 mm
scale B. 0.2 mm
scale C. 0.3 mm
scale D. 0.05 mm
1
2
3
4
5
6
7

Fig. 8-17 - *Anthessius dolabellae* n. sp., female (continued)

8 - First antenna, dorsal (B)
9 - Second antenna, anterior (B)
10 - Mandible (D)
11 - Paragnath below edge of labrum, ventral (E)
12 - First maxilla, anterior (D)
13 - Second maxilla, posterior (F)
14 - Process on second segment of second maxilla, posterior (E)
15 - Maxilliped, anterior (F)
16 - Area between maxillipeds and leg 1, ventral (C)
17 - Leg 1, anterior (B)

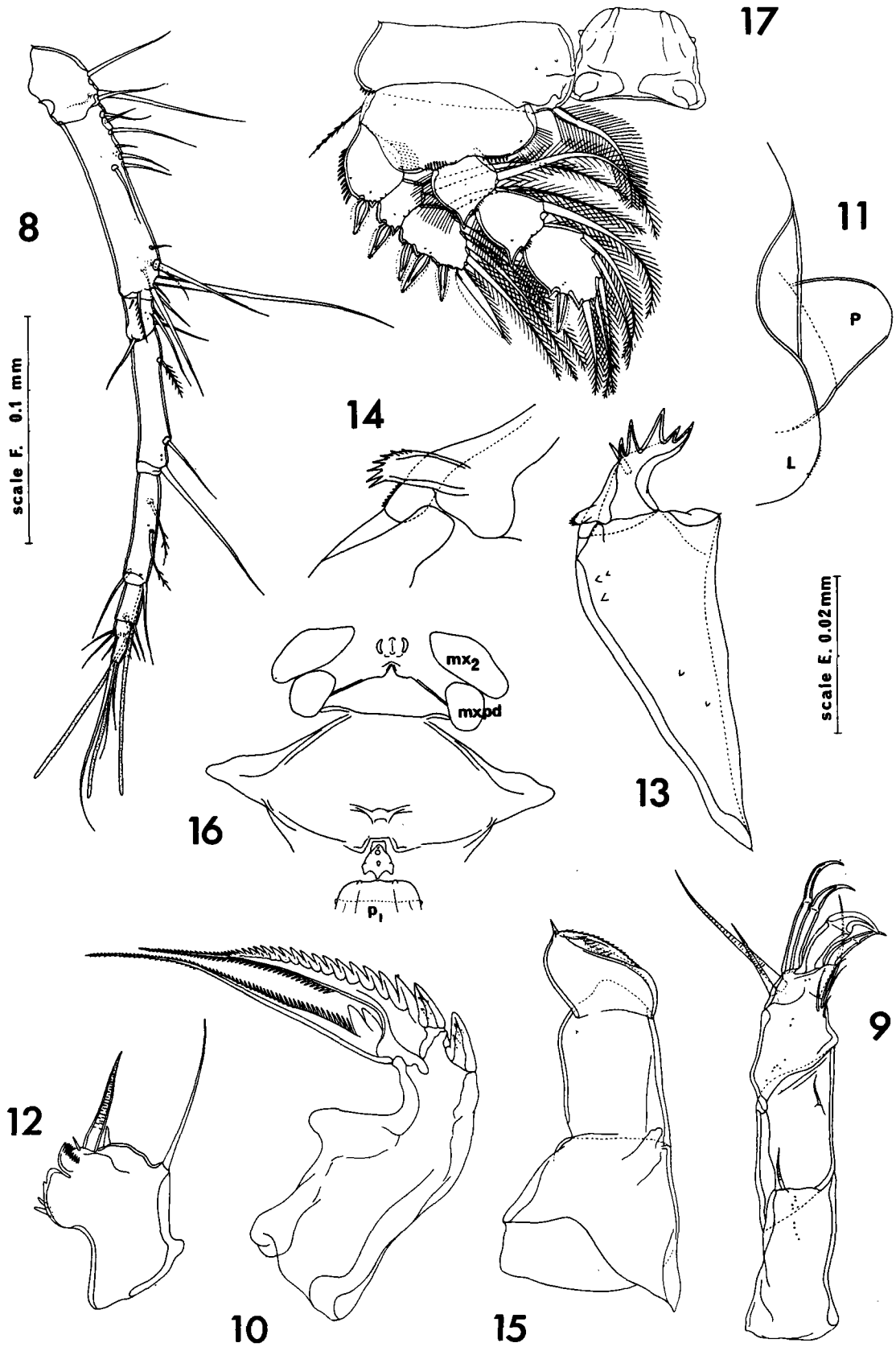
17
8
11
P
L
scale F. 0.1 mm
14
scale E. 0.02mm
mx2
mxpd
16
13
p1
9
12
10
15

Fig. 18-22 - *Anthessius dolabellae* n. sp., female (continued)

18 - Leg 2, anterior (B)
19 - Tip of endopod of leg 2, anterior (G)
20 - Leg 3, anterior (B)
21 - Leg 4, anterior (B)
22 - Leg 5, ventral (F)

Fig. 23-24 - *Anthessius dolabellae* n. sp., male

23 - Body, dorsal (A)
24 - Urosome, ventral (C)

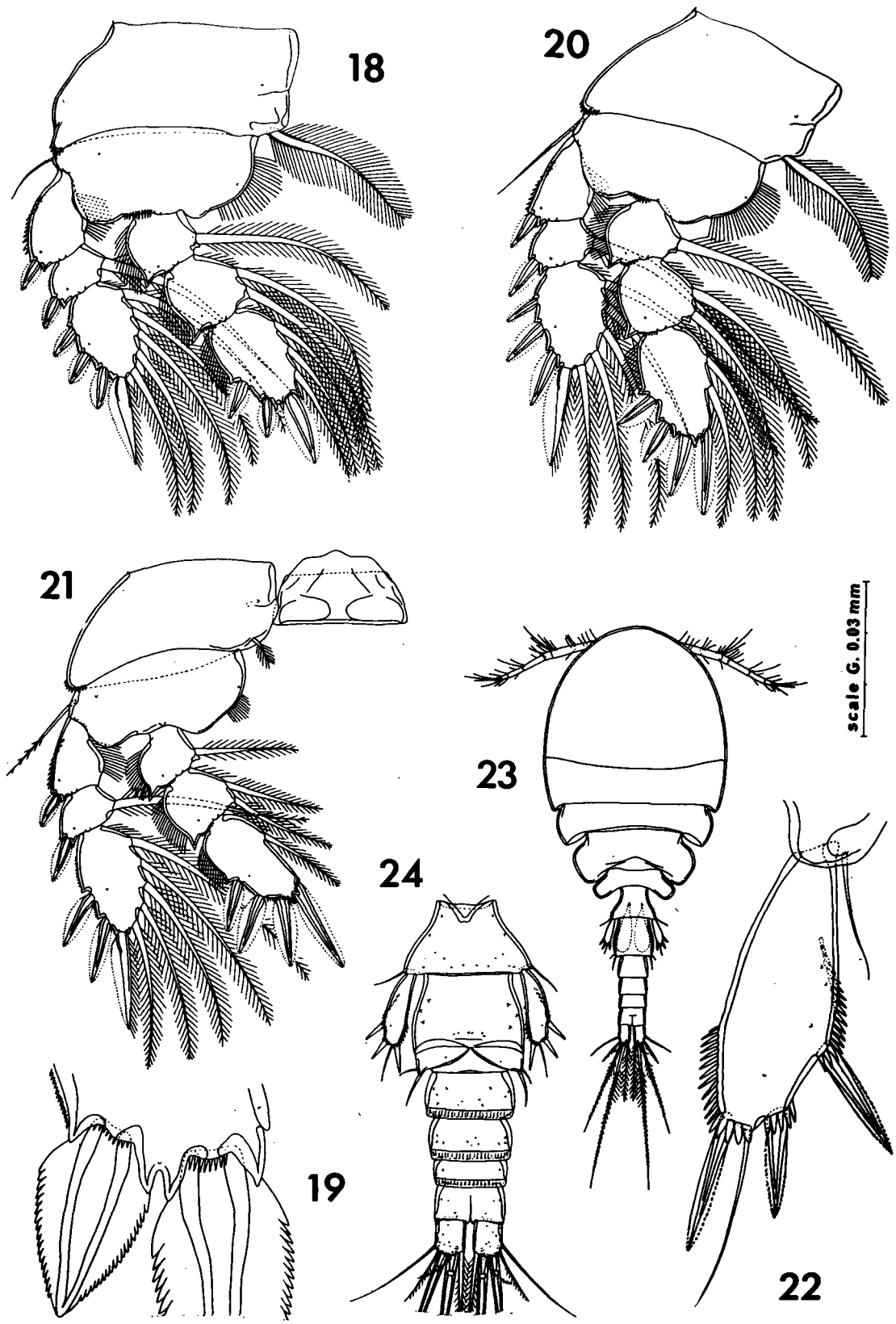
18
20
21
23
scale G. 0.03 mm
24
19
22

Fig. 25-34 - *Anthessius dolabellae* n. sp., male (continued)

25 - Caudal ramus, ventral (D)
26 - Second segment of first antenna, ventral (H)
27 - Second segment of second antenna, anterior (F)
28 - Second maxilla, posterior (F)
29 - Maxilliped, posterior and inner (F)
30 - Claw of maxilliped, posterior (F)
31 - Area between maxillipeds and leg 1, ventral (C)
32 - Third segment of endopod of leg 1, anterior (F)
33 - Leg 6, ventral (D)
34 - Spérmatophore inside body of male (H)

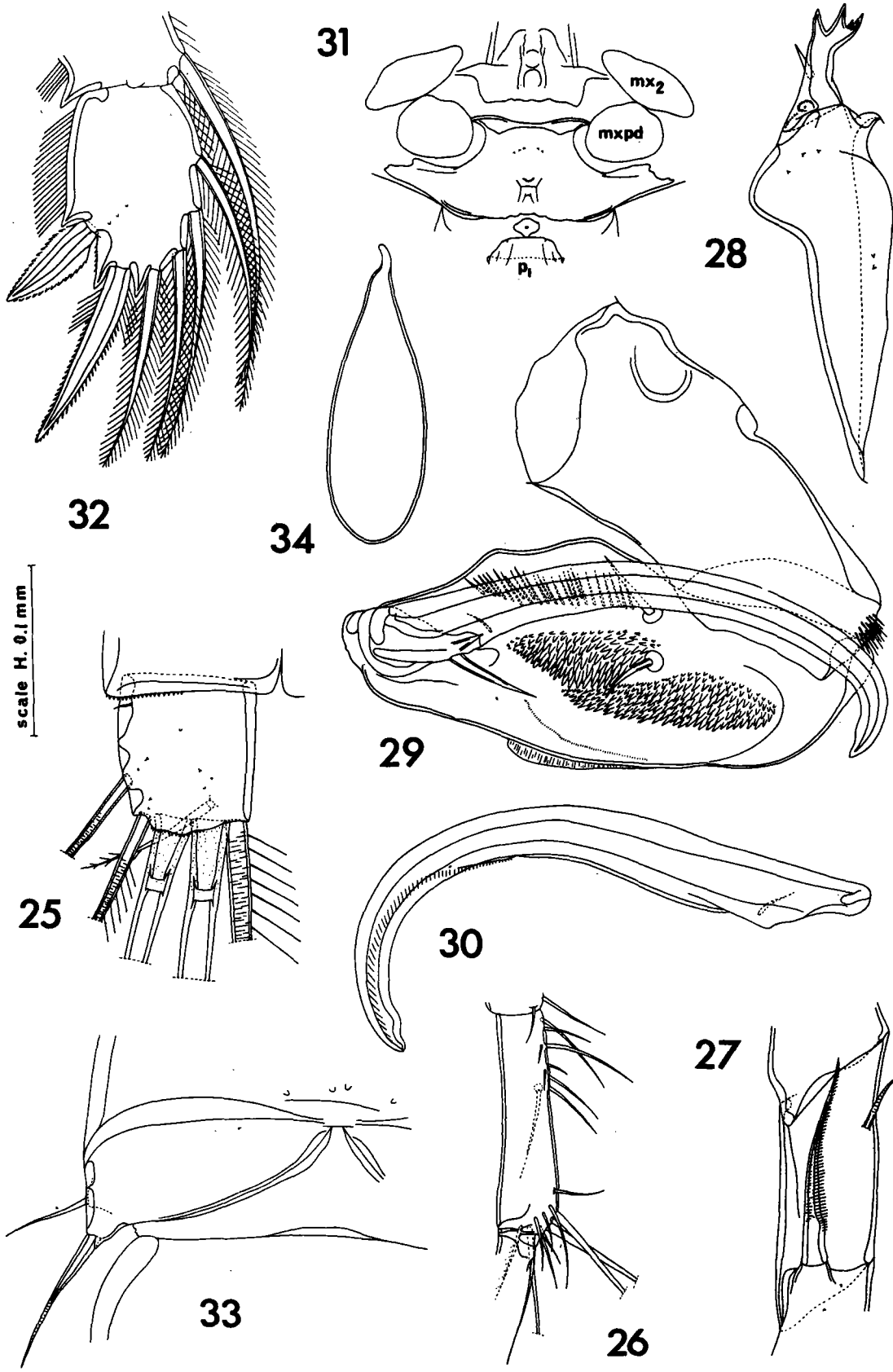
31
mx2
mxpd
p1
28
32
34
scale H. 0.1 mm
29
25
30
27
33
26

Fig. 35-46 - *Anthessius stylocheili* n. sp., female

35 - Body, dorsal (A)
36 - Urosome, ventral (I)
37 - Area of attachment of egg sac, dorsal (D)
38 - Caudal ramus, dorsal (B)
39 - Egg sac (A)
40 - First antenna, ventral (B)
41 - Tip of labrum, ventral (F)
42 - Detail of mandible (G)
43 - Paragnaths, ventral (H)
44 - Second maxilla, anterior (F)
45 - Tip of second maxilla, same individual as in fig. 44 but opposite side, anterior (D)
46 - Tip of second maxilla, anterior (D).

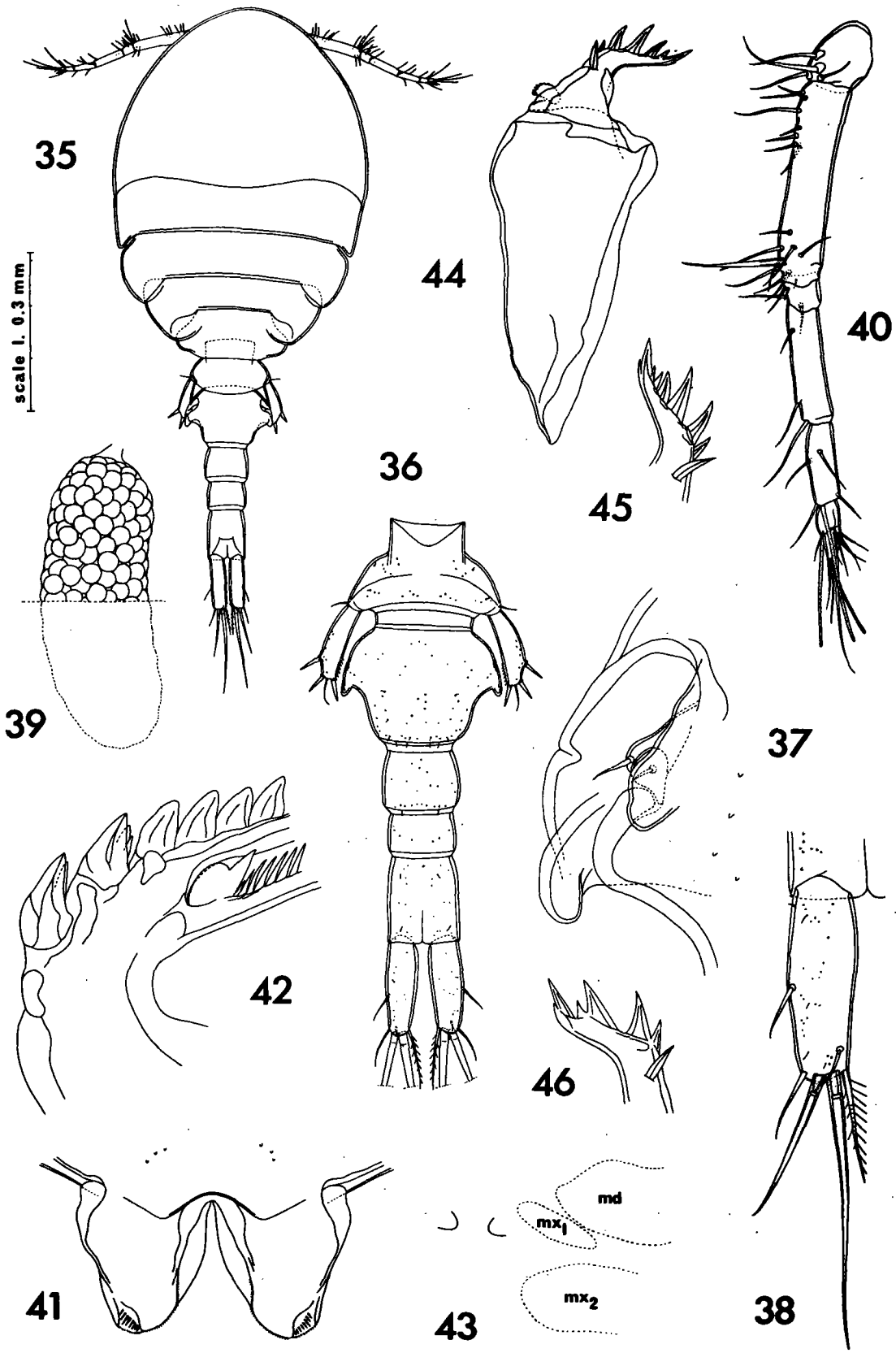
35
scale l. 0.3 mm
44
40
45
36
39
37
42
46
41
md
mx1
mx2
43
38

Fig. 47-51 - *Anthessius stylocheili* n. sp., female (continued)

47 - Area between maxillipeds and leg 1, ventral (C)
48 - Leg 1, anterior (B)
49 - Tip of endopod of leg 2, anterior (G)
50 - Exopod of leg 4, posterior (B)
51 - Leg 5, ventral (F)

Fig. 52-57 - *Anthessius stylocheili* n. sp., male

52 - Body, dorsal (A)
53 - Urosome, dorsal (I)
54 - First antenna, ventral (B)
55 - Second segment of second antenna, anterior (F)
56 - Second maxilla, posterior (H)
57 - Hyaline spine on second segment of second maxilla, anterior (E)

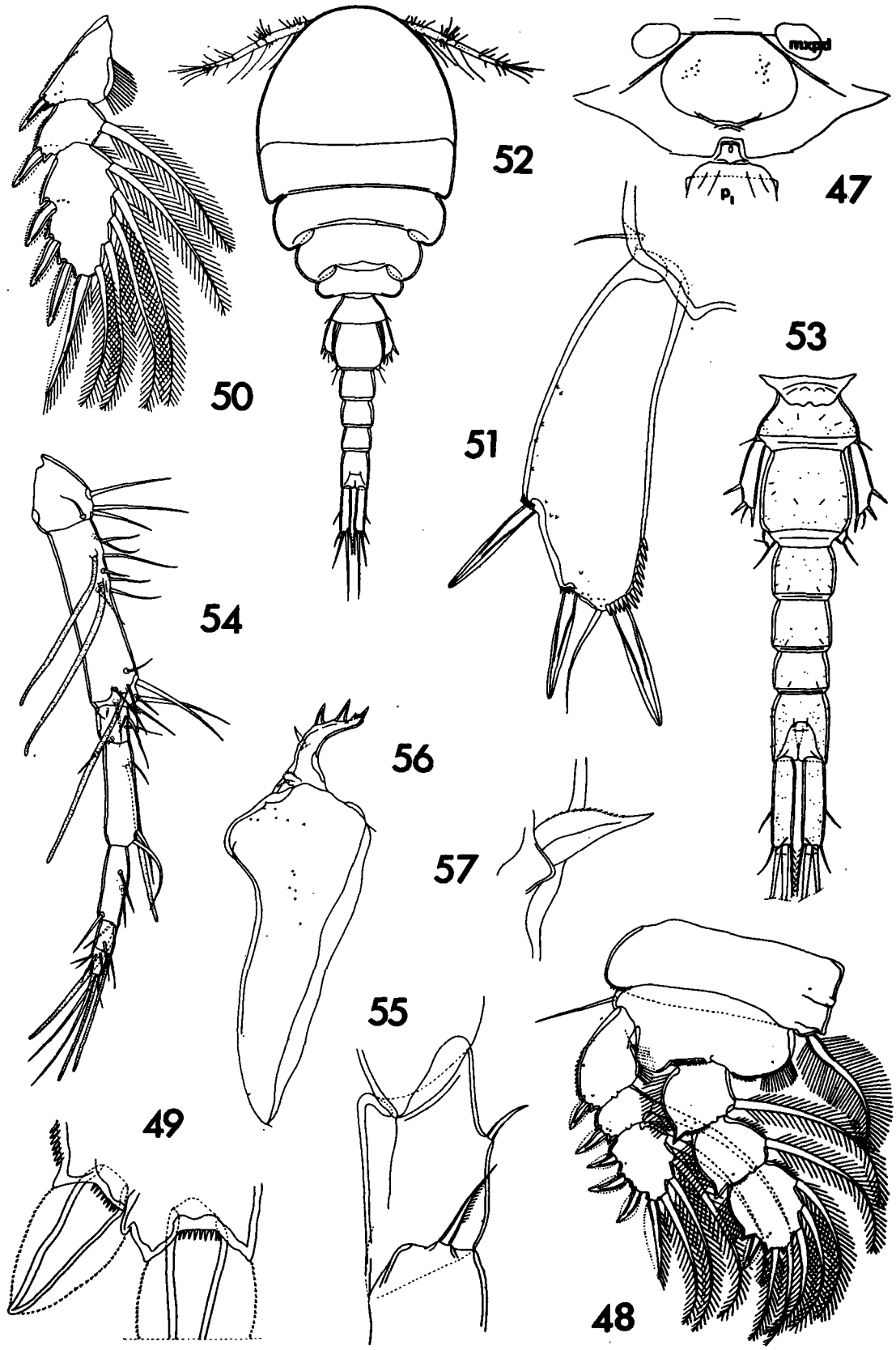
52
maxpd
47
P_1
53
50
51
54
56
57
55
49
48

Fig. 58-62 - *Anthessius stylocheili* n. sp., male (continued)

58 - Maxilliped, posterior and inner (H)
59 - Area between maxillipeds and leg 1, ventral (C)
60 - Tip of last segment of endopod of leg 1, anterior (F)
61 - Leg 5, ventral (F)
62 - Leg 6, ventral (D)

Fig. 63-64 - *Anthessius distensus* n. sp., female

63 - Body, dorsal (A)
64 - Urosome, dorsal (C)

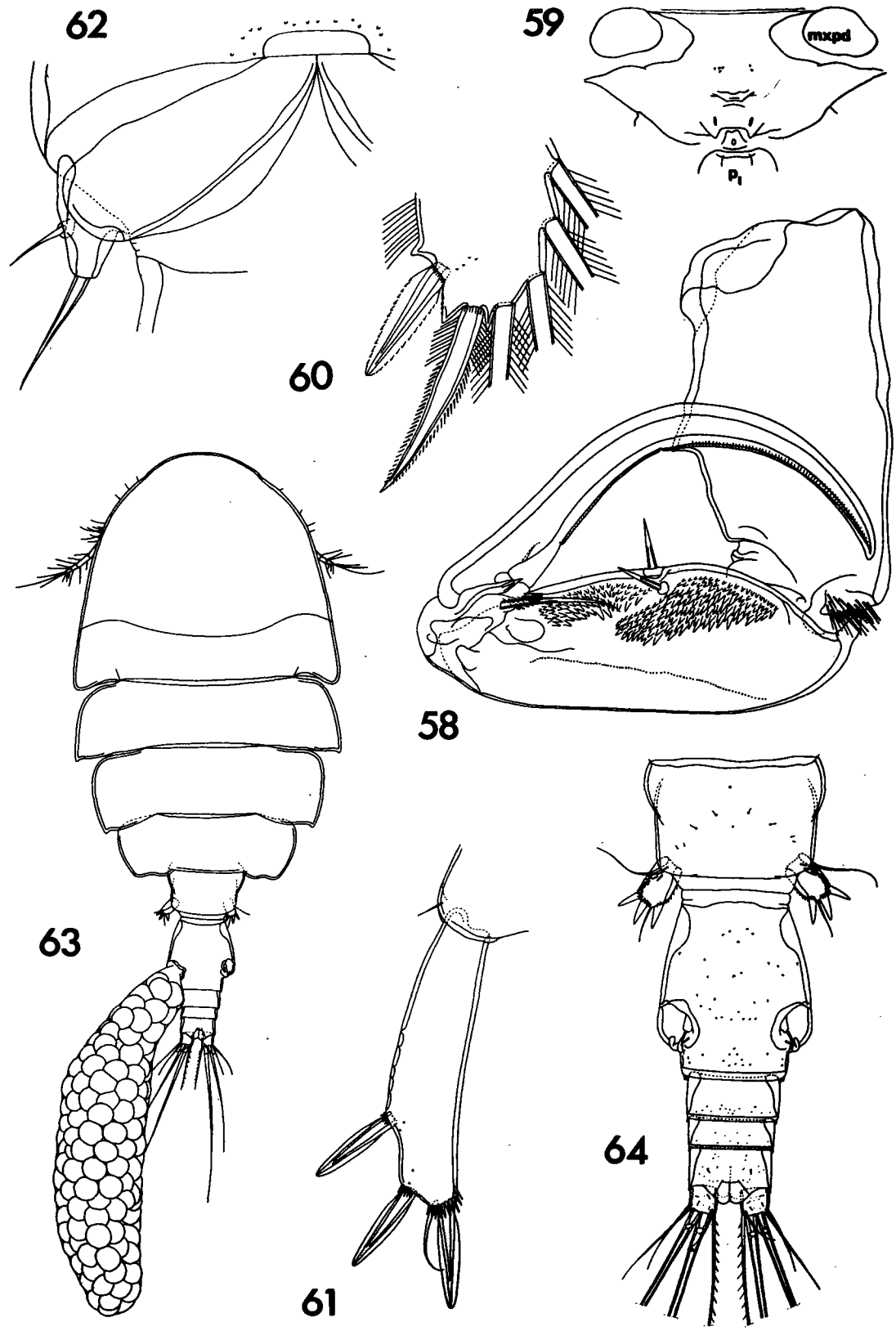
62
59
mxpd
P_1
60
58
63
61
64

Fig. 65-73 - *Anthessius distensus* n. sp., female (continued)

65 - Urosome, ventral (C)
66 - Area of attachment of egg sac, dorsal (D)
67 - Caudal ramus, ventral (G)
68 - Rostral area, ventral (B)
69 - First antenna, ventral (B)
70 - Third segment of first antenna, ventral (G)
71 - Second antenna, posterior (H)
72 - Second antenna, anterior (H)
73 - Labrum, with paragnaths indicated by dashed lines, ventral (H)

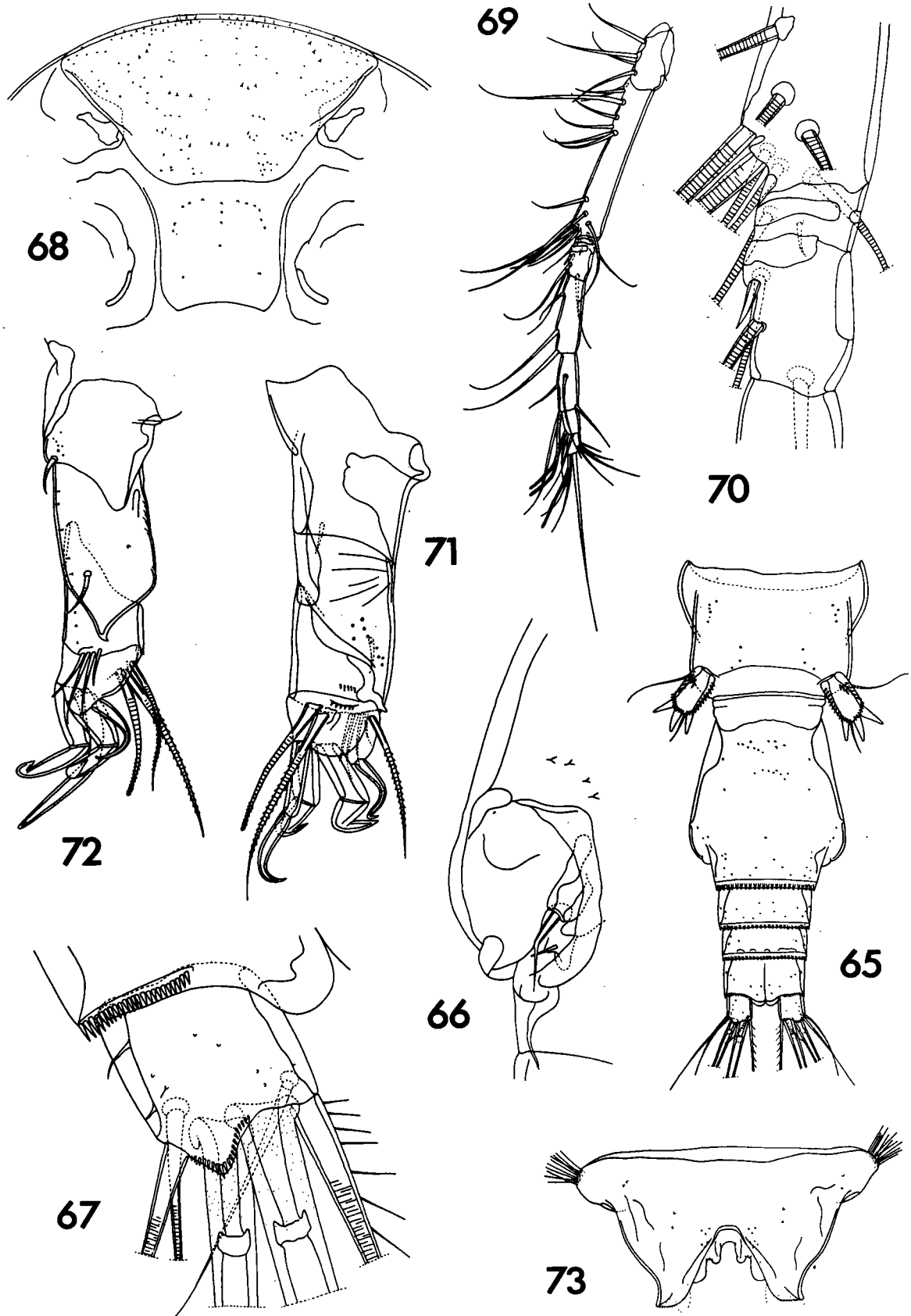
68
69
70
71
72
66
65
67
73

Fig. 74-81 - *Anthessius distensus* n. sp., female (continued)

74 - Mandible (D)
75 - First maxilla (D)
76 - Second maxilla, anterior (D)
77 - Maxilliped, posteroventral (D)
78 - Area between maxillipeds and leg 1, ventral (C)
79 - Leg 1, anterior (B)
80 - Leg 2, anterior (B)
81 - Leg 3, anterior (B)

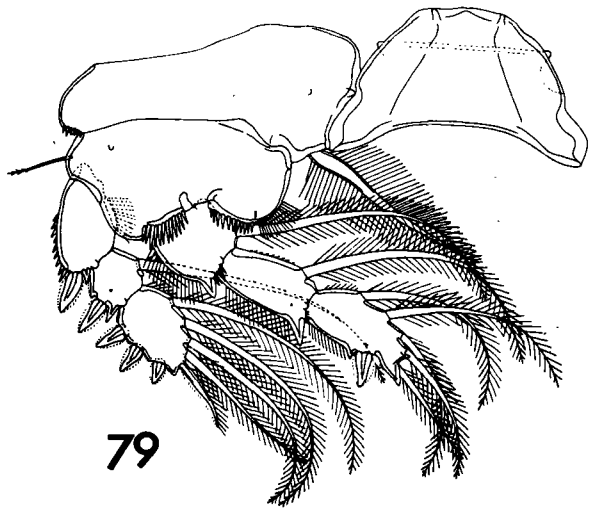

79

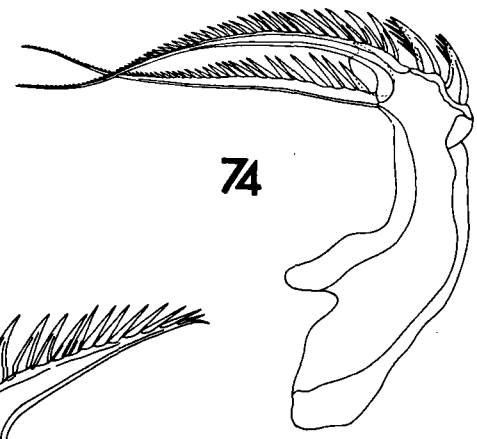

74

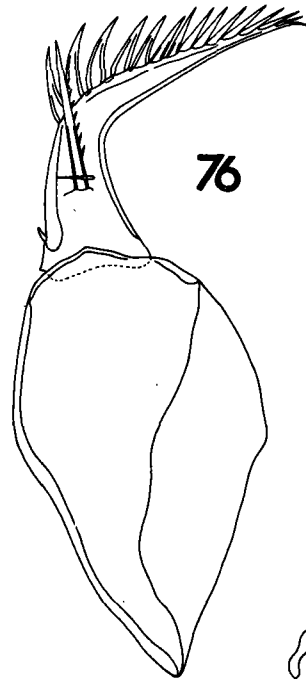

76

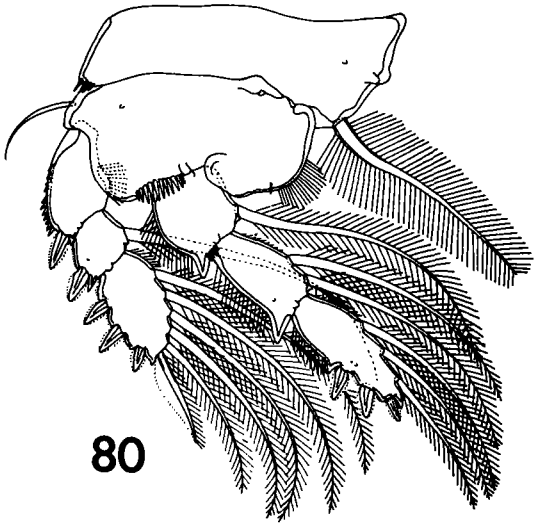

80

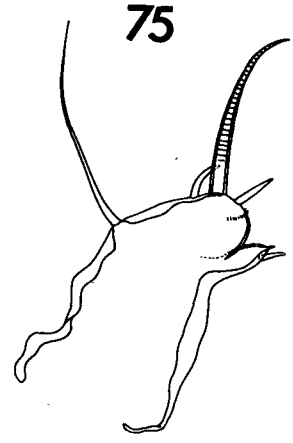

75

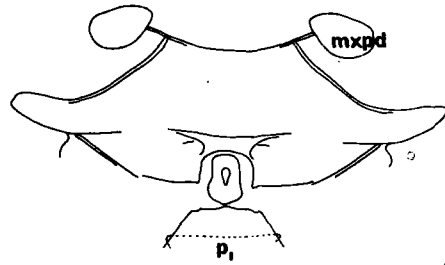

78

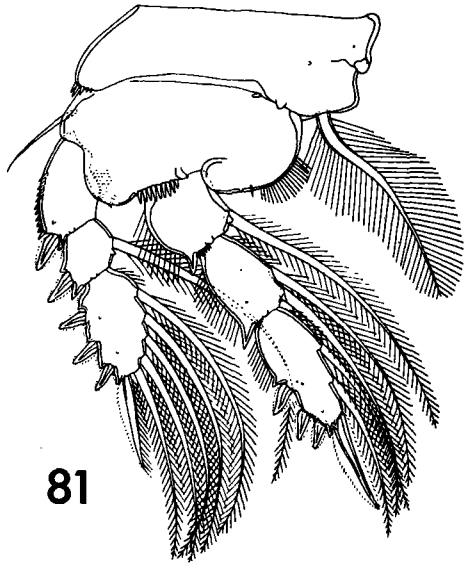

81

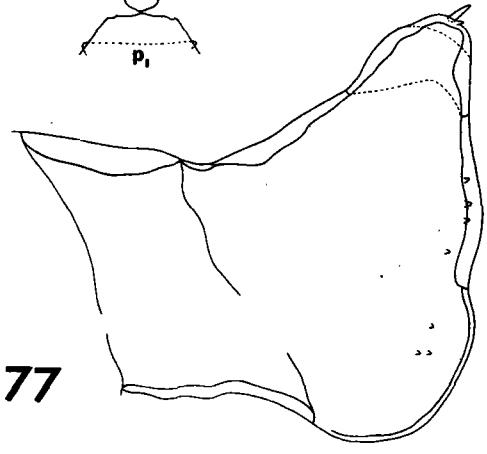

77

Fig. 82-83 - *Anthessius distensus* n. sp., female (continued)

82 - Leg 4, anterior (B)
83 - Leg 5, dorsal (D)

Fig. 84-88 - *Anthessius distensus* n. sp., male

84 - Body, dorsal (I)
85 - Urosome, ventral (B)
86 - Maxilliped, posterior and inner (F)
87 - Area between maxillipeds and leg 1, ventral (B)
88 - Leg 6, ventral (D)

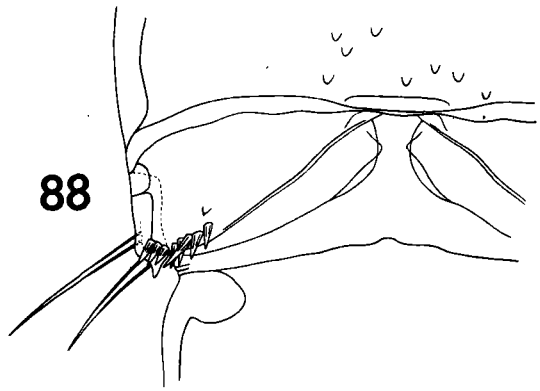

88

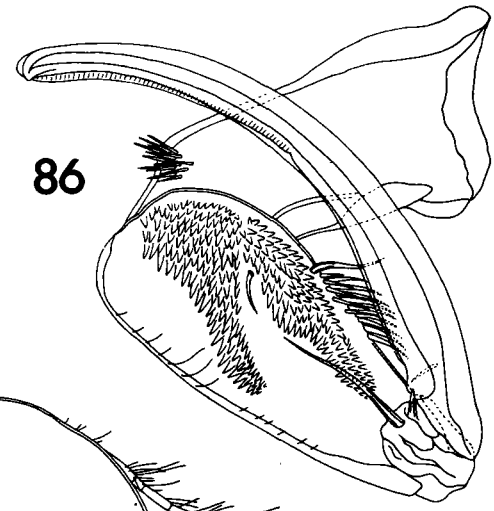

86

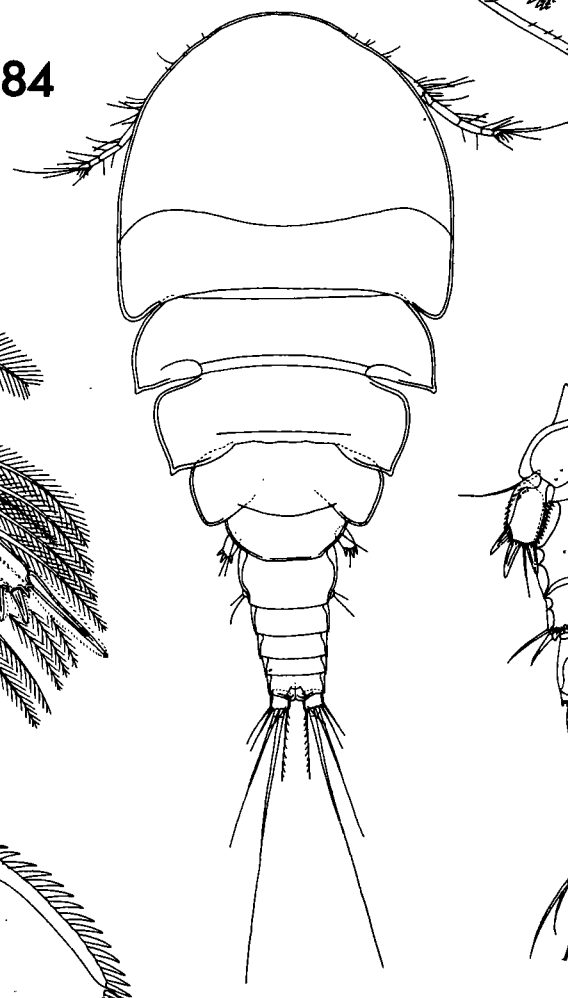

84

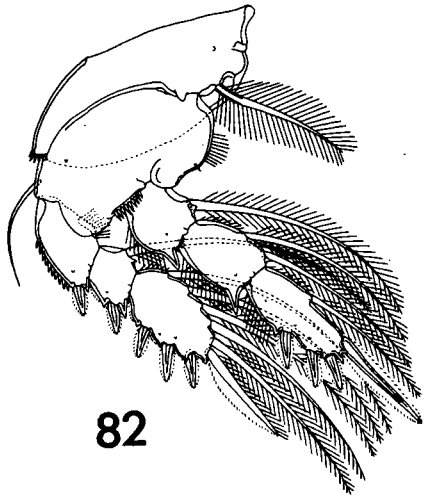

82

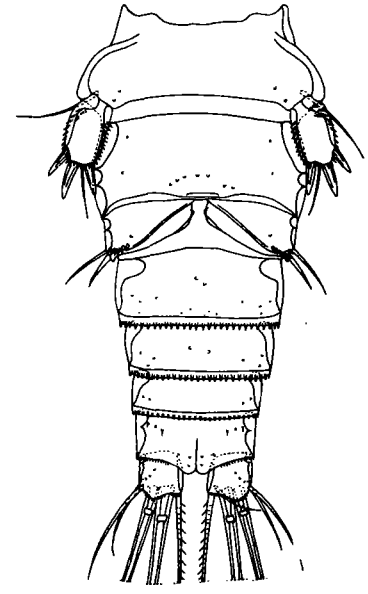

85

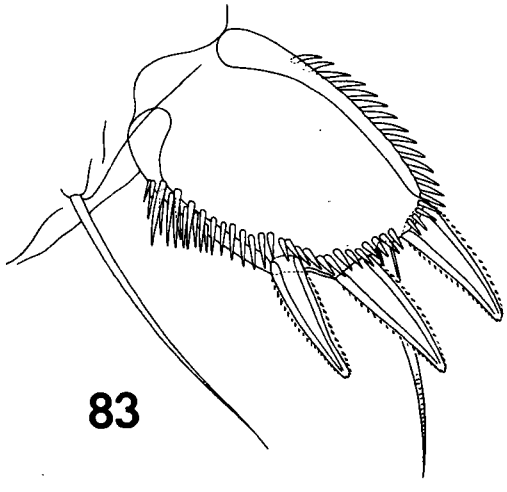

83

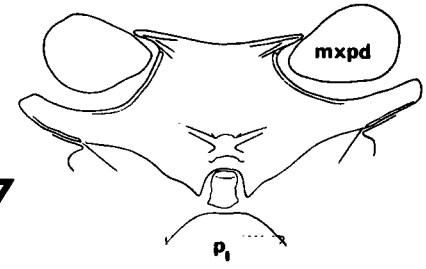

87

Reprinted from *Bull. Mus. comp. Zool.*, vol. 134, no. 6, 1965, p. 159-259.

NEW SPECIES OF *HEMICYCLOPS* (COPEPODA, CYCLOPOIDA) FROM MADAGASCAR

ARTHUR G. HUMES[1]

INTRODUCTION

One species of the genus *Hemicyclops*, *H. visendus* Humes, Cressey, and Gooding, 1958, is already known from Madagascar. This copepod lives at Nosy Bé in association with the thalassinidean shrimp *Upogebia* (*Upogebia*) sp., having been recovered by washing the bodies of the crustaceans in sea water with a small amount of ethyl alcohol.

As a result of extensive collecting in the region of Nosy Bé during 1960 and 1963–64, seven more species of *Hemicyclops* have been found, all of them new. Two of the species came from burrows known to be inhabited by a shrimp, one was washed from the body of a stomatopod, and the remaining four were recovered from water drawn from intertidal burrows of unknown origin by means of a small hand-operated bilge pump.

The island of Nosy Bé lies a few miles off the northwestern coast of Madagascar and is intersected by Lat. 13°20′S and Long. 48°15′E. (The map presented by Humes, 1962, p. 39, shows a French geographic grid based on a circle of 400°, with the longitude relative to the Paris meridian, instead of the more conventional degrees of latitude and longitude.) The spelling "Nosy Bé" (nosy = island, and bé = large, in Malgache) is the preferred form, although "Nossi Bé" is sometimes used.

The collecting in 1960 was supported by the Academy of Natural Sciences of Philadelphia, and that of 1963–64 by the U.S. Program in Biology of the International Indian Ocean Expedition. I wish to thank the directors of both the Institut de Recherche Scientifique de Madagascar and the Office de la Recherche Scientifique et Technique Outre-Mer (ORSTOM) for making certain facilities available to me at the Centre d'Océanographie et des Pêches at Nosy Bé. I am indebted to Dr. Richard U. Gooding for certain helpful suggestions in connection with the first four species described.

I wish also to thank Dr. Fenner A. Chace, Jr., for the identification of the thalassinidean and Dr. Raymond B. Manning for the generic name of the stomatopod.

The study of the material and the preparation of this paper have been aided by grants G 15911 and GB 1809 from the National Science Foundation of the United States.

The material covered in this work comprises copepods from (1) burrows of the thalassinidean shrimp *Axius* (*Neaxius*) *acanthus* A. Milne Edwards:

Hemicyclops axiophilus n. sp.
Hemicyclops amplicaudatus n. sp.

(2) burrows of unknown origin:

Hemicyclops carinifer n. sp.
Hemicyclops diremptus n. sp.
Hemicyclops kombensis n. sp.
Hemicyclops biflagellatus n. sp.

(3) the body of the stomatopod crustacean *Acanthosquilla* sp.:

Hemicyclops acanthosquillae n. sp.

[1] Boston University, Boston, Mass., and Associate in Marine Invertebrates, Museum of Comparative Zoology.

SYSTEMATIC DESCRIPTION

Hemicyclops axiophilus[1] n. sp.

Pls. I–VI; VII, figs. 39–40

Type material.—276 females, 282 males, and about 100 copepodids from water in the burrows of the thalassinidean crustacean *Axius* (*Neaxius*) *acanthus* A. Milne Edwards (determined by Dr. Fenner A. Chace, Jr.) in sand exposed at low tide at the northeastern end of the beach at Andilana (sometimes spelled Andilah), on the northern side of Nosy Bé, Madagascar. Collected by A. G. Humes September 4, 1960. Holotype female, allotype, and 110 paratypes (55 of each sex) deposited in the United States National Museum, Washington; the same number of paratypes in the Muséum National d'Histoire Naturelle, Paris, the British Museum (Natural History), London, and the Museum of Comparative Zoology, Cambridge, Mass. The remaining paratypes are in the collection of the author.

Other specimens (from burrows presumed to be of the same host).—68 females, 64 males, and 30 copepodids along the southwestern shore of Nosy Iranjà, about 55 kilometers southwest of Nosy Bé, September 7, 1960; 26 females, 6 males, and 3 copepodids in the same locality, October 7, 1960; 12 females, 9 males, and 3 copepodids at Andilana, October 8, 1960; 93 females, 96 males, and 3 copepodids at Andilana, August 8, 1960; 98 females, 47 males, and 3 copepodids at Nosy Iranja, November 4, 1963; 38 females, 60 males, and 40 copepodids at Antsakoabe, east of Andilana, November 1, 1963; 50 females, 41 males, and 22 copepodids at Navetsy, on the northernmost end of Nosy Bé, November 3, 1963; 19 females, 26 males, and 19 copepodids from Nosy N'Tangam, near Dzamandzar, Nosy Bé, December 2, 1963; and 97 females, 37 males, and 11 copepodids from the same locality, January 1, 1964.

Female.—The body length (not including the setae on the caudal rami) is 1.80 mm (1.66–1.89 mm) and the greatest width (near the posterior edge of the cephalosome) is 0.79 mm (0.70–0.86 mm), based on 10 individuals. The prosome is a little longer than the urosome, the ratio being about 1.4 : 1 (Fig. 1). The tergal plates of pedigerous segments 1–4 (Fig. 2) are well separated laterally (with acute posterolateral angles) and are ornamented, like the rest of the dorsal surface of the prosome, with small knobs and hairs. The segment of leg 5 is smaller, without produced epimera and with two groups of rather long hairs on the dorsolateral areas. An almost complete intersegmental sclerite occurs between this segment and the next. The genital segment (Fig. 3) is about 310 μ in length, without a trace of division into its two constituent somites. It is broadest in its anterior third (268 μ), has a moderate ventrolateral expansion in its middle third (211 μ), and is narrowest in its posterior third (169 μ), where the sides are nearly parallel. There is an extensive lateral invagination between the anterior and middle thirds. Details of the border of the anterior two-thirds of the genital segment are shown in Figures 4 and 5. The egg sacs are attached dorsolaterally on the anterior part of the broadened anterior third. Near the attachment of each sac there are two minute blunt spines, each about 9 μ in length (Fig. 6); posterior to the attachment area there is a single isolated small seta. Each egg sac is oval, about 507 × 253 μ (based on 3 individuals), and contains many small eggs (Fig. 1).

The spermatophores when attached to the female are carried along the posterior third of the genital segment (Fig. 1), behind the middle expansion. The three postgenital segments (Fig. 3) measure in length, respectively, 122, 96, and 72 μ, the last of these segments with a row of minute spinules on the ventral posterior margin near the insertion of the ramus. A row of smaller spinules continues laterally on the ventral posterior margin (see Fig. 7). Two diagonal rows of very fine spinules form a V on the dorsal anal area. A few minute refractile points

[1] The specific name *axiophilus* is derived from *Axius*, the generic name of the crustacean with which the copepod is associated, and φιλος, loving.

occur on the ventral surface of the first postgenital somite.

The caudal ramus (Fig. 7) measures 102 × 53 μ (2.0 times longer than wide), based on 5 individuals, the length measured ventrally along the inner edge. The lateral seta is 88 μ in length, without hairs or spinules, but with a narrow flange along the posterior edge. The dorsal seta is 100 μ long and haired. The innermost terminal seta is 226 μ long, with erect lateral hairs; the outermost terminal seta is 83 μ long, naked, with the proximal two-thirds having an inner flange and terminating in two pointed processes, the distal third forming a hyaline flagellum (Fig. 8). Of the two long terminal setae, the outer one is 437 μ in length, the inner one 728 μ, both with a basal peg and with lateral hairs. A minute hyaline setule (hair ?) occurs on the outer edge near the base of the ramus. There is a row of long setules along the distal half of the inner edge, and a small group of spinules at the inner distal corner of the ramus. The distal end of the ramus overlaps ventrally the insertions of the four terminal setae.

The rostral area (Fig. 9) bears two small hairs and a few refractile points.

The first antenna (Fig. 10) has 7 segments, their lengths (measured along their forward setiferous margins) beginning at the base: 56, 94, 55, 117, 62, 53, and 52 μ, respectively. The first segment bears 4 setae, the second 15 (some of them apparently with extremely short lateral hairs in their proximal halves), the third 6, the fourth 3, the fifth 4 and 1 aesthete, the sixth 2 and 1 aesthete, and the seventh 7 and 1 aesthete. All but 6 setae are annulate, these six being disposed as follows: 1 each on segments 5 and 6, 4 on the terminal segment. On the distal anterodorsal surface of the second segment there are a few transverse refractile lines as shown in the figure.

The second antenna (Fig. 11) is 4-segmented, with the third segment produced on the inner distal corner and bearing there 2 spines, the proximal one blunt and having a spinulose flange, the distal one attenuated and bearing a row of spinules, both spines with a subterminal setule. The fourth segment measures about 36 × 29 μ and has 3 hyaline, pectinate flanges, two on the outer side and one on its posterior surface. The remaining armature and ornamentation is shown in the figure.

The labrum in anterior (dorsal) view (Fig. 12) is slightly trilobed with a row of 5–10 setules along its free edge. In posterior (ventral) view (Fig. 13) the labrum has a complex ornamentation, as shown in the figure.

The metastomal areas have the ornamentation indicated in Figure 14, with the anterior area showing mostly hairs, the posterior one bearing spinules.

The mandible (Fig. 15) has the usual two stout elements and two spinulose setae. The paragnath (Fig. 16) is a large lobe bearing spinules and hairs. The first maxilla (Fig. 17), the second maxilla (Fig. 18), and the maxilliped (Fig. 19) present no outstanding differences from other species. Seen ventrally, the maxillipeds are connected by a line (Fig. 20) probably representing a trace of an intercoxal plate. The postoral protuberance is neither well defined nor particularly well developed.

The armature of legs 1–4 (Figs. 21, 22, 23, and 24) is as follows (the Roman numerals representing the spines, the Arabic numerals the setae):

P1	protopod	0:1	1:I	exp	I:0	I:1	I,7
				end	0:1	0:1	I,5
P2	protopod	0:1	1:0	exp	I:0	I:1	II,7
				end	0:1	0:2	I,II,3
P3	protopod	0:1	1:0	exp	I:0	I:1	II,7
				end	0:1	0:2	I,II,3
P4	protopod	0:1	1:0	exp	I:0	I:1	I,7
				end	0:1	0:2	I,II,2

The formula for the terminal segments of the exopods and endopods depends in some cases upon whether an element is interpreted as a "spine" or a "seta." Thus, when comparing the armature of the legs, reference should also be made to the figures.

Leg 1 bears on its basis an inner spine 70 μ in length, and its exopod spines have subterminal setules; both of these features

being absent on legs 2–4. On leg 3 the distalmost of the three spines on the last exopod segment is somewhat intermediate in form between a spine and a seta, and the distalmost of the three spines on the last endopod segment is nearly twice the length of the other two (48, 49, and 95 μ, respectively). The spines on all four legs have slight spinulose flanges.

Leg 5 (Figs. 25 and 26) has a rather short and broad free segment, measuring 134 × 84 μ (based on 4 specimens), or about 1.6 times longer than wide. There are rows of spinules on both outer and inner margins. The three terminal spines are 60, 57, and 68 μ in length, respectively, from outer to inner, and the terminal seta is 104 μ long. (One female from Nosy Iranja showed a normal right leg, but the left leg 5 was abnormal, lacking the innermost terminal spine and having a smooth inner margin on the free segment.) The seta arising from the body near the base of the free segment is about as long as the free segment. The area adjacent to the insertion of the free segment of leg 5 is ornamented with groups of slender setules and spines, as shown in the figures.

Leg 6 is apparently absent.

The color in living specimens in transmitted light includes red speckling along the sides of the prosome, a red eye, a gray ovary, and orange-red to gray egg sacs.

Male.—The body length (not including the setae on the caudal rami) is 1.57 mm (1.44–1.73 mm), and the greatest width is 0.67 mm (0.61–0.77 mm), based on 10 individuals. The body form (Fig. 27) in general resembles that of the female, with a similar ratio of prosome to urosome. The tergum of the fifth pedigerous segment appears to be not as clearly defined as in the female and lacks the two groups of hairs near the insertion of leg 5. The genital segment in dorsal or ventral outline is subcircular (Fig. 28), 190 μ long and 247 μ wide. The four postgenital segments are 125, 104, 72, and 62 μ in length, respectively. A few scattered refractile points and hairs may be seen on the dorsal surface of the genital and postgenital segments, as shown in the figure.

The caudal ramus is similar to that of the female but a little shorter, its average size (based on 5 individuals) being 88 × 51 μ, or about 1.7 times longer than wide.

The spermatophore attached to the body of the female (Fig. 29) is pyriform, 99 × 70 μ, not including the short neck; the spermatophore seen inside the body of the male (Fig. 30) appears to be a little smaller (86 × 62 μ).

The rostral area is like that of the female.

The first antenna is similar to that of the female, but there is an additional seta on the third and fourth segments (Fig. 31), so that the formula for the seven segments is: 4, 15, 7, 4, 4 + 1 aesthete, 2 + 1 aesthete, and 7 + 1 aesthete.

The second antenna resembles that of the female.

The labrum (Fig. 32) lacks the line of long setules on its anterior surface and shows a more extensive area of fine, close-set spinules medially below the free ventral edge (replacing the two rows of spinules in the female). The second metastomal area has only one row of blunt triangular spines (instead of two as in the female).

The mandible, paragnath, and first maxilla are similar to those of the female. The second maxilla (Fig. 33) shows the stout inner spine on the second segment here replaced by a strongly sclerotized, claw-like element lacking an articulation with the segment. The details of the compound element are also slightly modified (Fig. 34).

The maxilliped (Figs. 35, 36, and 37) has a single seta on the first segment. The proximal inner angle of the second segment is greatly expanded, the segment being 190 μ along its outer margin and 169 μ in greatest width. There are three rows of blunt spinules and two setae on the inner surface of this segment. It also shows three groups of cuticular furrows on its inner posterior surface, as indicated in Figure 36. The third segment is very short and unarmed. The fourth segment extends into a long claw 260 μ in length (measured along its axis and

not along the curvature) bearing near its base a slender setiform process, a slender seta, and a minute setule.

Leg 1 lacks the inner spine on the basis (Fig. 38); otherwise legs 1–4 are similar to those of the female, with the same armature.

Leg 5 (Fig. 39) has a free segment more slender than in the female, measuring about 138 × 68 μ, or about 2 times longer than wide, with its armature resembling that in the female (the three spines are 70, 68, and 74 μ in length from outer to inner, the seta 83 μ long). The processes at the outer sides of the bases of the two proximal spines are larger than in the female. The seta arising from the body near the base of the free segment is shorter than the segment; near this seta there is a row of spinules, but the group of slender setules seen in the female is absent.

Leg 6 (Fig. 40) consists of a sclerotized flap bearing laterally a seta 64 μ in length. The sclerotizations on the segment, against which these flaps fit, are particularly heavy.

The color in living specimens resembles that of the female.

Remarks on its biology.—H. axiophilus was found in water in the relatively small burrows of *Axius acanthus* but never in burrows of larger size and presumed to be inhabited by other animals. (In every collection of *H. axiophilus* the copepod next described also occurred.) It seems to show a distinct preference for the burrows of *Axius* in the Nosy Bé region. The copepod apparently lives in the burrow water and not on the body of *Axius*, since no copepods were found on the bodies of 16 *Axius* dug from their burrows. All specimens were recovered by drawing water from the burrows by means of a small bilge pump.

In artificial lighting under a binocular microscope, the copepods showed a fairly strong positive photokinesis, with the majority of them concentrating on the side of the dish nearest the light source.

Two specimens (one female and one male) were observed whose intestines contained fragments of copepods, suggesting that in part at least the food of *H. axiophilus* includes copepods.

Relationship to other species.—H. axiophilus belongs to the group of species in the genus *Hemicyclops* having four setae on the first segment of the first antenna and a short terminal segment on the second antenna. It seems to be closest to *H. visendus* Humes, Cressey, and Gooding, 1958 (found associated with *Upogebia* at Nosy Bé). It differs from that species, however, in several respects. In the female of *H. visendus* the caudal ramus is about 1.7 times longer than wide, a rather large number of the setae on the first antenna have conspicious lateral hairs, and the genital segment does not show two lateral expansions; in the male the body length is 2.06 mm, the genital segment is subrectangular in dorsal or ventral outline rather than subcircular, the second segment of the maxilliped is pyriform in outline rather than subtriangular, and the free segment of leg 5 is elongate, being 2.4 times longer than wide.

Hemicyclops amplicaudatus[1] n. sp.

Pl. VII, figs. 41–46; Pls. VIII–X; Pl. XI, figs. 71–72

Type material.—7 females and 17 males from water in burrows of *Axius* (*Neaxius*) *acanthus* A. Milne Edwards (determined by Dr. Fenner A. Chace, Jr.) in sand exposed at low tide along the southwestern shore of Nosy Iranja, about 55 kilometers southwest of Nosy Bé, Madagascar. Collected by A. G. Humes September 7, 1960. Holotype female, allotype, and 11 paratypes (2 females and 9 males) deposited in the United States National Museum, Washington; 6 paratypes (1 female and 5 males) in the Museum of Comparative Zoology, Cambridge, Mass.; and the remaining paratypes in the collection of the author.

Other specimens (from burrows pre-

[1] The specific name *amplicaudatus*, from Latin *amplus* = wide, broad, and *cauda* = tail, refers to the unusually wide genital segment in this species.

sumed to be of the same host). — 13 females and 13 males on the northeastern end of the beach at Andilana, on the northern side of Nosy Bé, September 4, 1960; 7 females from the same locality, October 8, 1960; 11 females, 3 males, and 1 copepodid again from the same locality, August 8, 1963; 9 females and 1 male from Nosy Iranja, November 4, 1963; 9 females and 1 male from Antsakoabe, east of Andilana, November 1, 1963; 6 females and 5 males from Navetsy, on the northernmost end of Nosy Bé, November 3, 1963; 30 females and 21 males from Nosy N'Tangam, near Dzamandzar, Nosy Bé, January 1, 1964; and 10 females and 2 males from the same locality, December 2, 1963.

Female.—The length of the body (not including the setae on the caudal rami) is 1.34 mm (1.24–1.42 mm), and the greatest width (in the posterior third of the cephalosome) is 0.57 mm (0.53–0.62 mm), based on 10 individuals. The prosome is distinctly longer than the urosome (Fig. 41), the ratio being about 1.5 : 1. The epimera of pedigerous segments 1–4 are laterally somewhat rounded and closely imbricate, those of the segment bearing leg 4 partly covered by the tergal area of the preceding segment. The dorsal surface of the prosome bears scattered hairs mounted on refractile points; these hairs extend around onto the ventral edges of the cephalosome (Fig. 42). The segment bearing leg 5 has dorsally two raised lobes, each bearing a somewhat ragged membranous fringe along the outer edge and resembling reduced epimera (Figs. 43 and 61). The genital segment (Figs. 43 and 44) is greatly widened, 280 μ in length (including the attached spermatophores) $\times$ 325 μ in greatest width. An intersegmental sclerite extends ventrally and laterally between the segment of leg 5 and the genital segment. The egg sacs are attached far forward and laterally on the genital segment, lying dorsally to the fifth legs. Each egg sac is moderately elongated (Fig. 41), about 430 $\times$ 154 μ, and contains many small eggs.

The spermatophores are cemented firmly to the posterolateral areas of the genital segment in all females observed (Figs. 43 and 44).

The three postgenital segments measure 75, 53, and 41 μ in length, respectively. The surfaces of these segments (and the genital segment) show a few hairs and refractile points, as indicated in the figures. The last postgenital segment has dorsally a flap-like operculum (Fig. 45) extending into the wide anal area. The sides of the aperture are finely rugose so as to produce the appearance of striations around the operculum. The last segment bears a short row of very small spinules on its ventral posterior margin near the insertion of each ramus.

The caudal ramus (Fig. 45) is inserted somewhat ventrally, and measures 71 $\times$ 20 μ, about 3.6 times longer than wide, the length being taken along the inner edge. A small hyaline hair (setule ?) is situated on the outer margin near the base. The dorsal seta has lateral hairs. The lateral seta and the outermost terminal seta have minute spiniform projections about midway along their lengths (two such projections on the former and one on the latter), beyond which the setae are annulated. The innermost distal seta is 112 μ in length, with conspicuous lateral hairs along the inner edge and less well-developed hairs along the outer edge. The inner long terminal seta is 414 μ in length, the outer 240 μ, both with short outer spinules and long inner hairs and both showing a basal peg. The distal end of the ramus overlaps ventrally the insertions of the four terminal setae.

The rostral area (Fig. 46) is slightly protuberant anteriorly but weakly developed, with a few hairs as shown in the figure.

The first antenna (Fig. 47) is 7-segmented, about 350 μ in length, the lengths of the segments from the base, respectively, 20, 49, 49, 58, 44, 50, and 38 μ (measured along their non-setiferous margins). The first segment bears 4 setae, the second 15, the third 6, the fourth 3, the fifth 4 and 1 aesthete, the sixth 2 and 1 aesthete, and the seventh 7 and 1 aesthete; the formula thus

being the same as in *H. axiophilus*. The aesthetes on segments 5 and 6 have their basal portions (about one-fifth) sclerotized like a seta. All the long setae are annulated and naked. The longest seta on the last segment is unusually long, about 290 μ.

The second antenna (Fig. 48) is 4-segmented, with the third segment considerably produced on the inner (anterior) corner and bearing four elements: two of them relatively short spines with a flange of spinules on the anterior side and a subterminal setule, the third very long and strongly recurved with annulations and a spinulose flange (Fig. 49), and the fourth a naked annulated seta. The fourth segment is subcylindrical, 40 × 20 μ, and bears 7 setae, of which the outermost has distinct lateral hairs and is relatively short; the remaining 6 setae are either naked or show very short lateral spinules as indicated in the figure.

The labrum (Fig. 50) is slightly trilobed, with teeth and setules as shown in the figure. The two metastomal areas have a complex ornamentation, as indicated in Figure 50.

The mandible (Figs. 51 and 52) is provided terminally with two stout elements of unusual shape for the genus, both of them edged with tooth-like serrations (perhaps modified spines ?) and the outer one having a dorsal protuberance that fits into a concavity on the adjacent element, and with two inner spinulose spines. The paragnath (Figs. 50 and 53) is an elongated hairy lobe. The first maxilla (Fig. 54) is similar to that of other species. The second maxilla (Fig. 55) has the same armature as in that of other species, but the ornamentation of the spines and setae is less strongly developed, and the accessory spinous processes of the terminal compound element are replaced by spinulose flanges. The maxilliped (Fig. 56) is small and rather slender. The bases of the two maxillipeds are connected ventrally by a weak line perhaps representing a trace of the intercoxal plate.

The armature of legs 1–4 (Figs. 57, 58, 59, and 60) has the same formula as in *H. axiophilus*. The element distal to the two outer spines on the third exopod segment of all four legs is here considered as a modified seta, since it shows annulations. The outer seta on the basis of legs 2 and 3 is relatively short, but in legs 1 and 4 this seta is long, reaching 200 μ in length in leg 4 (longer than the entire exopod which is about 140 μ long).

Leg 5 (Fig. 61) has two segments, the distal one elongate, 110 × 34 μ, or about 3 times longer than wide. There are rows of long spinules on both outer and inner margins. The three spines measure 49, 35, and 54 μ in length, respectively, from outer to inner. The seta is 99 μ long. The seta on the basal segment of the leg is 112 μ in length.

Leg 6 is apparently absent.

In life, in transmitted light, the body is nearly colorless, the eye red, and the spermatophores brownish.

Male.—The body length (not including the setae on the caudal rami) is 1.0 mm (0.92–1.0 mm) and the greatest width is 0.39 mm (0.35–0.41 mm), based on 10 individuals. The form of the body (Fig. 62) is much like that of the female. The ratio of the length of the prosome to that of the urosome is about 1.4 : 1. The segment bearing leg 5 shows dorsally the two raised lobes only weakly developed, and lacks the membrane seen in the female. The genital segment (Fig. 63) is widened, 195 μ in length × 234 μ in greatest width, with its lateral margins more evenly rounded than in the female. The four postgenital segments are 65, 55, 43, and 36 μ in length, respectively. There are scattered hairs and refractile points over the surface of the urosome as shown in the figure.

The caudal ramus resembles that of the female.

The spermatophore while inside the body of the male has the form shown in Figure 63, with its neck arising subterminally on the inner anterior margin. The greatest length of the spermatophore is 130 μ, the width anterior to the neck 78 μ, and the width in the posterior third 49 μ.

The rostral area is like that of the female.

The first antenna is similar to that of the female, but the third and fourth segments have an additional seta (7 and 4, respectively, as in the male of *H. axiophilus*), indicated in Figure 64.

The second antenna resembles that of the female.

The labrum, metastomal areas, mandible, paragnath, and first maxilla are essentially like those of the female.

The second maxilla (Figs. 65 and 66) has the large dorsal spine transformed into a very large, blunt, strongly sclerotized, claw-like process. The compound element is also modified.

The maxilliped (Fig. 67) has a single seta on the first segment. The second segment has its proximal inner angle greatly expanded, with the inner margin of the segment being distinctly curved (not almost straight as in *H. axiophilus*). The length of this segment is 150 μ along the outer edge and its greatest width is 117 μ. Along its inner surface there are two rows of stout spines and a row of slender spinules, plus the usual two small setae. The third segment is very short and unarmed. The fourth segment forms part of the long claw which is 179 μ in length (measured along its axis and not along the curvature). The claw has an interrupted membranous fringe along part of its concave edge, and near its base bears two small setae (the one on the anterior surface of the claw annulate) and a spinous process, as shown in the figure. A distinct transverse line may be seen ventrally between the bases of the maxillipeds (Fig. 68), probably representing the edge of the intercoxal plate.

Leg 1 lacks the inner spine on the basis (Fig. 69); otherwise legs 1–4 are similar to those of the female, with the same spine and setal formula but with somewhat larger endopod spines.

Leg 5 (Fig. 70) has a single free segment which is shorter than in the female, measuring 99 × 43 μ, or about 2.3 times longer than wide. Its armature resembles that of the female (the three spines being 53, 47, and 53 μ in length, respectively, from outer to inner, and the seta 66 μ). The seta on the basal area is shorter than in the female (about 60 μ in length).

Leg 6 (Figs. 71 and 72) consists of a ventrolateral posterior flap bearing a spine 47 μ in length with fine lateral spinules.

The color in life resembles that of the female.

Remarks on its biology.—Each time that *H. amplicaudatus* was collected it was found in company with *H. axiophilus*, though in smaller numbers. As in the case of *H. axiophilus*, this species seems to show a preference for *Axius* burrows, apparently living in the water rather than on the bodies of the crustaceans, since no copepods were recovered after washing the bodies of *Axius*.

Relationship to other species.—*H. amplicaudatus* differs in its unusually broad genital segment from all known species of *Hemicyclops* that have four setae on the first segment of the first antenna. Only one species, *H. aberdonensis* (T. and A. Scott, 1892), shows a genital segment approaching that of *H. amplicaudatus* in width, but here the shape is very different (see the Scotts' pl. VI, figs. 1 and 12). Other distinctive features are the form of the spermatophores, the unusually long, recurved, fringed spine on the third segment of the second antenna, and the unusual shape of the two stout elements on the end of the mandible.

Hemicyclops carinifer[1] n. sp.

Pl. XI, figs. 73–81; Pls. XII–XV; Pl. XVI, figs. 109–115

Type material.—16 females and 4 males from water in burrows 3–4 cm in diameter and more than 90 cm deep, of unknown origin, in intertidal sand at Bamoko, 3 kilometers north of Dzamandzar, Nosy Bé, Madagascar. Collected by A. G. Humes October 22, 1960. Holotype female, allotype, and 11 paratypes (10 females and 1

[1] The specific name *carinifer*, from Latin *carina* = a keel, and *ferre* = to bear, alludes to the keel-like ridge on the ventral area between the maxillipeds and the first pair of legs.

male) deposited in the United States National Museum, Washington; 6 paratypes (5 females and 1 male) in the Museum of Comparative Zoology, Cambridge, Mass.; and one dissected paratype male in the author's collection.

Other specimens (from similar burrows).—19 females in sand near the village of Antafiabe, on the western shore of Nosy Faly, an island to the east of Nosy Bé, October 21, 1960; 1 female in sand on the southeastern shore of Nosy Sakatia, opposite the village of Antanambe, about 3 kilometers west of Nosy Bé, October 23, 1960; 16 females, 11 males, and 1 copepodid in muddy sand at the Centre d'Océanographie et des Pêches, Pointe à la Fièvre, Nosy Bé, August 28, 1960; 2 females from the same locality, August 22, 1960; 1 female in muddy sand near mangroves at Ambanoro, across the bay from the Centre d'Océanographie et des Pêches, Nosy Bé, August 23, 1960; 36 females, 9 males, and 1 copepodid from sand west of Pte. Ambarionaomby, Nosy Komba, March 14, 1964; 10 females from the same locality, March 28, 1964; 21 females and 5 males in sand at Bamoko, Nosy Bé, February 29, 1964; 2 females and 1 male from sand at Antviabe, on the southern shore of Nosy Komba, March 16, 1964; 6 females from sand at Nosy Kisimany, 25 kilometers southwest of Nosy Bé, April 12, 1964; 2 females from sand at Madirokely, Nosy Bé, April 28, 1964; 12 females and 2 males from sand at Befotaka, Nosy Bé, April 29, 1964; 22 females and 12 males from sand at Nosy Roty, near Nosy Sakatia, May 12, 1964; 6 females and 2 males from muddy sand at Ampassipohe, Nosy Bé, May 11, 1964; and 1 female from sand at Boloboxo, Nosy Faly, May 13, 1964.

Female.—The length of the body (excluding the setae on the caudal rami) is 1.42 mm (1.32–1.55 mm), and the greatest width (in the posterior half of the cephalosome) is 0.50 mm (0.45–0.52 mm), based on 10 individuals. The body (Fig. 73) has a rather slender form, the prosome being only slightly longer than the urosome, with the ratio 1.18 : 1. The dorsal body surface has relatively few small hairs. The epimera are prominent but have subacute or rounded posterolateral angles in dorsal or ventral view. The genital segment (Fig. 74) is wider than long, 132 × 161 μ, broadest in its anterior third, and with the median posterior dorsal surface raised and abruptly truncated (Fig. 75), forming a transverse crescentic sclerotized line in dorsal view. The egg sacs are attached dorsolaterally near the widest part of the segment. Near the attachment of each egg sac there are three slender naked setae (Fig. 76), 62, 57, and 23 μ in length, respectively, borne within the genital area surrounding the oviducal opening. Each sac is slender and elongated, 560 × 123 μ, held parallel to the abdomen in preserved specimens, and containing 4 rows of approximately 12 eggs each (Fig. 77).

No spermatophore was found attached to the female.

The four postgenital segments measure 91, 78, 55, and 117 μ in length, respectively. The anal segment (Figs. 78 and 79) has a posterior fringe of small spinules extending from each side dorsally and ventrally near the insertions of the rami; this segment shows dorsally a large, oval, weakly sclerotized anal region and ventrally a pair of transverse rows of slender spinules near the anterior edge.

The caudal ramus (Fig. 80) measures 220 × 27 μ (the width taken at its midregion, the length along its inner edge), about 8.0 times longer than wide. A small hyaline hair (setule ?) is situated on the outer margin in the proximal third. The lateral seta is naked, 49 μ in length. The dorsal seta, borne on a minute basal segment, is naked, 122 μ long. The outermost terminal seta is naked, 59 μ long. Of the 2 long terminal setae, the outer one is 426 μ and the inner one 280 μ in length, both with a basal peg and with lateral hairs. The innermost terminal seta is 114 μ in length and haired along its inner edge. The distal end of the ramus slightly overlaps ventrally the insertions of the 4 terminal setae.

The rostral area (Fig. 81) is small and inconspicuous, set off from the anterior surface of the head by a furrow, and protruding ventrally.

The first antenna (Fig. 82) is about 582 μ in length, with 7 segments, in length from the base, 55, 91, 33, 130, 83, 83, and 106 μ (measured along their forward setiferous margins). The first segment bears 5 setae, the second 15, the third 6, the fourth 3, the fifth 4, the sixth 2 and 1 aesthete, and the seventh 7 and 1 aesthete. Certain of the setae have lateral hairs, as indicated in the figure. The terminal aesthete seems to insert independently of any seta.

The second antenna (Fig. 83) is 4-segmented, with the third segment not produced on the inner distal corner and bearing there 4 setae as indicated, the largest similar in structure to the 4 terminal curved setae; the last segment is slender and elongated, 105 × 22 μ, about 4.8 times longer than wide, with the usual 7 elements. The long spinules along the edges of the third and fourth segments are rather flattened and have brush-like tips (as in Fig. 84).

The labrum (Fig. 85) has the usual transversely oval shape, its free margin having a row of large teeth, its sublateral areas a few spinules, and its lateral areas groups of hairs.

The metastomal areas (Fig. 86) have an ornamentation as shown in the figure.

The mandible (Fig. 87) has a terminal armature consisting of a stout spine with teeth on each side, two more slender lamelliform spines bearing lateral spinules, and a very small spinule. The paragnath (Fig. 88; see also Fig. 86) is a lobe bearing a distal row of teeth (broad spinules ?), a small semicircular subapical lobe, and two groups of hairs on its posterior surface which merge into a proximal patch; the more ventral row of these hairs continues distally into a line of minute denticles. The first maxilla (Fig. 89) and the second maxilla (Fig. 90) have the number and arrangement of the spines and setae similar to other species, but with minor differences in their lateral spinules as indicated in the figures. The maxilliped (Fig. 91) has a large inner process on the fourth segment, this process being distinctly bent, approaching an S in contour; there are 2 slender setae arising from the terminal segment; the tips of the S-shaped process and of the terminal element are rather blunt, while the proximal seta on the first segment and the 2 setae on the second segment have minutely bifid tips (see Fig. 92). The bases of the maxillipeds are connected ventrally by a cuticular line (Fig. 93) probably representing a trace of the intercoxal plate.

The area between the bases of the maxillipeds and the first pair of legs, forming the postoral protuberance, lacks ornamentation but shows prominent lateral sclerites (Fig. 93), and is produced medially to form a longitudinal keel (Fig. 94).

The armature of legs 1–4 (Figs. 95, 96, 97, and 98) is as follows:

P1	protopod	0:1	1:I	exp	I:0	I:1	III,5
				end	0:1	0:1	I,5
P2	protopod	0:1	I:0	exp	I:0	I:1	III,6
				end	0:1	0:2	I,II,3
P3	protopod	0:1	1:0	exp	I:0	I:1	I,II,5
				end	0:1	0:2	I,III,2
P4	protopod	0:0	1:0	exp	I:0	I:1	I,II,5
				end	0:1	0:1	I,III

Leg 1 bears on the basis a straight inner spine 50 μ in length; the outer distal corner of the second endopod segment of this leg forms a spiniform process. Leg 4 shows the rami relatively more elongated than in the preceding legs; the last endopod segment has four spines, 31, 52, 87, and 26 μ in length from outer to inner, respectively. The coxa of leg 4 lacks an inner seta. All four legs show minute flagella near the tips of the outer exopod spines. Legs 1–3 show 2–3 unusually strong lateral spinules on the outer side of the bases of certain of the distal setae on the last endopod segment, as shown in the figures.

Leg 5 (Fig. 99) has a ventral row of spinules near the seta on the basal segment. The distal segment is elongated, 114 μ

along its inner edge; it is wider in its basal half (45 μ) than in its distal half (36 μ), and deeply indented at the insertion of the lateral seta. There is an outer marginal row of spinules on the basal half, and a similar inner row of spinules along part of the margin of the distal half. The outer margin forms a blunt projection near the insertion of the marginal spine and also near the distal outer spine; there is a row of slender spinules ventrally on these projections. There is also a row of minute spinules ventrally near the insertion of the inner distal spine. The 3 spines and the seta measure 42, 42, 77, and 49 μ in length from outer to inner, respectively.

Leg 6 is apparently absent, but may be represented by the 3 setae near the egg sac attachments.

The color in living specimens, in transmitted light, is translucid, slightly amber or reddish brown, with reddish orange globules in the prosome, the ovary dark gray, the eye red, and the egg sacs reddish gray to orange.

Male.—The body length (not including the setae on the caudal rami) is 1.61 mm (1.57–1.66 mm) and the greatest width is 0.55 mm (0.53–0.58 mm), based on 4 individuals. The ratio of the prosome to urosome is 1.35 : 1, with the prosome only slightly longer (Fig. 100) than in the female. The genital segment (Fig. 101) is nearly quadrate in dorsal or ventral view, measuring 156 × 151 μ. The 4 postgenital segments have proportions similar to those of the female. The ornamentation of the anal segment is also like that in the female.

The caudal ramus is as in the female.

Spermatophores were seen only inside the genital segment of the male (Fig. 101).

The rostral area resembles that of the female.

The first antenna is similar to that of the female, but the third segment has 7 setae and the fourth 4 setae (see Fig. 102).

The second antenna is like that of the female.

The labrum (Fig. 103) has a row of slender spines along its free edge and a row of additional, broad, scale-like denticles curving dorsally along the posteroventral face on either side. The metastomal areas are much like those of the female, but the most posterior rows of spines are smaller (Fig. 104).

The mandible, paragnath, first maxilla, and second maxilla are similar to those of the female.

The maxilliped (Figs. 105 and 106) has 2 unequal setae on the first segment, the proximal seta with prominent lateral spinules, the distal one naked. The second segment is slender, 239 × 101 μ, with 2 rows of broad spinules and 2 annulated setae on its inner surface; one of these rows is interrupted by the bases of the setae, proximal to which the row becomes a series of blunt serrations and then a group of broad spinules. The third segment is short and unarmed. The fourth segment forms part of the claw, which is 260 μ in length (measured along its axis and not along the curvature), slightly sinuous in outline, and with a distinct flexure near its tip, where there is a small outer lamella and 2 rows of denticle-like ridges which decrease in size proximally. Near the base of the claw there may be seen a setiform process and 3 slender setae (the one nearest to the process recurved and unilaterally haired) (see Fig. 107).

The postoral area between the bases of the maxillipeds and the first pair of legs (Fig. 108) is raised to form a ventral longitudinal keel (Fig. 109). This keel bears a row of serrations along its edge, a short transverse crescentic row of irregular serrations anteriorly, and laterally a few minute refractile points. Between the bases of the second maxillae there is a minute bifurcated sclerotization.

Legs 1–4 have the same number and arrangement of spines and setae as in the female. The inner spine on the basis of leg 1 (Fig. 110) is larger than in the female and slightly recurved, about 77 μ in length, with a transverse weakening in the sclerotization in its basal third, a row of minute refractile points, and a cluster of rather

blunt minute spinules near its tip (Fig. 111). The second endopod segment of leg 1 does not show a distal outer spiniform process as in the female. The middle spine on the outer side of the third exopod segment of leg 1 is relatively smaller than in the female. Leg 2 shows the 3 spines on the third endopod segment of different proportions than those of the female, their lengths from outer to inner being 38, 28, and 77 μ, the middle spine being distinctly shorter and more slender (Fig. 112). There is on this endopod only a single terminal spiniform process. (One male showed the distal margin of the third endopod segments of leg 3 with a single spiniform process between the 2 middle spines on one leg, and with a bifurcated process at this point on the opposite leg, as indicated in Fig. 113).

Leg 5 (Fig. 114) is similar to that of the female, but the row of spinules on the distal inner margin of the distal segment is shorter, and the processes near the bases of the 2 outermost spines are more acute than rounded.

Leg 6 (Fig. 115) consists of a small ventrolateral flap on whose extreme lateral portion a slender seta 34 μ in length is borne on a slight prominence.

The color in living specimens resembles that of the female.

Remarks on its biology.—H. carinifer frequently occurred in the same burrows with the following species (in 10 of 16 collections).

Relationship to other species. — This copepod falls in the group of *Hemicyclops* species having five setae on the first segment of the first antenna, an elongated terminal segment on the second antenna, and elongated caudal rami. Four species attributable to this group (*H. elongatus* Wilson, 1937, *H. adhaerens* (Williams, 1907), *H. subadhaerens* Gooding, 1960, and *H. arenicolae* Gooding, 1960) have in the female a caudal ramus which is much shorter than in *H. carinifer* (only a little more than 4 times longer than wide, or less). These species also appear (as nearly as can be ascertained from the published descriptions) to lack two features of *H. carinifer*, namely, the projections near the insertions of the two outer spines on the distal segment of leg 5, and the keel on the ventral surface between the maxillipeds and the first legs.

Hemicyclops diremptus[1] n. sp.

Pl. XVI, figs. 116–117; Pls. XVII–XX; Pl. XXI, figs. 147–152

Type material.—6 females and 5 males from burrows of unknown origin 3–4 cm in diameter and more than 90 cm deep in intertidal sand near the village of Antafiabe, on the western shore of Nosy Faly, an island to the east of Nosy Bé, Madagascar. Collected by A. G. Humes October 21, 1960. Holotype female, allotype, and 3 paratypes (2 females and 1 male) deposited in the United States National Museum, Washington; 2 paratypes (1 female and 1 male) in the Museum of Comparative Zoology, Cambridge, Mass.; and the remaining paratypes in the author's collection.

Other specimens (from similar burrows).—1 male from sandy mud in front of the Centre d'Océanographie et des Pèches, Nosy Bé, August 22, 1960; 8 females in sand west of Pte. Ambarionaomby, Nosy Komba, March 14, 1964; 2 females from the same locality, March 28, 1964; 1 male from sand north of Antafiabe, Nosy Faly, March 15, 1964; 5 females and 13 males from sand at Nosy Kisimany, April 12, 1964; 1 female and 2 males from sand at Madirokely, Nosy Bé, April 28, 1964; 176 females and 118 males from sand at Befotaka, Nosy Bé, April 29, 1964; 77 females and 21 males from sand at Nosy Roty, near Nosy Sakatia, May 12, 1964; 15 females and 22 males from muddy sand at Ampassipohe, Nosy Bé, May 11, 1964; and 1 female and 2 males from sand at Boloboxo, Nosy Faly, May 13, 1964.

Female.—The length of the body (not including the setae on the caudal rami) is

[1] The specific name *diremptus*, from Latin *dirempere* = to separate, divide, alludes to the divided condition of the genital segment in the female.

1.90 mm (1.82–1.97 mm), and the greatest width (in the posterior part of the cephalosome) is 0.81 mm (0.76–0.87 mm), based on 6 individuals. The prosome is moderately broad and a little longer than the urosome, the ratio being about 1.37 : 1 (Fig. 116). In dorsal or ventral view the epimera are conspicuous and angulate. The segment bearing leg 5 is narrow in front and broadened posteriorly at the level of the legs, where it shows a dorsal transverse sclerotized ridge (probably a remnant of the epimeron of this segment). An intersegmental sclerite occurs between the first two urosomal segments. The genital segment (Figs. 117, 118, and 119) is widened and divided transversely into an anterior portion bearing the attachments of the egg sacs and a slightly narrower posterior portion. The length of the genital segment is 195 μ, the anterior part being 117 × 273 μ and the posterior part 78 × 229 μ.

The egg sacs are attached dorsolaterally on the anterior half of the genital segment between small dorsolateral and more extensive ventrolateral flanges (see Fig. 119). Each egg sac is about 560 × 200 μ, and contains numerous small eggs (Figs. 116 and 117).

The three postgenital segments measure respectively 114 × 178 μ, 62 × 133 μ, and 62 × 114 μ, the first segment being longer, wider, and more globose than the other two, which are somewhat more closely associated. The last segment has near the insertion of each caudal ramus a ventral transverse row of about four small spinules followed by a row of much smaller spinules (see Figs. 119, 120, and 121). The thinly sclerotized anal area occupies virtually the whole dorsal side of the anal segment. There is no anal plate, but the posterior edge of the preceding postgenital segment is modified (see Fig. 121).

The dorsal surface of the prosome and the dorsal and ventral surfaces of the urosome are covered with minute hairs, each arising from a refractile point.

The caudal ramus (Fig. 121) is elongated, 117 × 24 μ (the length measured along the inner edge and the width at the middle of the ramus), nearly 5 times longer than wide. A small hyaline hair occurs on the basal outer margin and a few minute hairs are to be found on the ventral surface. The lateral seta is 47 μ in length and the outermost terminal seta is 65 μ, including the basal shaft and the distal flagelliform part. The dorsal seta is 91 μ long and bears only a few lateral hairs. The innermost terminal seta is 112 μ in length with an inner row of hairs. The inner long terminal seta is 728 μ and the outer one 437 μ in length, both with lateral spinules, these being at first widely spaced and long, then in the distal two-thirds of the setae short and closely spaced.

The rostral area (Fig. 122) is very weakly developed.

The first antenna (Fig. 123) is about 400 μ long, 7-segmented, the segments, beginning at the base, 20, 55, 52, 88, 51, 55, and 47 μ in length (measured along their non-setiferous margins). The formula for the armature is 4, 15, 6, 3, 4 + 1 aesthete, 2 + 1 aesthete, and 7 + 1 aesthete. Most of the setae are annulated with minute lateral hairs, but there are a few setae which are entire with longer lateral hairs (1 on the second segment, 2 on the fifth, 1 on the sixth, and 4 on the seventh).

The second antenna (Fig. 124) is 4-segmented, with the third segment produced on the inner distal corner where it bears four elements: proximally a small posterior seta, more distally a large and slightly sinuous spine, and distally two more slender and somewhat recurved spines with subterminal setules. The fourth segment is quadrate in flat view, 29 × 29 μ, and bears seven setae, the four long curved setae with their tips not as attenuated as the others, and the outermost of these seven setae lying across the bases of the others and having long lateral spinules.

The labrum (Fig. 125) is tilted forward, so that the ventral view shown in the figure is equivalent to posterior in other species.

The labrum is somewhat trilobed and has setules and teeth as shown in the figure; there is a curved row of long hyaline setules along the anteroventral margin. The metastomal areas have a complex ornamentation, as indicated in Figure 125.

The mandible (Fig. 126) has the usual two stout elements and two well-developed setae with lateral hairs. The paragnath (Figs. 125 and 127) is a stout hairy lobe. The first maxilla (Fig. 128) is similar in structure to that of other species; it has prominent lateral spinules on certain of the setae. The second maxilla (Fig. 129) is armed as in other species, the innermost spine on the second segment having long outer spinules. The maxilliped (Fig. 130) shows the two setae on the second segment with prominent lateral spinules, and the margin distal to these two setae bears a row of hairs. The last maxilliped segment (Fig. 131) bears two large setae (spines?) (one of them with about five very long slender spinules on its inner margin), four more slender setae, and a row of 4–5 slender hyaline setules on the outer side near the bases of the spines. The bases of the maxillipeds are connected by a ventral transverse line as indicated in Figure 125.

The postoral protuberance is poorly differentiated.

The armature of legs 1–4 (Figs. 132, 133, 134, and 135) is similar to that of *H. axiophilus* and *H. amplicaudatus*, although certain elements are difficult to classify as a "spine" or a "seta." In leg 1 the inner spine on the basis is 65 μ in length, its inner margin serrated and its outer margin with a row of short hairs; the margin of the basis medial to this spine is prominently rounded and smooth. In legs 2–4 this inner area of the basis has a broadly rounded margin and bears a row of short marginal setules and another row of hyaline spinules on its anterior surface. The ventral margin of the intercoxal plate of leg 1 bears on each side a row of hairs; in legs 2–4 this margin has on each side a patch of long spinules. The outer margin of the coxa of leg 4 lacks the long hairs seen in the preceding three legs.

Leg 5 (Fig. 136) has a rather broad and short free segment (its greatest diagonal length from the outer proximal corner to the inner distal angle 143 μ, its length along the inner side 125 μ, its greatest width 105 μ). There are rows of spinules on the distal half of both the outer and inner margins. The three spines are 48, 63, and 50 μ in length, respectively, from outer to inner; the seta is very short, only 34 μ in length. A row of spinules occurs laterally on the basal area of the leg just anterior to the insertion of the free segment. The seta on the basal area is 68 μ long. Traces of a basal segment may be seen in the pattern of sclerotization on the segment of leg 5; the fifth legs are joined ventrally by a strong ridge near the posterior edge of this segment.

Leg 6 is apparently absent.

The color in living specimens, in transmitted light, is translucid, the eye red.

Male.—The length of the body (not including the setae on the caudal rami) is 1.14 mm (1.04–1.28 mm) and the width in the posterior part of the cephalosome is 0.48 mm (0.44–0.52 mm), based on 4 individuals. The ratio of the length of the prosome to that of the urosome is about 1.36 : 1 (Fig. 137). The epimera are prominent as in the female. The genital segment (Fig. 138) is undivided and subcircular in dorsal or ventral view, 143 μ long × 174 μ wide. The spermatophore (seen only within the body of the male) is elongated (Fig. 139), 99 × 36 μ including the neck of 13 μ.

The four postgenital segments are respectively 68, 60, 40, and 40 μ in length.

There are hairs and refractile points on both the urosome and prosome as in the female, but the general sclerotization seems to be stronger.

The caudal ramus (Fig. 140) is shorter than in the female, 55 μ (the length along the inner edge) × 28 μ (the greatest width), or two times longer than wide. The setae are arranged as in the female.

The rostral area (Fig. 141) is a little better defined than in the female.

The first antenna is similar to that of the female, but the third segment has 7 setae and the fourth 4 setae (Fig. 142). The second antenna is like that of the female.

The labrum and the metastomal areas (Fig. 143) are generally like those of the female, but the long hyaline setules on the anteroventral margin of the labrum are absent, and the second metastomal area shows only a single row of broad tooth-like spines.

The mandible, paragnath, and first maxilla are like those of the female. The second maxilla (Fig. 144) is similar to that of the female, but the spinules on the innermost spine of the second segment are much less developed.

The maxilliped (Figs. 145 and 146) has a single long seta on the first segment. The second segment has its proximal inner angle greatly expanded, making the segment almost pyriform in outline. The length of this segment along the outer margin is 114 μ, its greatest length along the inner spinose margin is 143 μ, and the greatest width is 112 μ. There are three rows of stout, rather blunt spines along the inner margin, in addition to the usual two setae. The third segment is very short and unarmed. The fourth segment forms part of a long claw 148 μ in length (measured along its axis and not along the curvature), bearing near its base a small seta on the posterior side, and a spinous process and a minute setule on the inner curvature. The transverse line on the ventral surface between the bases of the maxillipeds is weakly developed.

Leg 1 lacks the inner spine on the basis (Fig. 147). Otherwise the spine and setal formula of legs 1–4 is like that of the female. There is a slight sexual dimorphism in the last endopod segment of legs 2–4 (Figs. 148, 149, and 150), where the terminal spine-like processes are reduced and the sclerotization at the base of the two distal spines is stronger.

Leg 5 (Fig. 151) has a free segment which is not as broad as in the female, measuring 85 μ long (along the inner side) × 51 μ in greatest width. Its armature is like that of the female.

Leg 6 (Fig. 152) consists of a ventral flap on the posterior part of the genital segment. It bears a stout spine 30 μ long with minute lateral spinules.

The color is like that of the female.

Remarks on its biology.—H. diremptus was often found in burrows along with *H. carinifer* (in 10 of 11 collections).

Relationship to other species.—H. diremptus belongs to the group of species with four setae on the basal segment of the first antenna, along with *H. axiophilus* and *H. amplicaudatus*. It differs from all other species in this group in having a distinctly divided genital segment in the female. In the original description of *H. bacescui* (Şerban, 1956) the genital segment is described as double, and Stock (1959), who has restudied the species, mentions a trace of a suture on its dorsal surface. The division is much weaker, however, than in *H. diremptus*. *H. bacescui* further differs from the new species in the form of the fifth legs and the caudal rami. *H. indicus* Sewell, 1949, shows lateral indentations on the female genital segment (see Sewell's fig. 16A), but the segment is single. Although this species shows certain similarities to *H. diremptus* (for example, in the form of the fifth legs and in the armature of the second maxilla), it differs in the form of the caudal ramus, in the relative length of the second and third segments of the first antenna, and in the size of the body. The female of *H. leggii* (Thompson and Scott, 1903) is unknown, but the male differs from that of the new species in its body length, in the relative lengths of the first antennal segments, in the form of the innermost terminal spine on the second segment of the second maxilla, in the shape of the second segment of the maxilliped, and in the size of the caudal ramus. The fifth leg of *H. leggii* seems to resemble closely that of the new species.

Hemicyclops kombensis[1] **n. sp.**

Pl. XXI, figs. 153–154; Pls. XXII–XXVI

Type material.—3 females and 2 males from water in burrows of unknown origin 3–4 cm in diameter and more than 90 cm deep in intertidal sand west of Pte. Ambarionaomby, Nosy Komba, near Nosy Bé, Madagascar. Collected by A. G. Humes March 14, 1964. Holotype female, allotype, and one paratype female deposited in the United States National Museum, Washington; the remaining female and male dissected and in the collection of the author.

Other specimens (from similar burrows).—1 male from sand in front of the village of Antviabe, on the southern shore of Nosy Komba, March 16, 1964; 1 female and 1 male from sand at Madirokely, Nosy Bé, April 28, 1964; and 1 female from sand at Nosy Roty, near Nosy Sakatia, May 12, 1964.

Female.—The length of the body (not including the setae on the caudal rami) is 2.27 mm (2.26–2.29 mm), and the greatest width is 0.83 mm (0.80–0.89 mm), based on 3 individuals. The prosome is moderately broad and only slightly longer than the urosome, the ratio being about 1.08 : 1 (Fig. 153). In dorsal or ventral view the epimera of the segments of legs 1–4 are conspicuous and angulate. The segment of the fifth legs shows a dorsal transverse sclerotized band, bearing a row of long slender spinules on each side (Fig. 154). An intersegmental sclerite, best seen from the ventral side, occurs between the first two segments of the urosome. The genital segment (Figs. 154 and 155) is elongated, with the sides nearly parallel except for slight swellings near the attachments of the egg sacs, and shows dorsally in the middle of the segment a transverse internal sclerotization. The segment measures 475 μ in length; its width in the anterior one-fourth is 305 μ and in the posterior half 271 μ.

The egg sacs are attached ventrolaterally far forward on the genital segment, between small dorsal and ventral flanges (Fig. 155). Near the point of attachment there are two minute, rather obscure spiniform processes, each about 10 μ in length. Each egg sac is elongated oval, 633 × 249 μ, and contains numerous rather small eggs (Fig. 156).

The three postgenital segments measure, respectively, 203 × 220, 140 × 184, and 92 × 158 μ. The last segment is thus shorter and narrower than the preceding ones; there is no apparent anal operculum. Above and below the insertion of each caudal ramus there are slight flanges, the dorsal one smooth, the ventral one with an outer row of minute spinules and an inner row of larger spinules (Fig. 157).

The dorsal surface of the prosome and the dorsal and ventral surfaces of the urosome bear minute hairs and refractile points.

The caudal ramus (Fig. 157) is moderately elongated, 170 μ in length, 70 μ wide near the base, 62 μ at the middle, and 54 μ near the distal end; taking the width at the middle, the ramus is 2.74 times longer than wide. A small hyaline hair arises from the outer basal margin. The lateral seta is 68 μ in length and shows only a slight differentiation into a basal shaft and a distal flagellum. The outermost terminal seta is 117 μ long, including the basal shaft of 68 μ and the distal flagelliform part of 49 μ. The dorsal seta is 149 μ long and bears a few lateral hairs. The innermost terminal seta is 260 μ in length and bears lateral spinules, those along the inner side being longer and better developed. The inner long terminal seta is 948 μ and the outer one 588 μ in length, the middle region of both bearing short outer spinules and longer inner hairs (see Fig. 153). The four terminal setae are inserted somewhat dorsally and the resulting ventral flange at the end of the ramus bears a row of minute spinules and a group of longer spinules on the inner angle. Along the distal third of the inner margin of the ramus there is a row of long slender spinules.

[1] The specific name *kombensis*, a combination made from Nosy Komba and Latin *-ensis* = living in, refers to the island where this species was first found.

The rostral area (Fig. 158) is moderately well defined.

The first antenna (Fig. 159) is about 510 μ long, 7-segmented, the segments, beginning at the base, 15, 74, 65, 110, 65, 73, and 56 μ in length (measured along their non-setiferous margins). The formula for the armature is 4, 15, 6, 3, 4 + 1 aesthete, 2 + 1 aesthete, and 7 + 1 aesthete. Most of the setae are annulated and a few of those on the second segment show minute lateral hairs. There are, however, certain entire setae with long lateral hairs (one on the second segment, one on the fourth, 2 on the fifth, one on the sixth, and 4 on the seventh). The armature is thus very similar to that in *H. diremptus*. On the distal anteroventral surface of the second segment there are a few transverse narrow refractile bars.

The second antenna (Fig. 160) is 4-segmented, with the third segment produced on the inner distal corner where it bears four elements: proximally a slender posterior seta, more distally a larger recurved annulated seta, and distally two slender spines bearing unilateral spinules and subterminal setules. The fourth segment is nearly quadrate in flat view, 35 μ in length × 30 μ, and bears seven setae, the four long recurved annulated setae with their tips less attenuated than the others, and the seta lying posteriorly across the bases of the long setae having conspicuous lateral spinules (Fig. 161).

The labrum (Fig. 162) is tilted forward as in *H. diremptus*, and in a ventral and somewhat posterior view has a rather trilobed appearance, with setules and teeth as shown in the figure. The metastomal areas have a complex ornamentation, as indicated in Figure 163.

The mandible (Fig. 164) has two stout elements and two well-developed setae with lateral hairs. The paragnath (Fig. 165) is a moderately elongated lobe bearing hairs and a row of delicate hyaline spinules as indicated. The first maxilla (Fig. 166) is similar in structure to that of *H. diremptus*; the lateral setules on the outermost seta, however, are longer than in that species. The second maxilla (Fig. 167) is in major respects similar to that of *H. diremptus*. The maxilliped (Fig. 168) has the same general form as in *H. diremptus*, but the two setae on the first segment are more slender, and the two setae on the second segment are relatively shorter; the last segment bears two large recurved setae (spines ?), one of them with conspicuous lateral spinules (four on one side and three on the other), and four slender setae. Between the bases of the maxillipeds there is a ventral transverse line as shown in Figure 169.

The area between the maxillipeds and the first pair of legs shows little differentiation.

The armature of legs 1–4 (Figs. 170–173) is similar to that of *H. axiophilus*, *H. amplicaudatus*, and *H. diremptus*, but again certain elements are difficult to classify as a "spine" or a "seta." In leg 1 the inner spine on the basis is 97 μ in length, with both margins bearing a narrow, finely serrated fringe. The margin of the basis medial to this spine is rounded and smooth except for a small tooth-like process near the base of the spine. In legs 2–4 this inner area of the basis bears a row of slender marginal spinules and another row of larger hyaline spinules on its anterior surface. The ventral margin of the intercoxal plate of leg 1 bears on each side a row of long hairs, but in legs 2–4 these hairs are replaced by rather stout spinules. The outer margin of the coxa of leg 4 lacks the long spinules seen on legs 1–3, but a row of slender spinules occurs on the outer posterior margin. On the last segment of the endopod of leg 4 the two inner elements are setiform, with long lateral hairs basally and short lateral spinules in the distal two-thirds.

Leg 5 (Fig. 174) has a free segment which is shaped rather like a petal, narrow at the base but broadened distally; its greatest length is 180 μ, its greatest width 98 μ, and its width basally 32 μ. There are rows of spinules on both outer and inner margins, those on the outer margin being longer than the others. The three spines are 65, 52, and 71 μ in length, respectively, from outer

to inner; the seta is 89 μ long. Rows of small spinules occur ventrally near the insertions of the three spines. The two outer spines are bilaterally fringed, but the inner spine is fringed outwardly and bears small spinules inwardly. The basal area of leg 5 shows a pattern of sclerotization which suggests a discrete segment; the seta is 110 μ long and lightly plumose distally. There is a row of small spinules adjacent to the seta.

Leg 6 is apparently absent.

The color in living specimens in transmitted light is somewhat opaque to light amber, with reddish globules in the prosome, the eye red, the egg sacs reddish brown.

Male.—The length of the body (without the setae on the caudal rami) is 2.09 mm (1.99–2.19 mm) and the greatest width is 0.77 mm, based on 2 individuals. The ratio of the length of the prosome to that of the urosome (Fig. 175) is about the same as that in the female. The epimera of the segment bearing leg 4 are less angular than in the female. The genital segment (Fig. 176) measures 240 × 287 μ, being wider than long, constricted anteriorly, with the posterolateral areas pointed. Spermatophores were not seen in any of the males collected.

The four postgenital segments measure, respectively, 221 × 205, 170 × 167, 124 × 148, and 82 × 140 μ.

As in the female, the prosome and the urosome bear hairs and refractile points. The general sclerotization of the body is stronger than in the female (see Fig. 187 below).

The caudal ramus (Fig. 177) is relatively shorter than in the female, 132 μ long, 58 μ wide basally, 54 μ in the middle, and 46 μ distally; thus, taking the middle width, the ramus is about 2.4 times longer than wide. The armature of the ramus is like that of the female.

The rostral area is similar to that in the female.

The first antenna is generally like that of the female, but as in the previous species shows an additional seta on the third and fourth segments, the formula being 4, 15, 7, 4, 4 + 1 aesthete, 2 + 1 aesthete, and 7 +1 aesthete.

The second antenna is similar to that of the female.

The labrum (Fig. 178) shows certain differences in details of the spinules and teeth. The number of large teeth at either side of the transverse row appears to be somewhat variable (see Figure 179 of these teeth in another male). There are two diagonal lines of very small refractile points (spinules ?) on each side of the ventral surface of the labrum. The metastomal areas (Fig. 178) are ornamented as indicated in the figure. (In the specimen from which Figure 178 was drawn, the two groups of tooth-like spines on the left side, indicated by broken lines, were missing and presumably broken off.)

The mandible resembles that of the female, but the teeth on the largest element appear to be more pointed (see Fig. 180). The paragnath (Fig. 181) is similar to that of the female, but has a protuberance on the inner margin, which in the female is regular. The first maxilla (Fig. 182) appears to be shorter and less slender than in the female, and, although the long spines and setae are much like those in the opposite sex, there is an additional row of short spinules on the inner margin. The second maxilla (Fig. 183) shows the stout inner element on the second segment here replaced by a strongly sclerotized, rather blunt, claw-like element lacking an articulation with the segment.

The maxilliped (Fig. 184) has a single long seta on the first segment. The second segment has its proximal inner angle greatly expanded. The length of this segment along the outer margin is 224 μ, its greatest length from the distal end to the tip of the inner expansion is 260 μ, and its greatest width is 189 μ. There are three rows of fairly stout spines along the inner surface, in addition to the usual two setae. The third segment is very short and unarmed. The fourth segment forms part of a long recurved claw 270 μ in length (measured along its axis and not along the curvature), bearing near its

base a small seta on the posterior side, and a spinous process and a minute setule on the inner curvature. The ventral surface between the bases of the maxillipeds (Fig. 185) does not show a transverse line. The region between the maxillipeds and the first pair of legs is unmodified as in the female.

Leg 1 lacks the inner spine on the basis (Fig. 186). Otherwise legs 1–4 have a spine and setal formula like that of the female. The sclerotization of the legs, illustrated in the endopod of leg 4 (Fig. 187), seems to be stronger than in the female. (This may be an individual difference, however, since only one male was dissected.)

Leg 5 (Fig. 188) has a free segment which is not broadened distally as in the female, its greatest dimensions being 173 × 73 μ. Its armature is like that of the female.

Leg 6 (Fig. 189) consists of a ventral flap on the posterior part of the genital segment, bearing a strong spine 51 μ in length. In dorsal view the sixth leg is completely hidden except for the tip of the spine.

The color in life is similar to that of the female.

Remarks on its biology.—H. kombensis was always found in burrows in company with other species of *Hemicyclops*, once with *H. carinifer* and three times with both *H. diremptus* and *H. carinifer*.

Relationship to other species.—H. kombensis is included in the group of species having four setae on the basal segment of the first antenna. It may be compared only with the male of *H. leggii* (Thompson and Scott, 1903), since the female of that species remains unknown. The male of *H. leggii*, however, differs in having nearly quadrate caudal rami and in having two setae on the basal segment of the maxilliped. *H. dilatatus* Shen and Bai, 1956, has a "squarish" genital segment in the female. *H. australis* Nicholls, 1944, has two setae on the basal segment of the male maxilliped and the caudal ramus is almost quadrate. *H. indicus* Sewell, 1949, has a genital segment which is very slightly wider than long and the caudal rami are but little longer than broad. In *H. purpureus* Boeck, 1873, as figured by Sars (1917), the fifth leg in the female is not markedly expanded distally and the caudal rami are relatively shorter than in *H. kombensis*. *H. thysanotus* Wilson, 1935, shows lateral expansions in the anterior part of the genital segment and the form of the fifth leg is different from that in the species from Madagascar. In *H. aberdonensis* (T. and A. Scott, 1892) the genital segment is much wider than long, and there are two setae on the basal segment of the male maxilliped. In *H. thompsoni* (Canu, 1888) the genital segment, though elongate, is expanded in its extreme anterior part. *H. tamilensis* (Thompson and Scott, 1903) has in the female broad lateral expansions on the genital segment, and short, almost quadrate caudal rami. In the female of *H. bacescui* (Serban, 1956) the caudal rami are two times longer than wide, the inner spine on the basis of leg 1 is strongly denticulated (Stock, 1959), and the lateral margins of the genital segment are not almost parallel as in *H. kombensis*. *H. visendus* Humes, Cressey, and Gooding, 1958, shows in the female a genital segment somewhat resembling that of *H. kombensis* but which has a pair of dorsolateral ridges; the caudal ramus is only 1.7 times longer than wide; the third segment of the second antenna bears spinules and setae of a different form than in the species from Madagascar; and the free segment of the fifth leg is oval rather than petal-like in outline. The inner side of the second segment of the male maxilliped of *H. visendus* is broadly inflated rather than angularly produced as in *H. kombensis*.

Hemicyclops biflagellatus[1] n. sp.

Pls. XXVII–XXXI; Pl. XXXII, figs. 221–222

Type material.—24 females and 6 males from water in burrows of unknown origin 3–4 cm in diameter and about 50 cm deep in intertidal muddy sand at Ampassipohe, on the southern shore of the bay of Ambato-

[1] The specific name *biflagellatus*, a combination from Latin *bis* = twice and *flagellum* = a whip, refers to the two setiform processes on the segment of leg 5 in the female.

zavavy, Nosy Bé, Madagascar. Collected by A. G. Humes May 11, 1964. Holotype female, allotype, and 22 paratypes (19 females and 3 males) deposited in the United States National Museum, Washington; one paratypic female in the Museum of Comparative Zoology, Cambridge, Mass.; and the remaining paratypes in the author's collection.

Female.—The length of the body (excluding the setae on the caudal rami) is 1.63 mm (1.51–1.80 mm) and the greatest width (in the cephalosome, although in some specimens the segment of leg 2 may be expanded laterally so that its width is slightly greater) is 0.56 mm (0.51–0.61 mm), based on 5 individuals. The prosome is not much broadened, and somewhat longer than the urosome, the ratio being about 1.46 : 1 (Fig. 190). In dorsal aspect the epimera of the segments of legs 1–4 are conspicuously angulate. The segment bearing the fifth legs has a posterior transverse ridge, and bears a pair of prominent posterolateral recurved setiform processes about 100 μ long, with delicate hyaline lateral hairs (?). These processes are perhaps true setae, but an articulation could not be established with certainty. A very narrow intersegmental sclerite, more evident in a ventral view, occurs between the first two segments of the urosome. The genital segment (Fig. 191) is elongated, with two rounded lateral wings in its anterior fourth and with the sides of the posterior three-fourths subparallel and only very slightly swollen. An extremely indistinct transverse indication of subdivision occurs internally near the middle of the segment in some specimens. The genital segment measures 294 μ in dorsal length; its width at the anterior lateral expansions is 270 μ, and in the posterior third 167 μ.

The egg sacs are attached dorsolaterally on the two expansions of the genital segment, the actual attachment being covered by a dorsal flange (Fig. 192). Near the point of attachment there are two strongly sclerotized spine-like processes each about 6 μ in length. Each egg sac (Fig. 190) is elongated, about 519 × 170 μ, and contains numerous small eggs.

The three postgenital segments measure, respectively, 122 × 143, 84 × 130, and 78 × 108 μ. There is no apparent anal operculum. The anal segment bears on its dorsal and ventral surfaces fine hairs, as indicated in the figure. The caudal rami are inserted dorsally and the posterior ventral border of the segment below each ramus bears an outer row of minute spinules and an inner submarginal row of prominent spinules (the longest about 15 μ in length), as shown in Figure 193.

The dorsal surface of the prosome and the dorsal and ventral surfaces of the urosome bear minute hairs and refractile points.

The caudal ramus (Fig. 193) is moderately elongated, 100 μ in length, 41 μ wide just proximal to the lateral seta and 35 μ wide distal to that seta. Taking the width as 41 μ, the ramus is 2.44 times longer than wide. A minute hyaline hair arises on the outer basal margin. The lateral seta (52 μ long) and the outermost terminal seta (90 μ long) are both composed of a basal shaft and a distal flagelliform part. The dorsal seta is 200 μ long and bears a few lateral hairs. The innermost terminal seta is 227 μ in length and bears lateral spinules, those on the inner side being slightly better developed. The inner long terminal seta is 746 μ and the outer one 407 μ in length, both bearing lateral hairs (see Fig. 190). The four terminal setae are inserted somewhat dorsally and the resulting terminal ventral flange on the ramus bears a row of minute spinules. Along the inner margin of the ramus there is a row of very slender setules. Both the dorsal and ventral surfaces of the ramus bear scattered hyaline hairs.

The rostral region (Fig. 194) is well defined and bears a pair of setules and pairs of small hairs as indicated.

The first antenna (Fig. 195) is about 410 μ long, 7-segmented, the segments, beginning at the base, 15, 54, 49, 85, 58, 54, and 52 μ in length (measured along their non-setiferous margins). The armature is 4, 15, 6, 3, 4 + 1 aesthete, 2 + 1 aesthete, and

7 + 1 aesthete (the same formula as in *H. axiophilus, H. amplicaudatus, H. diremptus,* and *H. kombensis*). A few of the setae on the second segment show very short lateral hairs. On the distal posteroventral surface of this segment there are a few short rows of minute refractile points. Certain setae bear long lateral hairs as in *H. kombensis.*

The second antenna (Fig. 196) is 4-segmented, with the third segment produced on the inner distal corner where it bears four elements: proximally a slender posterior seta, more distally a long recurved seta (which resembles the four long terminal recurved setae on the last segment), and distally two unequal recurved spines, both bearing subterminal setules and the longer one a row of prominent spinules. The fourth segment is nearly quadrate, 33 × 30 μ, and bears seven setae much like those in *H. kombensis.*

The labrum (Fig. 197), in addition to ornamentation suggesting that in *H. kombensis,* shows a crescentic row of long hyaline setules, with the surface posterior to this row bearing conspicuous obtuse scales. The metastomal areas have a complex ornamentation, as shown in Figure 198.

The mandible (Fig. 199) has two stout elements and two well-developed setae with lateral hairs. The paragnath (Fig. 200) is a moderately elongated lobe bearing long hairs (shorter at the tip) and a row of small spinules as indicated. The first maxilla (Fig. 201) is in general similar to that of *H. kombensis.* The second maxilla (Fig. 202) also resembles in major features that of *H. kombensis.* The maxilliped (Fig. 203) is also much like that of *H. kombensis,* but the second segment is relatively longer and more slender, and the setae (including the two terminal claw-like setae) tend to be relatively longer. From near the base of the shorter claw-like seta there arises a setiform process without clear articulation. Between the bases of the maxillipeds there is a conspicuous ventral transverse sclerotization as shown in Figure 198.

The area between the maxillipeds and the first pair of legs is without conspicuous features.

The armature of legs 1–4 (Figs. 204, 205, 206, and 208) is as follows:

P1	protopod	0:1	1:I	exp	I:0	I:1	I,I,6
				end	0:1	0:1	I,5
P2	protopod	0:1	1:0	exp	I:0	I:1	II,7
				end	0:1	0:2	I,II,3
P3	protopod	0:1	1:0	exp	I:0	I:1	II,I,6
				end	0:1	0:2	I,II,3
P4	protopod	0:1	1:0	exp	I:0	I:1	I,7
				end	0:1	0:2	I,II,2

This formula is somewhat different from that of *H. axiophilus,* the third exopod segment of leg 1 having two spines and the same segment in leg 3 having three spines. In leg 1 the inner spine on the basis is 105 μ in length, with short lateral spinules and with a blunt tip. The margin of the basis medial to this spine is rounded and smooth except for a tooth-like process near the base of the spine. In legs 2–4 this inner area of the basis bears a row of marginal hairs and a group of slender hyaline spinules on its anterior surface. The ventral margin of the intercoxal plate of leg 1 bears on each side rows of long hairs, but in legs 2–4 these hairs are replaced by spinules. The outer margin of the coxa of leg 4 lacks the long spinules seen on legs 1–3, but a row of slender spinules occurs on the outer posterior margin. In leg 3 the distalmost spine on the last segment of the exopod is distinctly spine-like rather than almost setiform as in *H. kombensis.* (An abnormal second segment of the exopod of leg 3, with two outer spines instead of one, is shown in Fig. 207.) On the last segment of the endopod of leg 4 the inner two elements are different from the outer three: the inner one being almost spine-like with lateral hairs basally and with a bilateral fringe of spinules in the distal three-fourths, the outer one being setiform with lateral hairs.

Leg 5 (Fig. 209) has a free segment which is somewhat constricted basally, broadened in the middle, and narrowed beyond the first outer spine. Its greatest length is 120 μ (91 μ along the outer edge to the base of the first spine and 94 μ along

UNESCO ARCHIVES

the inner edge), and its greatest width is 56 μ. The ratio of greatest length to width is 2.14 : 1. There are rows of prominent spinules on both outer and inner margins. The three spines are 63, 59, and 71 μ in length, respectively, from outer to inner. The first few inner lateral spinules on the innermost spine are unusually long. The outermost spine seems to lack outer spinules. The seta is 93 μ long and bears a few lateral hairs. The basal area of leg 5 suggests a discrete segment; it is armed with a plumose seta about 100 μ in length and a group of outer spinules.

Leg 6 is apparently absent.

The color in living specimens, in transmitted light, is slightly opaque, with reddish orange globules in the prosome, the eye dark red, the ovary gray, the egg sacs dark reddish orange.

Male.—The length of the body (not including the setae on the caudal rami) is 1.34 mm (1.25–1.46 mm) and the greatest width is 0.45 mm (0.41–0.50 mm), based on 5 individuals. The prosome is less expanded than in the female (Fig. 210). The ratio of the length of the prosome to that of the urosome is about the same as that in the female. The segment of leg 5 lacks the two setiform processes seen in the female. The genital segment (Fig. 211) is wider than long, 148 × 178 μ, with gently rounded lateral margins.

The four postgenital segments measure, respectively, 108 × 103, 95 × 101, 62 × 98, and 54 × 89 μ.

As in the female, the prosome and urosome bear hairs and refractile points.

The caudal ramus is similar to that of the female, but is relatively shorter, the greatest length being 80 μ, the width just proximal to the lateral seta 35 μ, and the width distal to that seta 31 μ. Taking the width as 35 μ, the ramus is 2.29 times longer than wide.

The spermatophore (Fig. 212), as seen attached to the female, is pyriform, 68 μ long (including the slender neck of 6 μ) and 40 μ wide.

The rostral area is like that of the female.

The first antenna resembles that of the female, but, as in previous species, has an additional seta on the third and fourth segments, so that the formula is 4, 15, 7, 4, 4 + 1 aesthete, 2 + 1 aesthete, and 7 + 1 aesthete.

The second antenna is similar to that of the female.

The labrum (Fig. 213) lacks the crescentic row of hyaline spinules, and the medial posteroventral surface has numerous scales and spinules, as shown in the figure. The metastomal areas (Fig. 214) are ornamented as indicated in the figure.

The mandible is like that in the female. The paragnath (Fig. 214) resembles that of the female, but seems to be somewhat more slender. The first maxilla is similar to that of the female. The second maxilla (Fig. 215) shows the stout inner element on the second segment here replaced by a strongly sclerotized, rather blunt, claw-like structure, sometimes pale yellowish in color, which lacks an articulation with the segment.

The maxilliped (Fig. 216) has a single long seta on the first segment. The second segment has its proximal inner angle expanded and rounded; the length of this segment along the outer margin is 137 μ, its greatest length from the distal end to the tip of the inner expansion is 173 μ, and its greatest width is 115 μ. There are three rows of fairly stout spines along the inner margin, in addition to the usual two setae. The third segment is very short and unarmed. The fourth segment forms part of the long recurved claw 189 μ in length (measured along its axis and not along its curvature), bearing near its base on the posterior surface a small seta 18 μ long, and on its inner curvature a spinous process 25 μ long and a minute setule 5 μ long. The ventral surface of the cephalosome between the bases of the maxillipeds (Fig. 217) shows only an incomplete transverse line, instead of the readily visible sclerotization seen in the female.

Leg 1 lacks the inner spine on the basis (Fig. 218). Otherwise legs 1–4 show the same spine and setal formula as in the fe-

male. The last endopod segments of legs 2 and 3 (Figs. 219 and 220) show the three terminal processes reduced and blunt, in contrast to their acute spiniform condition in the female.

Leg 5 (Fig. 221) has a free segment which is relatively longer and more slender than in the female. Its greatest length is 116 μ (81 μ along the outer edge to the base of the first spine and 93 μ along the inner edge) and its greatest width is 44 μ. The armature resembles in major respects that of the female, although the outermost spine has spinules along both sides. The basal area of leg 5 does not seem to show a clear separation from the body.

Leg 6 (Fig. 222) consists of a ventral flap on the posterior part of the genital segment, bearing a strong spine 44 μ in length. In a dorsal view of the animal this spine projects posterolaterally beyond the edge of the segment.

The color in life resembles that of the female.

Remarks on its biology.—*H. biflagellatus* was collected on only one occasion, and then from burrows which also contained *H. diremptus* and *H. carinifer.*

Relationship to other species.—This species seems to be unique among the previously described species of the genus in having two posterolateral setiform processes on the segment of leg 5. Otherwise, it resembles *H. thysanotus* Wilson, 1935, in certain respects. However, in the female of *H. thysanotus* the inner spine on the basis of leg 1 is recurved and rather blunt instead of straight, and in the male the form of the maxilliped is rather different from that of the Madagascar species. *H. biflagellatus* is unlike *H. leggii* (Thompson and Scott, 1903), of which only the male is known; in this species the caudal rami are nearly quadrate and the basal segment of the male maxilliped has two setae. *H. bacescui* (Şerban, 1956) has, in the female, less prominent expansions on the genital segment and the inner spine on the basis of leg 1 has strong denticulations. *H. purpureus* Boeck, 1873, has, in the female, a broader distal segment in leg 5 and shorter caudal rami, and the inner distal corner of the third segment of the second antenna is not prolonged. *H. thompsoni* (Canu, 1888) has a broad distal segment of leg 5 in the female.

The following species also has a pair of setiform processes on the segment of leg 5, but may be readily distinguished from *H. biflagellatus* as pointed out below.

Hemicyclops acanthosquillae[1] n. sp.

Pl. XXXII, figs. 223–227; Pls. XXXIII–XXXVI

Type material.—8 females and 5 males washed from the bodies of two stomatopods, *Acanthosquilla* sp., dug from intertidal sand at Antsakoabe, on the northwestern shore of Nosy Bé, Madagascar. Collected by A. G. Humes July 12, 1964. Holotype female, allotype, and 8 paratypes (5 females and 3 males) deposited in the United States National Museum, Washington; one paratypic female in the Museum of Comparative Zoology, Cambridge, Mass.; and the remaining paratypes in the author's collection.

Female.—The length of the body (not including the setae on the caudal rami) is 2.24 mm (2.00–2.44 mm) and the greatest width (taken at the level of the segment bearing leg 2) is 0.71 mm (0.68–0.80 mm), based on 5 individuals. The prosome is moderately broadened and of about the same length as the urosome (Fig. 223). In dorsal aspect the epimera of the segments of legs 1–4 are angulate posterolaterally. The segment bearing the fifth legs is rounded laterally and bears a pair of posterolateral smooth setiform processes about 72 μ in length (Figs. 224 and 225). (These resemble somewhat the two setiform processes described in the preceding species.) Medial to the two processes there is a pair of minute hyaline setules (hairs ?) about 8 μ long. An intersegmental sclerite may be seen ventrally between the first two urosomal segments. The genital segment (Fig. 224) is

[1] The specific name *acanthosquillae* is taken from the generic name of the crustacean upon whose body the copepod was found.

greatly elongated. In dorsal view it shows two pronounced lateral swellings in its anterior fifth, the remaining portion of the segment having the sides nearly parallel. Dorsally, just anterior to the midregion, there are four longitudinally oblique sclerotizations. The segment measures 486 μ in length; its width at the level of the two swellings is 289 μ, and in the posterior part 224 μ.

The egg sacs are attached slightly dorsally on the lateral swellings of the genital segment, between dorsal and ventral flanges. Each egg sac is elongated (Fig. 223), about 730 × 235 μ, and contains many small eggs, each about 53 μ in diameter.

The three postgenital segments measure, respectively, 243 × 205, 159 × 159, and 100 × 135 μ. There is no evident anal operculum. The anal segment is provided ventrally on each side along its posterior margin with an outer row of minute spinules and an inner row of spines (see Fig. 226). The dorsal surface of the urosome bears minute refractile points and hairs as shown in Figure 224.

The caudal ramus (Fig. 226) measures 116 × 54 μ (2.15 times longer than wide). All six setae are inserted somewhat dorsally. There is a minute hyaline hair on the basal outer margin. The lateral seta (58 μ long) and the outermost terminal seta (103 μ long) are both composed of a distinct basal shaft and a distal flagelliform part. The sparsely haired dorsal seta is 95 μ in length. The innermost terminal seta is 282 μ in length and bears lateral spinules. The inner long terminal seta is 1017 μ and the outer one 542 μ in length, both bearing lateral hairs (see Fig. 223). The posterior end of the ramus is prolonged ventrally to form a flange bearing a row of minute spinules and, near the base of the innermost terminal seta, a row of larger spinules. The distal half of the inner margin of the ramus bears a row of very slender spinules.

The rostral area (Fig. 227) is well defined and bears a pair of setules.

The first antenna (Fig. 228) is about 441 μ long, 7-segmented, the segments, beginning at the base, being 15, 68, 49, 94, 59, 58, and 54 μ in length (measured along their non-setiferous margins). The armature is similar to that of *H. biflagellatus*.

The second antenna (Figs. 229 and 230) is 4-segmented, with the third segment much produced on the inner distal corner, where it bears four elements: proximally a slender seta, more distally a stout recurved seta, and terminally two recurved unequal spines, both provided with subterminal setules and the longer one having a row of spinules. The fourth segment is quadrate, 23 × 23 μ, and bears the usual seven setae. The convex inner area of the second segment bears on its posterior surface numerous scale-like protuberances, and the concave inner area of the third segment bears also on its posterior surface short spine-like knobs (see Fig. 230).

The labrum (Fig. 231) has a group of broad irregular ventromedial lobes, in addition to the other ornamentation shown in the figure. The metastomal areas have a complex ornamentation, as indicated in Figure 232.

The mandible (Fig. 233) has the usual two stout elements and two well-developed setae with lateral spinules. The paragnath (Fig. 234) is a moderately elongated lobe with hairs and short spinules as indicated in the figure. The first maxilla (Fig. 235) resembles in major respects that of *H. biflagellatus*. The second maxilla (Fig. 236) is similar to that of the preceding species. The maxilliped (Fig. 237) also resembles in general structure that of the preceding species, but there is a greater number of small hyaline setae near the bases of the two terminal claw-like setae. There is a conspicuous ventral transverse sclerotization between the bases of the maxillipeds (see Fig. 232) as in *H. biflagellatus*.

The area between the maxillipeds and the first pair of legs lacks outstanding features.

The armature of legs 1–4 (Figs. 238, 240, 242, and 243) is similar to that of *H. axiophilus*. In leg 1 the inner spine on the basis is 52 μ in length, with short truncated lateral spinules, giving the edges the ap-

pearance of a saw blade (Fig. 239). The margin of the basis medial to this spine is smooth, except for a rather blunt tooth-like process near the base of the spine. In legs 2–4 this inner area of the basis bears a row of marginal hairs and a group of slender hyaline setules on its anterior surface. As in the preceding species, the ventral margin of the intercoxal plate of leg 1 bears hairs, while in legs 2–4 it bears spinules; and the coxa of leg 4 lacks the long slender spinules seen in legs 1–3, instead having a row of spinules on the outer posterior margin. In leg 1 the outer margin of the second segment of the endopod bears only a row of hairs, but in legs 2–4 this margin bears basally a group of small knobs (Fig. 241) followed by the usual hairs. On the last endopod segment of leg 4 the inner two elements are setae, the lateral hairs on the innermost being equal but those on the adjacent seta being longer near the base and shorter on the distal three-fourths of the seta; the fringed inner terminal spine is more than twice as long as either the outer terminal spine or the outer lateral spine.

Leg 5 (Fig. 244) has a free segment which is narrow basally but broadened distally, its greatest dimensions being 142 × 95 μ, with a ratio of length to width of 1.5 : 1. There are rows of long spinules on both outer and inner edges of the segment. The three spines measure 67, 73, and 86 μ in length, respectively, from outer to inner; the seta is 88 μ long. The basal area of the leg suggests a discrete segment and is armed as in the preceding species.

Leg 6 is apparently absent.

The color in living specimens in transmitted light is slightly amber, with the eye red and the egg sacs gray. The spermatophores attached to the female are golden brown.

Male.—The length of the body (not including the setae on the caudal rami) is 1.85 mm (1.79–1.91 mm), and the greatest width is 0.63 mm (0.60–0.66 mm), based on 5 individuals. The prosome is only slightly less expanded than in the female, and is somewhat longer than the urosome (Fig. 245), the ratio being 1.2 : 1. The segment of leg 5 lacks the two setiform processes seen in the female, but instead has dorsally on each side, medial to the seta associated with the leg, a somewhat triangular projection (Figs. 246 and 247). The genital segment (Fig. 246) is about as long as wide, 260 × 271 μ, with gently rounded lateral margins.

The four postgenital segments measure, respectively, 186 × 157, 157 × 130, 108 × 116, and 76 × 116 μ.

The dorsal surface of the urosome bears hairs and refractile points, as indicated in the figure.

The caudal ramus resembles that of the female, but is relatively shorter, the greatest dimensions being 92 × 49 μ. The ratio of length to width is 1.88 : 1.

The spermatophore (Fig. 248), as seen attached ventrally on the genital segment of the female, is somewhat irregularly ovoid. Its greatest dimensions are 124 × 99 μ plus a neck of 13 μ.

The rostral region (Fig. 249) is only slightly less defined than that of the female.

The first antenna resembles that of the female, but, as in previous species, has an additional seta on the third and fourth segments, thus giving the formula of 4, 15, 7, 4, 4 + 1 aesthete, 2 + 1 aesthete, and 7 + 1 aesthete.

The second antenna is like that of the female.

The labrum (Fig. 250) has a more complex ornamentation than in the female. The metastomal areas (Fig. 251) are ornamented as shown in the figure.

The mandible resembles that of the female. The paragnath appears to be similar to that of the female, but the notch on the outer edge is less apparent. The first maxilla is like that of the female. The second maxilla (Fig. 252), as in previous species, has the stout inner element on the second segment transformed to form a strongly sclerotized, rather blunt, claw-like structure, having a conspicuous yellowish amber color and lacking an articulation with the segment.

The maxilliped (Fig. 253) has a single long seta on the first segment. The second segment has its proximal inner angle rather acutely expanded. The length of this segment along its outer margin is 197 μ, its greatest length from the distal end to the tip of the inner expansion is 240 μ, and its greatest width is 159 μ. There are three rows of moderately stout but somewhat obtuse spines along the inner surface, plus the usual two setae. The third segment is very short and unarmed. The fourth segment forms part of the long, slightly recurved claw, 235 μ in length (measured along its axis and not along its curvature). The claw bears near the base on its posterior surface a slender seta 35 μ in length, and on its inner curvature a spinous process 28 μ long and a minute setule 10 μ long. The ventral surface of the cephalosome between the bases of the maxillipeds shows only an incomplete transverse line (Fig. 251), as in *H. biflagellatus*.

Leg 1 lacks the inner spine on the basis (Fig. 254) and the spinules in this region are longer and more slender than in the female. Otherwise legs 1–4 have the same spine and setal formula as in the female. The sclerotization of the rami appears to be stronger than in the opposite sex.

Leg 5 (Fig. 255) has an elongated free segment which is relatively much more slender than in the female. Its greatest dimensions are 132 × 57 μ, the ratio of length to width being about 2.3 : 1. The ornamentation resembles that of the female, but the lateral spinules on the three terminal spines are shorter. The basal area of leg 5 does not show a separation from the body. Leg 6 (Fig. 256) consists of a ventral sclerotized flap on the posterior region of the genital segment, bearing an outwardly directed spine 38 μ in length with minute lateral spinules on each side. This spine in dorsal view of the body projects posterolaterally beyond the edge of the genital segment (see Figs. 245 and 246).

The color in life resembles that of the female.

Remarks on its biology.—The two stomatopods from which these copepods were taken appeared in the water seeping into a hole 30 cm deep which had been dug in clean sand. They were quickly placed in a plastic bag with a small amount of sea water. Later a few drops of ethyl alcohol were added, the whole gently agitated, and the copepods recovered from the sediment. There seems to be justification for assuming that these *Hemicyclops* were living on the bodies of the *Acanthosquilla*. This is the first record of a member of the genus *Hemicyclops* occurring on a stomatopod.

Relationship to other species.—*H. acanthosquillae* belongs to the group of *Hemicyclops* species having four setae on the first segment of the first antenna. It possesses several very characteristic features by which it may be distinguished from other members of this group: on the segment of leg 5 in the female a pair of dorsolateral setiform processes and in the male a pair of triangular projections; the form, armature, and ornamentation of the second antenna, especially the greatly produced inner distal corner of the third segment and the very small quadrate fourth segment; the ornamentation of the outer edge of the second segment of the endopods of legs 2–4; and the acute inner proximal expansion of the second segment of the male maxilliped.

H. acanthosquillae bears certain resemblances to *H. biflagellatus*. For example, in the female, the elongated genital segment has anterior lateral expansions and there is a pair of setiform processes on the segment of leg 5. It may be distinguished from *H. biflagellatus*, however, by several readily observable characters, such as the form of the second antenna, the fifth leg, and the male maxilliped.

REMARKS ON THE SPECIES OF *HEMICYCLOPS* FROM MADAGASCAR

Gooding (1960) divided the American species of *Hemicyclops* into two groups on the basis of morphological characters. Later (1963, unpublished thesis), he developed further this concept of groups of species within the genus. Selecting a few typical

characters, the eight known species from Madagascar (comprising the seven described above and *H. visendus*) may be placed in two groups (corresponding to two of Gooding's):

1) those species with the urosome of the adult female having five segments, with four setae on the first segment of the first antenna, with a short terminal segment on the second antenna, and with a sexually dimorphic second maxilla, including:

H. axiophilus n. sp.
H. amplicaudatus n. sp.
H. diremptus n. sp.
H. kombensis n. sp.
H. biflagellatus n. sp.
H. acanthosquillae n. sp.
H. visendus Humes, Cressey, and Gooding, 1958;

2) that species with the urosome of the adult female having six segments, with five setae on the first segment of the first antenna, with an elongate terminal segment on the second antenna, and without sexual dimorphism in the second maxilla:

H. carinifer n. sp.

THE GENUS *HEMICYCLOPS* IN THE INDIAN OCEAN

Five species of *Hemicyclops* have been reported from the Indian Ocean area: *H. indicus* Sewell, 1949, from Nankouri Harbour, Nicobar Islands, in weed-washings; *H. leggii* (Thompson and Scott, 1903) in washings from dredgings, sponges, in the Gulf of Manaar, Ceylon; *H. intermedius* Ummerkutty, 1962, from weed-washings in the Gulf of Manaar, southeastern coast of India; *H. tamilensis* (Thompson and Scott, 1903) in Muttuvaratu pearl oyster washings, Ceylon; and *H. visendus* Humes, Cressey, and Gooding, 1958, from *Upogebia* sp. at Nosy Bé, Madagascar.

In addition, Pillai (1963) has reported *Hemicyclops* sp. from brackish water at Ashtamudi Lake, Quilon, Kerala State, India. The only specimen, a male, is 2.3 mm in length and belongs to the group of species having four setae on the first segment of the first antenna. Its size alone distinguishes it from all six of the species in this group from Madagascar described above. The caudal ramus is nearly three times longer than wide (in *H. amplicaudatus* it is 3.6 times, in *H. axiophilus*, *H. diremptus*, *H. kombensis*, *H. biflagellatus*, and *H. acanthosquillae* it is 2.4 times or less). The male of *H. kombensis* appears to be closest to the Indian specimen, having a length of 2.09 mm and the caudal ramus being 2.4 times longer than wide. In the Indian form, however, the free segment of leg 5 is broader, the genital segment is not constricted anteriorly, and hairs occur along the entire inner border of the caudal ramus.

The question arises whether Pillai's specimen may be one of the five Indian Ocean species mentioned above. This male shows the fourth segment of the first antenna distinctly longer than the second (Pillai's fig. 49), while in *H. indicus* the reverse is true. The free segment of leg 5 is broadened and the second segment of the male maxilliped has its inner side rather angularly expanded proximally, while in *H. visendus* the free segment is elongate and the second segment of the maxilliped has its inner side broadly expanded. The caudal rami are nearly three times longer than wide and the first segment of the male maxilliped has one seta, while in *H. leggii* the caudal rami are nearly quadrate and the first segment of the maxilliped has two setae. The male of *H. tamilensis* is unknown, but the female of this Ceylonese species has nearly quadrate caudal rami, and it is perhaps safe to assume for the present that *H. tamilensis* and Pillai's single male are distinct.

Only the female of *H. intermedius* is known. It belongs to the group of *Hemicyclops* species having four setae on the first segment of the first antenna. It appears to be distinct from all six new species in this group described above. In these the caudal ramus is two or more times longer than wide, while in *H. intermedius* it is quadrate; the contour of the genital segment in dorsal view is different from that in *H. intermedius*; the inner distal corner of the third segment

of the second antenna is produced, while in *H. intermedius* this region is rounded; and the armature of the four legs is somewhat different than in *H. intermedius*, where, for example, the formula for the third exopod segment of the first leg is III,I,4.

It is difficult to compare *H. intermedius* and Pillai's *Hemicyclops* sp., since the corresponding sexes are not known. These two copepods seem to be distinct, however, since in the male *Hemicyclops* sp. the caudal rami are nearly three times longer than wide, the inner distal corner of the third segment of the second antenna is produced, and the armature of the third exopod segment of the first leg is I,7.

Twelve described species and one unnamed form of *Hemicyclops* are now known from the Indian Ocean area: *H. indicus* from the Nicobar Islands, *H. leggii* and *H. tamilensis* from Ceylon, *H. intermedius* and *H.* sp. from India, and *H. axiophilus, H. amplicaudatus, H. carinifer, H. diremptus, H. kombensis, H. biflagellatus, H. acanthosquillae*, and *H. visendus* from Madagascar.

REFERENCES CITED

BOECK, A. 1873. Nye Slaegter og Arter af Saltvands-Copepoder. Forh. Vid. Selsk. Christiana (1872) **14**: 35–60.

CANU, E. 1888. Les copépodes marins du Boulonnais III. Les Hersiliidae, famille nouvelle de copépodes commensaux. Bull. Sci. France Belgique **19**: 402–432.

GOODING, R. U. 1960. North and South American copepods of the genus *Hemicyclops* (Cyclopoida:Clausidiidae). Proc. U.S. Nat. Mus. **112**(3434): 159–195.

———. 1963 (unpublished). External morphology and classification of marine poecilostome copepods belonging to the families Clausidiidae, Clausiidae, Nereicolidae, Eunicicolidae, Synaptiphilidae, Catiniidae, Anomopsyllidae, and Echiurophilidae. Ph.D. thesis, University of Washington, Seattle.

HUMES, A. G. 1962. Eight new species of *Xarifia* (Copepoda, Cyclopoida), parasites of corals in Madagascar. Bull. Mus. Comp. Zool. **128** (2): 37–63.

HUMES, A. G., R. F. CRESSEY, AND R. U. GOODING. 1958. A new cyclopoid copepod, *Hemicyclops visendus*, associated with *Upogebia* in Madagascar. J. Washington Acad. Sci. **48** (12): 398–405.

NICHOLLS, A. G. 1944. Littoral Copepoda from South Australia. (II) Calanoida, Cyclopoida, Notodelphyoida, Monstrilloida and Caligoida. Rec. South Australian Mus. **8**(1): 1–62.

PILLAI, N. K. 1963. Copepods associated with South Indian invertebrates. Proc. Indian Acad. Sci. **58**(section B, 4): 235–247.

SARS, G. O. 1917. Copepoda Cyclopoida. Clausidiidae, Lichomolgidae (part). An account of the Crustacea of Norway, etc. Vol. 6(11 & 12): 141–172. Bergen Museum, Bergen.

SCOTT, T. AND A. SCOTT. 1892. On new and rare Crustacea from the east coast of Scotland. Ann. Scot. Nat. Hist. Soc. **3**: 149–156.

ŞERBAN, M. 1956. *Pontocyclops bacescui* n. g., n. sp. (Crustacea Copepoda), ein neuer Cyclopide vom schwarzen Meere. Izdanija **1**(7): 169–184.

SEWELL, R. B. S. 1949. The littoral and semiparasitic Cyclopoida, the Monstrilloida and the Notodelphyoida. John Murray Expedition 1933–34, Sci. Repts., Vol. 9(2): 17–199.

SHEN, C-j. AND S. BAI. 1956. The marine Copepoda from the spawning ground of *Pneumatophorus japonicus* (Houttuyn) off Chefoo, China. Acta Zool. Sinica **8**(2): 177–234.

STOCK, J. H. 1959. Copepoda associated with Neapolitan invertebrates. Pubbl. Staz. Zool. Napoli **31**(1): 59–75.

THOMPSON, I. C. AND A. SCOTT. 1903. Report on the Copepoda collected by Professor Herdman, at Ceylon, in 1902. Rept. Gov. Ceylon Pearl Oyster Fish. Gulf of Manaar, Suppl. Rept. No. 7: 227–307.

UMMERKUTTY, A. N. P. 1962. Studies on Indian copepods 5. On eleven new species of marine cyclopoid copepods from the south-east coast of India. J. Mar. Biol. Ass. India, 1961, **3**(1 & 2): 19–69.

WILLIAMS, L. W. 1907. List of the Rhode Island Copepoda, Phyllopoda, and Ostracoda, with new species of Copepoda. 37th Ann. Rept. Comm. Inland Fish. Rhode Island (Special Paper no. 30), pp. 69–79.

WILSON, C. B. 1935. Parasitic copepods from the Pacific Coast. Amer. Midland Nat. **16** (5): 776–797.

———. 1937. Two new semi-parasitic copepods from the Peruvian coast. Parasitology **29** (2): 206–211.

(Received 25 January 1965.)

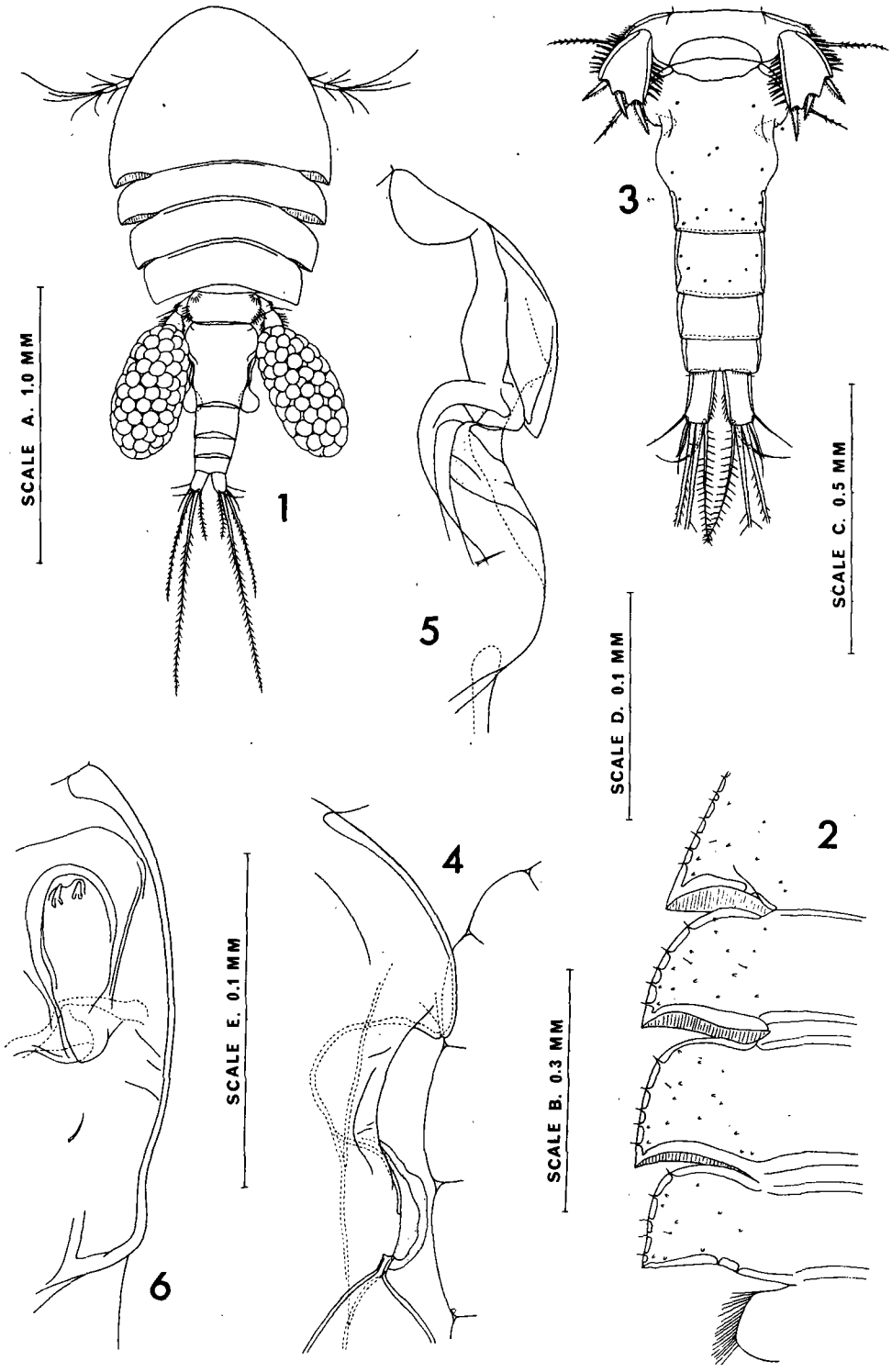
SCALE A. 1.0 MM
1
5
3
SCALE C. 0.5 MM
SCALE D. 0.1 MM
2
4
SCALE B. 0.3 MM
SCALE E. 0.1 MM
6

EXPLANATION OF FIGURES

All figures were drawn with the aid of a camera lucida. The letter after each figure refers to the scale at which it was drawn.

Plate I

Hemicyclops axiophilus n. sp., female

Fig. 1. Body, dorsal (A).
Fig. 2. Edges of somites of legs 1–5, dorsal (B).
Fig. 3. Urosome, ventral (C).
Fig. 4. Part of edge of genital segment showing areas of attachment of egg sac and spermatophore, ventral (D).
Fig. 5. Part of edge of genital segment, dorsal (D).
Fig. 6. Same, lateral (E).

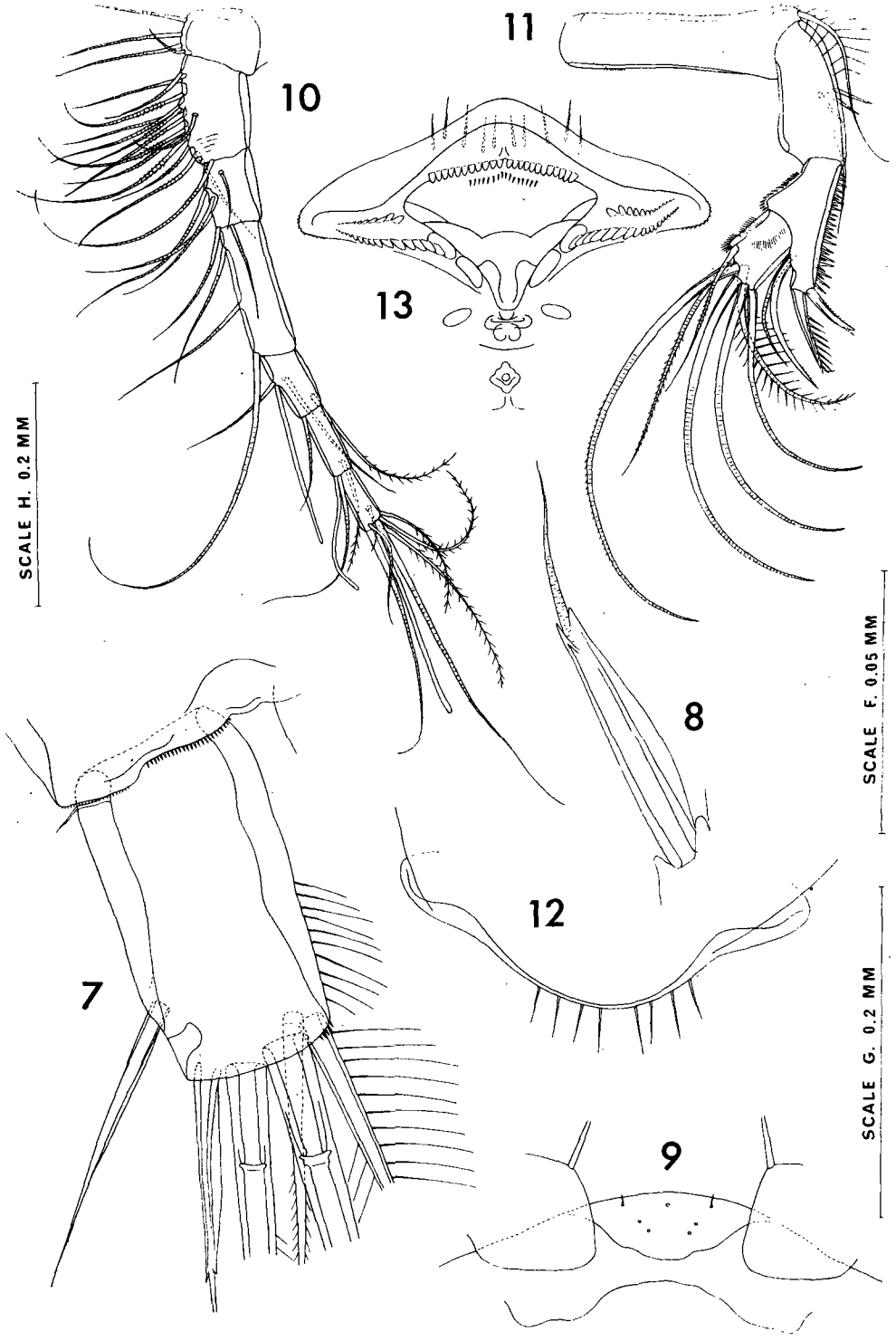
11
10
13
SCALE H. 0.2 MM
8
SCALE F. 0.05 MM
12
7
SCALE G. 0.2 MM
9

Plate 11

Hemicyclops axiophilus n. sp., female (continued)

Fig. 7. Caudal ramus, ventral (E).
Fig. 8. Outermost terminal seta on caudal ramus, dorsal (F).
Fig. 9. Rostral area, ventral (G).
Fig. 10. First antenna, anterodorsal (H).
Fig. 11. Second antenna, anterior or ventral (G).
Fig. 12. Edge of labrum, anterior and dorsal (E).
Fig. 13. Posterior surface of labrum, pushed forward (E).

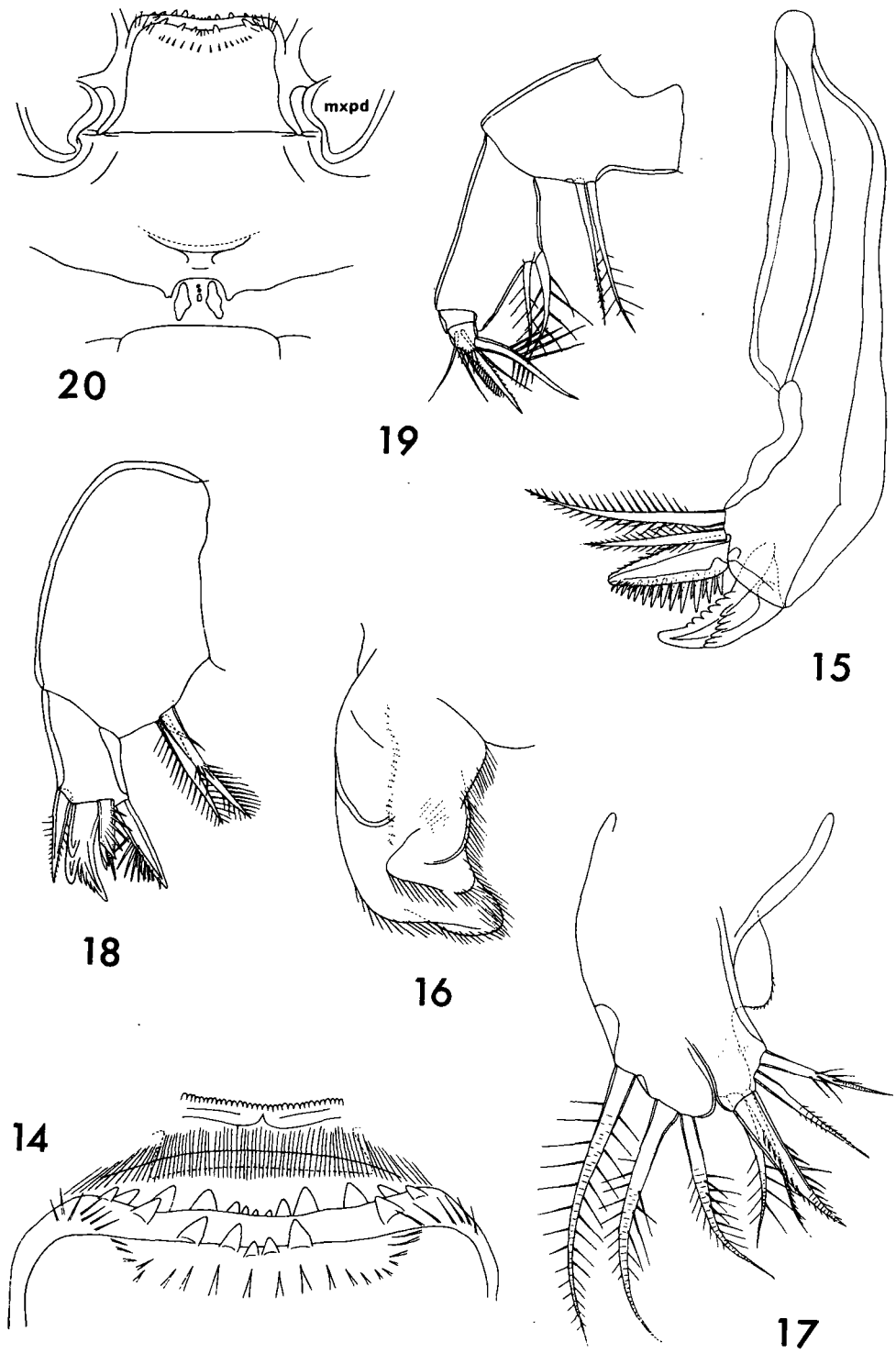
mxpd
20
19
15
18
16
14
17

Plate III

Hemicyclops axiophilus n. sp., female (continued)

Fig. 14. Metastomal areas, ventral (E).
Fig. 15. Mandible, anterior and dorsal (E).
Fig. 16. *Paragnath, anterior* (E).
Fig. 17.. First maxilla, posterior (E).
Fig. 18. Second maxilla, posterior (G).
Fig. 19. Maxilliped, anterior or dorsal (G).
Fig. 20. Region between maxillipeds and leg 1, ventral (H).

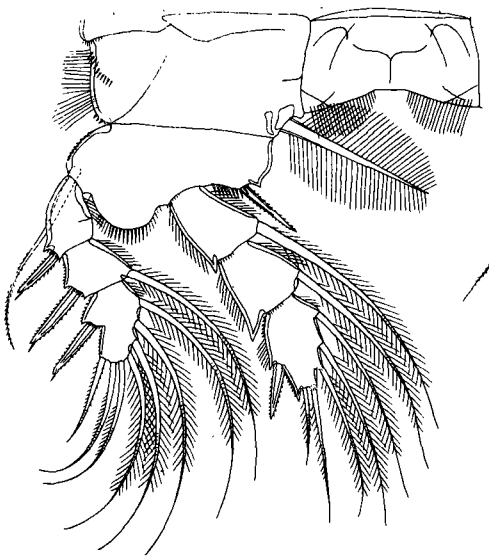

21

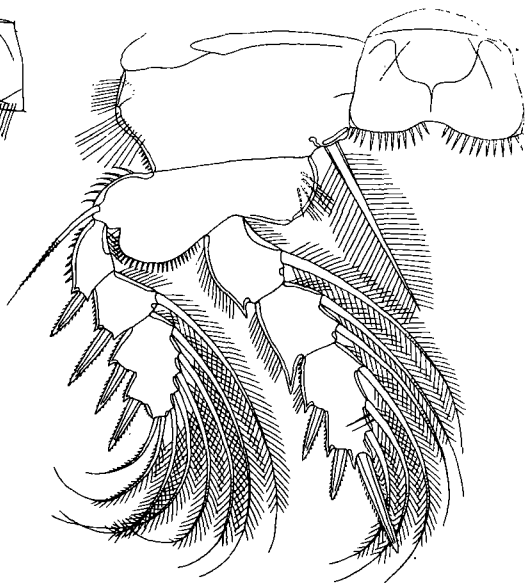

22

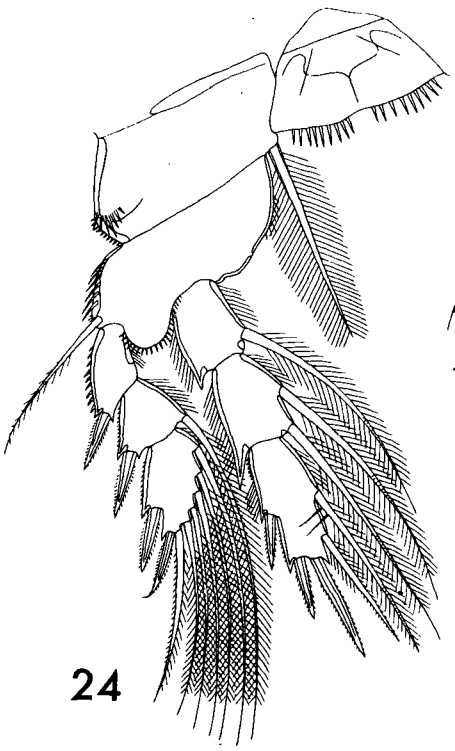

24

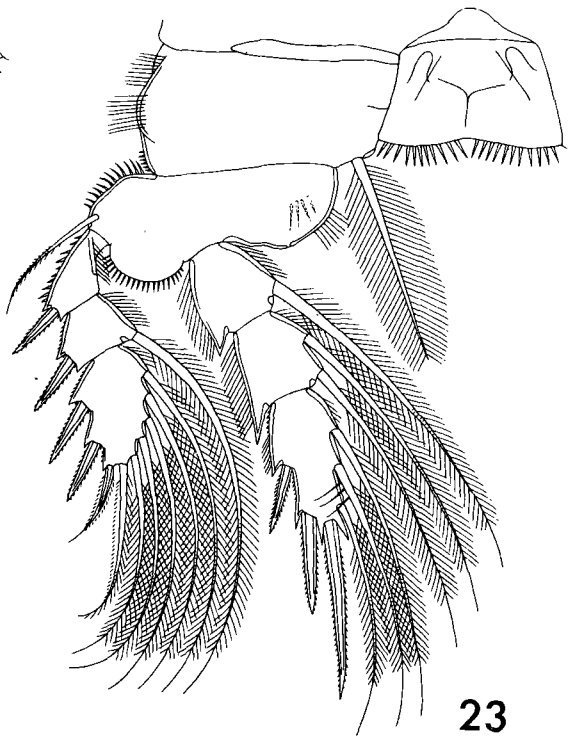

23

Plate IV

Hemicyclops axiophilus n. sp., female (continued)

Fig. 21. Leg 1, anterior (H).
Fig. 22. Leg 2, posterior (H).
Fig. 23. Leg 3, posterior (H).
Fig. 24. Leg 4, posterior (H).

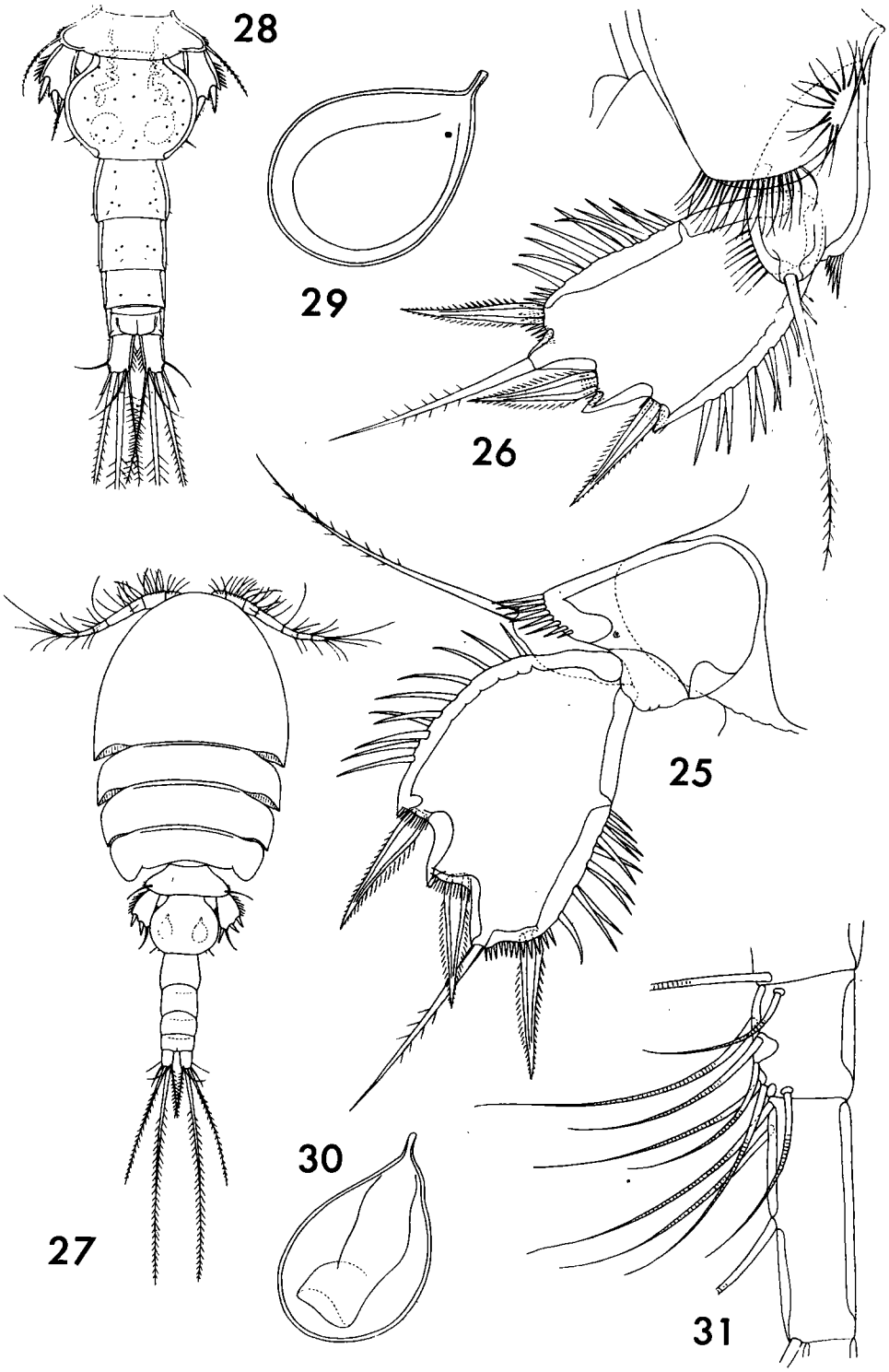
28
29
26
25
27
30
31

Plate V

Hemicyclops axiophilus n. sp., female (continued)

Fig. 25. Leg 5, ventral (D).
Fig. 26. Leg 5, dorsal (D).

Hemicyclops axiophilus n. sp., male

Fig. 27. Body, dorsal (A).
Fig. 28. Urosome, dorsal (C).
Fig. 29. Spermatophore attached to female (D).
Fig. 30. Spermatophore inside male (D).
Fig. 31. Segments 3 and 4 of first antenna, anterodorsal (D).

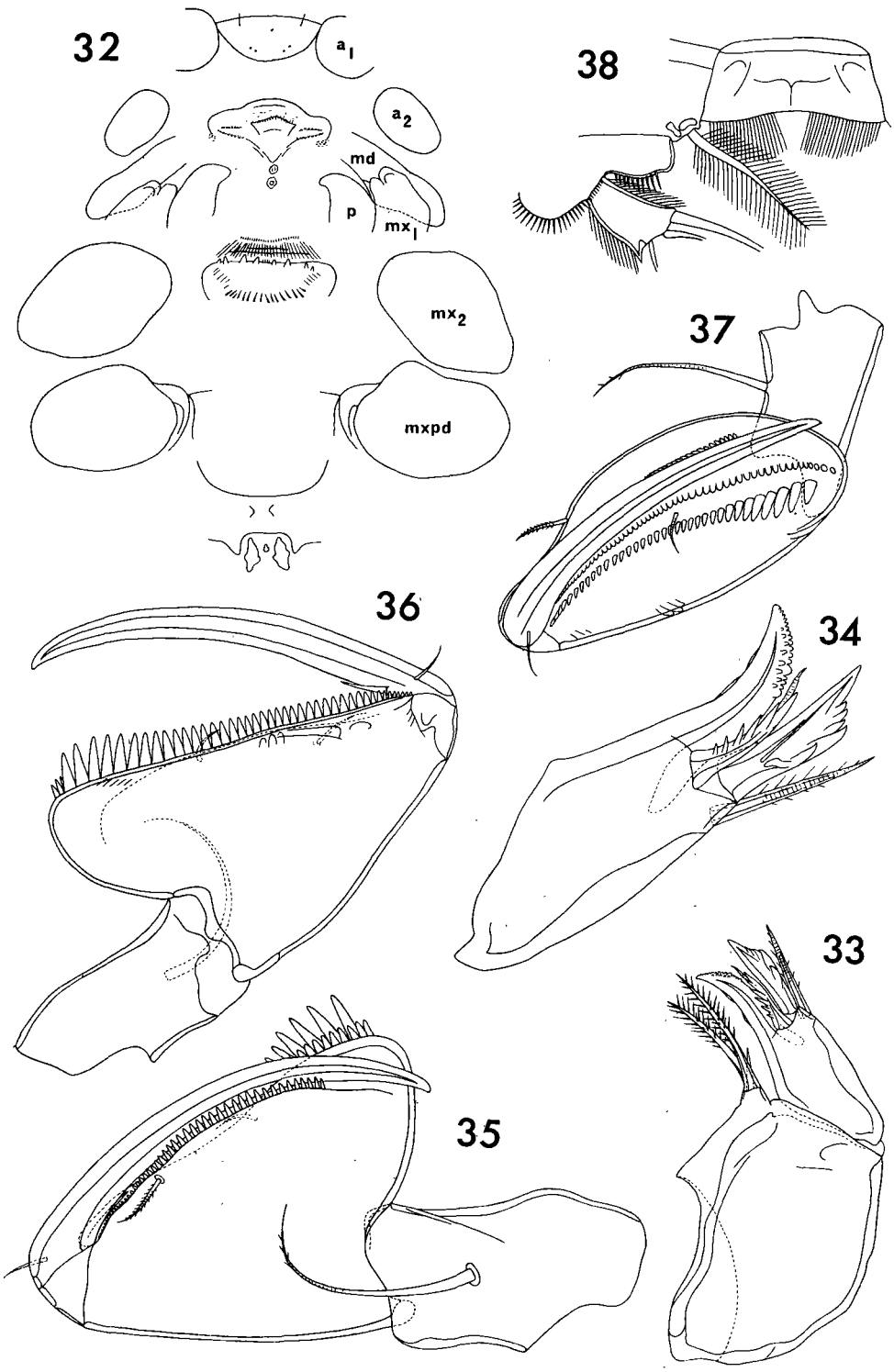
32
a_1
a_2
md
p
mx_1
mx_2
mxpd
38
37
36
34
33
35

Plate VI

Hemicyclops axiophilus n. sp., male (continued)

Fig. 32. Part of cephalosome, ventral (H).
Fig. 33. Second maxilla, posterior (G).
Fig. 34. Distal segment of second maxilla, posterior (E).
Fig. 35. Maxilliped, anterior (dorsal of large segment and claw) (G).
Fig. 36. Maxilliped, posterior (ventral of large segment and claw) (G).
Fig. 37. Maxilliped, inner surface (G).
Fig. 38. Detail of part of leg 1, posterior (H).

Abbreviations

a_1, first antenna	mx_1, first maxilla
a_2, second antenna	mx_2, second maxilla
md, mandible	mxpd, maxilliped
p, paragnath	p_1, leg 1

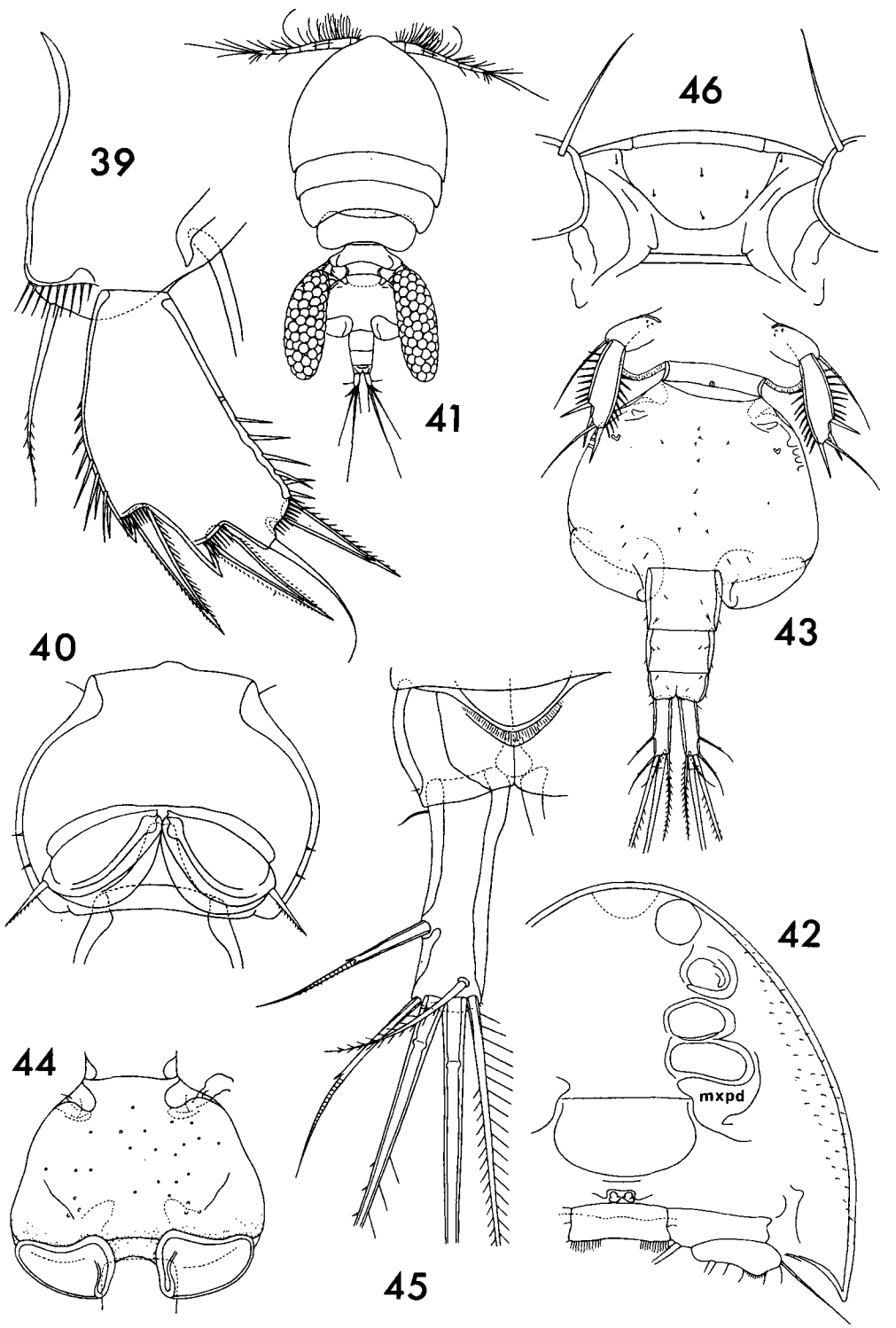
39
41
46
43
40
42
mxpd
44
45

Plate VII

Hemicyclops axiophilus n. sp., male (continued)

Fig. 39. Leg 5, ventral (D).
Fig. 40. Genital segment showing leg 6, ventral (H).

Hemicyclops amplicaudatus n. sp., female

Fig. 41. Body, dorsal (A).
Fig. 42. Part of cephalosome, ventral (B).
Fig. 43. Urosome, ventral (B).
Fig. 44. Genital segment, dorsal (B).
Fig. 45. Caudal ramus and part of anal segment, dorsal (E).
Fig. 46. Rostral area, ventral (D).

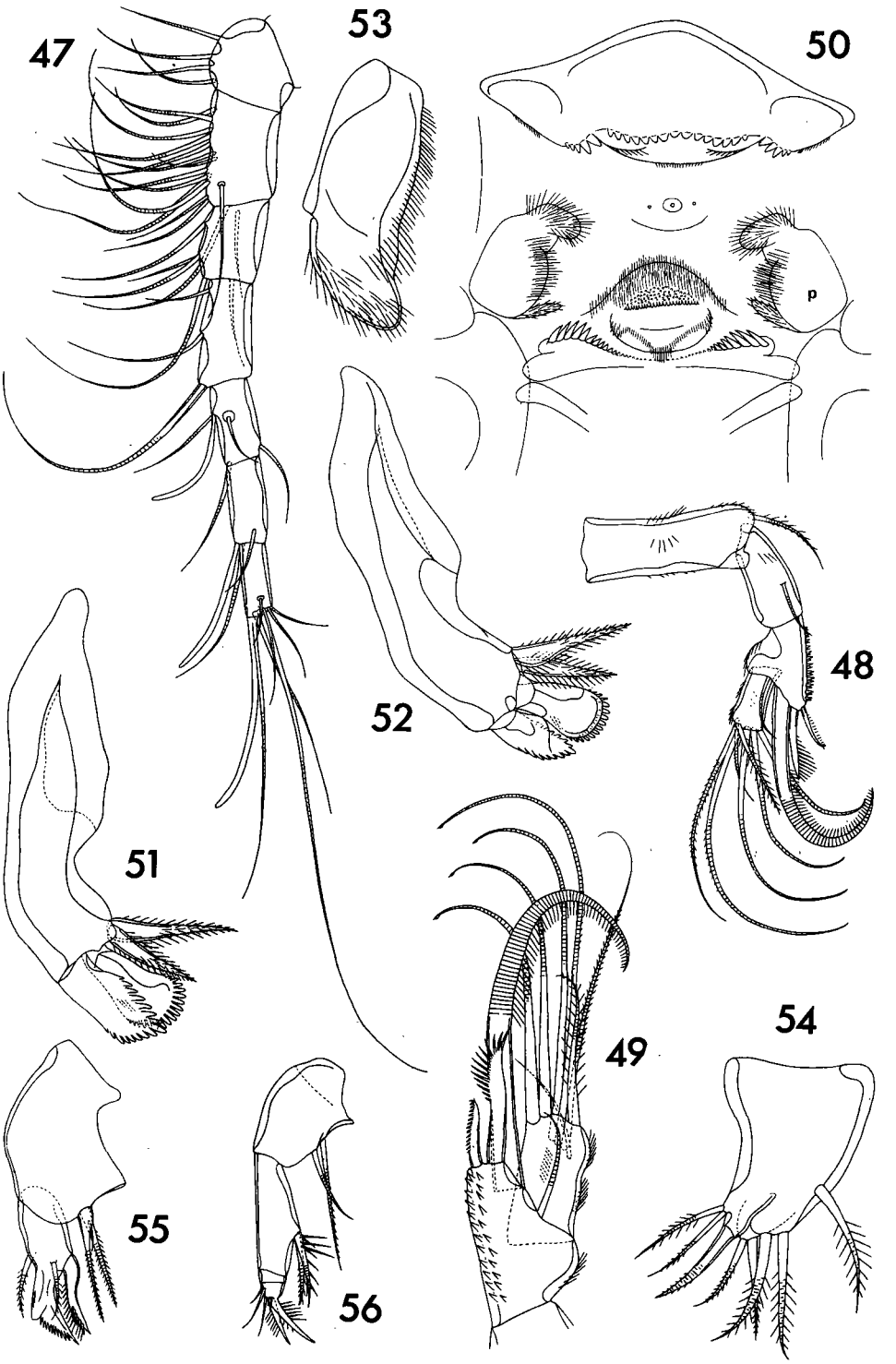
47
53
50
p
52
48
51
49
54
55
56

Plate VIII

Hemicyclops amplicaudatus n. sp., female (continued)

Fig. 47. First antenna, ventral (G).
Fig. 48. Second antenna, posterior (G).
Fig. 49. Last two segments of second antenna, posterior (E).
Fig. 50. - Oral area, ventral (E).
Fig. 51. Mandible, ventral (E).
Fig. 52. Mandible, dorsal (E).
Fig. 53. Paragnath, ventral and posterior (F).
Fig. 54. First maxilla, posterior (G).
Fig. 55. Second maxilla, posterior (G).
Fig. 56. Maxilliped, posterior and slightly outer (G).

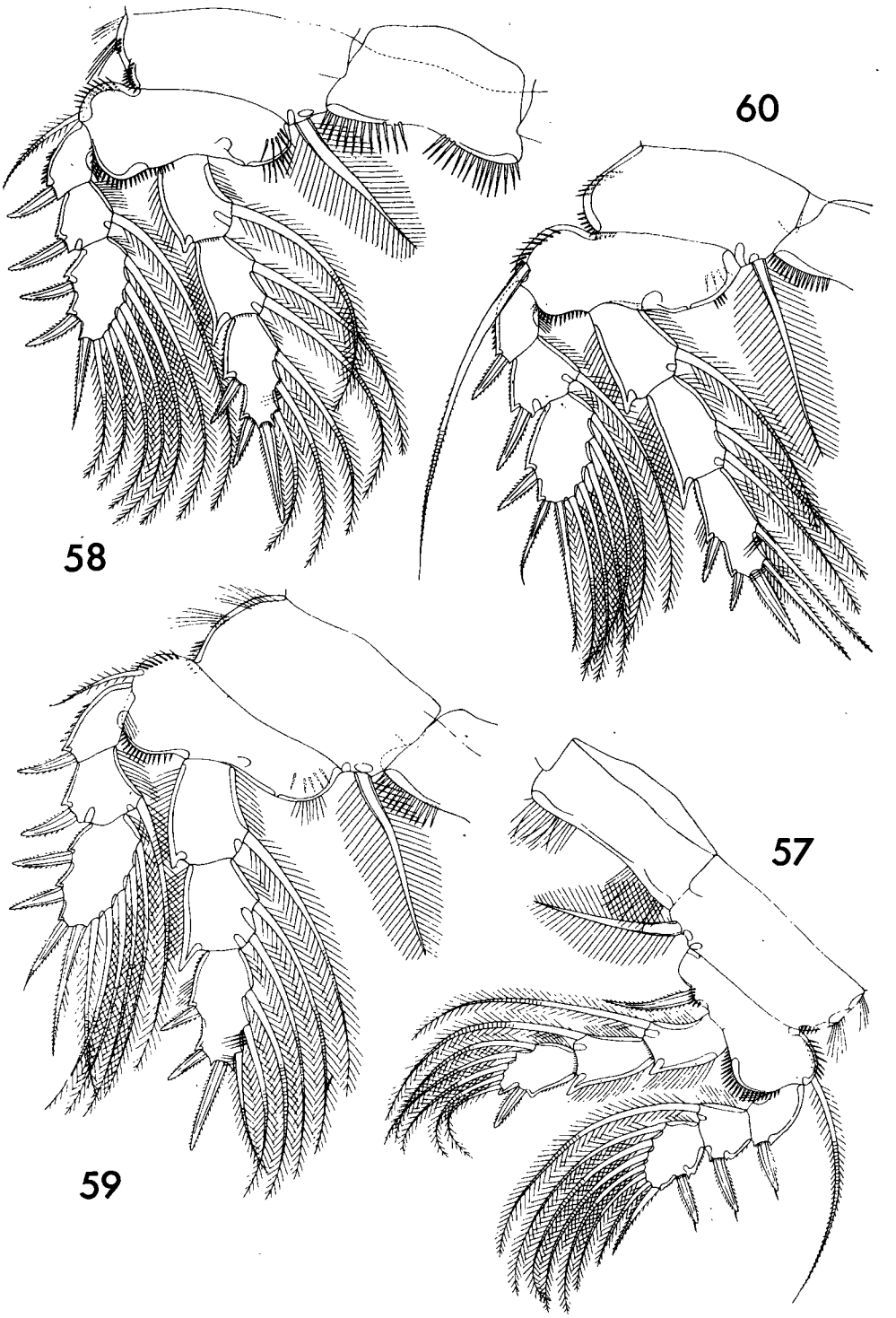
60
58
57
59

Plate IX

Hemicyclops amplicaudatus n. sp., female (continued)

Fig. 57. Leg 1, anterior (G).
Fig. 58. Leg 2, anterior (G).
Fig. 59. Leg 3, posterior (G).
Fig. 60. Leg 4, posterior (G).

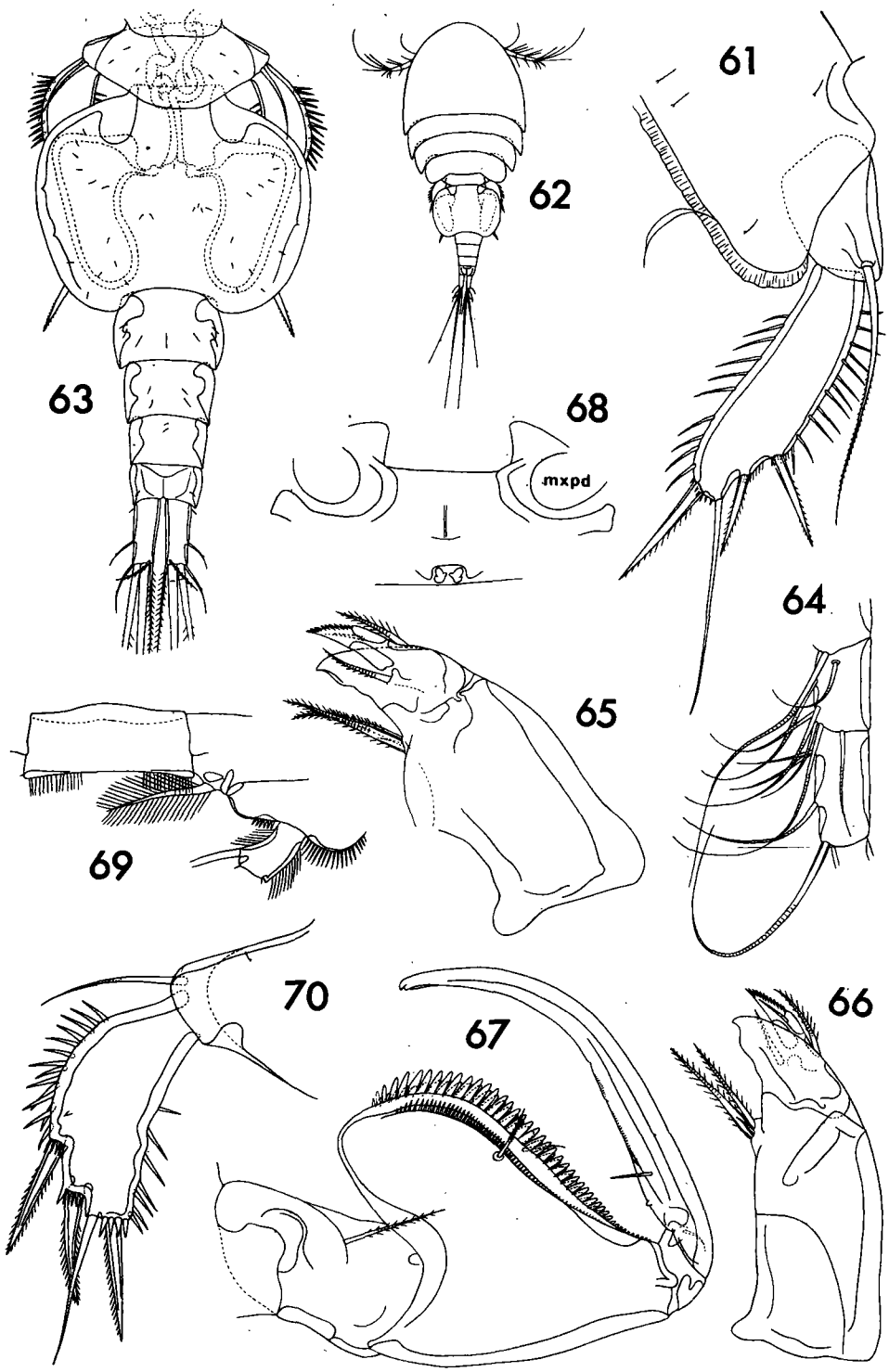
61
62
63
68
mxpd
64
65
69
70
67
66

Plate X

Hemicyclops amplicaudatus n. sp., female (continued)

Fig. 61. Leg 5, dorsal (D).

Hemicyclops amplicaudatus n. sp., male

Fig. 62. Body, dorsal (A).
Fig. 63. Urosome, dorsal (H).
Fig. 64. Segments 3 and 4 of first antenna, ventral (D).
Fig. 65. Second maxilla, anterior (D).
Fig. 66. Second maxilla, posterior (D).
Fig. 67. Maxilliped, anterior (D).
Fig. 68. Area between maxillipeds and leg 1, ventral (H).
Fig. 69. Portion of leg 1, anterior (G).
Fig. 70. Leg 5, ventral (D).

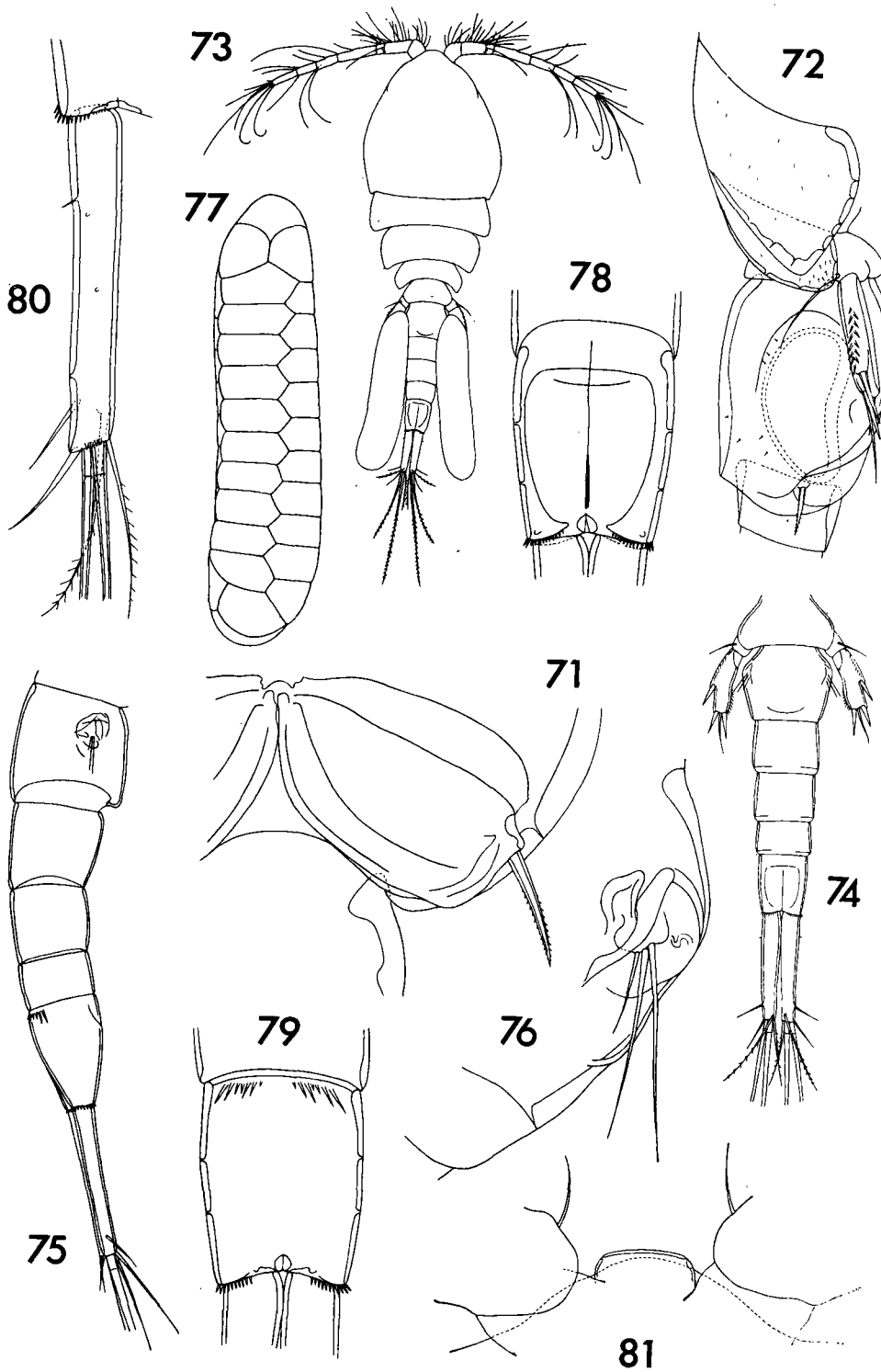
73
72
77
80
78
71
74
79
76
75
81

Plate XI

Hemicyclops amplicaudatus n. sp., male (continued)

Fig. 71. Leg 6, ventral (D).
Fig. 72. Segment of leg 5, genital segment, and adjacent areas, lateral (H).

Hemicyclops carinifer n. sp., female

Fig. 73. Body, dorsal (A).
Fig. 74. Urosome, dorsal (C).
Fig. 75. Urosome, lateral (B).
Fig. 76. Area of attachment of egg sac, dorsal and slightly lateral (E).
Fig. 77. Egg sac, dorsal (B).
Fig. 78. Anal segment, dorsal (G).
Fig. 79. Anal segment, ventral (G).
Fig. 80. Caudal ramus, ventral (G).
Fig. 81. Rostral area, ventral (D).

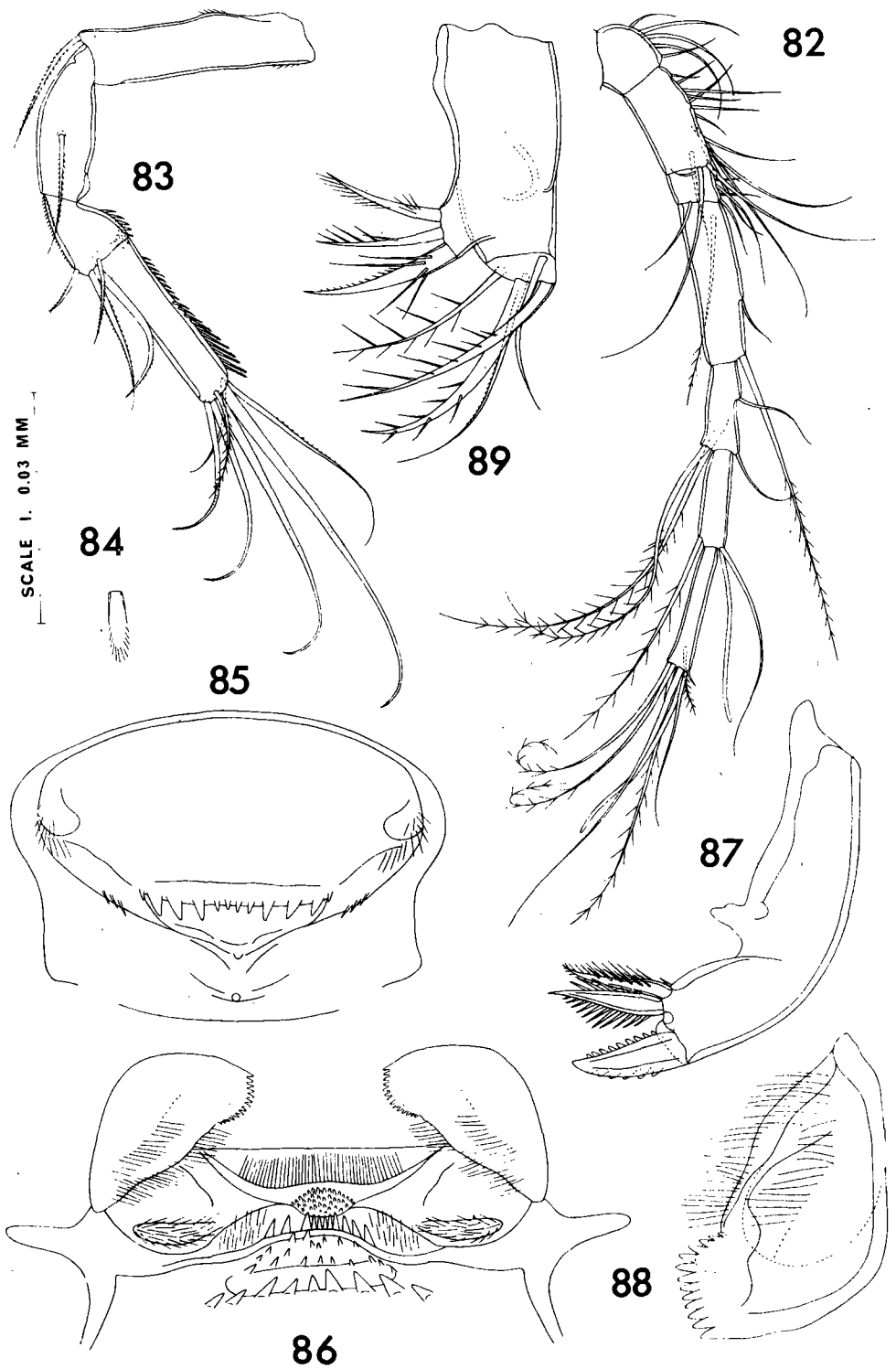
82
83
89
SCALE I. 0.03 MM
84
85
87
88
86

Plate XII

Hemicyclops carinifer n. sp., female (continued)

Fig. 82. First antenna, dorsal (H).
Fig. 83. Second antenna, posterior mesial (G).
Fig. 84. Seta on third segment of second antenna (I).
Fig. 85. Labrum, anterior and ventral (E).
Fig. 86. Metastomal areas and paragnaths, ventral (E).
Fig. 87. Mandible, posterior (E).
Fig. 88. Paragnath, ventral and posterior (F).
Fig. 89. First maxilla, posterior (E).

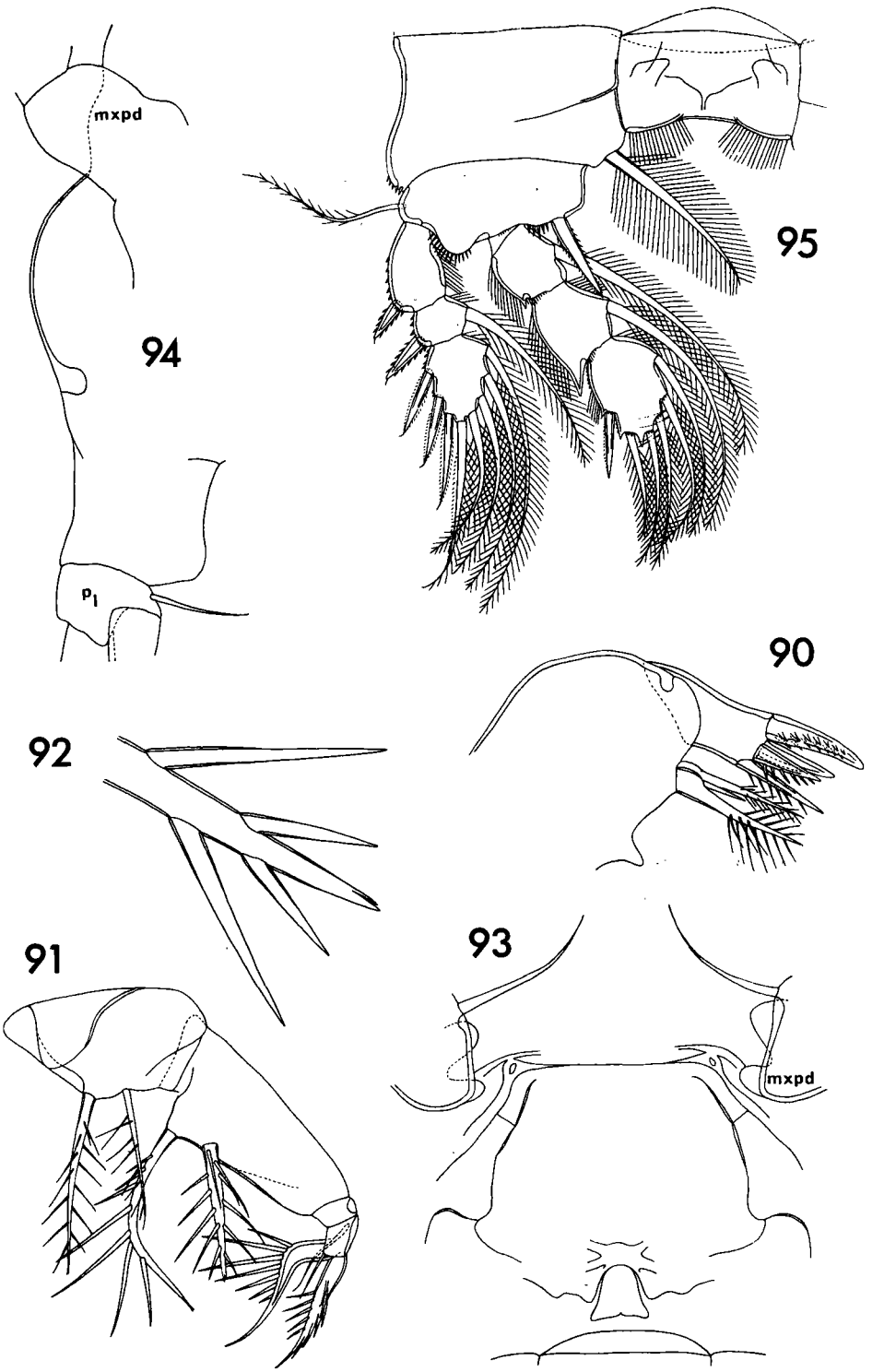
mxpd
94
p_1
95
90
92
91
93
mxpd

Plate XIII

Hemicyclops carinifer n. sp., female (continued)

Fig. 90. Second maxilla, posterior and dorsal (D).
Fig. 91. Maxilliped, dorsal (G).
Fig. 92. Terminal part of distal seta on second segment of maxilliped (I).
Fig. 93. Area between maxillipeds and leg 1, ventral (G).
Fig. 94. Area between maxillipeds and leg 1, lateral (G).
Fig. 95. Leg 1, anterior (G).

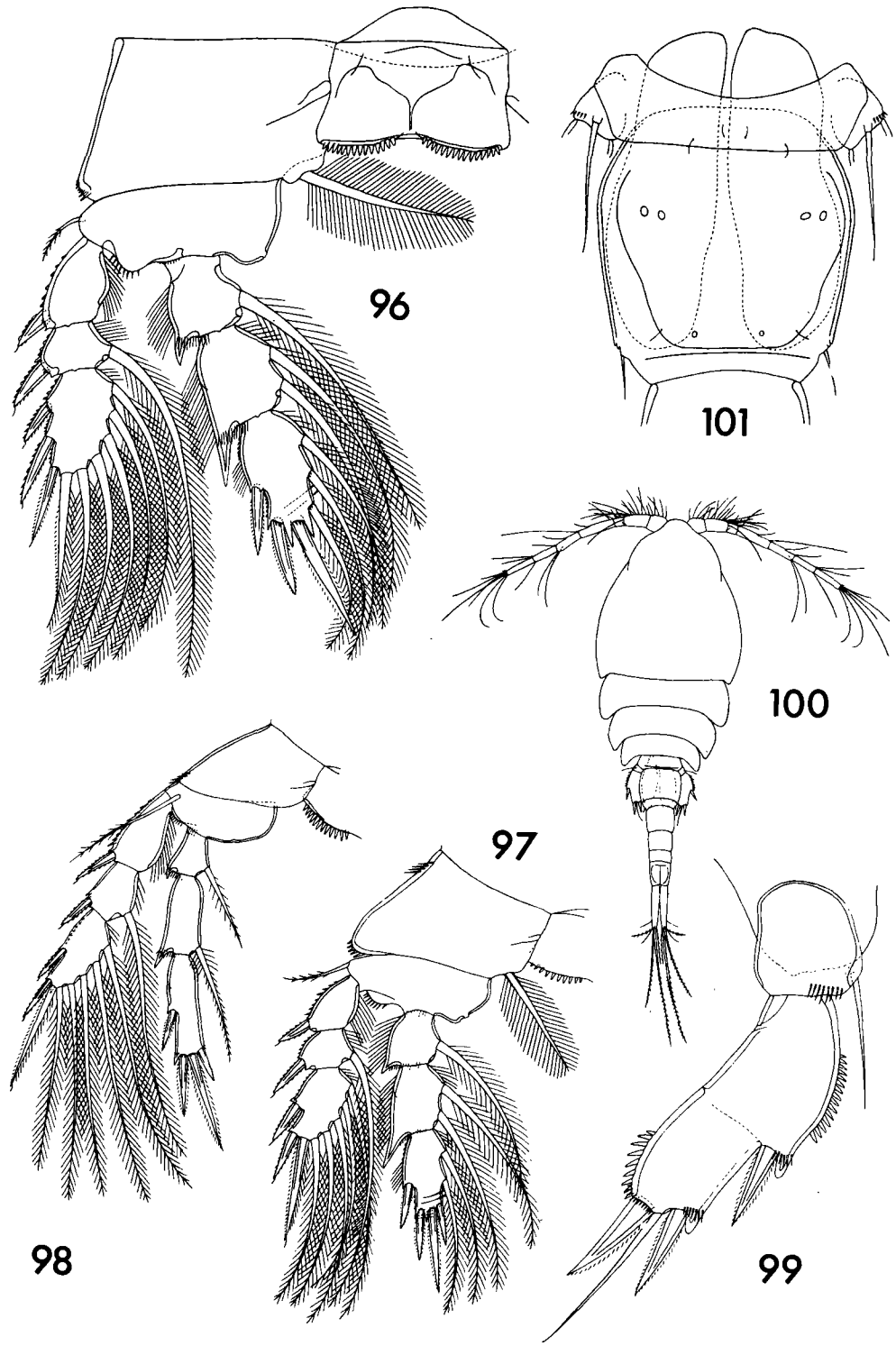
96
101
100
97
98
99

Plate XIV

Hemicyclops carinifer n. sp., female (continue

Fig. 96. Leg 2, anterior (G).
Fig. 97. Leg 3, posterior (H).
Fig. 98. Leg 4, posterior (H).
Fig. 99. Leg 5, ventral and lateral (D).

Hemicyclops carinifer n. sp., male

Fig. 100. Body, dorsal (A).
Fig. 101. Segment of leg 5 and genital segment, dorsal (G).

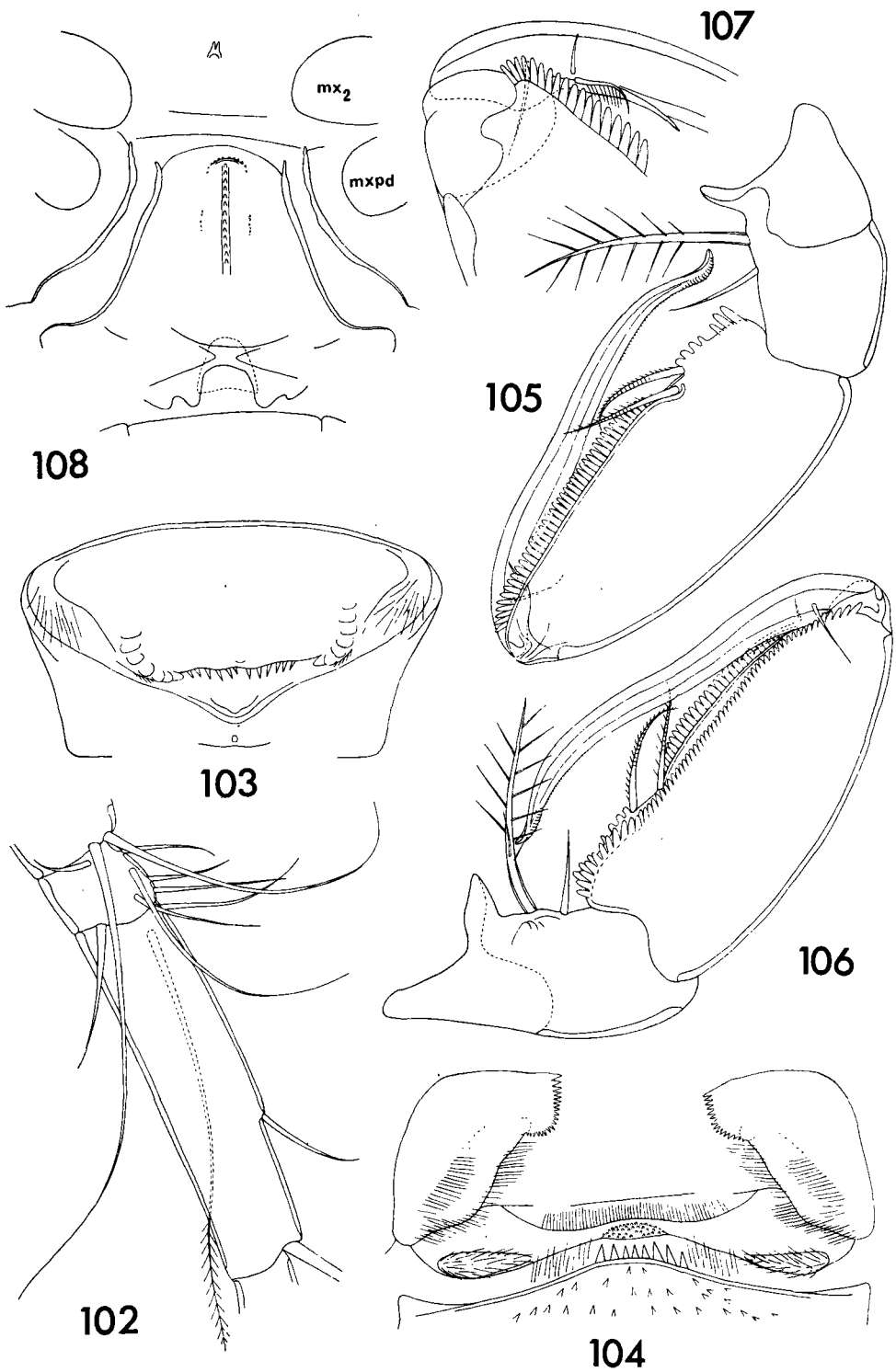
107
mx2
mxpd
105
108
103
106
102
104

Plate XV

Hemicyclops carinifer n. sp., male (continued)

Fig. 102. Third and fourth segments of first antenna, dorsal (D).
Fig. 103. Labrum, ventral and anterior (E).
Fig. 104. Metastomal areas and paragnaths, ventral (E).
Fig. 105. Maxilliped, anterior (G).
Fig. 106. Maxilliped, posterior (G).
Fig. 107. Detail of third and fourth segments of maxilliped, anterior (E).
Fig. 108. Area between maxillipeds and leg 1, ventral (G).

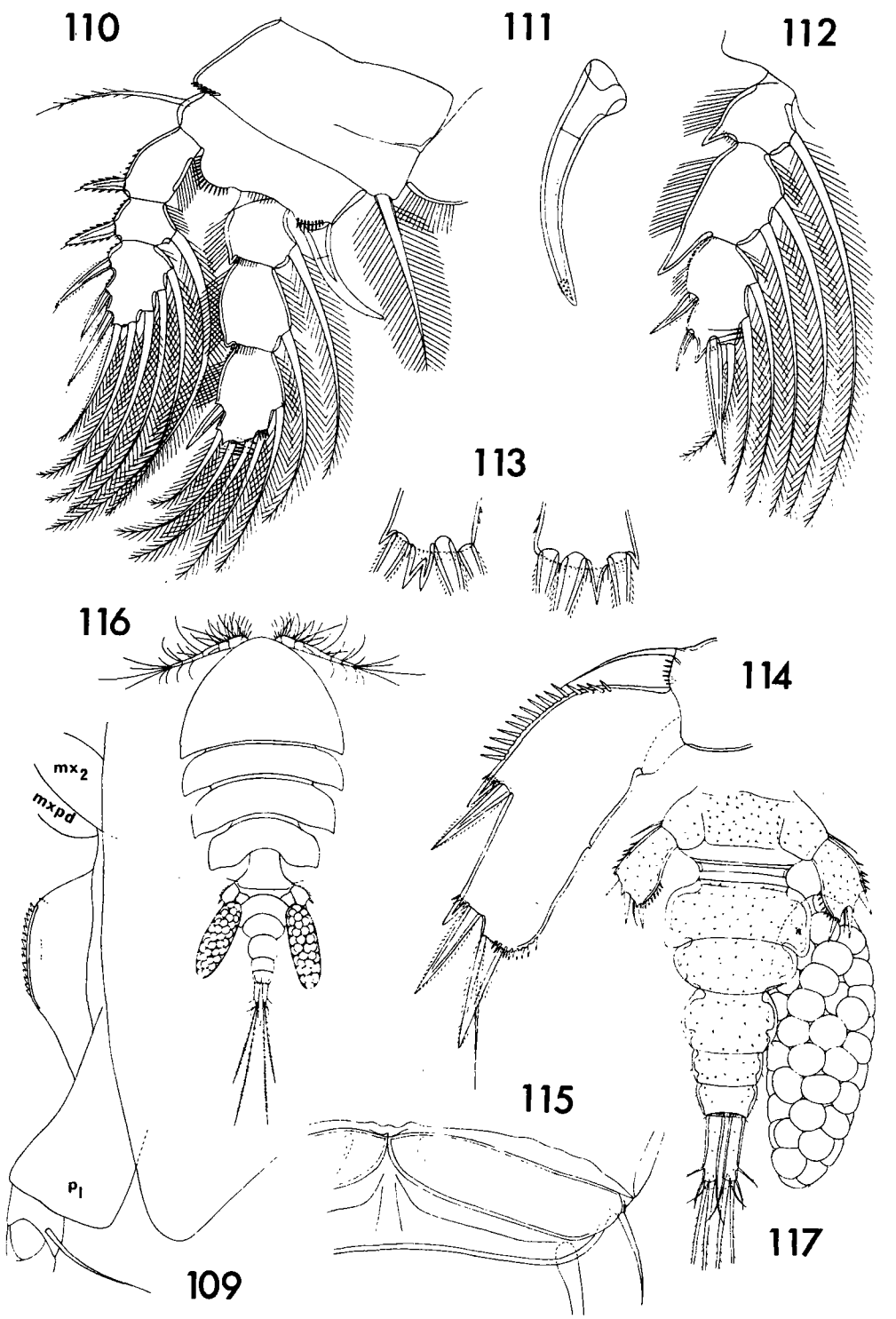
110
111
112
113
116
114
mx2
mxpd
115
P1
117
109

Plate XVI

Hemicyclops carinifer n. sp., male (continued)

Fig. 109. Area between maxillipeds and leg 1, lateral (G).
Fig. 110. Leg 1, anterior (G).
Fig. 111. Inner spine on basis of leg 1, posterior (E).
Fig. 112. Endopod of leg 2, posterior (G).
Fig. 113. Distal margins of endopods in leg 3 of 1 male, posterior (E).
Fig. 114. Leg 5, dorsomesial (D).
Fig. 115. Leg 6, ventral (E).

Hemicyclops diremptus n. sp., female

Fig. 116. Body, dorsal (A).
Fig. 117. Urosome, ventral (C).

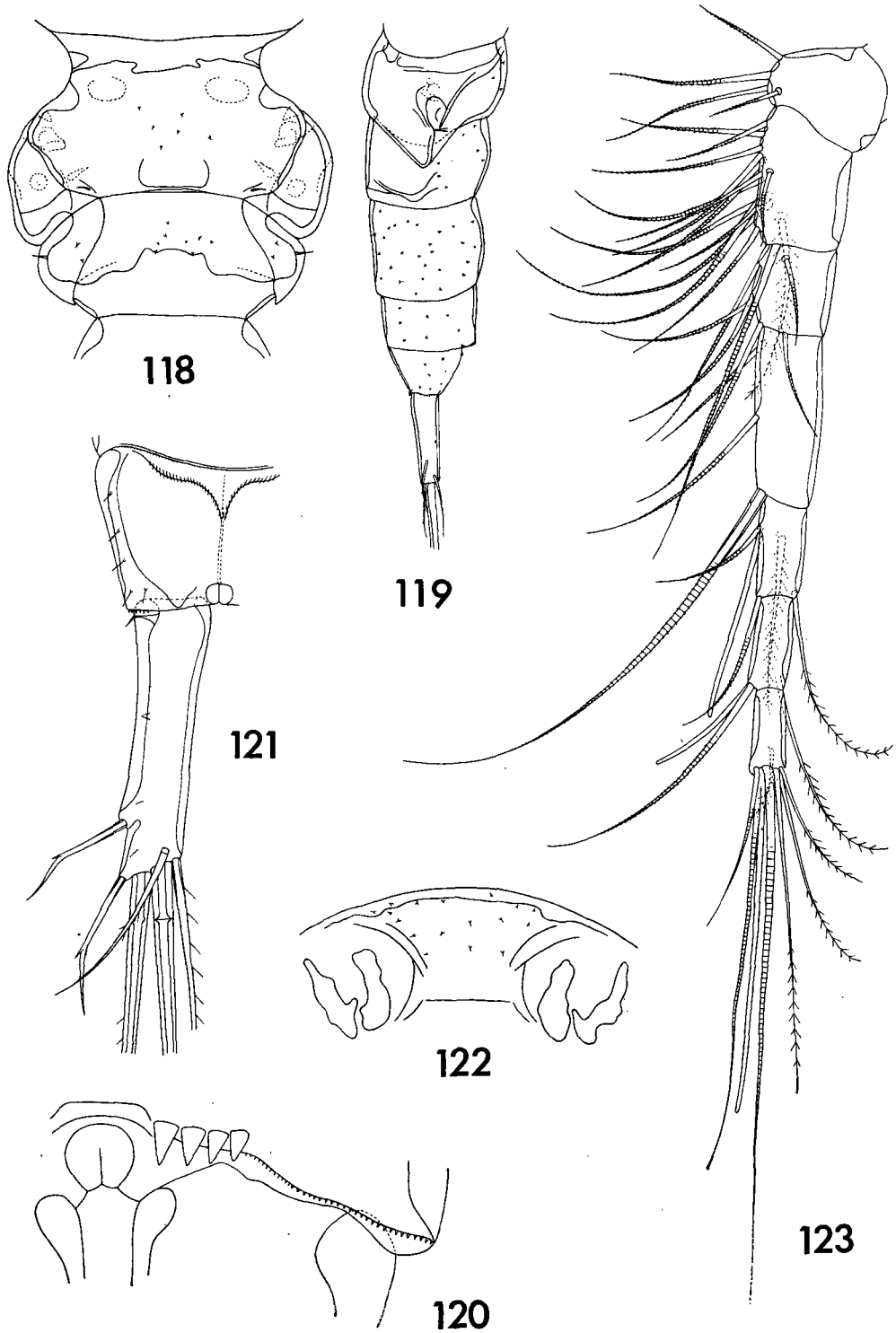
118
119
121
122
120
123

Plate XVII

Hemicyclops diremptus n. sp., female (continued)

Fig. 118. Genital segment, dorsal (H).
Fig. 119. Genital and postgenital segments, lateral (B).
Fig. 120. Area of insertion of a caudal ramus, ventral (I)
Fig. 121. Caudal ramus, dorsal (D).
Fig. 122. Rostral area, ventral (G).
Fig. 123. First antenna, ventral (G).

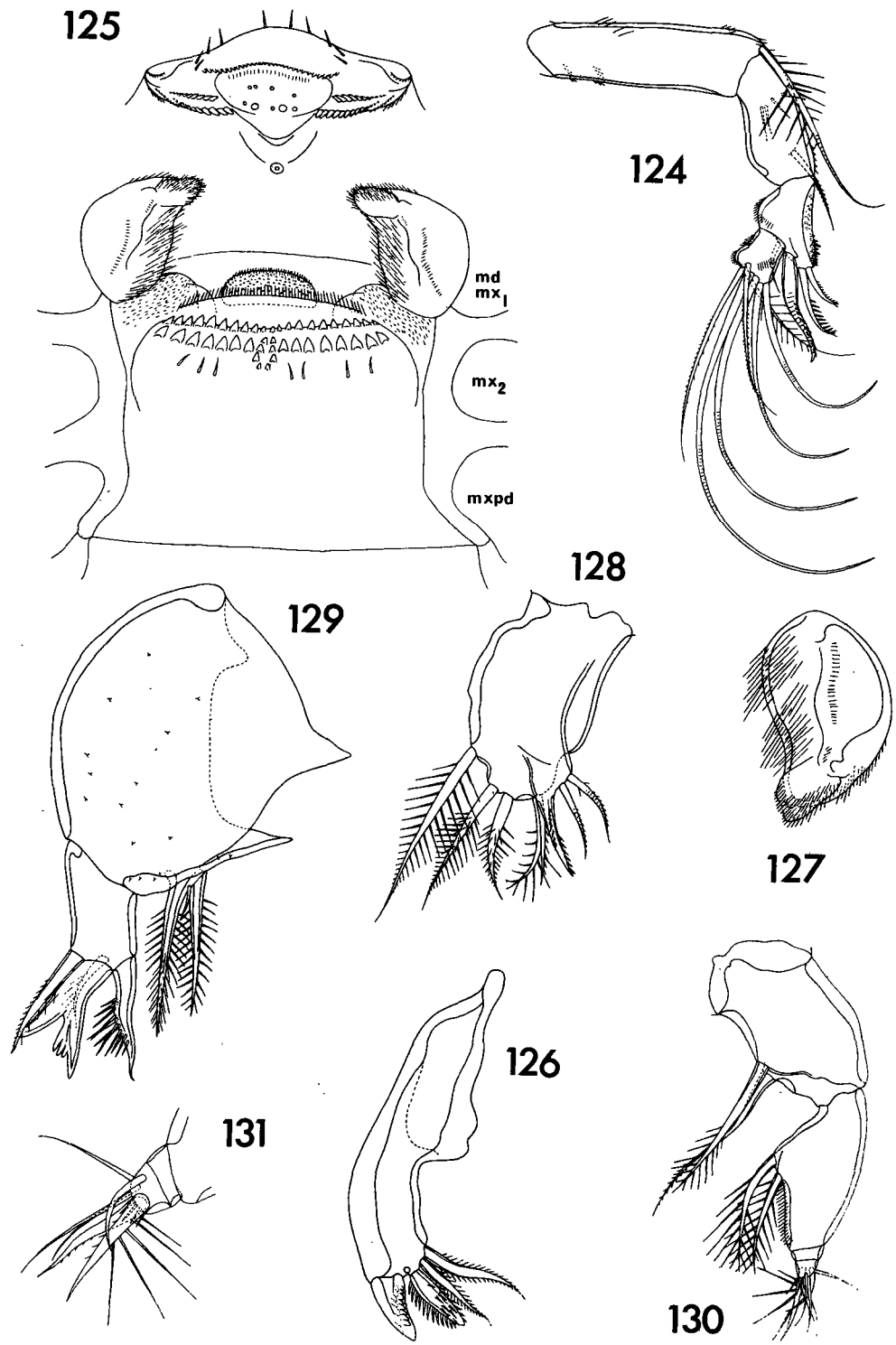
125
md
mx1
mx2
mxpd
124
128
129
127
126
131
130

Plate XVIII

Hemicyclops diremptus n. sp., female (continued)

Fig. 124. Second antenna, anterior (G).
Fig. 125. Oral area, ventral (D).
Fig. 126. Mandible, posterior and ventral (D).
Fig. 127. Paragnath, posterodorsal (E).
Fig. 128. *First maxilla*, posterior (D).
Fig. 129. Second maxilla, anterior (D).
Fig. 130. Maxilliped, anterodorsal (G).
Fig. 131. Tip of maxilliped, posteroventral (E).

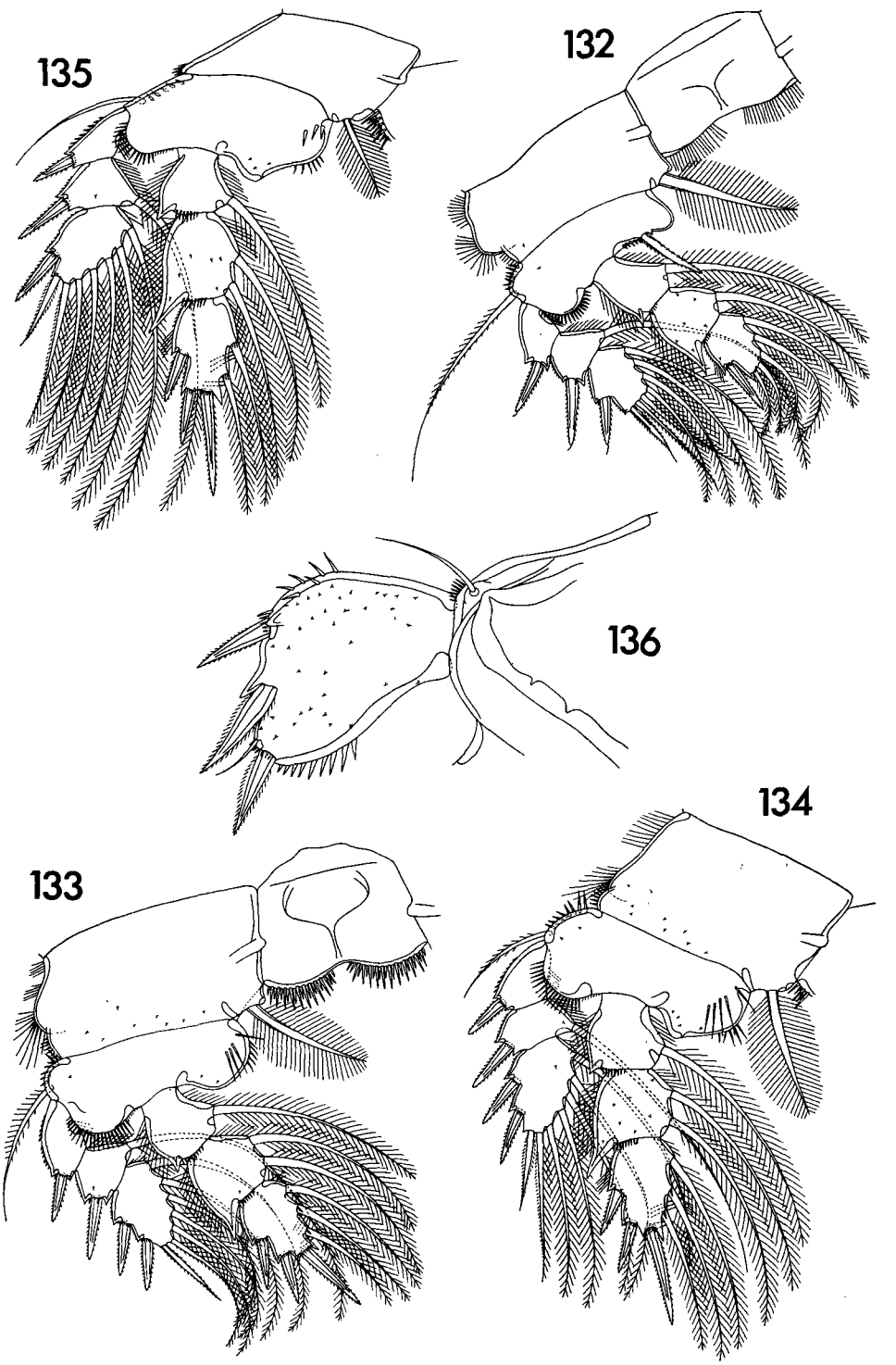
135
132
136
134
133

Plate XIX

Hemicyclops diremptus n. sp., female (continued)

Fig. 132. Leg 1, anterior (H).
Fig. 133. Leg 2, anterior (H).
Fig. 134. Leg 3, anterior (H).
Fig. 135. Leg 4, anterior (H).
Fig. 136. Leg 5, dorsal (G).

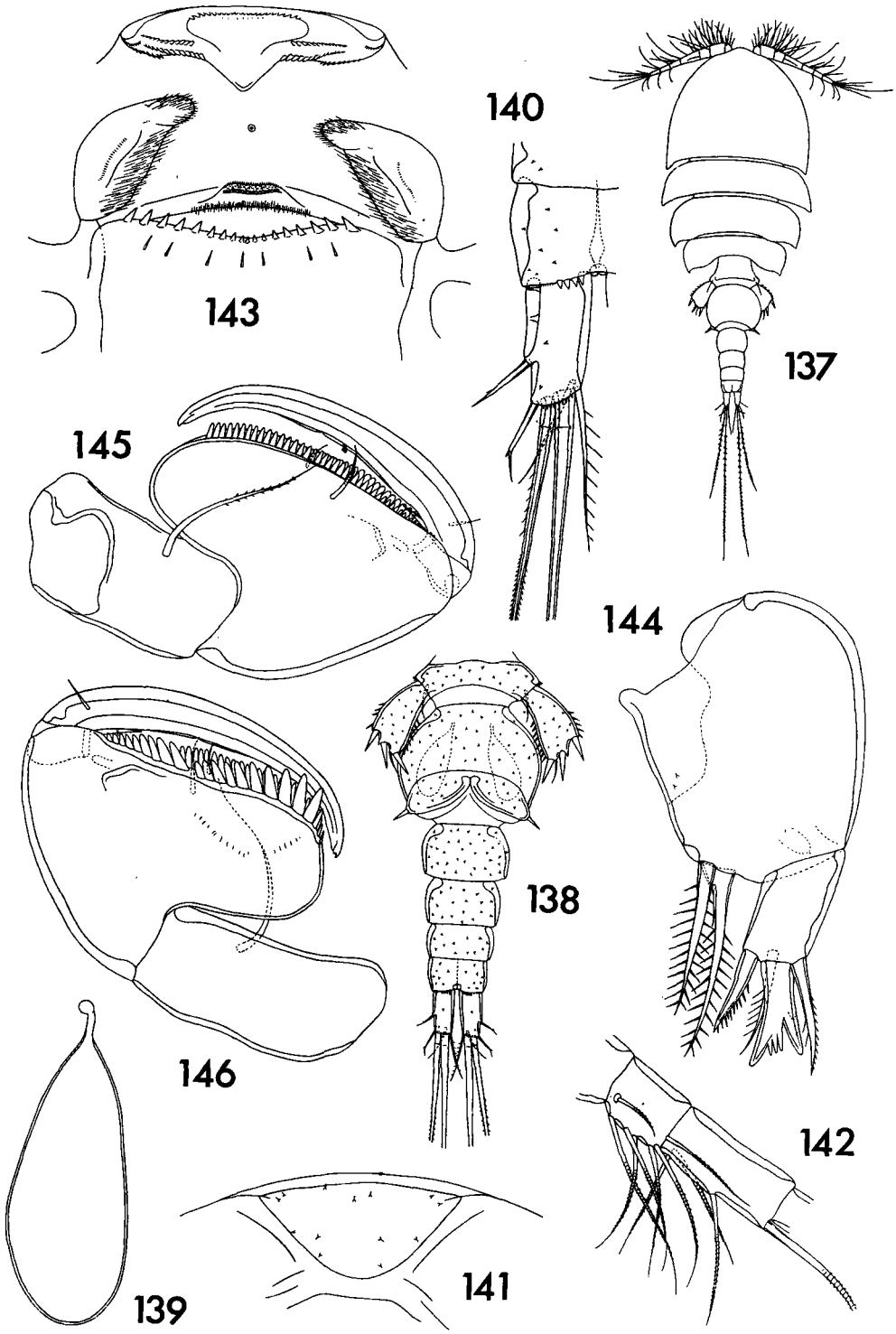
140
143
137
145
144
138
146
142
139
141

Plate XX

Hemicyclops diremptus n. sp., male

Fig. 137. Body, dorsal (A).
Fig. 138. Urosome, ventral (C).
Fig. 139. Spermatophore from inside body of male (E).
Fig. 140. Caudal ramus and part of anal segment, ventral (D).
Fig. 141. Rostral area, ventral (E).
Fig. 142. Third and fourth segments of first antenna, ventral (D).
Fig. 143. Oral area, ventral (E).
Fig. 144. Second maxilla, anterior (E).
Fig. 145. Maxilliped, anterior (D).
Fig. 146. Maxilliped, posterior (D).

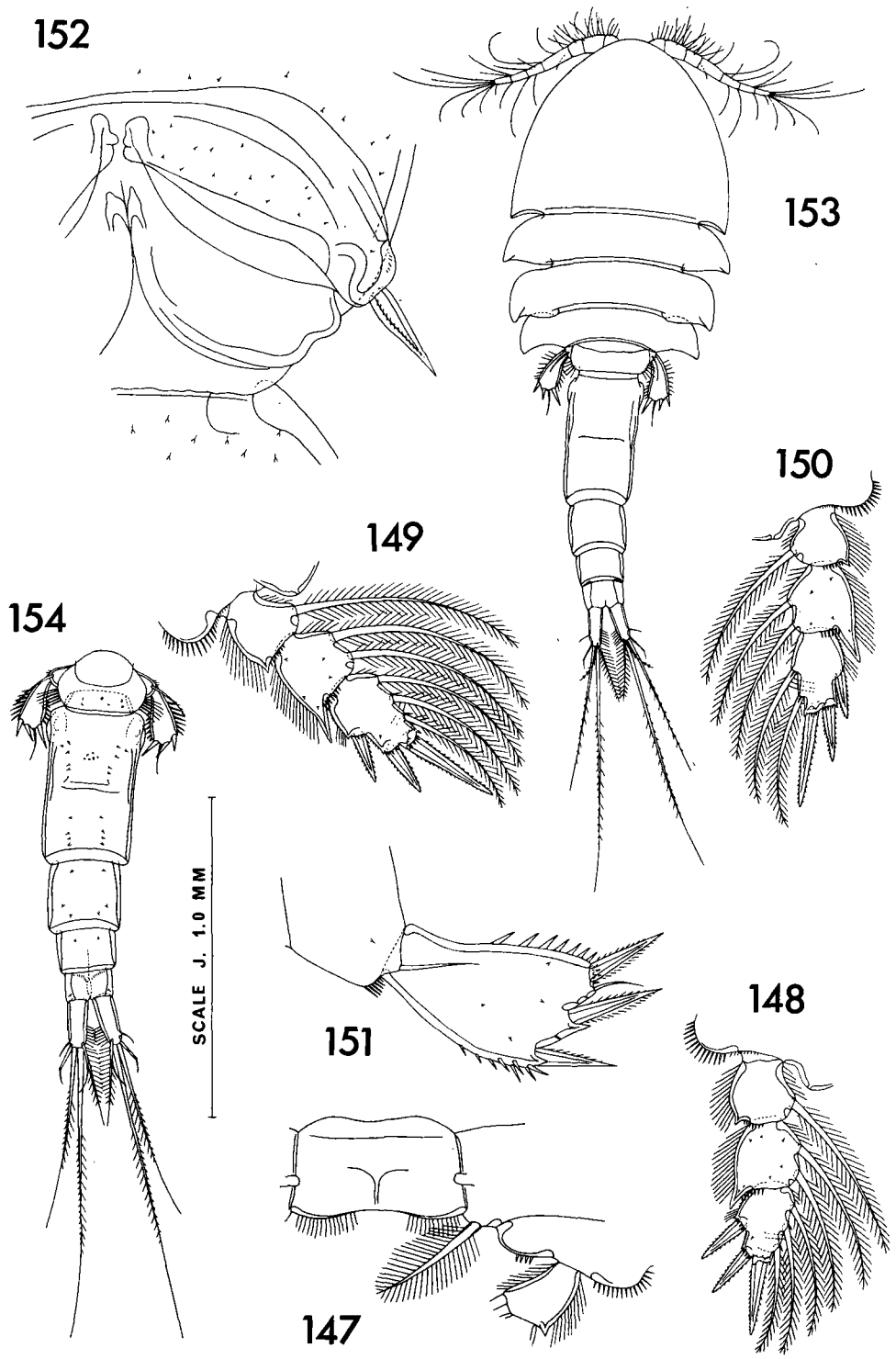
152
153
150
149
154
SCALE J. 1.0 MM
151
148
147

Plate XXI

Hemicyclops diremptus n. sp., male (continued)

Fig. 147. Portion of leg 1, anterior (G).
Fig. 148. Endopod of leg 2, anterior (G).
Fig. 149. Endopod of leg 3, anterior (G).
Fig. 150. Endopod of leg 4, anterior (G).
Fig. 151. Leg 5, dorsal (D).
Fig. 152. Leg 6, ventral (E).

Hemicyclops kombensis n. sp., female

Fig. 153. Body, dorsal (A).
Fig. 154. Urosome, dorsal (J).

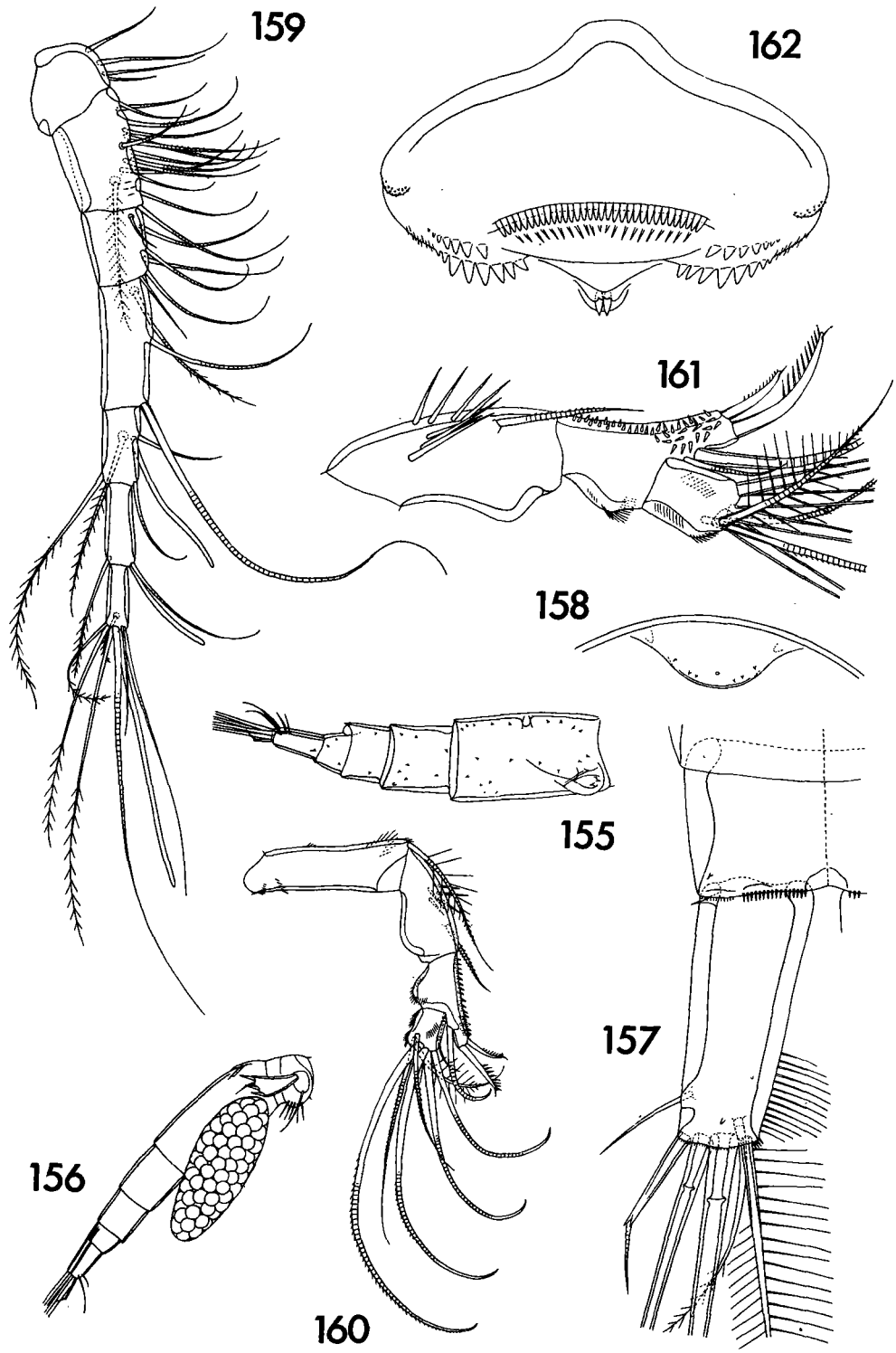
159
162
161
158
155
157
156
160

Plate XXII

Hemicyclops kombensis n. sp., female (continued)

Fig. 155. Genital and postgenital segments, nearly lateral (J).
Fig. 156. Egg sac attached to urosome, nearly lateral (A).
Fig. 157. Caudal ramus, ventral (G).
Fig. 158. Rostral area, ventral (G).
Fig. 159. First antenna, ventral (H).
Fig. 160. Second antenna, anterior (H).
Fig. 161. Last three segments of second antenna, posterior (D).
Fig. 162. Labrum, ventral and somewhat posterior (E).

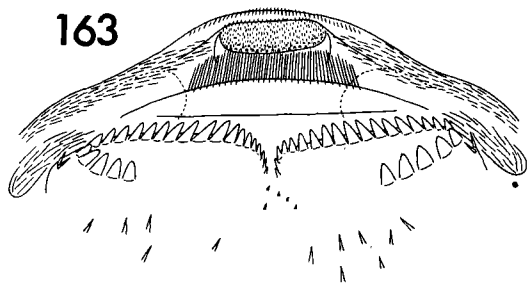
163

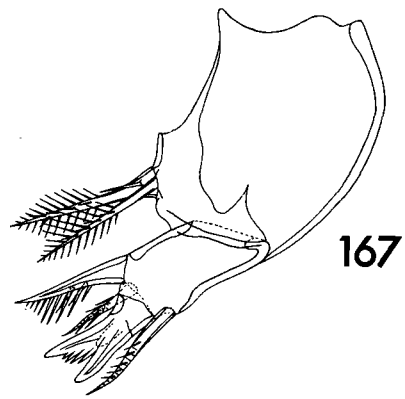
167

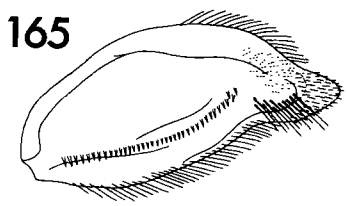
165

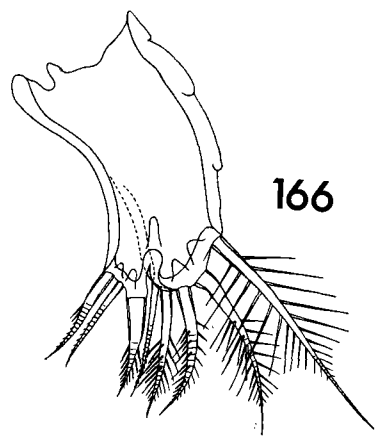
166

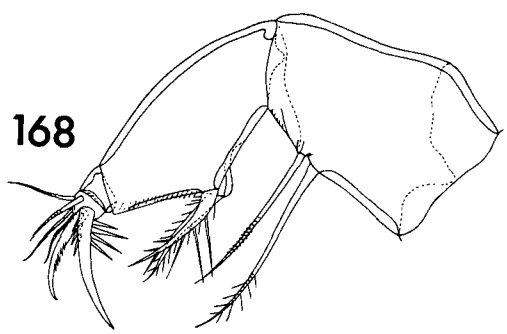
168

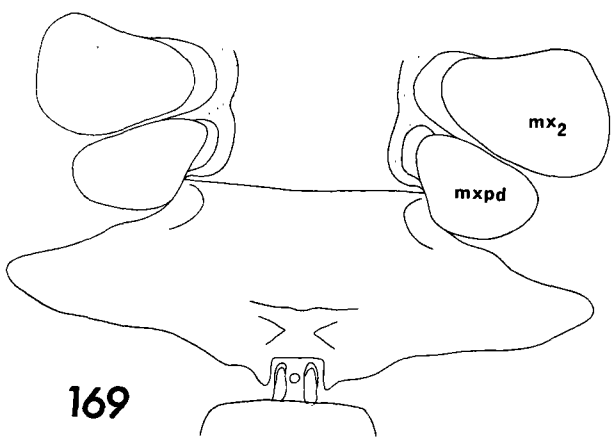
mx2
mxpd
169

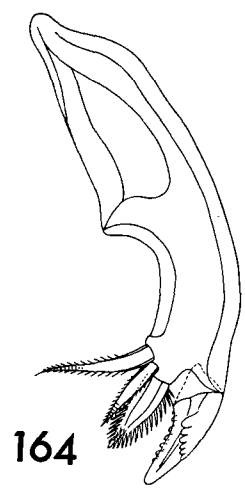
164

Plate XXIII

Hemicyclops kombensis n. sp., female (continued)

Fig. 163. Metastomal areas, ventral (E).
Fig. 164. Mandible, anterior and dorsal (D).
Fig. 165. Paragnath, posterior and ventral (E).
Fig. 166. First maxilla, posterior (D).
Fig. 167. Second maxilla, anterior (G).
Fig. 168. Maxilliped, posterior and ventral (G).
Fig. 169. Region between maxillipeds and leg 1, ventral (H).

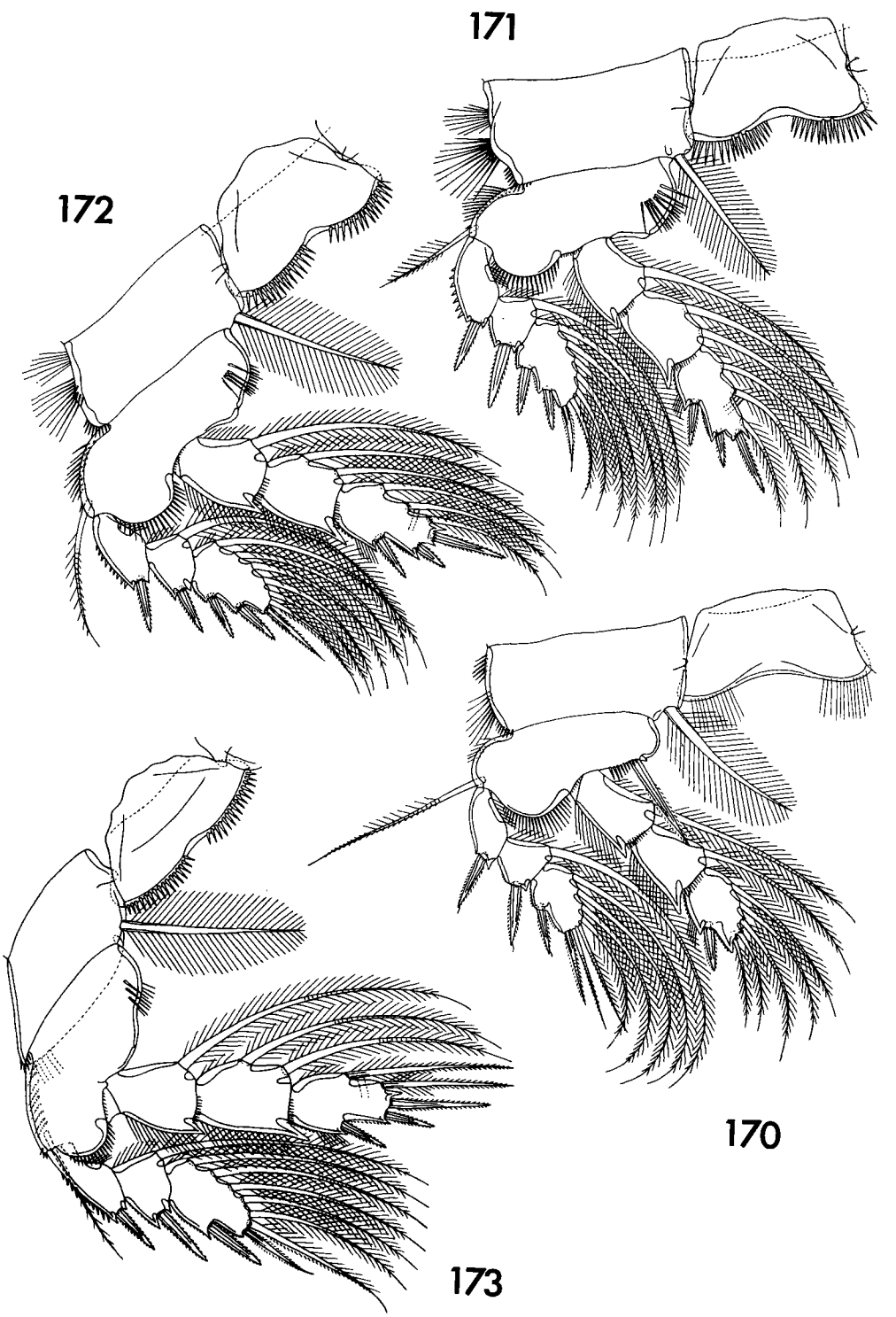
171
172
170
173

Plate XXIV

Hemicyclops kombensis n. sp., female (continued)

Fig. 170. Leg 1, anterior (H).
Fig. 171. Leg 2, anterior (H).
Fig. 172. Leg 3, anterior (H).
Fig. 173. Leg 4, anterior (H).

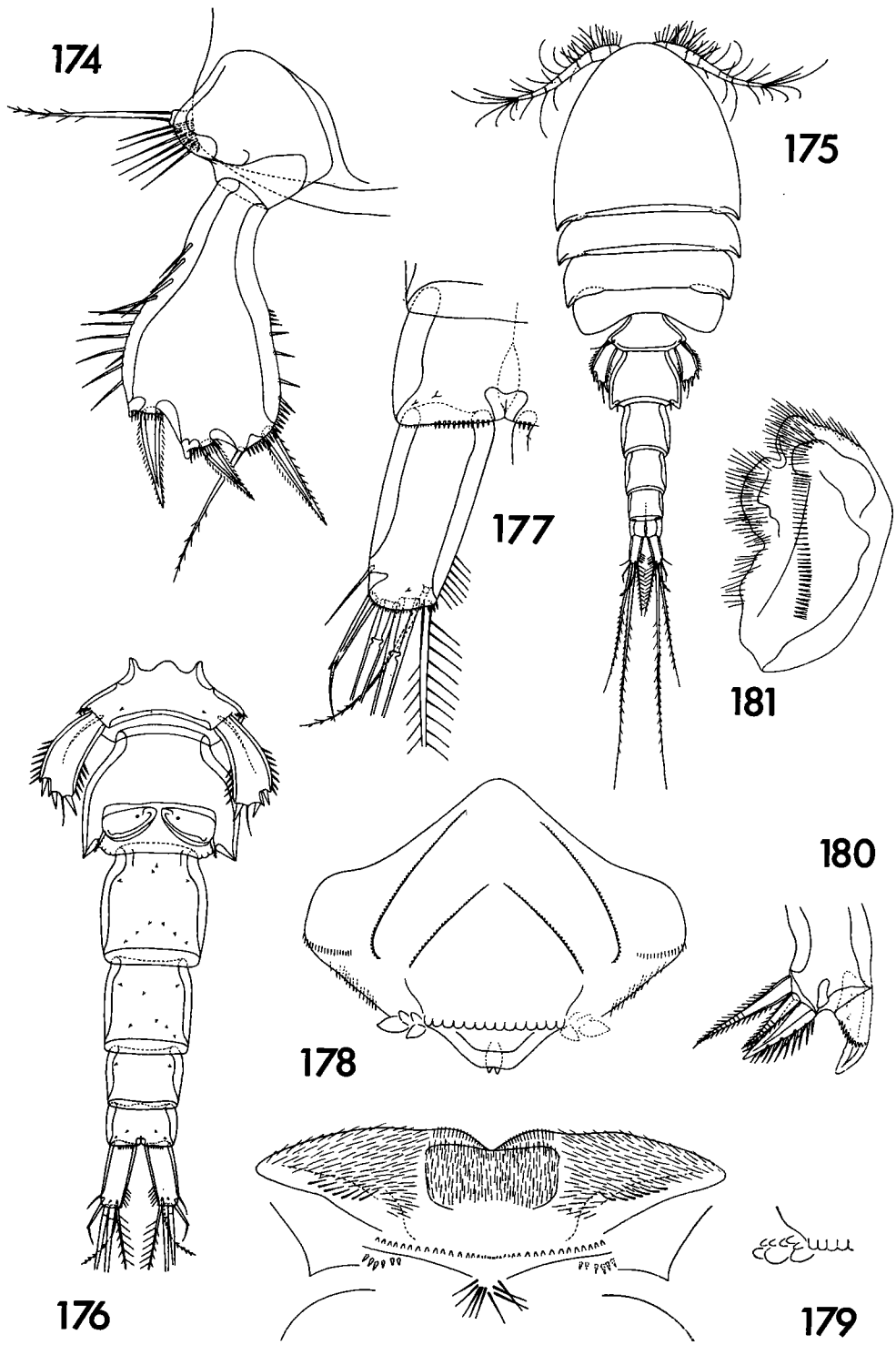
174
175
177
181
180
178
176
179

Plate XXV

Hemicyclops kombensis n. sp., female (continued)

Fig. 174. Leg 5, ventral (G).

Hemicyclops kombensis n. sp., male

Fig. 175. Body, dorsal (A).
Fig. 176. Urosome, ventral (C).
Fig. 177. Caudal ramus and part of anal segment, ventral (G).
Fig. 178. Labrum and metastomal areas, ventral (E).
Fig. 179. Spines at corner of labrum, ventral (E).
Fig. 180. Tip of mandible, anterior (D).
Fig. 181. Paragnath, posterior and ventral (E).

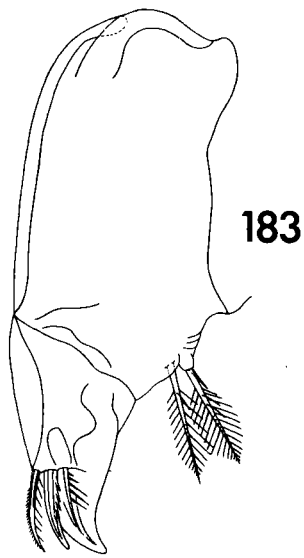
183

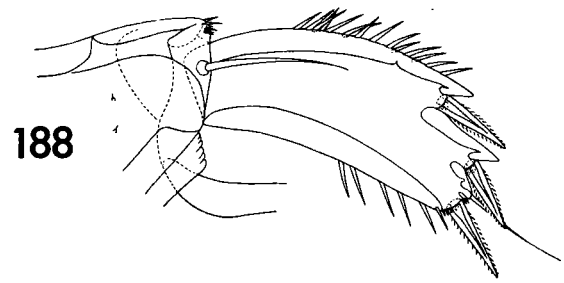
188

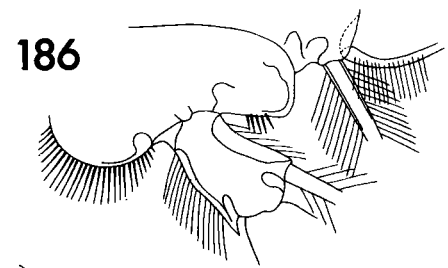
186

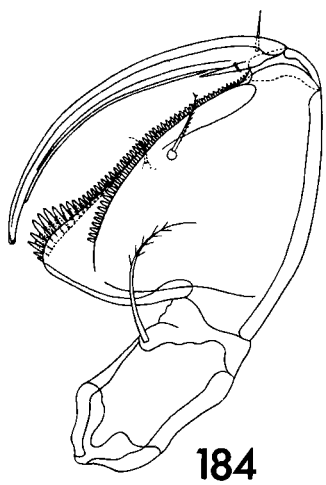
184

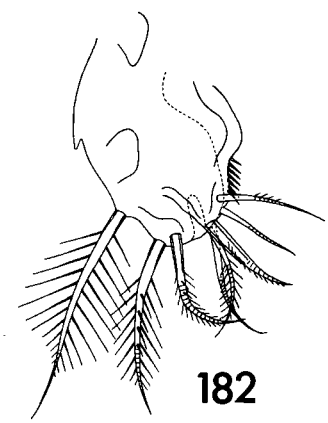
182

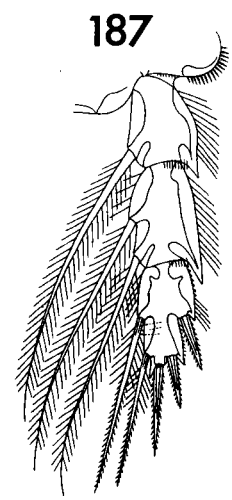
187

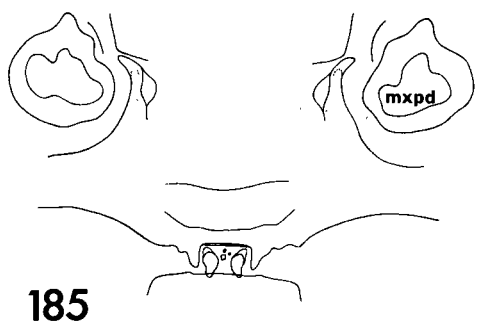
mxpd
185

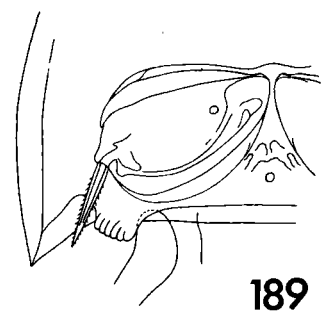
189

Plate XXVI

Hemicyclops kombensis n. sp., male (continued)

Fig. 182. First maxilla, posterior (D).
Fig. 183. Second maxilla, anterior (G).
Fig. 184. Maxilliped, anterior (H).
Fig. 185. Region between maxillipeds and leg 1, ventral (H).
Fig. 186. Detail of leg 1, anterior (G).
Fig. 187. Endopod of leg 4, anterior (H).
Fig. 188. Leg 5, dorsal (G).
Fig. 189. Leg 6, ventral (G).

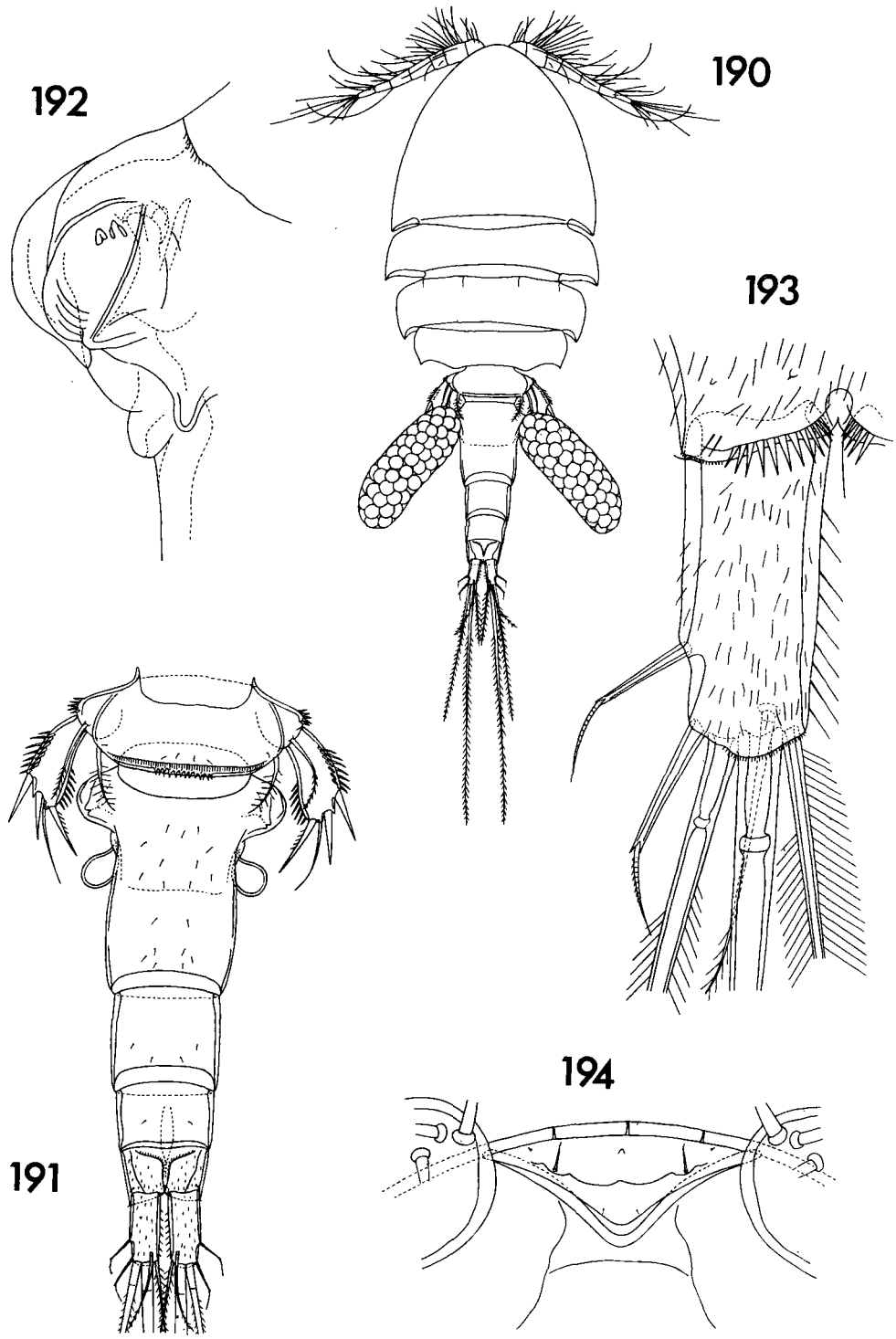
192
190
193
191
194

Plate XXVII

Hemicyclops biflagellatus n. sp., female

Fig. 190. Body, dorsal (J).
Fig. 191. Urosome, dorsal (B).
Fig. 192. Area of attachment of egg sac, dorsal (E).
Fig. 193. Caudal ramus, ventral (E).
Fig. 194. Rostral area, ventral (E).

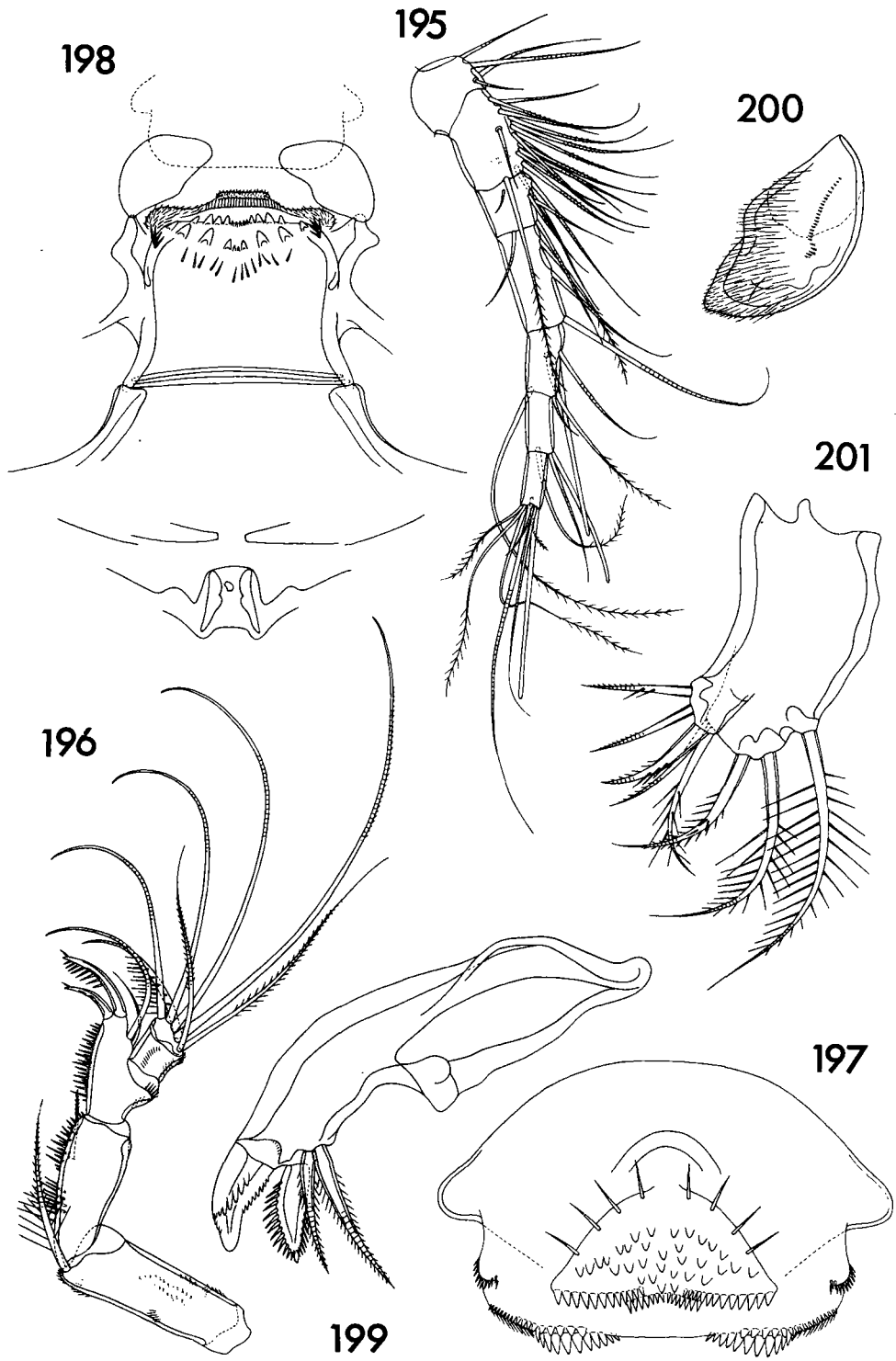
198
195
200
201
196
197
199

Plate XXVIII

Hemicyclops biflagellatus n. sp., female (continued)

Fig. 195. First antenna, anterodorsal (H).
Fig. 196. Second antenna, anterior (G).
Fig. 197. Labrum, ventral (E).
Fig. 198. Metastomal areas and region between maxillipeds and leg 1 (with outline of labrum in dashed lines), ventral (G).
Fig. 199. Mandible, anterior and dorsal (E).
Fig. 200. Paragnath, posterior (E).
Fig. 201. First maxilla, posterior (E).

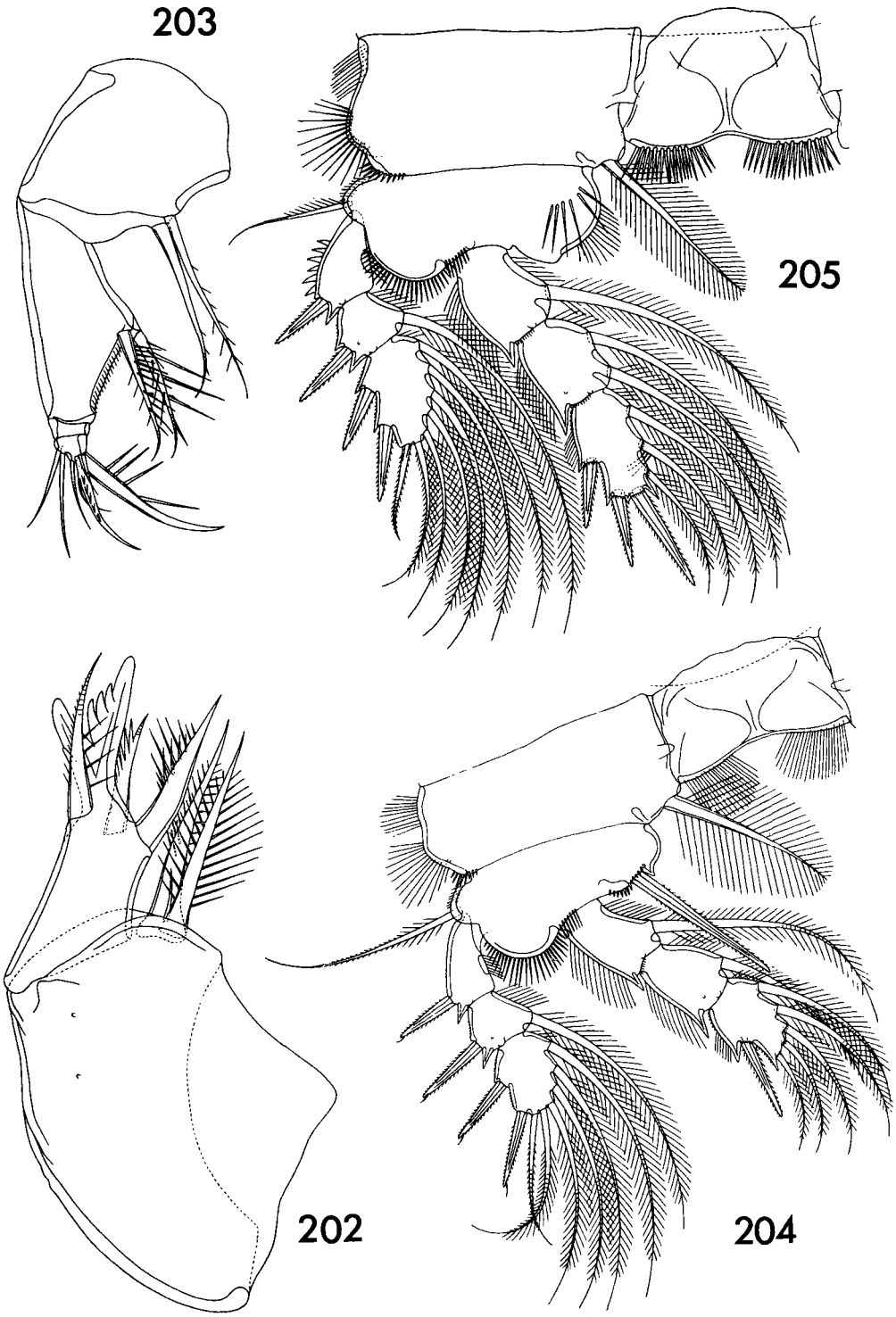
203
205
202
204

Plate XXIX

Hemicyclops biflagellatus n. sp., female (continued)

Fig. 202. Second maxilla, anterior (E).
Fig. 203. Maxilliped, dorsal (D).
Fig. 204. Leg 1, anterior (G).
Fig. 205. Leg 2, anterior (G).

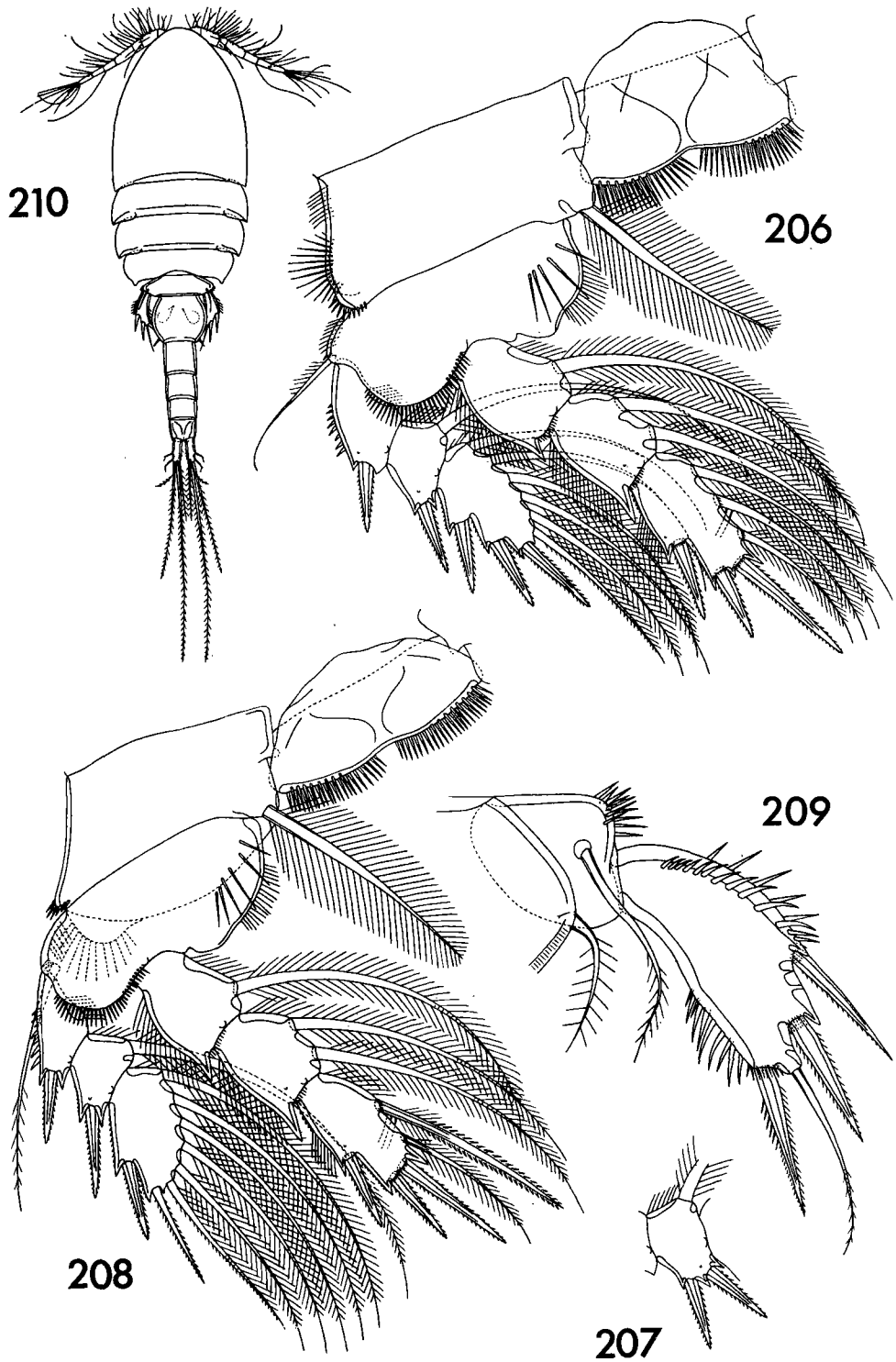
210
206
209
208
207

Plate XXX

Hemicyclops biflagellatus n. sp., female (continued)

Fig. 206. Leg 3, anterior (G).
Fig. 207. Abnormal second segment of exopod of leg 3, anterior (G).
Fig. 208. Leg 4, anterior (G).
Fig. 209. Leg 5, dorsal (D).

Hemicyclops biflagellatus n. sp., male

Fig. 210. Body, dorsal (J).

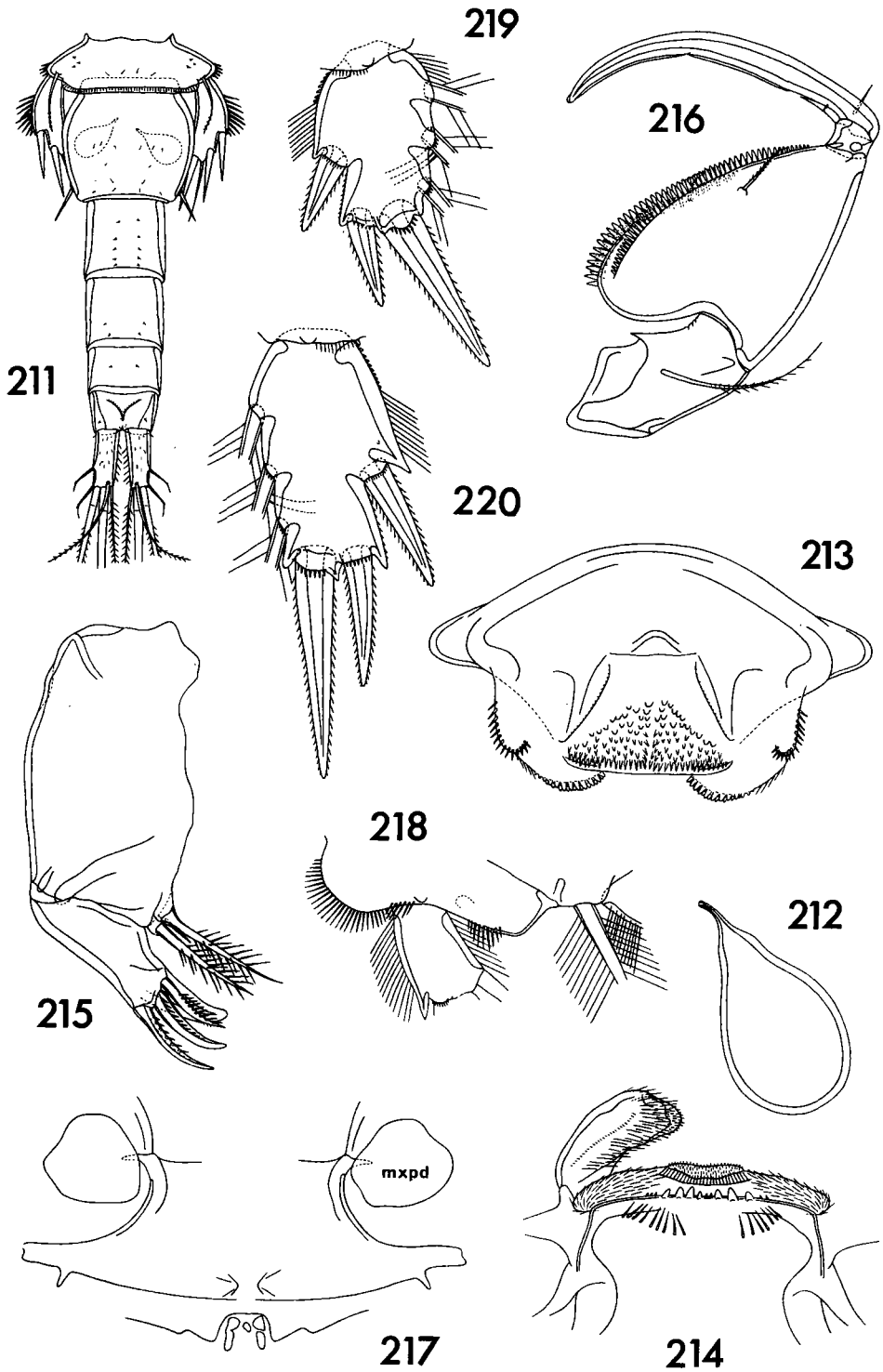
219
216
211
220
213
218
212
215
mxpd
217
214

Plate XXXI

Hemicyclops biflagellatus n. sp., male (continued)

Fig. 211. Urosome, dorsal (B).
Fig. 212. Spermatophore attached to female, ventral (E).
Fig. 213. Labrum, ventral (E).
Fig. 214. Metastomal areas, with one paragnath in position, ventral (D).
Fig. 215. Second maxilla, anterior (D).
Fig. 216. Maxilliped, anterior (G).
Fig. 217. Region between maxillipeds and leg 1, ventral (G).
Fig. 218. Detail of leg 1, anterior (D).
Fig. 219. Last segment of endopod of leg 2, anterior (E).
Fig. 220. Last segment of endopod of leg 3, anterior (E).

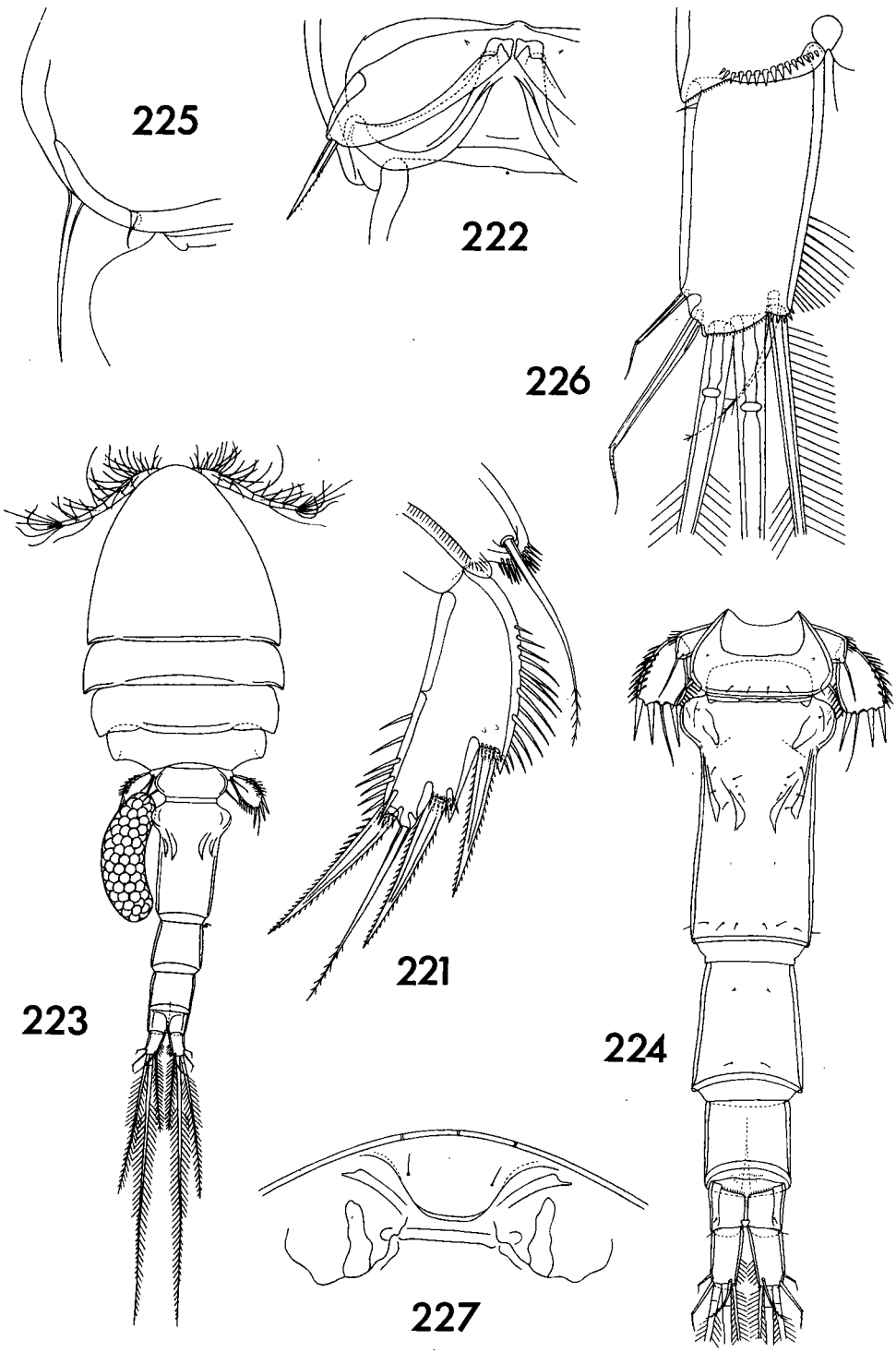
225
222
226
223
221
224
227

Plate XXXII

Hemicyclops biflagellatus n. sp., male (continued)

Fig. 221. Leg 5, dorsal (D).
Fig. 222. Leg 6, ventral (D).

Hemicyclops acanthosquillae n. sp., female

Fig. 223. Body, dorsal (A).
Fig. 224. Urosome, dorsal (C).
Fig. 225. Portion of segment of leg 5 showing setiform process, dorsal (D).
Fig. 226. Caudal ramus, ventral (D).
Fig. 227. Rostral area, ventral (G).

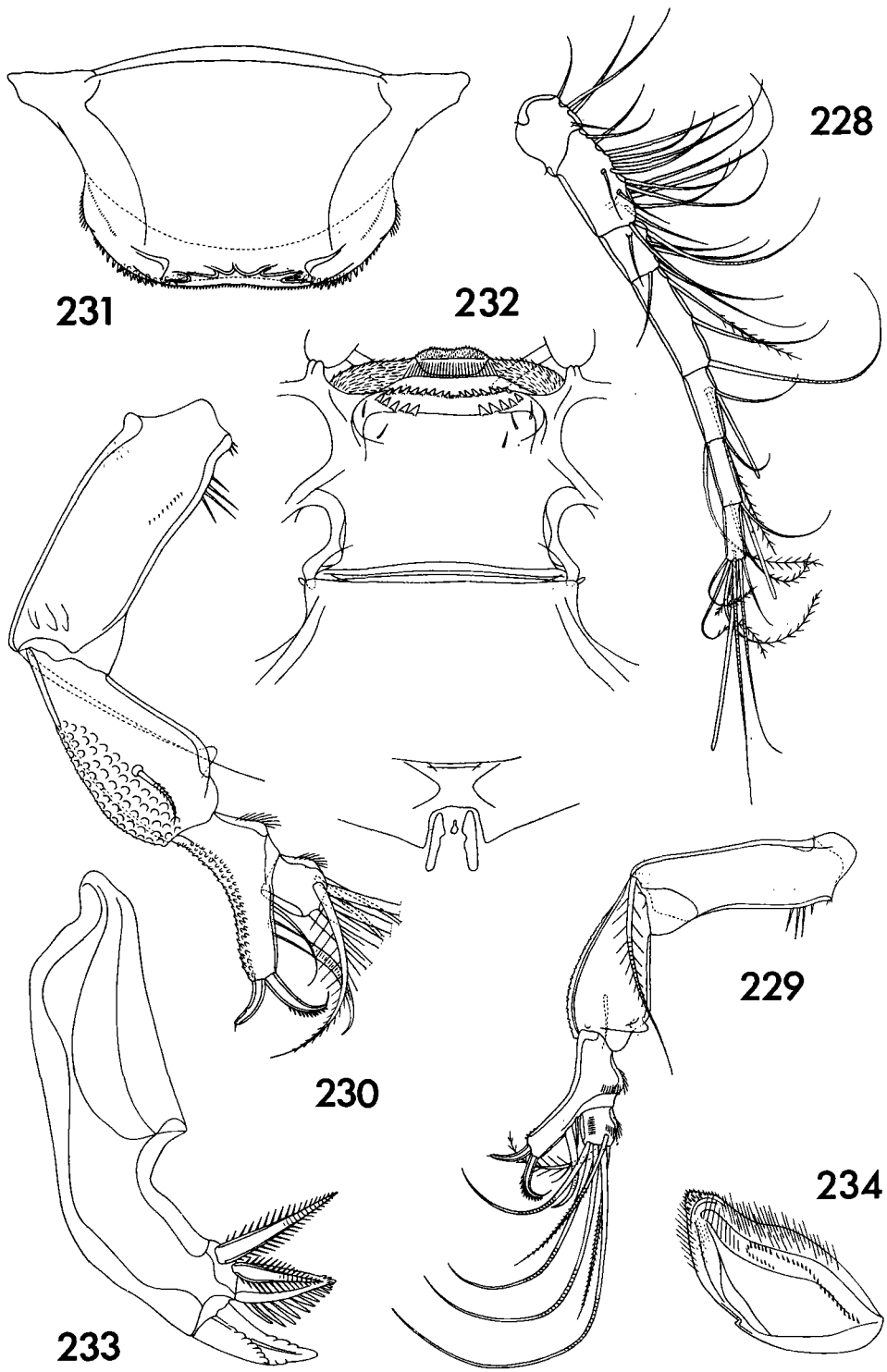
228
231
232
230
229
234
233

Plate XXXIII

Hemicyclops acanthosquillae n. sp., female (continued)

Fig. 228. First antenna, anterodorsal (H).
Fig. 229. Second antenna, anterior (G).
Fig. 230. Second antenna, posterior (D).
Fig. 231. Labrum, ventral (D).
Fig. 232. Metastomal areas and region between maxillipeds and leg 1, ventral (G).
Fig. 233. Mandible, anterior and dorsal (E).
Fig. 234. Paragnath, posterior and ventral (E).

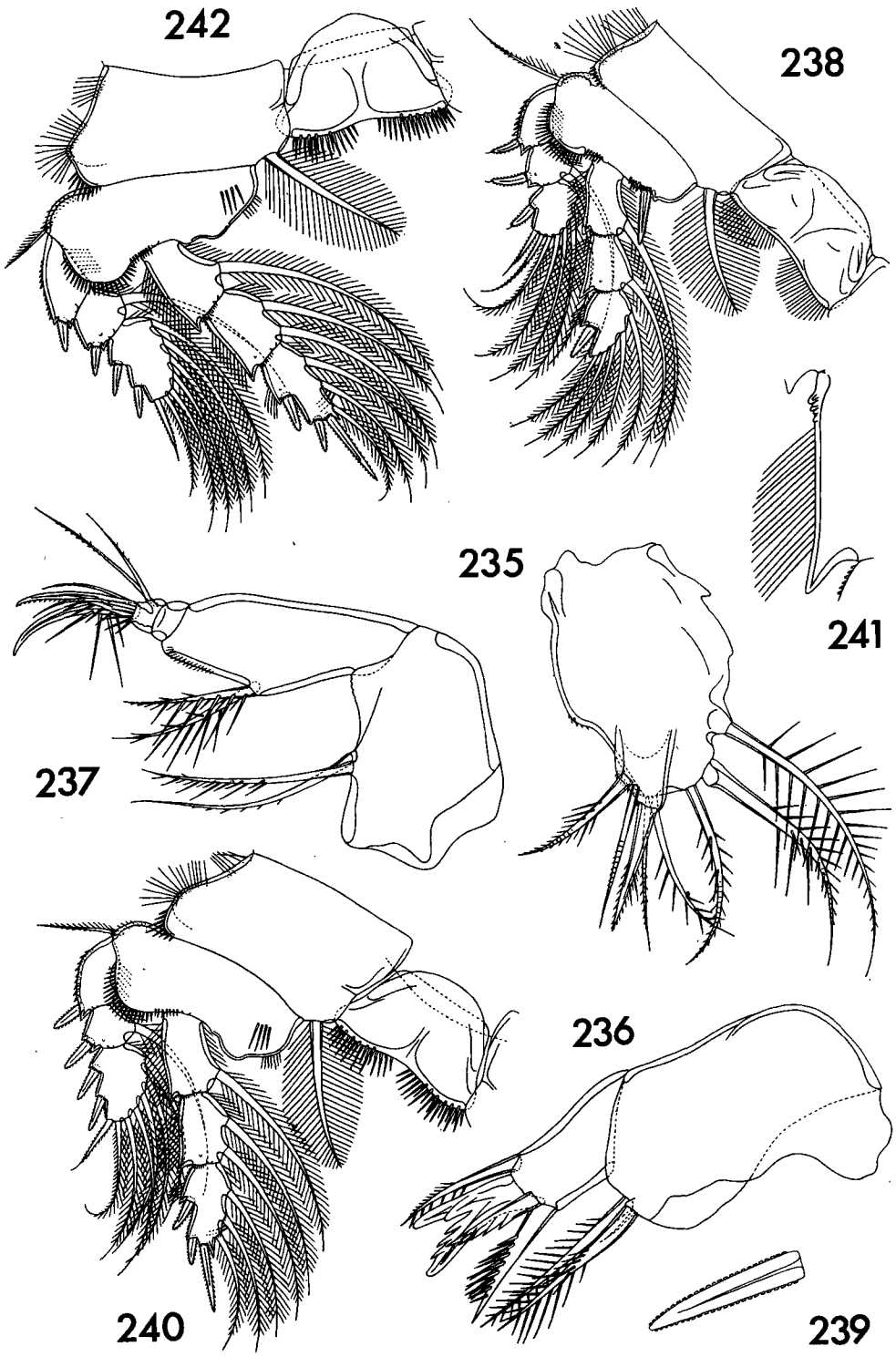
242
238
235
241
237
236
240
239

Plate XXXIV

Hemicyclops acanthosquillae n. sp., female (continued)

Fig. 235. First maxilla, posterior (E).
Fig. 236. Second maxilla, posterior (D).
Fig. 237. *Maxilliped, dorsal* (D).
Fig. 238. Leg 1, anterior (H).
Fig. 239. Inner spine on basis of leg 1, anterior (E).
Fig. 240. Leg 2, anterior (H).
Fig. 241. Outer edge of second segment of endopod of leg 2, anterior (E).
Fig. 242. Leg 3, anterior (H).

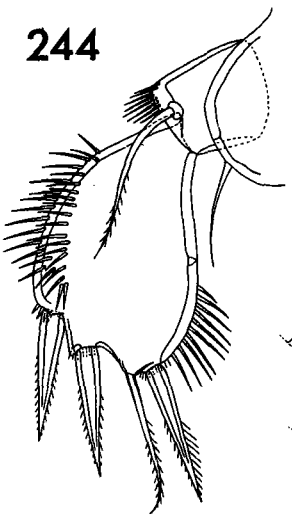
244

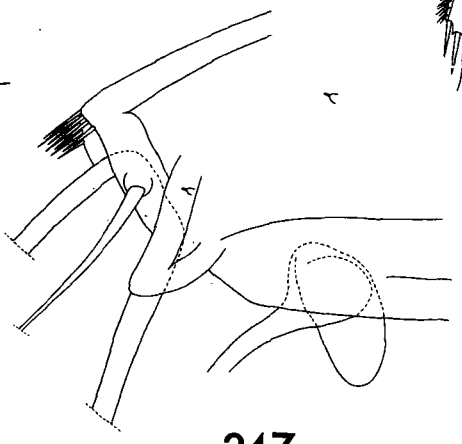
247

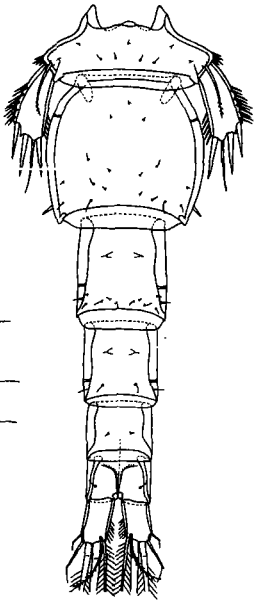
246

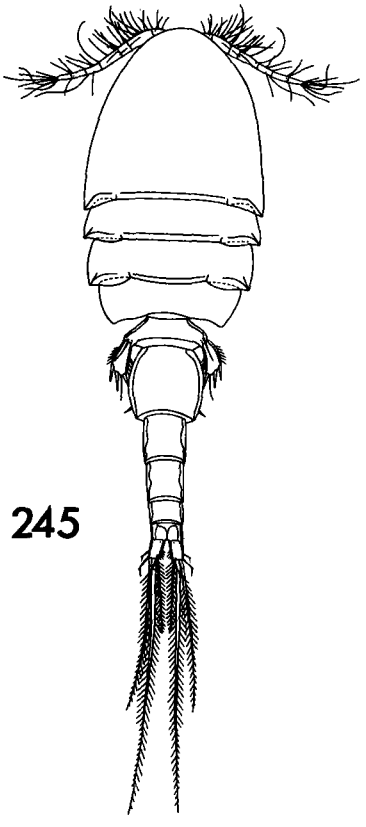
245

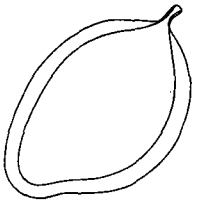
248

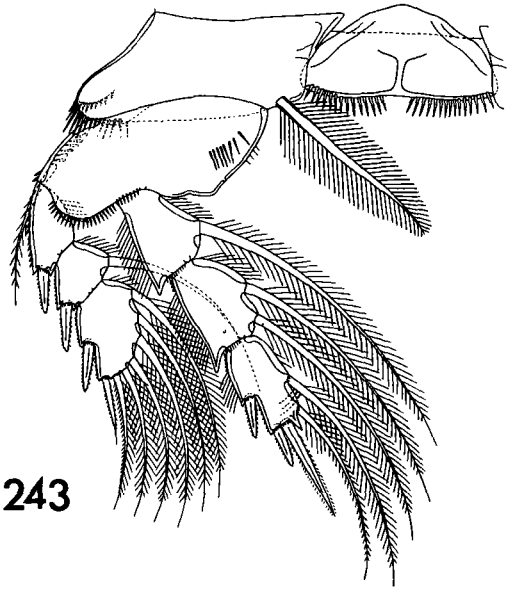
243

Plate XXXV

Hemicyclops acanthosquillae n. sp., female (continued)

Fig. 243. Leg 4, anterior (H).
Fig. 244. Leg 5, dorsal (G).

Hemicyclops acanthosquillae n. sp., male

Fig. 245. Body, dorsal (A).
Fig. 246. Urosome, dorsal (C).
Fig. 247. Portion of segment of leg 5 showing projection, dorsal (E).
Fig. 248. Spermatophore (G).

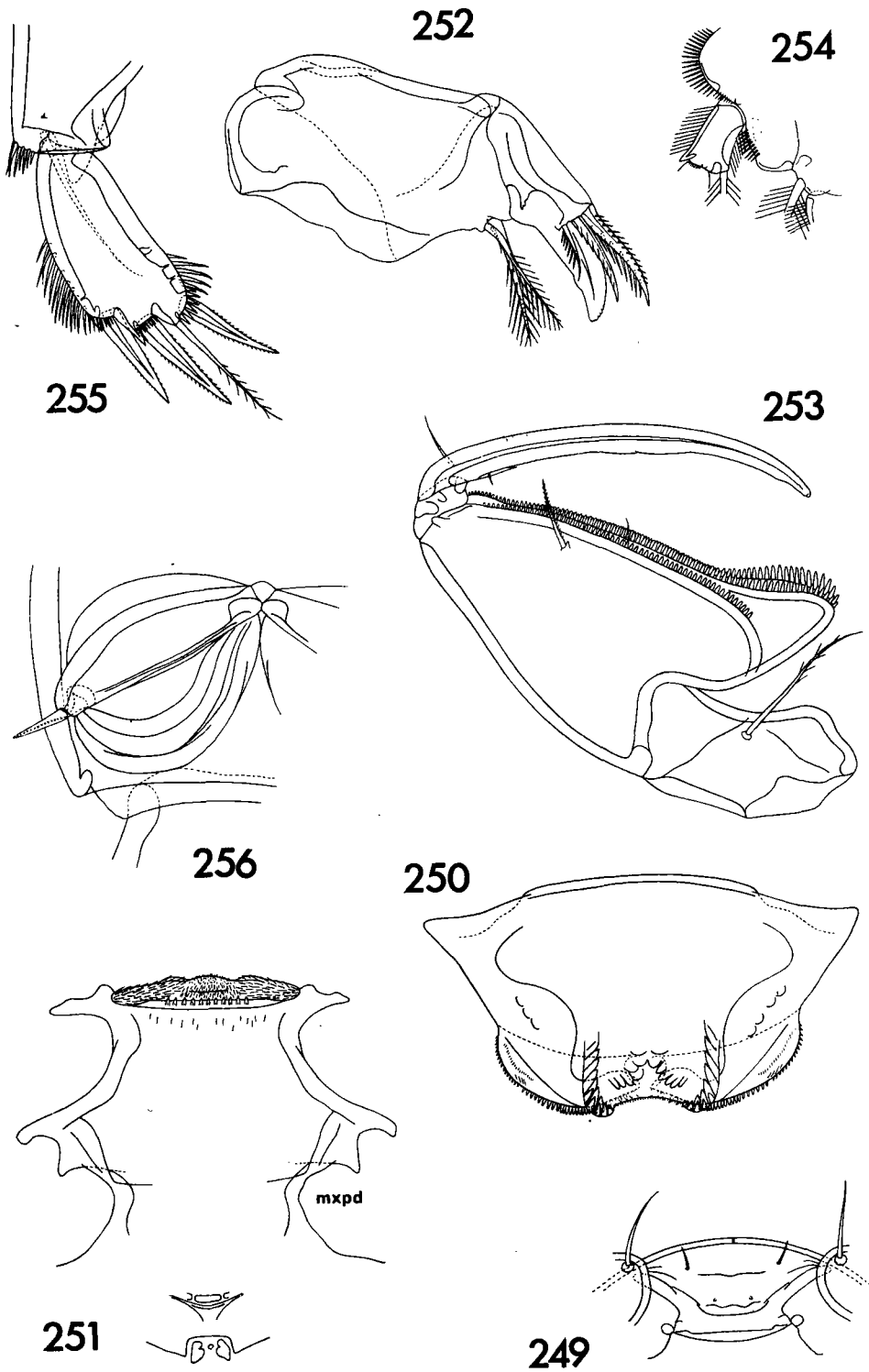
252
254
255
253
256
250
mxpd
251
249

Plate XXXVI

Hemicyclops acanthosquillae n. sp., male (continued)

Fig. 249. Rostral area, ventral (G).
Fig. 250. Labrum, ventral (D).
Fig. 251. Metastomal areas and region between maxillipeds and leg 1, ventral (H).
Fig. 252. Second maxilla, anterior (G).
Fig. 253. Maxilliped, anterior (G).
Fig. 254. Detail of leg 1, anterior (H).
Fig. 255. Leg 5, ventral (G).
Fig. 256. Leg 6, ventral (G).

Reprinted from *Bull. Mus. comp. Zool.*, vol. 134, no. 7, 1965, p. 261-274.

NEW OCEANIC CHEILODIPTERID FISHES FROM THE INDIAN OCEAN

GILES W. MEAD and J. E. De FALLA

ABSTRACT

The collections made in or adjacent to the Indian Ocean during voyages of R/V *Anton Bruun* and the "Monsoon" Expedition of Scripps Institution of Oceanography include six species of high-seas cheilodipterid fishes. Two, *Rosenblattia robusta* and *Florenciella lugubris*, are described here as new genera and species; the other four, *Howella brodiei, Bathysphyraenops simplex, Brinkmannella elongata*, and a second unidentified species of *Brinkmannella* are new records for the Indian Ocean. Included in the description of *Rosenblattia robusta* is material taken in the sub-Antarctic part of the Pacific Ocean during the Antarctic Research Program of the University of Southern California.

INTRODUCTION

In addition to the abundant mesopelagic malacopterygians such as myctophids and gonostomatids, midwater nets fished far from shore occasionally take spiny-rayed fishes which are related to coastal groups. We are concerned here with one such group, the midwater segment of the percomorph family Cheilodipteridae (Apogonidae), a family that is chiefly coastal, but that does contain a few off-shore species.

Although these fishes are customarily referred to the Cheilodipteridae, the family relationships have not properly been established. For example, Norman (1957:242A) tentatively placed the genera *Howella, Neoscombrops, Bathysphyraenops*, and *Apogonops* in the serranid subfamily Serraninae. The problem is the recognition of those characters which are adaptations for mesopelagic life as distinct or partially distinct from those which reflect ancestry and relationship to an inshore family or subfamily. Various features found in these fishes, such as reduction or loss of color pattern, lack of countershading, occasional presence of terminal and horizontal antrorse teeth in the jaws, increased development of the lateral line, etc., are certainly characteristic of many mesopelagic fishes of diverse relationships. Variability in other characters, such as number of anal spines, deciduous *vs.* adherent scales, presence or absence of opercular spines, and the extension of the lateral line onto the caudal fin, suggests that the group is not homogeneous. However, some of these features also may reflect the requirements of oceanic life as well as ancestry. A critical study of the family relationships is clearly in order, but cannot be attempted here.

The midwater species discussed below are so different from their coastal relatives that comparison is pointless. However, mindful of the possibility that these forms may represent the pelagic young or prejuveniles of benthic cheilodipterids from the continental shelf and abyssal plain, various benthic genera (e.g. *Brephostoma* Alcock, *Synagrops* Günther, *Epigonus* Rafinesque, *Neoscombrops* Gilchrist, *Paroncheilus*

Smith) were considered while arriving at the identifications which are given.

Only two oceanic cheilodipterids, *Oxyodon macrops* Brauer 1906 and *Hynnodus atherinoides* Gilbert, 1905 (Fourmanoir, 1957) have been previously reported from the Indian Ocean. Neither of these is represented in our collections.

The area with which we are primarily concerned is the Indian Ocean. The type locality of *Rosenblattia robusta* lies in the southwestern Pacific, but the species was also caught in the Indian Ocean. In addition, we have included in our description of this species a few specimens taken in the sub-Antarctic part of the Pacific Ocean. Our principal material was taken during Cruises III and VI of R/V *Anton Bruun* during the American Program in Biology, International Indian Ocean Expedition. Cruise III fished along the 60°E meridian from 12°N to 44°S, 13 August to 13 September, 1963. Cruise VI sampled waters along 65°E from 18°N to 41°S, 17 May to 4 July, 1964. Supplementing the *Anton Bruun* collections are several lots taken by Scripps Institution of Oceanography during its "Monsoon" Expedition to the Pacific and Indian Oceans, October, 1960 to March, 1961 (Clarke, 1963), and a few lots taken by the R/V *Eltanin* during the Antarctic Research Program of the University of Southern California.

Both cruises of the *Anton Bruun* used a 10-foot Isaacs-Kidd Midwater Trawl; the Foxton Trousers (see Foxton, 1963), an opening-closing device designed to separate a shallow from a deep fraction of the trawl haul; and occasionally a time-depth recorder. Attempts to calibrate the Foxton Trousers by repeated lowerings of the instrument on the hydrographic wire showed that the depth at which the device triggered varied greatly. The device did separate the shallow from the deep part of the catch, but the actual depth of such separation was imprecise. Even limits of error of half or double the nominal depth of separation may be unrealistically narrow.

Our methods of counting and measuring are chiefly those of Hubbs and Lagler (1947). The tip of the snout is taken as the midpoint of the upper jaw, even though this point may not be terminal. The length of the head is taken from the tip of the snout to the most posterior edge of the gill flap exclusive of opercular spines. The number of scales between the first dorsal fin and the lateral line is counted along the oblique row beginning at the base of the second dorsal spine. This count includes the small scale at the base of the fin but excludes the lateral line scale. The count between the lateral line and anal fin is made on the oblique row terminating at the base of the first anal spine. This count also excludes the lateral line scale, and is somewhat variable due to the occasional presence of a half scale at either end of the row. The last soft dorsal and the last anal rays may or may not be divided to the base, but in either instance the ray is counted as one.

The following abbreviations are used: IIOE (International Indian Ocean Expedition), IKMT (Isaacs-Kidd Midwater Trawl), l.s.t. (local standard time), t.d.r. (time-depth recorder), s.l. (standard length), ANSP (Academy of Natural Sciences of Philadelphia), LACM (Los Angeles County Museum), MCZ (Museum of Comparative Zoology, Harvard University), SIO (Scripps Institution of Oceanography), USC (University of Southern California), and USNM (United States National Museum).

We are indebted to Basil G. Nafpaktitis for the illustrations, to E. A. Lachner and D. M. Cohen for review of the manuscript, and to Richard H. Rosenblatt, R. H. Gibbs, Jr., Jay M. Savage, and John R. Paxton for the loan of specimens. We are particularly indebted to John H. Ryther of the Woods Hole Oceanographic Institution, Scientific Director of the American Program in Biology, International Indian Ocean Expedition, and to the National Science Foundation for the organization of the field pro-

gram of which the *Anton Bruun* cruises were a part. This study was aided by Grant GF147 from the National Science Foundation to Harvard University, whose support is here gratefully acknowledged.

ROSENBLATTIA, NEW GENUS

Type species: Rosenblattia robusta new species. Gender of generic name: feminine.

Generic characters. Rosenblattia is distinguished from all other known oceanic cheilodipterid fishes by the more robust body and by the pair of caudal keels formed by the scales of the mid-lateral series of the caudal peduncle. The high number (*ca.* 52) of scales in the lateral line and the antrorse teeth anteriorly in both jaws distinguish this genus from all others except *Florenciella* which is discussed below.

All scales strongly ctenoid; head almost completely covered, fins largely naked. Scales on body small and numerous; about four between base of dorsal fin and lateral line and about fifteen between lateral line and base of anal fin. Lateral line complete, uninterrupted, and continuing onto caudal fin. The scales along the caudal peduncle particularly spinulose and V-shaped. Strong spines in vertical fins. Anal fin with two spines. Body raised and stiffened at origins of unpaired fins. Procurrent caudal fin rays stiff and spiny, their tips free. Eye large, a small aphakic space present. A few discrete simple spines along the upper edge of opercle; opercle and subopercle elsewhere serrated. Upper edge of orbit spiny when viewed from above. Teeth present on jaws, vomer, and palatines; some of anterior jaw teeth antrorse.

This genus is named in honor of Dr. Richard Rosenblatt of Scripps Institution of Oceanography, friend and fellow ichthyologist.

ROSENBLATTIA ROBUSTA, NEW SPECIES

Holotype. An 84.8 mm s.l. specimen taken in the South Pacific by the Scripps Institution of Oceanography "Monsoon" Expedition; IKMT haul no. 17; 28 February to 1 March, 1961; 2206 to 0250 hrs. l.s.t.; 46° 53′S, 179°48′W to 46°42′S, 179°32′W; maximum calculated depth 1878 m, open net. SIO 61–45.

Paratypes. Two, 94.4 and 48.8 mm s.l.; same data as holotype. MCZ and SIO, respectively.

One, 75.8 mm s.l.; R/V *Eltanin*, USC Antarctic Research Program, Cruise II; Sta. 882; 30 December 1963; 0805 to 1210 hrs. l.s.t.; 55°10′S, 114°15′W to 55°52′S, 114° 22′W; IKMT; maximum depth of sampling 1737 m, open net. LACM 10075.

One, 67.0 mm s.l.; R/V *Eltanin*, USC Antarctic Research Program, Cruise 10; Sta. 846; 10 November 1963; 2315 to 0330 hrs. l.s.t.; 57°52′S, 74°43′W to 57°27′S, 74°42′W; IKMT; maximum depth of sampling 1829 m, open net. LACM 10074.

One, 61.0 mm s.l.; R/V *Eltanin*, USC Antarctic Research Program, Cruise 13; Sta. 1107; 24 May 1964; 0513 to 0855 hrs. l.s.t.; 57°59.6′S, 90°36.3′W to 58°20′S, 90°46.9′W; IKMT; maximum depth of sampling 713 m, open net. LACM 10077.

One, 49.9 mm s.l.; R/V *Eltanin*, USC Antarctic Research Program, Cruise 13; Sta. 1099; 22 May 1964; 1510 to 1845 hrs. l.s.t.; 56°59.9′S, 89°09.3′W to 57°03.1′S, 88°54.3′ W; IKMT; maximum depth of sampling 759 to 1207 m, open net. LACM 10076.

One, 49.5 mm s.l.; R/V *Eltanin*, USC Antarctic Research Program, Cruise 15; Sta. 1380; 17–18 November 1964; 2250 to 0250 hrs. l.s.t.; 54°01′S, 145°02′W to 53°53′S, 145°13′W; IKMT; maximum depth of sampling 841 m, open net. LACM 10078.

One, 49.0 mm s.l.; R/V *Eltanin*, USC Antarctic Research Program, Cruise 6; Sta. 348; 4 December 1962; 1125 to 1445 hrs. l.s.t.; 54°40.1′S, 58°57.8′W to 55°05.8′S, 59°05.3′ W; IKMT; maximum depth of sampling 896 m, open net. LACM 10073.

One, 35.1 mm s.l.; "Monsoon" Expedition; IKMT haul no. 13; 13 January 1961; 0004 to 0457 hrs. l.s.t.; 49°26′30″S, 132° 18′24″E to 49°21′00″S, 132°39′24″E; maximum calculated depth 1878 m, open net. SIO 61–41.

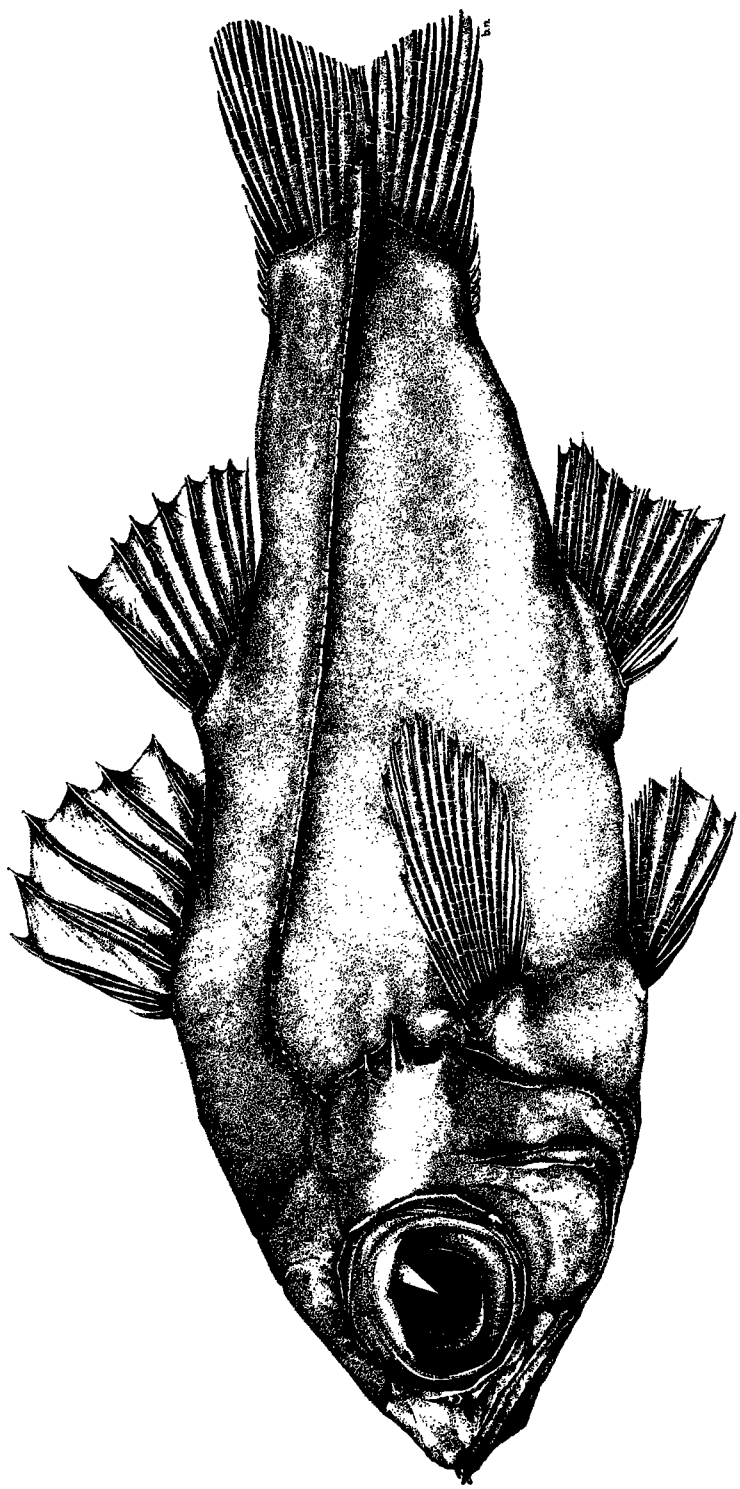

Figure 1. *Rosenblattia robusta*, new genus and species; holotype, 84.8 mm in standard length; SIO 61-45. Squamation not shown. Drawn by Basil G. Nafpaktitis.

TABLE 1. PROPORTIONAL DIMENSIONS (IN PER CENT OF STANDARD LENGTH) OF NINE SPECIMENS, INCLUDING THE HOLOTYPE, OF *Rosenblattia robusta*

	SIO 61-45	Holotype SIO 61-45	LACM 10075	LACM 10074	LACM 10077	LACM 10076	LACM 10073	SIO 61-45	SIO 61-41
Standard length (mm)	94.4	84.8	75.8	67.0	61.0	49.9	49.0	48.8	35.1
Fork length	112.0	113.1	111.2	110.6	115.1	114.2	112.4	111.2	118.2
Greatest depth of body	36.8	38.0	38.7	38.7	40.0	38.5	39.8	42.0	39.9
Least depth of caudal peduncle	16.2	17.3	15.0	14.9	14.9	13.6	14.7	14.5	14.0
Greatest width of body	23.3	23.6	22.3	24.2	26.4	24.0	25.1	25.0	27.4
Snout to origin of first dorsal fin	40.8	40.8	39.6	43.7	41.0	42.1	43.3	45.5	48.7
Snout to origin of anal fin	67.3	64.4	67.7	65.8	73.1	72.1	71.6	68.0	72.4
Snout to insertion of ventral fin	41.7	40.3	47.9	41.8	50.0	47.7	47.8	46.3	47.6
Snout to insertion of pectoral fin	36.7	36.0	38.4	37.0	41.0	39.3	40.4	41.0	43.9
Length of base of first dorsal fin	17.8	17.1	16.2	14.5	14.9	14.6	15.9	14.7	14.2
Length of base of second dorsal fin	11.6	11.2	11.2	10.9	10.5	13.0	11.8	10.6	11.7
Distance between first and second dorsal fins	7.6	8.1	7.7	7.5	7.4	8.2	7.1	7.4	7.4
Distance between anus and insertion of ventral fin	19.6	18.6	16.2	19.3	18.4	21.8	19.0	20.5	18.5
Distance between anus and origin of anal fin	5.9	6.1	4.4	4.9	5.1	5.2	5.3	5.5	8.3
Length of pectoral fin	24.9	24.8	25.7	27.6	26.7	28.7	28.6	28.7	29.9
Length of ventral fin	16.9	18.9	19.5	21.6	20.3	20.0	20.8	19.5	21.7
Length of head	35.5	35.1	34.7	36.3	38.0	37.3	39.0	38.9	42.2
Length of snout	8.5	7.9	8.6	8.1	8.7	7.6	8.4	8.4	8.8
Length of upper jaw	14.9	15.9	15.6	16.7	17.7	18.0	17.6	18.2	20.8
Horizontal diameter of eye	13.3	15.0	14.5	15.7	17.5	17.2	18.8	17.4	21.4
Width of interorbital space	9.7	12.0	12.3	14.6	14.4	13.8	14.7	10.0	11.4

Two juveniles, 25.0 and 27.5 mm s.l.; R/V *Anton Bruun*, IIOE, Cr. VI; Sta. 353A; 2 July 1964; 1115 to 1925 hrs. l.s.t.; 37°59′S, 64°56′E to 38°15′S, 64°45′E; maximum calculated depth 2394 m; IKMT, deep fraction of catch with Foxton Trousers nominally set at 350 m, specimens probably from below 175 m. MCZ.

One juvenile, 26.5 mm s.l.; R/V *Anton Bruun*, IIOE, Cr. VI; Sta. 354A; 4 July 1964; 0915 to 1510 hrs. l.s.t.; 40°48′S, 65°03′E to 40°51′S, 64°49′E; maximum calculated depth 1650 m; IKMT, considered to be an open net. USNM.

Two juveniles, 24.5 and 25.5 mm s.l.; R/V *Anton Bruun*, IIOE, Cr. VI; Sta. 354B; 4 July 1964; 1605 to 2210 hrs. l.s.t.; 40°51′S, 64°49′E to 40°56′S, 64°25′E; maximum calculated depth 885 m; IKMT, considered to be an open net. SIO.

Description. Morphometric data on the larger specimens are provided in Table 1. Meristic data (value, followed in parentheses by the number of specimens) as follows: first dorsal fin VII (14); second dorsal fin I, 7 (2) or 1, 8 (12); anal fin II, 8 (14); pectoral fin (left side) 18 (9) or 19 (5); gill rakers on first arch 5 (3), 6 (9) or 7 (2) + 1 +13 (1), 14 (1), 15 (5), 16 (5) or 17 (2) totaling 20 to 24; branchiostegal rays 4 + 3 (14); complete scale rows between origin of first dorsal fin and lateral line, 4 (14); between lateral line and origin of anal fin, 14 (1), 15 (11) or 16(2); scales in lateral line from origin to base of mid-caudal ray, 49 (1), 50 (3), 51 (3), 52 (5) or 53 (1); lateral line scales overlying central caudal rays 1 to 4, somewhat correlated with size of fish. Vertebrae, 10 + 14 + 1 = 25 (2).

The notes which follow are based chiefly on the four larger specimens. Observations of juvenile conditions are identified as such. Body compressed and relatively deep; its greatest depth (at origin of dorsal fin) 2.4 to 2.7 in s.l. Greatest width 1.5 to 1.7 in

greatest depth. All of body and head, except for the tip of the snout anterior to the eye and the isthmus, covered by heavy, strongly ctenoid, adherent scales, the cteni of which continue onto the surface of the scale as tranverse ridges. Squamation on the body is complete in our smallest juvenile (24.5 mm s.l.), although the cteni and ridges are poorly developed and the scale coverings on the head and fins are incomplete. The lateral line is well developed. The lateral line scales are produced laterally to form a pair of mid-caudal keels, the beginnings of which are evident in juveniles. Aside from the single simple tranverse tube, the anterior scales of the lateral line are similar to their neighbors. The lateral line continues onto the proximal half of the caudal fin. Other fins are naked.

Distance between snout and origin of first dorsal fin 2.1 to 2.5 in s.l.; preanal distance 1.4 to 1.6 in s.l., preventral distance 2.0 to 2.5 in s.l., prepectoral distance 2.3 to 2.8 in s.l. Spines in fins strong and sharp. Those in first dorsal lie alternately to the right or left of center when the fin is depressed. The second anal and ventral spines are as long or nearly as long as the succeeding soft rays. Pectoral fin set at about 45° with the horizontal, its length 1.4 in length of head. The anus is located about one-fourth of the distance from anal origin to the base of the ventral fin and is separated from the first anal spine by about four scales.

Head broad; interorbital slightly convex, 2.5 to 3.9 in length of head. Eye large, aphakic space small but prominent. Horizontal diameter of eye 2.0 to 2.7 in length of head. Dorsal, and to a lesser extent posterior, edge of orbit spinulose, the spines small and nearly uniform in size. Preopercle with two free edges, the posterior spinulose, the anterior less so or completely without serrations. Opercle, especially its lower half, armed with small simple cteni. Three simple spines, the longest in the middle, present along the upper edge of the opercle.

Gill openings wide. Branchiostegal membranes attached to isthmus but not overlapping. Pseudobranchs present, formed of about 14 filaments. Gill rakers on first arch long and of the usual lath-like shape, those on successive arches reduced to spinulose knobs. Gill filaments notably few and short, those on the first arch no more than half the length of the gill rakers opposite them.

Teeth present on jaws, vomer, and palatines. Tongue toothless. Posterior end of maxillary but little expanded posteriorly and incompletely covered by the suborbitals. Premaxillaries separate and protractile. Each premaxillary bears one to three large antrorse teeth that lie in a horizontal plane and are excluded from the mouth when it is closed. These, as well as the similar teeth at the tip of the lower jaw, are present in juveniles as well as in adults. Premaxillary with a row of minute teeth posterior to the anterior protruding series. Mandibular teeth similar, with antrorse fangs lateral to the median terminal bony boss followed posteriorly by a row of minute teeth. A transverse patch of small teeth present on the vomer, and an irregular band can be found on each palatine.

In alcohol, the adults are uniformly yellowish brown. All fins slightly dusky. Iris and linings of pharyngeal and abdominal cavities black. Juvenile coloration is far more striking. Pigmentation of the caudal part of the body appears last during development; and in young, shorter than 35 mm, the caudal peduncle and fin are completely colorless, while the more anterior part is dark brown or black. There is a darker broad vertical band at about the level of the second dorsal and anal fins, a narrower band through the rear part of the gill cover, and a dark patch on the body ventrally where the black peritoneum can be seen through the body wall. In these young the body coloration is not solid but formed of melanophores more or less closely spaced. When newly caught, the 20–30 mm young showed a ventral reflective zone anterior

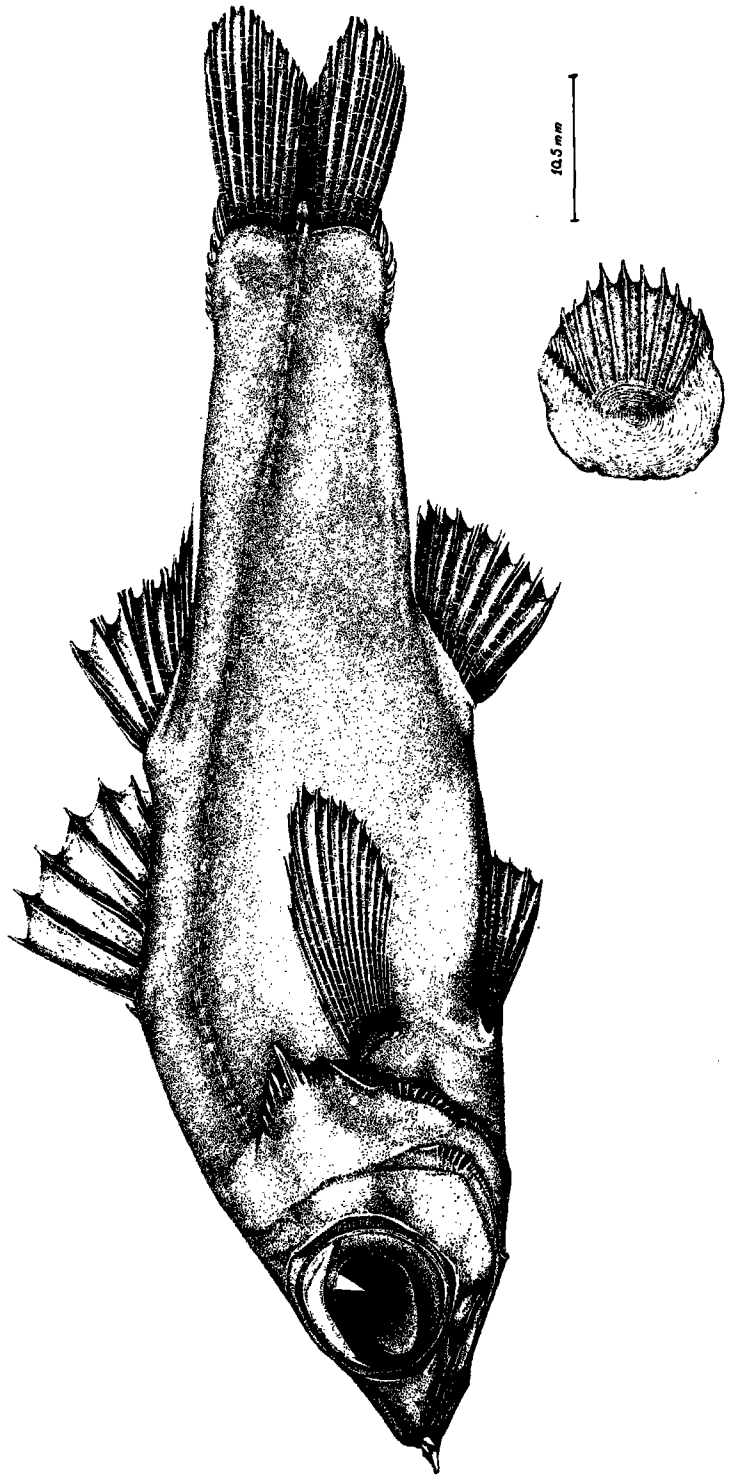

Figure 2. *Florenciella lugubris*, new genus and species; holotype, 89.2 mm in standard length; MCZ 43089. Squamation not shown; the scale illustrated is typical of those on the flank under tip of pectoral fin. Drawn by Basil G. Nafpaktitis.

to the pelvic fins reminiscent of some luminescent systems reported in other cheilodipterid genera (e.g. *Siphamia*, Haneda, 1961), but no structural evidence has been found.

FLORENCIELLA, NEW GENUS

Type species: Florenciella lugubris new species. Gender of generic name: feminine.

Generic characters. This genus most closely resembles *Rosenblattia*, especially by the presence of relatively large antrorse teeth in the anterior parts of both jaws. However, it lacks the mid-lateral caudal keels of *Rosenblattia* and has a less deep body than that genus.

All scales strongly ctenoid. Head almost completely covered by scales; fins largely naked. Lateral line complete, uninterrupted, and extending onto the caudal fin. Mid-lateral scales of caudal peduncle differing from those adjacent to them only by the presence of a lateral line channel. About three rows of scales between base of dorsal fin and lateral line, about seventeen between lateral line and base of anal fin. Strong spines in vertical fins. Two anal spines. Procurrent caudal spines stiff, spiny, and exposed. Eye large, aphakic space prominent. One prominent spine, simple or multifid, at upper end of gill flap which is flanked above and below by lesser spines. Subopercle and preopercle with feeble spines or serrations. Spines present along upper edge of orbit. Teeth present on jaws, palatines, and usually vomer.

FLORENCIELLA LUGUBRIS, NEW SPECIES

Holotype. A 89.2 mm s.l. specimen taken in the equatorial Indian Ocean by R/V *Anton Bruun*, IIOE, Cruise III; Sta. 6, coll. AE13B; 21 August 1963; 0155 to 0440 hrs. l.s.t.; 01°58′S, 60°06′E to 02°06′S, 60°02′E; maximum calculated depth 510 m (depth from t.d.r. 500 m); IKMT, considered an open net collection. MCZ 43089.

Paratypes. Fifty-seven specimens, 22.7 to 97.0 mm s.l.; same data as holotype. Eight specimens in USNM; eight in SIO; eight in ANSP; three in Zoological Museum, University of Copenhagen; remainder, including one cleared and stained individual, in MCZ.

One, 89.9 mm s.l.; R/V *Anton Bruun*, IIOE, Cr. III; Sta. 5, coll. AE12A; 19 August 1963; 2035 to 2350 hrs. l.s.t.; 01°23′N, 60°11′E to 01°22′N, 60°04′E; maximum calculated depth 750 m (maximum depth from t.d.r. 800 m); shallow fraction of catch with Foxton Trousers set for *ca.* 275 m, specimen probably from above 550 m. MCZ.

Seven, 22.7 to 65.5 mm s.l.; R/V *Anton Bruun*, IIOE, Cr. III; Sta. 6, coll. AE14B; 21 August 1963; 0445 to 1010 hrs. l.s.t.; 02°06′S, 60°02′E to 01°48′S, 59°50′E; maximum calculated depth 1600 m; deep fraction of catch with Foxton Trousers set for *ca.* 275 m, specimens probably taken below 140 m. MCZ and USNM.

Two, 24.7 and 25.9 mm s.l.; R/V *Anton Bruun*, IIOE, Cr. III; Sta. 7, coll. AE15D; 23 August 1963; 0250 to 0610 hrs. l.s.t.; 05°03′S, 60°10′E to 04°52′S, 60°02′E; maximum calculated depth 685 m; deep fraction of catch with Foxton Trousers set for *ca.* 150 m, probably taken below 75 m. MCZ.

One, 26.1 mm s.l.; R/V *Anton Bruun*, IIOE, Cr. III; Sta. 13, coll. AE24A; 8 September 1963; 1055 to 1500 hrs. l.s.t.; 31°58′S, 59°45′E to 32°11′S, 59°30′E; maximum calculated depth 1360 m (depth from t.d.r. 1350 m); deep fraction of catch with Foxton Trousers set for 275 m, probably taken below 110 m. Cleared and stained in MCZ.

One, 26.8 mm s.l.; R/V *Anton Bruun*, IIOE, Cr. VI; Sta. 336B; 27 May 1964; 0047 to 0530 hrs. l.s.t.; 01°50′N, 65°06′E to 01° 37′N, 65°07′E; maximum calculated depth 1250 m; deep fraction of catch with Foxton Trousers set for 275 m, probably taken below 140 m. USNM.

One, 26.0 mm s.l.; R/V *Anton Bruun*, IIOE, Cr. VI; Sta. 337A; 27 May 1964; 2130 to 0245 hrs. l.s.t.; 00°03′N, 65°00′E to 00° 14′S, 65°03′E; maximum calculated depth 525 m; deep fraction of catch with Foxton

TABLE 2. PROPORTIONAL DIMENSIONS (IN PER CENT OF STANDARD LENGTH) OF A SERIES OF 21 SPECIMENS, INCLUDING THE HOLOTYPE, OF *Florenciella lugubris* CAUGHT BY R/V *Anton Bruun*, IIOE, CRUISE III.

	Sta. 13 AE24A	Sta. 6 AE13B	Sta. 6 AE14B	Sta. 6 AE13B				Sta. 6 AE14B			Sta. 6 AE13B							Sta. 5 AE12A	Sta. 6 AE13B		
																	Holotype				
Standard length	26.1	28.8	33.1	36.6	45.6	54.4	57.7	58.9	61.6	65.5	66.2	70.5	73.0	76.0	78.5	84.7	89.2	89.9	90.3	95.4	97.0
Fork length	111.9	108.7	110.3	111.5	109.0	112.7	109.2	111.0	109.1	109.6	108.5	109.2	108.5	110.4	108.9	109.6	108.4	107.4	108.7	107.6	108.2
Greatest depth of body	27.2	26.7	27.8	25.1	26.3	27.6	27.6	28.5	28.4	28.1	25.5	26.9	25.9	27.4	27.4	26.2	29.1	29.6	28.2	28.3	27.5
Least depth of caudal peduncle	10.0	11.1	12.4	11.5	11.4	11.9	13.3	12.7	12.8	11.1	14.1	13.6	13.4	14.1	12.9	13.9	14.3	13.9	13.9	13.8	13.1
Greatest width of body	21.1	14.2	15.4	17.2	17.1	17.1	17.3	17.1	16.2	17.7	16.9	18.4	17.0	17.8	18.1	18.0	17.4	19.7	18.6	18.7	19.2
Snout to origin of first dorsal fin	46.7	44.1	41.4	37.7	41.0	38.8	37.1	38.9	39.9	39.9	39.1	39.0	38.1	38.4	37.5	35.3	38.2	38.3	36.8	38.3	36.8
Snout to origin of anal fin	65.1	62.5	65.0	64.7	63.6	62.5	60.7	61.5	60.5	60.9	60.3	59.4	60.7	60.8	61.5	57.0	59.6	59.3	60.8	58.3	60.4
Snout to insertion of ventral fin	43.7	39.6	37.2	39.6	35.7	37.3	37.3	37.7	36.2	37.3	36.1	35.0	36.3	37.4	35.8	36.4	33.7	34.6	35.2	34.6	35.4
Snout to insertion of pectoral fin	40.6	36.8	35.9	35.8	33.8	34.7	33.4	33.8	33.8	34.8	33.2	32.8	32.6	34.2	32.6	33.2	31.9	33.5	33.8	31.1	33.0
Length of base of first dorsal fin	16.1	13.9	13.9	14.2	13.6	12.5	13.7	13.4	16.2	15.1	12.5	13.6	15.8	15.7	12.7	13.3	13.7	13.7	13.5	14.5	14.3
Length of base of second dorsal fin	10.3	11.1	11.2	10.9	10.5	10.7	11.4	11.5	9.7	11.5	10.3	11.1	10.7	11.1	10.6	10.4	11.5	11.0	10.4	10.9	11.1
Distance between first and second dorsal fins	8.0	6.9	9.1	8.7	7.5	9.6	9.7	9.8	4.7	8.6	9.1	9.5	9.7	8.9	10.3	8.6	8.4	11.0	9.3	9.0	10.3
Length of base of anal fin	13.8	10.7	10.6	11.2	9.4	11.0	11.3	11.4	11.0	11.1	10.6	9.4	10.8	11.2	10.7	11.3	11.2	11.1	10.4	10.7	11.0
Distance between anus and insertion of ventral fin	17.6	19.4	18.1	18.9	19.5	18.9	18.2	17.1	18.8	17.7	19.9	20.8	19.9	19.0	19.5	18.1	20.2	19.7	18.8	19.8	16.4
Distance between anus and origin of anal fin	6.1	5.2	8.2	8.2	7.5	5.5	7.8	7.0	6.3	5.8	7.1	6.1	6.4	6.6	7.3	6.0	6.8	7.3	6.8	6.0	6.8
Length of pectoral fin	23.8	21.5	26.0	24.6	20.8	24.4	24.4	24.6	23.2	25.0	24.8	23.0	22.2	23.6	22.9	23.0	22.6	22.2	21.6	20.4	21.2
Length of ventral fin	19.9	16.7	17.8	18.3	16.7	17.6	16.5	17.1	17.9	15.1+	14.5	15.9	15.5	16.2	15.3	15.0	15.1	12.3+	15.5	14.7	14.9
Length of head	40.6	37.5	35.0	32.5	35.7	36.0	34.7	34.0	34.2	35.1	32.5	33.2	32.1	33.8	32.5	31.9	34.1	33.5	32.4	34.2	33.5
Length of snout	10.7	9.7	9.4	7.4	7.0	9.2	6.4	7.5	6.8	8.6	6.3	6.9	7.0	7.8	7.1	6.8	7.0	7.3	7.2	6.4	7.2
Length of upper jaw	19.5	19.1	18.2	18.0	16.9	16.5	16.1	16.8	16.4	16.3	15.9	15.9	15.6	15.8	14.9	14.4	15.0	13.6	14.6	15.0	15.2
Horizontal diameter of eye	19.5	16.7	16.0	15.8	15.4	14.3	15.6	15.8	15.1	15.3	13.8	13.8	14.5	14.2	13.4	13.2	13.5	11.2	12.7	12.8	13.6
Width of interorbital space	13.4	8.3	9.4	9.0	9.9	10.7	9.5	10.0	9.4	9.5	10.1	10.1	9.2	11.1	10.4	9.8	10.3	9.9	10.4	9.5	9.7

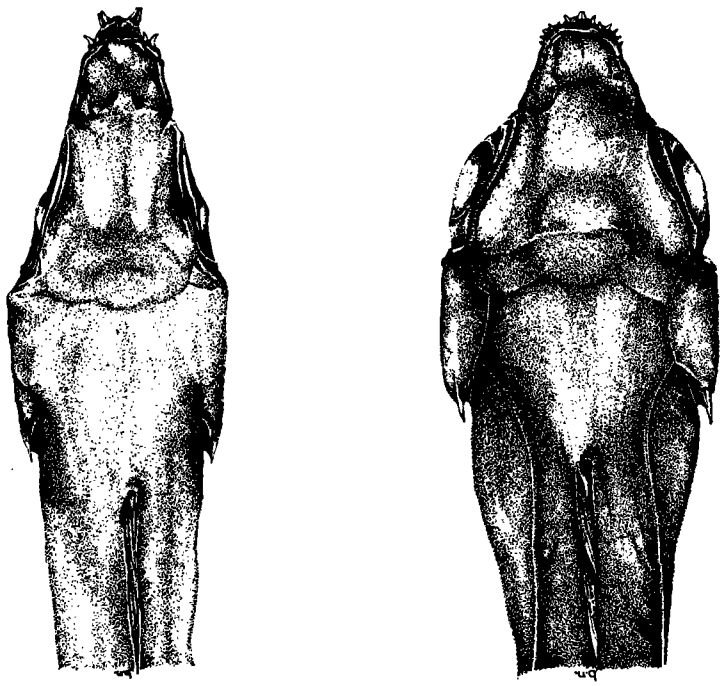

Figure 3. Dorsal views of heads of Rosenblattia robusta (left) and Florenciella lugubris (right). Squamation not shown. Drawn by Basil G. Nafpaktitis.

Trousers set for 275 m, probably taken below 140 m. MCZ.

Description. Morphometric data, taken from the type and a series of paratypes, are provided in Table 2. Meristic data were taken from fifty specimens including the type. These data (value, followed in parentheses by the number of specimens) follow: first dorsal fin VII (50); second dorsal fin I, 8 (50); anal fin II, 8 (49) or rarely II, 7 (1); pectoral fin (left side, or if damaged the right) 16 (1), 17 (28), 18 (20) or 19 (1); gill rakers on first arch 5 (1), 6 (39) or 7 (10) + 1 + 14 (16), 15 (32) or 16 (2) totaling 20 (2), 21 (13), 22 (24) or 23 (11); branchiostegal rays 4 + 3 (50); complete rows of scales between origin of first dorsal fin and lateral line 4 (50); between lateral line and origin of anal fin 15 (5), 16 (37) or 17 (8); scales in lateral line from origin to base of mid-caudal ray 49 (3), 50 (14), 51 (18), 52 (8) or 53 (7); one to four lateral line scales on caudal fin, some of these frequently missing and apparently more numerous in larger than in smaller specimens. Vertebrae, 10 + 14 + 1 = 25 (8) or 10 + 13 + 1 = 24 (1).

Body compressed and relatively shallow, its greatest depth (at origin of first dorsal fin) 3.3 to 3.8 in s.l., its greatest width (immediately behind orbit) 1.3 to 1.8 in greatest depth. All of body and head, except for the snout anterior to eye, covered by adherent ctenoid scales, the cteni of which are continuous with transverse ridges on the surface of each scale. Squamation essentially complete at 30 mm s.l., but at this size the cteni and associated ridges are scarcely evident. Scales of lateral line normal, the line terminating with one, two or three pored scales overlying central rays of the caudal fin. The other fins, both paired and vertical, are naked and there are no axillary scales.

Distance between snout and origin of first dorsal fin 2.2 to 2.8 in s.l.; preanal distance 1.5 to 1.8 in s.l.; preventral 2.3 to 2.9 in s.l.; prepectoral 2.5 to 3.2 in s.l. Spines in fins strong, high and sharp, those in the first dorsal fin lying alternately on the right or left of center when the fin is depressed. Dorsal and second anal spines about as long as the soft rays which follow them; spiny elements in the vertical fins longer than the soft. Base of pectoral fin set at about 45° angle with the horizontal, the fin relatively short and rounded, its length 1.4 to 1.7 in length of head. Anus located about one-fourth of the way from origin of anal to insertion of ventral fins and separated from the first anal spine by about five scales. Head broad and bony, its greatest width 1.7 to 2.3 in length of head, its length 2.5 to 3.1 in s.l. Interorbital nearly flat, its least bony width 3.0 to 3.7 in length of head. Eye large, its horizontal diameter 2.1 to 3.0 in length of head. Pupil elliptical, aphakic space prominent. Dorsal and posterior edges of orbit spinulose, the supraorbital ridge terminating anteriorly in a broad, flat spine. Free edge of preopercle single, usually smooth, but occasionally (especially in smaller individuals) bearing a few minute spines. A complex cluster of spines originate near the more posterior part of the opercular bone. The largest spine is the most posterior; it is usually simple in smaller specimens, but compound in the larger. Smaller and more or less simple spines lie above and below that at the angle of the operculum. Elsewhere the free edge of the gill cover is either smooth or weakly serrated.

Gill openings wide, the gill flaps and branchiostegal membranes meeting at the ventral midline but not overlapping. Pseudobranchs present, formed of about 14 filaments. Gill rakers on first arch of the usual lath-like shape and about half as long as diameter of eye. Gill filaments unusually short and few, those of first arch about two-thirds as long as the opposite rakers.

Symphysis of upper jaw toothless. On each side lateral to the midpoint is a patch of minute teeth and two or three conical, slightly recurved antrorse teeth. A single series of minute teeth is present on the more posterior biting edge of the premaxilla. The two or three conical antrorse canines on the mandible are followed by a row of small teeth. The vomer may bear a few minute, sharp teeth or be completely toothless. Palatines with teeth in a simple series or in a band. Tongue toothless.

In alcohol, the flanks are uniformly dusky, with more pigment along the margins of the scale pockets than elsewhere and with darker areas along the bases of the vertical fins. All fins are dark brown. The eye is dark, but elsewhere the head is similar in pigmentation to the body. Linings of mouth, pharynx, and abdominal cavity black. In young of about 35 mm s.l., the black linings of the body cavities are evident through the lighter dermal pigmentation, the black bases of the second dorsal and anal fins contrast in a more striking way with the pale flanks, the tip of the caudal is black, and there is a prominent dark vertical bar across the caudal peduncle in an area bounded by the upper and lower procurrent caudal rays.

HOWELLA BRODIEI OGILBY 1898

The three nominal species of *Howella* have never been critically compared. The type specimen of *Howella brodiei* was found on the beach at Lord Howe Island near Australia. The type locality for the second species, *H. sherborni* (Norman, 1930, as *Rhectogramma sherborni*) lies in the eastern Atlantic off South Africa, *ca.* 34°S, 17°E. The third species, *H. pammelas* (Heller and Snodgrass, 1903, as *Galeagra pammelas*) was first taken at Wenman Island in the Galapagos group.

The type of *H. pammelas* (Heller and Snodgrass, 1903: pl. 4) and additional eastern Pacific material of this species from the collections of Scripps Institution of Oceanography show both an upper and a lower opercular spine to be complex. In

contrast, only the upper opercular spine is complex in specimens of *Howella* from the western Pacific and Atlantic. On this basis alone, other morphometric data being similar, our Indian Ocean specimens, all of which have only an upper complex opercular spine, are referred here to *H. brodiei*, a species of which *H. sherborni* is tentatively considered conspecific. A critical and more detailed examination of the now considerable material from all oceans is obviously in order.

This genus is hitherto unknown from the Indian Ocean, the nearest records being the South African-Atlantic type locality of *H. sherborni*, the Australian type locality of *H. brodiei*, and a Philippine locality reported for the latter species by Herre and Herald (1951).

The *Anton Bruun* took specimens of *H. brodiei* at each of the following twelve stations:

One, 18.0 mm s.l.; Cr. III; Sta. 2, coll. AE6E; 15 August 1963; 0350 to 0715 hrs. l.s.t.; 10°09′N, 59°55′E to 10°00′N, 60°01′E; maximum calculated depth 560 m (depth from t.d.r. 520 m); IKMT, deep fraction of catch with Foxton Trousers nominally set for 150 m, specimen probably taken below 75 m. MCZ.

One, 14.5 mm s.l.; Cr. III; Sta. 3, coll. AE8B; 16 August 1963; 1845 to 2213 hrs. l.s.t.; 06°54′N, 59°55′E to 06°37′N, 59°57′E; maximum calculated depth 750 m; IKMT, shallow fraction of catch with Foxton Trousers set for 150 m, probably taken above 300 m. MCZ.

One, 13.6 mm s.l.; Cr. III; Sta. 5, coll. AE12B; 19 August 1963; 2035 to 2350 hrs. l.s.t.; 01°23′N, 60°11′E to 01°22′N, 60°04′E; maximum calculated depth 750 m (depth from t.d.r. 800 m); IKMT, shallow fraction of catch with Foxton Trousers set for 275 m, probably taken above 550 m. Zoological Museum, University of Copenhagen.

One, 65.0 mm s.l.; Cr. III; Sta. 7, coll. AE16D; 23 August 1963; 0625 to 1350 hrs. l.s.t.; 04°52′S, 60°02′E to 04°27′S, 59°55′E; maximum calculated depth 2030 m; IKMT, deep fraction of catch with Foxton Trousers set at 275 m, probably caught below 140 m. MCZ.

One, 42.5 mm s.l.; Cr. III; Sta. 16, coll. AE30B; 12 September 1963; 1110 to 1710 hrs. l.s.t.; 40°53′S, 60°01′E to 41°07′S, 59°52′E; maximum calculated depth 2750 m; IKMT, deep fraction of catch with Foxton Trousers set for 275 m, probably taken below 140 m. SIO.

One, 61.0 mm s.l.; Cr. III; Sta. 16, coll. AE31B; 12 September 1963; 1725 to 2105 hrs. l.s.t.; 41°07′S, 59°52′E to 41°07′S, 60°08′E; maximum calculated depth 635 m; IKMT, deep fraction of catch with Foxton Trousers set for 150 m, probably from below 75 m. MCZ.

Two, each 14.6 mm s.l.; Cr. VI; Sta. 334A; 24 May 1964; 1912 to 2345 hrs. l.s.t.; 06° 01′N, 64°59′E to 05°48′N, 64°57′E; maximum calculated depth 700 m; IKMT, deep fraction of catch with Foxton Trousers set for 275 m, probably taken below 140 m. MCZ.

One, 47.0 mm s.l.; Cr. VI; Sta. 335 B; 26 May 1964; 0100 to 0850 hrs. l.s.t.; 03°46′N, 65°05′E to 03°27′N, 65°07′E; maximum calculated depth 2575 m; IKMT, deep fraction of catch with Foxton Trousers set for 275 m, probably taken below 140 m. USNM.

One, 15.5 mm s.l.; Cr. VI; Sta. 337B; 28 May 1964; 0300 to 0930 hrs. l.s.t.; 00°14′S, 65°03′E to 00°29′S, 65°08′E; maximum calculated depth 2250 m; IKMT, shallow fraction of catch with Foxton Trousers set for 275 m, probably taken above 550 m. USNM.

Three, 11.8 to 14.6 mm s.l.; Cr. VI; Sta. 340B; 31 May 1964; 1945 to 0155 hrs. l.s.t.; 05°55′S, 64°48′E to 06°08′S, 64°58′E; maximum calculated depth 746 m; IKMT, shallow fraction of catch with Foxton Trousers set for 275 m, probably taken above 550 m. MCZ.

Two, 11.1 and 11.9 mm s.l.; Cr. VI; Sta. 341B; 1–2 June 1964; 2200 to 0300 hrs. l.s.t.; 07°56′S, 65°14′E to 07°57′S, 64°51′E; max-

imum calculated depth 504 m; IKMT, considered an open net. MCZ.

Three, 10.2 to 12.4 mm s.l.; Cr. VI; Sta. 342A; 2 June 1964; 1755 to 2250 hrs. l.s.t.; 09°57′S, 64°55′E to 10°01′S, 64°19′E; maximum calculated depth 580 m; IKMT, deep fraction of catch with Foxton Trousers set for 200–250 m, probably taken below 125 m. MCZ.

BATHYSPHYRAENOPS PARR 1933

Bathysphyraenops, a monotypic genus, has been known only from the type series of *B. simplex* Parr 1933, which was taken off the Bahamas and adjacent islands, and from unpublished catches made elsewhere in the Atlantic and Pacific. Our Indian Ocean collection contains two specimens, 84.5 and 90.8 mm s.l., which we have critically compared with the holotype of *B. simplex* (Bingham Oceanographic Lab. no. 2847). Meristic values, with the possible exception of the number of scale rows between the lateral line and origin of anal fin, are nearly identical, and differences in body proportions, armature, etc. are insignificant. These Indian Ocean *B. simplex* were taken at the following station:

R/V *Anton Bruun*, IIOE, Cr. III; Sta. 6, coll. AE13B; 21 August 1963; 0155 to 0440 hrs. l.s.t.; 01°58′S, 60°06′E to 02°06′S, 60°02′E; maximum calculated depth 510 m (depth from t.d.r. 500 m); IKMT, considered an open net. MCZ and USNM.

BRINKMANNELLA PARR 1933

Included within the small group of oceanic cheilodipterids with single anal spines and unarmed opercular flaps are *Brinkmannella elongata* Parr, previously known only from midwaters off the Bahama Islands (Parr, 1933:26), and *Brephostoma carpenteri* Alcock, an abyssal benthic species from the Bay of Bengal (Alcock, 1889:383). *Brinkmannella elongata* has deciduous scales and teeth in jaws, palatines, and vomer. *Brephostoma carpenteri* has adherent scales and a toothless mouth. In other respects the two genera are suspiciously similar.

Our Indian Ocean material contains two lots of specimens within this group. The first is a single individual, 104.5 mm s.l., which is larger but otherwise identical to the Atlantic *Brinkmannella elongata*. It was taken as follows:

Scripps Institution of Oceanography "Monsoon" Expedition; IKMT haul no. 9; 19 December 1960; 0324 to 0829 hrs. l.s.t.; 33°19′18″S, 72°34′24″E to 33°38′06″S, 72° 31′00″E; maximum calculated depth 1878 m, open net. SIO 61–37.

The second lot contains four fishes, *ca.* 64-*ca.* 103 mm s.l., all in poor condition, which are meristically more similar to *Brephostoma carpenteri* than to *Brinkmannella elongata* but show the generic characters diagnostic of this latter genus: teeth in jaw, palatines, and vomer; deciduous scales; and an area of relatively light pigmentation on the flanks posterior to the anal fin. These are characters which possibly could change as a pelagic young assumes a benthic adult life. Therefore, pending further study, the identity of this lot is left open as "*Brinkmannella* sp." The series came from the following locality:

R/V *Anton Bruun*, IIOE, Cr. III; Sta. 6, coll. AE13B; 21 August 1963; 0155 to 0440 hrs. l.s.t.; 01°58′S, 60°06′E to 02°06′S, 60° 02′E; maximum calculated depth 510 m (depth from t.d.r. 510 m); IKMT, considered an open net. MCZ.

LITERATURE CITED

ALCOCK, ALFRED. 1889. On the bathybial fishes of the Bay of Bengal and neighbouring waters, obtained during the seasons 1885–1889. (Natural history notes from H. M. *Investigator* no. 13.) Ann. Mag. Nat. Hist., ser. 6, vol. 4, pp. 376–399.

———. 1890. On the bathybial fishes collected in the Bay of Bengal during the season 1889–1890. (Natural history notes from H. M. *Investigator* no. 16.) Ann. Mag. Nat. Hist., ser. 6, vol. 6, pp. 197–222.

BRAUER, AUGUST. 1906. Die Tiefsee-Fische I. Systematischer Teil. Wiss. Ergeb. Deutschen

Tiefsee-Exped. auf dem Dampfer *Valdivia* 1898–99, vol. 15, 432 pp.

CLARKE, WILLIAM D. 1963. Field data for the Isaacs-Kidd midwater trawl collections of Scripps Institution of Oceanography, University of California. Data Report, SIO Ref. 63–29, 23 pp. + figs.

FOURMANOIR, P. 1957. Poissons téléostéens des eaux malgaches du Canal de Mozambique. Mém. Inst. Sci. Madagascar, Sér. F. Océanogr., vol. 1, pp. 1–316.

FOXTON, PETER. 1963. An automatic opening-closing device for large plankton nets and mid-water trawls. J. Mar. Biol. Ass. U. K., vol. 43, pp. 295–308.

HANEDA, YATA. 1961. Luminous organs of fish, which emit light indirectly. Rec. Oceanogr. Works Japan, vol. 7, no. 1, pp. 83–87.

HELLER, EDMUND AND ROBERT EVANS SNODGRASS. 1903. Papers from the Hopkins Stanford Galapagos Expedition, 1898–1899. XV. New fishes. Proc. Washington Acad. Sci., vol. 5, pp. 189–229.

HERRE, ALBERT W. AND EARL S. HERALD. 1951. Noteworthy additions to the Philippine fish fauna with descriptions of a new genus and species. Philippine J. Sci., vol. 79, no. 3, pp. 309–340.

HUBBS, CARL L. AND KARL F. LAGLER. 1947. Fishes of the Great Lakes Region. Cranbrook Inst. Sci. Bull. no. 26, 186 pp.

NORMAN, J. R. 1930. Oceanic fishes and flatfishes collected in 1925–1927. Discovery Rep., vol. 2, pp. 261–370.

———. 1957. A draft synopsis of the orders, families and genera of recent fishes and fish-like vertebrates. 649 pp. Duplicated and distributed by British Museum (Natural History).

OGILBY, J. DOUGLAS. 1898. Additions to the fauna of Lord Howe Island. Proc. Linn. Soc. New South Wales, vol. 23, pp. 730–745.

PARR, ALBERT E. 1933. Deepsea Berycomorphi and Percomorphi from the waters around the Bahama and Bermuda Islands. Bull. Bingham Oceanogr. Coll., vol. 3, art. 6, 51 pp.

(*Received 5 April 1965.*)

Reprinted from *Zool. Jb. Syst*, Bd. 92, 1965, S. 289-326.

Nachdruck verboten
Übersetzungsrecht vorbehalten

Aus dem Instituto Oceanografico Cumana, Venezuela

Über das Vorkommen von Nemertinen in einem tropischen Korallenriff 4. Hoplonemertini monostilifera

Ergebnisse der Österreichischen Indo-Westpazifik-Expedition 1959/60
Teil VII

Von Ernst Kirsteuer

Mit 19 Abbildungen im Text

Inhaltsverzeichnis

Einleitung

Die vorliegende Schrift behandelt die Hoplonemertini monostilifera aus dem Material der „Österreichischen Indo-Westpazifik-Expedition 1959/60". Die Aufsammlung erfolgte im Saumriff der nordwestlich von Madagaskar im Mozambique-Kanal gelegenen Insel Tanikely (48°14'9"O, 13°28'9"S). Die Proben wurden tauchend im Ostabschnitt des Riffes entlang eines abgesteckten Profiles abgetragen und im Feldlabor mittels Klimaverschlechterung aufbereitet. Um auch hinsichtlich der quantitativen Verteilung der Nemertinenfauna eine Aussage möglich zu machen, wurden die insgesamt 40 zur Aufarbeitung gelangten Proben volumengleich gehalten, wo-

bei eine Probe 3 Glaswannen zu je 30 Liter, gefüllt mit Substrat, entsprach. Die bei der Untersuchung berücksichtigten Bestandsbildner waren: *Seriatopora angulata* KLUNZINGER, *Acropora pharaonis* (EDWARDS & HAIME), *Acropora corymbosa* (LAMARCK), *Porites nigrescens* DANA, *Porites iwayamaensis* EGUCHI und *Millepora tenella* ORTMANN, sowie eine dicke Rasen bildende Alge, deren Bestimmung noch ausständig ist[1]). Die Nemertinen-Ausbeute der Expedition umfaßt 38 Arten mit zusammen 488 Individuen. Auf die Hoplonemertini monistilifera entfallen 9 Arten, von denen 8 nachfolgend dargestellt sind, während eine mit zwei Individuen vertretene *Tetrastemma*-Species wegen des schlechten Erhaltungszustandes nicht weiter determiniert werden konnte und nur kurz Erwähnung findet.

Für Unterstützung und Förderung der im Rahmen der „Österreichischen Arbeitsgemeinschaft für Meeresforschung" durchgeführten Expedition sei an dieser Stelle Herrn Prof. Dr. W. MARINELLI, Herrn Doz. Dr. R. RIEDL und Herrn Doz. Dr. F. STARMÜHLNER, I. Zoologisches Institut der Universität Wien, aufrichtig gedankt. Die Feldarbeit auf Tanikely wurde durch Herrn Prof. Dr. J. MILLOT, Herrn Prof. Dr. R. PAULIAN, Herrn Dr. A. CROSNIER, Herrn Dr. P. FOURMANOIR und Herrn M. BJØRNUM, Institut de Recherche Scientifique a Madagascar, Station Océanographique Nossi Bé, in dankenswerter Weise gefördert und erleichtert. Dank gebührt auch Herrn Dr. F. BALDA und Herrn Dr. R. CURRA vom Instituto Oceanografico Cumana, Venezuela, für gezeigtes Interesse an der Bearbeitung des vorliegenden Teiles. Für die Bestimmung der bestandsbildenden Madreporaria und Hydroidea möchte ich Frau Dr. L. ROSSI, Istituto e Museo di Zoologia, Universita di Torino, herzlichst danken.

Beschreibungen

Cratenemertes FRIEDRICH 1955

Im Genus *Cratenemertes* wurden von FRIEDRICH (1955) alle jene bis dahin unter *Amphiporus* geführten Arten zusammengefaßt, bei welchen in der Rhynchocoelomwand eine Verflechtung der Muskulatur auftritt. Es sind dies *Cratenemertes amboiensis* (BÜRGER) 1890, *C. drepanophoroides* (GRIFFIN) 1898, *C. pacificus* (COE) 1905, *C. occidentalis* (COE) 1905, *C. punctatulus* (COE) 1905 und *C. bergendali* (GERING) 1912. Hinzu kamen *Cratenemertes danae* FRIEDRICH 1957 und *C. pelagicus* KOROTKEVITSCH 1961 sowie die in der Folge beschriebene Form

Cratenemertes madagascarensis n. sp.

Habitus

Die aufgesammelten Exemplare der Art hatten eine Körperlänge von 5—7 mm und erreichten eine maximale Breite von 1,5 mm. Im Leben wirkten die dorsoventral

1) Da in den Algenproben keine Hoplonemertini monostilifera auftraten, ist das Fehlen einer Bestimmung ohne Bedeutung für die vorliegende Arbeit.

leicht abgeflachten Tiere etwas plump. Die terminad sich verjüngende Kopfregion ist nur schwach abgesetzt und weist 12 unregelmäßig angeordnete Augen auf, von denen je 6 auf eine Körperseite entfallen. Von der dorsal intensiver als ventral in Erscheinung tretenden ockergelben Grundfarbe heben sich auf der Rückenpartie der Tiere rostbraune Pigmentschollen ab (Abb. 3, C). Diese Pigmentschollenzone beginnt bald hinter der Kopfregion und reicht nicht bis ganz an das caudale Körperende heran. Damit ähnelt die vorliegende Form sehr *Amphiporus maculosus* (Coe 1944a), bei welcher rotbraune Flecken auf grauem Grund aufscheinen, wobei ebenfalls die Zeichnung auf die Dorsalseite beschränkt ist und der Kopf frei bleibt. Wenngleich von *A. maculosus* keine Habitusabbildung vorhanden ist, scheint doch auf Grund der von Coe (1944a, S. 30) gegebenen Beschreibung eine recht gleichartige lockere Verteilung der Pigmentflecken beiden erwähnten Formen zuzukommen, so daß zu deren habitueller Trennung, abgesehen von dem nicht sehr signifikanten Unterschied in der Grundfarbe, nur das Vorhandensein von Augen bei *Cratenemertes madagascarensis* und deren Fehlen bei *Amphiporus maculosus* herangezogen werden kann. Der gleichfalls von Coe (1901) beschriebene *Amphiporus nebulosus* als auch *Cratenemertes punctatulus* (Coe 1905) zeigen die dorsalen braunen Flecken dicht beisammen, oftmals ineinanderfließend und vor allem auch am Kopf vorhanden, wodurch sich die beiden Arten deutlich von der zur Rede stehenden Form distanzieren.

Anatomie

Das Epithel ist besonders in der vorderen Körperhälfte stark entwickelt, ebenso auch die Grundschicht, die in dieser Region die Dicke der Ringmuskulatur erreicht. Die Höhe des Epithels entspricht annähernd der Dicke von Grundschicht und Muskularis zusammen. Eine Diagonalmuskelschicht wie bei *C. punctatulus* und *C. bergendali* ist bei *C. madagascarensis* nicht realisiert. Die Kopfspitze wird größtenteils von der Kopfdrüse erfüllt, welche in schlauchförmige Lappen gegliedert, dorsomedian und bei einem der untersuchten Tiere auch ventral das Praecerebralseptum durchdringt, ohne dann noch erwähnenswert weiter caudad zu reichen (Abb. 1, kd). Eine gut ausgebildete Kopfdrüse ist auch bei den meisten der anderen *Cratenemertes*-Arten gefunden worden und lediglich von *C. pelagicus* wird berichtet, daß sie nicht vorhanden ist. Submuskulare Drüsenzellen, wie sie bei *C. drepanophoroides* und *C. punctatulus* beobachtet wurden, fehlen im vorliegenden Fall.

Der Cerebralkomplex ist im Vergleich zum Körperquerschnitt als sehr groß zu bezeichnen. In der terminalen Hälfte des Gehirns ist kaum eine Begrenzung der Ganglien an der Oberfläche zu bemerken, im caudalen Abschnitt hingegen sind Dorsal- und Ventralganglien vollständig isoliert. Die Seitennervenstämme gehen nach ihrem Austritt von den ventralen Ganglien erst über eine starke Bogenbildung in ihren Längsverlauf ein. Die ventrale Gehirnkommissur ist gering an Durchmesser

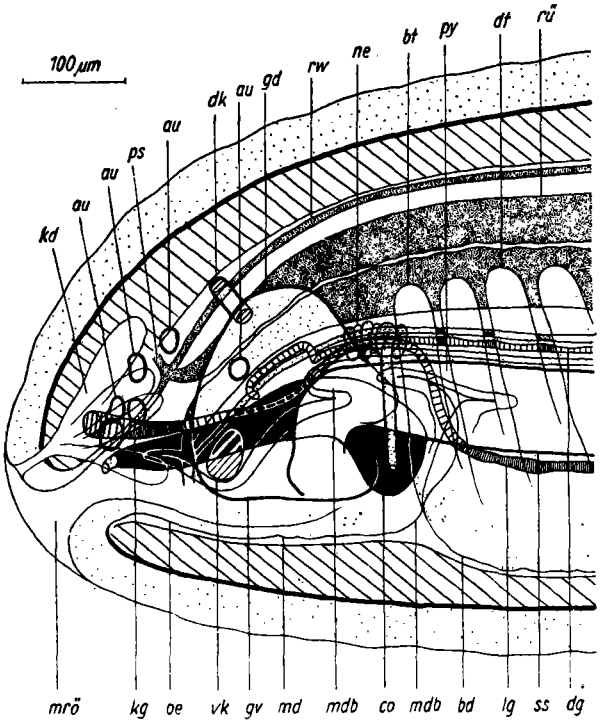

Abb. 1. *Cratenemertes madagascarensis* — Vorderende. Projektion der Organisation (der linken Körperseite) in die Median-Sagittale. (Erklärung der Abkürzungen s. S. 324.)

und extrem kurz, da sich die korrespondierenden Ganglien median berühren. Eingekeilt zwischen den kuppenförmigen Enden der Ganglien und den Bögen der Lateralstämme liegen die großen Cerebralorgane, die sich caudad noch ein kleines Stück über das Gehirn hinaus erstrecken (Abb. 1, co). Sie münden seitlich in den Kopffurchen aus.

Das Rhynchocoelom ist bis an das caudale Körperende zu verfolgen. Die Muskulatur der je nach Kontraktionszustand an Dicke variierenden Rüsselscheide wird in erster Linie von einer Ringfaserschicht gebildet, in welcher regellos eingebettet Längsfibrillen verlaufen, so daß eine Verflechtung der Muskulatur zustandekommt. Rhynchocoelomtaschen sind nicht vorhanden und wurden in der Gattung bislang nur von *C. bergendali* mitgeteilt. Der Rüssel selbst weist keine Besonderheiten auf, er wird von 9 Rüsselnerven versorgt, die in der von einer äußeren und inneren Ringfaserlage umgebenen Längsmuskulatur des vorderen Rüsselzylinders liegen (Abb. 2). Das Angriffstilett und die Form seiner Basis konnten an Hand des zur Verfügung stehenden Materials nicht rekonstruiert werden. In den beiden Reservestilettaschen sind 2 oder 3 Stilette gelagert.

Im Gegensatz zu *C. pelagicus*, wo nach Mitteilung KOROTKEVITSCHS der Mund von der Rüsselöffnung getrennt ist, ist bei der vorliegenden Form nur ein gemein-

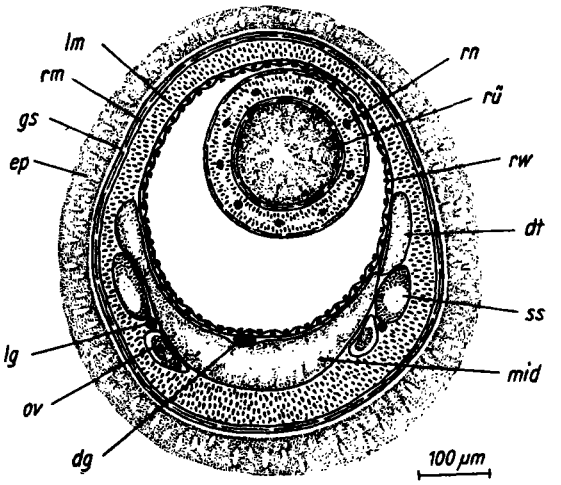

Abb. 2. *Cratenemertes madagascarensis.* Querschnitt durch die Mitteldarmregion. (Erklärung der Abkürzungen s. S. 324.)

samer Porus gegeben, welcher sich etwas subterminal an der Kopfspitze in einer seichten medianen Einbuchtung, in der auch die Kopfdrüse ausleitet, befindet. Das Rhynchodaeum ist kurz, ebenso auch der Ösophagus, der sich unmittelbar hinter der Ventralkommissur zum Magen erweitert. An letzterem ist dorsomedian ein kleiner, nicht ganz bis zur Gehirnmitte terminad reichender Blindsack zu beobachten (Abb. 1, mdb), sowie eine caudale Blindsackbildung, die durch den ein wenig terminad verschobenen Abgang des anhanglosen Pylorus bedingt ist. Die Taschen an dem kurzen Mitteldarmblindsack sind wie die des Mitteldarmes selbst unverzweigt und stiegen leicht terminad geneigt bis zur Mitte des Rhynchocoeloms dorsad auf (Abb. 1, bt,dt; Abb. 2, dt). Beginnend mit dem Mitteldarmblindsack ist eine relativ gut entwickelte Dorsoventralmuskulatur zu bemerken, deren Fibrillen lateral von der Rhynchocoelomwand ausgehen und zwischen den Darmtaschen hindurch lateroventral an den Darm heranführen. Differenzierungen am Vorderdarm sind auch von anderen Vertretern des Genus bekannt geworden. So ist bei *C. occidentalis* außer einem Blindsack am Magen auch ein solcher am Ösophagus vorhanden, während *C. bergendali* zwei Blindsackbildungen am Magen und eine am Pylorus aufweist. Unterschiedlich zur vorliegenden Situation ist auch der Beginn des Magens vor dem Gehirn sowie das Fehlen eines Mitteldarmblindsackes bei *C. pelagicus.*

Die Kopfgefäße ziehen nach ihrer Vereinigung in der Kopfspitze, sich zusehend verengend, durch den Cerebralring und setzen sich als Lateralgefäße fort, wobei sie noch in der Cerebralregion dorsad aufsteigend, im Endbereich der Dorsalganglien über den Seitenstämmen zu liegen kommen, hier von den Nephridien umgeben werden und in der Pylorusregion steil abfallend ihren weiteren Verlauf ventral von den Seitenstämmen einnehmen. Eine Gehirnanastomose ist nicht ausgebildet und das Dorsalgefäß zweigt vom rechten Lateralgefäß knapp hinter der Ventralkommissur

UNESCO ARCHIVES

ab, dringt darauf in das Rhynchocoelom ein und tritt aus diesem mit Beginn des dorsalen Magenblindsackes wieder aus. Sowohl die Lateralgefäße als auch das Dorsalgefäß zeigen stellenweise Erweiterungen und Anschwellungen (Abb. 1, lg, dg).

Die Nephridien befinden sich über den Endkuppen der Dorsalganglien und öffnen sich über je einen, die Seitenstämme lateral umgreifenden Ableitungskanal lateroventral hinter den Ventralganglien nach außen (Abb. 1, ne). Ein wesentlicher Unterschied ergibt sich daraus nur zu *C. pelagicus*, bei welcher Form überhaupt kein Nephridialapparat gefunden wurde (KOROTKEVITSCH 1961, p. 1420).

Die untersuchten Tiere erwiesen sich als geschlechtsreife Weibchen, deren Gonaden hauptsächlich in der caudalen Körperhälfte ventral von den Lateralnervenstämmen angeordnet sind (Abb. 2, ov). Die Ausfuhrgänge der Ovarien sind nach lateroventral gerichtet.

Verbreitung

Indo-westpazifischer Raum: Madagaskar (Tanikely) [Mozambique-Kanal].

Verteilung

Cratenemertes madagascarensis wurde im Untersuchungsgebiet auf abgestorbenen, stark ineinander verkeilten und von krustenbildenden Bryozoen bewachsenem Geäst von *Acropora pharaonis* mit einer Frequenz von 30 % bei einer Dominanz von 2,8 % registriert. Ebenfalls totes Material (zum Teil abgebrochene und übereinander geschichtete Platten) von *Acropora corymbosa* erbrachte die Art mit 16,7 % Fr. und 1,4 %Do. und auf Stöcken von *Seriatopora angulata* (60 % Totmaterial in den Proben) betrug die Fr. 11,2 % und Do. 1,5 %.

Paramphiporus n. g.

In seiner synoptischen Darstellung der Hoplonemertini monostilifera verweist FRIEDRICH (1955) mit Nachdruck auf die Heterogenität der Gattung *Amphiporus* und gliedert diese Sammelgattung durch Umstellung einer Reihe von Arten in neue Genera auf. Eine weitere Anzahl von Arten, zum Teil hinsichtlich ihrer anatomischen Verhältnisse nicht genügend bekannt, aber doch in dem einen oder anderen Merkmal von *Amphiporus* sensu FRIEDRICH abweichend, wird in Formengruppen zusammengefaßt. Von diesen ist im vorliegendem Fall die Hastatus-Gruppe von Interesse, da deren Vertreter *Amphiporus hastatus*, *A. bioculatus*, *A. nebulosus* und *A. korschelti* ähnlich der hier zu beschreibenden Form eine Spaltung der Längsfibrillenschicht in der vorderen Körperwandmuskularis zeigen. Ansonsten ist diese Gruppe uneinheitlich, wie aus dem Fehlen eines Praecerebralseptums bei *A. korschelti* und der eigentümlichen Ausbildung des Blutgefäßsystems bei letztgenannter Art und bei *A. hastatus* zu ersehen ist. Auch *A. nebulosus* dürfte entsprechend der Abbildung bei COE (1901, Taf. 11, Fig. 1) extracerebrale Gefäßäste besitzen. Hinzu kommt, daß bei

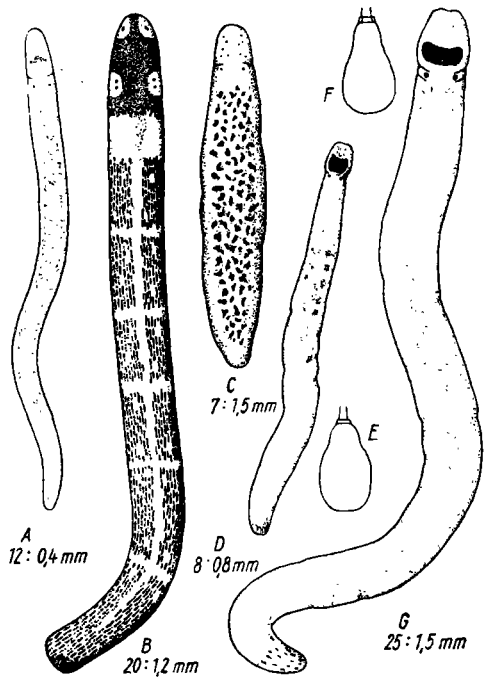

Abb. 3. *A. Tetrastemma* sp. Habitus von dorsal; B. *Friedrichia corallicola.* Habitus von dorsal; C. *Cratenemertes madagascarensis.* Habitus von dorsal; D. *Tetrastemma melanocephalum.* Habitus von dorsal; E. *Tetrastemma melanocephalum.* Basis und Knauf des Angriffstiletts; Basis und Knauf des Angriffstiletts; F. *Tetrastemma tanikelyensis.* Basis und Knauf des Angriffstiletts; G. *Tetrastemma tanikelyensis.* Habitus von dorsal.

A. nebulosus im Gegensatz zu den drei anderen Arten die Muskulatur nicht durch einen Bindegewebseinschub, sondern durch dicht angelagerte subepitheliale Drüsenzellen geteilt wird. Da FRIEDRICH (1955) auf Grund der von den erwähnten Arten bekanntgewordenen Merkmale eine Abtrennung der Gruppe von *Amphiporus* als vorerst noch ungerechtfertigt betrachtet, andererseits es nun aber nicht wünschenswert erscheinen kann, neue Arten in diese, in ihrer Bindung zu *Amphiporus* unsicheren und in sich nicht geschlossenen Gruppe einzureihen, wurde die vorliegende Art in eine eigene, neue Gattung gestellt. *Paramphiporus* n. g. unterscheidet sich von *Amphiporus* in erster Linie durch die Teilung der Längsmuskulatur im Vorderkörper, ist aber damit nicht identisch mit der Hastatus-Gruppe. Eine Nachuntersuchung der Anatomie von *Amphiporus bioculatus* könnte es vielleicht notwendig machen, die Art zu *Paramphiporus* zu ziehen.

Unklar ist vorerst noch die Beziehung der neuen Gattung zu *Paranemertes*, welch letztere sich nach der von FRIEDRICH (1955) gegebenen Diagnose von *Amphiporus* durch getrennte Längsmuskulatur und kurzes, nur über die halbe Körperlänge reichendes Rhynchocoelom und demnach von *Paramphiporus* nur durch die Rhynchocoelomlänge unterscheidet. Im Hinblick auf diese beiden Merkmale näher betrachtet,

erweist sich aber *Paranemertes* ebenfalls als eine uneinheitliche Gattung, zumal nicht von allen Arten die Spaltung der Muskulatur eindeutig nachgewiesen ist. COE (1901) erwähnt dieses Merkmal nicht bei *Paranemertes peregrina*, *P. pallida* und *P. carnea* und betont bei der Beschreibung der Muskelteilung von *P. californica* (COE 1904), daß „in no other species, so far as I am aware, has any such condition been described, though an approach to it is met with in *Amphiporus nebulosus*". Auch in seiner Revision der pazifischen Nemertinen von den amerikanischen Küsten hebt COE (1940) nur bei *Paranemertes californica* die Zweischichtigkeit als Charakteristikum hervor und vergleicht auch später (COE 1944b) die Teilung der Längsfaserschicht bei *P. biocellatus* nur mit der bei *P. californica*. Daß IWATA (1952) bei seiner *Paranemertes incola* keine Zweischichtigkeit erwähnt, wurde schon von FRIEDRICH (1955) vermerkt. Was nun die Länge des Rhynchocoeloms betrifft, so sind auch hier beachtliche Unterschiede gegeben, und zwar gerade bei den beiden Arten mit Muskelteilung, denn *Paranemertes californica* hat ein bis an die Körpermitte reichendes Rynchocoelom, während es bei *P. biocellatus* „nearly as long as the body" ist (COE 1944b).

Unterschiede zur Gattung *Nemertes*, deren Arten *N. antonina* und *N. rubrolineata* (vgl. S. 317) auch die Längsmuskulatur durch Bindegewebe geteilt haben, liegen hauptsächlich in der Körperform und der geringen Ausdehnung des Rhynchocoeloms bei *Nemertes*.

Die Diagnose für *Paramphiporus* hätte zu lauten: Kleinen *Amphiporus*-Arten ähnliche Form; Cerebralorgane normal ausgebildet und vor dem Gehirn gelegen; Ring- und Längsmuskulatur der Körperwand zieht bis in die Kopfspitze, die Längsmuskulatur ist caudal vom geschlossenen Praecerebralseptum in der Gehirnregion durch Bindegewebe in zwei Schichten zerlegt; Rhynchocoelom körperlang und ohne Anhänge; Ösophagus mündet in das Rhynchodaeum; Vorderdarm ohne Blindsackbildungen; Mitteldarmblindsack mit zwei terminad gerichteten Taschen; Dorsoventralmuskulatur fehlt; Lateralnervenstämme mit einem Faserkern; Blutgefäßsystem einfach; Nephridialapparat auf die Magenregion beschränkt.

Paramphiporus albimarginatus n. sp.

Habitus

Paramphiporus albimarginatus ist im Leben 25—30 mm lang und 1—1,5 mm dick. Bei kriechenden Tieren ist der Kopf deutlich von Rumpf abgesetzt und das hintere Körperende verjüngt und abgerundet (Abb. 12, A). In der Färbung zeigt die Art große Ähnlichkeit mit *Amphiporus texanus* COE 1951 (entsprechend der von CORREA (1961) gegebenen Beschreibung), indem die einheitliche dunkelbraune Grundfarbe von keiner Zeichnung unterbrochen wird und nur die Körperkonturen weiß erscheinen. Dieser eine Spur blau getönte weiße Saum wird nicht durch Fehlen von braunem Pigment, sondern durch das Irisieren der Epidermiszilien hervorgerufen und ist auf dem im Gegensatz zum fast drehrunden Rumpf dorsoventral stärker ab-

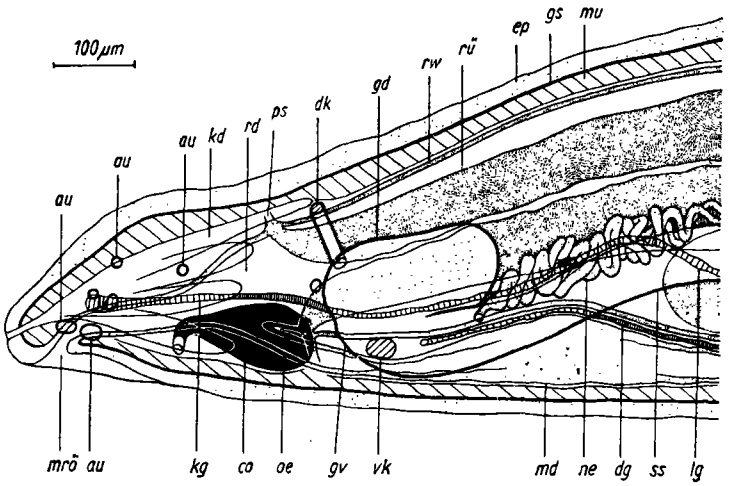

Abb. 4. *Paramphiporus albimarginatus* — Vorderende. Projektion der Organisation (der linken Körperseite) in die Median-Sagittale. (Erklärung der Abkürzungen s. S. 324.)

geflachten Kopf breiter als am übrigen Körper. Eine derartige Beeinflussung des Farbkleides durch Lichteffekte an den Zilien wurde u. a. auch von McIntosh (1873 bis 1874) bei *Emplectonema neesii* beobachtet. In einigen Fällen schimmerte das Rhynchocoelom stellenweise durch die dorsale Pigmentschicht, die Augen waren jedoch nie zu erkennen.

Anatomie

Epithel und Grundschicht sind vergleichsweise schwach ausgebildet und zeigen keine Besonderheiten. An der Körperwandmuskularis, welche an Dicke dem Epithel annähernd entspricht, fällt die Spaltung der Längsmuskulatur in der Cerebralregion auf. Von ventral bis dorsolateral wird die Längsfibrillenlage durch eine Bindegewebsschicht in eine äußere und innere Portion unterteilt (Abb. 5, A, bs). Die innere Komponente endet terminal mit dem geschlossenen Praecerebralseptum, während die peripheren Fasern ringsum bis in die Kopfspitze ziehen. Neben der gut entwickelten, dorsal das Septum durchdringenden und bis an die dorsale Gehirnkommissur heranreichenden Kopfdrüse sind praeseptal einige wenige subepitheliale Drüsen zu finden. Die 14—16 Augen sind nur an Schnittpräparaten zu sehen und liegen in je einer unregelmäßigen Reihe zu beiden Seiten der Kopfdrüse. Die vordersten Augen sind die größten und befinden sich im Bereich der Mundöffnung, nach caudad werden die Augen kleiner und das letzte in jeder Reihe ist unmittelbar vor dem Gehirn anzutreffen (Abb. 4, au). Etwa in der Mitte der praecerebralen Region beginnen die Cerebralorgane mit den in den Kopffurchen lateroventral angeordneten Pori. Sie sind einfach gebaut und erstrecken sich bis an das Septum, mit ihrem caudalen Ende dessen Muskelfasern teilweise verdrängend, so daß dieses an jenen Stellen schwächer erscheint (Abb. 4, co). Von den an der Oberfläche des umfangreichen Gehirns nur

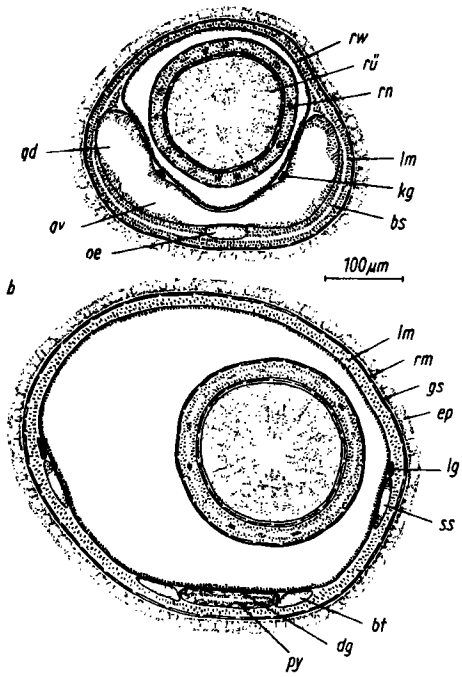

Abb. 5. *Paramphiporus albimarginatus.* A. Querschnitt durch die Gehirnregion auf Höhe der Ventralkommissur; B. Querschnitt durch die Pylorusregion. (Erklärung der Abkürzungen s. S. 324.)

undeutlich begrenzten Ganglien übertreffen die dorsalen die ventralen an Größe. Die sie verbindende Dorsalkommissur ist dünn und umgreift in einem weiten Bogen das Rhynchocoelom, welches sehr geräumig ist. Die caudal von den Ventralganglien abgehenden Lateralnervenstämme sind über ihre ganze Länge einfaserkernig. Nach ihrem Austritt vom Gehirn steigen sie langsam dorsal an und erreichen erst in der Pylorusregion ihre laterale Lage.

Das Rhynchocoelom ist körperlang und ohne Anhänge. In seiner dünnen Wand sind die Muskelschichten deutlich getrennt. Die bei den untersuchten Tieren vorgefundene enorme Erweiterung des Rhynchocoeloms postcerebral bis zur Körpermitte hin (Abb. 5, B), ist auf unterschiedliche Kontraktion bei der Fixierung zurückzuführen und daher ohne Bedeutung. Der Rüssel ist kräftig und zeigt in seinem proximalen Abschnitt eine dreischichtige Muskularis. Die Innervation erfolgt über 15 Nerven (Abb. 5, A, rü, rn). Die Bewaffnung besteht aus einem Angriffstilett, welches einer konischen, caudal abgerundeten Basis aufsitzt. Zwei Reservestilett-taschen mit je 2 oder 3 Stiletten sind vorhanden.

Der Ösophagus mündet nur wenig vor dem Praecerebralseptum in das Rhynchodaeum. Hinter der Ventralkommissur beginnt der äußerst einfache und englumige Magen, der sich caudal in einen sehr langen, dorsoventral abgeflachten und sich bis an das Ende des ersten Körperdrittels erstreckenden Pylorus fortsetzt. Der Mittel-

darmblindsack ist mit einer Länge von rund 25 μ bemerkenswert kurz und die beiden von ihm abgehenden Blindsacktaschen reichen, neben dem Pylorus verlaufend, nur über 240 μ terminad (Abb. 5, B, bt, py). Seichte, kaum über das dorsale Darmniveau aufsteigende Mitteldarmtaschen treten erst in der caudalen Hälfte des Körpers auf.

Die sich über der Mund-Rüsselöffnung verbindenden Kopfgefäße sind nach Durchlaufen des Gehirnringes als Lateralgefäße weiter zu verfolgen. Das Dorsalgefäß, welches keine Rhynchocoelombeziehung zeigt, nimmt seinen Abgang vom rechten Lateralgefäß.

Die Exkretionsorgane liegen dorsolateral von den Seitennervenstämmen und reichen caudal bis in die Pylorusregion hinein. Terminal kommen sie bis an das Gehirn heran, wo sie durch je einen, vor Eintritt in das Epithel leicht blasig erweiterten Ableitungskanal lateral ausmünden (Abb. 4, ne). Die Gonaden sind bei den vorliegenden Exemplaren der Art nicht ausgebildet.

Verbreitung

Indo-westpazifischer Raum: Madagaskar (Tanikely) [Mozambique-Kanal].

Verteilung

Mit 69 registrierten Individuen zählt *Paramphiporus albimarginatus* zu den häufigsten Arten im untersuchten Riffgebiet. Die Art schien in allen Proben von *Acropora pharaonis* und *Acropora corymbosa* auf (jeweil 100 % Frequenz), wobei sich auf ersterer eine Dominanz von 21,8 %, auf letzterer von 23,9 % ergab. Auf *Seriatopora angulata* wurde die Art mit einer Frequenz von 77,8 % bei eine Dominanz von 15,6 % vorgefunden.

Africanemertes Stiasny-Wijnhoff 1942

Die Gattung *Africanemertes* wurde von Stiasny-Wijnhoff für eine, selbst im fixierten Zustand noch an *Tetrastemma* erinnernde Nemertine von der westafrikanischen Küste errichtet. Die aus der sehr sorgfältigen Beschreibung der Typusart, *Africanemertes swakopmundi*, ersichtlichen und von Stiasny-Wijnhoff (1942, p. 188) zum Teil zur Gattungsdiagnose zusammengefaßten anatomischen Charakteristika sind: Rhynchodaeum mündet in den Ösophagus; vom Normalen abweichende Muskulatur in der Kopfspitze (horizontale Muskelplatte und den Ösophagus begleitende Längsmuskulatur); geschlossenes Praecerebralseptum; eigenartiger Ursprung der Seitennervenstämme vom Gehirn; Cerebralorgane in der Kopfspitze; Vorderteil des Rüssels schwach und mit nur zweischichtiger Muskularis; Rüsselnerven bilden eine zusammenhängende Schicht; Pylorus und Mitteldarmblindsack fehlen; zwei bis über das Gehirn reichende Mitteldarmtaschen; Längsgefäße bilden Schlingen.

Neben *Africanemertes swakopmundi*, der bisher einzigen Art des Genus, kann nun eine weitere Art gestellt werden, welche meinem Freund und Expeditionsgefährten Dr. Klaus Rützler gewidmet sei.

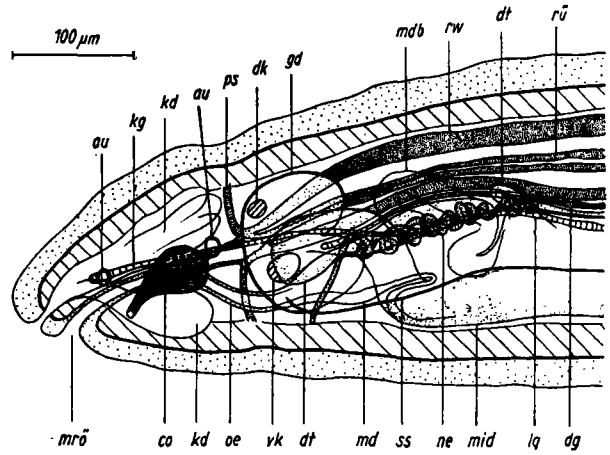

Abb. 6. *Africanemertes rützleri* — Vorderende. Projektion der Organisation (der linken Körperseite, ergänzt durch den Magendarmblindsack der rechten Seite) in die Median-Sagittale. (Erklärung der Abkürzungen s. S. 324.)

Africanemertes rützleri n. sp.

Habitus

Mit einer Länge von 15 mm bei einer Dicke von maximal 0,8 mm ist die vorliegende Form wesentlich schlanker als *Africanemertes swakopmundi*. Die Grundfarbe ist ein semitransparentes Weißgelb und läßt die Cerebralganglien rosa, den stark gewundenen Rüssel orangerot und den Darm dottergelb durchscheinen. Die beiden von vergleichsweise kleinen Ocellen dargestellten Augenpaare sind weit von einander entfernt und nur undeutlich im Leben zu erkennen. Der Kopf ist von dem dorsoventral leicht abgeflachten Rumpf kaum abgesetzt und letzterer läuft, sich im caudalen Körperviertel kontinuierlich verengend, in ein fast spitzes Hinterende aus. Mit diesem Habitus weist die Form wieder eine Ähnlichkeit zu *Tetrastemma* auf (Abb. 12, C).

Anatomie

Das Epithel ist über den ganzen Körper hin einheitlich entwickelt und ist postcerebral gleich hoch wie Grundschicht und Körperwandmuskularis zusammen. Praeseptal verändert sich das Dickeverhältnis zugunsten des Epithels durch die ein wenig schwächere Ausbildung der über das Septum bis in die Kopfspitze reichenden Längsmuskulatur. Das Septum ist geschlossen und normal gestaltet, d. h. es fehlt die bei *Africanemertes swakopmundi* beobachtete Verschiebung ventraler Septalmuskulatur durch den Ösophagus nach caudad, mit FRIEDRICH (1955, p. 156) bin ich aber der Meinung, daß es sich dabei um ein Artefakt gehandelt hat, zumal STIASNY-WIJNHOFF (1942, S. 185) hinsichtlich der verschobenen Rüsselinsertion und der das Gehirn umgebenden Rhynchocoelomblindsäcke selbst auf die starke Kontraktion des vorgelegenen Materials verweist und diese Bildungen als Artefakte anspricht. Eine Fort-

setzung des Sphincter rhynchodaei in Form einer Horizontalmuskulatur ist auch im vorliegendem Fall realisiert, kann aber nicht wie bei *A. swakopmundi* als Muskelplatte bezeichnet werden, da die Faserzüge eher locker angeordnet sind. Die Kopfdrüse nimmt den größten Teil der Kopfspitze ein und bedingt das fast vollständige Fehlen von Parenchym in dieser Region. Sie ist in drei Lappen gegliedert, von denen der dorsomediane bis dicht an das Septum heranreicht. Subepitheliale Drüsen sind in der Kopfregion in geringer Anzahl vorhanden.

Die kleinen Cerebralorgane liegen vor dem Gehirn (Abb. 6, co). Sie sind einfach gebaut und besitzen wie bei *Africanemertes swakopmundi* kein eigenes Neurilemma, im Gegensatz zur Situation bei letztgenannter Art führt aber der Cerebralkanal nicht vertikal aufsteigend direkt in das Organ, sondern weicht nach Durchdringen der Körperwand caudad ab und verläuft annähernd horizontal im Organ. Die Ausmündung der Cerebralorgane erfolgt in den kurzen Kopffurchen, die gleich hinter der Mund-Rüsselöffnung ventral beginnen und über lateral etwa zwei Drittel des Körperumfanges bedecken.

Das Gehirn liegt dem Praecerebralseptum zum Teil direkt auf. In seiner terminalen Hälfte zeigt es nur geringe Oberflächendifferenzierung und stellt im Querschnitt einen geschlossenen Ring dar, da sich sowohl die Ventral- als auch Dorsalganglien median berühren und die Länge der Kommissuren auf Null reduziert ist. Der Cerebralkomplex ist im vorliegenden Fall größer als bei *Africanemertes swakopmundi*, in der inneren Struktur und mit dem Abgang der Seitennervenstämme vom Gehirn sind jedoch weitgehende Übereinstimmungen gegeben. Die Lateralnerven entstehen nach Abtrennung der Fasermasse von den Dorsalganglien und Abbiegen nach lateral mehr minder zwischen den Dorsal- und Ventralganglien, durch Kontraktion können diese Lageverhältnisse aber kleinen Veränderungen unterworfen sein (Abb. 7, A). Postcerebral steigen die einfaserkernigen Seitenstämme leicht dorsad an, senken sich dann aber rasch wieder auf ein lateroventrales Niveau.

Das Rhynchocoelom erstreckt sich über vier Fünftel des Körpers. Seine Wand ist in der vorderen Hälfte auffallend dick, was vor allem durch eine starke Längsmuskulatur verursacht wird. Der Rüssel hingegen muß als bemerkenswert schwach bezeichnet werden, besonders im ersten Abschnitt des proximalen Zylinders ist er sehr eng und hat außer dem Epithel nur eine dünne zweischichtige Muskularis (Abb. 7, A, B, rü). Die Rüsselnerven bilden eine zusammenhängende Schicht, und erst in der mittleren Mitteldarmregion, wo der Rüssel durch das Auftreten einer dritten Muskellage an Dicke zunimmt, sind stellenweise die Nerven als Verdickungen zu erkennen. Insgesamt wurden 11 Rüsselnerven gezählt. Die Basis des Angriffstiletts ist tropfenförmig und ungefähr gleich lang wie die 20 μ langen Reservestilette, welche zu je zweien in den beiden Reservestilettaschen eingelagert sind.

Der an die subterminal gelegene Mundöffnung anschließende Vorderdarm ist in Ösophagus und Magen gegliedert. Wie bei *Africanemertes swakopmundi* ist kein

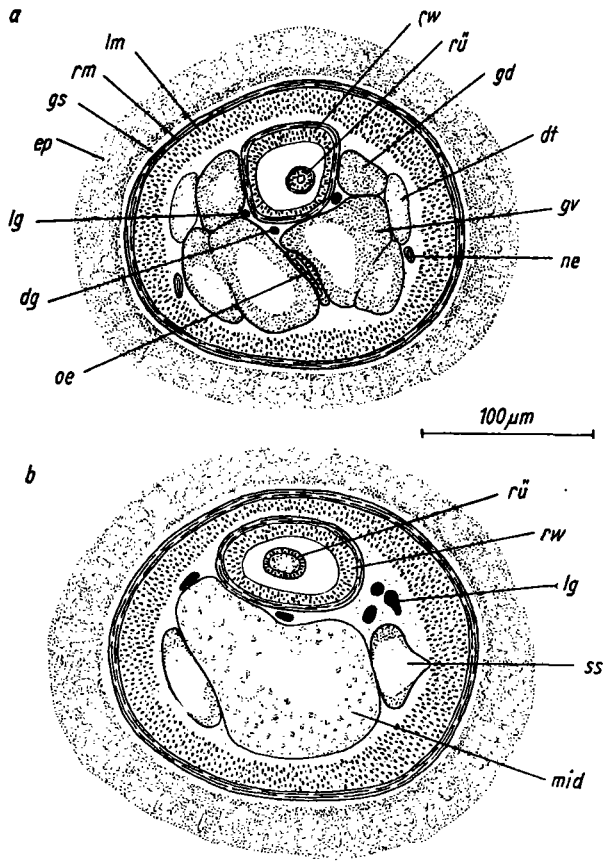

Abb. 7. *Africanemertes rützleri*. A. Querschnitt durch die Gehirnregion; B. Querschnitt durch die Mitteldarmregion. (Erklärung der Abkürzungen s. S. 324.)

Pylorus vorhanden und auch die Einmündung des kurzen Rhynchodaeums in den Ösophagus ist übereinstimmend mit den Verhältnissen bei der erwähnten Art. Die von STIASNY-WIJNHOFF (1942) beobachtete, den Ösophagus begleitende Längsmuskulatur tritt im vorliegenden Fall nicht auf. Es sind wohl in der Praecerebralregion einige von der Körperwand stammende Längsfibrillen nach innen verlagert und diese tangieren auch teilweise den Ösophagus, es kommt aber zu keiner mit der ventralen Muskulatur in Verbindung stehenden Kammbildung. Im Bereich des Gehirns ist der Ösophagus zwischen den Ventralganglien eingekeilt und abgeflacht (Abb. 7, A, oe), erweitert sich aber postcerebral rasch zum Magen. Dieser besitzt zwei laterale, tief eingreifende Längsfalten, welche den Magenhohlraum in zwei, nur über einen medianen Spalt in Verbindung stehende Kammern teilen. Kurz vor dem Magenende bricht die ventrale Kammer zum Mitteldarm durch und caudal von dieser Magen-Mitteldarmöffnung vereinigen sich die beiden Lateralfalten. Die Dorsalkammer setzt sich als caudaler Magenblindsack fort, während der ursprünglich die Ventralkammer dorsal begrenzende Faltenanteil unter Beibehaltung der histologischen Magenmerkmale noch ein Stück in die dorsale Mitteldarmwand wulstartig

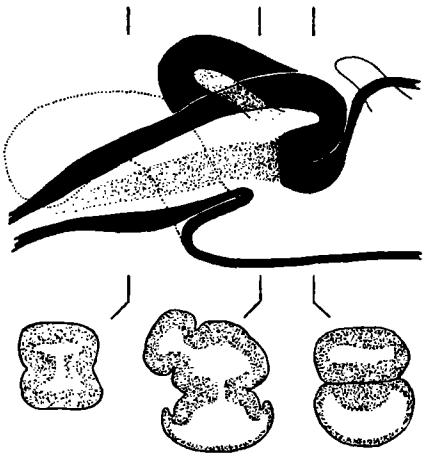

Abb. 8. *Africanemertes rützleri*. Magen und Vorderende des Mitteldarms. Rekonstruktion nach einer Querschnittserie, ergänzt durch drei stark vereinfachte Querschnittdarstellungen. Die eingetragenen Ebenen geben die Lage der Schnitte an.

einstrahlt. Zu diesen Differenzierungen kommt noch ein dorsolateraler, terminad gerichteter Blindsack an der rechten Magenseite hinzu, dessen Lumen mit der Dorsalkammer im Bereich der Magen-Mitteldarmverbindung kommuniziert (Abb. 8). Vom Vorderende des Mitteldarms gehen zwei kopfwärts geneigte unverzweigte Taschen ab, die den Cerebralganglien lateral aufliegen und bis in die terminale Gehirnregion reichen. Ein unpaarer medianer Mitteldarmblindsack fehlt. Die dorsolateralen Mitteldarmtaschen sind gut ausgeprägt, wenngleich der zentrale Darmraum sehr weit ist. Die ersten unmittelbar hinter dem Magen zu findenden Taschen stellen zwar nur kurze, hornförmige Ausstülpungen dar (Abb. 6, dt), größere, geräumigere Taschen folgen jedoch in einigem Abstand.

Das Blutgefäßsystem beginnt auf Höhe der vorderen Augen mit der Kopfschlinge. Auf ihrem Weg zum Gehirn kommen die Gefäße dicht an den Cerebralorganen vorbei, ob sie aber wie bei *Africanemertes swakopmundi* diese Organe netzartig umgeben, konnte an Hand des vorliegenden Materials nicht sichergestellt werden. Die Gehirnanastomose liegt relativ weit vorne, nämlich schon über dem Ende der Ventralkommissur, und die von ihr entspringenden Längsgefäße verlaufen zuerst dorsal von den Lateralnerven, später dann lateral und lateroventral. Das Dorsalgefäß zweigt noch in der Gehirnregion vom rechten Lateralgefäß ab, dringt aber nicht wie bei *A. swakopmundi* in die Rhynchocoelomwand ein und zeigt auch keine Netzbildung. Das Auftreten von Gefäßschlingen ist vorliegend auf die Lateralgefäße beschränkt, an denen sie im Mitteldarmbereich zwischen den Darmtaschen zu beobachten sind (Abb. 7, B, lg).

Die Nephridien erstrecken sich vom Gehirn bis zu den ersten dorsolateralen Mitteldarmtaschen. Die Ausleitungskanäle umgreifen die Seitennervenstämme von außen und münden lateroventral in der Cerebralregion (Abb. 6, ne).

Die Gonaden sind über die beiden caudalen Körperdrittel verteilt und stellen unregelmäßig aber durchweg dorsal von den Seitenstämmen angeordnete Ovarien dar, welche die Darmtaschen oft weitgehend verdrängen.

Auf Grund der angeführten Merkmale kann die zur Rede stehende Form in das Genus *Africanemertes* eingereiht werden und unterscheidet sich von der Typusart *A. swakopmundi* durch folgende Gegebenheiten: Es sind nur vier Augen vorhanden; die Cerebralorgane liegen horizontal in der Kopfspitze; die Rüsselinnervation erfolgt über 11 Nerven; es fehlen die bei *A. swakopmundi* den Ösophagus begleitenden Längsmuskelkämme, ebenso fehlt ein ventraler Magenblindsack, hingegen ist ein caudaler und dorsolateraler Blindsack am Magen ausgebildet; die zum Gehirn ziehenden Mitteldarmtaschen sind unverzweigt; das Dorsalgefäß zeigt keine Rhynchocoelombeziehung und auch keine Tendenzen zu Netzbildungen.

Verbreitung

Indo-westpazifischer Raum: Madagaskar (Tanikely) [Mozambique-Kanal].

Verteilung

Africanemertes rützleri wurde nur auf *Acropora pharaonis* mit einer Frequenz von 10% bei einer Dominanz von 0,7% angetroffen und zählt damit zu den seltensten Arten im Untersuchungsgebiet.

Nemertellina FRIEDRICH 1935

Die seit 1935 bekannt gewordenen drei Vertreter der Gattung, *Nemertellina oculata*, *N. canea* und *N. minuta* sind kleine schlanke Formen, die durch den Besitz von vier Augen einige Ähnlichkeit mit *Tetrastemma*-Arten zeigen. Als wichtigste anatomische Gattungsmerkmale haben zu gelten die Lage der Cerebralorgane in der Kopfspitze; das geschlossene Praecerebralseptum; das kurze, zwischen Körpermitte und Beginn des letzten Körperdrittels endende Rhynchocoelom; ein unpaarer taschenloser Mitteldarmblindsack; die Einfaserkernigkeit der Lateralnervenstämme sowie das nur bei dieser Gattung der Hoplonemertini bisher festgestellte Querseptum im Bereich des caudalen Rhynchocoelomendes, gebildet durch Ringmuskelfasern der Rhynchocoelomwand.

Die hier zu behandelnde Form war zufolge der inneren Organisationsverhältnisse in keine andere Gattung einzureihen, kann aber auch nur mit einem gewissen Vorbehalt *Nemertellina* zugeordnet werden, da sich das erwähnte Querseptum nicht genau erkennen läßt. Leider ist das vorhandene Material auf ein Individuum beschränkt, welches sich bei der Fixierung trotz vorangegangener Betäubung mit Urethanum in zwei Teile autotomisierte. Der die Gonaden führende hintere Körperhälfte abtrennende Bruch erfolgte im Endbereich des Rhynchocoeloms, dort wo das Septum zu erwarten wäre. Wenngleich zu beiden Seiten der Bruchstelle einige den

Körper durchsetzende Ringmuskelfasern zu finden sind, ist es nun nachträglich nicht sicherzustellen, ob sie als Reste des Septums angesprochen werden können. Sollte sich an Hand von weiterem Material die vorliegende Form als einwandfrei zu *Nemertellina* gehörig erweisen (abgesehen von der Unsicherheit hinsichtlich des Septums sprechen alle Merkmale dafür), so wäre die Lage der Trennlinie eine Stütze für die von FRIEDRICH (1935b, S. 322) geäußerte Vermutung, wonach das Septum der *Nemertellina*-Arten eine praeformierte Bruchstelle sein könnte.

Nemertellina tropica n. sp.

Habitus

Das Tier ist 3 mm lang und 0,3 mm dick. Die einheitliche weiße, mit einem schwachen gelblichen Ton versehene Grundfarbe des Körpers wird durch das Durchschimmern des grauen Darmes und der hell organgegelben Ovarien unterbrochen. Eine besondere Zeichung fehlt. Der Körper ist nur wenig dorsoventral abgeflacht, der Kopf vom Rumpf nicht abgesetzt und das Hinterende des Körpers stumpf abgerundet. Die vier Augen sind in einem Trapez angeordnet, die vorderen sind einander näher als die hinteren und der Abstand der beiden Augenpaare zueinander ist wie bei *Nemertellina minuta* relativ groß. Auffallend während der Lebendbeobachtung war die unregelmäßige Oberfläche des Tieres, verursacht durch Epithelwülste und Höcker, die auch beim Kriechen erhalten blieben (Abb. 12, B).

Anatomie

Das Körperepithel übertrifft fast durchweg die Muskularis an Dicke. Die stellenweise auftretenden Wülste sind Überwachsungen, die im Querschnitt (Abb. 10, ev) ein annähernd gleiches Bild ergeben wie bei *Tetrastemma pinnatum* (IWATA 1954a), nur daß im vorliegendem Fall die Grundschicht nicht in diese Verdickungen einstrahlt. Beide Komponenten der Körperwandmuskulatur reichen bis in die Kopfspitze, die Längsmuskulatur wird jedoch durch Abgabe von Faserzügen zur Bildung des geschlossenen Praecerebralseptums etwas schwächer. In das Parenchym der Kopfspitze eingesenkte Retraktoren sind vorhanden. Die Kopfdrüse ist klein und besteht nur aus einem dorsomedianen Drüsenbündel, welches noch vor dem Praecerebralseptum endet (Abb. 9, kd). Die Cerebralorgane liegen vor dem Gehirn in der Kopfspitze. Sie beginnen auf Höhe der vorderen Augen mit einem ventrolateralen Porus, welcher sich am oberen Ende einer histologisch nicht als Kopffurche gekennzeichneten Eintellung befindet. Das caudale Ende der Organe folgt bald nach dem hinteren Augenpaar (Abb. 9, co).

Die Abgrenzung der Ganglien zueinander ist an der Oberfläche des Gehirns nicht stark ausgeprägt. Dorsal- und Ventralganglien sind annähernd gleich groß, die ventrale Kommissur aber wesentlich kürzer und dicker als die dorsale. Die caudal von den Ventralganglien abgehenden Lateralnervenstämme führen nur einen Faserkern.

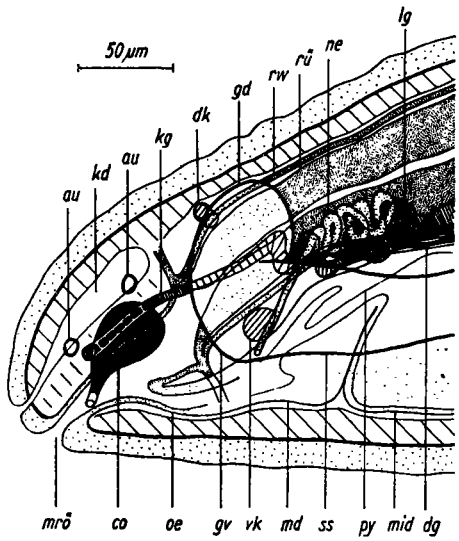

9

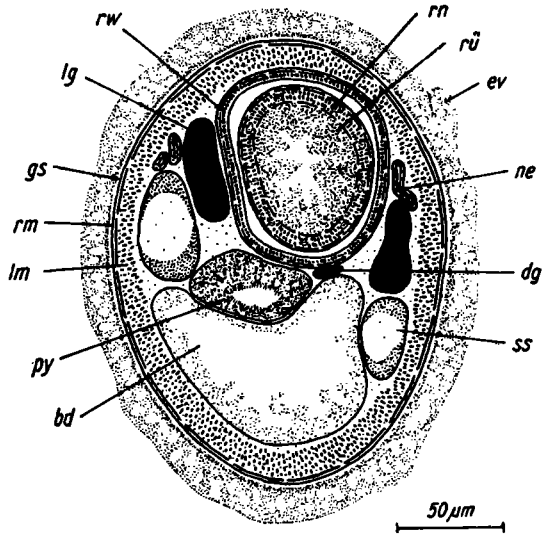

10

Abb. 9. *Nemertellina tropica* — Vorderende. Projektion der Organisation (der linken Körperseite) in die Median-Sagittale. (Erklärung der Abkürzungen s. S. 324.)

Abb. 10. *Nemertellina tropica.* Querschnitt durch die Pylorusregion. (Erklärung der Abkürzungen s. S. 324.)

Der von FRIEDRICH (1935a) bei *Nemertellina oculata* beobachtete kurze Rückennerv konnte im vorliegenden Material nicht gefunden werden.

Das Rhynchocoelom reicht bis an die Körpermitte heran. Die Ring- und Längsmuskulatur seiner Wand ist getrennt. Auf die im Endabschnitt der Rüsselscheide den Körper durchsetzenden Ringmuskelfasern wurde schon weiter oben verwiesen und es dürfte sich dabei um Reste des für *Nemertellina* charakteristischen Querseptums handeln. Der Rüssel ist nicht stark gewunden und demnach vergleichsweise kurz. Die Muskularis seines proximalen Zylinders ist dreischichtig und in der Längsfibrillenlage sind 9 Rüsselnerven eingebettet (Abb. 10). An der Rüsselbewaffnung sind keine Besonderheiten festzustellen. Die Basis des Angriffstilettes ist tropfenförmig. In der einen der beiden Reservestilettaschen sind zwei, in der anderen drei Stilette.

Der in das Rhynchodaeum mündende Ösophagus ist kurz und wird schon vor dem Praecerebralseptum zum Magen. Dieser zeigt insofern eine Gliederung, als von caudal her die Magenwand einen kuppenartigen Fortsatz in das Magenlumen entsendet. Die an der Dorsalseite dieser Kuppe anfänglich zu beobachtende Rinne wird durch Überwachsung von den beiden Lateralseiten her rasch zu einem Rohr, welches sich dann caudal in den Mitteldarm öffnet (Abb. 11). Wenngleich dieses, das zentrale Magenlumen mit dem Mitteldarm verbindende Rohr morphologisch einem Pylorus gleicht, zeigt doch der histologische Aufbau seiner Wand, daß nur ein kleiner Abschnitt unmittelbar vor dem Mitteldarm als solcher aufgefaßt werden kann. Der

Mitteldarm reicht nur wenig über die Pyloruseinmündung terminad (Abb. 9, md) und es sind keine Taschen an diesem kurzen Blindsack ausgebildet. Die nicht sehr zahlreich auftretenden Taschen am Mitteldarm sind seicht und liegen, sich kaum über die Seitennervenstämme dorsad erhebend, dem Darm eng an.

Die beiden in der Nähe des vorderen Augenpaares sich verbindenden Kopfgefäße bilden keine Cerebralanastomose und setzen sich caudad als Lateralgefäße fort. Das nicht in die Rhynchocoelomwand eintretende Dorsalgefäß zweigt vom linken Lateralgefäß ab. Auffallend sind die starken Erweiterungen der Seitengefäße im Bereich zwischen ventraler Gehirnkommissur und Mitteldarmbeginn (Abb. 9, 10, lg), wo auch der Exkretionsapparat gelegen ist, dessen Nephridialkanäle stellenweise die Blutgefäße tangieren (Abb. 9, 10, ne).

Die Ovarien des geschlechtsreifen Tieres befinden sich in der caudalen Körperhälfte und liegen nur dorsal von den Seitennerven.

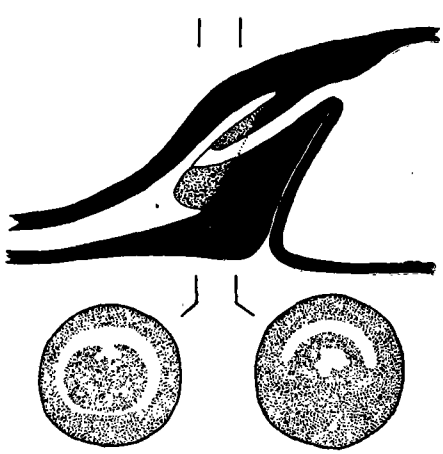

11

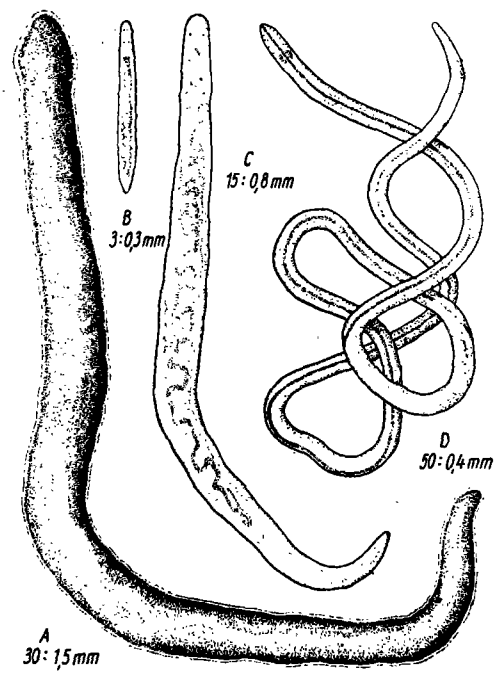

12

Abb. 11. *Nemertellina tropica*. Magen und Mitteldarmblindsack. Rekonstruktion nach einer Querschnittserie, ergänzt durch zwei stark vereinfachte Querschnittdarstellungen. Die eingetragenen Ebenen geben die Lage der Schnitte an.

Abb. 12. A. *Paramphiporus albimarginatus*. Habitus von dorsal; B. *Nemertellina tropica*. Habitus von dorsal; C. *Africanemertes rützleri*. Habitus von dorsal; D. *Nemertes rubrolineata*. Habitus größtenteils von dorsal.

Verbreitung

Indo-westpazifischer Raum: Madagaskar (Tanikely) [Mozambique-Kanal].

Verteilung

Während der Aufsammlungen wurde *Nemertellina tropica* lediglich auf *Acropora pharaonis* gefunden. Die sich für die Art ergebende Frequenz beträgt 10 %, die Dominanz 0,7 %.

Tetrastemma EHRENBERG 1831 (sensu FRIEDRICH 1955)

Ähnlich wie bei der Gattung *Amphiporus* wurde durch FRIEDRICH (1955) auch bei *Tetrastemma* mehr Klarheit durch Umstellung einiger Arten und Ausbau der Gattungsdiagnose geschaffen. Es verblieben allerdings noch viele Arten im Genus, die ursprünglich größtenteils nur auf Grund des Habitus eingereiht wurden und deren unzureichend bekannt gewordene anatomische Gegebenheiten zur Zeit keine Entscheidung über ihre systematische Stellung erlauben. Zu *Tetrastemma* sensu FRIEDRICH gehören kleine, schlanke, meist vieräugige Formen, deren anhangloses Rhynchocoelom körperlang ist, bei denen der Ösophagus in das Rhynchodaeum mündet und der Mitteldarmblindsack zwei terminad gerichtete Taschen besitzt. Weiter ist bei *Tetrastemma*-Arten die Ring- und Längsmuskulatur bis in die Kopfspitze hinein ausgebildet und das Praecerebralspektrum geschlossen. Die Cerebralorgane liegen vor oder in der Gehirnregion und die Seitennervenstämme sind einfaserkernig.

Tetrastemma melanocephalum (JOHNSTON)

T. m. VANSTONE & BEAUMONT 1894
T. m. BEAUMONT 1895 (part)
T. m. BÜRGER 1895
T. m. BERGENDAL 1903
Prostoma m. BÜRGER 1904
P. m. WIJNHOFF 1912
P. m. SOUTHERN 1913
P. m. MONASTERO 1930
P. melanocephala FRIEDRICH 1935b
P. melanocephalum, ders. 1936
Testrastemma m. GONTCHAROFF 1955
T. m. BÉNARD 1960
T. m. KIRSTEUER 1963

(Angaben älterer Literatur finden sich bei BÜRGER 1895 und 1904.)

Habitus

Die beobachteten Tiere entsprechen in der Färbung jenen von WIJNHOFF (1912) in der Umgebung von Plymouth aufgesammelten Individuen. Das Gelb der Dorsalseite zeigt einen zarten orangen Anflug und läßt teilweise den Rüssel, die Darmtaschen und die Gonaden dunkel durchscheinen. Die Ventralseite als auch die Ränder des stark abgesetzten Kopfes sind weißgelb. Der dunkelbraune Pigmentfleck am Kopf stimmt in Form und Anordnung mit dem bei adriatischen Vertretern der Art vorgefundenen überein (KIRSTEUER 1963). Er überlagert fast vollständig das vordere Augenpaar, reicht aber caudal nicht bis an die hinteren Augen heran. Vor dem Pig-

mentschild liegen drei kurze, längsgerichtete, weißgeflockte Felder, ein weiteres findet sich quergestellt caudal vom Kopffleck und ein ebenfalls weißer Saum umgibt das Hinterende des Körpers (Abb. 3, D). Die lebenden Tiere waren nur 8 mm lang und 0,8 mm dick, erwiesen sich aber trotz der unterhalb der bislang mitgeteilten Größenordnung gelegenen Ausmaße als bereits geschlechtsreif.

Anatomie

In der inneren Organisation stimmen die vorliegenden Individuen weitestgehend überein mit der auf Grund von adriatischen Funden gegebenen Beschreibung (KIRSTEUER 1963, p. 570). Wieder reichen beide Komponenten der Körperwandmuskularis bis in die Kopfspitze. Subepitheliale Drüsen sind vorwiegend lateroventral in der Praecerebralregion zu sehen. Die Kopfdrüse erscheint stärker ausgebildet und durchbricht dorsal das geschlossene Septum. Die zum Teil dem Cerebralkomplex aufliegenden Cerebralorgane reichen etwas über die ventrale Gehirnkommissur caudad (Abb. 13, co), der daraus entstehende Unterschied zur adriatischen Form ist jedoch sehr gering und muß wohl als Ausdruck verschiedener Kontraktion aufgefaßt werden. Rhynchocoelom und Rüssel sind ohne Besonderheiten, lediglich die Basis des Angriffstiletts (Abb. 3, E) wirkt gedrungener als die bei FRIEDRICH (1935b, S. 338, Abb. 30, b) abgebildete. Eine gut entwickelte Ringmuskulatur am Rhynchodaeum im Bereich des Ösophagus ist auch vorliegend realisiert. Die Gliederung des Vorderdarmes läßt Ösophagus, Magen und Pylorus erkennen und am Magen tritt wieder eine starke dorsale Einfaltung auf (Abb. 13, mdf). Von den Taschen des Mitteldarmblindsacks reicht das erste Taschenpaar bis an die dorsale Gehirnkommissur terminad. Blutgefäßsystem und Exkretionsapparat (Abb. 13) zeigen im großen und ganzen die schon früher bei der Art festgestellte Ausbildung und Lagebeziehung. Die vorliegenden Individuen sind geschlechtsreife Männchen, deren Gonaden bereits in der Pylorusregion beginnen und, mit den Darmtaschen alternierend, dorsal und ventral von den Lateralnervenstämmen angeordnet sind.

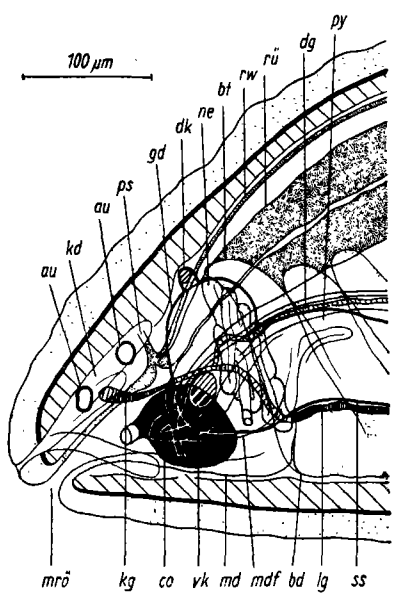

Abb. 13. *Tetrastemma melanocephalum* — Vorderende. Projektion der Organisation (der linken Körperseite) in die Median-Sagittale. (Erklärung der Abkürzungen s. S. 324.)

Verbreitung

Eine Zusammenstellung der bisher nur aus dem Atlantik und Mittelmeerraum gemeldeten Fundorte ist bei KIRSTEUER (1963, S. 571) gegeben. Zu ergänzen ist diese Übersicht mit

Indo-westpazifischer Raum: Madagaskar (Tanikely) [Mozambique-Kanal].

Verteilung

Bislang wurde die Art vornehmlich in gezeitennahen Bereichen gefunden, ihre bathymetrische Verteilung ist jedoch bis zu 60 m Tiefe nachgewiesen. Bei der Substratwahl werden offensichtlich seichte Phytalbestände wie *Ulva*, *Cystosira* und *Zostera* bevorzugt. Ein Vorkommen auf Sand und zwischen Steinen ist nur zweimal in der Literatur vermerkt.

Das Aufscheinen von *Tetrastemma melanocephalum* auf Korallenstöcken im Untersuchungsgebiet schließt sich, was den Substratcharakter betrifft, an das Vorkommen der Art auf *Corallina officinalis* und *Lithophyllum incrustans* an, indem es sich um Besiedlung von durch Organismenverkalkung zustandegekommene feste Lückenraumsysteme handelt. Auf *Porites nigrescens* war die Art mit einer Frequenz von 50 % bei einer Dominanz von 7,7 % vertreten. Auf *Seriatopora angulata* betrug die Frequenz 11,1 % und die Dominanz 0,7 %.

Tetrastemma tanikelyensis n. sp.

Habitus

Die in den Probenprotokollen aufscheinenden Individuen dieser Art maßen rund 25 mm in der Länge und maximal 1,5 mm in der Dicke. Der Körper wirkt etwas gedrungen und ist dorsoventral leicht abgeflacht. Im Leben ist der Kopf deutlich abgesetzt und bei kriechenden Tieren gewinnt man den Eindruck vom Vorhandensein zweier Kopffurchenpaare (Abb. 3, G), die Untersuchung der Schnittpräparate ergibt jedoch nur ein Paar Kopffurchen, welches dorsal zu den hinteren Augen zieht, während die andere beobachtete Einkerbung anscheinend eine den Kopf begrenzende Faltenbildung darstellt, die bei der fixationsbedingten Kontraktion verloren geht bzw. von weiteren auftretenden Falten nicht mehr unterscheidbar ist. Die sich von der hellen orangegelben Grundfarbe abhebende Zeichnung beschränkt sich auf einen dunkelbraunen Kopffleck, einem diesen vorgelagerten, nicht ganz terminad reichenden weißen Areal und locker verteilten ocker Schollen gegen das caudale Körperende zu (Abb. 3, G). Von den inneren Organen schimmern die Cerebralganglien rötlich und der Rüssel stellenweise braun durch.

Die im vorliegendem Fall auftretende, die vorderen Augen überdeckende und verbindende Pigmentbrücke macht es naheliegend, die Form mit jenen Arten des Genus *Tetrastemma* in Beziehung zu bringen, bei denen ähnliche Pigmentanlage-

rungen gefunden wurden. Hierbei sind vor allem die sich habituell um *Tetrastemma coronatum* gruppierenden Arten *Tetrastemma peltatum*, *T. melanocephalum*, *T. diadema* und auch *T. longissimum* zu erwähnen[1]). Eine vergleichende Betrachtung zeigt wohl, daß Umriß und Lage des Kopffleckes nicht ganz mit der Situation bei den genannten Arten übereinstimmt, die äußerlichen Trennungsmerkmale aber keineswegs markant sind und sich die Form leicht als Varietät der einen oder anderen Species auffassen ließe. Nicht zuletzt wurde ja auch schon früher des öfteren versucht, einige dieser Arten zu vereinigen (JOUBIN 1890, 1894, RICHES 1893) und in neuerer Zeit findet sich dieses Problem bei RIEDL (1959) und KIRSTEUER (1963) wieder aufgegriffen, wobei gezeigt werden konnte, daß auf Grund von anatomischen Fakten die Arten zu Recht bestehen. Es wird demnach auch für die zur Diskussion stehende Form vorerst nur an Hand der inneren Organisation Klarheit hinsichtlich ihrer systematischen Position zu erlangen sein. Neben den oben zitierten, hauptsächlich nordatlantischen und mediterranen Formen[2]) sind auch noch einige wenige indopazifische Arten in den Vergleich einzuschließen, zumal aus tiergeographischen Erwägungen eine Beziehung zur vorliegenden Form mit höherer Wahrscheinlichkeit zu erwarten ist. Es sind dies *Tetrastemma verinigrum* (IWATA 1954a) mit deren Varietät *T. v.* var. *meridianum* (IWATA 1954b), Formen, bei denen jedoch der Kopf nicht abgesetzt ist und keine Kopffurchen auftreten, weiter *Tetrastemma insolens* (IWATA 1952) mit zwei Paar Kopffurchen und Verdoppelung der hinteren Augen, *Tetrastemma yamaokai* (IWATA 1954a) mit einem orangeroten Schild auf dem vom Rumpf nicht abgesetzten Kopf, der auch keine Kopffurchen zeigt, und *Tetrastemma nigrifrons* (COE 1904), von der bislang 7 Varietäten beschrieben wurden, wobei die von IWATA (1954a, S. 30) gefundene *T. n.* var. *punctata* die meiste Ähnlichkeit mit der zu behandelnden madagassischen Form zeigt. Die aus den Abbildungen bei COE (1904) und IWATA (1954a) ersichtliche enorme Variabilitätsbreite von *Testrastemma nigrifrons* macht es unmöglich, dem Habitus in diesem Rahmen eine artdifferenzialdiagnostische Bedeutung beizumessen.

Anatomie

Das Epithel der Körperwand entspricht in seiner histologischen Struktur dem bei *Tetrastemma* gemeiniglich vorgefundenen Typus und ist verglichen mit dem von *Testrastemma nigrifrons* wesentlich schwächer, da es durchschnittlich nur die Dicke der Muskularis erreicht. Es liegt einer an Stärke der Ringfaserlage gleichkommenden

---

1) *Tetrastemma nimbatum* BÜRGER 1895, durch die braunrote Farbe des Rumpfes stark von der vorliegenden Form abweichend, aber doch auch eine schwarze Pigmentbinde zwischen den vorderen Augen aufweisend, kann hier nicht berücksichtigt werden, da die anatomischen Gegebenheiten ungenügend bekannt sind.

2) Nur für *Testrastemma peltatum*, *T. coronatum* und *T. melanocephalum* zeigen Einzelfunde ein Vorkommen außerhalb des Hauptverbreitungsgebietes an.

Grundschicht auf. Sowohl die Ring- als auch die Längsmuskelschicht reicht bis in die Kopfspitze. Das von inneren Lagen der Längsschicht gebildete Praecerebralseptum ist geschlossen, wird aber von dorsalen Anteilen der großen Kopfdrüse durchdrungen (Abb. 14, kd). Wie das Septum bei den erwähnten indopazifischen Formen gestaltet ist, läßt sich nicht genau beurteilen, da es weder COE noch IWATA beschreibt, allerdings vermerkt COE (1904, S. 162) bei *T. nigrifrons* hinsichtlich des stark entwickelten Körperparenchyms, daß "this parenchyma extends forward into the head in front of the brain", was aber vermutlich nur bei einem zumindest teilweise aufgelösten Septum möglich wäre. Das in der Kopfregion auftretende Parenchym selbst, bei den vorliegenden Individuen ist nur wenig vorhanden, bietet keine brauchbare Vergleichsgrundlage, da es soweit angegeben, bei allen Tetrastemmen gefunden wurde, die quantitativen Unterschiede vom Ausbildungsgrad der Kopfdrüse abhängig sind, letzterer jedoch kein Artcharakteristikum darstellt. Wie *Tetrastemma melanocephalum* und *T. diadema* hat die vorliegende Form subepitheliale Drüsen in der praecerebralen Region. Die im Bereich des vorderen Augenpaares den Kopffleck hervorrufenden dunkelbraunen Pigmentschollen sind subepithelial angeordnet und zeigen damit gleiche Lageverhältnisse wie bei *T. coronatum* und *T. nigrifrons*. Die Vierzahl der Augen liefert keine Handhabe zur Artunterscheidung, da, abgesehen von dem Umstand, daß über die Veränderung der Augenzahl innerhalb einer Art wenig bekannt ist, sowohl bei *Tetrastemma insolens* (IWATA 1952) als auch gelegentlich bei Individuen von *T. nigrifrons* 6 Augen ausgebildet sind. Bei den sechsäugigen *Tetrastemma nigrifrons* Exemplaren handelt es sich um *T. n.* var. *purpureum* (COE 1904, Taf. 17, Fig. 1), die nicht nur im Habitus *T. insolens* sehr ähnlich ist, sondern auch in allen von IWATA (1952) angeführten anatomischen Merkmalen mit dieser übereinstimmt und daher vorerst die Frage offen bleiben muß, ob die beiden Formen nicht identisch sind.

Die Cerebralorgane liegen größtenteils vor dem Septum. Sie beginnen lateroventral in den Kopffurchen und reichen mit ihrem caudalen Ende noch etwas in die Cerebralregion hinein (Abb. 14, co). Kleine Unterschiede ergeben sich daraus zu *Tetrastemma verinigrum*, bei welcher sich die Cerebralorgane über die ganze Gehirnregion erstrecken und zu *T. nigrifrons* als auch *T. insolens*, wo sie in einer ihrem eigenen Durchmesser gleichkommenden Distanz vor dem Gehirn liegen. Zu den übrigen in die Diskussion einbezogenen Arten sind die Abweichungen sehr gering und ohne Bedeutung. Der Cerebralkomplex ist ähnlich dem von *Tetrastemma diadema* wesentlich höher als lang (Abb. 14, gd, gv) und läßt nach außen hin keine Unterteilung in Ganglien erkennen. Die einfaserkernigen Seitennervenstämme verlaufen lateral im Körper.

Das von einer dünnen Ring- und Längsmuskellage umscheidete Rhynchocoelom reicht bis an das caudale Körperende heran. Im Gegensatz zu *Tetrastemma peltatum*, *T. melanocephalum* sowie *T. longissimum* und in Übereinstimmung mit *T. coronatum*

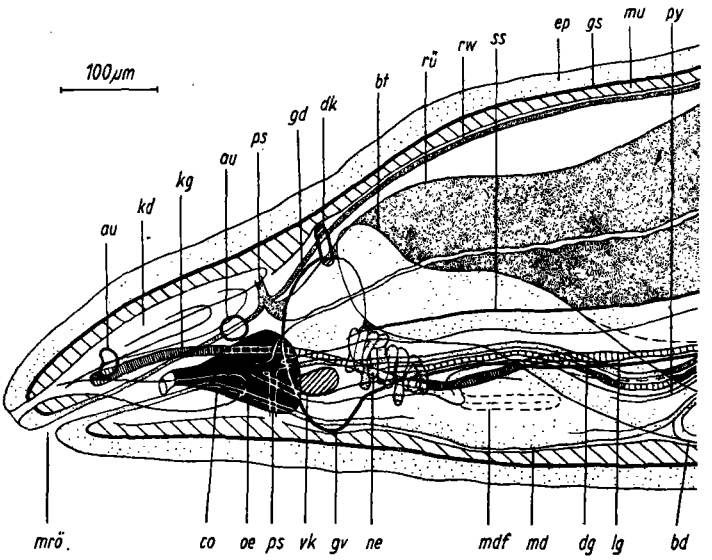

Abb. 14. *Tetrastemma tanikelyensis* — Vorderende. Projektion der Organisation (der linken Körperseite) in die Median-Sagittale. (Erklärung der Abkürzungen s. S. 324.)

ist vorliegend die Muskularis des vorderen Rüsselzylinders dreischichtig. Für die restlichen in Betracht kommenden Arten liegen keine diesbezüglichen Angaben vor, hingegen wird die Innervation durchweg erwähnt und es zeigt sich, daß fast immer 10 Rüsselnerven auftreten und nur bei den japanischen Varietäten von *T. nigrifrons* (IWATA 1954a und 1957) 11 Nerven vorhanden sind. Das Angriffstilett ruht auf einer Basis von der in Abb. 3, Fig. F, wiedergegebenen Form und der Knauf des Stilettes entspricht einem sechsseitigen Pyramidenstumpf. In den beiden Reservestilettaschen sind je zwei oder drei Stilette zu finden.

Der Ösophagus mündet nahe dem Praecerebralseptum in das Rhynchodaeum. Hinter der ventralen Gehirnkommissur geht er kontinuierlich in den Magen über, welcher bald darauf eine schwache, dorsale, terminad gerichtete Ausbuchtung und eine an diese anschließende auffallende Faltenbildung zeigt. Von den beiden Dorsolateralseiten des Magens senken sich zwei Horizontalfalten tief in das Lumen ein, so daß eine große ventrale und eine kleine dorsale Gastralkammer entsteht (Abb. 14, md, mdf), es kommt aber zu keiner vollständigen Abtrennung, da sich die Falten median nicht berühren. Mit Beginn des letzten Magendrittels ist dann wieder ein einheitlicher Hohlraum vorhanden und auf Höhe des Mitteldarmblindsack-Vorderendes liegt der Anfang des langen, mondsichelförmig gewölbten Pylorus. Das erste und einzig gut ausgebildete Taschenpaar des Mitteldarmblindsacks reicht, flach ansteigend, bis zur Dorsalkommissur nach vorne und ist extrem lang (Abb. 14, bt). Diese in ihrer terminalen Hälfte schlauchartigen Taschen erscheinen gegen den Blindsack zu mehr und mehr abgeplattet und umgreifen mit ihrer Innenseite lateroventral das Magenende und den ersten Teil des Pylorus, während sie sich nach außen hin der

Rundung der Körperwand anpassen. Die nachfolgenden Blindsacktaschen stellen nur seichte, kaum bis zu den Seitennerven sich erhebende Aussackungen dar und erst am Mitteldarm selbst ist ein Auftreten von normalen, höher aufsteigenden Taschen zu beobachten. Damit liegen Verhältnisse vor, die im Grundsätzlichen, i. e. einem Mitteldarmblindsack mit Seitentaschen und zwei terminad gerichteten Taschen, mit den bisher innerhalb der Gattung gemachten Feststellungen übereinstimmen, deren Analyse und graphische Wiedergabe jedoch ein vom Gewohnten stark abweichendes Bild liefern, welches nicht auf Kontraktion oder Darmfüllungszustand zurückzuführen ist. Eine ähnliche Situation wurde auch bei *Tetrastemma signifer* (COE 1904, S. 158) und *T. fulvum* (KIRSTEUER 1963, S. 582) gefunden, Unterschiede im Aufbau des Vorderdarms und des Blutgefäßsystems sowie in der Gesamtorganisation schließen jedoch eine Identität mit der vorliegenden Form aus. Zur Abgrenzung gegen die aufgezählten Vergleichsarten sind die Differenzierungen am Vorder- und Mitteldarm gut verwertbar, wobei sich aus dieser Gruppe besonders *Tetrastemma nigrifrons* var. *bilineatum* (IWATA 1957, S. 27) abhebt, da der Mitteldarmblindsack bis an das Gehirn heranreicht, weiter auch *Tetrastemma rerinigrum* (IWATA 1954a, S. 32), bei welcher die kurzen vorderen Blindsacktaschen bis in die terminale Gehirnregion ziehen.

Das Blutgefäßsystem gliedert sich in die Kopfschlinge und von dieser abgehende Lateralgefäße sowie Dorsalgefäß, welch letzteres nicht in das Rhynchocoelom eindringt (Abb. 14). Mit diesen Eigenschaften sind weitere Merkmale zur Abgrenzung gegeben, da bei *Tetrastemma nigrifrons* und *T. diadema* das Dorsalgefäß Rhynchocoelombeziehung zeigt, bei *T. coronatum*, *T. melanocephalum* und *T. longissimum* ebenfalls Eintritt in das Rhynchocoelom und außerdem noch Abgang von einem der beiden Lateralgefäße beobachtet wurde. Lediglich *Tetrastemma peltatum* weist in diesem Punkt keine andersartige Ausbildung auf — für die restlichen indopazifischen Formen fehlen leider Vergleichsmöglichkeiten.

Die relativ kleinen Exkretionsorgane liegen zwischen dem Gehirn und der erwähnten Magenfaltenbildung den Seitennerven lateral auf und münden über je einen Ableitungskanal lateroventral nach außen. Akzessorische Ableitungskanälchen, wie sie bei einigen Individuen von *Tetrastemma nigrifrons* (COE 1904, S. 163) gefunden wurden, sind vorliegend nicht ausgebildet.

Die Genitalregion der untersuchten weiblichen und männlichen Exemplare beginnt etwas nach dem ersten Körperdrittel. Die Ovarien liegen dorsal und ventral von den Seitenstämmen, die Testis nur dorsal von diesen und die Ausfuhrgänge der letzteren durchbrechen die Körperwand lateral bis zur Grundschicht, sind aber im Epithelbereich nicht mehr zu sehen.

Verbreitung

Indo-westpazifischer Raum: Madagaskar (Tanikely) [Mozambique-Kanal].

Verteilung

Die Aufsammlungen ergaben für *Tetrastemma tanikelyensis* auf *Acropora corymbosa* eine Frequenz von 33,3 % bei einer Dominanz von 11,3 %. Auf *Seriatopora angulata* waren 11,1 % Frequenz und 0,7 % Dominanz festzustellen.

Tetrastemma sp.

Wie schon eingangs vermerkt wurde, befindet sich unter den aufgesammelten Hoplonemertini monostilfera eine durch zwei Individuen repräsentierte Art, deren genaue Bestimmung durch den schlechten Erhaltungszustand der konservierten Tiere leider nicht möglich ist. Die beiden vorliegenden Schnittserien lassen die Art als Vertreter des Genus *Tetrastemma* erkennen, gestatten aber keine ins Detail gehende Beschreibung der anatomischen Verhältnisse. Da nach Abschluß der systematischen Bearbeitung des gesamten Nemertinenmaterials der Expedition eine allgemeine, zusammenfassende Darstellung der Gruppe geplant ist, sei die Form der Vollständigkeit halber hier kurz erwähnt.

Habitus

Die Tiere waren 10 und 12 mm lang und 0,3—0,4 mm dick. Die einheitliche Grundfarbe war ein milchiges, semitransparentes Weiß, welches den Darm dunkelgrau durchschimmern ließ, während der Rüssel nur stellenweise zu erkennen war. Von den vier in einem Rechteck stehenden, kleinen Augen wurden die vorderen von einem rotbraunen, dreieckigen Pigmentfleck überdeckt (Abb. 3, A).

Verbreitung

Indo-westpazifischer Raum: Madagaskar (Tanikely) [Mozambique-Kanal].

Verteilung

Die Form wurde auf *Acropora pharaonis* mit einer Frequenz von 10 % bei einer Dominanz von nur 0,7 % registiert. Fast gleiche Werte ergaben sich für das Vorkommen auf *Seriatopora angulata* mit einer Frequenz von 11,1 % und einer Dominanz von 0,7 %.

Nemertes Johnston 1837

Die Gattung *Nemertes* wurde von Friedrich (1955) restituiert, und zwar für *Nemertes* (*Emplectonema*) *antonina* Quatrefages, deren durch Bindegewebe geteilte Längsmuskulatur in der Cerebralregion sie deutlich von den übrigen *Emplectonema*-Arten distanziert. Von Brunberg (1959) wurde diese Abtrennung nicht akzeptiert, wird aber in der vorliegenden Schrift beibehalten, da sie den ersten konkreten Schritt zur Klärung der Verhältnisse in der als uneinheitlich zu betrachtenden

Gattung *Emplectonema* darstellt. Die nachfolgend beschriebene Form zeigt sowohl im Habitus als auch in der inneren Organisation weitgehende *Emplectonema*-Ähnlichkeit, vor allem zu jener Gruppe innerhalb der Gattung, bei deren Vertretern die Cerebralorgane vor dem Septum liegen. Da aber außerdem zwei durch Bindegewebe isolierte Längsmuskellagen im Bereich des Gehirns zu beobachten sind, steht ihre Zugehörigkeit zum Genus *Nemertes* außer Zweifel.

Nemertes rubrolineata n. sp.

Habitus

Die Exemplare dieser Art waren 25—50 mm lang, jedoch nur 0,2—0,4 mm dick. Die Grundfarbe des schwach dorsoventral abgeflachten Körpers ist ein semitransparentes Weiß oder Weißgelb, von dem sich ein weinroter dorsaler Medianstreifen abhebt, welcher am terminalen Körperende beginnt, aber nicht bis an das Caudalende heranreicht (Abb. 12, D). Die Cerebralorgane schimmern gelb, der Darm braun durch. Auf dem vom Rumpf nicht abgesetzten Kopf sind beiderseits vom roten Längsband mehrere Augen zu finden. Ihre Anzahl und Anordnung läßt sich an lebenden Tieren nur schwer feststellen, die Schnittuntersuchung erbrachte aber, daß in jeder Kopfhälfte 10—12 Augen in zwei übereinander verlaufenden Reihen gegeben sind (Abb. 15, au). Kopffurchen sind vorhanden, fallen jedoch bei einer Habitusbetrachtung nicht auf, da sie sehr seicht sind und kaum über die Lateralkontur dorsad aufsteigen. Die Tiere zeigten immer eine starke Neigung zu Knäuel- und Schlingenbildung, wobei dann nur der vorderste Körperabschnitt frei und etwas vorgestreckt blieb.

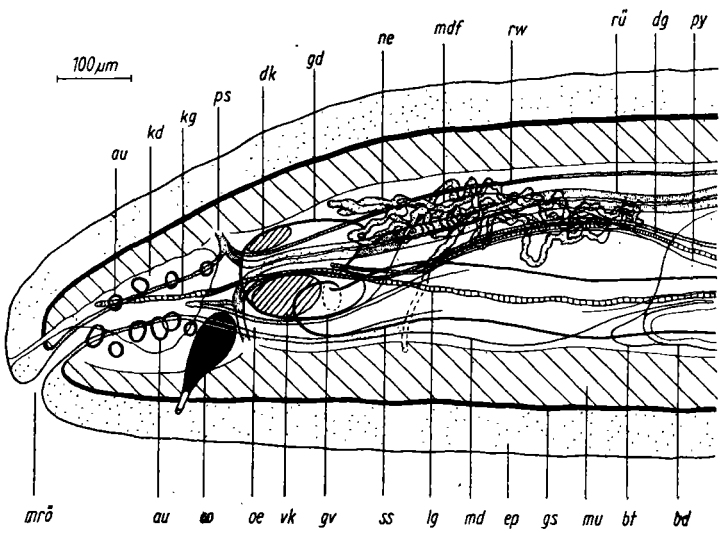

Abb. 15. *Nemertes rubrolineata* — Vorderende. Projektion der Organisation (der linken Körperseite) in die Median-Sagittale. (Erklärung der Abkürzungen s. S. 324.)

Anatomie

Die Elemente der Körperwand sind mit Ausnahme der Ringmuskelschicht alle sehr gut entwickelt. Das drüsenreiche Epithel ist bemerkenswert hoch und kommt an Dicke der Muskularis gleich, die Grundschicht ist in der Kopfregion annähernd gleich stark wie die Ringfaserlage, im mittleren Körperbereich aber übertrifft sie letztere um mehr als das Doppelte an Dicke. Beide Muskellagen ziehen bis in die Kopfspitze. Caudad vom ringsum geschlossenen Praecerebralseptum wird die Längsmuskulatur durch eine Bindegewebslage in eine äußere und innere Schicht zerlegt (Abb. 16, bs). Diese Aufspaltung beschränkt sich auf die Gehirnregion und ist, wie oben erwähnt, für die systematische Einordnung der Form von Bedeutung. Die beiden lateralen Lappen der Kopfdrüse füllen die Kopfspitze größtenteils aus und kommen dorsolateral nahe an das Septum heran. Die Cerebralorgane sind klein und einfach und liegen wohl noch vor dem Septum, aber doch näher beim Gehirn, als dies bei *Nemertes antonina* der Fall ist, münden aber wie bei der genannten Art ventral aus (Abb. 15, co). Subepitheliale Drüsen sind weder im Kopf noch im übrigen Körper zu finden.

Das Gehirn stellt in seiner terminalen Hälfte einen einheitlichen Komplex dar, an dessen Oberfläche keine Gliederung in Ganglien und die sie verbindenden Kommissuren zu erkennen ist (Abb. 16, gd, gv). Erst hinter der Ventralkommissur setzt eine rasch stärker werdende Abgrenzung der Ganglien ein und caudal enden sie kuppenförmig und vollständig voneinander getrennt. Die Seitennervenstämme treten

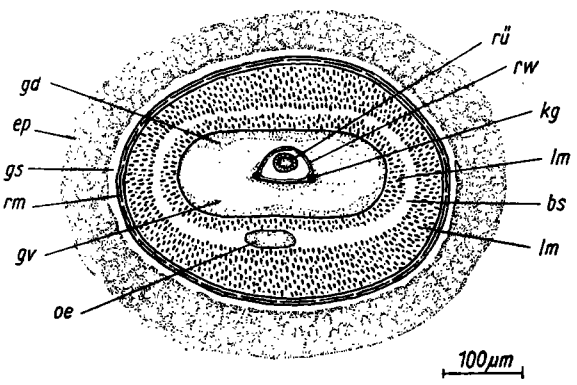

16

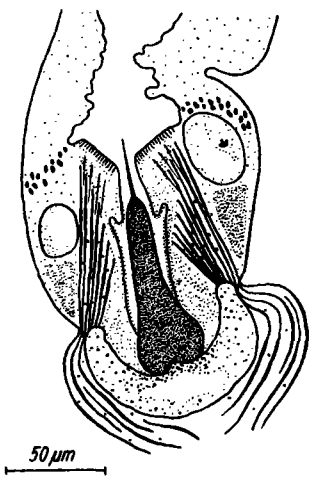

17

Abb. 16. *Nemertes rubrolineata.* Querschnitt durch die Cerebralregion im Bereich der Kommissuren. (Erklärung der Abkürzungen s. S. 324.)

Abb. 17. *Nemertes rubrolineata.* Mittlere Rüsselregion mit Angriffstilett und Basis. Gezeichnet nach einem Längsschnitt und etwas vereinfacht.

lateral von den Ventralganglien aus und nehmen über eine Bogenbildung ihren Längsverlauf ein. Wie bei *Nemertes antonina* sind auch vorliegend die Cerebralkommissuren außerordentlich breit, die dorsalen Ganglien sind aber caudal nicht in zwei Zipfel ausgezogen und es fehlen Anschwellungen der Seitenstämme im Bereich ihres Ursprunges.

Das Rhynchocoelom ist etwas länger als ein Drittel des Körpers, endet aber noch vor der Körpermitte. Seine Wand ist durchlaufend sehr dünn und Ring- als auch Längsmuskulatur meist nur in einfaserigen Schichten vorhanden. Auch der Rüssel ist, vor allem in seinem vorderen Abschnitt, sehr schwach ausgebildet (Abb. 15, 16, rü). Die Muskularis des proximalen Rüsselzylinders besteht aus einer Ring- und einer Längsfibrillenlage, die beide anfangs zart, gegen die Rüsselmitte zu etwas an Dicke zunehmen. Die Rüsselnerven bilden eine einheitliche Schicht, die in der Längsmuskulatur gelegen ist. Das Angriffstilett sitzt einer schlanken, birnenförmigen Basis auf (Abb. 17), die der von *Emplectonema gracilis* (CORREA 1955, Tafel 1, Fig. 2) ähnlich ist. In den beiden Reservestilettaschen sind ein oder zwei Stilette eingelagert.

Der Vorderarm ist wie normal in Ösophagus, Magen und Pylorus unterteilt. Der sich in das Rhynchodaeum öffnende Ösophagus verläuft in der Gehirnregion in der die Längsmuskulatur spaltenden Bindegewebeschicht und geht postcerebral in einen faltenreichen Magen über. Dieser, im Querschnitt hufeisenförmig, legt sich dem Rhynchocoelom an (Abb. 15, mdf). Der Pylorus ist kurz, ebenso der Mitteldarmblindsack, der nur wenig den Pylorus an Länge übertrifft und zwei kleine terminad gerichtete und lateroventral vom Magen liegende Taschen entsendet (Abb. 15, bd, bt). Wie der Magen umgreifen auch der Mitteldarmblindsack und der Mitteldarm mit ihren weiten geräumigen Taschen das Rhynchocoelom an den Lateralseiten.

Das Blutgefäßsystem besteht aus den beiden Kopfgefäßen, die sich nach Durchlaufen des Gehirnringes als Seitengefäße fortsetzen, und dem Rückengefäß, welches vom rechten Lateralgefäß abzweigt und keine Rhynchocoelombeziehung zeigt (Abb. 15).

Die Nephridien sind schon in der hinteren Gehirnregion zu finden und erstrecken sich bis an den Mitteldarmblindsackbeginn caudad (Abb. 15, ne). Sie sind dorsal von den Seitennervenstämmen in dem zwischen Vorderdarm und Körperwand eingeschobenen Bindegewebe gelagert. Ihre Ausmündung erfolgt vermutlich bald nach dem Gehirn lateroventral, mit Sicherheit konnte dies aber am vorliegendem Material nicht festgestellt werden.

Die bei einigen Individuen angetroffenen Ovarien sind ventral und dorsal von den Lateralstämmen angeordnet, wobei die vordersten noch in den Caudalbereich des Rhynchocoeloms fallen.

Verbreitung

Indo-westpazifischer Raum: Madagaskar (Tanikely) [Mozambique-Kanal].

Verteilung

Nemertes rubrolineata war eine im Untersuchungsgebiet relativ häufig auftretende Form. Auf *Acropora corymbosa* schien sie mit einer Frequenz von 16,7 % bei einer Dominanz von 2,8 % auf. Für das Vorkommen auf *Seriatopora angulata* ergab sich eine Frequenz von 33,3 % und eine Dominanz von 2,2 %, für *Acropora pharaonis* eine Frequenz von 40 % und Dominanz von 7 %, während auf *Porites nigrescens* 50 % Frequenz und 15,4 % Dominanz festgestellt wurden.

Friedrichia n. g.

Vorliegend ist eine Form, die zufolge ihrer inneren Organisation in keines der bestehenden Genera der monostiliferen Hoplonemertinen eingereiht werden kann. Auf Grund der Tetraneurie ergeben sich wohl Beziehungen zu einigen wenigen Gattungen, bei kritischer Prüfung unter Heranziehen weiterer Merkmale erweisen sich diese Bindungen aber nicht stark genug, um eine Einordnung der Form zu rechtfertigen. So zeigen sich Unterschiede zu *Gononemertes* BERGENDAL (1900) in der Länge des Rhynchocoeloms und durch das Fehlen eines Stilettapparates und eines Ösophagus sowie durch das Auftreten von terminad gerichteten Taschen am Mitteldarmblindsack und einer Diagonalmuskelschicht im Hautmuskelschlauch bei *Gononemertes parasita*, der einzigen Art des Genus. Bei *Antarctonemertes* FRIEDRICH (1955) hingegen sind es die großen, nahe beim Gehirn gelegenen Cerebralorgane, das körperlange Rhynchocoelom und Differenzierungen am Mitteldarmblindsack, welche die Gattung für die zur Rede stehende Form nicht in Betracht kommen lassen. Es sei auch darauf verwiesen, daß sich keine engere Beziehung zu der bislang als *Nemertopsis actinophila* BÜRGER (1904) geführten, jedoch wie FRIEDRICH (1955) mit Recht betont, nicht zur Gattung *Nemertopsis* gehörenden und 1958 in die Gattung *Nemertopsella* FRIEDRICH gestellten Form abzeichnet, da bei dieser die Seitenstämme nicht über die ganze Länge zweifaserkernig sind und auch durch die direkte Einmündung des Magens in das Rhynchodaeum und das kurze Rhynchocoelom eine sehr abweichende Situation geschaffen ist. Die größte Annäherung zeigt sich zu dem Gattungsdreieck *Oerstedia* — *Paroerstedia* — *Oerstediella*. Die Übereinstimmungen liegen in der Ausbildung und Anordnung der Cerebralorgane, Aufspaltung des Praecerebralseptums in Fixatoren, Fehlen einer postcerebralen Gefäßverbindung und weitestgehender Ähnlichkeit in der Körperform. Unterschiede zu *Oerstedia* sensu FRIEDRICH (1955) entstehen durch Vorhandensein eines Ösophagus und Erstreckung der Längsmuskulatur bis in die Kopfspitze, der vollkommen taschenlose Mitteldarmblindsack steht im Widerspruch mit den Diagnosen von allen drei oben genannten Genera, ebenso die Tatsache, daß vorliegend das Rückengefäß in das Rhynchocoelom eindringt. Hinzu kommt, daß bei *Oerstediella* FRIEDRICH (1955) der zweite Faserkern in den Lateralnervenstämmen nicht über deren große Länge reicht.

Es ergibt sich damit die Notwendigkeit der Errichtung einer neuen Gattung, und ich erlaube mir diese nach Herrn Prof. Dr. HERMANN FRIEDRICH zu benennen, der sich in den letzten Jahrzehnten um die Nemertinenforschung große Verdienste erworben hat.

Dem Genus *Friedrichia*, welches in den Verwandschaftskreis um *Oerstedia* einzuschließen ist, kommt die folgende Diagnose zu: Walzenförmige an *Oerstedia* erinnernde Form ohne Kriechsohle und Kopffurchen; Cerebralorgane klein, einfach und weit vorne in der Kopfspitze, diese mit Längsmuskulatur; Praecerebralseptum in Fixatoren aufgelöst; Rhynchocoelom einfach, vier Fünftel der Körperlänge; Ösophagus mündet in das Rhynchodaeum; Mitteldarmblindsack ohne terminale und laterale Taschen; Dorsoventralmuskulatur fehlt; Seitennervenstämme über ihre ganze Länge mit zwei Faserkernen; Blutgefäßsystem ohne Cerebralanastomose, das Dorsalgefäß dringt in das Rhynchocoelom ein. Die Typusart für die neue Gattung ist

Friedrichia corallicola n. sp.

Habitus

Der drehrunde, 20 mm lange und 1,2 mm dicke Körper erinnert an *Oerstedia*, es ist jedoch keine Kriechsohle ausgebildet und im Vergleich zu Beobachtungen an *Oerstedia dorsalis* wirkt *Friedrichia corallicola* weniger starr in den Bewegungen und zeigt auch eine stärkere Kontraktionsfähigkeit. Das Vorderende ist abgerundet und es ist keine abgegrenzte Kopfregion äußerlich zu erkennen, das Hinterende ist stumpf abgestutzt und wirkt rein optisch wie eine Bruchstelle. Von der ocker Grundfarbe wird der größte Teil durch rostbraune Pigmente überdeckt. In der terminalen Körperregion sind diese so dicht gelagert, daß eine einheitliche Färbung zustande kommt, innerhalb welcher nur im Bereich der Augen kreisrunde ocker Flächen erhalten bleiben. Ebenfalls ocker ist das dorsomediane, an das braune Vorderende anschließende Längsband, welches die weißen und braunen, gegeneinander nicht scharf begrenzten Querbinden dorsal unterteilt. Die erste der sechs weißen Querbinden ist 3—4mal so breit wie die nachfolgenden, die braunen Binden sind alle von annähernd gleicher Breite und setzen sich aus rostbraunen, länglichen Pigmentschollen zusammen (Abb. 3, B). Im Gegensatz zu den bisher bekannten Vertretern des *Oerstedia*-Kreises sind vorliegend mehr als nur vier Augen vorhanden, diese allerdings in vier Gruppen vereint. Das terminale Gruppenpaar besteht aus je einem Doppelauge und einem Einzelauge, die beiden hinteren Gruppen aus je zwei separierten Augen (Abb. 18, au).

Anatomie

Körperepithel und Grundschicht sind ohne Besonderheiten. Die Längsmuskulatur setzt sich terminad über das in Fixatoren aufgespaltene Praecerebralseptum bis in die Kopfspitze hinein fort. Zum Teil sind Längsfibrillen in das durch die enorme

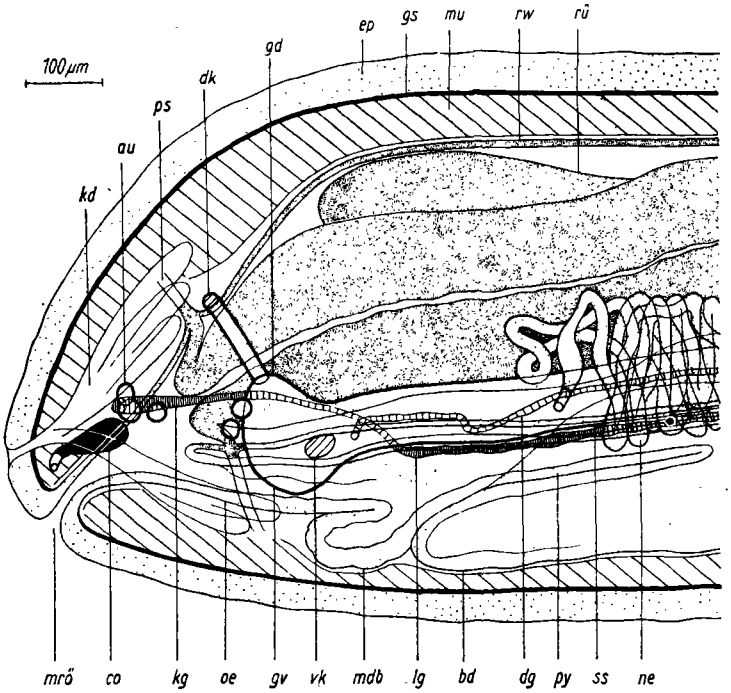

Abb. 18. *Friedrichia corallicola* — Vorderende. Projektion der Organisation (der linken Körperseite) in die Median-Sagittale. (Erklärung der Abkürzungen s. S. 324.)

Entwicklung der Kopfdrüse spärlich vorhandene Parenchym eingesenkt. Dorsal und ventral ziehen Lappen der Kopfdrüse bis in die Gehirnregion. Eine größere Anzahl von lateroventral gelagerten subepithelialen Drüsenzellen ist praecerebral festzustellen. Die Cerebralorgane sind klein und einfach und liegen weit vorne in der Kopfspitze (Abb. 18, co).

Das Gehirn ist vergleichsweise klein und zeigt an seiner Oberfläche keine Unterteilung in Ganglien. Die Seitennervenstämme treten caudal vom Gehirn aus und besitzen über ihre ganze Länge zwei Faserkerne (Abb. 19, A, B, ss, fk).

Das Rhynchocoelom erreicht vier Fünftel der Körperlänge. Bis zur Mitte hin ist es stark erweitert und der Rüssel liegt hier in vielen Windungen, im caudalen Abschnitt wird aber das Lumen rasch enger und die Rhynchocoelomwand legt sich meist dem Rüssel direkt an; möglicherweise ist aber diese Situation kontraktionsbedingt. Am Aufbau des proximalen Rüsselzylinders sind drei Muskelschichten beteiligt und in der Längsfibrillenlage verlaufen die 11 Rüsselnerven. Der Stilettapparat besteht aus dem Angriffstilett, dessen Knauf bemerkenswert groß und halbkugelförmig ist, der Stilettbasis, von der keine Details ermittelt werden konnten, und zwei Reservestilettaschen mit je drei Stiletten.

Anschließend an die subterminal gelegene Mund-Rüsselöffnung folgt das kurze Rhynchodaeum, in welches der ebenfalls kurze Ösophagus einmündet. Letzterer geht

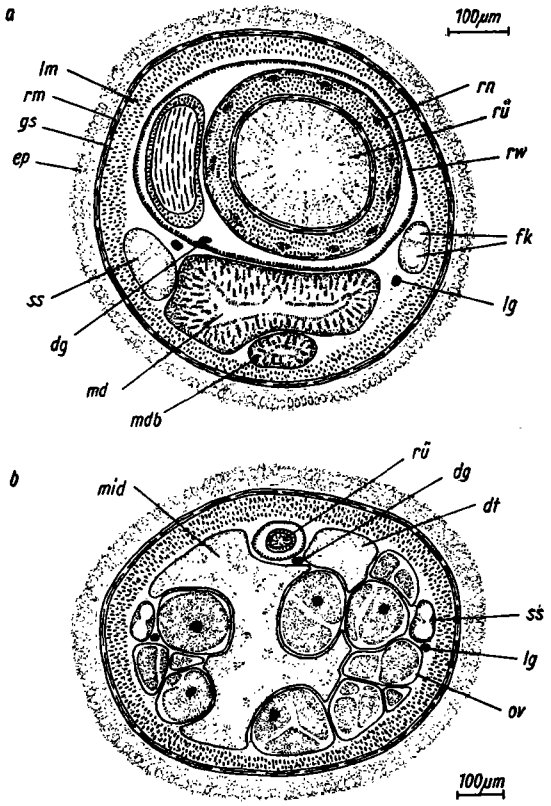

Abb. 19. *Friedrichia corallicola*. A. Querschnitt durch die Magenregion; B. Querschnitt durch die Mitteldarmregion. (Erklärung der Abkürzungen s. S. 324.)

schon im Bereich des Septums in den Magen über, der als besondere Differenzierung einen ventralen, bis unter die ventrale Gehirnkommissur reichenden Blindsack aufweist (Abb. 18, mdb). Caudad setzt sich der Magen in einen langen Pylorus fort. Auffallend ist die schwache Ausbildung von Taschen am mittleren Darmabschnitt. Dem Mitteldarmblindsack fehlen sowohl terminale als auch laterale Taschen und er stellt eine einheitliche Rinne dar, da er sich lateral bis zu den Seitenstämmen aufwölbt. Die Taschen am Mitteldarm selbst sind sehr seicht, bleiben stets unterhalb des dorsalen Darmniveaus und sind nur undeutlich zu erkennen.

Die beiden Kopfgefäße vereinigen sich auf der Höhe der ersten Augengruppen und setzen sich, da eine Gehirnanastomose fehlt, postcerebral als Lateralgefäße fort. Das Dorsalgefäß geht vom rechten Lateralgefäß ab und verläuft ab der Mitte des Magenblindsacks bis zum Ende des Magens im Rhynchocoelom (Abb. 18).

Die Nephridien liegen dorsal und lateral von den Seitenstämmen. Terminal enden sie nahe der Magen-Pylorusgrenze mit je einem lateral sich öffnenden, vor Durchbruch der Körperwand bulbusartig erweiterten Ableitungskanal; caudal reichen sie noch etwas über das Pylorusende in die Mitteldarmregion hinein (Abb. 18, ne).

Die Ovarien liegen rings um den Darm angeordnet und sind bereits mit Beginn des zweiten Körperdrittels zu beobachten.

Verbreitung

Indo-westpazifischer Raum: Madagaskar (Tanikely) [Mozambique-Kanal].

Verteilung

Friedrichia corallicola wurde auf *Acropora corymbosa* mit einer Frequenz von 16,7% bei einer Dominanz von 1,4% registriert.

Zusammenfassung

In der vorliegenden Arbeit wurden die im Verlauf der „Österreichischen Indo-Westpazifik-Expedition 1959/60" im Saumriff der Insel Tanikely aufgesammelten Hoplonemertini monostilifera behandelt. Das Material entstammt Proben von *Seriatopora angulata*, *Acropora pharaonis*, *A. corymbosa*, *Porites nigrescens*, *P. iwayamaensis* und *Millepora tenella*. Die anatomische Untersuchung ergab die Notwendigkeit der Errichtung von zwei neuen Genera, nämlich *Paramphiporus* und *Friedrichia*. Die dargestellten Arten sind: *Cratenemertes madagascarensis* n. sp., *Paramphiporus albimarginatus* n. sp., *Africanemertes rützleri* n. sp., *Nemertellina tropica* n. sp., *Tetrastemma melanocephalum* (Johnston), *Tetrastemma tanikelyensis* n. sp., *Nemertes rubrolineata* n. sp., *Friedrichia corallicola* n. sp. und eine nur kurz angeführte *Tetrastemma* sp. Daß von den neun monostiliferen Hoplonemertinenarten sieben neu für die Wissenschaft sind, ist zum einen darauf zurückzuführen, daß von der Nemertinenfauna des Indischen Ozeans vergleichsweise wenig bekannt ist, zum anderen ist es durch die Aufsammlungsmethode bedingt, da durch freitauchendes Einholen des Probensubstrates und anschließender Aufbereitung der Proben mit Hilfe der Klimaverschlechterung auch Klein- und Kleinstformen erfaßt werden konnten. Die quantitative Verteilung der Arten im Untersuchungsgebiet ist durch Prozentwerte ihrer Frequenz und Dominanz ausgedrückt (vgl. Riedl 1959 und Kirsteuer 1963).

Erklärung der Abkürzungen

au	Augen	md	Magendarm
bd	Blinddarm	mdb	Magendarmblindsack
bs	Bindegewebeschicht	mdf	Magendarmfalte
bt	Blinddarmtasche	mid	Mitteldarm
co	Cerebralorgan	mrö	Mund-Rüsselöffnung
dg	Dorsalgefäß	mu	Muskulatur
dk	Dorsalkommissur	ne	Nephridien
dt	Mitteldarmtasche	oe	Ösophagus
ep	Epithel	ov	Ovar
ev	Epithelverdickung	ps	Praecerebralseptum
fk	Faserkern	py	Pylorus
gd	Dorsalganglion	rd	Rhynchodaeum
gs	Grundschicht	rm	Ringmuskulatur
gv	Ventralganglion	rn	Rüsselnerven
kd	Kopfdrüse	rü	Rüssel
kg	Kopfgefäß	rw	Rhynchocoelomwand
lg	Lateralgefäß	ss	Seitennervenstamm
lm	Längsmuskulatur	vk	Ventralkommissur

Literatur

BEAUMONT, W. (1895), Report on Nemertines observed at Port Erin, Isle of Man. Trans. Biol. Soc. Liverpool **9**, 354—373.

BÉNARD, F. (1960), La faunule associée au *Lithophyllum incrustans* des cuvettes de la région de Roscoff. Cahiers de Biologie Marine **1**, 89—102.

BERGENDAL, D. (1900), Über ein Paar sehr eigentümliche nordische Nemertinen. Zool. Anz. **23**, 313—328.

— (1903), Till kännedomen om de nordiska Nemertinerna. IV. Förteckning öfver vid Sveriges vestkust iakttagna Nemertiner. Arkiv Zool. **1**, 85—156.

BRUNBERG, L. (1959), *Emplectonema bocki* n. sp., a Hoplonemertean epizoic on *Funiculina quadrangularis* (PALLAS). Vidensk. Medd. fra Dansk naturh. Foren. **119**, 59—66.

BÜRGER, O. (1895), Fauna und Flora des Golfes von Neapel. Monographie **22**.

— (1904), Nemertini. Das Tierreich, Lief. **20**.

COE, W. (1901), Papers from the Harriman Alaska Expedition. XX. Nemerteans. Proc. Washington Acad. Sci. **3**, 1—84.

— (1904), Nemerteans, Part II. Harriman Alaska Series **11**, 111—202.

— (1905), Nemerteans of the West and Northwest Coasts of America. Bull. Mus. Comp. Zool. Harvard **47**, 1—318.

— (1940), Revision of the Nemertean Fauna of the Pacific Coasts of North, Central and northern South America. Rep. Allan Hancock Exped. 1932—1938, **2**, Nr. 13, 247—323.

— (1944a), Geographical distribution of the nemerteans of the Pacific Coasts of North America, with desciptions of two new species. J. Washington Acad. Sci. **34**, 27—32.

— (1944b), A new species of hoplonemertean (*Paranemertes biocellatus*) from the Gulf of Mexico. J. Washington Acad. Sci. **34**, 407—409.

— (1951), The nemertean faunas of the Gulf of Mexico and of southern Florida. Bull. mar. Sci. Gulf & Caribbean **1**, 149—186.

Correa, D. (1955), Os generos *Emplectonema* Stimpson e *Nemertopsis* Bürger (Hoplonemertini monostilifera). Bol. Fac. Fil. Cién. Letr. Univ. Sao Paulo, Zoologia **20**, 67—78.

— (1961), Nemerteans from Florida and Virgin Island. Bull. mar. Sci. Gulf & Caribbean **11**, 1—44.

Friedrich, H. (1935a), Neue Hoplonemertinen der Kieler Bucht. Schr. Naturwiss. Ver. Schleswig-Holstein **21**, 10—19.

— (1935b), Studien zur Morphologie, Systematik und Ökologie der Nemertinen der Kieler Bucht. Arch. Naturgesch. Berlin, N. F. **4**, 293—375.

— (1936), Nemertini. Grimpe und Wagler, Die Tierwelt der Nord- und Ostsee. Leipzig **4**, 1—69.

— (1955), Beiträge zu einer Synopsis der Gattungen der Nemertini monostilifera nebst Bestímmungsschlüssel. Zschr. wiss. Zool. **158**, 133—192.

— (1957), Beiträge zur Kenntnis der arktischen Hoplonemertinen. Vidensk. Medd. fra Dansk naturh. Foren. **119**, 129—154.

— 1958), Nemertini. The Zoology of Iceland **2**, Part 18, 1—24.

Gering, G. (1912), Neue Nemertinen der schwedischen Westküste. Zool. Anz. **39**, 520—523.

Gontcharoff, M. (1955), Inventaire de la Faune Marine de Roscoff. Trav. Stat. Biol. Roscoff, Suppl **7**, 1—15.

Griffin, B. (1898), Description of some marine Nemerteans of Puget Sound and Alaska. Ann. New York Acad. Sci. **11**, 193—217.

Iwata, F. (1952), Nemertini from the Coasts of Kyusyu. J. Fac. Sci. Hokkaido Univ. Ser. VI, **11**, 126—148.

— (1954a), The Fauna of Akkeshi Bay. XX. Nemertini in Hokkaido. J. Fac. Sci. Hokkaido Univ. Ser. VI, **12**, 1—39.

— (1954b), Some Nemerteans from the Coasts of the Kii Peninsula. Publ. Seto Mar. Biol. Lab. **4**, 33—42.

— (1957), Nemerteans from Sagami Bay. Publ. Akkeshi Mar. Biol. Stat. Nr. **7**, 1—31.

Joubin, L. (1890), Recherches sur les Turbellariés des côtes de France. Arch. Zool. Exp. Ser. II, **8**, 548—602.

— (1894), Les Némertiens. Faune francaise par R. Blanchard et J. de Guerne, Paris 1894, 1—235.

Kirsteuer, E. (1963), Beitrag zur Kenntnis der Systematik und Anatomie der adriatischen Nemertinen (Genera *Tetrastemma*, *Oerstedia*, *Oerstediella*). Zool. Jb. Anat. **80**, 555—616.

Korotkevitsch, V. (1961), A new nemertean species and its position in the system. Zool. J. **40**, 1416—1420.

McIntosh, W. (1873), A Monograph of the British Annelids. Part I, The Nemerteans. Ray Soc. London 1873—1874.

Monastero, S. (1930), I Nemertini della spiaggia di Palermo. Atti R. Acc. Sci. Palermo **16**, 1—23.

Riches, P. (1893), A List of the Nemertines of Plymouth Sound. J. Mar. Biol. Ass. Plymouth, N. S. **3**, 1—39.

Riedl, R. (1959), Das Vorkommen von Nemertinen in unterseeischen Höhlen. Ergebnisse der Österreichischen Tyrrhenia-Expedition 1952. Teil XV. Pubbl. Staz. Zool. Napoli, Suppl. **30**, 529—590.

SOUTHERN, R. (1913), Nemertinea of Clare Island. Clare Island Survey Part 55. Dublin Proc. Roy. Irish Acad. **31**, 1—20.

STIASNY-WIJNHOFF, G. (1942), Nemertinen der Westafrikanischen Küste. Zool. Jb. Syst. **75**, 121—194.

VANSTONE, H., and BEAUMONT, W. (1894), Report upon the Nemertines found in the neighbourhood of Port Erin, Isle of Man. Trans. Liverpool Biol. Soc. **8**.

WIJNHOFF, G. (1912), List of Nemerteans collected in the neighbourhood of Plymouth from May bis Sept. 1910. J. Mar. Biol. Ass. Plymouth **9**, 407—434.

Anschrift des Verfassers: Dr. ERNST KIRSTEUER, The American Museum of Natural History, Department of Living Invertebrates, Central Park West at 79th Street, New York, N. J. (USA).

DEPARTMENT OF COMMERCE AND INDUSTRIES

DIVISION OF SEA FISHERIES

OBSERVATIONS ON THE ECOLOGY AND DISTRIBUTION OF COPEPODA IN THE MARINE PLANKTON OF SOUTH AFRICA

BY

A. DE DECKER.

INVESTIGATIONAL REPORT No. 49

Issued by the Division of Sea Fisheries, Beach Road. Sea Point, Cape Town

REPUBLIC OF SOUTH AFRICA

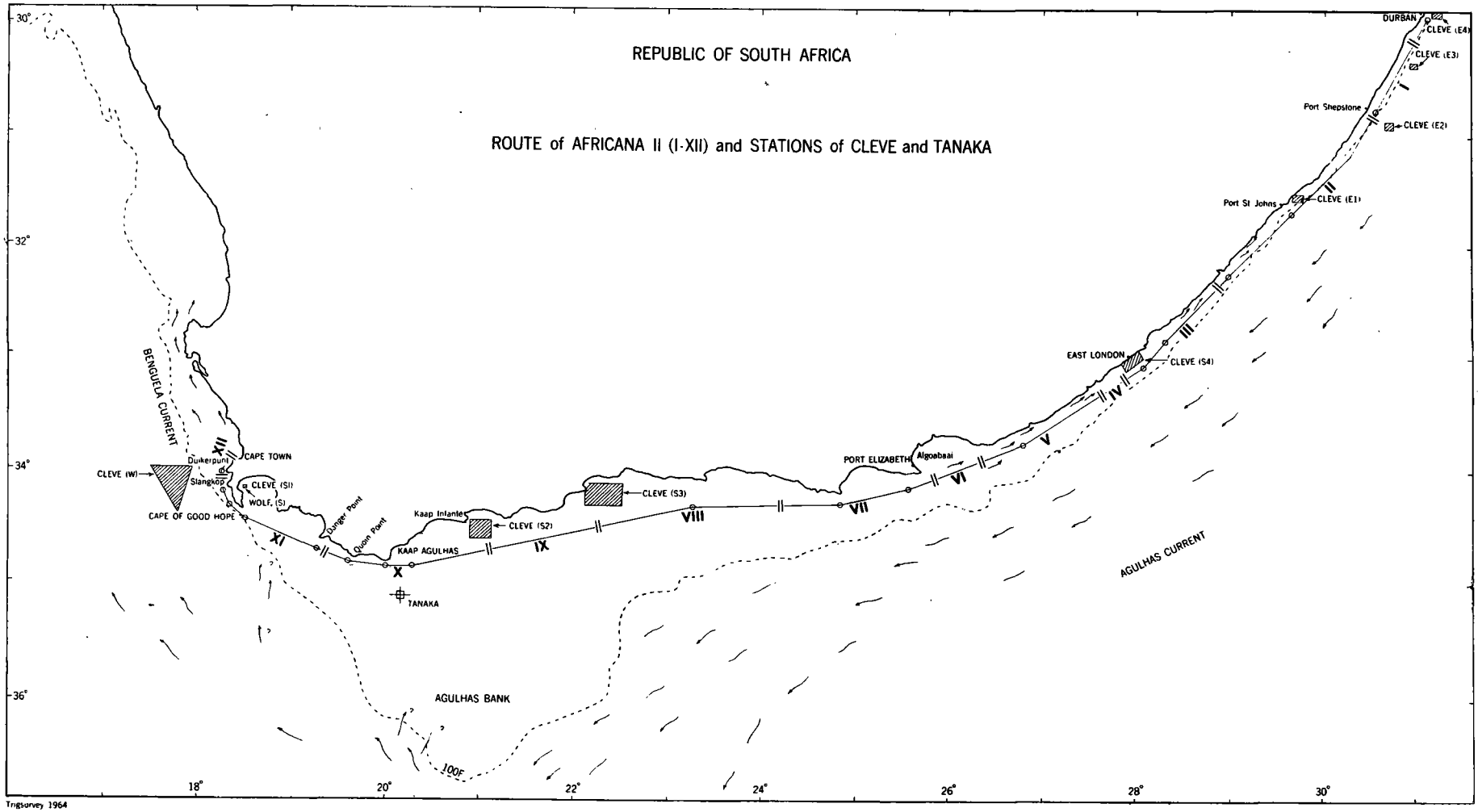

Trigsurvey 1964
5275733—2

Contents.

1. Summary.

During a non-stop voyage of the Division of Sea Fisheries' R.S. AFRICANA II from Durban to Cape Town during July, 1961, a continuous plankton catch was made by straining surface water pumped from the hull of the ship to deck level.

Simultaneously, a surface thermogram was obtained.

The catch extended over a distance of nearly 800 miles and was subdivided into 12 separate plankton samples by emptying the collecting gear at what seemed to be critical points along the route.

A brief outline of the bathymetric and hydrographic conditions in the area south of Africa is given, followed by an analysis of the temperature fluctuations recorded by the thermograph. This leads to a subdivision of the route into 4 main sections:—

(1) The Agulhas Current;
(2) a transitional stretch;
(3) the eastern part of the Agulhas Bank;
(4) the western part of the Agulhas Bank and the vicinity of the Cape Peninsula.

At the time, no important upwelling occurred in the western part of the route.

The plankton volumes showed a sharp increase during the dark hours, amounting to as much as six times the volumes obtained in daylight. They also showed that near the Cape of Good Hope the zooplankton density was about four times greater than that off Natal. The latter increase is correlated with the presence of nutrient-rich cold water near or at the surface.

Phytoplankton blooms were found twice along the coast of the Eastern Cape Province, each time in the vicinity of a sharp drop in the water temperature. The main components of both these blooms were the same species that cause blooms along the West Coast, in the Benguela Current system.

Ninety-two species of Copepods were identified, 28 of them being first records for the South African seas. Their local occurrence, general distribution and references by previous workers in this area are compared and discussed.

The Copepods of the Agulhas Current were a most sharply characterized group in this plankton collection, due to the presence of a high percentage of genuine Indo-Pacific species. This characteristic community disappeared as soon as the shelf started broadening towards the Agulhas Bank.

On the Bank itself, hardly any Indo-Pacific Copepods were found, but a local community comprising mainly cosmopolitan species seemed to be distinguishable. One of its features is the presence of an apparently isolated colony of *Calanus finmarchicus*.

The western part of the Agulhas Bank and the vicinity of the Cape Peninsula are characterized by a predominance of those species which are known to form a part of the huge zooplankton swarms that are typical of the Benguela Current system along the West Coast.

An isolated local occurrence of a number of warm water species near Danger Point seems to indicate that a northward directed arm of the Agulhas Current had reached the shore at that time.

2. Introduction.

The plankton life in South African seas is the source of food for an exceptionally rich fish population which itself serves as a basis for a fishing industry well-known for its remarkable development during the past few years.

Consequently this plankton and its environment have been investigated by the Division of Sea Fisheries for more than ten years. From the routine observations and mapping of many thousands of plankton samples by the staff of the Division's laboratories at Sea Point, a general picture of the plankton distribution in our coastal waters has gradually been built up over the course of years. That picture was broadly outlined during the Symposium of the CCTA/CSA held in Cape Town in September 1960, in so far as it related to the Copepoda, a group which constitutes an average of more than half of the total mass of zooplankton in the sea. In the meantime the investigation is proceeding and more particulars are continually coming to light. These will make it possible to give a much more accurate description of the plankton relationships in our waters within the foreseeable future.

This paper was a somewhat unexpected by-product of the abovementioned research programme. It contains the results of an experiment conducted outside the fixed programme. One of its values is perhaps that it may serve as a control for results usually obtained by completely different methods. The research ships generally carry out vertical or short horizontal hauls with a plankton net at a number of stations in the routine investigational area. Here the opportunity presented itself for obtaining plankton over almost 800 miles

in an uninterrupted and uniform manner even though such plankton came only from the surface layer of water.

Before the method is described in greater detail I should like to express my gratitude to the officers and crew of R.S. AFRICANA II who gave me greatly appreciated assistance in the experiment. I am particularly indebted to the Third Officer, Mr. H. HOY, who provided the accurate record of the ship's route illustrating the text.

Thanks are also due to my colleagues in the laboratory of the Division of Sea Fisheries at Sea Point for their critical reading of the manuscript and to Miss R. THORNTON, Technical Assistant, for the care with which she prepared the map and diagrams.

Finally I should like to express my special indebtedness to Mr. C. G. DU PLESSIS, the former Director of Sea Fisheries, for the assistance and encouragement received from him at all times.

3. Method.

In the afternoon of 17 July 1961, the R.S. AFRICANA II began the return voyage to its home port Cape Town, after the completion of a commission in the S.W. Indian Ocean. The cruise was made without interruption at the normal speed of 11 to 12 knots, so that the vessel reached Cape Town by the afternoon of 20 July.

Plankton was obtained by means of a permanent installation which pumped the sea water through a hole in the hull of the vessel, about 4 metres below the water line, through a pipe and into the laboratory. This installation, which was intended mainly for the replacement of water in the aquarium tanks of the ship's laboratory, can divert the water to the deck without first conducting it through any aquaria. This pipe was used for the collection of plankton samples. At the open end of the tube a cylinder of plankton gauze of medium-sized mesh was attached; its diameter was the same as that of the tube ($\pm$5 cm) and its length about 50 cm. A plankton bucket was attached to a ring at the free end of the cylinder. The pump delivered water at the rate of 27·3 litres (6 gallons) per minute. The pump was put into operation shortly after the ship had left Durban harbour. Initially no plankton was collected, the plankton bucket being attached for the first time only an hour later. In the meantime the water rushing through the pipe system cleared out all plankton remains which might still have been present after the earlier collection of plankton samples.

During the cruise the bucket was removed from time to time and immediately replaced by another (see Table 2). The contents were preserved in formalin and transferred to a measuring cylinder thereby measuring the settled volume of the plankton. In this manner the total catch was divided into 12 tubes with plankton from 12 contiguous parts of the route. It was the intention to ascertain from the contents of the 12 samples how the quantity and composition of the plankton varied along each section according to the locality, the hydrographic nature of the water and the time of the day.

Only one hydrographic factor, namely temperature, could be measured from the moving ship and this was done by a continuously registering thermograph.

It was the author's first intention to change the plankton buckets whenever any important variation occurred in the water temperature, the object being to avoid as far as possible two different plankton communities becoming mixed in a single sample. In practice, however, this was difficult to do because the irregular trend of the temperature curve made it impossible to predict whether any incipient rise or fall of the thermograph needle would continue long enough to be of significance. Generally such movements were of very short duration. Where large deviations actually did occur, they were frequently observed too late owing to the fact that the thermograph was located in a place on the ship where it could not be kept under continuous observation.

Since this experiment was undertaken outside the normal programme of work, there was very little time on land for the taxonomic processing of the available material. Quantitative determinations could not be carried out. The adult Copepoda and the recognisable juvenile stages were identified in all samples except in the case of certain " more difficult " genera, such as *Corycaeus*, *Oithona*, *Oncaea*, the representatives of which were investigated with reasonable completeness only in a small number of samples. The numbers for each species were estimated and reflected by means of symbols, as follows:—

r = 1 to 3 individuals per sample.
f = 4 to 20 individuals per sample.
+ = 20–50 individuals per sample.
c = 50 to 100 individuals per sample.
cc = 100 to 200 individuals per sample.
ccc = 200 to 400 individuals per sample.

For a comparison of the occurrence of a species in the different sections of the route, it is, of course, necessary to take account of the length of the relevant sections in addition to these symbols (see Table 2).

The plankton did not suffer greater damage in their passage through the pump than would have occurred in a classic catch with a vertical net. Their state of preservation was completely satisfactory.

4. Morphological and Hydrographic Conditions.

The general structure of the area concerned will first be described in broad outline.

Off the south-east coast of Africa the continental shelf is for the most part very narrow and the gradient steep. At hardly any point between Durban and East London is the 100-fathom line further than 12 miles from the coast, the distance generally being less than six miles. Between Port Shepstone and Port St. Johns the route of AFRICANA II consequently ran seawards of this depth. West of East London the shelf gradually becomes broader and off Port Elizabeth the 100-fathom line already lies 25 miles from the coast, bending more and more to the south further down while the coast line turns to the west. The Agulhas Bank lies in the form of a triangle along the whole length of the south coast since at its most southerly point, the 100-fathom line bends sharply to the north-west 120 miles south of Cape Infante to run close to the coast again near the Cape of Good Hope.

The hydrographic structure shows an unmistakable agreement with the bottom topography. Parallel to the south-west coast runs the broad Agulhas Current in a south-westerly direction with the water temperature above 20°C. Between this warm water mass and the coast there flows a very narrow but sometimes very rapid and appreciably colder counter current. At a later stage in its course the Agulhas Current ceases to follow the coast but flows along the south-eastern edge of the Agulhas Bank. As far as the author is aware, no water from the Agulhas Current flows over the south-eastern edge of the bank, despite the regular occurrence over the southern portion of a tongue of warm surface water (19°C to 23°C) which, however, runs from a south-westerly direction across this part of the bank. Except for this occasional and localised tongue of warm water, the water on the bank is influenced by colder water masses of southern origin which well up from the depths against the slope of the bank.

What subsequently happens to the Agulhas Current when it comes into contact with the South Atlantic water is a point on which oceanographers are still not agreed. The possibility, however, is not ruled out and it is even highly probable that a northward moving arm may occur at times and run to the south and west of the Cape of Good Hope in the vicinity of the coast. Part of the plankton dealt with in this report is derived from that area.

Along the last section of the route lies still another area which merits special mention, namely that to the west of Danger Point. The salient features of this area become increasingly regular and prominent towards the west coast of the Cape Peninsula. Here we find the Benguela Current which in its typical course appears at the surface near Slangkop in the form of a narrow strip of cold water (approximately 10°C) and then moves in a northerly direction. This typical form, however, seldom makes its appearance during the winter months, because of the absence during that season of the continuous, strong south-easterly winds which drive the warm Atlantic surface water away from the coast and cause cold water from the depths to take its place.

During the cruise of AFRICANA II no Benguela water was present at the surface and only a few elements of its typical cold-water plankton were found in the samples.

5. Surface Temperature.

Although there was no temperature decline to 10°C on this occasion, as would probably have happened towards the end of the cruise or during some other season, it nevertheless appears from the temperature curve that an area of sudden hydrographic changes had been crossed with rapid temperature fluctuations between limits of 24°C and 14°C (see Fig. 1).

In the curve of Figure I the following sections can be distinguished:

5.1 The Agulhas Current and its Margin (Sections I–III).

The counter current manifests itself in the curve in the form of repeated coolings.

The average temperature is approximately 22·5°C (maximum: 24°C, minimum: 21°C).

5.2 A Zone of Transition to the Agulhas Bank (Sections IV–VII).

A sudden temperature decline of 5·5°C over a distance of 10 miles brings us to an area with a distinct general trend towards cooling (from

Fig. 1

SURFACE TEMPERATURE

(Correction: + 0·5°C)

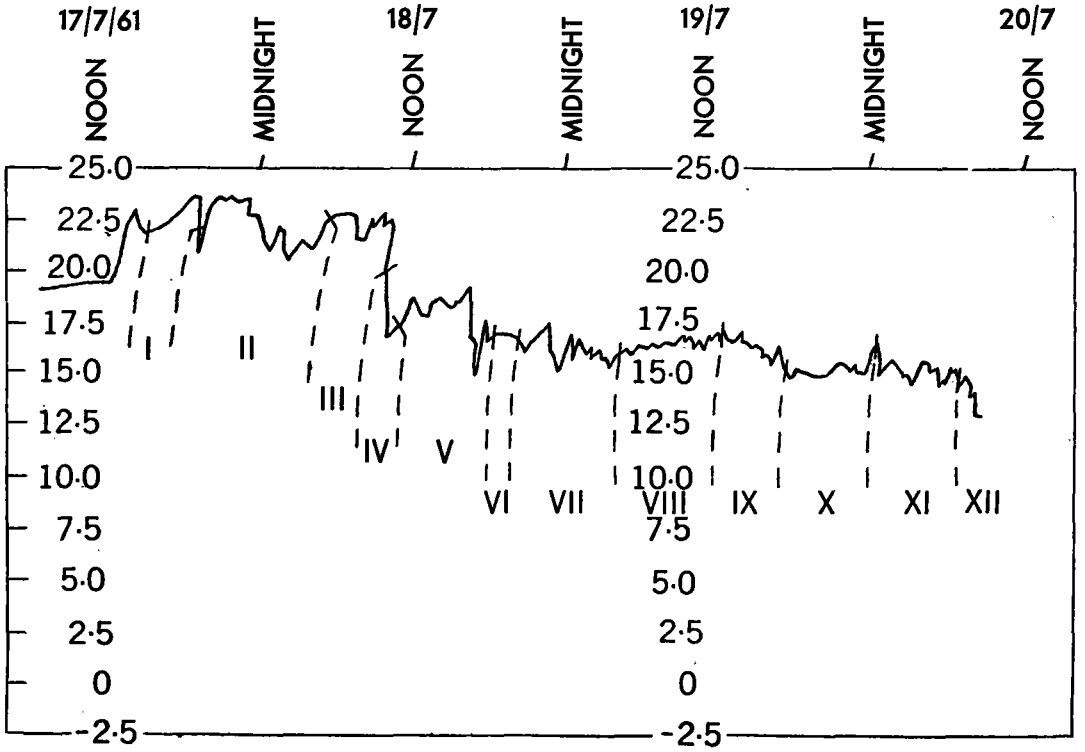

Trigsurvey 1964.

19°C to 16°C). Two further important temperature changes follow, namely one of 4°C (V) and one of 2·5°C (VII). Such sharp temperature differences may possibly be caused by the deflection of deeper cold water by submarine ridges, or a gyratory effect in the current as a result of irregularities in the coastline may force the cold deep water upwards.

The temperature average here lies at 17·5°C (maximum: 19·5°C, minimum: 15·5°C).

5.3 The Eastern Agulhas Bank (Sections VIII–IX).

For the first time during the cruise an area was now traversed where there were no large temperature fluctuations. It is clearly apparent from the irregular trend of the curve, however, that the water temperature was not yet quite stable.

Here the curve is in the form of an arc with its peak at 17·5°C during the afternoon hours. This particular form may be due to solar radiation or to the course taken by the vessel. The latter lies like a chord drawn under a wide arc of the coast and may consequently intersect a series of concentric isotherms running parallel to the coast. The temperature difference of 2°C between the morning and evening minima and the afternoon maximum may possibly also be caused simultaneously by both of the above-mentioned factors.

5.4 The Western Agulhas Bank and the Vicinity of the Cape Peninsula (Sections X–XII).

A small temperature fluctuation of 1·5°C twenty miles south-east of Cape Infante introduces the coldest part of the curve. With the exception of a single strictly local temperature increase between Quoin Point and Danger Point, also amounting to 1·5°C, the temperature nowhere exceeds 16°C. The minima remain above 14·5°C, except at the very end of the curve off Mouille Point which is the most northerly tip of the Cape Peninsula and the entrance to Table Bay.

In contrast with the relatively uniform temperature trend in the eastern half (X) of this area, the western half (XI) shows repeated coolings of brief duration. It seems that these may be regarded as upwelling of cold water and as precursors of that deep water mass which, under favourable conditions (a south-easterly wind), appears at the surface off the west coast of the Cape Peninsula and further to the north and, in the form of the Benguela Current, influences the environmental conditions along the entire west coast as far as Walvis Bay.

A characteristic feature is that the coldest point of the curve is at its extremity, i.e. at the entrance to Table Bay. Towards noon on the 20th July a strong south-easter was blowing across Table Bay, this being something unusual at that time of the year. The effect of this brief period of wind was sufficient to bring colder water to the surface.

In the accompanying table a summary is given of the sub-division of the route according to surface temperature.

TABLE 1.

Sections.	Temperature in °C.			Area.
	Maximum.	Minimum.	Average.	
I–III.....	24	21	22·5	Agulhas Current and its marginal area.
IV–VII..	19·5	15·5	17·5	Transitional area (counter current?).
VIII–IX	17·5	15·5	16·5	Eastern part of Agulhas Bank.
X–XII...	16·5	14·5	15·5	Western part of Agulhas Bank and Cape Peninsula.

TABLE 2.—Summary of Plankton Samples.

Sample No.	Date.	Hour.	Coastal Localities.	Distances in Sea Miles.	Plankton Volumes.		Remarks.
					Volume. (cc)	cc/Hour. (x 1,000).	
I.....	17th July	1715	Illovo.....	—	—	—	—
II.....		2115	Port Shepstone-Margate	45	0·5	125	—
III.....	18th July	0745	Bashee River.....	125	3	286	—
IV.....		1300	East London.....	80	1·25	238	—
V.....		1430	Keiskama Point..	20	0·5	333	phytoplankton bloom.
VI.....		2200	Bird Island.....	75	3·5	466	—
VII.....		2330	South-east of Port Elizabeth	30	0·75	500	phytoplankton bloom.
VIII.....	19th July	0800	Tsitsikama River.	85	7·5	882	—
IX.....		1600	Mossel Bay.....	95	1·5	188	—
X.....		2130	Cape Infante.....	60	3	545	—
XI.....	20th July	0500	Danger Point....	85	8	1,067	—
XII.....		1130	Duiker Point (Hout Bay)	75	2	308	—
		1230	Mouille Point...	10	Volume too small for accurate measurement		—

6. Plankton Volumes.

In order to compare the volumes of plankton samples from sections of varying length, the former were converted into *cubic centimetres per hour* (and then multiplied by one thousand in order to avoid fractional numbers).

From the histogram of the hour-volumes (Fig. 2) the following facts are clearly observable.

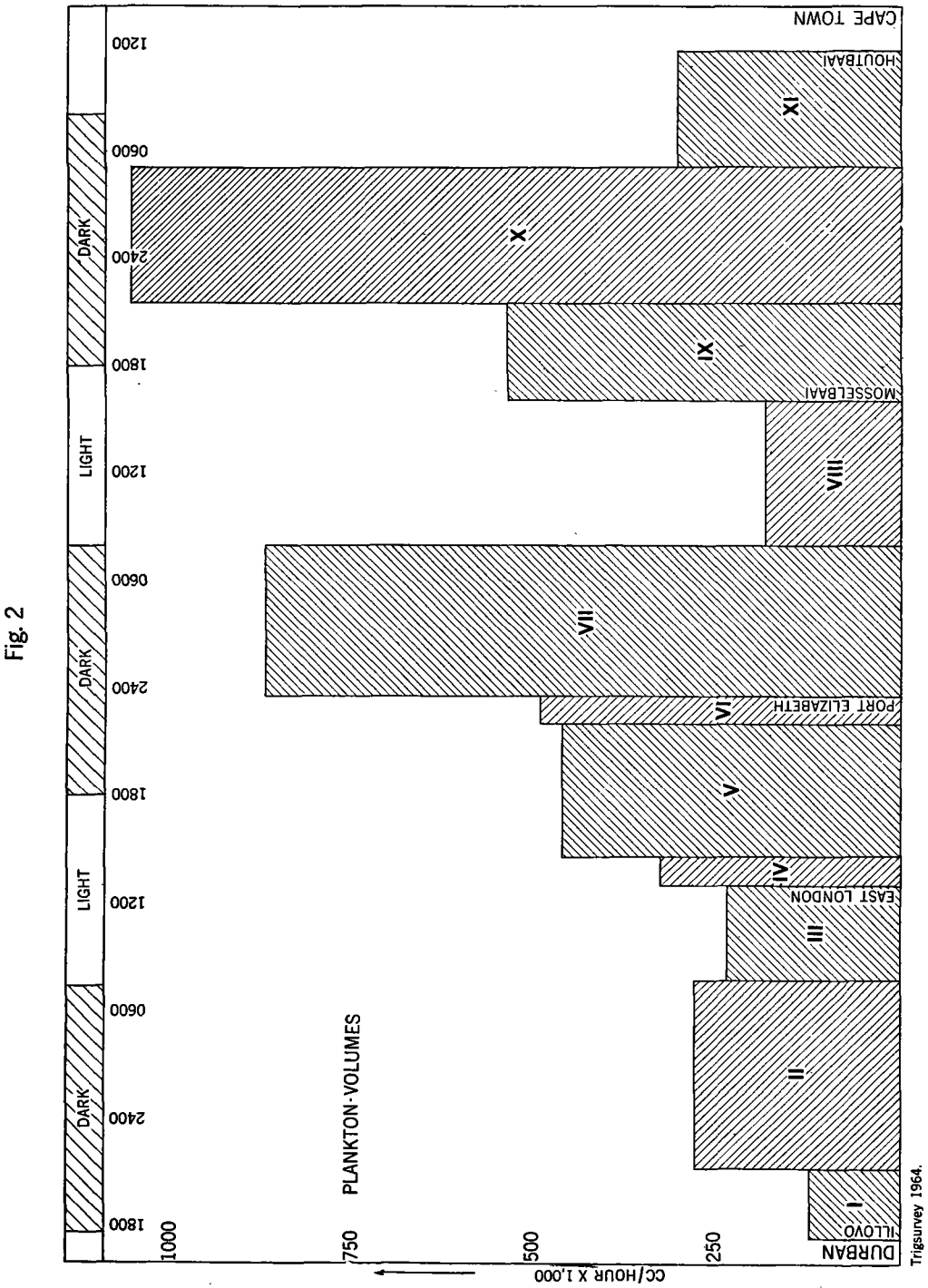

Fig. 2

6.1 Daily Fluctuations in Plankton Density near the Surface.

The three largest volumes were on each occasion obtained at night. The first night section (II) yielded twice as much plankton as the preceding section (I), although the catching time for sample I lasted until the earliest hours of the night and the volume was consequently without any doubt increased by the nocturnal ascent of the plankton. During the second night (VII) four times more plankton, and during the third night (X) six times more plankton, were obtained than during the preceding daylight sections (III and VIII).

6.2 Increase in the Quantity of Plankton in a Westerly Direction with Declining Temperature.

This increase is already visible in the small volumes from the consecutive daylight periods. Section VIII yielded 50 per cent more than section I although the latter was favoured by ascending plankton during the late evening. The volume in section V is still larger, but is not comparable with the above-mentioned two volumes since a phytoplankton bloom was traversed here. Section XI, however, yielded 60 per cent more than section VIII.

The catches made at night give an idea of the amount of plankton which sinks into deeper water during the day and which was consequently beyond the reach of the pump. A comparison of the three nocturnal catches shows that during the second night there was three times more plankton and during the third night almost four times more plankton than during the first.

The following comparison makes it clear that the temperature decline is not in itself the factor which causes the plankton to increase.

On the final part of its cruise through the south-western part of the Indian Ocean between 6 and 15 July AFRICANA II made observations at a number of oceanographic stations lying in a straight line from 38°S, 58°E as far as 100 miles S.S.E. of Durban. Between the stations, where the whole of the day was generally spent in making observations, plankton was caught at night with the pumping apparatus described above. The surface temperatures lay between 15·5°C and 17·5°C in the south-eastern half of the section, and between 17·5°C and 20°C in the north-western half. The average plankton volume per hour (x1,000) was 66 cc in the colder half and 138 cc in the warmer half. In both halves a short catch was also made during the day and these yielded 28 cc and 38 cc (per hour x 1,000) respectively. These values from the open sea are only fractions of those obtained two days later in the appreciably warmer coastal waters south-west of Durban during the cruise to the Cape.

The increase in the plankton of the South African coastal area is undoubtedly caused by a large number of factors. One of these is the influence of the continental shelf with its greater complexity of communities than the open sea. Another very important factor in the area concerned is the influx of nutrients from the depths, cold water rising to the surface along the south coast. The extent of this phenomenon becomes greater towards the west, the density of the plankton also increasing from east to west. In the plankton-deficient marine area in the S.W. Indian Ocean mentioned above, the 15°C isotherms lay between 200 and 400 metres below the surface and the 10°C isotherms between 700 and 400 metres. Along the edge of the Agulhas bank a sharp thermocline regularly occurs and rises towards the north, the 10°C isotherm there being only at 100 metres depth.

7. Distribution of Phytoplankton.

The main constituent of the plankton samples was made up of Crustacea, except in areas V and VII where the ship passed through dense masses of phytoplankton. This phytoplankton bloom was encountered in the same locality where the three large temperature declines occurred. It illustrates the effect of nutrient-rich deep water rising up and reaching the photic region. First there is a tremendous activation of algal growth (=primary production) on which the heterotrophic (animal) links of the living community can then subsequently feed in abundance.

It was impossible to determine accurately the place of occurrence, the density and the extent of the phytoplankton patches because of the limitations of the apparatus. The question of their location in respect of the temperature minima must unfortunately remain unanswered.

I am deeply indebted to Miss V. A. HILLHOUSE of the Division of Sea Fisheries, for the readiness with which she undertook the identification of the algae from these two samples. In both cases their composition was very similar in so far as the predominating species are concerned, only the five diatom species which were most abundant in both samples being mentioned here, namely:—

Schröderella schröderi.
Thalassionema nitzschioides.
Thalassiosira rotula.
Thalassiothrix longissima.
Chaetoceros decipiens.

It is noteworthy that this algal community shows little relationship to that known from the sea area along the south east and south coasts of South Africa as a whole but it does indeed reflect a good agreement with that occurring in the cold Benguela waters along the west coast.

8. The Copepoda.

8.1 Systematic Review.

Little research work has been done as yet on the Copepod fauna of South Africa. The most important and most exhaustive contribution hitherto made was that of CLEVE (1904). He had at his disposal a number of net catches from the western, southern and eastern parts of the area, obtained mainly from stations near the coast, as well as a few vertical hauls from greater depths (down to 780 metres). He found altogether 110 species.

STEBBING's Catalogue of South African Crustacea (1910) contains mainly the list of species given by CLEVE, plus three species which he had found in DANA's work (1852–55).

BRADY (1914–15) wrote three short contributions on material obtained from Durban, with approximately 48 " recognisable " species of which 18 were new to South Africa. In addition a number of " species novae " were mentioned in those publications. The description and illustration of the latter, however, are inadequate for identification.

In the meantime WOLFENDEN (1911) published his excellent work on the material obtained by the German Deep-sea Expedition, in which a number of samples from the South African marine area are also found. Sometimes, however, WOLFENDEN is very vague in his locality determinations, especially in regard to his species from the South Atlantic Ocean, with the result that it is often difficult to deduce from the text whether a species was found near the coast or a thousand miles away.

By applying the broadest geographic criteria the author found that 45 of WOLFENDEN's species were then new to South Africa.

Finally TANAKA (1960) obtained 37 near-surface species from material collected by the Second Japanese Antartic Expedition at a station south of Cape Agulhas (erroneously called the " Cape of Good Hope " in the work concerned). Of these, 22 were new to South Africa, It is worth mentioning that among the 17 plankton stations occupied by the Research Vessel SOYA between Japan and Antarctica, the one station on the Agulhas Bank was the richest in species and individuals.

The author identified 92 species in his material, 28 of these being new to the South African fauna. They are arranged below in alphabetical order.

The following *abbreviations* are used:—

Cl(eve), *Br*(ady), *Wo*(lfenden) and *Tan*(aka). When one of these is used after the name of a species, it means that the author concerned established the presence of the relevant species in the South African area.

St. . . . : is placed in front of the number (Roman) of the sample(s) in which the species was found.

L: this means the total length in millimetres (from the anterior point of the cephalothorax to the end of the furca) as established in specimens from the whole area (not merely those from the material dealt with here). Many of the South African species are larger than the sizes recorded in the literature for their congeners from other areas.

" (DF) " and " (IOP) " are placed after information extracted from unpublished data on Copepod material of the Division of Sea Fisheries. Dr. F. MOMBECK and the author have been busy processing this material for over three years. " (IOP)" relates more particularly to the results of the first cruise of AFRICANA II in connection with the International Indian Ocean Project undertaken in June–July, 1961.

TABLE 3.—Occurrence and Abundance.

	I.	II.	III.	IV.	V.	VI.	VII.	VIII.	IX.	X.	XI.	XII.
Acartia—												
amboinensis		r										
danae		f				r					r	
negligens			r		r	r	f					
Acrocalanus—												
gracilis	f	f	+	+	f	r	f		f			
monachus	r				r							
Calanoides—												
carinatus	r	f	r	r	r		f		+	f	f	f
Calanopia—												
minor		r				r	r					
Calanus—												
finmarchicus			r		f	r	c	f	+	+	f	
tenuicornis				r	r		r			r		

TABLE 3.—Occurrence and Abundance (*continued*).

	I.	II.	III.	IV.	V.	VI.	VII.	VIII.	IX.	X.	XI.	XII.
Calocalanus—												
contractus		r		r								
pavo	r	r	f		r	r						
plumulosus		r	f	r	f	r	f		r			
styliremis					r	r			r		r	
tenuis									f	f	r	
Candacia—												
armata(?)							f		r	r		
bipinnata							r		r	r		
catula	r		r			r						
curta		r										
truncata	r	r										
Canthocalanus—												
pauper			r	r	r	r	r					
Centropages—												
brachiatus								f	+	+	c	r
calaninus			r		r	r						
elongatus		r										
furcatus		f		f	r	r	r					
gracilis		r	r		r							
pacificus			r									
Clausocalanus—												
arcuicornis			f			r		f	cc	c	f	
furcatus	f	c	+	+	c	f	c	+	f		r	
paululus										r		
Clytemnestra—												
rostrata					r				r			
scutellata		r										
Copilia—												
mediterranea						r						
mirabilis		r	f									
Corycaeus—												
africanus							f					
agilis				f							f	
asiaticus	r	r	r				f	f				
crassiusculus	r		f				r				f	
dubius	r											
latus				r				r				
longistylis			r									
pacificus			f					f		f	f	
speciosus		f	f		r			r			f	
subtilis	r											
Corycella—												
concinna	r	+	+	f	+	f	f	r			r	
curta										r		
gibbula	f	f	f	r	f			r				
Ctenocalanus—												
vanus											r	
Eucalanus—												
attenuatus		r	f							r	r	
elongatus					r							
monachus							r					
mucronatus			r				r					
pileatus		r	r	r	r		f					
subcrassus						f						
Euchaeta—												
wolfendeni		r	r									
Euterpina—												
acutifrons	f	f	r	+	cc	cc	c	f	f	r	f	
Labidocera—												
acutum	r	f	r	f		r	r					
minutum									r			

TABLE 3.—Occurrence and Abundance (*continued*).

	I.	II.	III.	IV.	V.	VI.	VII.	VIII.	IX.	X.	XI.	XII.
Macrosetella—												
gracilis	r	f			r	r	r				r	
Mecynocera—												
clausi			r								r	
Metridia—												
lucens										r	f	
Microsetella—												
norvegica			r		r		r		r	r	r	r
rosea					r					r		
Nannocalanus—												
minor		f	r			f	f		+	ccc	cc	
Oithona—												
fallax											f	
nana							+	f	f		f	f
plumifera			f	f	f	f		r		+	c	r
rigida			r									
tenuis												r
Oncaea—												
clevei		r										
media	f		f								f	r
mediterranea						f	f			f	f	
subtilis							f			f	f	f
venusta	f	c	f		f					f		
Pachos—												
tuberosum			r									
Paracalanus—												
aculeatus	f	+	r	f	c	+					c	f
crassirostris		+			f			f	+	+	f	f
denudatus	r											
parvus		r				f	c	cc	cc	ccc	+	+
Pleuromamma—												
abdominalis						r	r					
gracilis					r							
robusta		f										
Pontellina												
plumata		r			r							
Pseudodiaptomus—												
nudus									f	f	f	
Rhincalanus—												
cornutus		r	f	r	f		f					
nasutus		r					r			r	r	
Sapphirina—												
gastrica			r									
nigromaculata		r										
ovatolanceolata-gemma	r				r							
Scolecithrix—												
danae		r										
Temora—												
discaudata		c		r	f	+	f		r		r	
turbinata	r	f	f	f	c	r	c	f	f	r	r	
Undinula—												
darwinii	f	f	r									
vulgaris	r											
TOTAAL	24	40	39	20	35	27	33	17	22	26	34	11

Acartia amboinensis CARL. New to South Africa.

In St. II one female and one male were found. The agreement with STEUER's description (1923) was very satisfactory in respect of both sexes.

L = ♀1·45, ♂1·32.

The same species which is new to the South African fauna, has in the meantime also been found in two surface catches (vertical haul 50–0 metres) 20 and 100 miles, respectively, east of Delagoa Bay (Mocambique), namely one female on each occasion. L = 1·43 (IOP).

In his list of species for Durban Bay, BRADY (1915) mentions the closely related species *A. erythraea* GIESBRECHT, which has not been found in the area again since that date. STEUER did not include these data in his monograph on the genes *Acartia*, obviously because BRADY's contribution was not accessible to him (see STEUER l.c., p. 37, Nachtrag).

Very little information on the distribution of *A. amboinensis* could be found by the author in the available literature.

STEUER's distribution map shows the Indonesian Archipelago, the Gulf of Bengal and the Gulf of Aden. SEWELL (1948) mentions in addition the Central Pacific Ocean, and he himself (1932, 1947) repeatedly encountered the species in the northern area of the Indian Ocean, on many occasions together with *A. erythraea.*

Acartia danae GIESBRECHT. *Cl*: W, S, E.

St. II, VI, XI (two night sections and one night and day section).

This species was fairly scarce in our material but otherwise it is abundant in the warm surface water around South Africa. It is frequently encountered in association with *A. negligens.* The latter is scarce off the west coast but frequently predominates over *A. danae* in the Agulhas Current (DF). L= ♀1·13–1·28, ♂ 0·82–0·86.

Acartia negligens DANA *Wo*: W, E. *Tan.*

St. III, V, VI, VII. (One daylight section with only juveniles; three night sections with adult females; males were present also in V).

This species is found everywhere in warm water around South Africa; for the rest it is distributed in the tropical and temperate parts of the Indo-Pacific and Atlantic areas.

L= ♀1·04–1·16, ♂1·04.

Acrocalanus gracilis GIESBRECHT. *Cl*: E: *Wo*: E; *Tan.*

St. I to VII and IX (in the last-mentioned St. only juveniles).

This was one of the most abundant representatives of the smaller zooplankton in the Agulhas Current. In the warm water it is present throughout the Indo-Pacific area. The author was unable to find any mention in the literature of its occurrence in the Atlantic Ocean; its distribution around South Africa (DF), however, shows that it occasionally penetrates into the Atlantic area as far as 100 miles west of the Cape of Good Hope and equally far northwards (30°S). L= ♀1·30–1·32.

Acrocalanus monachus GIESBRECHT. New to South Africa.

St. I and V.

This species is rare in the author's material, as indeed it is throughout the entire area where it is found only off the south and south-east coasts (DF). Its general distribution is Indo-Pacific.

L= ♀0·99–1·08.

Calanoides carinatus (KRÖYER). *Cl*: W, S, E. *Tan.* [=*Calanoides brevicornis* (LUBBOCK)].

This species was found at all stations except VI and VIII; in I to V juveniles predominated (only three adults), while in VII to XII mostly adults, and in XI also males were found.

This species is very numerous along the west coast and occurs there during the summer in gigantic swarms over the whole length of the Benguela Current as far as Angola. The species here occupies the biological niche filled by *Calanus finmarchicus* in other seas.

According to the author's material it would appear that the species gradually becomes rarer towards the east, at any rate near the surface. Off the coast of Natal it has never yet been found in vertical hauls between 100 and 0 metres (DF) in any quantities worth mentioning. South of Madagascar the author regularly found this species in closing nets operated between 700 and 3,000 metres.

BRADY (1914) described a new species from Durban Bay, namely *Calanoides natalis*, which has not been found again since that time, and SEWELL (1947) discovered a number of juvenile specimens in the N.W. Indian Ocean (partly at great depths) which he with reservations identified as *Calanoides patagoniensis* (BRADY), a species which is very closely related to *C. carinatus.* Since no *Calanoides* species has as yet been found in the Indian Ocean, a connection may exist between SEWELL'S find and the occurrence of *C. carinatus* in the South African area.

This species also occurs along the east and south coast of Australia; in addition it has been shown to the present in the Indo-Malayan area and appears to be widely distributed, but nowhere abundant, in the Atlantic Ocean.

L= ♀2·63–2·77, ♂2·33–2·50.

Calanopia minor A. SCOTT. New to South Africa.

St. II (1 ♀), VI (1 ♂) and VII (1 juv.). Night sections.

This species has also been caught off Delagoa Bay (IOP) and in Natal waters (DF), but is rare in our area. It occurs in the central and eastern areas of the Pacific Ocean, in the northern part of the Indian Ocean and in the Red Sea. (Also see BOWMAN, 1957). L= ♀1·28–1·46, ♂1·08–1·37.

Calanus finmarchicus (GUNNER). *Cl.*: W, S, E.

St. III (1 juv. ♂) and V to XI (predominantly adult ♀ ♀; 1 ♂ in VII).

Observations conducted over a number of years (DF) indicate that a fairly numerous colony of this species is consistently present over the Agulhas Bank. The distribution in the author's samples is in agreement with these observations (Table 3). Off the West Coast and off Natal it occurs only at certain times and in small numbers. CLEVE's quantitative data (1904) are also in agreement with this finding.

In the South Atlantic Ocean the species is scarce, and in the Indian Ocean, the only record known to the author is that by SEWELL (1947), who found one single male in a 1,000–0 metre haul in the Arabian Sea.

Never yet has any massive swarming been noticed in the *C. finmarchicus* colony of the Agulhas Bank, comparable to what happens in this species in other seas at certain times of the year. The author has also never found a specimen which had the well-nourished oil-rich appearance which is a general feature of the large Calanids during the swarming season. In our waters this is indeed the case with *Calanoides carinatus* and *Calanus tonsus*. This local *C. finmarchicus* colony gives the impression that it may be a relic which is trying to maintain itself under unfavourable conditions.

L= ♀2·77–2·98, ♂2·73–2·82.

Calanus tenuicornis DANA. *Cl*: W, E.

St. IV, V, VII and X (only juveniles). Night sections.

This species occurs regularly round South Africa but is nowhere abundant. It inhabits the warmer areas of all oceans but appears to be a rarity in the Indian Ocean. The author caught it in deep closing nets (down to 3,000 metres) south of Madagascar together with *Calanoides carinatus* and *Calanus tonsus* (IOP).

L= ♀2·13–2·19, ♂1·81–2·12.

Calocalanus contractus FARRAN. New to South Africa.

St. II and IV (only males, one with spermatophores).

This species is known from the Bay of Biscay and the Great Barrier Reef (FARRAN 1926, 1936), the N. Indian Ocean (SEWELL 1929), the N.E. Atlantic Ocean and the western part of the Mediterranean Sea (BERNARD 1960). This inconspicuous species may have remained unnoticed in many plankton samples. This find confirms SEWELL's (1948) hypothesis in regard to the migration of the species along the Cape of Good Hope. L= ♀0·74.

Calocalanus pavo (DANA). *Cl*: W, S, E.

St. I, II, III, V and VI.

Only females, partly juvenile.

This species is distributed in the warm water round South Africa (DF), being for the rest cosmopolitic (occurring not only in warm seas: WILSON 1950).

L= ♀0·94–1·05.

Calocalanus plumulosus (CLAUS). New to South Africa.

St. II to VII and IX (only females).

Its distribution is roughly the same as that of the foregoing species.

L= ♀1·10–1·13.

Calocalanus styliremis GIESBRECHT. New to South Africa.

St. V, VI and IX (night sections), and XI (day). All adults.

This species is abundant throughout the Pacific Ocean and round New Zealand, and is not rare in the Atlantic Ocean and the western Mediterranean. SEWELL (1929) found a few specimens near the Nicobar Islands; the author could find no other data on the Indian Ocean.

L= ♀0·68.

Calocalanus tenuis FARRAN. New to South Africa.

St. IX, X and XI. Mostly night sections. Only adult females.

The Bay of Biscay (FARRAN 1926) and the western Mediterranean Sea (BERNARD 1960) are the only places known to the author where this species has been found. The fact that such a conspicuous and by no means small species should have escaped the notice of planktologists is perhaps even more remarkable than its appearance off South Africa.

It occurs particularly along the west coast and becomes rarer along the south coast but is nowhere very abundant. Its most northerly occurrence in Southern Africa known to the author lies 20 miles off the mouth of the Kunene (southern boundary of Angola) (DF).

L= ♀1·06–1·28.

Candacia armata (BOECK) (?) [=*C. pectinata* (BRADY)].

Candacia bipinnata (GIESBRECHT). *Cl.*: S.

St.	VII.	IX.	X (Night Sections).
C. armata...	♀♀, ♂♂	♂♂	♀♀, ♂♂. ♀♀ have no spermatophores.
L=	♀ 1·82 ♂ 2·10–2·20	—	♀ 1·72. ♂ 2·20
C. bipinnata	♀♀	♀♀	♀♀ ♀♀ all have spermatophores.
L=			2·20

With the individuals given here as *C. armata*, the author is faced with a problem similar to that which apparently also troubled DAKIN & COLEFAX (1940) in their study of the plankton of New South Wales.

The female *armata* among the author's specimens not only lack the lateral points on the genital segment which are typical of *bipinnata*, but also do not have the asymmetrical growth on the second abdominal segment which is characteristic of *armata*. On the fifth leg there is no striking difference between the two species. The body length of the author's specimens corresponds to that of *armata*.

The females identified as *bipinnata* possess all the features of this species, including the body length.

The size and build of the males is the same as in the case of *bipinnata*, but the fifth leg has a large curved spine at the end of the chelate segment: this is a characteristic of *armata* which according to ROSE'S (1939) redescription does not occur in *bipinnata*. The fifth leg, however, is in complete agreement with the drawing of "*Candacia pectinata var. Sidney*" in DAKIN & COLEFAX (1940). It is noteworthy that in the Sidney variety the males are 2·3 mm. and the females only 1·9 mm. long, while the *bipinnata* females from the same area attain a length of 2·25 mm.

DAKIN & COLEFAX do not mention the exact place where their specimens were found but the author's specimens occurred together in all three samples. This simultaneous occurrence, the agreement in body size and the presence of spermatophores in the *bipinnata* females are regarded by the author as adequate reasons for accepting that these males belong to the latter species. The correct name of the *Sydney variety* should then be *Candacia bipinnata* Sidney variety. Neither DAKIN & COLEFAX nor the author found *bipinnata* males which agreed with ROSE'S description; the former were apparently not acquainted with the work of ROSE (1929).

The author's *armata* females may perhaps be juvenile stages of *armata* or of *bipinnata*. As far as the author is aware, the developmental stages of these two species have never yet been described.

Candacia bipinnata occurs along our south coast at least as far east as the eastern edge of the Agulhas Bank; along the west coast it avoids the cold water near the coast but for the rest it is widely distributed northwards (DF).

Candacia catula (GIESBRECHT). *Cl.*: E.
St. I (♀), III and VI (juvenile).

This species is rare in South African waters and has never yet been found west of the Agulhas Bank (DF). The general distribution is Indo-Pacific.

L= ♀1·46.

Candacia curta (DANA). *Cl*: E; *Br.*
St. II (♀).

This species had been found earlier south of the Agulhas Bank and 80 miles west of St. Helena Bay (West Coast, 33°S) (DF) as well as in the S.W. Indian Ocean (IOP). The general distribution is Indo-Pacific and South Atlantic.

L= ♀2·50, ♂2·20.

Candacia truncata (DANA). *Cl*: E; *Br.*
St. I and II (♀ ♀).

This species is rare in our waters but widely distributed in the Indo-Pacific and Atlantic areas.

L= ♀1·78–2·10, ♂2·05.

Canthocalanus pauper (GIESBRECHT). *Tan.*
St. III to VII.

This species must undoubtedly have escaped earlier notice here because the author found it in samples from other localities only after recognising it for the first time in the IOP material. TANAKA'S find (1960) off Cape Agulhas is up to the present the most westerly locality recorded. WOLFENDEN'S (1911) statement that this species occurs "in great abundance" in the Atlantic Ocean, appears to the author to be doubtful, firstly because this finding has never been confirmed and furthermore because the relevant text was compiled in such a manner that a printing or recording error could easily have slipped in here. For the time being therefore the author wishes to regard this species as Indo-Pacific.

L= ♀1·47–1·75, ♂1·34–1·40.

Centropages brachiatus (DANA). *Dana*: S(1853); (?) *Cl*: S, E.

St. VIII to XII (mostly adult ♀ ♀ and ♂ ♂).

This species is always abundant along the west and south coasts of South Africa and plays an important part in the large swarms of Copepoda which occur in the Benguela Current area at certain times of the year. Together with *Calanoides carinatus* it is one of the principal food organisms for fish in our area (DF).

It is surprising that, of all the earlier investigators of South African plankton, only DANA recognised this species as such. The author considers it highly probable that CLEVE's (1904) *Centropages typicus* was a wrongly identified *C. brachiatus*. The particulars given by CLEVE about the distribution of this species along our coasts are on the whole in agreement with the distribution of *C. brachiatus* as the present author knows it: " South of the Cape Colony ": c, r, r, +, r, (present in five out of eleven net catches)—" East of South Africa ": r, r, r, (in three net catches out of six). Its absence from the west coast catches of CLEVE can be explained by the fact that the stations were too far offshore, i.e. outside the dense plankton zone which occurs along the cold coastal water.

Apart from this, *C. typicus* has never yet been found in our area. TANAKA'S mention of this species on the Agulhas Bank (1960) was an error, as he has kindly mentioned to the author. The specimens were in fact *Centropages chierchiae*, the second most abundant *Centropages* species in our area.

The geographic distribution of *Centropages brachiatus* is noteworthy. Besides occurring in the Benguela Current area, it is also encountered in gigantic swarms along the Humboldt Current from Patagonia to Peru (DANA, BRADY, GIESBRECHT, SARS), and ROSE found it at times abundant off the coast of Mauritania (N.W. Africa). THOMPSON also mentions it as occurring near the Canary Islands and Malta (?), while ROSE found it near the Azores. No finds from other localities are known to the author.

L= ♀1·70–1·91, ♂1·58–1·75.

Centropages calaninus (DANA). New to South Africa.

St. III (♀ + ♂), V (♀) and VI (juven.).

L= ♀2·00, ♂1·76–1·88.

Centropages elongatus GIESBRECHT. New to South Africa.

St. II (juven.).

L = ♀1·42.

Centropages furcatus (DANA). *Cl*: E; *Wo*: S; *Br*.

St. II, IV to VII (adult ♀ ♀ and ♂ ♂).

L= ♀1·61–1·86, ♂1·61–1·69.

Centropages gracilis (DANA). New to South Africa.

St. II, III V (only ♀ ♀).

L = 1·85–1·88.

Centropages pacificus CHIBA. New to South Africa.

St. III (♂ ♂).

L = ♂1·63–1·75.

The last mentioned five *Centropages* species occurred in the author's samples only east of the distribution area for *C. brachiatus*. Only *C. furcatus* is known to the author from a more westerly location, namely 10 miles south of the Cape of Good Hope (DF).

C. furcatus, *C. calaninus* and *C. gracilis* are known in the tropical and temperate parts of the three oceans, while the rarer *C. elongatus* has up to the present been found only in the Pacific Ocean and in the northern part of the Indian Ocean.

C. pacificus was discovered in 1956 by TAKUO CHIBA in the vicinity of the Bikini Atoll. Shortly before the author found this species in his material, his colleague Dr F. MOMBECK had identified it in a 50–0 metre vertical haul from shallow water near Mauritius (IOP).

Clausocalanus arcuicornis (DANA). *Cl.*: W, S, E; *Tan.*

St. III, VI, VIII to XI (only ♀ ♀).

In the author's samples this species shows in respect of its occurrence and abundance a very close agreement with *Centropages brachiatus*, and it is on the whole more abundant round western South Africa than in the east (DF). It is one of the most widely distributed Copepoda.

L = ♀1·18–1·97, ♂0·96–1·09.

Two length groups can be distinguished in the females. There are ovigerous females measuring only 1·24 mm. The larger individuals (over 1·50 mm.) frequently have a bluish colour. It is possible that we have an example here of that dimorphism which was first described by SEWELL and later confirmed by numerous other investigators (*formae major* and *minor*). A morphological analysis of the South African forms must be held over for a later contribution. Large individuals were seen in this material at St. VIII only.

Clausocalanus furcatus (BRADY). *Cl*: W, E; *Tan.*

This species occurred in all samples except X and XII (ovigerous females in I; males in II, IV and V).

To the east of South Africa this species is much more abundant than the former. It lives in all warm seas.

L = ♀1·25.

Clausocalanus paululus FARRAN. New to South Africa.

St. X (♀).

L = 0·86.

This species occurs in the Bay of Biscay and has also been found in the south-western Pacific Ocean (FARRAN). It has recently also been recorded east of Mauritius by TANAKA (1960).

Clytemnestra rostrata (BRADY). New to South Africa.

St. V and IX.

L = 1·02. Night catches.

Clytemnestra scutellata (DANA). New to South Africa.

St. II. Night catches.

Both species occur in all oceans. Off South Africa they are rare in the surface plankton (100–0 m.) (DF).

Copilia mediterranea CLAUS. New to South Africa.

St. VI (juv. ♀).

L = ♀2·85–4·16, ♂5·20–6·20.

Copilia mirabilis DANA. New to South Africa.

St. II and III (♀ ♀).

L = ♀2·63–3·85, ♂4·84–5·15.

Both *Copilia* species are distributed in all warm seas. Off South Africa, however, *C. mirabilis* has not yet been found in the Atlantic area although its most western location lies 10 miles south of the Cape of Good Hope. *C. mediterranea* has already been encountered in the open ocean off Luderitz (South West Africa) and also off Natal (DF).

Corycaeus (*Ditricho-*) *africanus* F. DAHL. New to South Africa.

St. VII (♂).

L = 1·11.

Corycaeus (*Onycho-*) *agilis* DANA. *Br*; *Tan.*

St. IV (♀ ♀) and XI (♂ ♂).

L = ♂0·80–0·86.

Corycaeus (*Ditricho-*) *asiaticus* F. DAHL. *Tan.*

St. I to IV, VII, VIII (only ♂ ♂).

L = ♂1·07–1·15.

Corycaeus (*C.*) *crassiusculus* DANA. *Br. Tan.*

St. I (♂), III (♀), VII (♂), XI (ovigerous ♀, ♂).

L = ♀1·48–1·69, ♂1·47–1·49.

Corycaeus (*Ditricho-*) *dubius* FARRAN. New to South Africa.

St. I (♀).

L = 1·00.

Corycaeus (*Onycho-*) *latus* DANA. New to South Africa.

St. IV and VIII (♂ ♂).

L = 0·86–0·93.

Corycaeus (*Uro-*) *longistylis* DANA. *Br.*; *Tan.*

St. II (♀) and III (♂ ♂).

L = ♀2·38, ♂2·10.

Corycaeus (*Onycho-*) *pacificus* F. DAHL. *Tan.*

St. III (♀ ♀), VIII, X, and XI (only ♂ ♂).

L = ♀1·09–1·15, ♂1·08.

Corycaeus (*C.*) *speciosus* DANA. *Cl*: E; *Br.*; *Wo*: E.

St. II, III, V, VIII, and XI (♀ ♀ only in VIII, ♂ ♂ in others).

L = ♀1·89–1·97, ♂1·66–1·72 (in XI: 1·45–1·80).

Corycaeus (*Ditricho-*) *subtilis* F. DAHL. *Tan.*

St. I (♂).

L = ♂0·82.

Corycella concinna DANA. *Tan.*

St. I to VIII, and XI (I to IV: spermatophore-bearing ♀ ♀ and numerous ♂ ♂).

L = ♀0·86, ♂0·81.

Corycella curta FARRAN. New to South Africa.

St. X (♀).

L = ♀0·74.

Corycella gibbula GIESBRECHT. New to South Africa.

St. I to V, and VIII. (I to V: ♀ ♀ with spermatophores, and ♂ ♂).

L = ♀0·84.

Ctenocalanus vanus GIESBRECHT. New to South Africa.

St. XI (♀).

L = ♀1·18–1·30.

This species easily escapes notice, especially when the organisms occur among numerous specimens of *Paracalanus* or *Clausocalanus*, as is often the case in our waters.

In South African plankton this species is by no means rare, especially along the West coast, but its distribution appears to be irregular. The author gained the impression that it is encountered mainly in the coldest patches of fresh upwelled water (± 10°C) where the other Copepod species are poorly represented. This does not mean that it is a cold stenotherm because it also occurs in warmer waters (DF, IOP).

It occurs in tropical seas and in the Mediterranean, as well as in the Antarctic Ocean. It had not been recorded in the Indian Ocean, until it was found recently south of Madagascar in at least 20 samples of the IOP material, one of them being taken near the surface off Delagoa Bay, the others at various depths ranging from 750 to 1,000 metres. Its distribution in deep water shows an agreement with that of *Calanoides carinatus* and *Calanus tonsus*.

Eucalanus attenuatus (DANA). *Cl*: E; *Wo*: S, E; *Br*.

St. II, III, X and XI (only juven.).

L = ♀4·74–6·40, ♂5·76.

Eucalanus elongatus DANA. *Cl.*: E.

St. V (juven.).

L = ♀5·78–6·88, ♂4·4–4·54.

Eucalanus monachus GIESBRECHT. *Cl.*: E.

St. VII (♀).

Eucalanus mucronatus GIESBRECHT. *Cl*: E; *Tan*.

St. III (♀) and VII (juven. ♀).

L = ♀3·13.

Eucalanus pileatus GIESBRECHT. *Cl*: E.

St. II to V and VII (♀ ♀ + ♂ ♂).

L = ♀2·19–2·22.

Eucalanus subcrassus GIESBRECHT. *Cl.*: E.

St. VI (one ♀ + one ♂).

L = ♀2·10–2·81.

All of these *Eucalanus* species occur in the warm and temperate areas of the three oceans. Off South Africa, *E. attenuatus*, *E. elongatus*, *E. pileatus* and *E. subcrassus* are fairly abundant (DF).

Euchaeta wolfendeni A. SCOTT. New to South Africa.

St. II (ovigerous and juvenile ♀ ♀) and III (juven. ♀).

This species is Indo-Pacific. It has been found off Natal and Mocambique (DF, IOP).

L = ♀2·66–2·77.

Euterpina acutifrons (DANA). *Br.*; *Tan*

All samples, except XII, contained ♀ ♀, IV to VII ovigerous specimens, and VII also ♂ ♂.

L = ♀0·58–0·82, ♂0·62–0·64.

This species is present round South Africa and is known in all seas. Its occurrence in the author's material points to a distribution similar to that of *Calanus finmarchicus*, being more abundant on the Agulhas Bank. It is significant that on the whole voyage from Japan to Antarctica, the SOYA found this species only here, 17 individuals occurring in one sample.

Labidocera acutum (DANA). *Cl*: E; *Wo*: E; *Br*.

St. I to IV, VI and VII (adult ♀ ♀ and ♂ ♂ in I to III only, elsewhere juveniles).

L = ♀3·02–3·35, ♂2·95–3·30.

The above distribution is completely in agreement with the general findings round South Africa (DF), as well as with the literature: the species is more abundant in the Indo-Pacific than in the Atlantic area [cf. WOLFENDEN (1911), WILSON (1942)].

Labidocera minutum GIESBRECHT. New to South Africa.

St. IX (♀).

L = 1·94–2·04.

This species has hitherto been found in the South African area only along the south and east coasts (DF) and for the rest only in the Indo-Pacific area (GIESBRECHT, A. SCOTT, WILSON).

Macrosetella gracilis (DANA). *Wo*: S; *Br*; *Tan*.

St. I, II, V to VII (♂ ♂ here) and XI.

L = ♀1·30–1·40.

This species is distributed in the warm waters round South Africa, mostly in small patches, but occasionally it occurs in swarms. It is more abundant in the Agulhas Current (DF). The general distribution is cosmopolitic, including the Antarctic Ocean.

Mecynocera clausi I. C. THOMPSON. New to South Africa.

St. III and XI.

L = 1·09–1·29.

This species is cosmopolitic and is fairly abundant here and there round South Africa (DF).

Metridia lucens BOECK. *Cl*: W, S.

St. X and XI.

L = ♀2·24–2·92, ♂1·78–1·83.

This species is one of our most important food organisms for fish and plays a major role in many of the large plankton swarms in the Benguela Current area. It shows a preference for cold water and the densest swarms occur near the coldest patches of upwelling. Where warm Atlantic water lies near the surface along the west coast, this species can be found in deeper water or below the thermocline. It is also found regularly along the south coast in 100–0 metre vertical hauls, but swarms are rarer here than off the west coast (DF).

Its general distribution includes not only the North and South Atlantic and Pacific areas but also areas near the Galapagos and Philippine Islands where it has been found in small numbers. The author was unable to find any data on the Indian Ocean in the literature, except for one laconic observation of SARS (1925): "Mer Rouge". In the area south of Madagascar this species has, however, been taken in five closing net catches at depths between 500 and 1,500 metres (IOP).

Microsetella norvegica (BOECK). New to South Africa.

St. III, V, VII and IX to XII (only ♀).

L = ♀0·40–0·56.

Microsetella rosea (DANA). *Tan.*
St. V and X.
L = ♀0·79–0·93.

The distribution of these two species in our area compares well with that given by WILSON in the Carnegie plankton, i.e. *norvegica* more abundant in the Atlantic, *rosea* more abundant in the Indian (resp. Pacific) Ocean.

In the deep catches south of Madagascar both species show a certain agreement in their distribution with that of the calanids *Calanoides carinatus* and *Calanus tonsus*. *M. norvegica*, however, does not occur near the surface there, whereas *rosea* does (IOP).

Nannocalanus minor (CLAUS). *Cl*: W, S, E.; *Tan.*
St. II, III, VI, VII, IX, X and XI. Night sections.
L = ♀1·75–2·20, ♂1·67–1·84.

According to WILSON (1950), " this is one of the most widely distributed Calanids ". This statement is entirely pertinent in the South African area, since this species is absent only from a very narrow strip along the west coast where the temperature is too low. At times it represents more than 50 per cent of the Copepoda found in a catch (DF).

Oithona fallax FARRAN. *Tan.*
St. XI ♀ ♀.

Oithona nana GIESBRECHT. *Cl*: S; *Tan.*
St. VII to IX, XI and XII (mainly night sections).
L = ♀0·62.

This species is abundant round our coast, particularly in colder water.

Oithona plumifera BAIRD. *Cl*: W, S, E; *Wo*: W, E; *Br*; *Tan.*
St: Present everywhere except I, II, VII and IX.
L = ♀1·12–1·39.

Oithona rigida GIESBRECHT. *Cl.*: E.
St. III (♀).
L = ♀0·90.

Oithona tenuis ROSENDORN. New to South Africa.
St. XII (♀).
L = ♀1·27.

Oncaea clevei FRÜCHTL. *Tan.*
St. II (ovigerous ♀).
L = 0·68.

Oncaea media GIESBRECHT. *Cl*: W, E; *Tan.*
St. I, III, XI and XII (♀ ♀ everywhere, in III: ovigerous ♀ ♀ + ♂ ♂).
L = ♀0·62–0·97, ♀0·64–0·75.

Ocaea mediterranea (CLAUS). *Cl*: W, S, E.
St. VI, VII, X and XI (ovigerous ♀ ♀ everywhere).
L = ♀1·33.

Oncaea subtilis GIESBRECHT. *Cl*: S.
St. VII, X, XI and XII (only ♀ ♀, ovigerous in XI).
L = ♀0·58–0·59.

Oncaea venusta PHILIPPI. *Cl*: W, S, E; *Wo*: E; *Br*; *Tan.*
St. I, II, III, V, VIII and X (ovigerous ♀ ♀ in III).
L = ♀0·99–1·50 (mostly 1·42–1·46), ♂0·87.

Most of the *Oncaea* species are cosmopolitic in warm and temperate areas.

Pachos tuberosum (GIESBRECHT). *Cl*: E; *Br.* (?).
St. III (♂).
L = ♂2·58–2·63.

In our area this species is found only off the Natal coast where it occurs infrequently but nevertheless regularly. Hitherto only males were taken (DF).

Paracalanus aculeatus (GIESBRECHT). *Cl*: S; *Tan.*
St. I to VI, XI and XII (♂ ♂ in V and VI).

This is a cosmopolitic species which in our area avoids the proximity of cold patches of upwelled water near the coast but for the rest it is the commonest *Paracalanus* species round South Africa.

Paracalanus crassirostris F. DAHL. *f. typica* FRÜCHTL. *Tan.*
St. II, V, VIII to XII.
L = ♀0·57–0·66.

In these specimens the anterior antennae extend as far as the extremity of the furca, in agreement with TANAKA'S remarks (1960), whereas SEWELL observes about his specimens from the Indian Seas : " The antenna reaches back only to the level of the posterior thoracic margin ".

In our area the species is abundant in the west (DF). MARQUES (1953) found the *forma scotti* FRÜCHTL in all plankton samples from Angola and frequently in great abundance.

Paracalanus denudatus SEWELL. New to South Africa.
St. I (♀).
L = 0·83.

Its presence has also been established from the South China Sea (TANAKA 1960) and the Great Barrier Reef (FARRAN 1936) right through the Northern Indian Ocean as far as the Arabian Sea (SEWELL 1947).

Paracalanus parvus (CLAUS). *Cl*: S; *Br*; *Tan.*
St. II (♀), VI to XII (♀ ♀ + ♂ ♂).
L = ♀0·90–0·95.

This species takes the place of *P. aculeatus* almost everywhere in the colder waters along our western and southern coasts where it may occur in large quantities (DF). It is cosmopolitic.

Pleuromamma abdominalis (LUBBOCK). *Cl*: W, E; *Wo*: W, S; *Br.*
St. VI and VII (♀ ♀). Night section.
L = ♀2·77–3·60, ♂3·18–3·40.

Pleuromamma robusta (F. DAHL). *Cl*: W, E·
St. II (♀ + juv.). Night section.

Pleuromamma gracilis (CLAUS). *Cl*: W, S, E; *Wo*: S.
St. V (♀ + juv. ♀).
L = ♀2·00–2·25.

All three of these *Pleuromamma* species are cosmopolitic.

Pontellina plumata (DANA). *Cl*: E; *Br.*
St. III and V (juven.).
L = ♀1·75–1·85, ♂1·43–1·58.

This species is a warm-water cosmopolite which is never abundant in our area but which occurs regularly in the warm waters off our coast; off Natal it is more numerous than elsewhere (DF).

Pseudodiaptomus nudus TANAKA. *Cl*: S; *Tan.*
St. IX, X and XI (ovigerous ♀ ♀, ♂ ♂ and juveniles).
L = ♀1·22–1·52 (mainly 1·42–1·48), ♂1·20–1·29.

TANAKA (1960) discovered this species in material from the Agulhas Bank and described it as being different from *Ps. serricaudatus* (T. SCOTT).

There can be no doubt that the organisms which were obtained from the same area and which CLEVE (1904) called *Ps. serricaudatus*, were really *Ps. nudus.*

This species occurs on the Agulhas Bank throughout the year and can at places be fairly numerous. Sometimes its area appears to extend westwards beyond the Cape of Good Hope, after which it turns to the north and appears as a narrow strip parallel to the west coast at least as far as 30°S. (DF). This distribution picture suggests water transport according to the same pattern, possibly a northward sweeping arm of the Agulhas Current.

It is noteworthy that the author also repeatedly found this species off the Kunene River mouth (southern boundary of Angola). MARQUES (1953, 1958) mentions the occurrence of *Ps. serricaudatus* off Angola, and her measurements agree more closely with T. SCOTT'S (1894, as *Heterocalanus serricaudatus*) than with those of the author (DF).

The genus *Pseudodiaptomus* is well known for its numerous species, the majority of which are littoral forms with a limited distribution.

Rhincalanus cornutus DANA. *Cl*: E; *Br.*
St. I (♀), II to V (juven.) and VII (♀). Adults in night sections.

Rhincalanus nasutus GIESBRECHT. *Cl.*: W, S, E.
St. II, VII (adult ♀ ♀), and X and XI (juven. ♀ ♀). Night sections.
L = ♀3·60–4·52, ♂3·45–3·67.

Although both *Rhincalanus* species are represented in the waters round South Africa and in fact both live in the three great oceans, it is very clear from their distribution in our area that *Rh. cornutus* has a predilection for warmer water; its real habitat is the Agulhas Current since it is a rarity off the west coast. *Rh. nasutus* on the other hand, is abundant along the west coast, especially in the Benguela Current, and also over the Agulhas Bank (DF). Both species are present in the S.W. Indian Ocean, *cornutus* seldom being encountered deeper, and *nasutus* seldom higher, than the 500 m. level (IOP). This occurrence is in agreement with SEWELL'S diagram (1948, p. 366, Fig. 81) of the vertical distribution of the *Rhincalanus* species in the Indian Ocean.

Sapphirina gastrica GIESBRECHT. New to South Africa.
St. III (♂).
L = 1·85.

Sapphirina nigromaculata CLAUS. *Cl*: E.
St. II (ovigerous ♀ + juven.).
L = ♀2·16–2·34, ♂1·81–2·57.

Sapphirina ovatolanceolata-gemma (DANA). *Cl*: E; *Br*; *Tan.*
St. II (juv. ♀) and V (♀).
L = ♀2·22, ♂3·86.

These *Sapphirina* species occur in all three oceans.

Scolecithrix danae (LUBBOCK). *Cl*: W. E; *Wo*: W; *Br.*
St. II (juv. ♀).
L = ♀1·94–2·19, ♂2·05–2·39.

This is a cosmopolitic warm-water species which occurs regularly round South Africa but which is nowhere very abundant (DF).

Temora discaudata GIESBRECHT. *Cl*: E.

St. II, IV to VII, IX and XI (Both sexes, with juveniles also in V).

L = ♀1·73–2·05, ♂1·78–1·95.

This is an Indo-Pacific species, although THOMPSON and A. SCOTT recorded it on one occasion in the Mediterranean. At times it is fairly abundant along our south and east coasts; its most westerly point of occurrence hitherto recorded lies 10 miles south of the Cape of Good Hope (DF).

Temora turbinata (DANA). *Br.* (as T. *africana*); *Tan.*

Everywhere except in St. XII (♂ ♂ in VI and IX; juv. in I, IV, V and VIII).

L = ♀(1·16)–1·34–1·45, ♂1·18–1·28.

This species is more abundant in our area than the foregoing and is also fairly numerous off the west coast—but never in the upwelled water (DF). It is a cosmopolite.

Undinula darwinii (LUBBOCK). *Cl*: E; *Br.*

St. I to III (♀ ♀ + ♂ ♂).

L = ♀2·08–2·39, ♂1·97–2·30.

Undinula vulgaris (DANA). *Cl*: E; *Br.*

St. I (♀).

L = ♀2·80–3·00, ♂2·47–2·60.

Both *Undinula* species were frequently found together in our nets. They are far more abundant in the eastern area but nevertheless not rare in the west. From their distribution pattern for the west coast, it is clearly apparent that they avoid the cold water. In winter when the upwelling is slightest, they may occur fom the Cape of Good Hope to far in the north (DF).

Both are cosmopolites. WILSON (1942) found *vulgaris* abundant in the Atlantic Ocean and *darwinii* more abundant in the Pacific Ocean. TANAKA (1960) encountered *vulgaris* even in the Sub-Antarctic area (48°S).

8.2 Discussion.

Before proceeding to draw conclusions from the above results, we should first consider the following three sources of errors:—

I. Only a single plankton catch is discussed here and if taken in another season its composition might have been different.

II. Only surface plankton was collected (from a depth not exceeding 4 metres). Its composition could have been strongly influenced by the daily vertical migration of a number of species. For this reason the absence of a species from certain parts of a section should not necessarily be regarded as a gap in its distribution because the organisms may possibly have retreated temporarily to deeper water under the influence of sunlight.

III. Our knowledge of the general distribution of the Copepoda is still very incomplete and partly uncertain. Many data from the literature upon which one is dependent for a bio-geographic assessment of one's own findings will in course of time appear to be incomplete or sometimes even inaccurate as a result of incorrect identification.

In regard to points I and II, the following observations may be made:—

Ad I. Up to a certain point the possible occurrence of seasonal changes may be tested against the results of earlier investigations in this area and against the unpublished data in the archives of the Division of Sea Fisheries at Sea Point. Within the framework of this short communication it is not possible to enter into details, but none of the above-mentioned sources of information is in flagrant conflict with the author's results. Only TANAKA'S (1960) data on the Agulhas Bank station on 1/12/57 will be briefly mentioned here because they were obtained in the opposite season and by a method very similar to the author's, namely by filtration of the cooling water of the ship's engines.

Of the 37 species obtained by TANAKA at this station, 29 also occur in the author's list and of these 29 species common to both investigators the author caught only nine in another part of the section. Among these nine there were three *Corycaeus* species and one *Oncaea*, in other words, groups which, due to the author's method, have not correctly been reflected here (see " Method ", sixth paragraph, p. 8). The remaining five species were:—

Canthocalanus pauper (1 ♀, 2 ♂ ♂).
Eucalanus mucronatus (1 juv.).
Acrocalanus gracilis (5 ♀ ♀).
Acartia negligens (3 ♀ ♀, 1 juv.).
Sapphirina gemma (2 ♀ ♀).

Sapphirina gemma and *Eucalanus mucronatus* are isolated random catches of little significance. The presence of the other three species could possibly be

explained by seasonal fluctuations. In the author's material they were found in the Agulhas Current and in the transitional zone. In December easterly and south-easterly winds prevailed in this area and these may perhaps have shifted the boundary of the transitional zone to the west. It should be observed in this connection, however, that the SOYA approached this station from the east. The possibility exists that part of the plankton obtained at that station had been retained for some considerable time in the less well-flushed parts of the cooling system after being taken in at some point further to the east.

Ad II. In regard to the vertical migration of certain species, the following observations may be made.

Forty species were caught only in those sections traversed *wholly or partly* during night-time. Among these, 19 species were obtained *only at night*, the following five occurring in more than one sample:—

Acartia danae.
A. negligens.
Calanopia minor.
Candacia bipinnata.
Pleuromamma abdominalis.

Besides being taken in night catches, ten of the above-mentioned 40 species were also found in catches made partly during daylight in the evening or the morning. The following species occurred three to four times in nocturnal catches and one to three times in mixed catches:—

Macrosetella gracilis.
Nannocalanus minor.
Rhincalanus nasutus.
Temora discaudata.

Each of the remaining 11 was found only in one sample, and on each occasion in a sample which had been obtained partly during daylight and partly in the dark.

Finally there were further species which were found both at night and during the day but which were appreciably more abundant at night, namely:—

Calanus finmarchicus.
Centropages brachiatus.
Clausocalanus arcuicornis.
Cl. furcatus.
Euterpina acutifrons.
Paracalanus aculeatus.
P. crassirostris.

As will be seen from the distribution discussed below, the daily vertical migration caused no discernible disturbance in the distribution pattern of the numerically important species.

In his attempt at a *biogeographic subdivision* of the coastal waters investigated, the author has made use of the four areas identified in the description of the temperature curve (Table I).

The species occurring in each separate area or in various regional groupings were determined, and these populations were then subjected to closer investigation and compared with one another.

For simplicity's sake the respective areas will be indicated below by letters as follows:—

A for I–III: Agulhas Current and its marginal area,
B for IV–VII: Transitional area,
C for VIII–IX: Eastern Agulhas Bank, and
D for X–XII: Western Agulhas Bank and Cape Peninsula.

The four areas are similar in their length and light relationships:—

A: 250 miles—day and night;
B: 210 miles—day and night;
C: 180 miles—day and evening (till 2130); and
D: 170 miles—day and night.

Only in the case of C was the period of darkness shortened and this fact may perhaps explain the relative paucity of species found in that area.

TABLE 4.—Occurrence in Separate Areas.

	Species.	Atlantic Ocean.		Cape–Durban.												Indian Ocean.		Pac. Ocn.
				XII.	XI.	X.	IX.	VIII.	VII.	VI.	V.	IV.	III.	II.	I.			
				D.			C.		B.				A.					
		Literature.	DF.													DF.–IOP.	Literature.	Literature.
A	*Acartia amboinensis*													r		r	×	×
	Candacia curta	×	×											r		×	×	×
	Candacia truncata	×												r	r	×	×	×
	Centropages elongatus													r		×	×	×
	Centropages pacificus												r			×	×	×
	Clytemnestra scutellata	×												r		×	×	×
	Copilia mirabilis	rare											f	r		×	×	×
	Corycaeus dubius														r		×	×
	Corycaeus longistylis												r				×	×
	Corycaeus subtilis														r		×	×
	Euchaeta wolfendeni												r	r		×	×	×
	Oithona rigida												r				×	×
	Oncaea clevei													r			×	×
	Pachos tuberosum												r			×	×	×
	Paracalanus denudatus														r		×	×
	Pleuromamma robusta	×	×											f			×	×
	Sapphirina gastrica	×											r				×	×
	Sapphirina nigromaculata	×	×											r		×	×	×
	Scolecithrix danae	×	×											r		×	×	×
	Undinula darwinii	rarer	×										r	f	f	×	×	×
	Undinula vulgaris	×	×										r			×	rarer	rarer
AB	*Acartia negligens*	×	×						f	r	r		r			×	×	×
	Acrocalanus monachus										r				r	×	×	×
	Calanopia minor								r	r				r		×	×	×

TABLE 4.—Occurrence in Separate Areas (*continued*).

	Species.	Atlantic Ocean.		Cape–Durban.												Indian Ocean.		Pac. Ocn.
				XII. XI. X. D.			IX. VIII. C.		VII. VI. V. IV. B.				III. II. I. A.					
		Literature.	DF.													DF.–IOP.	Literature.	Literature.
	Calocalanus contractus	×									r		r			×	×	×
	pavo	×	×							r	r		f	r	r	×	×	×
	Candacia catula									r			r		r	×	:	×
	Canthocalanus pauper								r	r	r	r	r			×	×	×
	Centropages calaninus	×								r	r		r			×	×	×
	furcatus	×							r	r	r	f		f		×	×	×
	gracilis	×									r		r	r		×	×	×
	Eucalanus mucronatus	×							r				r				×	×
	pileatus	×							f		r	r	r	r			×	×
	Labidocera acutum	×	×						r	r		f	r	f	r	×	×	×
	Pontellina plumata	×									r			r		×	×	×
	Rhincalanus cornutus	×	×						f		f	r	f	r		×	×	×
	Sapphirina ovatol.-gemma	×	×								r				r	×	×	×
ABC	*Acrocalanus gracilis*	× (south)					f		f	r	f	+	+	f	f	×	×	×
	Calocalanus plumulosus	×					r		f	r	f	r	f	r		×	×	×
	Corycaeus asiaticus							f	f				r	r	r	×	×	×
	Corycella gibbula	(×)						r			f	r	f	f	f		×	×
B	*Copilia mediterranea*	×	×							r						×	×	×
	Corycaeus africanus	×							f								(× ?)	
	Eucalanus elongatus	×	×								r					×	×	×
	monachus	×	×						r							×	×	×
	subcrassus	×								f						×	×	×
	Pleuromamma abdominalis	×	×						r	r						×	×	×
	gracilis	×	×								r					×	×	×
BC	*Clytemnestra rostrata*	×	×				r				r					×	×	×
	Corycaeus latus	×						r				r					×	×
C	*Labidocera minutum*						r										×	×

TABLE 4.—Occurrence in Separate Areas (*continued*).

	Species.	Atlantic Ocean.		Cape-Durban.												Indian Ocean.		Pac. Ocn.
		Literature.	DF.	XII.	XI.	X.	IX.	VIII.	VII.	VI.	V.	IV.	III.	II.	I.	DF. IOP.	Literature.	Literature.
				D.			C.		B.				A.					
D	*Clausocalanus paululus*	×				r											×	×
	Corycella curta	×				r											×	×
	Ctenocalanus vanus	×	×		r											× (abyssal)		×
	Metridia lucens	×	×		f	r										× (abyssal)	× (S.A.)	×
	Oithona—																	
	tenuis	×		r													×	
	fallax	×			f												×	×
CD	*Centropages brachiatus*	×	×	r	c	+	+	f								×	(× ?) Cleve)	×
	Pseudodiaptomus nudus		×		f	f	f									×	×	
	Calocalanus tenuis	×	×		r	f	f									×	(S.A.)	
BCD	*Calanus tenuicornis*	×	×			r			r		r	r				×	rare	×
	Calocalanus styliremis	×			r		r			r	r						×	×
	Candacia bipinnata	×	×			r	r		r							×	×	×
	Corycaeus agilis	×			f							f					×	×
	Microsetella rosea	×	×			r					r					×	×	×
	Oithona nana	×	×	f	f		f	f	+							×	×	×
	Oncaea																	
	mediterranea	×	×		f	f			f	f							×	×
	subtilis	×	×	f	f	f			f							×		
ACD	*Corycaeus pacificus*				f	f		f					f			×		×
ABD	*Acartia danae*	×	×		r					f				f		×	×	×
	Corycaeus crassiusculus	(× ?)			f				r				f		r	×	×	×
	Macrosetella gracilis	×	×		r				r	r	r			f	r	×	×	×
	Paracalanus aculeatus	×	×	f	c					+	c	f	r	+	f	×	×	×
	Rhincalanus nasutus	×	×		r	r			r					r		×	×	×

TABLE 4.—Occurrence in Separate Areas (*continued*).

	Species.	Atlantic Ocean.		Cape–Durban.												Indian Ocean.		Pac. Ocn.
		Literature.	DF.	XII.	XI.	X.	IX.	VIII.	VII.	VI.	V.	IV.	III.	II.	I.	DF.–IOP.	Literature.	Literature.
				D.			C.		B.				A.					
ABCD	*Calanoides carinatus*.....	×	×	f	f	f	+		f		r	r	r	f	r	×	× (S.A.)	×
	Calanus finmarchicus.....	×	×		f	+	+	f	c	r	f		r			×	× (S.A.)	×
	Clausocalanus arcuicornis.....	×	×		f	c	cc	f		f			r			×	×	×
	furcatus.....	×	×		r		f	+	c	f	c	+	+	c	f	×	×	×
	Corycaeus speciosus.....	×	×		f			r			r		f	f		×	×	×
	Corycella concinna.....				r			r	f	f	+	f	+	+	r		×	×
	Euterpina acutifrons.....	×	×		f	r	f	f	c	cc	cc	+	r	f	f	×	×	×
	Microsetella norvegica.....	×	×	r	r	r	r		r		r		r			×	×	×
	Nannocalanus minor.....	×	×		cc	ccc	+		f	f			r	f		×	×	×
	Oithona plumifera.....	×	×	r	c	+		r		f	f	f	f			×	×	×
	Oncaea venusta.....	×	×			f		r			f		f	c	f	×	×	×
	Paracalanus crassirostris.....	×	×	f	f	+	+	f			f			+		×	×	×
	parvus.....	×	×	+	+	ccc	cc	cc	c	f				r		×	×	×
	Temora discaudata.....	? (South)			r		r		f	+	f	r		c		×	×	×
	turbinata.....	×	×		r	r	f	f	c	r	c	f	f	f	r	×	×	×
ACD	*Eucalanus attenuatus*.....	×	×		r	r							f	r		×	×	×
	Mecynocera clausi.....	×	×		r								r			×	×	×
	Oncaea media.....	×	×	r	f								f		f		×	×

In Table 4 the species are grouped according to their occurrence: A, B, C or D for only one area; AB, BC, CD; ABC or BCD for 2 (or 3) adjacent areas, ABCD for all four areas, and ABD, ACD or AD for non-adjacent areas.

The various groupings in Table 4 can be summarised as follows from the point of view of species-content.

(*a*) *Individual areas*:—

Area.	Number of Species Found.	
	Only there.	Also elsewhere.
A.....	21	42
B.....	7	48
C.....	1	28
D.....	6	34

The 21 A species were made up as follows:—

11 solely Indo-Pacific,
4 predominantly Indo-Pacific, and
6 cosmopolitic.

Amongst the seven B species there were:—

6 cosmopolites;
1 coastal species from W. Africa (F. DAHL), which possibly also occurs in the Indian Ocean (SEWELL 1947).

The six D species included:—

3 cosmopolites,
2 not previously found in the Indian Ocean, and
1 not yet found in the Pacific Ocean.

The solitary C species is a rarity which has not yet been encountered outside the Indo-Pacific area.

(*b*) *Adjacent areas.*

Area.	Number of Species Found.	
	Only there.	Also elsewhere.
AB.....	16	65
BC.....	2	59
CD.....	3	44

The easterly part (AB) is still the richest in species although it is poorer than A. The predominantly Indo-Pacific character of A is already diminishing here and it will not reappear further to the west.

The 16 AB species contain only—

4 Indo-Pacific specimens as against 12 cosmopolites.

Both BC species are cosmopolites, while the three CD species are bio-geographic curiosities (see " Systematic Review " above).

Further comparisons between areas do not reveal any important facts. As a conclusion from the above findings, the author wishes to emphasise that in the A area a Copepoda community with a strong Indo-Pacific character, which we will call the *Agulhas Current community*, was identified and that this community did not occur over the northern part of the Agulhas Bank in July, 1961. It had already disappeared from the coastal waters off East London. On the strength of observations made on other occasions (DF) the author is of the opinion that this community seldom if ever extends beyond the eastern edge of the Agulhas Bank. Proof of this assertion, however, must be reserved for a later contribution.

(*c*) The *whole section* (ABCD) yielded 15 species which occurred in all four areas. It will clearly be seen from the table, however, that they are not uniformly distributed. In addition, their group includes those species which were most abundant in the author's material: 10 of the 15 species were marked with the abundance symbol *c* in at least one sample, this symbol having been given only twice outside this group.

As *eastern* components the following are clearly distinguishable:—

Clausocalanus furcatus (warm-water cosmopolite),
Corycella concinna (Indo-Pacific),
Temora discaudata (Indo-Pacific).

In the *south* the following species were most abundant:—

Calanus finmarchicus,
Euterpina acutifrons,
Temora turbinata.

Together with *Pseudodiaptomus nudus* and *Calocalanus tenuis*, the latter are so constant in their occurrence on the Agulhas Bank (DF) that the author feels tempted to regard this group of species as part of a *plankton community peculiar to the Agulhas Bank*.

The following species appear to be *western* components:—

Calanoides carinatus (represented in AB almost exclusively by juveniles),
Clausocalanus arcuicornis,
Nannocalanus minor,
Paracalanus crassirostris,
Paracalanus parvus.

Together with *Centropages brachiatus*, *Metridia lucens* and perhaps also *Ctenocalanus vanus*, they occur in very great abundance along the whole

west coast and are associated with the Benguela Current (DF). Along the West Coast, the dispersion area of these species runs parallel to direction of the Benguela Current. Each of them seems to keep at an appropriate distance from the cold core, within the temperature limits that suits it. The author proposes to regard this group of species as members of the *plankton community of the Benguela Current.*

A striking feature in the case of the groups ABCD and ABD is the richness in species of sample XI. It contained 34 species, being surpassed in this respect only by samples II, III and V. It would be possible to regard at least 11 species in the author's material as southern and south-eastern warm-water inhabitants without further ado if they had not also cropped up in sample XI. They were the following:—

Acartia danae,
Calocalanus styliremis,
Cc ycaeus agilis,
Corycaeus crassiusculus,
Corycaeus speciosus,
Clausocalanus furcatus,
Corycella concinna,
Macrosetella gracilis,
Mecynocera clausi,
Paracalanus aculeatus
Temora discaudata.

Sample X also appears to share in this phenomenon because it contains six species which are distribute in a manner similar to that of the foregoing and of which four also occur in XI:—

Corycaeus pacificus,
Eucalanus attenuatus,
Oncaea media,
Oithona plumifera,
Calanus tenuicornis,
Oncaea venusta.

When one recalls the sharp temperature increase of 1·5°C which took place in a ten-mile strip on the boundary between sections X and XI, one cannot help feeling inclined to associate it with the local occurrence of so many warm-water species, and it would appear that a tongue of warm water penetrated to a point near the coast in this locality. The presence of the following four Indo-Pacific species, namely—

Corycaeus crassiusculus,
Corycaeus pacificus,
Corycella concinna,
Temora discaudata

gives an indication of the possible origin of this water; it could perhaps have been a northward moving off-shoot of the Agulhas Current.

9. Literature.

Only the papers quoted in the text are mentioned here.

BERNARD, M., 1958.—Révision des Calocalanus (Copépodes Calanoida) avec description d'un genre nouveau et de deux espèces nouvelles. *Bull. Soc. Zool. France*, T. LXXXIII. 15 pp.

——— 1960.—Famille des Calocalanidae. *Conseil Internat. Explor Mer.* Zooplankton, Sheet 36 (First Revision), 5 pp.

BOWMAN, TH. E., 1957.—A new species of *Calanopia* (Copepoda Calanoida) from the Carribean Sea. *Proc. U.S. Nat. Mus.*, 107, pp. 39–45.

BRADY, G. S., 1914.—On some pelagic Entomostraca collected by Mr. J. Y. Gibson in Durban Bay. *Ann. Durban Mus.*, Vol. 1, pp. 1–9..

——— 1914.—On further pelagic Entomostraca collected by Mr. J. Y. Gibson in Durban Bay. *Ann. Durban Mus.*, Vol.: 1, pp. 25–28.

——— 1915.—Notes on the pelagic Entomostraca of Durban Bay. *Ann Durban Mus.*, Vol. 1, pp. 134–146.

CHIBA, T., 1956.—Studies on the development and the systematics of Copepoda. *Jnl. Shimonoseki College of Fisheries*, Vol. 6, (1), 90 pp. (In Japanese with English summary).

CLEVE, P. T., 1904.—The Plankton of the South African seas. I. Copepoda. *Marine Investigations in South Africa*, Vol. 3 (1905), pp. 177–210.

DAHL, M., 1912.—Die Copepoden der Plankton-Expedition. I. Die Corycaeinen (mit Berücksichtigung aller bekannten Arten). *Ergebn. Plankton-Exped. Humboldt Stiftung*, II, f. 1, iv + 135 pp.

DAKIN, W. J. AND COLEFAX, A. N., 1940.—The plankton of the Australian coastal waters off New South Wales, Part 1. *Public University of Sidney, Department of Zoology, Monogr.* 1, 215 pp.

DANA, J. D., 1852–55.—Crustacea. U.S. Exploring Expedition during the years 1838–42 under the command of Charles Wilkes; 13 (2); 1019–1262.

DE DECKER, A., 1960. Communication provisoire sur la répartition des Copépodes planctoniques marins de l'Afrique du Sud. *CCTA/CSA, Lagos/Bukavu: Colloque de biologie marine et de pêches maritimes sur les côtes orientales de l'Afrique.* Le Cap, 12–17 Sept., 1960. 3 pp. (Roneoed).

FARRAN, G. P., 1926.—Biscayan plankton collected during a cruise of H.M.S. Research, 1900. Part XIV. The Copepoda. *Jnl. Linnean Soc. London*, Zoology, Part XXXVI, pp. 219–310.

——— 1936.—Great Barrief Reef Expedition 1928–29. Scientific Reports, Vol. V (3), Copepoda. *British Museum (Natural History)*, pp. 73–142.

FRÜCHTL, F., 1924.—Die Cladoceren und Copepodenfauna des Aru-Archipels. *Arb. Zool. Instit. Univers. Innsbruck.* II, pp. 25–136.

MARQUES, E., 1953.—Copépodes marinhos de Angola. I. Calanoida. *Lisboa, Trabalhos da Missao de Biologia Maritima*, 5, pp. 85–126.

——— 1957.—Copépodes dos mares de Angola. II. Ciclopoida e Harpacticoida. Ibid, 20, pp. 131–150.

——— 1958.—Copépodes marinhos de Angola. (2a Campanha 1952–53). *Ibid.*, 24, pp. 197–222.

ROSE, M., 1929.—Copépodes pélagiques, particulièrement de surface, provenant des campagnes scientifiques de S.A.S. le Prince Albert Ir de Monaco. *Rés. camp. scientif. Monaco*, 78, 132 pp.

ROSENDORN, I., 1917.—Die Gattung Oithona. *Wiss. Ergebn Deutschen Tiefsee-Expedit.* 23 (1), 58 pp.

SCOTT, A., 1909.—The Copepoda of the Siboga Expedition. Pt. I: Free-swimming, littoral and semi-parasitic Copepoda. *Siboga Expedition Monograph* 29 *A*, 323 pp.

SCOTT, TH., 1894.—Report on the Entomostraca from the Gulf of Guinea. *Trans. Linnean Soc. London*, Second Series, Vol. 6, Zoology, pp. 1–16.

SEWELL, R. B. S., 1929–32.—The Copepoda of the Indian Seas. Calanoida. *Calcutta, Memoirs Indian Mus.*, Vol. X, 407 pp.

——— 1947.—The free-swimming planktonic Copepoda. Systematic Account. *Sci. Repts. John Murray Exped.* 1933–34. Vol. 8 (1), 303 pp.

——— 1948.—The free-swimming planktonic Copepoda. Geographical Distribution. *Ibid*, pp. 317–592.

STEBBING, TH. R. R., 1910.—General Catalogue of South African Crustacea (Part V of 1 South African Crustacea for the Marine Investigations in South Africa). *Annals South African Mus.*, 6 (4), pp. 281–593.

STEUER, A., 1923.—Bausteine zu einer Monographie der Copepodengattung Acartia. *Arb. Zool. Instit. Univ. Innsbruck*, 1 (5).

TANAKA, O., 1960.—Biological Results of the Japanese Antarctic Expedition. 10. Pelagic Copepoda. *Special Public. Seto Marine Biol. Labor*, 95 pp.

WILSON, C. B., 1942.—Copepods of the plankton gathered during the last cruise of the Carnegie. *Washington Sci. Res. Cruise VII of the Carnegie* 1928–29. Biology I, 237 pp.

——— 1950.—Copepods gathered by the U.S. Fisheries Steamer Albatross from 1887 to 1909, chiefly in the Pacific. *Smithsonian Instit. U.S. Nat. Mus. Bull* 100, Vol. 14 (4), IX + 300 pp.

WOLFENDEN, R. N., 1911.—Die Marinen Copepoden der Deutschen Südpolar Expedition 1901–03. II. Die pelagischen Copepoden der Westwinddrift und des südlichen Eismeeres. *Deutsche Südpolar Expedition*, 12 (Zool. Vol. 4), pp. 181–380.

DEPARTMENT OF COMMERCE AND INDUSTRIES

DIVISION OF SEA FISHERIES

SOUTH AFRICAN CONTRIBUTION TO THE INTERNATIONAL INDIAN OCEAN EXPEDITION:

(4) A Preliminary Report on the Planktonic Copepoda

by A. DE DECKER & F. J. MÓMBECK.

INVESTIGATIONAL REPORT No. 51

Invest. Rep. Div. Sea Fish. South Africa. 51: 1—67

Issued by the Division of Sea Fisheries, Beach Road, Sea Point, Cape Town, South Africa.

REPUBLIC OF SOUTH AFRICA

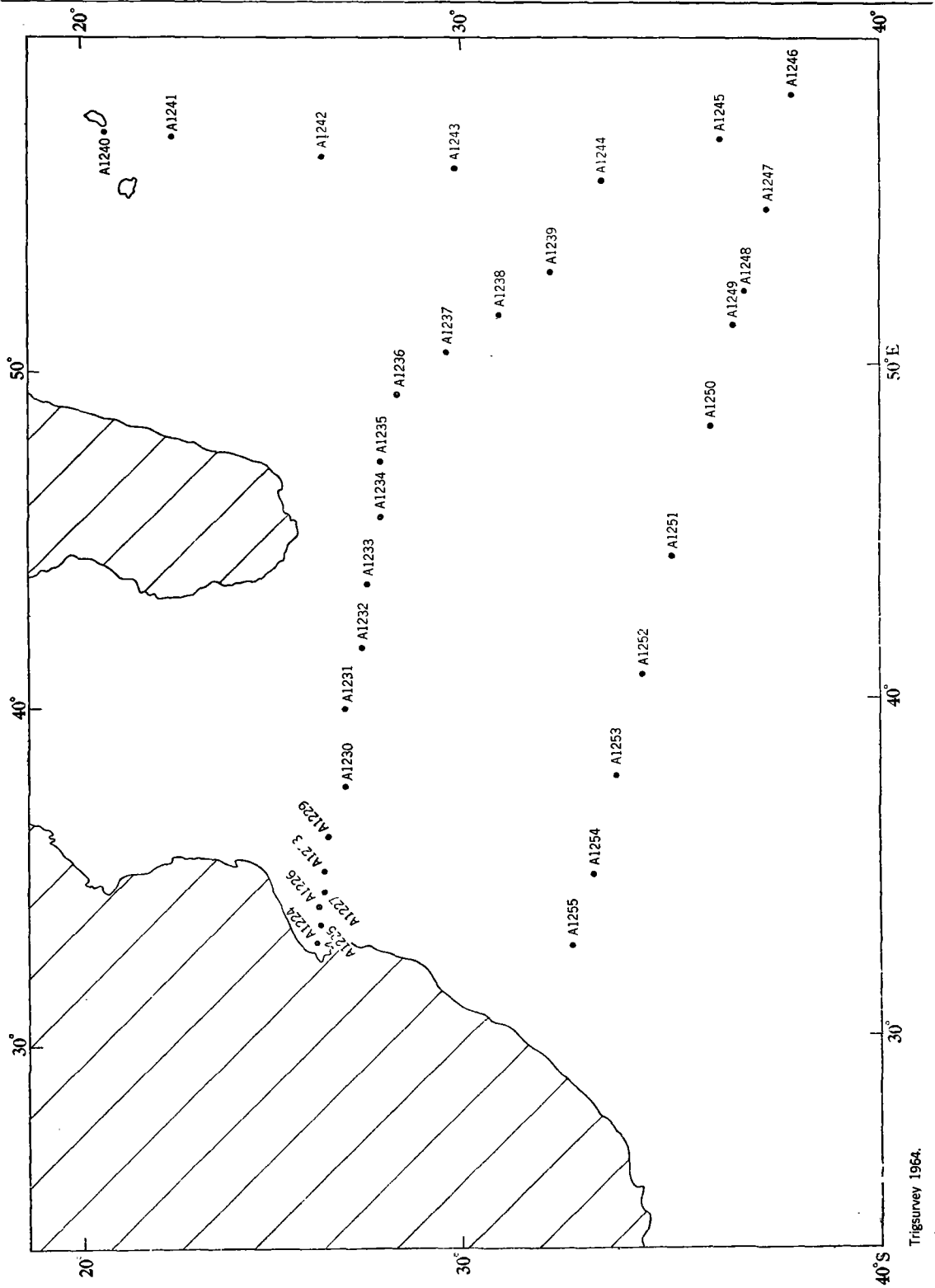
20°
30°
40°
50°
50° E
40° S
A1240
A1241
A1242
A1243
A1244
A1245
A1246
A1247
A1248
A1249
A1250
A1251
A1252
A1253
A1254
A1255
A1239
A1238
A1237
A1236
A1235
A1234
A1233
A1232
A1231
A1230
A1229
A1223
A1224
A1226
A1227
Trigsurvey 1964.

A PRELIMINARY REPORT ON THE PLANKTONIC COPEPODA

by

A. DE DECKER and F. J. MOMBECK.

1. Abstract.

Some 274 Copepod species were collected in the South Western Indian Ocean during 1961. Sixty-five of these species appear to be new to the Indian Ocean. They have been grouped into local communities and appear to indicate certain oceanographic phenomena. The bathypelagic Copepods are compared with those reported by SEWELL and A. SCOTT from the Northern Indian Ocean and the Indonesian Archipelago, respectively.

2. Introduction.

The area covered by the 1961 cruise of AFRICANA II is situated in one of the least known parts of the Indian Ocean as far as zooplankton, and especially the copepod fauna are concerned.

The examination of the AFRICANA II material yielded 274 Copepod species, among which 65 appear to be new to the Indian Ocean. It seems unlikely that further and more thorough processing of the samples will greatly add to the number of species stated above. Nevertheless, such a variety found during a relatively short cruise shows that the diversity in this part of the ocean is quite comparable with that of other oceanic areas where more intensive sampling was carried out in the past over greater areas and for longer periods. SEWELL's major papers (1929, 1932, 1947) on the Northern Indian Ocean make mention of a total of some 350 species found between Burma and East Africa. In samples taken by the Siboga Expedition in the Eastern Malay Archipelago, A. SCOTT (1909) identified 278 holoplanktonic species. Over 1,000 plankton samples collected by Prince ALBERT I of Monaco during his long cruises through the Atlantic north of the Equator included 348 Copepod species, as identified by SARS (1925) and ROSE (1929). C. B. WILSON (1942, 1950) found 281 species in the CARNEGIE collections and 473 species in those made by the ALBATROSS, both vessels having worked numerous stations scattered all over the Pacific as well as in some parts of the Western Atlantic north and south of the Equator. In the case of the ALBATROSS, this was carried on for over twenty-two years.

The variety of the Copepod fauna in our samples, together with a few observations on the spatial distribution of certain of its components, justifies this short preliminary report. The area concerned is of special biogeographical interest as it lies on the border of the Indian Ocean where influences of the South Atlantic and the West Wind Drift may, at times, interfere with the dominant features provided by the Mozambique-Agulhas system and the South Equatorial Current.

3. Methods.

The procedures followed at sea for catching and preserving the plankton are described in the general narrative of this cruise (R. W. RAND, pp. 4–9).

The information contained in this report was derived from—

(*a*) a routine general cataloguing of the entire contents of the N 70 V-samples; and

(*b*) a detailed identification of all the Copepods found in the N 200-net used as a mid-water trawl.

Out of the 199 N 70 V-samples, 14 day-light hauls (viz. the 100–50 m. hauls at alternate stations) and 18 hauls taken in the dark in 100–0 m. are as yet unprocessed. The remaining 167 samples were examined under a binocular dissecting microscope and their general contents catalogued on special record sheets. Each species or higher taxonomic group was given a symbol to indicate its estimated abundance in the sample, as follows:—

r= 1 to 5 indiv.	1= 50 to 100 indiv.
f= 6 to 20 indiv.	2=100 to 200 indiv.
+=20 to 50 indiv.	3=200 to 400 indiv.

The plankton of the N 200-samples was fully sorted into groups and all Copepods were identified and counted. It may be of interest to note that the N 200 catches yielded a total of 115 Copepod species, of which 43 were new additions to our list; the remaining 72 were also found in the N 70-nets. One of the authors of this report (F. J. M.) who has carried out all the taxonomic work on Copepods from the N 200-nets, will discuss his findings in greater detail in a separate paper.

The occurrence of each species in the N 70 V-samples has been plotted on a separate diagram, which shows the horizontal and vertical distribution of the species as well as their approximate abundance in each haul. Eighty-four of these diagrams form an appendix to this report. The distribution of the other species is detailed in the species list. In this list the serial number of the station is followed by a capital letter which indicates the depth range where the net was operated. Thus the stations A 1224 to A 1255 are given the serial numbers 1 to 32, and the depth ranges 50–0 m. to 1,500–1,000 m. are represented by the letters A to G, H being applied to some nets used in depths of more than 1,500 m.

As far as possible, the Copepods were identified according to species, free use being made of dissection and examination under high power. Where necessary, permanent mounts were made and specimens kept for future reference. This procedure, however, could only be followed with Copepod forms whose specific identification would not involve too great a delay in the routine cataloguing of the general zooplankton. Consequently, no consistent effort was made to identify all specimens belonging to such genera as *Oithona*, *Oncaea*, *Corycaeus*, *Paracalanus*, etc., which either through their large number and variety or through the technical difficulties associated with their taxonomy, could not be positively identified at this stage. They will receive closer attention in an exhaustive account of the Copepod fauna of the whole area.

4. List of Species and Occurrence.

Symbols used in the following species list and annexed diagrams of distribution are shown in Table I below:—

TABLE I.

Symbol used in List.	Symbol used in Diagrams.	Definition.
x		Found in N 200 nets only.
xx		Found in both N 70 V nets and N 200 nets.
N		New to Indian Ocean.
*	↑	Net has sampled all the way up to the surface, because closing mechanism failed to operate.
	•	Specimen of same genus present, but not identified to species.
	?	Species present, but no data on abundance.
	—	Sample not yet examined.

Species.	*Occurrence.*
Acartia amboinensis Carl	2A, 5A, 8A.
A. danae Giesbrecht	See diagram.
A. negligens Dana	See diagram.
Acrocalanus gibber Giesbrecht	See diagram.
A. gracilis Giesbrecht	See diagram.
A. longicornis Giesbrecht	See diagram.
A. monachus Giesbrecht	See diagram
Aegisthus mucronatus Giesbrecht	See diagram.
Aetidlopsis divaricata Esterly	14G N.
A. rostrata Sars?	6B N.
Aetideus armatus (Boeck)	See diagram xx.
Amallothrix emarginata (Farran)	13E, 28F.
Amallothrix sp. was also recorded in 4E, 16G, 26G, 30G and 30F.	
Arietellus aculeatus (T. Scott)	xN.
A. giesbrechti Sars	14F xx.
A. pavoninus Sars	xN.
A. plumifera Sars	x.
A. setosus Giesbrecht	15C xx.
A. simplex Sars	x.
Augaptilus glacialis Sars	30F N.
A. longicaudatus Claus	30F.
A. spinifrons Sars	15C N.
Augaptilus specimens occurred in ten other closing-nets, all between 100 and 1,000 m.	
Bathypontia elegans Sars	xN.
B. minor Sars	30F N.
Calanoides carinatus (Kröyer)	See diagram xx.
Calanopia elliptica (Dana)	2A, 7G, 8A, 11A.
C. minor A. Scott	2A, 11A.
Unidentified specimens of *Calanopia* were recorded at 1A, 3A, 4B, 5A, 23A.	
Calanus tenuicornis Dana	See diagram.
C. tonsus Brady	See diagram. N.
Calocalanus contractus Farran	6A, 28A?, 30A, 32A.
C. gracilis Tanaka	32A N.
C. pavo (Dana)	See diagram.
C. plumulosus (Claus)	See diagram.
C. styliremis Giesbrecht	See diagram.
C. tenuis Farran	32A N.
Calocalanus spp. were present in almost all catches from all depths (see diagram).	
Candacia aethiopica (Dana)	See diagram xx.
C. bipinnata (Giesbrecht)	3A, 6B, 17A xx.
C. bispinosa (Claus)	See diagram.
C. catula (Giesbrecht)	See diagram.
C. curta (Dana)	8A xx.
C. longimana (Claus)	See diagram xx.
C. pachydactyla (Dana)	5A, 6A.
C. simplex (Giesbrecht)	See diagram. xx.
C. truncata (Dana)	See diagram.
C. varicans (Giesbrecht)	11A.
Canthocalanus pauper (Giesbrecht)	See diagram. xx.
Centraugaptilus horridus (Farran)	x.
Centr. rattrayi (T. Scott)	x.
Centropages calaninus (Dana)	See diagram.
C. elongatus Giesbrecht	See diagram.
C. furcatus (Dana)	See diagram.
C. gracilis (Dana)	See diagram.
C. orsinii Giesbrecht	2A.
Cephalophanes sp.	13F N.
The species could not be identified with the literature at our disposal.	
Chiridiella macrodactyla Sars	26F N.

5640042—3

Species.	Occurrence.
Chiridius poppei Giesbrecht	27C.
Chiridius sp. was recorded in six other catches but has not yet been identified to species (see diagram).	
Chirundina streeti ii Giesbrecht	24E, 26E, 30E xx.
Clausocalanus arcuicornis (Dana)	See diagram.
C. furcatus (Brady)	See diagram.
C. paululus Farran	See diagram N.
C. pergens Farran	10A, 12A, 14A N.
Clytemnestra rostrata (Brady)	30F, 32A.
C. scutellata Dana	6E, 8B, 10A, 11A, 26G.
Conaea gracilis (Dana)	See diagram.
Copilia mediterranea Claus	12B, 13A, 32A, xx.
Copilia mirabilis Dana	See diagram. xx.
C. quadrata Dana	See diagram. xx.
C. vitrea Haeckel	14B, 14E*, 32A. xx.
Corina granulosa Giesbrecht	11G. N.
Cornucalanus chelifer (I. C. Thompson)	24F, 24G? xx.
Corycaeus agilis Dana	6A, 8A, 30A, 32A.
C. asiaticus F. Dahl	8A.
C. catus F. Dahl	26A.
C. clausii F. Dahl	12A, 14A, 20A.
C. crassiusculus Dana	6A, 8A, 10A, 20A, 30A, 32A.
C. flaccus Giesbrecht	6A, 8A, 12A, 14A, 20, 32A.
C. giesbrechti F. Dahl	12A.
C. latus Dana	30A. N.
C. limbatus Brady	8A, 14A.
C. longistylus Dana	12A, 32A.
C. pacificus F. Dahl	6A, 8A, 12A.
C. speciosus Dana	6A, 8A, 10A, 12A, 14A, 32A.
C. typicus Kröyer	6A.
Corycella carinata Giesbrecht	10A, 12A, 14A, 18A.
C. concinna Dana	6A, 8A, 10A, 12A, 14A, 32A.
C. curta Farran	10A, 12A, 28A, 30A, 32A.
C. rostrata Claus	10A, 12A, 14A, 20A, 21A, 26A, 28A, 30A, 32A,
The genera *Corycaeus* and *Corycella* were represented in the majority of the hauls and in all depths (see diagram). The data given here apply to a number of surface samples only.	
Ctenocalanus vanus Giesbrecht	See diagram. N.
Disseta palumboi Giesbrecht	30F.
Euaetidius acutus (Farran)	See diagram N.
E. giesbrechti Cleve	See diagram.
Euaugaptilus affinis Sars	x N.
E. angustus (Sars)	x.
E. bullifer (Giesbrecht)	12G. xx.
E. filigerus (Claus)	x.
E. gibbus (Wolfenden)	28F N.
E. laticeps (Sars)	x.

Species.	Occurrence.
E. magnus (Wolfenden)	27F xx.
E. nodifrons (Sars)	28F xx.
E. oblongus (Sars)	27F xx.
E. palumboi (Giesbrecht)	See diagram.
Eucalanus attenuatus (Dana)	See diagram. xx.
E. crassus Giesbrecht	See diagram. xx.
E. elongatus (Dana)	See diagram. xx.
E. longiceps Matthews	12B, 24G, 32B?
E. mucronatus Giesbrecht	4B, 5A, 7A, 8B, 32A.
E. subcrassus Giesbrecht	6A, 8A, 8B, 10A, 11A, 32A.
E. subtenuis Giesbrecht	1A, 3A, 8B, 32B.
Euchaeta acuta Giesbrecht	28A. xx.
E. concinna Dana	6G. xx.
E. longicornis Giesbrecht	6A.
E. marina (Prestandrea)	1A, 2A, 4A, 6A, 8A, 12A, 32A. xx.
E. media Giesbrecht	x.
E. spinosa Giesbrecht	x.
E. wolfendeni A. Scott	4A, 6A, 8A.
Euchirella amoena Giesbrecht	6A, 8A, 15A. xx.
E. bitumida With	x N.
E. curticauda Giesbrecht	16G, 25C xx.
E. maxima Wolfenden	x.
E. messinensis (Claus)	x.
E. rostrata (Claus)	31A.
E. formosa Vervoort	x N.
E. venusta Giesbrecht	x.
Euterpina acutifrons Dana	See diagrams.
Gaetanus curvicornis Sars	16G.
G. kruppi Giesbrecht	7E. xx.
G. latifrons Sars	30F. xx.
G. miles Giesbrecht	See diagram. xx.
G. minor Farran	See diagram.
G. pileatus Farran	7E, 14E, 24E, 28E. xx.
G. recticornis Wolfenden	x N.
Gaidius tenuispinus Sars	27F, 30F.
Haloptilus acutifrons Giesbrecht	28C, 30G.
H. angusticeps Sars	24F. N.
H. longicornis (Claus)	See diagram. xx.
H. mucronatus (Claus)	6G.
H. ornatus (Giesbrecht)	7E, 8B, 14D xx.
H. oxycephalus (Giesbrecht)	13A, 28C, 32B xx.
H. spiniceps (Giesbrecht)	28C xx N.
H. tenuis Farran	x N.
H. validus Sars	x.
Heterorhabdus abyssalis (Giesbrecht)	23A (Cast), 30F xx.
H. austrinus Giesbrecht	28F.
H. clausi (Giesbrecht)	7E, 14B.
H. compactus Sars	16G N.
H. norvegicus (Boeck)	29F, 4E N.
H. papilliger (Claus)	22A, 22B, 29C xx.
H. spinifrons (Claus)	See diagrams. xx.
Heterostylites longicornis (Giesbrecht)	23D, 27D, 30D xx.
Labidocera acutifrons (Dana)	x.

Species.	*Occurrence.*
L. acutum Giesbrecht	1A, 2A, 3A, 11A.
L. minutum Giesbrecht	4A, 11A.
Lophothrix frontalis Giesbrecht	14E, 26D xx.
L. latipes (T. Scott)	14D, 14E*. 24F, 28C, N.
L. varicans Wolfenden(?)	23F N.
Lubbockia aculeata Giesbrecht	7D, 14E, 15D.
L. squillimana Claus	See diagram. N.
Lucicutia clausi (Giesbrecht)	See diagram.
L. curta Farran	See diagram N.
L. flavicornis (Claus)	See diagram. xx.
L. magna Wolfenden	28A.
L. maxima Wolfenden	27F xx.
L. ovalis Wolfenden	8A, 24E, 26A, 28B, 32B.
L. simulans Sars	26F N.
Macrosetella gracilis (Dana)	See diagrams.
Mecynocera clausi I. C. Thompson	See diagrams.
Megacalanus princeps Wolfenden	13F., 23F. xx.
Mesorhabdus angustus Sars	x.
Mesundeuchaeta asymmetrica Wolfenden.	x.
Metridia bicornuta Davis	16G, 24F, 26F, 27F, 28F xx.
M. boecki Giesbrecht	27F.
M. brevicauda Giesbrecht	See diagram.
M. longa (Lubbock)	13G, 16G, 24G.
M. lucens Boeck	See diagram.
M. venusta Giesbrecht	See diagram.
Microcalanus pygmaeus Sars	10G, 12G. N.
Microsetella norvegica (Boeck)	See diagram.
M. rosea (Dana)	See diagram.
Miracia minor T. Scott	24B, 32A. N.
Monacilla tenera Sars	30G.
M. typica Sars	See diagram. N.
Mormonilla minor Giesbrecht	See diagram. N.
M. phasma Giesbrecht	See diagram N.
Nannocalanus minor (Claus)	See diagram. xx.
Neocalanus gracilis (Dana)	See diagram. xx.
N. robustior (Giesbrecht)	6A, 12A, 22C, 28B. xx.
Oculosetella gracilis (Dana)	4A, 27D, 30B.
Oithona atlantica Farran	24A, 28A.
O. attenuata Farran	30A, 32A.
O. fallax Farran	6A, 10A, 12A, 30A, 32A.
O. nana Giesbrecht	12A.
O. plumifera Baird	6A, 8A, 10A, 12A, 14A, 16A, 18A, 20A, 22A, 24A, 30A, 32A. xx.
O. rigida Giesbrecht	6A.
O. setigera (Dana)	10A, 12A, 14A, 20A, 30A, 32A.
O. similis Claus	10A, 16A, 22A, 24A, 28A, 30A, 32A.
O. simplex Farran	3B.
O. tenuis Rosendorn	6A, 10A, 12A, 14A, 30A, 32A.
Oncaea clevei Früchtl	6A, 8A, 10A, 12A, 32A.
O. conifera Giesbrecht	10A, 24A, 32A,

Species.	*Occurrence.*
O. curta Sars	20A. N.
O. dentipes Giesbrecht	20A. N.
O. media Giesbrecht	6A, 8A, 10A, 12A, 14A, 20A, 28A, 30A, 32A.
O. mediterranea Claus	14A.
O. obscura Farran	28A. N.
O. similis Sars	10A, 14A. N.
O. venusta Philippi	6A, 8A, 10A, 12A, 26A, 32A, xx.
Onchocalanus sp	27F.
Pachyptilus eurygnathus Sars	x.
Paracalanus aculeatus Giesbrecht	2A, 2B, 6A, 8A, 10A, 30A, 32A.
P. nanus Sars	6A, 6D, 10A, 12A, 16A, 26A, 26D, 28A, 30A, 32A.
P. nudus Sewell	6A, 10A, 30A, 32A.
P. parvus (Claus)	10A, 12A, 16A. 22A, 32A, xx.
P. pygmaeus (Claus)	8A, 10A, 24A, 26A, 28A, N.
Paraeuchaeta barbata (Brady)	13G, 26G, 30G. x.
P. biloba Farran	x N.
P. dubia Esterly	x N.
P. diegensis (Esterly)	x N.
P. exigua (Wolfenden)	x N.
P. gracilis Sars	x N.
P. hanseni With	x.
P. malayensis Sewell	x.
P. norvegica (Boeck)	30F. N.
P. sarsi Farran	x.
P. scotti (Farran)	x.
P. tonsa (Giesbrecht)	x.
Phaenna spinifera Claus	3A, 4E, 5C, 7A, 12C, 14E*, 14G, 14H, 22C, 25C.
Phyllopus aequalis Sars	23F. N.
P. helgae Farran	5E, 14E, 24E, 28F, 30E. xx.
Pleuromamma abdominalis (Lubbock)	3A, 8B, 14A, 16A. xx.
P. borealis Dahl	x N.
P. gracilis (Claus)	x.
P. piseki Farran	3A xx.
P. xiphias (Giesbrecht)	See diagram. xx.
Pontella diagonalis C. B. Wilson	10C. xx N.
Pontellina plumata (Dana)	See diagram.
Pontellopsis regalis (Dana)	4A, 10G.
Pontoeciella abyssicola (T. Scott)	6F, 14D. N.
Ratania atlantica Farran	14F. N.
R. flava Giesbrecht	32B N.
Rhincalanus cornutus Dana	See diagram. xx.
R. nasutus Giesbrecht	See diagram. xx.
Sapphirina angusta Dana	12C xx.
S. auronitens Claus	8A, 11A, 32A,
S. bicuspidata Giesbrecht	8A.
S. gastrica Giesbrecht	6A.
S. maculosa Giesbrecht	4E*. N.
S. metallina Dana	4E, 6B, 14B, 14C, 14E, 15C, 20A, 32B.
S. nigromaculata Claus	8A, 12A.

Species.	*Occurrence.*
S. opalina Dana	3A, 4B, 11A. xx.
S. ovatolanceolata Dana	10A, 14B, 30A, 32A. xx.
S. stellata Giesbrecht	x.
Scaphocalanus magnus (T. Scott)	x.
S. medius Sars	13F, 24 F.
Scolecithricella dentata (Giesbrecht)	See diagram. N.
S. dubia (Giesbrecht)	22C. N.
S. media Wolfenden	x N.
S. vittata (Giesbrecht)	27c, 28C, 29C N.
Scolecithrix bradyi Giesbrecht	See diagram. N.
S. danae (Lubbock)	See diagram.
Scottocalanus longispinus A. Scott	28F xx N.
S. persecans (Giesbrecht)	28F xx.
S. securifrons (T. Scott)	22F, 28E xx.

Species.	*Occurrence.*
Spinocalanus magnus Wolfenden	16G.
S. spinosus Farran	16G. N.
Temora discaudata Giesbrecht	See diagram.
T. stylifera Dana	See diagram.
T. turbinata Dana	See diagram.
Temoropia mayumbaensis T. Scott	See diagram. N.
Undeuchaeta intermedia A. Scott	22E, 30E xx.
U. major Giesbrecht	26F. xx.
U. plumosa (Lubbock)	See diagram. xx.
Undinula caroli (Giesbrecht)	See diagram.
U. darwinii (Lubbock)	See diagram. xx.
U. vulgaris (Dana)	See diagram. xx.
Xanthocalanus sp	4C, 14C, 16E, 16G, 19C, 22C, 30F xx.

Fig. 1

	1	2	3	4	5	6	7	8	9	10	11	12	13	14	15	16	Average
A	44	46	53	37	34	51	38	58	10	40	47	51	15	35	14	16	37
B		19	–	34	–	27	–	43	–	0	–	24	–	25	–	15	23
C		18	6	30	23	24	19	7	25	9	11	31	13	25	24	12	18
D		21	13	15	9	10	18	10	6	11	10	10	11	26	20	15	14
E				33	23	20	44		7	14	10	17	24	31	24	12	22
F						14	14			6	9	9	22	28	15	18	15
G						22	29			24	12	27	27	29	15	35	24
H													22	24		9	19
	32	31	30	29	28	27	26	25	24	23	22	21	20	19	18	17	
A	52	16	37	8	26	13	18	15	13	15	9	12	22	18	7	21	19
B	36	–	15	–	24	–	14	–	13	–	13	–	8	–	–		18
C	22	14	25	18	21	23	22	24	9	12	22	12	10	21			18
D	9	9	16	14	8	6	14		12	8	26	11	9	17	13		12
E		11	17	10	28	8	23		21	12	21	9		13			16
F		13	45	15	49	35	37		25	19	12	6		13			24
G			28	17		12	19		26	14	21	13					19

Trigsurvey 1964

5. Discussion.

Diversity distribution.

The total number of Copepod species found in each separate haul (=diversity) is recorded in Fig. 1. Although our taxonomic work is not complete, the present data already show two maxima: one in the surface layers along the northern line, the other in the deep hauls between 750 and 1,500 m. throughout the area. The occurrence of maxima in those levels has been observed on many occasions in all oceans, as SEWELL (1948) has already emphasized.

In the greater part of the southern area, however, the surface water was marked by a paucity of species as well as by low plankton volumes. In fact, comparatively few adult copepods were found near the surface at most of the southern stations and the populations were composed of a very high percentage of early copepodid stages of small Calanoids and *Oithona.*

Distribution of certain species within the area.

In more than 100 of our distribution diagrams of individual species some sort of pattern is apparent. When we compare these patterns, it is possible to classify them into four groups, which could well correspond to four separate communities. By utilizing one diagram on which was plotted the occurrence of all the species which appear to fall into the same group (or supposed community), we obtained the results shown in Figs. 2 to 5, where each dot represents the occurrence of one species of the group in a certain haul.

Table II shows that both groups C and D, occurring in deeper levels, contain a number of species known to occur in the Atlantic and Pacific, but not previously found in the Indian Ocean. The number of these species appears to increase with depth. Furthermore, from Table II, the per cent occurrence of each of the four groups is uniformly high in that area to which we have tentatively assigned it. This strengthens our supposition that the four groups correspond with real plankton communities.

The vertical distribution of the four groups closely agrees with that of the water masses as deduced from the hydrological data of the cruise (ORREN 1963):—

Mocambique and Agulhas Currents: Stat. 1–5, 0–500 m... Group A.

Surface and subsurface water: 0–200 m..... Group B.

Central water: 200–600 m..... Group C.

Antarctic Intermediate water: 600–1, 300 m..... Group D.

Deep water: 1,400–3,000 m: As the nets seldom reached further down than the upper limit of the "Deep water", it cannot be expected that a separate community (which might well occur here) would be distinguishable in our catches.

Again, the surface water at the southern line of stations did not yield any species falling within any of the four groups. This water mass seems to be inhabited by a few ubiquitous species only. The hydrological data here point towards a general sinking of the surface water (ORREN 1963), but we can find no connection between this phenomenon and the dearth of surface plankton.

TABLE II.

Group.	No. of species.	General distribution.			No. of occurrences in our catches.			Percentage occurrence in group area.
		Atlantic.	Indian.	Pacific.	In/Outside group area.		Total.	
A.....	12	10	12	12	52	10	62	84
B.....	21	15	21	21	166	37	203	82
C.....	14	14	10	14	107	41	148	72
D.....	81	75	50	75	491	83	574	85

Fig. 2

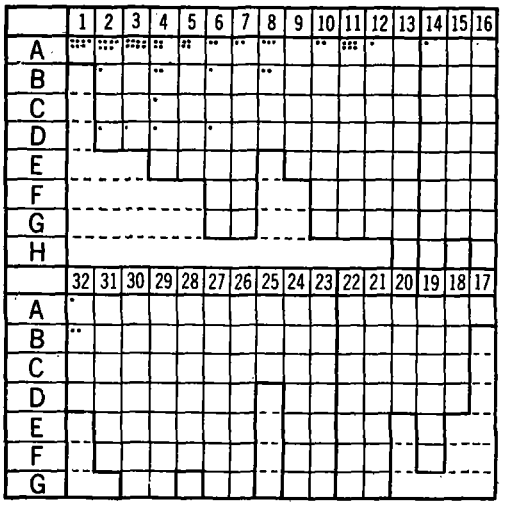

GROEP A

Canthocalanus pauper
Eucalanus crassus
E. subtenuis
Euterpina acutifrons
Labidocera acutum
L. minutum
Pontellina plumata
Sapphirina opalina
Temora discaudata
T. stylifera
T. turbinata
Undinula caroli

Fig. 3

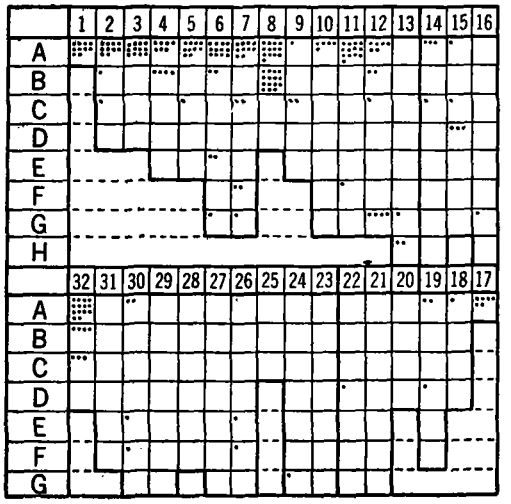

GROUP B

Acrocalanus gibber
A. gracilis
A. longicornis
A. monachus
Calanopia elliptica
Candacia simplex
C. truncata
Centropages calaninus
C. elongatus
C. furcatus
C. gracilis
Clytemnestra rostrata
C. scutellata
Copilia mirabilis
Eucalanus attenuatus
E. longiceps
E. mucronatus
E. subcrassus
Scolecithrix danae
Undinula darwinii
U. vulgaris

Trigsurvey 1964

Fig. 4

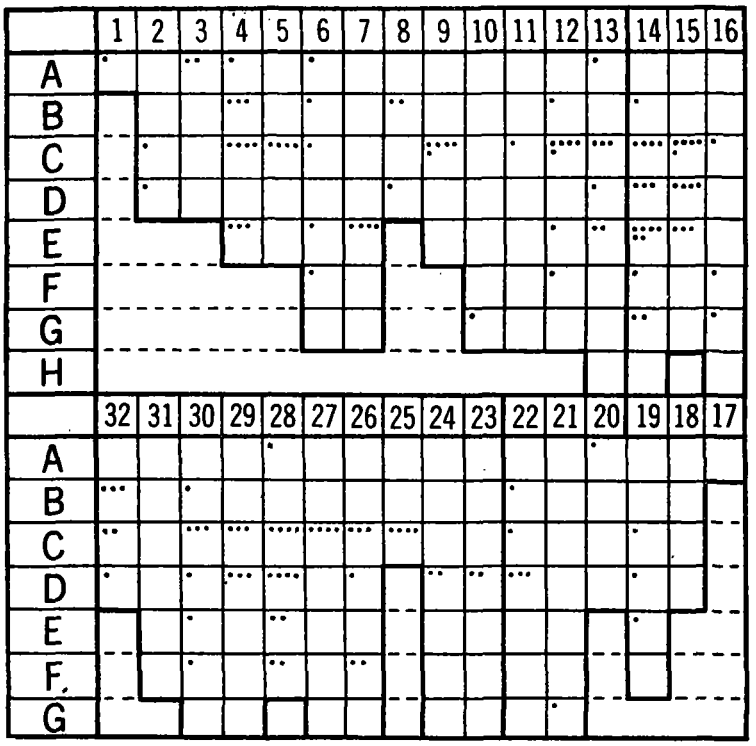

GROUP C

Aetidius armatus
Candacia longimana
Euaetidius giesbrechti
Haloptilus longicornis
H. ornatus
H. oxycephalus
H. spiniceps
Heterorhabdus papilliger
H. spinifrons
Phaenna spinifera
Sapphirina metallina
Scolecithricella vittata
Scolecithrix bradyi
Undeuchaeta plumosa

Trigsurvey 1964

GROUP D

Fig. 5

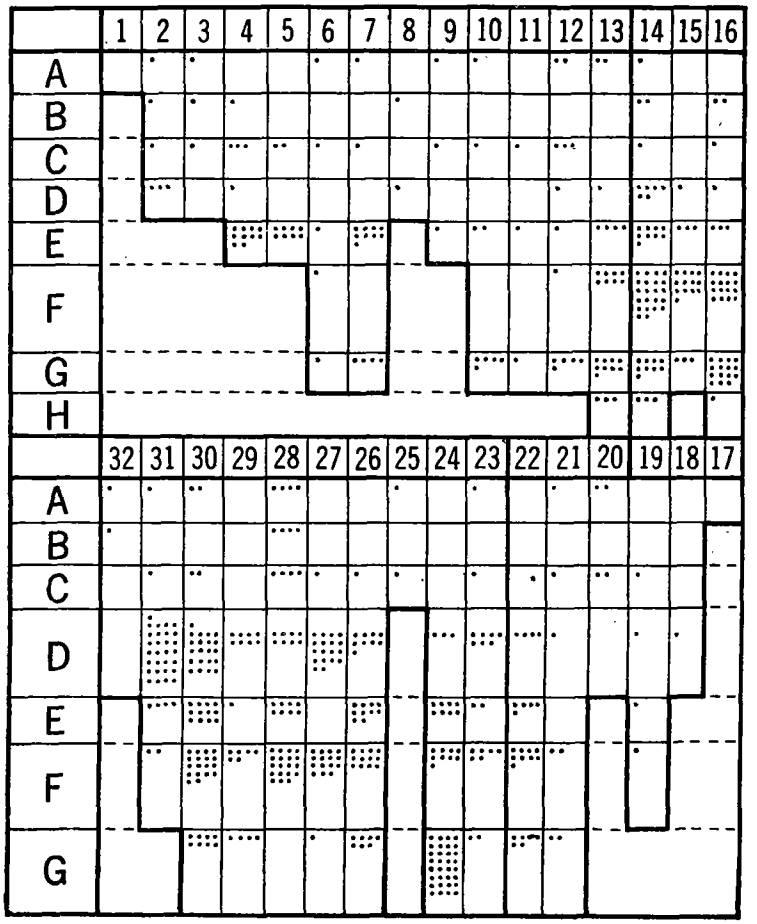

Amallothrix emarginata
Augaptilus glacialis
A. longicaudatus
Bathypontia minor
B. elegans
Calanoides carinatus
Calanus tonsus
Chiridiella macrodactyla
Chiridius poppei
Chirundina streetsi
Conaea gracilis
Cornucalanus chelifer
Ctenocalanus vanus
Disseta palumboi
Euaugaptilus (all 10 spp.)
Eucalanus elongatus
Gaetanus (all 7 spp.)
Gaidius tenuispinus
Haloptilus acutifrons
Haloptilus angusticeps
H. mucronatus
Lophothrix (all 3 spp.)
Lucicutia maxima
Megacalanus princeps
Metridia (all 6 spp.)
Mesundeuchaeta asymmetrica
Microcalanus pygmaeus
Monacilla (both spp.)
Mormonilla (both spp.)
Onchocalanus sp.
Paraeuchaeta (all 12 spp.)
Phyllopus (both spp.)
Pontoeciella abyssicola
Ratania atlantica
Rhincalanus nasutus
Scaphocalanus (both spp.)
Scottocalanus (all 3 spp.)
Spinocalanus (both spp.)
Temoropia mayumbaensis
Undeuchaeta intermedia
U.major

Trigsurvey 1964

A certain number of species showed no special distribution pattern as they were found in nearly every haul from all depths, including the surface nets along the southern traverse. Such species were among others, *Acartia danae*, *A. negligens* and *Mecynocera clausi*. It seems probable that after completion of the taxonomic work certain species of *Oithona*, *Paracalanus*, *Clausocalanus*, *Calocalanus* and perhaps a few others will show the same ubiquitous trend. They could be placed into a fifth group, which we will here call the " ubiquists ".

Macrosetella gracilis could be classified as a " ubiquist ", if only the northern profile (stations 1–12) were considered. Elsewhere, it is found only in the deepest nets (1,500–1,000 m.) and near the 250 m.-level, except at station 32 where it is again found at all depths down to 500 m. (no deeper hauls could be made at that station). Hydrologically, station 32 has the same type of water as the northern stations. *M. gracilis* provides an apt transition towards a sixth group of distribution patterns which is not uncommon in our material and which could be defined as " *dichotopic* ", i.e. occurring in two or more rather widely separated areas, and being conspicuously absent between them.

The following are some examples of dichotopic distribution:—

Acrocalanus gracilis and *A. monachus* are found regularly in the upper 50 (seldom 100)m. from station 1 to 11, at stations 17 and 32. However, they also appear below 500 m. and down to 1,500 m. at stations 6, 7, 11 and 12.

Centropages gracilis is rather scattered in the upper 250 m. at stations 1, 5 and 11, but occurs twice below 1,000 m. at stations 11 and 12.

Euaetidius acutus is found in the upper 100 m. in the Mocambique Current but also below 1,000 m. at stations 6 and 10. The waters between them accommodate *E. giesbrechti*.

Aetideus armatus occurs in the Central water in the north, but only in the Atlantic Intermediate water in the south.

Ctenocalanus vanus is found at six stations above the 100 m.-level and at four stations below the 750 m.-level along the northern profile, whereas in the south it occurs in one surface catch, five central water catches shallower than 500 m. and eight deep catches in over 1,000 m.

5640042—4

Although it is premature at this stage to theorise about these cases of " dichotopic " occurrence, we feel tempted to put forward the following considerations.

In many cases of " dichotopy " we are dealing with species known to occur in both the Indian and the Atlantic Oceans. It is known that Atlantic water flows eastward around the Cape of Good Hope at a certain depth and penetrates the Indian Ocean. This influx carries elements of Atlantic plankton into the deep layers of the Indian Ocean, whereas the autochthonous Indian population of the same species lives near the surface. Hence the appearance of such species at two separate levels in our cross sections.

There are other cases of dichotopy involving species which are rare or entirely absent in the Atlantic, such as *Acrocalanus gracilis* and *A. monachus*. Their occurrence in our deep nets seems to coincide with that of North Indian Deep water originating from surface water sinking in the Arabian Sea. Thus our northern transect would show these species to occur both as a " normal " epiplanktonic population and as a deep " displaced " one.

The distribution of meso- and bathypelagic Copepods throughout the Indian Ocean.

The frequent occurrence in our deep catches of such species as *Calanus tonsus*, *Calanoides carinatus*, *Ctenocalanus vanus*, *Metridia lucens* as well as many others considered to be representatives of the Atlantic and Subantarctic plankton, suggests a considerable influx of southern and western origin into this part of the Indian Ocean. The four species just mentioned are among those that have not been found elsewhere in the Indian Ocean. With the exception of *C. tonsus*, they are at times very common along the western and southwestern coasts of South Africa, where they reach the surface with the upwelling water masses (Benguela Current system). *C. tonsus* can be found in great numbers in the upper layers some 100 miles south of the Cape of Good Hope.

SEWELL (1948) has shown a correlation between a deep current of Antarctic Intermediate water flowing into the Arabian Sea and the occurrence in that area of a number of species which he considers to be of North Atlantic and Arctic origin and transported there by way of the Cape. Following the path of that current northward, he finds a decrease in the number of these species from 56 and 38, respectively, at two stations in the

southern and central Arabian Sea, to 32, 19 and 12, respectively, at three stations near the Gulf of Oman and the Gulf of Aden.

By applying SEWELL's standards (SEWELL 1948, pp. 498–506, list of species) we find that the Atlantic contribution to our SW-Indian bathypelagic fauna has reached 134 species so far, which agrees very well with SEWELL's views. This trend in the western part of the Indian Ocean, as shown by SEWELL, is seen to continue in the region east of the Laccadive–Maldive Ridge as well, if we compare the contents of the six mid-water trawls described by SEWELL (1929, 1932) with our list of meso- and bathypelagic species. Proceeding from west to east, we find—

20 of our " Atlantic " species at station 682 (Laccadive Sea, 1,260 m., 54 spp. in total);

11 of our " Atlantic " species at station 670 (W of Ceylon, 360 m., 40 spp. in total);

5 of our " Atlantic " species at station 393 (ESE of Ceylon, 720 m., 45 spp. in total);

2 of our " Atlantic " species at station 463 (E of Ceylon, 720 m., 8 spp. in total);

none of our " Atlantic " species at station 462 (central southern area of Bay of Bengal, 855 m., 9 spp. in total); and

none of our " Atlantic " species at station 461 (W of Andaman Islands, 675 m., 1 sp.).

From the foregoing figures it will be noted that a gradual decrease in the numbers of Atlantic species in a northerly and easterly direction is apparent in the Indian Ocean, and that a minimum is reached in the Bay of Bengal.

A similar regression seems to occur from the opposite direction, along the axis of the deep current penetrating into the Indian Ocean from the West Pacific through the Moluccan Passage, the Banda and Timor Seas.

In eleven deep hauls made by the Siboga Expedition in the Eastern Malay Archipelago, A. SCOTT (1909) found a number of our " Atlantic " species. When the number of species which each Siboga station has in common with the Central and Antarctic Intermediate waters in our area is plotted on a map, a decrease in a southerly and westerly direction becomes apparent. Isolines drawn around the stations with more than 15 species in common, and around those with more than 20 species in common with our southwestern deep fauna, follow much the same trend as the contour lines of the lower oxygen minimum given by WYRTKI (1961, plates 32 and 35); see Fig. 6.

We may conclude that the influxes of deep water into the Indian Ocean from the South Atlantic as well as from the Western Pacific are clearly indicated by the changes observed in the bathypelagic and mesopelagic Copepod fauna.

6. Literature.

ORREN, M. J., 1963.—Hydrological observations in the South West Indian Ocean. *Invest. Rep. Div. Sea Fish., South Africa.* 45: 61 pp. Pretoria.

ROSE, M., 1929.—Copépodes pélagiques, particulièrement de surface, provenant des campagnes scientifiques de S.A.S. le Prince Albert Ir de Monaco. *Res. Camp. Sci., Monaco,* 78: 374 pp.

SARS, G. O., 1925.—Copépodes, particulièrement bathypélagiques, provenant des campagnes scientifiques du Prince Albert Ir de Monaco. *Res. Camp. Sci. Monaco,* 69: 408 pp.

SCOTT, A., 1909.—The Copepoda of the Siboga Expedition, Pt. I: Free-swimming, littoral and semi-parasitic Copepoda. *Siboga Exp. Monogr.*, 29*A*: 323 pp.

SEWELL, R. B. S., 1929/32.—The Copepoda of the Indian Seas. ,Calanoida. *Mem. Indian Mus., Calcutta, X*: 407 pp.

SEWELL, R. B. S., 1947.—The free-swimming planktonic Copepoda. Systematic account. *Sci. Repts. John Murray Exp.*, 1933–34, 8 (1): 303 pp.

SEWELL, R. B. S., 1948.—The free-swimming planktonic Copepoda. Geographical distribution. *Sci. Repts. John Murray Exp.*, 1933–34, 8 (3): 317–592.

WILSON, C. B., 1942.—Copepods of the plankton gathered during the last cruise of the Carnegie. *Sci. Res. Cruise VII of the Carnegie*, 1928–29. *Washington, Carnegie Inst. Publ.*, 536: 233 pp.

WILSON, C. B., 1950.—Copepods gathered by the U.S. Steamer " Albatross " from 1887 to 1909, chiefly in the Pacific. *Smithsonian Inst., U.S. Nat. Mus. Bull.*, 100: 141–441.

WYRTKI, K., 1961.—Physical Oceanography of the South East Asian Waters. *Naga Rep.*, 2: 195 pp.

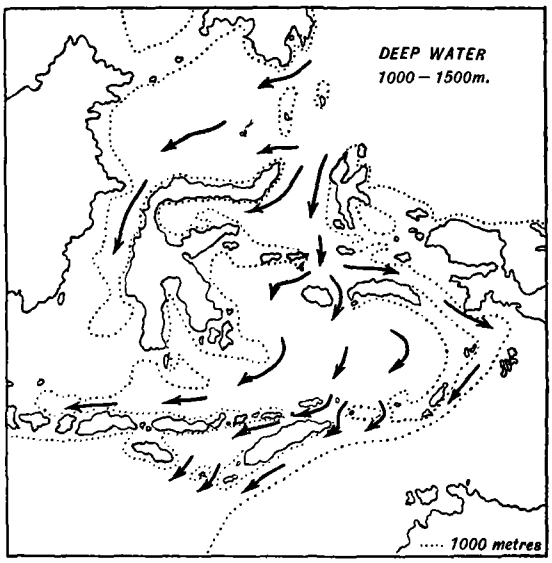

Water movements in 1000–1500m.
(from WYRTKI 1961)

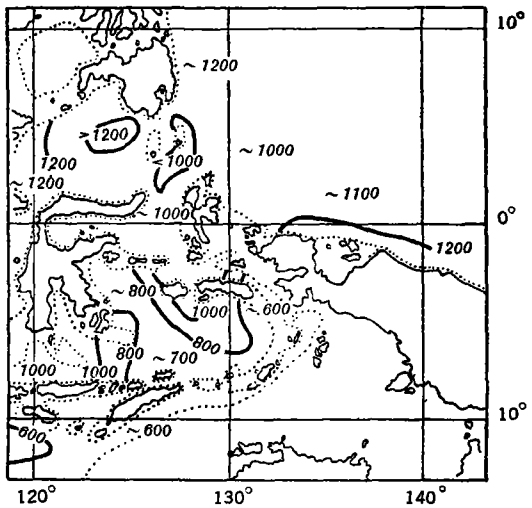

Depth (m.) of O_2 minimum
(from WYRTKI 1961)

Fig. 6

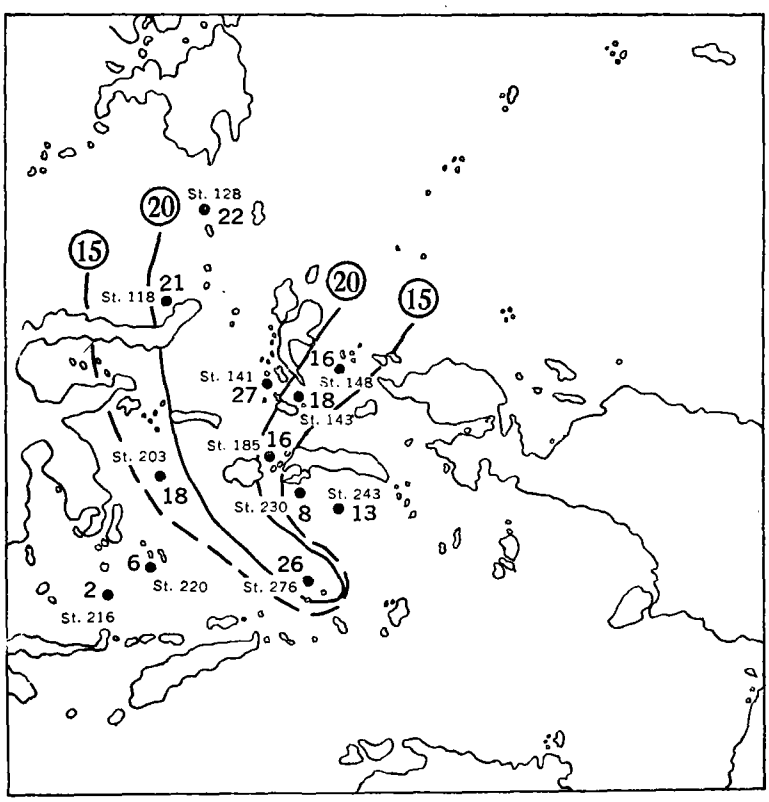

Trigsurvey 1964

Number of Atlantic and Polar Copepod species which each deep haul of the SIBOGA Expedition has in common with the S.W. Indian Ocean fauna as recorded from our N 70 V-nets.

Depths of the hauls:

St. 118: 900 – 0m.
St. 128: 700 – 0m.
St. 141: 1500 – 0m.
St. 143: 1000 – 0m.
St. 148: 1000 – 0m.
St. 185: 1500 – 0
St. 203: 1500 – 0
St. 216: 1000 – 400
St. 220: 200 – 0
St 230: 2000 – 0
St. 243: 1000 – 0
St. 276: 750 – 0

Acartia danae

(A)

	1	2	3	4	5	6	7	8	9	10	11	12	13	14	15	16
A	f	f	f					r		+	f	f	f	r		r
B				f								f		f		f
C				•	•	•	•		•	•	•	•	•	•	•	•
D							r			•		r		r		
E				•	•	•	•			•		•	•	•	•	•
F						r							r		r	
G						•	•			•	•	•	•	•	•	
H													•	•		

	32	31	30	29	28	27	26	25	24	23	22	21	20	19	18	17
A	f	f	+	f	+	f	+	r	r	r	f	f				
B	f		f		+		+		f		f					
C	f	f	f•	•	f		f			f		f				
D	•	•	•	•	•	•				•	•	•			•	
E		r	f	f						r		r				
F		•	•	•	•	•			•	•		•				
G			f	f												

Acartia negligens

	1	2	3	4	5	6	7	8	9	10	11	12	13	14	15	16
A	+	f	+	f	f	f	f	r		+	+	+	r	f	r	+
B				f		f		f				f		r		f
C				•	•	•	•		•	•	•	•	•	•	•	•
D				r	r		f	r		•	r					+
E				•	•	•	•			•		•	•	•	•	•
F						r	f					r	r	r		
G						•	•			•	•	•	•	•	•	
H													•	•		

	32	31	30	29	28	27	26	25	24	23	22	21	20	19	18	17
A	+		+	r	+	1	f	r	r	r	f	f		f		f
B	f		•		r		r		r		f					
C	f		•	•		f					f					
D	•	•	•	•	•	•				•	•	•		f	•	
E		f	f		+	r				f						
F		•	•	•	•	•			•	•		•				
G				f		f	r			r	r	r				

Acrocalanus gibber

	1	2	3	4	5	6	7	8	9	10	11	12	13	14	15	16
A			r		r		r	r			r					
B		•						r								
C		•					•		•							
D																
E				•		•										
F																
G																
H																

	32	31	30	29	28	27	26	25	24	23	22	21	20	19	18	17
A	r															
B																
C																
D																
E																
F																
G																

CORRIGENDUM and ADDENDUM.

Acartia negligens:

Insert . in square C 28.
Delete . in square C 30.

PLATE I

Trigsurvey 1964.

Acrocalanus gracilis

(B)

	1	2	3	4	5	6	7	8	9	10	11	12	13	14	15	16
A	+	r	f	f	f	f	r	f	r		f	r				
B		•						f								
C		•					•		•							
D																
E				•		•										
F																
G																
H																

	32	31	30	29	28	27	26	25	24	23	22	21	20	19	18	17
A															r	r
B																
C																
D														r		
E																
F																
G																

Acrocalanus longicornis

	1	2	3	4	5	6	7	8	9	10	11	12	13	14	15	16
A		r	f			f		f		r	r	r				
B		•						r				r				
C		•					•		•							
D																
E				•		•										
F																
G																
H																

	32	31	30	29	28	27	26	25	24	23	22	21	20	19	18	17
A	r															
B																
C																
D																
E																
F																
G																

Acrocalanus monachus

	1	2	3	4	5	6	7	8	9	10	11	12	13	14	15	16
A			r	r	r	r	r				f	r		r		
B		•														
C		•					•		•							
D																
E				•		r•										
F							r									
G																
H																

	32	31	30	29	28	27	26	25	24	23	22	21	20	19	18	17
A	f															r
B	r															
C																
D																
E																
F																
G																

ADDENDA.

Acrocalanus gracilis:

Insert r in squares: F7, F11 and G12.

PLATE I

Aegisthus spp. (m=A. mucronatus)

(A)

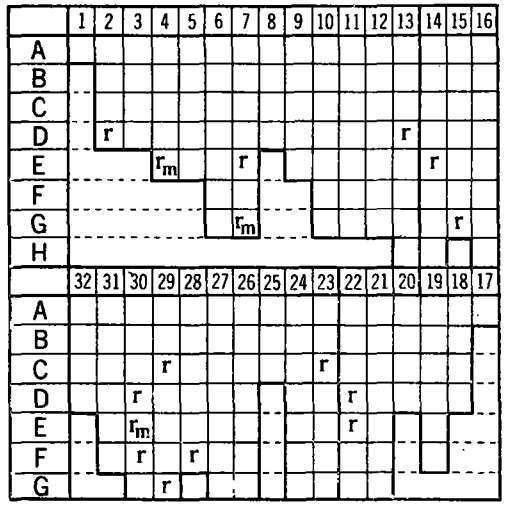

Aetideus armatus

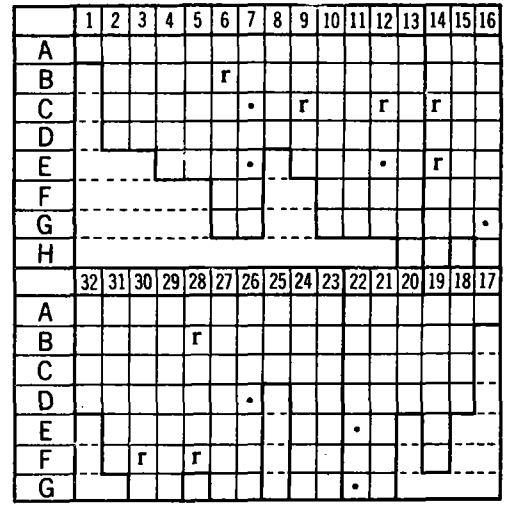

Calanoides carinatus

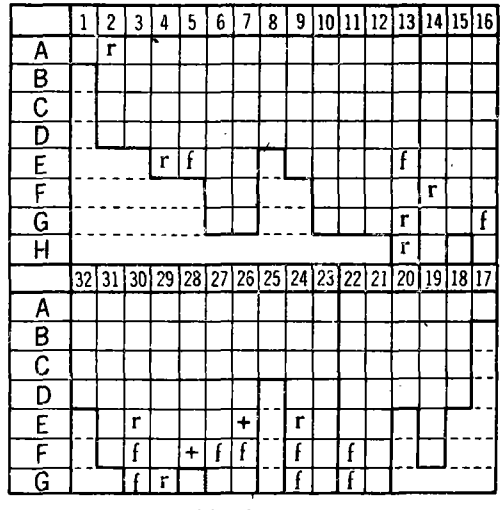

CORRIGENDUM and ADDENDUM

Aetideus armatus:

Insert r in square A 28.
Delete r in square B 28.

Trigsurvey 1964

PLATE II

Calanus tenuicornis

(B)

	1	2	3	4	5	6	7	8	9	10	11	12	13	14	15	16
A	•		•		•		•	f		r	r	r	r	f	r	
B		•		•		r		r				r		f		
C		r			•						•			•		
D		r					r							r		
E							•					•				
F							r							r		
G										r			r	•	•	•
H													r	•		

	32	31	30	29	28	27	26	25	24	23	22	21	20	19	18	17
A	f	r			r		+	f		•		r		r		r
B					r				•				r			
C	r		f		f	r	r	f			r		r			
D			•												r	
E			•											r		
F					•		•			•	•	•		•		
G			r	r						r	r					

Calanus tonsus

	1	2	3	4	5	6	7	8	9	10	11	12	13	14	15	16
A							r									
B																
C																
D																
E																
F													f	r		r
G										-	r		r			r
H																r

	32	31	30	29	28	27	26	25	24	23	22	21	20	19	18	17
A																
B																
C																
D																
E																
F						+				r						
G							r		r							

Calocalanus (all spp.)

	1	2	3	4	5	6	7	8	9	10	11	12	13	14	15	16
A	ı	ı	+	f	f	f	r	f	r	f	f	f	r	f	r	r
B		r		f		f		f				f		r		r
C				r		r	r	r		r	r	r		r	r	r
D		r	r	r	r	r		r	r	f	f	r				f
E				r		r	r			r	r	r	r	f	r	r
F						f				r		f	r		r	r
G						r	f			f	r	f	r	f	r	
H													r	f		r

	32	31	30	29	28	27	26	25	24	23	22	21	20	19	18	17
A	ı	+	ı	f	+	f	ı	f	f		r	f	f	+	f	f
B	+		+		f		f		+		f					
C	f	+	f	f	f	f	f	r		r	f	r	r	r		
D	+	f		f	f	f	r			f	f	r	r		r	
E		f	f	+		+	f		f	f	r			r		
F		f	f	f	f	r	f		f	f	f	r		r		
G			+			f	+		f	f		r				

ADDENDA.

Calanus tonsus:

Insert . in same squares as in *Calanus tenuicornis*, except where another symbol is already present in *C. tonsus*.

PLATE II

Calocalanus pavo

(A)

	1	2	3	4	5	6	7	8	9	10	11	12	13	14	15	16
A	•	•	•	•	•	r	•	r	•	f	•	f	•	f	•	r
B		•		•		•		•				•		•		•
C				•		•	•	•		•	•	•		•	•	•
D		•	•	•	•	•		•	•	•	•	•				•
E				•		•	•			•	•	•	•	•	•	•
F						•				•		•	•		•	•
G						•	•			•	•	•	•	•	•	
H													•	•		•

	32	31	30	29	28	27	26	25	24	23	22	21	20	19	18	17
A	f	•	f	•	f	•	l	•	•		•	•	r	•	r	•
B	•		•		•		•		•		•					
C	•	•	•	•	•	•	•	•		•	•	•	•	•		
D	•	•		•	•	•	•			•	•	•	•		•	
E		•	•	•		•	•		•	•	•					
F		•	•	•	•	•	•		•	•	•	•				
G			•			•	•		•	•		•				

Calocalanus plumulosus

	1	2	3	4	5	6	7	8	9	10	11	12	13	14	15	16
A	f	•	•	•	•	r	•	f	•	f	•	f	•	r	•	r
B		•		•		•		•				•		•		•
C				•		•	•	•		•	•	•		•	•	•
D		•	•	•	•	•		•	•	•	•	•				•
E				•		•	•			•	•	•	•	•	•	•
F						•				•		•	•		•	•
G						•	•			•	•	•	•	•	•	
H													•	•		•

	32	31	30	29	28	27	26	25	24	23	22	21	20	19	18	17
A	r	•	f	•	r	•	r	•	r		•	•	•	•	•	•
B	•		•		•		•		•		•					
C	•	•	•	•	•	•	•	•		•	•	•	•	•		
D	•	•		•	•	•	•			•	•	•	•		•	
E		•	•	•		•	•		•	•						
F		•	•	•	•	•	•		•	•	•	•				
G			•			•	•		•	•		•				

Calocalanus styliremis

	1	2	3	4	5	6	7	8	9	10	11	12	13	14	15	16
A	•	•	•	•	•	•	•	f	•	f	•	r	•	•	•	•
B		•		•		•		•				•		•		•
C				•		•	•	•		•	•	•		•	•	•
D		•	•	•	•	•		•	•	•	•	•				•
E				•		•	•			•	•	•	•	•	•	•
F						•				•		•	•		•	•
G						•	•			•	•	•	•	•	•	
H													•	•		•

	32	31	30	29	28	27	26	25	24	23	22	21	20	19	18	17
A	f	•	f	•	f	•	r	•	r		r	•	•	•	•	•
B	•		•		•		•		•		•					
C	•	•	•	•	•	•	•	•		•	•	•	•	•		
D	•	•		•	•	•	•			•	•	•	•		•	
E		•	•	•		•	•		•	•	•					
F		•	•	•	•	•	•		•	•	•	•				
G			•			•	•		•	•		•				

CORRIGENDA and ADDENDA.

Calocalanus pavo:

Insert . in squares E 19, F 19.

Calocalanus plumulosus:

Delete . in squares: A 2, A 4, A 18 A 20, A 22.

Trigsurvey 1964.

PLATE III

Candacia aethiopica

(B)

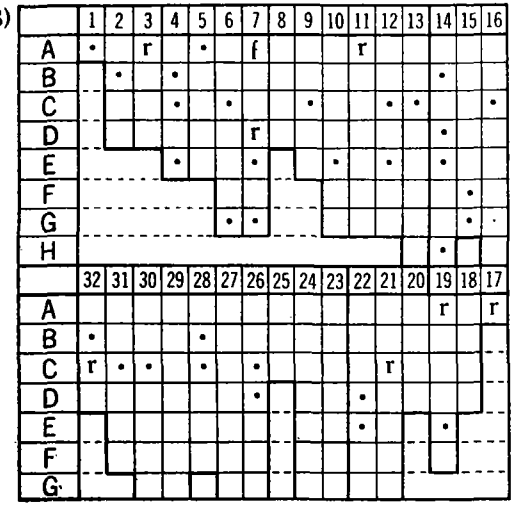

Candacia bispinosa

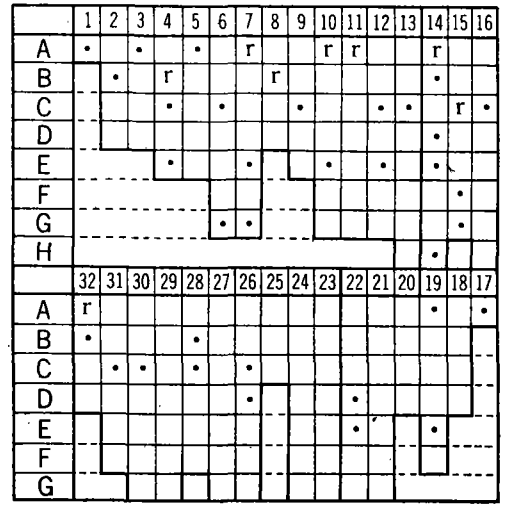

Candacia catula

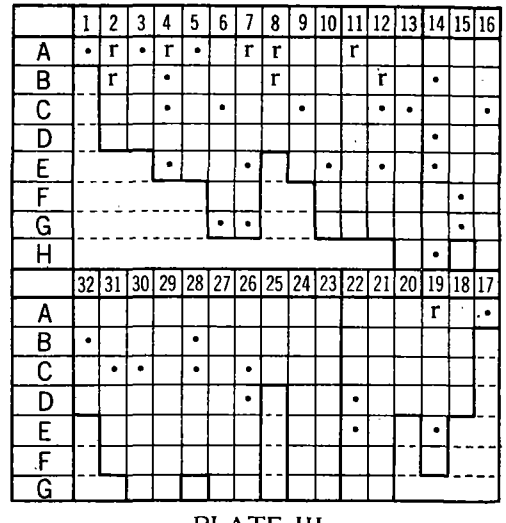

PLATE III

Candacia longimana

(A)

	1	2	3	4	5	6	7	8	9	10	11	12	13	14	15	16
A																
B																
C															r	
D																r
E													r	r		
F																
G																
H																

	32	31	30	29	28	27	26	25	24	23	22	21	20	19	18	17
A																
B																
C								r								
D					r											
E					r											
F																
G																

Candacia simplex

	1	2	3	4	5	6	7	8	9	10	11	12	13	14	15	16
A	f		r			r				r		r		r		
B						r		r								
C														r		
D															r	
E																
F																
G																
H																

	32	31	30	29	28	27	26	25	24	23	22	21	20	19	18	17
A	r		r													
B	f															
C	r												r			
D																
E																
F					r											
G																

Candacia truncata

	1	2	3	4	5	6	7	8	9	10	11	12	13	14	15	16
A	f		r	r			r	r			f					
B								r								
C																
D							r									
E																
F																
G																
H																

	32	31	30	29	28	27	26	25	24	23	22	21	20	19	18	17
A																
B																
C																
D																
E																
F																
G																

ADDENDA.

Candacia longimana, C. simplex, C. truncata:

Insert . in same squares as in other *Candaciae* (page 27), except where another symbol is already present in the square concerned.

Trigsurvey 1964.

PLATE IV

(B)

Canthocalanus pauper

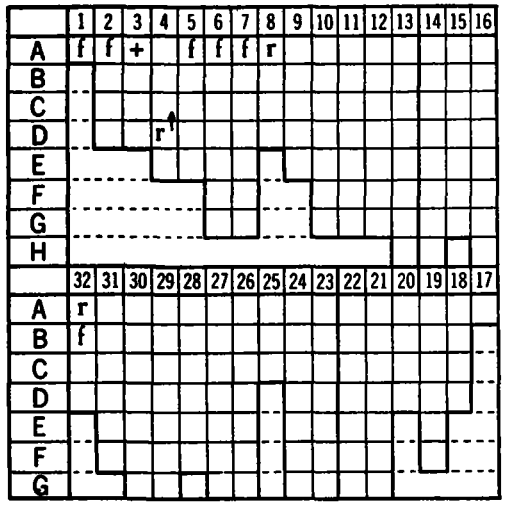

Centropages calaninus

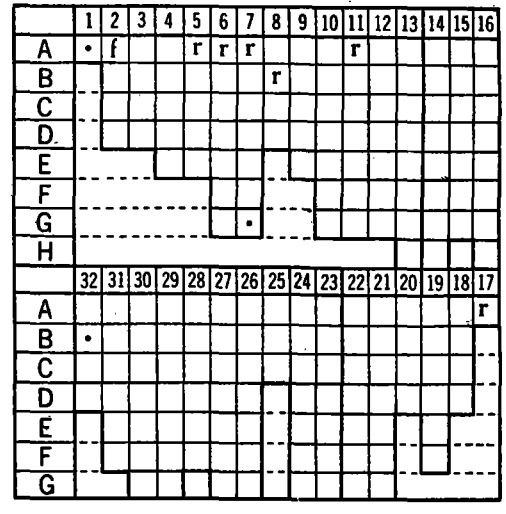

Centropages elongatus

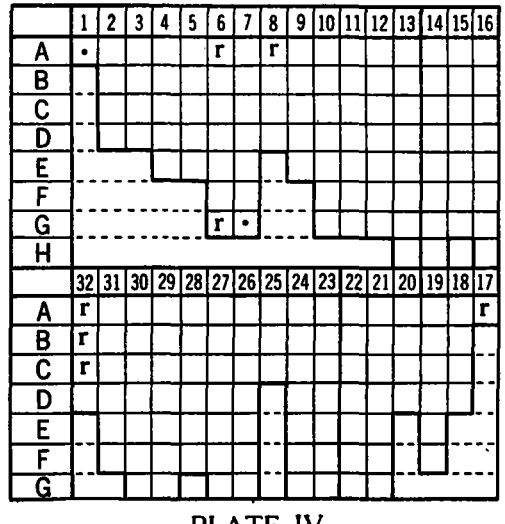

PLATE IV

Trigsurvey 1964.

Centropages furcatus

(A)

	1	2	3	4	5	6	7	8	9	10	11	12	13	14	15	16
A	+	+	f		r			r								
B								r								
C																
D																
E																
F																
G							•					r				
H																

	32	31	30	29	28	27	26	25	24	23	22	21	20	19	18	17
A																
B	•															
C																
D																
E																
F																
G																

Centropages gracilis

	1	2	3	4	5	6	7	8	9	10	11	12	13	14	15	16
A	f				r	f					r	r				
B																
C					r											
D																
E																
F																
G							•					r	r			
H																

	32	31	30	29	28	27	26	25	24	23	22	21	20	19	18	17
A	r		r													
B	•															
C																
D																
E																
F																
G																

Chiridius sp.

	1	2	3	4	5	6	7	8	9	10	11	12	13	14	15	16
A																
B																
C																
D														r		
E							r									
F																
G																
H																

	32	31	30	29	28	27	26	25	24	23	22	21	20	19	18	17
A																
B																
C						f										
D				r							r					
E			r													
F					r											
G																

PLATE V

Clausocalanus arcuicornis

(B)

	1	2	3	4	5	6	7	8	9	10	11	12	13	14	15	16
A	2	+	•	+	•	1	•	+	•	f	•	1		f	f	r
B		•		•		•		•				•		f		•
C		•		•	•	•	•	•	•		•	•		•	•	•
D		•		•	•	•	•	•	•	•	•		•	•		•
E				•		•	•		•	•	•	•	•	•	•	•
F						•	•			•	•		•	•	•	•
G						•	•			•	•	•	•	r	•	•
H													•	•		r

	32	31	30	29	28	27	26	25	24	23	22	21	20	19	18	17
A	+	•	f		r	•	r	•		•	f	•		f		•
B	•		•		•		•				•					
C		•	•	•	•	•	•	•	•	•	•			•		
D	•	•	•			•	•		•	•	•	•	•	•	•	
E			•	•	•	•	•				•	•		•		
F		•	•	•	•	•	•			•	•	•		•		
G						•	•			•	•	•				

Clausocalanus furcatus

	1	2	3	4	5	6	7	8	9	10	11	12	13	14	15	16
A	3	+	•	+	•	2	•	+	•	+	•	1			•	
B		•		•		•		•				•		•		•
C		•		•	•	•	•	•	•		•	•		•	•	•
D		•	r	r	•	•	•	•	•	•	•		•	•		•
E				f		•	•		•	•	•	•	•	•	•	•
F						•	•			•	•		•	•	•	•
G						•	•			•	•	•	•	•	•	•
H														•		

	32	31	30	29	28	27	26	25	24	23	22	21	20	19	18	17
A	f	•	f			•		•		•		•				•
B	•		•			•		•			•					
C		•	•	•	•	•	•	•	•	•	•	•		•		
D	•	•	•			•	•		•	•	•	•	•	•	•	
E			•	•	•	•	•				•	•		•		
F		•	•	•	•	•	•			•	•	•		•		
G						•	•			•	•	•				

Clausocalanus paululus

	1	2	3	4	5	6	7	8	9	10	11	12	13	14	15	16
A		•	•		•	r	•	r	•	r	•	•		f	•	r
B		•		•		•		•				•		•		•
C		•		•	•	•	•	•	•		•	•		•	•	•
D		•		•	•	•	•	•	•	•	•		•	•		•
E				•		•	•		•	•	•	•	•	•	•	•
F						•	•			•	•		•	•	•	•
G						•	•			•	•	•	•	•	•	•
H													•	•		

	32	31	30	29	28	27	26	25	24	23	22	21	20	19	18	17
A	r	•	r			•	r	•		•		•		•		•
B	•		•		•		•				•					
C		•	•	•	•	•	•	•	•	•	•			•		
D	•	•	•			•	•		•	•	•	•	•	•	•	
E			•	•	•	•	•				•	•		•		
F		•	•	•	•	•	•			•	•	•		•		
G						•	•			•	•	•				

ADDENDUM.

Clausocalanus furcatus:
Insert . in square H 13.

PLATE V

Trigsurvey 1964

Clausocalanus (all spp.)

(A)

	1	2	3	4	5	6	7	8	9	10	11	12	13	14	15	16
A	3	1	+	1	+	2	+	+	f	+	1	2		+	f	f
B		f		+		f		+				f		f		f
C		f		f	f	f	f	f	f		f	f		f	f	f
D		f	f	f	r	r	f	f	f	f	f		r	r		f
E				r		+	f		r	f	r	f	r	f	f	f
F						1	f			f	f		r	f	f	r
G						+	+			+	f	+	+	+	f	r
H													f	+		r

	32	31	30	29	28	27	26	25	24	23	22	21	20	19	18	17
A	+	f	f		r	f	f	+	r	r	f	f		f		f
B	+		f		+		+				f					
C		f	+	f	1	f	+	f	f	f	+	r		f		
D	f	f	r			r	f		f	r	f	r	r	f	r	
E			1	1	+	1	f				+	r		f		
F		f	f	+	f	r	f		f	r	r	f		f		
G						f	f		f	f	1	f				

Conaea gracilis

	1	2	3	4	5	6	7	8	9	10	11	12	13	14	15	16
A												r	r			
B														r		
C																
D		r														
E					f		r							r		r
F							r							r	r	r
G							r		f				r		r	r
H														f		

	32	31	30	29	28	27	26	25	24	23	22	21	20	19	18	17
A					r								r			
B																
C													r			
D						r										
E			f				r		r							
F		r	+	r	f	r	+		r		r					
G			f	r			f		r		r	r				

Copilia mirabilis

	1	2	3	4	5	6	7	8	9	10	11	12	13	14	15	16
A	r	f	f	r	r		r	r						r		
B								r								
C						•	•									
D																
E				r										•		
F																
G																•
H																

	32	31	30	29	28	27	26	25	24	23	22	21	20	19	18	17
A	r															
B	r															
C																
D																
E																
F																
G							•									

PLATE VI

Trigsurvey 1964.

(B) Copilia quadrata

	1	2	3	4	5	6	7	8	9	10	11	12	13	14	15	16
A								r							r	
B														r		
C						•	•								r	
D																
E														•		
F																
G																•
H																

	32	31	30	29	28	27	26	25	24	23	22	21	20	19	18	17
A	r															r
B																
C																
D																
E																
F							•									
G																

Ctenocalanus vanus

	1	2	3	4	5	6	7	8	9	10	11	12	13	14	15	16
A			r													
B		r	r	r				r						r		r
C																
D																
E																
F														r		
G							r			r				r		
H																

	32	31	30	29	28	27	26	25	24	23	22	21	20	19	18	17
A			r													
B					r											
C					r		r									
D						r						r				
E																
F			f	r			f		r		r	r				
G									r		r					

Corycaeus sensu lato (all spp., excl. Corycella)

	1	2	3	4	5	6	7	8	9	10	11	12	13	14	15	16
A	ı	ı	+	ı	+	+	+	+		f	+	+	f	+	r	
B		r		f		f		+				+		f		r
C		r		?	?	?	?		?	?	?	?	?		?	?
D			r	f	f	f	+	+	r	r	f	?	r	f		r
E				f		r	f		r	r	f	f	r	+	r	r
F						ı	r					f	f		r	
G						f	f			f	f	+	r	f		r
H													f	+		f

	32	31	30	29	28	27	26	25	24	23	22	21	20	19	18	17
A	+	f	+				r	f				f	f	+		f
B	+				r								r			
C		+	r	+	ı	r		r			r	r	f	?		
D		r	r								f	r	r	f	?	
E		r	f	f	r	f				r		r				
F			r			r						r				
G			f	r			r					f				

PLATE VI

ADDENDA.

Ctenocalanus vanus:

Insert r in squares A 12 and A 25.

Trigsurvey 1964.

Corycella (all spp.)

(A)

	1	2	3	4	5	6	7	8	9	10	11	12	13	14	15	16
A	f	f	f	r	f	f	f	f	f	+	f	l	f	+		
B						f		f				+		f		
C				?		?	?			?			?			
D			r			f				r					f	r
E				f	r	f						r		f		
F						r	r							r		
G						+	r				r	r	?	f		
H													f			

	32	31	30	29	28	27	26	25	24	23	22	21	20	19	18	17
A		+	+	l	l	f	f	f				r	r		r	f
B	+		+		+		f		r							
C	+				r	r	r	r			r	r		?		
D	f	+	f	f	f	f	r				f	r	r	r	?	
E					f							r		r		
F		l	f	l	f	f	r		r			r				
G			f	r		r			?		r	r				

Euaugaptilus palumboi

	1	2	3	4	5	6	7	8	9	10	11	12	13	14	15	16
A																
B																
C																
D																
E																
F																
G							r									r
H														r		

	32	31	30	29	28	27	26	25	24	23	22	21	20	19	18	17
A																
B																
C																
D																
E																
F			r		f	r										
G																

Euaetidius acutus

	1	2	3	4	5	6	7	8	9	10	11	12	13	14	15	16
A			r				r									
B				r		r										
C																
D																
E																
F																
G						r				r						
H																

	32	31	30	29	28	27	26	25	24	23	22	21	20	19	18	17
A																
B																
C																
D																
E																
F																
G																

ADDENDUM.

Corycella (all spp.):
Insert + in square A 32.

Trigsurvey 1964

PLATE VII

Euaetidius giesbrechti

(B)

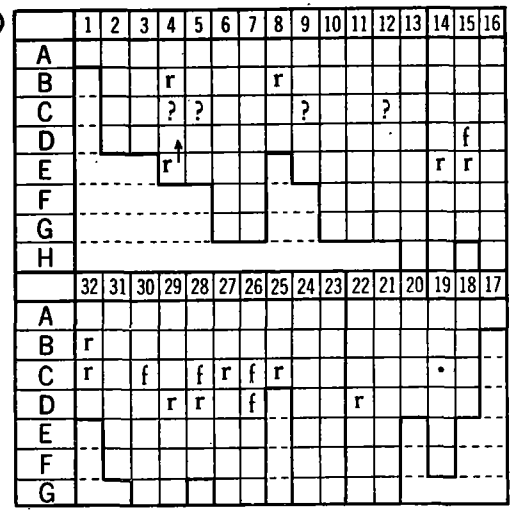

Eucalanus attenuatus

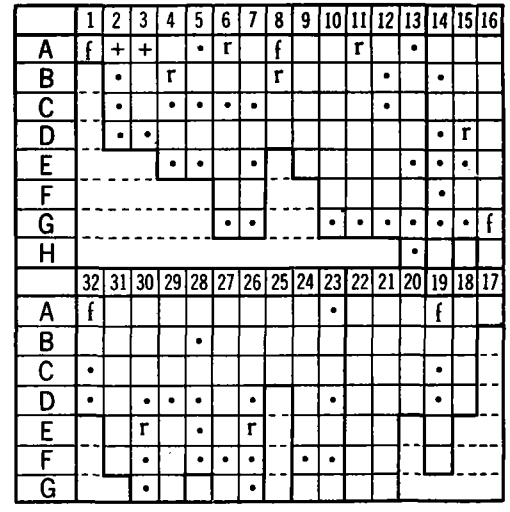

Eucalanus crassus

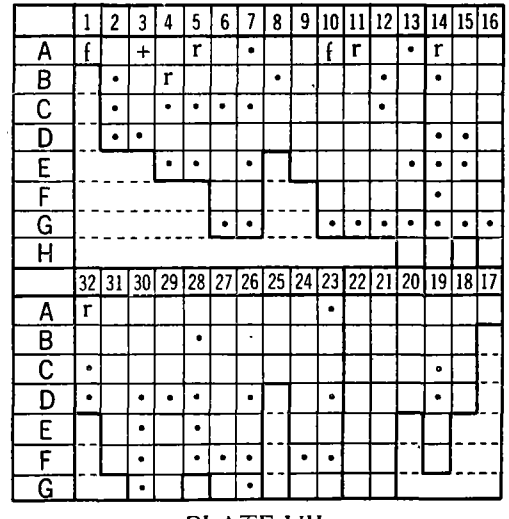

ADDENDUM.

Eucalanus crassus:
Insert . in square H 13.

PLATE VII

Eucalanus elongatus

(A)

	1	2	3	4	5	6	7	8	9	10	11	12	13	14	15	16
A	•		•		•		•			r	•		•			
B		•		•				•				•		•		
C		•		•	•	•	•					•				
D		•	•											•	•	
E				•	•		•						•	•	•	
F														r		r
G						•	•			•	•	•	•	•	•	f
H													•			

	32	31	30	29	28	27	26	25	24	23	22	21	20	19	18	17
A										•						
B					•											
C	•													•		
D	•		•	•	•		•			•				•		
E			r		•				r							
F			•		•	•	•		•	•						
G			r				•		r							

Euchaeta (all spp.)

	1	2	3	4	5	6	7	8	9	10	11	12	13	14	15	16
A	f	f	f	f	2	2	f	+		r	f	r				
B		r		f		r		+								r
C				?	?	?		?	?				?	?	?	
D		r					r				r				f	
E				r		r	r				r		r	r	r	
F																
G						r	r					r				r
H													r			

	32	31	30	29	28	27	26	25	24	23	22	21	20	19	18	17
A	f				r					f						r
B	f		r				r									
C			f	f	f	f	f	f	r	r	f					
D			f	f	f		+		f	f	+					
E			f		f		f		f		r					
F			f		r		r		r					r		
G									r		r					

Euchirella (all spp.)

	1	2	3	4	5	6	7	8	9	10	11	12	13	14	15	16
A						r		r							r	
B												r				
C						r			r					r		
D																
E				r	f		f							r		
F															r	
G													r			r
H																

	32	31	30	29	28	27	26	25	24	23	22	21	20	19	18	17
A		r														
B																
C					r		r	r								
D			f	f			r									
E					f											
F					r											
G			r								r					

Trigsurvey 1964,

PLATE VIII

Euterpina acutifrons

(B)

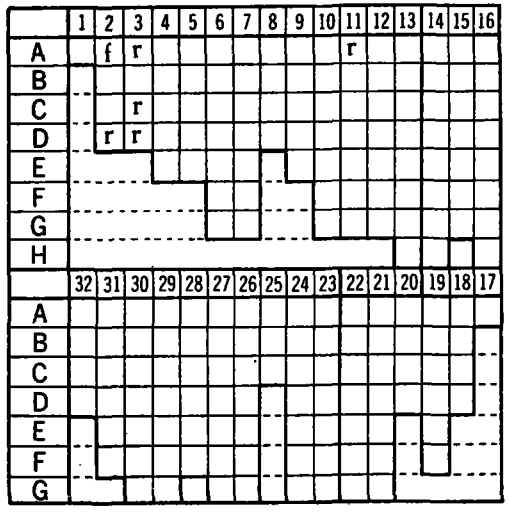

Gaetanus miles

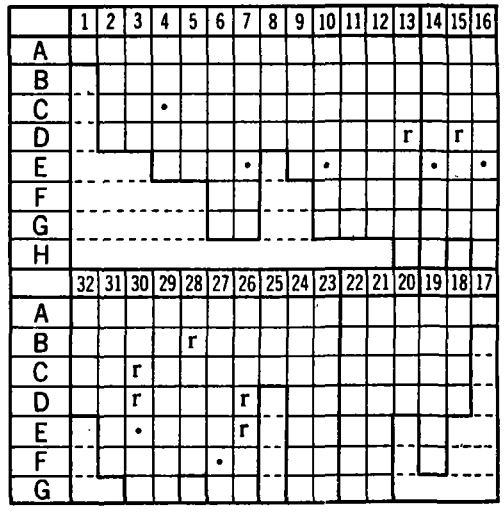

Gaetanus minor

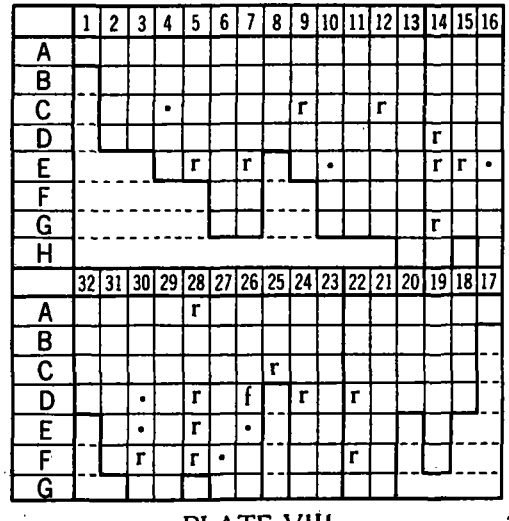

ADDENDUM.

Gaetanus minor:

Insert r in square A 21.

PLATE VIII

Trigsurvey 1964

Haloptilus longicornis

(A)

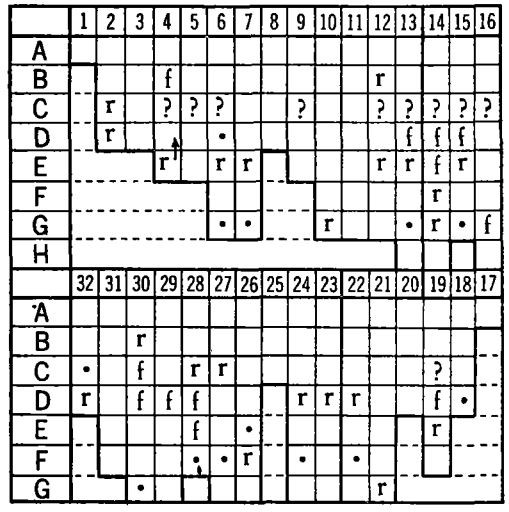

Heterorhabdus spinifrons

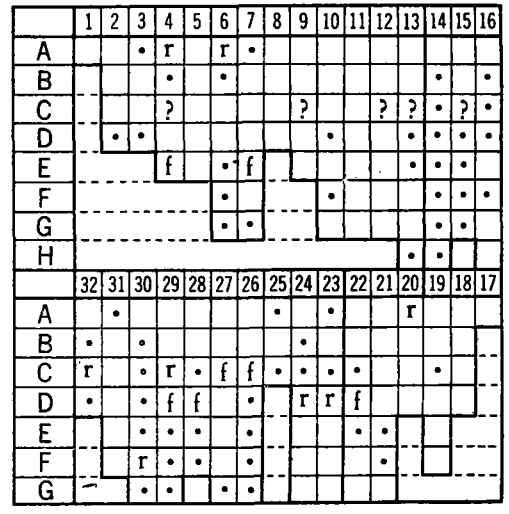

Lubbockia squillimana

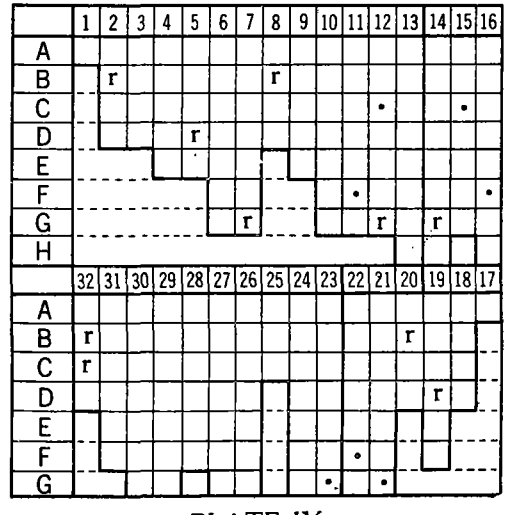

PLATE IX

Trigsurvey 1964

(B)

Lucicutia clausi

	1	2	3	4	5	6	7	8	9	10	11	12	13	14	15	16
A			•						r		•				•	
B		•														
C		•		•	•	•	•		•			•	•	•	•	•
D		•	•	•			•					•		r	f	
E				•	•	•	•			•		•			•	
F						•	•				•		•	•	r	•
G						•	•			r		•	•	•		•
H													•	•		•

	32	31	30	29	28	27	26	25	24	23	22	21	20	19	18	17
A		•						•		•				•		
B					•				•				r			
C	•	•	•	•	•	r	•	+		•	•					
D		•	•	•	•	•	•		•		•			•	•	
E		•	•	•	•		•		•	•	•			•		
F		•	•	•	•	•	•		•	•		•				
G			•	•					•		•	•				

Lucicutia curta

	1	2	3	4	5	6	7	8	9	10	11	12	13	14	15	16
A			r										r			
B				r				r				r		r		
C																
D																
E																
F																
G																
H																

	32	31	30	29	28	27	26	25	24	23	22	21	20	19	18	17
A	r	•						•		•				•		
B					r		r				r		•			
C	•	•	•	•	•	•	•			•	•					
D		•	•	•	•	•	•		•		•			•	•	
E		•	•	•	•		•		•	•	•			•		
F		•	•	•	•	•	•		•	•		•				
G			•	•					•		•	•				

Lucicutia flavicornis

	1	2	3	4	5	6	7	8	9	10	11	12	13	14	15	16
A			•								f			r	•	r
B		•		r		r		f						r		r
C		•		•	r	•	•		•			•	•	•	•	•
D		•	•	•			•					•			•	
E				•	•	•	•			•		•		•	•	
F						•	•				•		•	•		•
G						•	•			•		•	•	•		•
H													•	•		•

	32	31	30	29	28	27	26	25	24	23	22	21	20	19	18	17
A		•					r	•		•				•		
B	r				r		r		•				•			
C	•	•	•	•	•	•	•			•	•	r	r			
D		•	•	•	•	•	•		•		•			•	•	
E		•	•	•	•		•		•	•	•			•		
F		•	•	•	•	•	•		•	•		•				
G			•	•					•		•	•				

ADDENDA.

Lucicutia curta:

Insert . in same squares as in *L. clausi*, except where another symbol is already present in *L. curta*.

Insert . also in squares D 15, G 10.

PLATE IX

Macrosetella gracilis

(A)

	1	2	3	4	5	6	7	8	9	10	11	12	13	14	15	16
A	+	f	+	f	f	r	f	f		f	f	f		r		
B		r		r		r		f				f				
C				?	?	?	?	?	?		?			?		
D				r			r	r		r	f	?				
E				r	r	r	r					r				
F											r					
G							r				r	f		r		
H																

	32	31	30	29	28	27	26	25	24	23	22	21	20	19	18	17
A	f		r												r	
B	f															
C	r						r							r		
D	f	r													r	
E																
F					r									r		
G			r													

Mecynocera clausi

	1	2	3	4	5	6	7	8	9	10	11	12	13	14	15	16
A	r			r	r		r	r	r	+	f	f	f	f	r	r
B				r		f						ı		f		r
C			r	?	?		?			?	?	?		?	?	
D						r	r			f	f	?		f		
E				r		r	r			r	r	f	r	f	r	
F						r	f						f	r		r
G						r	r			r		r	r	r	r	r
H													r	f		

	32	31	30	29	28	27	26	25	24	23	22	21	20	19	18	17
A	+	f	+	ı	f	r	+	+	f		f	f	r	r		
B	+		f		f		+		f		f					
C	f	f	+	+	f	r	f	r	r	f	f	r	r	?		
D	+	+	+	f	f	f			r	r	f	r	r	r		
E		r	f	f		r	r			r		r		r		
F		f	f	ı	+	f	r		r	r	f					
G				+		r	r			r		r				

Metridia brevicauda

	1	2	3	4	5	6	7	8	9	10	11	12	13	14	15	16
A																
B																r
C		•	•	•									•			
D				•									•	•		•
E				f	•	•	•					•	•	•		•
F						•							•	•		•
G							•						•			•
H													•			

	32	31	30	29	28	27	26	25	24	23	22	21	20	19	18	17
A			r													
B																
C										•	•			•		
D			•	•	•		r			•						
E			•		•		•		r		•					
F		•	•	•	f	r	r		•	•	•	•		•		
G			•						•	•	•					

ADDENDUM.

Metridia brevicauda:

Insert . in square D 27.

Trigsurvey 1964.

PLATE X

Metridia lucens

(B)

	1	2	3	4	5	6	7	8	9	10	11	12	13	14	15	16
A														r		
B																
C		•	•	•									•			
D				•									•	•		•
E				f	•	•	•						•	•	•	•
F						•							•	•		•
G							•						•			•
H													•			

	32	31	30	29	28	27	26	25	24	23	22	21	20	19	18	17
A																
B																
C										•	•			•		
D			•	•	•	•	•			•						
E			•		r		•				•					
F		•	•	•	•	•	•			•	•	•		•		
G			•	r			f		?	•	•					

Metridia venusta

	1	2	3	4	5	6	7	8	9	10	11	12	13	14	15	16
A																
B																
C		•	•	•									•			
D				•									•	•		•
E					•	•	•						•	•		•
F						•							r	r		•
G							•						•			•
H													•			

	32	31	30	29	28	27	26	25	24	23	22	21	20	19	18	17
A																
B					r											
C										•	•			•		
D			•	•	•	•	•			•						
E			r		•		r				r					
F		•	•	•	r	f	•			•	•	f	•	•		
G			•							•	•	•				

Monacilla typica

	1	2	3	4	5	6	7	8	9	10	11	12	13	14	15	16
A																
B																
C																
D																
E				r												
F																
G																r
H																

	32	31	30	29	28	27	26	25	24	23	22	21	20	19	18	17
A																
B																
C																
D																
E			'													
F			f		r	r										
G			r						r							

PLATE X

UNESCO ARCHIVES

Trigsurvey 1964.

Microsetella norvegica

	1	2	3	4	5	6	7	8	9	10	11	12	13	14	15	16
A				r						r						
B																
C		•				•	•				•					
D				r	r											
E				•	•	•			•		•					
F																
G							•									
H																

	32	31	30	29	28	27	26	25	24	23	22	21	20	19	18	17
A	r															
B																
C	•	•	•		•			•								
D	•	•		•	•						•					
E		r								r	r					
F					r_i		r				•			•		
G																

Microsetella rosea

	1	2	3	4	5	6	7	8	9	10	11	12	13	14	15	16
A			r		r		r	r		r	r			r		r
B				r		r		r								
C		•				•	•				•					
D		r	r		r											r
E				•	•	•			•		•					
F						r						r	r			r
G							•			r				r		r
H														f		

	32	31	30	29	28	27	26	25	24	23	22	21	20	19	18	17
A	r		r						r							
B	r															
C	•	•	•		•			•								
D	•	•		•	•						•					
E			r				r									
F				r	r						•			•		
G			r							r						

Mormonilla spp.

m minor
p = phasma

	1	2	3	4	5	6	7	8	9	10	11	12	13	14	15	16
A						r_p			r			r_m	r_p			
B																
C		f		?	?							?				?
D		f		r				r						r		f
E				f	f	f	f		r	f	f	r	f	r	r	r
F												r		f	r	
G						r	r			f	f	f	f	f		f
H														+		

	32	31	30	29	28	27	26	25	24	23	22	21	20	19	18	17
A		r_m			r_m								r_p			
B																
C												r_m	r	?		
D	f		+	f	f	f	f		r	f				r	?	
E			+	f	f		r			r	r					
F		f	+	f	+	f	f		f	f	f	r		r		
G			+	+		f	r		?	+		f				

PLATE XI

Trigsurvey 1964

Nannocalanus minor

(B)

	1	2	3	4	5	6	7	8	9	10	11	12	13	14	15	16
A	+	+	2	r	f	r	f	f		r	+	f		r		
B				f		r		+				f		f		
C						?						?	?	?	?	
D							r	r					r	r	f	
E				r										f	r	
F							r								r	
G												f	?			
H													r	r		

	32	31	30	29	28	27	26	25	24	23	22	21	20	19	18	17
A	+	f	f	f	r	r	r	r		r		f	r	f		f
B	+		r		f		f		r		f		r			
C			+	r	r	r	r		r		f			?		
D				f	r		+		f		r		r		r	
E											r					
F					r											
G																

Neocalanus gracilis

	1	2	3	4	5	6	7	8	9	10	11	12	13	14	15	16
A	r	r		r			r	r		r	r					
B				f												
C				?	?	?						?	?	?		
D													r		r	
E							r							r	r	
F													r		r	
G												r	r	r		
H																

	32	31	30	29	28	27	26	25	24	23	22	21	20	19	18	17
A	r		r													
B											f					
C			f	r	f	r	f	f	f		f			?		
D			+	+	r				+		2					
E			r		f				r		r					
F			r		f	r										
G						r					f					

Oithona (all spp.)

	1	2	3	4	5	6	7	8	9	10	11	12	13	14	15	16
A	2	1	4	1	2	1	1	+	f	1	2	2	f	÷	f	f
B		f		2		1		1				1		+		+
C		f	f	?	?	?	?	?	?	?	?	?	?	?	?	?
D		f	f	f	+	f	1	+	f	+	+	?		f	r	÷
E				+	f	+	+		r	f	f	÷	f	1	+	÷
F						1				f	+	÷	f	f	+	+
G						+	+			+	f	÷	f	1	f	f
H													+	1		f

	32	31	30	29	28	27	26	25	24	23	22	21	20	19	18	17
A	1	1	2	+	1	1	1	1	+	+	÷		f	+	r	+
B	1		2		1		1		1		1		f			
C	+	1	+	+	1	+	+		+	1	+	f	r	?		
D	3	3	3	3	2	3	3		3	+	4	f	f	f	f	
E		1	1	1	1	1	1		÷	+	+	f		÷		
F		1	2	3	2	1	2		1	2	2	÷				
G			1	1		+	+		?	1	1	+				

PLATE XI

Trigsurvey 1964.

Oncaea (all spp.)

(A)

	1	2	3	4	5	6	7	8	9	10	11	12	13	14	15	16
A	2	2	4	1	2	2	1	+	f	f	2	+		f	f	r
B		+		2		1		+				1		f		f
C		f	f	?	?	?	?	?	?	?	?	?		?	?	?
D		f	f	f	f	f	+	+	f	+	f	?	r	f	r	f
E				+	f	+	+		r	f	f		f	+	f	+
F						1	+			f	f	+	f	+	f	f
G						+	+			+	f	+	r	+	+	f
H													+	1		f

	32	31	30	29	28	27	26	25	24	23	22	21	20	19	18	17
A	1	f	f		f	r	r	r	r	r		r	f	+		f
B	+		f				f		r		f		r			
C	+	1	1	r	1	+	+	1	f	r	f	r	r	?		
D	+	1	1	+	+	f	+				f	+	f	f	+	r
E		+	+	+	+	f	1		+	f	f	r		+		
F		1	1	2	1	+	1		+	+	+	f		f		
G			1	+		+	+		?	1	1	+				

Paracalanus (all spp.)

	1	2	3	4	5	6	7	8	9	10	11	12	13	14	15	16
A	2	1	1	f	1	f	+	f	f	f	+	1	r	f	r	r
B		r		+		+		+				f				r
C		r	r	?	?	?	?		?	?	?	?		?		
D			r	r		r			r	f	f	?			.	r
E				r	f	f	r		r	f	f	f	r	r	r	f
F										r	f	f		r	r	r
G						f	f			f	f	f	r	f	f	f
H													f	+		

	32	31	30	29	28	27	26	25	24	23	22	21	20	19	18	17
A	1	f	f	r	r	f	f	+	r		f	f	r	f	r	f
B	+		f		f		f				r					
C	f	+	r	f	f		r				r					
D	f	f		r		f	r			r			r	f		
E		f	r			f	r		f		f			r		
F		f	f	f	f	r	f		f	f	f	f		f		
G						r	r			r						

Phyllopus (all spp.)

	1	2	3	4	5	6	7	8	9	10	11	12	13	14	15	16
A																
B																
C																
D																
E					r		r							r	r	
F														r		
G										r			r	r		
H													r			

	32	31	30	29	28	27	26	25	24	23	22	21	20	19	18	17
A																
B					r											
C																
D			f	f	r		f		r		r					
E			f		f		r			r	r					
F		r		f			r			r						
G											r					

ADDENDA and CORRIGENDA.

Oncaea (all spp.):
Delete f in A 28.

Paracalanus (all spp.):
Delete ? in C 5.

Phyllopus (all spp.):
Insert r in E 24.

Trigsurvey 1964.

PLATE XII

Pleuromamma xiphias

(B)

	1	2	3	4	5	6	7	8	9	10	11	12	13	14	15	16
A			·				·									
B												·		·		
C		·		·	·	·	·		·			·	·	·	·	·
D		·	·	·			·						·	·	·	·
E				f	·		f			·			f	·	·	·
F													·	·	·	·
G						·	·			·		·	·	·	·	r
H													·	·		

	32	31	30	29	28	27	26	25	24	23	22	21	20	19	18	17
A		·			r	·				·						
B			·		r		·		·		·					
C	·	·	·	·	·	·	·	f	·		·			·		
D		·	f	·	·	·	+		·	·	f	·		·		
E		·	·		·		·		·		·			·		
F			·		r		·			·	·					
G			·	·		·			·	·	·					

Rhincalanus cornutus

	1	2	3	4	5	6	7	8	9	10	11	12	13	14	15	16
A	r	r	f													
B				f		?		r				r				
C		r		?		?			?			?				
D		r														
E				r			f									
F																
G																
H																

	32	31	30	29	28	27	26	25	24	23	22	21	20	19	18	17
A	r															
B	f															
C					r			r			r					
D														r		
E																
F			r													
G																

Rhincalanus nasutus

	1	2	3	4	5	6	7	8	9	10	11	12	13	14	15	16
A																
B																
C														?		
D																
E					r		f						f	f		
F													r	f		
G														r		
H														r		

	32	31	30	29	28	27	26	25	24	23	22	21	20	19	18	17
A	r				r					r						
B	r															
C		r								r						
D			f													
E			f		f		f		r		f					
F			r		+		f			r	f					
G									?		r					

ADDENDUM.

Rhincalanus cornutus:
Insert ? in C 5.

PLATE XII

Trigsurvey 1964.

Pontellina plumata

(A)

	1	2	3	4	5	6	7	8	9	10	11	12	13	14	15	16
A	r	f	r	f	r	r	f	r		r	r					
B																
C																
D																
E																
F																
G																
H																

	32	31	30	29	28	27	26	25	24	23	22	21	20	19	18	17
A																
B	r															
C																
D																
E																
F																
G																

Scolecithricella dentata

	1	2	3	4	5	6	7	8	9	10	11	12	13	14	15	16
A			•													
B								•				•				
C												•		•		
D		r												r	r	•
E				•			r						•	•		
F																r
G						•	•			•		•		•		
H														•		•

	32	31	30	29	28	27	26	25	24	23	22	21	20	19	18	17
A																
B	•															
C						r	r									
D	•			•					•	•						
E			•		•				•	•						
F			•				•				•					
G			r	•												

Scolecithrix bradyi

	1	2	3	4	5	6	7	8	9	10	11	12	13	14	15	16
A	r		f													
B				r		r										
C				?	?	•			•			•		?	•	
D							•	r						r	f	
E				•										r	r	
F						r						r				r
G																
H																

	32	31	30	29	28	27	26	25	24	23	22	21	20	19	18	17
A																
B																
C			r											•		
D																
E																
F			•		•											
G																

PLATE XIII

Trigsurvey 1964.

Scolecithrix danae

(B)

	1	2	3	4	5	6	7	8	9	10	11	12	13	14	15	16
A	l	+	+	f	+	l	f	f		f					r	
B				r		r		f								
C						•			•			•			•	
D							•								r	
E				•												
F																
G																
H													r			

	32	31	30	29	28	27	26	25	24	23	22	21	20	19	18	17
A	f													f		r
B																
C														•		
D																
E																
F			•		•		r									
G																

Temora discaudata

	1	2	3	4	5	6	7	8	9	10	11	12	13	14	15	16
A	+	f			r			r								
B								r								
C				•												
D																
E																
F																
G																
H																

	32	31	30	29	28	27	26	25	24	23	22	21	20	19	18	17
A																
B																
C																
D																
E																
F																
G																

Temora stylifera

	1	2	3	4	5	6	7	8	9	10	11	12	13	14	15	16
A		f	+								r					
B						r										
C																
D																
E																
F																
G																
H																

	32	31	30	29	28	27	26	25	24	23	22	21	20	19	18	17
A																
B																
C																
D																
E																
F																
G																

PLATE XIII

Trigsurvey 1964.

Temora turbinata

(A)

	1	2	3	4	5	6	7	8	9	10	11	12	13	14	15	16
A	r	f		r												
B		r														
C				•												
D						r										
E																
F																
G																
H																

	32	31	30	29	28	27	26	25	24	23	22	21	20	19	18	17
A																
B																
C																
D																
E																
F																
G																

Temoropia mayumbaensis

	1	2	3	4	5	6	7	8	9	10	11	12	13	14	15	16
A																
B																
C					r											
D												r				
E				r	r											
F														r		
G													r			
H																

	32	31	30	29	28	27	26	25	24	23	22	21	20	19	18	17
A																
B																
C																
D																
E														r		
F			r				r									
G										r						

Undeuchaeta plumosa

	1	2	3	4	5	6	7	8	9	10	11	12	13	14	15	16
A																
B																
C									r						r	
D																
E				r			r						•	•		
F													•			
G																
H																

	32	31	30	29	28	27	26	25	24	23	22	21	20	19	18	17
A																
B																
C								r								
D																
E			r													
F					f	r	•									
G									•		•					

ADDENDUM.

Undeuchaeta plumosa:
Insert . in D 2.

Trigsurvey 1964

PLATE XIV

Undinula caroli

(B)

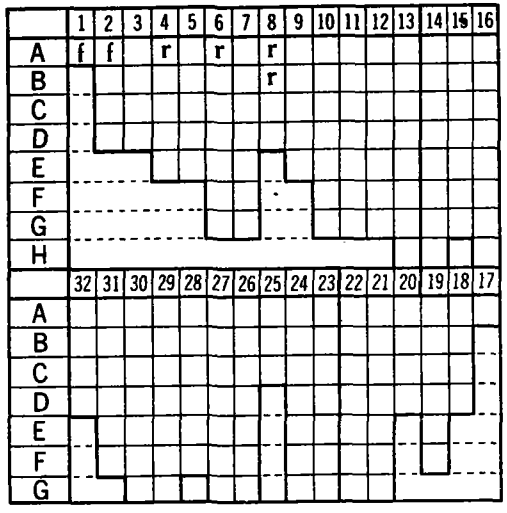

Undinula vulgaris

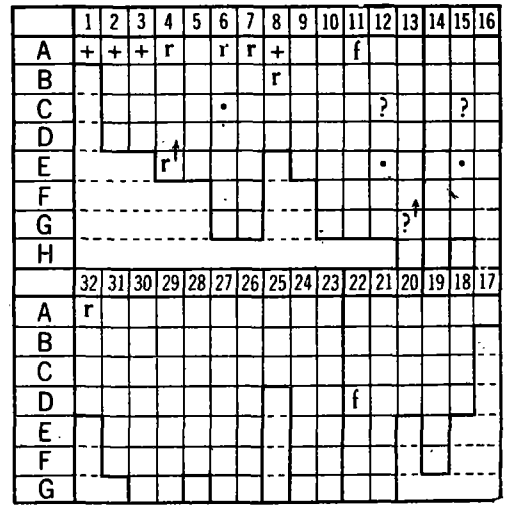

Undinula darwinii

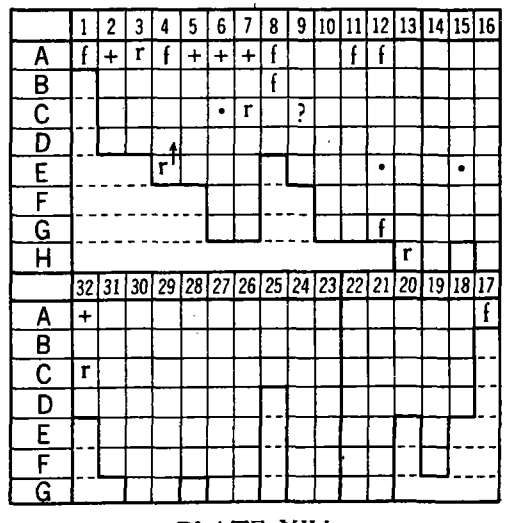

ADDENDA.

Undinula caroli:
Insert . in C 6, E 12, E 15.

PLATE XIV

Reprinted from *Zoologica Africana*, vol. 1, no. 2, 1965, p. 275-295.

NOTES ON THE BATHYPELAGIC FAUNA OF THE SEAS AROUND SOUTH AFRICA

J. R. GRINDLEY AND M. J. PENRITH*

South African Museum, Cape Town

INTRODUCTION

The bathypelagic fauna of the sea may be regarded as comprising those pelagic animals which dwell during daylight hours in the darkness of the mid-depths of the ocean, below the depth to which visible light penetrates. At night most of these bathypelagic animals migrate vertically upwards and some actually reach the surface. The present study was limited to animals obtained with a mid-water trawl, with netting of half-inch stretched mesh size, fishing down to a depth of approximately 500 metres. The area covered included southern African coastal waters and the South West Indian Ocean, as shown in Figure 1.

Until recently collecting in the bathypelagic zone was hampered by lack of suitable equipment. Available devices were based either on some sort of frame net, such as beam trawls and scaled up plankton nets, or adaptations of otter trawls, where the shearing effect of doors takes the place of the frame, as in the case of the Petersen young fish trawl and Parr's (1934) triangular trawl. Both types suffered from a number of disadvantages, the major ones being that to maintain depth they had to be towed slowly. They required a great length of cable to reach even moderate depths and, because of the slow speed of towing, they had to be large to capture the faster swimming animals and were therefore extremely unwieldy.

The Isaac-Kidd mid-water trawl (Devereaux & Winsett 1953) developed at the Scripps Institution of Oceanography, has to a large extent overcome many of the faults of earlier types. The diving action of the wide V-shaped steel depressor vane enables fast towing and the trawl maintains its fishing depth within wide margins of speed. If the ship's speed is increased, the additional drag on the cable tends to lift the net, but the depressing action of the vane also increases. The vane used in the present programme was slightly modified to increase its strength.

In 1960 the South African Museum began a survey of the biology of tuna in South African waters, including a study of their stomach contents. To make a reference collection of the possible forage organisms of the tuna a ten ft. Isaacs-Kidd mid-water trawl was obtained. This trawl proved so efficient for the collection of bathypelagic animals that its use was continued after the end of the tuna survey and it is hoped to continue this programme further to cover more intensively the seas around South Africa. Little work in this field had been done in these seas apart from the early trawling surveys by the S.S. *Pieter Faure* (1897–1907) and S.S. *Pickle* (1920–1929) and a few stations worked by the Danish Dana expedition (1928–1930).

The stations at which successful trawls have so far been made are shown on the chart

*Seconded from the Council for Scientific and Industrial Research, Oceanographic Unit, University of Cape Town.

Collected reprints of the International Indian Ocean Expedition, vol. IV, contribution no. 226

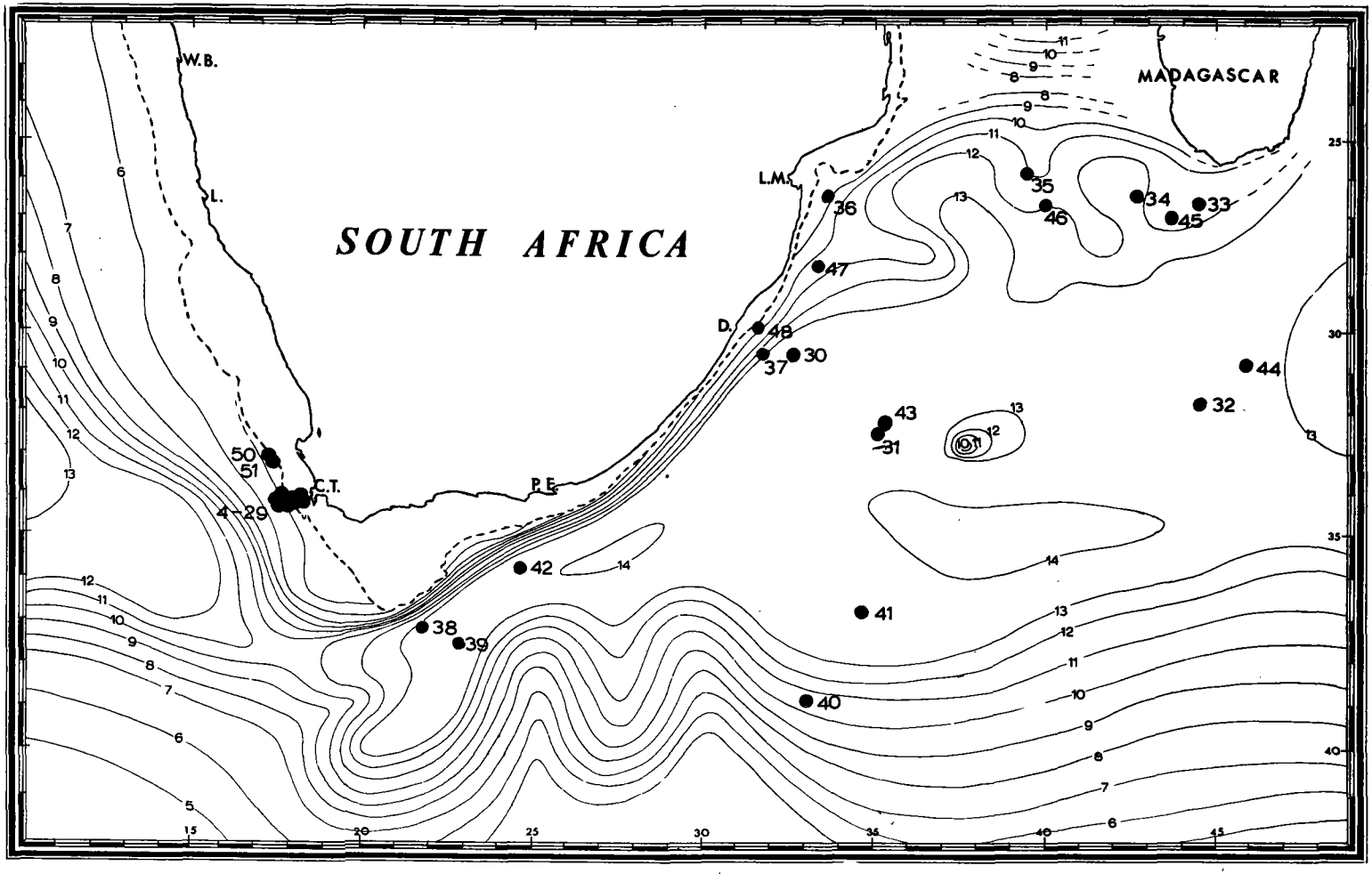

FIGURE 1. Chart showing positions of mid-water trawl stations and isotherms (°C) at the 500 metre depth level. The isotherms were plotted on the basis of published data from several sources enumerated in the text. To allow for seasonal and other variations recorded by different vessels at different times the isotherms have been smoothed in several places. The continental margin at the 500 metre level has been indicated by a broken line.

(Figure 1) and station list (Table 1), and were in the following six general areas: (1) Two trawls off Saldanha Bay (IK 50, 51) at estimated fishing depths (E.F.D.) of 120 and 280 metres. (2) Twenty-four trawls (IK 4–7 and 10–29) west of the Cape Peninsula at varying depths between 10 and 500 metres. (3) Three trawls south-east of Cape Agulhas (IK 38, 39 and 42) at E.F.D. 500 metres. (4) Five trawls east of Natal (IK 30, 36, 37, 47, 48) at E.F.D. 200 and 500 metres. (5) Nine trawls in the south-west Indian Ocean (IK 31–35, 43–46) E.F.D. 500 metres. (6) Two trawls (IK 40, 41) just north of the subtropical convergence, E.F.D. 500 metres. The estimated fishing depth has been assumed to be equal to half the length of cable out. King and Iversen (1961) give a table for estimating fishing depth at different wire angles, but the slightly modified trawl used in this programme appeared to go deeper. The depth factor of half cable out was confirmed on several occasions when the net touched the bottom. In the first three trawls the gear hit the bottom and no catch was made and the bottom was also touched at Station IK 16.

Except for certain of the trawls made off the Cape Peninsula and one off Durban, all were made at night. As the trawls made in daylight caught extremely few bathypelagic invertebrates and fish, and as time available for trawling was limited, especially in the Indian Ocean, it was felt that a large collection in this poorly known area was of the first importance.

Many of the species found are new records for the Indian Ocean, although usually known from the Atlantic and Pacific Oceans whereas off the Cape Peninsula and west coast, where there has long been much active scientific collecting and a large deep-sea trawling industry, few new South African records have been obtained.

It must be emphasised that this is a general report, and that more detailed taxonomic reports on the various animal groups will be published later. In the following account the first author is responsible for the work on invertebrates and hydrography, and the second author is responsible for the work on fishes. A preliminary report on this work was read at the Oceanography Symposium in Durban in 1963 (Penrith & Grindley 1963).

TABLE 1. STATION LIST

IK Station Number	Date	Time	Estimated Fishing Depth (Metres)	Water Depth (Metres)	Position (Approx.)
4	1/10/60	1415–1515	200	600	N.W. of Cape Town
5	23/ 4/61	1500–1515	10	2,000	West of Slangkop*
6	23/ 4/61	1800–2030	200	1,600	West of Cape Town
7	25/ 5/61	1900–2045	250	300	West of Slangkop
10	7/ 9/61	1310–1510	20	140	West of Slangkop
11	7/ 9/61	1820–2220	40	130	West of Slangkop
12	7–8/ 9/61	2230–0630	40	140	West of Slangkop
13	8/ 9/61	1345–1545	500	2,000	West of Slangkop
14	8/ 9/61	1830–2230	500	2,000	West of Slangkop

IK Station Number	Date	Time	Estimated Fishing Depth (Metres)	Water Depth (Metres)	Position (Approx.)	
15	8–9/ 9/61	2300–0300	15	400	West of Slangkop	
16	9/ 9/61	0345–0745	350	350	West of Slangkop	
17	9/ 9/61	1115–1315	400	1,600	West of Slangkop	
18	9/ 9/61	1800–2200	400	1,600	West of Slangkop	
19	11–12/11/61	2200–0700	100	200	West of Slangkop	
20	12/11/61	0800–1300	100	200	West of Slangkop	
21	12/11/61	1330–1800	10	200	West of Slangkop	
22	12–13/11/61	1830–0600	15	200	N.W. of Slangkop	
23	14–15/11/61	2000–0600	250	500	West of Slangkop	
24	15/11/61	0600–1200	100	300	West of Slangkop	
25	15/11/61	1200–1900	400	600	West of Slangkop	
26	15–16/11/61	1900–0600	400	700	West of Slangkop	
27	16/11/61	0600–1200	100	600	West of Slangkop	
28	16/11/61	1200–1900	15	300	West of Slangkop	
29	16/11/61	1900–2200	15	150	West of Slangkop	
30	10/ 8/62	1430–1700	500	3,120	30° 30′	32° 33′
31	12/ 8/62	0300–0500	500	1,320	32° 30′	35° 08′
32	15/ 8/62	0145–0440	500	1,880	31° 44′	44° 35′
33	17/ 8/62	2200–0420	500	2,900	26° 38′	44° 28′
34	18/ 8/62	1825–2125	500	4,540	26° 30′	42° 40′
35	19/ 8/62	1825–0745	500	4,320	25° 55′	39° 30′
36	21/ 8/62	1800–0725	500	710	26° 30′	33° 40′
37	23/ 8/62	1815–0330	200	930	30° 30′	31° 45′
38	7/11/62	2100–2340	500	3,300	37° 10′	21° 50′
39	10/11/62	2036–2345	500	5,750	37° 40′	22° 59′
40	13–14/11/62	2230–0050	500	5,000	38° 50′	33° 08′
41	14/11/62	2030–2300	500	3,920	36° 47′	34° 40′
42	17–18/11/62	2030–0015	500	4,810	35° 42′	24° 40′
43	14/ 2/63	2100–0330	500	1,390	32° 20′	35° 15′
44	19–20/ 2/63	2045–0005	500	1,980	30° 47′	45° 50′
45	21–22/ 2/63	2037–0045	500	4,310	27° 00′	43° 30′
46	22/ 2/63	2035–2337	500	4,760	26° 40′	40° 00′
47	24/ 2/63	2030–2335	500	1,820	28° 12′	33° 24′
48	25–26/ 2/63	2130–0040	500	810	29° 52′	31° 36′
50	17–18/ 4/63	1835–0710	280	450	33° 10′	17° 20′
51	18–19/ 4/63	1850–0700	120	400	33° 10′	17° 20′

*Slangkop is on the west coast of the Cape Peninsula (Pos. 34° 09′ S., 18° 19′ E.).

TABLE 2. DISTRIBUTION OF INVERTEBRATE SPECIES

	Off West Coast	West of Cape Peninsula	S.E. of Agulhas	Off Natal Coast	S.W. Indian Ocean	Stations 40 and 41
COELENTERATA						
Siphonophora		+	+	+	+	
*Periphylla periphylla (Péron and Leseur)		+	+		+	+
Unidentified medusae	+	+	+	+	+	+
CTENOPHORA						
Beroe sp.	+	+				+
Pleurobrachia sp.		+				
CHAETOGNATHA						
Sagitta bipunctata Quoy and Gaimard						+
*Sagitta gazellae Ritter-Zahony		+				
Sagitta hexaptera d'Orbigny				+		
Sagitta lyra? Krohn			+			
Sagitta sp. indet.					+	
ANNELIDA						
Polychaete larvae		+			+	
CRUSTACEA						
Hoplocarida						
Larval stages	+	+	+		+	
Amphipoda						
Cystisoma spp.		+	+		+	+
Hyperia galba Mont.		+				
Oxycephalus sp.		+				
Phronima sedentaria (Forskal)	+	+	+	+	+	
Phrosina semilunata Risso	+	+	+	+	+	+
Platyscelus c.f. armatus	+	+	+	+	+	
Scina c.f. crassicornis		+			+	
Scinids (other)			+	+		
Streetsia sp.		+				
Mysidacea						
Gnathophausia ingens (Dohrn)		+			+	
Euphausiacea						
*Euphausia longirostris Hansen		+				
Euphausia lucens Hansen	+	+				

	Off West Coast	West of Cape Peninsula	S.E. of Agulhas	Off Natal Coast	S.W. Indian Ocean	Stations 40 and 41
Euphausia recurva Hansen		+				
Euphausia similis var. armata Hansen.. ..	+	+				
Euphausia spinifera Sars			+	+		+
Nematobrachion flexipes (Ortman)	+					
Nematoscelis megalops Sars	+	+	+	+	+	+
Nematoscelis tenella Sars		+				
Stylocheiron abbreviatum Sars		+		+	+	
Stylocheiron maximum Hansen	+	+	+	+	+	+
Thysanoëssa gregaria Sars					+	
Thysanopoda acutifrons Holt and Tatt. ..	+		+	+	+	+
*Thysanopoda cristata Sars				+		
Thysanopoda monocantha Ortman	+	+	+	+	+	
Thysanopoda obtusifrons Sars		+			+	+
*Thysanopoda orientalis Hansen	+			+	+	+
*Thysanopoda pectinata Ortman			+		+	+
*Thysanopoda tricuspidata Milne-Edwards ..				+		
Juvenile Euphausiids	+	+		+		
Decapoda						
Acanthephyra haeckelii (von Martens) ..						+
Acanthephyra quadrispinosa Kemp	+	+	+	+	+	+
Aristeomorpha foliacea (Risso)..				+		
Chlorotocus crassicornis (Costa)	+					
Funchalia woodwardi Johnson		+	+	+	+	
Gennadas gilchristi Calman			+	+		+
Gennadas spp.	+	+		+	+	+
*Notostomus longirostris Bate		+				
Notostomus juv.				+		
Oplophorus grimaldi Coutière					+	
*Oplophorus typus Bate					+	
Oplophorus juv.		+				
*Pasiphaea acutifrons Bate		+			+	+
Plesionika longirostris Borradaile			+		+	
Plesiopenaeus nitidus Barnard					+	
Sergestes arcticus Kröyer	+	+				+

	Off West Coast	West of Cape Peninsula	S.E. of Agulhas	Off Natal Coast	S.W. Indian Ocean	Stations 40 and 41
Sergestes armatus Kröyer	+	+	+	+	+	
Sergestes gloriosus Stebbing	+	+	+	+	+	+
Sergestes phorcus Faxon		+		+	+	+
Sergestes splendens Sund	+	+		+	+	
Sergestes spp.	+	+	+	+	+	+
Solenocera africanum Stebbing		+				
Systellaspis debilis (Milne Edwards)	+	+	+	+	+	+
Decapod larvae						
Eryoneicus larva					+	
Megalopa larva		+			+	
Phyllosoma larva	+	+	+	+	+	
Puerulus larva		+				
Other decapod larvae		+		+	+	+
MOLLUSCA						
Pteropoda						
Cavolinia tridentata Forskal		+	+			
Heteropoda						
Carinaria lamarcki Péron and Leseur		+				
Pterotrachea coronata Forskal		+		+		
Pterotrachea hippocampus Philippi		+				
Pterotrachea scutata Gegenbaur	+			+	+	
Cephalopoda						
Spirula spirula Linnaeus				+	+	
Other cephalopods	+	+	+	+	+	+
PROTOCHORDATA						
Larvacea						
Oikopleura sp.		+				+
Thaliacea						
Doliolum spp.	+	+	+	+	+	+
Pyrosoma sp.	+	+		+	+	
Salpa spp.		+	+	+	+	+

* New records for South Africa

TABLE 3. DISTRIBUTION OF FISH SPECIES

	Off West Coast	West of Cape Peninsula	S.E. of Agulhas	Off Natal Coast	S.W. Indian Ocean	Stations 40 and 41
Alepocephalidae						
Xenodermichthys socialis Valliant				+		
Bathylagidae						
Bathymacrops macrolepis Gilchrist		+				
†*Bathylagus microcephalus Norman			+	+		+
Gonostomidae						
†*Margrethia obtusirostra Jespersen and Taning			+		+	+
Gonostoma elongatum Gunther		+	+	+	+	+
Vinciguerria sanzoi Jespersen and Taning ..				+		+
†Photichthys argenteus Hutton			+	+		
Diplophos taenia Gunther					+	
Maurolicus muelleri (Gmelin)	+	+				+
*Valenciennellus tripunctulatus Esmark ..	+	+				
Sternoptychidae						
*Argyropelecus aculeatus Cuvier and Valenc. ..	+		+	+	+	+
†*Argyropelecus amabilis Ogilby			+		+	
Argyropelecus hemigymnus Cocco	+	+	+	+	+	+
Polyipnus spinosus Gunther				+		
Chauliodontidae						
Chauliodus sloani Schneider				+	+	+
Stomiatidae (sensu lato)	+	+	+	+	+	
Idiacanthidae						
Idiacanthus niger Regan						+
Idiacanthus fasciola Peters				+		
Evermanellidae						
†*Evermanella balbo Risso			+	+	+	
Myctophidae						
*Electroma subasper (Gunther)	+					
*Electroma tenisoni (Norman)		+				
*Hygophum hygomi Lutken		+	+	+	+	+
*Hygophum hanseni (Taning)		+				
Hygophum reinhardti (Lutken)			+		+	
*Benthosema fibulata (Gilbert and Crane) ..				+		

	Off West Coast	West of Cape Peninsula	S.E. of Agulhas	Off Natal Coast	S.W. Indian Ocean	Stations 40 and 41
Myctophum evermanni Gilbert				+		
Myctophum humboldti (Risso)		+				
Diaphus gemellari (Cocco)					+	
*Diaphus brachycephalus Taning		+				
†*Diaphus dofleini Zugermayer				+		
Diaphus effulgens Goode and Bean				+	+	
*Diaphus diadematus Taning					+	
†*Diaphus fulgens Brauer		+	+	+		
†*Diaphus lutkeni Brauer			+		+	
†*Diaphus theta Eigenmann and Eigenmann	+		+	+		+
Lampanyctodes hectoris (Gunther)	+	+				
Lampanyctus niger Gunther					+	
†*Lampanyctus leucosaurus Eigenmann and Eigenmann					+	
†*Lampanyctus superlateratus Parr					+	
†Lampanyctus alatus Goode and Bean	+	+	+	+	+	+
*Lampanyctus pyrosobolus Alcock						+
Ceratoscopelus townsendi (Eigenmann and Eigenmann)				+		+
Neoscopelidae						
†*Notoscopelus elongatus (Costa)			+	+	+	
Scoleopsis multipunctatus Brauer		+	+	+	+	
Cetomimidae						
Rondeletia bicolor Goode and Bean						+
Nemichthyidae						
Nemichthys scolopacea Richardson		+		+	+	
Avocettina infans (Gunther)			+	+	+	+
Serrivomer beani Gill				+	+	
Gadidae						
Physiculus capensis Gilchrist	+					
Malacocephalus laevis (Lowe)	+					
Bregmaceros macclellandi Thompson					+	
*Melanonus gracilis Gunther					+	+
Merluccius capensis Castlenau	+	+				

	Off West Coast	West of Cape Peninsula	S.E. of Agulhas	Off Natal Coast	S.W. Indian Ocean	Stations 40 and 41
Trachipteridae						
Regalecus glesne (Ascanius)		+		+		
Trachipterus arcticus (Brunnich)		+				
Melamphaidae						
*Melamphaes microps Gunther					+	
*Sio nordenskjoeldi (Lonnberg)			+	+	+	
Zeidae						
Zeus faber Linn		+				
Oreosoma atlanticum Cuvier		+				
Scombropidae						
†Howella sherborni (Norman)				+		
Caragidae						
Trachurus trachurus Linn		+				
Bramidae						
Brama brama					+	
†*Collybus drachme Snyder				+		
†*Taractes asper Lowe				+	+	
Champsodontidae						
Champsodon capensis Regan		+				
Chiasmodontidae						
Chiasmodon niger Thompson		+				
Brotulidae						
†*Brotulotaenia crassa Parr					+	
Callionymidae						
Paracallionymus costatus (Boulenger)	+					
Gempylidae						
Thrysites atun (Euphrasen)		+				
Trichiuridae						
Benthodesmus tenuis Gunther				+	+	
Lepidopus caudatus (Euphrasen)	+	+				
Scomberidae						
Scomber japonicus Houttyn		+				
Scorpaenidae						
Helicolenus maculatus (Cuvier)		+				

* New South African records † New Indian Ocean Records

SYSTEMATIC NOTES ON SPECIES

Lists of the species of invertebrates (Table 2) and fishes (Table 3) taken during this survey have been given above. but it must be emphasised that these are not complete lists. Detailed taxonomic reports on the major groups will be published separately.

Among the Coelenterata was the characteristic bathypelagic medusa *Periphylla periphylla* (Péron and Leseur) which has been described under a number of different names throughout the world. Kramp (1961) has, however, indicated that there is only a single species with an extensive synonymy. This is apparently the first record of this species from the South African region.

Sagitta gazellae is a species new to the South African list but the other *Sagitta* species are previously known from South Africa (Heydorn 1959).

The Amphipoda obtained were mostly not typical bathypelagic forms and may have been caught near the surface, but two species of the rare and interesting bathypelagic genus *Cystisoma* are represented.

Some of the specimens of *Phronima sedentaria* were in their transparent gelatinous "houses". Others, however, were found inside *Pyrosoma* colonies and there were a number of houses that were clearly the remains of *Pyrosoma* colonies that had the zooids missing to varying degrees, until they formed a normal smooth, gelatinous house. *Phronima* is normally reported to live in the tests of salps and doliolids.

The giant mysid *Gnathophausia ingens* (Dohrn) is a remarkable example of evolutionary convergence, resembling closely the bathypelagic prawns. It is large and red and has a long serrated rostrum like a bathypelagic prawn and it is many times the size of a normal mysid. This genus has seven abdominal segments instead of six. Typical mysids have seven abdominal segments as embryos, of which the last two fuse, while in *Gnathophausia* they remain separate (Manton 1928). The specific identification of the *Gnathophausia* specimens proved problematical as they showed a wide range of size and proportions, particularly in the length of the rostrum and carapace spines. The forms they appeared to resemble were regarded by Fage (1943) as synonymous and grouped under the name *ingens*.

Various characters such as the lengths of the rostrum and carapace spines, and the numbers of teeth on the rostrum and antennal scale were compared graphically with total lengths. These morphometric data when plotted indicated that all our material could be regarded as a single species, *G. ingens*, and that the striking differences in appearance were merely due to allometric growth.

Amongst the Euphausiacea four species of Thysanopoda, (*T. cristata*, *T. orientalis*, *T. pectinata* and *T. tricuspidata*) as well as *Euphausia longirostris* appear to be new records for South Africa, although *T. cristata* is the only species not included in Boden's (1951) review which includes records from neighbouring regions.

The Decapoda have not yet all been identified and there appear to be some new records for South Africa in several genera. Earlier records of bathypelagic prawns obtained by trawling around South Africa are included in Barnard's (1950) monograph, while Lebour (1954) has discussed material from the Benguela current off South West Africa.

Further work is required particularly on the species of the genus *Sergestes*. The *Notostomus* obtained has been referred to *N. longirostris* Bate although the rostrum is relatively shorter than in the small original specimen. The specimens of *Plesionika* obtained have been referred to *P. longirostris* but the rostral teeth are rather more widely spaced than is normal for the species. The erioneicus larva appears to be the form described as "*Kempi*" which is the larva of *Polycheles typhlops*.

Most of the phyllosoma and puerulus larvae obtained off the west coast appeared to be *Jasus lalandii* as described by Gilchrist (1916), whereas the phyllosomata obtained elsewhere represented other genera and species.

The small squid *Spirula spirula* (Linnaeus) is generally regarded as rare throughout the world although its characteristic spiral shell is found on beaches everywhere. It was, however, found in large numbers in the southern Mozambique channel by the *Dana* expedition (Bruun 1943). This expedition also obtained a single juvenile specimen from south of Cape Point and there is a specimen in the South African Museum believed to be from Table Bay. During this survey we obtained live specimens of *Spirula* from three stations off Natal and in the South West Indian Ocean.

Pelagic molluscs other than Cephalopoda included the pteropod *Cavolinia tridentata* and four species of Heteropoda. One specimen of *Pterotrachea coronata* was exceptionally large, measuring approximately 300 mm. in total length, which is larger than any known to Tesch (1949).

The list of the fishes identified (Table 3) does not include Stomiatid fishes (*sensu lato*), larval fishes, and some of the myctophid fishes, which still require study.

Schultz (1961) in his review of the hatchet fishes states that *Argyropelecus hemigymnus* is confined to the Mediterranean and Atlantic while in the Indo-Pacific it is replaced by the related *A. intermedius*, and he places *A. hemigymnus* recorded off South Africa by Gilchrist (1913), Barnard (1925) and Smith (1949) in the synonomy of *A. intermedius*. Unfortunately no Cape or Indian Ocean specimens of this fish were available to Schultz at the time. All specimens found in this survey having a barbed dorsal blade, clearly fitted *A. hemigymnus* rather than *A. intermedius*. Both seem to be very closely related and rather variable species. It was also surprising that although large numbers of *Argyropelecus* species were taken, only one specimen of the related genus *Polyipnus* was caught.

A single specimen of *Brotulotaenia* was found and has been assigned to *B. crassa*; the two known species *B. nigra* Parr (1933) and *B. crassa* Parr (1934) are very similar, but the present species seems to be closer to *crassa*. This catch is not only the first record of the genus outside the Caribbean but is also believed to be only the fourth example of the genus ever found.

Bathylagus microcephalus was formerly only recorded from the South Atlantic. These further records indicate that it is present in the southern Indian Ocean also.

Smith (1949) placed *Lampanyctus alatus* in the synonymy of *L. pusillus* although they can be separated easily by the presence of a luminous organ at the adipose fin in *alatus*. All the specimens recorded here were clearly *alatus* rather than *pusillus*. All examples in the collections of the South African Museum on which Barnard's (1925) records of *alatus* were based were re-examined and found to be correctly identified as *alatus*.

Included in the table are a few species taken off the Cape Peninsula which do not form part of the bathypelagic fauna, but are rather the juveniles of common Cape fishes. It is presumed that they were caught while the net was being hauled. They are mostly the juveniles of the bottom-dwelling species *Lepidopus caudatus*, *Merluccius capensis* and *Helicolenus maculatus*, but other juveniles included *Trachurus trachurus* and *Scomber japonicus*.

One of the most unexpected results of the survey has been the complete absence of *Cyclothone* species. Of all bathypelagic fish genera this is considered to be the most abundant in number of individuals (Marshall 1954), yet apart from one doubtful and badly damaged specimen, no fish of this genus were found. Most *Cyclothone* are small, but the posterior end of the trawl was lined with half inch stretched mesh netting which captured many other very small species of fishes.

HYDROGRAPHY OF THE ENVIRONMENT

Most specimens obtained in this survey were caught at night at a depth of about 500 metres, and it is well known that most bathypelagic animals migrate down to a deeper level diurnally. To understand their distribution it is thus necessary to know something of the hydrographic conditions in the seas around South Africa at a depth of 500 metres and perhaps a few hundred metres below this. Conditions at these depths differ greatly from surface conditions and data on their hydrography is limited and scattered in the literature. It has, however, been possible to obtain a picture of the hydrographic environment of this bathypelagic fauna by extracting data from the following published reports: Clowes and Deacon (1935), Dietrich (1935) Clowes (1950), Zoutendyk (1960), le Pichon (1960), Trotti and Welsh (1961), Fukase (1962), Kort (1962), Menaché (1963), Orren (1963), Zoutendyk (1963), Taft (1963), Darbyshire (1963), Darbyshire (1964), Shipley and Zoutendyk (1964), Station lists in the Discovery Reports, and Annual Reports of the Division of Sea Fisheries.

In the south-western part of the Indian Ocean there are three main water masses that concern us (Figure 2). In vertical sections Agulhas water, which, following the delimitations of Darbyshire (1964), may be regarded as water above the 17° C isotherm, extends down to approximately 300 metres below the main stream of the Agulhas current. Further offshore, however, the Agulhas water does not extend down so far, and near the coast it may be considerably less than 100 metres thick. The southern limit of the Agulhas water varies but the 17° C isotherm reaches the surface between about 35° and 40° south, where Fukase (1962) has described the "Agulhas Convergence".

Below the Agulhas water is the South Indian Central Water which may be regarded as extending down from the 17° C isotherm to the 5° C isotherm. Salinities in this water mass lie between approximately 35·5‰ and 34·5‰, and there is an approximately linear temperature-salinity gradient within this range. It extends down to about 1,300 metres in the open ocean but only to about 800 metres at the continental margin (Darbyshire 1964). The origin of this water mass is problematical, probably involving sinking at the subtropical convergence, northward drift, and mixing with adjoining water along its path (Orren 1963). In the south of

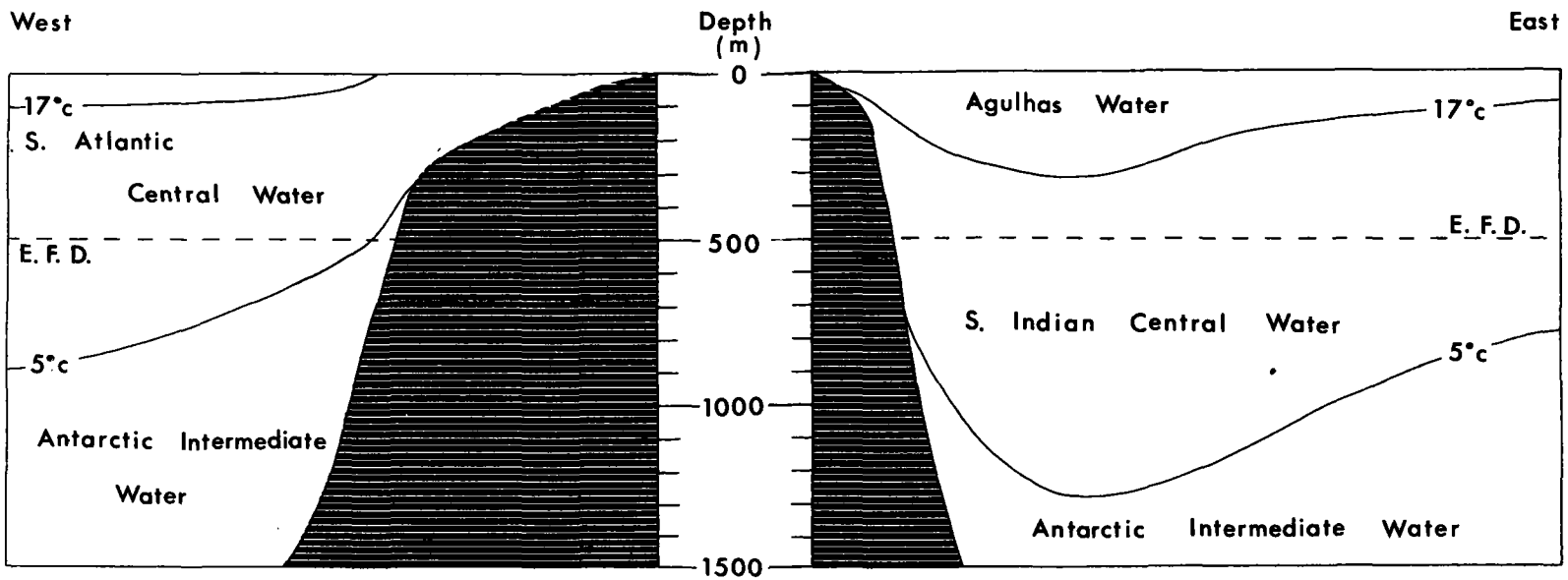

FIGURE 2. Diagrammatic hydrographic section to show the general pattern of the water masses present down to a depth of 1,500 metres off the west and east coasts of South Africa, in the South Atlantic and South-west Indian Oceans. The broken line E.F.D. represents the Estimated Fishing Depth of the 500 metre deep trawls. The offshore water above 17°C in the West (not labelled) is part of the South Atlantic Gyral.

the region covered it lies closer to the surface and may extend down to a depth of less than 700 metres. Under the Agulhas Current, Le Pichon (1960), Kort (1962) and Taft (1963) have suggested that the South Indian Central Water has a strong westward component and tends to follow the Agulhas water. In the north of the region covered the South Indian Central Water lies closer to the surface and the work of Menaché (1963) has shown that it extends steeply upwards to within about 150 metres of surface at the divergence at 24° S in the southern end of the Mozambique channel.

Under the South Indian Central Water lies the Antarctic Intermediate Water which may be regarded as being below 5° C and which is characterised by a marked salinity minimum. This water originates by sinking just north of the Antarctic Convergence, and drifts northwards under the South Indian Central Water, except under the Agulhas Current where it may also drift towards the south-west.

In the south-eastern Atlantic, west of the Cape, the same pattern of three water masses is present. The warm waters of the South Atlantic Gyral, which may also be delimited by the 17° C isotherm, are only found offshore and in the area concerned only extend down about 100 metres.

The Central Water, here known as the South Atlantic Central Water, occupies the layer between about 100 and about 700 metres. Clowes (1950) showed that there was a well marked linear T-S relationship between 6° C, 34·4‰ and 16° C, 35·5‰ and that the same T-S characteristics were found in water along the west coast right up to the surface indicating upwelling of South Atlantic Central Water.

The Antarctic Intermediate Water delimited by the 5° C isotherm and characterised by the salinity minimum is usually below 700 metres but marked fluctuations occur. It may be below 1,000 metres, or as suggested by the data of Trotti and Welsh (1961), may come up to less than 300 metres over the shelf in August, 1959).

It is thus apparent that all the mid-water catches which were made at a depth of about 500 metres were in Central Water (South Indian and South Atlantic). Shallower hauls made near the coast would also have been in the same water mass owing to the tendency of the Central Water to approach the surface at the coast. Even during the hours of daylight when these bathypelagic animals may migrate downwards a few hundred metres they would in most areas remain within the Central Water.

Conditions within the Central Water mass vary considerably at any particular level in different parts of the area concerned. Using all the data available it was possible to get a picture of the temperature distribution at the 500 metre level over the region covered by this survey (Figure 1). The isotherms were plotted on the basis of published data from a number of sources enumerated above. To allow for seasonal and other variations recorded by different vessels at different times the isotherms were smoothed in a few places. Periodic variations appear to occur particularly in the area south of the Cape Province (Darbyshire 1963), in the eddies in the northern and southern parts of the South West Indian Ocean (Darbyshire 1964), and in the extent of the upwelled water west of the Cape Peninsula (Trotti and Welsh, 1961), and further north (Hart and Currie 1960, Stander 1964). Over most of the South West Indian Ocean temperatures at the 500 metre level range between 12° and 14° C. Where the Antarctic Inter-

mediate Water is not far below, temperatures at the 500 metre level are lower. In the south they may be as low as 8° C at 38° S. Near the east coast of South Africa the isotherms curve up sharply so that near the continental margin temperatures fall in places to 10°C and well below, particularly off the southern coast. The low temperature shown in Figure 1 at a point in the middle of the South West Indian Ocean (33° 02′ S., 37° 35′ E.) is based on a single series of observations at Station NIOE-102 (Shipley and Zoutendyk, 1964). This anomaly has not been found in any other data and it may not be a normal feature. Off the south-west Cape coast in the region of upwelling temperatures are even lower. The data of Trotti and Welsh (1961) for this area show considerable seasonal fluctuations in the temperature at the 500 metre level between 8° C and 5° C and occasional incursions of Antarctic Intermediate Water onto the shelf probably occur.

Regional differences in the bathypelagic fauna may be associated in some way with the variations of temperature at the 500 metre level described above. They might also be related to the depth of the Antarctic Intermediate Water, because many bathypelagic animals are capable of making extensive vertical migrations, and where this lower water mass is closest, animals from it may be represented in catches.

NOTES ON DISTRIBUTION OF FISHES AND INVERTEBRATES

Several interesting features in the distribution of the invertebrates and fishes represented in these collections appear worthy of discussion although it would be premature to draw final conclusions.

Vertical distribution

Hauls made during daylight were remarkably poor. No prawns at all were obtained, only two euphausiids (and those at 500 metres) and few fish. Even at night most prawns and euphausiids appeared only in the deep hauls at 500 metres. *Solenocera africanum* was however obtained at night at only 100 metres and *Funchalia woodwardi* came up to only 20 metres at night. Amphipods, salps and medusae appeared in both day and night hauls but many of these should perhaps be regarded as epipelagic, as should many of the juvenile fishes.

Regional distribution

It has been shown above that the Central Water Mass extends throughout the region concerned so that many species may be expected to occur throughout the region. In fact few species have so far been found in all areas, but this may be due to differences in depth of the Central Water Mass in different parts of the region. Many species were not obtained in the warmer central area of the South West Indian Ocean (Figure 1), where they may occur deeper down than 500 metres. Several species obtained only in the upwelled water off the Cape Peninsula and West Coast may also be more widely distributed at greater depths.

Amongst the prawns most species were found in both the Atlantic and Indian Oceans. Five species (*Plesiopenaeus nitidus*, *Aristeomorpha foliacea*, *Gennadas gilchristi*, *Acanthephyra haeckelii* and *Plesionika longirostris*) were found only in the Indian Ocean samples while *Solenocera africanum* was only obtained from the Atlantic. *Acanthephyra haeckelii* only appeared in the extreme south (Station 40). The closely related form *A. acanthitelsonis* was recorded by Lebour (1954) in the Benguela Current off South West Africa. *Sergestes arcticus* also appeared in the extreme south and otherwise only in the cold upwelled water west of the Cape. *Gnathophausia ingens* appeared only in the colder regions, and it is interesting to note that Fage (1941) found that this species in the north Atlantic was limited to regions below a temperature of 10° C at 600 metres. (There are large areas above 13° C at this depth in the N. Atlantic also.)

Many fish also showed very wide ranges, and the scattered incidence of many rarer species suggests that they are probably also widely if sparsely distributed. A distinct distribution pattern was however evident in the presence of vast numbers of *Maurolicus muelleri* and large numbers of *Lampanyctodes hectoris* in the cold water off the west coast and their almost complete absence in the Indian Ocean. Only one example of *M. muelleri* was found in the extreme south (IK 40). Inshore off the east coast it appeared that the place of *M. muelleri* was taken by *Scoleopsis multipunctatus* which was not found off the west coast and only once off the Cape Peninsula.

Two specimens of *Sagitta gazellae* were obtained in the cold upwelled water west of the Cape Peninsula. David (1955) in his study of the distribution of *Sagitta gazellae* found that it was limited to waters south of the region of the subtropical convergence. David (1955), however, did find specimens in some hauls just north of the subtropical convergence where subantarctic water was present below the surface. He remarked that they might penetrate further north in deeper waters but regarded this as unlikely as a large number of hauls in areas further north had not revealed a single specimen. The present specimens thus represent a very interesting extension of the range of this characteristically antarctic and subantarctic species. The other *Sagitta* species appearing in Table 2 represent too few specimens to draw any conclusions as to their regional distribution.

Spirula spirula which is generally regarded as a tropical species was only found in the northern part of the region.

Amongst the amphipods *Phrosina semilunata* was found throughout the area and *Phronima sedentaria* and a species of *Platyscelus* appeared everywhere except in the extreme south.

One of the most striking distributional features was the great abundance of *Euphausia similis* var. *armata* off the west coast and its complete absence elsewhere. Numerically there were far more of this species than of all the other euphasiids together. It occurred associated with very large numbers of the fish *Maurolicus muelleri*. It would appear that this strikingly distinct population was related to the cold water upwelling and possibly to the presence of Antarctic Intermediate Water in this area. It is interesting that Nepgen (1957) in his study of the euphausiids of this same region west of the Cape found that *Euphausia similis* var. *armata* "did not occur in large numbers or often". It seems probable that this anomaly is due to his work being based mainly on shallower plankton hauls, taken mainly in daylight.

Euphausia spinifera appeared at almost all of the southern stations in this survey and otherwise only inshore off Durban. This species is known to occur in waters north of the subtropical convergence while it is replaced by a closely related species *E. longirostris* south of the convergence (Boden 1951). The occurrence of *E. spinifera* off Durban is not surprising as the temperatures at the 500 metre level are much lower close to the coast than in the regions offshore. *E. spinifera* occurred at most of the southerly stations while the prawns *Sergestes arcticus* and *Acanthephyra haeckelii* only appeared at the most southerly station (IK 40) and west of the Cape in the case of *S. arcticus*. In both these areas the Antarctic intermediate water is not far below 500 metres and they may have migrated up from this water. These prawns are larger and perhaps migrate further than *Euphausia spinifera*, which would probably be confined to the Central Water Mass. However more work is required before the apparent differences in distribution pattern can be explained.

It is interesting that *Euphausia longirostris* was obtained in the cold upwelled water west of the Cape Peninsula. Boden (1951) regarded it as characteristically subantarctic and reported that it was rarely encountered north of the subtropical convergence, and he did not find it in the Benguela Current off South West Africa either (Boden, 1955).

ACKNOWLEDGEMENTS

We are grateful to Dr. F. H. Talbot who initiated this programme and made it possible for the South African Museum to carry it out; to Messrs. Irvin & Johnson Ltd., who provided the first Isaacs-Kidd trawls; and to the following for the use of ships: The South African Navy, S.A.S. *Natal*; Messrs. Irvin & Johnson Ltd., trawlers *Cape Point*, *Illovo* and *Natalia*; and the University of Cape Town, R.V. *John D. Gilchrist*. We acknowledge the help of Mrs. M.-L. Penrith, Miss D. du Plessis and Mr. B. Kensley in sorting and preliminary identification of some of the collections, Dr. G. W. Mead of the Museum of Comparative Zoology, Harvard, for the identification of the bramid fishes, Mrs. S. Talbot of the University of Cape Town for checking the identification of Euphausiacea and Mr. J. Stone of the University of Cape Town for identifying the Chaetognatha.

We are indebted to the Council for Scientific and Industrial Research of South Africa who paid the salary and subsistence allowance for sea time for the second author, paid the salary of Mrs. M.-L. Penrith as research assistant to the first author, and granted funds for the replacement of the mid-water trawl.

SUMMARY

The results of a mid-water trawling survey for bathypelagic fauna in the seas around South Africa and in the South West Indian Ocean is described. The programme was carried out by the South African Museum using a 10 ft Isaacs-Kidd mid-water trawl down to a depth of 500 m from several vessels. A station list gives details of the trawling stations and the species

of invertebrates and fishes obtained are listed for six areas resulting from a grouping of these stations. Many species new to the South African fauna list and new to the Indian Ocean fauna list are recorded. Brief systematic notes have been included where necessary. The hydrography of the environment of the bathypelagic fauna at a depth of 500 m is discussed on the basis of data extracted from published reports and the temperature distribution at this level is described. Outstanding features of the distribution of species are discussed in relation to the hydrographic background. Distribution patterns appear to be related largely to the depth of the central water mass and some interesting records appear where this water upwells to near the surface. Two species, *Sagitta gazellae* and *Euphausia longirostris*, previously regarded as characteristically sub-antarctic are recorded in the cold upwelled water west of the Cape.

REFERENCES

This list of references includes only papers referred to in the text, and does not include all taxonomic papers used in the course of the work. These will be cited separately in the taxonomic reports on different animal groups.

BARNARD, K. H. 1925–27. A monograph of the marine fishes of South Africa. *Ann. S. Afr. Mus.* 21: 1–1065.

BARNARD, K. H. 1950. Descriptive catalogue of South African decapod crustacea (Crabs and Shrimps). *Ann. S. Afr. Mus.* 38: 1–837.

BODEN, B. P. 1951. The Euphausiid crustaceans of southern African waters. *Trans. roy. Soc. S. Afr.* 34: 181–243.

BODEN, B. P. 1955. Euphausiacea of the Benguela current. First Survey, R.R.S. "William Scoresby", March 1950. *Discovery Rep.* 82: 337–376.

BRUUN, A. 1943. The biology of *Spirula spirula* (Linn.). *Dana Rep.* 24: 1–46.

CLOWES, A. J. 1950. An introduction to the hydrology of south African waters. *Invest. Rep. Fish mar. biol. Surv. S. Afr.* 12: 1–42.

CLOWES, A. J. and DEACON, G. E. R. 1935. The deep water circulation of the Indian Ocean. *Nature, Lond.* 136: 936–938.

DARBYSHIRE, J. 1964. A hydrological investigation of the Agulhas Current area. *Deep Sea Res.* 11: 781–815.

DARBYSHIRE, M. 1963. Computed currents off the Cape of Good Hope. *Deep Sea Res.* 10: 623–632.

DAVID, P. M. 1955. The distribution of *Sagitta gazellae* Ritter-Zahony. *Discovery Rep.* 27: 237–278.

DEVEREAUX, R. F. and WINSETT, R. C. 1953. Isaacs-Kidd midwater trawl, final report. *Scripps Inst. Oceanogr. Equipment Rept.* 1: 1–21.

DIETRICH, G. 1935. Aufbau und Dynamik des Südlichen Agulhasstromgebietes. *Veröff. Inst. Meeresk. Univ. Berl.* (*Ser. A*) 27: 1–79.

FAGE, L. 1943. Mysidacea, Lophogastrida—1. *Dana Rep.* 19: 1–52.

FUKASE, S. 1962. Oceanographic conditions of surface water between the south end of Africa and Antarctica. *Oceanogr. results, Japanese Antarct. Res. Exp.* 15: 54–104.

GILCHRIST, J. D. 1916. Larval and post-larval stages of *Jasus lalandii* (M.Ed.). *J. Linn. Soc. Lond. (Zool.)* 33: 101–124.

HART, J. H. and CURRIE, R. I. 1960. The Benguela current. *Discovery Rep.* 31: 123–298.

HEYDORN, A. E. F. 1959. The Chaetognatha off the west coast of the Union of South Africa. *Invest. Rep. Div. Fish, S. Afr.* 36: 1–56.

KING, J. E. and IVERSEN, R. T. 1962. Midwater trawling for forage organisms in the central Pacific, 1951–1956. *Fish. Bull. U.S. Fish Wildl. Ser.* 62: 271–319.

KORT, V. G. 1962. The Antarctic Ocean. *Scientif. Amer.* 207 (3): 113–128.

KRAMP, P. L. 1961. Synopsis of the Medusae of the world. *J. mar. biol. Ass. U.K.* 40: 1–469.

LEBOUR, M. V. 1954. The planktonic decapod crustacea and stomatopoda of the Benguela current Part 1. First Survey, R.R.S. "William Scoresby", March 1950. *Discovery Rep.* 27: 219–234.

LE PICHON, X. 1960. The deep water circulation in the southwest Indian Ocean. *J. Geophys. Res.* 65: 4061–4074.

MANTON, S. M. 1928. On some points in the anatomy and habits of the lophogastrid crustacea. *Trans. roy. Soc. Edin.* 56: 103–119.

MARSHALL, N. B. 1954. *Aspects of deep sea biology.* London: Hutchinson.

MENACHÉ, M. 1963. Première campagne océanograe que du "Commantant Robert Giraud" dans le canal de Mozambique, 11 Octobre—28 Novembre 1957. *Cahiers océanogr.* 15: 224–285.

NEPGEN, C. S. de V. 1957. The Euphausiids of the west coast of South Africa. *Invest. Rep. Div. Fish., S. Afr.* 28: 1–30.

ORREN, M. J. 1963. Hydrological observations is the South West Indian ocean. *Invest. Rep. Div. Sea Fish., S. Afr.* 45: 1–61.

PARR, A. E. 1933. Deepsea Berycomorphi and Percomorphi from the waters around the Bahama and Bermuda Islands. *Bull. Binghum Oceanogr. Coll.* 3 (6): 1–51.

PARR, A. E. 1934. Report on the experimental use of a triangular trawl for bathypelagic collecting with an account of the fishes obtained and a revision of the family Cetomimidae. *Bull. Bingham. Oceanogr. Coll.* 4 (6): 1–59.

PENRITH, M. J. and GRINDLEY, J. R. 1963. A preliminary report on the bathypelagic fauna of South African seas. (Abstract only). *S. Afr. Assoc. Adv. Sci., Congress Abstracts,* 1963: 35–36.

SCHULTZ, L. P. 1961. Revision of the marine silver Hatchet Fishes (family Sternoptychidae). *Proc. U.S. nat. Mus.* 112: 587–649.

SHEARD, K. 1942. The genus *Thysanopoda* (Crustacea: Euphausiaea) *Trans. roy. Soc. S. Austral.* 66 (1): 60–65.

SHIPLEY, A. M. and ZOUTENDYK, P. 1964. Hydrographic and plankton data collected in the south west Indian Ocean during the S.C.O.R. International Indian Ocean Expedition, 1962–1963. *Data Rep. Univ. Cape Town Oceanogr. Dep.* 2: 1–210.

SMITH, J. L. B. 1949. *The sea fishes of southern Africa.* Cape Town: Central News Agency.

STANDER, G. H. 1964. The Benguela current off South West Africa. *Invest. Rep. S.W. Afr. mar. Res. Lab.* 12: 1–43.

STATION LISTS: *Ann. Rep. Div. Sea Fisheries*, Cape Town.

STATION LISTS: *Discovery Reports*, Cambridge.

SUZUKI, O. 1961. Mechanical analysis on the working behaviour of midwater trawl. *Bull. Japan. Soc. sci. Fish.* 27: 903–907.

TAFT, B. A. 1963. Distribution of salinity and dissolved oxygen on surfaces of uniform potential specific volume in the south Atlantic, south Pacific and Indian Oceans. *J. Mar. Res.* 21: 129–146.

TESCH, J. J. 1949. Heteropoda. *Dana Rep.* 34: 1–53.

TROTTI, L. and WELSH, J. G. 1961. Hydrographic and plankton observations made during cruises on board the "John D. Gilchrist" 1959–1960. *Publ. Univ. Cape Town Oceanogr. Dep.* 2: 1–107.

ZOUTENDYK, P. 1960. Hydrographic and plankton data collected in the Agulhas current during I.G.Y. *Publ. Univ. Cape Town Oceanogr. Dep.* 1: 1–14, and Station lists.

ZOUTENDYK, P. 1963. Hydrographic and plankton data collected in the Agulhas current by R.V. "John D. Gilchrist" during July, 1959. *Publ. Univ. Cape Town. Oceanogr. Dep.* 7: 1–27.

ADDENDUM

Since this paper was written a number of other publications have appeared which have some bearing on this work. A paper on towing characteristics of plankton-sampling gear by Aron, W., Ahlstrom, E. H., Bary B.McK., Bé, A. W. H., and Clarke, W. D. (*Limnol.Oceanogr.*10: 333–340, 1965) shows that the fishing depth of an Isaacs-Kidd midwater trawl is reduced considerably with increased towing speed. In the present work low towing speeds of the order of two knots were used. Alvarino, A., in his review on chaetognaths (*Oceanogr. Mar. Biol. Ann. Rev.* 3: 115–194, 1965) records *Sagitta gazellae* north of the subtropical convergence in deep waters, reaching 21° S. in the Pacific and 36° S. in the Indian Ocean. De Decker, A. and Mombeck, F. J. in their preliminary report on the planktonic Copepoda (*Invest. Rep. Div. Sea Fish. S.Afr.* 51: 10–67, 1965) show clearly there are groups of species of Copepoda associated with the water masses at different levels in the south west Indian Ocean, and that species previously considered Atlantic or Sub-Antarctic occur frequently, as bathypelagic species in this region. The work of Visser, G. A. and van Niekerk, M. M. on ocean currents and water masses at 1,000, 1,500 and 3,000 metres in the south west Indian Ocean (*Invest. Rep. Div. Sea. Fish. S. Afr.* 52: 1–46, 1965) gives data for these deeper levels which may be compared with the conditions at 500 metres described in the present work.

BREVIORA

Museum of Comparative Zoology

CAMBRIDGE, MASS. FEBRUARY 25, 1966 NUMBER 241

AVOCETTINOPS YANOI, A NEW NEMICHTHYID EEL FROM THE SOUTHERN INDIAN OCEAN

By GILES W. MEAD and IRA RUBINOFF

Museum of Comparative Zoology, Harvard University

The oceanic eels of the genus *Avocettinops* lack the prolonged jaws or snout typical of other snipe eels, although they do have fleshy anterior appendages; and they can be distinguished from all other apodal fishes by the complete absence of teeth, if not from their bizarre physiognomies alone. The number of known specimens is small: the type of *A. schmidti* (Roule and Bertin, 1924); a second specimen taken off Zanzibar during the "John Murray" expedition (Norman, 1939; the specimen rather casually christened *Avocettinops normani* by Bertin in 1947); a specimen collected from the *Arcturus* by William Beebe, New York Zoological Society, off New York and reported as *A. schmidti* by Böhlke and Cliff (1956) (SU 47758); and the fish described below. Böhlke and Cliff (1956) also discussed in some detail the nomenclatorial and taxonomic entanglements generated by earlier authors, and reviewed the relationship of the genus to other snipe eels.

AVOCETTINOPS YANOI, new species
Figure 1

Holotype. — A specimen 620 mm long collected by R/V *Anton Bruun* during the International Indian Ocean Expedition, Cruise VI, Sta. 350 B, APB label 7314; 27 June 1964; 28°05′ S, 64°58′ E to 28°28′ S, 65°04′ E; depth of bottom 2200-4000 m; 10-ft. Isaacs Kidd Midwater Trawl with catch dividing device nominally set to operate at 350 m; deep fraction of catch the probable depth of capture between the maximum depth reached, 1750 m and 125 m. MCZ Catalog No. 44404.

Distinctive characters. — *Avocettinops yanoi* differs from its congeners in the position of the dorsal fin, which originates well in advance of the gill slit, and by the more anterior anal origin, the preanal distance being about 1.3 times the length of the head (*cf.* 2.0 or 2.1 in specimens hitherto described). The species has a correspondingly low number of preanal vertebrae (13 *cf.* 20 or more), and of lateral line pores between the temporal pore and that above the origin of the anal fin (13 *cf.* 18 or more).

Description. — Meristic data and measurements, which are expressed in per cent of head length to facilitate comparison with prior catches, are provided in Table 1.

Body about two-thirds as broad as deep anteriorly, becoming more compressed posteriorly. Head 12 in total length. Jaws coterminal and bearing fleshy protuberances anteriorly both of which were damaged during capture. Angle of gape under posterior edge of eye. Mouth without teeth but with minute denticles on skin overlying jaws and roof of mouth. Anterior nostril before center of orbit, the tube anteriorly directed. Posterior nostrils large deep pits, the posterior edges of which lie on a tangent with anteriormost points of orbits. Gill slits short (13 in length of head), ventrally directed, and placed below bases of pectoral fins. Eye circular, its diameter 7 in length of head. Acustico-lateralis system on head well developed (Fig. 1), the pores large. The system includes series of lappets, which are presumably sensory, such as the vertical row behind and the horizontal series above and behind the eye. Similar lappets are interspersed at irregular intervals between pairs of pores in the lateral line along the flank. These lappets are not bilaterally symmetrical. The lateral line is continuous and complete.

Dorsal and anal fins originating far forward and nearly continuous around tip of tail. Predorsal distance 17 in total length, preanal 10 in length. Pectoral fin broad, short, and lying in a horizontal plane when expanded. Anus and urogenital openings immediately anterior to origin of anal fin. The fish is completely black externally. Internally, the peritoneum, linings of mouth, and pharyngeal cavities are white. The coelom extends posteriorly far beyond the anus to about the midpoint of the total length. Most of this space is filled by the swollen, convoluted and apparently mature pair of gonads. These appear to be ovaries, although they are too decomposed for close study. The muscular stomach, which is placed anterior to the anus, is empty.

The success of any trawling expedition is dependent in no small measure on those responsible for the maintenance and operation of the nets and associated equipment. Throughout the trawling activities which produced the collections of which this specimen is a part, Mr. Shigeru Yano and his associate, Mr. C. P. Lee, devoted themselves to this equipment with ability, understanding, and scrupulous care; without these master fishermen these cruises would have fallen short of their goals. With respect and professional admiration we take pleasure in naming this new eel in honor of Shigeru Yano, friend and fellow fisherman.

Remarks. — The identity of the nominal species of *Avocettinops* remains in doubt. The type of *A. schmidti* has been cleared in potassium hydroxide and stained with alizarine. Norman's "John Murray" specimen from off Zanzibar lacks the tail, and has a fragmentary head which has also been cleared and stained, while the Atlantic individual discussed by Böhlke and Cliff is also fragmentary. Hence meaningful morphological comparison is impossible. A qualitative study of the latter specimen and the published accounts of the two others, in comparison with *A. yanoi,* suggests that the Zanzibar specimen is probably identical with *A. schmidti,* while the western North Atlantic specimen of Böhlke and Cliff probably represents a distinct and unnamed species.

This specimen was taken during the American Program in Biology, International Indian Ocean Expedition, a program financed by the National Science Foundation and under the general scientific direction of Dr. John H. Ryther of the Woods Hole Oceanographic Institution. To the National Science Foundation, which has also financed the research of which this is a part through GF 147 with Harvard University, and to Dr. Ryther the authors express here their sincere appreciation.

TABLE 1

Proportional dimensions, expressed as per cent of length of head, of *Avocettinops schmidti* and *A. yanoi*. Data for the type of *A. schmidti* taken from the descriptions and figures of Roule and Bertin (1924, 1929); those of the Stanford University specimen from Böhlke and Cliff (1956), and from the specimen.

	Type of *A. schmidti*	Western North Atlantic (SU 47758)	Type of *A. yanoi*
Total length (mm)	510.0	—	620.0
Length of head (mm)	32.0	32.0	50.0
Depth of body at anus (% of h.)	21.9	—	24.4
Greatest depth of body	43.8	28.4	35.8
Width of body at anus	9.4	*ca.* 7.8	15.4
Greatest width of body	10.9	—	16.4
Greatest depth of head	25.6	*ca.* 23.4	26.4
Greatest width of head	18.8	17.5	19.8
Length of snout	25.0	25.0	24.0
Diameter of orbit	15.6	12.5?	13.4
Postorbital length of head	59.4	55.9	62.4
Length of upper jaw	39.1	33.1	34.8
Length of lower jaw	32.8	24.7	32.8
Length of gill slit	13.1	17.2	7.6
Interorbital width	14.1	—	16.6
Predorsal length	90.6	108.8	73.8
Preanal distance	203.1	207.8	127.4
Width of base of pectoral fin	14.1?	9.7	9.0
Length of pectoral fin	28.1	24.7	29.0
Dorsal fin rays	340	—	285
Anal fin rays	315	—	266
Pectoral fin rays	16-17	15-15	12-13
Total number of vertebrae	194	—	184
Preanal vertebrae (±1)	20	24	13
Total number pores in lateral line	188	—	185
Lateral-line pores, temporal pore to anus	18?	23	13

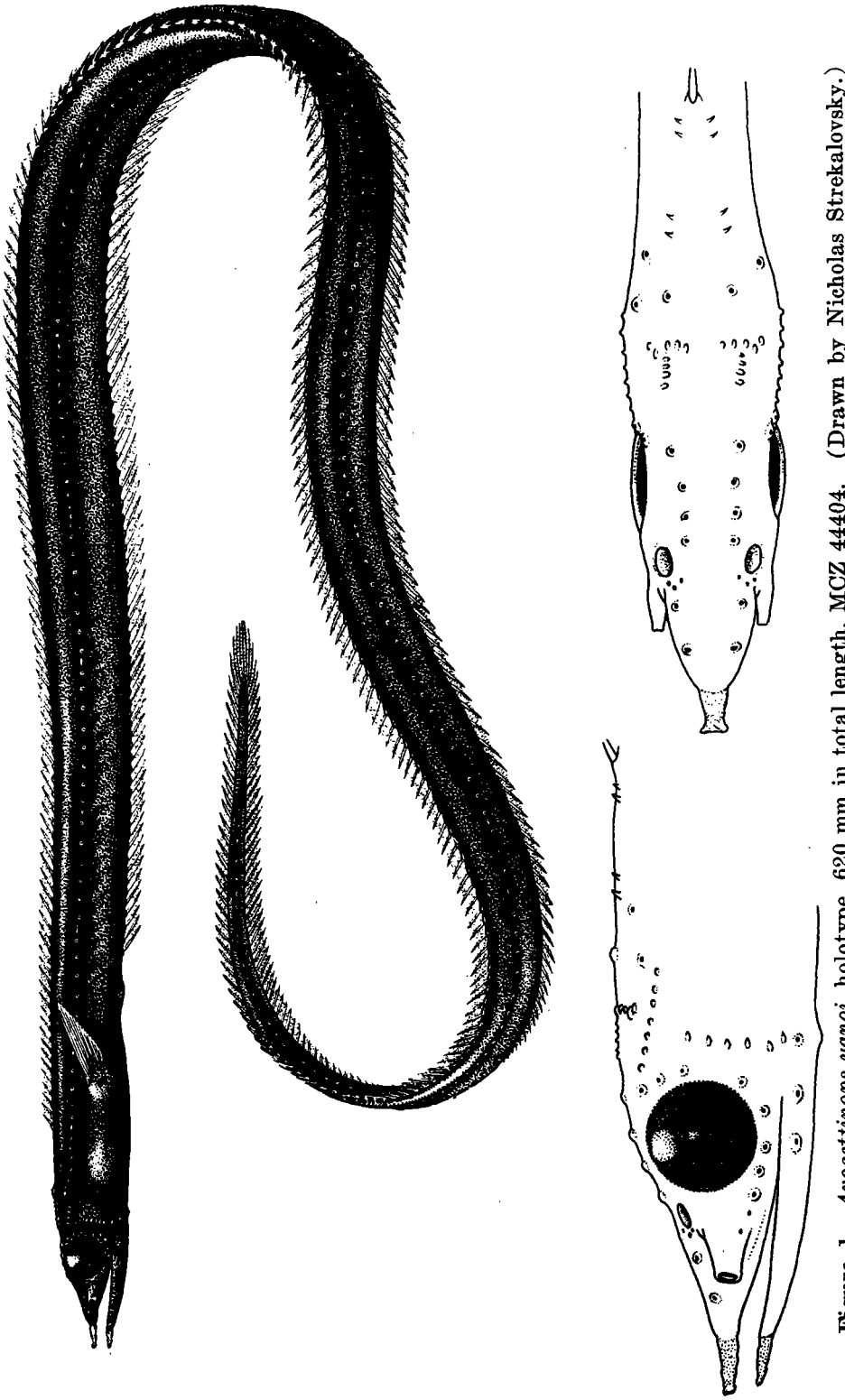

Figure 1. *Avocettinops yanoi*, holotype, 620 mm in total length, MCZ 44404. (Drawn by Nicholas Strekalovsky.)

LITERATURE CITED

BERTIN, LÉON

1947. Notules ichthyologiques. 1. — Compléments sur le genre *Avocettinops*. Bull. Soc. Zool. France, **72**:54-55.

BÖHLKE, JAMES E., and FRANK S. CLIFF

1956. A discussion of the deep-sea eel genus *Avocettinops*, with notes on a newly discovered specimen. Copeia, 1956:95-99.

NORMAN, J. R.

1939. Fishes. Sci. Rep. "John Murray" Expedition, **7**(1):116 pp.

ROULE, LOUIS, AND LÉON BERTIN

1924. Notice préliminaire sur la collection des nemichthydés recueillie par l'expédition du "Dana," (1921-1922), suivie de considérations sur la classification de cette section des poissons apodes. Bull. Mus. Nat. Hist. Natur., Paris, **30**:61-67.

1929. Les poissons apodes appartenant au sous-ordre des Nemichthydiformes. Rep. "Dana" Exp., 1920-1922, No. 4, 113 pp., 19 pls.

(Received 9 November 1965.)

Reprinted from *Some contemporary studies in marine science*, 1966, p. 545-554.

SELECTIVE FEEDING BY CALANOID COPEPODS FROM THE INDIAN OCEAN*

MICHAEL M. MULLIN

Institute of Marine Resources, University of California at San Diego

Planktonic copepods form an important part of marine food webs, but the assignment of the various populations of an area to trophic levels is difficult because the feeding of most oceanic species has not been thoroughly studied. Where closely related species are sympatric in distribution and their populations are limited by food supply, a difference in selective feeding may provide the ecological distinctness which permits the populations to coexist.

The probable food of planktonic copepods has been deduced from the morphology of their mouthparts, by examining the contents of the guts of preserved animals, testing the feeding of living animals on one type of food at a time, or by measuring the feeding rate on various types of food in a mixture. All four methods were used in the present study, since each provides a different type of information.

An abundance of fine setae on the second maxilla and other mouthparts and blunt, grinding mandibular teeth are generally thought to indicate a herbivorous food habit, while spined or grasping mouthparts and long, sharp mandibular teeth suggest that the copepod is a carnivore. This conclusion is supported by experimental studies (Anraku and Omori, 1963). An examination of the mouthparts alone does not, however, tell what food the species eats, but only indicates what general type of food the species may be morphologically best adapted to eat. Analysis of the gut contents of preserved animals may tell what the animal had actually eaten just prior to capture, but the majority of animals generally have empty guts when examined, either because they had rapidly voided their gut contents or because they had not fed recently. Even when food is found in the gut, many types of food organisms, such as the naked flagellates, leave no recognizable remains; true rates of feeding cannot be estimated by this method or by examination of mouthparts.

Measurement of the feeding of a copepod on a single type of food determines to what extent the copepod will eat that food when no other food is available. Comparison between different foods in different experiments is difficult, however,

* Contribution No. 1593 from the Woods Hole Oceanographic Institution.

S

TABLE I

Copepods used in feeding experiments; the locations from which the experimental animals were taken; the production of fecal pellets when fed Thalassiosira; *and the organisms present in the gut contents of preserved specimens, listed in order of decreasing abundance*

Symbols: D —diatoms; Di —dinoflagellates; C —coccolithophorids; S —silicoflagellates; R —radiolarians; F —foraminiferans; T —tintinnids; Cr —crustaceans; [1] from Heinrich, 1958; [2] from Wickstead, 1962; N.E.—not examined

Family	Genus and species	Locations collected	Fecal pellet production	Gut contents
Calanidae	*Neocalanus* (*Calanus*) *gracilis* (Dana)	02°N–10°S, 55°E; 32°S, 55°E 27°–39°S, 62°–70°E	good	D, R, S, Cr, C
	Nannocalanus (*Calanus*) *minor* (Claus)	26°–33°S, 75°E	good	D, R, Cr
Eucalanidae	*Rhincalanus nasutus* Giesbrecht	16°–15°N, 58°–62°E	good	D, R
	R. cornutus (Dana)	15°–05°N, 55°E; 08°S, 75°E	good	D
	Eucalanus attenuatus (Dana)	16°N–03°S, 55°–62°E 02°–08°S, 75°E	good	D, C, S, Di, F, Cr[1] D, R, S, Cr, F, C
Metridiidae	*Pleuromamma xiphias* (Giesbrecht)	02°N, 55°E; 25°–35°S, 55°E	fair	D, S, C, T, F, R, Cr[1, 2]
	P. abdominalis (Lubbock)	02°–00°N, 55°–75°E; 25°–35°S, 55°E	fair	D, R, F, S, Cr[2]
	P. gracilis (Claus)	21°S, 75°E	poor	D, R, Cr[1], D, R, S, F, Cr[2]
	P. piseki Farran	21°S, 75°E	poor	N.E.
Aetideidae	*Euchirella curticauda* Giesbrecht	25°–35°S, 55°E	poor	Di(?), S, F, C
	E. bella Giesbrecht	15°–30°S, 75°E; 08°–02°N, 75°E	fair	Di(?), Cr, S, C
	Chirundina indica Sewell	16°–34°S, 55°E	poor	Cr, S
Scolecithricidae	*Scolecithrix danae* (Lubbock)	19°S–05°N, 75°E	poor	R, Cr
	Lophothrix latipes (Scott)	26°–43°S, 75°E	poor	N.E.
Euchaetidae	*Euchaeta acuta* Giesbrecht	23°–39°S, 55°–70°E; 26°–33°S, 75°E	poor	Cr, S
	E. marina (Prestandrea)	05°–02°N, 75°E	poor	Cr
Pontellidae	*Labidocera acutifrons* (Dana)	27°S, 61°E	N.E.	N.E.
Candaciidae	*Candacia aethiopica* (Dana)	33°S, 67°E	poor	N.E.
Augaptilidae	*Haloptilus ornatus* (Giesbrecht)	10°–21°S, 55°E; 04°–08°S, 75°E	poor	N.E.

because so many other factors affect the rate of feeding (Mullin, 1963). Measurement of feeding on various kinds of food in a mixture overcomes this difficulty since any factor other than selective feeding affects consumption of all foods equally. This type of experiment only shows what kind of food of those offered in the mixture the copepod will eat most readily; it does not necessarily show what food the copepod eats in nature unless the mixture is a good approximation to the types of food actually available in the sea.

METHODS

Copepods for experimental work were collected at night in the upper 200 m of water with a plankton net and sorted into species and developmental stages under a dissecting microscope, using Rose (1933) and Grice (1962) as taxonomic references. These identifications were later verified in a shore laboratory using animals preserved in formaldehyde after the experiments. The mouthparts of preserved male and female animals were removed for examination. Living animals on shipboard were kept in the dark at 20°C in filtered sea water. The species used and the locations where they were collected are shown in Table I; the table shows only those locations from which the experimental animals were taken, and not all the locations at which the species were encountered.

Animals containing food were picked out of preserved zooplankton collections from the *Lusiad* Expedition (equatorial Indian Ocean). The guts of these animals were dissected out, crushed under a cover glass on a glass slide, and examined at 645× magnification.

Three species of phytoplanktonic organisms, *Coscinodiscus perforatus*, *Thalassiosira fluviatilis*, and *Cyclotella nana*, were grown in enriched sea water as unialgal cultures (medium "f–1" of Guillard and Ryther, 1962). These cells, plus newly hatched *Artemia* nauplii, were used in selective feeding experiments (Table II). All the phytoplankters were centric diatoms living as isolated cells and differing greatly in cell size but not in shape.

The feeding of each species of copepod on *Thalassiosira* was tested by placing the animals in a suspension of the diatom (about 10^4 cells/ml) and examining the

TABLE II

The sizes of various food organisms computed from linear dimensions, and their initial concentrations in experimental mixtures

Food organism	Approximate volume, μ^3	Approximate initial concentration
Artemia nauplius	9×10^6	1 per ml
Coscinodiscus perforatus[1]	8×10^5	2 per ml
Thalassiosira fluviatilis[2]	$3{\cdot}5 \times 10^3$	2,000 per ml
Cyclotella nana[2]	$1{\cdot}5 \times 10^2$	18,000 per ml

[1] isolated by the author from Mauritius waters and identified by R. W. Holmes.
[2] from the culture collection of the Woods Hole Oceanographic Institution.

containers for fecal pellets after 48 or 72 hours. Selective feeding experiments with mixtures of food were run at 20°C in the dark for 18 to 24 hours, using the method described by Mullin (1963). A mixture of *Artemia* nauplii and at least one diatom was usually used. In order to measure grazing on phytoplankton in the absence of animal food, *Artemia* was omitted from the food mixture in some experiments. The food organisms present in the control and experimental containers after an experiment were counted after concentration by sedimentation or by filtration on to a membrane filter with a printed grid. The volume of water swept clear of food per copepod per day was then computed for each type of food in the mixture

The fecal pellet production of each species when fed *Thalassiosira* was rated on a qualitative scale as 'good', 'fair', or 'poor', and the relative abundance of the

TABLE III

Results of selective feeding experiments. Each horizontal row represents a separate experiment; for any experiment, N.P. means that the particular food organism was not present in the mixture of food tested

T.B.L. is the total body length of the copepod, in mm.
G.R. is the grazing rate, in ml/day/copepod, significant ($P < \cdot 05$) by rank sum test.
I.R. is the ingestion rate, in number of food organisms eaten/day/copepod

Copepod, species and stage	T.B.L.	Food organisms in mixture				
		Artemia G.R.	*Artemia* I.R.	*Coscinodiscus* G.R.	*Thalassiosira* G.R.	*Cyclotella* G.R.
Neocalanus gracilis female	3·0–3·7	172·4	44	N.P.	20·4	0
,,	,,	52·0	58	0	0	0
,,	,,	N.P.	—	222·0	37·2	12·0
male	3·0–3·2	0	0	N.P.	0	0
stage V	2·5–3·0	152·6	26	N.P.	0	0
,,	,,	29·6	32	0	0	0
stage IV	2·0–2·3	35·2	20	N.P.	0	0
Nannocalanus minor female	1·8–1·9	21·8	19	17·8	18·4	0
Rhincalanus nasutus female	3·8–4·3	16·7	14	N.P.	0	N.P.
R. cornutus female	3·1–3·4	15·8	14	N.P.	51·7	N.P.
,,	,,	119·9	41	0	0	0
stage V	2·5–2·9	0	0	N.P.	30·7	N.P.
,,	,,	64·0	28	0	0	0
Eucalanus attenuatus female	3·8–5·8	37·8	26	N.P.	14·8	N.P.
,,	,,	105·1	43	54·6	0	0
stage V	3·0–3·1	0	0	N.P.	45·1	N.P.
Pleuromamma xiphias female	4·2–5·0	520·2	155	N.P.	0	0
,,	,,	359·0	108	0	0	0
male	4·3–4·5	180·0	246	N.P.	0	0
stage V	3·4–4·3	178·6	86	N.P.	0	0
,,	,,	250·0	97	0	0	0

(continued opposite)

TABLE III (continued)

Copepod, species and stage	T.B.L.	Food organisms in mixture				
		Artemia G.R.	*Artemia* I.R.	*Coscinodiscus* G.R.	*Thalassiosira* G.R.	*Cyclotella* G.R.
P. abdominalis female	3·0–3·4	210·4	150	N.P.	0	0
,,	,,	250·0	97	0	0	0
,,	,,	N.P.	—	38·4	0	0
male	2·9–3·6	527·0	167	N.P.	0	0
,,	,,	280·0	128	0	0	0
P. gracilis female	1·7–1·8	73·0	27	0	0	0
P. piseki female	1·7–1·8	110·0	49	0	0	0
Euchirella curticauda female	3·6–3·7	264·0	180	0	0	0
stage V	3·1–3·3	127·5	112	0	0	0
stage IV	2·1–2·5	51·3	53	0	0	0
E. bella female	3·1–3·9	231·5	70	0	0	0
,,	,,	N.P.	—	0	0	0
stage V	2·6–3·1	550·0	60	0	0	0
stage IV	2·0–2·2	290·0	42	0	0	0
stage III	1·7–1·8	117·0	54	111·2	0	0
Chirundina indica female	3·3–3·9	197·0	75	0	48·7	68·3
stage V	2·4–3·1	126·0	59	0	0	0
Scolecithrix danae female	1·7–2·0	117·5	48	0	0	0
,,	,,	N.P.	—	0	0	0
Lophothrix latipes female	2·9–3·1	57·5	43	31·0	0	0
stage V	2·2–2·5	33·8	28	33·0	0	0
Euchaeta acuta female	3·2–3·9	84·5	83	0	0	0
male	3·4–3·5	0	0	0	0	0
stage V	2·7–3·4	99·5	80	0	0	0
E. marina female	3·1–3·6	N.P.	—	0	0	0
male	2·9–3·4	0	0	0	0	0
Labidocera acutifrons female	3·3–3·9	86·0	91	0	0	0
Candacia aethiopica female	2·1–2·4	0	0	0	0	0
male	2·0–2·3	0	0	0	0	0
Haloptilus ornatus female	3·8–4·3	0	0	0	0	0

various types of food organisms identified in the guts of preserved specimens was estimated (Table I). Table III summarizes the quantitative results of the experiments in which the copepods grazed on a mixture of foods. All the results will now be summarized by copepod families (ref. Table I). Some of the mouthparts referred to are illustrated by Giesbrecht (1892).

RESULTS

Calanidae

Both species have 'typical' herbivorous mouthparts, i.e. abundant setae on the second maxilla; many heavy, rather blunt mandibular teeth; and no major spines

or raptorial appendages. Diatom and radiolarian fragments constituted the major portion of the recognizable gut contents, although crustacean and other remains were also present. Similar gut contents are usually found in *Calanus* (see, Marshall, 1924; Beklemishev, 1954). *Nannocalanus* fed on both plant and animal food in the experiments. *Neocalanus* grazed *Artemia* almost exclusively in the food mixture, even the copepodid stage IV preferring *Artemia* to the diatoms. *Neocalanus* thus exhibits more carnivorous tendencies than found in the genus *Calanus*, since although female *Calanus finmarchicus* grazes *Artemia* nauplii at higher rates than diatoms (Mullin, 1963), this preference is reversed in the copepodid stages IV and V (Anraku and Omori, 1963). The mandibular teeth of *Neocalanus* are somewhat sharper in appearance than those of *Calanus*. Female *Neocalanus* ate the diatoms readily in the absence of *Artemia*, showing a direct relationship between grazing rate and cell size as does *Calanus* (Harvey, 1937; Mullin, 1963).

Male *Calanus* have greatly reduced grazing rates compared to the females (Raymont and Gross, 1942; Mullin, 1963) and the mandibular blade and the second maxilla are reduced in size. Both these observations also apply to *Neocalanus*, where the reduction in male mouthparts is much more pronounced. As in *Calanus*, the male second antenna and mandibular palp are not reduced. These appendages are presumably necessary for normal swimming during the finding of potential mates.

Eucalanidae

The mandibular teeth of *Eucalanus* are quite blunt and heavy; those of *Rhincalanus* are somewhat sharper. The other mouthparts also fit the herbivorous pattern, although the setae on the second maxillae are rather coarse. The gut contents suggest a basically herbivorous diet, although protozoans are equally abundant in the gut. *Thalassiosira fluviatilis* was eaten readily (see, Conover, 1960) and both *Artemia* nauplii and diatoms were eaten in the selective feeding experiments. Different experiments gave rather contradictory results.

Metridiidae

The mandibular teeth are quite sharp, especially in *Pleuromamma xiphias* and *P. abdominalis*, but the other mouthparts are herbivorous. The gut contents include phytoplankton, protozoans, and crustaceans. Beklemishev (1954) reports similar gut contents for *Metridia pacifica* and *M. ochotensis*. Although some fecal pellets were produced when only the diatom *Thalassiosira* was provided as food, all species of *Pleuromamma* fed exclusively on *Artemia* when it was available. This is also true for female *Metridia lucens* and *M. longa* from the Gulf of Maine (Mullin, unpubl.). Very high grazing and ingestion rates were found, e.g. the ingestion rate of *P. piseki* is equivalent to a consumption of about twice its body volume per day. *P. abdominalis* grazed *Coscinodiscus* at low rates when *Artemia* was not present. Males fed just as voraciously as females, and no reduction in their mouthparts was noted.

Aetideidae

All three species have stout spines on the second maxilla and *Chirundina* has a raptorial maxilliped and sharp mandibular teeth. In *Euchirella* the mandibular blade is rather narrow and its teeth are heavy and rather blunt. Both species of *Euchirella* contained large numbers of what appeared to be fragments of armoured dinoflagellates, while *Chirundina* contained abundant crustacean remains. There was little feeding on diatoms in the experiments, even in the absence of *Artemia* (see Conover, 1960, for *E. rostrata*). The apparent feeding by female *Chirundina* on the two small diatoms is difficult to interpret. All three species grazed *Artemia* at high rates, even in the younger copepodid stages.

Scolecithricidae

Neither species has obviously carnivorous modifications of the mouthparts; in both, the mandibular blade is narrow, its teeth are not particularly sharp, and the second maxilla is rather stumpy and equipped with thread-like as well as stout setae. The gut contents of *Scolecithrix* suggest predominantly carnivorous feeding, although Wickstead (1962) reported diatoms and silicoflagellates as well as protozoans and crustaceans from the gut of *Lophothrix frontalis*. *Scolecithrix* did not feed on any of the diatoms used, although *Lophothrix* grazed *Coscinodiscus* at about the same rates as it did *Artemia* nauplii.

Euchaetidae

The enlarged raptorial second maxilla and maxilliped, both armed with heavy setae, and the edged cutting teeth of the mandible suggest predaceous feeding. Gut contents and feeding experiments supported this conclusion. Males of both species have virtually lost the mandibular blade and second maxilla, and did not feed during the experiments.

Pontellidae

The enlarged maxilla with its stout setae, the modified maxilliped, and the sharp mandibular teeth are suited for the selective predation shown by *Labidocera* in the feeding experiments (see Anraku and Omori, 1963, for *L. aestiva*). No reductions in male mouthparts were noted.

Candaciidae and Augaptilidae

Neither *Candacia* nor *Haloptilus* fed during the present experiments on either diatoms or *Artemia*. Both have stout spines on the first and second maxillae, the second maxilla of *Candacia* being highly modified for grasping prey. Both have a very slender mandibular blade terminating in two sharp points. Wickstead (1959) suggested that *Candacia bradyi* feeds on large animals such as *Sagitta*, grasping them with the second maxilla (= first maxilliped) and piercing them with the pointed mandibular blade. It is tempting to suggest, by analogy, that *Haloptilus* feeds in the same way on animals larger than itself, although *Haloptilus* does not

look nearly so robust as *Candacia;* however, opposed to this suggestion, is Heinrich's (1958) report of diatoms, radiolarians, foraminiferans, and tintinnids in the guts of three species of *Haloptilus*.

DISCUSSION

No obligate herbivores were found; all species tested fed on *Artemia* nauplii and contained animal protozoans in the guts. Rather than classifying copepods as herbivores or carnivores, it seems more useful to use terms such as particle grazers and predators, realizing that even these terms impose an artificial division on a continuum of types of feeding behaviour.

The particle grazers (the Calanidae and Eucalanidae) ingested *Artemia* and diatoms at high rates, although sometimes showing a marked preference for *Artemia*. The genus *Acartia* also seems to fit into this category (Lebour, 1922; Anraku and Omori, 1963). These copepods have no obvious morphological adaptations for capturing motile prey and apparently eat most types of available particles of suitable size, such as diatoms and radiolarians, without regard to the taxonomic character of the particles. They feed, at least in part, by filtration, often removing larger particles preferentially. An intermediate situation is exemplified by the Metridiidae, which never fed as readily on diatoms as on *Artemia*. However, the gut contents and mouthparts suggest that these copepods are basically particle grazers. *Lophothrix* and *Centropages* (Lebour, 1922; Anraku and Omori, 1963) present a rather similar situation. In all the particle grazers, selective feeding on certain types of food is particularly marked when food is abundant, as in the feeding experiments, and probably involves behavioural mechanisms in addition to mechanical selection based on particle size. The extent to which the copepods 'search' for particular types of food and the mechanism permitting discrimination between food particles of similar size, such as *Artemia* nauplii and *Coscinodiscus*, are not known.

Most of the so-called predatory forms (the Aetideidae, Euchaetidae Pontellidae and probably *Scolecithrix* and the Candaciidae) are adapted to catch and hold motile animals, or at least to grasp large masses of food, and seldom capture small particles by filtration. *Tortanus* should be included here (Anraku and Omori, 1963). Prey is presumably detected by contact, but the mechanism of discrimination and selection of particular food requires further study (see, however, Horridge, this Volume, p. 395).

Available evidence suggests that less than one-fourth of the total particulate carbon in the surface waters of the Indian Ocean is in the form of particles larger than 30 μ (Mullin, 1965). The preference for large food particles shown by almost all copepods tested therefore provides indirect evidence as to the possible importance of micro-zooplankton and large aggregates of detritus in marine food webs. Estimation of the biomass and dynamics of production and utilization of these categories of organic matter is only beginning (Banse, 1962; Riley, 1963; Riley, Wangersky and Van Hemert, 1964). Since feeding on detritus was not tested

experimentally and cannot be readily distinguished from feeding on living organisms by examination of gut contents, this possibility cannot be further discussed.

Cases of rather specialized feeding by a particular genus, such as the utilization of dinoflagellates by *Euchirella* or the possible predation by *Candacia* on large animals, are suggested by this study. In general, however, the particle grazers on the one hand and the predators on the other, seem to be rather unselective as to diet and opportunistic in what they ingest. Neither the analyses of gut contents nor the selective feeding experiments reveal significant differences in the food materials utilized by most of the different species within each category. Specializations in feeding behaviour sufficient by themselves to provide the ecological distinctness theoretically necessary for the coexistence of food-limited sympatric populations thus have not been demonstrated by the present investigation.

SUMMARY

Selective feeding experiments were used to investigate the food preferences of 19 species of planktonic copepods, and the mouthparts and gut contents of these species were examined. All species consumed animal food at least as readily as phytoplankton, and several species ate only animal food. Most species could be tentatively classified as either particle grazers or predators, but there seems to be considerable overlap in the food preferences of different species.

ACKNOWLEDGMENTS

The experiments reported here were carried out during Cruise 5 of the R. V. *Anton Bruun* as part of the International Indian Ocean Expedition; the co-operation of the scientific staff on the vessel is gratefully acknowledged. Dr. A. Fleminger kindly provided preserved samples from the *Lusiad* Expedition and, together with Dr J. D. H. Strickland, suggested improvements in the manuscript. The U.S. National Science Foundation provided funds for ship time and equipment through Grant NSF-G20952 and supported the investigator with a Postdoctoral Fellowship. The U.S. Atomic Energy Commission supported the investigator during the preparation of the manuscript through Contract No. AT(11-1)-34, Project 108.

REFERENCES

Anraku, M. and Omori, M., 1963. Preliminary survey of the relationship between the feeding habit and the structure of the mouth-parts of marine copepods. *Limnol. Oceanogr.*, Vol. 8, pp. 116–126.

Bause, K., 1962. Net zooplankton and total zooplankton. *Rapp. Cons. Explor. Mer*, Vol. 153, pp. 211–215.

Beklemishev, K. V., 1954. [The feeding of some abundant plankton copepods in Far-Eastern seas.] *Zool. Zhurn.*, Vol. 33, pp. 1210–1230, [Eng. trans.].

Conover, R. J., 1960. The feeding behaviour and respiration of some marine planktonic Crustacea. *Biol. Bull., Woods Hole*, Vol. 119, pp. 399–415.

Giesbrecht, W., 1892. Systematik und Faunistik der pelagischen Copepoden des Golfes von Neapel. *Fauna und Flora des Golfes von Neapel und der angrenz Meeres-abschnitte*, Vol. 19, 831 pp.

Grice, G. D., 1962. Calanoid copepods from equatorial waters of the Pacific Ocean. *U.S. Fish. Bull.*, Vol. 61, No. 186, pp. 171–246.

Guillard, R. R. L. and Ryther, J. H., 1962. Studies of marine planktonic diatoms. I. *Cyclotella nana* Hustedt, and *Detonula confervacea* (Cleve) Gran. *Canad. J. Microbiol.*, Vol. 8, pp. 229–239.

Harvey, H. W., 1937. Note on selective feeding by *Calanus*. *J. mar. biol. Ass. U.K.*, Vol. 22, pp. 97–100.

Heinrich, A. K., 1958. [On the nutrition of marine copepods in the tropical region.] *Dokl. Akad. Nauk S.S.S.R.*, Vol. 119, pp. 1028–1031, [Eng. trans.]

Lebour, M. V., 1922. The food of plankton organisms. *J. mar. biol. Ass. U.K.*, Vol. 12, pp. 644–677.

Marshall, S. M., 1924. The food of *Calanus finmarchicus* during 1923. *J. mar. biol. Ass. U.K.*, Vol. 13, pp. 473–479.

Mullin, M. M., 1963. Some factors affecting the feeding of marine copepods of the genus *Calanus*. *Limnol. Oceanogr.*, Vol. 8, pp. 239–250.

Mullin, M. M., 1965. Size fractionation of particulate organic carbon in the surface waters of the western Indian Ocean. *Limnol. Oceanogr.*, Vol. 10, pp. 495–462; 610–611.

Raymont, J. E. G. and Gross, F., 1942. On the feeding and breeding of *Calanus finmarchicus* under laboratory conditions. *Proc. roy. Soc. Edinb.*, Vol. 61, pp. 267–287.

Riley, G. A., 1963. Organic aggregates in sea water and the dynamics of their formation and utilization. *Limnol. Oceanogr.*, Vol. 8, pp. 372–381.

Riley, G. A., Wangersky, P. J. and Van Hemert, D., 1964. Organic aggregates in tropical and subtropical surface waters of the North Atlantic Ocean. *Limnol. Oceanogr.*, Vol. 9, pp. 546–550.

Rose, M., 1933. Copépodes pélagiques. *Faune de France*, Vol. 26, Office Central de Faunistique, Paris, 374 pp.

Wickstead, J. H., 1959. A predatory copepod. *J. anim. Ecol.*, Vol. 28, pp. 69–72.

Wickstead, J. H., 1962. Food and feeding in pelagic copepods. *Proc. zool. Soc. Lond.*, Vol. 139, pp. 545–555.

Reprinted from *Okeanologia*, vol. VI, no. 2, 1966, p. 314-325.

УДК 550.42 : 517/475(267)

В. Г. БОГОРОВ, О. К. БОРДОВСКИЙ, М. Е. ВИНОГРАДОВ

БИОГЕОХИМИЯ ОКЕАНИЧЕСКОГО ПЛАНКТОНА. РАСПРЕДЕЛЕНИЕ НЕКОТОРЫХ ХИМИЧЕСКИХ КОМПОНЕНТОВ ПЛАНКТОНА В ИНДИЙСКОМ ОКЕАНЕ

Институт геологии и разработки горючих ископаемых
Институт океанологии АН СССР

Основная проблема современной морской планктонологии — изучение экологических систем пелагиали. При этом особенно существенно оценить поток энергии, идущей через эти экосистемы, через их трофическую сеть.

Совершенно очевидно, что для выяснения переноса энергии, ее концентрации и потерь на различных трофических уровнях, недостаточно иметь сведения только о биомассе или даже продукции планктона. Для количественной оценки энергетического баланса необходимо детальное знание химического состава планктона и, прежде всего, соотношения в нем основных химических компонентов, таких, как углеводы, белки, жиры, характеризующихся различной энергоемкостью. Эти компоненты с различным энергетическим эффектом могут усваиваться и трансформироваться организмами.

Один из важнейших законов биоэнергетики заключается в том, что все последующие превращения органического вещества, созданного автотрофными организмами, осуществляются экзотермическим путем, т. е. с освобождением некоторого количества энергии [1]. При этом на каждой последующей стадии превращения органическое вещество в целом будет характеризоваться все более низким запасом потенциальной энергии по сравнению с исходным.

Изменчивость экосистем в различных районах и климатических зонах океана служит одним из основных моментов, определяющих всю биологическую структуру океана. С этой точки зрения чрезвычайно существенно выяснение химического состава всей массы планктона (тотального планктона), изменения его в разных районах океана и влияния внешних — абиотических факторов, с которыми связаны эти изменения.

Наконец, от химического состава планктона в значительной степени зависит его роль как осадкообразователя. Карбонатные осадки отлагаются в тех районах, где в планктоне преобладают животные с известковистыми раковинами — птероподы и глобигерины. Осадки с высоким содержанием кремнезема характерны для районов массового развития пелагических диатомовых водорослей или же для больших глубин океана, где скелетные остатки, состоящие из карбоната кальция, не встре-

[1] Вальтерс [29] указывает, что на каждый моль окисленной глюкозы при переходе от одного пищевого уровня к следующему теряется примерно 275 *ккал*.

чаются, благодаря растворению в недонасыщенных CO_2 глубинных водах. Существенным компонентом таких осадков обычно оказываются скелеты радиолярий.

Изучением химического состава планктона занимались многие исследователи, и в настоящее время уже накоплен значительный материал, характеризующий как отдельные виды и целые группы животных [6—7, 10, 12, 16, 24, 27 и мн. др.], так и тотальный планктон различных участков морей и некоторых районов океана [11, 13—15, 22, 25—27 и др.]. Однако вопрос об изменчивости химического состава океанических планктонных сообществ и его связи с внешними факторами все еще остается одним из наименее изученных. Только в последние годы исследования обширных океанических акваторий, предпринятые рядом стран, позволили подойти к постановке подобных задач.

Особенно широко развернулись исследования взвеси поверхностного слоя воды, в значительной степени состоящей из микропланктона [17—19]. Был исследован, в частности, состав взвеси в южных и центральных районах Индийского океана. К сожалению, по отношению к более крупному сетному зоопланктону подобных наблюдений сделано несоизмеримо меньше.

Определение жирности планктона проводилось на меридиональных разрезах через Тихий и Атлантический океаны [2—3], а также на нескольких станциях в Индийском и Атлантическом океанах [30].

В дальнейшем исследования биохимического состава океанического планктона были расширены. Некоторым результатам этих исследований и посвящается настоящее сообщение.

МАТЕРИАЛ И МЕТОДИКА

Материал был собран во время 31-го рейса э/с «Витязь» в Индийский океан сетью типа Джеди с площадью входного отверстия 0,5 *м*^{2} и с фильтрующим конусом из мельничного сита № 38 (размер ячеи 0,18 *мм*). На станциях облавливался слой 0—100 *м*. Полученные пробы без фиксации фильтровались, взвешивались, а затем высушивались. В дальнейшем в них определялось содержание карбоната кальция, органического углерода и липидов.

Карбонатность образцов и содержание органического углерода определялись по Кноппу. Далее карбонатный CO_2 пересчитывали на $CaCO_3$. При этом следует иметь в виду, что, хотя $CaCO_3$ и является преобладающим компонентом в составе карбонатных скелетов планктонных организмов, в некоторых случаях он в значительной степени может замещаться $MgCO_3$. Установлено, что с повышением температуры окружающей воды роль $MgCO_3$ в составе карбонатных скелетов возрастает и, например, у фораминифер колеблется в зависимости от температуры и некоторых других факторов от 0,3 до 16% [23].

Содержание липидов определяли путем экстракции на аппарате Сокслета смесью, состоящей из 70% бензола, 15% ацетона и 15% метанола.

Для анализов был использован материал, собранный на 142 станциях. В связи с тем, что количество планктона, получаемое с одной станции, часто было недостаточным для анализа, то станции, сделанные в районе со сходными гидрологическими условиями и близким таксономическим составом и количеством планктона, объединялись в небольшие группы. Определение таксономического состава, биомассы планктона и подсчет массовых видов проводили в пробах, которые брались на каждой станции параллельно с пробами для химического анализа[2]. Результаты химических анализов приведены в таблице, где материал по отдельным станциям объединен по естественным био-гидрологическим

[2] Сведения о составе планктона приведены в ряде статей [4, 9, 21].

Химический состав планктона Индийского океана

(в слое 0—100 *м*)

№ районов	№№ станций в каждом районе	Характеристика района	Биомасса (сухой вес), *мг/м³*	$CaCO_3$	$C_{орг}$	Липиды	Относительное содержание липидов в органическом веществе планктона (в % от $C_{орг}$)	$CaCO_3$	$C_{орг}$	Липиды
				в % на сухой вес планктона				в объеме воды, *мг/м³*		
1	4546—551	Район взаимодействия суматранских вод и вод Южного экваториального течения	4,02	21,0	29,46	7,26	16,52	0,84	1,19	0,29
2	4556—559	Район смешения вод прияванского района и центральных индоокеанских вод	3,75	15,56	33,71	7,62	15,19	0,58	1,26	0,24
3	4555	Локальный район чрезвычайно интенсивного стационарного подъема вод	29,5	8,29	24,17	9,04	25,1	2,44	7,11	2,66
4	4518, 4521—525, 4553, 4554	Периферическая часть прияванского района	5,78	10,5	31,41	8,08	17,21	0,61	1,82	0,47
5	4508, 4515, 4527, 4530, 4531, 4533, 4534	Высокопродуктивный прияванский район	15,5	9,85	31,58	9,84	20,9	0,15	4,89	1,52
6	4560—562, 4570	Воды Западно-Австралийского течения	5,60	21,0	26,95	7,37	18,35	1,17	1,51	0,41
7	4564—565	Прибрежные воды северо-западной Австралии	13,5	5,38	30,86	6,42	13,92	0,73	4,16	0,87
8	4573—581	Центральные воды восточной части океана	2,1	11,6	30,38	6,83	15,1	0,24	0,64	0,14
9	4599, 4600, 4605—609	Воды Южного экваториального течения	3,5	9,87	31,84	9,9	20,81	0,35	1,11	0,35
10	4595, 4596, 4598, 4610, 4612	Зона дивергенции между водами Экваториального противотечения и Южного экваториального течения	7,0	14,3	30,95	10,06	21,82	1,00	2,16	0,70
11	4590—592, 4594, 4613—616	Район опускания вод на южной периферии Муссонного течения	3,44	14,05	28,41	7,51	17,72	0,48	0,98	0,26
12	4617—622	Прибрежные воды и зона подъема вод, вызванного расхождением ветвей Муссонского течения перед Мальдивскими о-вами	5,73	7,85	29,13	7,82	18,0	0,45	1,68	0,45
13	4625—632	Подъем вод в зоне расхождения ветвей Муссонного течения	10,69	11,2	26,65	13,63	34,38	1,20	2,84	1,45

14	4635—640, 4642	Подъем вод, вызванный циклонической циркуляцией части вод Экваториального противотечения, разворачивающихся западнее архипелага Чагос	10,21	13,4	30,95	12,45	27,0	1,37	3,16	1,27
15	4648—650, 4653	Центральные воды западной части океана	4,01	4,84	35,61	9,37	20,6	0,19	1,43	0,38
16	4664—665, 4667	Зона дивергенции между Экваториальными противотечениями и Южным экваториальным течением	11,93	8,9	31,41	11,09	23,6	1,06	3,75	1,32
17	4660, 4662—663, 4668	Воды Южного экваториального течения в западной части океана	7,31	12,1	30,29	9,24	20,4	0,88	2,22	0,67
18	4666,4676,4677,4690,4692,4694, 4695, 4697, 4699, 4700	Воды Экваториального противотечения в западной части океана	7,24	9,25	25,9	10,77	27,9	0,67	1,87	0,78
19	4675	Район Коморских о-вов	12,3	8,03	31,16	9,23	19,89	0,99	3,82	1,14
20	4703	Зона интенсивной дивергенции в месте расхождения ветвей Муссонного течения	27,3	7,85	28,02	9,58	22,8	2,14	7,65	2,62
21	4678, 4680—682, 4686	Продуктивные прибрежные воды в зоне стыка Южного экваториального и Сомалийского течений	10,4	13,29	29,0	10,66	24,6	1,38	3,02	1,11
22	4701, 4702	Район Сейшельских о-вов	16,25	18,7	25,94	8,00	20,7	3,04	4,21	1,30
23	4704—709	Южная часть Аравийского моря	8,03	9,4	32,17	9,06	18,9	0,75	2,58	0,73
24	4714—717	Прибрежные воды северо-восточной части Аравийского моря	18,35	7,96	29,85	10,09	22,6	1,46	5,49	1,85
25	4710—713, 4718—723, 4725	Высокопродуктивная северная часть Аравийского моря	13,34	12,26	27,15	6,78	16,8	1,63	2,03	0,90
26	4726, 4727	Район подъема вод к западу от о. Сокотра в истоках Сомалийского течения	20,6	11,1	30,27	11,17	24,7	2,29	6,24	2,30
27	4728—732	Устьевая часть Аденского залива	14,34	10,85	30,55	13,62	29,9	1,55	4,38	1,96

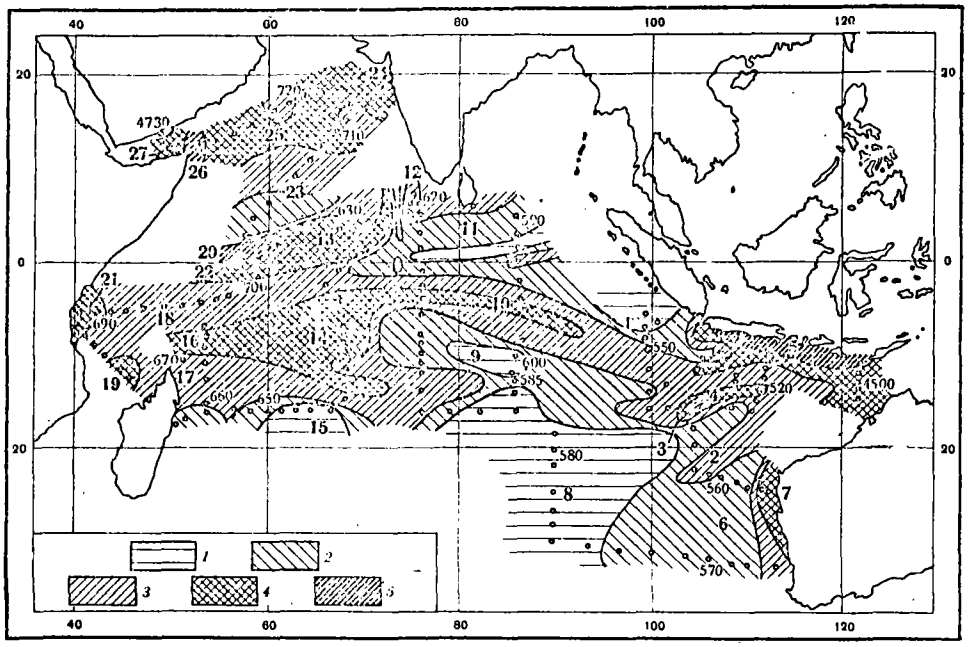

Рис. 1. Распределение биомассы планктона (*мг/м*³) в слое 0—100 *м* [по 4]

1 — <25; *2* — 25÷50; *3* — 50—100; *4* — 100—250; *5* — >250 *мг/м*³

Точки — положение станций, на которых проводились сборы планктона; мелкие цифры — номера станций; крупные цифры — номера районов (см. таблицу).

районам (рис. 1). Данные, приведенные в таблице, дают возможность количественно охарактеризовать особенности распределения основных химических компонентов поверхностного сетного планктона и наметить связь этого распределения с некоторыми абиотическими факторами.

ОРГАНИЧЕСКИЙ УГЛЕРОД

Содержание органического углерода в исследованном планктоне довольно постоянно в разных районах и составляет в среднем 29,9%, колеблясь от 24,2 до 35,6% от сухого веса. Колебания эти не слишком закономерны, но тем не менее можно отметить, что более низкое содержание $C_{орг}$ в планктоне наблюдается в районах интенсивного поднятия вод, где существенную часть в общей массе сестона составляет фитопланктон (диатомеи) с тяжелыми кремневыми створками. Наиболее высокое содержание $C_{орг}$ имеет место в некоторых сравнительно бедных районах, где роль фитопланктона мала. Однако, например, в таком высоко продуктивном районе, как Прияванский, где развивается большое количество фитопланктона, содержание органического углерода довольно высокое (до 3—7 *мг/м*³).

Благодаря мало меняющемуся относительному количеству $C_{орг}$ в планктоне картина распределения его абсолютного количества (рис. 2) в верхнем стометровом слое в общем довольно полно повторяет картину распределения общей биомассы планктона (см. рис. 1). Наибольшая концентрация планктоногенного органического углерода наблюдается в водах Прияванского района, в зоне подъема вод к юго-западу от него, в зонах подъема вод на 6—8° ю. ш. и на экваторе в западной части океана, а также в прибрежных районах северной части Аравийского моря, т. е. в наиболее продуктивных районах. Наименьшая его концентрация отмечена в центральных водах и в водах южной периферии

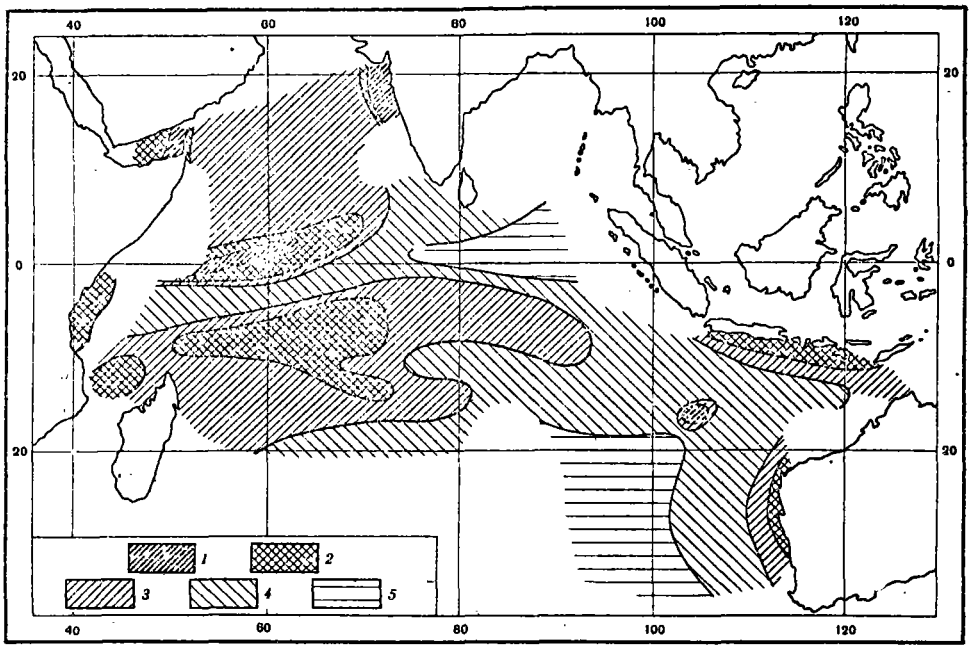

Рис. 2. Схема распределения $C_{орг}$ (*мг/м*³), содержащегося в планктоне в слое 0—100 *м*:
1 — >7; *2* — 7—3; *3* — 3—2; *4* — 2—1; *5* — <1 *мг/м*³

Муссонного течения в восточной части океана, т. е. в водах, особенно бедных планктоном.

Интересно сравнить количество органического углерода, заключенного в планктоне, с общим количеством органического углерода, растворенного в воде. По данным Мензеля [28], концентрация растворенного органического углерода в поверхностных водах западной части Индийского океана обычно составляет 0,5—0,3 *мг/л*. Эта величина примерно в десять раз больше, чем содержание $C_{орг}$ во взвеси, и в сотни раз больше, чем его содержание в планктоне, что подтверждает резкое преобладание мертвого — «косного» органического вещества над живым.

ЛИПИДЫ

В качестве одного из основных компонентов, характеризующих химический состав планктона и его энергетические особенности, рассматривалась липидная фракция органического вещества. Это мотивировалось прежде всего тем соображением, что именно жировые вещества в организмах обладают наибольшим запасом энергии и характеризуются высокой калорийностью. Известно также, что в планктонных организмах жиры представляют, по-видимому, основной резерв энергии и содержание их динамично связано с энергетическими затратами организма [20].

Жировые вещества можно рассматривать как весьма важный и лабильный компонент, тесно связанный с процессами обмена и энергетическими состояниями всех остальных компонентов организма. В липидах постоянно осуществляются процессы синтеза и распада нейтральных жиров, переход одних жирных кислот в другие и новообразование жировых веществ из углеводов и, частично, белков. Следует подчеркнуть, что образование и накопление жировых веществ в организмах происходит не столько за счет жиров, содержащихся в пище, сколько благодаря превращениям углеводов. В свою очередь, при дефиците угле-

водов или недостаточном их использовании, жиры используются организмом в качестве источника энергии. Таким образом, жиры являются показателем, суммирующим многие обменные процессы и в известной мере отображают энергетическое состояние организма.

Тесная связь между липидной фракцией планктонных организмов с их другими важнейшими компонентами, в частности с белками, проявляется в наличии в составе липидов широкого спектра аминокислот, весьма прочно с ними связанных. После кислотного гидролиза липидов нами были определены методом бумажной хроматографии следующие аминокислоты: цистин, лизин, гистидин, аспарагиновая и глютаминовая кислоты, аланин, изопролин, аргинин, тирозин, метионин, валин, фенилаланин и триптофан. Наличие аминокислот, по-видимому, обусловлено присутствием пептидов, и, таким образом, выделенные липиды относятся к группе липопротеидов.

По элементарному составу исследованные липиды в среднем на 67% состоят из углерода и на 10% из водорода, что свидетельствует о заметной роли в их составе гетероатомов и, в частности кислорода, связанного скорее всего с жирными кислотами. Это подтверждается также заметным содержанием омыляемых веществ и в то же время относительно небольшой ролью (около 10%) наиболее восстановленных компонентов-углеводородов.

На всей исследованной акватории содержание липидной фракции в планктоне колебалось от 6,4 до 13,6%, составляя в среднем 9,4% сухого веса. Примерно такое же содержание липидов характерно также для планктона в пределах тропической зоны Атлантического и Тихого океанов. Лишь в субтропических и умеренно холодноводных районах полярнее 20—30° содержание липидной фракции иногда превышает 15—20% [2, 3].

Меньшее содержание липидов в планктоне тропических и экваториальных районов дает основание считать, что их содержание связано обратной зависимостью с температурой воды. В тех районах, где эта температура высока, процессы метаболизма идут быстро, время существования каждой генерации планктонных животных невелико и животным нет необходимости создавать большие запасы жира. В соответствии с этим содержание липидов в планктоне оказывается низким.

Однако четкое соответствие между температурой воды и количеством липидной фракции в планктоне прослеживается только при обобщенном сравнении теплых тропических и более холодных вод высоких широт. Внутри тропической зоны такого соответствия обнаружить не удается. В обследованной нами северной части Индийского океана, целиком лежащей в тропической зоне, соотношение между температурой в ограниченных районах и содержанием липидов в планктоне оказывается далеко не таким четким. Так коэффициент корреляции между содержанием липидов L (в процентах от сухого веса) в планктоне слоя 0—100 *м* и температурой T на глубине 50 *м* для 27 рассматриваемых нами районов очень невелик $r_{LT}=0{,}15$ и статистически недостоверен ($t_r=0{,}764$, т. е. $p\ll 0{,}95$). В общем планктон обычно оказывается наиболее обогащен липидами в районах его максимальных концентраций, т. е. там, где условия для развития планктона оказываются наиболее благоприятными. Действительно, коэффициент корреляции между биомассой планктона P и содержанием липидов L выше ($r_{LP}=0{,}25$), чем между содержанием липидов в планктоне и температурой на глубине 50 *м*.

Как известно, в тропической зоне, и в частности в экваториальной части Индийского океана, планктон получает оптимальные условия для развития и имеет наибольшую биомассу в районах квазистационарных подъемов вод, о которых можно судить по подъему верхней границы слоя скачка плот-

ности [8]. Оказывается, что между количеством липидов в планктоне L и глубиной залегания верхней границы слоя термоклина H корреляция выше, чем с другими рассмотренными нами гидрологическими факторами ($r_{LH} = -0{,}32$). Почти столь же велика корреляция между содержанием липидов в планктоне и температурой на глубине 100 *м* ($r_{LT} = -0{,}26$), понижение

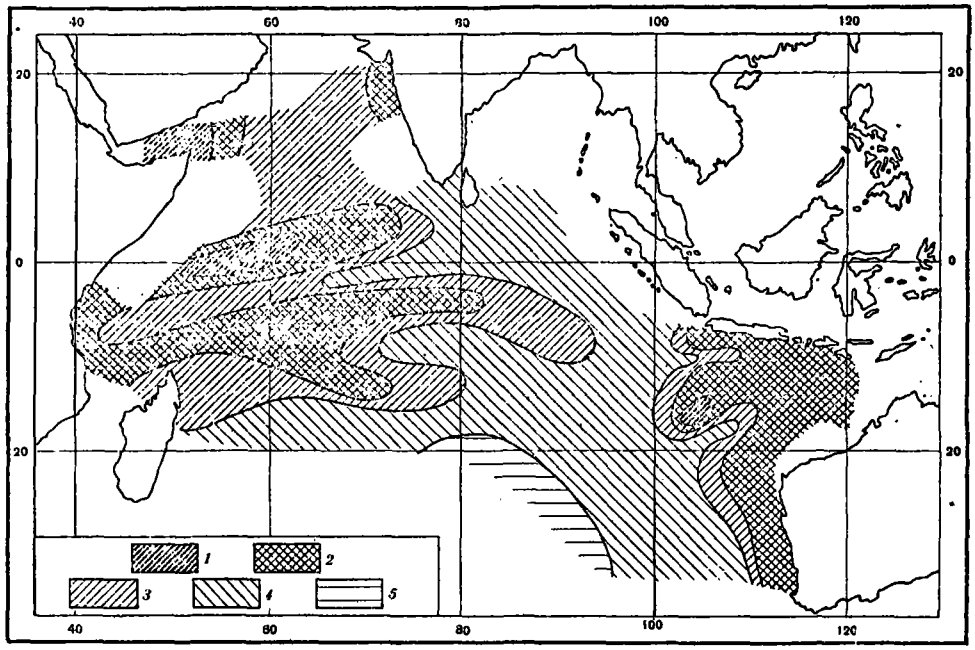

Рис. 3. Схема распределения липидной фракции планктона в слое 0—100 *м* (*мг/м*³): *1* — >2,0; *2* — 2,0—1,0; *3* — 1,0—0,5; *4* — 0,5—0,25; *5* — <0,25 *мг/м*³

которой указывает на подъем глубинных вод, а повышение — на опускание поверхностных.

В связи с тем, что нет полной уверенности в прямолинейности связи между содержанием липидов в планктоне и рассмотренными выше гидрологическими факторами, кроме коэффициента корреляции, была рассчитана величина коррелятивного отношения между ними. Величины коррелятивного отношения указывают на большее влияние гидрологических факторов, связанных с подъемом вод, чем это следовало из величин коэффициентов корреляции. Так, коррелятивное отношение между содержанием липидов L и температурой на глубине 100 *м* (t) $\eta_{tL} = 0{,}514$ при $m_\eta = 0{,}171$ и $t_\eta = 3{,}0$, т. е. при $p > 0{,}99$, а между количеством липидов L и глубиной верхней границы слоя скачка H $\eta_{HL} = 0{,}506$ при $m_\eta = 0{,}188$ и $t_\eta = 2{,}62$, т. е. при $p > 0{,}95$.

Полученные данные позволяют считать, что увеличение или уменьшение содержания липидной фракции в планктоне (во всяком случае в пределах тропической зоны) тесно связано с условиями его обитания. Оно зависит прежде всего от изменения всего комплекса факторов, связанного с подъемом глубоких вод в эвфотическую зону, при котором создаются оптимальные условия для развития планктона. Понижение или повышение температуры в данном случае влияет на количество липидов в планктоне не само по себе, а служит лишь индикатором суммы благоприятных условий для существования (питания) планктона.

Картина распределения абсолютного количества липидов, содержащихся в сетном планктоне верхнего стометрового слоя (рис. 3), повторяет в очень обобщенном виде картину распределения биомассы планктона (см. рис. 1). Максимальное количество липидов (более 1—2 *мг/м*³) содержится в австрало-яванском районе океана, в зоне дивергенций у экватора и на 5—8° ю. ш., а также и в северо-западной части Аравийского моря; наименьшее — в центральных водах восточной части океана.

КАРБОНАТ КАЛЬЦИЯ

Широко известна ведущая роль планктонных организмов в концентрации карбонатов кальция и в образовании различных карбонатных осадков. Все осаждение кальция в океане происходит биогенным путем, поэтому оценка кальциевой функции планктона служит необходимым звеном в количественной характеристике круговорота этого элемента в океане.

Содержание $CaCO_3$ в планктоне рассмотренных районов составляет в среднем 11,7% и изменяется от 4,8 до 21%, т. е. колеблется в гораздо большей степени, чем содержание любого из химических компонентов, рассмотренных выше. В центральных водах западной части океана и в приавстралийском районе оно едва достигало 5% от сухого веса планктона, а в присуматранском районе и в водах Западно-Австралийского течения превышало 20%.

Основные носители карбоната кальция в планктоне — птероподы и глобигерины. Однако соответствия между карбонатностью тотального планктона и количеством птеропод в нем мы не обнаружили. Более того, низкая карбонатность планктона оказалась характерной для ряда прибрежных районов (Коморские и Сейшельские о-ва, южная оконечность Индостана и др.), где широко развиты карбонатные донные отложения, в первую очередь птероподовые илы.

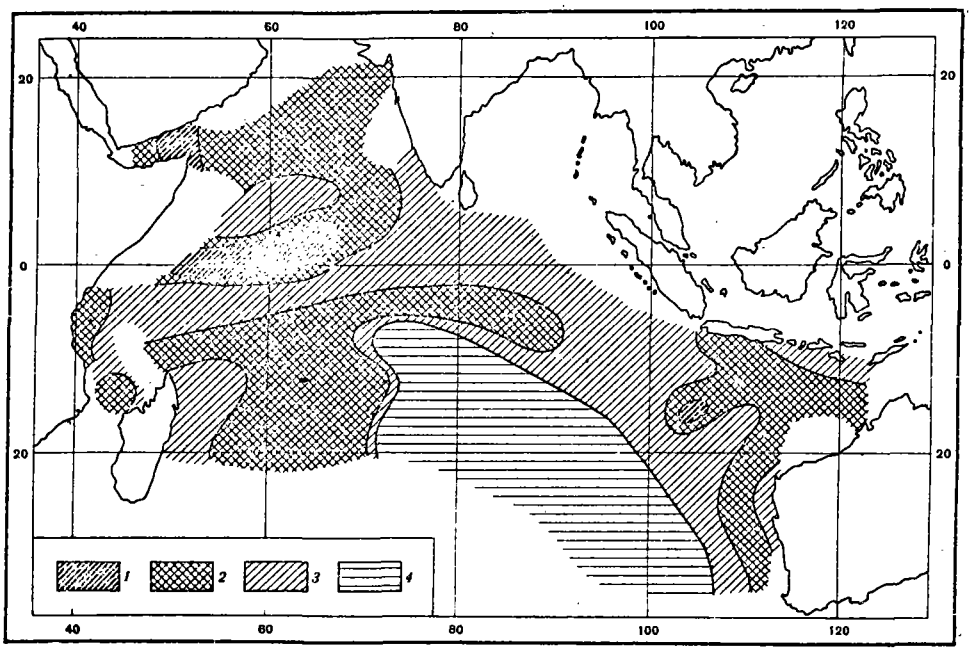

Рис. 4. Схема распределения $CaCO_3$(*мг/м*³), содержащегося в планктоне в слое 0—100 *м*:
1 — >2,0; *2* — 2,0—1,0; *3* — 1,0—0,5; *4* — <0,5

Иная картина наблюдается при сравнении распределения карбонатности планктона со схемой количественного распределения глобигерин, составленной Беляевой [1]. Оказалось, что районы с наиболее высокой карбонатностью планктона (южная часть Аравийского моря, приявайский и приавстралийский районы) совпадают с районами относительно высокой численности глобигерин. В то же время наиболее бедные планктоногенным карбонатом кальция центральные воды также обеднены и глобигеринами. Создается впечатление, что содержание карбоната кальция в тропическом планктоне определяется прежде всего количеством глобигерин.

Благодаря сравнительно большим колебаниям в содержании $CaCO_3$ в планктоне картина распределения его абсолютных значений (рис. 4) в меньшей мере, чем для других рассмотренных выше компонентов, согласуется с картиной распределения биомассы планктона (рис. 1).

Наиболее высокое содержание планктоногенного карбоната кальция оказалось характерным для зоны дивергенции на экваторе в западной части океана и в водах у входа в Аденский залив; несколько меньшее — в Аравийском море, к востоку от Мадагаскара и между Явой и Австралией (но не в прибрежных водах). Наименьшее содержание карбонатов отмечено в центральных водах восточной части океана и в водах Южного экваториального течения к востоку от архипелага Чагос.

* * *

Интересно проследить, как отражается распределение химических компонентов поверхностного планктона на характере накопления тех же веществ в донных отложениях.

Как уже говорилось, между распределением планктоногенного карбоната кальция и размещением карбонатных осадков не наблюдается четкой зависимости. По-видимому, растворение кальцита агрессивными глубинными водами в процессе седиментации, а также разбавляющее влияние терригенного и обломочного карбонатного материала в прибрежной зоне нарушают ее.

В то же время между битуминозностью донных отложений и распределением биомассы планктона в поверхностных водах наблюдается достаточно четкая, прямая связь [5]. Аналогичная связь проявляется и между распределением липидной фракции планктона и битуминозностью осадков, что подтверждает положение о ведущей роли липидов планктонных организмов в генерации битуминозных компонентов донных отложений.

Намечается также соответствие между обилием планктонных организмов и концентрацией органического вещества в донных отложениях открытых районов океана.

Участие различных планктоногенных компонентов в осадкообразовании в открытом океане в значительной мере зависит от их устойчивости по отношению к внешним воздействиям. Поэтому такие, относительно стабильные вещества, как липидная фракция, в гораздо большей степени запечатлевают в осадках общую картину своего распределения в планктоне, чем более лабильные карбонаты.

ЛИТЕРАТУРА

1. Беляева Н. В. 1964. Распределение планктонных фораминифер в водах и на дне Индийского океана. Тр. Ин-та океанол. АН СССР, 68.
2. Богоров В. Г. 1960. Географические изменения жирности планктона в океане. Докл. АН СССР, 134, № 6.
3. Богоров В. Г., Виноградов М. Е. 1960. Распределение биомассы зоопланктона в центральной части Тихого океана. Тр. Всес. гидробиол. о-ва, X.

4. Богоров В. Г., Виноградов М. Е. 1961. Некоторые черты распределения биомассы планктона в поверхностных водах Индийского океана зимой 1959/60 гг. Океанол. исслед., № 4.
5. Бордовский О. К. 1961. К характеристике органического вещества донных отложений Тихого и Индийского океанов. В сб. Среда и процессы нефтеобразования. Изд. «Наука», М.
6. Виноградов А. П. 1938. Химический состав морского планктона. Тр. Всес. н.-и. ин-та рыбн. х-ва и океаногр., VII.
7. Виноградов А. П. 1939. Химический состав планктона. Тр. Биогеохим. лабор., V.
8. Виноградов М. Е., Воронина Н. М., Суханова И. Н. 1961. Пространственное распределение тропического планктона и его связь с некоторыми особенностями структуры вод открытых районов океана. Океанология, 1, вып. 2.
9. Виноградов М. Е., Воронина Н. М. 1962. Некоторые черты распределения зоопланктона северной части Индийского океана. Тр. Ин-та океанол. АН СССР, 58.
10. Виноградова З. А. 1956. К познанию химического состава кормовых организмов и рыб Черного моря. Тр. Совещ. по физиол. рыб, М.
11. Виноградова З. А. 1957. Биохимический состав планктона Черного моря. Докл. АН СССР, 116, № 4.
12. Виноградова З. А. 1960. К изучению биохимического состава антарктических черноглазок Euphausia superba Dana. Докл. АН СССР, 133, № 3.
13. Виноградов З. А. 1961. Особенности биохимического состава и калорийность фито- и зоопланктона северо-западной части Черного моря в 1955—1959 гг. Уч зап. Одесск. биол. ст. АН УССР, вып. 3.
14. Виноградова З. А. 1964. Некоторые биохимические аспекты сравнительного изучения планктона Черного, Азовского и Каспийского морей. Океанология, IV, вып. 2.
15. Кизеветтер И. В. 1954. О кормовой ценности планктона Охотского и Японского морей. Изв. Тихоокеанск. н.-и. ин-та рыбн. х-ва и океаногр., 39.
16. Лапская Л. В., Пшенина Т. И. 1961. Содержание белка, жира, углеводов и золы в некоторых массовых планктонных водорослях Черного моря, выращенных в культурах. Тр. Севаст. биол. ст., 14.
17. Лисицын А. П. 1959. Новые данные о составе и распределении взвешенных веществ в морях и океанах в связи с вопросами геологии. Докл. АН СССР, 126, № 4.
18. Лисицын А. П. 1961. Распределение и состав взвешенного материала в морях и океанах. В сб. Современные осадки морей и океанов. Изд. АН СССР, М.
19. Лисицын А. П. 1964. Распределение и химический состав взвеси в водах Индийского океана. *Результаты исслед. по программе МГГ. Океанология, IV, вып. 10.*
20. Петипа Т. С. 1964. Суточный ритм расхода и накопления жира у Calanus helgolandicus (Claus) в Черном море. Докл. АН СССР, 156, № 6.
21. Суханова И. Н. 1962. О видовом составе и распределении фитопланктона в северной части Индийского океана. Тр. Ин-та океанол. АН СССР, 58.
22. Цхомелидзе О. Н. 1958. К биохимическому составу планктона восточной части Черного моря. Сообщ. АН Груз. ССР, 21, № 2.
23. Chave K. E. 1954. Aspects of the Biogeochemistry of Magnesium. 1. Calcareaus marine organisms. J. Geol., 62, No 3.
21. Fisher L. R. 1962. The total lipid material in some species of marine zooplankton. Cons. Perm. Intern. Explor. Mer. Rap. et Proc-Verb., 153.
25. Hagmeier E. 1964. Zum Gehalt an Seston und Plankton im Indisched Ozean zwichen Australien und Indonesien. Kieler. Meeresforsch., 20, H. 1.
26. Harris E., Riley G. A. 1956. Chemical composition of the plankton. Bull. Bingham Oceanogr. Coll., 15.
27. Krey I. 1958. Chemical determinations of net plankton with special reference to equivalent albumin content. J. Marine Res., 17.
28. Menzel D. W. 1964. The distribution of dissolved organic carbon in the Western Indian Ocean. Deep-Sea Res., 11, No 5.
29. Walters V. 1961. A contribution to the biology of the Giganturidae, with desceiption of a new genus and species. Bull. Museum Compar. Zool. Harv., 125, No. 10.
30. Wimpenny R. S. 1941. Organic polarity, some ecological and physiological aspects. Quart. Rev. Biol., 16, No. 4.

Поступила в редакцию
24.XII.1966 г.

B. G. BOGOROV, O. K. BORDOVSKY, M. E. VINOGRADOV

BIOGEOCHEMISTRY OF THE OCEANIC PLANKTON. THE DISTRIBUTION OF SOME CHEMICAL COMPONENTS OF THE PLANKTON IN THE INDIAN OCEAN

Summary

The material for the present study has been collected during the 31st cruise (October 1959 — April 1960) of the R/V «Vityaz» in the Indian Ocean. The 0—100 m layer was sampled. The samples were dried without fixing. Calcium carbonate, organic carbon and lipid content determinations were made.

The organic carbon content of the investigated plankton amounts to an average of 29.9% ranging from 24.2 to 35.6% of the dry weight. The lowest carbon content of the plankton is observed in the areas of the intensive upwelling where an essential part of the total seston biomass is composed of phytoplankton (diatoms). Due to little fluctuations in the relative amount of organic carbon in the plankton its absolute amount distribution in the upper 100 m layer generally follows rather closely the distribution pattern of the total plankton biomass.

The lipid fraction content ranges from 6.4 to 13.6% with an average of 9.4% of the dry weight. Plankton is especially rich in lipids in the areas of its maximum concentrations. A high correlation was found between the amount of lipids in the plankton and the depth of the upper boundary of the thermocline. A similarly high correlation exists between the lipid content of the plankton and temperature at a depth of 100 m. The obtained data lead to the conclusion that an increase or decrease in the lipid fraction content of the plankton is closely connected with environmental conditions. The distribution pattern of the lipid absolute amounts follows in a very general form the plankton biomass distribution pattern.

The calcium carbonate content averages 11.7% ranging from 4.8 to 21% of the dry weight. The comparison of the carbonate content of the plankton with the distribution of pteropods and globogerins shows that, apparently, the calcium carbonate content of the tropical plankton is determined, first of all, by the globigerins abundance.

B R E V I O R A

Museum of Comparative Zoology

CAMBRIDGE, MASS. MAY 3, 1966 NUMBER 246

PSEUDANTHESSIUS PROCURRENS N.SP., A CYCLOPOID COPEPOD ASSOCIATED WITH A CIDARID ECHINOID IN MADAGASCAR

BY ARTHUR G. HUMES

Boston University, Boston, Massachusetts

and

Associate in Marine Invertebrates, Museum of Comparative Zoology

INTRODUCTION

During an extensive search in 1963-64 for copepods associated with marine invertebrates at Nosy Bé, in northwestern Madagascar, 109 adults and 9 copepodids of the new lichomolgid copepod described below were recovered from the sediment obtained after washing 30 large pencil urchins, *Phyllacanthus imperialis* (Lamarck), in weakly alcoholized sea water. (The host echinoid is widespread in the Indo-Pacific region, where it occurs, for example, in Australia, the Marshall Islands, the Philippine Islands, Ceylon, the Red Sea, and Zanzibar). This new form brings the total number of species known in the genus *Pseudanthessius* to 24 (including the 22 species listed by Stock, Humes, and Gooding, 1963, and a new species from a polychaete annelid in Madagascar whose description by Humes and Ho is in press).

ACKNOWLEDGMENTS

The copepods were collected by the author while participating in the 1963-64 activities of the U.S. Program in Biology of the International Indian Ocean Expedition.

The study of the specimens has been aided by a grant (GB-1809) from the National Science Foundation of the United States.

I wish to thank Dr. H. Barraclough Fell, Professor of Invertebrate Zoology at the Museum of Comparative Zoology, for the identification of the echinoid host, and to acknowledge the assistance to the field work given by the staff of the Centre d'Océanographie et des Pêches at Nosy Bé.

DESCRIPTION

Family LICHOMOLGIDAE Kossmann, 1877

Genus PSEUDANTHESSIUS Claus, 1889

PSEUDANTHESSIUS PROCURRENS[1] n.sp.

Figures 1-29

Type material. — 16 females, 9 males, and 1 copepodid from washings of 3 pencil urchins, *Phyllacanthus imperialis* (Lamarck), in 1 meter depth among dead coral (*Acropora*) at Pte. Ambarionaomby, Nosy Kómba, near Nosy Bé, Madagascar. Collected November 28, 1963. Holotype female, allotype, and 19 paratypes (13 females and 6 males) deposited in the U. S. National Museum, Washington, and the remaining paratypic adults (dissected) together with the copepodid in the collection of the author.

Other specimens (all from *Phyllacanthus imperialis* collected in 1963 at the type locality). — 2 females from 1 host, July 3; 10 females and 7 males from 3 hosts, July 18; 14 females and 5 males from 6 hosts, August 23; 13 females, 6 males, and 4 copepodids from 7 hosts, October 30; and 16 females, 11 males, and 4 copepodids from 10 hosts, December 14. This last collection is deposited in the Museum of Comparative Zoology.

Female. — The body (Figs. 1 and 2) has a broadened prosome. The length (excluding the setae on the caudal rami) is 0.95 mm (0.90-1.01 mm) and the greatest width is 0.44 mm (0.42-0.46 mm), based on 10 specimens. The ratio of the length to the width of the prosome is 1.28:1. The segment bearing leg 1 is almost completely fused with the head, the only indication of separation being a short weak crease on each side. The lateral areas of the metasomal segments are rounded.

The segment of leg 5 (Fig. 3) is expanded laterally, being 50 μ in length and 133 μ in width. Between the segment of leg 5 and the genital segment there is a ventral intersegmental sclerite (see Fig. 2). The genital segment (Fig. 3) is 127 μ long. Anteriorly its lateral margins form 2 rounded, strongly sclerotized lobes (the width of the segment at this level being 115 μ). The width at the level of the dorsolateral areas of attachment of the egg sacs is 107 μ. Behind each attachment area the segment is slightly

[1] The specific name *procurrens*, from Latin *procurrere*, meaning to bulge out or project, alludes to the outer expansion on the coxa of leg 1 and to the 2 rounded lobes on the anterior part of the genital segment in the female.

constricted with nearly parallel margins (the width in this region being 86 μ). Each egg sac attachment area (Fig. 4) bears anteriorly a slender, slightly haired seta (21 μ long) and just posterior to it a short naked seta (6.5 μ long) composed of an expanded sclerotized basal portion and a slender hyaline distal part. Medial to the latter seta there are 2 small spinelike processes. The three postgenital segments are 44 x 81, 39 x 75, and 65 x 72 μ from anterior to posterior. The anal segment bears on each side on its distal margin a dorsal and ventral row of spinules.

The caudal ramus (Fig. 5) is elongated, with a terminal ventral expansion whose margin bears a row of spinules. The length along the inner side of the ramus to the end of the expansion is 114 μ, along the outer side 104 μ, and the width at the level of the outer seta is 24 μ. The ratio of length to width is about 4.5:1. The outer seta, inserted 70 μ from the base of the ramus, is naked and 56 μ in length. The pedicellate dorsal seta is 33 μ and slightly haired. The outermost terminal seta (100 μ) and the innermost terminal seta (72 μ) are haired. The 2 long median terminal setae are 177 and 250 μ in length respectively and haired. A minute lateral setule is borne on the outer basal margin of the ramus. The dorsal and ventral surfaces of the ramus bear a few refractile points.

The dorsal surface of the prosome and the dorsal and ventral surfaces of the urosome bear minute setules and refractile points. In addition, the outer ventral areas of the head carry a submarginal row of refractile points (Fig. 6). The ratio of the length of the prosome to that of the urosome is 1.53:1.

The egg sacs (Fig. 1) are moderately elongated, often rather pointed posteriorly, and contain numerous eggs. In one female the egg sacs measured 385 x 220 μ, with each egg about 57-60 μ in diameter.

The rostral area (Fig. 7) is moderately well developed. Between this area and the front of the labral region there is a slight protrusion on the ventral surface of the head.

The first antenna (Fig. 8) is 7-segmented, with the lengths of the segments (measured along their posterior non-setiferous margins) 24 (39 μ along the anterior margin), 103, 21, 39, 33, 20, and 17 μ respectively. The formula for the armature is 4, 13, 6, 3, 4 + 1 aesthete, 2 + 1 aesthete, and 7 + 1 aesthete. All the setae are naked.

The second antenna (Fig. 9) is 4-segmented, with the last segment elongated (69 μ along the shorter ventral margin, 93 μ along

the dorsal margin, and 19 μ in width). Each of the first two segments bears a small ventral seta, the third segment bears 4 slender setae (one of them very small), and the last segment bears 2 unequal slender recurved claws (47 and 25 μ respectively along their axes) and 5 setae, one of them very long (99 μ). The extremity of the last segment is swollen, so that the 2 claws insert at one side rather than directly on the tip of the segment. All the setae are naked.

The labrum (Fig. 10) consists of 2 diverging, pointed lobes with their medial edges straight and finely dentate, both arising from a large, conspicuous, sclerotized area which projects (Fig. 2) from the ventral surface of the head. On the posterior wall of the labrum, in front of the mouth area, there is a pair of small sclerotized lobes. The surface of the labrum lacks fine ornamentation.

The mandible (Fig. 11) has on the concave side of the blade an oblique row of spinules followed distally by a spinelike process lying parallel to the blade and evidently not articulated with it. The convex side of the blade bears a fringe of graduated spiniliform structures without definite articulations. The paragnath (Fig. 12), lying medial to the base of the first maxilla (as in Fig. 16), is a rounded lobe bearing a small sclerotized outer process, a small postero-inner knob, and a posterior group of hairs. The first maxilla (Fig. 13) is a single segment bearing 4 naked elements, comprising terminally 2 obtuse subequal spines (10 and 8 μ long) and a shorter pointed spine (5 μ) and subterminally a naked hyaline seta (11 μ). The second maxilla (Fig. 14) is 2-segmented. The first segment is unarmed but has a small sclerotized protuberance on its expanded margin. The second segment is produced to form a long bilaterally spinulose lash; the dorsal surface bears a proximal seta 29 μ in length (bearing lateral spinules along one edge) and a distal row of 3-5 spinules. The maxilliped (Fig. 15) is 3-segmented. There are 2 naked setae on the second segment. The terminal segment bears proximally a spine with unilateral spinules, a hyaline naked setule, and near the base of the latter a minute setule; the segment is produced to form an attenuated spinelike structure with a row of long spinules along one side and a row of minute spinules near the opposite margin.

The postoral area (Fig. 16) shows between the paragnaths a shield-shaped area which projects ventrally to form a low median process. Posterior to the sclerotization which almost joins the

bases of the maxillipeds, the ventral surface of the cephalosome protrudes slightly (best seen in a lateral view, as in Fig. 2).

Legs 1-4 (Figs. 17, 18, 19, and 20) have trimerous rami except for the endopod of leg 4 which is unimerous. The armature of the legs is as follows (the Roman numerals indicating spines, the Arabic numerals setae):

P 1	protopod	0-1;	1-0	exp	I-0;	I-1;	III,I,4
				end	0-1;	0-1;	I,2,3
P 2	protopod	0-1;	1-0	exp	I-0;	I-1;	III,I,5
				end	0-1;	0-2;	I,II,3
P 3	protopod	0-1;	1-0	exp	I-0;	I-1;	III,I,5
				end	0-1;	0-2;	I,II,2
P 4	protopod	0-1;	1-0	exp	I-0;	I-1;	II,I,5
				end	II		

The inner seta on the coxa of legs 1-3 is long and plumose, but in leg 4 this seta is minute (7 μ long) and naked. In the first 3 legs the inner margin of the basis bears a short row of hairs, but in leg 4 these hairs are lacking. The outer coxal margin of leg 1 is expanded to form a prominent lobe (Fig. 17); in legs 2 and 3 this expansion is much less prominent and in leg 4 it is apparently absent. The tips of the outer spines on the exopods are slightly recurved posteriorly and the more proximal ones have minute terminal flagella. The 3 spines on the last segment of the endopod of leg 2 are 14, 10, and 13 μ in length from proximal to distal, with the middle one having a short terminal flagellum. In leg 4 the exopod is longer than in any of the preceding legs. The endopod measures 53 x 16 μ and has nearly parallel margins without a constriction or notch. It bears a row of hairs on its outer proximal third and an anterior row of small spinules near the insertions of the 2 divergent terminal spines (the outer 18 μ long with a minute flagellum, the inner 37 μ long with a more strongly spinulose flange along the outer side than along the inner side).

Leg 5 (Fig. 21) consists of a strong spine (33 μ long) and an adjacent seta (21 μ), together with a dorsal seta (22 μ), ornamented as in the figure. External to the spine and seta there is a row of minute blunt spinules at the apex of the segment. Although, as in other species of *Pseudanthessius,* there is no free segment of leg 5, it is likely that the spine and its adjacent seta correspond to the terminal armature in other lichomolgids.

Leg 6 is probably represented by the 2 setae near the attachment of each egg sac (see Fig. 4).

The color in life in transmitted light is translucid, the eye red, the intestine black, the ovary gray, the egg sacs opaque gray. (Although in specimens preserved in 70 per cent ethyl alcohol the color is an opaque grayish brown, the color changes quickly to a bright red when the copepods are placed in lactic acid.)

Male. — The body (Figs. 22 and 23) has a much narrower prosome than in the female, but otherwise resembles that sex in general form. The length (not including the setae on the caudal rami) is 0.76 mm (0.73-0.78 mm) and the greatest width is 0.27 mm (0.25-0.28 mm), based on 10 specimens (including the allotype, 8 paratypes, and 1 specimen from Pte. Ambarionaomby on October 30). The ratio of length to width of the prosome is 1.57:1.

The segment of leg 5 is similar to that of the female, and measures 31 x 94 μ. The genital segment (Fig. 24) is nearly as long as wide, 104 x 110 μ, and in dorsal view has a subspherical outline. In lateral view (Fig. 25) the anteroventral part of the segment projects noticeably. There is no intersegmental selerite between the segment of leg 5 and the genital segment. The 4 postgenital segments are 39 x 52, 32 x 51, 30 x 50, and 43 x 53 μ from anterior to posterior.

The caudal ramus resembles that of the female, but is a little shorter, the inner length being 78 μ, the outer length 73 μ, the width 23 μ, and the ratio of length to width 3.26:1.

The surfaces of the prosome and urosome bear minute setules as in the female. The ratio of the length of the prosome to that of the urosome is 1.31:1.

The rostral area, first antenna, second antenna, labrum, mandible, paragnath, and first maxilla are like those in the female. The second maxilla also resembles that of the female, but lacks the small sclerotized protuberance on the expanded margin of the basal segment. The maxilliped (Fig. 26) is much elongated, slender, and 4-segmented (assuming that the fourth segment is represented by the proximal part of the claw). Its entire length including the claw is about 300 μ. The first segment is unarmed. The second bears 2 unequal inner setae and 2 rows of hairs, one along the inner margin distal to the setae and another starting on the proximal inner margin and passing obliquely to the distal posterior surface of the segment. The very short third segment is unarmed. The terminal recurved claw, 135 μ in length along its axis, bears a conspicuous terminal lamella. The slightly crenated fringe along its concave margin is interrupted about midway. Near the base of the claw on its posterior surface there is a seta

42 μ long with minute lateral spinules, and on its anterior surface there are 2 small naked setules, one 10 μ, the other 4 μ long.

The postoral area is like that of the female.

Legs 1-4 resemble those of the female except that the last segment of the endopod of leg 1 is more elongated (Fig. 27), and the terminal segment of the endopod of leg 2 is more elongated, and its 3 spines are longer (24, 22, and 25 μ from proximal to distal), as seen in Figure 28.

Leg 5 is similar to that of the female.

Leg 6 (Fig. 29) consists of a posteroventral flap on the genital segment. Beyond the rim of the segment the leg projects conspicuously (see Fig. 24) as a large, pointed, ventral sclerotized process dorsal to which there is a shorter rounded process bearing 2 naked setae 22 and 24 μ in length.

The spermatophore, seen only inside the body of the male (Fig. 24), is oval, about 72 x 45 μ, with a short neck.

The color in life in transmitted light resembles that of the female.

RELATIONSHIP TO OTHER SPECIES IN THE GENUS

Twelve species of *Pseudanthessius* may be readily distinguished from *P. procurrens* in that they lack the prominent outer expansion on the coxa of leg 1 and do not bear the two rounded sclerotized lobes on the anterior part of the genital segment in the female. These species are: *P. aestheticus* Stock, Humes, and Gooding, 1963, *P. concinnus* Thompson and A. Scott, 1903, *P. deficiens* Stock, Humes, and Gooding, 1963, *P. dubius* G. O. Sars, 1918, *P. graciloides* Sewell, 1949, *P. luculentus* Humes and Cressey, 1961, *P. mucronatus* Gurney, 1927, *P. nemertophilus* Gallien, 1935, *P. notabilis* Humes and Cressey, 1961, *P. pectinifer* Stock, Humes, and Gooding, 1963, *P. tortuosus* Stock, Humes, and Gooding, 1963, and a new species (Humes and Ho, in press) from a polychaete annelid in Madagascar.

Eight other species may be separated from *P. procurrens* in that they lack the two lobes on the anterior part of the genital segment in the female and have a different armature on the last segment of the second antenna. (Unfortunately, in the original descriptions of these species, definite information on the condition of the outer coxal margin of leg 1 was not given.) These species are: *P. gracilis* Claus, 1889, *P. latus* Illg, 1950, *P. obscurus* A. Scott, 1909, *P. sauvagei* Canu, 1892, *P. spinifer* Lindberg 1945, *P. tenuis* Nicholls, 1944, *P. thorelli* (Brady, 1880), and *P. weberi* A. Scott, 1909.

Three species remain to be compared with *P. procurrens*: *P. liber* sensu Sewell, 1949, *P. liber* (Brady, 1880), and *P. assimilis* G. O. Sars, 1917. The species referred to as *P. liber* (Brady and Robertson) by Sewell (1949) is probably a new and unnamed species of the genus (see Humes and Cressey, 1961, pp. 80-81). It differs from *P. procurrens* chiefly in the presence of two long elements (aesthetes ?) on the basal segment of the first antenna, in the inwardly curving terminal spine on the last segment of the exopod of legs 2-4, and in the notch on the outer margin of the endopod of leg 4. No information was given for this form regarding the nature of the genital segment in the female, and the condition of the outer coxal margin of leg 1 is not clearly shown in Sewell's text figure 32 D.

P. liber (Brady, 1880)[2] lacks the two lobes on the anterior part of the genital segment of the female, has a caudal ramus about twice as long as wide, and has a different armature on the last segment of the second antenna. Brady did not mention an outer coxal expansion on leg 1, but Sars (1917) both mentioned and figured such an expansion in specimens taken in Norway. The expansion illustrated on Sars' plate XCIV is, however, less pronounced than in *P. procurrens.* The armature for the last segment of the endopod of leg 3 in the female is, according to Sars, I,II,3, instead of I,II,2 as in the Madagascan species.

P. assimilis G. O. Sars, 1917, is said by Sars to be closely allied to *P. liber* (Brady, 1880). Like the latter species it lacks the two lobes on the genital segment of the female and has an armature on the last segment of the second antenna unlike that of *P. procurrens.* Sars stated that the legs are "almost exactly as in *P. liber,*" implying that there is a similar outer coxal expansion on leg 1.

Judging from the available information, *P. procurrens* appears to be near both *P. liber* (Brady, 1880) and *P. assimilis* G. O. Sars, 1917, resembling them in having an outer coxal expansion on leg 1, but differing in having two lobes on the anterior part of the genital segment in the female and in having a different armature on the last segment of the second antenna.

SUMMARY

The new species *Pseudanthessius procurrens* is associated with the cidarid echinoid *Phyllacanthus imperialis* (Lamarck) in the

[2] Not Brady and Robertson, 1876. See Stock, Humes, and Gooding, 1963, p. 10, footnote.

region of Nosy Bé, northwestern Madagascar. Within the genus the copepod may be recognized by the conspicuous expansion on the outer coxal area of leg 1 and by the two rounded lateral lobes on the anterior part of the genital segment in the female. The species nearest to the new form appear to be *P. liber* (Brady, 1880) and *P. assimilis* G. O. Sars, 1917. Although the host echinoderm is widely distributed in the Indo-Pacific area, the new copepod associated with it is known at present only from the type locality in Madagascar.

REFERENCES CITED

BRADY, G. S.

1880. A monograph of the free and semi-parasitic Copepoda of the British Islands. Ray Society, London, **3**:1-83.

BRADY, G. S. AND D. ROBERTSON

1876. Report on dredging off the coast of Durham and North Yorkshire in 1874. Rept. British Ass. Adv. Sci. (Bristol), **45**: 185-199.

CANU, E.

1892. Les Copépodes du Boulonnais, morphologie, embryologie, taxonomie. Trav. Lab. Zool. mar. Wimereux-Ambleteuse (Pas-de-Calais), **6**:1-354.

CLAUS, C.

1889. Über neue oder wenig bekannte halbparasitische Copepoden, insbesondere der Lichomolgiden- und Ascomyzontiden-Gruppe. Arb. Zool. Inst. Univ. Wien, **8**(3):327-370.

GALLIEN, L.

1935. *Pseudanthessius nemertophilus* nov. sp., copépode commensal de *Lineus longissimus* Sowerby. Bull. Soc. Zool. France, **60**:451-459.

GURNEY, R.

1927. Zoological results of the Cambridge expedition to the Suez Canal, 1924, XXXIII. Report on the Crustacea: — Copepoda (littoral and semi-parasitic). Trans. Zool. Soc. London, **22**(4):451-477.

HUMES, A. G. AND R. F. CRESSEY

1961. Deux nouvelles espèces de *Pseudanthessius* (Copepoda, Cyclopoida) parasites des oursins à Madagascar. Mém. Inst. Sci. Madagascar, sér. F, 1959, **3**:67-82.

HUMES, A. G. AND J.-S. HO

In press. New cyclopoid copepods associated with polychaete annelids in Madagascar. Bull. Mus. Comp. Zool.

ILLG, P.

1950. A new copepod, *Pseudanthessius latus* (Cyclopoida:Lichomolgidae) commensal with a marine flatworm. Jour. Washington Acad. Sci., **40**(4):129-133.

LINDBERG, K.
1945. Un nouveau copépode poecilostome de l'Inde de la famille des Lichomolgidae; *Pseudanthessius spinifer*, n. sp. Bull. Soc. Zool. France, **70**:81-84.

NICHOLLS, A. G.
1944. Littoral copepods from South Australia (II). Calanoida, Cyclopoida, Notodelphyoida, Monstrilloida and Caligoida. Rec. So. Austr. Mus., **8**(1):1-62.

SARS, G. O.
1917. An account of the Crustacea of Norway with short descriptions and figures of all the species. Vol. 6, Copepoda, Cyclopoida, pts. 11 and 12, Clausidiidae, Lichomolgidae (part), pp. 141-172. Bergen Museum, Bergen.
1918. An account of the Crustacea of Norway with short descriptions and figures of all the species. Vol. 6, Copepoda, Cyclopoida, pts. 13 and 14, Lichomolgidae (concluded), Oncaeidae, Corycaeidae, Ergasilidae, Clausiidae, Eunicicolidae, Supplement, pp. 173-225. Bergen Museum, Bergen.

SCOTT, A.
1909. The Copepoda of the Siboga Expedition. Part I. Free-swimming, littoral and semi-parasitic Copepoda. Siboga Exped., **29a**:1-323.

SEWELL, R. B. S.
1949. The littoral and semi-parasitic Cyclopoida, the Monstrilloida and Notodelphyoida. John Murray Exped. 1933-34, Sci. Repts., **9**(2):17-199.

STOCK, J. H., A. G. HUMES, AND R. U. GOODING
1963. Copepoda associated with West Indian invertebrates IV. The genera *Octopicola, Pseudanthessius* and *Meomicola* (Cyclopoida, Lichomolgidae). Studies Fauna Curaçao and other Caribbean Is., **18**(77):1-74.

THOMPSON, I. C. AND A. SCOTT
1903. Report on the Copepoda collected by Professor Herdman at Ceylon in 1902. Rept. Govt. Ceylon Pearl Oyster Fish. Gulf of Manaar, pt. I, Suppl. Rept. No. 7:227-307.

(Received December 10, 1965.)

EXPLANATION OF THE FIGURES

All the figures have been drawn with the aid of a camera lucida. The letter after the explanation of each figure refers to the scale at which the figure was drawn.

Abbreviations: a_1 = first antenna, md = mandible, p = paragnath, mx_1 = first maxilla, mx_2 = second maxilla, mxpd = maxilliped, p_1 = leg 1.

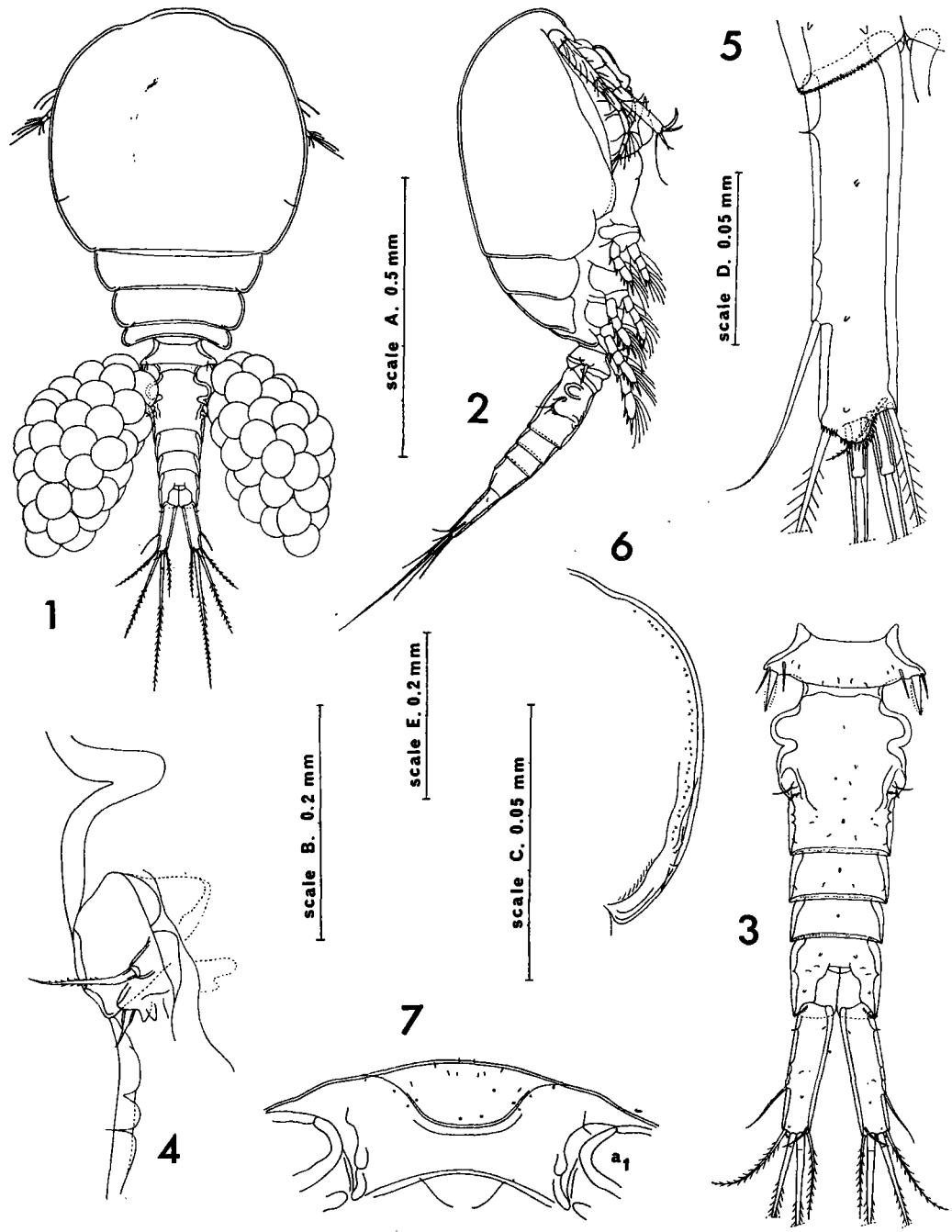

FIGURES 1-7. *Pseudanthessius procurrens* n.sp., female. 1, dorsal (A); 2, lateral (A); 3, urosome, dorsal (B); 4, area of attachment of egg sac, dorsal (C); 5, caudal ramus, ventral (D); 6, edge of cephalosome, ventral (E); 7, rostral area, ventral (F).

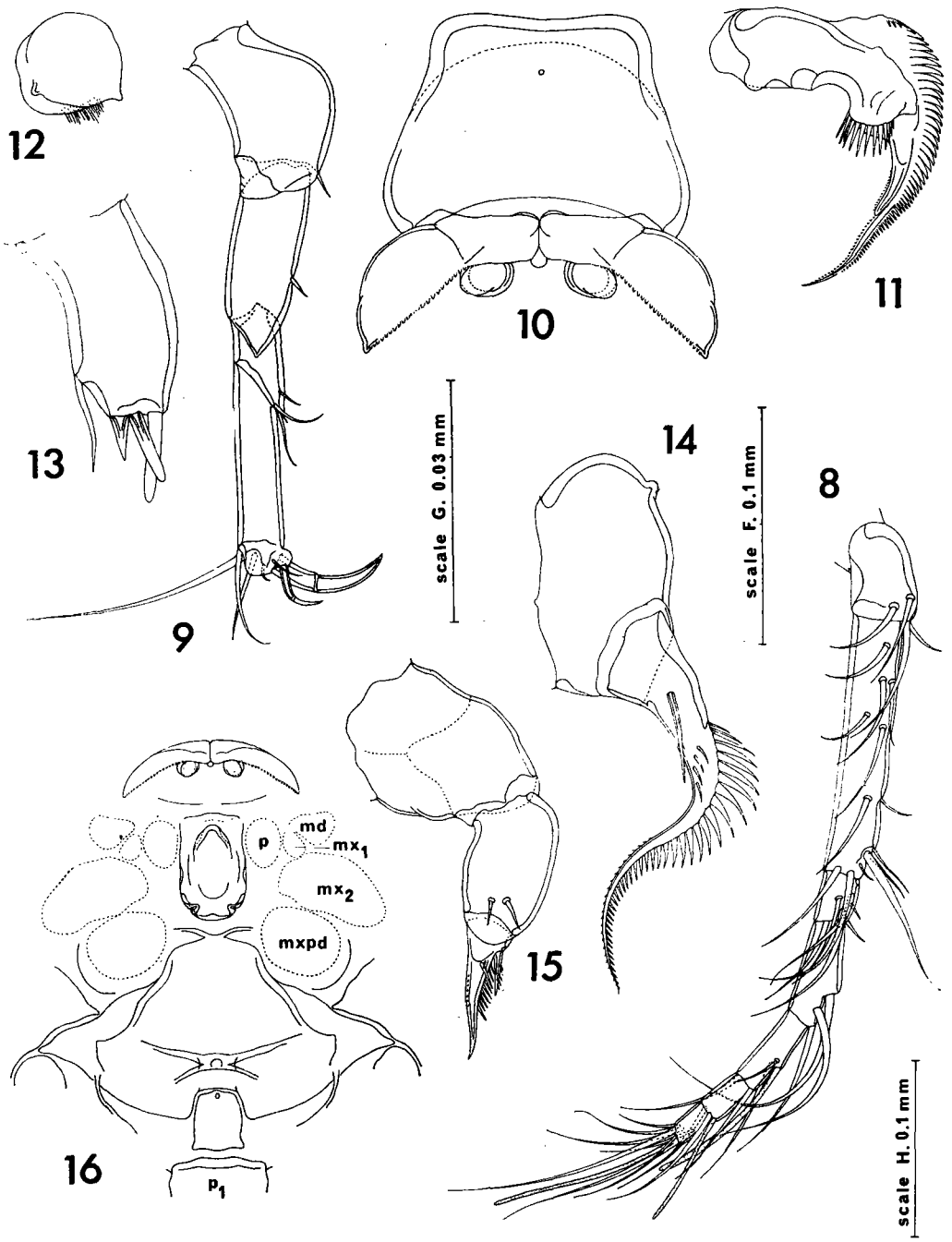

FIGURES 8-16. *Pseudanthessius procurrens* n.sp., female (continued). 8, first antenna, anterodorsal (F); 9, second antenna, inner (F); 10, labrum, ventral (D); 11, mandible, inner (D); 12, paragnath, ventral (D); 13, first maxilla, outer (G); 14, second maxilla, dorsal (D); 15, maxilliped, inner (D); 16, postoral area, ventral (H).

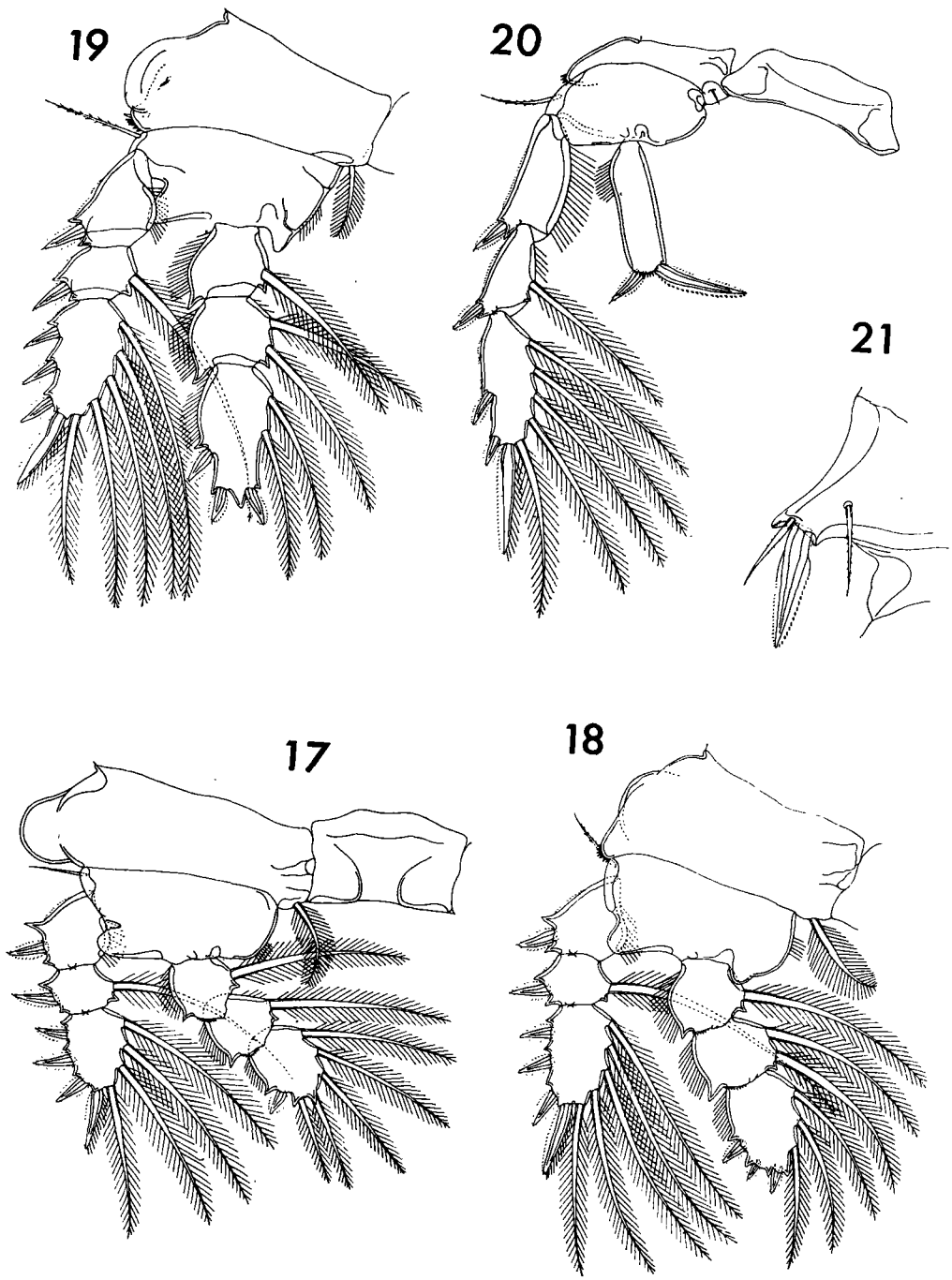

FIGURES 17-21. *Pseudanthessius procurrens* n.sp., female (continued). 17, leg 1, anterior (F); 18, leg 2, anterior (F); 19, leg 3, posterior (F); 20, leg 4, anterior (F); 21, leg 5, dorsal (D).

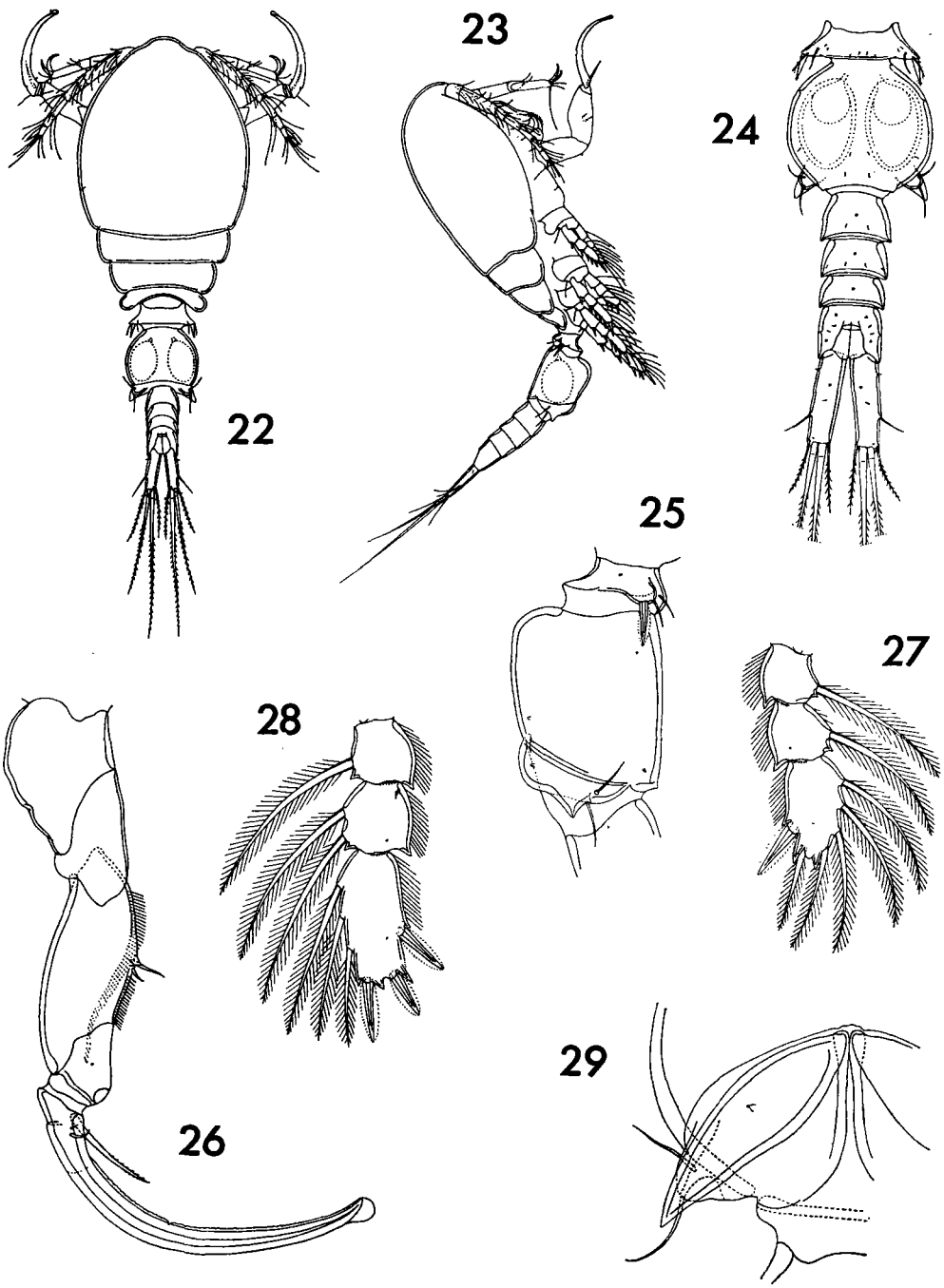

FIGURES 22-29. *Pseudanthessius procurrens* n.sp., male. 22, dorsal (A); 23, lateral (A); 24, urosome, dorsal (B); 25, genital segment, lateral (H); 26, maxilliped, anterior (F); 27, endopod of leg 1, anterior (F); 28, endopod of leg 2, anterior (F); 29, leg 6, ventral (D).

Part II Marine chemistry

Reprinted from *Aust. J. mar. freshw. Res.*, vol. 16, 1965, p. 273-280.

THE MEASUREMENT OF TOTAL CARBON DIOXIDE IN DILUTE TROPICAL WATERS

By D. V. SUBBA RAO*

[*Manuscript received November* 16, 1964]

Summary

A shipboard conductivity technique to measure the total carbon dioxide in dilute tropical water is described. The standard error of a single determination in the range 40–100 mg CO_2/l is 6·0 mg/l. There were 41–102 mg CO_2/l in waters of the Gulf of Thailand. In these waters, primary production determined with the usually assumed value of 90 mg CO_2/l gave errors ranging from 11 to 120% for the individual depth samples and from 6 to 92% for column values as compared to the values obtained using the measured CO_2 concentration.

I. INTRODUCTION

The concentration of total CO_2 in oceanic water has been found to vary between 85 and 103 mg/l (Clarke 1954; Rotschi, Angot, and Legand 1959). Based on the constancy of CO_2/pH and CO_2/salinity (‰) relationships, Buch (1951) presented tables to determine the total CO_2 in seawater. In studies on oceanic primary production employing the radiocarbon method it is sufficient to assume a value of 90 mg CO_2/l. However, in dilute tropical waters such as those in the present study, owing probably to $CaCO_3$ precipitation, the CO_2/pH and CO_2/salinity (‰) relationships do not remain constant, and the total CO_2 cannot be interpolated from Buch's tables. Therefore there is need for a suitable shipboard method for the direct determination of total CO_2 in dilute tropical waters.

In the present study a modified conductivity method based essentially on the method given by Milburn and Beadle (1960) is employed. The CO_2 is removed by acidification of the sample and absorbed by a standard volume of NaOH, whose change in conductance is measured. This method was used in conjunction with studies on primary production in the Gulf of Thailand.

II. METHODS

The apparatus (Fig. 1) is made from Pyrex glass and is mounted against a plywood board. The details of the temperature-compensated conductivity bridge are given by Dal Pont and Newell (1963).

Before each series of measurements the apparatus is flushed for 30 min with CO_2-free air without introducing samples or NaOH. By this procedure the blank is reduced to 0·5 mg CO_2/l.

* Division of Fisheries and Oceanography, CSIRO, Cronulla, N.S.W. (Reprint No. 568.)

Samples of 20 ml of seawater are pipetted into tube (1) and the tube connected to the apparatus by a ground-glass joint; 40 ml of 0·005 N NaOH solution are drawn from a tower (5) into absorption unit (6). With suction at (2), air is drawn through a soda lime tower (3) and a flowmeter (4), at a rate of 900 ml/min. Tap T_1 is then opened and 2·5 ml of concentrated H_3PO_4 (7) are added to the sample. After 15 min a further 2·5 ml of acid are added. This double addition of acid gave slightly higher results than a single addition of 5 ml. The CO_2 thus liberated is sucked through the diffuser into the absorption unit containing NaOH solution. The aeration and absorb-

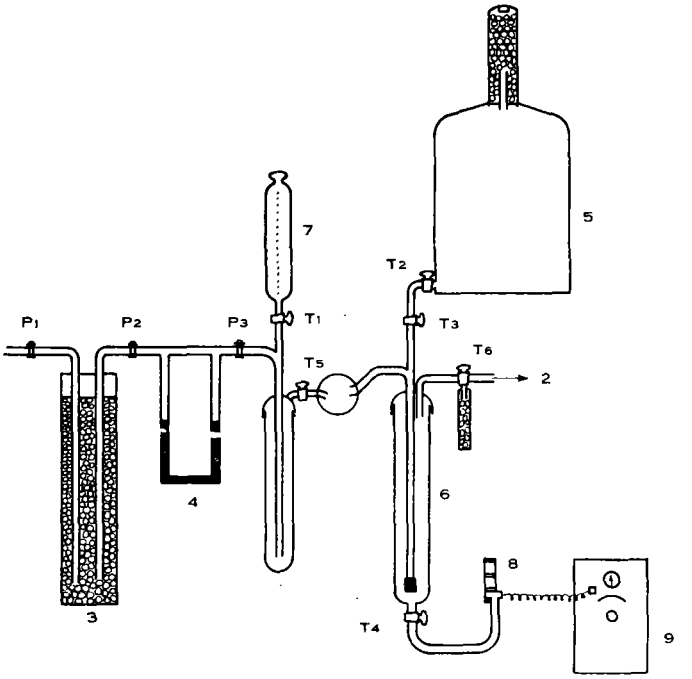

Fig. 1.—The CO_2 apparatus. Key: (1) CO_2 liberation unit; (2) suction; (3) soda-lime tower; (4) flowmeter; (5) NaOH tower with a CO_2 guard; (6) CO_2 absorption unit; (7) orthophosphoric acid tower; (8) conductometric cell; (9) conductivity bridge; P_1, P_2, P_3, screw clamps; T_1, T_2, T_3, T_4, T_5, two-way taps; T_6, three-way tap with a CO_2 guard.

tion are continued for 25 min, after which the solution is passed into the conductometric cell (8). The bridge reading of the solution is taken and the initial reading of the 0·005N NaOH solution subtracted.

After every estimation, tap T_6 is opened to admit CO_2-free air to the apparatus and the absorption unit is drained, flushed with fresh 0·005N NaOH, and drained again. After closing tap T_5, tube (1) is disconnected and the stem of the acid tower washed in a jet of distilled water. Tube (1) is rinsed with CO_2-free distilled water before admitting a subsequent seawater sample for analysis.

For calibration, 20-ml of standard Na_2CO_3 solutions containing 37·5–250 mg CO_2/l were used. Such calibration showed a linear relation between dial readings and CO_2 present (Fig. 2). A change of 2·04 divisions on the dial was equivalent to

1 mg CO_2/l in the standard or sample. In each series of measurements a standard solution was included. The standard error of a single determination in the range 40–100 mg CO_2/l was 6·0 mg/l.

During cruise Dm 3/64 of H.M.A.S. *Diamantina* in May 1964, water samples were taken at eight stations in the Gulf of Thailand. Samples were transferred from the plastic samplers to glass bottles, and the total CO_2 content determined immediately. The surface sample was analysed first and the other samples in order of increasing depth. Analyses for salinity, dissolved oxygen, and inorganic phosphate were carried out as reported in CSIRO Aust. (1963). Primary production was measured by the radiocarbon technique described by Dyson, Jitts, and Scott (1965), using 300-ml Pyrex bottles and incubation under constant artificial light of about 1100 f.c. for 4 hr.

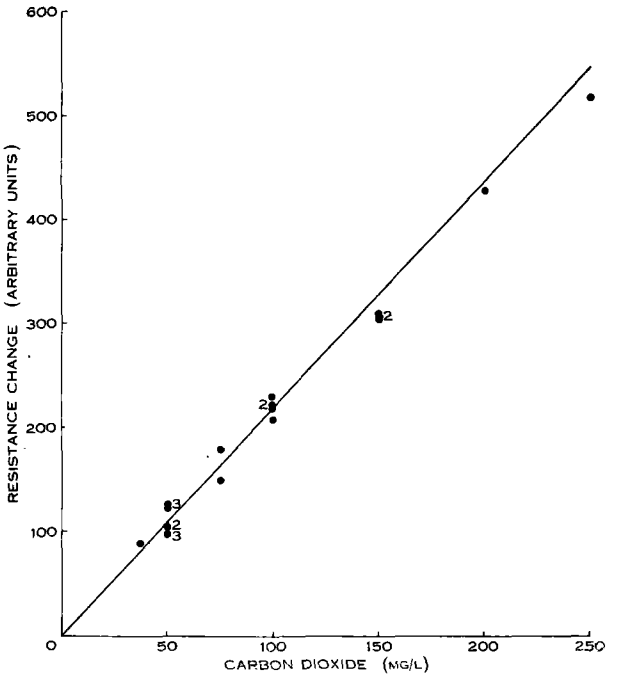

Fig. 2.—Relation between the change in resistance and CO_2 concentration. The numbers indicate superimposed identical values.

III. Results

Table 1 summarizes the hydrological data and the total CO_2 concentration at the stations in the Gulf of Thailand. The CO_2 content varied from 41 to 102 mg/l; only on two occasions was it more than 81 mg/l. In general, the CO_2 content was higher in the subsurface waters (41–102 mg/l) than at the surface (44–74 mg/l). At stations 140–144 the CO_2 concentration ranged from 41 to 68 mg/l (mean 55 mg/l). At stations 137–139 the CO_2 content was higher and ranged from 58 to 102 mg/l (mean 73 mg/l). There were no major differences in the hydrological characteristics (Table 1) between these two groups of stations.

TABLE 1

HYDROLOGICAL CONDITIONS IN THE GULF OF THAILAND

Date	Station No.	Longitude (E.)	Latitude (N.)	Sonic Depth (m)	Sample Depth (m)	Temperature (°C)	Salinity (‰)	Oxygen (ml/l)	Inorganic PO_4 (μg atom/l)	Total CO_2 (mg/l)
21.v.64	137	104°27·7′	1°34·6′	24	0	28·78	32·660	4·28	0·24	74
					5	29·70	32·672	4·23	0·24	81
					10	29·40	32·926	4·16	0·23	101
					15	29·18	33·188	4·08	0·20	72
					20	29·05	33·188	4·03	0·40	102
22.v.64	138	103°50′	4°15′	57	0	29·95	31·887	4·46	0·07	66
					10	31·13	32·616	4·44	0·07	62
					20	29·64	33·689	4·54	0·05	64
					30	28·04	33·767	4·33	0·13	76
					40	27·88	33·791	4·23	0·15	76
					50	—	—	—	—	61
22.v.64	139	103°34′	5°15·2′	57	0	29·80	32·396	4·37	0·01	58
					10	30·20	32·958	4·47	0	65
					20	29·91	33·452	4·46	0	80
					30	28·16	33·702	4·26	0·07	76
					40	27·57	33·776	4·31	0·08	76
					50	—	—	—	—	58
26.v.64	140	100°36′	13°15′	17	0	30·47	30·683	4·53	0·06	58
					5	30·43	30·660	4·55	0·07	51
					10	30·40	31·066	4·31	0·07	63
27.v.64	141	100°33′	10°14′	57	0	29·38	32·151	4·43	0·02	51
					10	29·32	32·154	4·44	0	46
					20	29·31	32·154	4·41	0	57
					30	29·27	32·162	4·42	0	46
					40	29·24	32·210	4·16	0·04	64
					50	29·90	32·284	4·32	0·17	61
27.v.64	142	100°28′	9°08′	31	0	29·59	32·103	4·38	0·05	44
					5	29·59	32·105	4·39	0·04	49
					10	29·58	32·105	4·41	0·02	43
					15	29·54	32·099	4·41	0·05	43
					20	29·53	32·130	4·33	0·05	41
					25	29·63	32·220	4·26	0·13	66
28.v.64	143	103°05′	5°02′	48	0	28·80	33·278	4·43	0·10	49
					10	27·78	33·729	4·46	0·09	51
					20	27·66	33·781	4·46	0·12	53
					30	27·60	33·785	4·46	0·07	57
					40	27·62	33·780	4·41	0·11	65
28.v.64	144	103°28·8′	4°51·2′	31	0	28·33	33·507	4·34	0·11	49
					5	28·28	33·509	4·31	0·11	56
					10	28·17	33·595	4·31	0·12	66
					15	27·63	33·708	4·26	0·11	68
					20	27·05	33·818	3·89	0·16	68
					25	26·87	33·845	3·65	0·23	61

TABLE 2

CO_2 CONCENTRATION AND PRIMARY PRODUCTION

Primary production was calculated using measured (*A*) and assumed (90 mg/l) CO_2 concentrations (*B*).

Station No.	Sample Depth (m)	Total CO_2 (mg/l)	Primary Production (mg C/hr/m³)		Error $[100(B-A)/A]$	Primary Production (g C/day/m²)		Error $[100(B-A)/A]$
			A	*B*		*A*	*B*	
137	0	74	5·44	6·62	22	0·78	0·83	6
	5	81	3·98	4·42	11			
	10	101	5·30	4·73	11			
	15	72	2·56	3·20	25			
	20	102	2·11	1·86	12			
138	0	66	0·59	0·80	36	0·45	0·63	40
	10	62	0·75	1·09	45			
	20	64	0·56	0·78	39			
	30	76	1·25	1·48	18			
	40	76	1·36	1·61	18			
	50	61	0·54	0·80	48			
139	0	58	0·63	0·97	54	0·58	0·53	9
	10	65	0·66	0·92	39			
	20	80	0·62	0·70	13			
	30	76	1·29	1·52	18			
	40	76	1·07	1·26	18			
	50	58	0·59	0·91	54			
140	0	58	4·14	6·42	55	0·44	0·73	66
	5	51	5·40	9·53	76			
	10	63	2·52	3·60	43			
141	0	51	1·11	1·97	77	0·65	1·12	72
	10	46	1·18	2·32	97			
	20	57	1·85	2·92	58			
	30	46	1·44	2·81	95			
	40	64	1·21	1·70	40			
	50	61	0·60	0·89	48			
142	0	44	1·70	3·48	105	0·52	1·00	92
	5	49	2·14	3·93	84			
	10	43	1·88	3·94	110			
	15	43	1·91	3·99	109			
	20	41	1·49	3·28	120			
	25	66	4·29	5·85	36			
143	0	49	0·82	1·51	84	0·48	0·84	75
	10	51	1·00	1·77	77			
	20	53	1·23	2·09	70			
	30	57	1·50	2·37	58			
	40	65	1·27	1·76	39			
144	0	49	3·00	5·51	84	0·84	1·20	43
	5	56	2·97	4·77	61			
	10	66	3·72	5·07	36			
	15	68	5·43	7·18	32			
	20	68	2·60	3·44	32			
	25	61	1·05	1·55	48			

The primary production calculated from the measured CO_2 ranged from 0·59 to 5·44 mg C/hr/m³ for the surface samples (Table 2). Higher values were observed at the shallow water stations 137, 140, 142, and 144 (mean 3·18 mg C/hr/m³) compared to those for deeper stations (mean 1·01 mg C/hr/m³). The column values were from 0·44 to 0·84 g C/day/m² (mean 0·65 g C/day/m²) for the shallow stations and from 0·45 to 0·65 g C/day/m² (mean 0·54 g C/day/m²) for the deeper stations.

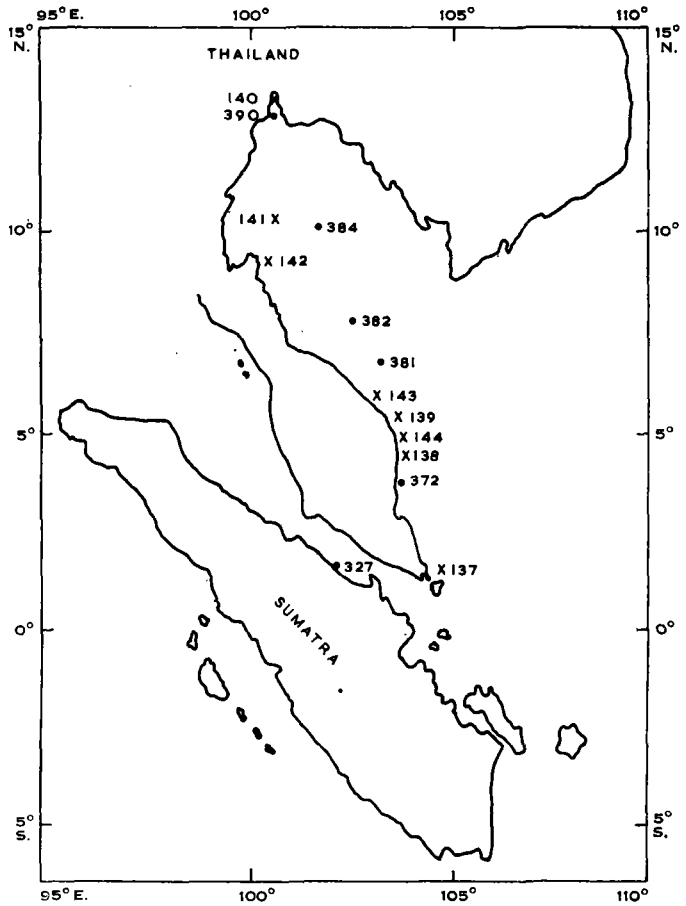

Fig. 3.—Positions of *Galathea* (●) and the *Diamantina* (X) stations.

When the concentration of CO_2 was assumed to be 90 mg/l the primary production ranged from 0·80 to 6·62 mg C/hr/m³ at the surface with column values of 0·53–1·20 g C/day/m². Table 2 shows that the error caused by assuming a value of 90 mg CO_2/l ranged from 11 to 120% for the individual depth samples and from 6 to 92% for column values.

IV. Discussion

The range of concentration of total CO_2 in the Gulf of Thailand (41–102 mg/l) is lower than that found in oceanic waters. Also it is lower than the 88–93 mg/l

reported for the Tortugas (Wells 1922) and the 70–140 mg/l reported for the Texan bays (Park, Hood, and Odum 1958) but comparable to the range (10·69–91·7 mg CO_2/l) reported for the coastal waters of Japan by Matsudaira (1964). It is possible that precipitation of $CaCO_3$ is responsible for the low total CO_2 content found in the Gulf of Thailand. Such precipitation has been described already from several shallow seas, notably around Japan (Miyake 1958) and on the Bahama Bank (Smith 1940, 1941).

TABLE 3

COMPARISON OF PRIMARY PRODUCTION

Values are in g C/day/m³; the results for stations at similar positions are on the same line

Diamantina			*Galathea*		
Station No.	Assuming 90mg CO_2/l	Using Measured mg CO_2/l	Station No.	Original	Recalculated
137	0·83	0·78	—		
138	0·63	0·45	372	0·39	0·35
139	0·53	0·58	—		
140	0·73	0·44	390	1·26	1·13
141	1·12	0·65	384	1·51	1·36
142	1·00	0·52	—		
143	0·84	0·48	381	0·70	0·63
144	1·20	0·84	—		
			327	0·97	0·87
			382	0·97	0·87

The only published measurements of primary production in the Gulf of Thailand are those of Steemann Nielsen and Jensen (1957) during the *Galathea* Expedition. The *Galathea* stations 327–390 were in the same region (Fig. 3) and were during the same season as the *Diamantina* stations. In addition to differences in techniques, Steemann Nielsen and Jensen corrected (by +10%) for isotope effects and respiration. They also assumed a CO_2 concentration of 90 mg/l. Since no corrections for isotope effects and respiration were made for the *Diamantina* data, the *Galathea* data have been recalculated by a factor of −10%. For both *Galathea* and *Diamantina* stations the column values (g C/day/m²) were calculated by integration of the results at the individual depths.

Primary production in the water column (Table 3) ranged from 0·35 to 1·36 g C/day/m² with a mean of 0·87 g C/day/m² for the recalculated *Galathea* stations and from 0·44 to 0·84 g C/day/m² with a mean of 0·59 g C/day/m² for the *Diamantina* stations. The difference between the *Galathea* and *Diamantina* values is due partly to the error caused by using an assumed CO_2 concentration, partly to a difference in technique, and partly to a difference in locality and time.

V. References

Buch, K. (1951).—Das Kohlensäure gleichgewichtssystem im Meerwasser. *HavsforskInst. Skr., Helsingf.* **151**: 1–16.

CSIRO Aust. (1963).—Oceanographical observations in the Indian Ocean in 1961. H.M.A.S. *Diamantina.* Cruise Dm2/61. *CSIRO Aust. Oceanogr. Cruise Rep.* **9**.

Clarke, G. L. (1954).—"Elements of Ecology." p. 534. (John Wiley & Sons: New York.)

Dal Pont, G., and Newell, B. (1963).—Suspended organic matter in the Tasman Sea. *Aust. J. Mar. Freshw. Res.* **14**: 155–65.

Dyson, N., Jitts, H. R., and Scott, B. D. (1965).—Techniques for measuring oceanic primary production using radioactive carbon. CSIRO Aust. Div. Fish. Oceanogr. Tech. Pap. No. 18.

Matsudaira, Y. (1964).—Cooperative studies on primary productivity in the coastal waters of Japan 1962–63. *Inform. Bull. Planktol. Japan* **11**: 24–73.

Milburn, T. R., and Beadle, L. C. (1960).—The determination of total carbon dioxide in water. *J. Exp. Biol.* **37**: 444–60.

Miyake, Y. (1958).—A study of the organic productivity and solubility product of $CaCO_3$ in the ocean by means of radiocarbon C-14. Int. Conf. Radioisotopes in Sci. Res. Vol. 4, pp. 651–7.

Park, K., Hood, D. W., and Odum, T. H. (1958).—Diurnal pH variations in Texan bays and its application to primary production estimation. *Publs Univ. Texas Inst. Mar. Sci.* **5**: 47–64.

Rotschi, H., Angot, M., and Legand, M. (1959).—ORSOM III. Resultats de la croisière "Boussole" 2ème partie: Chimie, Productivité et Zooplancton. O.R.S.T.O.M., I.F.O., Rapp. Sc. No. 13, p. 81.

Smith, C. L. (1940).—The Great Bahama Bank. II. Calcium carbonate precipitation. *J. Mar. Res.* **3**: 171–89.

Smith, C. L. (1941).—The solubility of calcium carbonate in tropical sea water. *J. Mar. Biol. Ass. U.K.* **25**: 235–42.

Steemann Nielsen, E., and Jensen, A. E. (1957).—Primary oceanic production, the autotrophic production of organic matter in the oceans. *Galathea Rep.* **1**: 47–135.

Wells, R. G. (1922).—Carbon dioxide content of sea water at Tortugas. *Pap. Dep. Mar. Biol. Carnegie Instn. Wash.* **18**: 89–93.

Reprinted from *Bull. Inst. océanogr., Monaco*, vol. 65, no. 1,347, 1965.

Teneur en radiocarbone des eaux profondes et superficielles du nord de l'océan Indien (mer d'Oman)

par

Jean THOMMERET, Yolande THOMMERET et Jean GALLIOT

Laboratoire de radioactivité appliquée, Centre scientifique de Monaco

---

(Manuscrit reçu le 4 octobre 1965)

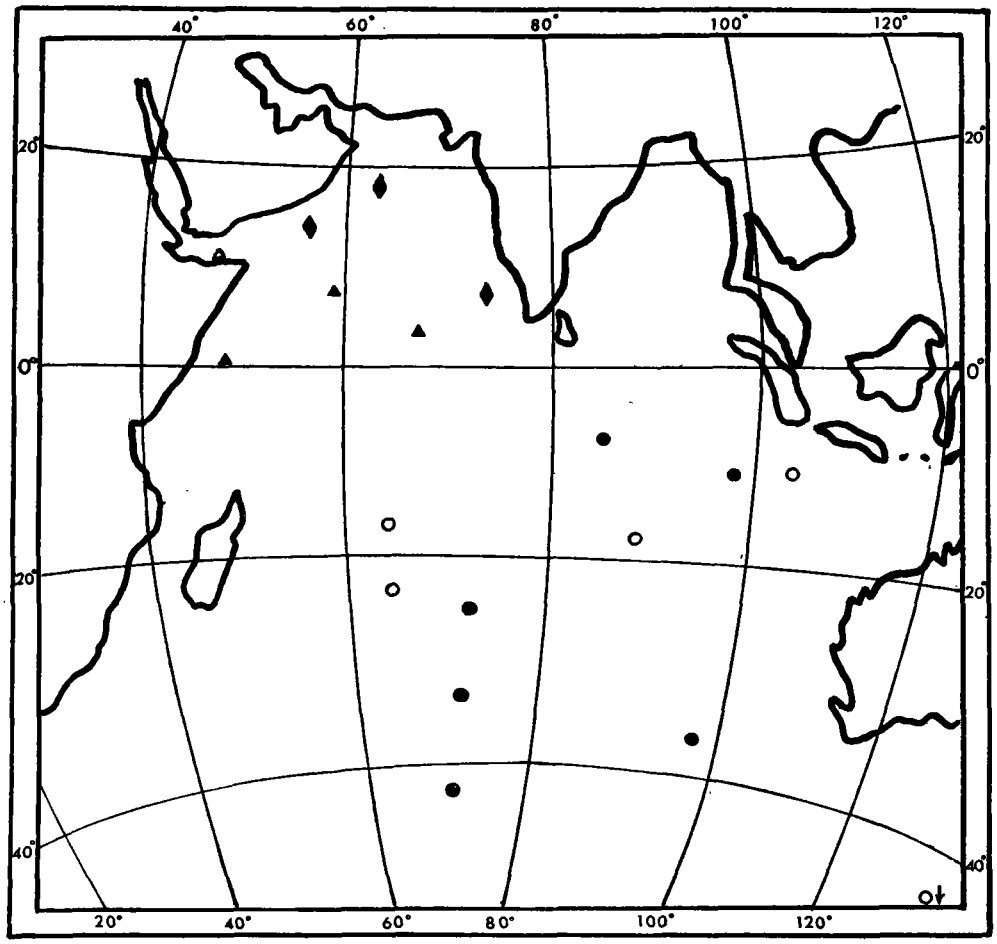

Emplacement des points où ont été prélevés les échantillons d'eau

- ● prélèvement sur un profil vertical (N.W. RAKESTRAW)
- ○ prélèvement d'eau de surface (N.W. RAKESTRAW)
- ◆ prélèvement sur un profil vertical (C.S.M.)
- △ prélèvement d'eau de surface (C.S.M.)
- ▲ prélèvement d'eau de profondeur (C.S.M.)

Introduction

L'étude des mouvements des masses d'eaux océaniques au moyen de l'analyse de la teneur en isotope 14 du carbone provenant des carbonates dissous dans les eaux de mer, a été traitée par plusieurs auteurs qui ont utilisé diverses méthodes d'extraction du gaz carbonique marin [2, 3, 4, 6, 10].

Au cours de l'Expédition internationale de l'océan Indien de la *Woods Hole Oceanographic Institution* sur l'*Atlantis II* (cruise 8) pendant l'été 1963, nous avons effectué une série de 10 prélèvements d'eau de mer de surface et de profondeur (2 400 à 4 500 m) dans le secteur nord de l'océan Indien : golfe d'Aden et mer d'Oman, aux latitudes comprises entre 0 et 20° nord.

Les résultats des mesures de radiocarbone de ces échantillons d'eau de mer nous ont permis de les comparer à ceux qui ont été obtenus par BIEN, RAKESTRAW et SUESS en 1960 dans le secteur sud de l'océan Indien entre les latitudes 10° et 40° sud [2].

Techniques et Mesures

Les prélèvements exécutés à l'aide d'une bouteille d'acier de 100 litres construite à l'Université de Göteborg, Institut océanographique, ont été traités immédiatement à bord de l'*Atlantis II* par J. GALLIOT en utilisant sans modification la méthode mise au point par FONSELIUS et ÖSTLUND [6]. Le gaz carbonique dissous dans l'eau de mer sous forme de bicarbonates ou d'ions carbonate, déplacé par de l'acide sulfurique concentré, sous courant d'azote, est fixé sur une solution de soude 2N décarbonatée. Les opérations terminales — transformation en carbonate de baryum, régénération et purification du gaz carbonique — et les mesures de l'activité du carbone 14 ont été effectuées au laboratoire suivant les techniques que nous utilisons habituellement [11].

Résultats

La mesure de l'activité en carbone 14 permet de déduire la valeur

$$\delta C^{14} = \frac{A_{éch.} - A_{st.} \times 0{,}95}{A_{st.} \times 0{,}95} \times 1\,000$$

$A_{éch.}$: activité de l'échantillon,
$A_{st.}$: activité du standard N.B.S.

Selon les conventions du *Lamont geological observatory*, la valeur Δ est obtenue en appliquant la formule de BROECKER [5].

$$\Delta = \delta C^{14} - (2\,\delta C^{13} + 50)(1 + 0{,}001\,\delta C^{14})$$

Nous avons calculé les âges correspondants aux valeurs de Δ d'après la formule donnée par ÖSTLUND, BOWMAN et RUSNAK de l'*Institute of marine science*, Université de Miami [9]

$$\text{Age} = \frac{-T\,½}{\text{Ln } 2} \text{ Ln } \frac{1\,000 + \Delta}{1\,000 + \Delta_0}$$

où Δ_0 est égal à — 50 pour les échantillons dérivant leur carbone de l'eau de mer et $T\,½ = 5\,568$ ans.

Les mesures de fractionnement isotopique du carbone 13 n'ont pu être effectuées dans des conditions satisfaisantes de précision. Pour nos calculs, nous avons choisi des δC^{13} égaux à

+ 0,6 pour 1000 pour les eaux de surface

− 0,6 pour 1 000 pour les eaux profondes

ces valeurs étant les moyennes des valeurs de δC^{13} mesurées par BIEN *et al* dans l'océan Indien en 1960. Nos résultats sont résumés dans le tableau (voir ci-contre).

BIEN *et al* ont établi que dans l'océan Pacifique l'activité en carbone 14 des eaux de surface décroît du nord au sud, tandis que l'activité des eaux profondes décroît du sud au nord. Des valeurs obtenues, ils déduisent que le taux moyen de la composante vers le nord du mouvement des masses d'eaux profondes du Pacifique est d'environ 0,05 cm/s. Les mesures de l'activité en carbone 14 des eaux profondes prélevées dans le secteur sud de l'océan Indien aux latitudes comprises entre 10° et 40° ne semblent pas permettre d'établir clairement, malgré la supposition des auteurs, l'existence d'une composante de déplacement sud-nord des masses d'eaux de l'océan Indien.

Nos mesures ont été effectuées dans le secteur nord de l'océan Indien aux latitudes comprises entre 0 et 20°. Elles sont en accord avec celles de BIEN *et al*, en ce qui concerne la valeur de Δ pour les eaux profondes. Les valeurs des âges apparents figurant dans notre tableau différent de 410 ans du fait de l'utilisation de la formule d'ÖSTLUND [9]. Pour les eaux de surface, l'accroissement des valeurs Δ que nous avons mesurées correspond à un enrichissement en carbone 14 par rapport aux valeurs Δ des eaux de surface de l'océan Indien sud mesurées en 1960 par BIEN *et al*; cette augmentation s'explique par l'importante élévation de la teneur en carbone 14 de l'air due aux explosions nucléaires postérieures à 1960. Relevée en divers points du globe, celle-ci a pour valeurs :

$\delta C^{14} = 961$ pour 1 000 à Abisko, Suède, septembre 1963 [8],

$\delta C^{14} = 950$ pour 1 000 à Trondheim, Norvège, août 1963 [7],

$\delta C^{14} = 794$ pour 1 000 à China Lake, Californie, sept. 1963 [1],

$\delta C^{14} = 754$ pour 1 000 à Monaco, août 1963 [12],

que l'on peut comparer à la valeur moyenne $\delta C^{14} = 250$ pour 1 000 (Abisko, 1960).

On peut remarquer la grande dispersion des valeurs Δ des eaux de surface qui reflète l'hétérogénéité et la durée relativement importante du mélange des eaux au-dessus de la thermocline.

Les eaux de profondeur dont les taux de mélange *(mixing rate)* sont extrêmement faibles ne présentent pas de modification par rapport aux résultats obtenus en 1960 par BIEN *et al* dans le Sud-Est de l'océan Indien. Les résultats que nous avons obtenus ne permettent donc pas d'établir par la méthode du radiocarbone l'existence d'un mouvement des eaux océaniques profondes. Ce mouvement ne pourrait être mis en évidence que par un grand nombre de mesures effectuées sur de très nombreux prélèvements simultanés couvrant tout l'océan Indien.

MC N°	Station	Date	Latitude	Longitude	Salinité (‰)	Temp. (°c)	Profondeur de prélèvements (mètres)	δC^{14} (‰)	δC^{13} (‰)	Δ (‰)	Age* B.P.**
35	77	21.8.63	19°58' N	64°58' E	36,37	26,79	Surface	+ 51±10	(+0,6)	- 3± 9	
36		21.8.63	19°58' N	64°58' E	34,74	1,71	3000	-154±11	(-0,6)	-195±10	1330 ans
37	61	11.8.63	14°56' N	56°59' E	35,91	25,10	Surface	+121±13	(+0,6)	+ 64±12	
38		11.8.63	14°56' N	56°59' E	non transmises		3121	-133± 9	(-0,6)	-175± 9	1133 ans
39	50	8.8.63	12°28' N	47°44' E	36,34	27,01	Surface	+ 76±14	(+0,6)	+ 21±13	
40	94	31.8.63	9°58' N	58°17' E	non transmises		3200	-112± 9	(-0,6)	-155± 8	940 ans
41	106	6.9.63	9°59' N	74°31' E	33,08	28,19	Surface	+ 78± 8	(+0,6)	+ 23± 7	
42		6.9.63	9°59' N	74°31' E	non transmises		2460	-117±11	(-0,6)	-160±10	988 ans
43	119	15.9.63	5°00' N	67°26' E	34,74	1,79	2930	-130±11	(-0,6)	-172±10	1105 ans
44	139	25.9.63	0°13' N	50°39' E	34,72	1,34	4500	-108±12	(-0,6)	-152±11	912 ans

* Calculés avec une différence de 410 ans plus jeunes que ceux donnés par BIEN et AL.

** B.P. sont les initiales anglaises ``Before present´´ adoptées pour la datation avec l´année 1950 prise comme année 0.

En examinant les résultats des trois stations où des prélèvements d'eau de surface et de profondeur ont été effectués sur un profil vertical, nous constatons que la différence entre la valeur moyenne Δ entre eau de surface et eau profonde est sensiblement égale à 200 pour 1 000, qui correspondrait à une différence d'âge d'environ 1 400 ans, mais comme pratiquement la teneur en carbone 14 des eaux de surface est en constante évolution, par suite du transfert du carbone 14 atmosphérique aux réservoirs de surface, il est difficile d'attribuer une signification à cet âge.

Remerciements

Nous remercions le Dr R. MILLER de la *Woods Hole Oceanographic Institution*, qui a permis à J. GALLIOT de participer aux travaux des équipes scientifiques, les officiers et l'équipage de l'*Atlantis II* pour l'aide apportée dans les prélèvements des échantillons d'eau de mer ainsi que le Professeur I. HELA, directeur du laboratoire de radioactivité marine de l'Agence internationale de l'énergie atomique à Monaco pour le prêt de la bouteille de prélèvements d'eau.

Résumé

Dix mesures de concentration en carbone 14 d'échantillons d'eaux de surface et de profondeur du Nord de l'océan Indien (mer d'Oman) prélevés en août et septembre 1963 pendant l'Expédition internationale de l'océan Indien *(Atlantis II)*, ont confirmé les résultats obtenus par BIEN, RAKESTRAW et SUESS en 1960 dans le même océan (partie sud-est). Le mélange des eaux de surface, au-dessus de la thermocline, prend plusieurs années et n'affecte qu'une mince couche superficielle de la mer. Une augmentation sensible de la teneur en carbone 14 a été observée en 1963 pour les eaux de surface.

Il n'y a aucune différence significative d'âge entre les eaux profondes du Sud-Est et celles du Nord-Ouest de l'océan Indien. L'emploi de la méthode du radiocarbone semble impuissante à assigner aux masses d'eaux profondes un mouvement vers le nord, d'après le même critère que BIEN, RAKESTRAW et SUESS ont utilisé pour les eaux profondes du Pacifique pour lesquelles ils ont estimé une composante de vitesse vers le nord de 0,05 cm/s en considérant la différence d'âge de 400 ans, mesurée par le radiocarbone entre 40° S et 40° N.

Summary

Ten carbon 14 concentration measurements of surface and deep sea water samples of the north Indian ocean (Arabian sea), collected in August and September 1963, during the International Indian Ocean Expedition *(Atlantis II)*, have confirmed the results obtained by BIEN, RAKESTRAW and SUESS in 1960 in the same ocean (south-east part).

The mixing of surface water, above the thermocline, takes several years and affects only a thin surface layer of the sea. A marked increase in the carbone 14 amount of surface waters has been observed in 1963.

There is no significant difference of age between deep waters from water masses, using the same criteria as BIEN, RAKESTRAW ans SUESS have taken for the deep waters of the Pacific for which they calculated a northward speed component of 0,05 cm/sec, on the consideration of the 400 years difference of age measured by the radiocarbon, between 40° S and 40° N.

Содержание радиоуглерода в глубинных и поверхностных водах северной части Индийского океана / Оманский залив/

Жан ТОММЕРЭ, Иоланда ТОММЕРЭ и Жан ГАЛЛИО

Краткое содержание

Десять проб концентрации углерода 14 в поверхностных и глубинных образцах Северной части Индийского Океана / Оманский залив /, взятых в августе и сентябре 1963 года во время Международной экспедиции в Индийский океана / *Atlantis II*/, подтвердили данные, полученные BIEN'ом, RAKESTRAW'ом и SUESS' ом в 1960 году в том же океане / в юго–восточной части/. Смешивание поверхностных вод, выше термического уровня, занимает несколько лет и касается только тонкого слоя морской поверхности.Значительное увеличение содержания углерода 14 наблюдалось для поверхностных вод в 1963 году.

Между глубинными водами Югов-осточной и Северно-западной частей Индийского океана не существует значительной разницы в возрасте. Повидимому, применение радиоуглеродного способа не может заставить глубинные воды перемещаться к северу на том же основании, на котором BIEN, RAKESTRAW и SUESS применяли его в Тихом океане в глубинных водах, для которых ими определялась составная скорости для передвижения к северу в 0,05 см/сек, принимая во внимание разницу возраста в 400 лет, измеренную с помощью радиоуглерода между 40° Южной и 40° Северной широты.

Addendum

Page 7, entre les quatrième et cinquième lignes, veuillez ajouter :
Page 7, between the fourth and fifth lines, please add :

« *(from)* south - east and those from north - west of the Indian ocean. The radiocarbon method seems unable to reveal a northward movement in deep *(water)* ».

Bibliographie

[1] BERGER (R.), FERGUSSON (G.J.) & LIBBY (W.F.), 1965. — UCLA radiocarbon dates IV. *Radiocarbon*, **7**, pp. 336-371.

[2] BIEN (G.S.), RAKESTRAW (N.W.) & SUESS (H.E.), 1963. — Radiocarbon dating of deep water of the Pacific and Indian oceans, *in : Radioactive dating*, pp. 159-172. — Vienna, International atomic energy agency [*Bull. Inst. océanogr. Monaco*, **61**, nº 1278, 16 p.]

[3] BROECKER (W.S.), TUCEK (C.S.) & OLSON (E.A.), 1959. — Radiocarbon analysis of oceanic CO_2. *Int. J. appl. Radiat. Isot.*, **7**, pp. 1-18.

[4] BROECKER (W.S.), GERARD (R.), EWING (M.) & HEEZEN (B.C.), 1960. — Natural radiocarbon in the Atlantic Ocean. *J. geophys. Res.*, **65**, 9, pp. 2903-2931.

[5] BROECKER (W.S.) & OLSON (E.A.), 1961. — Lamont radiocarbon measurements VIII. *Radiocarbon*, **3**, pp. 176-204.

[6] FONSELIUS (S.) & ÖSTLUND (G.), 1959. — Natural radiocarbon measurements on surface water from the North Atlantic and the Arctic sea. *Tellus*, **11**, 1, pp. 77-82.

[7] NYDAL (R.), 1963. — Increase in radiocarbon from the most recent series of thermonuclear tests. *Nature, Lond.*, **200**, nº 4903, pp. 212-214.

[8] OLSSON (I.U.) & KARLEN (I.), 1965. — Uppsala radiocarbon measurements VI. *Radiocarbon*, 7, pp. 331-335.

[9] ÖSTLUND (H.G.), BOWMAN (A.L.) & RUSNAK (G.A.), 1965. — Miami natural radiocarbon corrections I-III. *Radiocarbon*, 7, pp. 153-155.

[10] RAFTER (T.A.) & FERGUSSON (G.J.), 1957. — Recent increase in the C14 content of the atmosphere, biosphere and surface waters of the oceans. *N.Z. J. Sci. Tech.* (B), **38**, pp. 871-883.

[11] THOMMERET (J.) & RAPAIRE (J.L.), 1964. — Monaco radiocarbon measurements I. *Radiocarbon*, **6**, pp. 194-196.

[12] THOMMERET (J.) & THOMMERET (Y.). — Monaco radiocarbon measurements II. *Radiocarbon* (à paraître).

Reprinted from *Deep-sea Res.*, vol. 13, 1966, p. 413-425.

Distribution of particulate and dissolved nitrogen in the Western Indian Ocean*

F. FRAGA†

(*Received* 12 *November* 1965)

Abstract—Determinations were made of particulate and dissolved organic nitrogen in the waters of the western Indian Ocean from 20°S to 25°N. The vertical distribution of particulate nitrogen had a maximum at ten meters and a very clear diurnal variation extending down to 340 m. During the night the nitrogen increased from 0 to 60 m and decreased from 60 to 340 m. It is supposed that this is due to zooplankton migration.

The vertical distribution of the dissolved organic nitrogen had a peak at 20 m and another very large one between 100–170 m.

The relationships were studied between dissolved nitrogen, dissolved organic carbon, particulate nitrogen, and also particulate carbon and phosphorus, chlorophyll and the fixation of carbon-14.

The distribution of organic nitrogen is shown for a north–south section and for sections perpendicular to the Arabian coast.

INTRODUCTION

THE INVESTIGATIONS reported here are part of a general survey of the Indian Ocean 1963–1964. The samples were taken aboard the Oceanographic vessel *Anton Bruun* of the U.S. National Science Foundation on its Cruise 4-A, September to November 1963, from Mauritius to Bombay (Fig. 1). Further details may be found in Bulletin No. 5, U.S. Program in Biology, I.I.O.E. and the Final Cruise Report (WOODS HOLE OCEANOGRAPHIC INSTITUTION, 1964; 1965).

The distribution of dissolved organic nitrogen and of suspended particulate nitrogen were studied. The two fractions were separated by filtration with a fiberglass filter (" Gelman A "). The particulate matter consisted of detritus, bacteria, phyto- and zooplankton of a size larger than 13 μ. " Dissolved organic nitrogen " included particulate matter of less than 13 μ. Hence the pore-size must be especially considered when comparing these with results published elsewhere.

This is a preliminary paper outlining the vertical distribution of organic nitrogen. The basic data has already been distributed rather widely (WOODS HOLE OCEANOGRAPHIC INSTITUTION, 1965). The final analysis of the data must await publication of other oceanographic data.

Vertical distribution of organic nitrogen

To obtain the average vertical distribution of dissolved and particulate organic nitrogen (Tables 1 and 2), the average value at each standard depth interval was calculated for all the stations studied. These intervals were not always the same

*Part of the work was supported by the U.S. National Science Foundation through participation in the United States Biological Program of the International Indian Ocean Expedition.

†Instituto de Investigaciones Pesqueras, Vigo, Spain.

because the samples came from various depths depending on the transparency of the water. Thus, the samples were taken at depths to which 50, 25, 10 and 1 % of the light at the surface penetrated and at some intermediate depths. In highly productive areas, these depths were consequently shallower than in the less productive areas. In calculating the average value for each interval in order to avoid including samples from the richer and poorer waters in any definite proportion, the greatest possible number of samples were included which corresponded to the same penetration of light in such a way that in each average there would be the same ratio of stations with

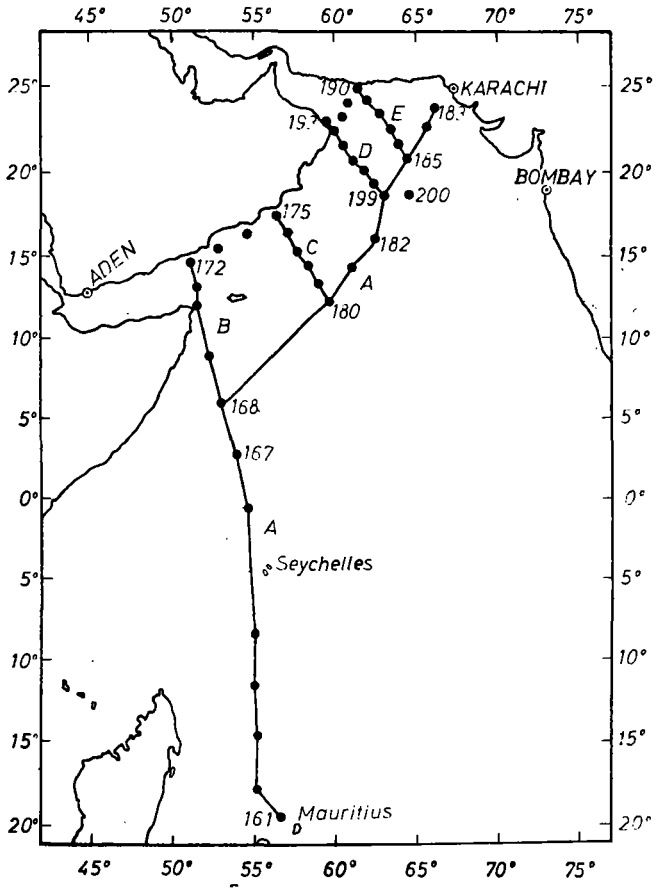

Fig. 1. Location of Oceanographic Stations E-161–E-200 along sections AA, B, C, D and E.

different degrees of productivity. For depths greater than 120 m a sufficient number of samples were included to obtain a probable error of the average of less than 0·1 μg-at N/l. for the particulate matter and 0·5 μg-at N/l. for the dissolved matter.

Particulate nitrogen (Table 1). The curve for particulate nitrogen (Fig. 2) is similar to that for photosynthesis with a maximum at 10 m. Deeper than this it decreases linearly in proportion to the light, but from 20–30 m, there is a sharp drop, quite distinct from the curve for photosynthesis. Considering the samples taken during the day and during the night, separately, it appears that the curve represents the sum of these two curves (cf. Fig. 3a). At night there is a higher concentration of organic nitrogen in

Table 1. Average values of particulate organic nitrogen

Depth intervals (m)	m	*Total samples* No.	μg-at N/l.	*Day* μg-at N/l.	± r	*Night* at-μg. N/l.	± r	*Light penetration* $K = 0{\cdot}07$ to $0{\cdot}05$ (%)
1	1	35	1·47	1·22	0·03	1·69	0·20	100
5–14	11	33	2·12	2·04	0·20	2·17	0·20	50
15–25	20	33	1·58	1·20	0·06	1·79	0·20	
26–32	28	34	1·50	1·12	0·08	1·81	0·10	25
33–47	37	35	1·21	1·03	0·08	1·35	0·10	10
50	50	14	0·65	0·60	0·10	0·68	0·20	
52–120	79	46	0·55	0·75	0·09	0·45	0·04	1
125–200	175	18	0·32	0·38	0·07	0·23	0·06	
300–400	336	14	0·28	0·19	0·06	0·20	0·06	
600	600	11	0·11					
800–1300	945	20	0·09					
1400–4000	2325	20	0·03					

Day : Samples taken during the day from 6 : 00 a.m. to 6 : 00 p.m.
Night : Samples taken during the night from 6 : 00 p.m. to 6 : 00 a.m.
m : Average depth in metres taking into account the frequencies.
No. : Number of samples used in obtaining the average.
± r : Probable error of the average $= 0{\cdot}67\ \sigma\ \sqrt{\text{No.}}$

Table 2. Dissolved organic nitrogen

Depth intervals	m	*Concentration of* N *No. obsvns.*	μg-at N/l.	± r	C/N *Ratio* m	C/N at.
1	1	38	8·1	0·2	1	11·1
5–14	11	35	8·0	0·2	11	11·2
15–25	20	32	8·8	0·3	21	8·5
26–32	28	34	7·5	0·1	27	9·6
33–47	37	32	7·4	0·2	37	8·1
50	50	14	6·2	0·2	72	9·6
52–120	79	45	6·5	0·1		
125	125	6	8·0	0·6	125	12·1
200	200	12	7·3	0·3	200	9·7
300–400	336	14	6·7	0·4	338	9·5
600	600	11	6·4	0·4	600	9·5
800	800	12	5·6	0·4	944	8·3
900–1400	1175	8	5·5	0·5		
1600–2000	1846	13	5·0	0·3	2300	6·3
2800–4000	3300	7	4·3	0·2		

the surface layer down to 60 m than during the day while deeper, from 60 to 340 m, the concentration is lower. Below 340 m, the diurnal difference is less than the probable error.

The only explanation at present for this phenomenon is the nocturnal migration of the zooplankton from 60–340 m to the surface, a minimal distance of about 60 m. Thus, during the day, organic matter with a high concentration of chlorophyll (Fig. 3C) especially at 20 m occurs in the superficial layer (0–70 m), where most of the phytoplankton is to be found. Then, during the night the zooplankton invades this layer and causes a considerable increase in the nitrogenous organic matter there. This in turn decreases the chlorophyll/N_p ratio. On the contrary, the chlorophyll/N_p ratio increases in the lower layers during the night when there is less nitrogen as a result of the upward migration of zooplankton.

The difference in particulate nitrogen between day and night (Fig. 3B) which indicates the migration of the zooplankton during the night from 60–340 m to 60–0 m,

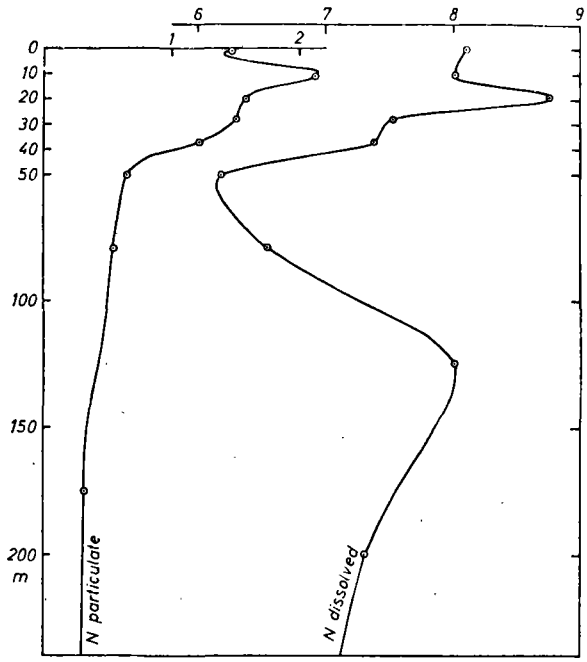

Fig. 2. Vertical distribution of particulate and dissolved organic nitrogen, both shown in microgram atoms of nitrogen per liter. The curves show the average values for all stations.

reaches its maximal variation at 80 and 28 m respectively. At 60 m there is no quantitative difference whatever between day and night. This does not indicate that there is no migration but that the quantity which comes from deeper layers compensates for the zooplankton which has migrated thence toward the surface (i.e. area *d* in Fig. 3B

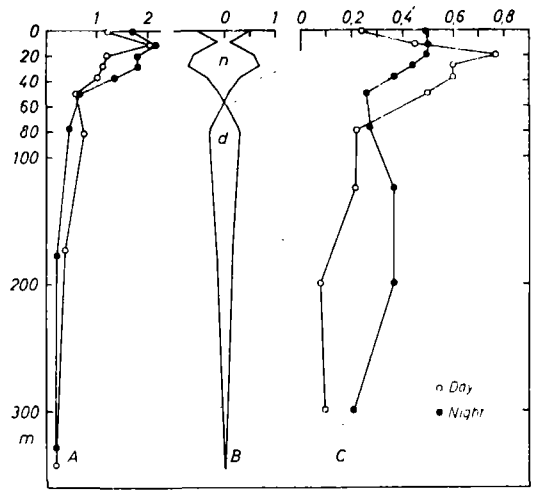

Fig. 3. *A*, particulate nitrogen; open circles, average for all stations made during the day; solid black circles, average of all stations taken during the night. *B*, difference between particulate nitrogen during the day and night; *n*, increase during the night, *d*, increase during the day. *C*, ratio of chlorophyll *a* in grams/particulate nitrogen in atoms.

is approximately equal to *n* corresponding to this migration). The total mass transported from one level to another is one of 500 Nμg-at/dm^2 in an average distance of 136 m, the difference between the centers of the two areas (160 and 24 m) (*n* and *d* in Fig. 3b).

Dissolved organic nitrogen (Table 2). The curve for the vertical distribution of dissolved organic nitrogen (Fig. 2) has the same type of inflection as that for particulate nitrogen though at a somewhat lower level. It also has another extraordinary and large, poorly-defined peak between 100 and 200 m. This peak is unrelated to that of particulate nitrogen. We suppose that it is produced by phytoplankton which had died and sunk below the level of compensation. The cellular membranes become permeable and thus free the soluble part of the protoplasm. Also augmenting the soluble nitrogen in this layer are the metabolites excreted by the zooplankton during the day. Thus, there is a daily transport of soluble nitrogen from the superficial layer where the zooplankton feeds to the deeper waters where it retreats to spend the day. Hence, an accumulation of soluble organic substances produced both by chemical and by bacterial decomposition occurs at the deeper level.

Relationship between dissolved and particulate organic nitrogen (Table 3). In an earlier investigation (FRAGA and VIVES, 1961) in coastal water there was a linear correlation between the two forms of nitrogen, expressed by the formula, where *a* is merely the slope of the line :

$$N_d = a\,N_p + I$$

However, a simple inspection of the curves for dissolved nitrogen N_d and particulate nitrogen N_p (Fig. 2) indicates that there is no correlation to be found for the Indian Ocean data. On the other hand, the particulate nitrogen has enormous diurnal variation with a 68% increment at 28 m. For this reason, correlations for N_d, N_p were sought for each level and also for samples taken by day or at night. This form

Table 3. Correlation between dissolved organic nitrogen N_d *and particulate nitrogen* N_p $N_d = a\,N_p + I$

Depth intervals (m)	m	*Day* *a*	I	*c*	*No.*	*Night* *a*	I	*c*	*No.*
1	1	1·2	6·8	0·2	16	1·4	5·9	0·4	17
5–25	15	—	—	0·0	28	0·7	7·1	0·2	35
26–32	28	1·7	5·7	0·6	15	1·0	5·7	0·7	17
33–47	37	5·1	3·3	0·2	14	2·1	4·0	0·2	18
50–120	71	3·6	4·6	0·6	24	3·2	4·3	0·4	30
125–400	233	7·2	4·3	0·8	9	12·3	4·4	0·3	9
		Day and night							
600–2000	1053	7·8	4·3	0·4	15				

As in some series the correlation is low, to obtain the true values of *a* and *I*, one calculates for each one :

$$N_d = a_1 N_p + I_1 \text{ and } N_p = \frac{1}{a_2} N_d - \frac{1}{a_2} I_2 \text{ and give as the slope}$$
$$a = \sqrt{(a_1/a_2)} \text{ and the } c = \sqrt{(a_1/a_2)}.$$

of correlation for the two forms of nitrogen is acceptable and the value of I ("inert" material) is approximately equal at all levels during the day and at night, with an average value of 5·1 μg-at N/l. This value is analogous to the Atlantic coastal water

from northwest Spain where the value most recently found (unpublished) was 5·9 μg-at N/l. between 0 and 100 m. It consisted of organic matter in a period when decomposition was great (which in the investigation previously cited we called "inert" material). Thus, only the slope of *a* which increases with depth and naturally varies also from day to night in the surface layers.

In Table 3 there is a summary of the values found.

RELATIONSHIP OF NITROGEN WITH OTHER COMPONENTS OF THE ORGANIC MATTER (Table 4)

Relationship of dissolved organic carbon–dissolved organic nitrogen. The vertical distributions of N_d and dissolved organic carbon C_d are very similar. Both have a minimum between 50–80 m and typically a maximum between 120–180 m, decreasing gradually toward the bottom.

In seeking a correlation between the two, using data for C_d made available by Menzel (W.H.O.I., 1965), an approximately linear correlation was found for the values of carbon between 0·5 and 1·5 mg C/l., but with a rather large scatter to the points. For high values of carbon, there is practically no correlation because the nitrogen does not increase, after reaching a determined level, an anomaly already observed in the North Atlantic by DUURSMA (1961).

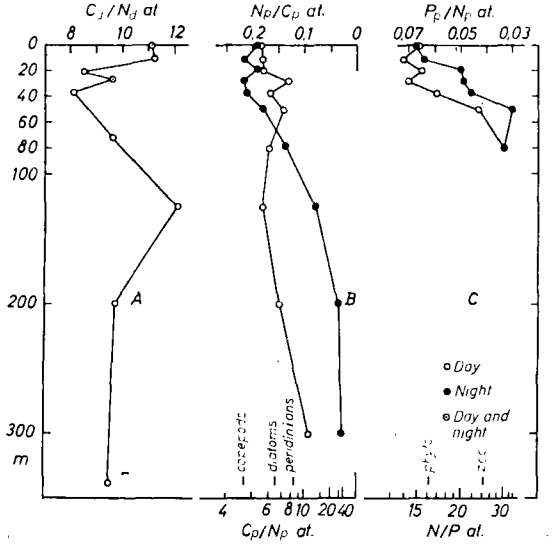

Fig. 4. *A*, ratio of carbon/dissolved nitrogen in atoms. *B*, the same ratio as the previous one for particulate organic material shown in atoms C/N on the lower scale and the inverse, N/C, on the upper scale; Vinogradov's values of C/N for copepods, diatoms and peridinians are also shown. *C*, ratio of phosphorus/particulate nitrogen shown in atoms and the inverse on the lower scale; also included are the Harris and Riley values for zooplankton and phytoplankton.

The ratio C/N varies with depth (Fig. 4 and Table 2). This variation is analogous to that of N_d which indicates that the variations in the vertical distribution of carbon are still larger but for the same depth there are large local variations from one zone to another. In general, it would seem that the relation C_d/N_d is greater in dissolved

organic matter of recent formation, despite DUURSMA's (1961) opinion to the contrary. Below 120 m the C_d/N_d ratio decreases with depth contrary to what happens with the ratio C_p/N_p for particulate matter.

The ratio C_d/N_d on the average ordinarily varies between 12 below the photosynthetic zone to 8 atoms of C for one atom of N and even less at great depths, but for high values of carbon, more than 1·5 mg/l. the ratio can be exceptionally high.

Particulate nitrogen–particulate carbon. As might be expected the C_p/N_p ratio has a diurnal variation presumably caused by zooplankton migration which differs from that of the phytoplankton. A. P. VINOGRADOV (1935, 1938) gave the following values for C/N in atoms (as cited in SVERDRUP, JOHNSON and FLEMING, 1946) : diatoms, 6·4; peridinians, 8·5; and copepods, 4·7. Thus, the zooplankton migration to the surface layer (0–60 m) during the night causes a lowering of the C/N ratio there similar to that occurring in the deeper layer (60 to 300 m) during the day when the zooplankton retreats to that level (Fig. 4B, Table 4). However, the series of events are not as simple as just indicated for photosynthesis also takes place during the day, a process which has not been considered in this report.

Table 4. Particulate organic matter. Ratio of nitrogen and phosphorus, carbon and chlorophyll a

Depth intervals (m)	m	C/N at. *day*	C/N at. *night*	N/P at. *day*	N/P at. *night*	*Chlorophyll a*, g/N at. *day*	*Chlorophyll a*, g/N at. *night*
1	1	5·4	5·2	15·3	15·0	0·24	0·50
5–14	12	5·5	4·6	13·8	15·6	0·45	0·50
15–25	20	5·6	5·2	15·4	19·9	0·77	0·50
26–32	28	7·6	4·6	14·3	20·6	0·60	0·44
33–47	38	6·0	4·5	16·9	21·6	0·60	0·37
50	50	7·0	5·6	23·1	32·8	0·45	0·26
52–120	78	5·9	7·3	30·6	30·0	0·22	0·27
125	125	5·5	12·3			0·21	0·37
200	200	6·7	29·5			0·08	0·37
300	300	10·8	37·0			0·10	0·21
		Day and night					
600	600	∞					
1000	1000	∞					
2000	2000	∞					

Owing to these variations in the C/N ratio, the correlation between the two shows a considerable scatter. Furthermore, it is not linear having considerable curvature for low values of C and N and the curve does not pass through the origin. When N equals zero, C is about 46 μg C/l. which in some areas ordinarily takes place at 400 m. In deep water particulate organic matter may be formed almost uniquely by non-nitrogenous compounds.

Particulate nitrogen–particulate phosphorus. The correlation between particulate organic nitrogen and phosphorus is linear and very good. The regressions found for samples between 0 and 107 m are :

$$\text{day} \quad N_p\ \mu\text{g-at} = 13{\cdot}0\ P_p\ \mu\text{g-at} + 0{\cdot}2;\ c = 0{\cdot}7$$
$$\text{night} \quad N_p\ \mu\text{g-at} = 15{\cdot}0\ P_p\ \mu\text{g-at} + 0{\cdot}3;\ c = 0{\cdot}8$$

(c = index of correlation)

The coefficient is higher at night when the zooplankton with a greater proportion of nitrogen is at the surface. The independent term is the concentration of nitrogen when phosphorus is equal to zero; these concentrations come up to 140 m at night and 340 m during the day. Therefore these are the lower limits from which comes the principal zooplankton biomass.

Although the correlation N : P is linear, the N/P ratio is not constant (Fig. 4c), because the regression line does not pass through the origin. For this reason, this ratio increases while their concentrations decrease. In this figure, are also shown, the values given by HARRIS and RILEY (1956) for the phyto- and zooplankton respectively.

Ratio of particulate nitrogen and chlorophyll a. This ratio can vary from zero to average values with limits of 1·0 and 1·8 μg chlorophyll a/μg-at N for dinoflagellates and diatoms respectively, calculated from the HARRIS and RILEY (1956) data.

The reasons for the variations in this ratio have already been discussed for particulate nitrogen. Here, the unique inversion between 0 and 12 m, should be mentioned. To ascertain whether it is real or whether it is due to an insufficient number of samples in determining the average, the probable error for this relationship was calculated and 0·03 and 0·07 μg chlorophyll a/μg-at N for day and for night respectively, was obtained, which gives a probability of 90%. The cause of this inversion between 0 and 12 m is due to a greater concentration of chlorophyll in the night samples and a slight lowering to 20 m, possibly due to the slight diurnal migration of dinoflagellates, but this point cannot be ascertained due to insufficient data. Deeper than this there is no significant difference between day and night.

Relation between particulate nitrogen and the fixation of ^{14}C *by the phytoplankton. Velocity of the renewal of nitrogenous material.* Phytoplankton, during photosynthesis at the same time that it fixes CO_2 also assimilates nitrogen compounds for the synthesis of proteins maintaining a relationship between both processes. Depending on various factors an average value of 7·5 : 1 atom C : N, based on A. P. VINOGRADOV's analysis of phytoplankton can be assigned to this.

The correlation between carbon fixed during the day and particulate nitrogen (Fig. 5) is not linear because the lower values for carbon fixation correspond to the

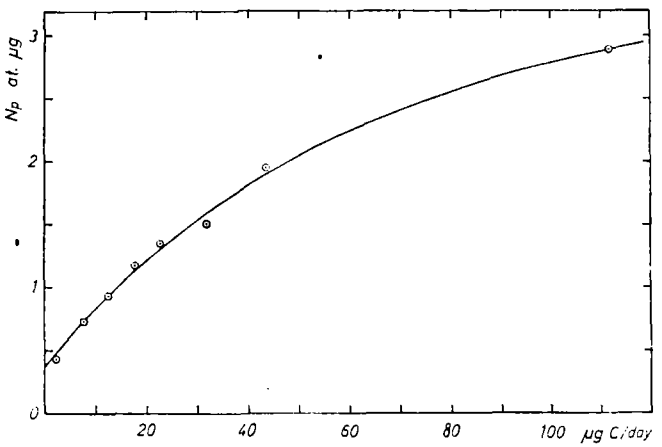

Fig. 5. Correlation between the concentration of particulate nitrogen in μg-at/l. and the carbon fixed by the phytoplankton in Cμg/l. per day. Each point is the average of twenty observations.

deeper samples where in addition to the organic material synthesized there, there is other material sinking down from the superficial layers which supplies more organic nitrogen than that being synthesized at this level. On the other hand the lower temperature in the deeper layers considerably reduces the velocity of decomposition of organic matter which tends to increase $N_p/\Delta C$ ratio.

When there is no carbon fixation, there is still about 0·4 μg-at N_p/l. of organic matter decomposing very slowly as it sinks down to the lower layers down to several hundred meters.

Table 5. Ratio of nitrogen assimilated by day, computed from ^{14}C data, and particulate nitrogen

Depth interval	m	N_p μg-at/l.	*Fixed carbon* μg/l./day	ΔN (μg-at/l./day)	*Nitrogen renewed daily* 100 $\Delta N/N_p$ (%)	*Temperature* (°C)
1	1	1·46	38·4	0·43	29	27·7
5–17	12	1·84	48·4	0·54	29	26·8
19–28	24	1·46	44·9	0·50	34	25·4
29–60	40	1·17	14·7	0·16	14	23·8
65–120	82	0·51	0·8	0·01	2	21·6

ΔN is calculated from fixed carbon by 0·0112.

At the level where organic matter which is being synthesized and decomposed is in dynamic equilibrium, it is possible to calculate the velocity of the decomposition

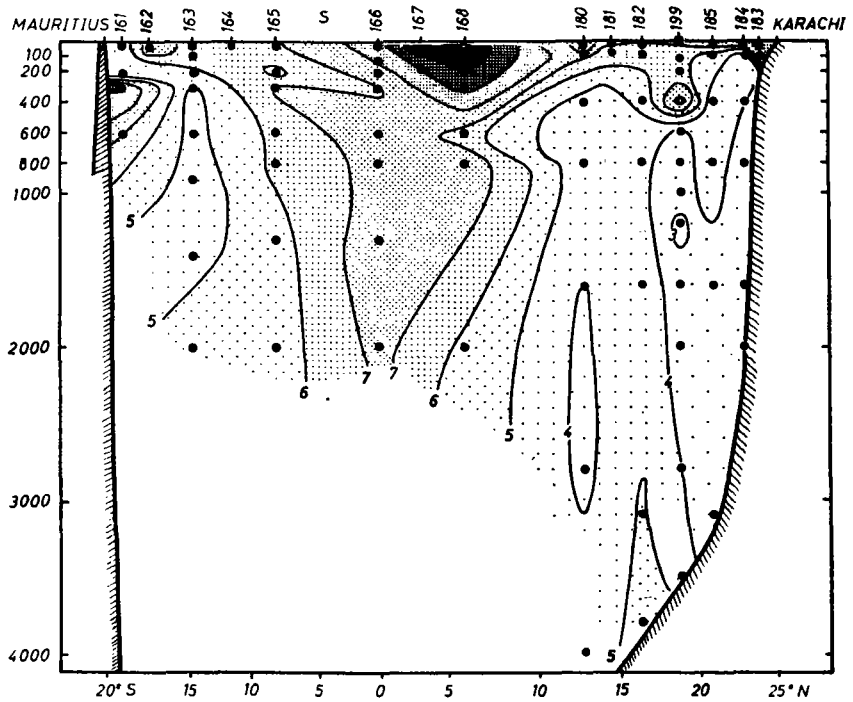

Fig. 6. Distribution of dissolved organic nitrogen, September to October along Section AA of Fig. 1; the numbers on the curves are μg-at N/l. The values at the surface are the average for 0–80 m, due to considerable variation with just a few meters in the shallower layers.

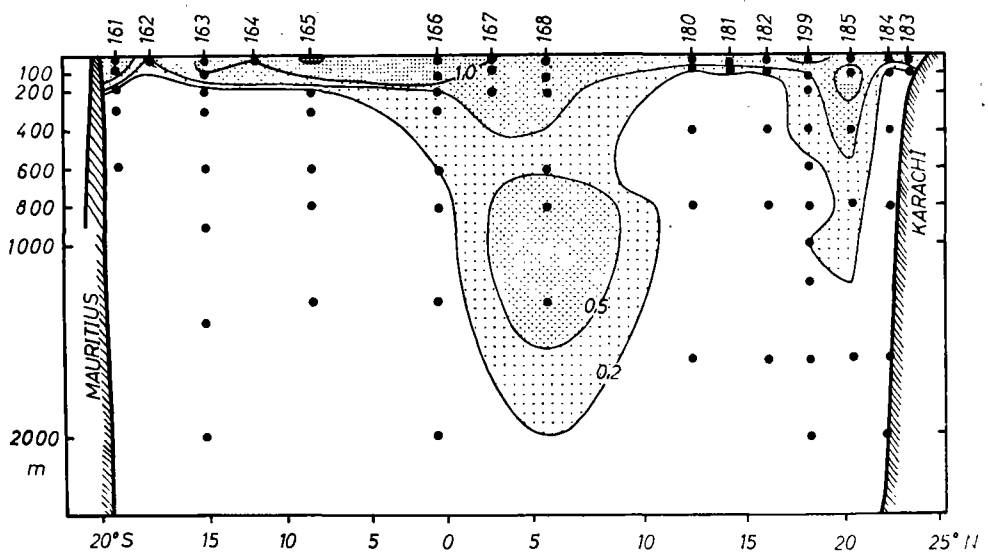

Fig. 7. Distribution of particulate nitrogen along the same section as in Fig. 6, also shown as μg-at N/l.

of the nitrogen compounds. From the values for fixed carbon (Table 5) the equivalent nitrogen assimilated during the day can be calculated by the factor $1/12{\cdot}01 \times 7{\cdot}45 = 0{\cdot}0112$ (12·01 = p.a. of C; 7·45 = C/N atoms in the phytoplankton). The quotient of assimilated nitrogen, which is equal to the decomposition, to total particulate nitrogen gives us the proportion of that which is renewed daily at each level, or that

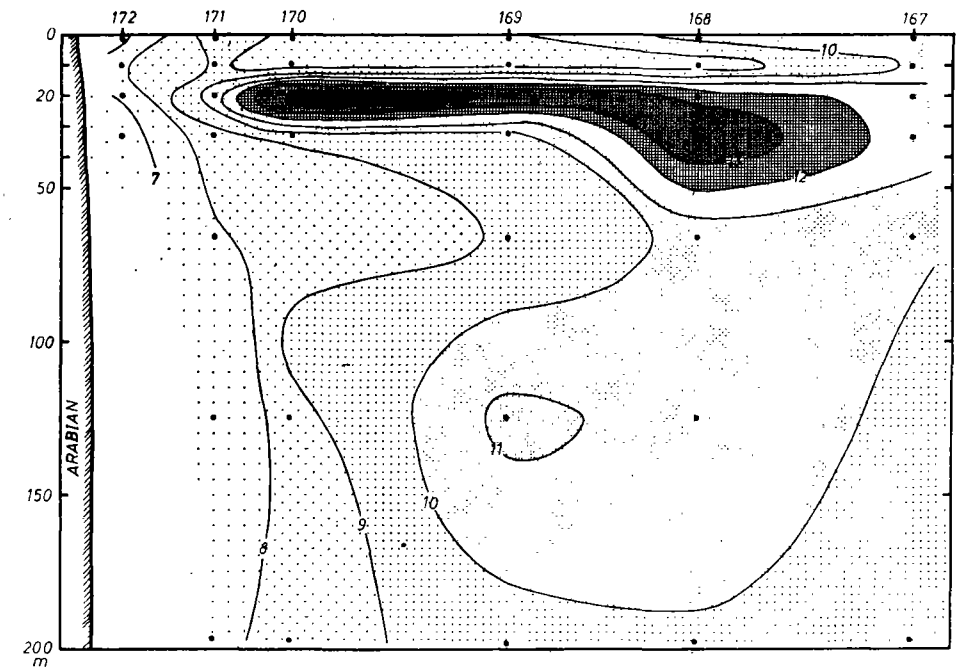

Fig. 8. Distribution of dissolved organic nitrogen in the superficial layers of Section B, Fig. 1, in μg-at N/l. in October.

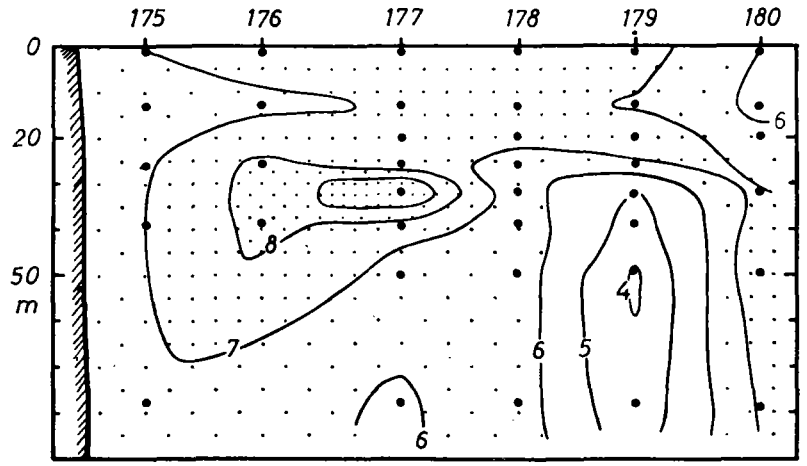

Fig. 9. Distribution of dissolved organic nitrogen, along Section C, Fig. 1, in October.

is, that which decomposes more than that which is sedimented down to the lower layer. The average daily values are similar to those in the Atlantic (FRAGA and VIVES, 1961) of 7·5% at 15·8°C which, if one considers that there is a five-fold increase for each 10° of temperature, corresponds to 37% at 25·8°.

SPATIAL DISTRIBUTION OF ORGANIC NITROGEN

Along Section A (Fig. 1) there was a high concentration of dissolved organic matter in the surface layer in the equatorial region from 0° to 8°N extending down to the deep layers, but at latitudes 20°N and 20°S, there are two zones with a lower

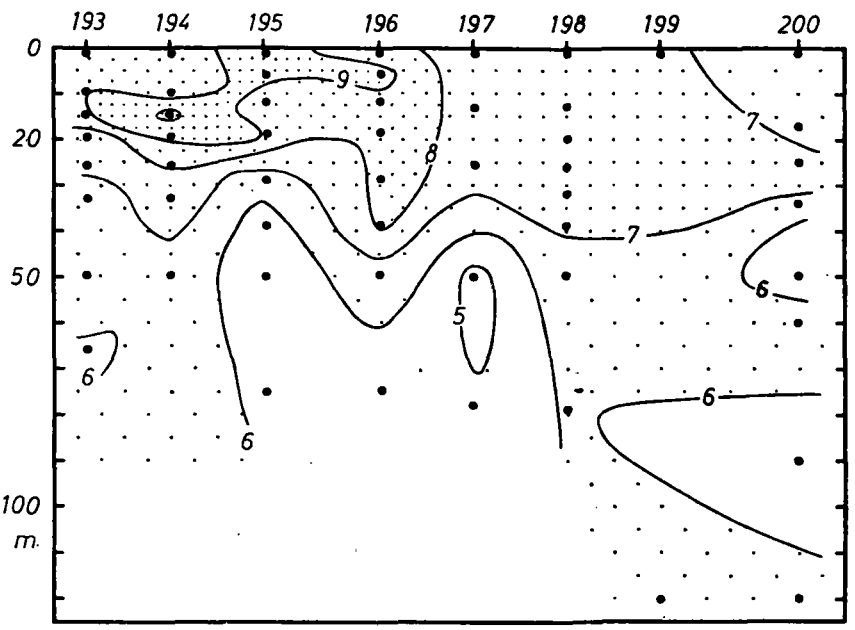

Fig. 10. Distribution of dissolved organic nitrogen along Section D, Fig. 1, in November.

nitrogen concentration extending from the bottom up to 500 to 300 m. The distribution of particulate nitrogen for this same section (A) (Fig. 7) is analogous to that of the dissolved nitrogen; both seem to indicate a convergence in the equatorial region. This is not constant because there is no continual decrease in organic nitrogen concentration with depth. Pockets may be formed at about 1000 m which could be due to seasonal variations in the organic matter produced at the surface with the change of the monsoon or transported horizontally from other richer areas, a question to be settled at a later date.

Particularly interesting is the water mass below 800 m between 18° and 23°N where the content of dissolved organic nitrogen is much lower in the amount of "inert" organic nitrogen (i.e., about 5·1 μg-at N_d/l.). The decomposition of this fraction is extraordinarily slow so that it is presumably a very old water mass. The

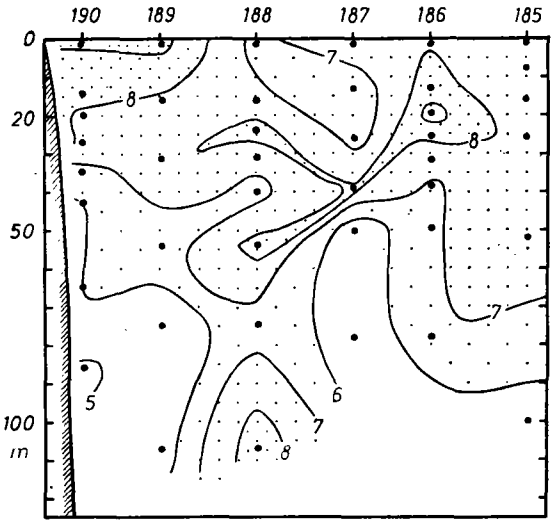

Fig. 11. Distribution of dissolved organic nitrogen along Section E, Fig. 1, October–November.

determination of the residence time of this water mass could be used to calculate the average " life " of substances resistant to mineralization.

The spatial distribution of dissolved organic nitrogen in the surface waters for Sections B, C, D and E are shown in Figs. 8, 9, 10 and 11, but figures for particulate nitrogen were not drawn because it is subject to large diurnal variations at the surface. On Section B, there is a typical distribution with a maximum at about 20 m and with another smaller one between 100 and 130 m separated by a minimum between 60–70 m approximately coinciding with its average distribution (Fig. 2). On the other sections C and D there was a similar distribution but less clearly defined than farther north and in section E it is confused.

Acknowledgements—I would like to express here my thanks to Dr. J. H. RYTHER for giving me the opportunity of participating in the expedition and providing me with the data for the particulate phosphorus, to Dr. D. W. MENZEL for allowing me to use this carbon analyses and to the permanent staff on shipboard for their great cooperation. Equally, I want to thank Drs. M. E. and S. W. WATSON, R. D. DUGDALE, J. J. GOERING and R. J. BARSDATE for their friendly encouragement while I was aboard the *Anton Bruun*, as well as Dr. MARY SEARS for the translation of this paper from the Spanish.

REFERENCES

DUURSMA E. K. (1961) Dissolved organic carbon, nitrogen and phosphorus in the sea. *Netherlands J. Sea Res.* **1**, pp. 1–148.

FRAGA F. y VIVES F. (1961) La descomposicion de la materia organica nitrogenada en el mar. *Inv. Pesq.* **19**, pp. 65–79.

HARRIS E. and G. A. RILEY (1956) Chemical composition of the plankton. *Bull. Bingham Ocean. Coll.* **25**, 135–323.

SVERDRUP H. U., M. W. JOHNSON and R. H. FLEMING (1946). *The Oceans*. Prentice-Hall, New York, 1087 pp.

WOODS HOLE OCEANOGRAPHIC INSTITUTION (1964). Narrative Report : *Anton Bruun* cruise 4-A. News Bull., U.S. Program Biol., Int. Indian Ocean Exped., No. 5, 15 pp., 11 figs. (Unpublished manuscript).

WOODS HOLE OCEANOGRAPHIC INSTITUTION (1965) Final Cruise Report, *Anton Bruun* cruises 4A and 4B, Oceanographic data, bathythermograph positions, stations lists for biological collections. U.S. Program in Biology, Int. Indian Ocean Exped., unnumbered pp. (Unpublished manuscript).

Reprinted from *Aust. J. mar. freshw. Res.*, vol. 17, 1966, p. 1-30.

SOURCE REGIONS OF OXYGEN MAXIMA IN INTERMEDIATE DEPTHS OF THE ARABIAN SEA

By D. J. ROCHFORD*

[*Manuscript received September* 24, 1965]

Summary

Oxygen maxima, in relation to σ_t, salinity maxima and minima, and other hydrological structural features, have been examined along three meridional sections of the Indian Ocean. These relations have provided a background for the interpretation of the water mass sources of oxygen maxima of the whole Indian Ocean. After grouping these oxygen maxima according to density, their salinities have been used to identify mixing circuits in which the following waters are involved: from the south (1) South Indian Central, (2) Subtropical oxygen maximum, (3) Antarctic Intermediate; from the east (4) Equatorial Frontal water; and from the north (5) Persian Gulf, and (6) Red Sea. The principal routes whereby oxygen-rich mixtures of these waters enter the Arabian Sea, during the south-west monsoon, have been determined. The directions of flow along several of these routes agreed with measured directions of current flow. Where these currents disagreed the measured current was generally very weak.

I. INTRODUCTION

The mid-depth waters of the Arabian Sea are very low in oxygen (Neyman 1961). Recent data of *Atlantis II* in 1963 and of *Discovery* in 1964 have shown layers of oxygen maxima in these waters, which must be formed by advection of waters richer in oxygen from outside the region. The origin and, wherever possible, the routes of such waters into the Arabian Sea during the south-west monsoon are examined in this paper.

II. DATA AND METHODS

The figures presented in this paper are based on the following sources:

FIGURES	VESSEL	REFERENCE
2–4	*Ob*	U.S.S.R. Acad. Sci (1959)
5–7	*Discovery*	Private communication
8–10	*Discovery*	Private communication
11–12	*Diamantina*	CSIRO (1962*a*)
	Diamantina	CSIRO (1963)
	Diamantina	CSIRO (1962*b*)
	Diamantina	CSIRO (1964*a*)
	Diamantina	CSIRO (1964*b*)
11–12	*Gascoyne*	CSIRO Cruise 4/62 (unpublished data)
	Vityaz	*Vityaz* (1960)
14–15	*Discovery*	Private communication
	Discovery	*Discovery* Commission (1942)
	Atlantis II	Private Communication
	Ob	U.S.S.R. Acad. Sci. (1958)
17–24		Data from above sources

The identification of the various high salinity water masses of the Arabian Sea and north Indian Ocean is based upon their salinity and density characteristics (Rochford 1964*a*, 1964*b*). Oxygen maxima have been identified on smoothed temperature–oxygen curves. Maxima were considered real whenever their oxygen values were greater by at least 0·1 ml/l than the values at their temperatures on the

* Division of Fisheries and Oceanography, CSIRO, Cronulla, N.S.W. (Reprint No. 581.)

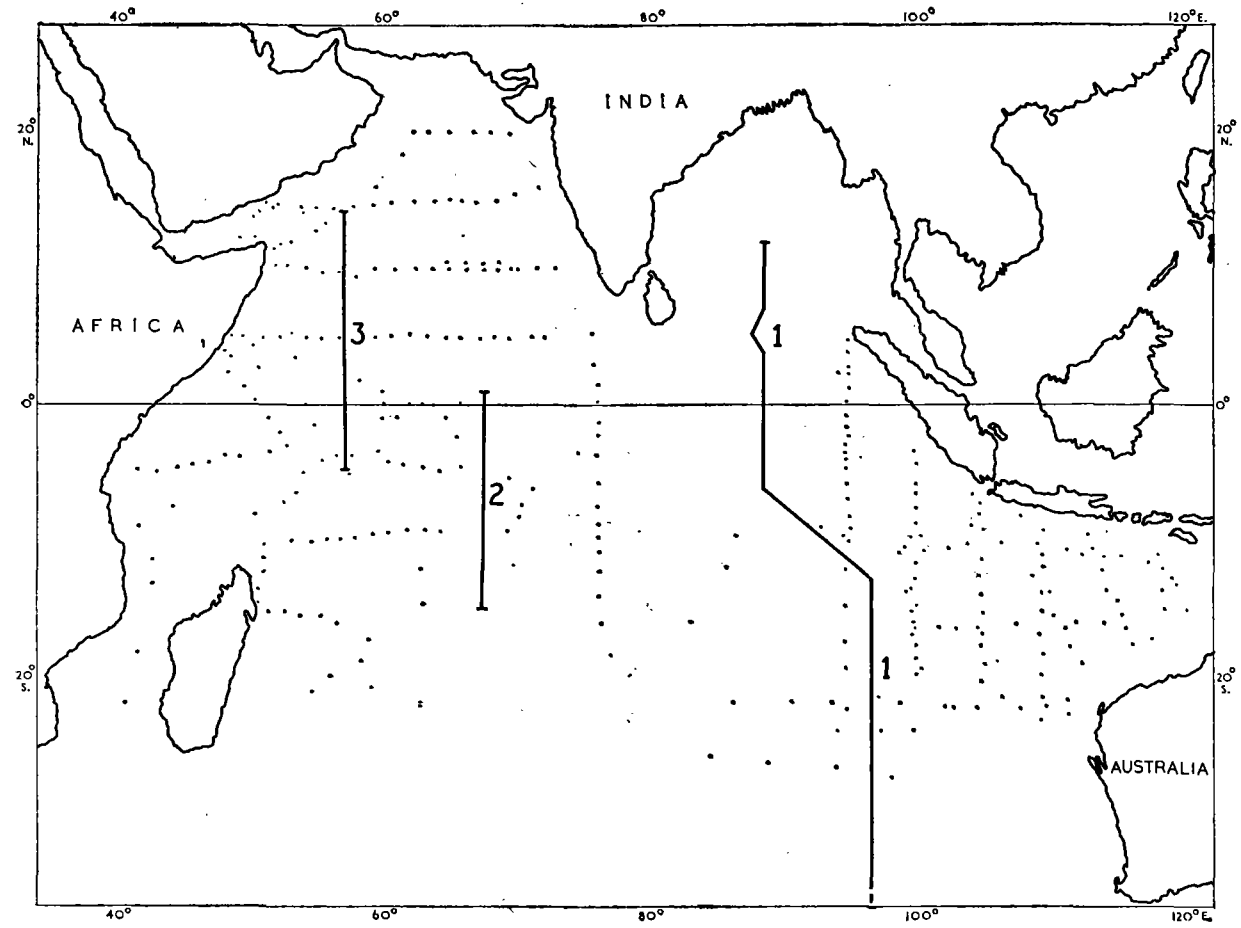

Fig. 1.—Chart of the hydrological sections and of the stations during the south-west monsoon.

line connecting adjoining oxygen minima of the curve. Curves illustrating this principle for salinity maxima have been published (Rochford 1964*b*, Fig. 7). In the absence of evidence to the contrary, it is assumed that an increase in oxygen at depths below 200 m cannot have a biological explanation and must be caused by the horizontal advection and mixing of waters richer in oxygen. It is assumed that such waters in the Arabian Sea must have an external origin.

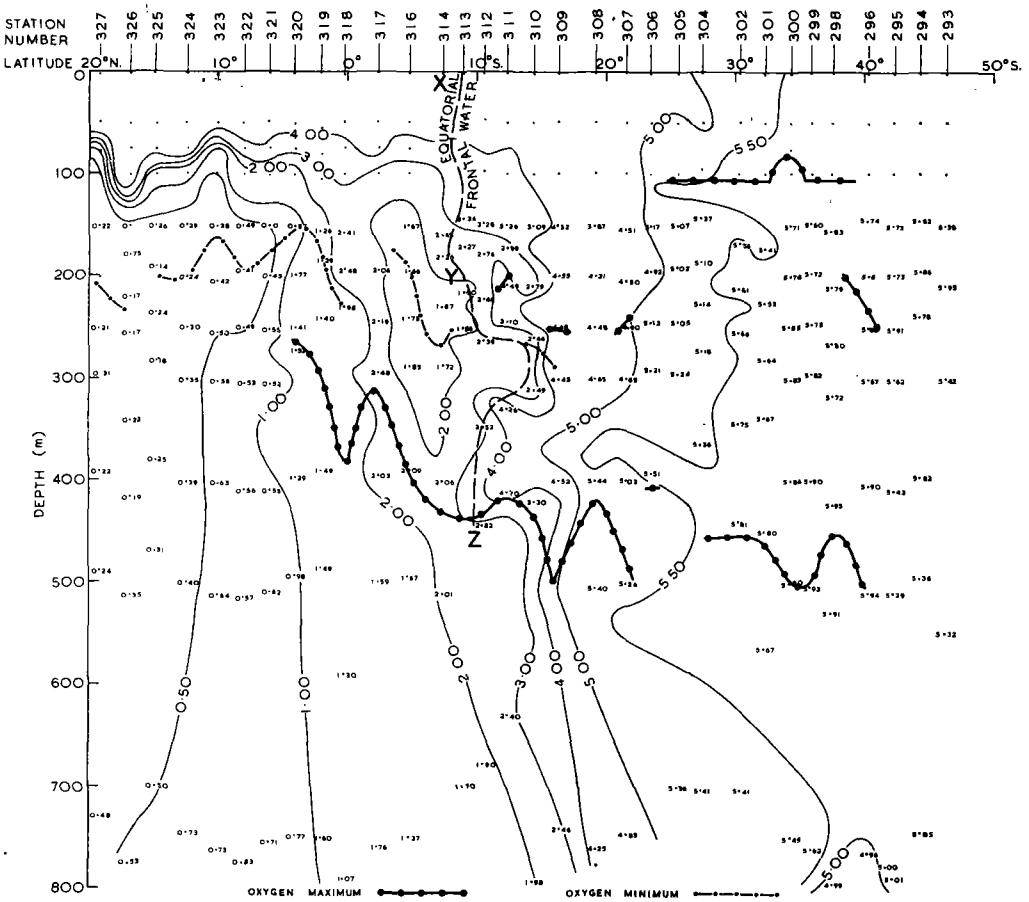

Fig. 2.—Oxygen (ml/l) distribution along Section 1 (*Ob*, 1956–57).

III. Oxygen Maxima and Hydrological Structure

Before examining the oxygen maxima of the Arabian Sea it is necessary to look at the oxygen maxima that occur in the Indian Ocean as a whole. This will show what relations, if any, exist between these oxygen maxima and such features as bands of salinity maxima and minima, whose water mass origin can be identified. One would expect such relations, since subsurface oxygen maxima can be maintained only by horizontal advections; these occur in the Indian Ocean principally within layers defined by a salinity maximum or minimum. The relations between oxygen maxima and hydrological structure along the three selected meridional sections (Fig. 1) are

then used to group and classify the various oxygen maxima of all station data (Fig. 1) of the Indian Ocean during the south-west monsoon. Finally, the distribution of oxygen and other properties of each of these groups of oxygen maxima is studied along certain sections, to show the principal routes of movement.

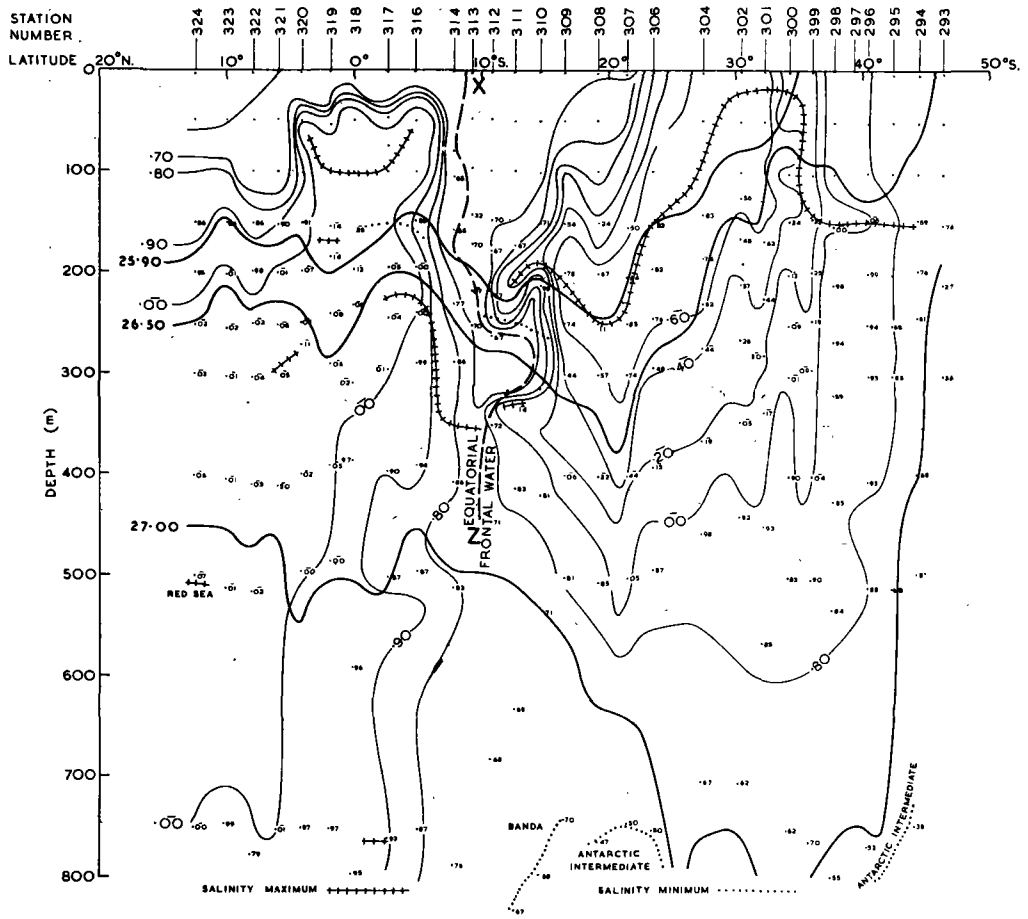

Fig. 3.—Salinity distribution along Section 1 (*Ob*, 1956–57). In this and other figures containing salinity values the following notation will be used: S‰ between 34·00 and 34·99‰—without the 34·00 prefix; S‰ between 35·00 and 35·99‰—without the 35·00 prefix and remainder barred.

(*a*) *Section 1* (Fig. 1)

An oxygen maximum layer, with approximately uniform oxygen content, occurred at 450–500 m at all stations between 10 and 42°S. (Fig. 2) except Station 305. As shown in Figure 2, north of 10°S., the concentration of this oxygen maximum layer decreased sharply (Fig. 2), and its depth decreased to about 250 m at 5°N. This almost continuous oxygen maximum layer, from about 40°S., will be subsequently referred to as the subtropical oxygen maximum. The origin, and therefore the nomenclature of this layer, is in doubt. Wyrtki (1962) considers it principally of Antarctic Polar Front origin, whilst Rochford (1960) claims that it originates at the Subtropical Convergence.

Along Section 1 (Fig. 2), this oxygen maximum first appears around 40°S., without any continuity with surface waters, and at a depth some 300 m above the Antarctic Intermediate salinity minimum (Fig. 3). It maintains a similar depth and relatively high content of oxygen to about 10°S. (Fig. 2). The Antarctic Intermediate salinity minimum, however, has disappeared by about 20°S. (Fig. 3), and therefore cannot transport the oxygen-rich waters above it beyond 20°S. It is therefore proposed to consider this subtropical oxygen maximum layer as a separate water mass.

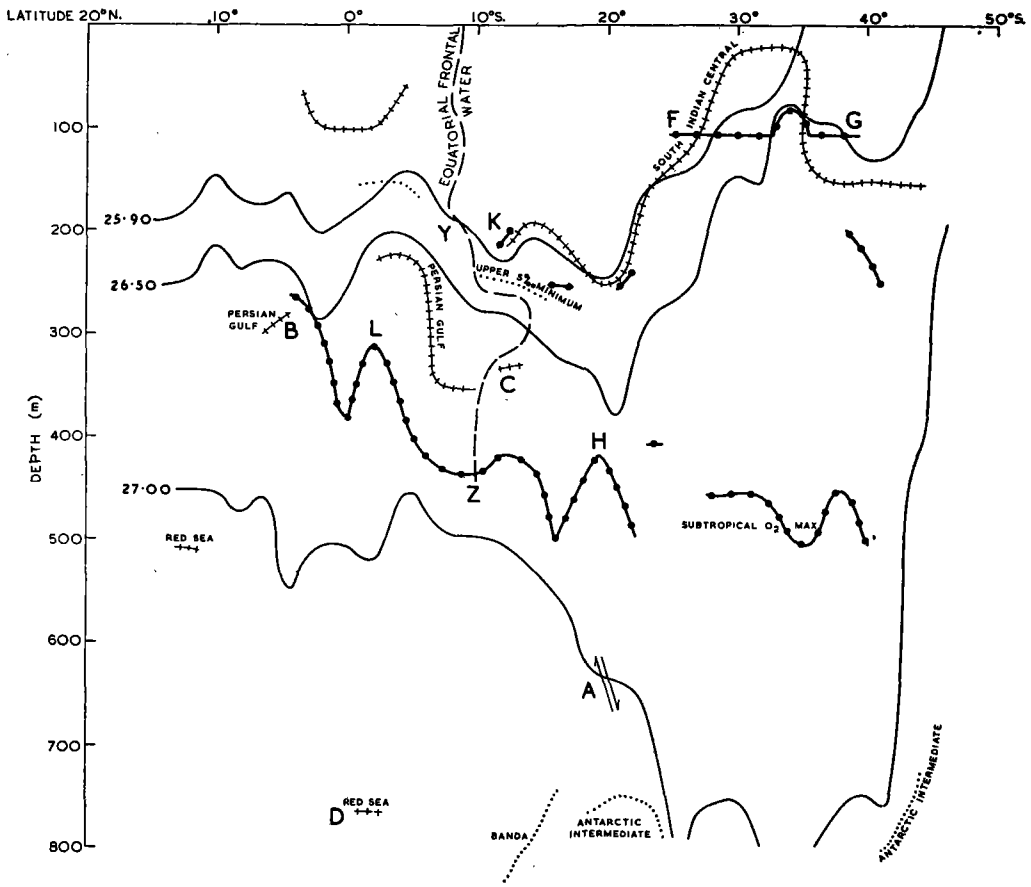

Fig. 4.—Principal structural features of the hydrology along Section 1.

Along this section there occurred a salinity maximum which showed highest values at the surface around 30°S. and which extended north and south at depths of 100–300 m (Fig. 3). This maximum was caused by the spreading of the south-east Indian high salinity water (Rochford 1964*a*), which forms the eastern end of the subtropical high salinity gyre with the general name of south Indian Central water. For convenience, any high salinity water from any part of this subtropical region will be called south Indian Central in this paper.

The northern limit of south Indian Central water along Section 1 was found at about 10°S. within a low salinity column which will be called Equatorial Frontal

water. This Frontal water occurred just south of the northern boundary of the south Equatorial current which from the elevation and depression of the 25·90 and 26·50 σ_t surfaces was located between stations 316 and 307 (Fig. 4). North of the south Equatorial current, Persian Gulf water was found as a salinity maximum to about 10°N. Comparison of the position of the oxygen maxima of Figure 2 with those of the various water mass layers of Figure 3 shows that the subtropical oxygen maximum

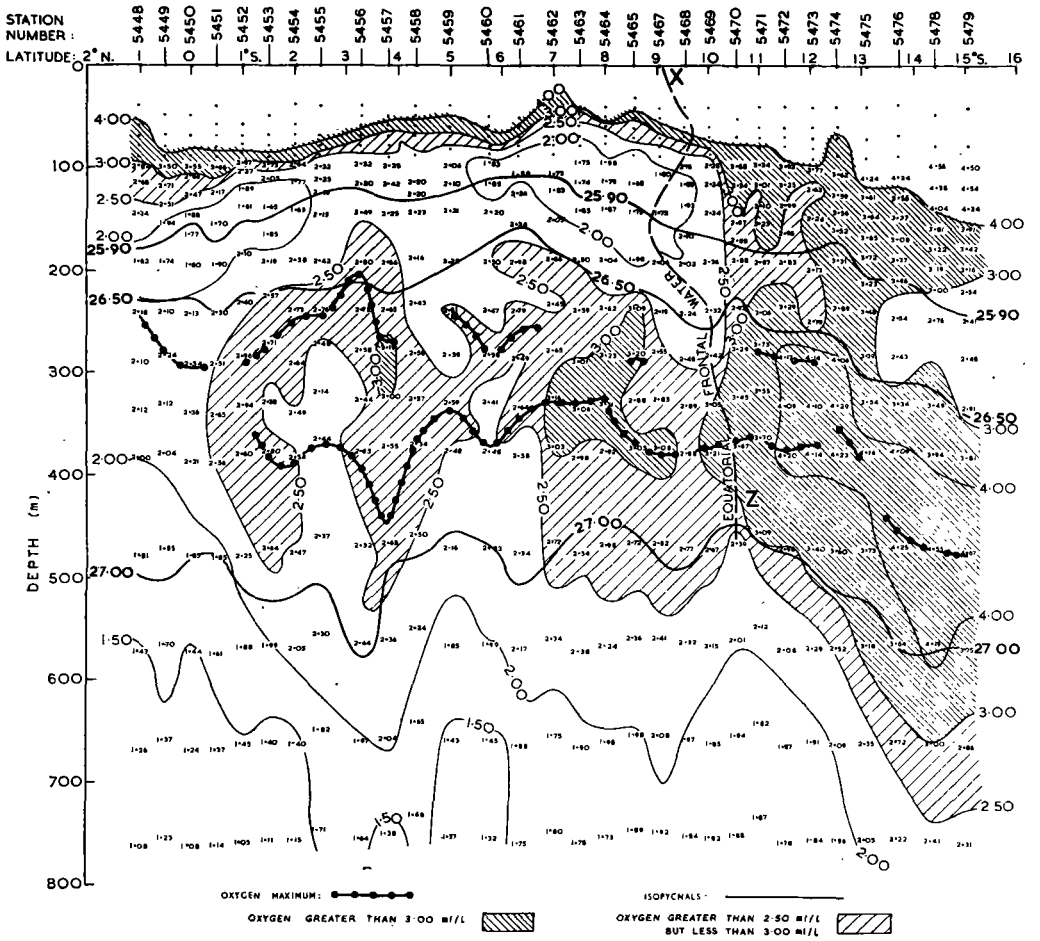

Fig. 5.—Oxygen (ml/l) distribution along Section 2 (*Discovery II*, 1964). Close shading indicates an oxygen value greater than 3·00 ml/l; open shading indicates an oxygen value greater than 2·50 but less than 3·00 ml/l.

occurred at a depth between the south Indian Central water above and the Antarctic Intermediate below, south of the Equatorial Frontal water. North of 10°S. this oxygen maximum is uplifted some 200 m and eventually merges with the Persian Gulf water mass at around 5°N. South Indian Central water was sometimes at the same depth as an oxygen maximum (Fig. 4).

(*b*) *Section 2* (Fig. 1)

In the west Indian Ocean, the subtropical oxygen maximum had oxygen values greater than 4 ml/l, south of 10°S. (Fig. 5). At this latitude, as in the east Indian Ocean (Fig. 3), a vertical column of low salinity water (Fig. 6) marked the position of the Equatorial Frontal water. North of this Frontal water, oxygen maxima occurred at every station but at greatly different depths and densities (Fig. 5). The oxygen concentration in the oxygen maxima north of 10°S. was greater along Section 2 than along Section 1 (Figs. 2 and 5). This difference is attributed to a stronger northward transfer of oxygen-rich waters along Section 2, where the salinity shows (Fig. 6) a much weaker Equatorial Frontal water barrier than along Section 1 (Fig. 3).

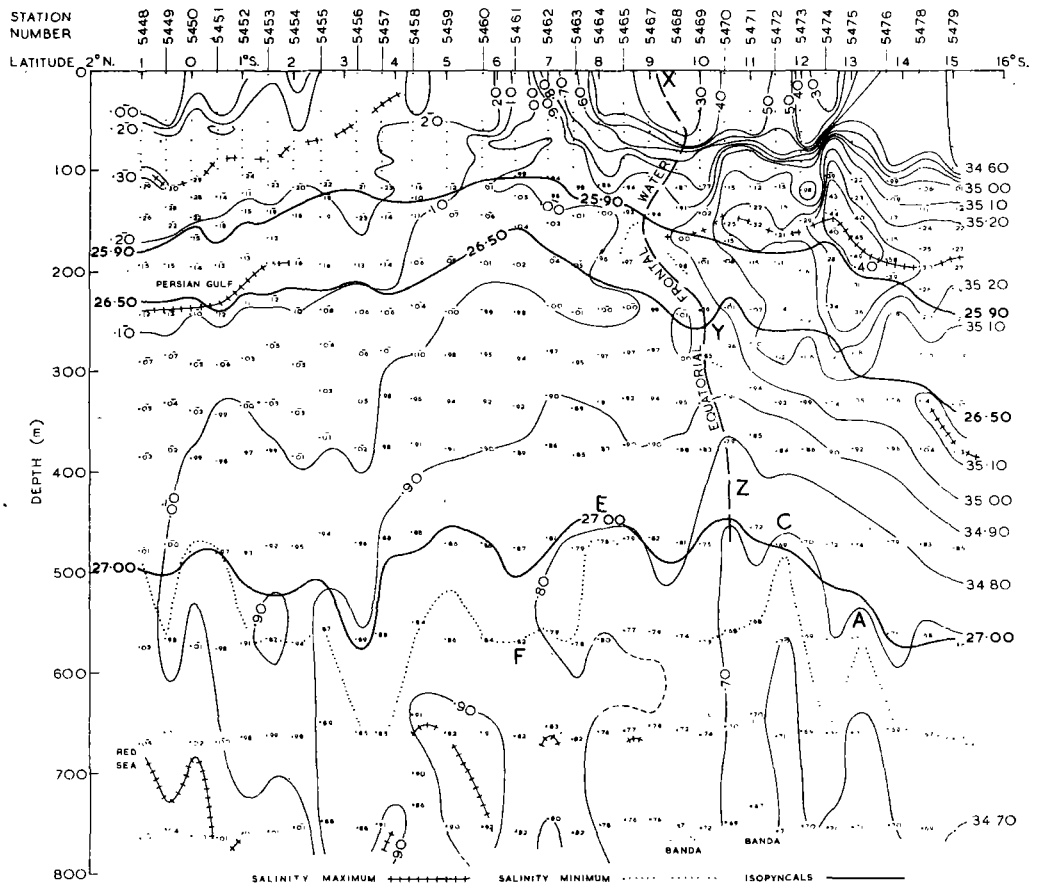

Fig. 6.—Salinity distribution along Section 2 (*Discovery II*, 1964).

South Indian Central water was found as a high salinity layer south of 10°S. (Fig. 6). In contrast to the previous section (Fig. 3), Persian Gulf water did not occur south of about 2°S. (Fig. 6). The doming of the 26·50 σ_t surface at 6°S. (Fig. 7) indicates the northern boundary of the south Equatorial current. The Equatorial Frontal water occupies the same relative position within the south Equatorial current as in the east (Fig. 4). An almost continuous salinity minimum from the southern

to the northern limits of this section, at about the depth of the 27·00–27·20 σ_t surfaces (Fig. 6), was caused by northward spreading of Antarctic Intermediate waters. Below this salinity minimum, a salinity maximum at around 700–800 m was formed by Red Sea water. There was little agreement (Fig. 7) between the depths at which the various identifiable water masses (Fig. 6) and oxygen maxima (Fig. 5) occurred, except around 1°N. where oxygen maxima merged into the Persian Gulf water mass.

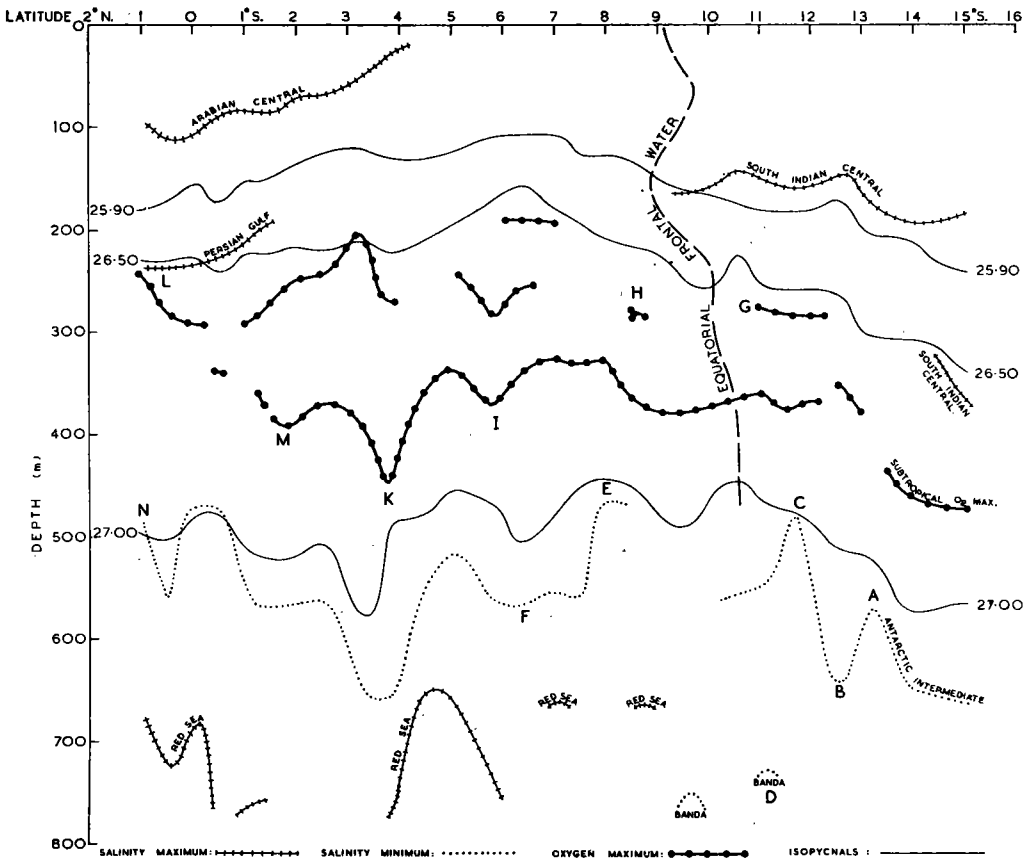

Fig. 7.—Principal structural features of the hydrology along Section 2.

(*c*) *Section 3* (Fig. 1)

In the west Indian Ocean along the 58°E. meridian, the single branch of the subtropical oxygen maximum, at about 300 m at the south end of the section, became separated into at least three branches further to the north (Fig. 8). The upper of these branches occurred near the depth of the 25·90 σ_t surface, the middle near the 26·50 σ_t surface, and the lower near 26·80 σ_t. An almost continuous salinity minimum (Fig.9) between 3°S. and 11°N. occurred near σ_t 26·80. Persian Gulf water occurred near the 26·50 σ_t surface, between 10 and 13°N., and at several stations between 3 and 6°N. near the 26·80 σ_t surface (Fig. 9). Antarctic Intermediate waters were found as a salinity minimum near the 27·20 σ_t surface in the south between 1°N. and 4°S. Further

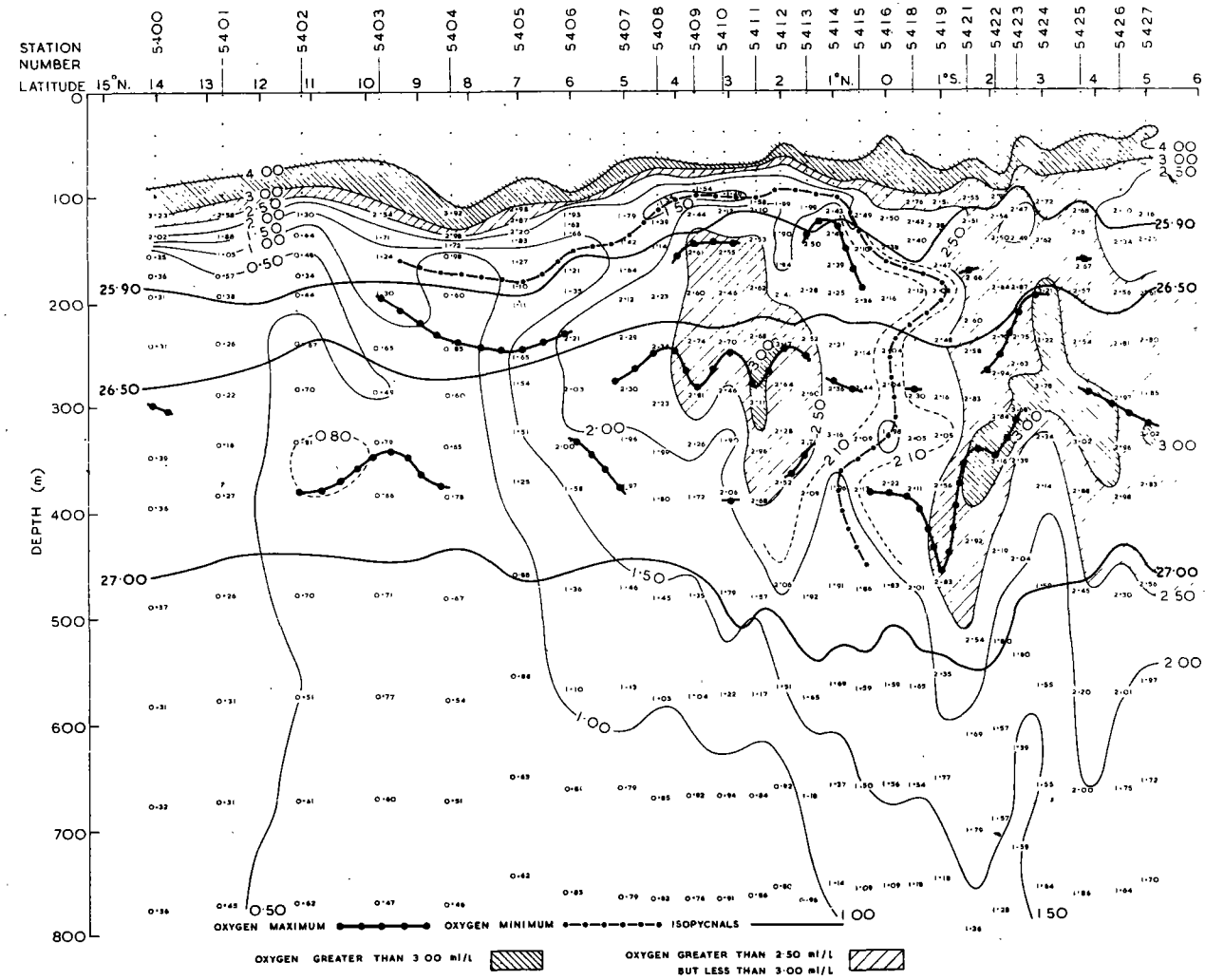

Fig. 8.—Oxygen (ml/l) distribution along Section 3 (*Discovery II*, 1964). Close shading indicates an oxygen value greater than 3·00 ml/l; open shading indicates an oxygen value greater than 2·50 but less than 3·00 ml/l.

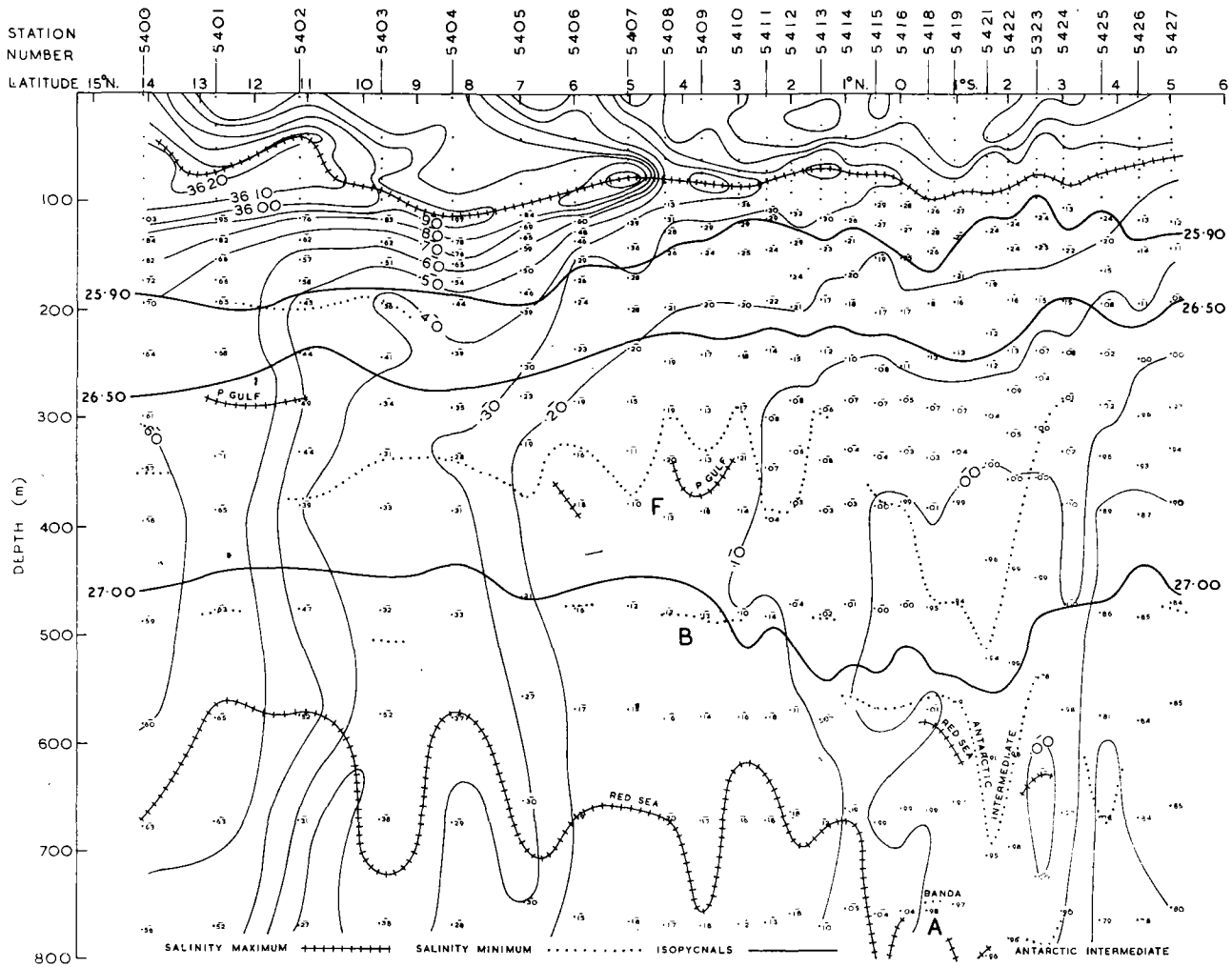

Fig. 9.—Salinity distribution along Section 3 (*Discovery II*, 1964).

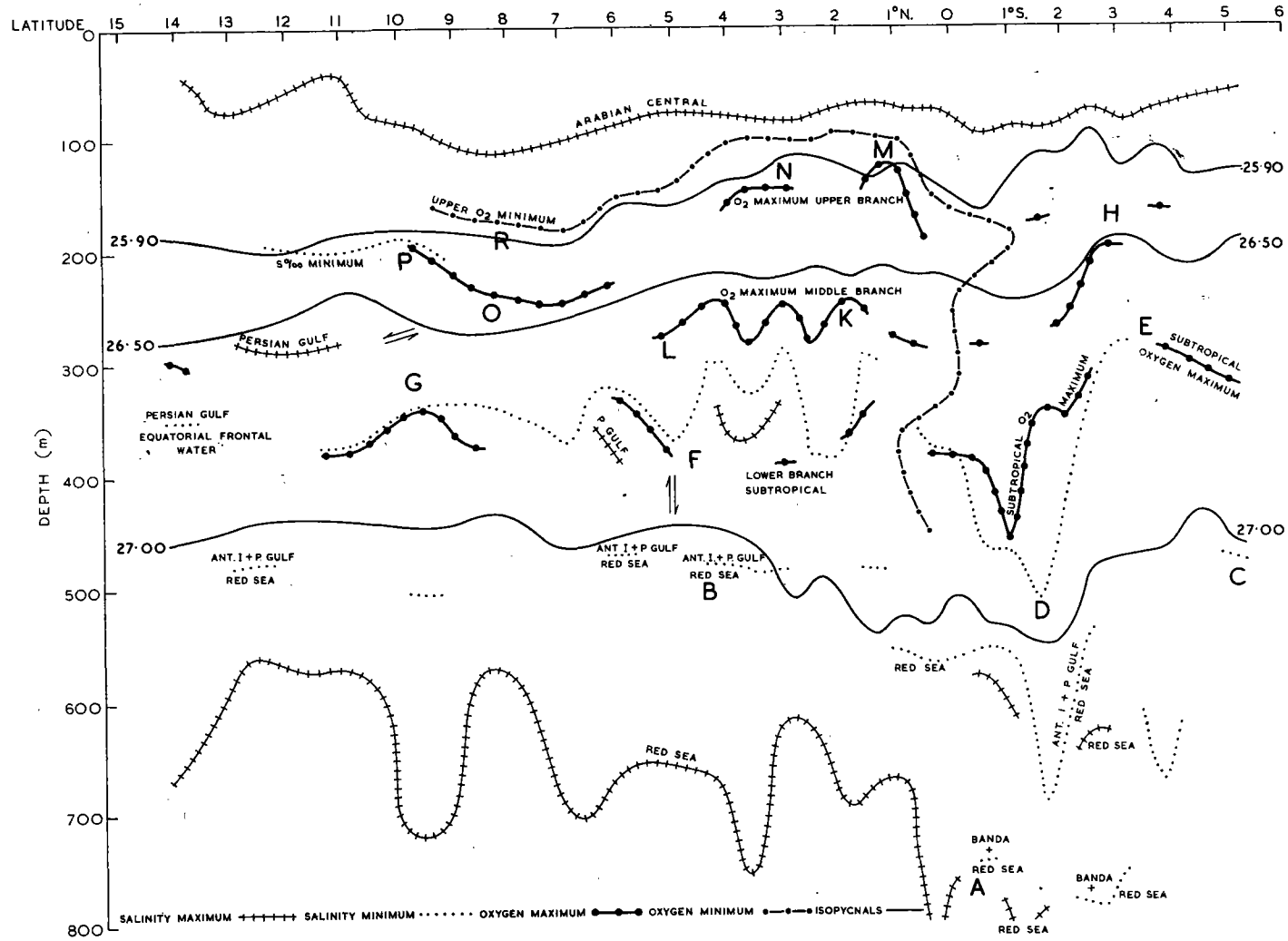

Fig. 10.—Principal structural features of the hydrology along Section 3.

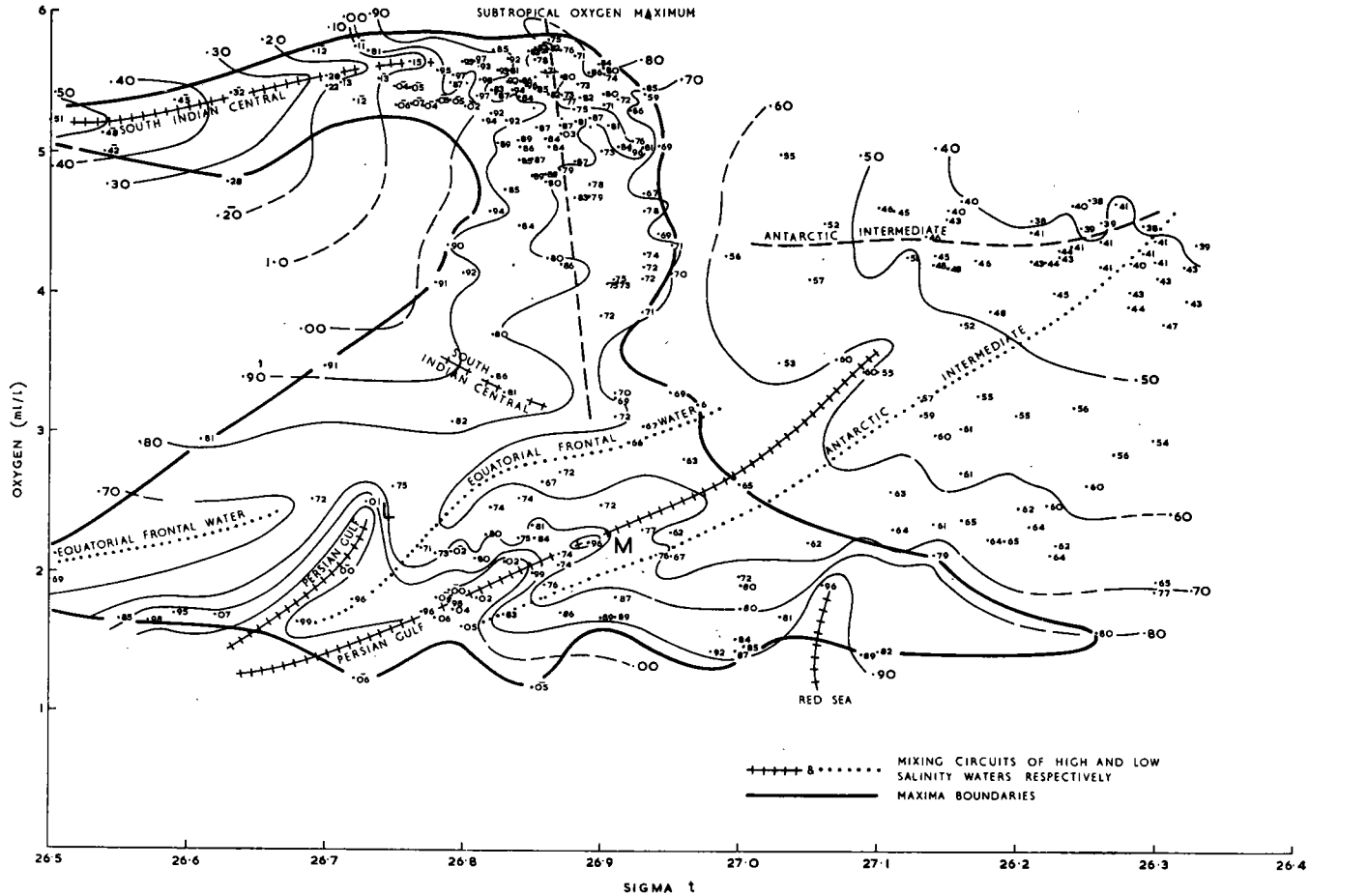

Fig. 11.—The salinity (‰) of the σ_t–oxygen relations of oxygen maxima north of 35°S. in the east Indian Ocean, where σ_t was greater than 26·50. Values outside the boundaries of these oxygen maxima show oxygen and salinity in relation to σ_t of the Antarctic Intermediate salinity minimum.

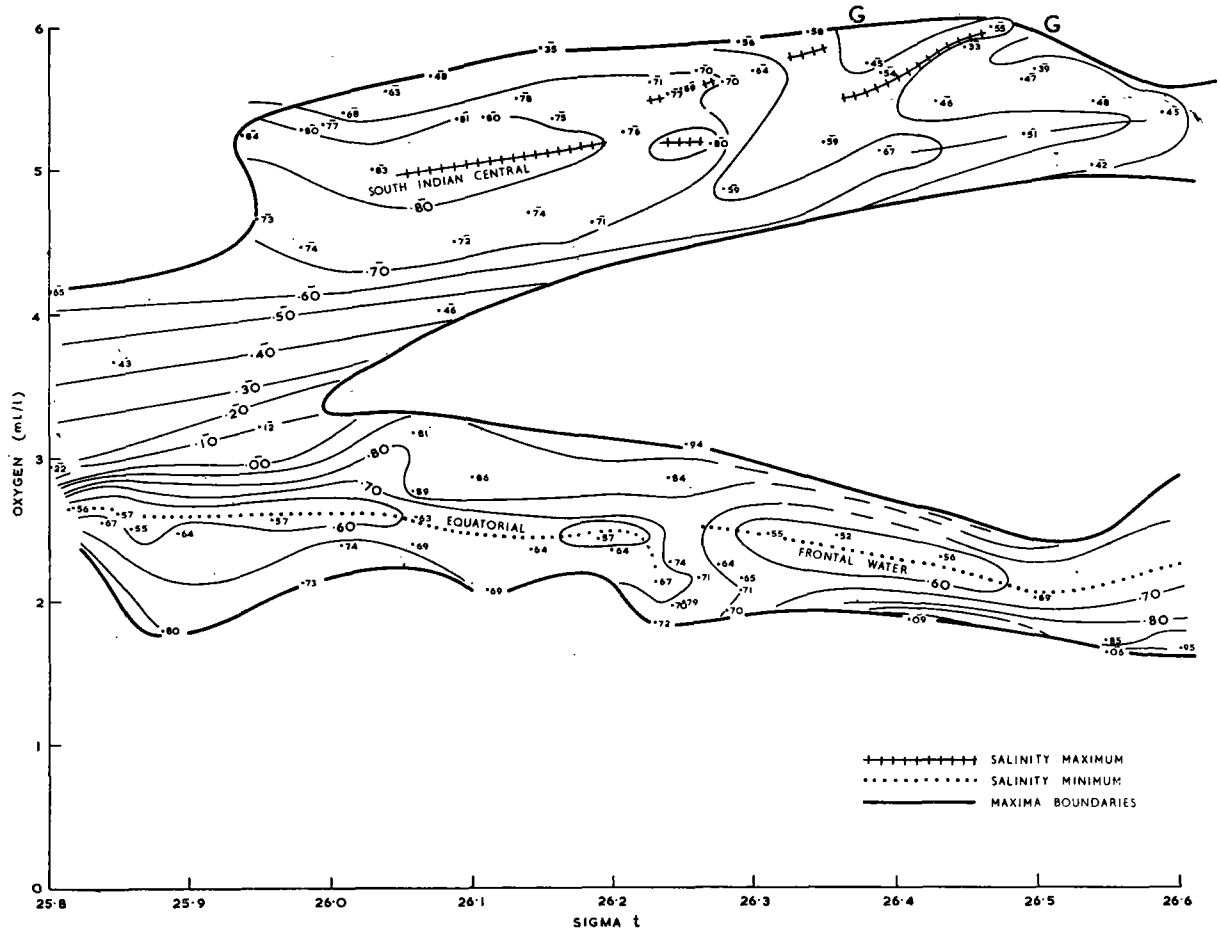

Fig. 12.—Salinities as for Figure 11, of oxygen maxima with σ_t less than 26·60.

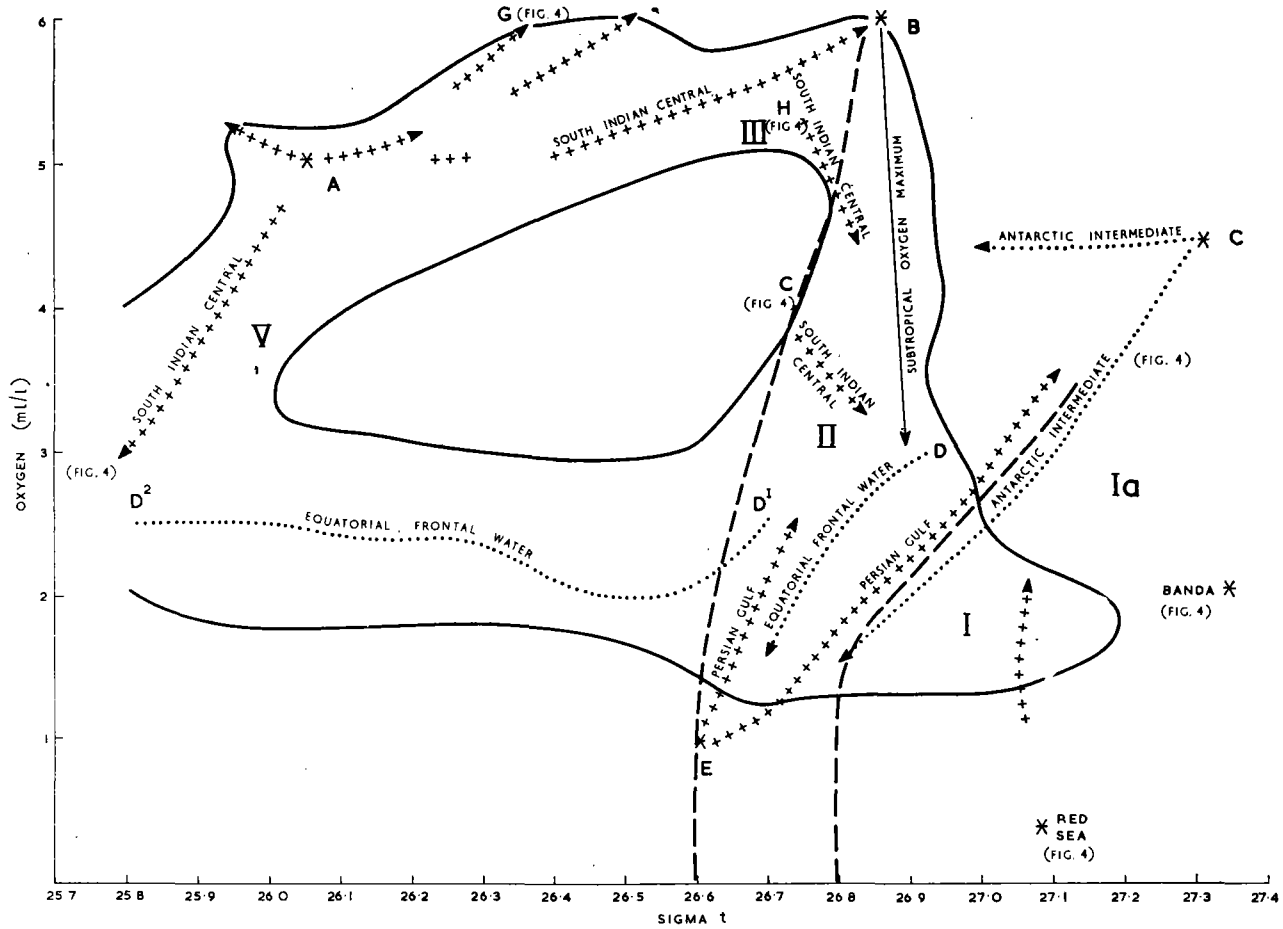

Fig. 13.—A simplification of the principal mixing features of Figures 11 and 12 and of the principal water masses involved. *A*, South Indian Central; *B*, subtropical oxygen maximum; *C*, Antarctic Intermediate; *D*,D^1,D^2, Equatorial Frontal water; *E*, Persian Gulf; I, I*a*, II, III, and V indicate mixing groups examined in Section V of this paper.

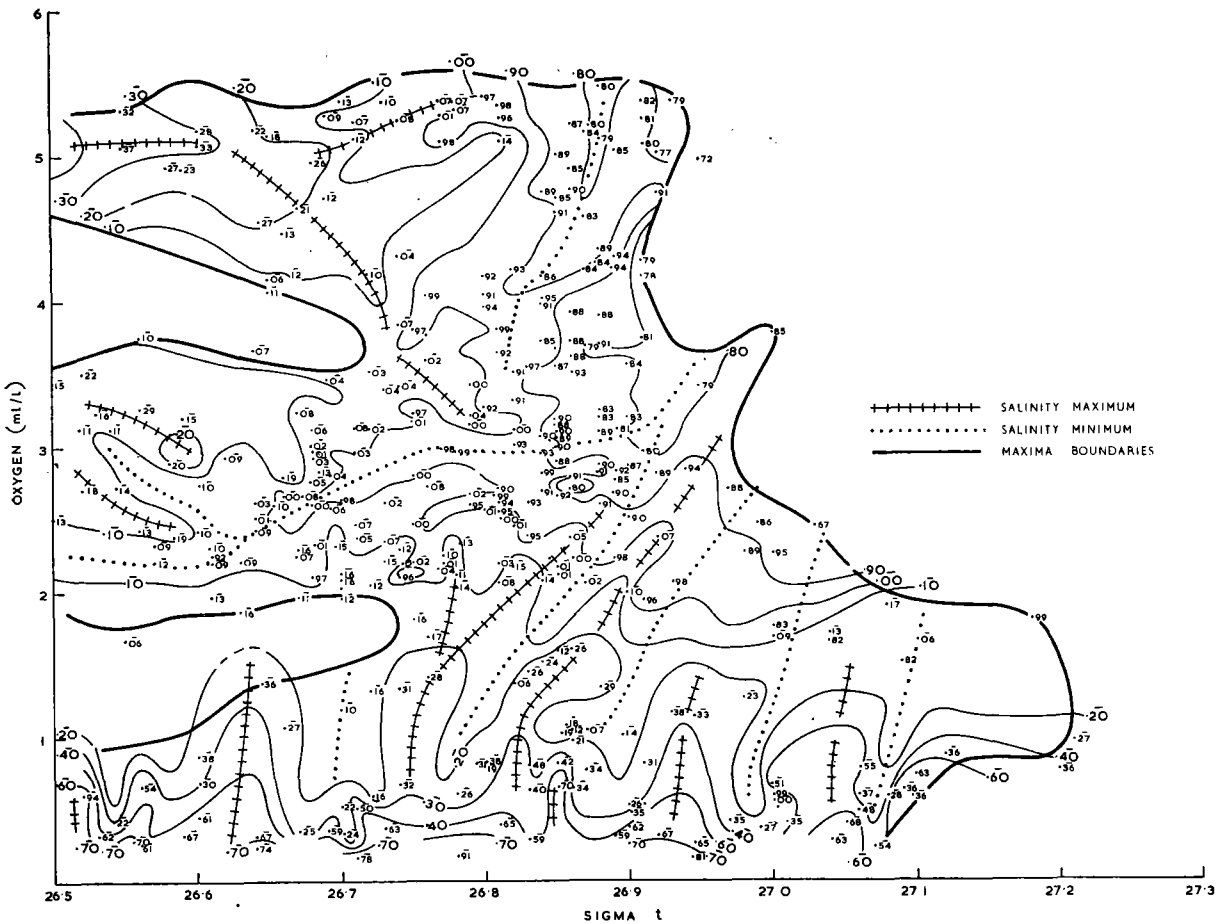

Fig. 14.—Salinities as for Figure 11 of oxygen maxima of the west Indian Ocean.

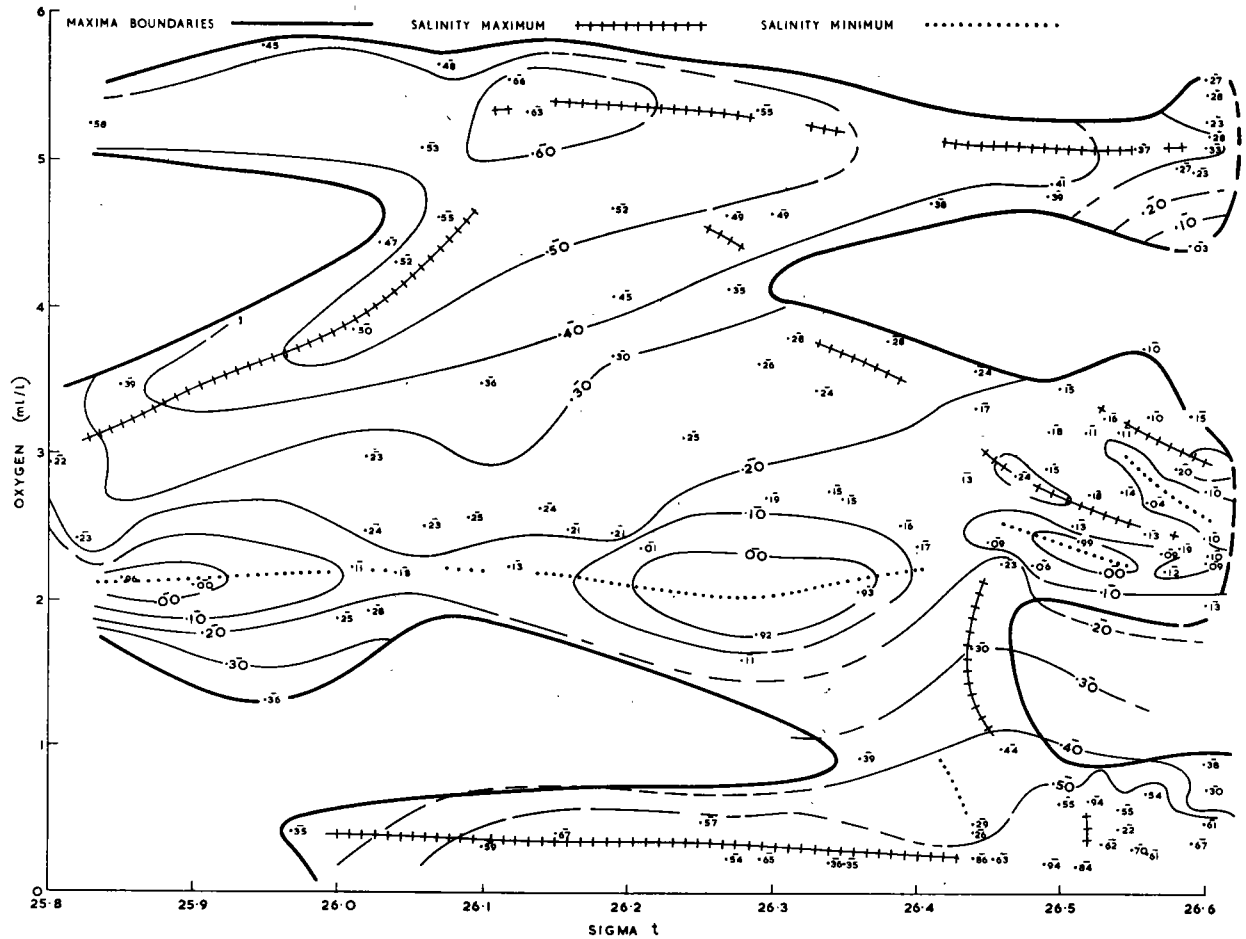

Fig. 15.—Salinities as for Figure 12 of oxygen maxima of the west Indian Ocean.

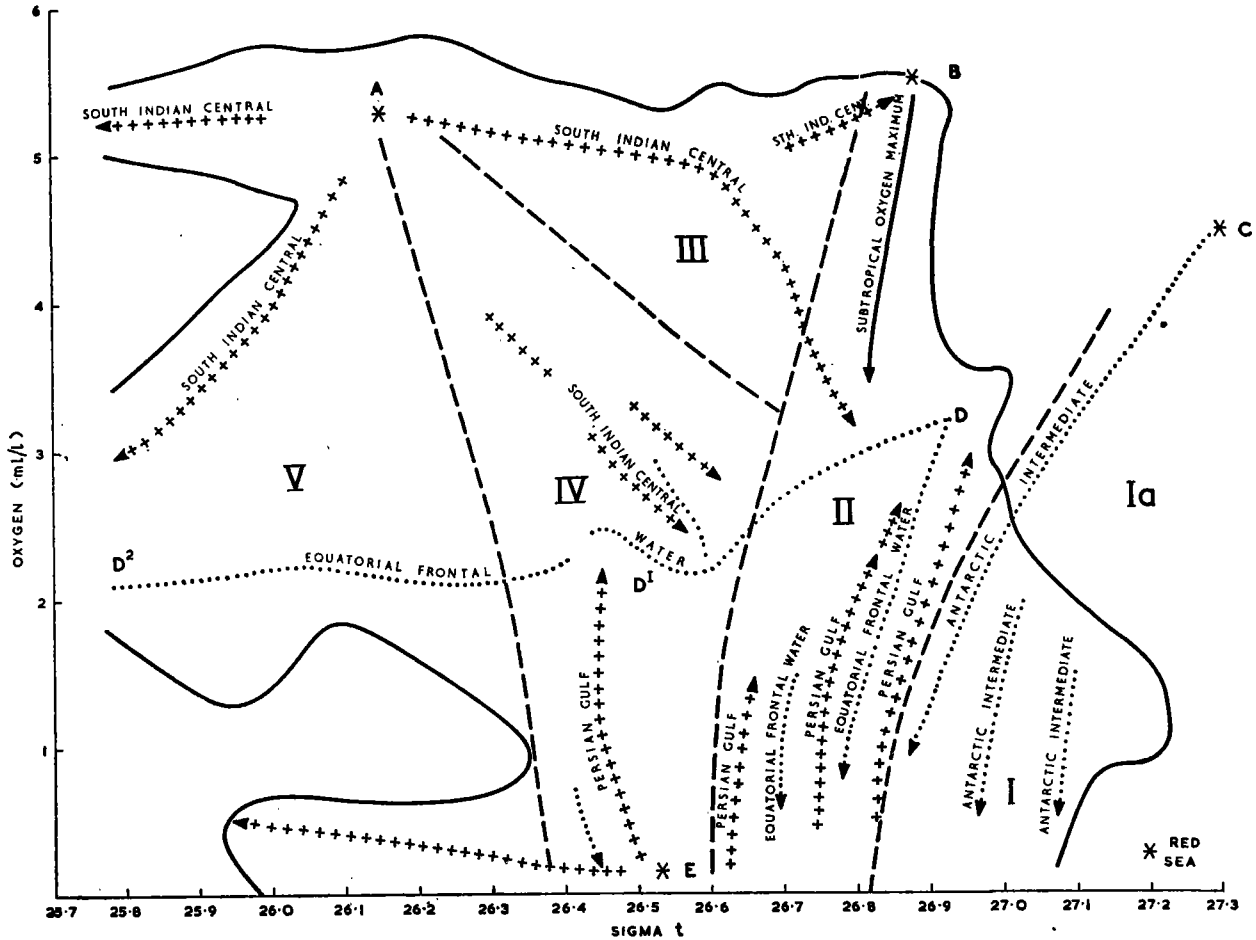

Fig. 16.—A simplification of the principal mixing features of Figures 14 and 15 and of the water masses involved; these have the same letter identification as in Figure 13. I, I*a*–V Denote mixing groups examined in Section V of this paper.

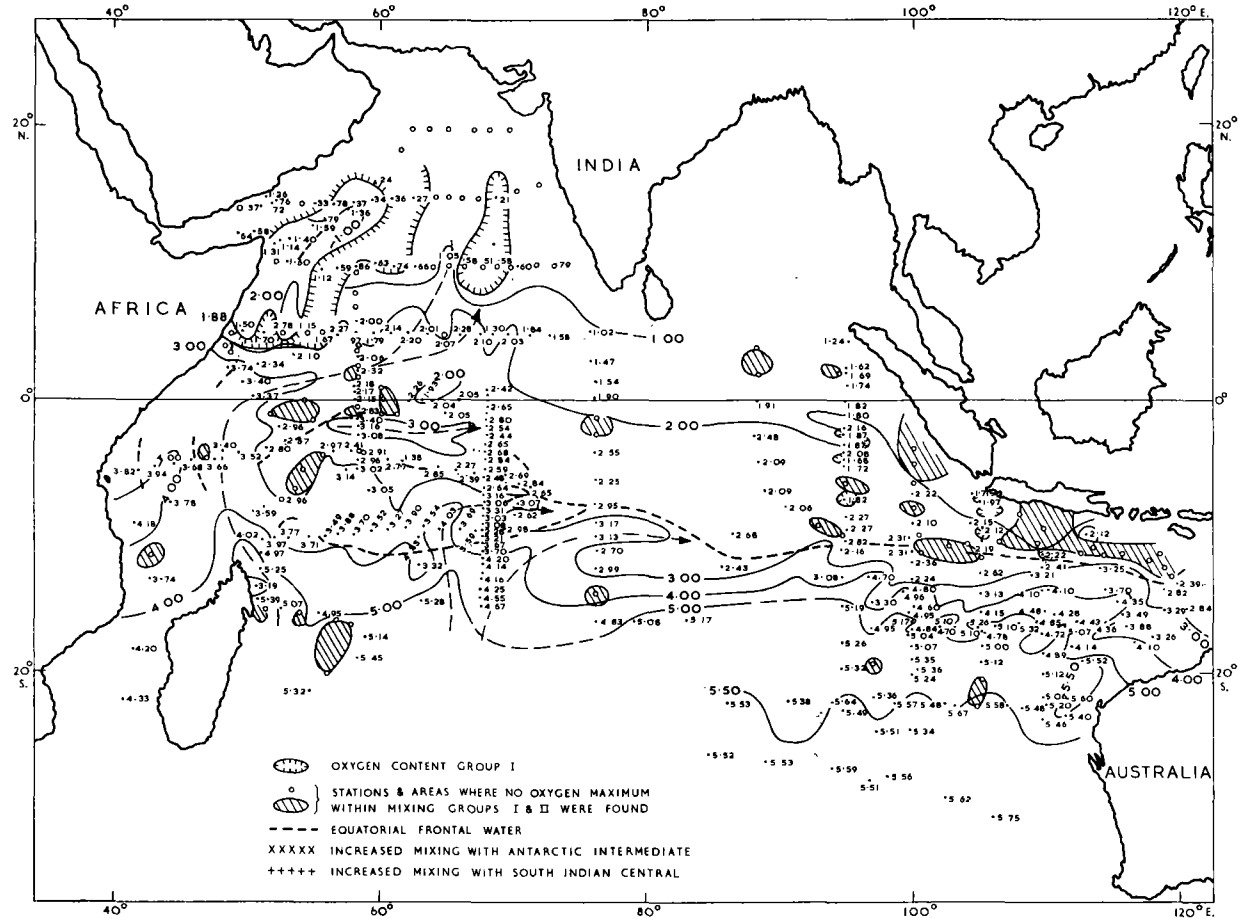

Fig. 17.—Oxygen content (ml/l) of the oxygen maxima within mixing groups I and II of Figures 13 and 16.

to the north, however, only isolated regions of such water, with σ_t values more than 27·00, were encountered (Fig. 9). A continuous layer of Red Sea water at between 600–800 m occurred northward from the equator (Fig. 9). The depth of the lower branch of the subtropical oxygen maximum coincided quite often with that of the salinity minimum around 26·80 σ_t (Fig. 10). The other branches of this oxygen maximum did not, however, show any affinity with the salinity structure, except near 10°N., where the upper branch merged into a salinity minimum.

IV. Water Masses Associated with the Oxygen Maxima of the Indian Ocean

Figures 2–10 show that north of the Equatorial Frontal water and extending into the Arabian Sea, a number of oxygen maxima occurred at different σ_t values. In some cases these maxima were associated with a salinity maximum or minimum. The origin of waters forming these oxygen maxima was determined, therefore, by the use of both σ_t (for the initial separation into groups) and salinity (for the water mass identification within these groups). This was done by (1) plotting the oxygen concentration of all oxygen maxima of the Indian Ocean (Fig. 1) against their σ_t (e.g. Fig. 11); (2) superimposing upon the position of each oxygen maximum of such a diagram (e.g. Fig. 11), the salinity of the oxygen maximum. These salinity values were then contoured to show bands or areas of high or low salinity, whose water mass source was identified by use of Figures 2–10. For convenience the oxygen maxima of the Indian Ocean were divided into an eastern group (east of 80°E.) and a western group. These groups were further subdivided into oxygen maxima with σ_t less than 26·50 and those with σ_t greater than 26·50.

(*a*) *Eastern*

In the east Indian Ocean (Figs. 11 and 12), two sources of well-oxygenated water, the south Indian Central (mean σ_t 26·10, Fig. 12) and the Subtropical oxygen maximum (mean σ_t 26·85, Fig. 11), spread towards the equator and mixed almost isentropically with the upper and lower parts of the Equatorial Frontal water (Figs. 11 and 12). This mixing provides the source of the oxygen maxima at various σ_t values within the column of Equatorial Frontal water. North of this Frontal water, oxygen maxima are mostly found within mixtures of Persian Gulf and Equatorial Frontal water (*L* and *M*, Figs. 4 and 11), or Persian Gulf and Antarctic Intermediate water (Fig. 11). At σ_t values greater than 27·00, a small number of oxygen maxima was formed by the mixing of Red Sea and Antarctic Intermediate waters. Oxygen maxima formed by the mixing of Antarctic Intermediate and Persian Gulf waters did not occur below σ_t 26·80 (Fig. 11). This agrees with the limit of 26·90, previously determined (Rochford 1963), for Antarctic Intermediate water in this eastern region. To facilitate comparison with the western Indian Ocean, the principal mixing circuits (based upon salinity) of Figures 11 and 12 were combined into a single simplified diagram (Fig. 13).

(*b*) *Western*

Figures 14 and 15 show that the salinity–oxygen–σ_t relations of oxygen maxima in the west Indian Ocean. Figure 16 summarizes the principal mixing circuits. Comparison of Figures 13 and 16 shows that, whereas mixing of south Indian Central

and Equatorial Frontal waters at σ_t values around 25·80 and 26·80 occur throughout, mixing of these waters at around σ_t 26·60 was a feature of the west Indian Ocean only. Oxygen maxima within a σ_t range of 26·00–26·60, and oxygen 3–4 ml/l were therefore found only in the west Indian Ocean. These maxima formed the middle branch of the oxygen maxima of Section 3 (Fig. 10). The shallow oxygen maxima of both the east and west Indian Oceans (Figs. 13 and 16), however, were formed by the mixing of south Indian Central and Equatorial Frontal waters in both cases. North of the Equatorial Frontal water in the west Indian Ocean, semi-isentropic mixing of Persian Gulf and this Frontal water occurred around σ_t 26·40–26·50 (Fig. 16). In the Arabian Sea mixing of Persian Gulf and Red Sea water masses formed a series of waters with σ_t values between those of the two parent water masses. These mixed so-called Persian Gulf waters spread southward (according to the salinity contours, see Fig. 14) and mixed with a northward movement of Equatorial Frontal water on about the same σ_t surfaces (Fig. 16). At σ_t values greater than 26·90, however, the Equatorial Frontal water was not present and Antarctic Intermediate water became the source of the low salinity water contributing oxygen to the Arabian Sea (Fig. 16). This Antarctic Intermediate water mixed with Persian Gulf water above and Red Sea water below. Along Section 3 this Intermediate water formed the almost continuous salinity minimum extending northward to 6°N. and beyond (Fig. 10).

V. Mixing Transport of Oxygen from the South to the North Indian Ocean

Figures 13 and 16 show that oxygen maxima with σ_t values less than 26·90 in the Indian Ocean north of the Equatorial Frontal waters are formed by a spreading northward of Frontal waters richer in oxygen, and by their near-isentropic mixing with a southward-spreading Persian Gulf or mixtures of Persian Gulf and Red Sea water masses. The upper layers of these Equatorial Frontal waters receive oxygen by near-isentropic mixing with south Indian Central at σ_t 25·80 (east Indian Ocean), and at σ_t values of 25·80 and 26·50 (west Indian Ocean). The deep layers of these Frontal waters receive oxygen by isentropic mixing with waters of the subtropical oxygen maximum. At σ_t values greater than 26·90, oxygen maxima in the Arabian Sea are formed by the spreading northward and mixing of Antarctic Intermediate waters with the Red Sea water mass below and the Persian Gulf water mass above. Oxygen maxima formed by the advection of these various waters into the north Indian Ocean and Arabian Sea have been divided into Groups I–V (Figs. 13 and 16), centred about these principal mixing circuits. The geographic distribution of oxygen maxima from mixing groups I, II and IV shows the location of the waters involved (Part V), and of their probable movements (Part VI).

(*a*) *Group I* (Figs. 13 and 16)

Oxygen maxima of this mixing group occurred east of the Somali coast along a strip running north-east from 5 to 15°N. near the mouth of the Gulf of Aden, and towards the west coast of India between 10 and 15°N. (Fig. 17). In general these maxima had greater salinities (Fig. 18), and occurred at greater depths (Fig. 19) than maxima of mixing Group II adjoining them. In the east Indian Ocean, only a small number of oxygen maxima of mixing Group I (Fig. 13) was found south of Java and west of Sumatra. Oxygen values within this mixing group off the Somali coast decreased

northward. Those in the east Indian Ocean decreased westward (Fig. 17). These changes in oxygen concentration in conjunction with a general increase in salinity in the same direction (Fig. 18) indicate that the oxygen maxima of Group I are formed by a northward movement of Antarctic Intermediate water into the north Arabian Sea, and by a north-westward movement in the east Indian Ocean towards the equator. However, the exceptionally high oxygen and low salinity values of this oxygen maximum at one station close to the central Arabian coast can be caused only by a stronger and more direct movement of Antarctic Intermediate water into the Gulf of Aden than Figure 18 shows during the south-west monsoon. During the north-east monsoon, surface currents move Arabian Sea water into the gulf and it is probable that intensification of the movement of Antarctic Intermediate water in the same direction occurs during this season. (See also Part VI of this paper.)

(*b*) *Group II* (Figs. 13 and 16)

The oxygen content of these maxima was greater, north of about 15°S., in the west than in the east Indian Ocean (Fig. 17). A tongue of waters with relatively high oxygen maximum values was found along the Somali coast and to the north-east towards the central Arabian coast (Fig. 17). Salinities within this oxygen-rich tongue were relatively low (Fig. 18), because of the accumulation of Equatorial Frontal water. Lower salinity values of oxygen maxima along the south-west coast of India (Fig. 18), on the other hand, were found in waters of low oxygen and are of a different mixing origin. Salinities of Group II (Fig. 13) show a fairly wide but clearly defined zone of Equatorial Frontal waters in the east Indian Ocean, which can be traced with little change in salinity or latitudinal position to about 85°E. West of this longitude the zone of minimum salinity, characteristic of these Equatorial Frontal waters, increases in salinity, narrows and finally bifurcates into a number of branches which terminate around 50°E. However, low salinities within the oxygen maxima of Group II (Fig. 16), at isolated stations along the Somali coast (Fig. 18), indicate that a northward movement of these Frontal waters must occur.

The depths of the oxygen maxima of Group II (Figs. 13 and 16) generally decreased northward (Fig. 19) except along the zone of Equatorial Frontal water, where the oxygen maxima were found at a greater depth than immediately north or south. This increase in depth of the oxygen maximum in the vicinity of a zone of Equatorial Frontal water occurred just to the south (Station 5456, Fig. 7) or just to the north (Station 5421, Fig. 10) of regions where a maximum vertical separation of the 26·50 and 27·00 σ_t surfaces occurred. This separation indicates a zonal flow in these regions between these two σ_t surfaces. This deepening of the oxygen maximum is thought, therefore, to be caused by intensified zonal flow of Equatorial Frontal waters.

(*c*) *Group IV* (Figs. 13 and 16)

Oxygen maxima of this mixing group occurred between 10°S. and 10°N. when west of 60°E., but between 0 and 10°S. only, from 60°E. to 80°E. (Fig. 20). Maxima of this mixing group were absent from the east Indian Ocean. The oxygen content (Fig. 20), together with the salinity (Fig. 21) of these maxima, identified regions in which south Indian Central, Equatorial Frontal water and Persian Gulf water pre-

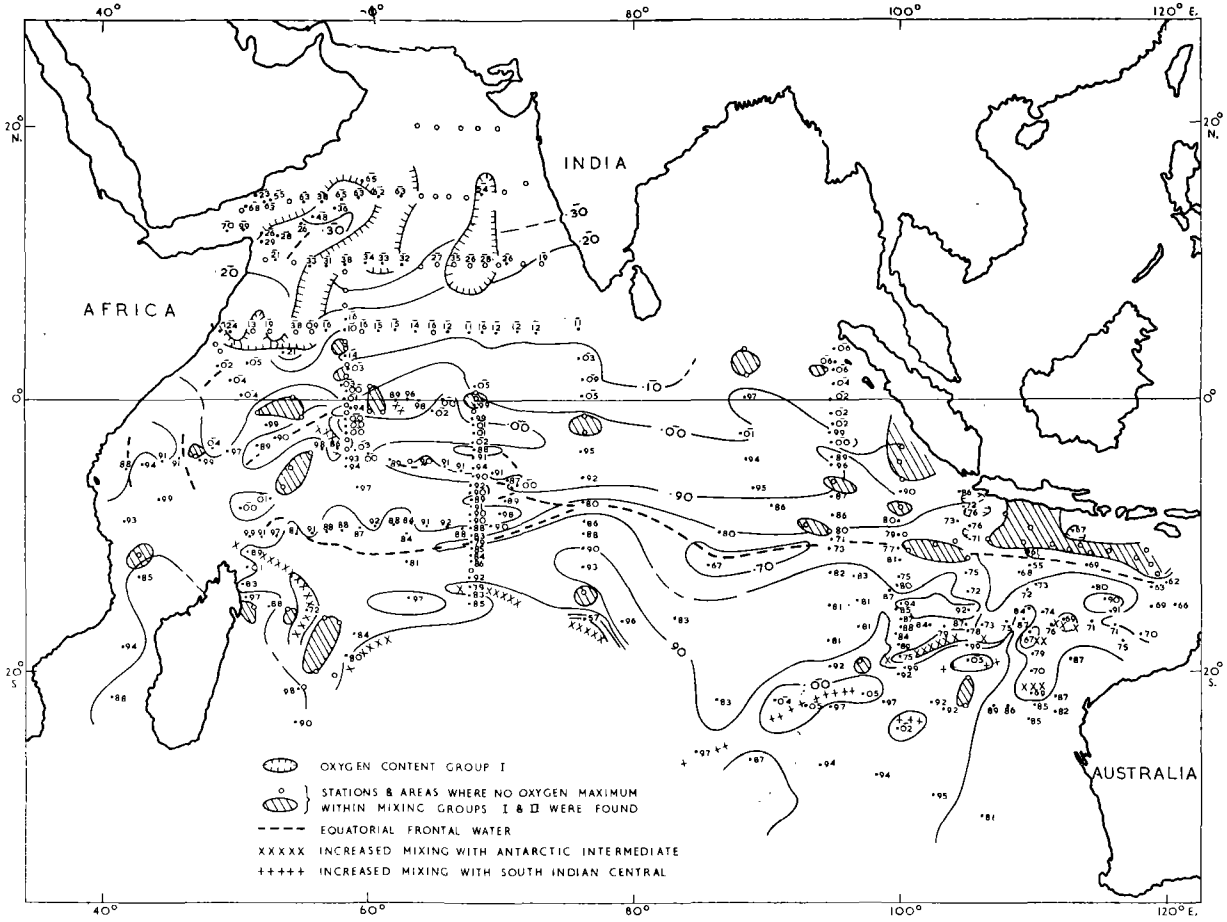

Fig. 18.—Salinities of the oxygen máxima of Figure 17.

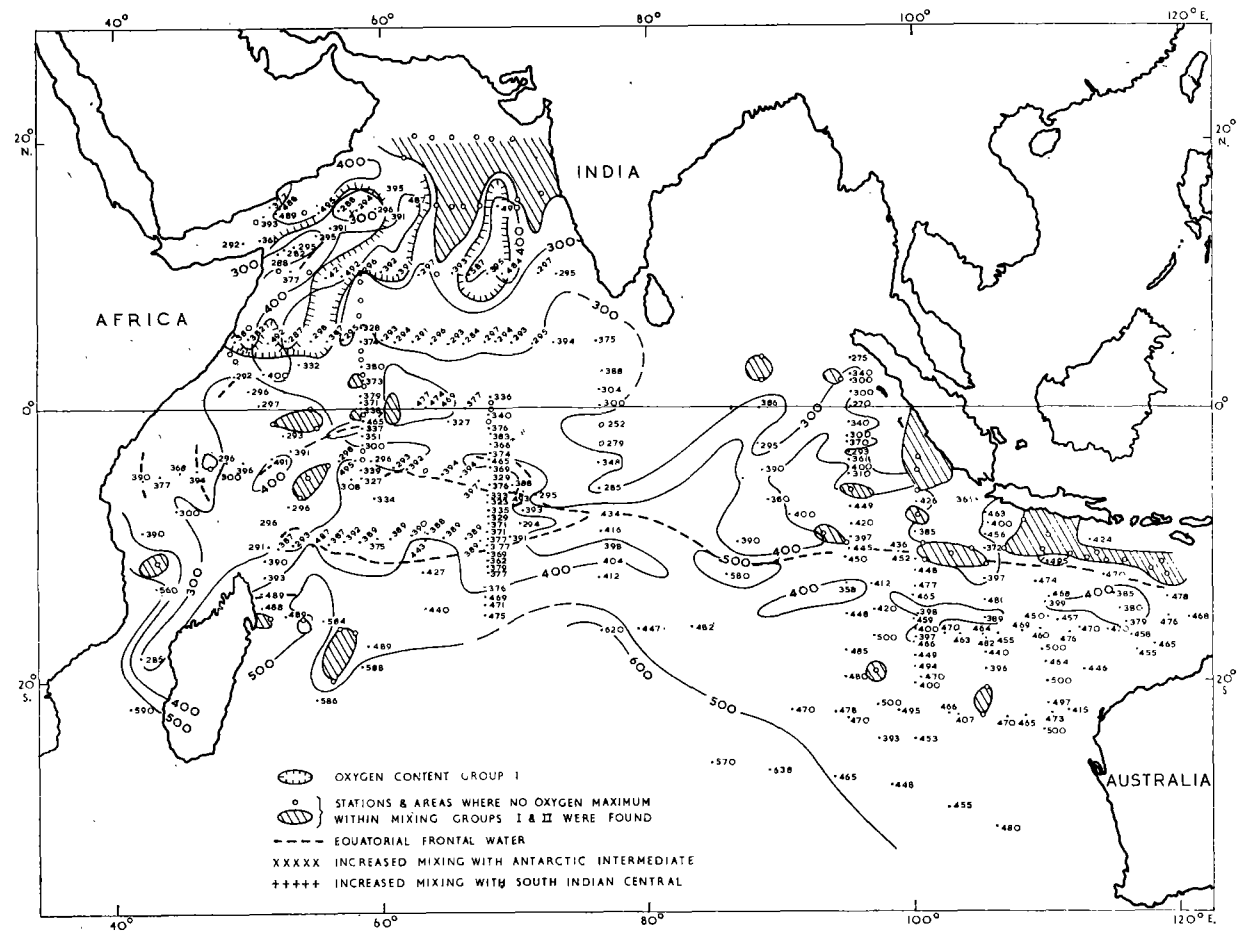

Fig. 19.—Depth (m) of the oxygen maxima of Figure 17.

dominated (Fig. 21). Based upon this identification and the source regions of these waters, directions of movement have been deduced (Fig. 21). Direct current measurements were made along the 58°E. section at the time of working that stations upon which Figures 20 and 21 are based. The zonal velocity section between 3°S. and 3°N. shows (Swallow 1964) a westward movement of about 25 cm per sec at about 200 m between 0 and 1°S. in agreement with the direction of movement based upon hydrological structure (Figs. 20 and 21) at 200–250 m (Fig. 22). At about 2°N. on this same

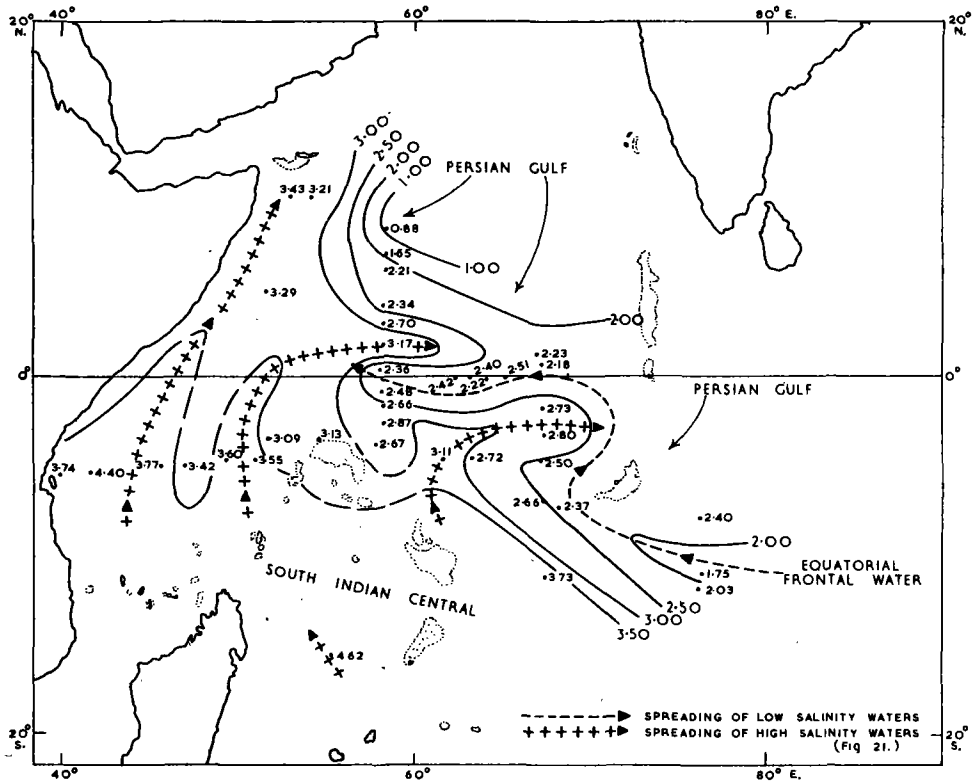

Fig. 20.—The oxygen content (ml/l) of the oxygen maxima within mixing group IV (Figs.13 and 16).

section measured velocities were zero or easterly in direction at 200 m in agreement with the direction of movement shown in Figure 22. At 200 m between 1°N. and 1°S. Swallow's (1964) measured currents between 58 and 68°E. were to the west and south-west. These currents again agree in direction with the inferred movement of Equatorial Frontal waters along the Equator (Fig. 22). At about 3°S. Swallow (1964) found no currents at 200 m along 68°E. in the region where an easterly flow of south Indian Central waters was indicated at the appropriate depth (Fig. 22).

VI. Circulation of Oxygen-enriching Water Masses

Figure 23 shows the principal circulation paths during the south-west monsoon (deduced from Figs. 17, 18, 20, and 21), of the water masses that enrich the oxygen content of the Arabian Sea within the 200–600 m depth range. The broad current

arrows indicate persistent surface currents with velocities of at least 25–50 cm per sec during September, which is the modal month of the observations of Figures 17–21. Equatorial Frontal waters at about 400 m are carried by the south Equatorial current (as indicated by broad surface current arrows) in one main branch as far as 75°E. (Fig. 23). Here these Equatorial Frontal waters separate into two branches. The northern branch follows a northern branch of the south Equatorial current to the Saya de Mahla Bank and mixes with the east-flowing waters of the subtropical oxygen

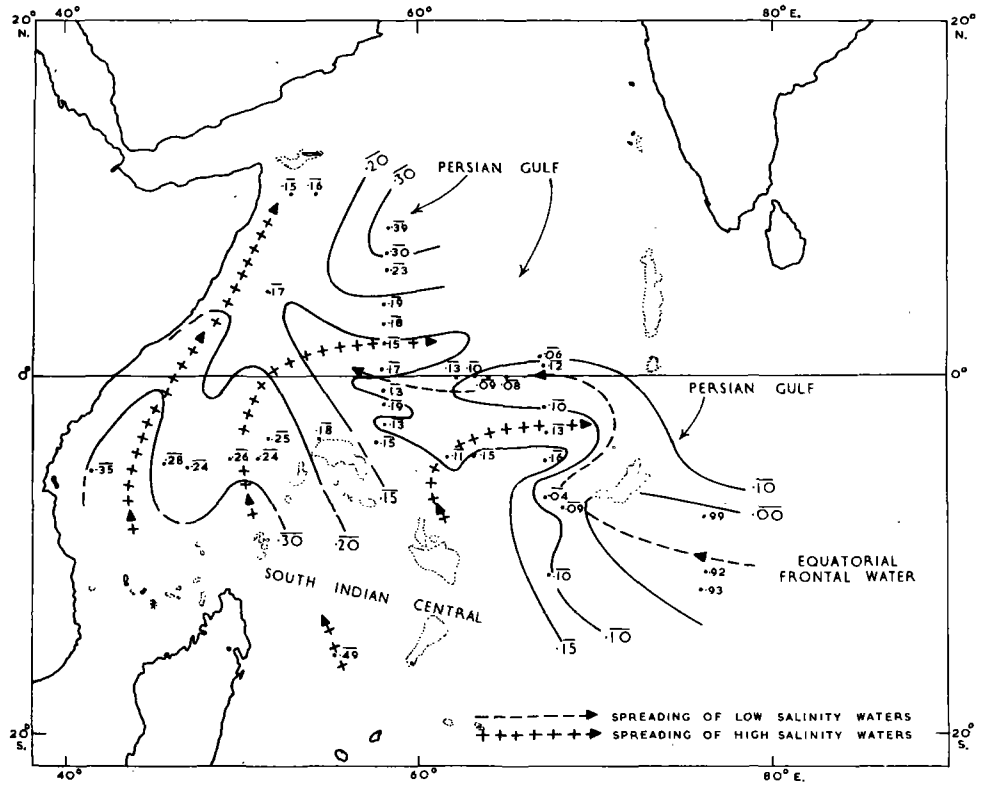

Fig. 21.—Salinity of the oxygen maxima of Figure 20.

maximum within the monsoon current at 2–5°S. The southern branch of this Frontal water follows the south Equatorial current as far as northern Madagascar. Here, this Frontal water mixes with a stream of north-flowing waters of the subtropical oxygen maximum, forming waters of relatively high oxygen content which spread north and north-east within the Somali current and the monsoon current, respectively, at depths of 300–400 m.

The middle zone of Equatorial Frontal waters at around 200 m mixes with south Indian Central waters between the Chagos Is. and the Saya de Mahla Bank to form waters of relatively high oxygen content. However, a stream of this Frontal water continues north at about 70°E. to the equator. Here it curves back to flow westward along the equator, in agreement with measured currents (page 21), but in opposition

to surface currents in September (Fig. 23). The apparent complexity of hydrological features in the Chagos Is.–Saya de Mahla Bank–Seychelles region could arise from the use of all data regardless of the month of sampling. Only seasonally representative data can decide the month by month sequence of ocean currents and water mass distribution in this region. Within the Somali and monsoon currents, oxygen maxima, at around 200–250 m, with σ_t values less than 26·50, are formed by the mixing of Equatorial Frontal waters and south Indian Central waters maintaining salinities below 35·20‰ (Fig. 21) and oxygen above 3·00 ml/l (Fig. 20). Elsewhere however, these

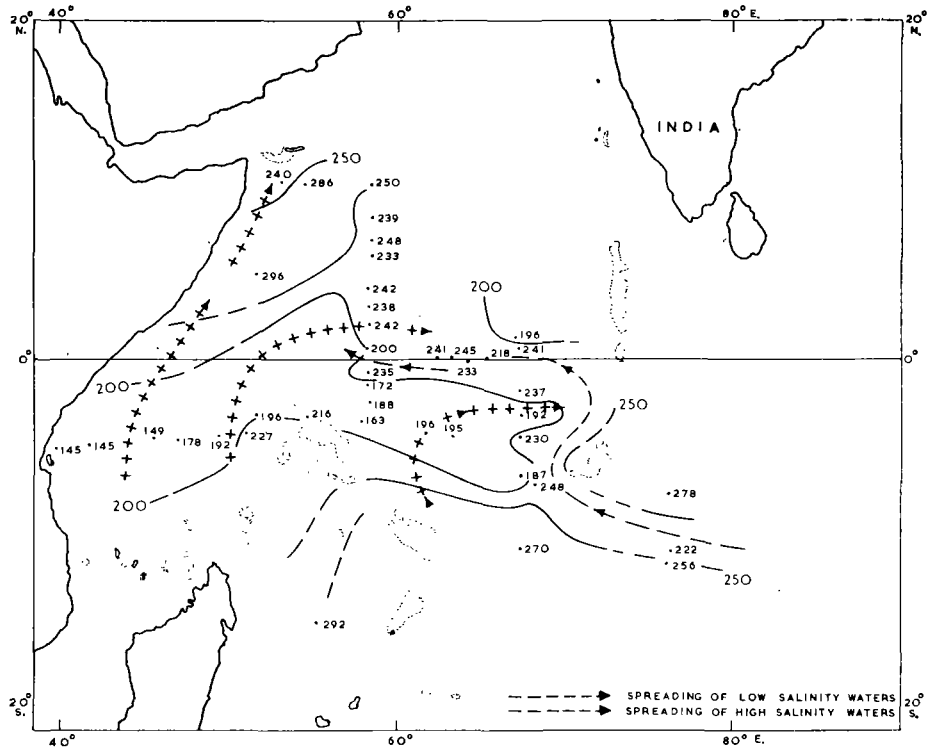

Fig. 22.—Depth (m) of the oxygen maxima of Figure 20.

mixed waters are absorbed into the general south-easterly spread of Persian Gulf waters (Rochford 1964*b*) and the resulting oxygen maxima are generally less than 2·50 ml/l. Figure 17 shows that some oxygen maxima in the central Arabian Sea and near the Gulf of Aden are formed by the mixing of Antarctic Intermediate water with Persian Gulf and Red Sea water masses.

Figure 24 shows the distribution of salinity of a salinity minimum, separated by its σ_t–oxygen relations from the salinity minimum formed by Equatorial Frontal waters, and considered, therefore, Antarctic Intermediate in origin. (Groups I and I*a* as distinct from Group II, Fig. 16). Although the station network allows other contour interpretations, it is thought that the separation of the northward spread of Antarctic Intermediate water into a number of district meridional paths (Fig. 24) is justified,

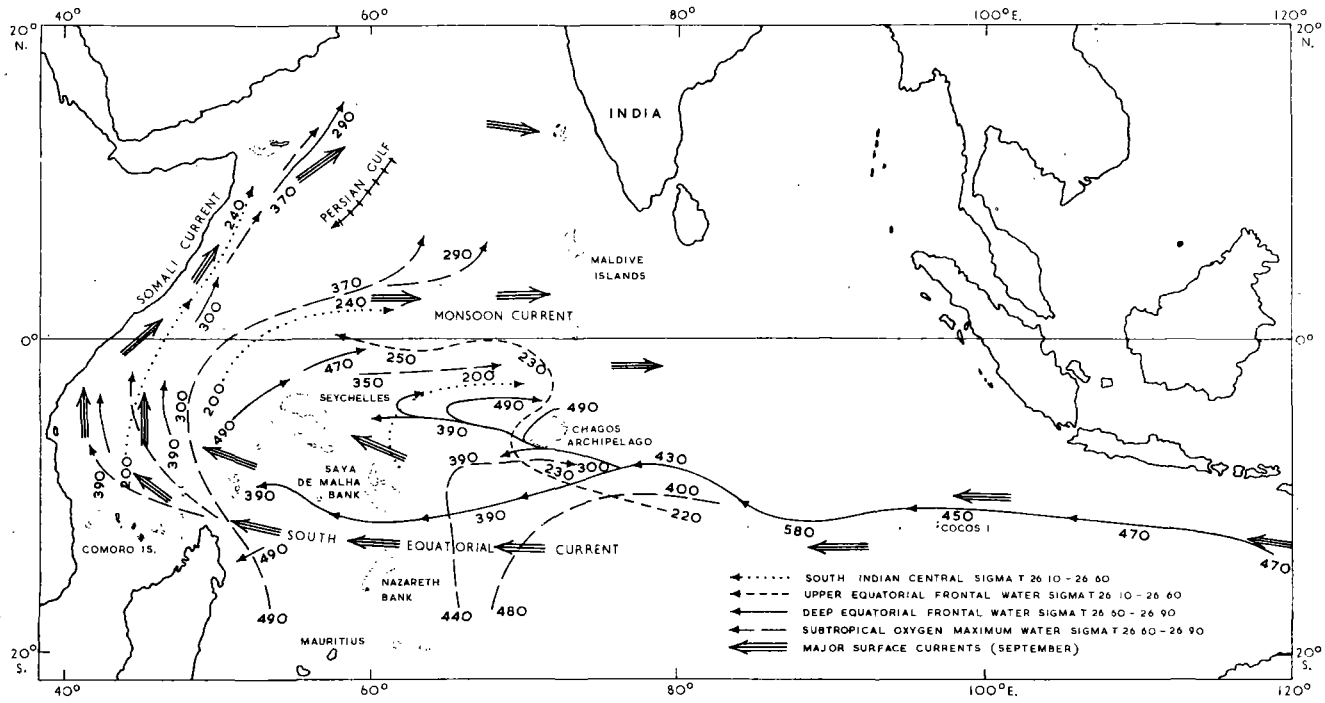

Fig. 23.—Circulation of the principal water masses carrying oxygen into the western Equatorial and Arabian Sea regions. Numbers along circulation paths indicate depth of the water mass at that point.

since a similar separation into alternate high and low salinity bands is found within the salinity pattern of the σ_t–oxygen relations of oxygen maxima (Fig. 18). Such meridional paths can persist only if the mixing involved is steady and continuous. This condition of mixing is indicated by the close agreement in salinity of this minimum

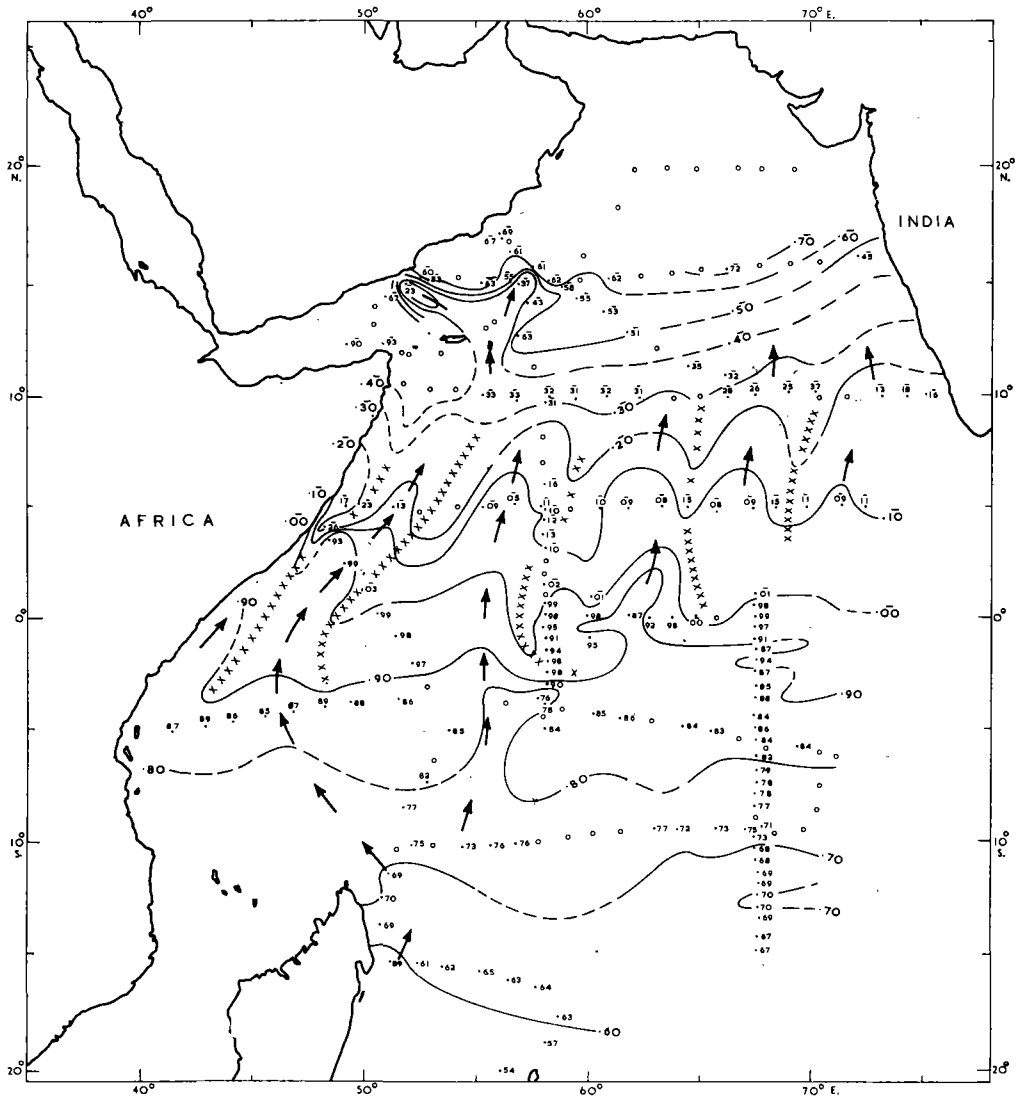

Fig. 24.—Salinity of a salinity minimum of Antarctic Intermediate origin. Lines of Stations north and south *Discovery II* (June 1964), east and west *Atlantis II* (August–November 1963).

(Fig. 24) at overlapping stations along the north–south section of *Discovery* (1964) and the east–west sections of *Atlantis* (1963). The exception to this state occurs along the Somali coast and east of the Gulf of Aden where north–south continuity of Antarctic Intermediate water cannot be shown (Fig. 24).

VII. Conclusions

(1) Three water masses from the south Indian Ocean and one from the east Indian Ocean are the external sources of oxygen-rich water of the Arabian Sea (200–600 m) during the south-west monsoon.

(2) Subtropical oxygen maximum water spreads northward on about the $26{\cdot}85\,\sigma_t$ surface, with little change in oxygen, to about 10°S. near the northern side of the west-flowing south Equatorial current. In the east Indian Ocean, waters of this subtropical oxygen maximum are absorbed into this current, but in the west Indian Ocean, streams of this water spread to the equator and beyond.

(3) South Indian Central water spreads northward along several σ_t surfaces. In the east Indian Ocean most of this spreading occurs within a σ_t band $25{\cdot}70$–$26{\cdot}10$ and terminates around 10°S. In the west Indian Ocean, however, spreading northward additionally occurs within a σ_t band $26{\cdot}10$–$26{\cdot}50$, carrying south Indian Central waters to the equator and beyond.

(4) Antarctic Intermediate low salinity water spreads northward within a σ_t band $26{\cdot}90$–$27{\cdot}30$, moving beneath the south Equatorial current and then between Persian Gulf above and Red Sea water below, to about 15°N. off the Arabian coast.

(5) Equatorial Frontal water occurs as a vertical band of low salinity water within the south Equatorial current at about 10°S. This water maintains about the same oxygen content throughout the Indian Ocean by a balance of mixing between it and the south Indian Central and subtropical oxygen maximum waters from the south and the Persian Gulf, and other waters of low oxygen content from the north. Streams of this Equatorial Frontal water mix with Persian Gulf water and form oxygen maxima in the central Arabian Sea, within a $26{\cdot}50$–$26{\cdot}90\,\sigma_t$ band.

VIII. References

Academy of Sciences, U.S.S.R. (1958).—I.G.Y. Reports of the complex Antarctic Expedition of the Academy of Sciences of the U.S.S.R. Hydrological, hydrochemical, geological, and biological studies. Research Ship *Ob*, 1955–56. (Hydro-Meteorological Publishing House: Leningrad.)

Academy of Sciences, U.S.S.R. (1959).—I.G.Y. Reports Second Oceanographic Expedition R.V. *Ob* (1956–57). (Publishing House of Marine Transport: Leningrad.)

Anon. (1960).—Data from *Vityaz* Cruise 31, 1959–60, on file at I.G.Y. World Data Centre *B*, Moscow, U.S.S.R.

CSIRO Aust. (1962*a*).—Oceanographical observations in the Indian Ocean in 1959. H.M.A.S. *Diamantina*, Cruise Dm 2/59. *CSIRO Aust. Oceanogr. Cruise Rep.* **1**.

CSIRO Aust. (1962*b*).—Oceanographical observations in the Indian Ocean in 1960. H.M.A.S. *Diamantina*, Cruise Dm 3/60. *CSIRO Aust. Oceanogr. Cruise Rep.* **4**.

CSIRO Aust. (1963).—Oceanographical observations in the Indian Ocean in 1960. H.M.A.S. *Diamantina*, Cruise Dm 2/60. *CSIRO Aust. Oceanogr. Cruise Rep.* **3**.

CSIRO Aust. (1964*a*).—Oceanographical observations in the Indian Ocean in 1961. H.M.A.S. *Diamantina*, Cruise Dm 3/61. *CSIRO Aust. Oceanogr. Cruise Rep.* **11**.

CSIRO Aust. (1964*b*).—Oceanographical observations in the Indian Ocean in 1962. H.M.A.S. *Diamantina*, Cruise Dm 2/62. *CSIRO Aust. Oceanogr. Cruise Rep.* **15**.

DEUTSCHES HYDROGRAPHISCHES INSTITUT (1960).—Monatskarten für den Indischen Ozean. Deutsches Hydrographisches Institut Hamburg Nr. 2422.

'DISCOVERY' COMMITTEE (1942).—Station List 1933–35. XXII, pp. 3–196. (Cambridge.)

NEYMAN, V. G. (1961).—Factors controlling the oxygen minimum in the subsurface waters of the Arabian Sea. Oceanological Research Articles, I.G.Y. Program (Oceanology), Acad. Sci. U.S.S.R., Moscow, Vol. 4, pp. 62–5.

ROCHFORD, D. J. (1960).—The intermediate depth waters of the Tasman and Coral Seas. II. The 26·80 σ_t surface, *Aust. J. Mar. Freshw. Res.* **11**: 148–65.

ROCHFORD, D. J. (1961).—Hydrology of the Indian Ocean. I. The water masses in intermediate depths of the south-east Indian Ocean. *Aust. J. Mar. Freshw. Res.* **12**: 129–49.

ROCHFORD, D. J. (1963).—Mixing trajectories of intermediate depth waters of the south-east Indian Ocean as determined by a salinity frequency method. *Aust. J. Mar. Freshw. Res.* **14**: 1–23.

ROCHFORD, D. J. (1964*a*).—Hydrology of the Indian Ocean. III. Water masses of the upper 500 m of the south-east Indian Ocean. *Aust. J. Mar. Freshw. Res.* **15**: 25–55.

ROCHFORD, D. J. (1964*b*).—Salinity maxima in the upper 1000 m of the north Indian Ocean. *Aust. J. Mar. Freshw. Res.* **15**: 1–24.

SWALLOW, J. C. (1964).—Equatorial undercurrent in the western Indian Ocean. *Nature, Lond.* **204** (4957): 436–7.

WYRTKI, K. (1962).—The subsurface water masses in the western South Pacific Ocean. *Aust. J. Mar. Freshw. Res.* **13**: 18–47.

REPUBLIC OF SOUTH AFRICA

DEPARTMENT OF COMMERCE AND INDUSTRIES

DIVISION OF SEA FISHERIES INVESTIGATIONAL REPORT

No. 54

DISTRIBUTION OF INORGANIC PHOSPHATE AND DISSOLVED OXYGEN IN THE SOUTH WEST INDIAN OCEAN

by

S. A. MOSTERT

Collected reprints of the International Indian Ocean Expedition, vol. IV, contribution no. 235

CONTENTS

1. ABSTRACT

Oxygen and phosphate data were collected in the South-West Indian Ocean during 1961, 1962 and 1963. Inorganic phosphate increased southwards and was correlated with dissolved oxygen in a horizontal plane. Oxygen and phosphate were inversely related with depth. Oxygen and sigma-t correlations were analysed for identification of water masses while the oxygen minimum layer was generally at 1,500 m. and sigma-t = 27·6.

2. INTRODUCTION

Up to the time of the International Indian Ocean Expedition very little was known about the South-West Indian Ocean. Scientific Expeditions that traversed this area were undertaken, amongst others by H.M.S. *Challenger* (1873—1876), the *Gazelle* (1874—1876), the *Gauss* (1901—1903), R.R.S. *Discovery* (1934, 1935, 1938 and 1951) and lately by S.A.S. *Natal* (1962—1963) of the South African Navy. The routes sailed by the early explorers invariably stretched from Cape Town to the island of Kerguelen.

The cruises of R.R.S. *Discovery II* (1934, 1935, 1938 and 1951) were the only expeditions that made extensive studies of the phosphate and oxygen distribution in part of this area. This ship's data show no or extremely little phosphate in the upper 100 metres of the Sub-tropical and Tropical Waters, but south of the Sub-tropical Convergence the phosphate content was found to be relatively high, which is in accordance with our findings. The dissolved oxygen figures agree very well with our results for the entire area. The *Discovery's* main investigation, however, was concentrated on the circumpolar Antarctic Oceans, well south of the area which is discussed in this report.

The present report describes the distribution of inorganic phosphate and dissolved oxygen in the South-West Indian Ocean. This area was investigated by the R.S. *Africana II* of the Division of Sea Fisheries, during the periods June/July 1961, June/July 1962 and March 1963. Altogether 70 stations were worked, and all sampling depths were in accordance with the international standards, extending to a maximum depth of 4,000 metres. Stations on the completed cruise tracks are shown in Figure 1.

This report only discusses the inorganic phosphate data collected during the 1961 and 1962 cruises as other data collected during the 1963 cruise were altogether unreliable. The distribution of dissolved oxygen, however, is discussed from all cruises.

A partial station and data list for the June/July 1961 cruise is published by ORREN (1963). A further complete station list, covering all data used in this report, will be published shortly in the "Annual Report" series of this Division.

3. METHODS

3.1 Inorganic Phosphate Determination.

Inorganic phosphate was determined on board, according to the molybdenum-blue technique, using acid ammonium molybdate, $(NH_4)_6Mo_7O_{24}.4H_2O$ and stannous chloride, made up freshly for each determination by dissolving 0·25 g. pure tin in 5 c.c. concentrated hydrochloric acid and making up to 500 c.c. with distilled water.

The sea-water samples were filtered through Whatman No. 1 fluted filters and after the water had reached room temperature, 1 c.c. of each reagent was added from a burette to 50 c.c. sea water and thoroughly mixed. After seven minutes the developed colours were compared with a blank consisting of a phosphate-free saline solution treated the same way as the samples, in a Gallenkamp photo-electric colorimeter, using a red filter (Ilford 608) and 1 cm. cells. The results are recorded in μg.atom P/litre. The precision of the method is about 5% (ROBINSON 1948).

3.2 Dissolved Oxygen Determination.

The amount of dissolved oxygen in sea water was determined on board by means of the classical method of Winkler, in which manganous hydroxide is allowed to react with the oxygen giving a tetravalent manganese compound; in the presence of acidified potassium iodide an equivalent quantity of iodine is liberated which is then titrated with a standard sodium thiosulphate solution. The amount of oxygen is recorded as c.c. oxygen/litre sea water.

3.3 General.

The data in this report are illustrated by means of vertical sections along lines of stations, which are discussed separately for each year. No horizontal distribution charts were drawn as the distance between lines was far too great for any reasonable degree of accuracy and the times of the year during which the stations were worked differed too widely. The bottom topography as shown in the sections is purely schematic, as only the soundings at each station were plotted.

4. DISCUSSION

4.1 Phosphate distribution.

4.1.1 General.—In general the distribution of phosphate with depth is characterized by four different layers: (i) a surface layer (0—100 m.) in which the concentration is low and relatively uniform with depth; (ii) a layer (100—500 m.) in which the concentration increases rather rapidly with depth; (iii) a layer of maximum concentration which in the area investigated falls between 1,000 m. and 1,500 m. and (iv) a thick bottom layer in which there is relatively little change with depth. As discussed in the following section there were some instances at stations between the island groups

where high phosphates were found at the surface and the layers of low surface concentration and rapid increase with depth were absent. This is in general agreement with other findings in the Indian Ocean (SVERDRUP *et al* 1942).

When the lines of equal density (isopycnals) are plotted together with the phosphate isolines it is clear that the transportation of phosphate occurs in a general way along the same lines (Figs. 2—5). As the isopycnals are very closely related to the current system in the oceans, this phenomenon explains how the water from the sea surface in higher latitudes, namely the Antarctic and Sub-antarctic, where its characteristics are acquired, is transported to the depths at which oxygen and phosphate maxima and minima are observed.

4.1.2 Variations during 1961.—The surface inorganic phosphate content is very low over the whole area, ranging between 0·25—0·50 μg.at.P/l. The highest surface phosphate content of 1·14 μg.at.P/l. is found at station 1 whence it decreases rapidly to 0·35 μg.at.P/l. at station 6. At station 1, being an inshore station, upwelling could well have occurred, thereby increasing the phosphate content.

Thus, throughout the area the phosphate distribution is characterized by (i) a phosphate deficient surface layer and (ii) a region of increasing phosphate. The 1·0 μg.at.P/l. isoline at 250—550 metres and the 2·0 μg.at.P/l. isoline at 500—1,250 metres. Below the 2·0 μg.at.P/l. isoline phosphate increases very slightly with depth, but an ill-defined maximum of about 2·8 μg.at.P/l. is reached at a depth of 2,500—3,500 metres (ORREN 1963).

Pockets of high phosphate content (up to 3·6 μg.at.P/l.) appear throughout the area, and may perhaps be attributed to the regeneration of phosphate from decaying matter sinking to the bottom.

4.1.3 Variations during 1962.—The vertical sections of phosphate distribution (Figs. 4 and 5) show that the surface phosphate values vary from 1·95 μg.at.P/l. in the south, around and between the islands, to 0·30 μg.at.P/l. near the South African coast. It is probable that the region of maximum decomposition of plankton always corresponds to the region of greatest phosphate content; this occurs in the boundary zones separating the north-going Sub-antarctic Surface Water, the Antarctic Intermediate Water and the south-going Warm Deep Water, between 40° and 45° S. In this region the greatest vertical mixing between these currents also takes place (CLOWES 1938) so that the phosphate released by the decomposition of plankton passes into the mixed water in the upper layers of the south-going deep water. Maximum phosphate occurs in 47° S, 45° E at a depth of between 300 and 900 metres in the Antarctic Intermediate Water.

Phosphate, which attains its highest value in the Antarctic surface waters near the ice-edge, enters the area around and between the islands in the Antarctic Intermediate Water, which sinks north of the Antarctic Convergence to form the Antarctic Intermediate Current. Between 40° S and the South African coast this current reaches its greatest depth at 1,000—1,900 metres (salinity minimum at *c.* 1,300 metres). The reason for this increased depth may be due to the vast body of Sub-tropical Water which is brought into the area by the Agulhas current system, depressing the level of the Antarctic Intermediate Water (CLOWES 1938).

The maximum phosphate content encountered throughout almost the whole area under survey, amounted to 2·4 μg.at.P/l. at a depth of between 600 and 2,000 metres; that is in the upper part of the Warm Deep Water (ORREN 1963) from where it returns south in this current. Between the island groups, however, a water mass between the depths of 200 to 2,000 metres has a phosphate content of 2·2 μg.at.P/l. at its upper and lower limits. The phosphate gradually increases towards the nucleus of the water mass to reach a value of 2·8 μg.at.P/l. at 340 metres and 960 metres, but finally decreasing again to form a nucleus of water with a phosphate content of 2·6 μg.at.P/l. This water mass seems to come from a south-easterly direction and spreads over the whole area between the islands, having its nucleus in the vicinity of station 43. Here the Antarctic Intermediate Water flows at a shallow depth, between 200 and 400 metres, having its core at about 300 metres.

The large area of intense mixing of Antarctic Intermediate Water and the upper layer of the Warm Deep Water may be deduced from the T/S diagram (Fig. 9). This area stretches between 400 and 2,000 metres, but below 2,000 metres the Warm Deep Water flows as an almost homogenous mass. A large amount of upwelling and mixing is also evident in the surface waters as far as phosphate content is concerned, but this is not so clearly evident in the vertical diagrams of dissolved oxygen content. It is difficult to draw any definite conclusions about the character and behaviour of the water between the islands as the ship steered a rather erratic, zig-zag course and the stations were relatively far apart; each station was separated from the next by a distinct ridge on the sea bottom.

The Sub-tropical Convergence was crossed at about 41° S on the outward cruise and again at about 42° S on the homeward cruise. This Convergence divided the area into two distinctly different water masses as far as surface characteristics are concerned. The surface water north of the Convergence is poor in phosphate, 0·30 μg.at.P/l. to 1·0 μg.at.P/l.; while the surface water south of the Convergence is relatively rich in phosphate, 1·0 μg.at.P/l. to 1·95 μg.at.P/l. A third area can also be added, this is that part of the continental shelf covered by the Agulhas Current and having warm water relatively high in phosphate; this well-known current flows along the South-east coast of South

Africa and can be traced as far south as Cape Agulhas.

At the Convergence the colder Sub-antarctic Water rapidly descends to a depth of about 600 to 1,200 metres. This water is known to be richer in phosphate than the Sub-tropical surface water and a phosphate maximum is encountered at an average depth of about 1,000—1,200 metres. Below this there is a slight decrease towards the bottom, the phosphate content reaching a secondary maximum at the bottom again (Fig. 5).

The sudden depression of phosphate content between stations 48 and 49 may tentatively be attributed to the presence of the eddy found in that area (ORREN 1965, in press).

Unfortunately the distribution of inorganic phosphate in the area covered by the same ship during March 1963 cannot be discussed because many of the phosphate determinations appear to be at fault.

Summarising, it can be said that the inorganic phosphate content of surface waters gradually increases along the lines of stations stretching from the African continent to the Sub-antarctic island groups of Prince Edward and Crozet.

The concentration of inorganic phosphate is correlated in a general way with the distribution of density.

4.2 Oxygen Distribution.

4.2.1 Generalized Oxygen/Density (Sigma-t) Relationship.—The whole area investigated can be divided into three distinct regions according to the surface characteristics of the water, namely (i) Tropical area; (ii) Sub-tropical area and (iii) Sub-antarctic area. These three regions can be identified clearly from the oxygen/sigma-t scatter diagrams (Figs. 6 and 7).

Tropical and Sub-tropical surface water have more or less the same characteristics, being relatively poor in dissolved oxygen and not very dense (sigma-t = *c.* 24·0); but below the surface these water masses are very different. Oxygen of the Tropical water reaches a minimum (4·0 c.c./l.) at about 75 metres but then increases with depth to *c.* 5·3 c.c./l. at a depth of 500 metres in Indian Central Water (Fig. 6). The Sub-tropical water has no sub-surface oxygen minimum, but oxygen content increases steadily with depth to the core of Indian Central Water, from 5·0 c.c./l. at the surface to 5·7 c.c./l. at 400 metres (Fig. 6) which in both cases is a maximum oxygen content. This demonstrates that the core of the Indian Central Water is slightly shallower in Sub-tropical than in Tropical waters (Fig. 8).

In Sub-antarctic Water there is no noticeable minimum or maximum from the surface downwards (Fig. 8). The oxygen content decreases rapidly with depth (from 7·4 c.c./l. to 4·8 c.c./l. at a depth of *c.* 700 metres) and shows a very small change with sigma-t (26·7—27·4).

The minimum oxygen content in all cases lies at an average depth of 1,500 metres on the sigma-t = 27·6 surface which is the boundary between Antarctic Intermediate and Warm Deep Waters according to the temperature/salinity characteristics of Indian Ocean Water (Fig. 9).

On comparing the three water masses, the minimum oxygen layer is found to be richest in dissolved oxygen in Sub-antarctic regions (4·1 c.c./l. as compared with 3·4—4·0 c.c./l. in the Sub-tropics) although the minimum layer is found at similar depths (1,500 metres and sigma-t = 26·7) throughout.

Below the minimum layer, the Warm Deep Water, of slightly higher oxygen content for a higher sigma-t value, has much the same oxygen content throughout, and the oxygen content increases downward almost to the bottom where a slight decrease again appears.

4.2.2 The Oxygen Minimum.—The presence of the oxygen minimum layer in the oceans has been investigated by several investigators. Darbyshire, using data obtained by R.S. *Africana II* during June/July 1962, could find very little evidence, if any, of the presence of such a layer in the Indian Ocean (DARBYSHIRE 1964). However, we found that there is indeed an oxygen minimum layer present at the sigma-t = 27·6 surface, and this layer was detected throughout the whole area irrespective of the time of the cruises (Figs. 6 and 7). This sigma-t = 27·6 layer actually coincides with the boundary area between the Antarctic Intermediate and the Warm Deep Water and in fact was found everywhere at an average depth of 1,500 m. This can be seen in the T/S diagram of Figure 9 (Compare ORREN 1963, Fig. 11). It was proposed by CLOWES and DEACON (1935) that this upper stratum of the Warm Deep Water is a continuation of the North Indian Deep Water which sank off the coastal region of the Arabian Sea and neighbouring gulfs, particularly the Red Sea.

From the vertical distribution of oxygen (Fig. 13) it is suggested that the Warm Deep stratum of about 2,000 metres, at least in the southern section of the whole area investigated, has its source in an eastward current of Atlantic Deep Water (VISSER and VAN NIEKERK 1965). At station 58 the oxygen minimum lies at a depth of approximately 1,900 metres (sigma-t = 27·6). This significant depression of the oxygen minimum is caused by the huge mass of water from the Agulhas Current pushing southwards and being joined by the West Wind Drift thereby forcing the Antarctic Intermediate Water to a greater depth. The Return Agulhas Current and the West Wind Drift are clearly illustrated by VISSER and VAN NIEKERK's (*op. cit.* 1965) horizontal current distribution charts.

In the northwestern section of our area the lowest oxygen content of 3·26 c.c./l. is recorded at a depth

of 1,600 metres at station 7. This very poorly oxygenated water seems to be a continuation of the North Indian Deep Water, as suggested by CLOWES and DEACON (*op. cit.*).

4.2.3 Oxygen Variation during 1961.—From station 1 near Lourenço Marques, where the dissolved oxygen content is relatively low (probably due to the presence of warm (±24° C) and highly saline ($S°/_{oo}$ = *c.* 35·4$°/_{oo}$) tropical water streaming southward down the coast), to station 8, the oxygen content increases very slightly (4·67—4·73 c.c./l.) and the water is all of tropical origin (c.f. ORREN 1963). From station 9 eastwards the increase becomes more noticeable over the whole area, and a maximum surface oxygen content of 5·70 c.c./l. occurred at station 26 in the easternmost part of the area investigated. In the extreme north around Mauritius, the surface oxygen is also low (4·75 c.c./l.) and the water is again of tropical origin. The rest of the area is covered by cooler sub-tropical water, the oxygen content being uniformly higher in the south of the area than in the north.

Summarising, we see that in tropical waters (Stations 2—8) the oxygen concentration attains a sub-surface minimum at a depth of ±75 metres (3·5—4·3 c.c./l.) and again a maximum (4·6—5·0 c.c./l.) at a depth of ±500 metres in Indian Ocean Central Water with sigma-t = 26·6. The minimum oxygen concentration lies at the sigma-t = 27·6 surface with a value of 3·5 c.c./l. and at a depth of *c.* 1,500 metres.

4.2.4 Oxygen Variation during 1962.—Dissolved oxygen is distributed very evenly over the entire area, and as the oxygen content is directly related to the temperature of the water, oxygen variations can be closely correlated with temperature changes throughout the area (Figs. 10—12).

Water with an oxygen content of 5 c.c./l., flowing at a depth of between 600 to 800 metres between the islands (800 metres deep at Marion Island), rises slowly towards the north to reach the surface near the South African coast outside Port Elizabeth. At station 48 this water suddenly sinks from about 400 metres to 800 metres, only to rise again at station 49 to 200 metres at which depth it remains until it reaches the coast. This sudden change in depth at station 48 can be attributed to an eddy found in the vicinity (ORREN 1965 in press).

In brief, we find that in the sub-tropical region the dissolved oxygen content of the surface water is higher than that of the tropical regions (5·5 c.c./l. as compared with 4·8 c.c./l.) and the oxygen content decreases gradually with depth to a depth of 500 metres (sigma-t = 26·6, 5·0 c.c./l.) and then rapidly to a minimum of 4·0 c.c./l. at a depth of 1,500 metres at the sigma-t = 27·6 surface.

At the Sub-tropical Convergence colder water with an oxygen content of 6·0 c.c./l. is encountered at the surface. This water appears to sink gradually southwards and can be traced between the islands at depths varying from 300 to 400 metres, but rising again to the surface between stations 46 and 47, where the Convergence was crossed once again.

Water with a surface oxygen content of 7·0 c.c./l. is encountered for the first time in the vicinity of Marion Island from where it sinks slightly and flows from 20 to 100 metres depth between the islands returning to the surface at the Convergence, encountered on the line of stations 44—50 (Fig. 12). The apparent effect of the oxygen isolines sinking in a southward direction is illusory and is no doubt brought about by the temperature which decreases southwards. In this way more oxygen can dissolve in the surface water to give a southward oxygen increase in the surface layer, causing the isolines to sink deeper.

Oxygen is more or less evenly distributed throughout the area, decreasing from the surface to the bottom except at station 36 where a secondary maximum of 5·0 c.c./l. lies at a depth of 1,800 to 2,200 metres. This seems to be an area where the lower layers of the Antarctic Intermediate Water mix with the upper layers of the Warm Deep Water. The core of the Warm Deep Water is at a depth greater than 2,500 metres. The depth of the core of the Antarctic Intermediate Water, however, varies considerably.

4.2.5 Oxygen Variation 1963.—The dissolved oxygen content of the surface water increases from 5·4 c.c./l. near the continent (36° 30′ S) to 7·1 c.c./l. at about 47° S (Fig. 13). The 5·0 c.c./l. isoline sinks from near the surface at station 56 to 500 metres at station 60 then rises to 50 metres again at station 61 from where it sinks once more to 950 metres at station 62 to stay at that level throughout the remaining stations. The depth of the minimum oxygen concentration (4·4 c.c./l.) varies considerably before station 61 (from 1,100 to 2,000 metres) but subsequently remains at a more or less constant depth of about 1,500 metres. A marked minimum of 4·0 c.c./l. is seen at station 58 between depths of 1,500 and 1,900 metres and is again very marked at station 61 between depths of 400 and 1,100 metres.

From the vertical oxygen distribution section (Fig. 13) it is very clear that strong upwelling occurs at station 61 from depths of more than 2,000 metres. This area of upwelling is in the immediate vicinity of the Sub-tropical Convergence and the upwelling is most probably caused by an eddy. This eddy is clearly shown in the horizontal current distribution charts of VISSER and VAN NIEKERK (1965).

The sigma-t/oxygen correlation chart (Fig. 14) shows that the large pocket of poorly oxygenated water between 400 and 1,100 metres at station 61 consists of Antarctic Intermediate Water brought

near the surface by the upwelling caused by this eddy.

At station 60, however, Sub-antarctic Surface Water with relatively high oxygen content was found at the surface, mixed with Indian Central Water (that is, Sub-tropical Surface Water with low oxygen content) giving an oxygen value of 6·5 c.c./l. (Fig. 14). This phenomenon is clearly caused by the abovementioned eddy which also lies in the region of the Sub-tropical Convergence. The surface water at station 61 is of pure sub-tropical origin. Station 63, on the other hand, had the characteristics of Sub-antarctic Water (Fig. 14).

From station 61 southwards the oxygen content of the surface water steadily increases as the temperature decreases. A sudden drop in temperature from 17·32° C to 10·79° C between stations 61 and 62 is accompanied by an increase in dissolved oxygen from 5·5 to 7·1 c.c./l. This is a clear indication that the Sub-tropical Convergence was crossed in this area in the vicinity of 43° S.

In general then, the dissolved oxygen content of the water in Sub-antarctic regions south of the Sub-tropical Convergence is much higher (7·0 c.c./l.) than in either the tropical or sub-tropical regions. The decrease with depth is rapid over a relatively small sigma-t range to a minimum of 4·3 c.c./l. at a depth of ±1,500 metres, which is again the sigma-t = 27·6 surface.

A definite linear relationship (Figs. 15 and 16) exists between the concentrations of dissolved oxygen and inorganic phosphates on a horizontal plane, i.e. the variations in phosphate concentrations are directly proportional to the oxygen concentrations (RILEY 1951). The correlation coefficient (r) was calculated by the linear least square regression method and it was found that $r = 0{\cdot}94$ for surface water and 0·92 for water at the 100 metre level. Although oxygen and phosphate are directly related on a horizontal plane, they seem to be inversely related with depth (Fig. 17).

4.2.6 Oxygen Saturation of Surface Water.—The percentage oxygen saturation of the sea water has been calculated and illustrated (Fig. 18) for the surface waters of the whole area. Although the water is 100% saturated at station 44 and super-saturated at stations 53 and 55, it was found later that a plankton bloom was present in the surface waters in these areas. The phosphate concentration was accordingly relatively low here. The high percentage of oxygen saturation can be ascribed to the photosynthetic process of the phytoplankton. Similar reasoning applies to the vicinity of station 36 where the surface water is also super-saturated with oxygen. For the calculation of the solubility of oxygen in sea water at different temperatures and chlorinities a nomograph published by TULLY (1949) was used.

4.2.7 The Whole Area.—Over the whole area investigated during the three consecutive years, the surface oxygen content increases southwards. North of the Sub-tropical Convergence the southward increase is slight and the Sub-tropical Surface water is very uniform in oxygen content varying very little from 4·80 c.c./l. in the north to 5·80 c.c./l. in the south, that is, in the Convergence area. At the Convergence with its colder water, however, the increase in oxygen content is relatively large (from 5·80—7·00 c.c./l.) over a very short distance. The Convergence was in the vicinity of 42° S ±1°. South of this Convergence the dissolved oxygen content is uniformly high again, being over 7·0 c.c./l. and reaching a maximum of 7·30 c.c./l. near the two island groups of Prince Edward and Crozet.

5. ACKNOWLEDGEMENTS

I am indebted to the Director of Sea Fisheries, Mr. B. v. D. de Jager, Mr. M. J. Orren and other staff members of the Division of Sea Fisheries for their critical reading of this report and for their many useful suggestions.

Finally I must also thank my colleagues and the officers and crew of *Africana II* for their help in the collection and processing of the data on which this report is based.

6. LITERATURE CITED

BARNES, H., 1959.—*Apparatus and Methods of Oceanography (Chemical)*. G. Allen and Unwin: 341 pp. London.

CLOWES, A. J. and G. E. R. DEACON, 1935.—The Deep-water circulation of the Indian Ocean. *Nature*, 136: 936.

CLOWES, A. J., 1938.—Phosphate and Silicate in the Southern Ocean. *Discovery Rep.*, 19: 3—120.

CLOWES, A. J., 1950.—An Introduction to the Hydrology of South African Waters. *Invest. Rep. Fish. Mar. Biol. Surv., S. Afr.* 12: 1—29.

DARBYSHIRE, J., 1964.—A Hydrological investigation of the Agulhas Current area. *Deep Sea Res.*, 11 (5): 781—815.

HARVEY, H. W., 1928.—*Biological chemistry and Physics of sea water*. Cambridge Univ. Press: Cambridge.

JAYARAMAN, R., 1959.—The vertical distribution of dissolved Oxygen in the deeper waters of the Arabian Sea in the neighbourhood of the Laccarides during the summer of 1959. *J. Mar. Biol. Assoc.*, India, 1 (2): 206—211.

ORREN, M. J., 1963.—Hydrological observations in the South West Indian Ocean. *Invest. Rep. Div. Sea Fish.*, S. Afr., 45: 1—61.

ORREN, M. J., 1965.—Hydrology of the South West Indian Ocean. Invest. Rep. Div. Sea Fish. S. Afr. 55: in press.

REDFIELD, A. C., 1942.—The processes determining the concentration of oxygen and phosphate and other organic derivatives within the depths of the Atlantic Ocean. *Pap. Phys. Oceanogr. and Met.*, Woods Hole, 9 (2): 1—22.

REID, J. C., 1962.—The distribution of dissolved Oxygen in the summer thermocline. *J. Mar. Res.* 20 (2): 138—148.

RICHARDS, F. A. and A. C. REDFIELD, 1955.—Oxygen density relationships in the western North Atlantic. *Deep Sea Res.*, 2 (3): 182—199.

RILEY, G. A., 1951.—Oxygen, Phosphate and Nitrate in the Atlantic Ocean. *Bingham Oceanogr. Fdn. Bull.* 13 (1): 1—124.

ROBINSON, R. J. and T. G. THOMPSON, 1948.—The determination of phosphates in sea water. *J. Mar. Res.* 7 (1): 33—41.

SEIWELL, H. R., 1937.—The minimum Oxygen concentration in the western basin of the North Atlantic. *Pap. Phys. Oceanogr. and Met.*, Woods Hole, 5 (3): 1—24.

SVERDRUP, H. U., M. W. JOHNSON and R. H. FLEMING, 1942. —*The Oceans, their Physics, Chemistry and general Biology*. Prentice-Hall, Inc.: 1087 pp. New York.

TULLEY, J. P., 1949.—Oceanography and prediction of pulp mill pollution in the Alberni inlet. *Fish. Res. Bd. Canada, Bull.* 83: 1—169.

VISSER, G. A. and M. M. VAN NIEKERK, 1965.—Ocean currents and water-masses at 1,000, 1,500 and 3,000 metres in the South-West Indian Ocean. *Invest. Rep. Div. Sea Fish.*, S. Afr. in press.

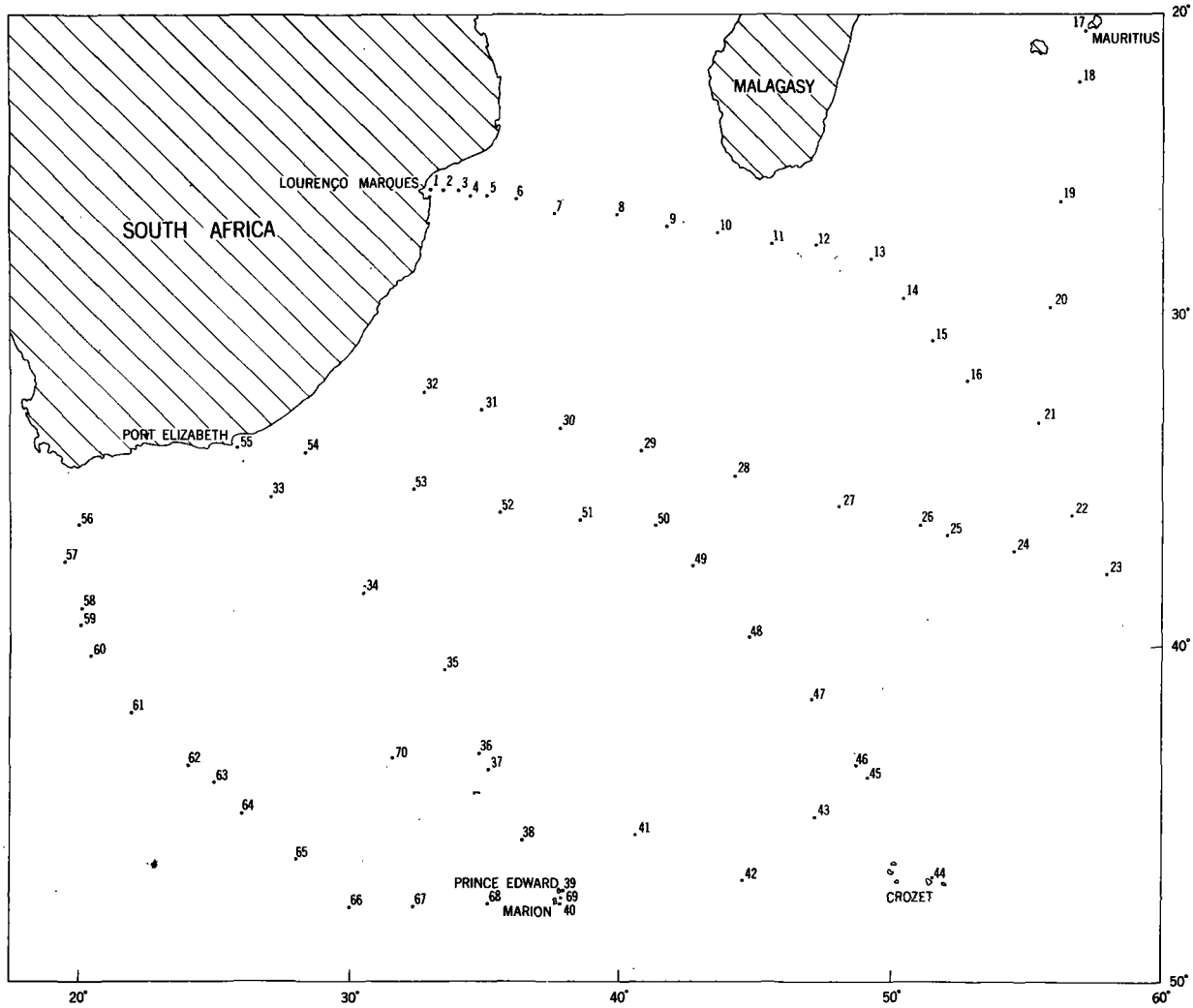

FIG. 1 POSITION OF STATIONS IN AREA INVESTIGATED DURING 1961, 1962 AND 1963.

Trigsurvey 1965.

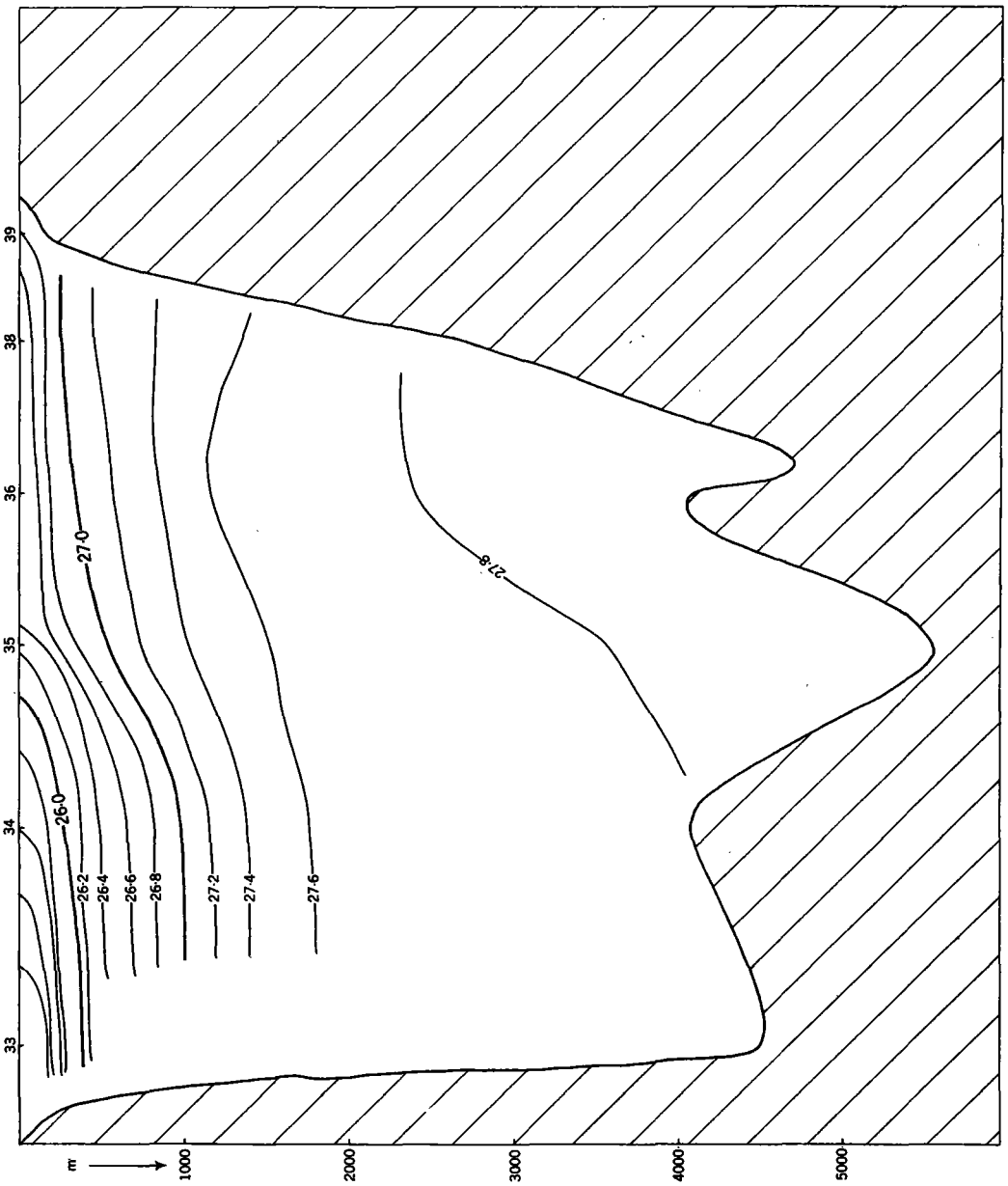

FIG. 2 DENSITY DISTRIBUTION–PORT ELIZABETH/MARION LINE

Trigonway 1965.

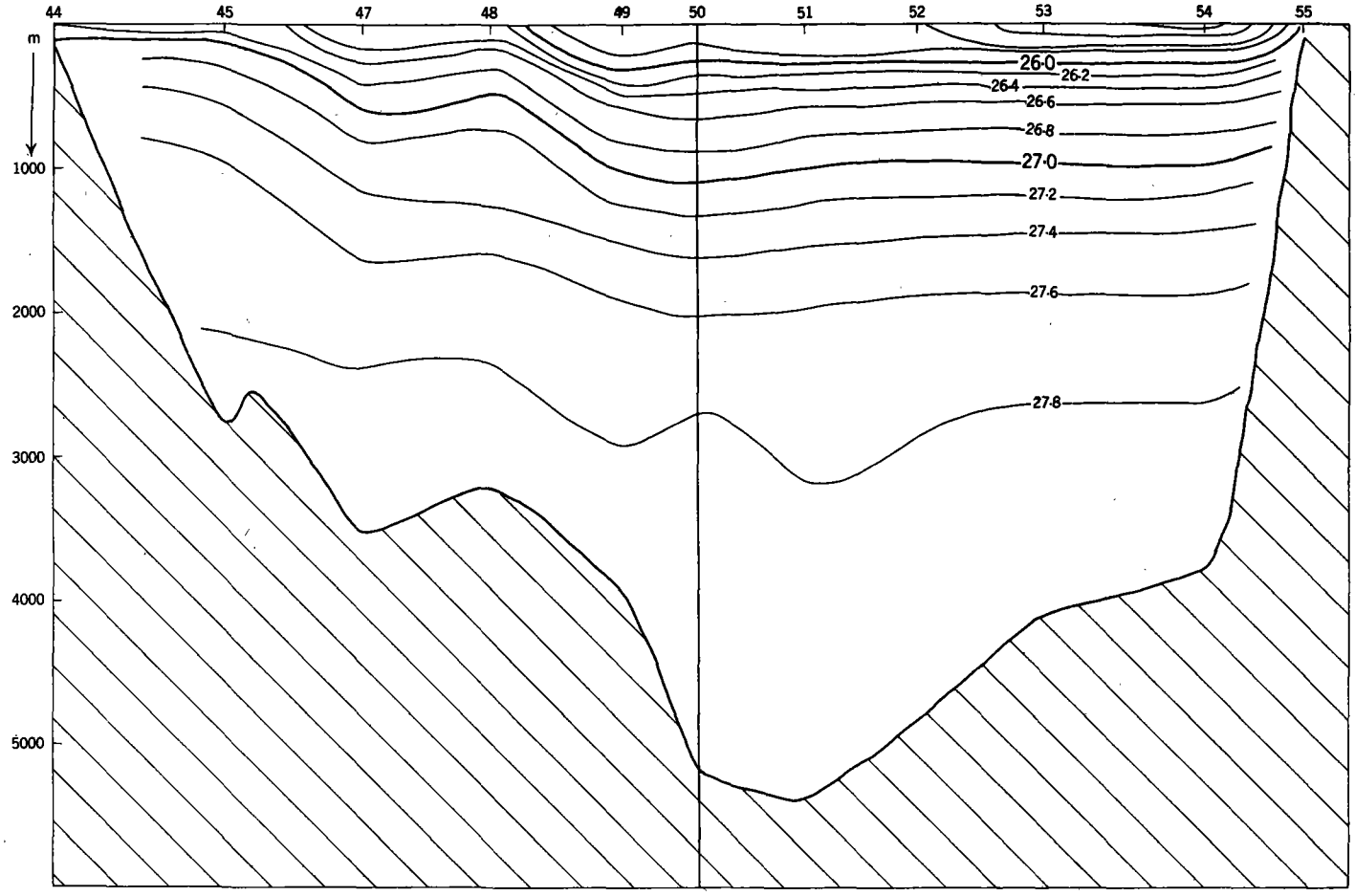

FIG. 3 DENSITY DISTRIBUTION—SLOT VAN CAPELLE/PORT ELIZABETH LINE

Trigsurvey 1965.

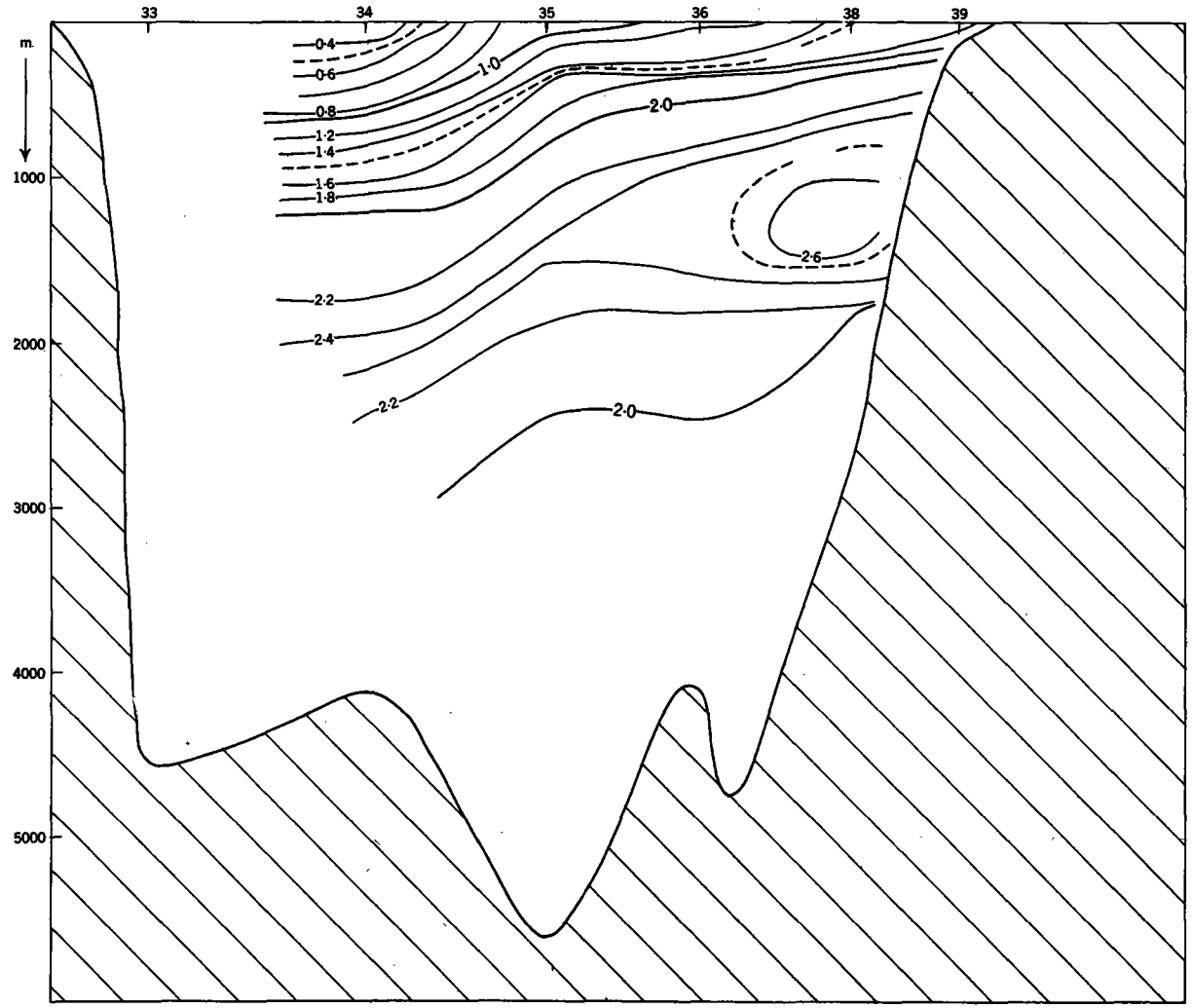

FIG. 4 PHOSPHATE DISTRIBUTION—PORT ELIZABETH/MARION LINE

Trigsurvey 1966

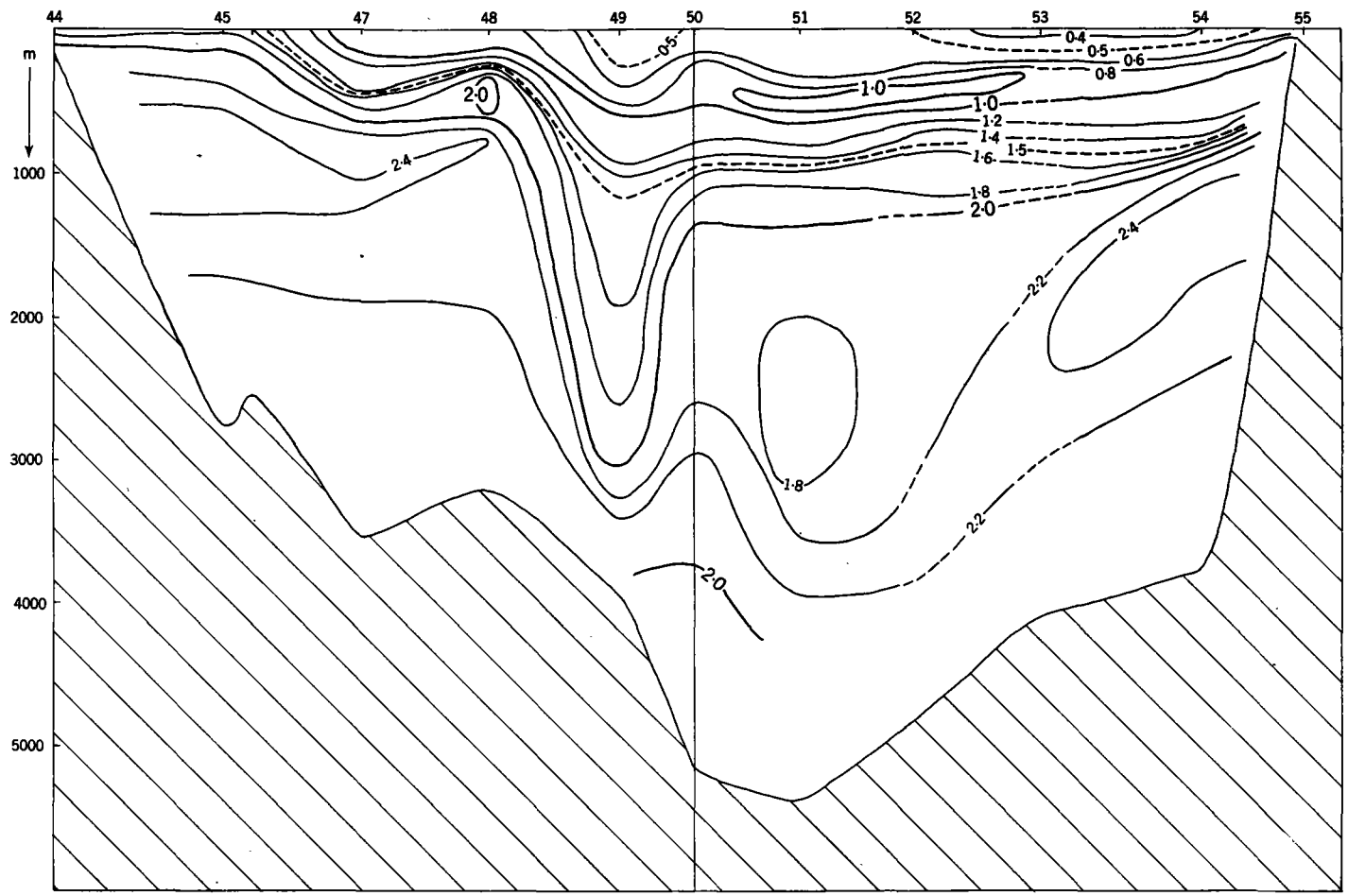

FIG. 5 PHOSPHATE DISTRIBUTION — SLOT VAN CAPELLE / PORT ELIZABETH LINE.

Trigsurvey 1965.

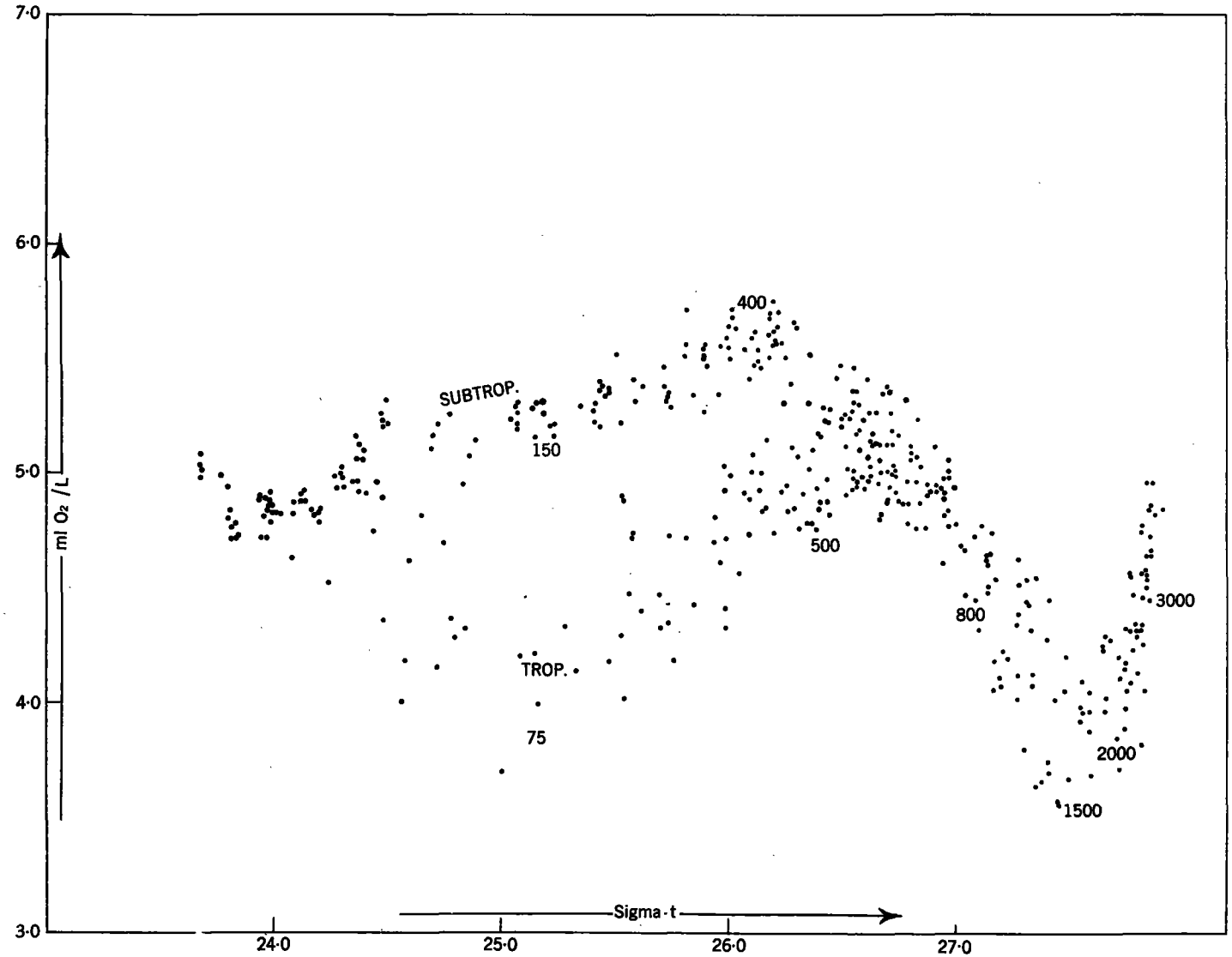

FIG. 6 OXYGEN/DENSITY RELATIONSHIP FOR TROPICAL AND SUBTROPICAL WATERS.

Trigsurvey 1965.

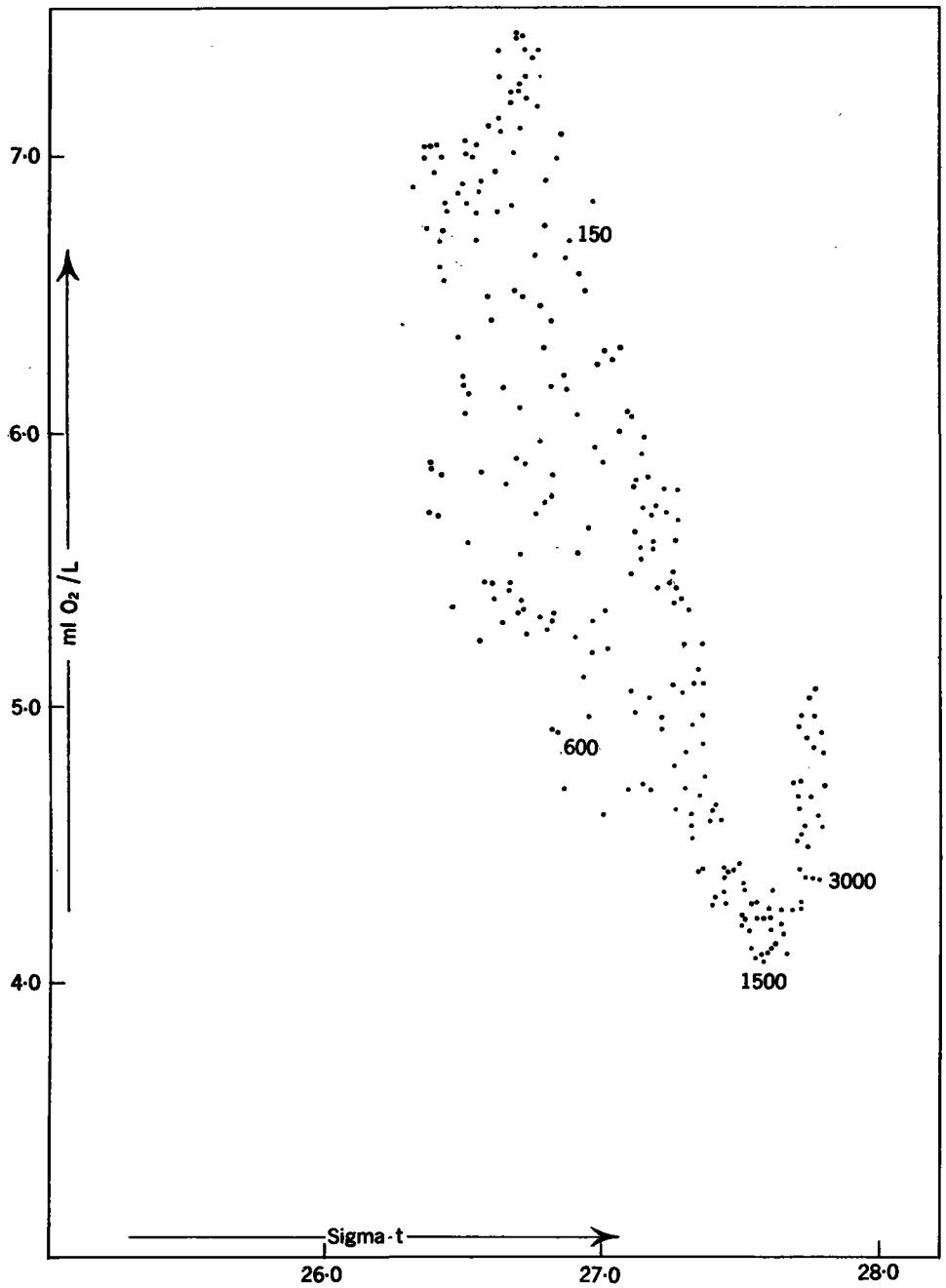

FIG. 7 OXYGEN/DENSITY RELATIONSHIP FOR SUBANTARCTIC WATERS.

Trigsurvey 1965.

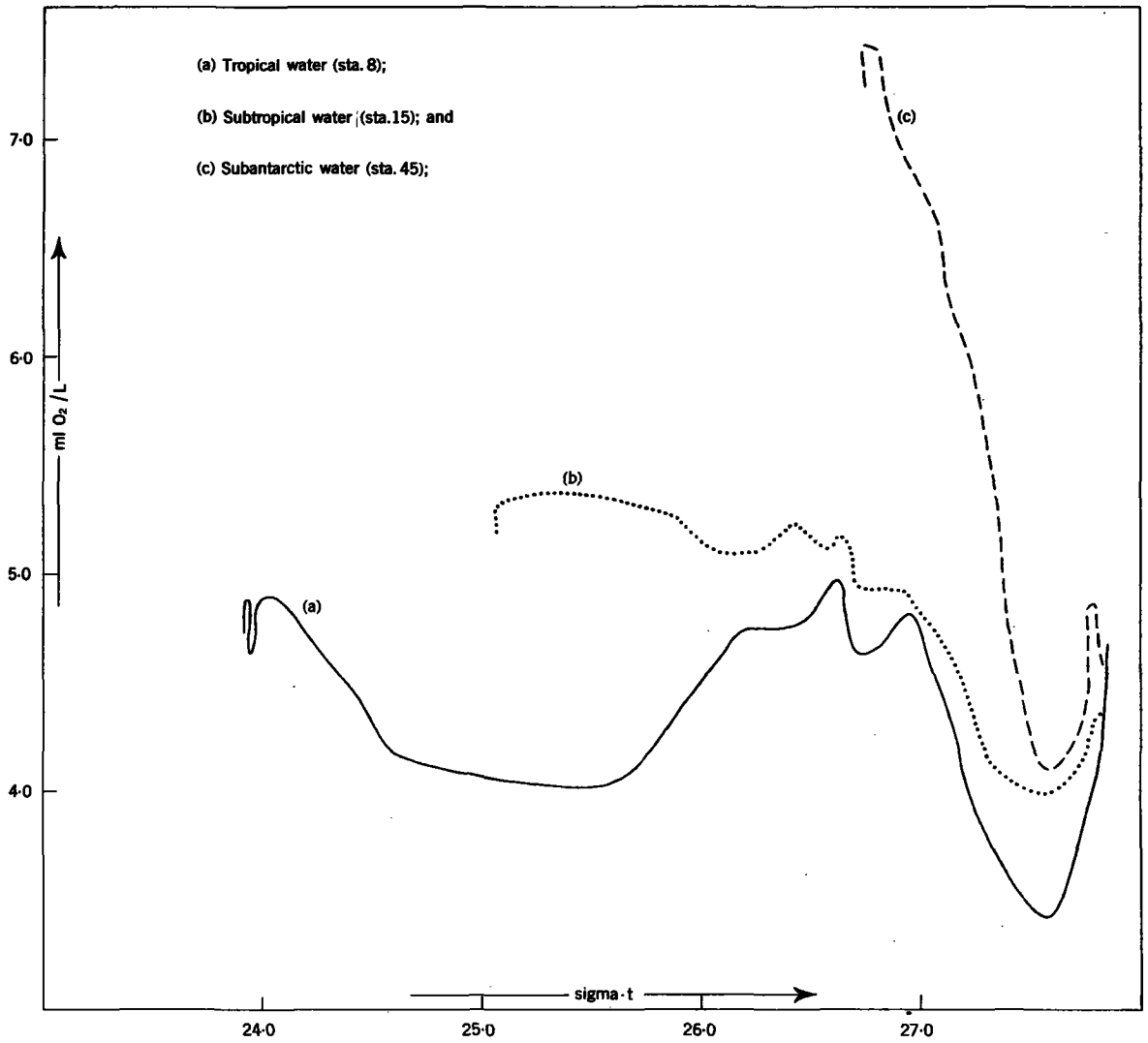

FIG 8 TYPICAL OXYGEN/DENSITY RELATIONSHIPS

Trigsurvey 1965.

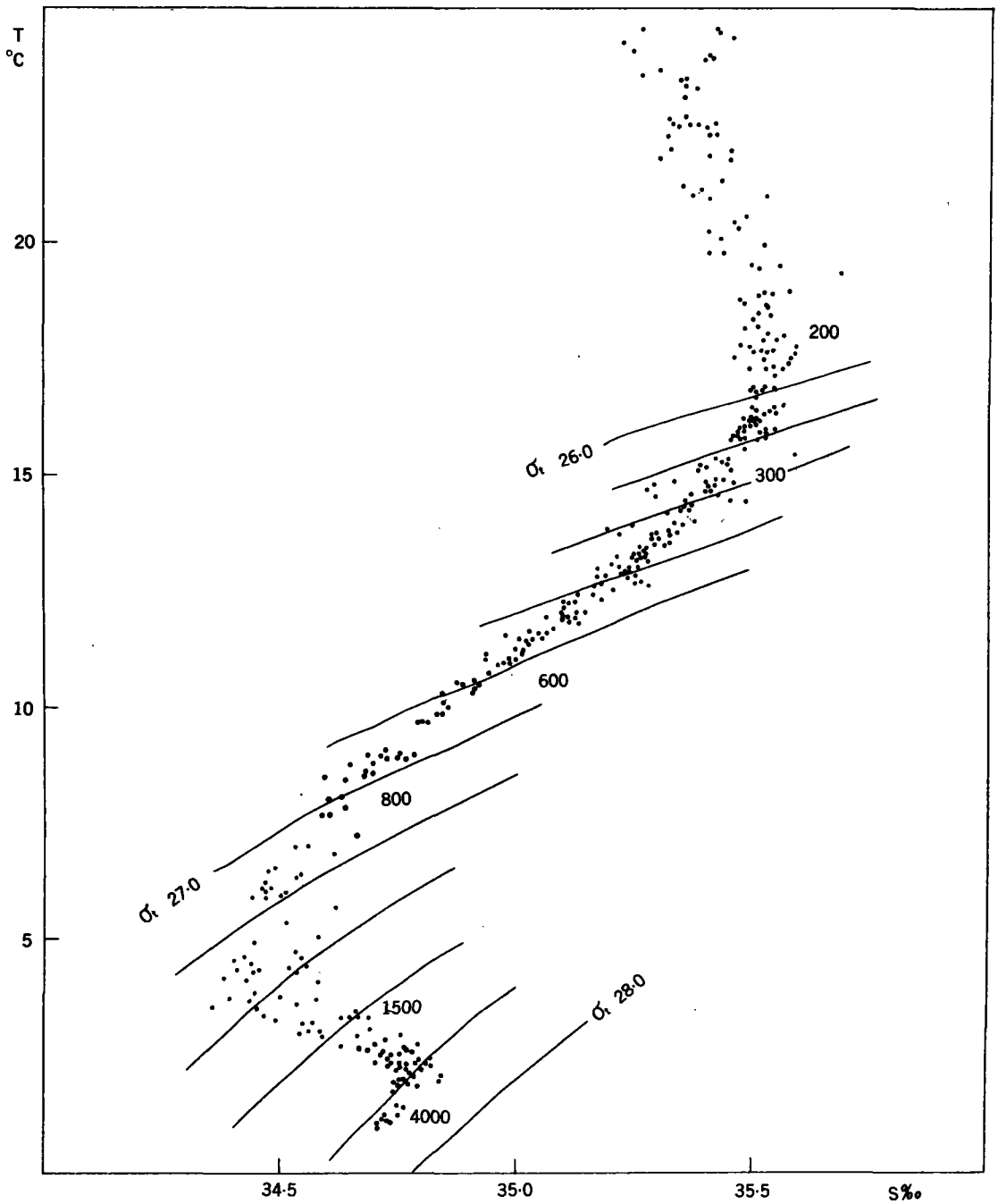

FIG. 9 T/S RELATIONSHIP— INDIAN OCEAN WATERS.

Trigsurvey 1965.

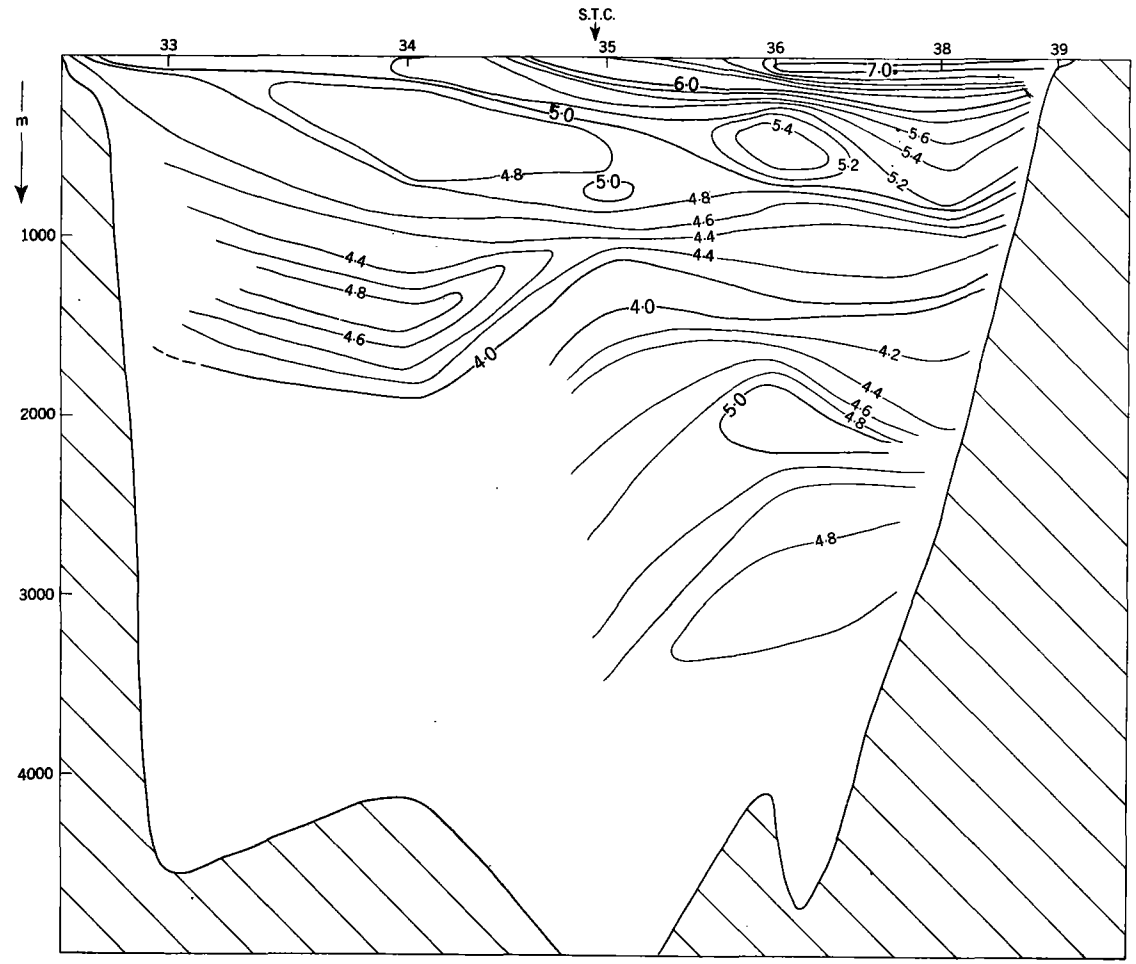

FIG. 10 OXYGEN DISTRIBUTION—PORT ELIZABETH/MARION LINE, 1962.

Trigsurvey 1965

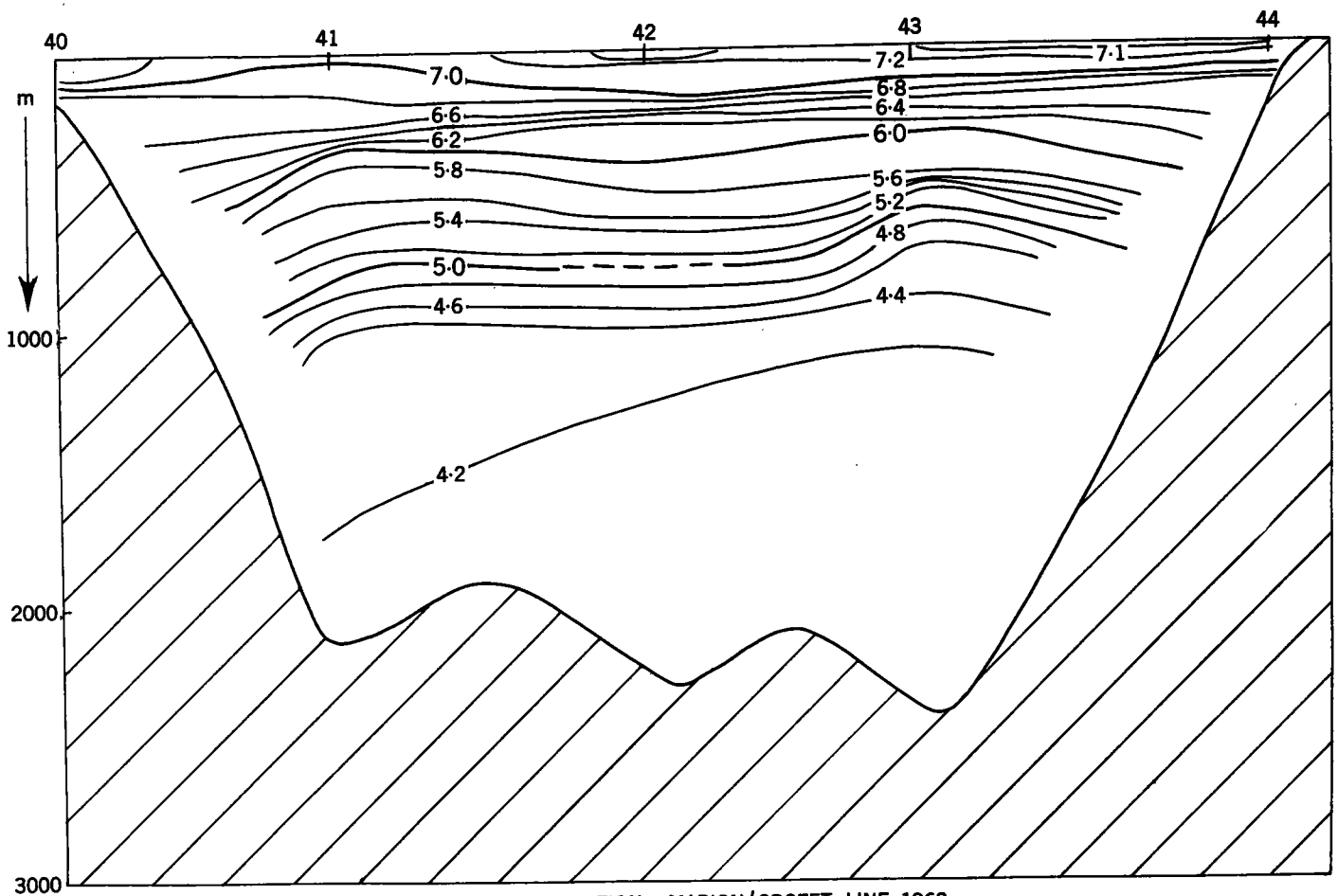

FIG. 11 OXYGEN DISTRIBUTION—MARION/CROZET LINE, 1962.

Trigsurvey 1965.

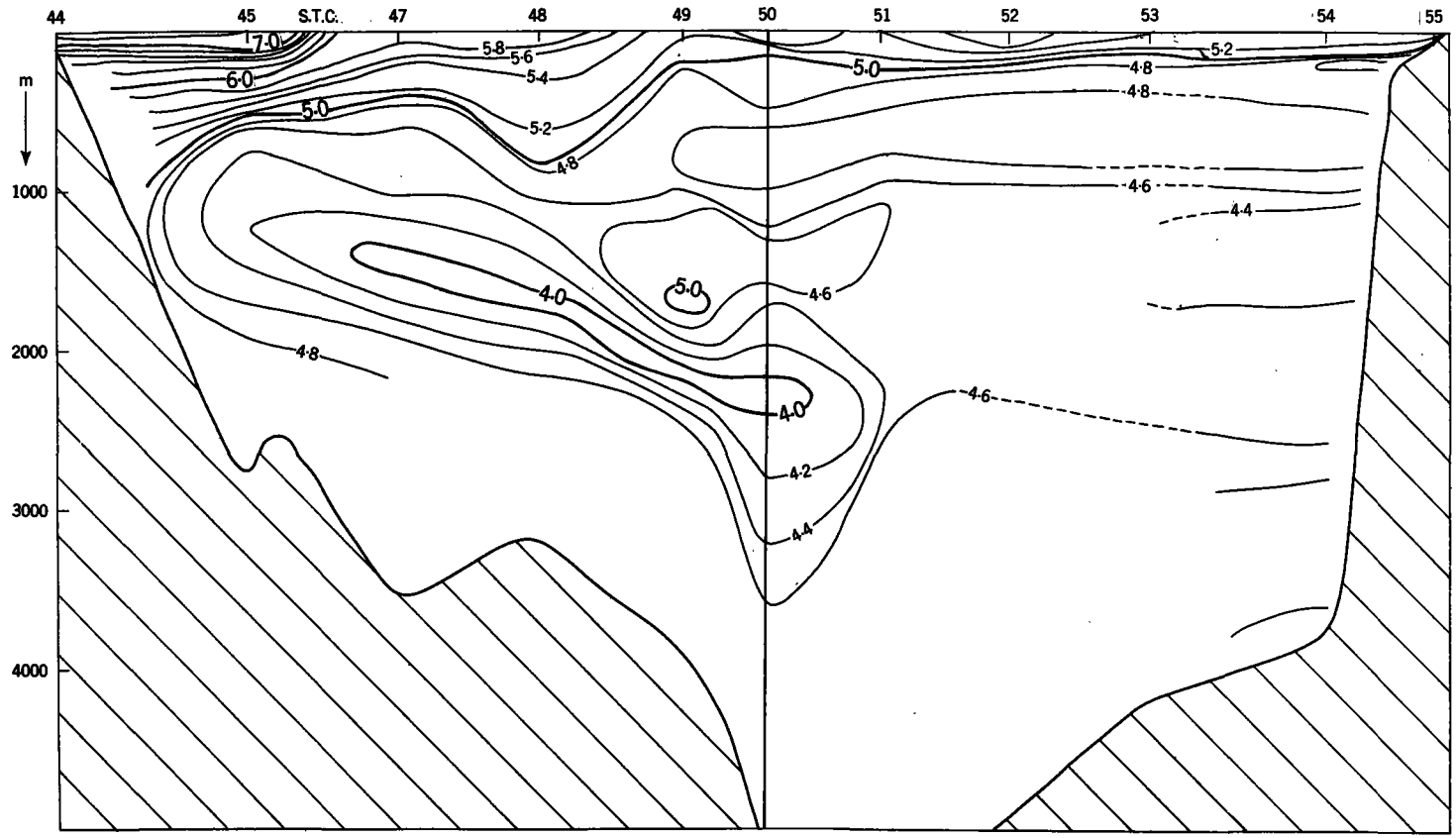

FIG. 12 OXYGEN DISTRIBUTION—CROZET/SLOT VAN CAPELLE/PORT ELIZABETH LINE, 1962.

Trigsurvey 1965.

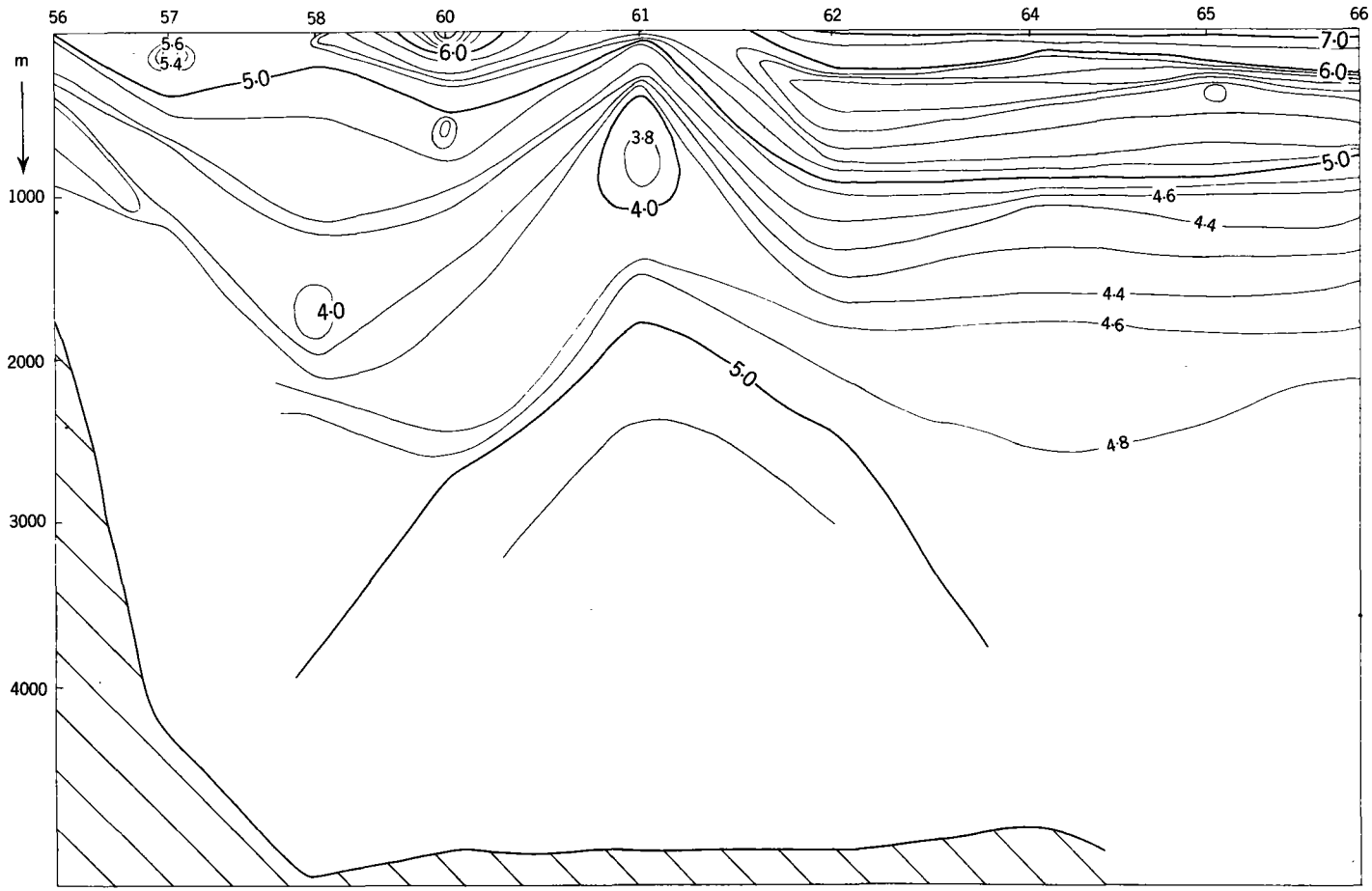

FIG. 13 OXYGEN DISTRIBUTION — CAPE AGULHAS/ MARION LINE, 1963.

Trigsurvey 1965.

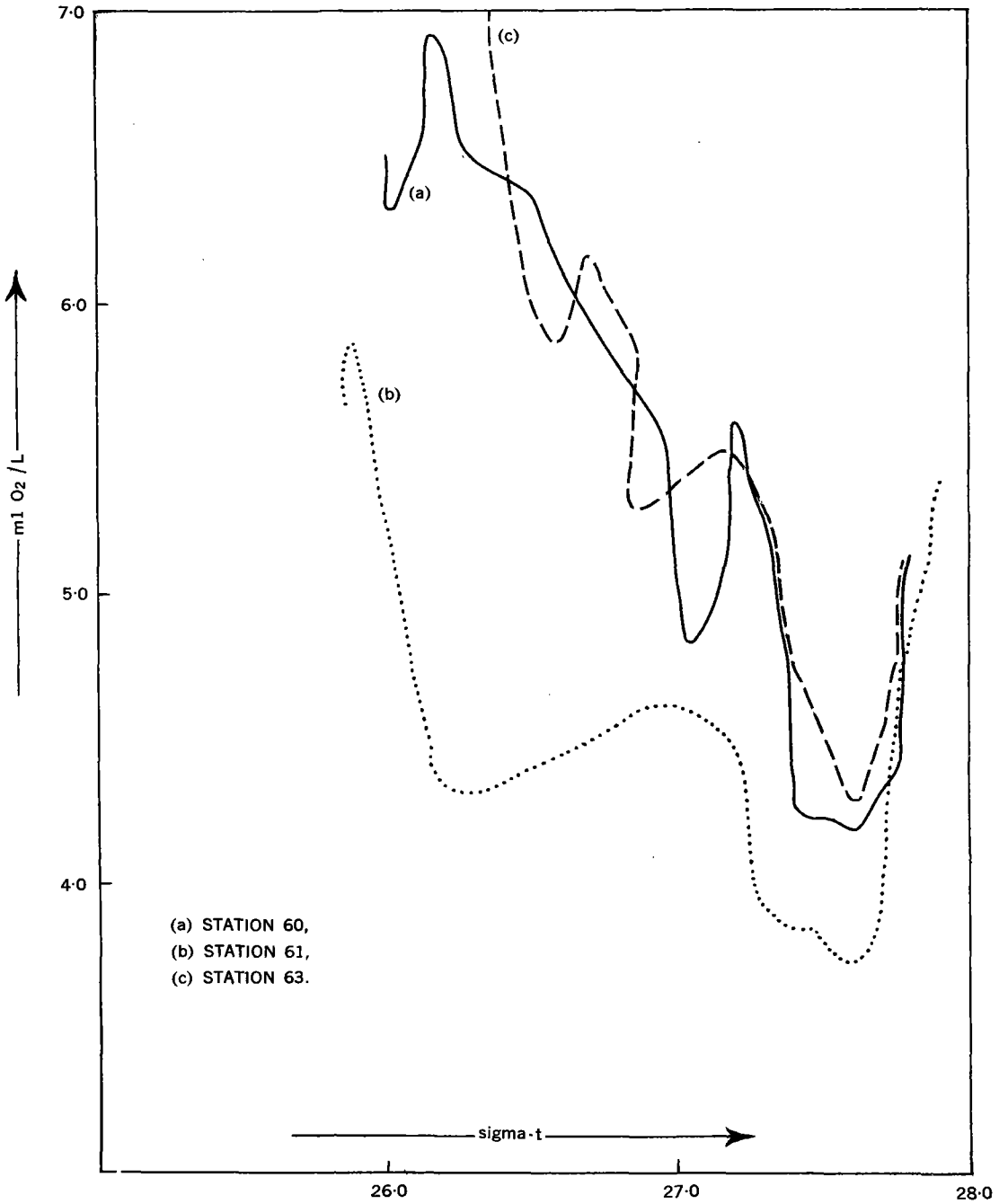

FIG. 14 OXYGEN/DENSITY RELATIONSHIPS

Trigsurvey 1965.

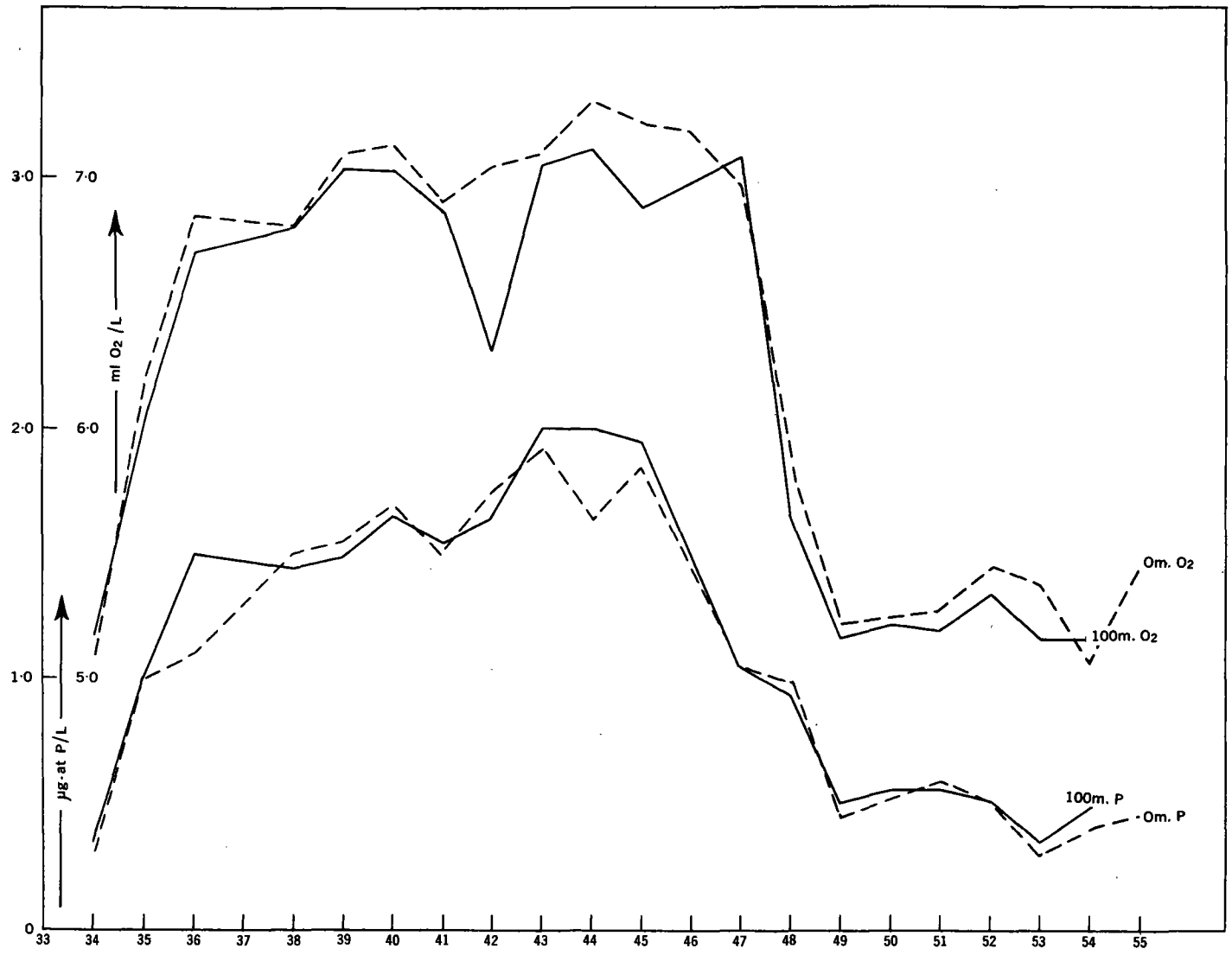

FIG. 15 OXYGEN/PHOSPHATE DISTRIBUTION AT SURFACE AND AT 100m.

Trigsurvey 1965.

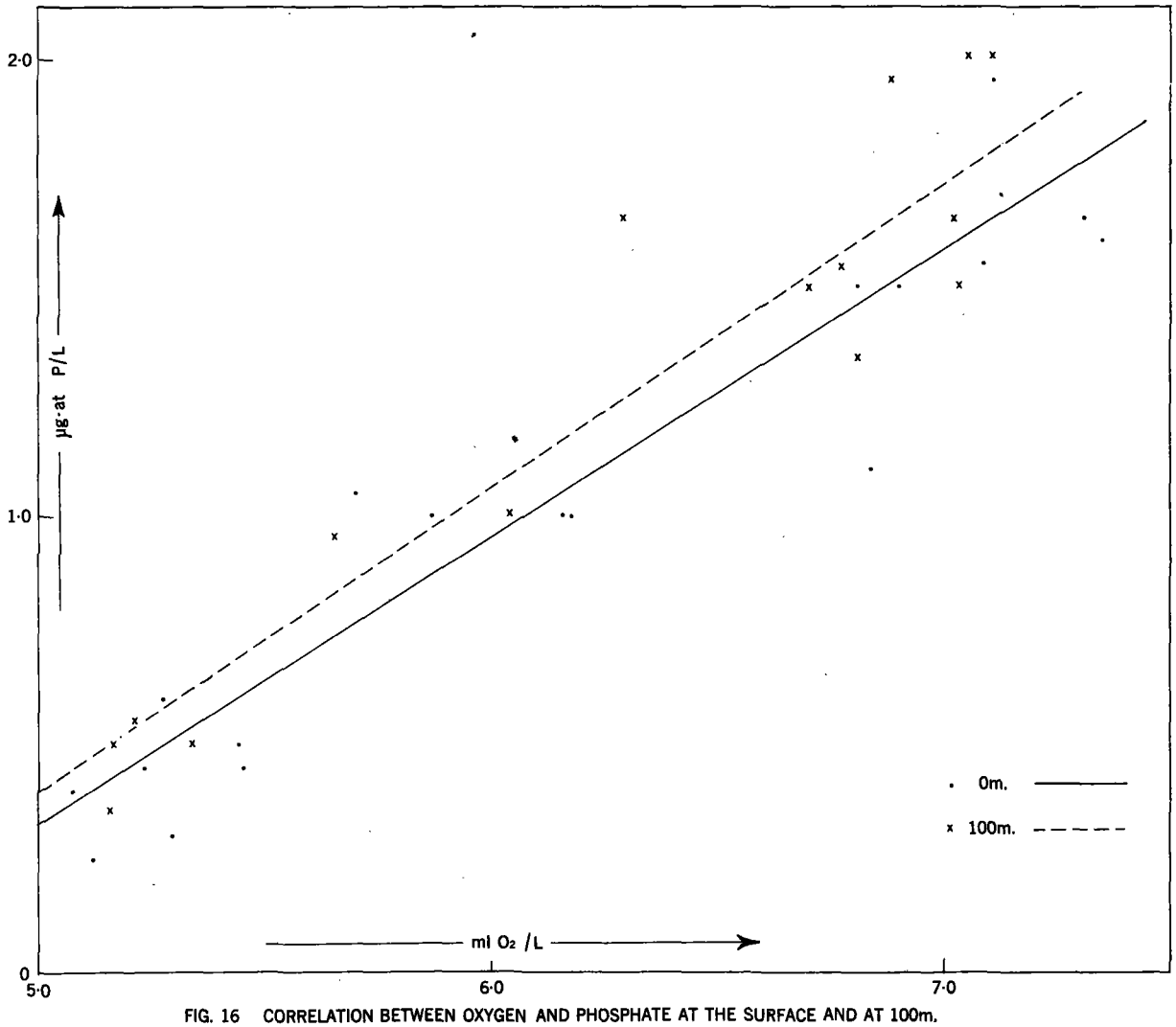

FIG. 16 CORRELATION BETWEEN OXYGEN AND PHOSPHATE AT THE SURFACE AND AT 100m.

Trigsurvey 1965.

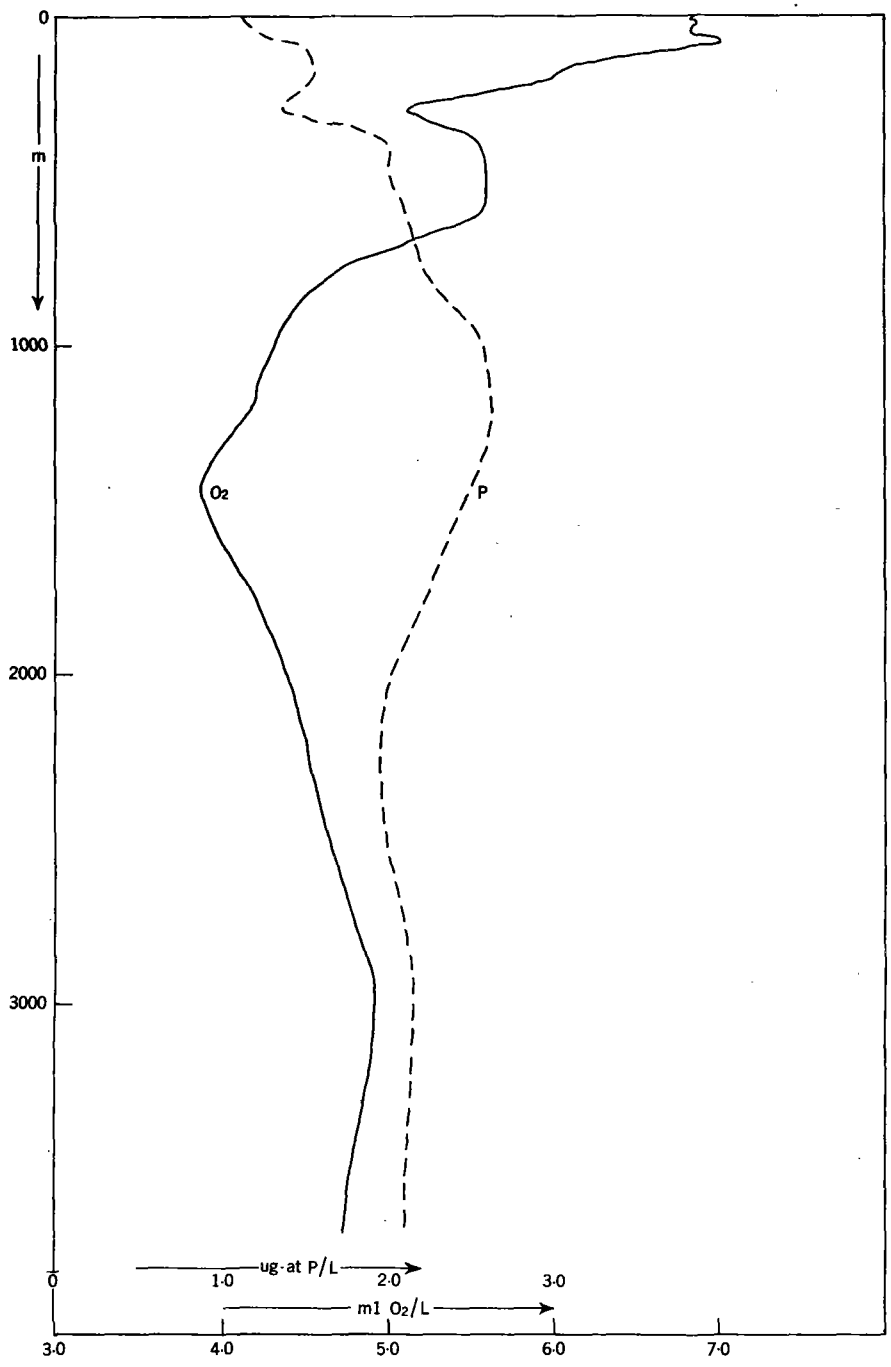

FIG. 17 INVERSE RELATIONSHIP BETWEEN OXYGEN AND PHOSPHATE WITH DEPTH AT STATION 36.

Trigsurvey 1965.

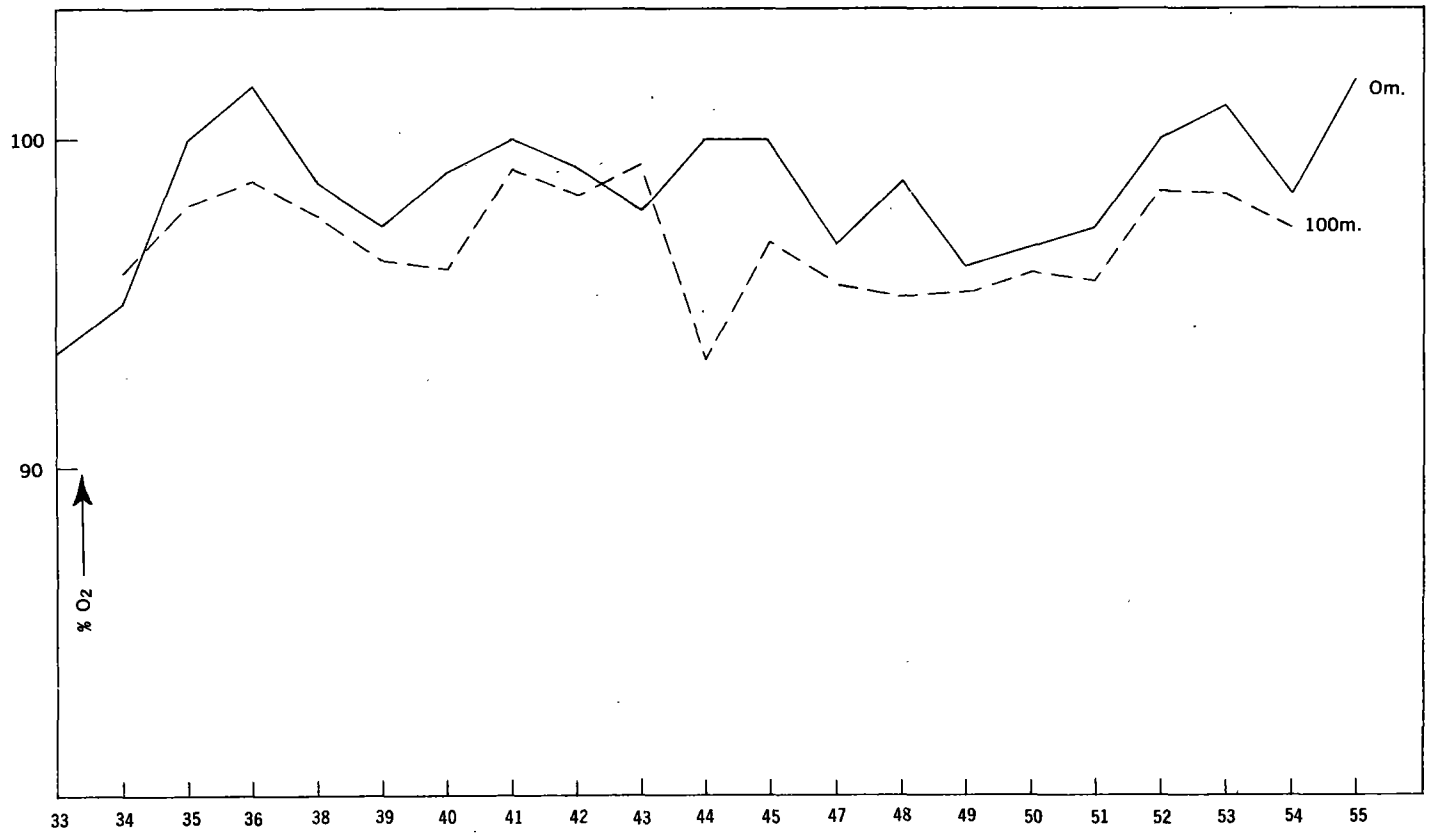

FIG. 18 PERCENTAGE OXYGEN SATURATION AT THE SURFACE AND AT 100m.

Trigsurvey 1965.

Part III

Physical oceanography

Reprinted from *Aust. J. mar. freshw. Res.*, vol. 16, 1965, p. 255-271.

GEOSTROPHIC CURRENTS IN THE SOUTH-EASTERN INDIAN OCEAN

By B. V. HAMON*

[*Manuscript received March* 10, 1965]

Summary

Dynamic topographies and geostrophic currents in the upper 1750 m are presented for several cruises between 1960 and 1963. The mean zonal surface circulation is shown to consist of the south equatorial current, 9–14° S., and a weak easterly current between 14° and 32° S. From 0° to 9° S., and again from 32° to 45° S., the mean dynamic height anomalies are independent of latitude, so that mean geostrophic zonal currents are negligible in these latitudes. Changes in dynamic height of the surface relative to 300 decibars within 2–4 weeks are shown for five "seasonal biological cruises", along 110° E. The significance of these changes in interpreting the dynamics of the region is discussed. Cyclonic and anticyclonic eddies appear occasionally off Fremantle, but no seasonal pattern was found. Cyclonic eddies south of Java are postulated, mainly during the south-east monsoon. A bathythermograph section across the equator on 95° E. is included; it shows no evidence of the equatorial undercurrent.

I. INTRODUCTION

This paper presents dynamic topographies and geostrophic currents in the upper 1750 m of the south-eastern Indian Ocean. Data obtained by Australian ships between 1960 and 1963 are used (CSIRO Aust. 1963*a*, 1963*b*, 1963*c*, 1964*a*, 1964*b*, 1964*c*, 1965*a*, 1965*b*, 1965*c*, 1965*d*, 1965*e*, 1965*f*, 1965*g*). Data from three earlier cruises of the Australian oceanographic frigate H.M.A.S. *Diamantina* in 1959 and 1960 (Dm 2/59, 1/60, and 2/60) have already been interpreted by Wyrtki (1962*a*).

II. CALCULATION OF DYNAMIC HEIGHT ANOMALIES

Anomalies of dynamic height were computed first for observed depths, using standard methods. Anomalies of dynamic height for standard depths were then computed by linear interpolation.

Following Wyrtki (1962*a*), a reference level of 1750 decibars was chosen for all cruises except Dm 3/61, and the anomalies of dynamic height computed relative to this reference level. Where the maximum sampling depth was less than the depth of the reference level, but greater than 1000 m, dynamic height anomalies were extrapolated, using data from adjacent stations. This extrapolation should not introduce appreciable errors in geostrophic currents or dynamic topographies above 700 m.

The results for each cruise have been presented separately, except in one case (Dm 2/62 and G 4/62) when two ships were operating simultaneously in the one area.

Since the geostrophic currents in tropical regions often vary rapidly with depth in the upper few hundred metres (Wyrtki 1962*a*), it was decided to present topo-

* Division of Fisheries and Oceanography, CSIRO, Cronulla, N.S.W. (Reprint No. 574.)

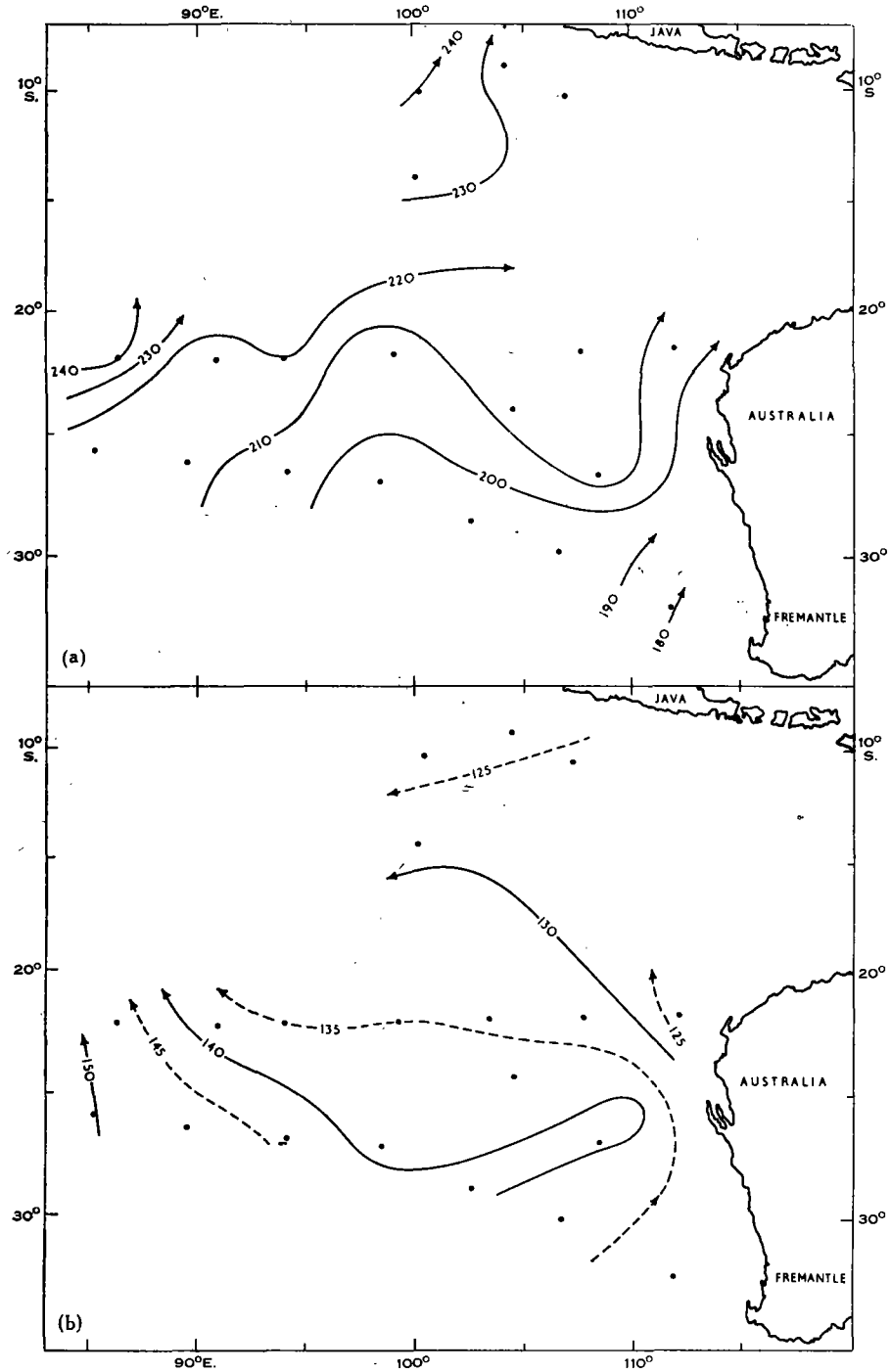

Fig. 1.—Dynamic topography of (*a*) the sea surface, and (*b*) the 300-decibar surface, relative to 1750 decibars. Cruise Dm 3/60 (October 16–November 15, 1960). Units: dyn cm. [An estimate of geostrophic current can be made from Figures 1–6 by noting the dynamic height change in 111 km (= 1 degree of latitude). This change (in dyn cm) is numerically equal to the current in cm/sec at latitude 38°S. At other latitudes, the current is inversely proportional to the sine of the latitude.]

graphies of both the surface and the 300-decibar level, relative to the assumed 1750-decibar level. Although this does not give as much detail as is sometimes presented, it should show the regions where there are rapid changes of circulation with depth.

The cruises reported here were planned to study chemical or biological problems. The station spacing, and more particularly the spacing between lines of

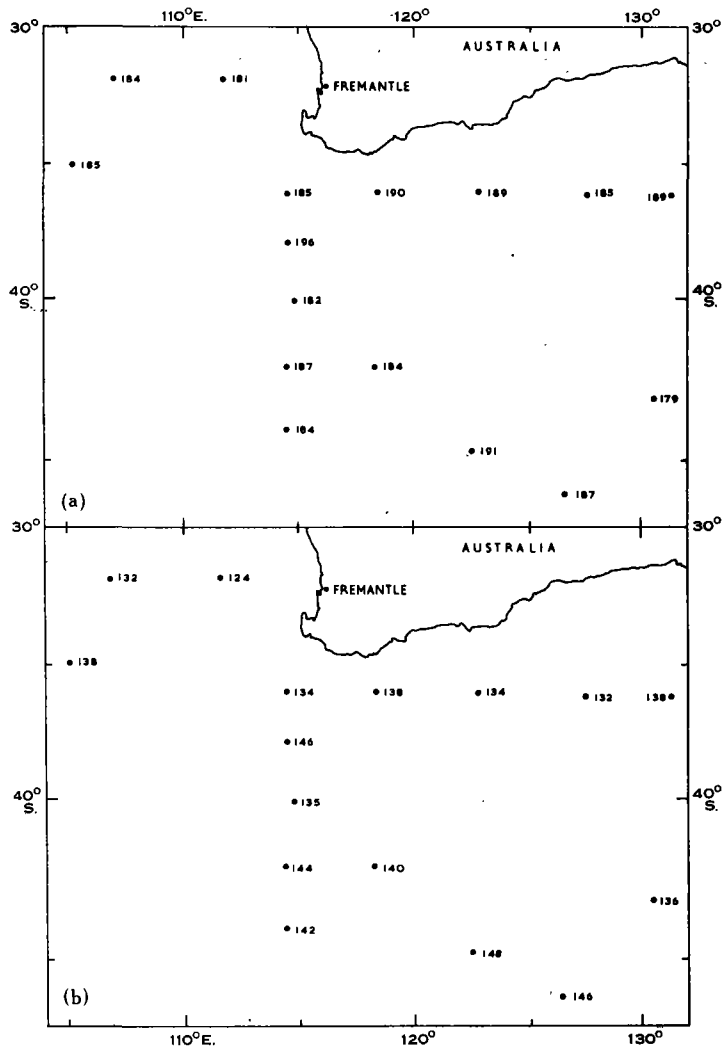

Fig. 2.—Dynamic height anomalies in dyn cm for (*a*) the sea surface, and (*b*) the 300-decibar surface, relative to 1750 decibars. Cruise Dm 1/61 (February 14–March 10, 1961).

stations, are often too large to permit contours of dynamic height anomaly to be drawn confidently. It is hoped that the results presented will suggest areas in which more detailed studies of the physical structure and circulation can be made.

III. Results

(*a*) *Cruise Dm* 3/60 (October 16–November 15, 1960)

The dynamic topographies of the 0 and 300-decibar surfaces, relative to 1750 decibars, are shown in Figures 1(*a*) and 1(*b*).

Figure 1(*a*) shows surface currents to the north and east throughout the whole area of the cruise. Figure 1(*b*) shows that at 300 m the north-easterly currents

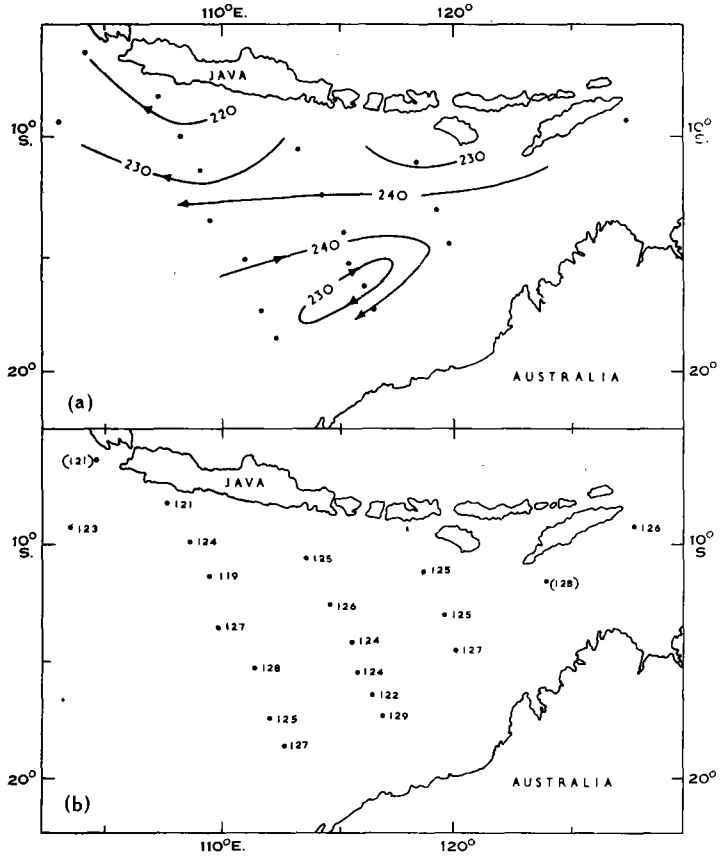

Fig. 3.—Dynamic topography of (*a*) the sea surface, and (*b*) the 300-decibar surface, relative to 1750 decibars. Cruise Dm 2/61 (May 1–June 12, 1961). Units: dyn cm.

have been replaced by north-westerly or westerly currents, except in the area off Fremantle.

(*b*) *Cruise Dm* 1/61 (February 14–March 10, 1961)

The anomalies of dynamic height relative to 1750 decibars for the surface and 300 decibar levels are shown in Figures 2(*a*) and 2(*b*), respectively. It will be seen that there is little variation in dynamic height on either surface. The station spacings and small range of dynamic height made it impossible to draw contours. The

southernmost station is in 46°S.; this is not far enough south to pick up the edge of the Antarctic convergence.

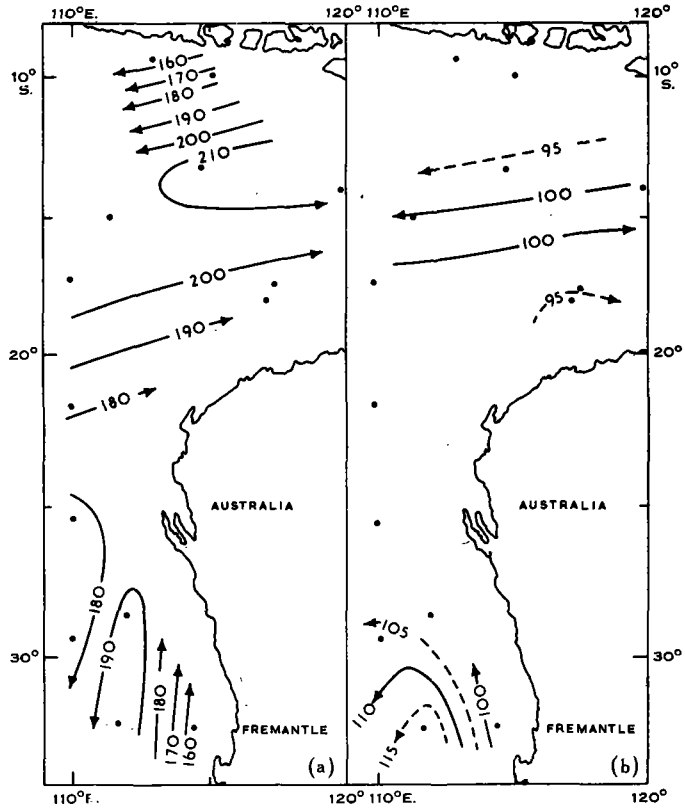

Fig. 4.—Dynamic topography of (*a*) the sea surface, and (*b*) the 300-decibar surface, relative to 1300 decibars. Cruise Dm 3/61 (July 20–August 26, 1961). Units: dyn cm.

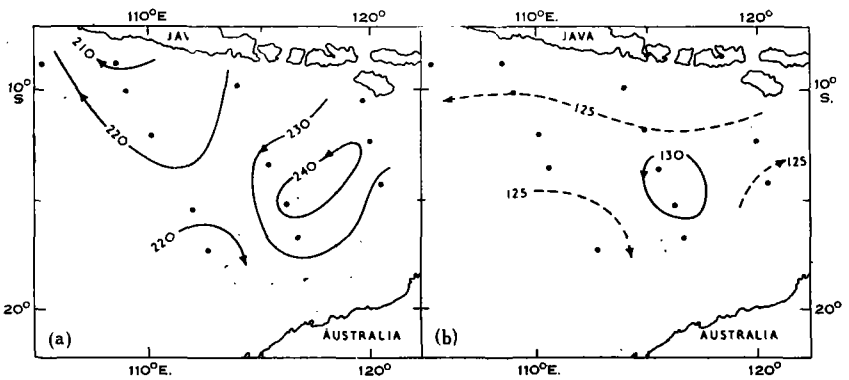

Fig. 5.—Dynamic topography of (*a*) the sea surface, and (*b*) the 300-decibar surface, relative to 1750 decibars. Cruise Dm 1/62 (February 12–March 25, 1962). Units: dyn cm.

Cruise Dm 3/62 (September 24–October 6, 1962), a meridional section on 110°E. from 32°S. to 45°S., showed a similar lack of feature in the surface and 300-decibar dynamic height anomalies.

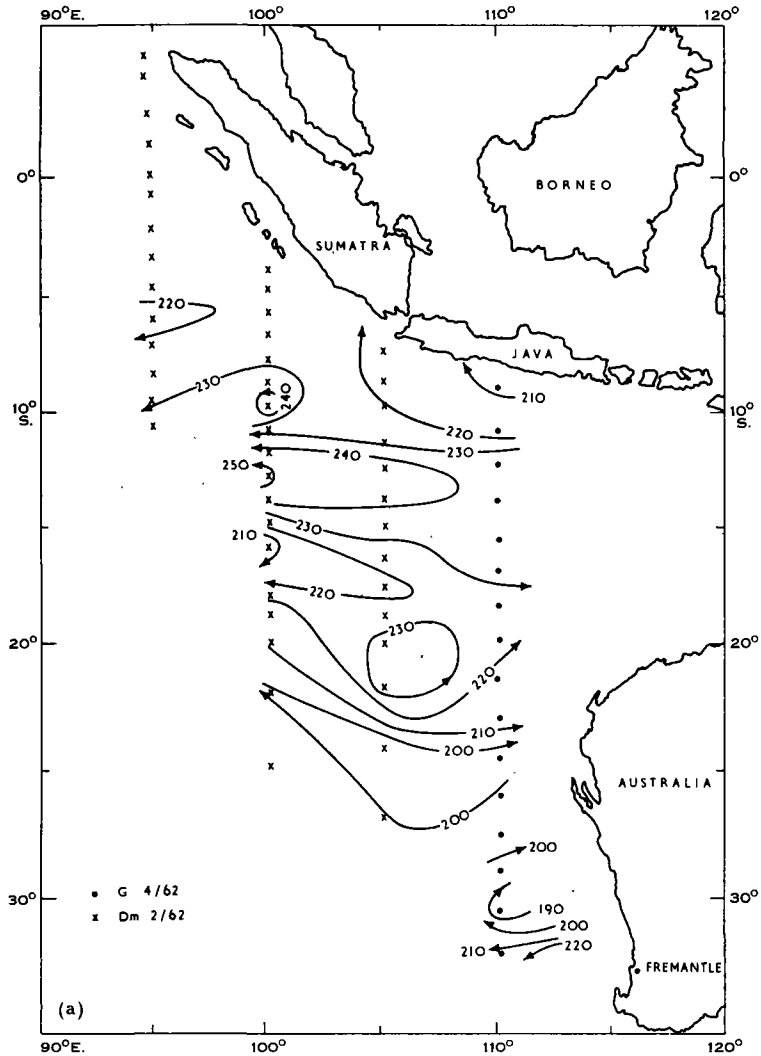

Fig. 6.—Dynamic topography of (*a*) the sea surface, and (*b*) the 300-decibar surface, relative to 1750 decibars. Cruises Dm 2/62 (X) (July 16–August 25, 1962) and G 4/62 (●) (August 19–September 16, 1962). Units: dyn cm.

(*c*) *Cruise Dm* 2/61 (May 1–June 12, 1961)

Figure 3 shows the dynamic topographies of the 0 and 300-decibar surfaces. Appreciable surface currents towards the west occur north of 13°S., and there is evidence of a weak cyclonic surface eddy at 17°S., 115°E. Only a slight trace of the eddy can be seen in the 300 decibar dynamic height anomalies (Fig. 3(*b*)).

(*d*) *Cruise Dm* 3/61 (July 20–August 26, 1961)

Stations were worked to a nominal depth of only 1500 m on this cruise, so that 1300 decibars was chosen as the reference level.

Figure 4(*a*) shows a strong westerly surface flow north of 13°S., within 200 miles of Java, and an eastward flow between 13°S. and 21°S. There is a strong current

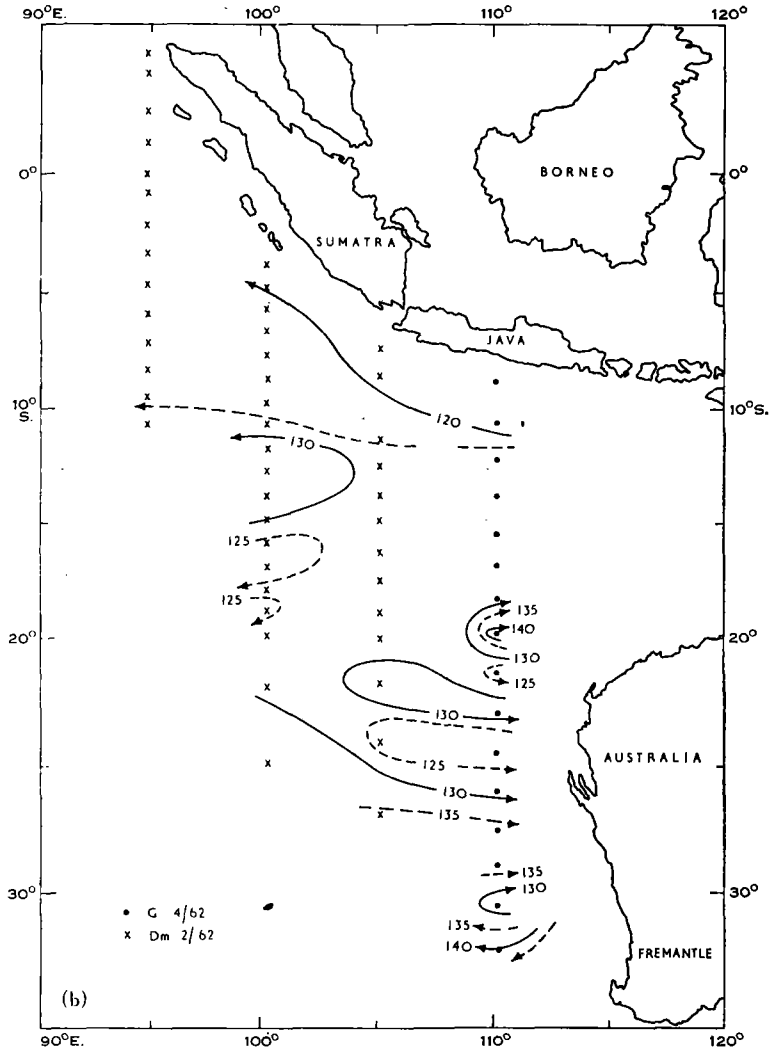

Fig. 6 (*Continued*)

to the north off Fremantle, but it is not clear where this current leaves the coast. The data suggest an anticyclonic eddy.

As in Cruise Dm 2/61, the westward flow south of Java has almost disappeared at a depth of 300 m (Fig. 4(*b*)). The northward current off Fremantle, however, is still well developed at this depth.

(e) *Cruise Dm* 1/62 (February 12–March 25, 1962)

The dynamic topography for the stations west of 122°E. on Cruise Dm 1/62 are shown in Figure 5. Some deep stations were worked in the Banda Sea on this

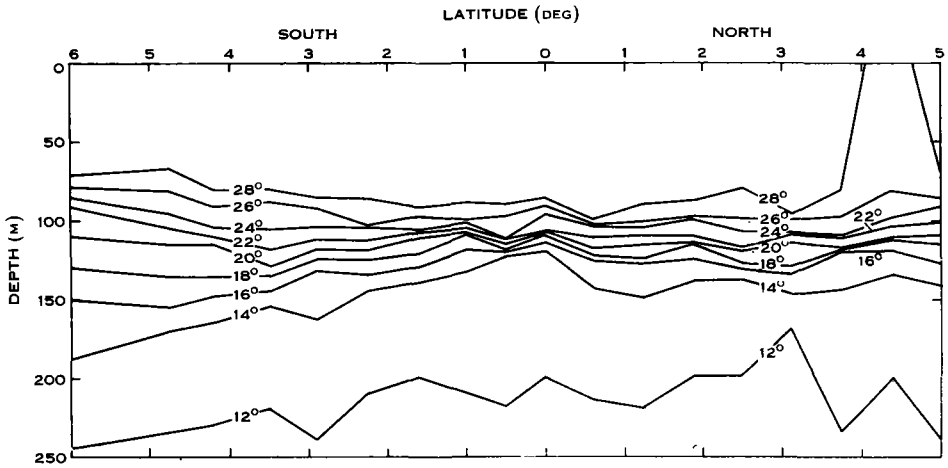

Fig. 7.—Temperature section (in °C) at 95°E., from 6°S. to 5°N., from bathythermograph results. Cruise Dm 2/62 (July 16–August 25, 1962).

cruise, but the results have not been included. Figure 5 shows a weak westward current between Java and 13°S., and a weak anticyclonic eddy centred at 15°S., 117°E.

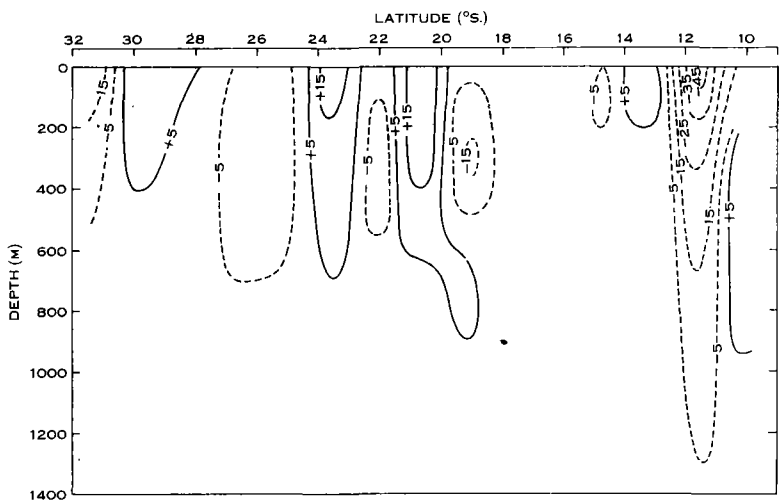

Fig. 8.—Zonal currents across 110°E. Cruise G 4/62 (August 19–September 16, 1962). Broken lines: contours of currents towards the west; solid lines: contours of currents towards the east. Contour interval 10 cm/sec.

(f) *Cruises Dm* 2/62 (July 16–August 25, 1962) *and G* 4/62 (August 19–September 16, 1962)

Cruise Dm 2/62 consisted of three north–south sections, on 95°E., 100°E., and 105°E. These sections have been combined with that of the first seasonal biological

cruise (G 4/62), on 110°E. The dynamic topographies of the 0 and 300-decibar surfaces are shown in Figures 6(*a*) and 6(*b*). The 5° spacing between sections makes contouring difficult.

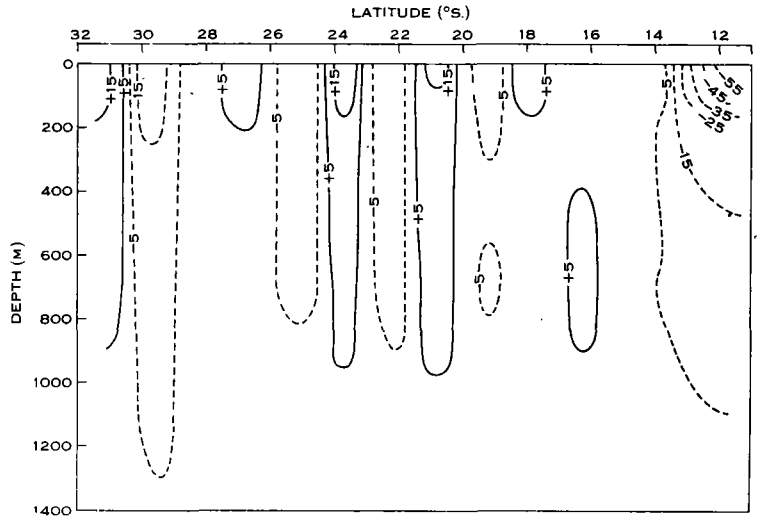

Fig. 9.—Zonal currents across 110°E. Cruise Dm 4/62 (October 15–November 13, 1962). Broken lines: contours of currents towards the west; solid lines: contours of currents towards the east. Contour interval 10 cm/sec.

There is little structure along the 95°E. section; apparently the section did not extend far enough south to show clear evidence of the South Equatorial Current. The

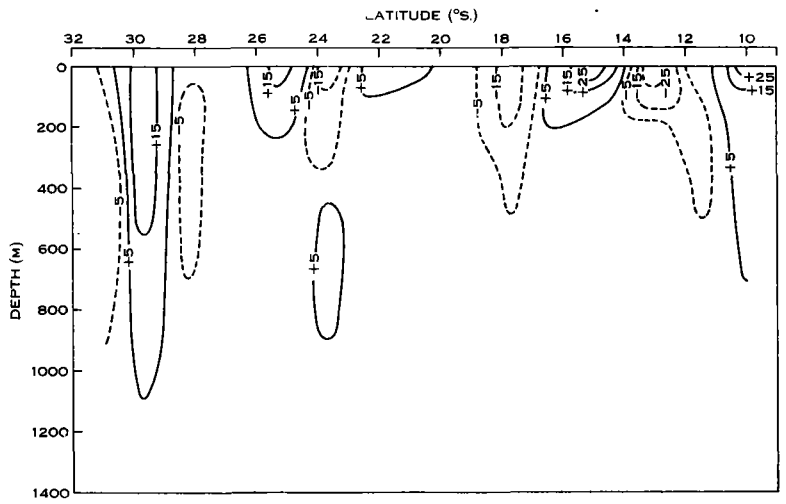

Fig. 10.—Zonal currents across 110°E. Cruise G 1/63 (January 17–February 17, 1963). Broken lines: contours of currents towards the west; solid lines: contours of currents towards the east. Contour interval 10 cm/sec.

South Equatorial Current appears at about 12°S. on the 100°E., 105°E., and 110°E. sections. On the 105°E. section, and more particularly on the 100°E. section, there are appreciable eastward currents south of the South Equatorial Current.

On Dm 2/62, a bathythermograph section was obtained across the equator, from 6°S. to 5°N., on 95°E. (94°30′E. at the north end of the section). The results

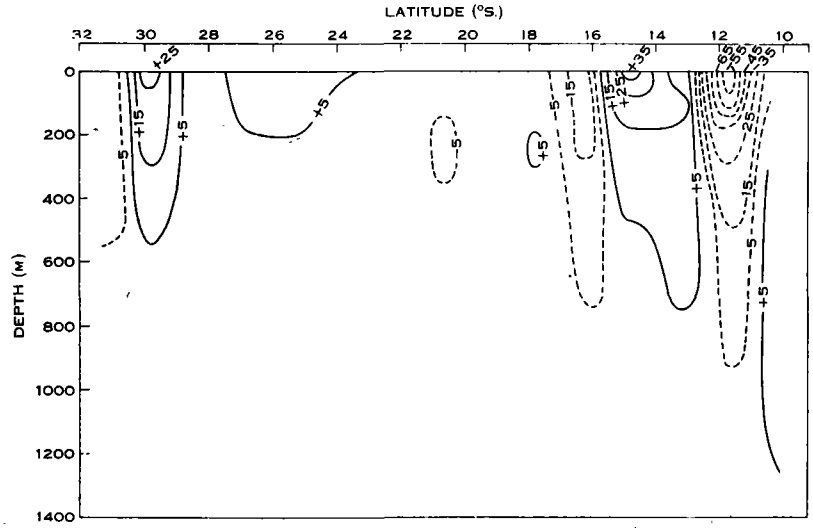

Fig. 11.—Zonal currents across 110°E. Cruise Dm 1/63 (March 28–April 27, 1963). Broken lines: contours of currents towards the west; solid lines: contours of currents towards the east. Contour interval 10 cm/sec.

are shown in Figure 7. There is no evidence of spreading of the isotherms near the equator, as has been found in the Pacific Ocean when an equatorial undercurrent is

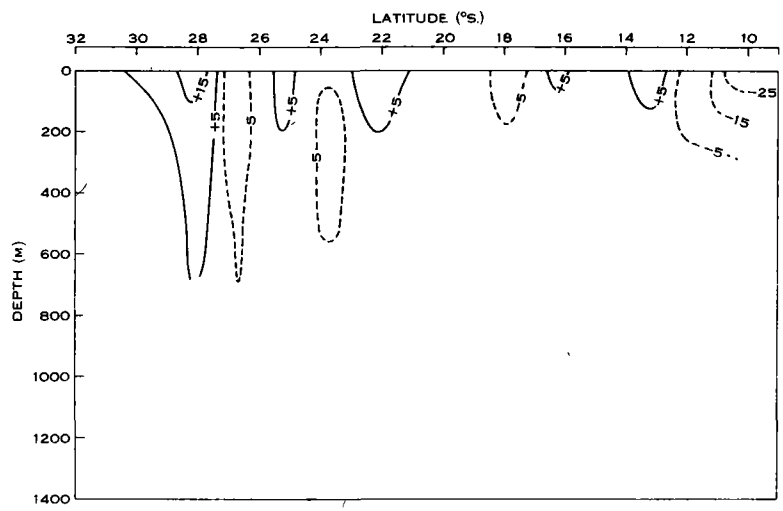

Fig. 12.—Zonal currents across 110°E. Cruise Dm 2/63 (May 6–June 3, 1963). Broken lines: contours of currents towards the west; solid lines: contours of currents towards the east. Contour interval 10 cm/sec.

present (Knauss 1960). Figure 7 shows a crowding together of the isolines, rather than a spreading.

(g) *The Seasonal Biological Cruises*

Between August 1962 and July 1963, six cruises were made to study the seasonal variation of biological conditions along 110°E. longitude, between Java and 32°S. The zonal geostrophic currents found on these six cruises are shown in Figures 8–13.

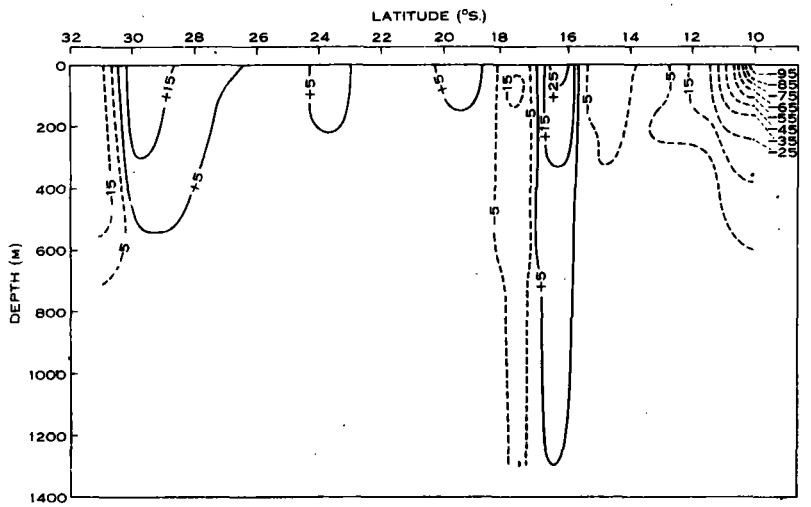

Fig. 13.—Zonal currents across 110°E. Cruise Dm 3/63 (July 9–August 11, 1963). Broken lines: contours of currents towards the west; solid lines: contours of currents towards the east. Contour interval 10 cm/sec.

On each cruise, stations were worked when steaming north, and again when steaming south along the same track, about 2 weeks later, after calling at Singapore.

TABLE 1

MEAN LATITUDE AND SURFACE VELOCITY OF THE SOUTH EQUATORIAL CURRENT ON LONGITUDE 110°E.

Cruise	Dates	Surface Geostrophic Current (cm/sec)	Mean Latitude
G 4/62	19.viii–16.ix.62	50	11°45′S.
Dm 4/62	15.x–13.xi.62	64	11°45′S.
G 1/63	17.i–17.ii.63	34	13°15′S.
Dm 1/63	28.iii–27.iv.63	75	11°45′S.
Dm 2/63	6.v–3.vi.63	35	10°15′S.
Dm 3/63	9.vii–11.viii.63	96	10°15′S.

Alternate deep and shallow (500 m) stations were worked 1½ degrees apart on both the northward and southward traverses. All deep stations were worked to the bottom:

the position of the deep station on the one traverse coinciding with the position of the shallow station on the other traverse. In preparing Figures 8–13, the deep station results for the northward and southward traverses have been combined without regard to the time difference between them, and the shallow station results have been disregarded.

In Figures 8–13, contours of equal zonal currents are shown in a vertical section along 110°E. The contour spacing is 10 cm/sec (approx. 0·2 knot). Currents less than 5 cm/sec are not regarded as significant.

The most prominent feature of the zonal currents in Figures 8–13 is the west-flowing South Equatorial Current. The computed surface current and the mean

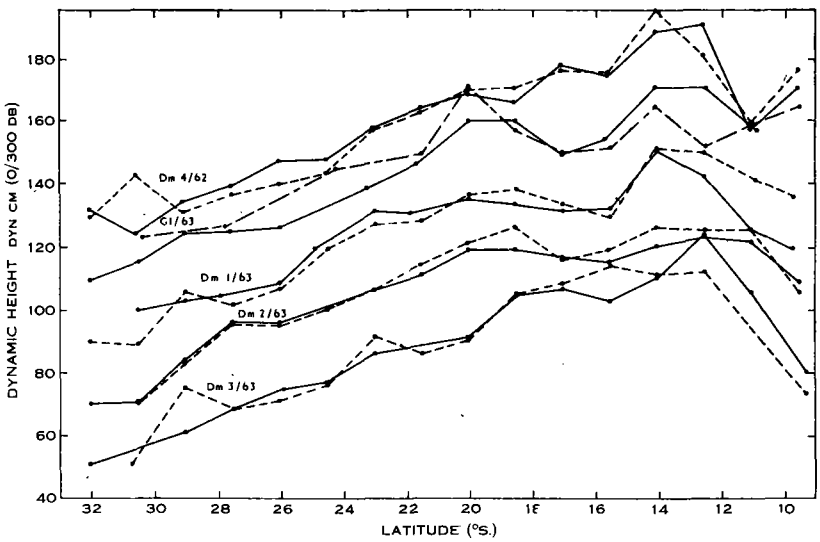

Fig. 14.—Dynamic height anomalies of the surface relative to 300 decibars, for five of the seasonal biological cruises. (●———●) Northward traverses; (●- - - -●) southward traverses. The ordinate scale is for Dm 3/63; it is to be moved upwards 20 dyn cm for each of the other cruises.

latitude of the South Equatorial Current for each cruise are given in Table 1. The width of the current appears to be of the same order as the station spacing (90 miles).

An indication of changes in the upper 300 m between the northward and southward traverses of each cruise can be obtained from Figure 14. This figure shows the dynamic height anomaly of the surface relative to 300 decibars, for the two traverses separately, on five of the seasonal biological cruises (shallow stations were worked to only 200 m on G 4/62). The average separation in time was 13 days at the north end of the traverses, increasing to 27 days at the south end. The differences between north and south traverses on each cruise are on the average small compared to the differences between cruises for the pair Dm 2/63 and Dm 3/63, but not for the other consecutive pairs of cruises. Because Dm 1/63 and 2/63 were separated by only 9 days, little change would be expected between them. It appears from Figure 14 that features with a scale of the order of several hundred miles (for

example, the dip in dynamic height between 14°S. and 20°S. on Dm 1/63 and Dm 2/63) are more persistent than features with a scale of the order of the station spacing (90 miles), as would perhaps be expected. The main conclusion to be drawn from Figure 14 is that much of the "station-to-station" detail in Figures 8–13 is probably unreliable.

A SCOR-UNESCO Reference Station (No. 1) was occupied at 32°S., 112°E. on all cruises. The north–south geostrophic currents between the reference station and 32°S., 110°E. on the six seasonal biological cruises are shown in Figure 15. The currents are small, and are mainly towards the south. There is no obvious seasonal variation.

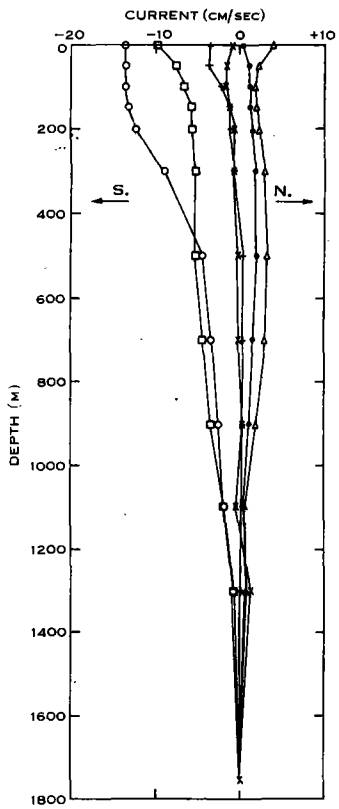

Fig. 15.—North–south currents between the reference station (32°S., 112° E.) and 32°S., 110°E., for the six seasonal biological cruises. ○ G 4/62; × Dm 4/62; + G 1/63; ● Dm 1/63; □ Dm 2/63; △ Dm 3/63.

IV. Discussion

The results presented here, and the earlier work reported by Wyrtki (1962*a*), show that the circulation in the south-eastern Indian Ocean is variable. This variability, particularly in the upper 300 m, makes it difficult to study the average circulation by combining the results of different cruises, and even more difficult to study seasonal variation.

Figures 1–6 suggest that with a few exceptions the dynamic height anomaly might be considered a function of latitude.

Figure 16 shows the surface dynamic height anomalies as a function of latitude from the equator to 45°S., and between 90°E. and 120°E. Data from all *Diamantina*,

Gascoyne, *Discovery*, *Ob*, and *Vityaz* cruises up to 1963 have been used. The mean curve in Figure 16 was fitted by eye, and shows the following main features: (1) a constant mean dynamic height anomaly from the equator to 9°S.; (2) an increase in dynamic height as the South Equatorial Current is crossed from 9°S. to 14°S.; (3) a gradual decrease from 14°S. to 32°S., implying a mean geostrophic current of 5 cm/sec towards the east; (4) constant mean dynamic height from 32°S. to 45°S. [The dynamic height anomaly would again decrease south of 45°S., in the circumpolar current.]

The mean dynamic height anomaly curve of Figure 16 summarizes the main features of the surface zonal geostrophic circulation in the south-eastern Indian Ocean. It does not include the easterly Java coastal current, which develops during the north-west monsoon (Soeriaatmadja 1957). This current appears on only one of

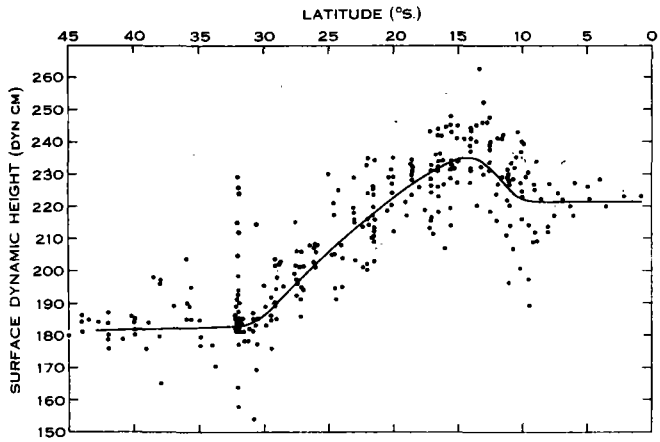

Fig. 16.—Dynamic height anomalies of the surface relative to 1750 decibars as a function of latitude, for all available data between 90 E. and 120 E.

the seasonal biological cruises (G 1/63, January–February), between 9°30′S. and 11°S., but as discussed below, this Java coastal current might have been present on other cruises, between 9°30′S. and the coast of Java.

The data in Figure 16 were separated into two groups on a seasonal basis, and mean curves fitted by eye for each group. The grouping was December–May, representing summer, and June–November, representing winter. The mean curve for summer was on the average about 6 dyn cm higher than that for winter, south of 17°S. Since this difference is small compared to either the scatter or the range of the mean in Figure 16, the separate figures have not been included.

Comparison of Figures 16 and 14 shows the importance of the upper 300 m in determining the surface dynamic topography in tropical and subtropical regions. By subtraction, it is seen that the mean dynamic height anomaly of the 300-decibar surface relative to 1750 decibars actually decreases slightly (about 10 dyn cm) in going north from 32°S. to 15°S., instead of increasing as found for the 0/1750-decibar surface (Fig. 16). This decrease implies an average geostrophic flow to the west at 300 m depth, but this would be too weak to appear in the vertical sections of Figures 8–13.

The data presented here give little indication of the West Australian Coastal Current, which, from current atlas data, flows north off the Australian coast between 20°S. and 30°S. (Wyrtki 1957). There is slight evidence of this northward current in Figure 1, but on other cruises station positions have been unfavourable.

The South Equatorial Current varies in position and strength, and at any one time is narrower than suggested by the mean curve of Figure 16. Table 1 shows that the south equatorial current, on 110°E., was furthest south in January–February 1963, and furthest north the following May–August. This agrees with the seasonal shift of the South Equatorial Current towards the coast of Java during the south-east monsoon

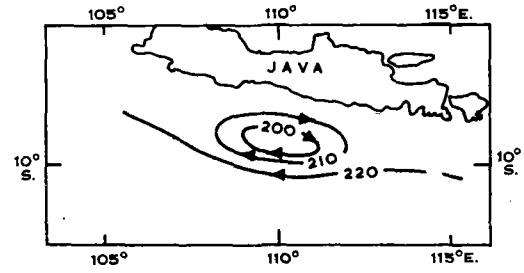

Fig. 17.— Suggested cyclonic eddy south of Java, when dynamic height anomalies less than about 200 dyn cm (0/1750 decibars) are found at 9°30′–11°S., 110°E.

(May–September) (Wyrtki 1957; Soeriaatmadja 1957) and its more southerly location during the north-west monsoon (October–April). The South Equatorial Current may at times be much further south than indicated in Table 1 or Figure 16; for example, there is no clear evidence of an appreciable west-flowing surface current north of latitude 16°S. on either 100°E. or 105°E. during *Vityaz* cruise 31 (October–November 1959).

The more extreme departures from the mean curve in Figure 16 deserve comment. It is probably safe to assume that departures from the mean greater than ± 15 or 20 dyn cm would be found only in limited areas, so that, if geostrophic balance is assumed, these extreme departures indicate the presence of cyclonic (low anomaly) or anticyclonic (high anomaly) eddies. Figure 16 shows that the largest departures from the mean are found near 10°S. and near 32°S.

The large negative departures between 9°30′S. and 11°S. were all on 110°E., so that they suggest the existence occasionally of closed cyclonic eddies south of Java (Fig. 17). No observations closer than 90 miles from the Java coast were made on the cruises which showed the low values in Figure 16, so the eddy structure of Figure 17 is at present hypothetical. When present, the eddy would locally reinforce the east-flowing Java coastal current (Soeriaatmadja 1957), and the South Equatorial Current.

The four lowest values of dynamic height anomaly between 9°30′S. and 11°S., Figure 16, were on the following cruises: Dm 2/59 (October), Dm 4/62 (October), Dm 1/63 (April), and Dm 3/63 (July). Except Dm 1/63, these cruises were during the south-east monsoon, when upwelling would be expected off the coast of Java (Wyrtki 1962*b*). The low values of dynamic height are associated with a shallow thermocline and a doming of isopycnal surfaces, but this structure is not necessarily evidence of upwelling.

TABLE 2

EXTREME VALUES OF DYNAMIC HEIGHT ANOMALY, 0/1750 DECIBARS, 30–32°S., 90–120°E.

Ship	Cruise	Station No.	Date	Position	Dynamic Height Anomaly (dyn cm)
Discovery	1/32	875	10.v.32	32°13′S., 113°48′E.	224
Diamantina	2/59	128	17.xi.59	31°50′S., 107°30′E.	164
Diamantina	2/59	131	17.xi.59	31°59′S., 109°57′E.	158
Diamantina	2/59	134	18.xi.59	32°03′S., 112°45′E.	205
Diamantina	3/61	193	26.viii.61	32°02′S., 111°45′E.	215
Gascoyne	4/62	181	19.viii.62	31°58′S., 111°48′E.	229
Gascoyne	4/62	182	20.viii.62	32°08′S., 110°00′E.	212
Diamantina	2/62	101	24.viii.62	32°00′S., 112°00′E.	226
Diamantina	4/62	159	11.xi.62	30°30′S., 110°00′E.	215
Diamantina	1/63	52	26.iv.63	30°30′S., 110°00′E.	169
Diamantina	3/63	123	10.viii.63	30°41′S., 110°03′E.	154

Table 2 gives details of the more extreme dynamic height anomalies between 30°S. and 32°S. They are all east of 107°E., that is, within 500 miles of the Australian coast. If the interpretation in terms of eddies is correct, it will be seen from Table 2 that anticyclonic eddies were present in May 1932, November 1959, August 1961,

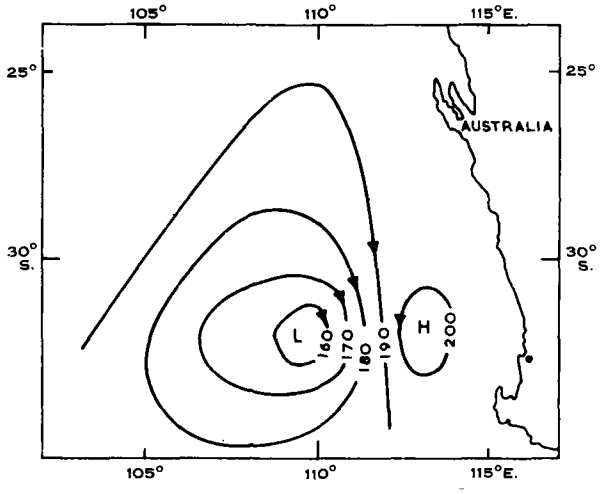

Fig. 18.—Suggested double eddy structure west of Fremantle (west Australia) in October–November 1959.

August 1962, and November 1962. Cyclonic eddies were present in November 1959, April 1963, and August 1963. No seasonal pattern is apparent. With this interpretation, a double eddy system may have been present off Fremantle in November 1959, as sketched in Figure 18.

The highest dynamic height anomaly in Figure 16, 263 dyn cm, was at 14°S., 110°E., and has been discussed by Wyrtki (1962*a*). This eddy moved or weakened rapidly, as it does not appear in the results of *Vityaz* cruise 39, 1 month later. It was not present the following year (Fig. 1; cruise Dm 3/60).

It should be emphasized that strong eddies, of the type discussed above, seem to be rare, particularly off Fremantle. For example, the reference station at 32°S., 112°E., was occupied 12 times between 1960 and 1963, but dynamic height anomalies greater than 200 dyn cm were observed only twice, and no value lower than 179 dyn cm was found. The four low values south of Java on 110°E. appeared in a total of 10 cruises that sampled the area, and there is evidence of another low value on 113°E. on cruise Dm 3/61 (Fig. 4).

V. References

CSIRO Aust. (1963*a*).—Oceanographical observations in the Indian Ocean in 1960. H.M.A.S. *Diamantina*, Cruise Dm 3/60. *CSIRO Aust. Oceanogr. Cruise Rep.* **4**.

CSIRO Aust. (1963*b*).—Oceanographical observations in the Indian Ocean in 1961. H.M.A.S. *Diamantina*, Cruise Dm 1/61. *CSIRO Aust. Oceanogr. Cruise Rep.* **7**

CSIRO Aust. (1963*c*).—Oceanographical observations in the Indian Ocean in 1961. H.M.A.S. *Diamantina*, Cruise Dm 2/61. *CSIRO Aust. Oceanogr. Cruise Rep.* **9**.

CSIRO Aust. (1964*a*).—Oceanographical observations in the Indian Ocean in 1961. H.M.A.S. *Diamantina*, Cruise Dm 3/61. *CSIRO Aust. Oceanogr. Cruise Rep.* **11**.

CSIRO Aust. (1964*b*).—Oceanographical observations in the Indian Ocean in 1962. H.M.A.S. *Diamantina*, Cruise Dm 1/62. *CSIRO Aust. Oceanogr. Cruise Rep.* **14**.

CSIRO Aust. (1964*c*).—Oceanographical observations in the Indian Ocean in 1962. H.M.A.S. *Diamantina*, Cruise Dm 2/62. *CSIRO Aust. Oceanogr. Cruise Rep.* **15**.

CSIRO Aust. (1965*a*).—Oceanographical observations in the Indian Ocean in 1962. H.M.A.S. *Gascoyne*, Cruise G 4/62. *CSIRO Aust. Oceanogr. Cruise Rep.* **17** (In press.)

CSIRO Aust. (1965*b*).—Oceanographical observations in the Indian Ocean in 1962. H.M.A.S. *Diamantina*, Cruise Dm 3/62. *CSIRO Aust. Oceanogr. Cruise Rep.* **18** (In press.)

CSIRO Aust. (1965*c*).—Oceanographical observations in the Indian Ocean in 1962. H.M.A.S. *Diamantina*, Cruise Dm 4/62. *CSIRO Aust. Oceanogr. Cruise Rep.* **20** (In press.)

CSIRO Aust. (1965*d*).—Oceanographical observations in the Indian Ocean in 1963. H.M.A.S. *Gascoyne*, Cruise G 1/63. *CSIRO Aust. Oceanogr. Cruise Rep.* **21** (In press.)

CSIRO Aust. (1965*e*).—Oceanographical observations in the Indian Ocean in 1963. H.M.A.S. *Diamantina*, Cruise Dm 1/63. *CSIRO Aust. Oceanogr. Cruise Rep.* **23** (In press.)

CSIRO Aust. (1965*f*).—Oceanographical observations in the Indian Ocean in 1963. H.M.A.S. *Diamantina*, Cruise Dm 2/63. *CSIRO Aust. Oceanogr. Cruise Rep.* **24** (In press.)

CSIRO Aust. (1965*g*).—Oceanographical observations in the Indian Ocean in 1963. H.M.A.S. *Diamantina*, Cruise Dm 3/63. *CSIRO Aust. Oceanogr. Cruise Rep.* **25** (In press.)

Knauss, J. A. (1960).—Measurements of the Cromwell Current. *Deep Sea Res.* **6**: 265–86.

Soeriaatmadja, R. E. (1957).—The coastal current south of Java. *Mar. Res. Indonesia* **3**: 41–55.

Wyrtki, K. (1957).—Die Zirkulation an der Oberfläche der südostasiatischen Gewässer. *Dt. Hydrog. Z.* **10**: 1–13.

Wyrtki, K. (1962*a*).—Geopotential topographies and associated circulation in the south-eastern Indian Ocean. *Aust. J. Mar. Freshw. Res.* **13**: 1–17.

Wyrtki, K. (1962*b*).—The upwelling in the region between Java and Australia during the south-east monsoon. *Aust. J. Mar. Freshw. Res.* **13**: 217–25.

Reprinted from *Bull. Inst. océanogr. Monaco*, vol. 65, no. 1,348, 1965.

Mesure de l'absorption de l'ultraviolet dans les eaux côtières de Nossi-Bé (Madagascar)

par

Alain SOURNIA

Laboratoire des pêches outre-mer,
Muséum national d'histoire naturelle, Paris

(Manuscrit reçu le 2 avril 1965)

Le problème de la pénétration des rayons ultraviolets dans la mer peut être abordé de deux façons : tout d'abord, on peut étudier *in situ* les modalités de la propagation du rayonnement et rechercher les variations qualitatives et quantitatives de la composition du spectre en fonction de la profondeur et des conditions du milieu.

On peut aussi mesurer l'absorption de l'ultraviolet par un échantillon d'eau de mer dans le but de caractériser la composition de celui-ci. L'absorption résulte en effet de la présence des différents constituants : eau pure, particules en suspension, sels minéraux et substances organiques. C'est ce second aspect que nous aborderons ici, en nous attachant particulièrement au rôle des matières organiques.

Les données que nous allons présenter concernent principalement la baie d'Ambanoro, à Nossi-Bé, et s'inscrivent dans l'étude générale du phytoplancton et de la production primaire de cette région [SOURNIA, 1965]*.

Historique

TSUKAMOTO [1927] a mesuré l'absorption de l'eau de mer à Roscoff, dans l'ultraviolet lointain; il remarque que l'extinction, croissant vers les courtes longueurs d'onde dans l'intervalle étudié (2 336 à 2 123 Å), est supérieure à celle de l'eau distillée, et attribue exclusivement cette différence aux sels dissous, à tort. HULBURT [1928] compare la pénétration de l'ultraviolet dans l'eau de mer, l'eau pure, et diverses solutions de sels dont il définit quantitativement le rôle. Les recherches de CLARKE et JAMES [1939], bien que n'intéressant que le spectre visible et le proche ultraviolet, montrent le rôle des particules en suspension vers les courtes longueurs d'onde. JOSEPH [1949, 1950] dans la Baltique et pour le proche ultraviolet, JERLOV [1950, 1951, 1953] dans les divers océans et jusqu'à 310 mμ, ont mesuré la pénétration des radiations *in situ :* celle-ci croît vers les courtes longueurs d'onde; elle est notablement supérieure dans les eaux littorales et les eaux à forte productivité, et fournit une intéressante caractéristique des masses d'eaux. Elle traduit essentiellement la présence de la substance jaune de KALLE [1937, 1949, 1961]. LENOBLE [1956, *a*, *b*, *c*, *d*] a mesuré l'absorption de l'ultraviolet en différents points des côtes françaises et recherché, à la suite de HULBURT, les coefficients d'absorption des divers sels. CHANU [1959] voit lui aussi dans la substance jaune l'origine de la différence entre l'absorption de l'eau de mer naturelle et celle de l'eau de mer artificielle, et isole cette substance en utilisant la technique développée par SHAPIRO pour

* Nous remercions vivement l'Office de la recherche scientifique et technique Outre-Mer de nous avoir accueilli au Centre d'océanographie et des pêches de Nossi-Bé pour y effectuer ces recherches.

les eaux lacustres. Enfin ARMSTRONG et BOALCH [1961 *a*, *b*], ont confirmé ces données, étudié dans la Manche les variations locales et saisonnières et recherché la nature des substances en cause.

Méthodologie

Nous avons suivi dans ses grandes lignes la méthode d'ARMSTRONG et BOALCH [1961 *a*] et utilisé un spectrophotomètre Beckman DU avec des cuves de quartz de 10 cm.

Les prélèvements à la mer se font au moyen de bouteilles non métalliques du type Van Dorm. Dans le but d'éliminer les particules en suspension, on filtre les échantillons sur membrane Millipore HA (porosité : 0,45 μ). Les mesures spectrophotométriques se font le plus tôt possible après le prélèvement; cependant les échantillons une fois filtrés conservent une absorption constante pendant plusieurs heures.

Mesure de référence : ARMSTRONG et BOALCH mesurent l'absorption de l'échantillon d'eau de mer par rapport à l'air, considérant cette référence comme plus sûre qu'une eau distillée dont on ignore exactement le degré de pureté. Les valeurs obtenues dans ces conditions représentent non seulement l'absorption des sels minéraux et des matières organiques, mais aussi celle de l'eau pure, ainsi que la réflexion sur les parois de la cuve. Il est préférable d'éliminer ces deux derniers effets en utilisant comme référence une eau déminéralisée et bidistillée préparée à l'abri des poussières de l'air. On prend de plus la précaution d'étalonner les deux cuves en comparant leurs spectres d'absorption de l'eau distillée; le facteur de correction qu'on en déduit est généralement négligeable. Finalement, l'absorption mesurée ne dépend plus que des teneurs en sels minéraux et matières organiques et la précision de la méthode se trouve notablement accrue.

Il serait également intéressant d'utiliser comme référence l'eau de mer artificielle; cependant, les impuretés des sels du commerce rendent ces mesures assez aléatoires.

Longueurs d'onde : Vers les plus courtes longueurs d'onde, à partir de 220 mμ, l'absorption devient très élevée et rend les mesures imprécises. Elle devient par ailleurs très faible dans le proche ultraviolet. Aussi limitera-t-on les mesures à l'intervalle 220-350 ou 220-400 mμ.

Le problème du choix des longueurs d'onde caractéristiques, qui n'est pas sans rappeler celui des pigments phytoplanctoniques, est à résoudre en trois étapes :

1. Réalisation du spectre complet de nombreux échantillons d'origines diverses, mesuré par intervalles de 5 ou 10 mμ, ou mieux, obtenu de façon continue au moyen d'un spectrophotomètre enregistreur.

2. Choix de quelques longueurs d'onde caractéristiques pour les mesures de routine.

3. Identification chimique des différentes substances en cause.

Provisoirement, la compilation des quelques spectres fournis par les divers auteurs et obtenus par nous-même à Barcelone et Nossi-Bé conduit à sélectionner les rayonnements : 220, 250, 265, 300 et 350 mμ, accessoirement 330 et 370 mμ. Notons que le pic 265 mμ est attribué aux doubles liaisons des bases puriques et pyrimidiques [YENTSCH & REICHERT, 1962].

Résultats

La figure 1 reproduit le spectre de trois échantillons prélevés dans la baie d'Ambanoro. Les deux stations **L** et **J** sont situées à l'ouverture de la baie; la station **A**, au fond de la baie, montre les absorptions les plus élevées.

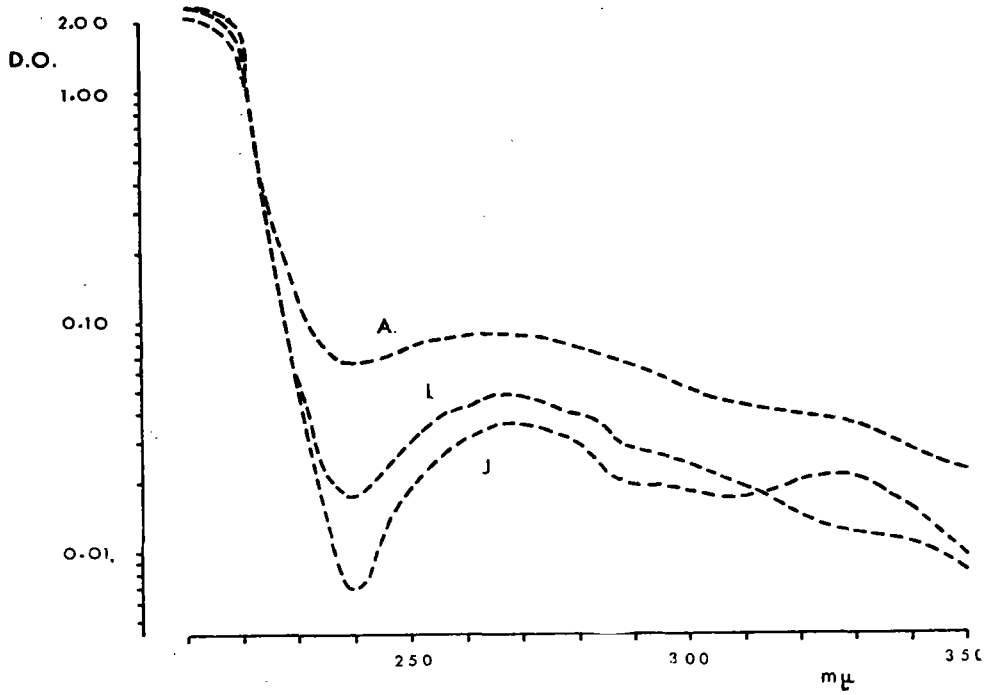

FIG. 1. — Spectres d'absorption des filtrats.

Des mesures hebdomadaires (figure 2) ont été poursuivies de mars à juin 1963 aux deux stations **L** et **A**, dont les caractères sont nettement opposés :

A : au fond de la baie, fond 4 m, eaux turbides (voisinage de la mangrove, apports d'eaux douces);

L : à l'ouverture de la baie, fond 8 m, eaux claires (récifs coralliens).

Les marées sont assez fortes (2 à 3 m) et leur périodicité telle que le niveau se trouve alternativement haut et bas de semaine en semaine à l'heure du prélèvement – celle-ci étant fixe. Les absorptions à 265 mμ, jugées bien représentatives, ont seules été représentées sur la figure.

Les salinités subissent un relèvement général pendant la période étudiée, qui se situe à la fin de la saison des pluies. Seules les salinités de la station **A**, la plus côtière, sont affectées par le rythme de la marée : valeurs plus élevées à marée haute, plus faibles à marée basse (le drainage des eaux littorales dessalées par les eaux du large exerce son effet maximal à la fin du reflux).

L'absorption de l'ultraviolet, à la station **L**, est en décroissance générale de mars à juin, en même temps que s'élèvent les salinités. Ces deux faits traduisent le changement de saison et l'influence décroissante

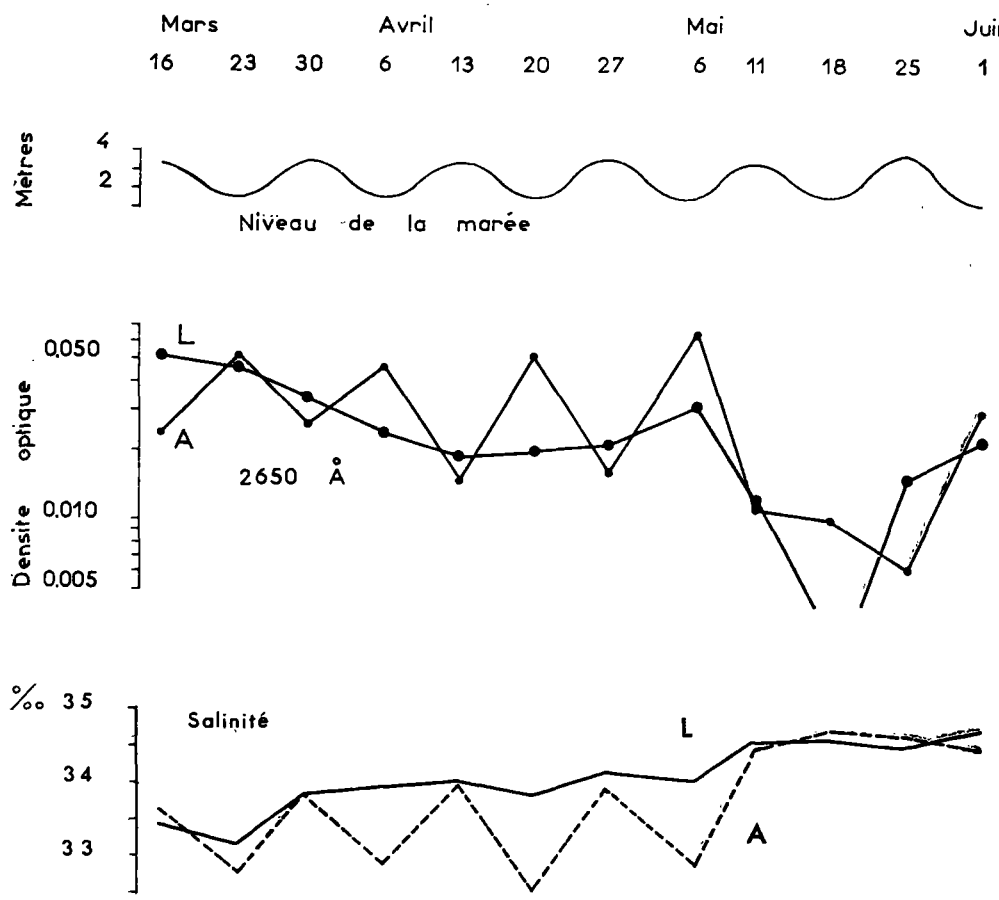

FIG. 2. — Mesures hebdomadaires.

des apports terrigènes. La station **A** montre des oscillations englobant de façon approchée les variations de la station **L**, mais reproduisant dans leur détail le rythme de la marée : valeurs plus élevées à marée basse, plus faibles à marée haute : de même que pour la salinité, l'influence continentale est dominante à marée basse et se traduit par une plus forte teneur en matières organiques. Ces variations dans le temps

à la station A peuvent être rapportées à des variations dans l'espace, les eaux de marée haute étant assimilables à des eaux du large, celles de marée basse à des eaux littorales.

Enfin la figure 2 montre, aussi bien dans l'évolution générale de mars à juin que dans les variations hebdomadaires, une relation inverse entre la salinité et l'absorption de l'ultraviolet. Ceci prouve que, du moins dans la région étudiée, les principaux sels minéraux ne jouent, par rapport aux substances organiques, qu'un rôle mineur dans l'absorption de l'ultraviolet.

Les valeurs relatives à cette série de mesures sont reportées dans le tableau 1.

TABLEAU 1

Absorption de l'ultraviolet et salinité aux deux stations

Mesures hebdomadaires

Date (1963)	Densité optique à 265 mμ (× 1 000)		Salinité (‰)	
	L	A	L	A
16/3	52	24	33,43	33,65
23/3	46	54	33,17	32,80
30/3	34	26	33,84	33,86
6/4	24	47	33,96	32,91
13/4	19	15	34,05	33,99
20/4	20	51	33,86	32,57
27/4	21	16	34,14	33,94
6/5	31	65	34,03	32,91
11/5	12	11	34,54	34,49
18/5	1	10	34,63	34,70
25/5	15	6	34,51	34,63
1/6	22	29	34,73	34,43

Le tableau 2 résume les données relatives à une prolifération de la Cyanophyte *Trichodesmium* observée le 2 avril 1963 à la station J. De tels phénomènes sont en effet fréquents dans la région à la saison des pluies [SOURNIA]. Les caractères physico-chimiques particuliers de cette « eau rouge » sont les témoins d'une masse d'eau différenciée au voisinage du littoral, à la faveur d'apports terrigènes, et dérivant par la suite au gré des courants. L'absorption de l'ultraviolet, plus élevée dans cette masse d'eau, peut n'être qu'une propriété concomitante, comme elle peut aussi résulter du métabolisme des algues [FOGG & BOALCH, 1958].

TABLEAU 2

« *Eau rouge* » à Trichodesmium *dans la baie d'Ambanoro, le 2 avril* 1963

	Eau à *Trichodesmium*	Eaux environnantes
Salinité	33,23	33,69
Chorophylle *a* (mg/m³)	17,03	0,60
Absorption U.V.		
230 mμ	0,140	0,100
250 mμ	0,075	0,030
265 mμ	0,040	0,020
300 mμ	0,020	0,003

Discussion

Il convient d'examiner successivement les diverses composantes de l'absorption de l'ultraviolet par l'eau de mer.

1 — ***L'eau pure***

L'absorption de l'eau pure est très faible et difficilement mesurable dans le visible; elle est minimale entre 400 et 540 mμ, et croît de part et d'autre de cet intervalle vers l'ultraviolet et, plus rapidement, vers l'infra-rouge [DAWSON & HULBURT, 1934; JAMES & BIRGE, 1938]. Dans l'ultraviolet, l'absorption croît régulièrement vers les courtes longueurs d'onde. Les phénomènes de diffusion moléculaire n'ont qu'un rôle restreint évalué au dixième de l'absorption totale [DAWSON & HULBURT].

L'effet de l'eau pure est éliminé dans les mesures, comme nous l'avons vu plus haut.

2 — ***Les particules en suspension***

CLARKE et JAMES [1939] puis BURT [1953] ont comparé dans le visible et le proche ultraviolet les spectres d'eaux naturelles et d'eaux filtrées : la différence met en évidence l'action des particules en suspension, qui apparaît prépondérante dans les régions côtières. Les particules en suspension ont un effet plus marqué vers la gauche du spectre, où le rapport : longueur d'onde/diamètre de la particule prend des valeurs de plus en plus petites.

Comme le montre JERLOV [1955], les particules de dimensions inférieures à 2 μ, bien que les plus nombreuses, interviennent peu dans la diffusion, puisque leur surface totale reste faible.

Aussi peut-on éliminer par filtration fine (porosité maximale : 1 μ) la presque totalité des phénomènes de diffusion et la plus grande partie des effets d'absorption dus aux particules.

3 — *Les sels minéraux*

Certains auteurs ont attribué aux sels minéraux l'exclusivité de l'absorption de l'ultraviolet, d'autres les ont au contraire totalement négligés. Les résultats sont par ailleurs souvent contradictoires.

On ne note pas de différence significative entre l'absorption de l'eau pure et celle de l'eau de mer artificielle dans le spectre visible [CLARKE & JAMES, 1939]. L'absorption devient manifeste dans l'ultraviolet et croît vers les courtes longueurs d'onde. Elle se décompose, selon HULBURT [1928], de la façon suivante : de 340 à 300 mμ, $Ca\ SO_4$ représente la moitié de l'absorption totale, H_2O le quart, les divers sels l'autre quart. De 300 à 250 mμ, $Mg\ Cl_2$, $Ca\ SO_4$ et H_2O en représentent chacun le tiers, les autres sels n'ayant qu'une importance minime. Selon LENOBLE [1956 *c*, *d*] aucun sel n'a de bande spécifique dans l'ultraviolet (les mesures de cet auteur couvrent l'intervalle 250-400 mμ): les coefficients d'absorption croissent vers la gauche du spectre, et l'importance de chaque sel est surtout fonction de sa concentration. L'ensemble des sels selon LENOBLE ajoute une absorption équivalente à la moitié ou au quart de celle de l'eau pure. Pour l'eau de la Manche, ARMSTRONG et BOALCH [1961 *a*] attribuent aux sels minéraux la moitié de l'absorption mesurée, pour les longueurs d'onde inférieures à 240 mμ.

Une mention particulière doit être faite concernant les nitrates, en raison de leur forte absorption aux environs de 200 mμ, qui a donné lieu à diverses techniques de dosage dont la plus récente est celle d'ARMSTRONG [1963].

4 — *Les matières organiques*

L'absorption d'une eau de mer filtrée est notablement supérieure à celle de l'eau de mer artificielle [CHANU, 1959; ARMSTRONG & BOALCH, 1961 *a*]. La différence est à attribuer à une substance ou un groupe de substances essentiellement organiques, dissoutes ou colloïdales, et dont la nature exacte est encore mal connue.

Distinction entre matières organiques et particules en suspension :

Elle est loin d'être aisée. JAMES et BIRGE [1938], CLARKE et JAMES [1939] appelent « suspensoids » l'ensemble des particules retenues sur filtre Berkefeld V, et « colors » les substances du filtrat. Cependant ils admettent que, d'une part, les « suspensoids » les plus fins passent à travers le filtre, de l'autre, qu'une partie des « colors » est associée aux particules. La distinction est donc dans ce cas tout à fait arbitraire. YENTSCH [1962] et divers auteurs admettent également qu'une fonction de la substance colorée se trouve sous forme figurée ou liée à des particules suspendues.

Il faut donc penser que la filtration, nécessaire pour éliminer les suspensions, retient une partie de la matière organique qui échappera ainsi aux mesures.

Essais d'identification

Un certain nombre de substances organiques ont été mises en évidence sur les extraits et les filtrats d'eau de mer. Il convient peut-être

mieux de dire qu'un certain nombre de propriétés ont été mises en évidence, car, dans leur ensemble, les données demeurent fragmentaires, et les analogies entre les divers composés décrits assez confuses.

Nous avons personnellement testé la présence de matières organiques dans nos filtrats de la façon suivante : dans une série d'échantillons (diverses cultures et eaux naturelles), nous avons simultanément mesuré le taux d'oxydation (permanganate de potassium en milieu basique) et l'absorption de l'ultraviolet. Les densités optiques sont directement proportionnelles aux volumes de permanganate consommé par l'oxydation.

La substance colorée à laquelle il est le plus souvent fait allusion est la « substance jaune » ou *Gelbstoff* de KALLE [1937, 1949, 1961], qui absorbe fortement les radiations violettes, mais n'a pas été étudiée par cet auteur aux longueurs d'onde inférieures à 387 mμ. Il s'agit d'un mélange de diverses matières organiques, colorées du jaune clair au brun foncé, se trouvant à l'état dissous dans toutes les eaux naturelles, mais considérablement mieux représentées dans les régions côtières. La substance jaune est souvent comparée, du moins quant à sa fonction, aux acides humiques des sols.

Il faut en rapprocher les substances appelées « colors » par JAMES et BIRGE [1938], définies comme des produits de décomposition organique, dissous ou colloïdaux; à la différence des « suspensoids », leur absorption est sélective dans le proche ultraviolet et leur présence caractéristique des eaux côtières.

SHAPIRO [1957] a donné pour l'eau des lacs une technique d'extraction de la matière jaune (évaporation sous vide et extraction par l'acétate d'éthyle), technique étendue par CHANU à l'eau de mer : la « substance jaune » obtenue par CHANU [1959] est reconnue de nature organique, non volatile, et présente un maximum d'absorption à 250 mμ.

Dans des cultures d'*Ectocarpus*, FOGG et BOALCH [1958] ont mis en évidence un produit extracellulaire azoté comportant un pic d'absorption à 260 mμ, ainsi qu'un autre composé, soluble dans l'éther et que son maximum d'absorption à 400 mμ rapproche de la *Gelbstoff*.

Enfin une fraction volatile a été isolée par ARMSTRONG et BOALCH [1960]; elle est en partie seulement organique et joue un rôle restreint (5 p. cent) dans l'absorption de l'ultraviolet.

Conclusions

1. L'absorption de l'ultraviolet par l'eau de mer, mesurée selon la technique décrite ci-dessus, est principalement due à la présence des matières organiques, et, pour une plus faible part, aux sels minéraux. L'effet des particules en suspension est en grande partie écarté.

2. La nature exacte des matières organiques en cause, et le rôle des « substances jaunes », restent à préciser, ainsi que la part de certains sels.

3. Cette méthode, simple et rapide, fournit en même temps une caractéristique des masses d'eau et une évaluation des matières orga-

nisues qui demeurent, à l'heure actuelle, mal connues et difficilement dosables par voie chimique.

4. L'étude d'une région côtière tropicale a, par ce moyen, mis en évidence les variations locales et saisonnières, l'abondance des matières organiques au voisinage de la mangrove et l'influence de la marée.

Résumé

L'absorption de l'ultraviolet par l'eau de mer est étudiée ici en tant que résultante des absorptions des divers constituants : eau pure, particules en suspension, sels minéraux et matières organiques dissoutes. La méthode spectrophotométrique utilisée élimine les deux premiers effets et fournit une estimation des matières organiques. La nature exacte et le rôle de ces dernières substances restent à préciser. Les variations locales et saisonnières, ainsi que le rôle de la marée, sont étudiés dans une baie tropicale.

Summary

Ultra-violet absorption by coastal waters of Nossi-Bé (Madagascar)

The absorption of ultra-violet light by sea-water is discussed here as the result of the absorption of its four components : pure water, suspended matter, inorganic salts and dissolved organic matter. A spectrophotometric method is used, which eliminates the effects of both pure water and suspended matter, and provides an estimation of organic matter. The exact nature and effects of the latter remain to be determined. Local, seasonal and tidal changes in a tropical bay are studied.

Zusammenfassung

Die Messungen der ultravioletten Absorption in den Strandzonen-gewässern von Nossi-Bé (Madagascar)

Die Absorption der ultravioletten Strahlen durch das Meerwasser wird hier als Ergebnis der Absorption der verschiedenen Bestandteile studiert : reines Wasser, suspendierte Teilchen, Mineralsalzen und gelöste organische Stoffe. Die angewandte spektrophotometrische Methode schaltet die beiden ersten Effekte aus, und liefert eine Abschätzung der organische Stoffe. Die exakte Natur und die Rolle dieser beiden Substanzen bleiben zu erwägen. Die lokalen und in die Jahreszeit passenden Variazionen sowie die Wirkung der Flut sind in einer tropischen Bucht studiert.

Измерение абсорбции ультра-фиолетовых лучей в прибрежных водах Носси-Бэ/Мадагаскар/

Алэн СУРНИА

Краткое содержание

Абсорбция морской водой ультра-фиолетовых лучей изучена здесь, как производная абсорбций различных составных частей: чистой воды, плавающих частиц, минеральных солей и растворенных органических веществ. Примененный спектрофотометрический способ удаляет два первых влияния и дает возможность оценить органические вещества. Остается уточнить истинную природу и роль этих последних веществ. Местные и сезонные изменения, как и роль морского прилива и отлива, изучены в тропической бухте.

Bibliographie

ARMSTRONG (F.A.J.), 1963. — Determination of nitrate in water by ultraviolet spectrophotometry. *Analyt. Chem.*, **35**, 9, pp. 1292-1294.

ARMSTRONG (F.A.J.) & BOALCH (G.T.), 1960. — Volatile organic matter in algal culture media and sea water. *Nature, Lond.*, **185**, n° 4715, pp. 761-762.

ARMSTRONG (F.A.J.) & BOALCH (G.T.), 1961 *a*. — The ultra-violet absorption of sea water. *J. mar. biol. Ass. U.K.*, **41**, 3, pp. 591-597.

ARMSTRONG (F.A.J.) & BOALCH (G.T.), 1961*b*. — Ultra-violet absorption of sea water. *Nature, Lond.*, **192**, n° 4805, pp. 858-859.

BURT (W.V.), 1953. — Extinction of light by filter passing matter in Chesapeake Bay waters. *Science*, **118**, pp. 386-387.

BURT (W.V.), 1955. — Interpretation of spectrophotometer readings on Chesapeake Bay waters. *J. Mar. Res.*, **14**, 1, pp. 33-46.

CHANU (J.), 1959. — Extraction de la substance jaune dans les eaux côtières. *Rev. Opt. (théor. instrum.)*, **38**, 12, pp. 569-572.

CLARKE (G.L.) & JAMES (H.R.), 1939. — Laboratory analysis of the selective absorption of light by sea water. *J. opt. Soc. Amer.*, **29**, pp. 43-55.

DAWSON (L.H.) & HULBURT (E.O.), 1934. — The absorption of ultraviolet light by water. *J. opt. Soc. Amer.*, **24**, pp. 175-177.

FOGG (G.E.) & BOALCH (G.T.), 1958. — Extracellular products in pure cultures of a brown alga. *Nature, Lond.*, **181**, n° 4611, pp. 789-790.

HULBURT (E.O.), 1928. — The penetration ol ultraviolet light into pure water and sea water. *J. opt. Soc. Amer.*, **17**, 1, pp. 15-22.

JAMES (H.R.) & BIRGE (E.A.), 1938. — A laboratory study of the absorption of light by lake waters. *Trans. Wis. Acad. Sci. Arts Lett.*, **31**, pp. 1-154.

JERLOV (N.G.), 1950. — Ultra-violet radiation in the sea. *Nature, Lond.*, **166**, nº 4211, pp. 111-112.

JERLOV (N.G.), 1951. — Optical studies of ocean waters. *Rep. Swed. Deep-Sea Exped.*, **3**, 1, pp. 1-59.

JERLOV (N.G.), 1953. — Influence of suspended and dissolved matter in the transparency of sea water. *Tellus*, **5**, 1, pp. 59-65.

JERLOV (N.G.), 1955. — The particulate matter in the sea as determined by means of the Tyndall meter. *Tellus*, 7, 2, pp. 218-225.

JOSEPH (J.), 1949. — Durchsichtigkeitsmessungen im Meere im ultravioletten Spektralbereich. *Dtsch. hydrogr. Z.*, **2**, 5, pp. 212-218.

JOSEPH (J.), 1950. — Durchsichtigkeitsregistrierungen als ozeanographische Untersuchungsmethode. *Dtsch. hydrogr. Z.*, **3**, 1/2, pp. 69-77.

KALLE (K.), 1937. — Meereskundliche chemische Untersuchungen mit Hilfe des Zeißschen Pulfrich-Photometers. VI. Mitteilung. Die Bestimmung des Nitrits und des « Gelbstoffs ». *Ann. Hydrogr. Berl.*, **65**, 6, pp. 276-282.

KALLE (K.), 1949. — Fluoreszenz und Gelbstoff im Bottnischen und Finnischen Meerbusen. *Dtsch. hydrogr. Z.*, **2**, 4, pp. 117-124.

KALLE (K.), 1961. — What do we know about the « Gelbstoff »? *Monogr. Un. géod. int*, **10** [Symposium on radiant energy in the sea, ed. by N.G. JERLOV], pp. 59-62.

LENOBLE (J.), 1956 *a*. — Sur la pénétration du rayonnement ultraviolet dans les eaux méditerranéennes. *C. R. Acad. Sci., Paris*, **243**, 22, pp. 1781-1783.

LENOBLE (J.), 1956 *b*. — Étude de la pénétration du rayonnement ultraviolet dans les eaux côtières de Bretagne. *Ann. Géophys.*, **12**, 3, pp. 225-227.

LENOBLE (J.), 1956 *c*. — Absorption du rayonnement ultraviolet par les ions présents dans la mer. *Rev. Opt. (théor. instrum.)*, **35**, 10, pp. 526-531.

LENOBLE (J.), 1956 *d*. — Sur le rôle des principaux sels dans l'absorption ultraviolette de l'eau de mer. *C. R. Acad. Sci., Paris*, **242**, 6, pp. 806-808.

SHAPIRO (J.), 1957. — Chemical and biological studies on the yellow organic acids of lake water. *Limnol. & Oceanogr.*, **2**, 3, pp. 161-179.

SOURNIA (A.), 1965. — Phytoplancton et production primaire dans une baie de Nossi-Bé (Madagascar). *C. R. Acad. Sci., Paris*, **261**, 11, pp, 2245-2248.

TSUKAMOTO (K.), 1927. — Transparence de l'eau de mer pour l'ultraviolet lointain. *C. R. Acad. Sci., Paris*, **184**, 4, pp. 221-223.

YENTSCH (C.S.), 1962. — Measurement of visible light absorption by particulate matter in the Ocean. *Limnol. & Oceanogr.*, **7**, 2, pp. 207-217.

YENTSCH (C.S.) & REICHERT (C.A.), 1962. — The interrelationship between water-soluble yellow substance and chloroplastic pigments in marine algae. *Bot. mar.*, **3**, 3/4, pp. 65-74.

Reprinted from *Mar. Obs., London,* July 1965, p. 125-130.

The Somali Current

SOME OBSERVATIONS MADE ABOARD R.R.S. "DISCOVERY" DURING AUGUST 1964

By J. C. SWALLOW, PH.D.
(National Institute of Oceanography)

Although well known as one of the fastest currents to be found in the open sea, the Somali* current has until recently received relatively little attention from oceanographers.

Like the Gulf Stream and the Kuro Shio, it is a 'western-boundary current', a consequence mainly of the distribution of wind stress over the whole of the Indian Ocean, and not just driven by the local winds in its own area. Unlike the other western-boundary currents though, this one runs right across the equator (if the East African coast current is included as well), and it undergoes a seasonal reversal of direction.

Because of these unique features, one might hope that a study of the Somali current would lead to a better understanding of the mechanism of ocean currents in general, and how they respond to changes in wind stress, as well as being a necessary part of the exploration of the Indian Ocean.

Besides its significance for dynamical oceanography, the Somali current is important in relation to the biology of the Indian Ocean and, perhaps, its fisheries, since it appears to be connected with the upwelling of cold water off the northern part of the east coast of Somalia, near Ras Hafun. This upwelling water is rich in the chemical nutrients needed for the growth of plankton, and can have a great effect on the biological productivity of the sea.

In the course of the International Indian Ocean Expedition there have been opportunities for research ships to make observations on this neglected current. The work described here was done during August 1964—a month when under the influence of the south-west Monsoon, the Somali current is setting strongly to the northward—in co-operation with the U.S. research vessel *Argo*, operated by the University of California. Compared to the intensive surveys carried out in the Gulf Stream and other more accessible currents, this two-ship survey lasting little more than a month can only be regarded as a reconnaissance, and as yet only part of the results collected by the two ships have been worked up and compiled together. Nevertheless, they represent the most detailed survey yet made of the Somali current, and some features of interest in the results can already be pointed out.

The observations made by the two ships comprised mainly water-sampling, current-measuring by various different means, and plankton-sampling with vertical nets. Tracks were chosen to cross the current working from south to north in irregular zig-zags, interlaced to give the best coverage of the area in the available time. After meeting in Mombasa to discuss final details of the programme, the two ships worked independently, though in daily radio contact, coming within sight of each other only once during the cruise when they met off Ras Mabber to transfer equipment and data. This account will be confined to *Discovery's* share of the work, but first some explanation of the kind of observations made would perhaps be appropriate.

Water-sampling provides the basic means of identifying the water masses being transported by the current. It also makes possible the calculation of relative

* The Somali current is the name given nowadays by oceanographers to that portion of the East African coast current which is north of the equator, alongside the east coast of Somalia, and which reverses its direction during the north-east monsoon. In the *Indian Ocean Current Atlas*[1] and in Hydrographic Office publications (e.g., the *Africa Pilot*, Vol. 3) the whole of this current is termed the East African coast current.

geostrophic currents, since the distribution of density in the water, and hence pressure, can be calculated from measurements of temperature and salinity of the water at different depths.

These indirect calculations of currents are similar to the much more familiar process of estimating winds from the spacing of the isobars on a weather map, but they suffer from the disadvantage that only differences of current, from one level to another, can be calculated. On these sections across the Somali current, *Discovery* occupied water-sampling stations at 10-mile intervals close to the coast, opening out the spacing gradually to about 50 miles at the offshore ends of the longer sections. Samples were collected from about 30 depths between surface and bottom at typical deep stations, though at some stations sampling was limited to the upper 1,200 metres, with 22 sampling depths. Temperature and salinity were measured at all sampling depths, dissolved oxygen, phosphate, nitrate and silicate were measured in the upper layers and at selected depths in the deep water.

Current measurements were made by various means. At each water-sampling station, current shear was measured in the near-surface layers, using a pair of direct-reading current meters. One meter was streamed at a constant depth of 10 metres while the other was lowered and read at 10-metre intervals down to 200-metres depth. At stations where radar fixing was possible, whether on the coast or on an anchored buoy, the ship's movement over the ground could be determined and combined with the current-meter readings to give true currents. At other stations, the current-shear profiles were fitted to surface currents deduced in the usual way from dead-reckoning and celestial navigation. Fortunately the weather was reasonably clear.

Surface currents were also measured by the electromagnetic method, in which a cable carrying a pair of electrodes is towed astern of the ship. The voltage between the electrodes depends on the rate at which the cable is cutting the vertical component of the earth's magnetic field, and is a measure of the component of surface current across the ship's track. The component along the track is obtained by altering course at right angles for a few minutes, then returning to the original line. Unfortunately, the magnetic equator passes through the region where the Somali current becomes strongest, and the vertical component of the earth's magnetic field was too small for satisfactory working of the method north of 4°N.

For measuring deep water-movements, at depths of 1,000 metres and below, neutrally-buoyant floats were used. These consist of sealed aluminium tubes, loaded so as to sink to a pre-determined depth, where they have the same density as the surrounding water, but a lower compressibility so that they do not sink deeper. They carry small sound transmitters by means of which they can be located, as they drift freely with the deep current. Such deep-current measurements are slow and laborious to make, they need to extend over at least half a day, preferably more, and call for continuous accurate knowledge of the ship's position which, in that area, could only be obtained by radar fixing on the coast or on an anchored buoy. Consequently, only a few such measurements were made, but they are very useful as an indication of the speed and variability of deep-water movements, and as a guide in choosing a reference level for geostrophic calculations of currents.

Biological sampling consisted of vertical hauls with a closing net for zooplankton, through standard depth-intervals between 1,000 metres and the surface, measurements of chlorophyll and fine-mesh net hauls in the upper 100 metres of water, and surface tows with a net designed to sample only the top few centimetres of water.

Bathythermograph observations were made every half-hour on passage between stations, and sea surface temperature was recorded continuously. An account of the meteorological equipment and observations has already been published.[2]

Discovery's observations of the East African coast current began in late July, with a section of 9 stations extending from 300 miles offshore in towards the coast, on the way from Cape Amber towards Mombasa. At the offshore stations, surface currents were weak (less than $\frac{1}{2}$ kt) and directed mainly in towards the coast.

Within 120 miles of the coast, the northward component of current increased, reaching 1 kt at 60 miles offshore, the maximum current observed being 2·7 kt only 20 miles from the coast. Closer in, there was a slight decrease. The current-shear measurements showed generally weak flow at 200 metres depth, most of the shear being within the thermocline below the warm surface-water. A buoy was anchored at the station 60 miles offshore, and a neutrally-buoyant float at 1,200 metres depth (only 200 metres off the bottom) moved north-east at nearly 0·4 kt. Although that may seem a weak current compared to those found at the surface, it is more than twice the average speed found at similar depths earlier in the cruise, and may imply substantial transport of deep water, below the main surface current. Unfortunately time did not permit any more deep-current measurements on that section. Approaching the coast, biological sampling with vertical nets was intensified, as plankton volumes increased from the usual low oceanic values.

Leaving Mombasa on 2nd August, the *Discovery* made a quick passage along the coast as far as 1°N, with a favourable wind and increasing surface current. At the first station, within 10 miles of the coast, combined current-meter observations and radar fixes indicated a surface current of 4·2 kt, decreasing with depth to about half-value at 100 metres. Working south-eastwards across the current, four more stations were occupied in a short section out to 60 miles from the coast. The current was narrow, decreasing to 2 kt at the surface at 23 miles offshore, though still running north-eastwards, parallel to the coast. Farther out along the section it decreased to about 1 kt and turned more northward. The current-shear at the two inshore stations was too strong for more than one wire to be used over the side at a time. Usually in the *Discovery* it had been possible to do water-sampling, current-meter observations, and vertical net hauls simultaneously but with each wire straying differently in the strong current, according to the depth and drag of the gear being used, each kind of observation had to be made separately, and the vessel manoeuvred to keep the single wire as near vertical as possible.

A second short section was then worked at 3°N, where a 2½-kt current was found in shallow water 8 miles offshore, but at 15 miles off, in deep water, the current was 4·7 kt, decreasing with depth to less than a knot at 200 metres. Farther out the current decreased, but not so sharply as in the first section; it was still 3 kt at 50 miles off. There were no signs of upwelling of cold water near the coast, on these short sections near the equator.

Next, a longer line of 10 stations, eastwards from the coast at 4½°N, was begun. Two sections made by the U.S. research vessel *Atlantis II* in 1963 had indicated a weak, broad countercurrent outside the main Somali current, and this was again observed by the *Discovery*. At the first station of this longer section, 5 miles from the coast, there was again a relatively weak current, but 10 miles farther out the current was running at 6 kt, to the northward with 4 kt of shear between surface and 100 metres depth. It was difficult working with even one wire over the side in the strong current, and only by rapid manoeuvring could anything like a vertical net haul be achieved. The water bottles sometimes failed to close properly, due to the drag of the current, and some casts had to be repeated several times. Despite the slow progress along the section, a full series of observations were made, with water sampling to the bottom and to 1,200 metres depth at alternate stations. The surface current decreased to 3 kt at 60 miles offshore, and was below 1 kt at 140 miles off. A buoy was anchored at that station, and a deep current of 0·4 kt towards the south-east, at 1,000 metres depth, was observed. Beyond 200 miles from the coast, a weak surface countercurrent, towards the south, was found.

Returning on a north-westward course, the *Discovery* soon came back into the main current, which exceeded 1 kt at 160 miles from the coast, and 2 kt at 100 miles. Further increase in current made it uneconomic to maintain the north-westward course of the section, and the later stations fall on a line running almost due north. The strongest surface current encountered was 6·9 kt, 22 miles offshore near 8°N, where the current was already beginning to turn away from the coast.

As would be expected in crossing a current from right to left, north of the equator, the depth of the near-surface isotherms had decreased steadily along the section, and within 20 miles of the coast the thermocline came to the surface, with a rapid decrease in surface temperature and current. Temperatures as low as 13·2°C (55·8°F) were found close inshore a little farther north, and as expected the cold water was relatively rich in nutrients. There was little evidence of plankton growth, however, in the coldest water, in fact the most obvious biological feature of that area was the number of dead fish seen on the surface, most probably killed by a sudden invasion of cold water. *Discovery* then worked north along the coast to Ras Hafun, and made another section north-eastwards towards Socotra. Surface temperatures remained below 20°C (68°F) out to 100 miles offshore, and currents in the cold water were relatively weak and variable, but predominantly northward. Returning from south of Socotra towards Cape Guardafui, warm water spreading from the Gulf of Aden was found on the surface, with the cold water moving northward below it. Only at these stations in the northern part of the cold-water area were abundant quantities of plankton found, with large numbers of larval fish. Remarkably few birds were seen, though they are usually abundant in upwelling areas.

After a brief visit to Aden, *Discovery* returned to the cold-water area to make further chemical and biological studies in the upwelling water. Seven station positions were chosen where it was hoped to find successive stages in the growth of plankton, and some further deep current measurements were made.

So far, there had been no measurements of deep currents under the strongest part of the surface current, although two observations, both showing only weak motion at 1,000 metres, had been made farther offshore during the last long section. Since the strongest current observed had been just within radar range of the coast, it was possible to keep track of neutrally-buoyant floats there without attempting to anchor a reference buoy (the buoys and moorings available were unsuitable for more than a 3-kt current, 100 metres thick). The surface current was found to be 6 kt on this second visit, and a weak southward movement was observed at 1,000 metres depth.

The ship then headed northward in a series of zig-zags, making half-hourly bathythermograph observations to delineate the boundary of the cold-water area, and the edge of the current, which turned more markedly eastward before reaching 10°N. A surface current measurement was made near 53°E, well out of radar range of the coast, by putting out a drogue attached to a buoy and tracking it relative to an acoustic marker laid on the sea floor. The surface current was 4·7 kt, slightly south of east. Soon after recovering the drogue and setting course northwards, the thermograph showed the expected drop in temperature on leaving the current, but this was followed quickly by a sharp rise, of 7°C (13°F), and next morning's stars indicated a north-westward set.

The cold water seemed to be drawn out into a narrow filament near 9½°N 54°E, with opposing currents in the warm water on either side. The *Argo* noticed what was probably an extension of this feature, in the form of a less marked brief temperature drop in a north–south section on 55°E. *Discovery's* observation was made on 3rd September, in the dark, and shortage of time prevented further investigation of this strange situation. Two days later, however, the m.v. *Border Pele* passed through the same area, fortunately in daylight. The Master, Captain E. L. Lloyd, reported sighting a continuous line of breakers running NW–SE. Passing through the disturbance, the ship's head was deflected in a manner consistent with the suspected strong current-shear, and a drop in sea surface temperature was observed.*

Two more stations in the northern part of the cold-water area completed *Discovery's* work on the Somali current. In all, 61 stations had been occupied, and nearly 1,000 bathythermograph observations made. The work of checking thermo-

* I am indebted to Lieut.-Cdr. L. B. Philpott for passing on this report from the *Border Pele*.[3]

meter corrections, sorting plankton samples and identifying them, correcting current-meter readings and compiling the data into a usable form, is continuing, and the results will be published elsewhere as they become available. From the current measurements, it seems clear that there is a great increase in volume transport of the current, above the 200-metre level, once it has crossed the equator, and the extra water comes partly from below 200 metres and is partly drawn in from the eastern side of the current. The inflow from the side is most marked at a depth of about 150 metres, near the bottom of the warm surface layer and the top of the thermocline on the oceanic side of the current. The surface water, which by geostrophic calculation should follow the same course, seems to be held off by the frictional effect of the local wind. One is tempted to speculate whether this may stabilize the transport against variations in local winds, or whether perhaps the transport of the current may even be greater when the local wind is weaker.

As an aid in planning the Somali current work, charts of the winds and sea surface temperatures in the area were prepared on a larger scale than is used in M.O. 519,[4] from information kindly made available by the Meteorological Office. All the accumulated ship's reports from that area, for the months of July and August, were plotted, and the logs of ships reporting abnormally low temperatures were consulted. This information is essential in estimating to what extent the oceanographic observations, limited to very few years, may be representative of average conditions. The winds in August 1964, although strong enough, were somewhat weaker than had been expected. Abnormally low temperatures were found by the *Discovery* in the cold-water area, though these were generally close inshore and might not have been observed by ships on passage. The Naval Weather Service is co-operating in further study of surface temperatures in this area.

The upwelling of cold water near 8°N seems clearly to be related to the speed of the current and the increasing slope of the isotherms as the water moves northward from the equator. If the current had been weaker, it could have travelled farther north before the thermocline came to the surface, but when that has happened the current cannot continue north at the same speed and its only course is to turn east. The filament of cold water going south-eastwards, with opposing currents on either side, is a more puzzling feature, with some resemblance to an almost closed-off meander.

Any further reports of its occurrence, in 1964 or in other years, would be most welcome.

There are two practical points concerning the *Discovery's* observations which it may be appropriate to mention here. First, in cases where radar fixing was not available, and surface currents were calculated from dead reckoning and celestial fixes, the biggest uncertainty was in estimating leeway on passage, and its variation with the relative bearing of the wind. (Movement through the water on station was measured by the shallow current-meter, which was read at 5-minute intervals throughout each station.)

The second point concerns surface temperatures in the cold-water area. Temperatures observed with the bucket thermometer were systematically higher than those recorded on the thermograph, the discrepancy being greater at lower surface temperatures (or at larger air-sea temperature differences), and reaching 0·6°C (1·1°F) in extreme cases. Evidently the heat-exchange between warm air and cold sea was affecting only a thin layer of surface water and not reaching the thermograph sensor, which is sited well forward (not in the engine-room intake) at a depth of approximately 4 metres. At water-sampling stations in that area, it was noted that the thermometers on the shallowest bottle, at a nominal depth of 1 metre, showed temperatures intermediate between the bucket and the thermograph. This is mentioned here as an example of one way in which apparently genuine differences between bucket and intake temperatures could occur.

In conclusion, may I take this opportunity of expressing my thanks to all those concerned with collecting and processing the ships' observations that we have used,

UNESCO ARCHIVES

and are using, in studying this area. May I also thank all those involved in the work of the R.R.S. *Discovery*, in particular Captain R. H. A. Davies, for his consistently helpful understanding in difficult conditions, and Mr. G. L. Swanson, Chief Officer, for his care in taking star sights.

REFERENCES

1. London, Meteorological Office. Indian Ocean Currents, (M.O.392), 2nd edn. London, 1939 (reprinted 1963).
2. Cox, W. J. Meteorological Observations aboard R.R.S. "Discovery". *Mar. Obs., London*, **35**, 1965, p. 21.
3. m.v. *Border Pele*. Marine Observers' Log, disturbed water. *Mar. Obs., London*, **35**, 1965, p. 113.
4. London, Meteorological Office. Monthly Meteorological Charts of the Indian Ocean, (M.O.519). London, 1949 (reprinted 1959).

Printed in England for Her Majesty's Stationery Office by
William Clowes and Sons, Ltd., London and Beccles

Reprinted from *Aust. J. mar. freshw. Res.*, vol. 17, 1966, p. 61-76.

DISTRIBUTION OF BANDA INTERMEDIATE WATER IN THE INDIAN OCEAN

By D. J. ROCHFORD*

[*Manuscript received December* 24, 1965]

Summary

Banda Intermediate water has been identified as a salinity minimum (salinity 34·58–34·70‰) on the 27·40 σ_t surface, separated from Antarctic Intermediate to the south by an oxygen minimum of Red Sea origin. Banda water of these characteristics has been found as far west as Madagascar within a 0–20°S. zone of the Indian Ocean. Along 110°E. Banda water was in maximum concentration at about 10°S. in August–December 1962. At this latitude and time of the year relatively strong (7–11 cm per sec) geostrophic currents to the west were found. Between January and July 1964 little or no net westward movement along 110°E. occurred. A strong (22 cm per sec) easterly flow of Red Sea water south of the Chagos Is. seems to retard the westward movement of Banda water and to divert its flow to the south.

I. INTRODUCTION

Wyrtki (1957) first showed that Banda Sea water spreads at intermediate depths into the east Indian Ocean. Rochford (1961) using more extensive *Diamantina* data and more accurate salinity values, traced Banda Intermediate water as far west as 95°E. Recent cruises of *Atlantis II*, *Discovery*, *Vityaz*, *Umitaka Maru*, and *Diamantina* in the region west of 95°E. provide enough data for a study of the limit of westward spreading of Banda Intermediate water. During 1962–63 a series of cruises along 110°E. by *Gascoyne* and *Diamantina* provided data for an examination of seasonal changes in the westward drift of Banda Intermediate water.

TABLE 1

DATA AND REFERENCE SOURCES

Vessel	Date	Plotting Symbol			Reference
		Fig. 5	Fig. 6	Fig. 7	
Diamantina	Apr.–May 1965	△	▲	▲	CSIRO AUST. (1966)
Atlantis II	Sept.–Oct. 1963	+	+	+	Personal communication
Discovery	May–June 1964	△	△	△	Personal communication
Vityaz	Oct.–Nov. 1959	□	□	□	*Vityaz* (1959)
Vityaz	Jan.–Feb. 1961	×	×	×	*Vityaz* (1961)
Umitaka Maru	Dec. 1962	×	●	●	Tokyo University of Fisheries (1964)
Diamantina	July–Aug. 1962	●	●	●	CSIRO AUST. (1964)
No Banda Intermediate water present			○		

* Division of Fisheries and Oceanography, CSIRO, Cronulla, N.S.W. (Reprint No. 569.)

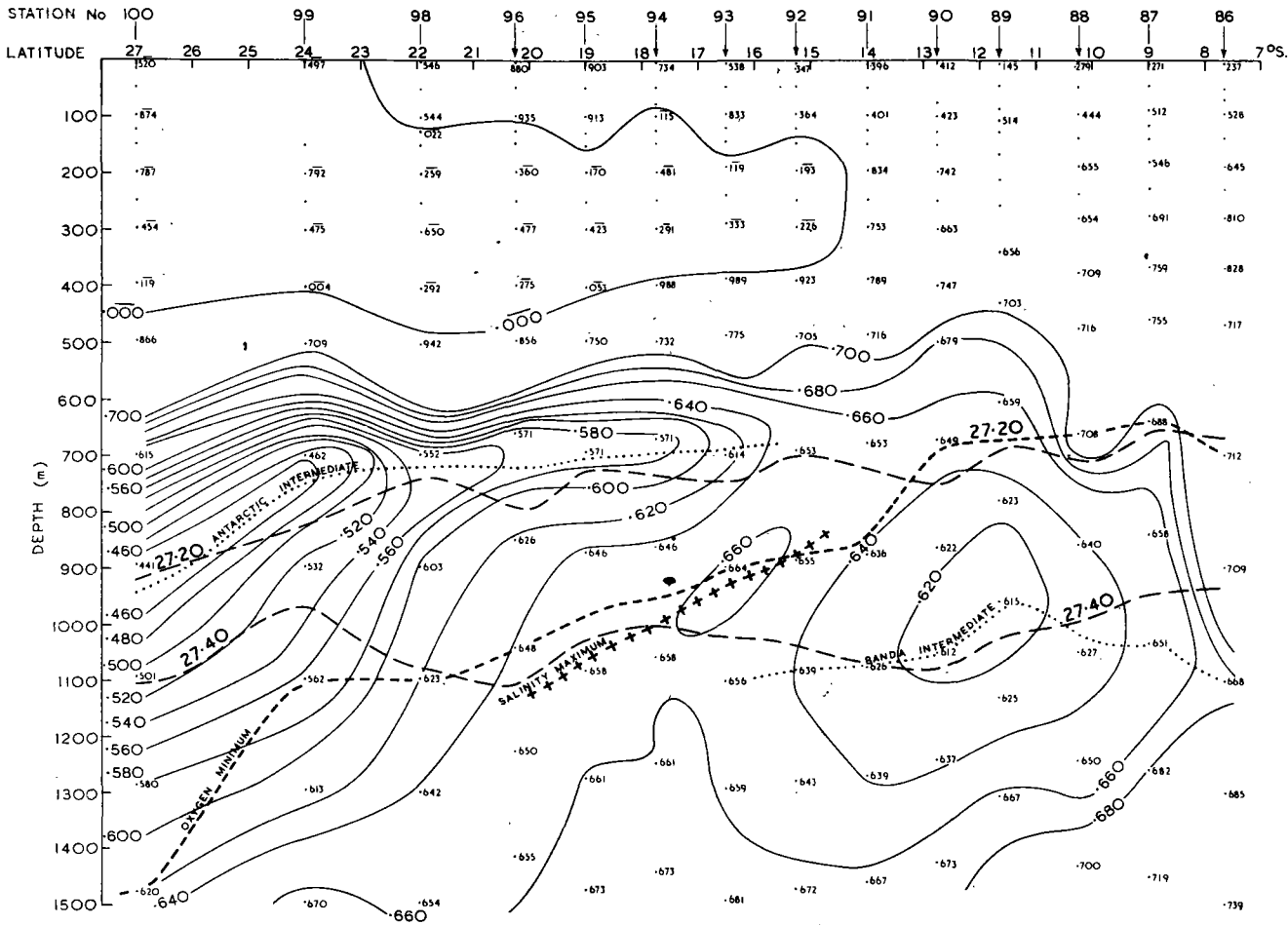

Fig. 1.—Salinity along a 105°E. section in August 1962 (*Diamantina* cruise 2/62). In Figures 1–5 and 10 salinity values unbarred are quoted without the 34 prefix and those barred are quoted without the 35 prefix. In Figures 1–4 salinity contours below 34·700‰ are at 0·020‰ intervals but above 34·700‰ only the 35·000‰ contour has been shown.

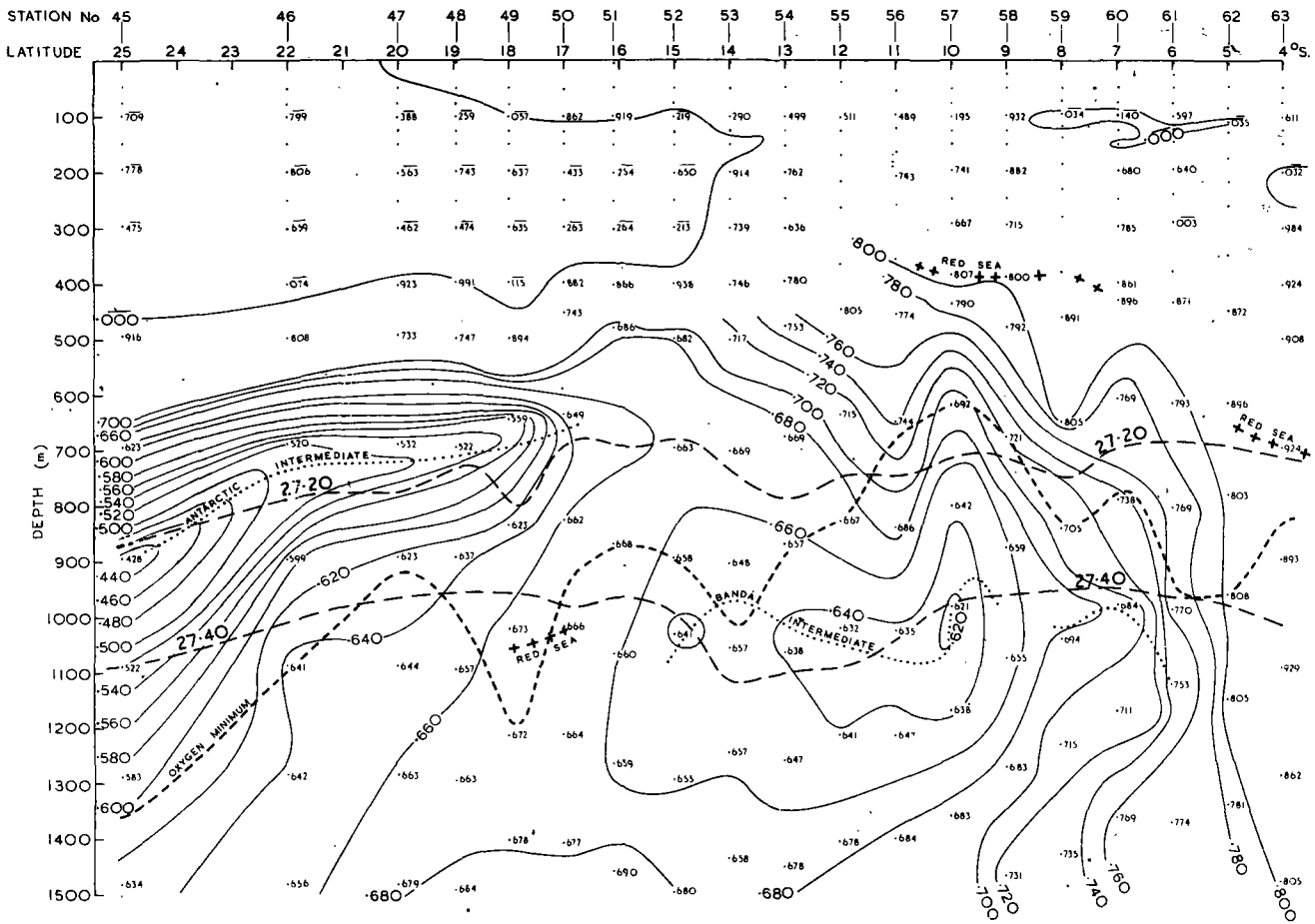

Fig. 2.—Salinity along a 100°E. section in July 1962 (*Diamantina* cruise 2/62).

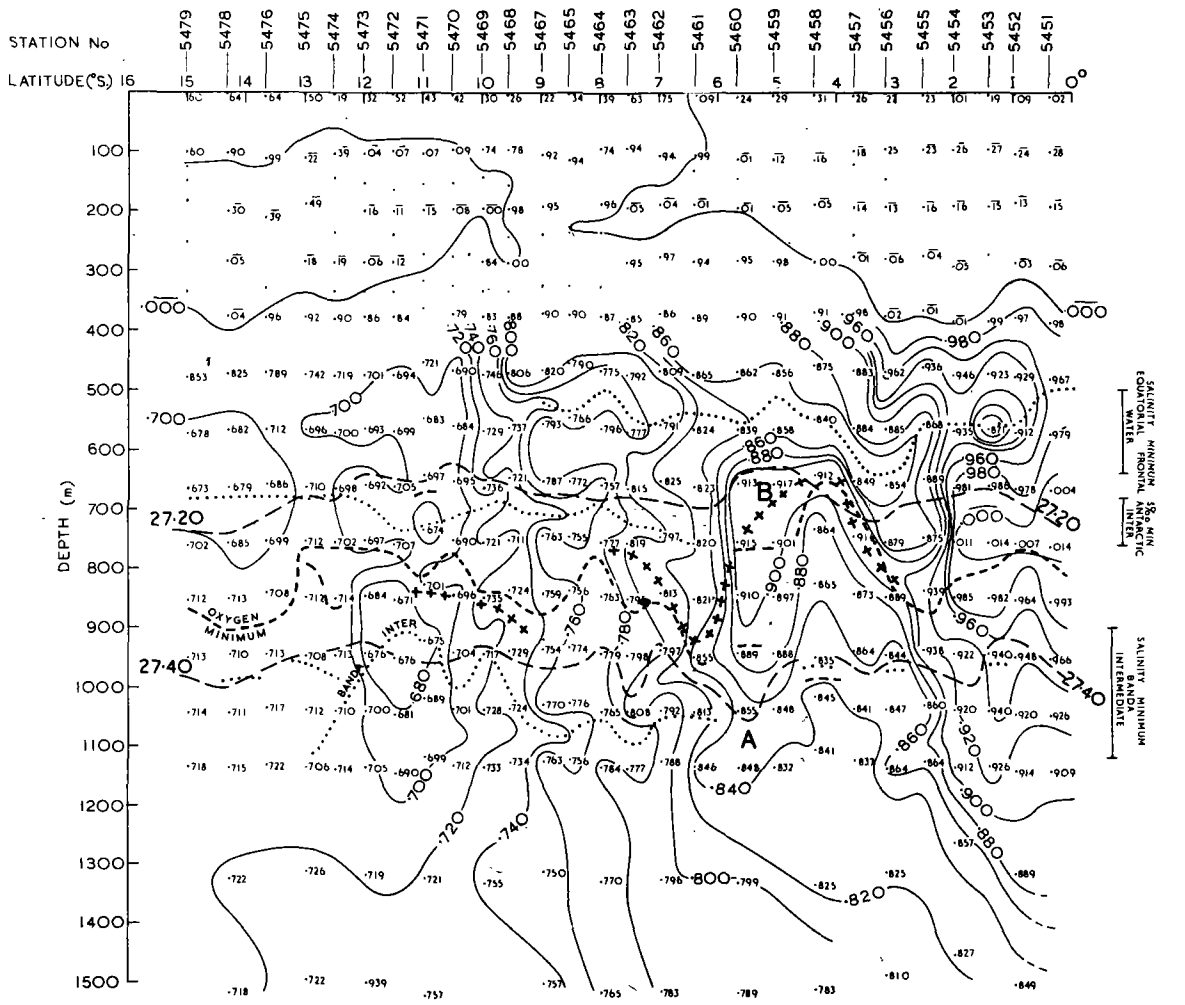

Fig. 3.—Salinity along a 67°30′E. section in June 1964 (*Discovery*).

II. Data and Methods

The data used and their reference sources are listed in Table 1. At many stations where the sampling interval was 100 m or less within the intermediate depth range 500–1300 m, salinity minima and maxima and their properties were found by inspection of the serial data. However, at a smaller number of stations, where the sampling interval exceeded 100 m the salinity minima and maxima had to be determined from smoothed temperature–salinity curves and their properties interpolated as required. It is considered that the first method introduces less error into the salinity value of any salinity minimum or maximum and in any case avoids the possibility of introducing, by the smoothing itself, a salinity minimum into the temperature–salinity curve that has no real existence.

III. Identification of Banda Intermediate Water

In the east Indian Ocean the Banda Intermediate salinity minimum occurs on about the $27{\cdot}40\ \sigma_t$ surface (900–1100 m) and is separated from the Antarctic Intermediate salinity minimum on about the $27{\cdot}20\ \sigma_t$ surface (700–900 m), by an oxygen minimum which is generally also a weak salinity maximum of Red Sea origin (Figs. 1 and 2). Generally, too, the Banda salinity minimum occurs only in the region 10–15°S. in the east Indian Ocean. In the west Indian Ocean this same structural separation is found (Figs. 3 and 4), and this is claimed, in association with a zonal continuity of such waters, as sufficient identification of Banda Sea water in this region. Additionally, however, in the west Indian Ocean, a salinity minimum is found north of 10°S. at lower σ_t ($27{\cdot}00$–$27{\cdot}10$) and shallower depths (500–650 m) than the Antarctic Intermediate below (Figs. 3 and 4). This salinity minimum is formed from a northward extension of Equatorial Frontal waters (Rochford 1966) and is not derived from either Antarctic Intermediate or Banda Intermediate waters.

It is claimed, therefore, that Banda Intermediate water can be identified throughout the Indian Ocean as the salinity minimum on about the $27{\cdot}40\ \sigma_t$ surface, mostly at depths of 900–1100 m, within latitude limits of 0–20°S., and always lying below an oxygen minimum with salinity characteristics of Red Sea origin.

IV. Distribution of Banda Intermediate Water

West of 90°E. all data with sufficiently accurate salinities have been used to prepare Figures 5–7. These show the salinity, σ_t, and depth of the core layer of the Banda Intermediate water mass. Table 1 shows that these data have been obtained at different times of the year. In contouring the data, therefore, greater emphasis has been given to those between May and October corresponding to the period of the south-east trade winds. However there were regions, notably in the centre of the region, where only data from the north-west monsoon period were available and these have had to be used without any selection. For this reason Figures 5–7 must be regarded principally as geographical summaries of the properties of the core layer of Banda Intermediate water.

Figure 5 shows that Banda Intermediate water occurs as far west as Madagascar within the 0–20°S. zone. It is probable also that this water occurs west and north-west of Madagascar, within the deep structure of the south Equatorial current, but data

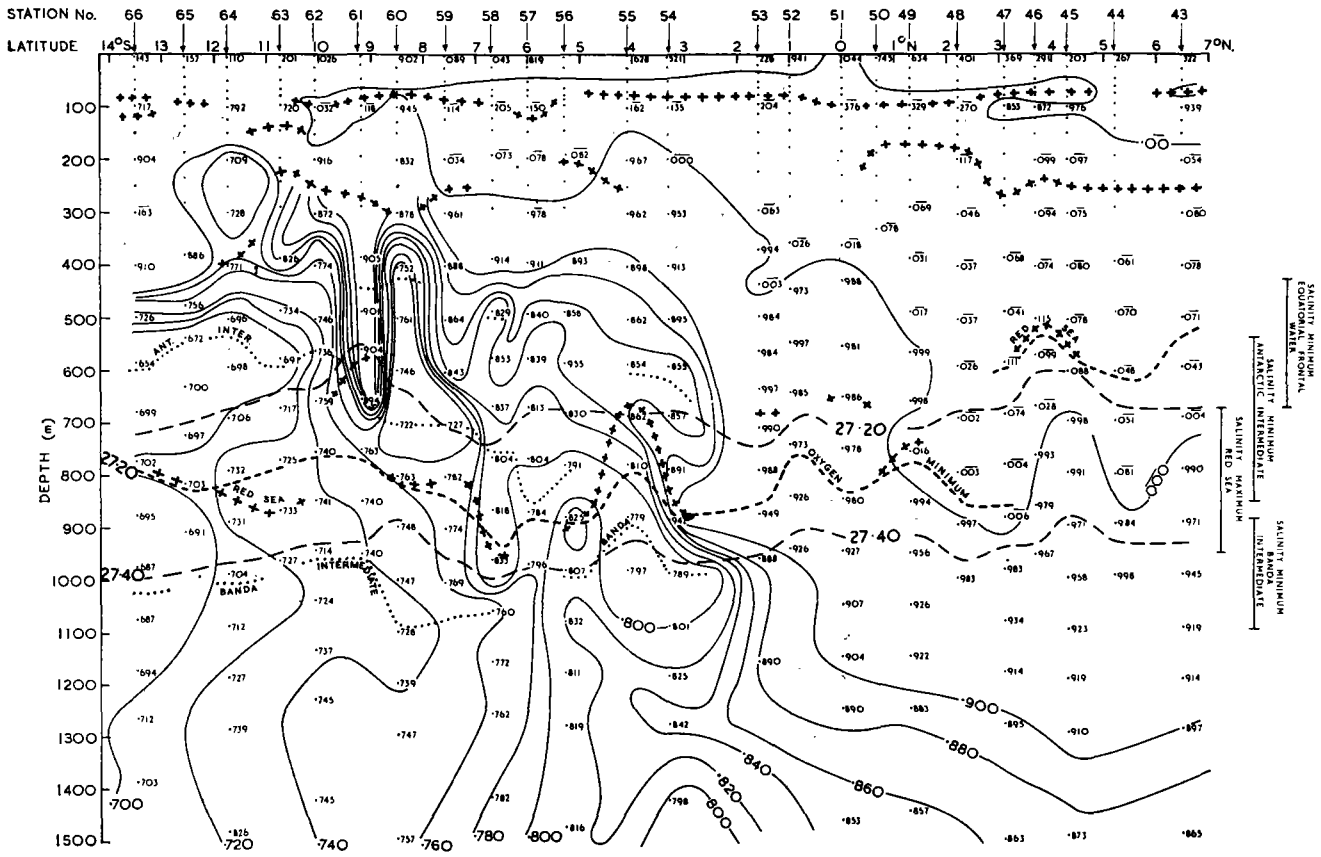

Fig. 4.—Salinity along a 76°E. section in May 1965 (*Diamantina* cruise 1/65).

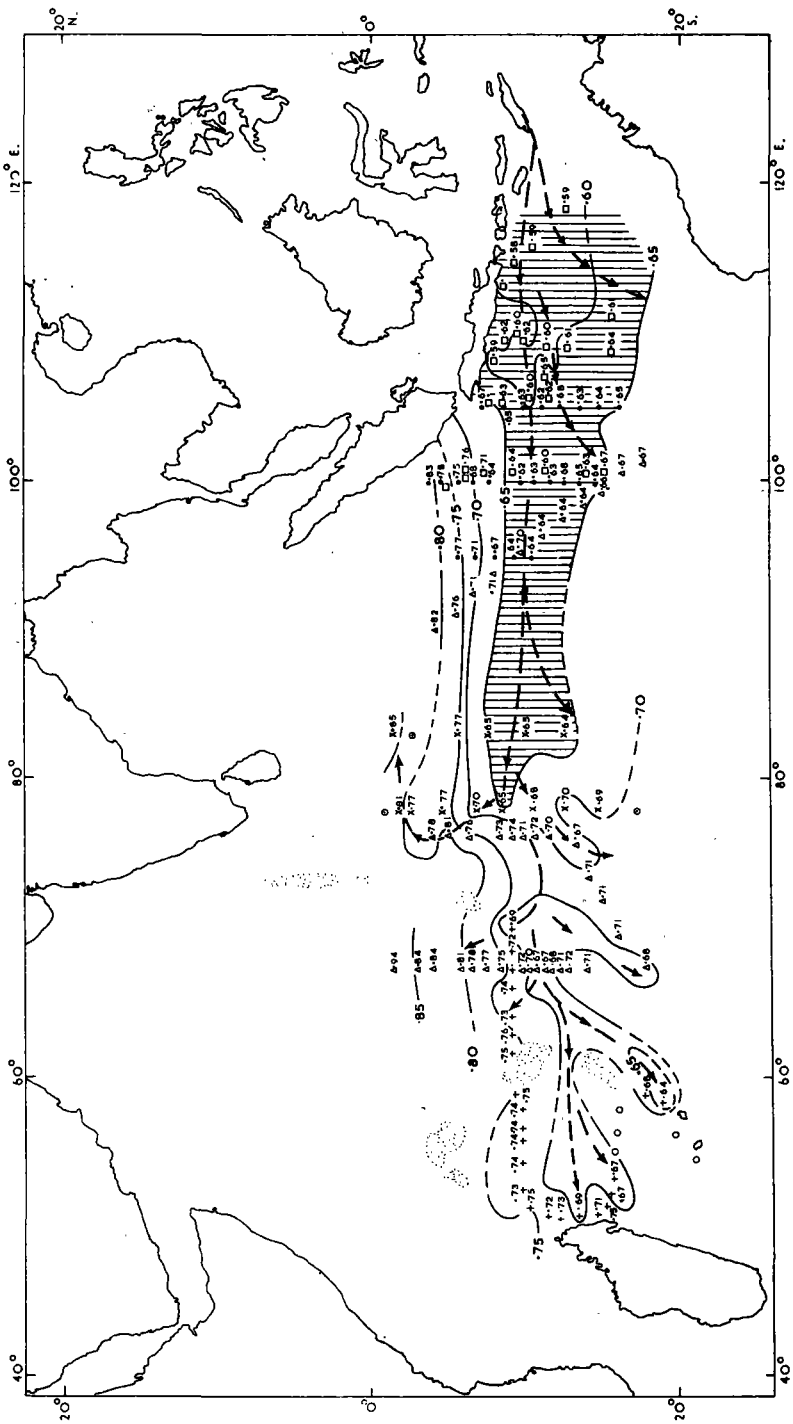

Fig. 5.—Salinity of the Banda Intermediate salinity minimum. All values quoted without a 34· prefix. Broken lines and arrows show the major concentrations and direction of drift of Banda Intermediate water. Shaded area indicates salinity less than 34·65‰. For data sources see Table 1.

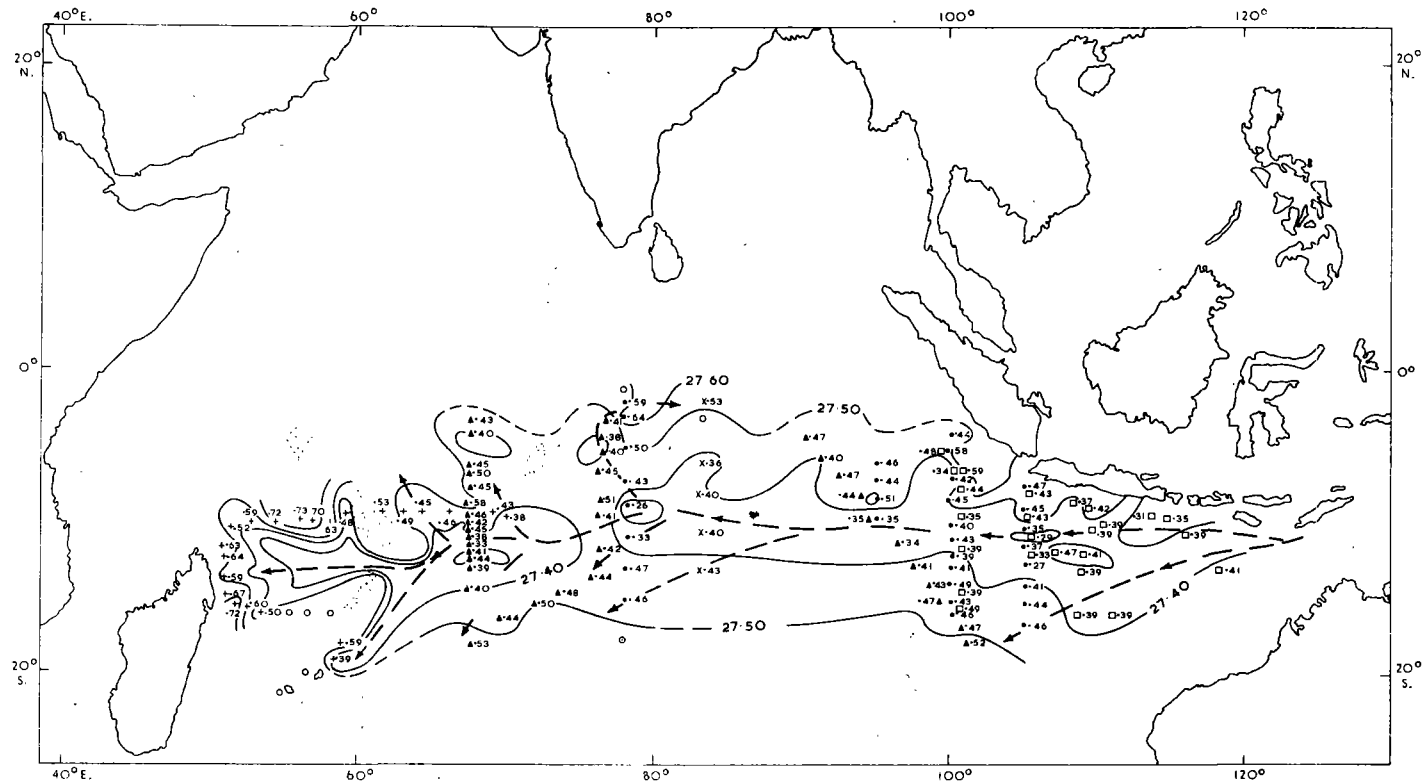

Fig. 6.—σ_t of the Banda Intermediate salinity minimum. Broken lines and arrows show the major concentrations and direction of drift of Banda Intermediate water. Cruise legends as in Figure 5.

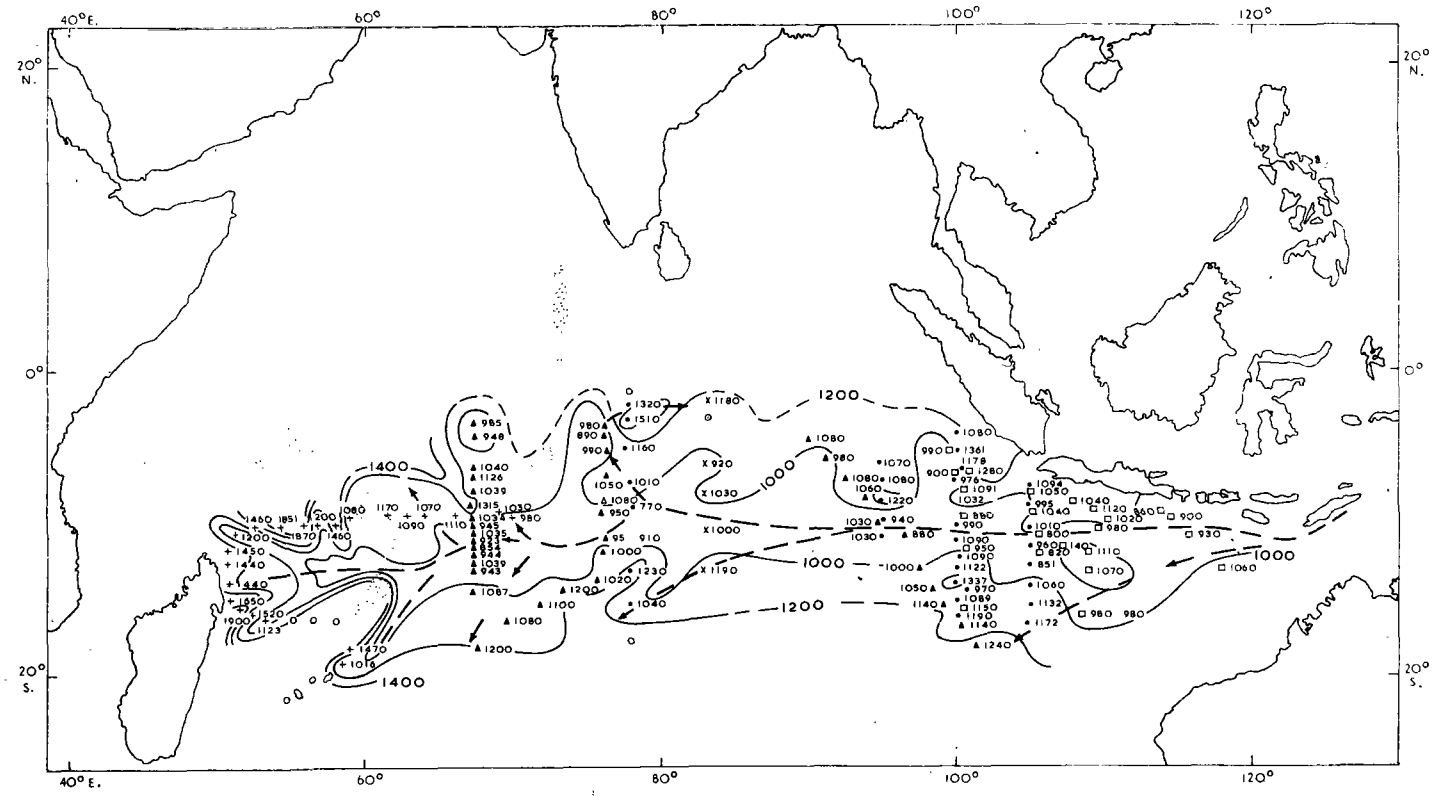

Fig. 7.—Depth (m) of the Banda Intermediate salinity minimum. Broken lines and arrows show the major concentrations and direction of drift of Banda Intermediate water. Cruise legends as in Figure 5.

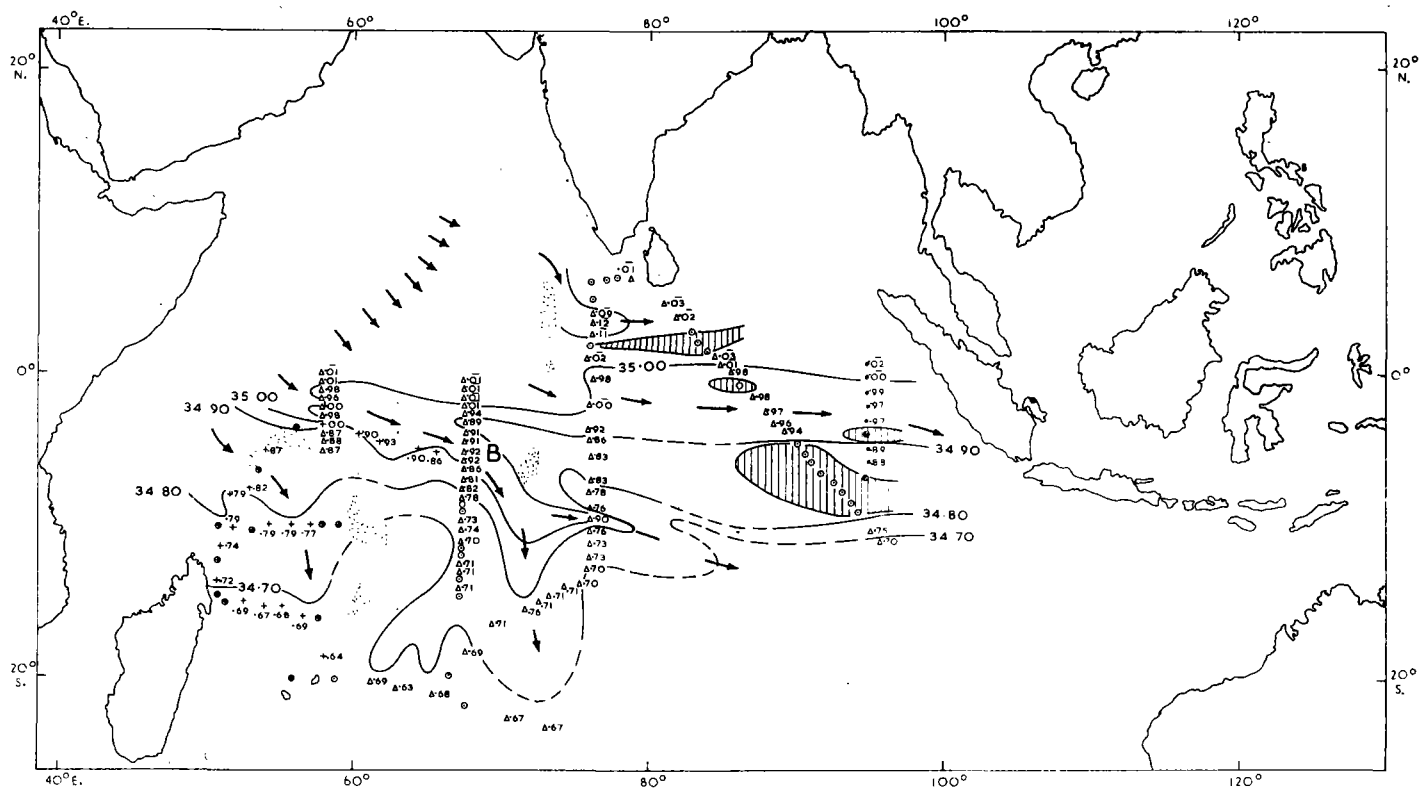

Fig. 8.—Salinity of the Red Sea water mass in the central Indian Ocean. Data sources as in Table 1. Arrows show paths of major concentrations.

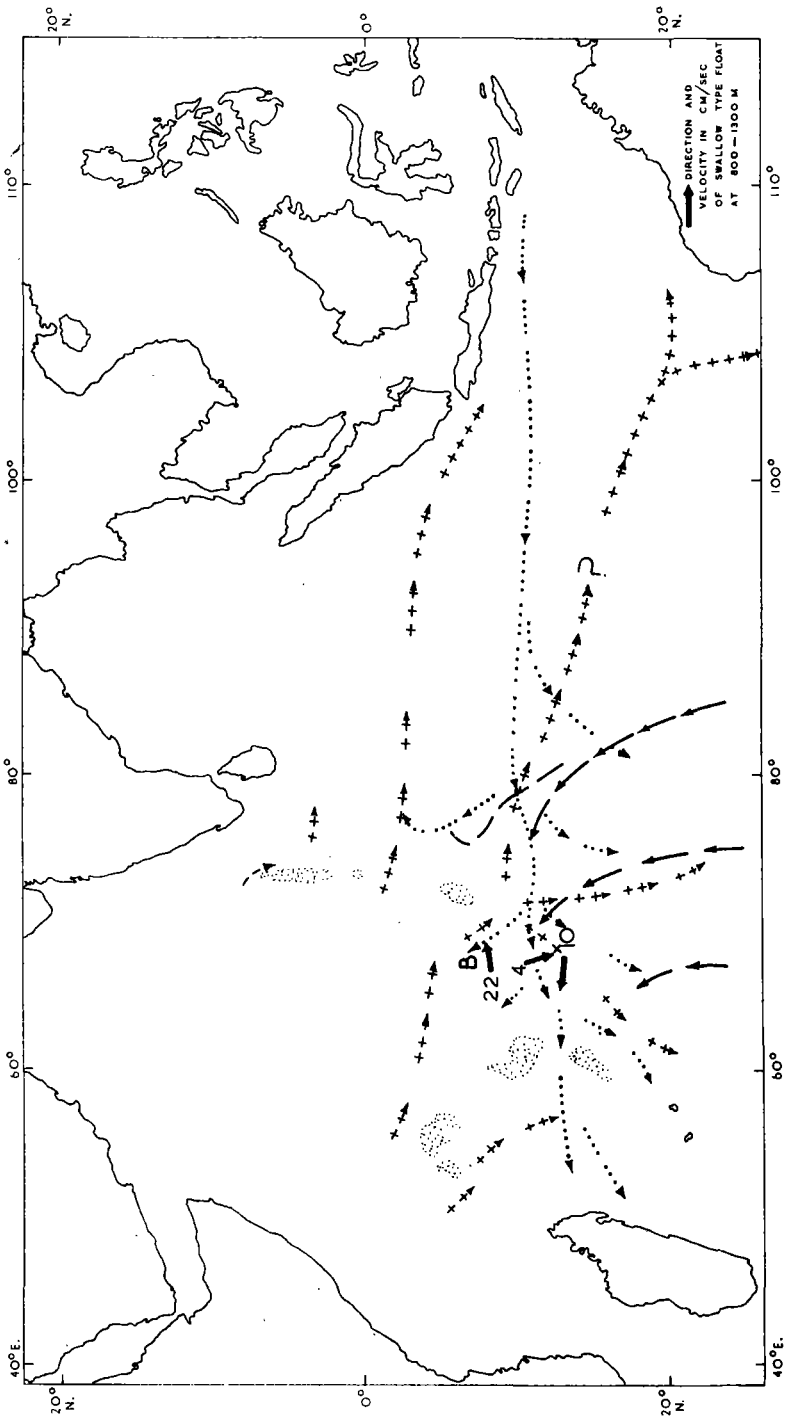

Fig. 9.—Principal paths of distribution of Banda Intermediate (. . . . .) from Figure 5, Red Sea (+ + +) from Figure 8 and Rochford (1961), and Antarctic Intermediate (———) from *Diamantina* cruise 1/65.

were insufficient in number and not accurate enough in salinity to verify this. Throughout the distribution of this Banda Intermediate water, the lowest salinities were generally found on the 27·40 σ_t surface (Fig. 6) and at a nearly uniform depth around 1000 m (Fig. 7). Increases in salinity (Fig. 5) were always associated with increases in $\bar{\sigma}_t$ (Fig. 6) and increases in depth (Fig. 7).

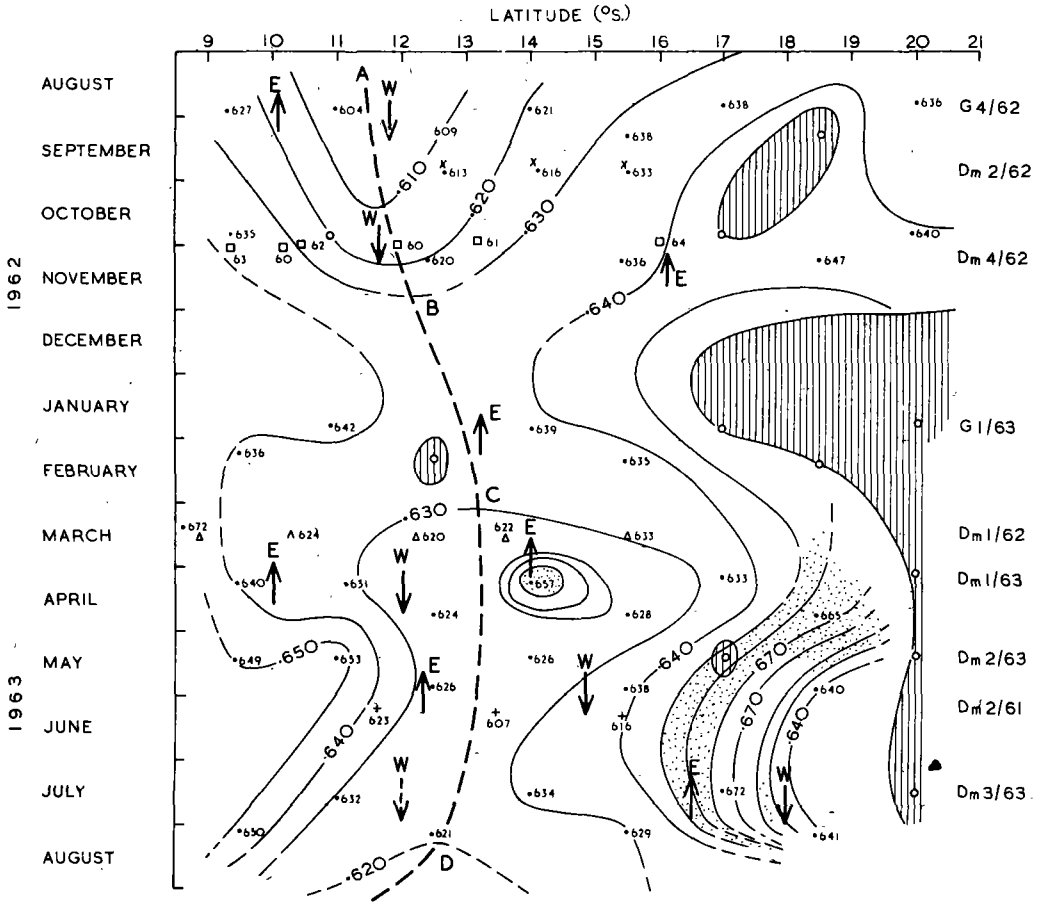

Fig. 10.—Changes in salinity of the Banda Intermediate salinity minimum along 110°E. during 1962–63. Values plotted (·) are from the following: CSIRO Aust. 1965*a*, 1965*b*, 1965*c*, 1965*d*, 1966*a*, 1966*b*. Other values are from the following sources: × CSIRO Aust. 1964*b*, □ *Vityaz* 1959, △ CSIRO Aust. 1964*a*, + CSIRO Aust. 1963. *ABCD* shows the position of the lowest salinity for each cruise. Arrows show position of geostrophic currents to east (*E*) and to west (*W*).

Since the Banda Intermediate water originates in the east (Rochford 1961) its major distribution westward must be maintained by a westerly flow. The 27·40 σ_t surface deepens very slightly to the south (14°S., Figs. 2 and 3) and to the north (4–6°S., Figs. 2 and 3) of the low salinity core of this Banda water. On the assumption of a deeper level of no motion the geostrophic flow to the west must occur between this low salinity core and 14°S. Further to the north the flow would be predominantly easterly. Along the 67°30′E. section the 27·40 σ_t surface was found at a deep level

at Station 5460 at about 5°30′S. (*A*, Fig. 3). This corresponds in position with the highest salinities and shallowest depth of the Red Sea salinity maximum (*B*, Fig. 3). Salinities of this Red Sea salinity maximum show that *B* (Fig. 8) lies within a tongue of the Red Sea water mass drifting to the east around the southern end of the Chagos Is. Current measurements at this position in May 1964 at around 1000 m showed

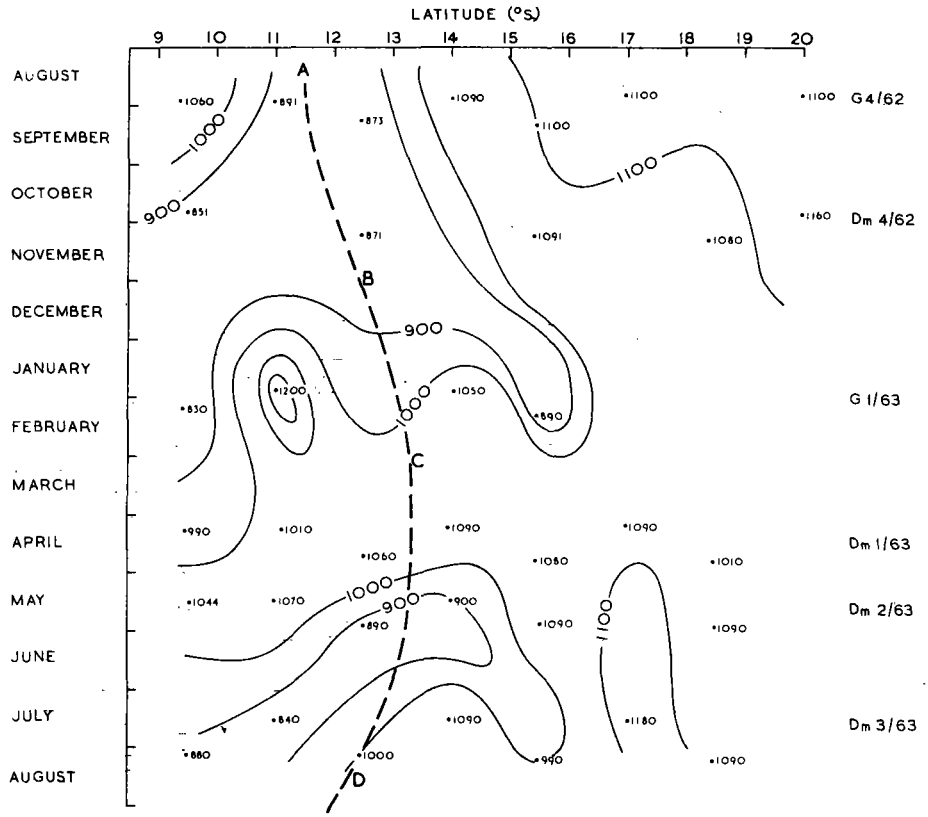

Fig. 11.—Depth (m) of the Banda Intermediate salinity minimum along 110°E. in 1962–63. *ABCD* from Figure 10.

exceptionally strong currents (22 cm per sec) to the east (Brit. Natn. Comm. Ocean Res. 1965). Some 12 months later, in May 1965, the doming of the Red Sea salinity maximum associated with this easterly flow along 67°30′E. (*B*, Fig. 3) was found at about the same latitude along a 76°E. section (Station 55, Fig. 4). This easterly flow of Red Sea water seems, therefore, to be a persistent feature of the region south of the Chagos Is. Such a flow provides an explanation for the more restricted northern distribution and for the southward curvature of Banda Intermediate water, south and west of the Chagos Is. (Fig. 9).

In the east Indian Ocean, Rochford (1961) found the Banda Intermediate water confined largely to a region bounded by a northern and a southern band of north-west Indian (Red Sea) water (Fig. 9). These eastern bands of Red Sea water, however, can be linked with the major drift of this same water, west of 80°E., only if

(1) there is a persistent movement of Red Sea water across the Banda flow to the west (Fig. 9) or, (2) there is a marked seasonal alternation of zonal flow around 1000 m in the central Indian Ocean permitting Red Sea flow at one time and Banda Intermediate at another.

V. Seasonal Changes in the Westward Drift of Banda Intermediate Water

Figure 10 shows the changes in salinity of the Banda Intermediate salinity minimum along 110°E. during 1962–63. Salinities varied from 34·604 to 34·672‰ with the lowest values for each month along a median zone *ABCD* (Fig. 10). Salinities along *ABCD* were less than 34·620‰ between August and November, greater than

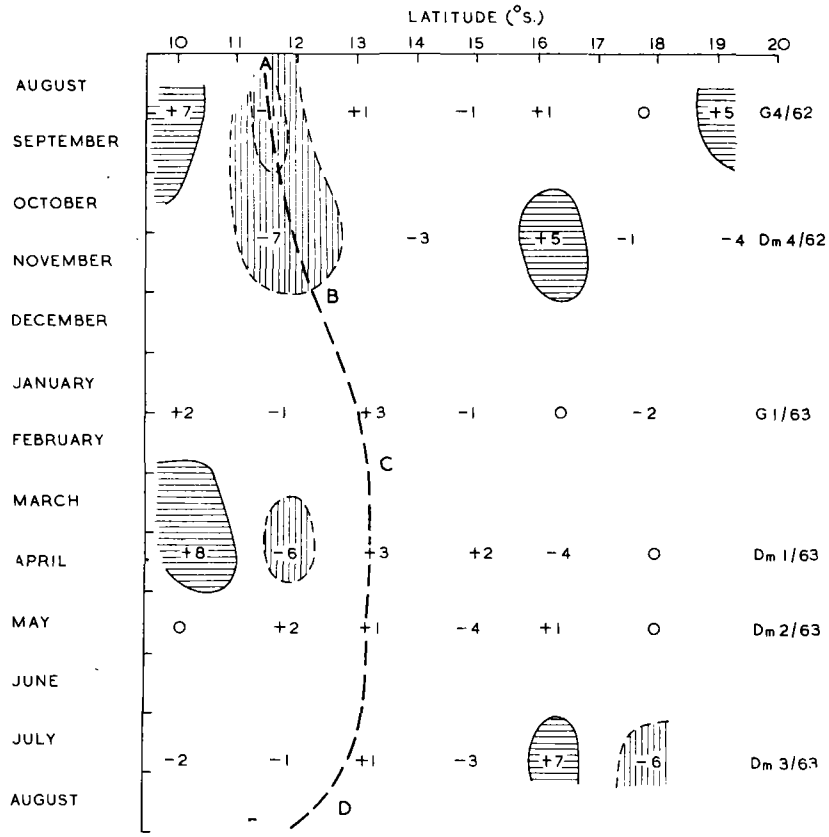

Fig. 12.—Geostrophic currents (cm per sec) of the 1000-decibar level relative to the 1750-decibar level along 110°E. in 1962–63. *ABCD* from Figure 10.

34·630‰ between December and January, and very gradually decreased to 34·620‰ from March onwards (Fig. 10). The position of *ABCD* varied from about 11°30′S. in winter to about 13°S. in summer, following the seasonal changes in position of the south Equatorial current along 110°E. (Hamon 1965). Salinities of Banda water along 110°E. from earlier cruises, have in general similar values to those of the 1962–63 cruises (Fig. 10). However, there are sufficient differences (e.g. *Vityaz* 59 in October and Dm2/61 in June, Fig. 10) to suggest that year by year departures from the 1962–63 salinity cycle do occur.

Geostrophic currents (Hamon 1965) at 1000 m, the average depth of Banda water along 110°E. (Fig. 11), were for the most part so weak (less than 5 cm per sec) as to be considered not significantly different from zero (Fig. 12). In August–December, however, the region of maximum concentration of Banda water (*AB*, Fig. 12) was found within a region of relatively strong (7–11 cm per sec) westward movement. In August some of this westward transport would have been absorbed into the east-flowing current around 10°S., but despite this, there would have been a net transport to the west beyond 110°E. during August–December. At other times of the year geostrophic currents along *BCD*, the zone of maximum concentration of Banda water, were virtually absent or directed eastwards (Fig. 12). Stronger westerly currents to the north of *BCD* in March–April and to the south of *BCD* in July (Fig. 12) were always matched by an adjacent easterly current of about the same strength. However, these easterly currents always had much higher core layer salinities than their adjoining westerly counterpart, showing that these currents are to some extent independently maintained. There could be some transport of Banda water westward in January–July but the amount involved is likely to be quite small. The strong easterly flow of high salinity Red Sea water south of the Chagos Is. (Fig. 9) was measured in June. It is thought likely that this easterly flow propagates eastwards and generates the easterly currents at 110°E. in the period March–July (Fig. 12). If this is the case, the weakening of westward transport of Banda water across 110°E. in March–July might not be caused by any seasonal diminution of flow out of the Banda Sea itself, but by its seasonal absorption into an increased eastward flow of Red Sea water. The southward diversions of Banda water, shown by the salinity distribution (Fig. 9), under these circumstances could be the resultant path of such waters when the opposing Red Sea flow intensifies.

VI. Conclusions

(1) Banda Intermediate water has been identified as a salinity minimum on about the 27·40 σ_t surface, below an oxygen minimum of Red Sea origin, throughout most of the 0–20°S. zone of the Indian Ocean.

(2) Lowest salinities within this zone occur around 10°S., where the depth is everywhere around 1000 m and the σ_t is nearly uniform at 27·40.

(3) The slope of the 27·40 σ_t surface indicates that westward movement of Banda water occurs only south of 10°S.

(4) North of 10°S., Banda water is absorbed into an easterly movement of Red Sea water.

(5) During 1962–63 the salinity of Banda water along 110°E. varied not only with latitude (lowest values always between 11–13°S.) but also with time (lowest values overall in August–November; highest values overall in December–January).

(6) Geostrophic currents associated with Banda water along 110°E. were generally less than 5 cm per sec. The strongest westerly currents (7–11 cm per sec) between 11–13°S. were found in August–December. At other times of the year westerly currents between 11–13°S. were either absent or matched by almost equally strong currents to the east.

(7) The strong (22 cm per sec) easterly flow of Red Sea water south of the Chagos Is., measured in June 1964, is thought to divert Banda water southward as well as retard its westward transport.

VII. REFERENCES

ANON. (1959).—Data from *Vityaz* Cruise 31, 1959–60, on file at I.G.Y. World Data Centre *B*, Moscow, U.S.S.R.

ANON. (1961).—Data from *Vityaz* Cruise 33, 1961, on file at I.G.Y. World Data Centre *B*, Moscow, U.S.S.R.

BRITISH NATIONAL COMMITTEE ON OCEANIC RESEARCH (1965).—I.I.O.E. R.R.S. *Discovery* Cruise 3 Report, p. 14. (Royal Society: London.)

CSIRO AUST. (1963).—Oceanographical observations in the Indian Ocean in 1961. H.M.A.S. *Diamantina*, Cruise Dm2/61. *CSIRO Aust. Oceanogr. Cruise Rep.* **9.**

CSIRO AUST. (1964*a*).—Oceanographical observations in the Indian Ocean in 1962. H.M.A.S. *Diamantina*, Cruise Dm1/62. *CSIRO Aust. Oceanogr. Cruise Rep.* **14.**

CSIRO AUST. (1964*b*).—Oceanographical observations in the Indian Ocean in 1962. H.M.A.S. *Diamantina*, Cruise Dm2/62. *CSIRO Aust. Oceanogr. Cruise Rep.* **15.**

CSIRO AUST. (1965*a*).—Oceanographical observations in the Indian Ocean in 1963. H.M.A.S. *Gascoyne*, Cruise G1/63. *CSIRO Aust. Oceanogr. Cruise Rep.* **21.**

CSIRO AUST. (1965*b*).—Oceanographical observations in the Indian Ocean in 1963. H.M.A.S. *Diamantina*, Cruise Dm1/63. *CSIRO Aust. Oceanogr. Cruise Rep.* **23.**

CSIRO AUST. (1965*c*).—Oceanographical observations in the Indian Ocean in 1963. H.M.A.S. *Diamantina*, Cruise Dm2/63. *CSIRO Aust. Oceanogr. Cruise Rep.* **24.**

CSIRO AUST. (1965*d*).—Oceanographical observations in the Indian Ocean in 1963. H.M.A.S. *Diamantina*, Cruise Dm3/63. *CSIRO Aust. Oceanogr. Cruise Rep.* **25.**

CSIRO AUST. (1966*a*).—Oceanographical observations in the Indian Ocean in 1962. H.M.A.S. *Gascoyne*, Cruise G4/62. *CSIRO Aust. Oceanogr. Cruise Rep.* **17.**

CSIRO AUST. (1966*b*).—Oceanographical observations in the Indian Ocean in 1962. H.M.A.S. *Diamantina*, Cruise Dm4/62. *CSIRO Aust. Oceanogr. Cruise Rep.* **20.**

HAMON, B. V. (1965).—Relative currents in the south-eastern Indian Ocean. *Aust. J. Mar. Freshw. Res.* **16**: 255–71.

ROCHFORD, D. J. (1961).—Hydrology of the Indian Ocean. I. The water masses in intermediate depths of the south-east Indian Ocean. *Aust. J. Mar. Freshw. Res.* **12**: 129–49.

ROCHFORD, D. J. (1966).—Source regions of oxygen maxima in intermediate depths of the Arabian Sea. *Aust. J. Mar. Freshw. Res.* **17**: 1–30.

TOKYO UNIVERSITY OF FISHERIES (1964).—Physical and chemical data. I.I.O.E. Reps. *Umitaka Maru* (1962–63).

WYRTKI, K. (1957).—The water exchange between the Pacific and the Indian Ocean in relation to upwelling processes. *Proc. 9th Pacif. Sci. Congr.* **16**: 61–6.

Reprinted from *J. atmosph. Sci.*, vol. 23, no. 2, 1966, p. 144-150.

The Summer Atmospheric Circulation over the Arabian Sea

C. S. RAMAGE
University of Hawaii Honolulu

The Summer Atmospheric Circulation over the Arabian Sea[1]

C. S. RAMAGE
University of Hawaii, Honolulu

(Manuscript received 23 September 1965)

ABSTRACT

The summer heat low system extending from Somalia across southeast Arabia to northwest India is the most extensive and intense on earth. Although it develops in the normal way over desert regions in response to the sun's zenithal march, it is maintained and intensified through the summer by subsidence of air originally lifted and warmed by the release of latent heat in monsoon rain systems to the east and south. The subsidence not only dominates West Pakistan, Arabia, and Somalia, but severely restricts low cloud formation over the central and western Arabian Sea.

The heat low exports cyclonic vorticity in the middle and upper troposphere to the northern Arabian Sea. When a deep layer of moist air is present over the eastern part of this area, subtropical cyclogenesis occurs, producing a burst of west Indian monsoon rains. This in turn, by increasing subsidence above the heat low, intensifies the heat low and its associated low-level monsoon circulation. When the supply of moist air is cut off, the subtropical cyclone fills, the heat low weakens, and a break takes place in the monsoon rains. With renewal of the moisture supply, the sequence is repeated.

1. Introduction

During the International Indian Ocean Expedition oceanographers have concentrated more on studying the western Arabian Sea than any other part of the Indian Ocean. The reason is not hard to find since nowhere else is the difference between summer and winter monsoons so sharp—strong southwesterly winds with vigorous coastal upwelling in summer and moderate to fresh northeasterly winds and near-uniform sea surface temperatures in winter. So far the summer monsoon has been probed more extensively than the winter monsoon and since several of the research vessels made regular radiosonde ascents and U. S. Weather Bureau and Woods Hole Oceanographic Institution research aircraft made drop soundings in the summers of 1963 and 1964, a detailed study of the summer atmospheric circulation over the western Arabian Sea appears to be feasible.

To prepare for this study, I attempt to construct in this paper a climatological framework interrelating gross features of the normal distributions of pressure, temperature, winds, and weather over the Arabian Sea and its littoral.

For surface climatology I have relied on the atlas published by the Royal Netherlands Meteorological Institute (1952) and for upper climatology on Raman and Dixit (1964), Frost and Stephenson (1965), and on observations from research vessels and aircraft.

Traditionally, meteorologists have linked the Arabian Sea summer monsoon circulation with a heat low system over Arabia, West Pakistan, and northern India. The heat low, developing during May, establishes the low-level monsoon wind regime a full month before heavy monsoon rains set in over western India south of the heat low. By mid-July, the low is deepest, the southwest monsoon is strongest, and the west Indian rains are heaviest, while all diminish through August and September. As long ago as 1887, W. L. Dallas questioned how a heat low dependent for its existence on hot sun and clear skies can persist once clouds and rain develop. Surface charts for the Arabian Sea show winds converging into the West Pakistan heat low. Surface relative humidities are high and the air is rising. Why then does the low remain cloud-free and intense while rain falls well to the south? This question and the related question—Why does so little rain fall over the western Arabian Sea?—will be discussed in the remainder of this presentation.

2. Undisturbed heat low circulation

The surface southwesterly winds of the heat low circulation force cold water to upwell along the coast of Somalia and Arabia. The cold water, by modifying the temperature and hence the pressure distribution of the overlying air, produces two pronounced effects; a persistent wind speed maximum offshore from the zone of upwelling (Bunker, 1965) and deflection of inflow to flow parallel to the coast (Fig. 1). Consequently, with moist inflow over West Pakistan and little or none over Somalia and Arabia, we should expect to find a rather weak moist heat low over West Pakistan with plentiful rain, a return current in the middle troposphere, evidence for some compensatory sinking

[1] Contribution No. 128 of the Hawaii Institute of Geophysics. This paper was presented at the Symposium on Meteorological Results of the International Indian Ocean Expedition, 22–26 July 1965, Bombay, India.

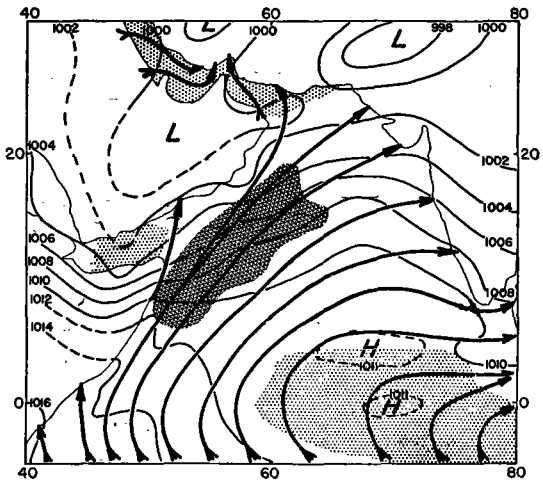

FIG. 1. August mean sea level pressure and mean resultant winds. Speeds less than 10 kt stippled; greater than 25 kt cross-hatched.

over the Arabian Sea (a situation similar to that observed over North Viet Nam and the South China Sea in summer), and a rather vigorous heat low over Arabia and Somalia.

3. Interaction between monsoon rains and heat low

What we do observe is a cloudless heat low which attains its maximum intensity over West Pakistan, and which is so shallow there that cyclonic inflow gives way to anticyclonic outflow below 700 mb. We also observe a subsidence inversion based between 500 and 2000 m over the western Arabian Sea, where precipitation is almost never recorded (Fig. 2).

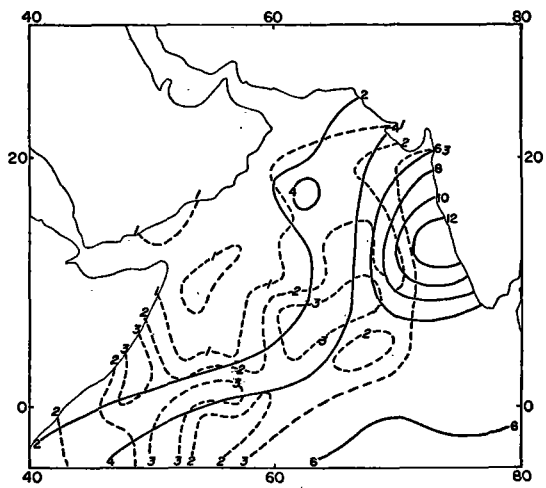

FIG. 2. Percentage duration of precipitation during summer from ship observations (full lines) and level of the inversion base in km from 130 aerological soundings made during the summers of 1963 and 1964 (dashed lines).

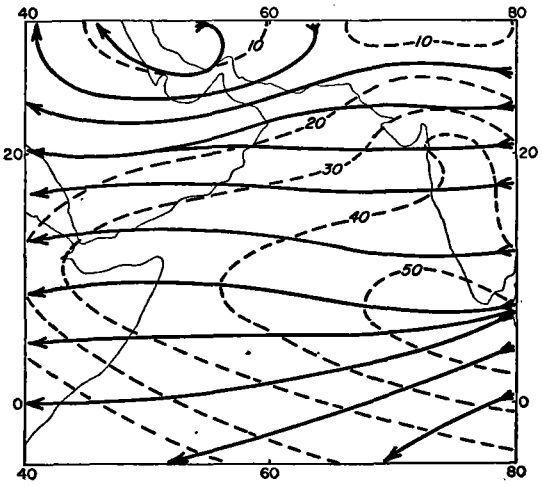

FIG. 3. August 200 mb mean resultant winds. Isotachs are labelled in kt.

To find an explanation, we must take cognizance of conditions over the eastern Arabian Sea and western India. By mid-June monsoon rains have set in over western India. South of Kutch and north of Goa, the precipitation agency is almost always a quasi-stationary mid-tropospheric depression which develops, intensifies, and dissipates over a period of one to three weeks in the vicinity of Bombay. A detailed case study by Miller and Keshavamurthy (1965) shows this "subtropical cyclone" (Simpson, 1952; Ramage, 1962) to be most intense at around 600 mb and to have a cold core

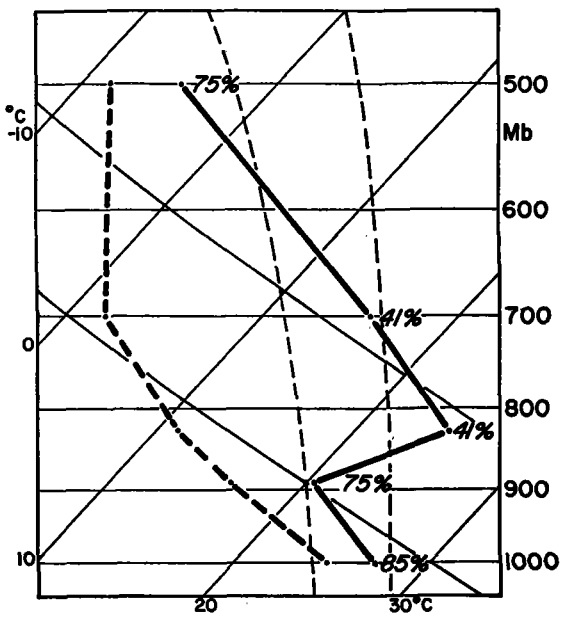

FIG. 4. Median sounding for Karachi (24°55'N; 67°09'E) for August 1963 at 0500 local time.

character below that level and a warm core character above. Convergence is weak at the surface and strongest in the middle troposphere, while above 300 mb the sub-tropical cyclone is overlain by persistent easterlies. Great sheets of cirrostratus or cirrus densus visible day after day over most of the Arabian Sea testify to the role of the easterlies in the energetics of the subtropical cyclone. Subtropical cyclones, and warm-cored systems further east over the Ganges Valley, release massive amounts of latent heat into the upper troposphere. This effect was noted by Raman and Ramanathan (1964) who demonstrated that heavy

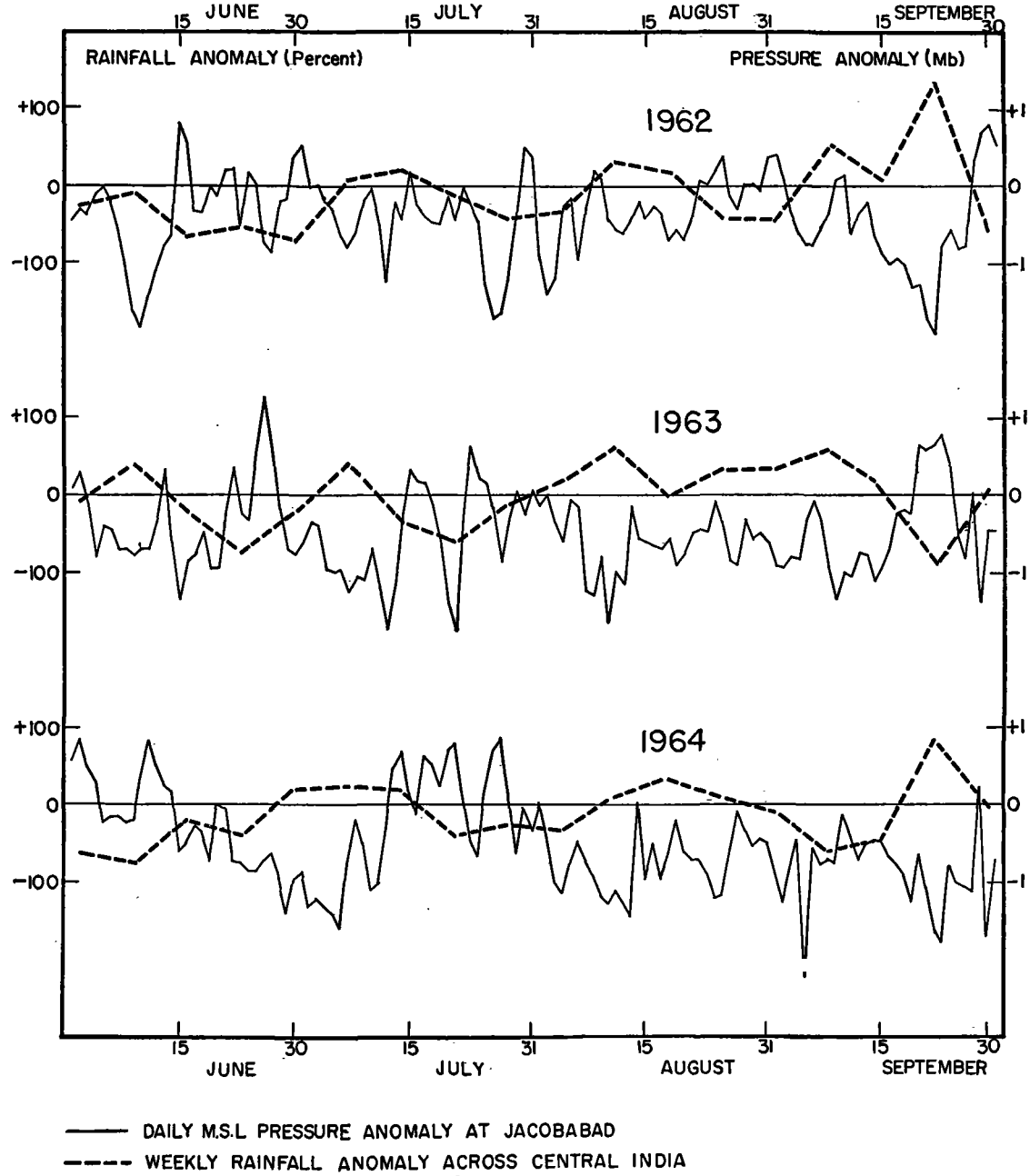

FIG. 5. Daily anomalies in mb of mean sea level pressures measured at 0800 local time at Jacobabad (28°18′N; 68°28′E); 56 m above MSL) (full lines) and weekly percentage anomalies of rainfall for Indian subdivisions lying roughly between 18 and 27N (dashed lines) for the summers of 1962, 1963, and 1964.

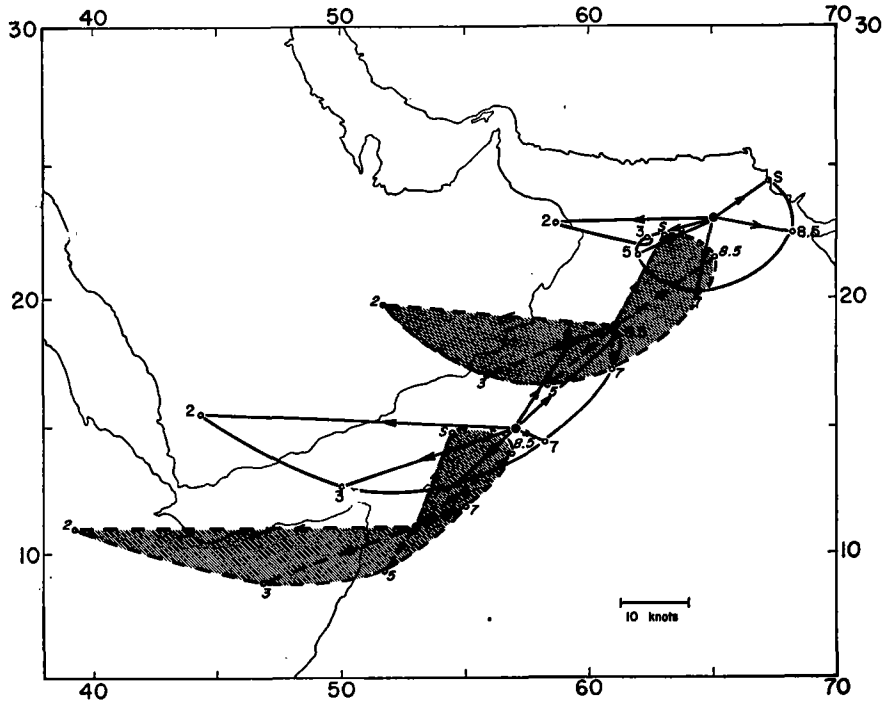

FIG. 6. Hodographs of August mean resultant winds at standard pressure levels (centibars) at four locations in the western Arabian Sea.

monsoon rains over Indo-Pakistan usually precede by several hours, and are found to the north of, a sharply defined jet in the upper tropospheric easterlies, while the easterlies possess a climatological speed maximum roughly coincident with the west coast of India (Fig. 3). Thus, above the heat low and over most of the Arabian Sea, northeast Africa and Arabia, the upper easterlies are convergent and subsidence prevails through the middle troposphere (Flohn, 1964).

Computation of the divergence (Bellamy, 1949) of the mean resultant winds at standard pressure levels over the eastern portion of the heat low (Indo-Pakistan border area) indicates net ascent below 700 mb associated with the heat low circulation and net descent above 700 mb associated with the convergent easterlies.

Observations reveal that the subsidence affects the heat low in two ways:

a) A median August 1963 sounding for Karachi at 0000 GMT (0500 local time) (Fig. 4) shows that the lower layers, originating over the Arabian Sea, are moist. There is a sharp inversion at around 850 mb and relative humidity increases with height above 700 mb. A similar vertical distribution is common inland at Jodhpur, although insolational heating often breaks down the inversion by early afternoon. Subsidence limits the height to which surface air from the Arabian Sea can ascend, restricting cloud development and thus favoring strong insolational heating.

b) Fig. 5 suggests that surface pressure at Jacobabad, near the center of the heat low, is inversely related to the intensity of monsoon rains over a strip of the subcontinent extending eastward to the south and east of the station, while Dixit and Jones (1965), in comparing a monsoon rain with a monsoon lull along the west coast of India, located by far the greatest middle and upper tropospheric temperature differences above the heat low, with the rain situation 2–6C warmer than the lull situation. Hence subsidence over the heat low by raising the temperature of the middle and upper tropospheric air reduces surface pressure below what is observed in heat lows elsewhere.

Both these effects then operate to maintain the heat low circulation and consequently the strength of the low-level monsoon flow. Similar but less marked effects are probably produced over Arabia. However, subsidence into the heat low waxes and wanes in unison with the monsoon rains. When the rains are heavy, the heat low is vigorous, and stronger than normal surface winds prevail over most of the Arabian Sea, hundreds of kilometers distant from the rain systems. When the rains break, the southwest monsoon over the Arabian Sea is weak.

Figs. 6 and 7 illustrate related reasons why the

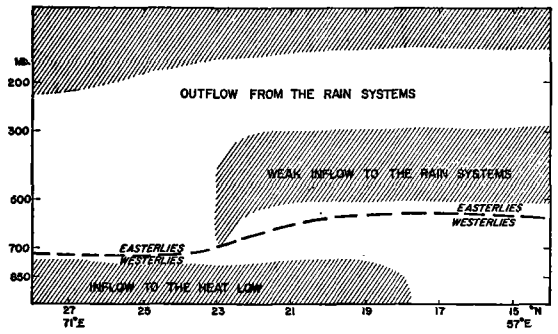

FIG. 7. Schematic section extending southwest from the Indo-Pakistan heat low. Layers with upward motion hatched.

western Arabian Sea, where the subsidence inversion is usually below 1000 m (Fig. 2), probably experiences as little rain as the deserts of Arabia and Somalia.

Fig. 6 shows that the mean resultant vertical wind shear over the western Arabian Sea parallels the Arabian and Somali coasts below 500 mb and is directed from east to west between 500 and 200 mb, reflecting the heating effect of Arabia and Somalia on the lower troposphere and the effect of latent heat release in monsoon rain systems on the upper troposphere. This shift in the shear pattern means that, between 800 and 600 mb, the western Arabian Sea is overlain by desert-dried air from the west.

A schematic cross section of the vertical circulation between the heat low (27N 71E) and 15N 57E (Fig. 7) suggests shallow inflow into the heat low and upward motion downstream from the southwest monsoon speed maximum (Fig. 1). In the middle troposphere south of 23N air is converging into a subtropical cyclone centered just west of Bombay. This results in sinking motion in the lower troposphere accentuated by low-level divergence upstream from the southwest monsoon speed maximum, and rising motion between 500 and 300 mb. In the upper troposphere the section lies west of the easterly jet maximum which in turn is an effect of intense condensation over India. Thus massive subsidence between 200 and 700 mb maintains the intensity of the heat low. The effect of the Arabian and Somali troughs, not explicitly included here, is to elongate the circulation toward the southwest.

4. Subtropical cyclone development

The heat low circulation always develops before the first of the subtropical cyclones which produce western India's monsoon rains. Therefore, an hypothesis that the heat low "causes" subtropical cyclogenesis seems worth exploring.

Because of its nature the heat low is likely to exert a thermodynamic effect rather than a mechanical effect on its environment. Petterssen (1956) discusses large scale thermodynamic influences on the behavior of cyclones and anticyclones. He begins with the vorticity equation for a surface of constant potential temperature and by assuming steady state and neglecting the contribution of vertical advection of the tangential vorticity vector derives the equation

$$\nabla\cdot(Q\mathbf{V})=F-\frac{\partial Q}{\partial\theta}\dot{\theta},$$

in which Q is the component of the absolute vorticity normal to a surface of constant potential temperature, $\mathbf{V}$ is the horizontal wind vector, F is the vorticity of the frictional force, and θ is the potential temperature.

Over Arabia and West Pakistan the heat low slowly intensifies from late May until mid-July then slowly weakens until it disappears after mid-September. Thus one might be justified in assuming steady state condi-

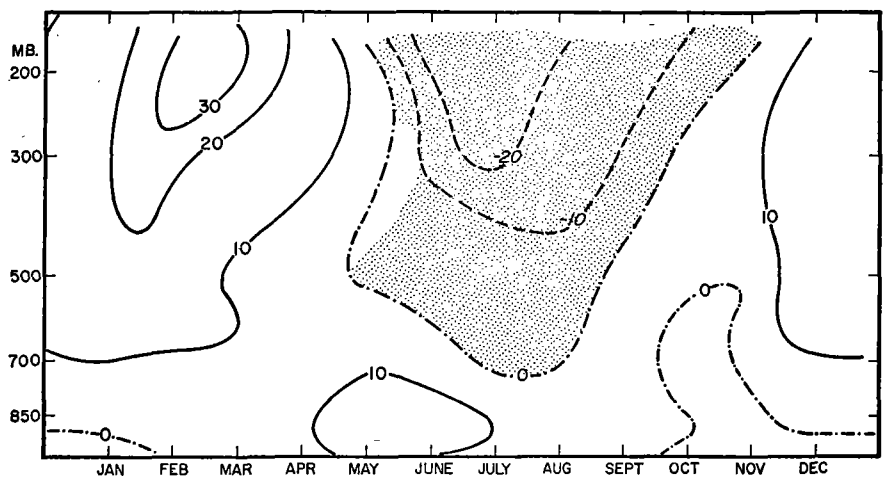

FIG. 8. Relative vorticity of the mean monthly resultant winds over the triangle Peshawar (34°01'N; 71°35'E); Karachi, (24°55'N; 67°09'E); Jodhpur (26°18'N; 73°01'E) in units of 10^{-6} sec^{-1}.

tions and in exploring the implications of Petterssen's equation.

The term on the left measures the intensity of the vorticity source, i.e., the export per unit time of vorticity through the boundaries of a unit area in a surface of constant potential temperature. The export depends on F, the intensity of the heat or cold source, $\dot{\theta}$, and the sign of $\partial Q/\partial\theta$ which differs insignificantly from $\partial Q/\partial Z$.

In only one part of the heat low are mean resultant tropospheric winds available for computing vorticity, the triangle enclosed by the rawinsonde stations of Pehsawar, Jodhpur, and Karachi. Fig. 8 depicts the mean distribution through the year and through the troposphere of the relative vorticity computed by the Bellamy (1949) method for the triangle, whose centroid is located at about 28N 71E, on the axis of the heat low.

If F and $[-\dot{\theta}(\partial Q/\partial\theta)]$ have the same sign, the sign of the vorticity export is known. During summer over the heat low, $\dot{\theta}$ is always positive while in the stippled area of the diagram, $F>0$ and $(\partial Q/\partial\theta)<0$. Fig. 8 shows that beginning in early June cyclonic vorticity is exported from the triangle in the middle and upper troposphere. If vorticity is similarly exported from Arabia then cyclonic vorticity accumulates over the northern Arabian Sea. As long as the air remains dry development is unlikely but by mid-June moist air reaches the northeast Arabian Sea, usually from the south or east. Then buoyancy forces come into play, a subtropical cyclone develops, and the first burst of monsoon rains drenches the Bombay district. The subtropical cyclone through the agency of subsidence further intensifies the heat low which then exports additional cyclonic vorticity to the middle and upper troposphere over the northern Arabian Sea. It may be no accident that the rains of western India set in (latitude for latitude) later than the rains of eastern India and Burma for the latter probably play a part in initiating the sharp increase in anticyclonic vorticity above the West Pakistan heat low in late May.

As Miller and Keshavamurthy (1965) show, a subtropical cyclone lasts from one to three weeks, modifying its environment so as finally to reduce the supply of moist air to the circulation below the sustaining point. The cyclone fills, and a monsoon "break" ensues. Then when a new supply of moist air becomes available, subtropical cyclogenesis may once more occur in the favored location.

In a more general discussion, Pisharoty (1964) accounts for diminution of monsoon rains in terms of decreasing slope of isentropic surfaces resulting from the release of latent heat in the condensation process.

Fig. 8 shows that the depth of the layer of positive $[F-\dot{\theta}(\partial Q/\partial\theta)]$ over the heat low decreases rapidly through September. At the same time, $\dot{\theta}$ also decreases. By mid-September, in most years, positive vorticity is no longer exported to the northern Arabian Sea and no further subtropical cyclogenesis occurs there. One consequence of the model, indicated by crudely quantitative computations, is that the Arabian Sea subsidence inversion may so limit the supply of moisture as to make appreciably heavy monsoon rains over western India unlikely without significant incursions of deeply moist air from the Bay of Bengal across the peninsula. A burst of west Indian monsoon rains is usually preceded by increased depth of the moist layer to the east.

The worst west Indian summer drought in history occurred in 1899. Over northwest India both surface temperatures *and* pressures were above normal. Over the Arabian Sea surface winds were below normal. Intense insolation favored heat low development but the absence of subsidence above the heat low resulting in turn from the absence of rain systems to the south and east outweighed the effect of insolation. Presumably if "feedback" between rain systems and heat low is interrupted, export of mid-tropospheric cyclonic vorticity to the northern Arabian Sea is reduced, chances of subtropical cyclogenesis are lessened, the heat low remains relatively weak, and drought tightens its grip.

5. Concluding remarks

The foregoing discussion implies a symbiotic relationship between heat lows and subtropical cyclones. Because cold upwelling coastal waters keep Somalia and Arabia dry and hot throughout the summer, because a complex of desiccating influences are at work over West Pakistan, because topography concentrates mid-tropospheric cyclonic vorticity over the northern Arabian Sea, and because deep moist air can reach the region only from south or east, the relationship is strongly developed over West Pakistan and the northeast Arabian Sea.

However, rain-producing systems similar in character to subtropical cyclones have been observed south of the Saharan heat low (Gilchrist, 1960). In early summer, south of the thermal equator over the South China Sea and the Bay of Bengal, subtropical cyclones may also develop (Ramage, 1959, 1964), but as summer advances, warm-cored cyclones dominate these seas and moving inland displace the dry cloud-free air of the heat lows. Thus many meteorologists maintain that the summer lows of North Viet Nam and the Ganges Valley are in reality only the statistical effects of stagnating, dissipating tropical storms (Palmer, 1951).

The summer regime over the Arabian Sea is a strange one whose character seems basically determined by the vast desert arc extending from northeast Africa to northwest India and by coastline orientation. The heat low develops over the deserts but then is maintained and protected by its offspring, upwelling along the west coast and subtropical cyclones in the northeast. The result is the most intense monsoon system on earth, gale force southwesterlies overlain by jet strength easterlies. Despite such vigor, no moving cyclone

system ever enters the region during summer. Tropical hurricanes are unknown (Ramage, 1959), while the subtropical cyclones develop, intensify and fill *in situ* equally as captive to orography as the heat low.

Acknowledgments. This work forms part of an investigation of the general atmospheric circulation of the Indian Ocean region made possible by grant G-22413 from the National Science Foundation.

REFERENCES

Bellamy, J. C., 1949: Objective calculations of divergence, vertical velocity, and vorticity. *Bull. Amer. Meteor. Soc.*, **30**, 45–49.

Bunker, A. F., 1965: Interaction of the summer monsoon air with the Arabian Sea (preliminary analysis). Paper presented at Symposium on Meteorological Results of the International Indian Ocean Expedition, Bombay, 22 July 1965.

Dallas, W. L., 1887: Memoir on the winds and monsoons of the Arabian Sea and north Indian Ocean. Calcutta, Supt. of Govt. Printing, India, 45 pp.

Dixit, C. M., and D. R. Jones, 1965: A kinematic and dynamical study of active and weak monsoon conditions over India during June and July, 1964. International Meteorological Center, Bombay (prepub.) 28 pp. (Available from International Meteorological Center, Colaba Observatory, Bombay-5, India.)

Flohn, H., 1964: Investigations on the tropical easterly jet. *Bonner Meteor. Abhand.*, 4, 80 pp.

Frost, R., and P. M. Stephenson, 1965: Mean streamlines and isotachs at standard pressure levels over the Indian and west Pacific Oceans and adjacent land areas. *Geophys. Mem.*, **109**, 24 pp.

Gilchrist, A., 1960: Contour charts for July 1960 in the West African area. *Tech. Notes, Brit. W. African Meteor. Services*, **19**, 5 pp.

Miller, F. R., and R. N. Keshavamurthy, 1965: The Arabian Sea summer monsoon. Paper presented at Symposium on Meteorological Results of the International Indian Ocean Expedition, Bombay, 26 July 1965.

Palmer, C. E., 1951: Tropical meteorology. *Compendium of Meteorology*, Boston, Amer. Meteor. Soc., p. 873.

Petterssen, S., 1956: *Weather Analysis and Forecasting, Second Edition*. Vol. I, Motion and motion systems, New York, McGraw-Hill, 428 pp.

Pisharoty, P. R., 1964: Monsoon pulses. Proc. WMO Symposium on Tropical Meteorology, Rotorua, New Zealand, 373–379.

Ramage, C. S., 1959: Hurricane development. *J. Meteor.*, **16**, 227–237.

——, 1962: The subtropical cyclone. *J. Geophys. Res.*, **67**, 1401–1411.

——, 1964: Some preliminary research results from the International Meteorological Center. Proc. WMO Symposium on Tropical Meteorology, Rotorua, New Zealand, 403–408.

Raman, C. R. V., and C. M. Dixit, 1964: Analyses of monthly mean resultant winds for standard pressure levels over the Indian Ocean and adjoining continental areas. Proc. WMO Symposium on Tropical Meteorology, Rotorua, New Zealand, 107–118.

——, and Y. Ramanathan, 1964: Interaction between lower and upper tropical tropospheres. *Nature*, **204**, 31–35.

Royal Netherlands Meteorological Institute, 1952: *Indian Ocean Oceanographic and Meteorological Data, Second Edition*, 31 pp. and 24 charts.

Simpson, R. H., 1952: Evolution of the kona storm, a subtropical cyclone. *J. Meteor.*, **9**, 24–35.

DEPARTMENT OF COMMERCE AND INDUSTRIES

DIVISION OF SEA FISHERIES

OCEAN CURRENTS AND WATER MASSES AT 1,000, 1,500 AND 3,000 METRES IN THE SOUTH-WEST INDIAN OCEAN

BY

G. A. VISSER AND M. M. VAN NIEKERK

INVESTIGATIONAL REPORT No. 52

INVEST. REP. DIV. SEAFISH. S. AFR. 52: 1-46

Issued by the Division of Sea Fisheries, Beach Road, Sea Point, Cape Town

REPUBLIC OF SOUTH AFRICA

Contents.

1. Summary.

This report deals with data collected during the three cruises of R.S. *Africana II* undertaken in the South-West Indian Ocean during 1961, 1962 and 1963.

During these investigational cruises observations were made of the temperature, salinity, dissolved oxygen and inorganic phosphate of the waters at international sampling depths. The sigma-t values were calculated by means of temperature and salinity data which were in turn used for dynamic calculations.

In the determination of current directions according to isobaths at the various sigma-t surfaces, use was made of the principle that, if the surface of discontinuity has a downward gradient towards the left, the current will flow in the direction in which an observer is looking when standing between the two relevant stations (SVERDRUP *et al.* 1942).

If a comparison is made between the current directions according to the dynamic topographical charts and the sigma-t charts, a very close agreement is observed. Up to the present research workers have made use mainly of identifying properties such as sigma-t, salinity and temperature for determining the direction of ocean currents and for identifying water masses on a theoretical basis.

According to the isobaths at the three selected sigma-t surfaces there is a possibility that water flows from an easterly direction over the Madagascar Ridge to the Agulhas Current, this flow being marked between stations 5 to 13 and 26 to 30. As appears clearly from an analysis of the temperature and salinity, the water at great depths at the above-mentioned stations is mainly of Atlantic origin or otherwise of Indian Ocean origin. Consequently it is very probable that the isobaths indicate the actual path of water transportation. Apparently the current directions shown by the isodynamic lines are also confirmed. The trend of isohalines and isotherms at the various sigma-t surfaces further supports this conclusion.

In the area just to the south of Madagascar the current directions, according to the sigma-t charts, confirm the supposition that water first moves south-eastwards, to flow over the Madagascar Ridge and curve north-westwards. Water gyrals, cyclonic or anticyclonic, as indicated by the dynamic topographic lines are confirmed by the isobaths, isotherms and isohalines at the sigma-t surfaces 27·20, 27·40 and 27·60.

Furthermore the isobaths on the sigma-t charts distinctly indicate that water flows from an easterly direction towards Madagascar. Part of this water is apparently deflected in a northerly direction along the east coast of Madagascar and the remainder moves around the southern tip of Madagascar.

In regard to the water masses of the area, it may be assumed with a large degree of certainty that Antarctic Intermediate Water, Warm Deep Water (originating from the Atlantic Ocean and the Mozambique Channel) and Bottom Water form a large anticyclonic movement of water in this area. The intensive anticyclonic swirls are clearly observable around station 50 and in the region of the returning Agulhas Current around stations 57 and 60. The rapidly flowing Agulhas Current and the West Wind Drift may also be readily identified.

It would, therefore, appear that the method of dynamic calculations for the theoretical determination of relative ocean currents at great depths is valid and gives a good picture of the general current directions.

2. Introduction.

In general the South-West Indian Ocean is an area where little intensive research has been done on the deep water masses. Only a few stations have been completed during wide-spread cruises. As a result of this deficiency earlier research workers for example, DIETRICH (1935) and CLOWES (1950), could not achieve absolute finality in their findings. The three cruises of R.S. *Africana II* were spread over a relatively short period during which quite a large number (70) of stations were occupied. As a result of the fairly stable nature of the deep water masses it appears that these data agree very well. Close agreement exists between the results obtained by the above-mentioned research workers, and those from data amassed during the voyage of R.S. *Africana II.*

For convenience when analysing the data, the stations were numbered from 1 to 70. These numbers are given first and then followed by the corresponding formal station numbers (Fig. 1). The data constitute only part of the hydrological particulars and additional information may be found in the complete station list under the formal station numbers as published in the " Annual Report " series of the Division of Sea Fisheries. Stations 1 to 32 (A 1,224 to A 1,255) south of Madagascar, were worked during 1961, while stations 33 to 55 (A 1,875 to A 1,897) from Port Elizabeth to the sub-antarctic islands were worked during 1962, and stations 56 to 70 (A 2,386 to A 2,400) from Cape Agulhas to Marion Island, during 1963.

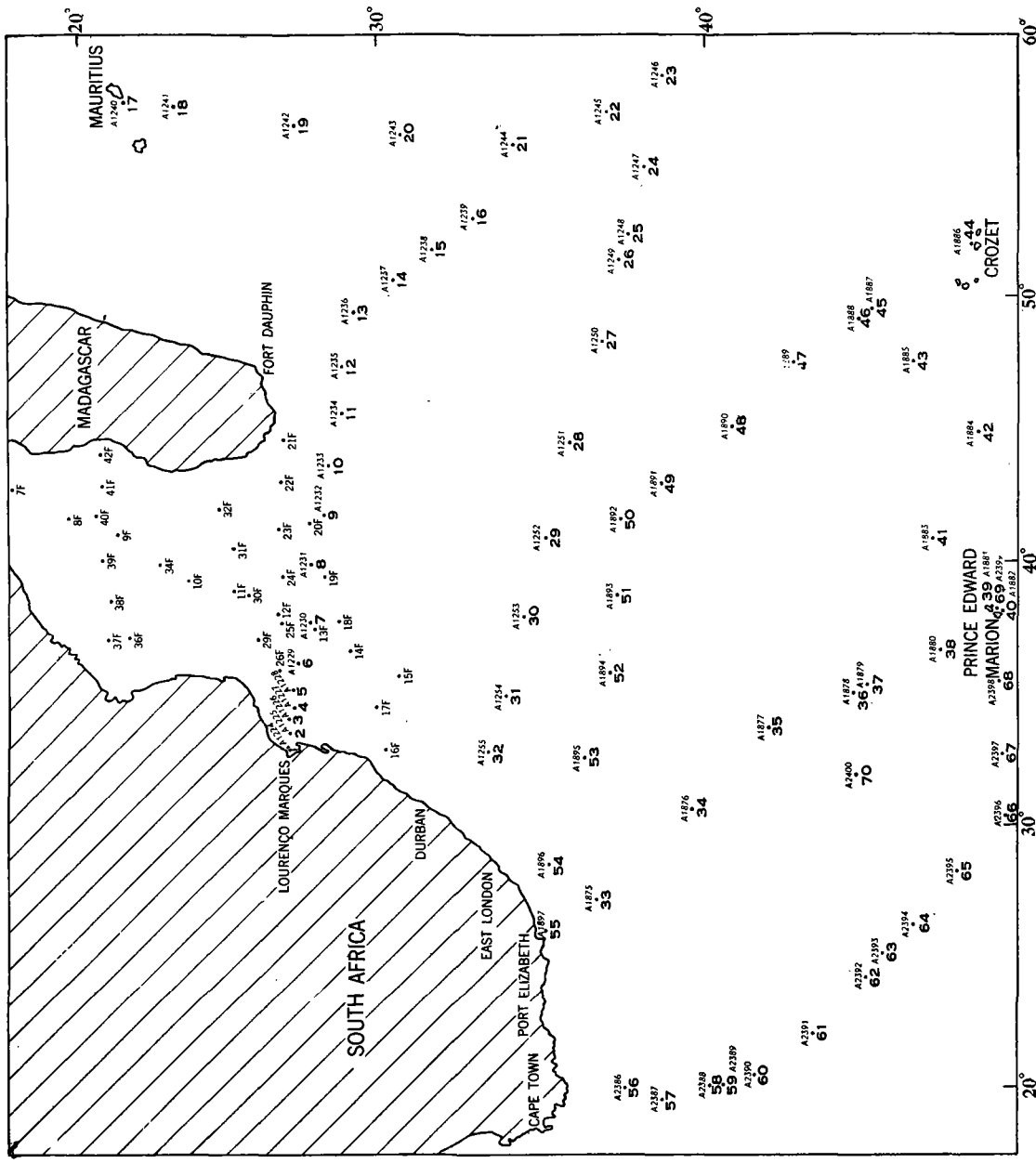

FIG. 1 POSITION OF STATIONS IN AREA INVESTIGATED.

Charts were plotted for the ocean currents existing at three different depths, namely 1,000 metres (Fig. 2), 1,500 metres (Fig. 3) and 3,000 metres (Fig. 4). Shading of parts of the charts indicates the location of plateaux, which are shallower than the relevant depths at which the ocean currents were calculated. In Figure 2 the geopotential gradient is indicated at intervals of ·05 dynamic metres, and in Figures 3 and 4 the spacing is ·02 and ·01 dynamic metres respectively. For the sake of completeness, charts of the temperature and salinity data have been plotted at the same depths (Figures 6 to 11).

The velocity of the ocean currents was calculated at each station at depths of 1,000 metres, 1,500 metres and 3,000 metres. The results are given in Table 1.

The chart indicating the position of stations in the area investigated by *Africana II* (Fig. 1), includes a number of stations occupied by the French research ship *Commandant Robert Giraud* in 1957 in the vicinity of the Mozambique Channel. All these foreign stations are indicated by an " F ". Furthermore, charts of depth, salinity and temperature have been plotted for the $\sigma t = 27{\cdot}20$, $\sigma t = 27{\cdot}40$ and $\sigma t = 27{\cdot}60$ surfaces (Figures 12–20). Depths, temperatures and salinities at the various sigma-t surfaces are chiefly interpolated values. In the salinity charts (Fig. 13, 16 and 19) only the figures following the decimal point are given, because the salinity at all three surfaces lies in the range $34{\cdot}00°/_{oo}$ to $34{\cdot}99°/_{oo}$. Station 20 was only worked to a depth of 800 metres and isobaths between stations 19 and 21 have for the most part been omitted.

A vertical section of salinity was also plotted between stations 62, 35, 49, 27, 16 and 19 (Fig. 35). As an annexure to the present investigational report and in support of certain assertions, part of a chart has been taken from *Cahiers Océanographiques*, showing work done by the French research ship *Commandant Robert Giraud* (Fig. 36).

The purpose of this report is mainly to identify the direction of currents between 1,000 metres and 3,000 metres in the area investigated. An attempt has also been made to test the validity of dynamic calculations for the determination of current directions by comparing these results with others obtained from the use of the identifying properties such as sigma-t, salinity and temperature in the South-West Indian Ocean.

3. Ocean Currents.

3.1. Dynamic Calculations.—

The determination of ocean currents and their directions by means of dynamic calculations does not give a complete picture of absolute currents but rather of relative currents (LAFOND 1951).

PARR (1937–38) has discussed in detail his objections against the use of hydrodynamic calculations and considerations in the determination of ocean currents. This writer's objections are based mainly on the fact that the dynamic method of analysis deals only with states of motion and not with the actual trajectories or paths of transportation. PARR regards the use of identifying properties of water masses such as sigma-t, salinity, temperature, etc., for the determination of the current directions as a better method than that of dynamic calculations.

According to VON ARX (1962) relative surface currents deviate by about 15 per cent from the actual current direction. Since the dynamic calculations of the present report were made for great depths, where slight differences would not result in any noteworthy current deviation, it may be accepted that the current pattern as shown in the charts of dynamic topography (Figures 2 to 4), in general, gives a good picture of ocean currents and water movements in the South West Indian Ocean. Here we have consistently endeavoured to substantiate current directions obtained with the aid of dynamic calculations by means of the analysis of sigma-t, salinity, etc.

Previous research workers, such as DARBYSHIRE (1963), have supposed that at a certain depth there is no noteworthy movement of water. This depth is known as the " Depth of no motion ". It is postulated that at this " Depth of no motion " the isobaric surface i.e. the surface at which the pressure is uniform, is horizontal and consequently no gradient current exists. In the present report use was made of a graphic method to determine the most suitable " Depth of no motion ", a graph being plotted to indicate the variation of dynamic height anomalies at the various isobaric surfaces. From this graph it appeared very clearly that at the 2,000 db surface there is very little variation. We subsequently computed the currents relative to the 2,000 db surface. The current lines will therefore indicate the movement of water relative to this surface.

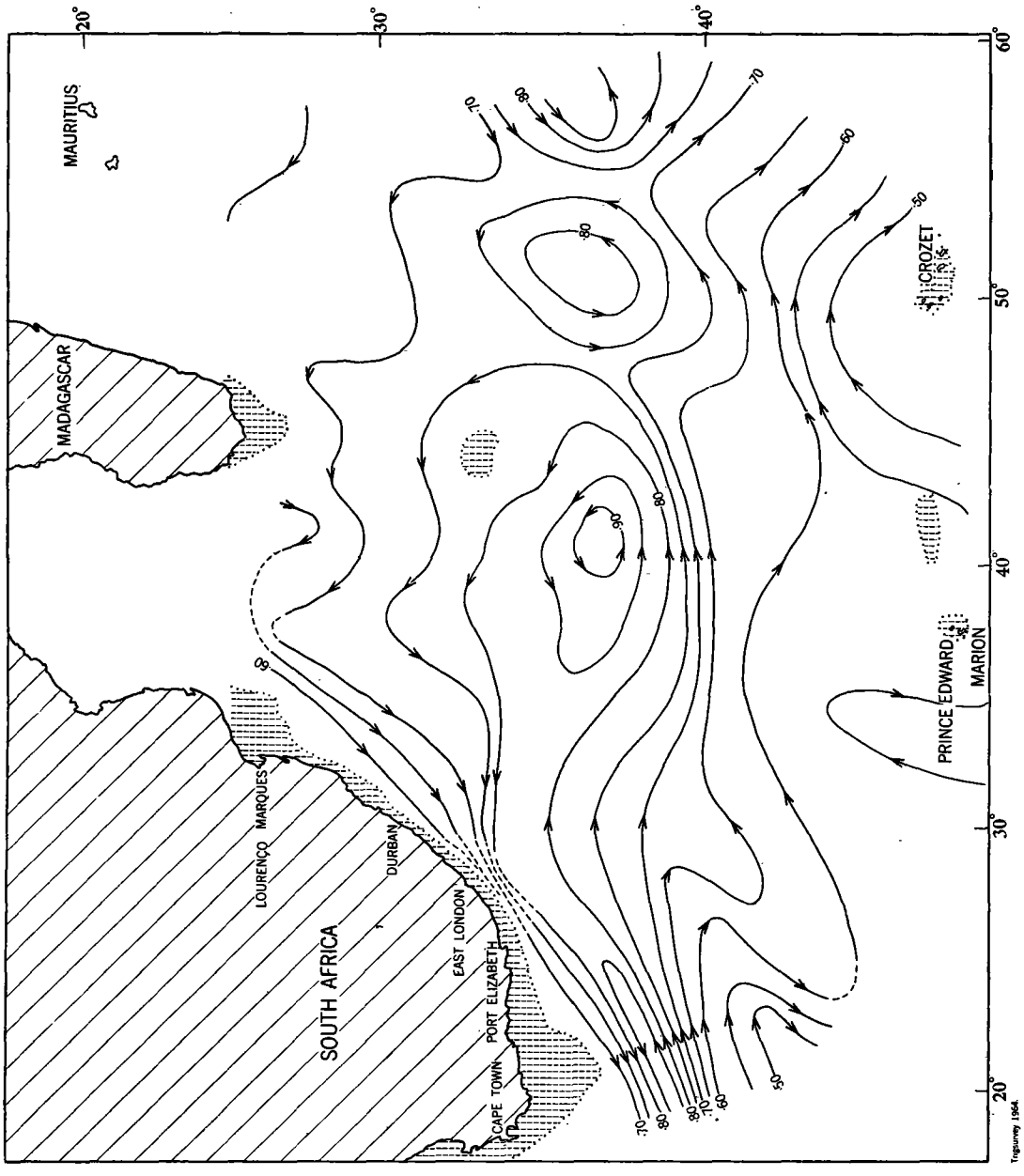

FIG. 2 CONTOURS OF DYNAMIC HEIGHT ANOMALIES (DYN. METRES) FOR 1000 db RELATIVE TO 2000 db.
(Shaded areas less than 1000 metres deep).

In this way the dynamic gradient of an isobaric surface, relative to the " Depth of no motion " can be obtained from the variation of specific volume over the relevant isobaric surface. Consistent use has been made of the hypothesis that the direction of flow will always be at right angles to the geopotential gradient; in other words, parallel with the dynamic contour lines (PARR 1937–38).

The dynamic calculations in this investigational report were made separately for each station and the results of all stations of the three cruises of R.S. *Africana II* were subsequently grouped together in order to obtain the general current pattern. The following equation was used for the calculation of the dynamic thickness:—

$$D_2 - D_1 = \int_{p_1}^{p_2} \alpha \, dp \text{ (LAFOND 1951) (1)}$$

where: $D_2 - D_1$ = dynamic thickness of the isobaric layer,
α = specific volume,
dp = pressure interval,
p_1 and p_2 = pressure at the isobaric surfaces.

The specific volume *in situ*, $\alpha_{s,t,p}$ consists of two parts, namely a standard term for dynamic thickness $\alpha_{35,o,p}$ and the anomaly of specific volume, namely δ.

Thus it may be written:—

$$\alpha = \alpha_{35,o,p} + \delta$$

The total dynamic thickness, therefore, consists of the dynamic thickness of the layer of water with a standard specific volume and an increment in dynamic thickness.

Thus:

$$D_2 - D_1 = \int_{p_1}^{p_2} \alpha_{35,o,p} \, dp + \int_{p_1}^{p_2} \delta \, dp$$

$$= (D_2 - D_1) \text{ standard} + \triangle D \text{ (LAFOND 1951)}$$

Since the standard dynamic thickness, $(D_2 - D_1)$ standard, is the same at all stations, it is merely necessary to obtain the difference in dynamic height between consecutive stations. This is indicated by $\triangle D$ and it is therefore merely necessary to calculate $\triangle D$ at each station. The following formula is used for this purpose:—

$$\triangle D = \int_{p_1}^{p_2} \delta \, dp \ldots\ldots\ldots\ldots\ldots\ldots (2)$$

There is a very close relationship between linear metres and pressure in decibars. Thus for an increase of one metre in depth, the pressure will increase by 1·006 decibars. Consequently p_1 and p_2 in (2) are replaced by linear metres at that particular depth.

Limitations of the method of dynamic calculations are as follows:—

(i) The calculated ocean currents are relative and not absolute.
(ii) The acceleration of ocean currents, which could result in changes, is not taken into account.
(iii) Frictional forces are disregarded.
(iv) Observations made at various stations at various times are regarded as simultaneous observations, as is almost always the case (LAFOND 1951).

In order to determine the direction of the relative currents use is made of the principle that, if the surface of discontinuity in the Southern Hemisphere has a downward slope, the isobaric surface will yield an upward gradient (PROUDMAN 1952). If, therefore, there are two stations A and B, and A lies west of B and the dynamic height anomaly at A is larger than at B, then it is found that the isobaric surface shows an upward slope towards the west, since the surface of discontinuity shows a downward slope towards the west. The present writers have further applied the principle that the current between A and B in this specific case flows in a northward direction (PROUDMAN 1952).

Since the depth of the water at all stations does not extend to 2,000 metres or 3,000 metres, consistent use has been made of a system of extrapolation for the dynamic calculations. When the station was shallower than 2,000 metres but deeper than 1,500 metres, or shallower than 3,000 metres but deeper than 2,500 metres, use was made of the dynamic height anomalies of the relevant stations at 1,500 metres, or of neighbouring stations at 2,500 metres (SVERDRUP *et al.* 1942, Fig. 109). The dynamic topography lines therefore were plotted throughout as though the depth at the relevant stations was 2,000 metres or more and 3,000 metres or more.

3.2. Current Directions at the 1,000/2,000 db Surface.—

The general directions of flow of currents in the area investigated point to the existence of a large anticyclonic movement of water (Fig. 2). The most clearly recognisable currents are the Agulhas Current, the " Return Agulhas Current " and the West Wind Drift. By the " Return Agulhas Current " is meant that part of the Agulhas Current which turns eastward south of the Cape of Good Hope and which is subsequently deflected in a northerly and north-easterly direction.

6315631—2

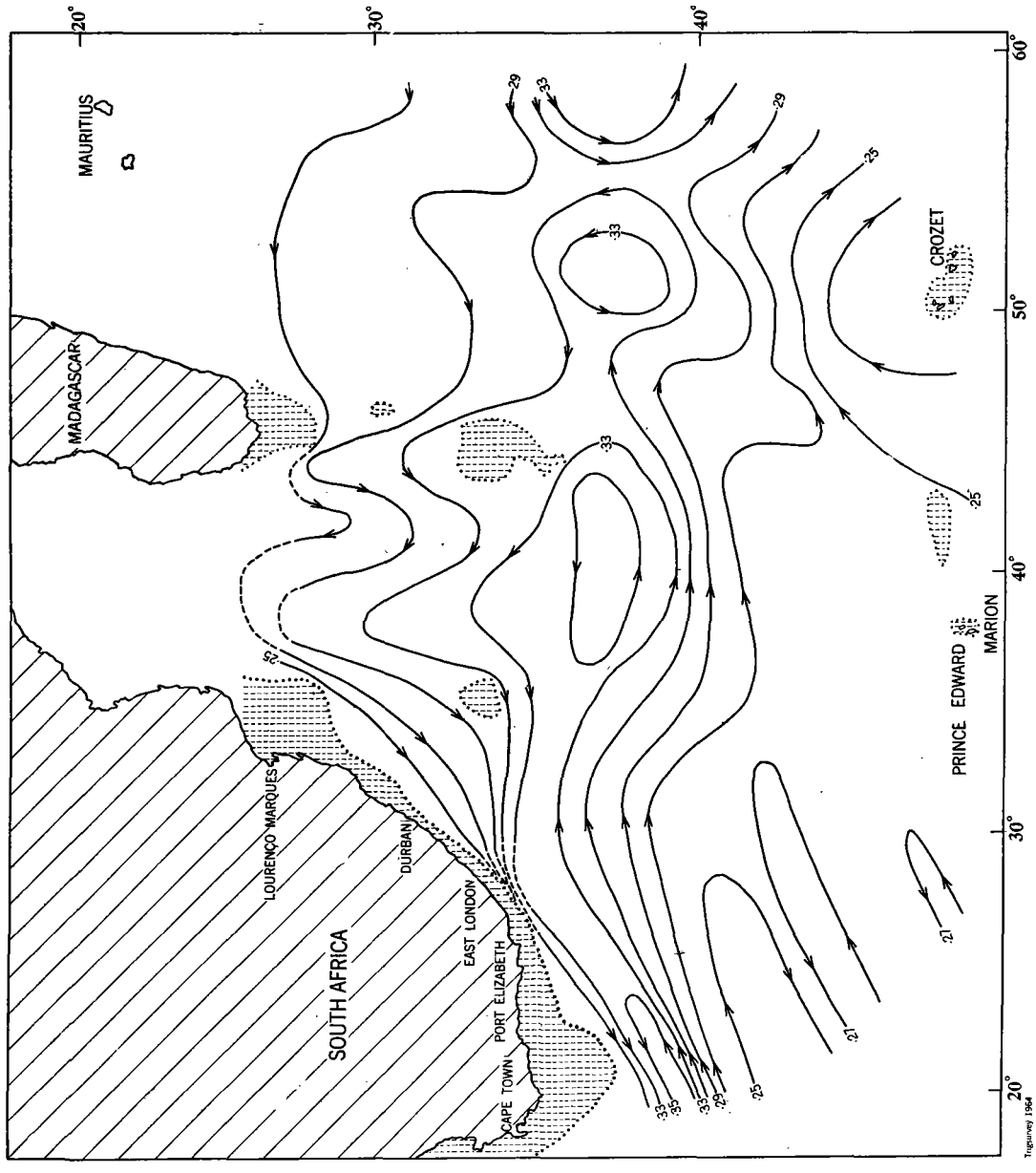

FIG. 3 CONTOURS OF DYNAMIC HEIGHT ANOMALIES (DYN. METRES) FOR 1500 db RELATIVE TO 2000 db.
(Shaded areas less than 1500 metres deep).

Off Lourenco Marques the current moves in a southerly direction and tends to curve inshore. Further east there is a cyclonic movement of the current, the water moving southward and turning back after a short distance before being deflected in the direction of the Mozambique Channel. South of this cyclonic water movement a well-marked westward current occurs, moving closer to the east coast of South Africa until the edge of the broadening Agulhas Bank is reached. Here the current is deflected in a more southerly direction and passes around the outside of the Agulhas Bank and then apparently turns in an easterly direction.

In the vicinity of ± 30° S and ± 38° E southerly branches of the current occur at the 1,000/2,000 db surface (Fig. 2). These intrusions indicate the presence of water from the Mozambique Channel penetrating as far as ± 30° S in the South-West Indian Ocean.

An interesting current pattern occurs at the southern tip of South Africa. Here part of the Agulhas Current flows over the southern edge of the Agulhas Bank and bends in a north-westerly direction towards Cape Point. The principal part of the current, however, shows an anticyclonic trend and apparently turns south of the Agulhas Bank to move eastward. The distance penetrated by the Agulhas Current in a south-westerly direction could unfortunately not be determined as a result of a lack of data collected at the time of the relevant three cruises of the R.S. *Africana II.* The current lines of the Return Agulhas Current continue, keeping approximately to the direction of the 40° S line of latitude which is also near the position of the Subtropical Convergence. As a result of the reversal of the Agulhas Current, a fairly large anticyclonic swirl is caused, which is clearly manifest in the centre of the turning area. The distinctive West Wind Drift also moves in an easterly direction together with the Return Agulhas Current.

The curving current line, which can be observed at the 1,000/2,000 db surface south of the West Wind Drift indicates the tendency of water to form a cyclonic movement around station 61. This cyclonic movement of water corresponds very closely to the course of isobaths at the various sigma-t surfaces.

In the region of ± 38° S and ± 30° E a part of the Return Agulhas Current branches off, moving first in a north-easterly direction before being deflected towards the south-east and then again in a westerly direction.

The same phenomenon of branching occurs at ± 38° S, ± 42° E. Current lines show that part of the current first moves north-eastward, but gradually turns northward in the direction of the Madagascar Basin. The current lines then turn westward towards South Africa. At the commencement of this branching there are again two well-marked anticyclonic swirls of water, one on the west side of the branch and another fairly large swirl on the east side. The latter apparently occurs as a result of the convergence of currents from various directions.

The southern part of the current which moves past the Agulhas Bank in a west-east direction, may be regarded as the West Wind Drift. This Drift curves slightly southward and a clear anticyclonic tendency is observable at ± 41° S and ± 45° E. In the above-mentioned area there is also a current which flows from a southerly direction to join the West Wind Drift near station 45.

On the southern side of the West Wind Drift we also find a current line which first runs eastward, then turns towards station 62 and then continues in an easterly direction.

At the southern tip of Madagascar there is a current which moves westward and then curves around the tip of the island. This is in agreement with what earlier research workers such as PAECH (1926), found for the movement of surface water. This occurrence will be dealt with in the discussion of southerly protrusions in the Mozambique Channel.

3.3. Current Directions at the 1,500/2,000 db Surface.—

Basically the same current directions are encountered at the 1,500/2,000 db surface (Fig. 3) as at the 1,000 db surface, except that branches, divergences and swirls are generally much less clearly discernible and less intensive according to the pattern of the current lines.

A very striking fact is that the current lines at the 1,000/2,000 db surface in the protrusions off Lourenco Marques are much less intensive than those at the 1,500/2,000 db surface. The water apparently also moves in a cyclonic direction in these protrusions at 1,500 metres while at 3,000 metres it moves in an anticyclonic direction (Fig. 4). At the latter depth the current directions are evidently influenced by the bottom topography.

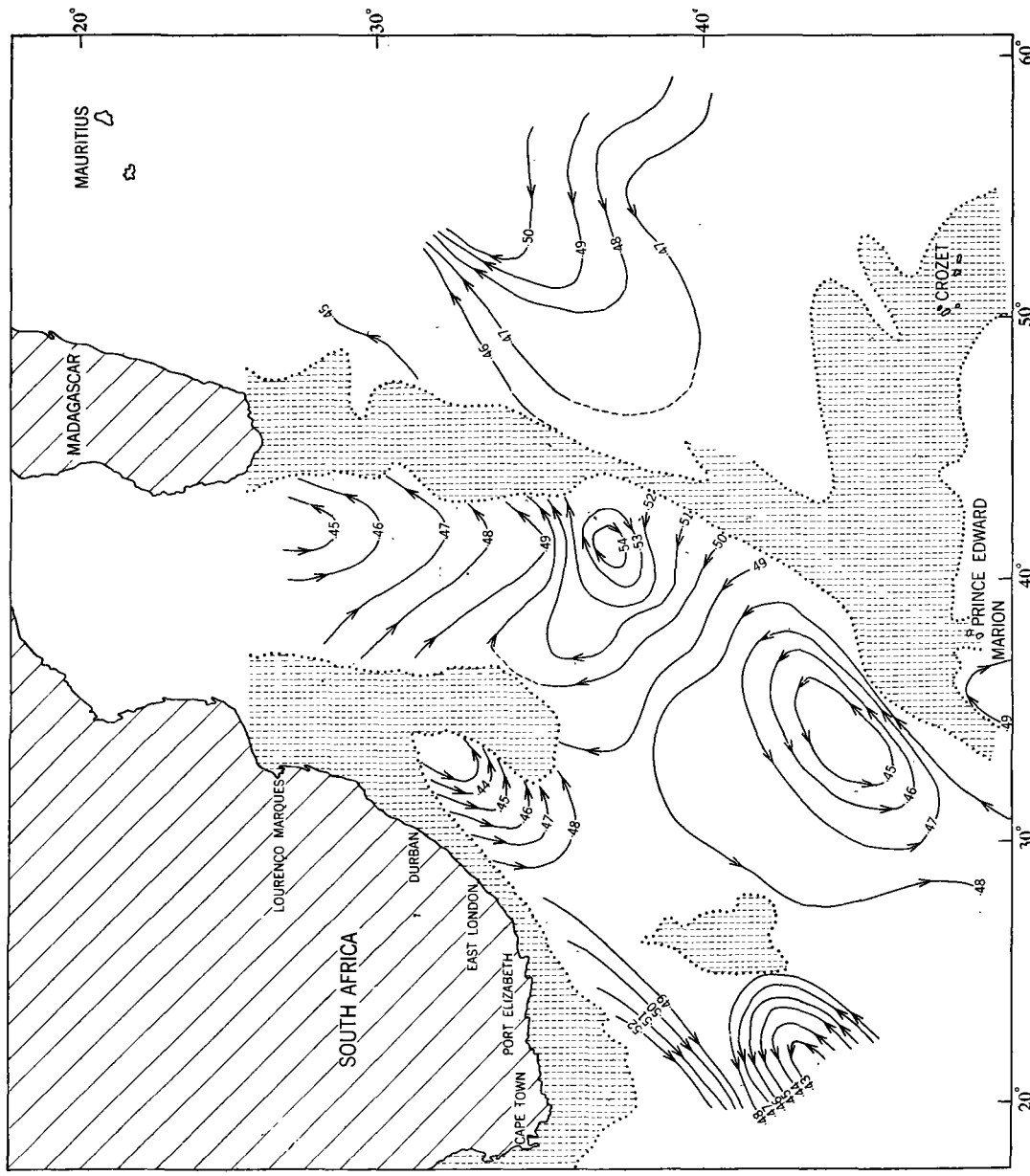

FIG. 4 CONTOURS OF DYNAMIC HEIGHT ANOMALIES (DYN. METRES) FOR 3000 db RELATIVE TO 2000 db.
(Shaded areas less than 3000 metres deep).

South-east of and opposite Durban the westward moving current tends to turn south and then to move towards the east coast of South Africa again between stations 32 and 54.

On the east side of the Madagascar Ridge the current lines indicate that at the 1,500/2,000 db surface around stations 21–23 there is a southward flowing current, part of which moves in the direction of Madagascar and joins the current flowing westward from the direction of station 19.

South-west of Madagascar in the vicinity of stations 8–10 well-defined southward current tendencies occur on the 1,500/2,000 db surface. The tendency of the current to turn back is apparently due to Atlantic water which has a northward component in the direction of the Mozambique Channel.

The most prominent anticyclonic swirl noticeable at both the 1,000/2,000 db and 1,500/2,000 db surfaces is that found around station 50. In addition there are well-marked anticyclonic swirls around stations 62 and 65 at the deeper surface. The fact that the Agulhas Current tends to move at an ever-decreasing rate around Cape Point towards the west coast of South Africa at the deeper surface may very clearly be observed.

In general, therefore, a part of the water moves south-ward along the east coast of South Africa, turns back in an easterly direction and then curves again in the direction of the Mozambique Channel, forming in this way a large anticyclonic water movement in the South-West Indian Ocean.

3.4. **Current Directions at the 3,000/2,000 db Surface.—**

The ocean currents as indicated by current directions at 3,000 metres, relative to the 2,000 db surface, are shown in Figure 4. Current lines have been plotted only where the area is deeper than 3,000 metres.

An important characteristic of ocean currents at this depth is that in general they flow in opposite directions to those at 1,000 and 1,500 metre depths. There is, for example, a well-marked cyclonic swirl around station 50. From a northerly direction there is also a tendency for the water from the Mozambique Channel to penetrate the Natal Basin and cause an anticyclonic movement of the current. In the same way, between stations 32 and 54 there is also a perceptible anticyclonic swirl, part of which apparently branches off and forms the deeper part of the Agulhas Current. According to the distribution of the current lines, it appears that the water between stations 6 and 31 flows over the shallow part, including the Mozambique Terrace and is then deflected by the southward-stretching Agulhas bank.

Other distinct anticyclonic swirls are perceptible around stations 36 and 61. According to the course of the current line between stations 66 and 67, the current flows north-eastward and turns back in the Natal Deep in the direction of station 65. The cyclonic swirl around station 50 is apparently due to the southward movement of water from the Mozambique Channel and the northward-moving water from the direction of stations 66 and 67.

On the eastern side of the Madagascar Ridge there is a westward movement of water, which later changes into a north-eastward current. Around station 68 there is a current line which gives a slight indication of a cyclonic movement of water.

3.5. **Current Velocities.—**

The velocities of ocean currents in the area are given in Table I. These velocities were calculated according to the basic formula:—

$$V = \frac{10(D_A - D_B)}{L\ 2\omega Sin.\ \varphi} \quad \text{....(LAFOND 1951)}$$

Where V = Relative current velocity in cm./sec. at right angles to the line joining the two stations.

$D_A - D_B$ = Difference between dynamic height anomalies at stations A and B in dynamic metres.

L = Distance between stations in nautical miles.

ω = Angular velocity of the earth's rotation = $0{\cdot}729 \times 10^{-4}$ radians per sec.

φ = Average latitude between stations.

This formula was reduced to the following:—

$$V = \frac{c\,(D_A - D_B)\,n}{L} \text{ (LAFOND 1951).}$$

where $c = \dfrac{1}{2\omega\ Sin.\varphi.\ 10^5}$ and is called the current factor.

n = 53959 and is called the unit conversion factor, dependent on the units of the other variables.

From Table I it is clear that even at relatively great depths there are relatively rapid currents between certain stations. At a depth of 1,000 metres, for example, velocities of 15·6 cm./sec. and 21·8 cm./sec. were obtained between stations 57 and 58, and 58 and 60. At 1,500 metres there is a velocity of 7·0 cm./sec. between stations 58 and 60. A fairly high velocity of 10·5 cm./sec is also found

at 1,000 metres between stations 6 and 7. In each of the above-mentioned cases the line joining the stations is at right angles to the direction of flow of the current.

At certain stations there is little or no movement of the water. It was found, for example, that between stations 29 to 30 there was no movement at 1,000 metres, while movement does occur to an increasing extent at 1,500 metres and 3,000 metres.

At certain localities it also happens that the velocity decreases down to 1,500 metres and then increases again at greater depths. An example of this phenomenon is found between stations 35 and 36. From 1,000 metres to 1,500 metres the velocity decreases from 2·0 cm./sec. to 0·7 cm./sec., increasing again to 1·1 cm./sec. at the 3,000 metre depth. The same phenomenon takes place between stations 29 and 50. This is apparently due to the fact that at 3,000 metres the current flows in the opposite direction to that at 1,000 and 1,500 metres (Figures 2 to 4).

TABLE 1.

Between Stations.	Current Velocity (in cm./sec.)		
	at 1,000 metres.	at 1,500 metres.	at 3,000 metres.
6 and 7	10·5	4·8	—
7 and 8	2·2	0·6	0·3
8 and 9	2·8	1·8	0·9
9 and 10	4·2	2·1	0·8
10 and 11	0·8	1·6	—
11 and 12	2·3	1·0	—
12 and 13	1·5	0·3	—
13 and 14	0·8	0·6	0·6
14 and 15	0·5	0·1	0·4
15 and 16	2·1	1·1	3·8
16 and 21	1·7	1·1	—
21 and 22	5·8	2·3	—
22 and 23	1·9	0·4	0·3
23 and 24	3·0	1·0	0·6
24 and 26	3·9	1·3	0·7
26 and 27	4·1	1·2	0·6
27 and 29	1·2	0·3	—
29 and 30	0	0·1	0·8
30 and 32	3·0	1·4	—
34 and 35	2·2	0·3	—
35 and 36	2·0	0·7	1·1
36 and 38	0·4	0·3	—
38 and 41	0·1	0·1	—
41 and 43	0·3	0·4	—
43 and 45	1·4	1·2	—
45 and 47	6·5	2·3	—
47 and 48	0·8	0·2	—
48 and 49	0·8	2·7	—
49 and 50	3·2	1·2	1·4
50 and 51	2·0	0·3	1·1
29 and 50	4·1	1·5	2·6
30 and 51	1·7	0·9	0·5
32 and 54	3·4	1·7	1·7
57 and 58	15·6	3·7	—
58 and 60	21·8	7·0	3·6
60 and 61	4·5	1·5	2·5
61 and 62	5·7	1·8	2·4
62 and 64	2·1	0·6	0·1
64 and 65	0·2	0·5	—
65 and 66	0·3	0·5	—
66 and 67	1·7	0·2	—
67 and 68	0·5	0·2	—
38 and 68	0·5	0·3	—

In general the highest current velocities are found in the Agulhas Current area and the area of the Return Agulhas Current, except between stations 6 and 7.

Between almost all stations it is found that with increasing depth the current flows more slowly. This reaction is apparently due to the fact that the bottom topography influences the velocity to an increasing extent. The effect of ridges and plateaux (according to contour lines) would be much greater at 3,000 metres than at 1,000 metres. The Madagascar Ridge, for example, serves as a natural obstacle to the currents flowing over it and the flow of deeper water is retarded as a result of friction.

A possible explanation for the increased velocity with increasing depth between stations 48 and 49 is that the current which flows north-eastward here, moves in an ever-narrowing area between the Madagascar Ridge and the Mid-Ocean Ridge. The effect of these two ridges will definitely increase as the depth increases. This may clearly be seen according to the 1,500 and 2,000 fathoms contour lines (Fig. 5). ISELIN (1936) described the increasing velocity of the Gulf Stream, east of North America, as follows: " The Yucatan Channel has a width of about 105 miles, while the Florida Straits opposite Bimini are only 44 miles wide. Thus in cross section the current is successively reduced as it flows northward and, therefore, must increase correspondingly in velocity ". The same effect is applicable to the current system in our area, although to a much lesser extent. The same principle may be applied between stations 10 and 11.

Data are given below in Table II in regard to the stations between which the current flowed more rapidly, more slowly, etc., with increasing depth:

TABLE II.

Velocity: more rapid between Stations.	Velocity: slower between Stations.	Velocity: constant between Stations.	Velocity: first slower and then more rapid between Stations.
10 and 11.....	6 and 7	38 and 41	14 and 15
29 and 30.....	7 and 8		15 and 16
41 and 43.....	8 and 9		35 and 36
48 and 49.....	9 and 10		49 and 50
64 and 65.....	11 and 12		50 and 51
65 and 66.....	12 and 13		29 and 50
	13 and 14		60 and 61
	16 and 21		61 and 62
	21 and 22		
	22 and 23		
	23 and 24		
	24 and 26		
	26 and 27		
	27 and 29		
	30 and 32		
	34 and 35		
	36 and 38		
	43 and 45		
	45 and 47		
	47 and 48		
	30 and 51		
	32 and 54		
	57 and 58		
	58 and 60		
	62 and 64		
	66 and 67		
	67 and 68		
	38 and 68		

From the above table it is clear that the current velocity decreases with increasing depth between by far the greater majority of stations. The velocity first decreases and then increases only between eight pairs of stations, while it increases with increasing depth between six pairs of stations. The fact that between the majority of stations the current velocity decreases with increasing depth may probably be ascribed to the increasing influence of the bottom topography on the deeper currents. According to Figure 4, for example, at a depth of 3,000 metres the Madagascar Ridge and the Mocambique Terrace would not only reduce the flow of the current but even constitute barriers.

A further cause to which the reduced velocity of the currents may be ascribed, is that many currents at the 3,000 db surface flow in an opposite direction to those at the 1,000 db and 1,500 db surfaces (Figures 3 and 5).

DEACON (1937) finds that the surface velocity of the Agulhas Current ranges between 3 and 4½ knots. A feature of the current velocities obtained at 1,000, 1,500 and 3,000 metres is that the greatest velocities were obtained between stations situated in the Agulhas Current area and the area of the Return Agulhas Current. As mentioned before, a velocity of as much as 21·8 cm./sec. was found at 3,000 metres between stations 58 and 60.

3.6. Influence of the Bottom Topography.—

According to a study of currents at the $\sigma t = 27{\cdot}70$ surface made in the Drake Passage to the east of the South Sandwich Islands (SVERDRUP *et al.* 1942), it is clear that an ocean current turns towards the left while passing over a ridge. This applies to currents in the Southern Hemisphere and the converse is true for currents in the Northern Hemisphere.

The explanation for this phenomenon is that when water near the bottom approaches a ridge, it will rise, the isosteric surface then being curved upwards in the direction of the current. It, therefore, follows that the lines of maximum gradient of the isosteric surface will be curved towards the left and, consequently, also the current. An isosteric surface is defined as a surface over which the density or the specific volume of water is uniform (PROUDMAN 1952).

When a current near the ocean bottom reaches a deep trough, the water sinks, the isosteric surface curves downwards and the lines of maximum gradient of the isosteric surface, and, consequently, also the current, are curved towards the right (PROUDMAN 1952).

In his study of the Gulf Stream system, ISELIN (1936) demonstrates that in the Labrador Basin the water tends to curve perceptibly eastward, ascribing this to the ridge which partially obstructs the deep channel. He also concludes that at a great depth the current is still apparent and follows various courses, the flow direction of which is not determined by the influence of the wind but apparently by the bottom topography.

Figure 5 was drawn from basic bottom-topography charts plotted by the Trigonometrical Survey Office at Mowbray, Cape Town. To avoid confusion, only the 500 (914 m.), 750 (1,371 m.), 1,000 (1,829 m.) and 1,500 (2,743 m.) fathom contour lines were plotted. A part of the general current directions of the 1,500 db surface relative to the 2,000 db surface are projected on this figure.

Off the east coast of South Africa it is clear that the current moves more or less in the trough between the continent and the Mozambique Terrace towards the Transkei Basin. The current, however, meets the Agulhas Bank which extends south-westward, and is apparently deflected in a south-easterly direction (Figs. 2 and 3). A fairly shallow terrace then forms an obstruction in the path of the current (because great depths are involved) and the current turns away partly in a westerly and partly in an easterly direction.

Since the water of the Agulhas Current flows over the deeper parts of the Agulhas Bank, it is possible that the Agulhas Current is thereby influenced to turn back as described earlier in this report.

The eastward-moving Return Agulhas Current and the West Wind Drift come into sharp contact with a ridge at a depth of 2,743 metres (1,500 fathoms) south of Madagascar. This is evidently the reason why some current lines diverge towards the left and make a complete turn. Certain current lines, however proceed over the ridge and are also curved towards the left, but move on the eastern side of the Madagascar Ridge towards the Reunion Basin.

One of the current lines on the west side of the Madagascar Ridge turns back completely on itself after it has encountered the shallow Walters Shoal, and this indicates that water again moves westwards, then meets the southern tip of the Mozambique Terrace and in this way gradually curves in the direction of the continent (Fig. 5).

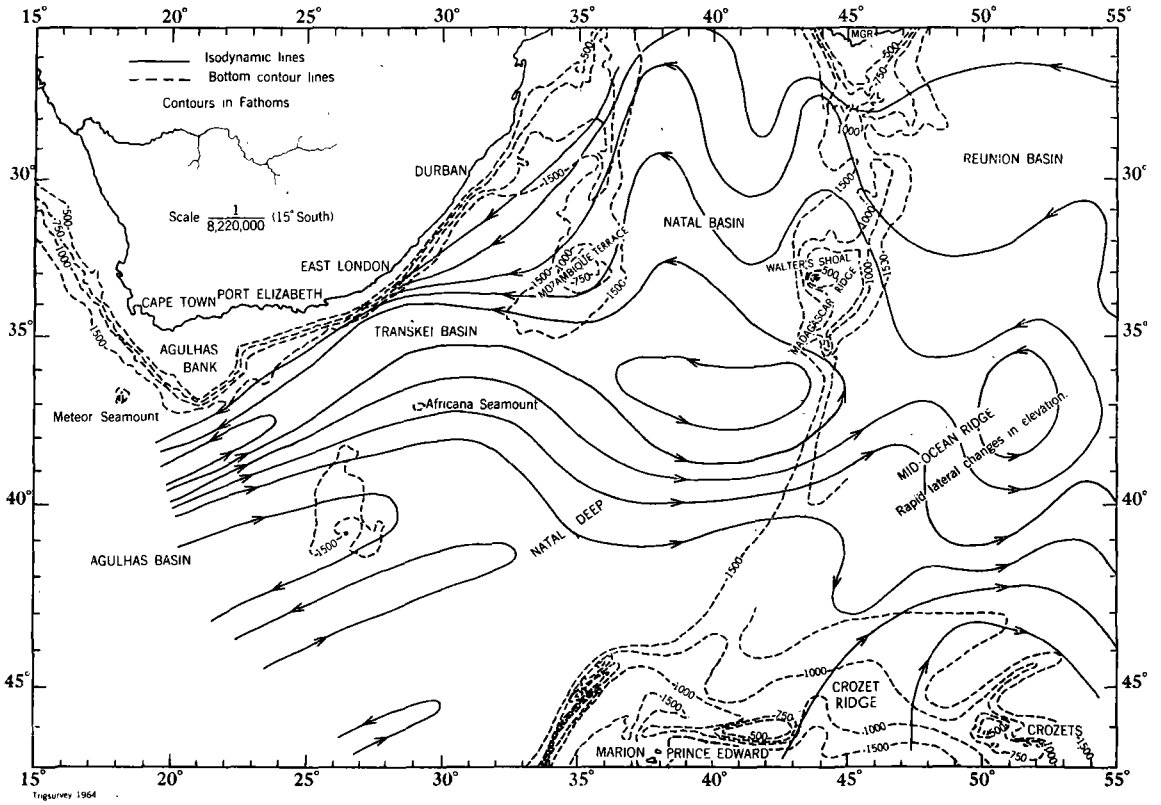

FIG. 5 INFLUENCE OF BOTTOM TOPOGRAPHY ON OCEAN CURRENTS

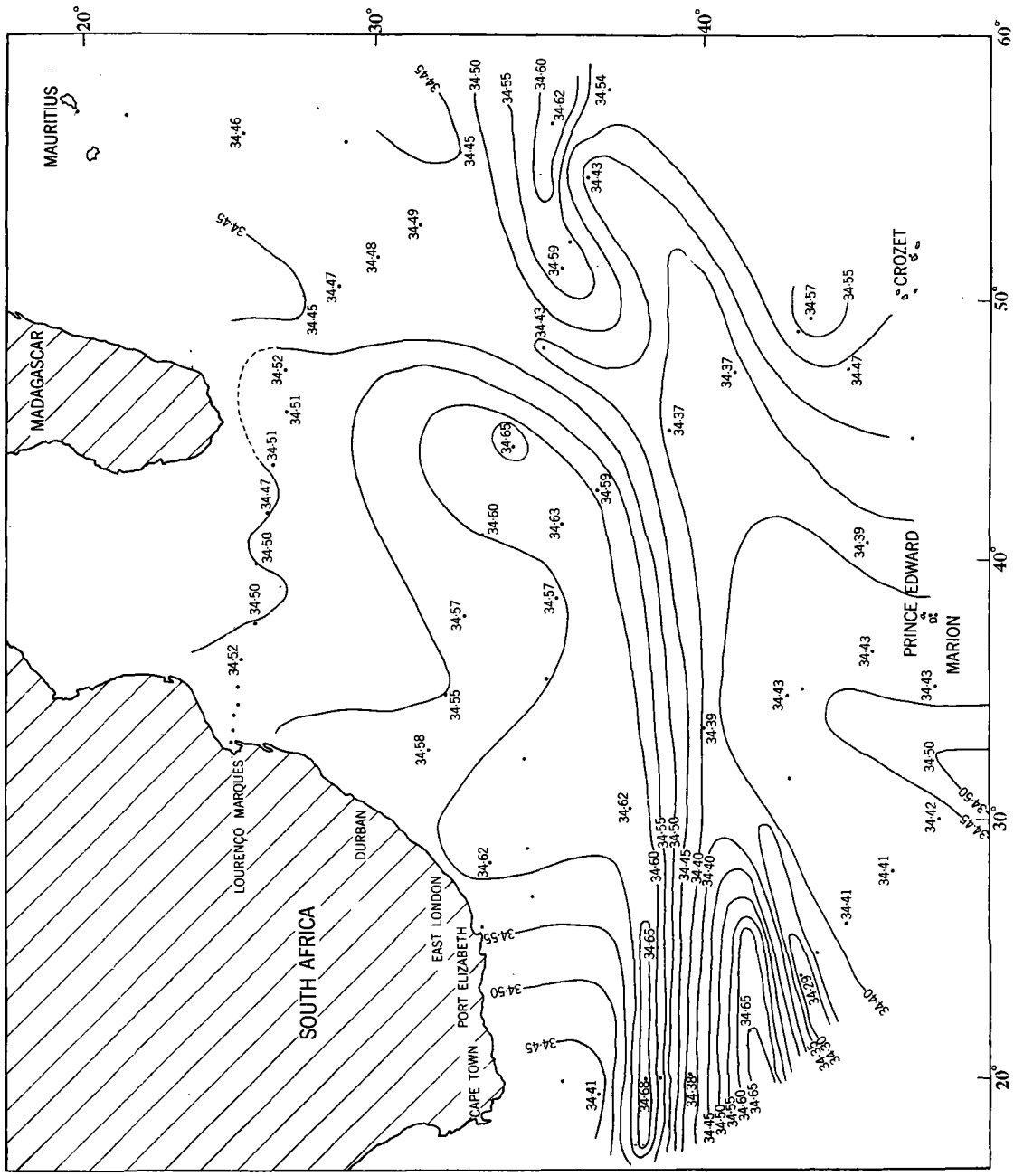

FIG. 6 SALINITY AT 1000 METRES.

6315631—3

The characteristic of currents in the Southern Hemisphere to turn to the left when passing over a ridge also explains further why water moving from the Mozambique Channel around the southern tip of Madagascar should be further deflected towards the left in a south-westerly direction. The water from the Return Agulhas Current and that from the Indian Ocean, which are evidently compressed between the shallow part at the southern tip of Madagascar and Walters' Shoal, apparently help to force this water back still further. Part of the water from the Mozambique Channel apparently moves (according to current lines at the 1,500/2,000 db surface) along the west side of the Madagascar Ridge in a southerly direction and is forced back as a result of the northward-moving Return Agulhas Current and flows back again in a northerly direction.

According to the contours of the Madagascar Ridge, the ocean first becomes deeper in a southerly direction and then shallows to Walters' Shoal. The deepest part is approximately due east of Durban. In this narrow part water from the Indian Ocean converges with Atlantic water and a measure of mixing is likely.

Another topographical feature which has a considerable effect on the ocean currents is the Mozambique Terrace. This shallow area apparently forces the Agulhas Current to move nearer to the continent.

According to Figure 4, it is clear that the bottom topography exercises a considerable influence at 3,000 metres, separating Atlantic Ocean water from Indian Ocean water.

At a depth of 1,000 metres the effect of the bottom topography on the current directions becomes less marked as is definitely evident from the current patterns at this depth (Fig. 2).

Over the whole area there is, therefore, adequate evidence that the bottom topography does, indeed, exercise an important influence over the deeper ocean currents.

4. Influence of Salinity.

4.1. Salinity and Water Masses at 1,000 Metres.—DEACON (1937) gives the following definition of Antarctic Intermediate water:—

> " The path taken by the intermediate current lies below the subsurface current and above the warm deep current and in longitudinal sections through each of the three main oceans it appears as a poorly saline layer between these highly saline waters ".

According to this quotation, it is possible that the Central Water (SVERDRUP *et al.* 1942) and Antartic Intermediate Water may be regarded as one water mass. SVERDRUP, however, furnishes a better understanding of Antarctic Intermediate Water in the following way: " Below the Central Water the Antarctic Intermediate Water shows up by the characteristic salinity minimum . "

According to CLOWES (1950), the salinity of Antarctic Intermediate Water ranges between $34{\cdot}30°/_{oo}$ and $34{\cdot}60°/_{oo}$, the depth of the nucleus varying between 1,000 metres and 1,500 metres in this area. CLOWES also finds that Antarctic Intermediate Water follows the direction of the Agulhas Current and the Return Agulhas Current in that it flows northwards together with the Return Agulhas Current and is then carried back in the southern part of the Mozambique Channel together with the Agulhas Current.

In his investigational report of the first cruise of the R.S. *Africana II* during 1961, ORREN (1963) found that the nucleus of the Antarctic Intermediate Water varied between 850 and 1,300 metres and the salinity between $34{\cdot}40°/_{oo}$ and $34{\cdot}50°/_{oo}$ in the north of the investigation area discussed in this report.

If the distribution of salinity values in general is considered, it appears that such values vary between $\pm\ 34{\cdot}40°/_{oo}$ and $\pm\ 34{\cdot}60°/_{oo}$ (Fig. 6), except in a few cases where they are higher or lower than these two limits. On the strength of these data it may therefore be said that, according to the salinity distribution, the water at a depth of 1,000 metres consists mainly of Antarctic Intermediate Water.

From a comparison of the results obtained during the cruises of the South African ship *Africana II*, and those of the French ship *Commandant Robert Giraud* during 1956, it appears that there is a fairly clear distinction between salinity values between 25° S and 27° S. In order to distinguish between stations worked by the *Commandant Robert Giraud* and R.S. *Africana II*, the stations of the former are indicated by an " F " after the station numbers, as has been mentioned above.

In the Mozambique Channel salinity values [stations 7F–11F and 31F–42F (Fig. 1)] were obtained which were mainly higher than $34{\cdot}70°/_{oo}$ at 1,000 metres. South of 27° S the salinities were for the most part lower than $34{\cdot}60°/_{oo}$. According to salinities it is therefore clear that there is a distinct separation between water in the Mozambique Channel and that in the South-West Indian Ocean (Cahiers Oceanographiques—April, 1963).

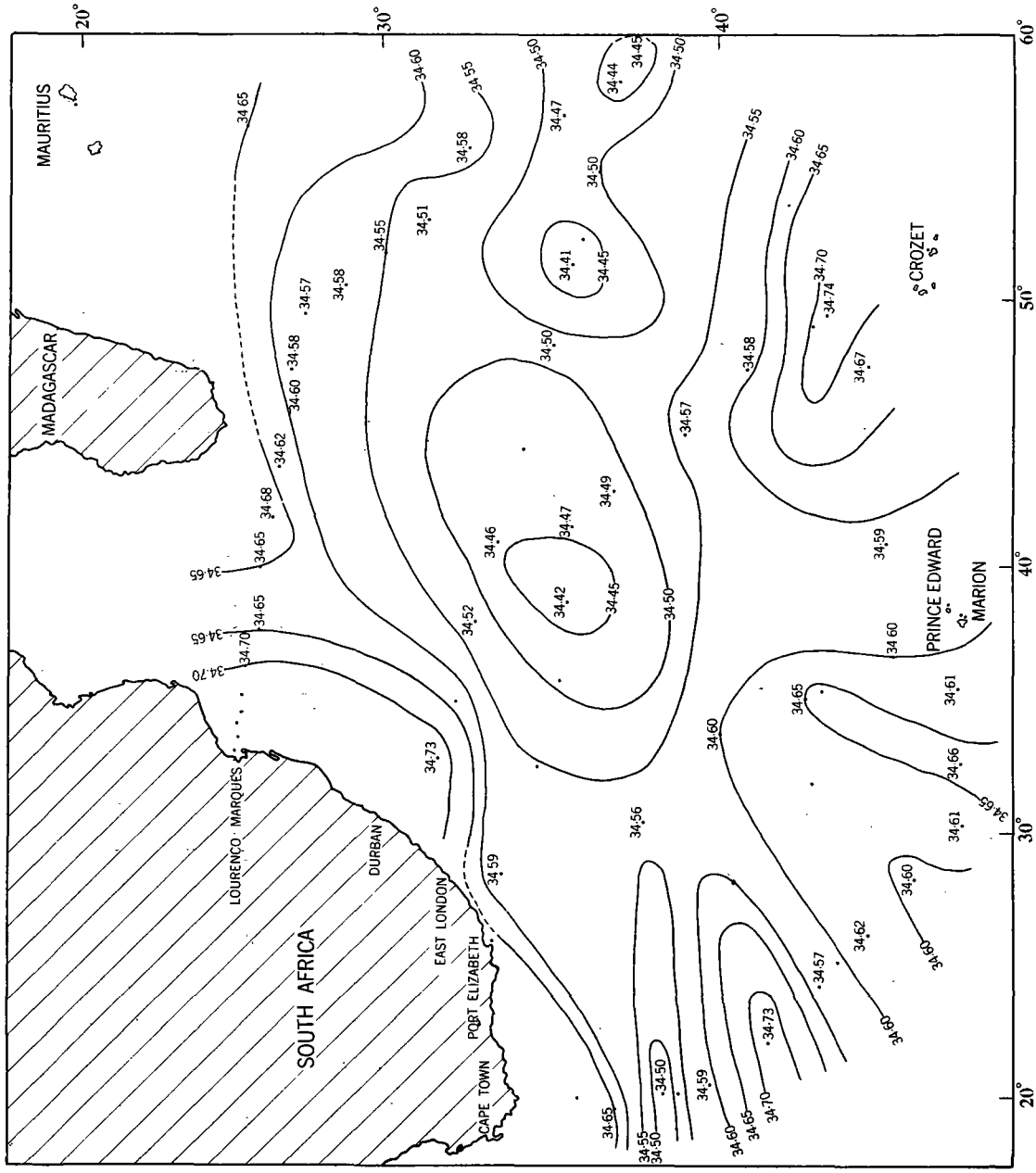

FIG. 7 SALINITY AT 1500 METRES.

At stations 21F and 24F we still find water with a salinity higher than 34·70°/$_{oo}$. A salinity of 34·66°/$_{oo}$ at station 20F is also very close to the above-mentioned salinities. The salinities of stations 42F, 32F and 21F at 1,000 metres compare as follows:—

42F = 34·70°/$_{oo}$;
32F = 34·66°/$_{oo}$;
21F = 34·70°/$_{oo}$.

From these data it appears, therefore, that the possibility exists at station 21F that water in the Mozambique Channel originates from the Indian Ocean moving around the southern tip of Madagascar.

If an imaginary line is drawn through stations 12, 29, 51 and 63, it is clear that, generally speaking, the salinities on the eastern side of this line are lower than those on the western side. Salinities in the Agulhas Current area fall mainly between 34·50°/$_{oo}$ and 34·60°/$_{oo}$ and the values east of the imaginary line mainly between 34·40°/$_{oo}$ and 34·50°/$_{oo}$. The higher salinity on the west side of the line is apparently due to the more intensive mixing of Antarctic Intermediate Water with sub-surface water, this mixing possibly occuring in the rapidly flowing Agulhas Current. The phenomenon may also be ascribed to the Antarctic Intermediate Water which intermingles in the southern part of the Mozambique Channel with water of higher salinity originating from the Indian Ocean, and which is then carried further southwards with the Agulhas Current.

Salinities lower than 34·40°/$_{oo}$ are found at only six stations, namely, 60, 62, 47, 48 41 and 35. The lowest value is found at station 62, namely 34·29°/$_{oo}$, while the salinities at the other four stations were in the region of 34·40°/$_{oo}$. The low salinity at station 62 is apparently due to the sinking of sub-surface water of Sub-antarctic origin, According to the sigma-t surfaces (Figures 12, 15 and 18), the water at station 61 rises and this must necessarily result in the water at station 62 sinking.

At station 22 a salinity of 34·62°/$_{oo}$ was obtained, this being strikingly higher than the surrounding salinities at stations 21 (34·45°/$_{oo}$) and 23 (34·54°/$_{oo}$). This phenomenon is apparently due to the fact that water of Indian Ocean origin penetrates this area. This fact is emphasised by the current lines at the 1,000/2,000 db surface. The temperature is also considerably higher, namely, 8·34° C in contrast with temperatures of 5·82° C and 7·20° C at stations 21 and 23, respectively.

In the rest of the area salinities higher than 34·60°/$_{oo}$ were usually encountered in the vicinity of swirls in the current. Salinities of between ± 34·60°/$_{oo}$ and 34·69°/$_{oo}$ were encountered at stations 28, 29, 34, 50, 54, 58 and 61. It is apparent that here the possibility exists that Antarctic Intermediate Water might intermingle in these swirls with water masses of the sub-surface layer or the layers below 1,000 metres, and in this way be responsible for the higher salinities. ORREN (1963) is of the same opinion. According to the dynamic height anomaly charts (Figures 2 to 4) and sigma-t charts (Figures 12, 15 and 18), this supposition is quite acceptable since swirls are distinctly shown around the above-mentioned stations on these charts.

According to the data obtained and the work of earlier workers, it is, therefore, obvious that, in regard to salinity, the water in the area investigated at the depth of 1,000 metres answers the requirements for identification as Antarctic Intermediate Water.

4.2. Salinity and Water Masses at 1,500 Metres.— Over the major part of the area investigated the salinities at 1,500 metres (Fig. 7) lie between the limits of 34·41°/$_{oo}$ and 34·62°/$_{oo}$. The temperatures at the relevant stations varied between 2·50° C and 4·85° C. No salinity was found lower than 34·41°/$_{oo}$, but at a few stations salinities were obtained which were higher than 34·62°/$_{oo}$, namely, at stations 6–9, 19, 32, 36, 43, 45, 57, 61 and 67. Out of 44 stations there were, consequently, only 12 stations with a salinity higher than 34·62°/$_{oo}$. The salinity was higher than 34·70°/$_{oo}$, only at stations 32, 45 and 61, but it was never higher than 34·74°/$_{oo}$. The salinities and temperatures, therefore, fall mainly within the salinity limits of Antarctic Intermediate Water (see discussion and quotations in section 4.1.).

The high temperature of 4·85° C at station 50 may be due to the deeper penetration of warmer Antarctic Intermediate Water as a result of swirling. The salinity of 34·42°/$_{oo}$ bears out such a possibility. Low temperatures are apparently due to the cold water in the vicinity of the Subtropical Convergence and the area southward thereof.

According to ORREN (1963), North Indian Deep Water extends from 1,600 metres and deeper and lies between Antarctic Intermediate Water and the Atlantic Deep Water. CLOWES (1950) asserts that Warm Deep Water from the Arabian Sea

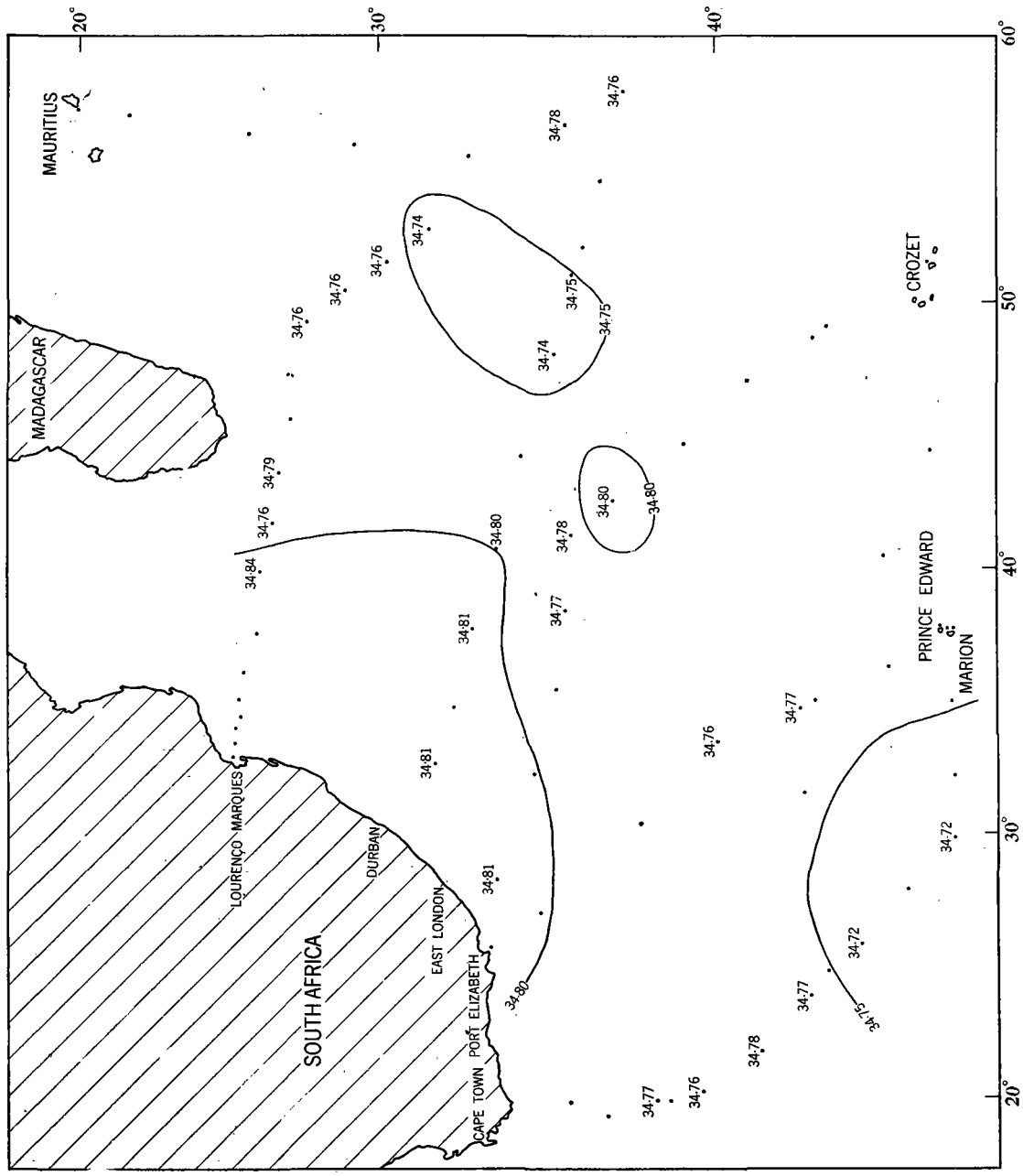

FIG. 8 SALINITY AT 3000 METRES.

certainly moves as far as 20° S and may even continue further as North Indian Deep Water with a salinity lower than 34·80°/₀₀. It may, therefore, be said with reasonable certainty that the high salinities at stations 6 to 9 are due to North Indian Deep Water. The temperatures at these stations are also noticeably higher than at neighbouring stations. The high salinity at station 19 is apparently due to the penetration of water from the Indian Ocean, as appears clearly from the vertical section of salinity in the area (Fig. 35). The high salinity at station 32 may apparently be ascribed to the upwelling of Warm Deep Water which mixes with warmer water as appears from the isobaths at the sigma-t surfaces (Figures 12, 15 and 18). It may also be seen from these charts that around stations 61 and 45 there are intensive cyclonic water movements which result in water here rising from the depths. It is, consequently, very possible that the high salinities at the above-mentioned two stations are due to the upwelling of Atlantic Deep Water. The same argument may be used to explain the high salinities at stations 36, 43 and 67, although the cyclonic water movement is less intensive, this fact also explaining why the salinities are lower than those at stations 61 and 45. The high salinity at station 57 is apparently due to the fact that the Agulhas Current in this region flows over the edge of the Agulhas Bank, curves towards the left and results in the upwelling of deeper water. It may, therefore, be stated with a large measure of certainty that high salinities at 1,500 metres are due to the presence of some Atlantic Deep Water or North Indian Deep Water. From the available data it appears that the dominant water mass is Antarctic Intermediate Water, although it is possible that at this depth the Antarctic Intermediate Water could well have undergone a fair measure of mixing with deeper-lying water masses.

4.3. Salinity and Water Masses at 3,000 Metres.—
A noticeable feature of the salinities for the 3,000 metre depth (Fig. 8) is their slight variation. This fell mainly between 34·71°/₀₀ and 34·80°/₀₀, except in the case of four stations, namely 8, 30, 32 and 54, where the salinity was higher than 34·80°/₀₀. At the last-mentioned three stations the salinity was 34·80°/₀₀ exactly. At station 8 the salinity was 34·84°/₀₀, while that at station 9 was 34·76°/₀₀.

Judging from the oxygen content at 3,000 metres at station 8 (between 4·67 c.c./l. and 4·65 c.c./l.), this high salinity cannot be attributed to pure, oxygen-poor North Indian Deep Water, since water with an oxygen minimum lies much shallower in this region. This water is apparently a mixture of highly saline North Indian Deep Water and oxygen-rich deeper water. The water throughout the rest of the area is chiefly recognisable as Atlantic Deep Water with a salinity maximum of ± 34·80°/₀₀. ORREN (1963) supports this view.

At stations 13–16, 22, 23, 26, 27, 36 and 60–66 there is a very strong possibility that Bottom Water may be present, especially at stations in the northern part of the area. In this report Bottom Water is regarded as water lying deeper than ± 3,000 metres. At these stations the salinity at 3,000 metres is in the vicinity of 34·75°/₀₀, and according to ORREN (1963), this indicates the possibility of Bottom Water. A study of the general T/S relationships (Figures 21 to 34) strengthens this supposition. The curves definitely turn away from the salinity maximum of the Warm Deep Water and for a short distance follow the characteristic curve of Bottom Water.

According to the current lines at the 3,000/2,000 db surface, it is clear that the water moves in opposite directions to that at the higher-lying surfaces. The possibility of the presence of Bottom Water is, therefore, not excluded.

5. Temperature Characteristics.

5.1. Temperature and Water Masses at 1,000 Metres.—
At a depth of 1,000 metres (Fig. 9) temperatures varied from 2·53° C at station 45 to 8·70° C at station 58. Temperatures higher than 8·0° C were encountered only at stations 22, 50 and 58. The high temperature at station 22 may be due to the penetration of water eastwards from the Indian Ocean into this region. The current lines plotted according to dynamic calculations support this supposition (Figures 2 to 4). The water mass with this high temperature is probably Indian Ocean Central Water, since isobaths at the sigma-t surfaces around station 22 and neighbouring stations indicate a well-marked anticyclonic swirl which would result in the sinking of water.

According to current lines around stations 50 and 58, there are also distinct anticyclonic swirls around these stations. Temperatures higher than 8·0° C are, therefore, apparently due to the sinking of Indian Ocean Central Water. This supposition is supported by the characteristics of the isobaths (Figures 12, 15 and 18) which definitely demonstrate that water around these stations sinks. According to SVERDRUP *et al.* (1942), the temperature limits of Indian Ocean Central Water are

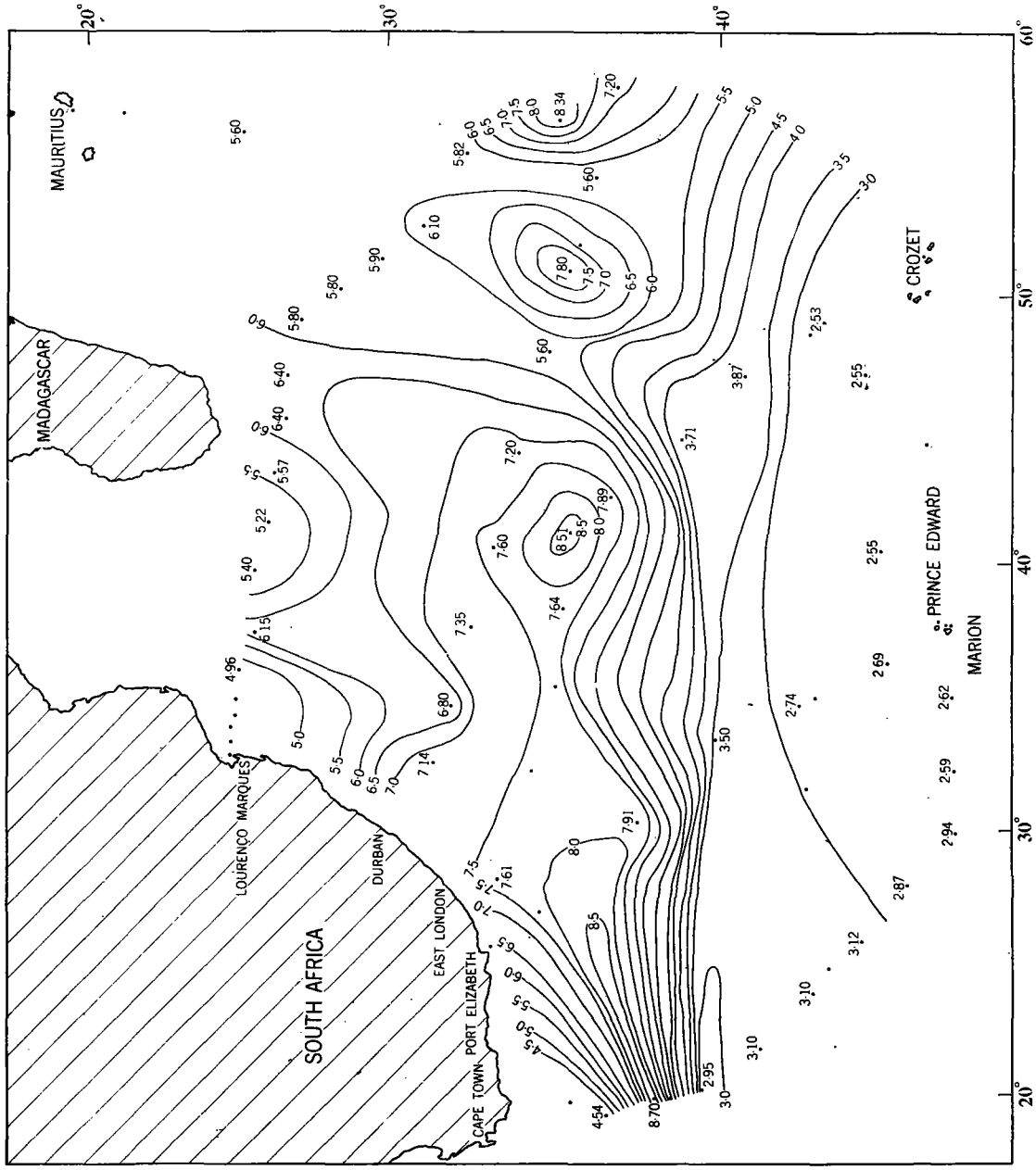

FIG. 9 TEMPERATURE AT 1000 METRES.

8° C and 15° C. Salinities of 34·62°/$_{oo}$ at station 22, 34·63°/$_{oo}$ at station 50 and 34·68°/$_{oo}$ at station 58 indicate that it is possible that at 1,000 metres the last traces of Indian Ocean Central Water might be present at these stations.

Temperatures ranging between 7·14° C and 7·96° C were encountered at stations 23, 26, 28–30, 32, 34, 49 and 51–54. These temperatures are a little high for "pure" Antarctic Intermediate Water and may be ascribed to the mixing of the above-mentioned water mass with Central Water.

Temperatures falling between 6·10° and 6·80° C were encountered only at isolated stations, namely, stations 7, 11, 12, 16 and 31. A feature was the constant temperature of 6·40° C at stations 11 and 12. The fact that the temperature was higher at stations 11 and 12 than at stations 10 and 13 further supports the supposition that water flows from the Indian Ocean around the southern tip of Madagascar. The higher temperature may also be due to water flowing northwards from stations 28 and 29 because the water temperatures at these two stations are considerably higher than at the more northerly stations.

Temperatures between 5·20° C and 5·90° C were encountered at stations 8–10, 13–15, 19–21, 24 and 27. These temperatures obviously fall between the limits of 3° C–7° C set by SVERDRUP *et al.* (1942) for Antarctic Intermediate Water. ORREN (1963) considers that the nucleus of Antarctic Intermediate Water falls between 4° C and 5° C in the vicinity of the above-mentioned stations. At these stations salinities at 1,000 metres, however, all fall between 34·40°/$_{oo}$ and 34·50°/$_{oo}$, these limits being set by the last-mentioned writer for the nucleus of Antarctic Intermediate Water in the northern part of the area investigated. We are, consequently, of the opinion that the higher temperature is due to the mixing of Antarctic Intermediate Water with shallower, warmer water masses.

A feature of the temperatures encountered in the vicinity of the West Wind Drift at stations 35, 47–48 and 61–64, is that they all fell between 3·10° C and 3·80° C. As appears from Figure 6, the salinities at these stations are very low, except in the case of station 61. According to salinity and temperature, the water at stations 62–64, 35 and 47–48 is therefore Antarctic Intermediate Water.

Temperatures between 2·53° C and 2·95° C were encountered only at the most southerly stations, namely stations 36–45, 60 and 65–68. These low temperatures are apparently due to the cold water of the Sub-antarctic region since all these stations, except station 60, lie south of the Subtropical Convergence.

It may, therefore, be stated with a large measure of certainty that, as regards temperature, most of the water at the 1,000 metre depth, is Antarctic Intermediate Water, or the product of intermingling between this water mass and Indian Ocean Central Water.

5.2. Temperature and Water Masses at 1,500 Metres.—

The temperatures of water at the 1,500 metres depth (Fig. 10) show a much smaller variation than those at 1,000 metres. In general temperatures north of stations 56, 34 and 48 are higher than 3·0° C and south of these stations lower than 3·0° C, with a few exceptions. Temparatures ranging between 4·15° C and 4·85° C were found at only three stations, namely, stations 50, 54 and 58. According to the current lines at 1,500 metres (Fig. 3), stations 50 and 58 lie in the vicinity of swirls, this fact explaining how it is possible that the mixing of cold water at 1,500 metres with warmer, shallower water could occur and in this way result in increased temperatures.

According to current lines, it is found that the Agulhas Current in the region of station 54 is deflected in a southerly direction. Consequently, mixing is also not excluded in this case.

The low temperature of 2·87° C at station 11 is apparently due to the rising of cold water since the current here flows over the Madagascar Ridge. Temperatures between 3·0° C and 3·85° C at 1,500 metres clearly still fall within the accepted limits for Antarctic Intermediate Water, namely 3 °C to 7° C.

Temperatures between 2·36° C and 2·92° C are encountered mainly in the vicinity of the Subtropical Convergence. In regard to salinity, however, this water still answers to the requirements for Antarctic Intermediate Water. The low temperature may probably be ascribed to the fact that the water here is apparently of Sub-antarctic origin since Antarctic Intermediate Water mixes with cold Sub-antarctic surface and sub-surface water at the Subtropical Convergence.

5.3. Temperature and Water Masses at 3,000 Metres.—

Temperatures at the 3,000 metre depth (Fig. 11) fell between 1·50° C and 2·50° C. An outstanding feature of water at the above-mentioned depth is that temperatures east of the Madagascar Ridge were lower than temperatures west of it, except in

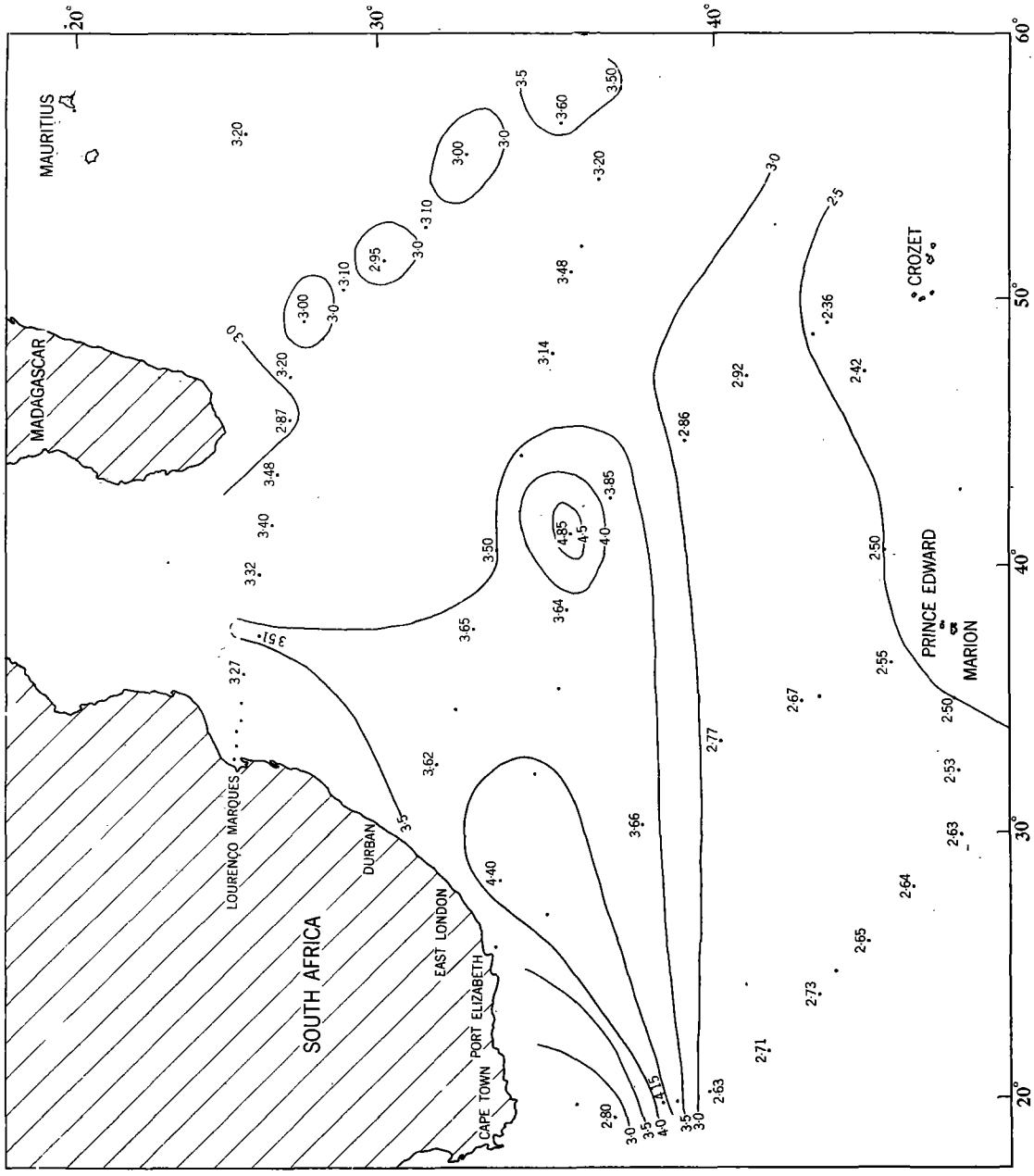

FIG. 10 TEMPERATURE AT 1500 METRES.

the case of stations 36, 61 and 66. This phenomenon is substantiated by the distinct separation caused by the Madagascar Ridge in the deeper water. Throughout the larger part of the area the temperature falls between 2·0° C and 2·44° C. This water is immediately recognisable (especially according to salinity distribution) as Atlantic Deep Water (ORREN 1963 and CLOWES 1950).

The oxygen content at stations 13–16 was conspicuously lower than in the rest of the area and the salinity was more or less constant, namely ± 34·75°/$_{oo}$. It is possible, therefore, according to temperature and salinity, that Bottom Water is present at these stations. If, however, the oxygen content of the water is taken into account, it appears that it is possible that North Indian Deep Water has mixed with Atlantic Deep Water, this mixing being responsible for the low oxygen content.

6. Depth, Salinity and Temperature at the σt = 27·20, 27·40 and 27·60 Surfaces.

According to SVERDRUP *et al.* (1942), the distribution of the sigma-t surface will give a good picture of water transportation. Isohalines and isotherms will therefore be parallel to isobaths at a particular sigma-t level and will indicate the direction in which a current flows.

(a) The sigma-t = 27·20 surface.—

The depth, salinity and temperature of the σt = 27·20 surface are shown in Figures 12 to 14. Isobaths for ever 50 metres, isohalines for every 0·05°/$_{oo}$ and isotherms for every 0·5° C have been plotted.

According to Figure 12, the depth of the σt = 27·20 surface varies between 315 metres at station 45 and 1,305 metres at station 50. On the northern side of the Sub-tropical Convergence the sigma-t surface lies for the most part at a depth of very close to 1,000 metres, and the isobaths will consequently give a good picture of ocean currents at 1,000 metres. An intense crowding of isobaths was obtained between stations 56 and 58, to the north of the Sub-tropical Convergence and around station 61.

Anticyclonic swirls are clearly perceptible at stations 22, 50, 58 and 66. Cyclonic swirls are encountered at stations 9 and 61. A feature of these swirls is that the relevant sigma-t surface descends to a deeper level at anticyclonic swirls and rises in a cyclonic swirl. The sigma-t surface rises perceptibly between stations 54, 56 and 57 where the water meets the Agulhas Bank. According to bottom topography influences, this will result in the current being deflected towards the left. This deflection will, therefore, be a further contributory factor in causing the Agulhas Current to turn back on itself. The swirl around station 58 is shown definitely not only by the isobaths but also by the course of isohalines and isotherms. The swirls indicated by the isobaths correspond closely to those demonstrated by the isodynamic lines (Fig. 2). The distribution of isobaths over the relevant sigma-t surface distinctly shows the tendency of water to sink at the Subtropical Convergence.

Salinities at the σt = 27·20 surface (Fig. 13) vary between 34·14°/$_{oo}$ at station 42 and 34·61°/$_{oo}$ at station 61. For the most part salinities north of the Subtropical Convergence are higher than those south of it. The high salinity of 34·61°/$_{oo}$ at station 61 is apparently due to the fact that the sigma-t surface here lies near to the surface at a depth where sub-surface water is present. This water has a higher salinity than the deeper water at ± 1,000 metres.

An intensive crowding of isohalines around stations 58–60 clearly indicates that there is a marked swirl in this area. The isohalines follow more or less the course of computed ocean currents on this surface.

The temperature of the relevant sigma-t surface (Fig. 14) varies between 3·00° C at station 45 and 6·83° C at station 18. It is quite noticeable that the temperatures in the Agulhas Current area are much higher than in the rest of the area. Temperatures south of the Subtropical Convergence are conspicuously lower than temperatures further north. Here, too, the isotherms follow more or less the course of the ocean currents.

From the above data it can readily be seen that the sigma-t surface north of the Subtropical Convergence corresponds well with the isodynamic lines at the 1,000/2,000 db surface. The 1,050 metres isobath south of Madagascar shows the northward trend of the Return Agulhas current.

(b) The sigma-t = 27·40 surface.—

The pattern of isobaths, isohalines and isotherms at the σt = 27·40 surface is shown in Figures 15 to 17. The spacing of the above values is exactly the same as in the case of the σt = 27·20 surface.

According to Figure 15, the depth of the relevant sigma-t surface varies between 520 metres at station 61 and 1,600 metres at station 50. Noticeable anticyclonic swirls are perceptible around stations 26, 50 and 58 and cyclonic swirls around stations 9 and 61. At this surface it is again

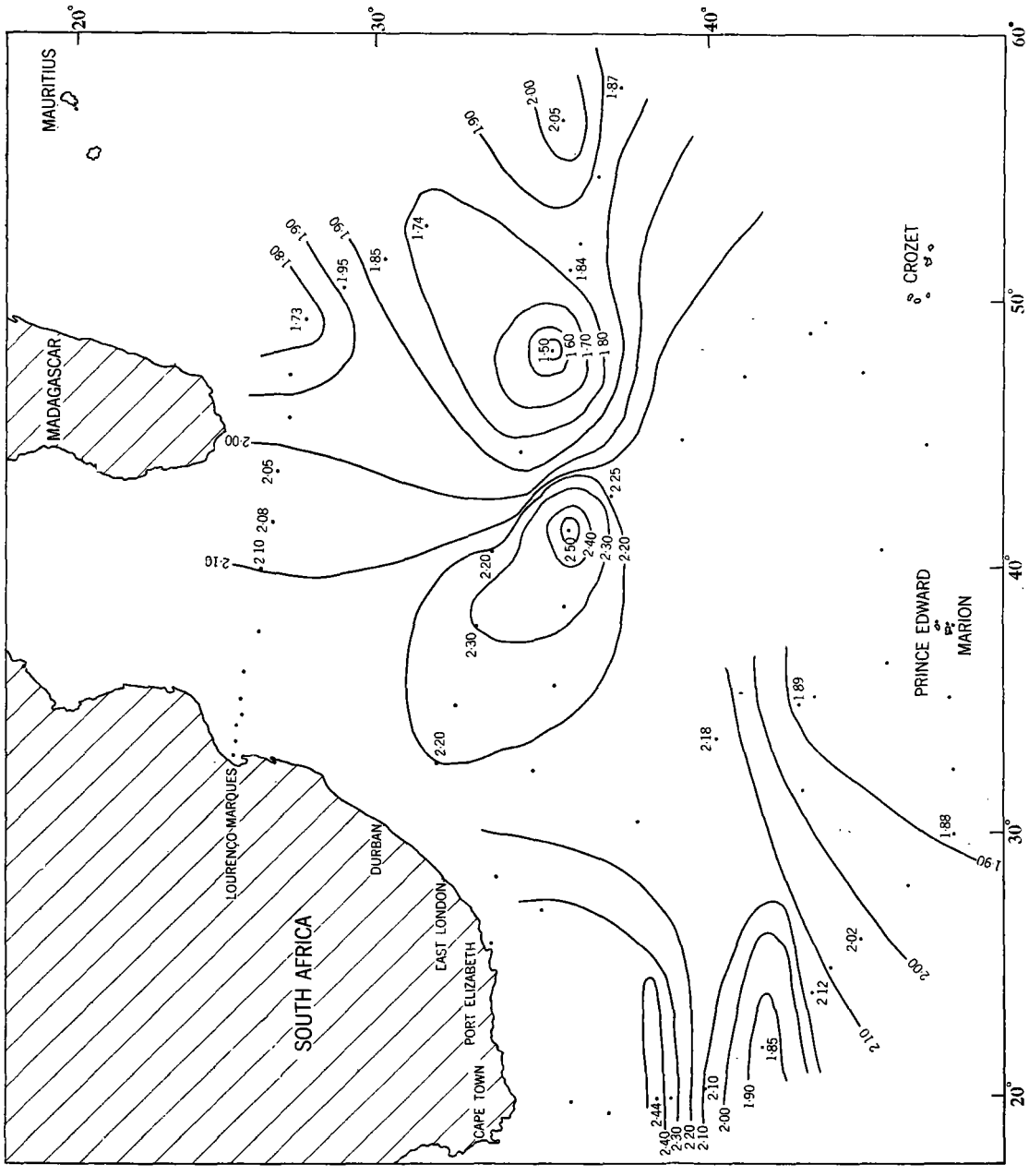

FIG. 11 TEMPERATURE AT 3000 METRES.

apparent that water of a certain density rises in cyclonic swirls and sinks in anticyclonic swirls. The intensive crowding of isobaths around stations 58 and 51 definitely indicates the presence of swirls. In the area of the Subtropical Convergence the isobaths are also very close together and show that the sigma-t surface sinks rapidly over a fairly short distance. This phenomenon is especially noticeable between stations 58 and 60 and between stations 45 and 47. The isobaths between stations 32 and 54 apparently run very close together between the coastline and station 54 and join the isobaths south of Port Elizabeth. In this case, too, the course of the isobaths shows the rising trend of the sigma-t surfaces at the Agulhas Bank. North of the Subtropical Convergence the course of the isobaths gives a fairly good picture of currents between ± 1,000 metres and ± 1,500 metres.

Salinities at the $\sigma t = 27{\cdot}40$ surface (Fig. 16) vary between $34{\cdot}32°/_{oo}$ at stations 41, 43 and 45 and $34{\cdot}64°/_{oo}$ at station 32. The highest salinities were encountered mainly in the Agulhas Current area and the lowest south of the Subtropical Convergence. A well-marked swirl of water is perceptible between stations 58 and 61 according to the isohalines. The closed isohaline around stations 49 and 50 gives an indication of the swirl around these stations which was obtained by means of dynamic calculations. The isohalines follow more or less the course of the dynamic topographic lines at the 1,000 db and 1,500 db surfaces, especially the $34{\cdot}50°/_{oo}$ and $34{\cdot}45°/_{oo}$ isohalines between stations 61 and 62. This isohaline pattern gives an indication that the isobaths over the Madagascar Ridge reflect a fairly reliable picture of actual water movements.

Temperatures at the $\sigma t = 27{\cdot}40$ surface (Fig. 17) range from 2·55° C at station 45 to 5·0° C at station 32. As above, temperatures south of the Subtropical Convergence are much lower than temperatures in the northern part of the area.

Just as was the case with the $\sigma t = 27{\cdot}20$ surface, the highest temperature is encountered in the Agulhas Current area off the east coast of South Africa. In general the isotherms follow the same direction as the isohalines and give a sure indication that water from the Subtropical Convergence moves northwards. The course of the 4·0°C and 3·5° C isotherms between stations 61 and 62 further substantiates the course of the $34{\cdot}50°/_{oo}$ and $34{\cdot}45°/_{oo}$ siohalines, as explained in the above paragraphs. It also further shows the tendency of water to flow from the Subtropical Convergence in a north-easterly direction over the Madagascar Ridge.

(c) The sigma-t = 27·60 surface.—

The pattern of isobaths, isohalines and isotherms at the $\sigma t = 27{\cdot}60$ surface is presented in Figures 18 to 20. The spacing of the above-mentioned values are identical to the $\sigma t = 27{\cdot}20$ and $\sigma t = 27{\cdot}40$ surfaces.

According to Figure 18, the depth of the $\sigma t = 27{\cdot}60$ surface varies between 953 metres at station 61 and 2,000 metres at station 50. This distribution of isobaths gives a good picture of the ocean currents and directions of flow between ± 1,500 and ± 2,000 metres. The intensive crowding of isobaths between stations 54 and 32, 57 and 60 and 45 and 47 indicates sinking of water over a relatively short distance. Around station 61 there is a perceptible upward motion of water. Other very clear features are the vertical movement of water over the edge of the Agulhas Bank and the deflection of the Agulhas Current in a southerly direction.

Anticyclonic swirls are perceptible around stations 9, 11, 26, 50 and 58, with the result that water with the same sigma-t value is found much deeper here than at neighbouring stations. Cyclonic swirls of water may be seen around stations 36, 45 and 61. At these stations water with a sigma-t value of 27·60 moves closer to the surface.

The closely spaced isobaths between station 54 and the coastline indicate that water from the Agulhas Current strikes the coast from a north-easterly direction and is then deflected towards the south between Port Elizabeth and East London. The distribution of isobaths apparently also gives a good indication of the deflection of water towards the left when passing over a ridge, and this effect is especially noticeable over the Madagascar Ridge.

Another noticeable feature is the tendency to sink manifested by water at the Subtropical Convergence even at the depths indicated in Figure 18. Between stations 45 and 47, for example, the $\sigma t = 27{\cdot}60$ surface sinks from 960 metres at station 45 to 1,630 metres at station 47.

In general the course of isobaths agrees closely with the current directions indicated by the dynamic topographic lines at the 1,500 db surface, except between the northern stations south of Madagascar. From a consideration of the isohalines and isotherms, the course of the isodynamic lines appears to be more correct.

The salinity at the $\sigma t = 27{\cdot}60$ surface (Fig. 19) varies between $34{\cdot}52°/_{oo}$ at station 36 and $34{\cdot}75°/_{oo}$ at station 50. A small number of isohalines could be plotted here to indicate that the

salinity is fairly constant throughout this sigma-t surface. The isohaline of 34·60°/$_{oo}$ gives a good impression of the distribution of salinity over this surface. West of the above-mentioned isohaline the salinity lies mainly between 34·60°/$_{oo}$ and 34·70°/$_{oo}$ and east of it between 34·50°/$_{oo}$ and 34·60°/$_{oo}$. These few isohalines give a further indication of the tendency of water of Atlantic origin to move in a north-easterly direction and thence to bring about a large anticyclonic movement in the South-West Indian Ocean.

Only a few isotherms could be plotted on the σt = 27·60 surface (Fig. 20), showing that the temperature on this surface is fairly constant, varying from 2·47° C at station 43 to 3·62° C at station 32. The course of the 3·0° C isotherm gives an indication of the temperature variation over the relevant sigma-t surface in this area.

In conclusion, it further appears that all three sigma-t surfaces have an upward trend around station 32 and this is probably the reason for the high temperatures and salinities experienced here.

7. Mean Temperature/Salinity Relationships.

Only mean T/S curves have been charted in this investigational report (Figures 21 to 34). In order to obtain them, all the curves for individual stations were drawn and from these curves the corresponding mean T/S curves were grouped. Approximate depths were also indicated on each general curve. Where depths of individual stations on the same curve differed greatly, approximate station depths are indicated separately.

All the mean curves have been charted in Figure 34. In this case only parts of the curves have been reproduced since only those at 1,000 metres and deeper are applicable to this report.

Sections of the curves giving a more or less linear T/S relationship are classified by SVERDRUP *et al.* (1942) as Central Water. The curved part with a distinct salinity minimum very obviously represents Antarctic Intermediate Water.

According to the general T/S curves, the 1,000 metre temperatures and salinities of only stations 22, 23, 26 and 58 lie clearly on the linear parts of the curves. This probably demonstrates the presence of Central Water. Station 58 lies more or less in the centre of an intensive anticyclonic swirl between the Agulhas Current and Return Agulhas Current, and at this station there is apparently a sinking of Central Water which is encountered even at depths of 1,000 metres. It may, therefore, be accepted with a large measure of certainty that the high temperatures and salinities at the stations are brought about by Central Water.

With the exception of the above, the T/S curves at 1,000 metres depth have values between the limits of ± 4·5° C, ± 34·40°/$_{oo}$ and ± 8° C ± 34·60°/$_{oo}$ north of the Subtropical Convergence. South of the Convergence these limits are ± 2·5° C, ± 34·50°/$_{oo}$ and ± 4° C, ± 34·30°/$_{oo}$. At stations in the last-mentioned area there is occasional indication that the temperatures and salinities of water at 1,000 metres lie on that part of the curve which indicates Warm Deep Water with a maximum salinity. The last-mentioned parts of the T/S curves lie in an almost horizontal direction with little variation in temperature but with a tendency towards a salinity maximum. This tendency is particularly noticeable at stations 38–45 and 60–68. The water at the 1,000 metre depth at these stations is, therefore, apparently already Warm Deep Water of Atlantic origin.

In general the mean T/S curves show a tendency to move from a maximum towards a minimum salinity and then again towards a maximum salinity. At stations 38–45 and 67–68 (Fig. 30) however, there is a noticeable tendency for the salinity to move from a minimum at the surface to a maximum at ± 1,500 metres and deeper. The variation in temperature is generally small in comparison with that at stations north of the Subtropical Convergence. The curves of stations 38–45 and 67–68 confirm the opinion that water with a minimum salinity in the Sub-antarctic region sinks at the Subtropical Convergence (from ± 200 metres to ± 1,000 metres) and then, as Antarctic Intermediate Water, forms an anticyclonic circulation in the South-West Indian Ocean.

At a depth of 1,500 metres temperatures varied between ± 2.40°C and ± 4.30°C and salinities between ±34·45°/$_{oo}$ and ± 34·70°/$_{oo}$ according to the T/S curves. At 1,500 metre depths the curves clearly show the presence of Warm Deep Water of Atlantic and Indian Ocean origin. In the northern part of the area this section of the curve is not as distinctly separated from the part indicating Antarctic Intermediate Water as in the southern part of the area, and at station 58 (Fig. 31) the 1,500 metre water layer is still mainly Antarctic Intermediate Water. As has already been mentioned, water sinks at this station in an eddy and Antarctic Intermediate Water, therefore, lies at greater depths here.

Most of the mean T/S curves show the presence of Bottom Water at 3,000 metres. The evidence for the presence of this water, however, is slight and

Bottom Water can be identified with certainty at only a few stations. It is definitely present at stations 13–16 (Fig. 24) and 60–66 (Fig. 32) and at these stations temperatures were generally ± 2·0° C or less and the salinity ± 34·75°/$_{oo}$. According to the bottom topography chart (Fig. 5), these stations lie in areas where the ocean is very deep, and the presence of Bottom Water is, therefore, likely.

According to the composite chart of mean T/S relationships (Fig. 34), it is apparent from the location of the curves that water at stations south of the Subtropical Convergence differs considerably (especially sub-surface water) from water at stations north of the Convergence. The curves of the northern stations show a close relationship and are well defined.

From the above discussion it appears that at depths of 1,000 metres to 3,000 metres the principal water masses encountered, according to the T/S relationships, were Antarctic Intermediate Water, Warm Deep Water and Bottom Water.

8. Southward Protrusions and the Current South of Madagascar.

According to the current pattern at the 0/1,000 db surface obtained during a cruise of the French research ship *Commandant Robert Giraud* during October–November, 1957 (Fig. 36), the Mozambique Current moves along the east coast of Africa and turns back completely at ± 25° S, moving northwards off the coast of Madagascar. Where this current comes into contact with the east-west current south of Madagascar, there is a tendency for the latter current to penetrate far to the south. These observations are similar to the anticyclonic and cyclonic disturbances in the current pattern perceptible at the line between Lourenco Marques and the southern tip of Madagascar (Figures 2 to 4).

A noteworthy feature is the good agreement obtained between deep currents and surface currents (compare Figures 2, 3 and 36). Although the observations of R.S. *Africana II* and *Commandant Robert Giraud* were made during different seasons, they nevertheless, show a close correspondence.

If the current directions according to the sigma-t surfaces (especially $\sigma t = 27{\cdot}60$ and $\sigma t = 27{\cdot}20$, Figures 12 and 18) are compared with current directions obtained with the aid of dynamic calculations in this area, it is clear that water in the southern part of the Mozambique Channel moves southwards near Madagascar, causing large protrusions. Such a comparison also definitely shows that water moving from a north-easterly direction between stations 11 and 13, moves southwards between stations 9 and 11.

According to a vertical section of salinity made by MÉNACHÉ from Lourenco Marques to Port Dauphin (*Cahiers Océanographiques*, April, 1963), the water in this area, as indicated by the tongued structure of isohalines, tends to move westward towards the coast of Africa even at fairly great depths. Such characteristics of the current south of Madagascar further confirm the supposition that water from the Indian Ocean flows round the southern tip of Madagascar in a westerly direction at depths greater than 1,000 metres.

Charts drawn by PAECH (1926) indicate that only during July is there a slight tendency for the currents south of Madagascar to flow, even at the surface, in a north-esaterly direction. According to the directions shown, this phenomenon is not, however, observable in the deep water during this period of the year (Figures 2 to 4).

9. Movement of Atlantic Water in the South-West Indian Ocean.

A vertical section of salinity was drawn between stations 62, 35, 49, 27, 16 and 19 (Fig. 35), and an interesting pattern was obtained.

Between stations 62 and 35 it is clear that water coming from a southerly direction with a salinity of ± 34·30°/$_{oo}$ to 34·70°/$_{oo}$ sinks from the surface and sub-surface to depths of between ± 800 metres and ± 1,350 metres. Between stations 35 and 49 there is marked sinking of water from the surface to ± 800 metres as clearly shown by the isohalines 34·80°/$_{oo}$ to 35·50°/$_{oo}$. According to the course of these isohalines, water which sank between stations 62 and 35, moves in a north-easterly direction as indicated by the tongued structure of the 34·30°/$_{oo}$ and 34·40°/$_{oo}$ isohalines. This water then apparently rises at station 19 where it meets water from the Indian Ocean moving in a south-westerly direction between stations 16 and 19. The water with a salinity of 34·30°/$_{oo}$ is apparently of Atlantic origin as demonstrated by the course of the isohalines. It may further be deduced from the course of the isohalines that Antarctic Intermediate Water constitutes the major part of the water south of the Subtropical Convergence, and is not only perceptible in sub-surface water but even extends to fairly great depths.

The sinking of Atlantic water is completely understandable since the Subtropical Convergence is crossed between stations 62 and 35. During the 1963 cruise of R.S. *Africana II* the Subtropical Convergence was encountered between stations 61 and 62 and again north-west of station 70.

At stations 49, 27, 16 and 19 it is clear that at depths shallower than ± 800 metres there is a sub-surface layer of water which apparently moves north-eastward and sinks to depths greater than ± 800 metres between stations 35 and 49. The salinity of this water ranges between ± 34·80°/$_{oo}$ and ± 35·50°/$_{oo}$. The currents between the surface and ± 800 metres, therefore, evidently move in the same direction as the currents at a depth of ± 1,000 metres and deeper. The water masses very obviously originate from two different oceans, namely, the Atlantic Ocean and the Indian Ocean, and according to the dynamic current pattern it is very likely that Atlantic water flows into the South-West Indian Ocean since the trend of the isohalines distinctly indicates the same tenddency as the current lines.

From a depth of ± 1,200 metres the course of the isohalines of 34·50°/$_{oo}$, 34·60°/$_{oo}$ and 34·70°/$_{oo}$ is fairly uniform. At station 19 the first mentioned two isohalines show an upward tendency which might be due to the penetration here of water from the Indian Ocean since station 19 is situated in the deep Reunion Basin. The current lines in Figures 2 and 4 further support this supposition.

If the general T/S curves of stations 16 and 19 (Figures 24 and 25) are compared with those of surrounding stations, it appears that Antarctic Intermediate Water lies much shallower at station 19 than at station 16. At depths greater than 1,000 metres, the T/S curve of station 19 shows a completely different tendency to that at station 16, and the two deep water masses which come into contact here are consequently of different origin.

According to LE PICHON (1960), the circulation of deep water below 2,000 metres in the South-West Indian Ocean is determined chiefly by the influx of Atlantic Deep Water into this area. As appears from charts published by the above-mentioned writer, there is a definite northwards movement of Atlantic water in the Natal Deep and the Natal Basin on the western side of the Madagascar Ridge. The Madagascar Ridge apparently forms an obstruction in the path of the Atlantic deep water, as shown by the current lines at the 3,000 db surface.

According to DE DECKER and MOMBECK (1964), certain species of plankton were for the most part only encountered in fairly high concentrations at ± 1,000 metres and deeper in the vicinity of stations 16 and 27. For example, *Calanus tonsus* was encountered at a depth of ± 1,000 metres in high concentration at station 27. This species of plankton is indigenous to the area ± 100 miles south of Cape Point and even further south. A second example is *Calanoides carinatus* which is found in medium to fairly high concentration at a depth of ±1,000 metres in the vicinity of station 27. This species is found in high concentrations off the west coast of South Africa where upwelling of cold water occurs in the important fishing area.

DE DECKER and MOMBECK (1964) state further that: " The frequent occurrence in our deep catches of such species as *Calanus tonsus*, *Calanoides carinatus*, *Ctenocalanus vanus*, *Metridia lucens* as well as many others considered to be representatives of the Atlantic and Subantarctic plankton, suggests a considerable influx of southern and western origin into this part of the Indian Ocean. The four species just mentioned are among those that had not been found elsewhere in the Indian Ocean. With the exception of *C. tonsus* they are at times very common along the western and southwestern coasts of South Africa, where they reach the surface with the upwelling water masses (Benguela Current System). *C. tonsus* can be found in great numbers in the upper layers some 100 miles south of the Cape of Good Hope ".

That these species of plankton which are indigenous to the Atlantic water, occur at great depths in the Indian Ocean, is further evidence of the movement of Atlantic water in the deeper layers of the South-West Indian Ocean.

10. Acknowledgements.

The authors would like to take this opportunity of thanking the Director of Sea Fisheries for his guidance and interest in this investigational report.

We would also like to express our appreciation to Messrs. M. J. Orren and S. A. Mostert of the Division of Sea Fisheries for their valuable assistance regarding the interpretation of data and the editing of the report.

We would also like to thank Mr. G. H. Stander of the Administration of South West Africa for his assistance and advice.

11. References

ARX, W. S. VON, 1962.—*Introduction to Physical Oceanography*, 422 pp. Addison-Wesley Publishing Company, Inc., Massachusetts.

CLOWES, A. J., 1950.—An introduction to the hydrology of South African waters. *Invest. Rep. Fish. and Mar. Biol. Survey Div. S. Afr.*, 12: 42 pp. Pretoria.

DARBYSHIRE, M., 1963.—Computed surface currents off the Cape of Good Hope. *Deep-Sea Res.*, 10: 623–632.

DEACON, G. E. R., 1937.—The Hydrology of the Southern Ocean. *Discovery Rep.*, 15: 1–123. Cambridge.

DE DECKER, A., AND F. MOMBECK, 1964.—South African contribution to the International Indian Ocean Expedition. *Invest. Rep. Div. Sea Fish. S. Afr.*, 51: 49 pp. Pretoria.

DIETRICH, G., 1935.—Aufbau und Dynamik des Südlichen Agulhas—stromgebietes. *Veröff Inst. Meeresk. Univ. Berlin*, 27: 79 pp. Berlin.

ISELIN, C. O'D., 1936.—A study of the circulation of the Western North Atlantic. *Pap. phys. Oceanogr.*, 4 (4): 101 pp. Cambridge.

LAFOND, E. C., 1951.—Processing Oceanographic Data. *H.O. Pub.*, 614: 114 pp. Washington.

LE PICHON, X., 1960.—The Deep Water circulation in the Southwest Indian Ocean. *J. geophys. Res.*, 65 (12): 4061–4074. Baltimore.

MÉNACHÉ, M., 1963.—Premiére campagne océanographique du "Commandant Robert Giraud" en canal de Mozambique (11 Octobre–28 Novembre, 1957) *Cahiers Océanographiques*, 15 (4): 224–234. Paris.

ORREN, M. J., 1963.—Hydrological observations in the South-West Indian Ocean. *Invest. Rep. Div. Sea Fish. S. Afr.*, 45: 61 pp. Pretoria.

PAECH, H., 1926.—Die Oberflächenströmungen im Madagaskar in ihrem Järlichen Gang. *Veröff. Inst. Meeresk. Univ. Berlin*, 16: 37 pp. Berlin.

PARR, A. E., 1937–1938.—*J. Mar. Res.* 1 (2): 119–132.

PROUDMAN, J., 1953.—*Dynamical Oceanography*. 409 pp. Methuen, London.

SVERDRUP, H. U., JOHNSON, M. W., AND R. H. FLEMING, 1942.—*The Oceans, their Physics, Chemistry and General Biology*, 1,087 pp. Prentice Hall, Inc., New York.

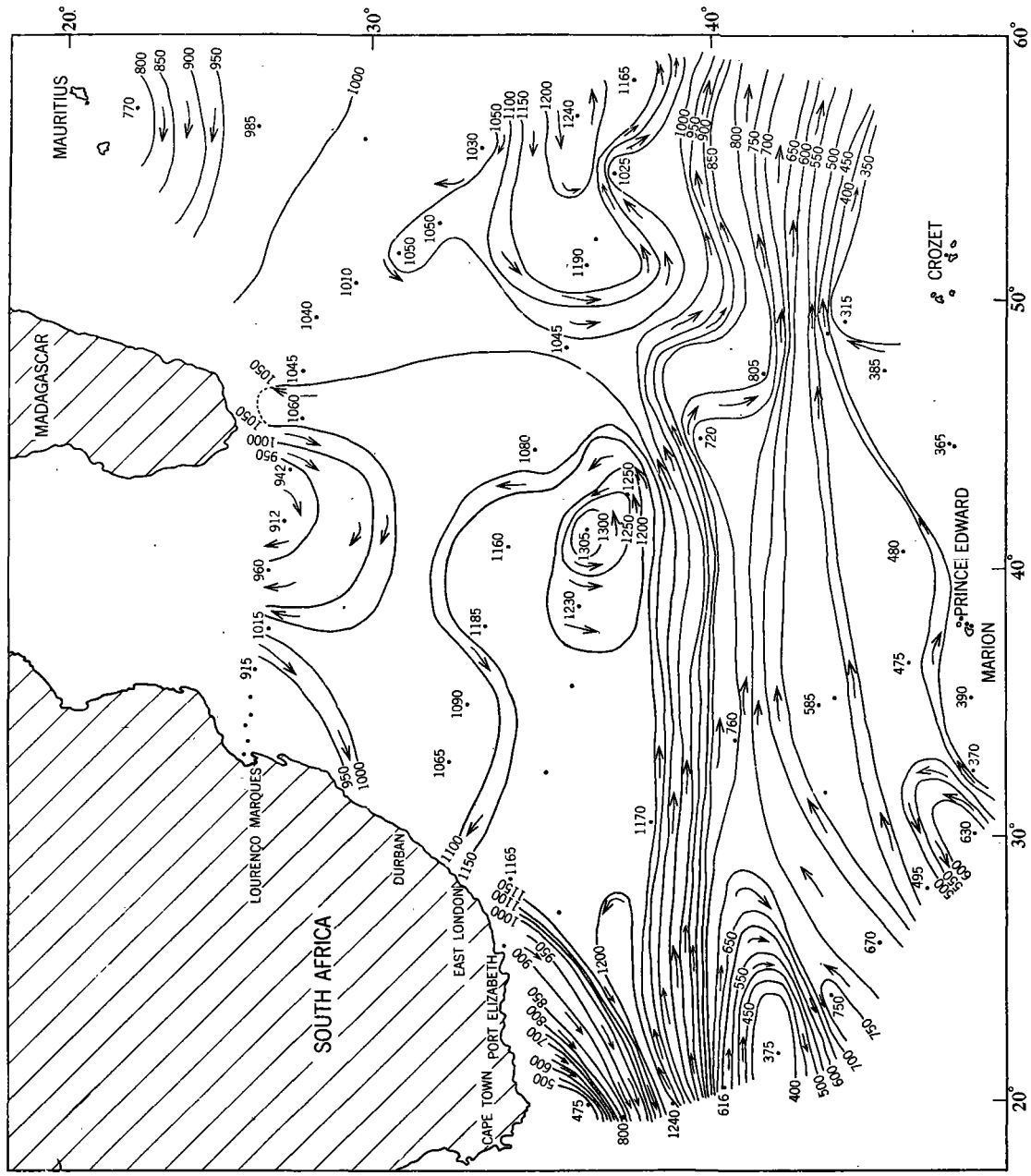

FIG. 12 DEPTH IN METRES OF THE σ_t = 27·20 SURFACE

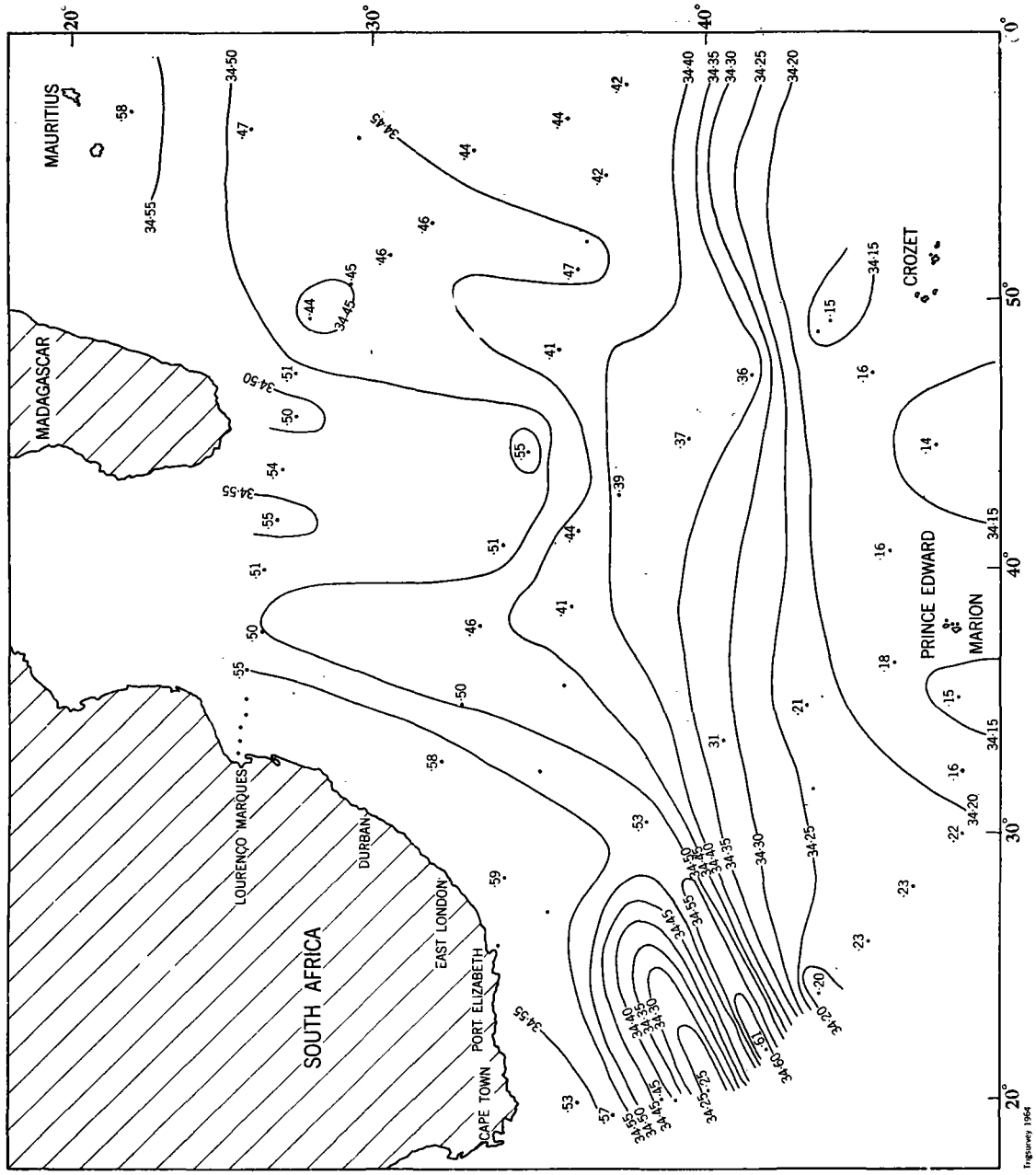

FIG. 13 SALINITY AT THE σ_t = 27·20 SURFACE

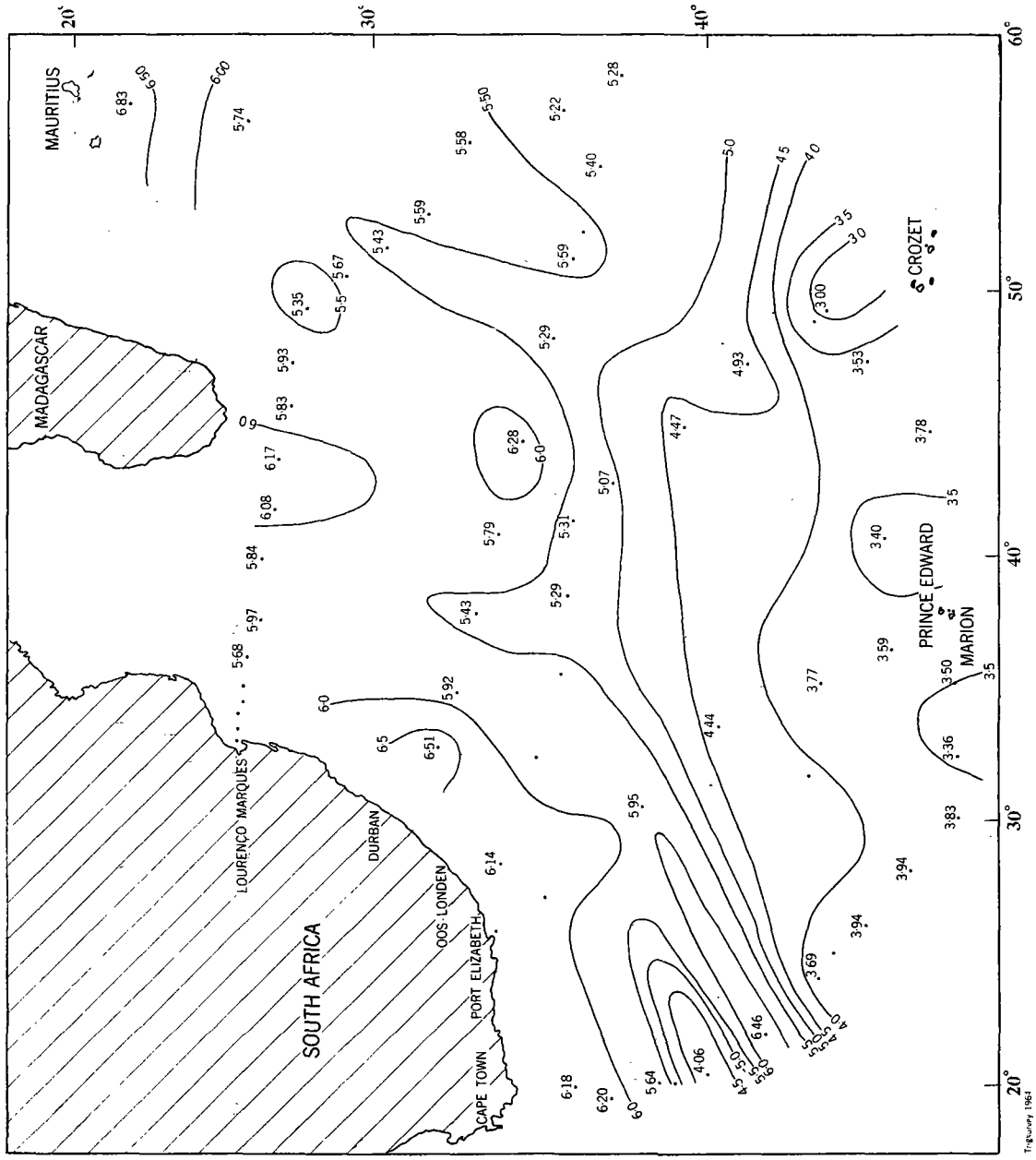

FIG. 14 TEMPERATURE AT THE σ_t = 27·20 SURFACE

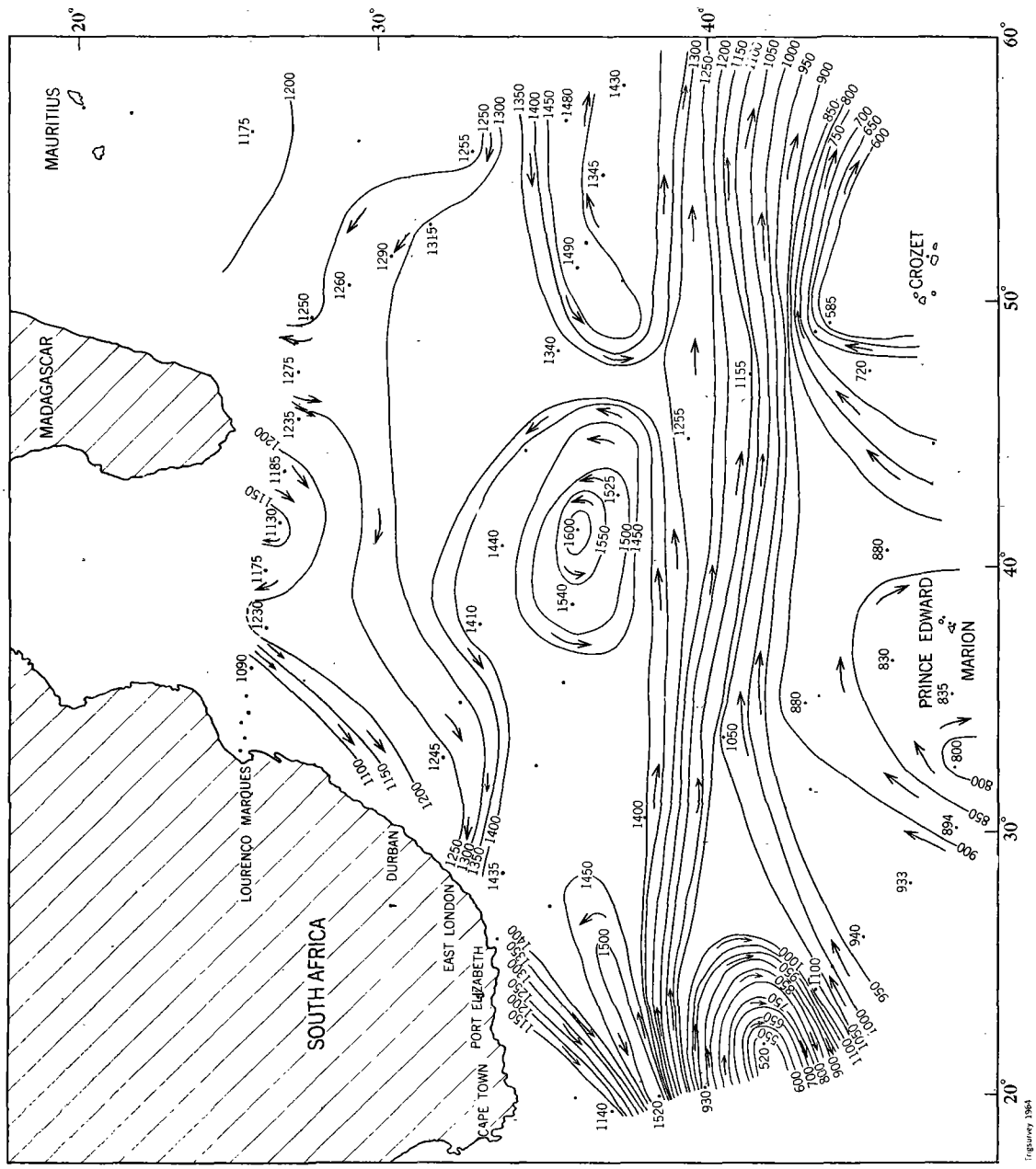

FIG. 15 DEPTH IN METRES OF THE σ_t = 27·40 SURFACE

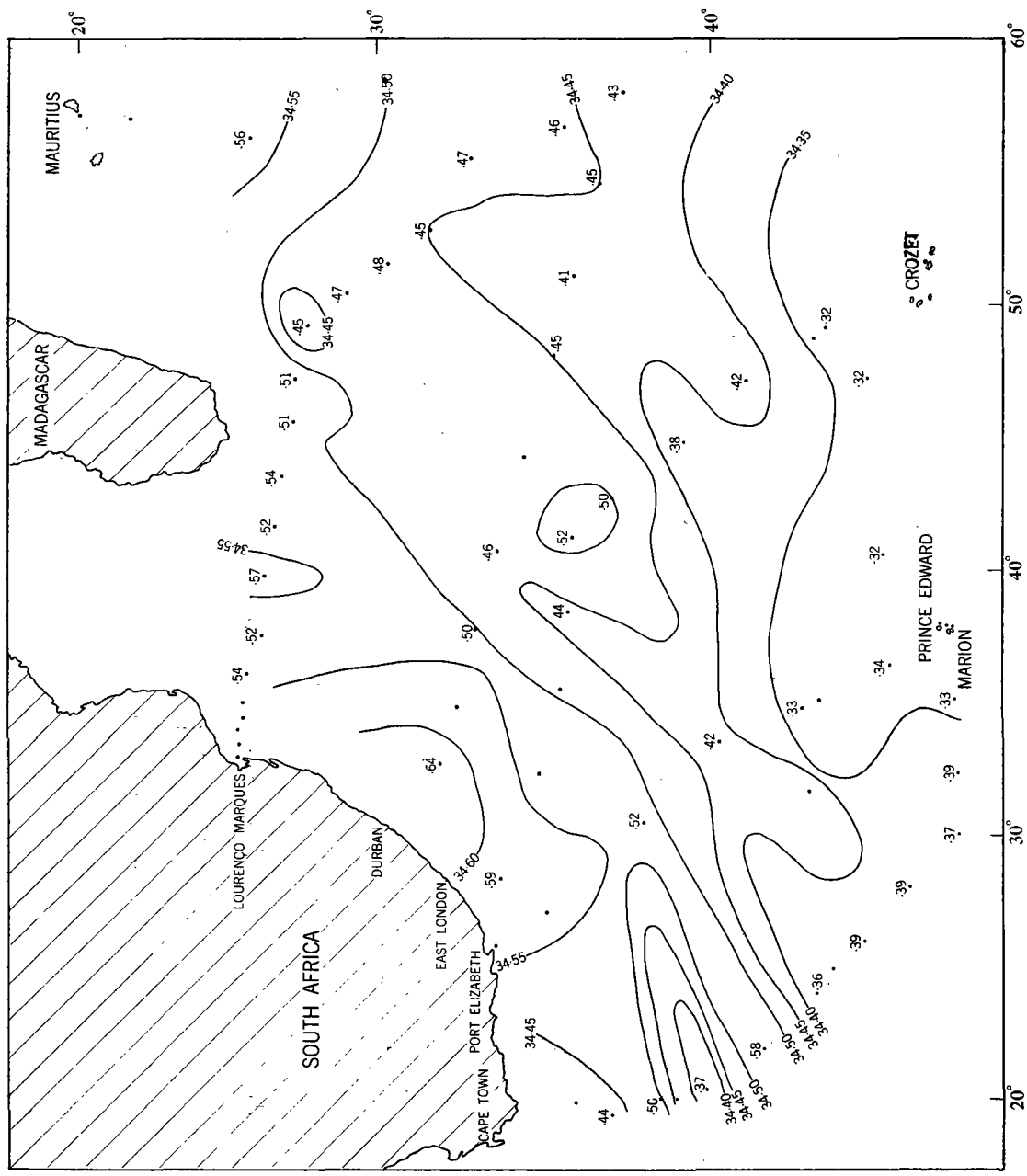

FIG. 16 SALINITY AT THE σ_t = 27·40 SURFACE

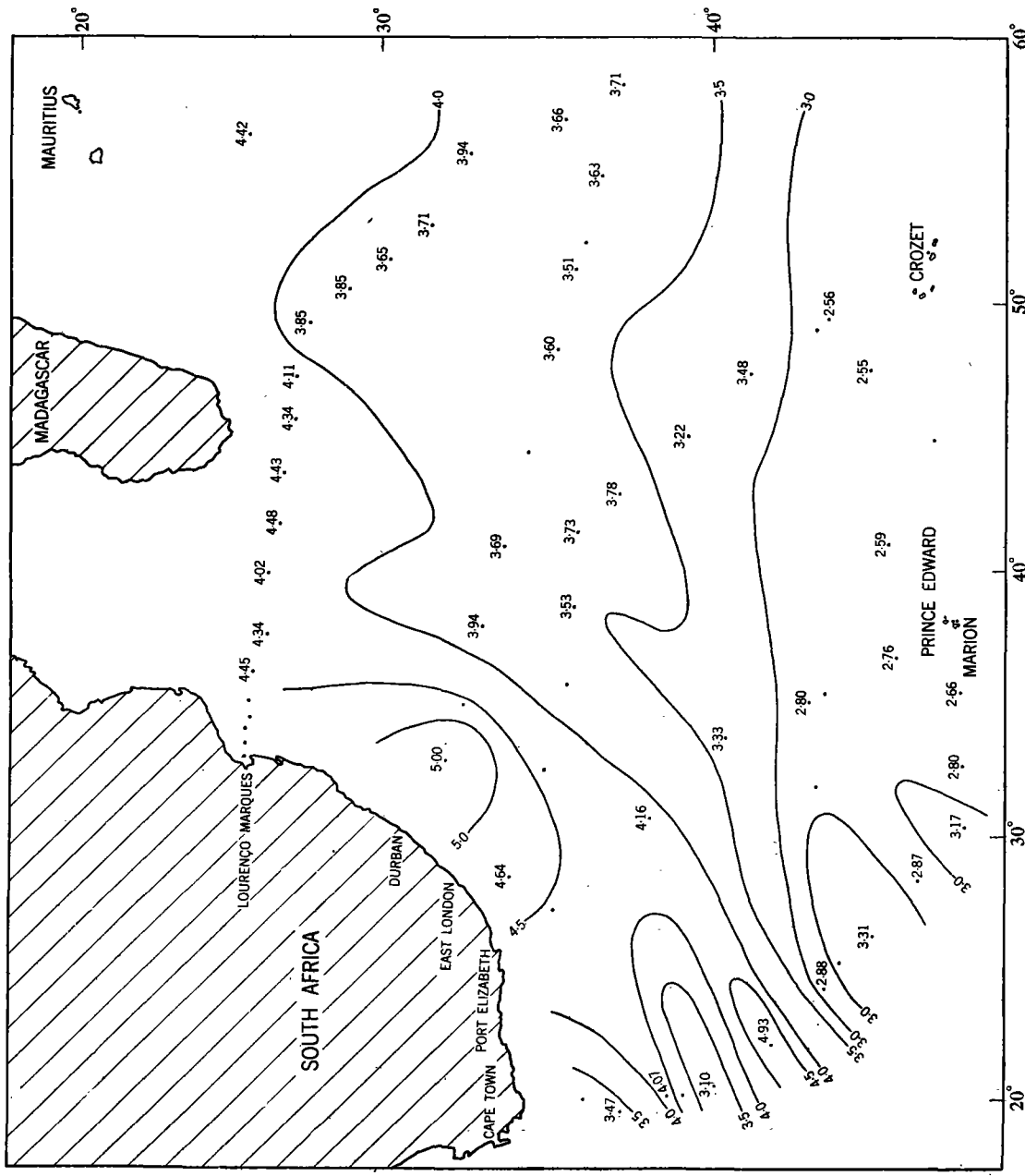

FIG. 17 TEMPERATURE AT THE σ_t = 27·40 SURFACE

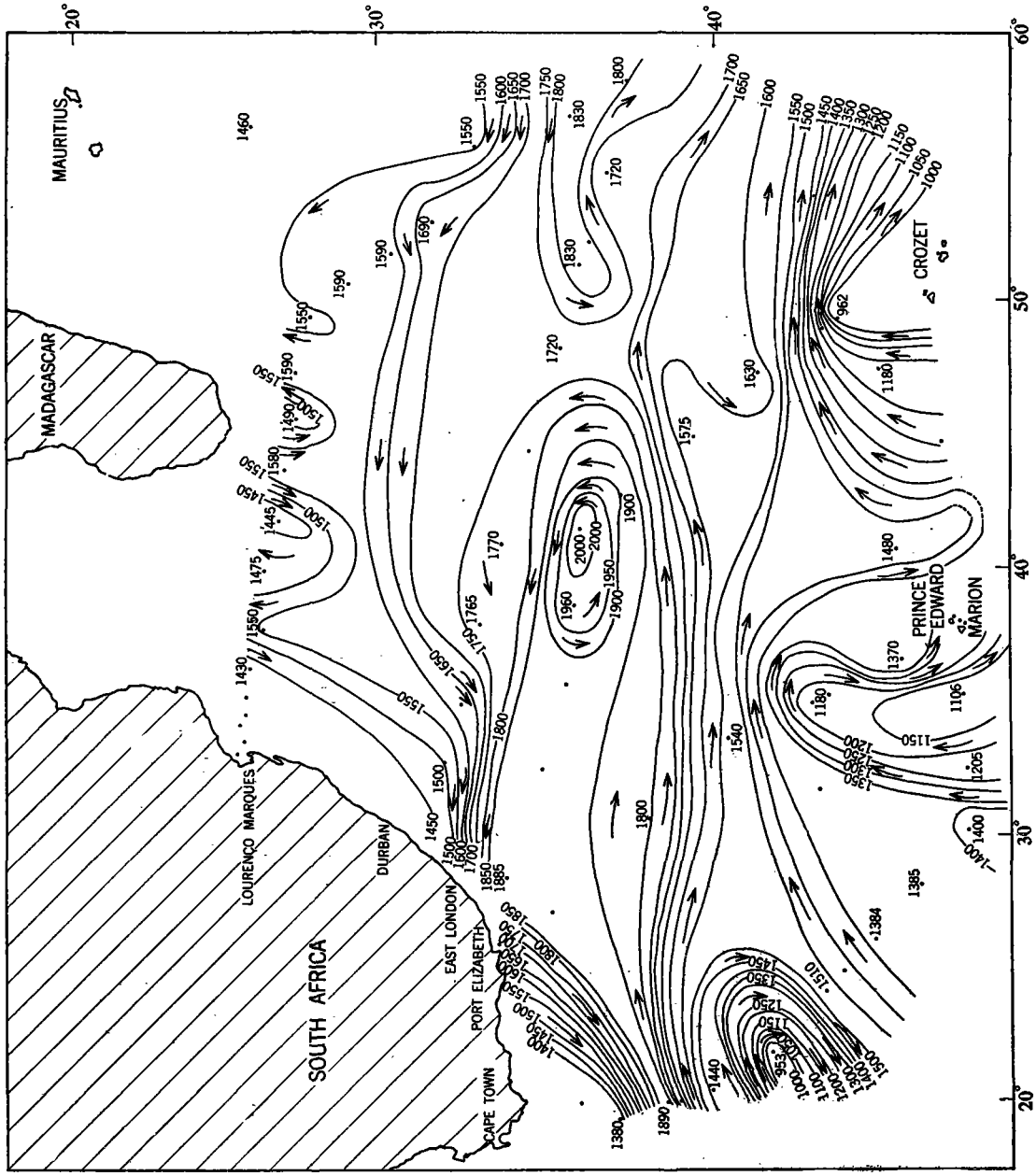

FIG. 18 DEPTH IN METRES OF THE OT -27·60 SURFACE

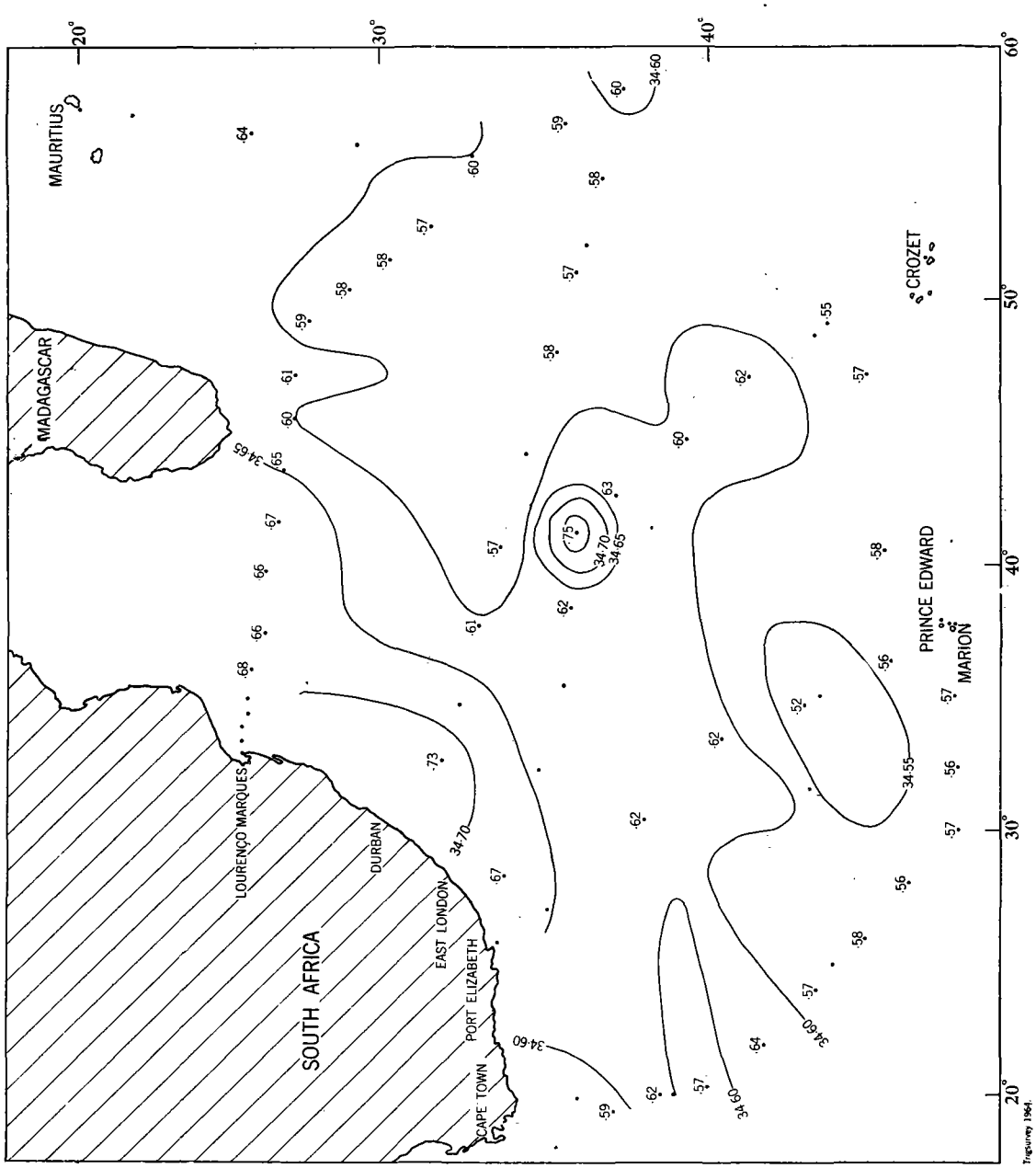

FIG. 19 SALINITY AT THE σ_t =27·60 SURFACE

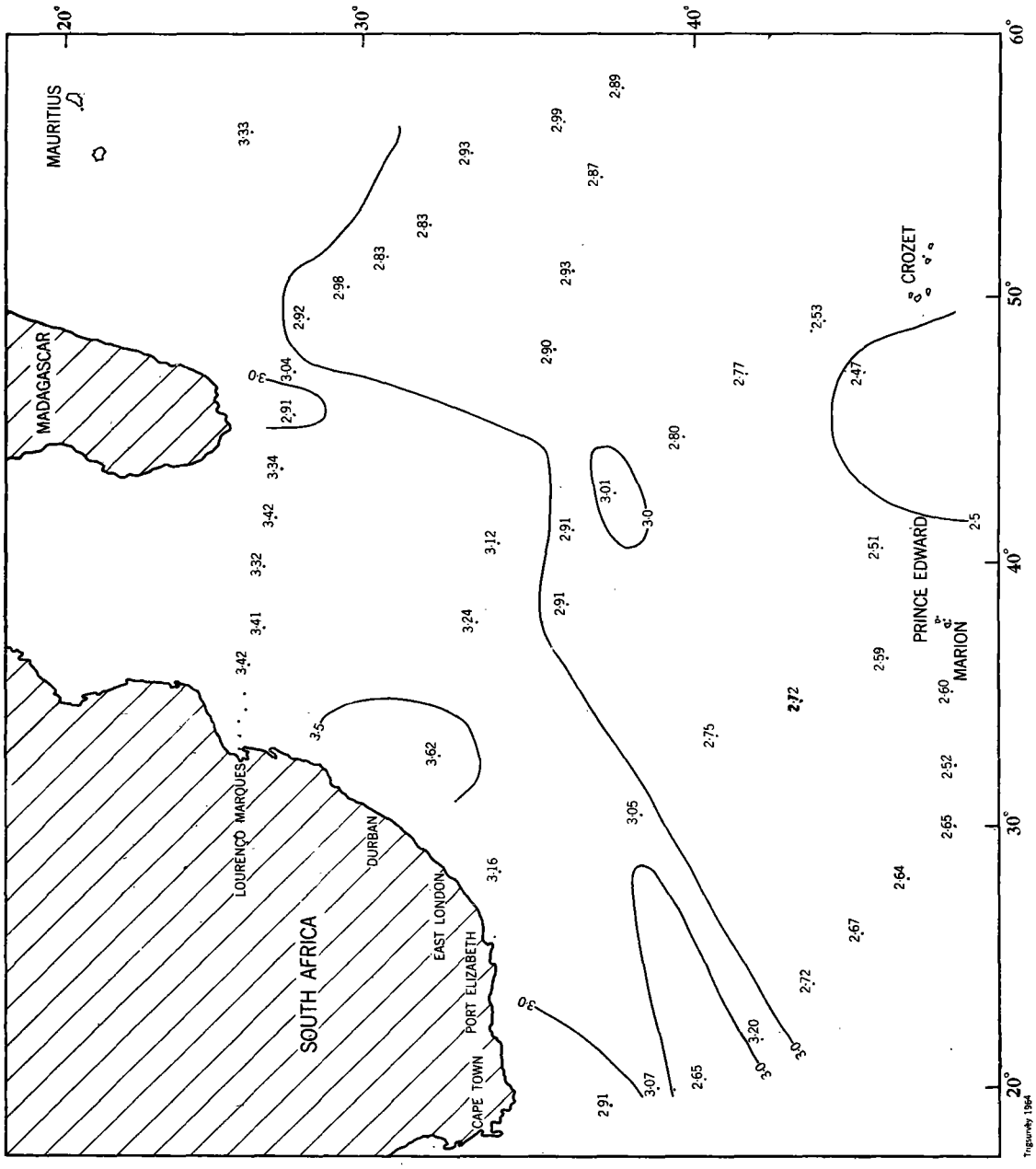

FIG. 20 TEMPERATURE AT THE O_T = 27·60 SURFACE

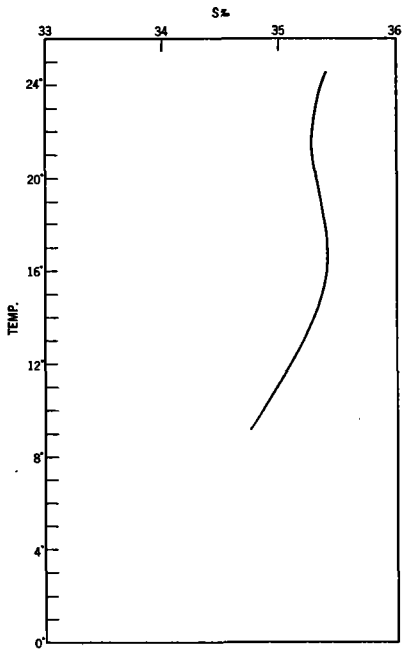

FIG. 21 MEAN T/S GRAPH ST. 2, 3, 4, 5.

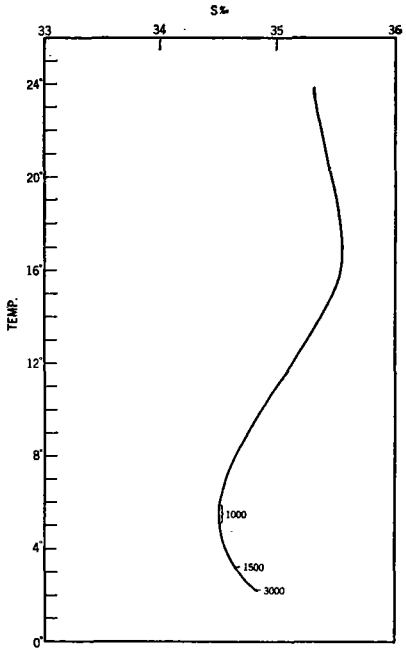

FIG. 22 MEAN T/S GRAPH ST. 6, 7, 8.

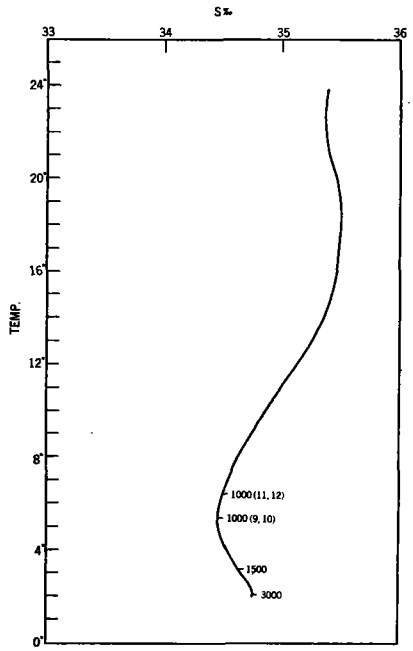

FIG. 23 MEAN T/S GRAPH ST. 9, 10, 11, 12.

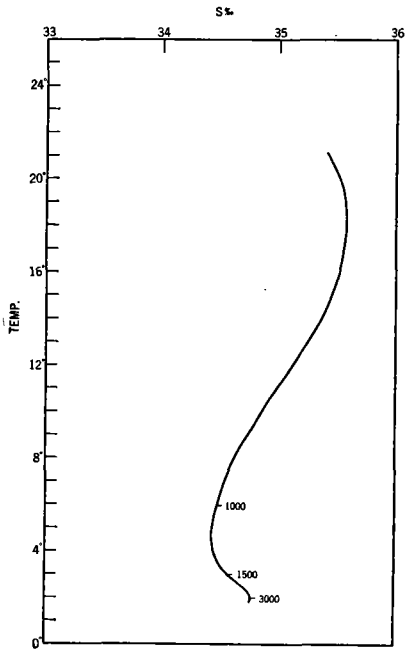

FIG. 24 MEAN T/S GRAPH ST. 13, 14, 15, 16.

Trigsurvey 1964

PLATE 1

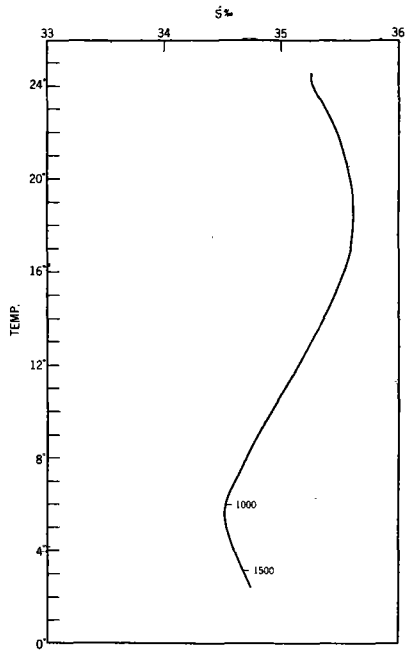

FIG. 25 MEAN T/S GRAPH ST. 18, 19, 20.

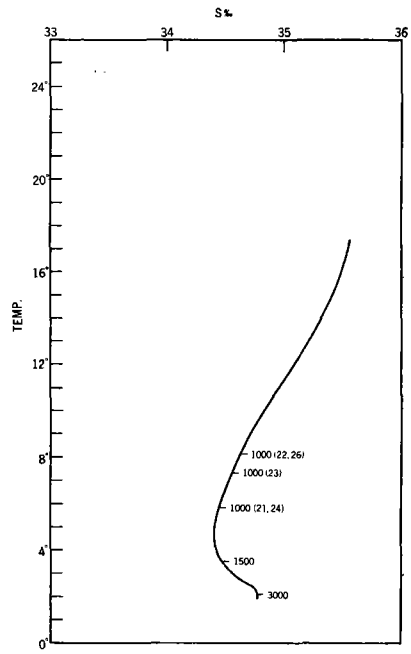

FIG. 26 MEAN T/S GRAPH ST. 21, 22, 23, 24, 26.

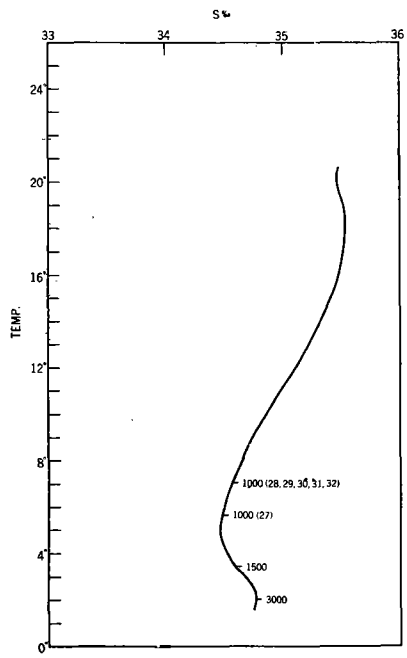

FIG. 27 MEAN T/S GRAPH ST. 27, 28, 30, 31, 32.

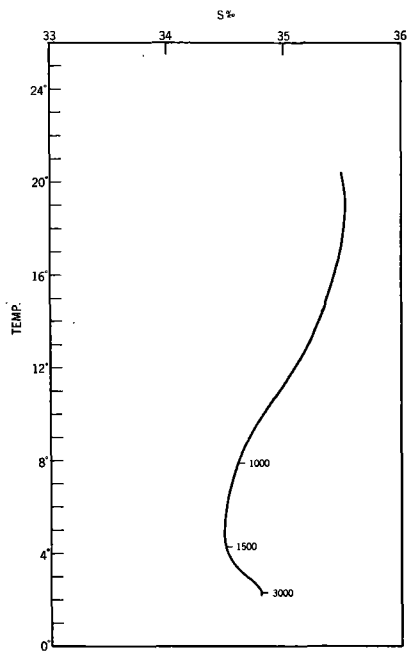

FIG. 28 MEAN T/S GRAPH ST. 33, 34, 49, 50, 51, 52. 54.

Trigsurvey 1964

PLATE 2

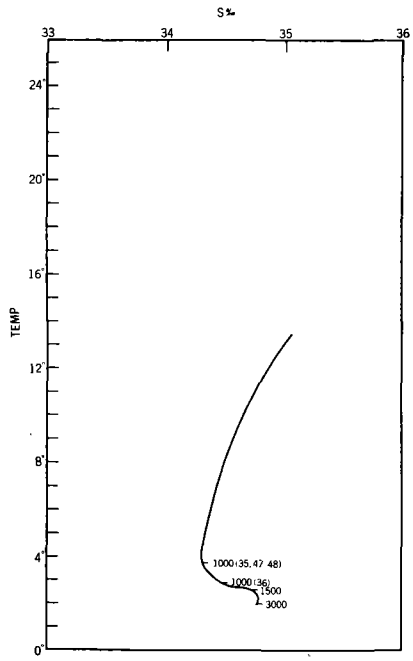

FIG. 29 MEAN T/S GRAPH ST. 35, 36, 47, 48.

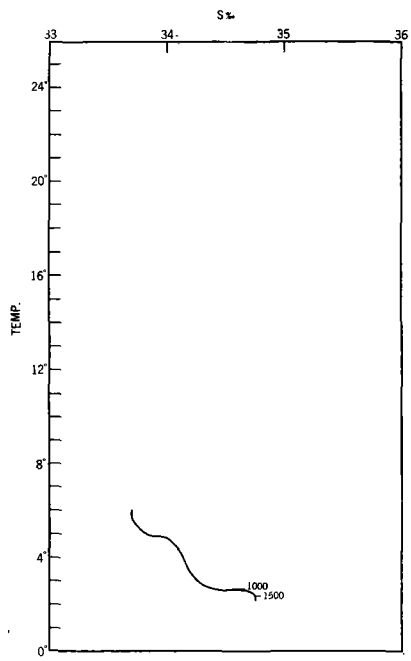

FIG. 30 MEAN T/S GRAPH ST. 38, 41, 42, 43, 45, 67, 68.

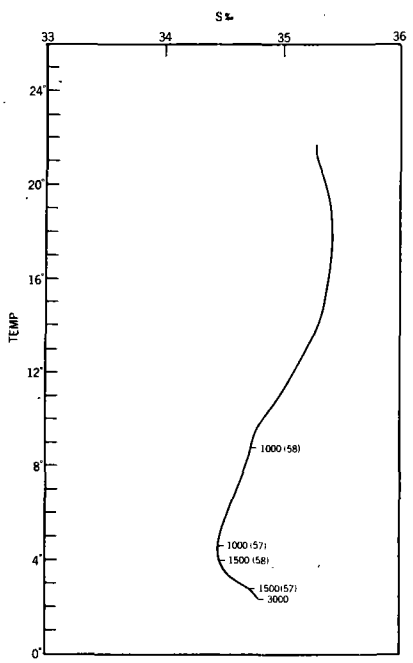

FIG. 31 MEAN T/S GRAPH ST. 56, 57, 58.

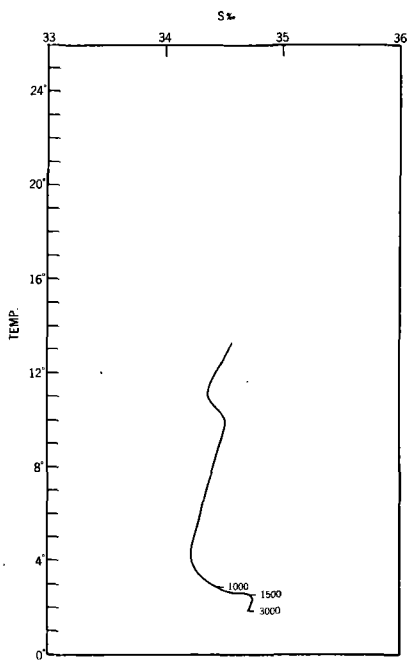

FIG. 32 MEAN T/S GRAPH ST. 60, 62, 64.

PLATE 3

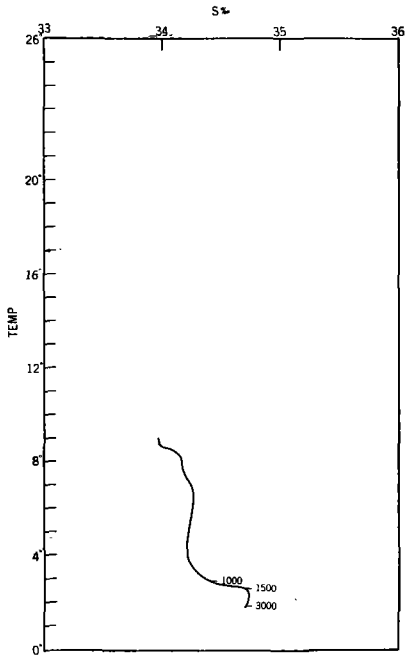

FIG. 33 MEAN T/S GRAPH ST. 61, 65, 66.

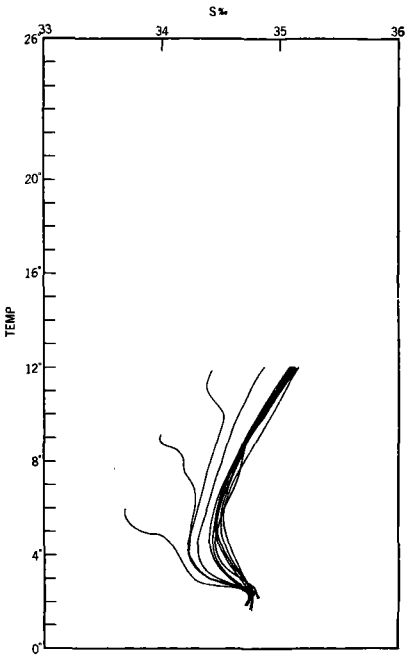

FIG. 34 GROUPED MEAN T/S GRAPHS.

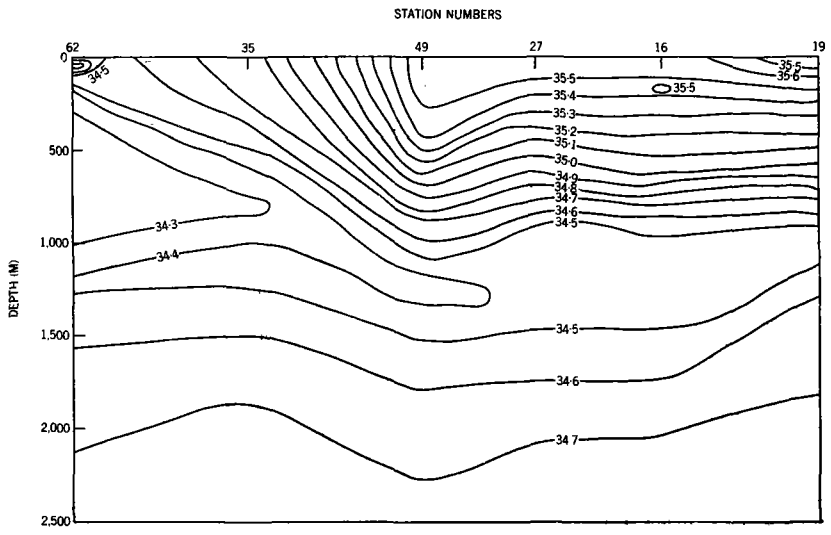

FIG. 35 SALINITY PROFILE - STATIONS 62, 35, 49, 27, 16 and 19

Tregurvey 1964

PLATE 4

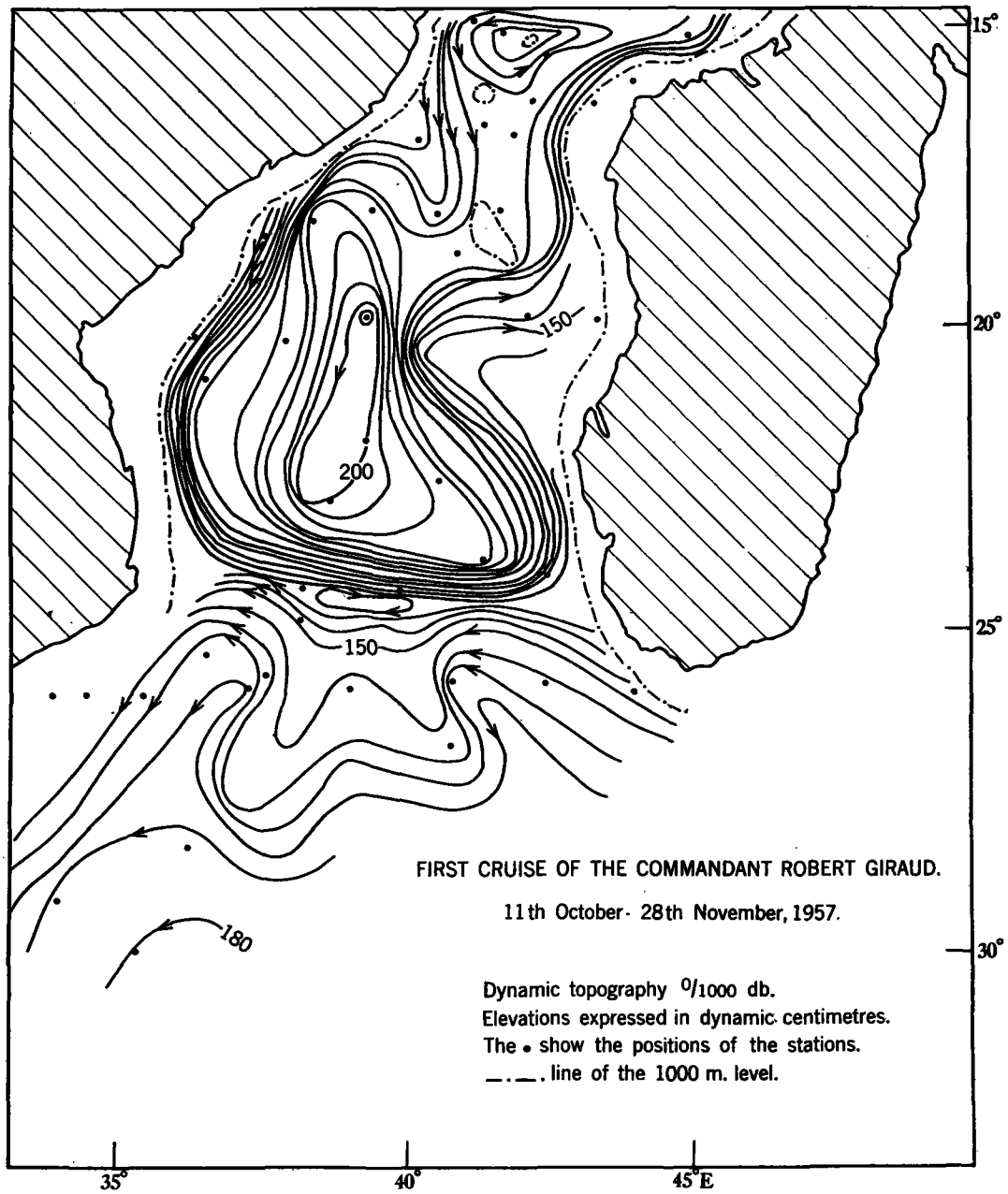

FIG. 36 DYNAMIC TOPOGRAPHY AT THE 0/1000 db SURFACE IN THE MOZAMBIQUE CHANNEL (TAKEN FROM CAHIERS OCÉANOGRAPHIQUES WITH THE PERMISSION OF THE COMITÉ CENTRAL d'OCÉANOGRAPHIE ET d'ETUDE DES CÔTES)

Driehoeksmeting 1964.

REPUBLIC OF SOUTH AFRICA

DEPARTMENT OF COMMERCE AND INDUSTRIES

DIVISION OF SEA FISHERIES INVESTIGATIONAL REPORT

No. 55

HYDROLOGY OF THE SOUTH WEST INDIAN OCEAN

by

M. J. ORREN

Collected reprints of the International Indian Ocean Expedition, vol. IV, contribution no. 242

CONTENTS

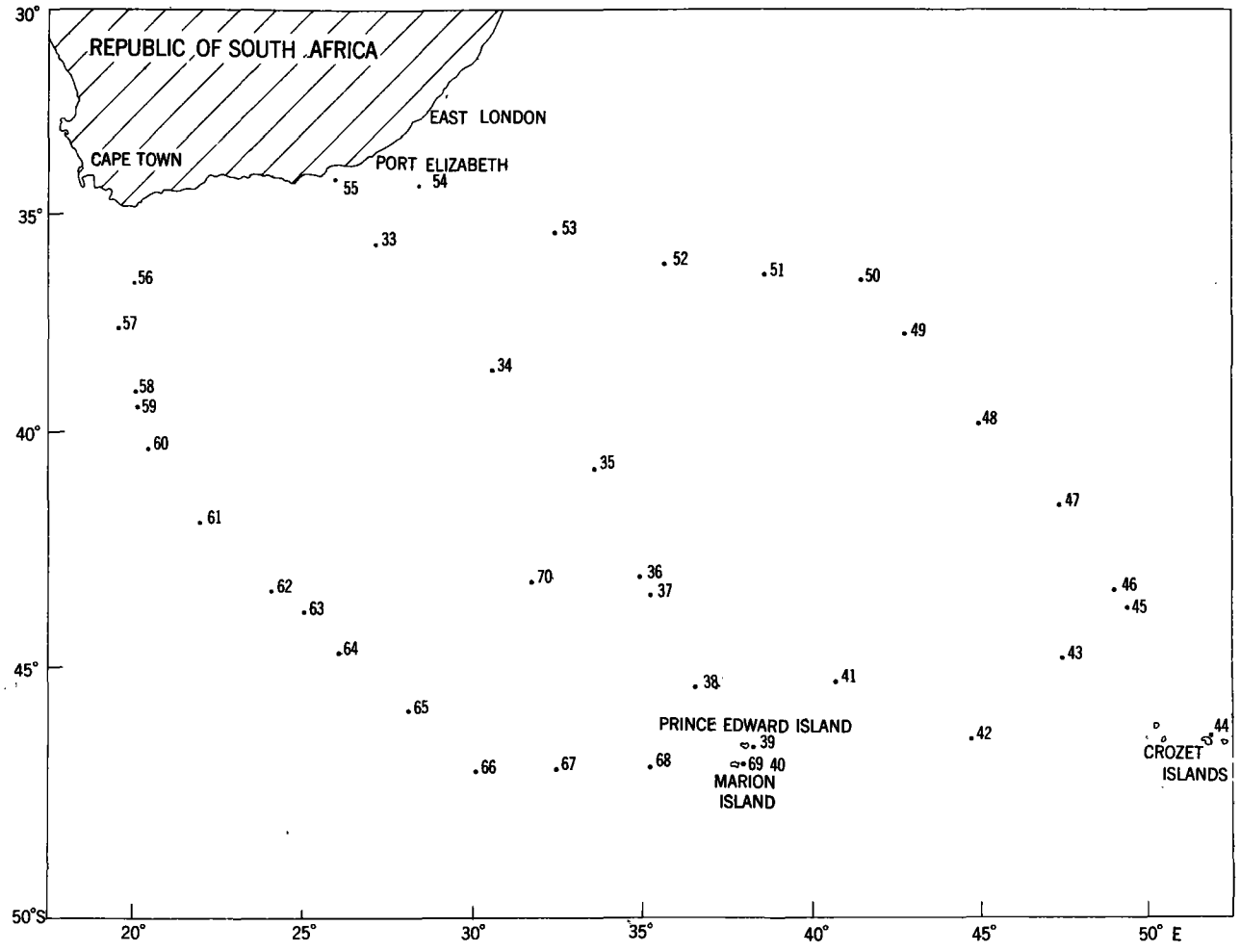

FIG. 1. POSITION OF STATIONS INVESTIGATED BY AFRICANA II DURING 1963 AND 1964

Trigsurvey 1965

1. ABSTRACT

During two cruises into an area of the Indian Ocean bounded by latitudes 34° S and 47° S and longitudes 20° E and 52° E, the sea water was sampled for temperature, salinity, oxygen and phosphate down to 4,000 m. Surface drift was obtained from navigational data. The Agulhas current varied from 50 to 100 miles in width and flowed at 2 to 4 knots. Little movement occurred in the Subtropical Water. The Subtropical Convergence was found to lie at 42° S ±1°. The West Wind Drift was only marked near the Crozets, where a northward thrust of Antarctic Surface Water appeared.

Subsurface currents were absent in the Subtropical Water, but were found in both the Agulhas Water and the Subantarctic Water. Possible sources of these currents are discussed. Central Water, originating from mixed Subtropical and Subantarctic Water, moved northwards at depths of 200 to 800 m. The movements of Intermediate Water and the North Atlantic and North Indian Deep Water masses are discussed.

2. INTRODUCTION

This report supplements Investigational Report 45 (ORREN 1963) and further describes the hydrological features of the South West Indian Ocean, using data obtained during two cruises by R.S. *Africana II* in 1962 and 1963 respectively. These cruises completed the field contribution of the Division of Sea Fisheries to the SCOR/UNESCO International Indian Ocean Exploration programme.

The area covered by the cruises is shown in Figure 1. Stations 33 to 55 were completed in June/July 1962, (Southern Winter) and the remainder in April 1963 (Southern Autumn). The 1963 cruise was curtailed due to an accident at Marion Island and no deep stations were done on the return part of the cruise. The stations have been numbered consecutively and in chronological order and the numerals follow those used in Investigational Report 45 (op cit.).

At each station the water column was sampled for temperature, salinity, dissolved oxygen and dissolved inorganic phosphate at the international depths to a maximum of 4,000 m., while simultaneously extensive biological sampling was carried out. At stations 37, 46, 59 and 63 only a surface sample was taken. The hydrological data on which this report is based will be published separately at a later date.

For the purpose of graphical presentation of the data the stations were divided into five lines named as follows:

(*a*) The "Marion Line", i.e. stations 33—40.
(*b*) The "Crozet Line", i.e. stations 40—44.
(*c*) The "Slot Line", i.e. stations 44—50.
(*d*) The "Port Elizabeth Line", i.e. stations 50—55.
(*e*) The "Agulhas Line", i.e. stations 56—69.

Stations 39, 40, 44 and 69 were worked in shallow water close to the islands. Vertical profiles of the hydrological variables have been constructed for each line and used for the deduction of water movements. The bathymetric terminology used in this report follows that of SIMPSON (1964).

3. METHODS

3.1 Temperature and Salinity.

Samples for temperature and salinity determination taken at the international depths down to 4,000m. were processed in the manner described by ORREN (1963).

3.2 Drift Measurements.

Surface currents were qualitatively estimated by noting the navigational set between two accurate astronomical position sights. During extended periods of overcast skies accurate sights were not possible and in these circumstances the drift was calculated as an average over 24 hours or more. Wind direction and velocity were noted at regular intervals during both cruises.

Figure 2 shows the current and wind vectors for the area and it may be noted that, in general, wind had little effect on the ship's drift when under way. Had this not been the case, the direction of the apparent surface current would have corresponded with the wind direction. Drifts observed on station with the ship stopped showed the latter tendency and consequently only drift measurements taken under way were included in the figure.

Although the surface drift thus arrived at is largely qualitative, it is felt that a fair picture of the actual movements may be obtained.

3.3 Miscellaneous.

Continuous depth records were obtained throughout the cruises with an Elac precision echo-sounder. Meteorological observations were made at the start of each station as well as at the synoptic hours, and a distant-reading thermograph recorded surface temperature continuously.

4. DISCUSSION

4.1 General.

The surface water of the area may be divided into three main water masses separated by more or less marked frontal discontinuities. These water masses are:

(*a*) The Agulhas system, composed mainly of Indian Ocean Tropical Water mixed with Subtropical Water;
(*b*) Subtropical Surface Water extending from the Tropical Convergence at 24° S (ORREN 1963) to the Subtropical Convergence at about 42° S;

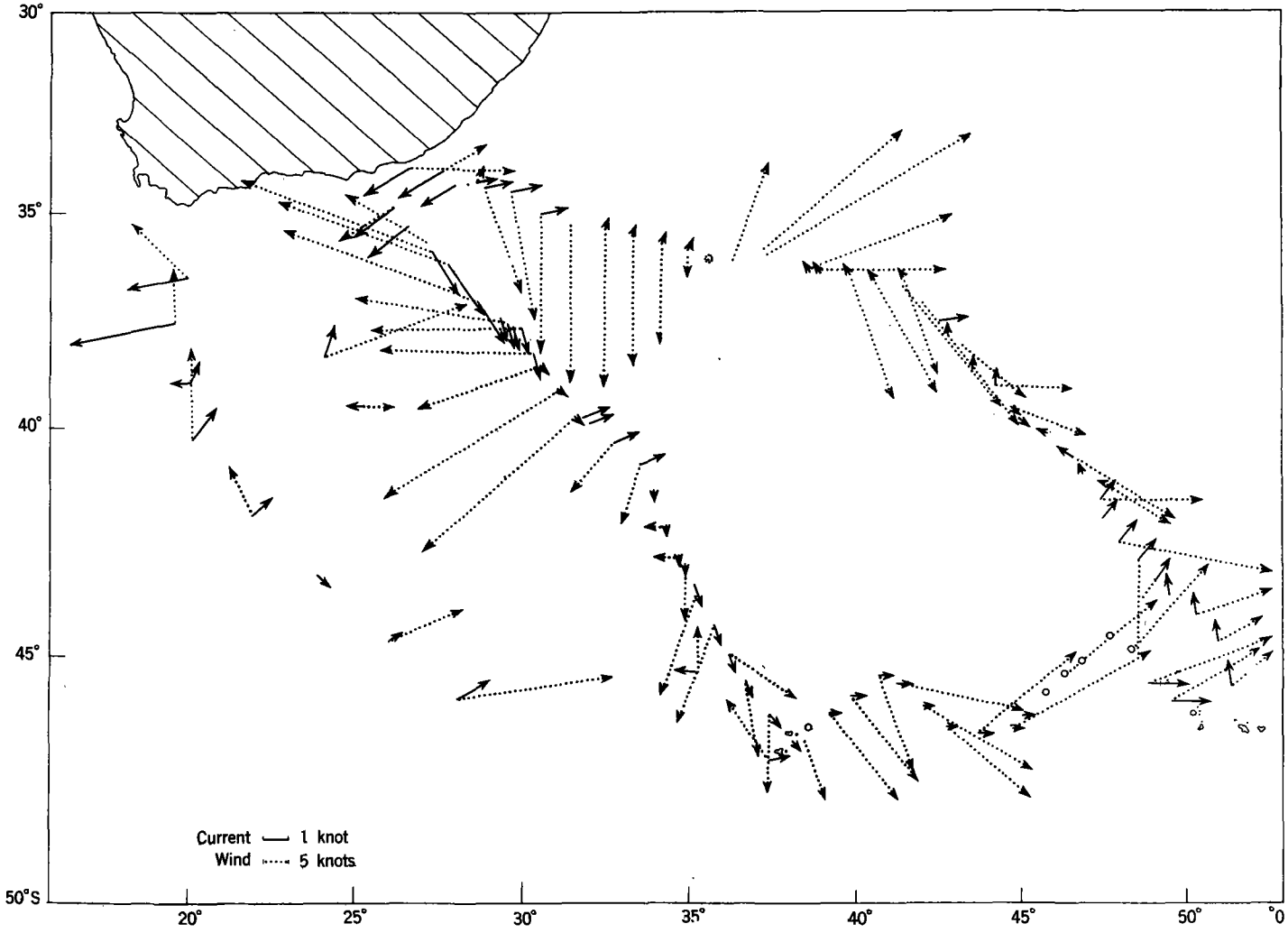

FIG. 2. SURFACE CURRENTS (UNBROKEN LINE) AND WIND VECTORS (DOTTED LINE) IN THE SOUTH-WEST INDIAN OCEAN (0 REPRESENTS ZERO VECTOR)

Trigsurvey 1965

(c) Subantarctic Surface Water stretching from the Subtropical Convergence to the Antarctic Convergence at *c.* 50° S.

Deeper down, the water masses can be further subdivided into the Subsurface, Central, Antarctic Intermediate, Deep and Bottom Waters. In the Northern part of the area all these water masses were present; southwards the Central Water source was passed at the Subtropical Convergence, and here also marked changes occurred in the distribution of the other water masses. For example, Figure 3 shows typical T/S curves for the water masses on either side of the Subtropical Convergence.

Figure 4 was used to distinguish surface water masses. Surface values of all stations, with the addition of stations 1 to 32 (quoted in ORREN 1963), are included in the surface T/S diagram. The boundary between Tropical and Subtropical masses was drawn at 23°C — the temperature of the Tropical Convergence—while the clustering of points was largely used to position the other limits. The large region between Subtropical and Subantarctic water is designated the "transition region", and the most likely position of the Subtropical Convergence (station 35) is entered as a dotted line.

The limits proposed by FUKASE (1962) for the "Agulhas", "North Edge" and "Subantarctic" water masses have been entered as lines of dashes on Figure 4. Fukase's "Agulhas Water" limit of 19° C appears low for this region, and his Agulhas region covers a large number of points found in this investigation to be typical of Subtropical Water despite the fact that his values were taken in summer whereas the data used here for Figure 4 were collected largely in winter, when lower temperatures could be anticipated.

The "North Edge Water" limits agree more or less with the lower part of the Subtropical Water and the upper part of what has been designated here as a "transition" region (Fig. 4).

Fukase's "Subantarctic Water" limits enclose water which is both warmer and more saline than was found in this investigation, and Fukase's results further agree with those of HORI (1962). It appears that the difference is purely seasonal since the *Africana II* cruises described here were undertaken in autumn and winter (April 1963 and June/July 1962) whereas the Japanese researchers crossed the area in summer. The temperature variation from autumn to winter is further discussed in section 4.2.4 below. The T/S envelope produced by Hori for the area between Cape Town and Antarctica generally agrees well with Figure 4.

4.2 Surface Water.

4.2.1 The Agulhas System.—The Agulhas current is a narrow, fast-flowing western boundary type current generally believed to originate in the southward moving part of the South Equatorial current, although recent studies by MENACHÉ (1961) show that the Moçambique current apparently returns to the north and does not form part of the Agulhas current. However, this phenomenon may be seasonal. The Agulhas region will be discussed only briefly here since other more detailed inshore surveys have been completed recently, for example DARBYSHIRE (1964).

From thermograph data, i.e. the rapid temperature change, the Agulhas current was encountered 10 to 20 miles off Port Elizabeth (Fig. 5) and extended about 100 miles off shore with temperatures of 21 to 23° C. On the 20° E meridian the current lay about 150 miles south of Cape Agulhas and was about 50 miles wide. South of Plettenberg Bay (24° E) the Agulhas current was evident as a 90 mile wide strip of warm water with temperatures in excess of 23° C. Between the current and a cool (less than 17° C) 50-mile wide strip of coastal water was a uniform layer of water moving westward at about two knots (probably a branch of Agulhas Water) which may later flow round the edge of the Agulhas Bank into the Atlantic.

Surface velocities in the current were generally high, namely two knots off Port Elizabeth and Plettenberg Bay and over four knots south of Cape Agulhas (See Fig. 2).

Station 57 (37½° S, 20° E) in the centre of the strong Agulhas flow in this area had a surface temperature and salinity which placed in it the Tropical Surface Water category, that is temperatures in excess of 23° C, and salinity ranging from 35·2 to 35·4‰, as shown in Figure 4, in common with stations from the Moçambique Channel and near Mauritius (compare stations 7 and 18 in ORREN 1963). No other station lay in the current core, but thermograph data indicated similar water throughout the Agulhas current in the study area. The T/S data from the Moçambique and Agulhas currents seem to indicate a common origin in equatorial water, but further stations north of Lourenço Marques would be required for investigating whether the phenomenon observed by MENACHÉ (1961) was an isolated or seasonal disturbance.

FUKASE (1962) considers the southern edge of the Agulhas current to be the "Agulhas Convergence" on the basis mainly of temperature measurement. This view is supported by DARBYSHIRE (1964), but this author admits the "Convergence" is not well marked, especially as regards salinity change. It is felt that the concept involves a rather unnecessary subdivision since the Agulhas current region is generally regarded as a separate hydrological entity and the edge of the Agulhas current may in fact perhaps be considered as a southward extension of the Tropical Convergence, especially since Tropical Water is present in the Agulhas current. If the concept of an "Agulhas Conver-

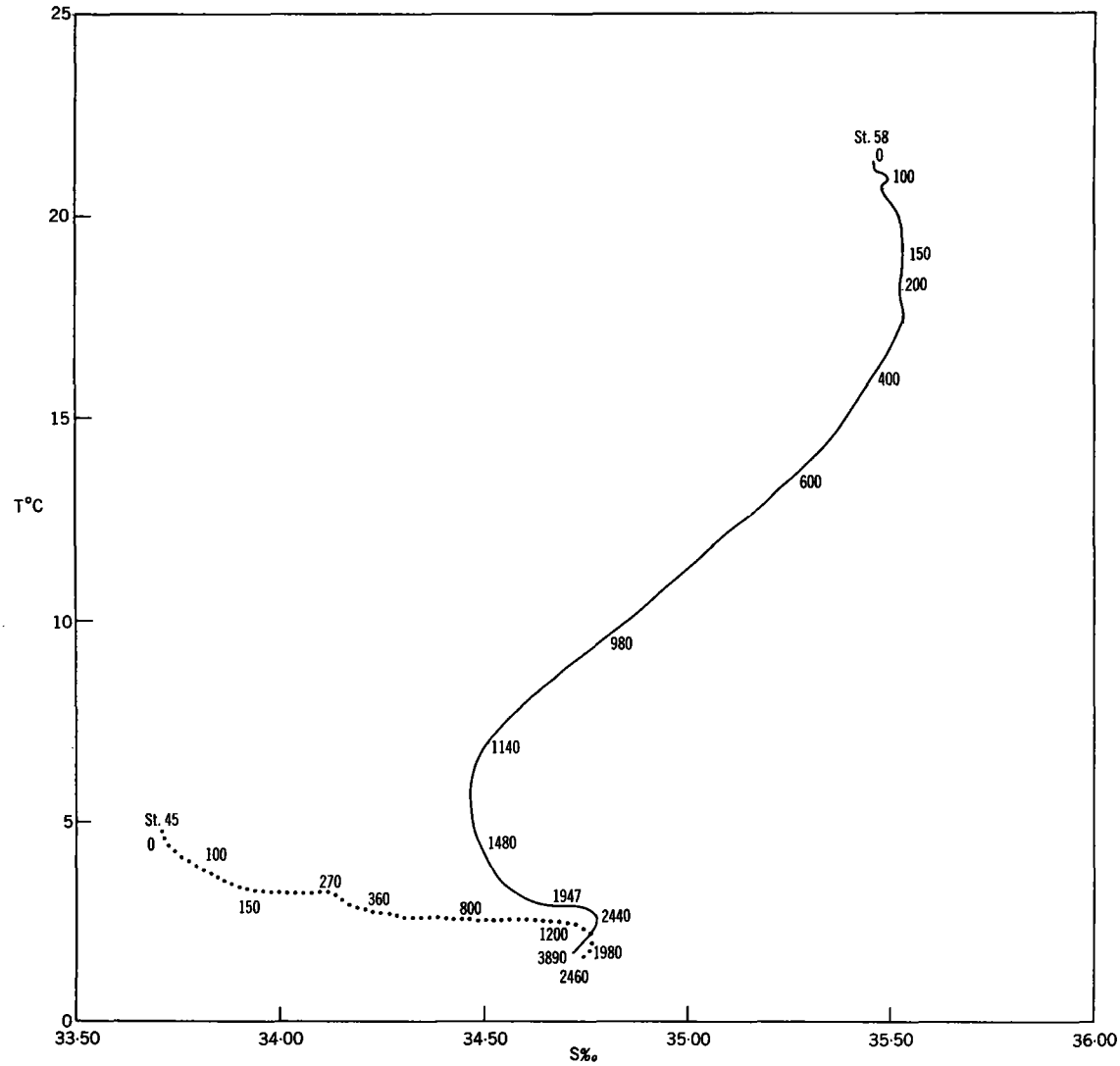

FIG. 3 TYPICAL T/S RELATIONSHIPS FOR STATIONS 45 (SUBANTARCTIC WATER) AND 58 (TROPICAL AND SUBTROPICAL WATER)

gence" is allowed, we are faced with two such convergences bounding each side of the current, that is a "North Agulhas Convergence" separating cool coastal water from the warm stream, and a "South Agulhas Convergence" separating Agulhas and Subtropical Water masses. Fukase also mentions a temperature of 18° C at the centre of the Agulhas Convergence, but on the Marion line temperatures of 18° C were maintained right up to the Subtropical Convergence (Fig. 5). The North Edge water of Fukase is almost certainly mixed Agulhas current and Atlantic water (brought in by the West Wind Drift), but the situation is rendered complex by the many eddies formed at the meeting of the two strong water movements, which bring about upwelling and sinking. Fukase's samples were from the surface only, so deep eddies and upwelling would not be detected directly. Analysis of unpublished hydrological data from the Division of Sea Fisheries has shown the presence of these eddies in this region.

An eastward moving counter current lying to seaward of the Agulhas current off East London (Fig. 2) had an apparent velocity of ¾ to one knot, and no appreciable salinity difference from Agulhas Water, while its temperature was about 3° C lower (i.e. about 20° C) than Agulhas current core water. On departing from station 54 a rise of almost 3° took place within a few miles, and this station must lie almost on the outer edge of the Agulhas current. This counter current was also apparent in a section from Madagascar to Port Elizabeth constructed by HORI (1962). The weak surface eddy centred on the Moçambique Terrace (ORREN 1963) may perhaps be brought about by interaction of the counter current with the Agulhas current, the shallowing water intensifying the motion.

No counter current is evident on recent charts (DARBYSHIRE 1964) of computed surface currents, data for which were obtained almost simultaneously with those collected for this report. Although the agreement between computed and measured currents is generally excellent, the computed current velocities are systematically too low by about one knot. Darbyshire's velocities of 10 to 60 cm./sec. are low for the strong Agulhas current (cf., measured values in Fig. 2) and it is suggested here that this is brought about by the choice of 1,000 db. as reference level, since our data show appreciable southward movement even at 1,500 m. in the Agulhas current region. Indeed, VISSER and VAN NIEKERK (1965) found 2,000 db. to be a far more satisfactory reference surface. The effect would be to reduce the relative surface velocity, and thus the ¾ knot counter current flow might not be detected.

To sum up, the Agulhas current varied from 50 to 100 miles in width and had measured velocities of 2 to 4 knots. A northward moving counter current (¾ to 1 knot) lay on the outer boundary of the current.

4.2.2 Subtropical Surface Water.—This includes all water lying between the Tropical and Subtropical Convergences with the exception of the Agulhas system. Near the Subtropical Convergence there is a zone denoted as a "transition region" between the Subtropical and Subantarctic Surface Waters. The above defines Subtropical Surface Water as having a temperature range of from 15° to 23° C and a salinity range of 35·3 to 35·7‰ with a salinity maximum at about 20° C surface temperature (Fig. 4).

In the north, between stations 50 and 53, the temperature change was very gradual, rising from 17·81° C at station 50 to 17·89° C at station 52, then rising rather faster to 19·71° C at station 53. Farther inshore the rapid temperature gradient on the border of the Agulhas system was encountered, with an increase of 3° C (20° to 23° C) in about 20 miles. The water along this line had a slight northward component of motion (about ½ knot) despite strong (30-knot) north winds between stations 52 and 54. This motion intensified and became a counter current near 54 (Fig. 2).

South-east of Port Elizabeth a strong (1½ to two knots) current of Subtropical Water moved generally southwards, and this movement is no doubt due to the deflection of Agulhas Water by the broadening continental shelf south and west of Port Elizabeth. In support of this, the 20° C isotherm lay about 90 miles south-east of East London and about 240 miles off-shore on the Marion line (Fig. 5). South of Cape Agulhas, Agulhas Water encounters the West Wind Drift and a large well-developed eddy was centered on about 40° S, 21° E. The southward moving warm water penetrated as far as 40° S on the Marion line and to about 41° S on the Agulhas line. South of station 49 a large eddy caused a complex distribution of surface water. Just to the north of the Convergence on the Marion line (at about 38° S) the temperature dropped to 18·4° C and the salinity increased from 35·47‰ at station 33 to 35·55‰ at station 34. The mixed Subtropical Water then moves in an arc curving round to the east, and is most probably augmented by more Agulhas Water, mixed with Atlantic West Wind Drift Water brought in from the west. Comparison of Figure 2 with the July current chart of MICHAELIS (1923) shows that there is a slight southward movement south of Port Elizabeth. It appears that this southerly current is strongly developed in winter since a layer of warm water extends right to the Subtropical Convergence and the current is stronger than recorded by Michaelis. The current chart for July 1962 of DARBYSHIRE (1964) supports the above findings.

In conclusion, Subtropical Water showed little movement apart from a slight northward flow (½ knot) along 35° S and a strong southward flow (1½ to two knots) south of Port Elizabeth. The latter current is almost certainly of Agulhas

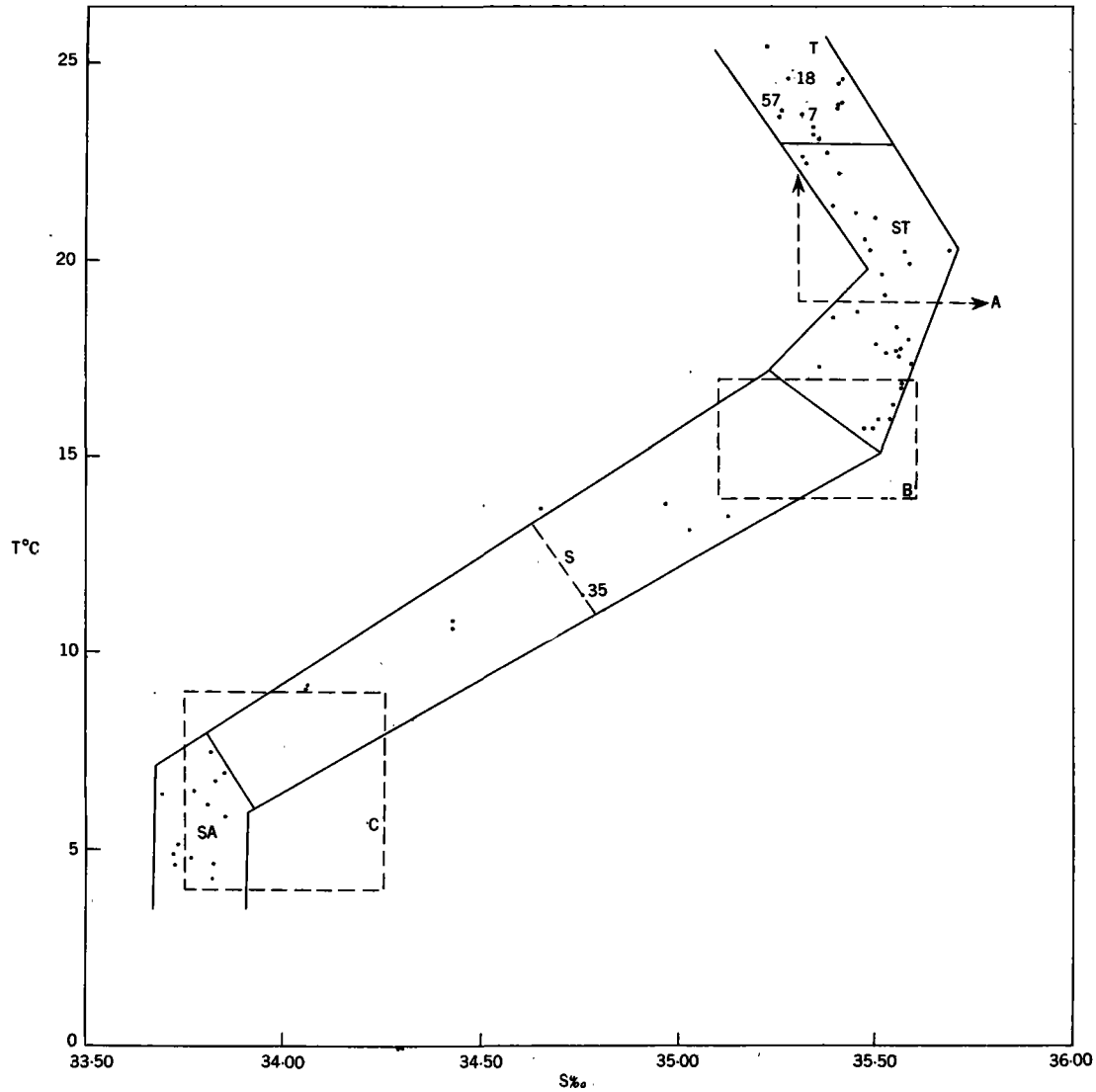

FIG. 4 SURFACE T/S RELATIONSHIPS IN THE SOUTH-WEST INDIAN OCEAN

(T = Tropical; ST = Subtropical; S = Subtropical Convergence (station 35); S.A. = Subantarctic Water)

[A = Agulhas Water; B = North edge Water; and C = Subantarctic Water according to Fukase (1962)]

Trigsurvey 1965

current origin and appears strongly developed in winter.

4.2.3 The Subtropical Convergence Region.— Perhaps the most interesting hydrological feature in this area of the Indian Ocean is the Subtropical Convergence region. Frontal discontinuities such as this are of great biological interest, since an accumulation of plankton, and a consequent accumulation of fish and marine mammals, is generally found in the neighbourhood of such a front (see, for example GRIFFITHS 1962). The Subtropical Convergence is also of considerable interest to meteorologists. The formation of Central Water here (see Section 4.4 below) is vitally important, since this is the water mass which upwells on the south west coast of Africa and is responsible for the vast abundance of marine life in the upwelled coastal water.

The Subtropical Convergence is generally recognized as the boundary region between Subantarctic and Subtropical Surface Waters. In general, however, the area of sharp temperature and salinity change at the surface does not coincide with the area of current convergence shown by stream lines. DEFANT (1961) distinguishes the "Subtropical Convergence"—the current convergence—and the "Subtropical Boundary" between the water masses. Since the transition region lies entirely in the region of strong Westerlies, DEACON (1937) believes the Convergence is formed between southward moving Subtropical Water and northward moving Subantarctic Water. The northward movement of Subantarctic Water is slight since the wind-induced northward drift is largely counterbalanced by a thermohaline southward flow due to climatic difference; a northward flow of water is produced by that part of the Antarctic Water which moves north across the Antarctic Convergence (DEACON 1937). At the Subtropical Convergence the denser Subantarctic Water sinks and mixes with subsurface water (see Section 4.4. below).

The position of the Convergence in the Atlantic is subject to much fluctuation (in fact DEACON (1937) has shown this to be as much as 6° of latitude), and is believed to lie further south in summer than in winter.

Figure 6 shows the approximate position of the Subtropical Convergence centre (centre taken as 13° C) in relation to longitude. Data have been taken from Discovery Committee, Le Pichon, Hori, Fukase, Deacon and Taljaard. Although the vast majority of observations were made in summer, the available winter points are all in the area 41° to 42° S, while the summer points seem to cluster nearer 43° S. By far the largest number of observations lie in the range 42° $\pm$1° S, and it is thus likely that in the region between 20° E and 50° E the Subtropical Convergence is found near 41° to 42° S in winter and near 42° to 43° S in summer—a seasonal variation of about 120 miles.

For example, S.A.S. *Transvaal* (TALJAARD 1957) crossed the Convergence at about 41° 20′ S, 36° E in April, i.e. autumn, and this station lay between two *Discovery* stations completed in summer and winter respectively in the same area.

The Subtropical Convergence divided the region roughly in two parts, and Figure 7 gives some idea of the large variation in surface properties across the Convergence, and the contrast between the high temperature, high salinity, low oxygen and low phosphate Subtropical Water and the cool, low salinity, high oxygen and nutrient rich Subantarctic Water may easily be seen.

The Convergence was most marked on the Marion line, where at about 40° S the surface temperature was still 18·5° C. On steaming south the temperature fell rapidly to 11·5° C, and at this point the ship was stopped and station 35 was completed. On leaving this station a further sharp decrease reduced the surface temperature to about 7·5° C (See Fig. 5). A temperature fall of 10° C thus took place in 90 miles—a decrease of 6·7° C/deg. lat. This figure agrees well with the 6·9° C/deg. lat. observed by FUKASE (1962). No continuous record of salinity was available but the surface salinity at stations 34, 35 and 36 was 35·55°/$_{oo}$, 34·75°/$_{oo}$ and 33·81°/$_{oo}$ respectively. The abrupt nature of the change, in conjunction with the very uniform water north of the Convergence, is further evidence for a strong southward movement of Subtropical Water.

On both the Agulhas and Slot lines the position of the Convergence was made more uncertain due to large eddies in the warmer water to the north. The stepwise decrease in temperature made it difficult to estimate the gradient, which was of the order of 3·3° C/deg. lat. for the Agulhas line and 4° C/deg. lat. for the Slot line. The salinity decreased from 35·35°/$_{oo}$ at 61 to 34·42°/$_{oo}$ at 62 on the Agulhas line and from 35·52°/$_{oo}$ at 49 to 33·76°/$_{oo}$ at 46 on the Slot line.

A large cyclonic eddy lay near station 48 (about 40° S, 45° E), and brought about a change in current direction (Fig. 2) and a small drop in surface temperature and salinity (Fig. 7). The surface water was greatly disturbed by the eddy, and irregular temperature variations with a range of 2·5° C were encountered while drifting on station 48. This eddy was also found by LE PICHON (1960), and is almost certainly brought about, as he suggests, by the junction of the Atlantic-Indian Ridge to the Madagascar Ridge here. A rough plot of the bottom, taken from soundings along the Slot line, was drawn in Figure 8 and the Atlantic-Indian Ridge can be seen at about 40° S with the Madagascar Ridge slightly to the North. The Rift Valley is also a notable feature of the section. Part of the salinity section (Fig. 19) has been entered in Figure 8 to show the eddy which lies just above the branching of the two ridges, and upwelling takes place in the region near station

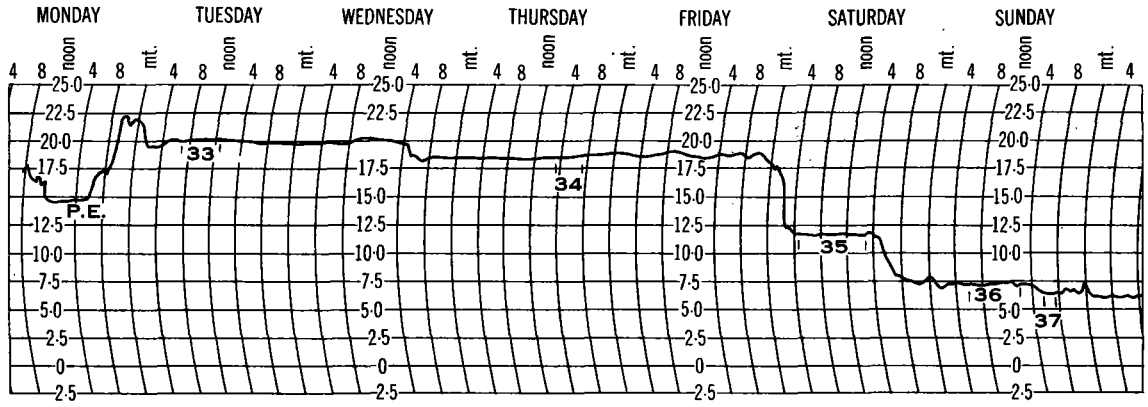

FIG. 5 THERMOGRAPH TRACE FROM PORT ELIZABETH TO STATION 37.

Trigsurvey 1965

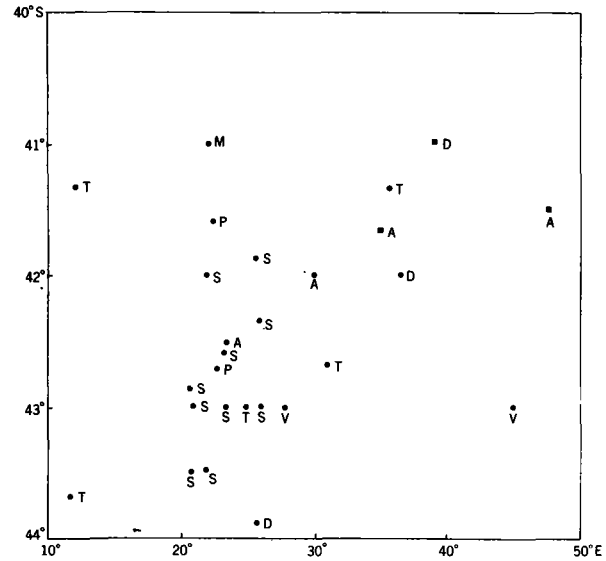

FIG. 6. POSITION OF SUBTROPICAL CONVERGENCE ACCORDING TO VARIOUS OBSERVATIONS.

A = Africana II; D = Discovery II; M = Meteor; P = Planet; S = Soya; V = Vema; T according to TALJAARD (1957)

Winter values are shown as squares and other seasons as circles

Trigsurvey 1965

48. This is a clear example of the bottom topography influencing the entire water column.

A strong cyclonic eddy was present on the Agulhas line at about 41° S, 21° E (See Figs. 2 and 7) and was responsible for the large temperature and salinity decrease at station 60. The presence of this eddy is also seen in the temperature diagrams of FUKASE (1962). The current chart suggests a surface velocity of about 1 knot in the eddy. From the sigma-t section (Fig. 26) it may be seen that the eddy form resembles that calculated for a cyclonic vortex in a two-layer ocean (DEFANT 1961), with the rotation increasing with depth to about 100 to 150 m., while below this, rotation decreases with depth. The upwelling in the centre of the vortex is very marked with an upward movement of about 700 m. present in the salinity section. The sharp fall in temperature and salinity and the sudden increase in oxygen content at the surface is also very well-marked (Fig. 7). The cause of the vortex is not apparent but it may be due to an isolated seamount not yet charted, or to the interaction of the Agulhas current with the West Wind Drift. Some indirect evidence of an eddy was found in the thermograph trace for the area near 41° S, 29° E. This eddy appeared as an intrusion of cold water near 40° S on the charts of DARBYSHIRE (1964).

In summary, the Convergence between 20° E and 50° E was found to lie at 42° S ±1°, moving to about 41° S in winter and to 43° S in summer. On crossing the Convergence from north to south temperature fell by as much as 11° C, salinity by 1·7‰, while oxygen content rose from 5 c.c./l. to 7 c.c./l., all within about 1° of latitude.

4.2.4 Sub-Antarctic Surface Water.—This water mass was comparatively uniform between stations 36 and 46, the variation in salinity being only 33·69 to 33·82‰ while temperatures ranged between 4·2° and 7·5° C. To the west of 37° E both temperature and salinity were appreciably higher and this is thought to be due to seasonal (autumn to winter) differences. A further contributory factor could be the seasonally increased strength of the south moving branch of the Agulhas current in this area which would tend to increase temperature and salinity by lateral mixing, thrusts of warm water forcing their way south through the Convergence. A T/S scatter diagram of all points in the Subantarctic region is shown in Figure 9.

Stations 62 and 64 had almost exactly the same temperature, salinity and oxygen, and it thus appeared that the surface water mass was common to these two stations. A large drop of approximately 2° C and 0·40‰ in salinity then took place and the current vector showed a westerly drift. DEACON (1937) showed the presence of a large cyclonic eddy in 46° to 48° S and 26° to 27° E, i.e. near to station 65, and it is very probable that the Agulhas line crossed the edge of this eddy and this gave rise to the sudden drop in surface temperature and salinity, the complex distribution of temperature and salinity in the deeper layers (see Figs. 16 and 21), and the fact that stations 65 and 66 were very similar in physical character. A further large decrease in temperature and salinity took place in the vicinity of station 67 and this is probably due to upwelling of deep water in the cyclonic vortex presumably formed when the West Wind Drift flows over the Atlantic-Indian Ridge here (see Section 4.6). Unfortunately no drift measurements are available due to adverse weather.

The Subantarctic Water showed a slight southerly drift for the area between the Subtropical Convergence and Marion Island and while the temperature decreased steadily southwards, the salinity remained almost constant at 33·80‰. This southerly drift, though slight, is in conflict with the general current charts for the area which indicate steady easterly drifts. A possible explanation for this unusual drift is the fact that only light northerly to easterly winds were experienced in this particular area during June (WEATHER BUREAU 1962) and that the absence of strong westerlies has weakened the West Wind Drift. On the Crozet Ridge the steady West Wind Drift again made itself felt, flowing east at ½ to 1 knot.

Station 41, north of the Crozet Ridge, was much warmer (6·3° C) than stations 40 (4·1° C) (at Marion Island) and 42 (5·1° C), the latter stations lying to the south of the Ridge. Stations 43, 44, 45 and 46, all of which are north of the Ridge, were in very much cooler water (3·9° to 4·7° C), and the coldest water at the surface on the two cruises was found at station 44 (off Possession Island). Further the temperature at 43° S, 35° E (Station 36) was 7·4° C, while at 43° S, 49° E (Station 46) the surface temperature was only 4·7° C, and the surface salinity was 0·05‰ lower at the latter station. The above temperature distribution in conjunction with the northerly drift shown between stations 44 and 47 indicates a northward flow of cold Subantarctic Water, probably occasioned by a northward movement of the Antarctic Convergence south of the Crozets. This may be anticipated on theoretical grounds—a true gradient current will deflect to the left as the sounding decreases (DEACON 1937) and in the case of the eastward flowing West Wind Drift, a northward movement is to be expected.

The strengthening of the West Wind Drift near 43° S, 50° E shown by the dynamic topography of LE PICHON (1960) is confirmed by the fairly strong (one knot) currents setting approximately north-east between stations 46 and 47 and by the sudden increase in temperature gradient. (See Figure 10, which shows the horizontal surface temperature distribution for the 1962 cruise only; seasonal variation made it very difficult to include the 1963 results.)

Thermoclines were almost completely absent in the Subantarctic Water, which was well-mixed

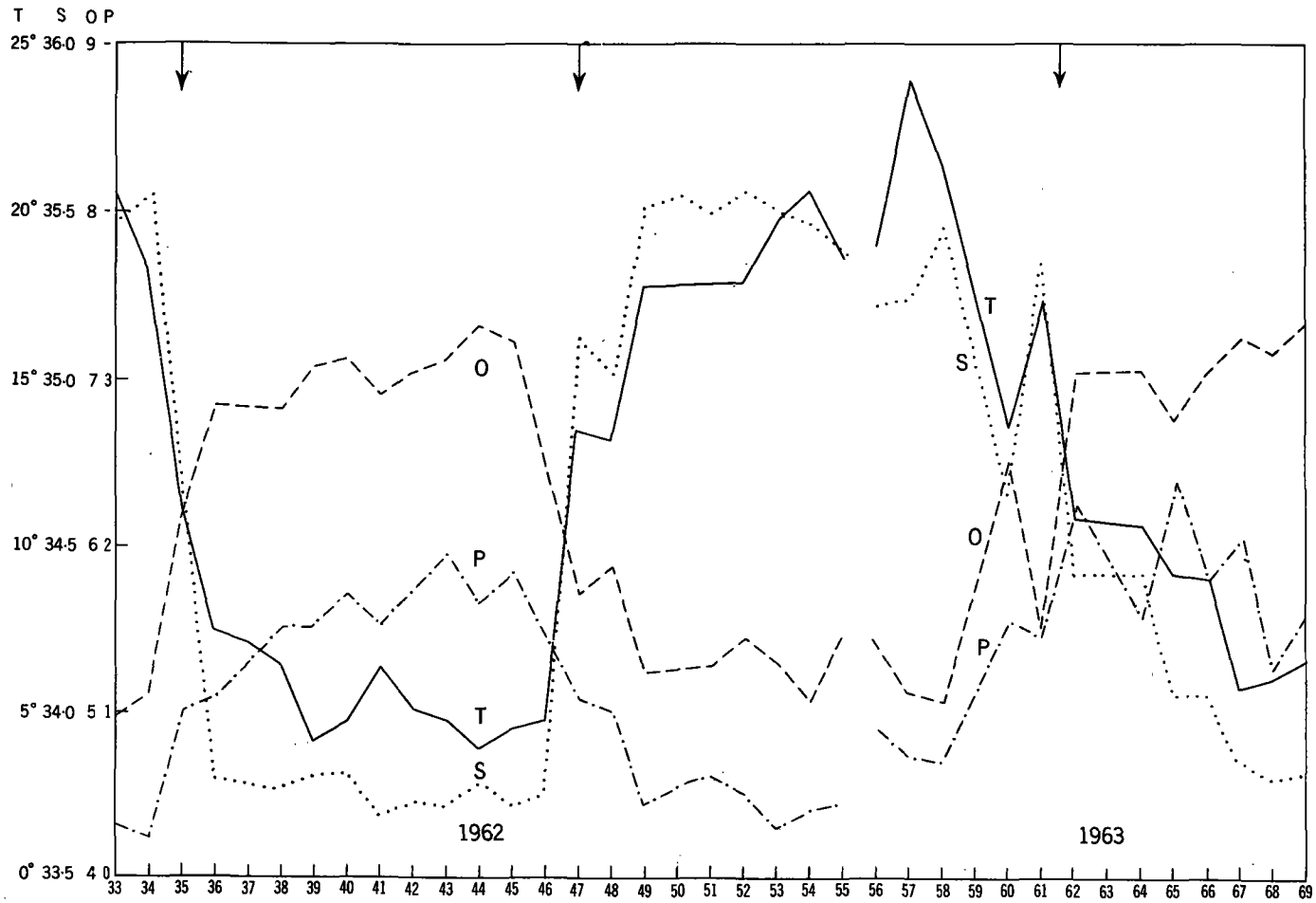

FIG. 7. SURFACE HYDROLOGICAL VARIABLES AT STATIONS 33 TO 69.

(T = Temperature; S = Salinity; O = Oxygen; P = Phosphate)

Arrows show the position of the Subtropical Convergence.

Trigsurvey 1965

throughout. Many slight temperature inversions associated with subsurface currents were found in this water, which appeared to be isothermal and isohaline to depths of about 60 to 100 m. in the west and to about 30 to 150 m. in the east. These differences in surface layer thickness may well be a seasonal effect, due to greater mixing in winter. (Only station 45 had a 30 m. thick surface layer and appears to be exceptional; the vast majority of stations had a surface layer 50 to 150 m. thick.)

It thus appeared that the Subantarctic Water was fairly uniform with temperature and salinity ranging round 5° C and 33·8°/$_{oo}$ respectively. The West Wind Drift was absent in the area between the Subtropical Convergence and Marion Island, but reappeared north of the Crozets. A tongue of cold, poorly saline water moving northwards over the eastern end of the Crozet Ridge was believed to have been caused by a northward thrust of the Antarctic Convergence.

4.3 Subsurface Water.

Subsurface currents were detected as subsurface salinity maxima. In the Subtropical Water north of the Subtropical Convergence, subsurface currents were only marked at stations 51, 54, 57 and 58. The latter three stations were near the Agulhas current system and the subsurface maximum salinity was considered to be brought about by sinking of the Subtropical Surface Water when it encounters the light, low salinity Tropical Water carried south in the Agulhas system. In all cases in which a subsurface salinity maximum was found in the area north of the Subtropical Convergence, including stations 1 to 32 of ORREN (1963), the salinity at the maximum layer and the corresponding temperature lay in the range given for Subtropical Surface Water in Figure 4. It appears that the northward moving Subtropical Water (Fig. 2) sinks beneath the Tropical Water and maintains the salinity maximum, mixing along its path with Tropical and Central Waters above and below respectively. Subtropical Water sinking beneath the Agulhas (Tropical) Water would also give a similar effect as it is swept southwards in the main stream. (Sigma-t sections indicate no change of direction of flow at the depth of the salinity maximum.) In general, the apparent lack of a winter subsurface current in the region from the Subtropical Convergence to about 33° S noted by ORREN (1963) was confirmed.

The subsurface current between stations 57 and 58 shows a decrease of oxygen content at the maximum salinity core from 5·09 c.c./l. at 58 to 4·52 c.c./l. at 57. It appears that the water at 57 is thus "older" than that at 58 and if the above description of the formation of this water is valid, the water at 57 would have been carried southwards in the Agulhas current and would thus be "older" than recently-sunk water at 58.

Irregular distribution of subsurface salinity noticed at stations 47, 48, 60 and 61 was related to eddy-induced circulation discussed below.

The Subantarctic Water showed signs of southward moving subsurface currents at most stations. In areas of intense vertical mixing (station 43) little subsurface current was detected and as there was an apparent salient of Antarctic Surface Water here, the mixed water present probably forms the source of the Antarctic Intermediate current.

The Subantarctic subsurface currents are believed to originate from mixed Subtropical and Subantarctic Water, which sinks at the Subtropical Convergence, with most of this mixed water sinking northwards as the Central Water and the remainder returning southwards, mixing strongly with Subantarctic Surface and Antarctic Intermediate Waters.

The clearest evidence for the southward movement of the subsurface current, apart from the deduction of southward motion from the observed maximum salinity layer between two low salinity layers, may be found in the oxygen distribution at the maximum salinity core of the current on the Agulhas line. At stations 62, 64 and 65 the oxygen content was 5·86, 5·76 and 5·31 c.c./l. respectively, showing a loss of oxygen southwards. In most cases the subsurface current also appeared as a temperature inversion on the bathythermograph slides.

Along the Agulhas line near station 61 Subtropical Water mixes both with upwelled Antarctic Intermediate Water (rising in the eddy) and Subantarctic Surface Water. This mixed water then sinks and the southward returning part extends as a high salinity (34·4 to 34·5°/$_{oo}$) tongue from stations 62 to 65 at 150 to 250 m. As the water proceeds to the south the salinity maximum is rapidly destroyed by mixing, but is still detected at 250 to 275 m. at stations 66 to 68 (Figs. 43, 44, 45) along about 47° S. The eddy near station 65 (see Section 4.2.4.) caused remarkable subsurface conditions and three weak northward moving currents alternated with three moving south (Fig. 42). The most marked southward moving current at 260 m. was probably the southward extending general subsurface current. The complex array of currents here must produce much turbulent mixing and the observed flow is probably subject to large fluctuations. The current along this line was of a slightly greater salinity than that along the Crozet line—presumably a seasonal variation.

A similar mechanism of sinking and southward movement applied to the Marion line. The mixed water sinks between stations 35 and 36 (Figs. 12, 17) and moves southwards at 250 to 300 m., the maximum salinity rapidly diminishing southwards near station 38. The T/S diagram for station 38 (Fig. 31) indicates that the current here is probably composed of core water at station 36 mixed with Antarctic Intermediate and, to a lesser extent, Subantarctic Surface Water from station 38. Inspection of the sigma-t depth curve for station 38

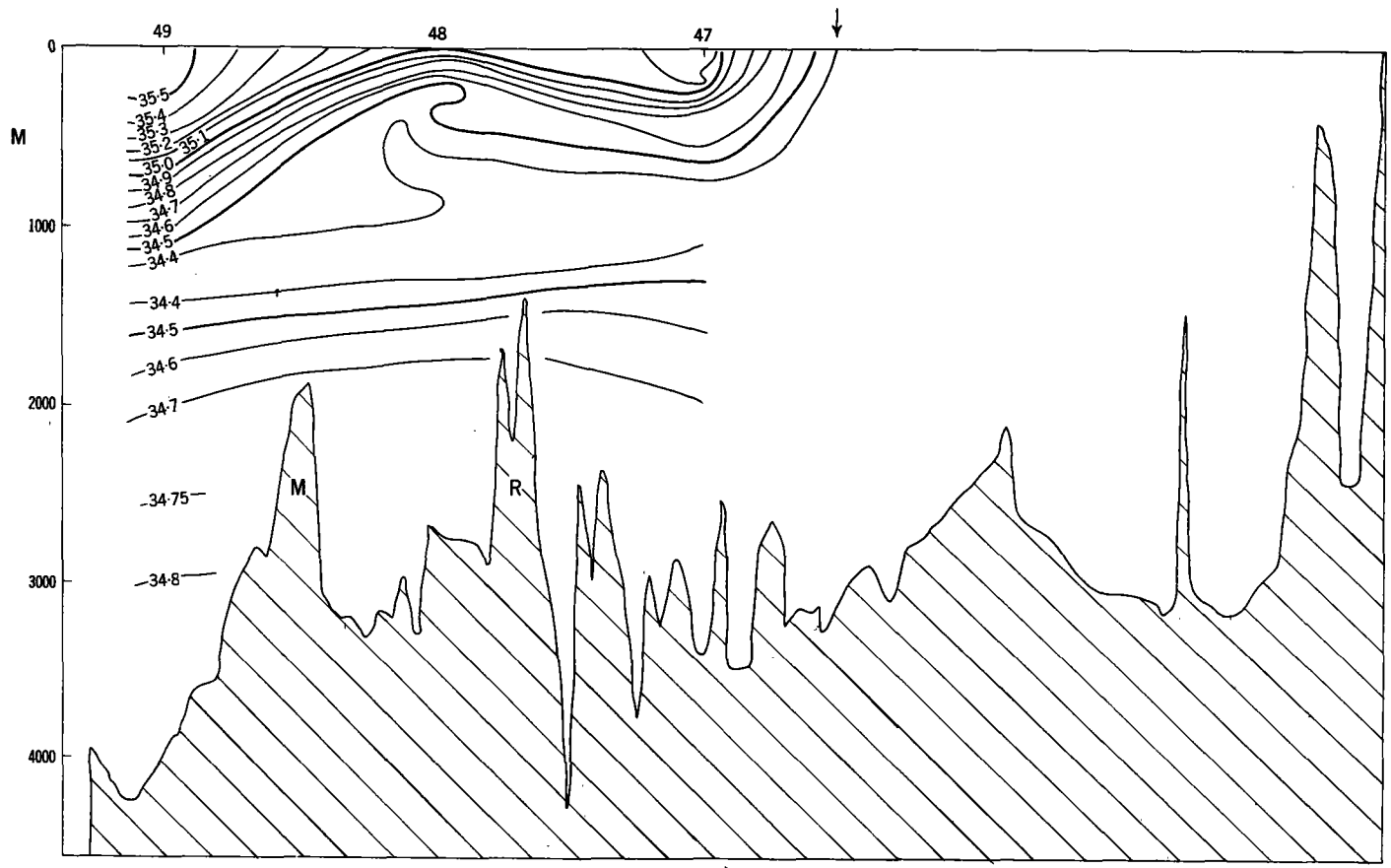

FIG. 8. SALINITY DISTRIBUTION AT SELECTED STATIONS ALONG THE SLOT LINE.
(M = Madagascar Ridge; R = Atlantic- Indian Ridge) Arrow indicates position of Subtropical Convergence.

Trigsurvey 1965

shows maximum vertical stability at about 150 m., making mixing with deeper layers easier than with the upper layers.

The Crozet Ridge forces the Deep Water nearer the surface along the Crozet line and brings about intensive mixing in the upper layers. Stations 41 and 42 (Figs. 32, 33) show the usual fairly weak subsurface current as observed along the Agulhas line (stations 66 to 68), but station 43 shows almost no subsurface current. Here the Subsurface, Surface and Intermediate Water lose their identity and become one strongly mixed layer, which is probably the source water of the Intermediate layer further north.

Between stations 45 and 49 across the Subtropical Convergence on the Slot line a most interesting cell-like circulation is apparent. Station 45 shows the usual weak subsurface current at about 300 m. caused by the southward return of water sunk at the Convergence between stations 46 and 47. The mixed water which sinks at the Convergence moves north at about 340 m. to near station 48 where it mixes with Antarctic Intermediate Water, part returning south at 440 m. to the Convergence, where it mixes with the sinking water once more. The mixed Subtropical and upwelled Antarctic Intermediate Waters sink to form the Central Water north of station 48. This indicates that intense turbulent mixing must occur between the eddy and the Convergence due to the conflicting currents. A schematic outline of these processes is given in Figure 11.

A similar circulation may be seen on the Agulhas line with station 60 corresponding to station 49 in Figure 11 and 62 corresponding to 45. Station 61 would lie just to the south of station 48 in Figure 11. The intense turbulence at station 62 is probably caused by the close proximity of the Convergence. Some sinking water at station 60 apparently turns back at about 400 m., but the remainder sinks northwards as Central Water.

The intense mixing to which the Antarctic Intermediate Water is subjected is no doubt responsible for the large increase in the core salinity (34·2‰ to 34·5‰) in the Convergence region.

It was thus apparent that subsurface currents are absent in winter in the area between 34° S and 42° S in the Subtropical Water. The marked subsurface salinity maxima in the Agulhas Water were probably brought about by sinking of the denser Subtropical Water beneath the light Tropical Water. Well-developed southward moving subsurface currents were present in Subantarctic regions and probably originated in the mixing region of the Subtropical Convergence.

4.4 Central Water.

The Central Water is found in the entire Subtropical region as a layer of linear T/S relation (Fig. 3) separating the Subsurface from the Intermediate layers, that is between about 300 m. and 800 m. This water mass is formed by the sinking and northward spreading of mixed Subtropical and Subantarctic Water masses in the Subtropical Convergence region. The centre of the water mass may be generally deduced to lie at 11° C, 35·0‰ (see Fig. 11 of ORREN 1963). The oxygen content at this level varied from 4·62 to 5·20 c.c./l., most values lying in the range 4·9 to 5·2 c.c./l. Data for stations 1 to 32 have again been included. The low values of 4·6 to 4·9 c.c./l. were obtained in the Moçambique Channel and Reunion Basin areas where North Indian Deep Water, probably influences oxygen concentration.

Central Water below 300 m. has a general T/S line which lies wholly in the space enclosed by lines joining the Subantarctic (taken as 7°, 33·8‰), Antarctic Intermediate (taken as 3·5°, 34·15‰ near the Subtropical Convergence), and Subtropical (15°, 35·5‰) Water types, showing that these water masses are the most probable source waters.

The sinking and sluggish northward motion of the Central Water may be seen from Table I, showing the distribution of oxygen on sigma-t surfaces along the Agulhas and Slot lines. Too few stations were available for this purpose on the Marion line. Although in all cases there is an initial decrease on moving northwards, the oxygen is fairly constant in the Central Water decreasing slightly northwards. Three of the four *Africana II* crossings of the Subtropical Convergence showed vortical disturbances to the north of the Convergence. Published sections (DEACON 1957: Fig. 15 and sections 7 and 10) also show the presence of cyclonic eddies to the north of the Convergence, and it appears likely that the large eddies, mixing upwelled Intermediate Water with the upper layers, form the main source of the Central Water (see also DEFANT 1961).

The T/S diagram of station 57 (Fig. 38) shows an intrusion of a different water mass at about 600 m. The intrusion is also visible in the Agulhas line salinity section (Fig. 21). The temperature and salinity characters of the upper water mass agree with the general Indian Ocean Central Water but the lower mass (below 600 m.) shows characteristics more in keeping with South Atlantic Central Water (ORREN 1963: Fig. 12). To test the possibility of an eastward flow of South Atlantic Central Water around the Agulhas Bank the Central Waters of both Atlantic and Indian Oceans were compared with regard to oxygen content. The level chosen was that of the 35‰ isohaline as this lies at about 600 m. generally. As mentioned above, the Indian Ocean oxygen range was 4·9 to 5·2 c.c./l. Oxygen values in South Central Water at 35‰ salinity were taken from *Discovery* stations D 673 to 679, D 1170 to 1175, and D 2042 to 2048, a total of 15 stations, and the measured range was from ±4·3 to ±4·8 c.c./l. It thus appears that

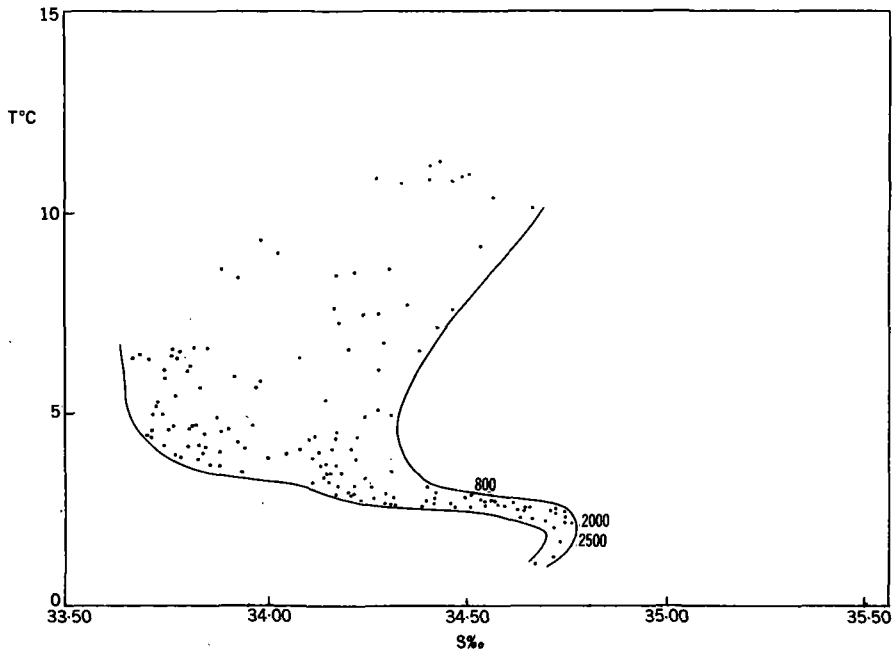

FIG. 9. T/S SCATTER DIAGRAM OF SUBANTARCTIC WATER

Trigsurvey 1965

South Atlantic Central Water has a lower oxygen content than South Indian Central Water. On inspection of oxygen data for station 57 it was noted that a sudden decrease of $\pm 0 \cdot 5$ c.c./l. took place between 560 and 680 m., oxygen values decreasing to 4·34 to 4·40 c.c./l. It is very likely therefore that an intruding current of South Atlantic Central Water flows east in this region. The eastward flow of Central Water shown by the sigma-t section (Fig. 26) cannot be positively identified as Indian or Atlantic Water by the above method as the oxygen content at $35 \cdot 0^{\circ}/_{\circ\circ}$ was about 4·8 to 4·9 c.c./l.—intermediate between Atlantic and Indian Ocean values. The question now arises as to whether the Antarctic Intermediate Water here also has an eastward component in common with the known eastward flow of Deep Water from the Atlantic to the Indian Ocean, and this will be considered below.

The Central Water thus originates from sinking of mixed Subtropical Water north of the Subtropical Convergence and moves northwards at 200—800 m., mixing with high salinity subsurface water and low salinity Antarctic Intermediate Water along its path.

4.5 Antarctic Intermediate Water.

Antarctic Intermediate Water, identified by its minimum salinity core, was found in the entire area studied and lay at 300 to 400 m. in the Subantarctic region, then sinking rapidly northwards to 900 to 1,300 m. north of the Convergence. In the Subtropical Region this water mass then rose slightly northwards, and part of the water appears to turn round and return southwards in the lower levels of the Agulhas current.

Along the Agulhas line from stations 56 to 58 the sigma-t section (Fig. 26) shows the water to have a strong south-westerly movement even at 2,000 m. The minimum salinity water in this region must accordingly be moving southwards and since it cannot originate in the Tropical or Subtropical regions, the water must be returning Antarctic Intermediate Water. Strong east-flowing water is present between 58 and 61 from the sigma-t sections and the high oxygen at the salinity minimum shows that this water is apparently flowing from the South Atlantic into the Indian Ocean. This flow could be traced by the progressive decrease of oxygen and increase of salinity at the salinity minimum (Table II). Since bad weather along the Marion and Port Elizabeth lines prevented deep sampling, and the sigma-t sections thus do not show much detail of the deep movements, use was made of data collected by S.A.S. *Natal* during May and July, 1962 in the same area (SHIPLEY and ZOUTENDYK 1964). Their sigma-t sections both along the Marion and near the Port Elizabeth line ("Natal line B") (Figs. 27, 28) show three parallel zones of movement within the Antarctic Intermediate Water, namely (1) A strong south-westward flow in the inshore core water, (2) A northward flowing counter current off shore of this, (3) A southward flowing current to seaward of (2). The eddy centred on the Moçambique Terrace just north of the "Natal line B" caused southward thrusts of core water near station NIOE 11, and this flow was probably strengthened by additional water turning back on encountering shallower depths.

In the Natal Deep and Natal Basin strong northerly flows were noted and it appears that this water turns round in the Moçambique Channel area and returns south again. Some evidence for this appears in the two separated "loops" of minimum salinity along the Lourenço Marques line (ORREN 1963: Fig. 20) while the sections of MENACHÉ (1961 and 1963) show that Antarctic Intermediate Water rapidly loses its identity on encountering the North Indian Deep Water at about 24° S in the Moçambique Channel, indicating a much weakened northward flow here. Table II shows the oxygen at the minimum salinity core, and Table III shows the northward increase in salinity and decrease in oxygen at the core along a section through stations 60, 35 and 48 and stations 29, 11 and 7 of the previous cruise (ORREN 1963). Southwestward flowing water at stations NIOE 78, 15 and 16, that is in the deeper layers of the Agulhas current, has a high salinity and low oxygen as would be expected if the water is returning south. Some southward movement occurs along the Marion line between NIOE 80 and 82 and it appears that the south-westward flow is reinforced by mixing with the northward moving Intermediate Water near Cape Agulhas, since the oxygen at stations 57 and 58 is rather higher and the salinity lower than expected, although these values differ markedly from the low salinity, high oxygen north-flowing current near station 60.

Some water from the strong flow in the Natal Basin (near station 50) appears to be deflected by the Atlantic-Indian Ridge and returns to some extent between 47 and 48 (Fig. 24) in the deeper layers of the eddy.

An interesting point arising from the strong southwesterly flow of the Agulhas current minimum salinity layer is the fate of this current on encountering the vigorously northward flowing South Atlantic Antarctic Intermediate Water. It may be expected that large eddies would form and the resultant upwelling zones be rich in marine life. It will be of interest to see if further cruises in the South Atlantic show any signs of these eddy zones, and it is considered that the unpredictable currents and eddies south and west of Cape Point may well be caused by this encounter of two strong water masses at both surface and intermediate levels.

The above findings are in general agreement with the dynamic topography of the 1,000 db. surface put forward by VISSER and VAN NIEKERK (1965), although this surface lies about 600 m. below the minimum salinity layer in the south and

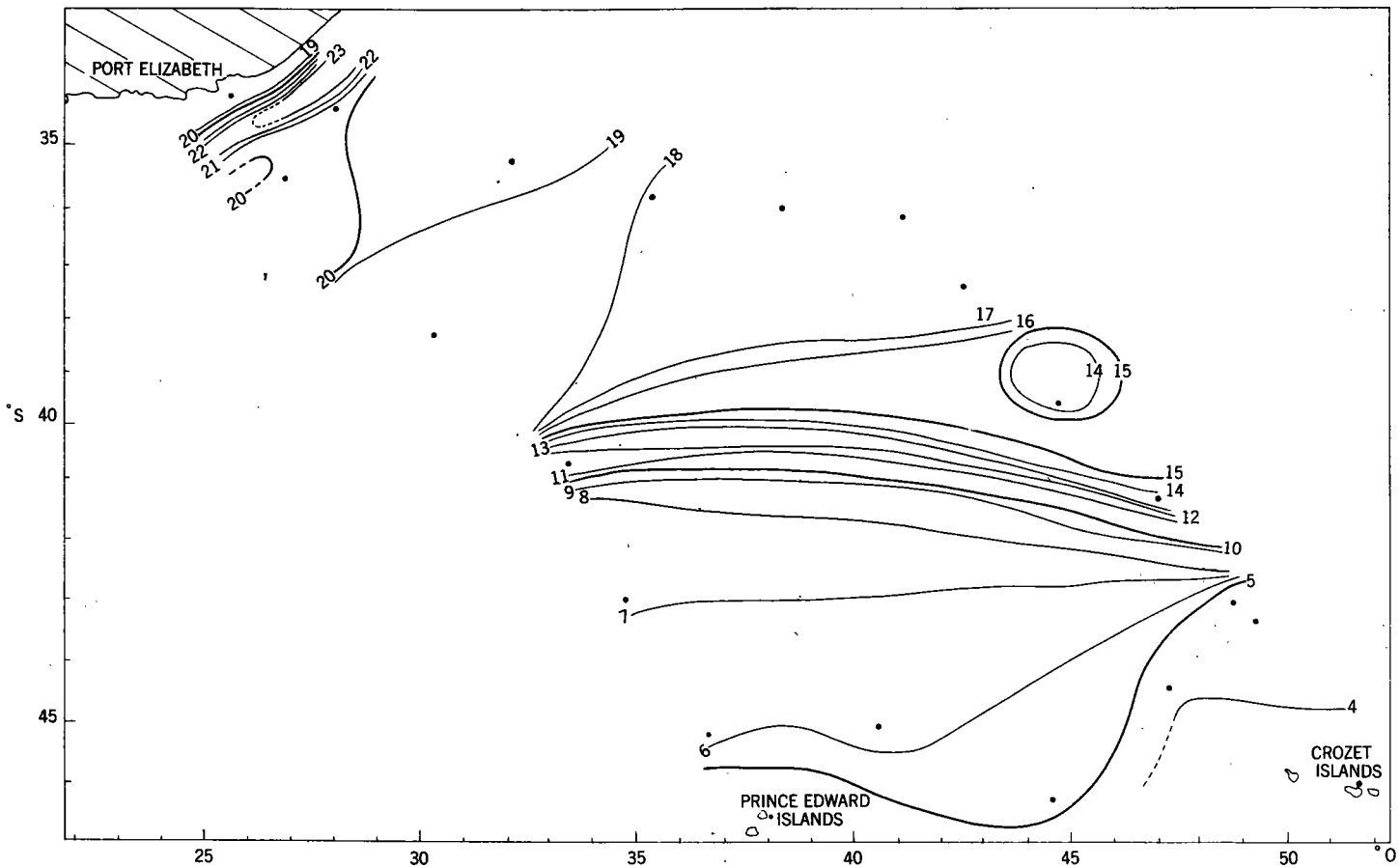

FIG. 10. SURFACE TEMPERATURE IN THE SOUTH-WEST INDIAN OCEAN DURING 1962

Trigsurvey 1965

about 300 m. above it in the north .These authors' choice of 2,000 db. as their reference level also introduces some further difficulty in interpretation since the sigma-t sections at 2,000 m. in this report show comparatively strong current movement at this level in much of the area, especially in the Agulhas current system.

4.6 Deep Water.

The generally sluggish flow and small variation in conservative properties in the Deep Water raise difficulties in interpreting the flow of this water mass. The discussion below must therefore be considered to be of a preliminary nature—further actual measurement of the deep layer movements is a requirement which should be borne in mind in future research cruises.

The Deep Water salinity maximum lay at 2,500 to 3,000 m. over the greater part of the area, and since relatively few samples deeper than 3,000 m. were obtained, the lack of observations further limits detailed conclusions.

The T/S diagrams for stations 66 and 68 show an intermediate salinity minimum in the Deep Water at depths of about 2,400 m. It is felt that this is due to upwelling of Antarctic Bottom Water on the Atlantic-Indian Ridge (sill depth about 2,000 m.) and the upwelled water then mixes with the Deep Water and forms a low salinity layer.

From the sigma-t sections (Fig. 22 to 26), a strong current of North Atlantic Deep Water of salinity near 34·80‰ flows from the Atlantic to the Indian Ocean across the Agulhas line. This flow then apparently splits on meeting the Agulhas Plateau—one stream follows the coast just off the outer edge of the Agulhas current, while the other flows up the deep Natal Basin. A further flow of water appears to be deflected completely by the Agulhas Plateau and returns to the west near station 62.

The inshore flow is seen between NIOE 79 and NIOE 80 (Fig. 27). To seaward of this there is a weaker return flow, which is perhaps water deflected from the main Natal Basin flow by the Moçambique Terrace and outlying ridges. The northward moving current in the Natal Basin appears to be concentrated more to the eastern side (Fig. 25). It appears likely that the northward moving water meets North Indian Deep Water in the Moçambique Channel, mixes, and returns south in the western part of the region (LE PICHON 1960). Some water apparently flows over the 2,800 m. sill joining the Natal and Reunion Basins near station 49 (Fig. 24) and further flow into the Reunion Basin may take place near station 10 (ORREN 1963: Fig. 20). There is some indication that a limited return flow from the Reunion Basin into the Natal Basin takes place near station 50 (Fig. 24).

The flow of Deep Water in the Agulhas current itself cannot be easily elucidated. Only station NIOE 15 showed a southward movement in the Deep Water under the Agulhas current and no other deep records are available for this region. The difficulties of working deep casts of sampling bottles in the strong surface current and inclement weather of the Agulhas current region are probably responsible for this. It is considered likely that the inshore stream of Deep Water is deflected by the Moçambique Terrace and returns south with some admixture of North Indian Deep Water, flowing in the channel between the Moçambique Terrace and the coast as a deep narrow southward moving current under the Agulhas current.

Further evidence for the above scheme of water movements may be gleaned from a study of the dissolved oxygen content at the salinity maximum (Table IV). All oxygen values along the Agulhas line are in excess of 4·7 c.c./l. with the important exception of station 57 (4·29 c.c./l.). The stations situated in the Natal Basin (35, 36, 49, 50 and 51 and also 8, 9, 10, 27, 29 and 30 of ORREN 1963), with the exception of station 50, all have oxygen values greater than 4·6 c.c./l. Low oxygen (less than 4·3 c.c./l.) was found at stations 47 and 50 and at NIOE 11, 15, 69 and 72.

The general northward flow may be demonstrated by examining stations 61, 35 and 51, which lie approximately along the axis of the Natal Basin; the oxygen values at the maximum salinity level are 5·14, 4·68 and 4·62 c.c./l. respectively.

The low oxygen recorded at station 50, lying on the eastern edge of the Natal Basin, may perhaps be brought about by traces of poorly oxygenated North Indian Deep Water moving over the 2,800 m. sill from the Reunion Basin. LE PICHON (1960) has shown that Reunion Basin Deep Water has about 4·0 c.c./l. oxygen at the salinity maximum, and this compares favourably with the value of 4·12 c.c./l. at station 50.

The inshore work of S.A.S. *Natal* (SHIPLEY and ZOUTENDYK 1964) yields an insight into near shore movements of the Deep Water. Figure 27 shows a section of sigma-t from NIOE 78 to NIOE 82, which line of stations was completed within a few weeks of the *Africana* cruise. Their line is essentially identical to the "Marion line" and stations 33 and 34 are marked on the section. Strong northward components of flow are evident at 2,000 to 3,000 m. from NIOE 79 to 80, and southward motion from NIOE 80 to 82. In agreement with this, the core oxygen at NIOE 79 (5·01 c.c./l.) is higher than for NIOE 80 or 82, the latter being 4·6 to 4·8 c.c./l. (Table IV). This low oxygen water may have been turned back by the Moçambique Terrace and is mixing with water flowing north near NIOE 79.

"Natal line B" data are plotted in Figure 28. This line extends 500 miles south-east of Port St. Johns. Stations NIOE 14 and 15 show southward flow at 2,000 m. under the Agulhas current with very low oxygen at NIOE 15. The low oxygen at station NIOE 11 is probably due to North Indian Deep Water penetrating southwards along the eastern

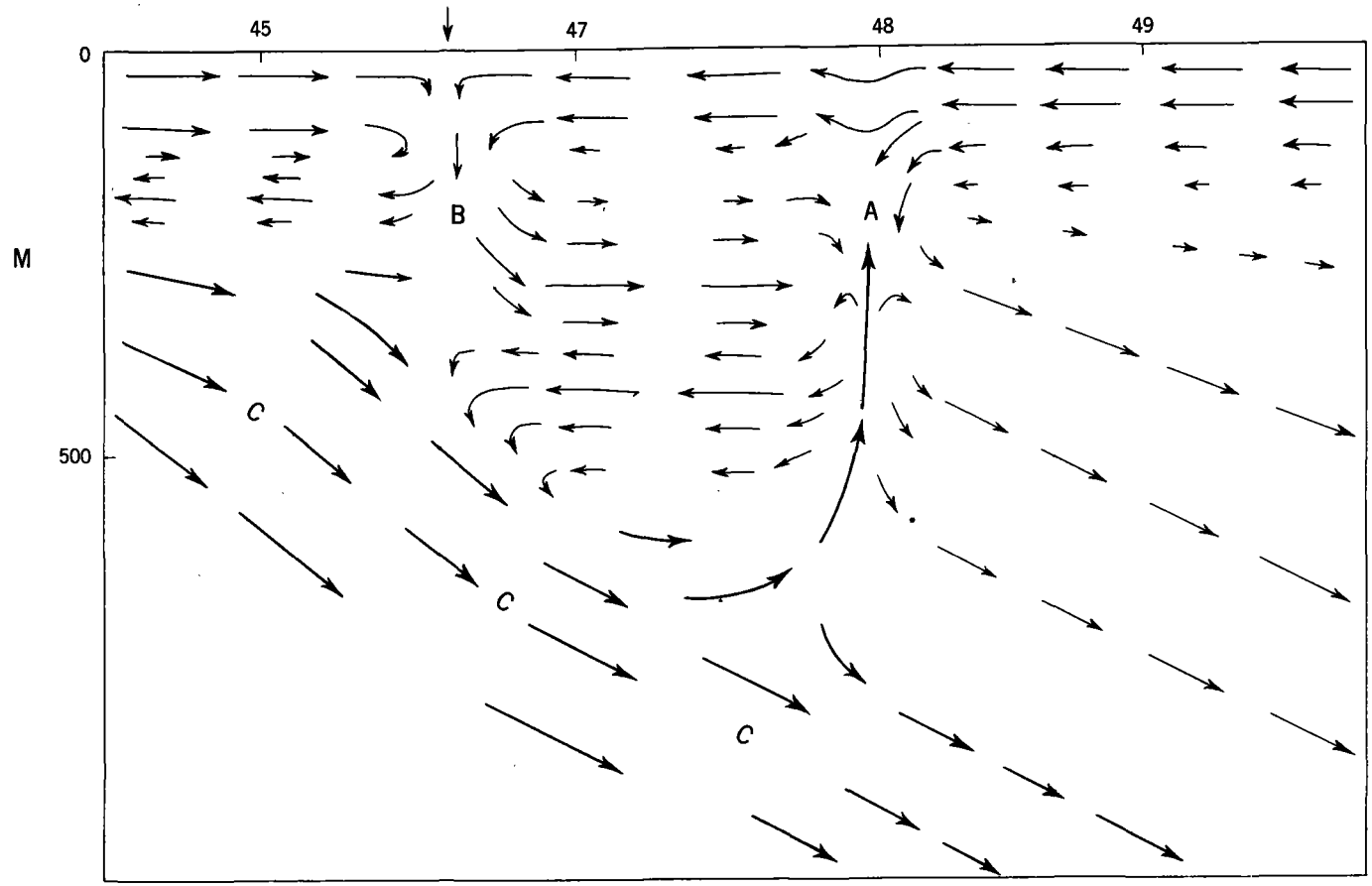

FIG. 11. SCHEMATIC OUTLINE OF CIRCULATION ON THE SLOT LINE.

(A = Eddy Zone in which upwelled Antarctic Intermediate Water mixes with Surface and Sub-surface Water.
B = Sinking Zone at convergence (marked with arrow).
C = Core of the Antarctic Intermediate Water).

Trigsurvey 1965

edge of the Moçambique Terrace, i.e. the western edge of the Natal Basin. ORREN (1963) has shown that traces of North Indian Deep Water are present at the edge of the shelf off Lourenço Marques at *c.* 1,600 m. and the low oxygen values here indicate further southward penetration of this water mass. The low oxygen in the deep layers of the Agulhas current (NIOE 15) may be brought about by North Indian Deep Water flowing over the sill joining the Moçambique Terrace to the coast and then mixing with the returning North Atlantic Deep Water. These low values are apparently maintained as far south as Cape Agulhas, for example at station 57.

It thus appears that the Deep Water under the Agulhas current is slowly moving southwards and is composed of returning North Atlantic Deep Water mixed with North Indian Deep Water.

From the above discussion (see Sections 4.5 and 4.6), it may be noted that southward components of flow are present at all depths sampled in the Agulhas current, which thus apparently extends from the surface to at least 3,500 m. Recent studies of the Gulf Stream (FUGLISTER 1963) have shown that this current extends to at least 3,500 m. and no "level of no motion" was found. Similar conditions seem to apply to the Agulhas current, but actual measurements of deep currents would be required to confirm these findings.

Lack of samples deeper than 3,000 m. has precluded any discussion of Bottom Water.

5. ACKNOWLEDGEMENTS

The author would like to thank the Director of Sea Fisheries, Mr. B. v. D. de Jager and the Assistant Director, Mr. R. W. Rand, for their critical reading of the manuscript and helpful advice. Further useful criticism was gratefully accepted from my colleagues at the Division.

Thanks are also due to Messrs. Mostert, Campbell and Paterson for help in collecting the data, and I should also like to thank Captain J. D. Richardson of R.S. *Africana II* for his surface drift computations.

6. LITERATURE CITED

DARBYSHIRE, J., 1964.—A Hydrological Investigation of the Agulhas Current area. *Deep Sea Res.*, 11 (5): 781.

DISCOVERY COMMITTEE, 1941.—*Discovery Rep.*, 21, 24.

DEACON, G. E. R., 1933.—A General Account of the Hydrology of the South Atlantic Ocean. *Discovery Rep.*, 7: 171—238.

DEACON, G. E. R., 1937.—The Hydrology of the Southern Ocean, *Discovery Rep.*, 15: 1—123.

DEFANT, A., 1961.—*Physical Oceanography* Vol. 1, London.

FUGLISTER, F. C., 1963.—Gulf Stream 1960. *Progress in Oceanography* 1, Pergamon Press.

FUKASE, S., 1962.—Oceanographic Condition of Surface Water between South Africa and Antarctica, *Oceanography Met., Nagasaki*, 12: 53.

GRIFFITHS, R. C., 1962.—Studies of oceanic fronts in the mouth of the Gulf of California. *FAO. Fish. Rep.*, (6), Vol. 3: 1583—1605.

HORI, S., 1962.—Preliminary Report of the Oceanographical Observations of the Fifth Japanese Antarctic Research Expedition (1960 to 1961). *Antarctic Rec.*, 14: 1182—1191.

LE PICHON, X., 1960.—The Deep Water Circulation in the Southwest Indian Ocean. *J. Geophys. Res.*, 65 (12): 4061—4074.

MENACHÉ, M., 1961.—Découverte d'un phénomène de remontée d'eaux profondes au Sud du Canal de Mozambique. *Mém. Inst. Scient. Madagascar*, Serie F, Tome IV: 167—173.

MENACHÉ, M., 1963.—Première campagne océanographique du "Commandant Robert Giraud" en Canal de Mozambique. *Cah. Oceanogr.*, 15 (4): 224—235.

MICHAELIS, G., 1923.—Die Wasserbewegung an der Oberfläche des Indischen Ozeans im Januar und Juli. *Veröff. Inst. Meeresk. Univ. Berl.*, Heft 8: 1—32.

ORREN, M. J., 1963.—Hydrological Observations in the South West Indian Ocean. *Invest. Rep. Div. Sea Fish. S. Afr.*, 45: 1—61.

SHIPLEY, A. M. and P. ZOUTENDYK, 1964.—Hydrographic and Plankton data collected in the South West Indian Ocean during the SCOR International Indian Ocean Expedition, 1962—1963. *Univ. Cape Town, Inst. Oceanography, Data Report* 2: 210 pp.

SIMPSON, E. S. W., 1964.—A new world of marine science awaits research. *Optima*, June 1964: 68—75.

TALJAARD, J. J., 1957.—Subtropical Convergence in the South Atlantic and Indian Oceans. *Weather Bureau News Letter* 99, *Pretoria.*

VISSER, G. A. and M. M. VAN NIEKERK, 1965.—Currents and Water Masses at 1,000, 1,500 and 3,000 m. in the South West Indian Ocean. *Invest. Rep. Div. Sea Fish. S. Afr.*, 52: 1—20.

WEATHER BUREAU, 1962.—*Daily weather bulletin for the month June 1962.* Weather Bureau, Department of Transport, Pretoria.

TABLE 1: DISTRIBUTION OF OXYGEN ON SIGMA-T SURFACES 26·4, 26·6 AND 26·8 FOR SELECTED STATIONS

STATION	56	57	58	60	48	49	50	54
Oxygen at sigma-t = 26·4	(4·9)	4·9	4·8	6·4	5·9	4·7	4·9	4·8
Oxygen at sigma-t = 26·6	4·6	4·9	4·9	6·2	5·4	4·8	4·8	4·8
Oxygen at sigma-t = 26·8	4·7	4·8	4·8	5·8	(5·6)	4·9	4·9	4·8

TABLE II: DISTRIBUTION OF OXYGEN AT THE MINIMUM SALINITY LEVEL, INCLUDING DATA FROM SHIPLEY AND ZOUTENDYK (1964) AND ORREN (1963)

Station	Oxygen at Salinity Minimum c.c./l.	Minimum Salinity °/₀₀	Station (NIOE)	Oxygen at Salinity Minimum c.c./l.	Minimum Salinity °/₀₀
34	5·0	34·42	11	4·1	34·56
35	5·0	34·28	12	4·4	34·30
47	4·6	34·35	13	4·3	34·42
48	4·9	34·32	14	±3·8	34·73
49	4·7	34·37	15	3·7	34·48
50	4·5	34·39	16	3·5	34·56
51	4·6	34·36	67	4·0	34·43
54	4·3	34·53	68	4·3	34·44
56	±4·1	34·40	69	3·6	34·44
57	4·4	34·41	70	4·0	34·44
58	4·6	34·47	71	4·1	34·81
60	5·6	34·24	72	3·6	34·35
61	3·8	34·55	73	3·6	34·60
62	5·3	34·09	78	3·3	34·56
64	5·9	34·17	79	4·3	34·48
65	6·1	34·18	80	4·1	34·44
66	5·8	34·21	81	4·2	34·48
67	±6·5	34·12	82	3·9	34·56
68	6·4	34·09			
28	4·6	34·40			
29	4·3	34·44			
30	4·2	34·46			

TABLE III: DISTRIBUTION OF OXYGEN AT THE MINIMUM SALINITY LEVEL ALONG SELECTED STATIONS IN THE ANTARCTIC INTERMEDIATE WATER, INCLUDING DATA FROM ORREN (1963)

Station	Minimum Salinity °/₀₀	Oxygen c.c./l.
60	34·24	5·6
35	34·28	5·0
48	34·32	4·9
29	34·44	4·3
11	34·49	3·8
7	34·51	3·6

TABLE IV: DISTRIBUTION OF OXYGEN AND TEMPERATURE AT THE MAXIMUM SALINITY LEVEL IN THE DEEP WATER, INCLUDING DATA FROM SHIPLEY AND ZOUTENDYK (1964) AND ORREN (1963)

Station	Oxygen at Salinity Maximum c.c./l.	Temperature at Salinity Maximum °C	Maximum Salinity °/₀₀	Station (NIOE)	Oxygen at Salinity Maximum c.c./l.	Temperature at Salinity Maximum °C	Maximum Salinity °/₀₀
35	4·68	2·47	34·78	11	3·68—3·72	2·36—3·43	34·84
36	4·61	2·33	34·79	12	4·51	2·30—2·36	34·82
38	4·50	2·27	34·75*	13	4·30	2·13	34·82*
43	4·38	2·06	34·75*	14	4·49	2·31	34·84
45	4·86	2·04	34·76*	15	3·89	2·34	34·85*
47	4·26	2·48	34·71*	67	4·52	2·31	34·82
48	4·57	2·37	34·74*	68	4·65	2·28	34·82*
49	4·71	2·24	34·80*	69	3·93	2·57	34·78*
50	4·12	2·50	34·79	70	4·35	2·29	34·83*
51	4·62	2·64	34·78	72	3·88	2·77	34·76*
54	4·94	2·39	34·81	79	5·01	1·89	34·84*
57	4·29	2·77	34·67*	80	4·62	2·11	34·85*
58	4·84—4·94	2·50—2·71	34·77	81	4·83	2·52	34·84*
60	4·74—4·86	2·61	34·77	82	4·81—4·86	2·54—2·65	34·88
61	5·14	2·46	34·81				
62	5·09	2·17	34·77				
64	4·64—4·99	2·51—2·61	34·73				
66	4·69	2·56	34·73				
8	4·67	2·16	34·84				
9	4·67	2·19	34·77*				
10	4·57—4·89	1·72—2·31	34·79				
27	4·48—4·65	1·62—2·36	34·74				
29	4·84	2·31	34·82				
30	4·96	2·32	34·81				

* Indicates deepest sample obtained—may not necessarily be a salinity maximum but is close to it.

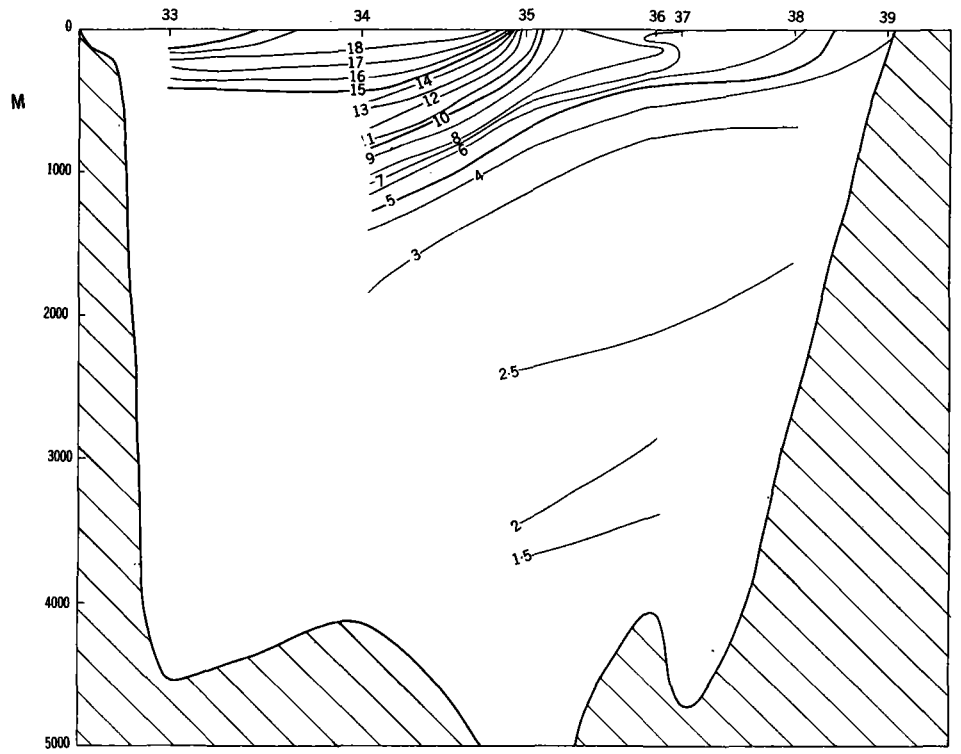

FIG. 12. TEMPERATURE DISTRIBUTION ALONG THE MARION LINE.

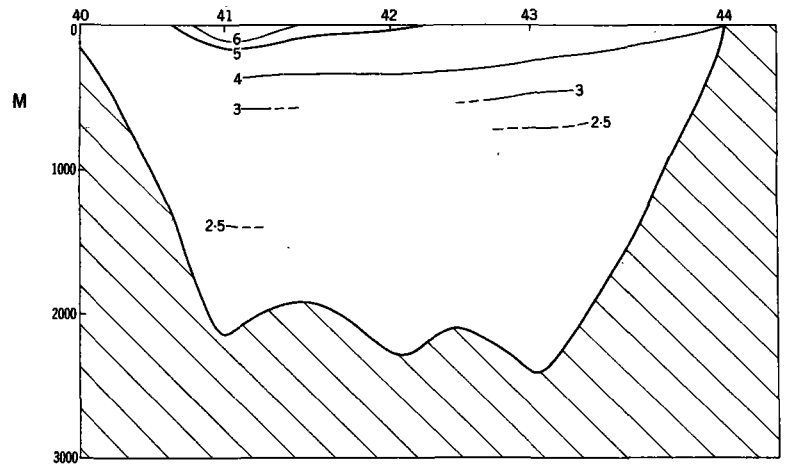

FIG. 13. TEMPERATURE DISTRIBUTION ALONG THE CROZET LINE.

Tri... ...ey 1965

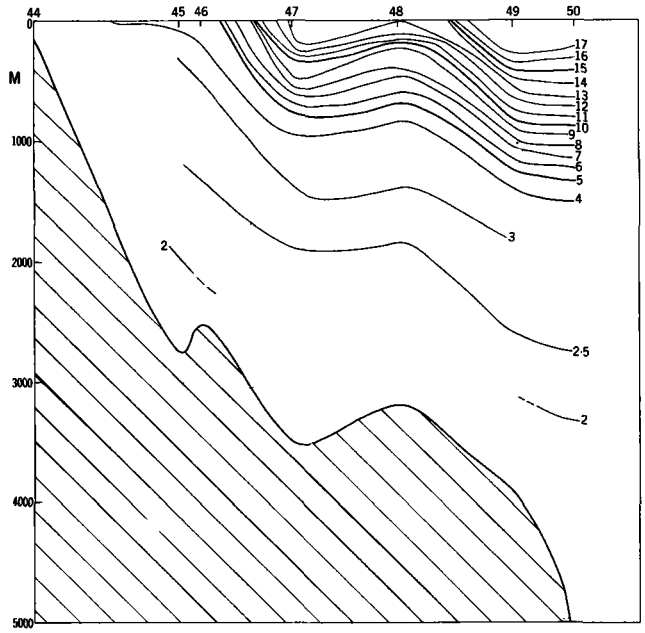

FIG. 14. TEMPERATURE DISTRIBUTION ALONG THE SLOT LINE.

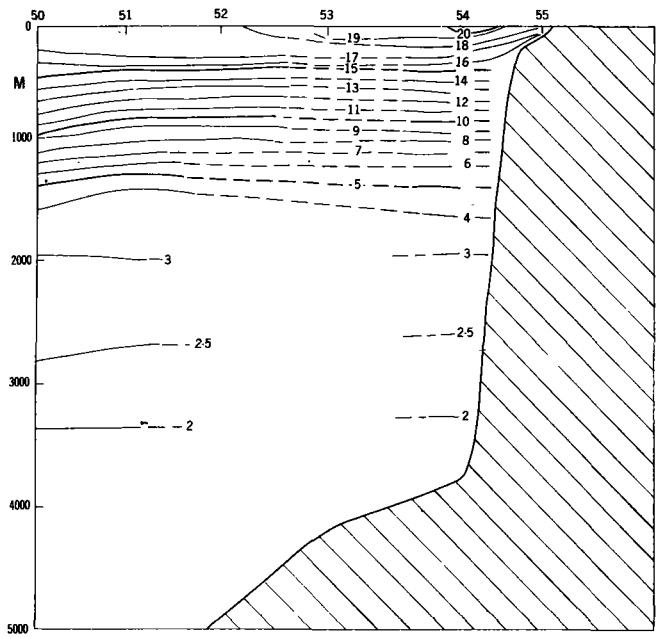

FIG. 15. TEMPERATURE DISTRIBUTION ALONG THE PORT ELIZABETH LINE.

Trigsurvey 1965

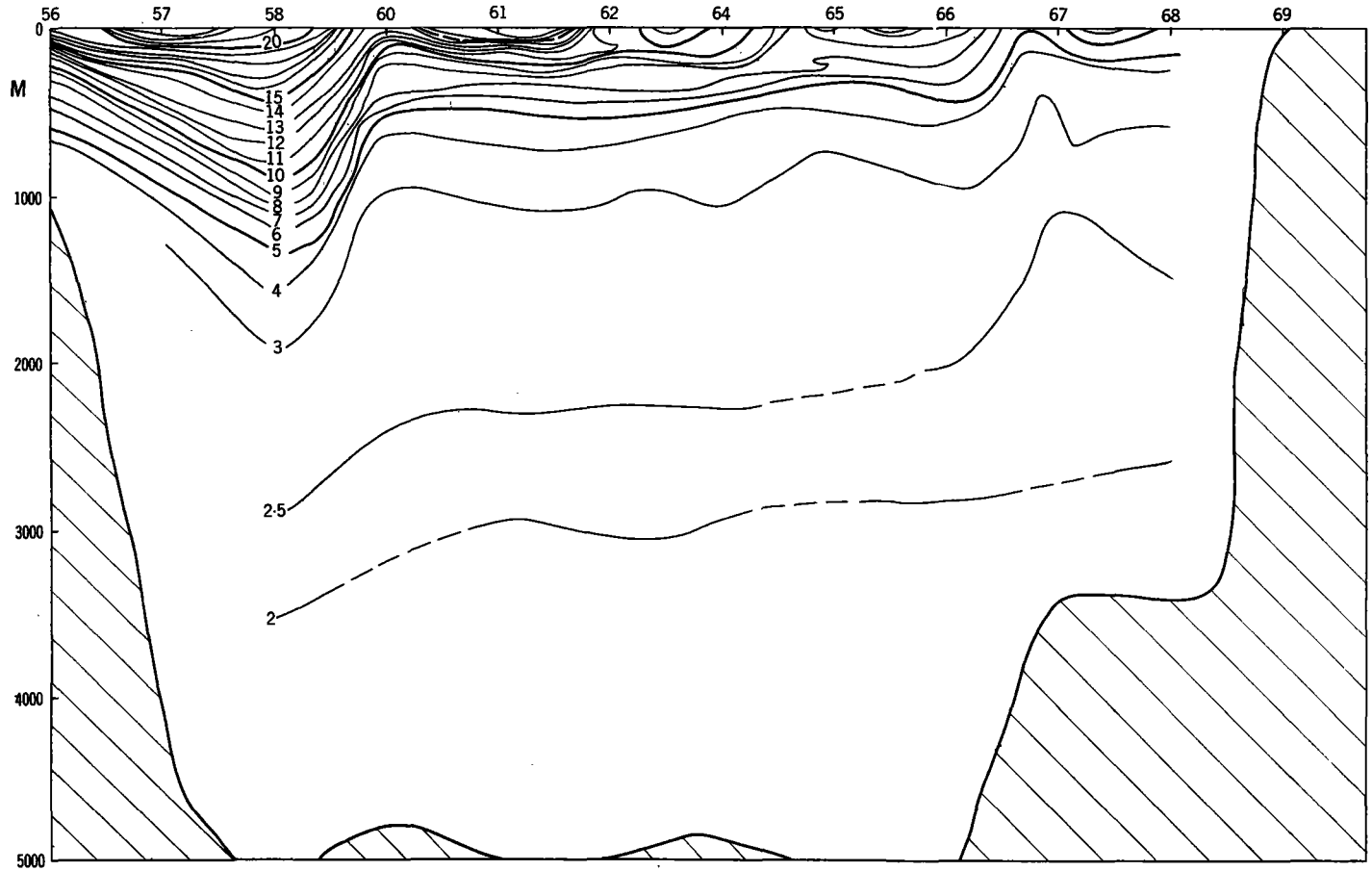

FIG. 16. TEMPERATURE DISTRIBUTION ALONG THE AGULHAS LINE

Trigsurvey 1965

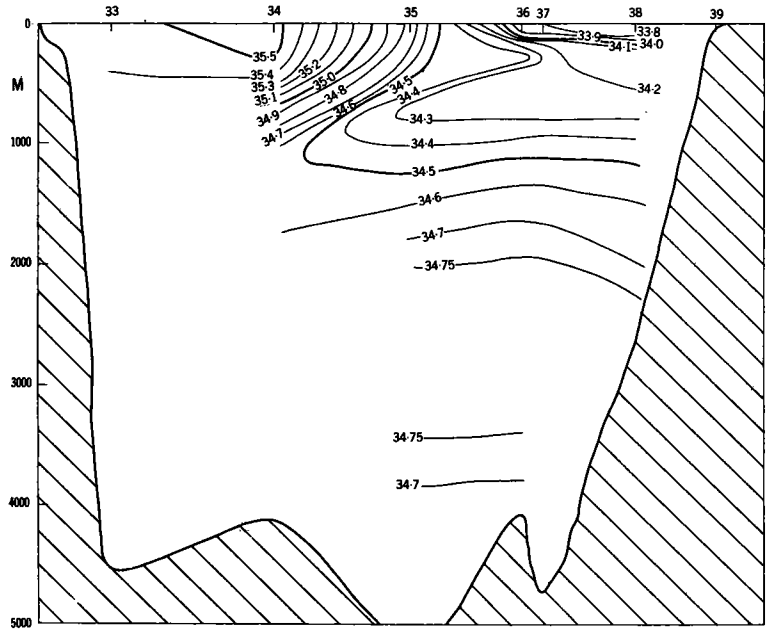

FIG. 17. SALINITY DISTRIBUTION ALONG THE MARION LINE.

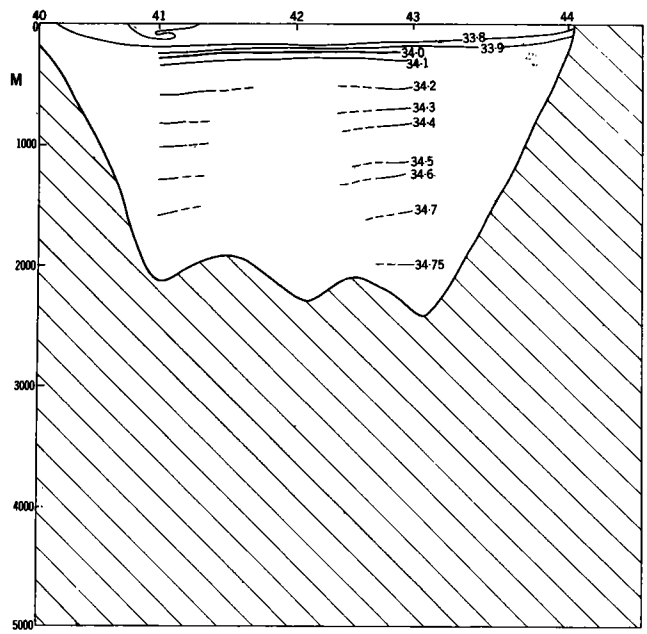

FIG. 18. SALINITY DISTRIBUTION ALONG THE CROZET LINE.

Trigsurvey 1965

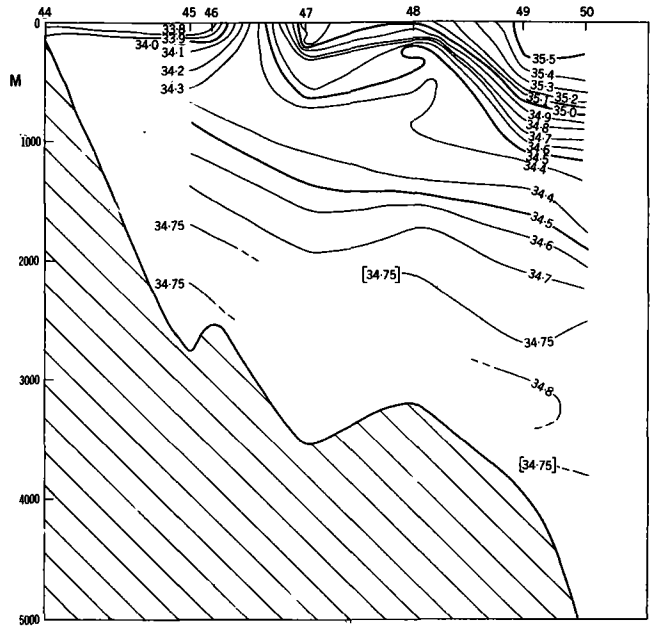

FIG. 19. SALINITY DISTRIBUTION ALONG THE SLOT LINE.

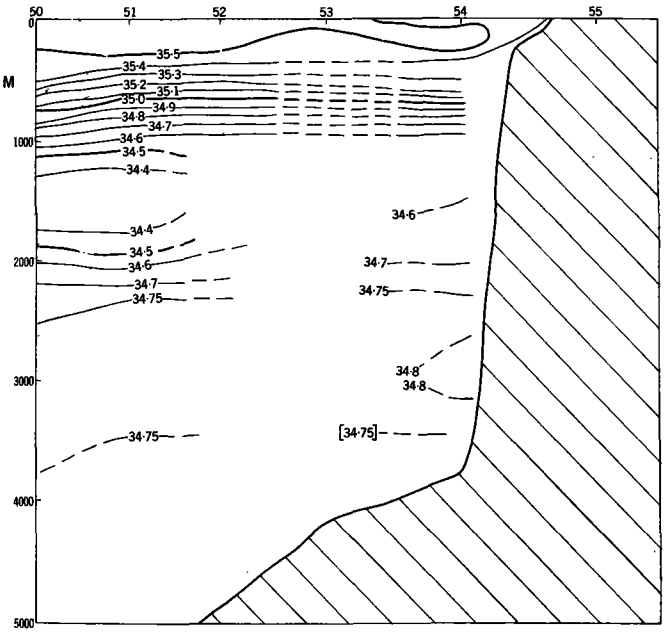

FIG. 20. SALINITY DISTRIBUTION ALONG THE PORT ELIZABETH LINE.

Trigsurvey 1965

UNESCO ARCHIVES

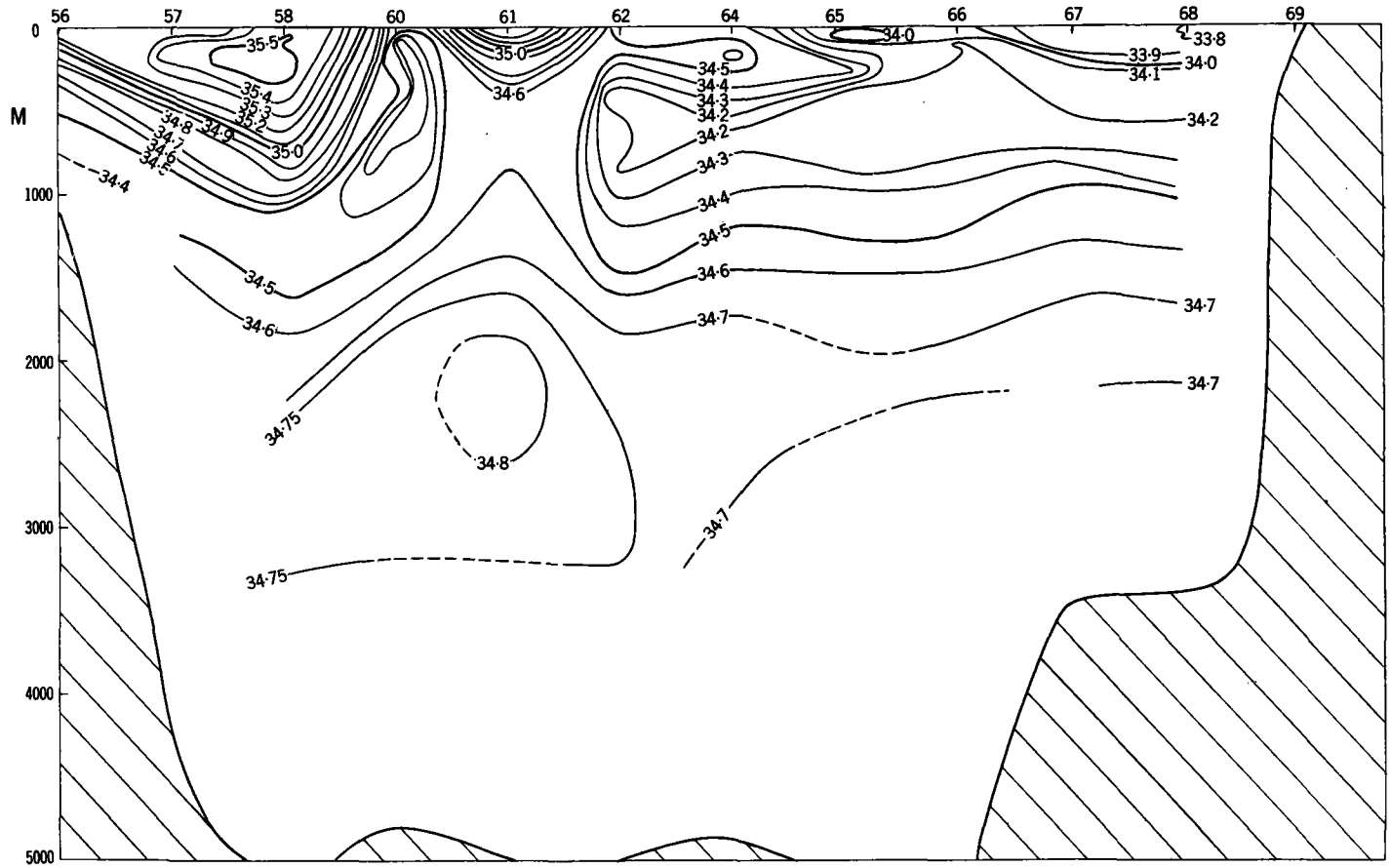

FIG. 21. SALINITY DISTRIBUTION ALONG THE AGULHAS LINE.

Trigsurvey 1965

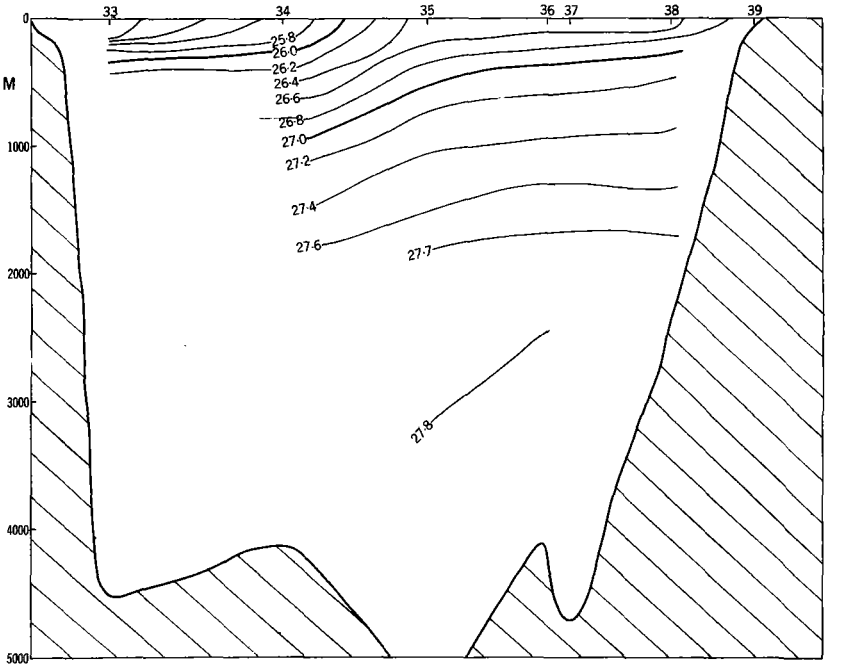

FIG. 22. SIGMA-T DISTRIBUTION ALONG THE MARION LINE.

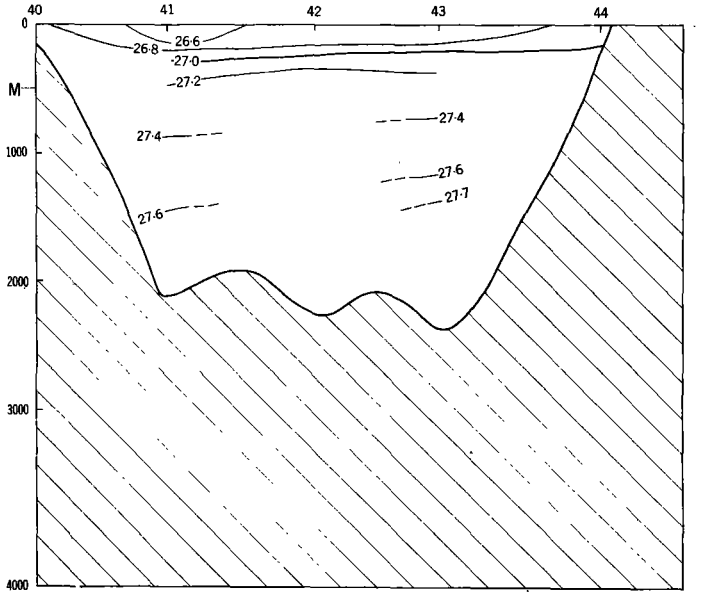

FIG. 23. SIGMA-T DISTRIBUTION ALONG THE CROZET LINE.

Trigsurvey 1965

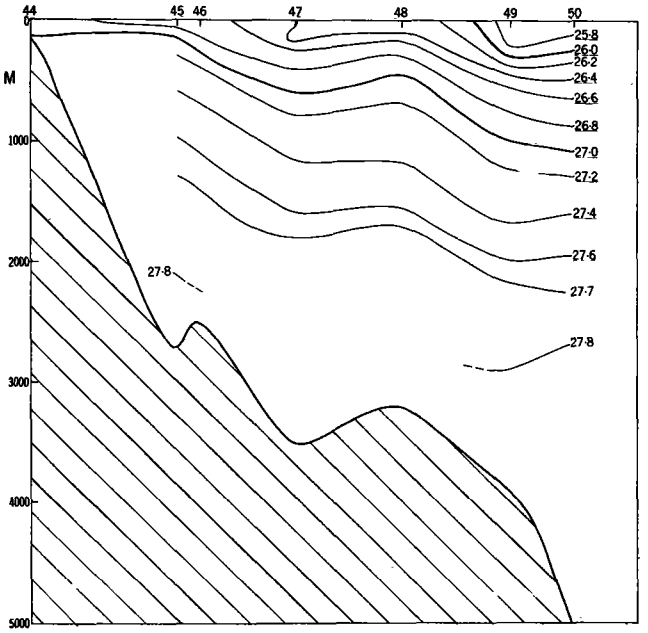

FIG. 24. SIGMA-T DISTRIBUTION ALONG THE SLOT LINE.

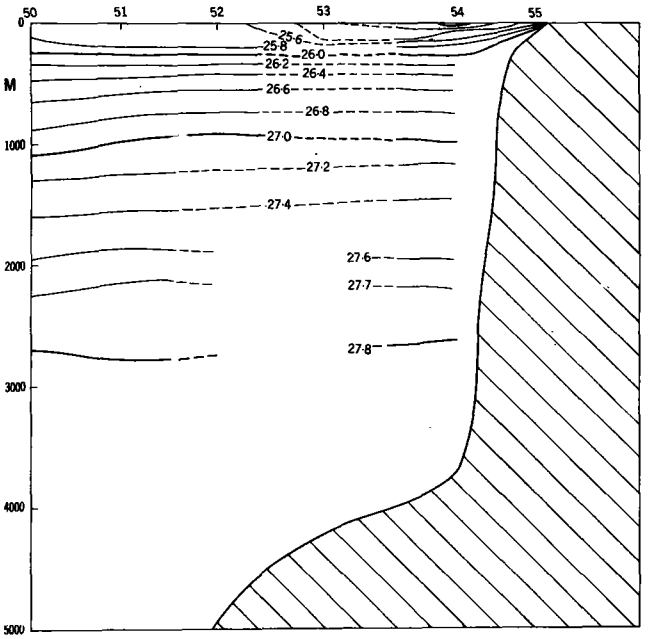

FIG. 25. SIGMA-T DISTRIBUTION ALONG THE PORT ELIZABETH LINE.

Tngsurvey 1965

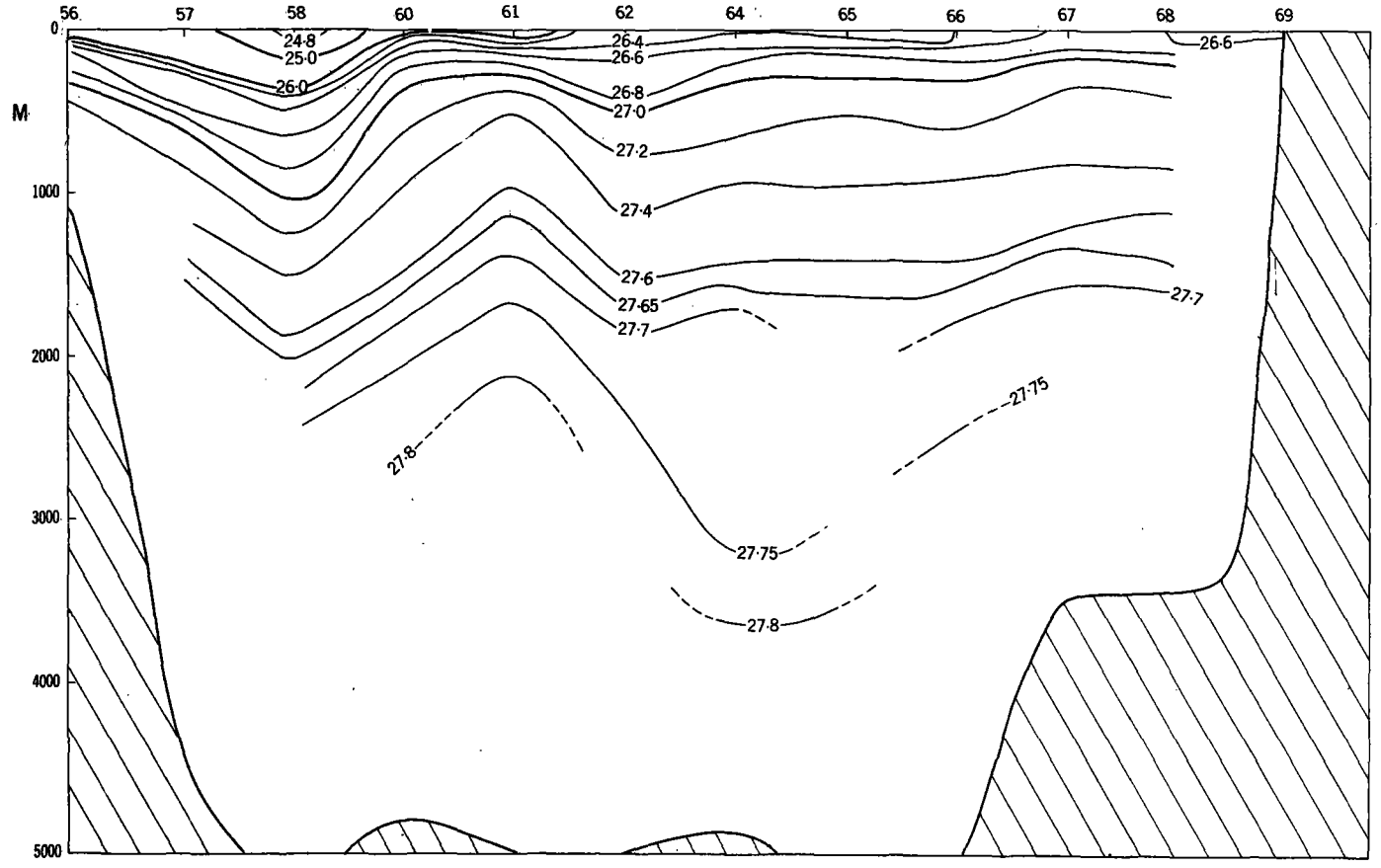

FIG. 26. SIGMA-T DISTRIBUTION ALONG THE AGULHAS LINE.

Trigsurvey 1965

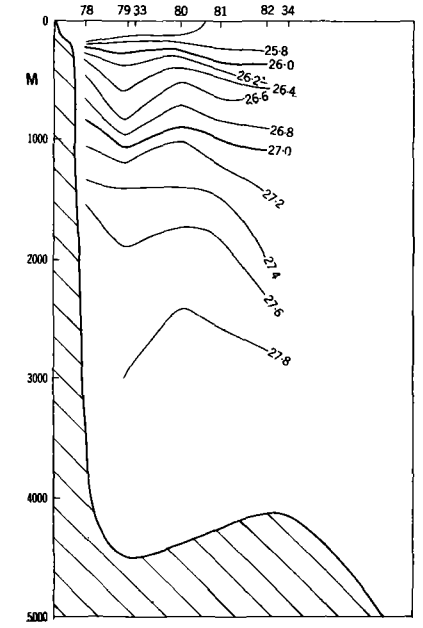

FIG. 27. SIGMA-T DISTRIBUTION ALONG THE "NATAL C" LINE.
(Stations N10E 78 to 82)

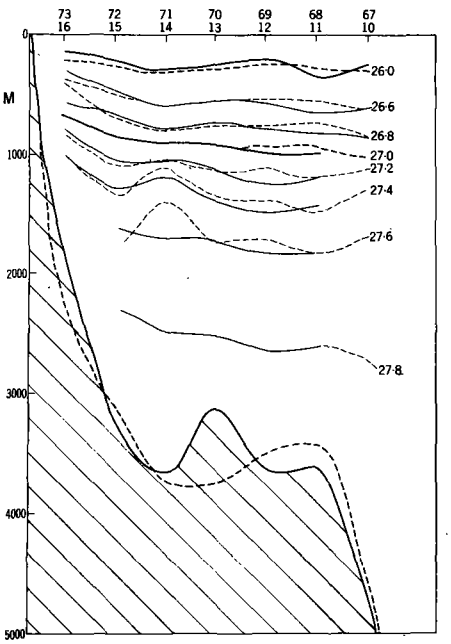

FIG. 28. SIGMA-T DISTRIBUTION ALONG THE "NATAL B" LINE.
[Stations N10E 10 to 16 (full line) and 67 to 73 (broken line)]

Trigsurvey 1965

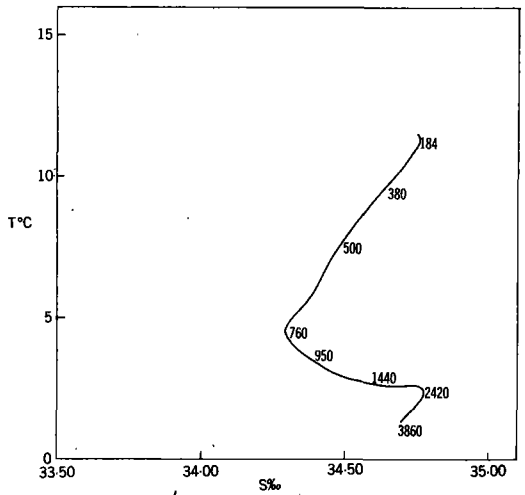

FIG. 29. T/S-VERHOUDING BY STASIE 35

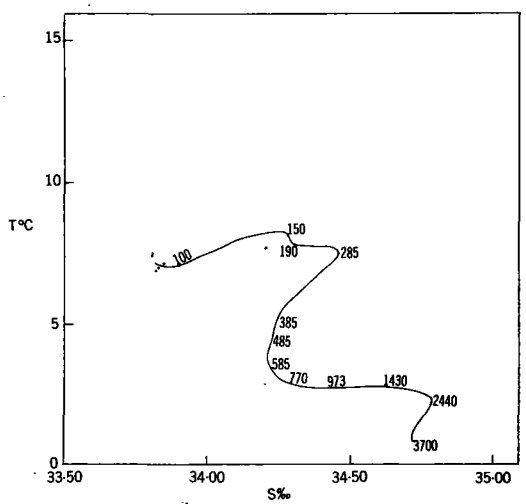

FIG. 30. T/S-VERHOUDING BY STASIE 36

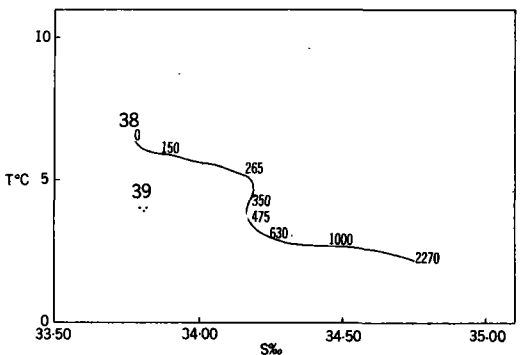

FIG. 31. T/S-VERHOUDINGS BY STASIES 38 EN 39

Driehoeksmeting 1965

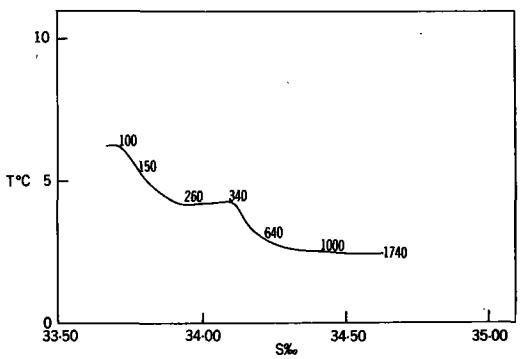

FIG. 32. T/S-VERHOUDING BY STASIE 41

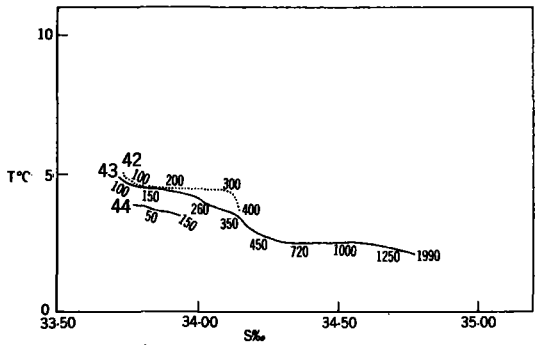

FIG. 33. T/S RELATIONSHIPS AT STATIONS 42, 43 AND 44

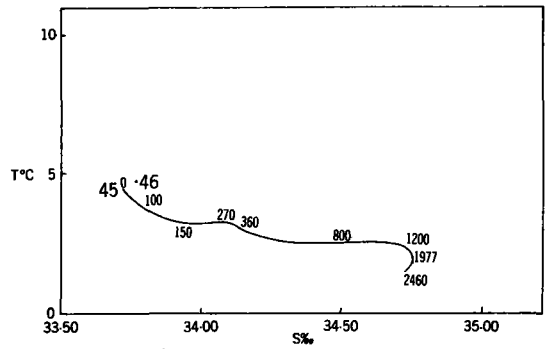

FIG. 34. T/S RELATIONSHIPS AT STATIONS 45 AND 46

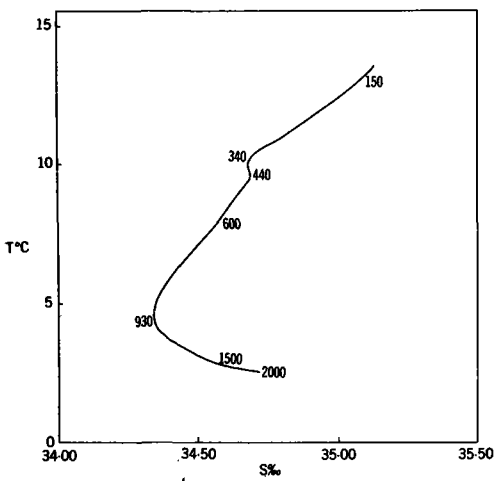

FIG. 35 T/S RELATIONSHIP AT STATION 47

Trigsurvey 1965

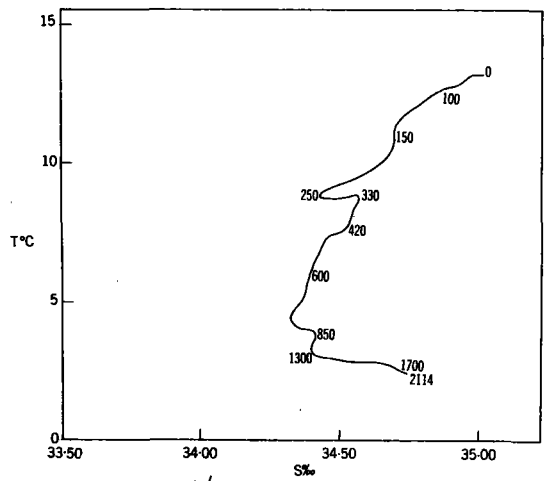

FIG. 36 T/S RELATIONSHIP AT STATION 48

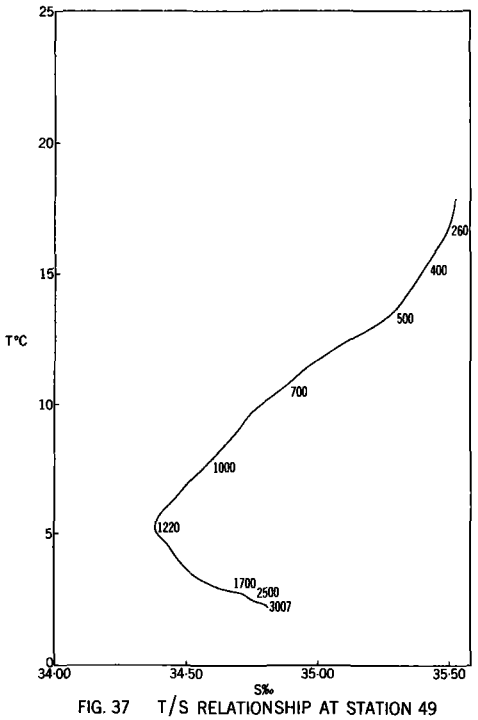

FIG. 37 T/S RELATIONSHIP AT STATION 49

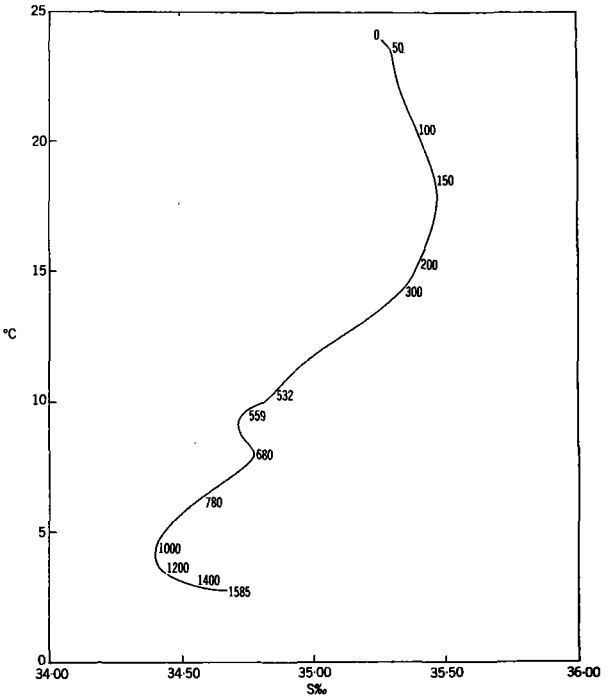

FIG. 38. T/S RELATIONSHIP AT STATION 57.

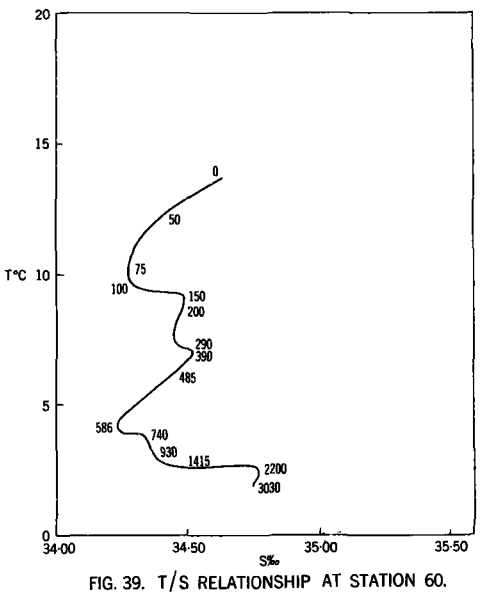

FIG. 39. T/S RELATIONSHIP AT STATION 60.

Trigsurvey 1965

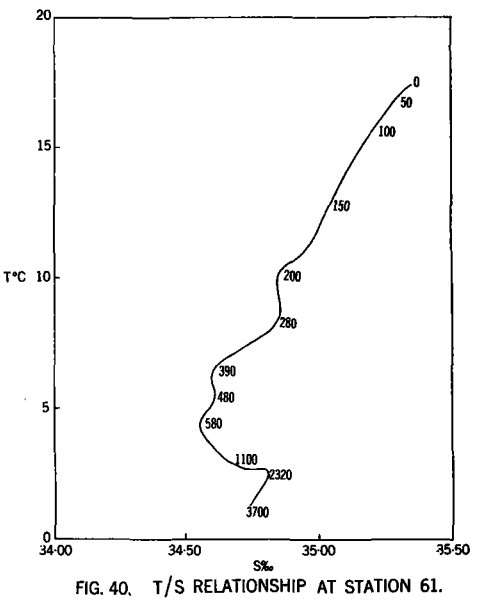

FIG. 40. T/S RELATIONSHIP AT STATION 61.

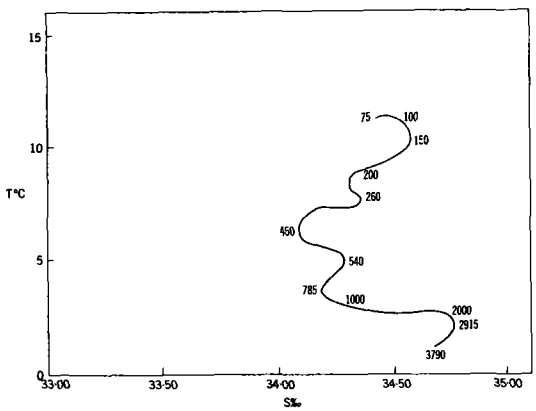

FIG. 41. T/S RELATIONSHIP AT STATION 62.

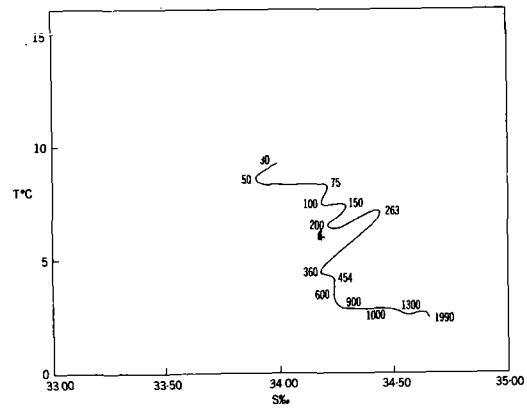

FIG. 42. T/S RELATIONSHIP AT STATION 65.

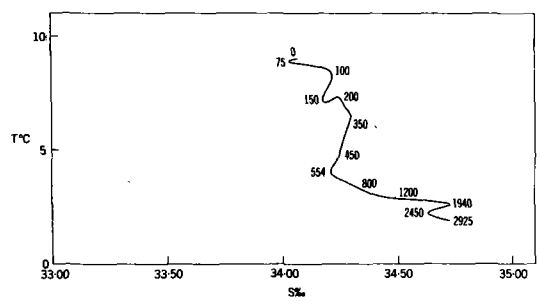

FIG. 43. T/S RELATIONSHIP AT STATION 66.

Trgsurvey 1965

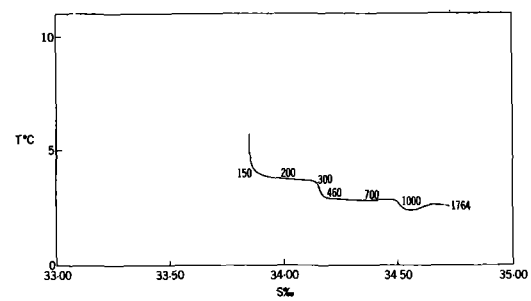

FIG. 44. T/S RELATIONSHIP AT STATION 67

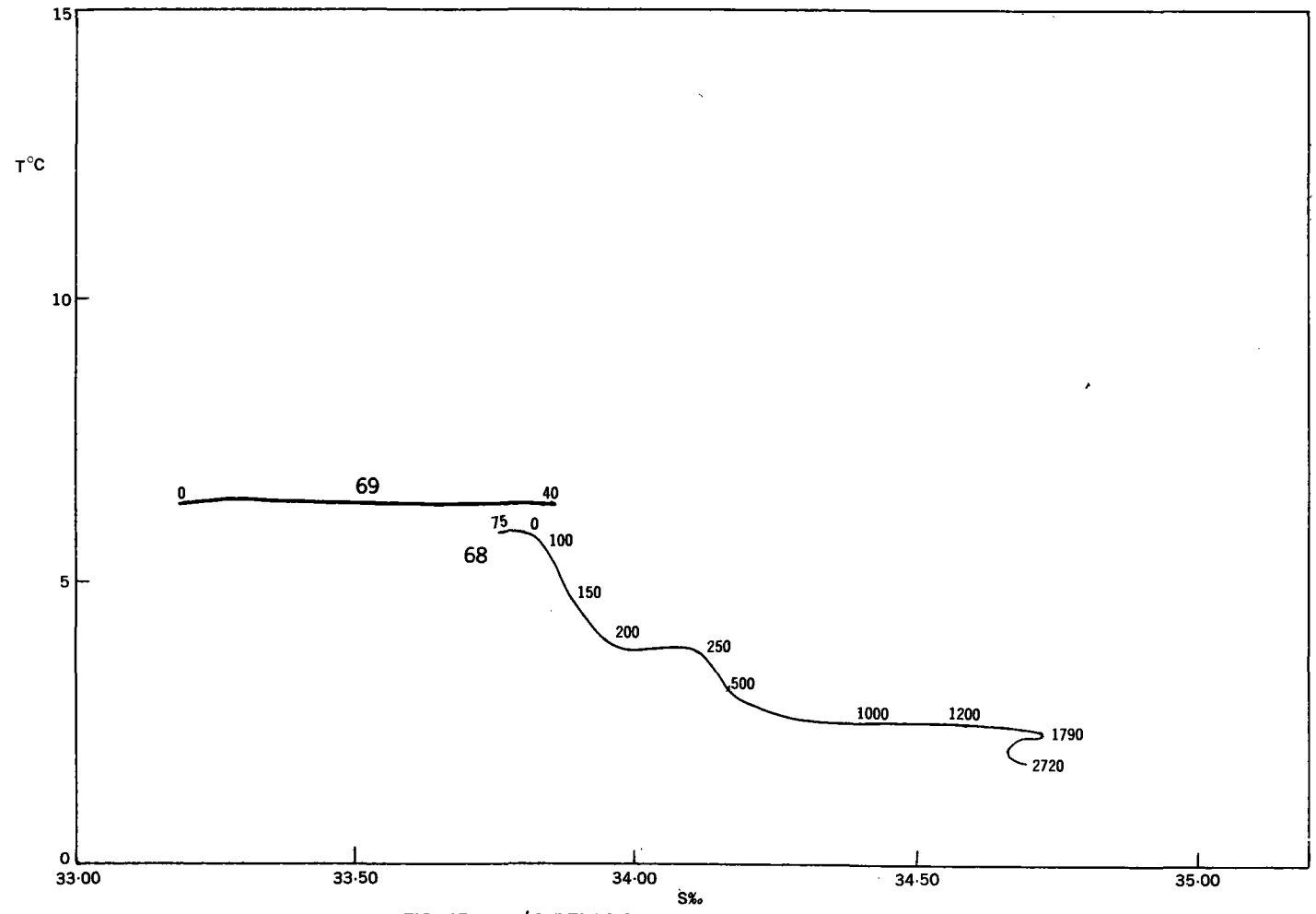

FIG. 45. T/S RELATIONSHIPS AT STATIONS 68 AND 69

Trigsurvey 1965

Part IV

Marine geology and geophysics

Reprinted from *J. Indian Geophys. Un.*, vol. 1, no. 1, 1964, p. 25-32.

ANDHRA, MAHADEVAN, AND KRISHNA SUBMARINE CANYONS AND OTHER FEATURES OF THE CONTINENTAL SLOPE OFF THE EAST COAST OF INDIA

BY

E. C. LAFOND

(U. S. Navy Electronics Laboratory, San Diego 52, California)

INTRODUCTION

Echo sounding profiles taken in the Indian Ocean off the central east coast of India have disclosed several interesting sea-floor topographic phenomena not yet discernible in the widely spaced soundings shown in published navigational charts. These phenomena consist of at least six submarine canyons that are cut into the continental slope off the Andhra Coast.

The discovery of these submarine canyons was made possible by the U. S. Program in Biology of the Indian Ocean Expedition. In the course of Cruise One of this program, echo sounding profiles, made by the writer from the research vessel ANTON BRUUN, revealed the presence of six hitherto unknown canyons while the expedition was conducting an integrated program of data collection concerning the life cycle of marine organisms throughout the Bay of Bengal. The ultimate goal of the over-all program is to furnish knowledge that will permit the development of marine resources for use by the population of Southeast Asia. It includes marine meteorology (the wind and radiant energy); physical oceanography (water movement, especially upwelling); chemical oceanography (nutrient distribution); primary production (initial plant life); plankton production (fish food); and harvestable organisms (fish, prawns).

The sea-floor topographic data, which led to the discovery of the six canyons, consisted of four profiles of the bottom off the east coast of India. These were obtained by echo sounders from the ANTON BRUUN as it cruised between oceanographic stations. The locations of individual lines of sounding are shown in Fig. 1 as straight lines marked A-B, C-D, E-F, and G-H, and additional details are given in Table I.

The sounding lines were made as the ship cruised on a straight course between stations at a speed of 10 to 12 knots. Although the general topography of the Bay of Bengal will be analyzed separately, four short sections across the Indian continental slope can be presented to show the nature of the new submarine canyons, and the continental terrace, that have been disclosed in this region of the world. The descriptions of the bottom features begin with the most northerly section and proceed to the south.

In addition to the measurement of sea-floor topography that established the existence of these offshore underwater canyons of India, Cruise One of the U.S. Program in Biology of the Indian Ocean Expedition conducted several related programs. These included the collection of all types of biological specimens for both museums and taxometric studies. The exploration of the offshore sea-floor was intended to supplement the active marine geological programs of India.[1] Although data from all phases of the expedition's general program have not yet been completely analyzed, the success of the enterprise is evident from a preliminary inspection. The final results will be presented after particularized analysis by experts in the various disciplines covered by the coordinated program.

The three largest canyons of the six revealed by the expedition were given identifying names. Andhra Canyon was named after the University at Waltair where modern Indian oceanography developed. Mahadevan Canyon bears the name of the late Professor C. Mahadevan, the internationally acclaimed Indian geologist and former Principal of Andhra University. The name of the late Vice-Chancellor of Andhra University, who was instrumental in providing facilities and inspiration to Indian marine science, was given to Krishna Canyon. The three

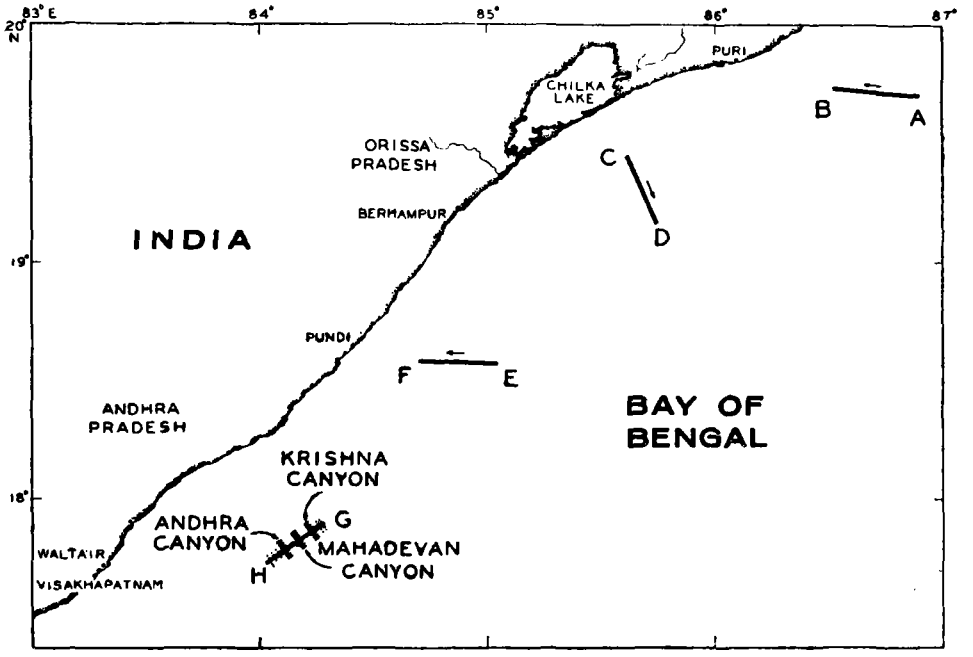
83° E
84°
85°
86°
87°
20° N
19°
18°
PURI
CHILKA LAKE
ORISSA PRADESH
BERHAMPUR
INDIA
PUNDI
ANDHRA PRADESH
BAY OF BENGAL
KRISHNA CANYON
ANDHRA CANYON
MAHADEVAN CANYON
WALTAIR
VISAKHAPATNAM
A
B
C
D
E
F
G
H

FIG. 1

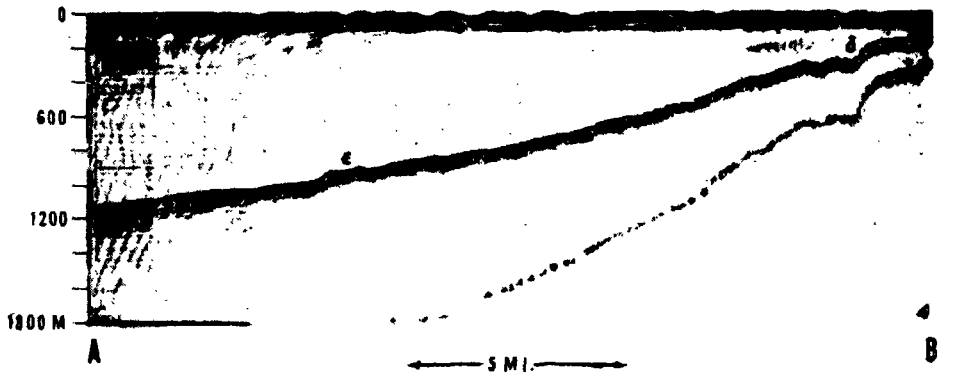
0
600
1200
1800 M
A
B
5 MI.

FIG. 2

smaller canyons have not yet been named, and need additional surveying to delineate their characteristics.

TABLE I

Location of Bathmetric Sections

Position	Date (April 1963)	Time (Local)	Lat. (N)	Long. (E)	Course (True)	Speed (Knots)
A	23	0600	19°42.0′	86°53.8′	280°	11
B		0800	19°43.9′	86°31.5′		
C	23	1830	19°33.9′	85°33.3′	154°	12
D		2030	19°10.2′	85°44.8′		
E	24	0505	18°34.8′	85°02.3′	272°	10
F		0655	18°35.9′	84°42.0′		
G	11	1940	17°54.0′	84°16.2′	234°	10
H		2130	17°44.0′	84°01.8′		

Section A–B

The first profile of the sea-floor runs up the continental slope near the head of the Bay of Bengal (Fig. 2). The bottom slope between 1100 and 280 meters is relatively gentle and has a slightly concave shape. The upper portion of the profile has minor irregularities that give this slope a hummocky appearance which might be associated with minor slumping or gravity creep of sediment downslope. The prominent rise (ϵ) with an elevation of 20 meters at a depth of 850 meters, appears at the deepest boundary of the hummocky topography. The slope is much smoother below this depth and probably represents a depositional surface.

At the major break in slope at the edge of the continental shelf, a depth of 190 meters, the bottom steepens abruptly and is associated with a slight depression. The sharp break in slope (δ) at a depth of 190 meters forms a 100-meter nick point in the axial profile of the slope. It is the only sudden drop in the section and is markedly different from the topography usually associated with the base of the break in slope at the continental shelf. A second depression is also found about half a mile seaward and is also about 20 meters deep. The

roughness of the bottom in the areas of the depressions indicates that they are probably either of tectonic origin or the result of an ancient lowering of sea level.

Section C–D

The next southerly topographic section runs seaward across the continental shelf (Fig. 3). The ship's course was 154° and its speed was 11 knots. The scale of the echogram is 0 to 400 fathoms (0–732 meters) during the time from before 1830 to 1946. Where the bottom trace ran off scale, it was changed to a new scale of 0 to 1000 fathoms (0–1829 meters).

In this section the bottom profile differs from the first in that it is convex. This is more typical of India's east coast.[2] Slight undulations in slope are found on the edge of the continental shelf at a depth of about 120 meters. Another terrace-like irregularity occurred between 270 and 280 meters just shoreward of the break in slope at 280 meters, but in general, the bottom was unusually smooth. These features lead to the assumption that they are terraces, but they may be the seaward beds of submerged deltas or represent successive lenses of recent sediment deposited on the continental shelf.[3] This area is noted for the large amount of sediment transported north along the coast.[4,5]

After the steep increase in bottom at the continental slope, two V-shaped, canyon-like features occur with bottom depths of around 700–880 meters marked x and ξ. The second one, marked ξ, is about 250 meters deep at this crossing. Its profile is not typical for most canyons in that it runs parallel to the trend of the continental slope. In addition, the inner crest is double and has what appear to be natural levees. The seaward crest is exceptionally sharp. It may well be that this is not a canyon but the effect of faulting. The terrace-like features on the shelf might be the result of tectonic activity. However, until further work is done in the region by sonic profiles, such an assumption must remain speculative.[3,6]

Section E–F

The next section was conducted up the continental slope onto the shelf (Fig. 4). This section was started at 0505 and ended at 0655

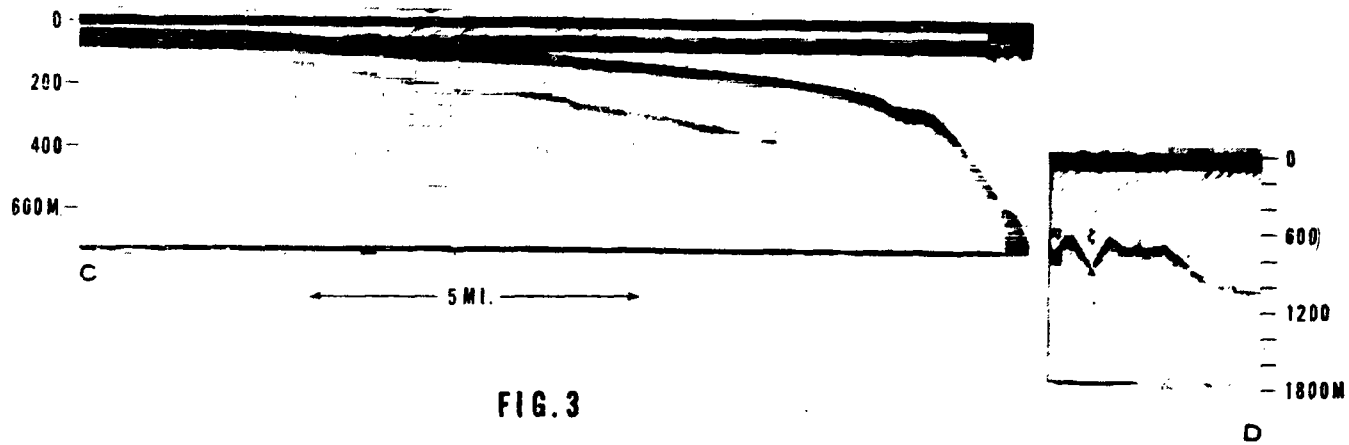

FIG. 3

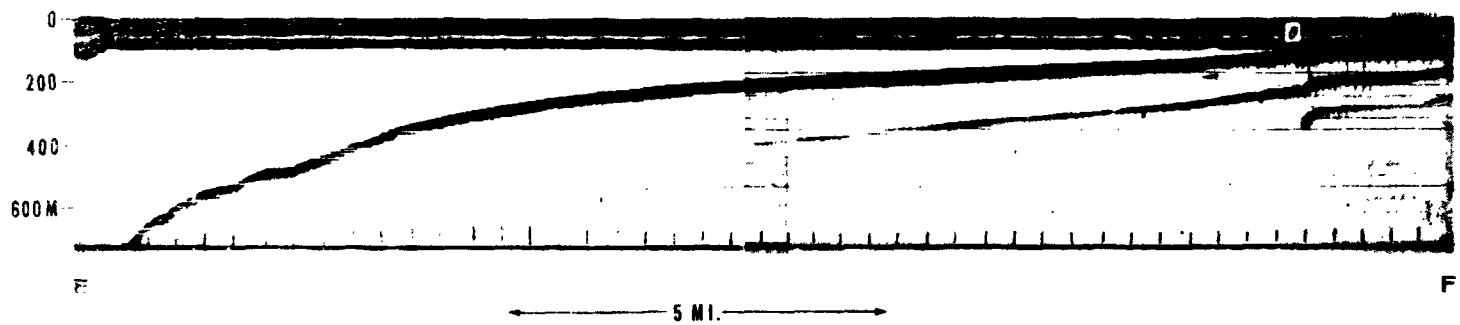

FIG. 4

on 24 April, 1963. The ship was proceeding on a course of 272° at a speed of 10 knots. This section did not begin until the depth was on the scale; therefore it is not known if the canyon-like features at the base of the slope were present at the greater depth as in the previous section.

The bottom profile in general is convex with but one small break that forms a small plateau or terrace at a depth of about 550 meters. There is a significant lack of a sharp break in slope at the edge of the continental slope. It is unusually rounded, and there is no indication of a break, as on other sections. Up to a depth of about 100 meters marked θ there is an indication of a higher reflectivity and possibly a harder bottom.

Section G–H

The most significant section is shown in Fig. 5. This record was made on a previous passage through the area. The echo sounder profile started at 1940 on 11 April at point G of the right of the upper part of the figure and ended at 2130 on 11 April, 1963 at point H in the lower part of the figure.

The profiles were made as the ship was proceeding on a course of 234° which is converging on the edge of the continental shelf at an angle of about 5 degrees. To all practical purposes, echograms represent a profile nearly parallel to the continental slope and thus have a greater chance of crossing submarine canyons trending down the continental slope. The upper part of Section G–H (Fig. 5) was made on a depth scale of 750 to 1500 meters. In the lower part of the figure, there is some duplication of the upper part which has a scale of both 750 to 1500 meters, and a surface to 750 meters.

Both profiles are typical for slopes cut by submarine canyons.[7] The profile shows major canyons 3 to 5 miles apart all along the track. The slopes of larger canyons have breaks in the slope of their transverse profiles marked x that could be small tributaries or slump blocks. As the profile moves closer to the slope and is shallower, around 1000 meters, the canyon profiles also become shallower and smaller, and this is a feature commonly observed in other regions. The bottoms

of the canyons appear to slope, one on its left side and one on its right side. This indicates that they are being crossed at an angle not at right angles to their trend. It is noteworthy that the bottom of Mahadevan Canyon does not show this sloping bottom and is extremely narrow. The bottoms of the two adjacent canyons have slopes in opposite directions. It thus appears that the canyons are not running down-slope at the same angle and in all probability they have meandering courses as do the canyons off Southern California and Baja Califorina.[7,8] The most northerly canyon on the right is Krishna Canyon. It lies between crests of 900 meters and 840 meters. The latter crest is broader and appears to be flatter than other crests and composed of three domes with small, what may be subsiding tributaries to the main channel lying between. The Krishna Canyon floor is at 1180 meters at this crossing.

Toward the south is a more narrow, V-shaped area now named Mahadevan Canyon. At this angle of crossing, the sides are steep, about 1 to 5 in slope. The narrow, flat floor is about 400 meters wide. The crest of the ridges on either side of this canyon are at 850 and 800 meters, probably due to crossing the canyon at a slight angle. The floor is at 1370 meters. The sides are symmetrically shaped, but the crests have irregularities suggestive of additional minor tributaries.

Six miles to the south is the large area known as Andhra Canyon. The crests on either side of this crossing are at around 850 meters and the trough is at 1300 meters. The base of the Canyon is lower toward the north, probably due to the angle of crossing. The bottom of the canyon floor is also harder, and is evidenced by the stronger return signal recorded on the echogram. The slope of the north and south sides is asymmetrical, a feature common in canyons that have meandering channels.

To the south, are the three small, and as yet unnamed, V-shaped-canyons. The first (γ) has a crossing depth of 1100 meters is followed by a second (β) with a depth of 1080 meters and a third (α) at 1000 meters. There is a possibility of a fourth at about 850 meters, but it is lost in the outgoing signal.

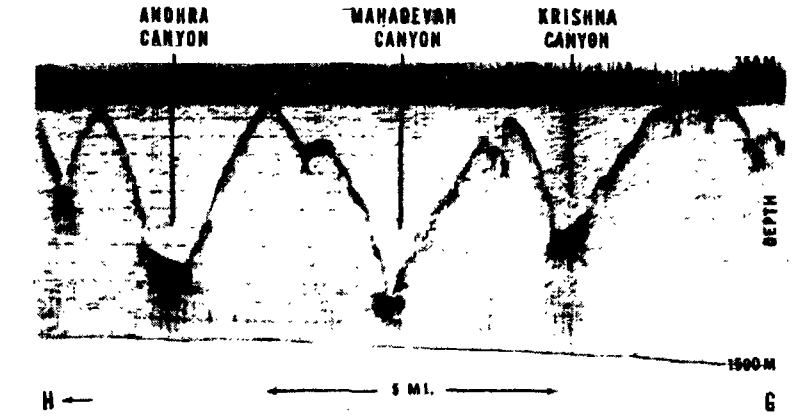
ANDHRA CANYON
MAHADEVAN CANYON
KRISHNA CANYON
DEPTH
1500 M
H
5 MI.
G

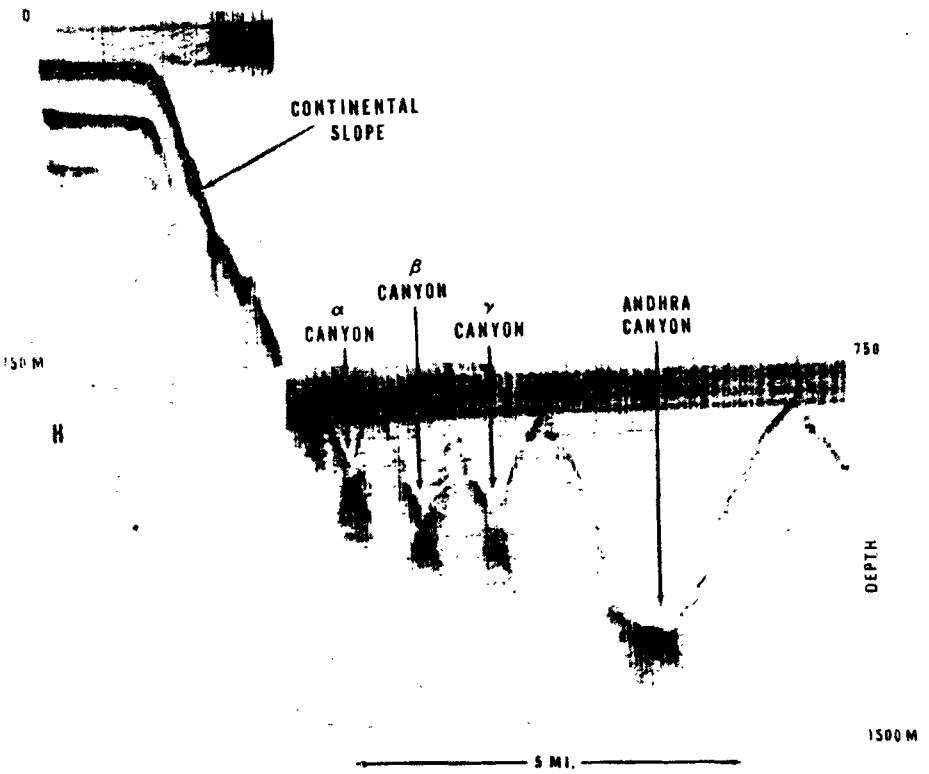
0
CONTINENTAL SLOPE
β CANYON
α CANYON
γ CANYON
ANDHRA CANYON
750
750 M
H
DEPTH
1500 M
5 MI.
G

FIG. 5

The unique aspect of these multiple canyons is that they are found at the base of the continental slope. The shape of all canyons is similar and their crests are much closer than is normal.

Discussion

The shape of the canyon walls shows the typical V-shaped profile found in canyons cut into continental slopes. Their narrow bottoms indicate that they are not being filled with sediment. It is not known whether they extend up to the break in slope nor if they cut across the shelf and intersect the longshore transport of nearshore sediments. The soundings on published navigation charts are so widely spaced that it is not possible to contour canyons with existing soundings. It is known from the work of R. F. Dill off Baja California and Southern California that canyons are often a focal point of fish concentrations. The canyons of the east coast of India therefore deserve future investigation to determine if such is also the case in the Indian Ocean.

Acknowledgment

The author wishes to express appreciation to the U. S. Program in Biology of the Indian Ocean Expeditions, which made possible the opportunity to collect the sounding records. Thanks are also extended to R. F. Dill and G. H. Curl for suggestions in the manuscript.

References

1. LaFond, E. C. (1957) "Oceanographic Studies in the Bay of Bengal." Proc. Indian Academy of Sciences, Vol. XLVI, pp. 1-46.

2. Rao, B. Kukkuteswara and E. C. LaFond (1954) "The Profile of the Continental Shelf off Visakhapatnam Coast." Andhra University Memoirs, Vol. 1, pp. 78-85.

3. Moore, D. G. (1960) "Acoustic Reflection Studies of the Continental Shelf and Slope off Southern California." Bull. Geol. Soc. America, Vol. 71, pp. 1121-1136.

4. Rao, R. Prasad and C. Mahadevan (1958) "Evolution of Visakhapatnam Beach." Andhra Univ. Memoirs, Vol. 2, pp. 33-47.

5. Mahadevan, C. and R. Prasad Rao (1958) "Cause of the Growth and Sand Spit North of Godavari Confluence." Andhra Univ. Memoirs, Vol. 2, pp. 69-74.

6. Moore, D. G. and J. R. Curray (1963) "Structural Framework of the Continental Terrace, Northwest Gulf of Mexico." Jour. Geophys. Res., Vol. 68, No. 6, pp. 1725-1747.

7. Shepard, F. P. (1963) "Submarine Geology." Chapter XI, Harper and Row, New York, N.Y.

8. Shepard, F. P., and R. F. Dill (1964) "Submarine Canyons," Rand McNally Co., N. Y. (Manuscript).

Reprinted from *Nature, London*, vol. 204, no. 4,965, 1964, p. 1245-1248.

MAGNETIC, GRAVITY AND DEPTH SURVEYS IN THE MEDITERRANEAN AND RED SEA

By T. D. ALLAN
Saclant ASW Research Centre, La Spezia
H. CHARNOCK
National Institute of Oceanography, Wormley, Godalming
AND
C. MORELLI
Osservatorio Geofisico Sperimentale, Trieste

ALTHOUGH a relatively small and land-locked basin, the Mediterranean has many oceanic features. About three-quarters of the area is deeper than 1,000 fathoms, with extensive areas deeper than 1,500 fathoms and isolated depths of more than 2,500 fathoms. The western and eastern basins are geophysically different.

In both western basins there are extensive areas of abyssal plain, whereas the floor of the eastern basin, in spite of the sediment from the Nile, is characterized by an unusual type of small-scale relief. To the north of the eastern basin the Cretan island arc bounds the irregular topography of the Aegean Sea. Geophysical investigations of the differences between the eastern and western basins may provide clues as to their origin.

The Red Sea is another area where systematic observations may be of more than local interest. Previous observations have shown the similarity between the rift valley of the southern Red Sea and that of the mid-Atlantic Ridge.

The Saclant ASW Research Centre was commissioned in 1959 and its Oceanography Group formed the following year. Submarine geophysical observations in both the Mediterranean and the Red Sea have formed part of the group's programme. A summary of the geophysical work is given in this article.

Facilities

S.S. *Aragonese*, a freighter 293 ft. long, displacing 3,000 tons, was chartered for conversion into a marine research vessel. Radar, gyrocompass, precision depth recorder and other essential equipment were fitted initially. A Loran-*C* receiver and an electromagnetic log were fitted later.

The number of scientific personnel directly involved

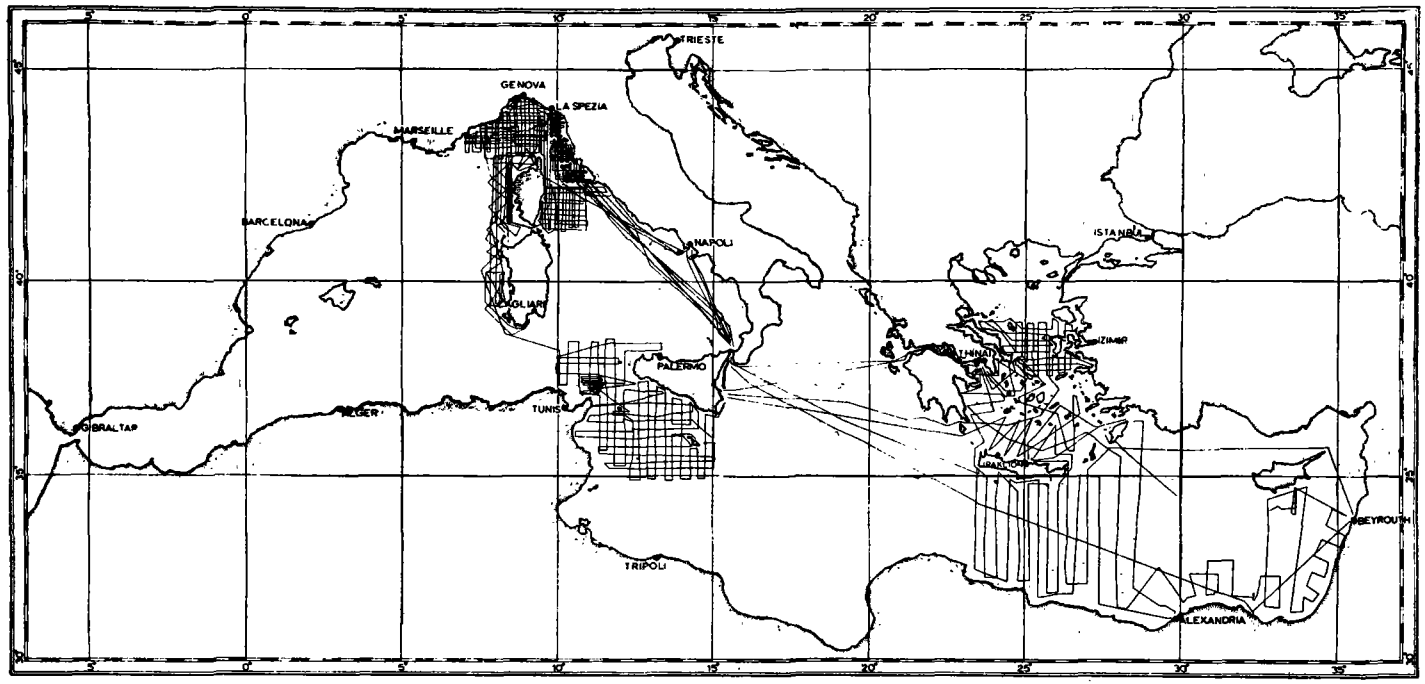

Fig. 1. Tracks of S.S. *Aragonese* in the Mediterranean Sea during the period July 1961–March 1963

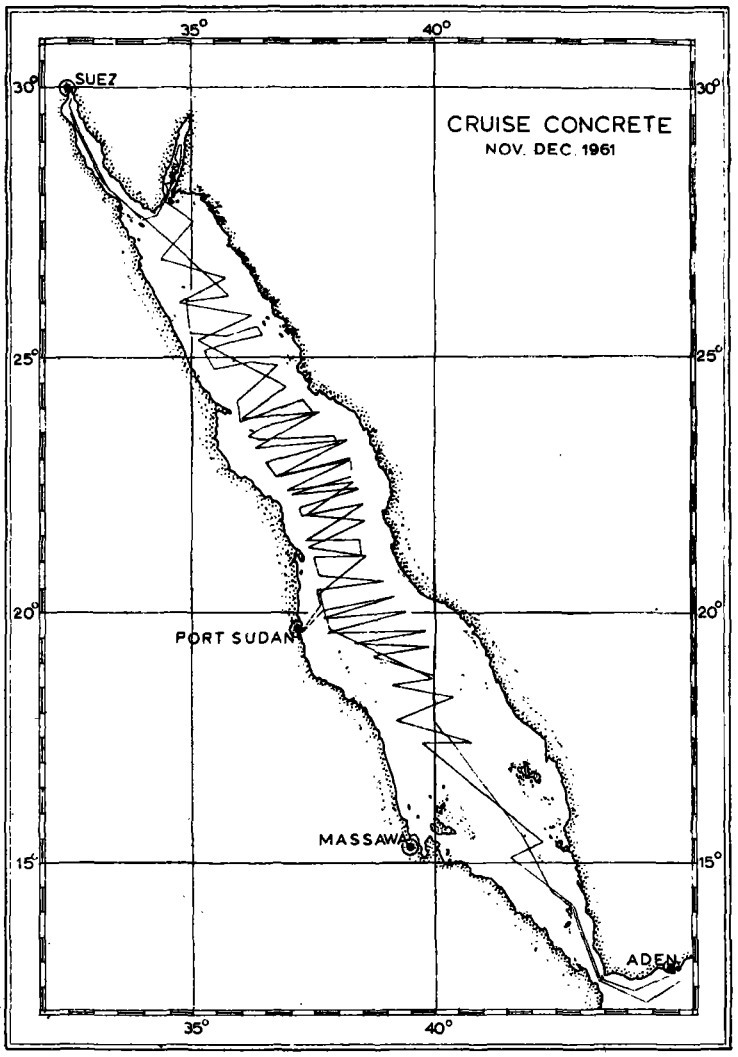

Fig. 2. Tracks of S.S. *Aragonese* in the Red Sea during November–December 1961

with the geophysical programme was small and the group frequently co-operated with other research establishments.

An agreement was reached with the Osservatorio Geofisico Sperimentale, Trieste, on a joint programme of gravity, magnetic and bathymetric survey work. The gravity meter, a Graf-Askania, was owned by the Osservatorio and operated by its staff throughout the cruises.

The gravity values were usually tabulated at 15-min intervals. The accuracy of the free-air gravity value depends not only on the performance of the meter and stabilized platform but also on the accuracy of the Eötvös correction which is calculated from the ship's speed and course. In this respect the Mediterranean

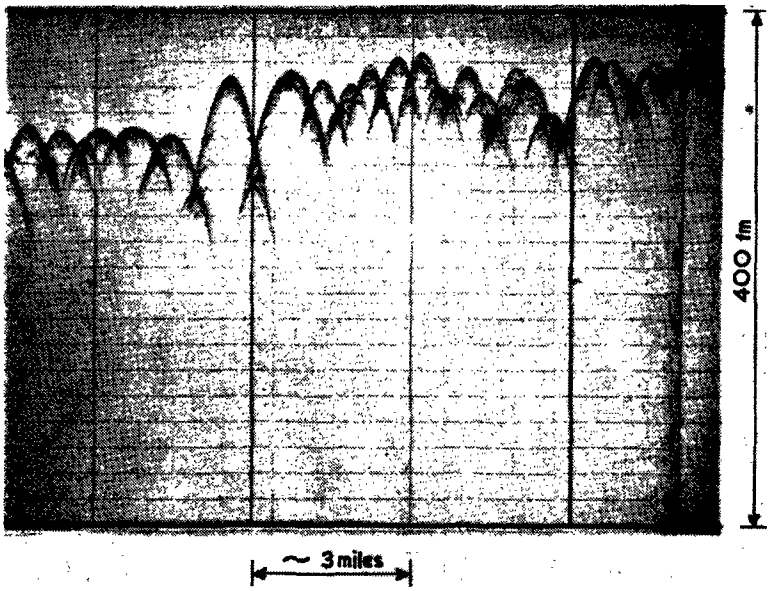

Fig. 3. Profile across the unusual floor of the eastern Mediterranean Sea

has presented fewer problems than those in the ocean generally. In the earlier cruises radar signals on numerous islands provided good control: for most of the work the probable error in position was $\pm 0{\cdot}25$ mile. For the later surveys, in areas far from land, Loran-*C* positions proved reliable to better than $\pm 0{\cdot}5$ mile.

The magnetometer was the nuclear spin model described by Hill[1] and manufactured by Bruce Peebles, Ltd. It had a sensitivity of $\pm 0{\cdot}5$ γ. Readings were taken every 30 sec and recorded on punched paper for later reduction on the Centre's computer. The greatest inaccuracy in the measurement of the absolute value of the field lay in the uncertain knowledge of its diurnal variation.

Depth was recorded on a precision depth recorder which could be read to ± 1 fathom.

During the period July 1961–March 1963 seven cruises were made. These were devoted almost entirely to magnetic, gravity and depth surveys of selected areas, but brief trials of other techniques, such as coring and seismic reflexion profiling, were also made.

About 40,000 miles of track have been covered: the distribution in the Mediterranean and Red Sea is shown in Figs. 1 and 2.

Western Mediterranean

The first cruise was used to compare the performance of different types of gravity meter. The Trieste Graf-Askania and a LaCoste-Romberg instrument provided by the U.S. Office of Naval Research were installed in

the ship. Observations were made in three areas between La Spezia and Sicily where earlier bottom gravity readings[2] provided a precise reference. Consequently, not only relative but absolute comparisons of the surface-ship meters were possible. In the area near La Spezia precise navigational control was achieved by using theodolites on nearshore hills.

The gravity meters agreed within 10 m.gal in calm conditions, but modifications to the LaCoste-Romberg were necessary to allow for the 'Browne' corrections in rougher weather. An account of the comparisons has been published[3].

Other cruises in the western basin have examined the continental slopes which border the Balearic and Tyrrhenian abyssal plains. These slopes are cut by submarine canyons resembling those found in other parts of the continental margin but which have been interpreted as former sub-aerial valleys.

Between Sicily and Malta the survey did not appear to change the existing conception of the geology of the area. There were large magnetic anomalies around volcanic islands such as Pantelleria and the negative Bouguer gravity anomaly known to exist in western Sicily was shown to change to a positive anomaly in the centre of the Strait.

Eastern Mediterranean

In the eastern Mediterranean the islands of Crete, Scarpanto and Rhodes appear to form an island arc structure with contrasting geophysical properties in the areas to the north and south of the arc. These areas have been extensively surveyed during three of our cruises. Dr. K. O. Emery took part in one of these, during which a relief map of the sea-floor was prepared from a study of the type of bottom displayed on the echo-sounder.

Much of the sea-floor in the eastern basin is characterized by the type of small-scale relief shown in Fig. 3. The lack of deposition appears to be caused by a series of trenches which borders the area and acts as a trap for sediment spreading from the Nile.

Perhaps the most interesting aspect of the eastern basin, in spite of the lack of sedimented area, is the dullness of its magnetic field. Thus, apart from the latitudinal variation, there is no significant change of magnetic field between North Africa and Crete. This can be seen from Fig. 4, which shows a typical north–south profile of magnetic field, gravity and depth across the island arc. To the north there are several isolated magnetic anomalies, probably associated with vulcanism.

The gravity field is broadly similar to that associated with the island arcs of the major oceans. Generally negative in the southern part of the eastern basin, there

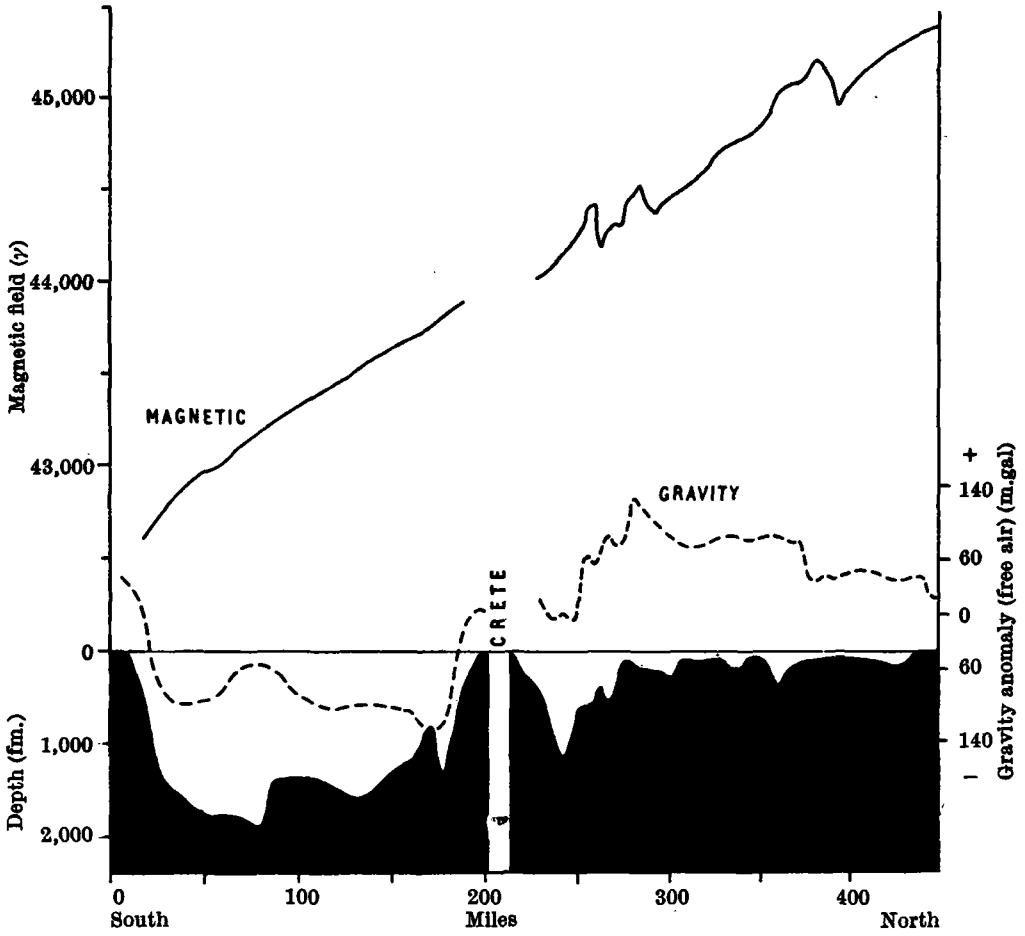

Fig. 4. Profile along meridian 26° E. of gravity (free-air) anomaly, total magnetic field and depth. The southern limit is the African coast and the northern limit lies at latitude 39° N. in the central Aegean

is a free air anomaly of about −100 m.gal in a band associated with the deep trenches just to the south of the arc. To the north the gravity field is generally positive, reaching +140 m.gal.

The Red Sea

A survey of the Red Sea and Gulf of Aqaba was made between October and December 1961. A second Graf-Askania gravity meter, supplied and operated by scientists of the German Hydrographic Institute and the Bundesanstalt für Bodenforschung, was embarked for this cruise and provided a good opportunity of comparing the performance of two meters of the same type. Over most of the cruise the agreement was excellent.

Preliminary surveys in the Red Sea[4,5] had shown the existence of a magnetic anomaly associated with a steep-sided medial valley about 30 miles wide. This anomaly

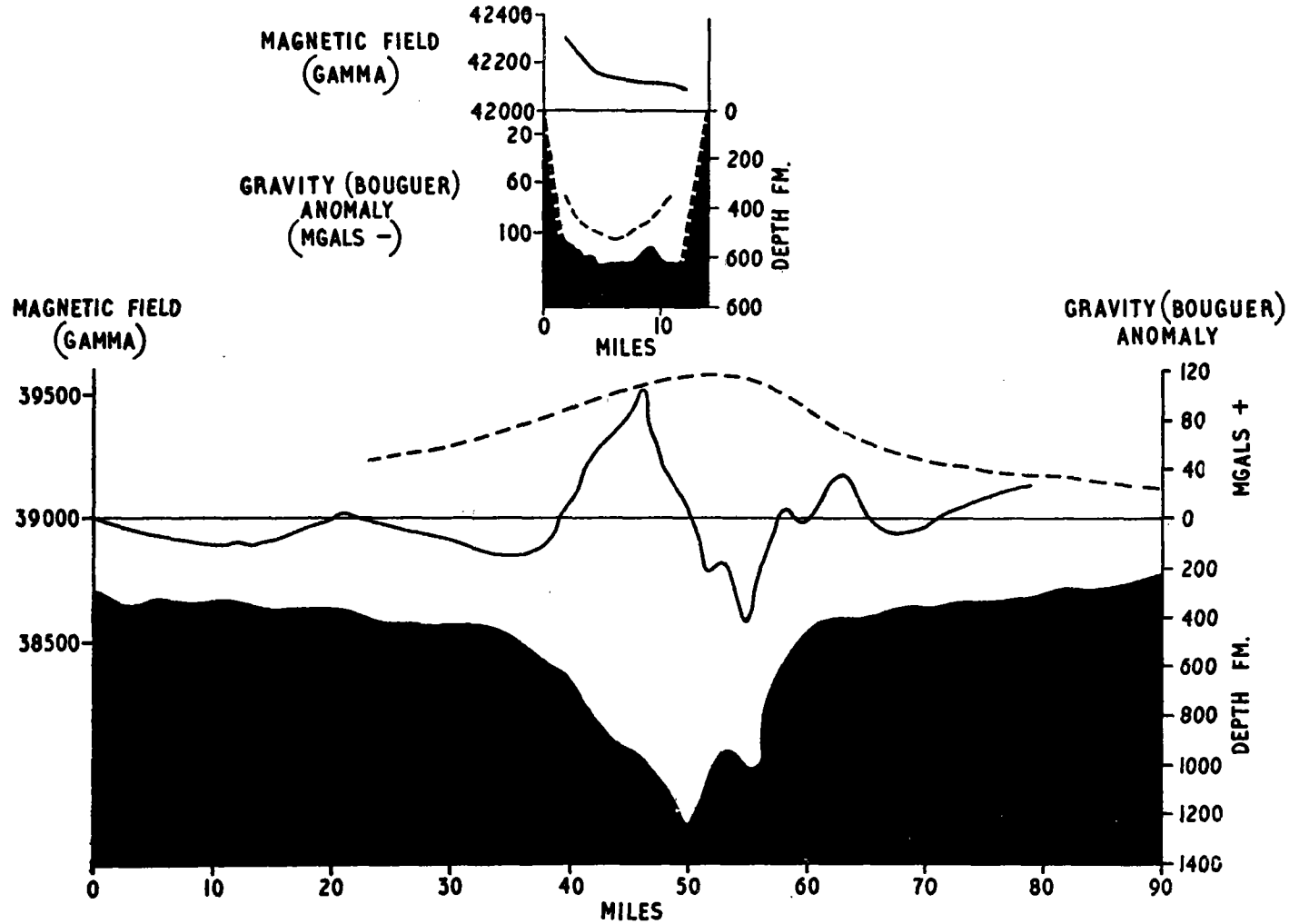

Fig. 5. Gravity and magnetic profiles across the Gulf of Aqaba (top), and across the Red Sea at 20° N. (bottom). The profiles are drawn to the same scale

was studied in much more detail during the 1961 cruise. A total of fifty-four transverse crossings were made. Records from a typical crossing (20° N.) are shown in Fig. 5.

A preliminary analysis of the results shows that the median valley, which is more fully developed in the south, is underlain by a considerable thickness of dense, magnetic rock. The lateral extent of this material appears to be confined to the width of the valley.

At the northern end of the Red Sea the Gulf of Suez is shallow and dull both in its magnetic and gravity structure. The Gulf of Aqaba, however, provides an interesting contrast. The Aqaba rift is everywhere less than 15 miles wide and about 600 fathoms deep. It is flanked on both sides by steep mountains. There is a strongly negative gravity anomaly, reaching -200 m.gal (free air) and -100 m.gal (Bouguer), while the magnetic field is featureless. The structure of the Gulf of Aqaba resembles that of the Gulf of Corinth; both may be thickly sedimented grabens.

The contrasting geophysical properties of the Gulf of Aqaba and the Red Sea, shown in Fig. 5, must be taken into account in any attempted interpretation of the origins of the Rift system.

We thank Dr. E. T. Booth and Dr. J. M. Ide for their advice during their service as scientific director of the Saclant ASW Research Centre; and our colleagues, ashore and afloat, and the captain, officers and crew of S.S. *Aragonese* for their assistance.

[1] Hill, M. N., *Deep Sea Res.*, **5**, 309 (1959).
[2] Ciani, A., Gantar, C., and Morelli, C., *Boll. Geofisica teor. appl.*, **2**, A, 289 (1960
[3] Allan, T. D., Dehlinger, P., Gantar, C., Morelli, C., Pisani, M., and Harrison, J. C., *J. Geophys. Res.*, **67**, 5157 (1962).
[4] Allan, T. D., *Boll. Geofisica teor. appl.*, **6**, 199 (1964).
[5] Drake, C. L., and Girdler, R. W., *Geophys. J.*, **8**, 473 (1964).

Printed in Great Britain by Fisher, Knight & Co., Ltd., St. Albans.

Reprinted from *Okeanol. Issled.*, no. 13, 1964, p. 157-162.

В. Ф. Канаев, Н. А. Марова

БАТИМЕТРИЧЕСКАЯ КАРТА СЕВЕРНОЙ ЧАСТИ ИНДИЙСКОГО ОКЕАНА

В результате работ э/с «Витязь», выполнившего в северной части Индийского океана в 1959—1962 гг. три рейса (31, 33, 35), были собраны обширные материалы по рельефу дна, которые внесли существенные изменения в прежние представления о геоморфологии дна Индийского океана [2,4]. На основании этих данных, а также материалов иностранных экспедиций, проводившихся как по планам Международного геофизического года 1957—1959 гг., так и по плану Международной индоокеанской экспедиции в Институте океанологии АН СССР И. М. Белоусовым, Л. К. Затонским, В. Ф. Канаевым и Н. А. Маровой, была составлена Батиметрическая карта северной части Индийского океана масштаба 1 : 5 000 000 в проекции Меркатора с изобатами через 500 *м*. Южная рамка карты проходит по 40° ю. ш. На рис. 1 приведена уменьшенная копия карты: северо-западный лист, ограниченный 15° ю. ш. и 78° в. д., рассматривается в работе И. М. Белоусова (см. наст. сборник стр. 163).

При составлении Батиметрической карты северной части Индийского океана, которая для краткости в дальнейшем называется Батиметрической картой Индийского океана, в качестве основных были использованы материалы э/с «Витязь». Они характеризуют значительную часть океанического дна и представлены подробными эхограммами и профилями, позволяющими дать правильную геоморфологическую интерпретацию другим данным. Сведения о подводном рельефе, собранные иностранными экспедициями на судах «Вима» (14 рейс), «Арго», «Диамантина», «Оуэн» и рядом английских судов, были представлены большим количеством отметок глубин, нанесенных вдоль эхолотных галсов на планшеты масштаба 1 : 1 000 000, которые были получены в порядке международного обмена. Материалы д/э «Обь», выполнившего эхолотный промер на пути из Антарктики в Бенгальский и Аденский заливы, представлены подробными профилями, которые составлены по эхограммам. Сведения о рельефе дна, собранные другими экспедициями, имелись в распоряжении авторов также в виде таблиц глубин («Планет» — 1906—1907 гг., «Дана» — 1930 г., «Альбатрос» — 1947 г., «Галатея» — 1952 г., «Махабис» — 1933—1934 гг.), в виде отметок глубин, нанесенных на батиметрические или навигационные карты («Снеллиус» — 1930 г., «Бугенвиль» — 1939 г., «Лаперуз» — 1949 г., «Шарко» — 1948 г. и др.) или в виде небольших обзорных профилей («Вима» — 16 рейс 1959—1960 гг.). Кроме данных океанографических экспедиций, при составлении карты использованы отметки глубин морских навигационных карт и Генеральной батиметрической карты океанов [10] (рис. 2).

БАТИМЕТРИЧЕСКАЯ КАРТА СЕВЕРНОЙ ЧАСТИ ИНДИЙСКОГО ОКЕАНА

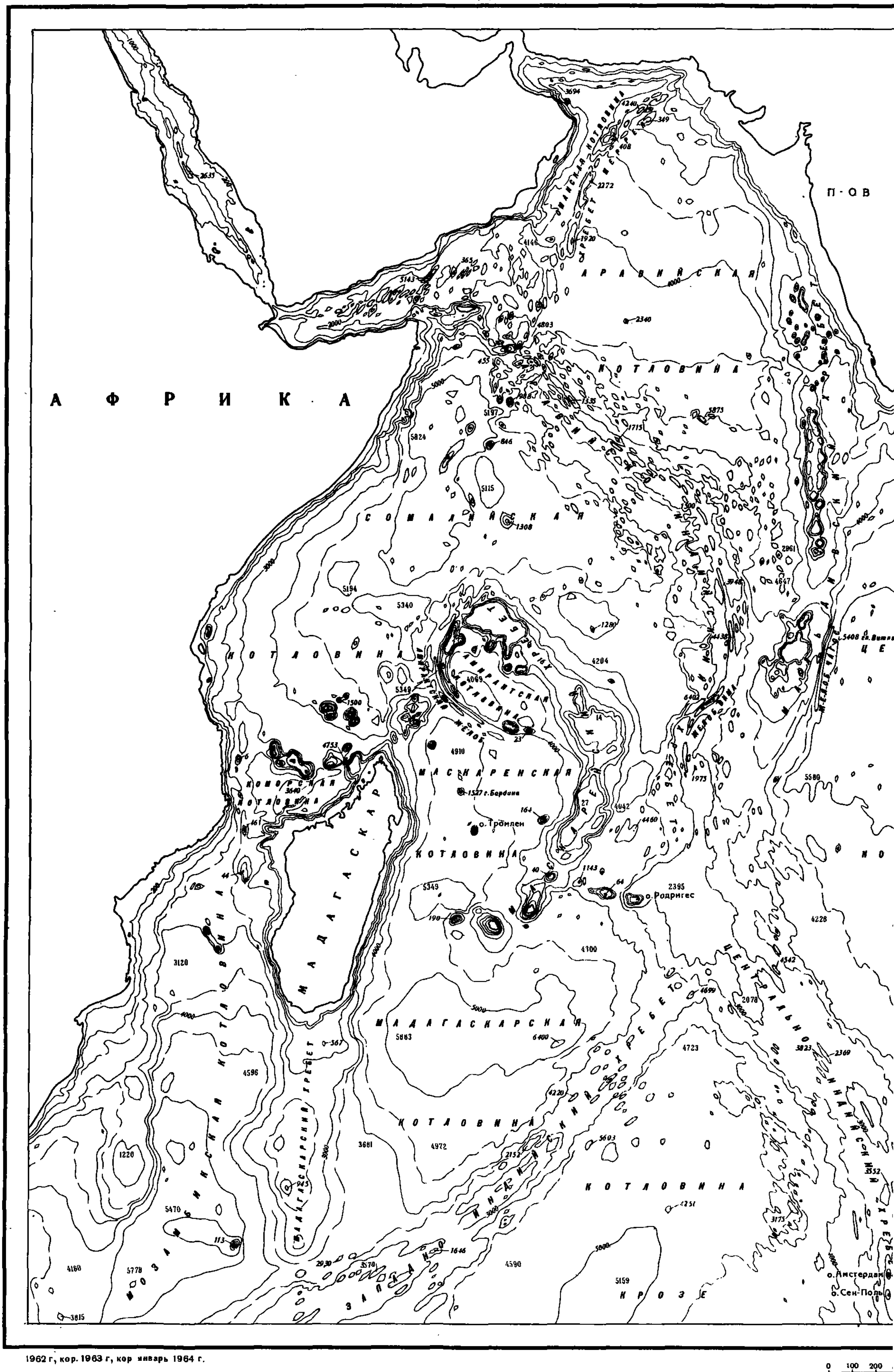

1962 г, кор. 1963 г, кор январь 1964 г.

0 700 600 900 км

Карту составили Белоусов И. М. Затонский Л. К.
Кашеев В. Ф. Марова Н. А.

Батиметрическая карта Индийского океана составлялась в масштабе 1 : 5 000 000; при составлении ее западной половины, района Яванского желоба и Андаманского моря были использованы навигационные карты более крупных масштабов. Обработка материалов и составление батиметрической карты велись в соответствии с разработанной в Институте океанологии методикой [5, 7].

Новая батиметрическая карта Индийского океана сильно отличается от предыдущих карт. На Генеральной батиметрической карте океанов масштаба 1 : 10 000 000 [10] рельеф дна Индийского океана изображен очень схематично. Это в значительной степени связано с ограниченностью данных, имевшихся при ее составлении. Подобными недостатками обладают и карты первого тома Морского атласа [8]. Физико-географические карты второго тома Морского атласа [8], Атласа мира [1], а также карта Индийского океана [6] более совершенны, так как они дают более правильное с геоморфологической точки зрения представление об изображаемых формах. Мелкомасштабная схематическая карта Стокса [16] интересна тем, что на ней частично уже были использованы данные, полученные экспедициями на «Альбатросе», «Оби», «Шарко», что позволило автору показать ряд новых форм. Однако наряду с этим на карте дано много гипотетических форм рельефа, что значительно снижает ее ценность.

Не имея возможности в краткой статье дать подробную характеристику рельефа дна всей площади, охватываемой батиметрической картой, ограничимся описанием новых форм рельефа и тех изменений, которые были внесены в изображение ранее известных форм.

Наиболее крупным горным сооружением Индийского океана является система Срединно-Индоокеанских хребтов, являющихся частью единой системы срединных хребтов Мирового океана. В Индийском океане она состоит из трех частей, соединяющихся в районе о-ва Родригес. Две ее южных ветви уходят в Атлантический и Тихий океаны, а третья (Аравийско-Индийский хребет) подходит к Аденскому заливу. До последнего времени юго-западная ветвь хребта на батиметрических картах не показывалась. Лишь в 1959—1960 гг. исследованиями «Вимы» [11] было установлено, что в юго-западной части Индийского океана протягивается хребет, названный Западно-Индийским.

Система Срединно-Индоокеанских хребтов в пределах карты представляет собой очень раздробленное довольно широкое поднятие, подножие которого находится на глубине около 4500 *м*. Средняя относительная высота единого основания хребта равна 1500 *м*, но отдельные вершины поднимаются значительно выше. Юго-западная ветвь (Западно-Индийский хребет) морфологически отличается от юго-восточной (Центрально-Индийский хребет). Первая имеет сильно раздробленную поверхность, которая постепенно переходит в менее расчлененное дно прилежащих котловин. Ширина этой части хребта в среднем равна 210 милям, относительная высота меняется от 1210 до 3300 *м*. Поверхность хребта представляет собой сочетание небольших хребтов и депрессий, размеры которых увеличиваются по мере приближения к оси хребта. К оси хребта также приурочены наиболее высокие горы, между которыми располагается рифтовая долина, представляющая собой ряд отдельных замкнутых узких глубоких депрессий — желобов. Глубина дна долины относительно вершин гор достигает 2000—2300 *м*. В отдельных местах дно рифтовой долины расположено глубже, чем дно соседних котловин. Ширина долины на высоте 1000 *м* от ее дна равна 17—20 милям.

Центрально-Индийский хребет отличается от Аравийско- и Западно-Индийских хребтов большей шириной и меньшей относительной высотой. Средняя ширина хребта составляет 550 миль; склоны его более пологие. На поверхности хребта расположены отдельные горы относительной высотой около 2500 *м*; острова Амстердам и Сен-Поль представляют две таких горы, вершины которых поднимаются над водой. Расчленение поверхности

Центрально-Индийского хребта более мелкое. Рифтовая долина выражена менее четко, чем у Аравийско- и Западно-Индийского хребтов, но также представлена цепочкой мелких депрессий, вытянутых вдоль хребта. К востоку от Мадагаскара, близ о-ва Родригес, начинается северная ветвь системы Срединно-Индоокеанских хребтов — так называемый Аравийско-Индийский хребет.

При изображении на батиметрической карте особенностей морфологии системы Срединно-Индоокеанских хребтов возник ряд трудностей, обусловленных недостатком фактического материала. На карте все формы рельефа, как правило, изображены на основании фактических данных и никаких гипотетических гор, холмов и котловин не показано, в том числе и на Срединно-Индоокеанских хребтах, хотя в действительности, судя по эхограммам и по профилям, вся поверхность этих хребтов покрыта небольшими горами, хребтами и котловинами. В связи с этим при изображении рельефа Срединно-Индоокеанских хребтов дан извилистый рисунок изобат, который в какой-то степени показывает, как проходила бы изобата при огибании многочисленных неровностей на поверхности хребтов, хотя в большинстве случаев эти извилины и не обоснованы фактическими данными.

Вторым по величине горным сооружением Индийского океана является Восточно-Индийский хребет, расположенный в северо-восточной части океана примерно вдоль 90° в. д. Существование этого хребта было установлено лишь в самые последние годы на основании работ многих судов различных государств [9]. Восточно-Индийский хребет представляет собой узкое (около 100 миль) длинное (2650 миль) поднятие относительной высотой от 1000 до 3500 *м*. Местами над хребтом возвышаются отдельные вершины с минимальными глубинами над ними до 870 *м*. На отдельных участках гребень хребта опускается, образуя седловины. В средней части Восточно-Индийский хребет резко расширяется в результате причленения крупного горного массива. Вдоль восточного подножия хребта протягивается узкое понижение — Восточно-Индийский желоб.

К западу от Австралии примерно на 30° ю. ш. находится массивный хребет, называемый Западно-Австралийским. Этот хребет обладает ярко выраженной асимметрией: его южный склон очень крутой, а северный пологий. Гребень хребта представляет широкую, слегка выпуклую поверхность. На склонах хребта встречаются горы и узкие гребни. Вдоль южного подножия хребта располагается узкий желоб.

К югу от Мадагаскара протягивается в меридиональном направлении очень широкий (средняя ширина порядка 270 миль) Мадагаскарский хребет с довольно пологими (до 1°) склонами. Относительная высота хребта около 2500 *м*. Широкая вершинная поверхность хребта расположена на глубине 2500 *м*. Над ней поднимаются отдельные горы. На юге хребет соединяется с Западно-Индийским хребтом. Седловина между хребтами расположена на глубине около 4000 *м*.

Кроме хребтов, на дне Индийского океана имеются горные массивы и горы. Некоторые из них были детально обследованы и названы [2—4]. Много крупных подводных гор расположено вдоль внешнего края Яванского желоба, между Кокосовыми островами и о-вом Рождества и к западу от Австралии, не говоря о небольших горах, широко распространенных на дне котловин в центральной части океана.

Отдельные горы обычно имеют крутые склоны, в среднем 10—15°, а местами до 25°, округлое или овальное основание диаметром от 15 до 70 миль. Относительная высота подводных гор, к которым мы относим поднятия, начиная с 500 *м*, достигает нескольких тысяч метров, а максимальная — 4300 *м*. Вершины отдельных гор поднимаются близко к поверхности океана или возвышаются над водой, образуя банки и небольшие острова. Такие горы имеют относительную высоту до 5500 *м*. Довольно часто основания нескольких гор сливаются одно с другим, иногда горы располагаются

по прямой линии. Например, между Кокосовыми островами и о-вом Рождества имеется цепочка крупных подводных гор, возвышающихся над широким пологим валом.

Близ побережья западной Австралии располагается несколько крупных поднятий дна, называемых нами горными массивами. Два из них присоединяются к материковому склону, а два расположены на дне котловины. Массив, расположенный к северу от северо-западного мыса Австралии, представляет выступ материкового склона, который Фейрбридж называет Эксму [12]. Массив Натуралиста, находящийся к западу от одноименного мыса, также сливается с основанием материкового склона. Вблизи подножия материкового склона Австралии на широте южного тропика находится горный массив Кювье с несколькими вершинами. От подножия материкового склона он отделен довольно глубоким понижением. Северо-западнее имеется еще один горный массив, имеющий в плане округлые очертания и плоскую вершину. Общей чертой всех перечисленных горных массивов является значительная крутизна склонов и плоская слегка волнистая вершинная поверхность.

Системой горных хребтов и валов впадина Индийского океана делится на ряд более или менее крупных котловин. К югу от Индии располагается Центральная котловина, включающая Бенгальский залив. На востоке она ограничена Восточно-Индийским хребтом, а на юге и западе — Центрально-Индийским и Мальдивским хребтами. К востоку от Восточно-Индийского хребта находится несколько крупных котловин: Кокосовая, Западно-Австралийская, Северо-Австралийская. Эти котловины соединяются одна с другой. К югу от Западно-Австралийского хребта располагается Юго-Западно-Австралийская котловина. От Южно-Австралийской котловины она отделена невысоким валом, в котором имеется проход, расположенный у самого подножия материкового склона Австралии.

До выявления Западно-Индийского хребта к юго-востоку от Мадагаскара на картах отмечалась большая котловина, иногда называвшаяся Центральной [12]. Северная часть этой котловины, названная Мадагаскарской, ограничена на западе поднятием о-ва Мадагаскар и продолжающимся от него к югу Мадагаскарским хребтом, на юго-востоке — Западно-Индийским хребтом, а на севере — южной частью Маскаренского хребта. Дно котловины, судя по профилям, выровнено и расположено на глубине немного более 5000 *м*. Южная котловина — Крозе — находится между двумя ветвями Срединно-Индоокеанских хребтов, а на юге ограничена поднятием островов Кергелен и Крозе.

Различная степень расчлененности дна котловин Индийского океана нашла отражение в рисунке изобат. Там, где развиты выровненные пространства аккумулятивных равнин, например в северной половине Центральной котловины с Бенгальским заливом и в Кокосовой котловине изобаты имеют плавные изгибы. Наоборот, в центральных частях океана, где дно котловин сильно расчленено, изобаты более извилистые.

В Индийском океане имеется один краевой глубоководный желоб — Яванский, протянувшийся вдоль Зондской островной дуги, вследствие чего его правильнее было бы называть Зондским. На севере желоб оканчивается в Бенгальском заливе примерно на 18° с. ш. Юго-восточное окончание желоба расположено примерно на 123° в. д. в районе о-ва Роти. Продолжением Яванского желоба к востоку является Тиморский желоб. Параллельно Яванскому глубоководному желобу вдоль островов Суматра, Ява и западной части Малых Зондских протягивается система межгорных желобов: Сималурский, Ментавей и Балийский. От Яванского желоба они отделены хребтами Ментавей и Балийским. Вершины первого около о-ва Суматра поднимаются над водой, образуя цепочку небольших островов; второй хребет полностью скрыт под водами океана. Северо-западное окончание Сималурского желоба через глубокий пролив между о-вом Суматра и поднятием Никобарских островов входит в котловину Андаманского моря.

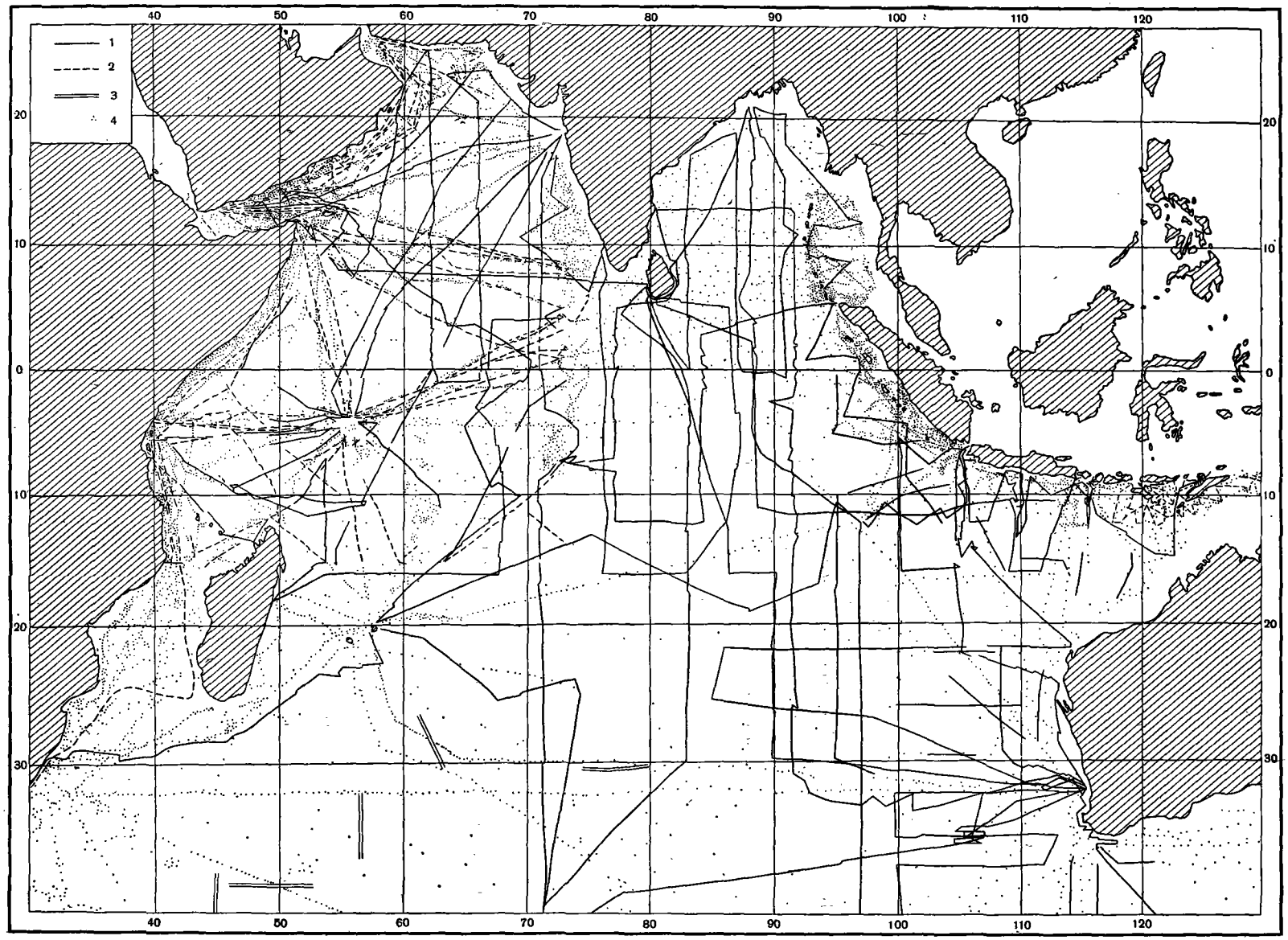

Рис. 2. Схема материалов, использованных при составлении батиметрической карты северной части Индийского океана

1 — галсы с непрерывным промером; *2* — галсы с разреженным эхолотным промером; *3* — положение обзорных профилей, выполненных «Вимой»; *4* — отдельные глубины (более 200 *м*)

Яванский глубоководный желоб представляет непрерывную узкую депрессию длиной около 2900 миль с широким (до 20 миль) плоским аккумулятивным дном. Наибольшая глубина желоба равна 7450 *м*. Желоб имеет асимметричное строение: крутой и высокий внутренний склон и более пологий низкий внешний. Внутренний склон желоба отличается сложным рельефом: местами его расчленяют глубокие долины и борозды, встречаются уступы и ступени. Крутизна нижней части внутреннего склона составляет 4—7°. Внешний склон Яванского желоба обладает более простым рельефом: лишь местами на нем встречаются небольшие ступени и уступы. Высота внешнего склона увеличивается в направлении с северо-запада на юго-восток от 500 до 2000 *м*.

С внешней стороны Яванского желоба протягивается краевой океанический вал, представляющий собой ряд пологих поднятий высотой 600—800 *м*, разделенных седловинами. Над поверхностью вала поднимаются отдельные горы, по-видимому, вулканического происхождения. Местами вал представляет собой сильно расчлененный горный хребет.

В Индийском океане имеются небольшие желоба, расположенные либо у подножия горных хребтов, либо на дне котловин. Вдоль восточного подножия Мальдивского хребта в районе островов Чагос протягивается одноименный желоб, обнаруженный в 33 рейсе «Витязя» [2]. В 35 рейсе «Витязя» были собраны дополнительные сведения по морфологии этого желоба [9]. Наибольшая глубина желоба равна 5408 *м*. Дно желоба плоское широкое (до 10 миль). Внутренний склон круче (до 20°) и выше, чем внешний. Вдоль западной стороны желоба протягивается узкий хребтик, а с восточной — широкий вал, над которым поднимаются небольшие горы.

Восточно-Индийский желоб протягивается вдоль восточного подножия одноименного хребта. Желоб состоит из нескольких частей, разделенных невысокими порогами. Наибольшая глубина 6335 *м* [13] приурочена к северной части желоба. Ширина желоба составляет 10—20 миль, ширина же плоского аккумулятивного дна достигает 15 миль. На склонах и дне желоба местами поднимаются холмы и горы. Крутизна склонов желоба достигает 20°. С внешней стороны желоба возвышаются горы и возвышенности, образующие слабо выраженный в рельефе вал.

Вдоль южного склона Западно-Австралийского хребта протягивается желоб, который был впервые пересечен на д/э «Обь», а затем подробно обследован в 35 рейсе «Витязя», после чего он был назван желобом Оби. Наибольшая глубина желоба Оби составляет 5761 *м*. Дно желоба также плоское, шириной около 7 миль, склоны крутые — до 15°. С южной стороны вдоль желоба тянется невысокий вал с отдельными горами. Восточнее желоба Оби и Западно-Австралийского хребта дно котловины сильно раздроблено. Здесь имеется много небольших желобов — разломов, гор и холмов.

К югу от этой зоны дробления океанического ложа в середине Юго-Западно-Австралийской котловины находится желоб Диамантина, названный в честь австралийского судна, впервые сообщившего о наличии в этом районе больших — до 6857 *м* — глубин [15]. Этот желоб представляет собой систему из нескольких желобов, имеющих *V*-образный профиль, узкое дно и крутые склоны. Вдоль краев желоба протягиваются небольшие валы и поднимаются отдельные горы.

Все небольшие желоба Индийского океана обладают общими морфологическими чертами (небольшая ширина, крутые склоны, наличие вдоль краев валов и гор), которые свидетельствуют о том, что образование данных форм рельефа связано с разломами океанического ложа, аналогичными разломам Тихого океана [14].

Многие из показанных на Батиметрической карте Индийского океана форм подводного рельефа были обнаружены в самые последние годы и не подвергались детальному обследованию. Поэтому при дальнейших исследованиях их изображение может подвергнуться изменению, могут появиться

также новые формы рельефа, так как обширные участки дна Индийского океана остались еще плохо исследованными. Но несмотря на это, новая карта по сравнению с прежними батиметрическими картами Индийского океана, представляет собой значительный шаг вперед, подводя итог первому этапу работ Международной Индоокеанской экспедиции, основной вклад в который был сделан э/с «Витязь».

ABSTRACT

Based on investigations of the research vessels «Vityaz», «Ob», «Vyma», «Argo», «Diamantina», etc. a bathymetric chart of the northern Indian Ocean (to 40°S) has been compiled at the Institute of Oceanology of the USSR Academy of Sciences on a scale of 1 : 5 000 000. The article contains new data on the Indian Ocean bottom topography (except for its north-western part). The greatest geographical discovery was the finding of the East Indian Ridge stretching along 90° E from 10° N to 34° S. The East Indian Ridge and West Australian Ridge, and rises divide the north-eastern part of the ocean into a number of basins : Central with the Bay of Bengal, Cocos, West Australian, North Australian, South-West Australian. New data on the geomorphology of the Java (Sunda) trench are introduced. A description is also given of some new troughes: Chagos, East Indian, Ob, Diamantina. The morphology of the Mid Indian and West Australian ridges has been specified.

ЛИТЕРАТУРА

1. Атлас мира. М. ГУГК, 1954.
2. Безруков П. Л. Исследования Индийского океана в 33 рейсе «Витязя».— Океанология, 1961, № 4.
3. Безруков П. Л., Затонский Л. К., Сергеев И. В. Гора Афанасия Никитина в Индийском океане.— Докл. АН СССР, 1961. **139**, № 1.
4. Белоусов И. М. 31 рейс «Витязя».— Океанология, 1961, № 2.
5. Буданова Л. Я., Затонский Л. К., Ларина Н. И., Марова Н. А. К вопросу о методике составления батиметрических карт.— Труды ИОАН, 1950, т. 44.
6. Индийский океан. Масштаб 1 : 10 000 000, М., НРКЧ ГУГК, 1956.
7. Канаев В. Ф., Удинцев Г. Б. Изучение подводного рельефа в океанографических экспедициях.— Труды ИОАН, 1960, т. 44.
8. Морской атлас. Изд. Морского Генерального штаба, т. I, 1950; т. II, 1953.
9. Безруков П. Л., Канаев В. Ф. Основные черты строения дна северо-восточной части Индийского океана.— Докл. АН СССР, 1963. 153, № 4.
10. Carte Générale Bathymétrique des Océans, M 1 : 10 000 000. 3 éd. Bureau Hydrogr. Internat. Monaco, AIV-1938, A-III-1940; A'IV - 1938, A'III-1942.
11. Ewing M., Heezen B. Continuity of Mid-Oceanic Ridge and Rift Valley in the Southwestern Indian Ocean confirmed.— Science, 1960, **131**, № 3414.
12. Fairbridge R. W. Some bathymetric and geotectonic features of the eastern part of the Indian Ocean.— Deep-sea Res., 1955, **2**, p. 161.
13. Koczy F. F. Echo Soundings.— Repts Swed. Deep-Sea Expedit., 1956, **4**, N 3, fasc. 2.
14. Menard H. W. Deformation of the Northeastern Pacific Basin and West Coast North America.— Bull. Geol. Soc. America, 1955, **66**, N 9.
15. Oceanographical cruise report № 2. Oceanographical Observations in the Indian Ocean in 1960 H. M. A. S. «Diamantina», Cruise DM 1/60, Melbourne, 1962.
16. Stocks T. Zur Bodengestalt des Indischen Okeans.— Erdkunde, 1960, **14**, H. 3.

Reprinted from *Okeanologia*, vol. V, no. 4, 1965, p. 760-762.

ИНДИЙСКИЙ ОКЕАН

Новая географическая карта

В 1963—1964 гг. Научно-редакционная картосоставительская часть ГУГК Госгеолкома СССР выпустила серию справочных физико-географических карт Тихого, Атлантического и Индийского океанов, а также северного и южного полушарий Земли. Благодаря этому сейчас имеются карты, охватывающие весь Мировой океан, причем изображение подводного рельефа на них дано по единой методике и основано на современных данных. Это обстоятельство имеет большое значение, так как рельеф дна является важнейшим элементом физико-географической среды, влияющим на многие процессы, происходящие в океане.

Необходимость создания новой карты Индийского океана возникла давно, потому что все ранее изданные карты, даже самые новейшие [29, 33], основывались исключительно на сведениях, полученных до второй мировой войны. Новые данные, собранные в послевоенные годы и, особенно, в течение Международного геофизического года 1957—1959 гг. большей частью не нашли отражения на картах. До этого в печати появились лишь отдельные частные работы и схематические батиметрические и тектонические карты Индийского океана и отдельных его частей [12, 20, 21, 32].

В связи с организацией Международной индоокеанской экспедиции [4] изучение рельефа дна Индийского океана стало осуществляться в широких масштабах. Наиболее крупный вклад в изучение рельефа дна океана в самом начале работ этой экспедиции внесли исследовательские суда: «Витязь» (СССР), «Вима» и «Арго» (США), «Оуэн» и «Далримпл» (Англия), «Диамантина» (Австралия).

Новая карта Индийского океана [17] издана в конце 1963 г. Она имеет масштаб 1 : 15 000 000 и составлена в равновеликой азимутальной проекции Ламберта (редактор карты Е. М. Шуран, рельеф дна океана отредактирован В. Ф. Канаевым и Н. А. Маровой).

Основным содержанием карты является рельеф дна океана и окружающей суши, показанный при помощи изолиний (изобат и изогипс) с послойной окраской по ступеням высот и глубин. Основные изолинии на карте даны через 1000 *м*. Для более подробной характеристики равнинных пространств проведены дополнительные изолинии: на суше 200 и 500 *м* и на дне 200, 3500, 4500, 5500 *м*. Изобата 200 *м* в подавляющем большинстве случаев хорошо показывает положение края материковой отмели, остальные изобаты необходимы для передачи характерных особенностей рельефа дна океанических котловин.

Основными материалами, использованными для составления новой карты Индийского океана, явились батиметрические карты, выполненные в 1963 г. в Институте океанологии АН СССР [8] и в Институте географии АН СССР. Рельеф дна Атлантического и Тихого океанов был взят с соответствующих ранее изданных карт [1, 24].

В основу батиметрической карты Института океанологии АН СССР, охватывающей северную часть океана, были положены материалы, собранные в трех рейсах НИС «Витязь» в 1959—1962 гг. [2,3,7], а для карты Института географии, охватывающей южную часть океана,— материалы, собранные в трех рейсах д/э «Обь» в 1957—1960 гг. [13, 14, 21]. Использование материалов «Витязя» и «Оби», представленных в виде профилей дна [9—11, 22—23], а также эхограмм, в том числе и полученных на прецизионных самописцах [2, 18], позволило достаточно полно и правильно изобразить на карте рельеф дна океана в целом и его частей, а также отдельные крупные формы рельефа. Вследствие того, что работами «Витязя» и «Оби» была охвачена большая часть Индийского океана, собранные материалы позволили более правильно интерпретировать другие сведения о подводном рельефе, представленные гораздо менее детальными данными в виде промерных планшетов, морских навигационных карт, списков глубин и мелкомасштабных профилей.

Промерные планшеты масштаба 1 : 1 000 000, полученные в порядке международного обмена, содержали отметки глубин, нанесенные вдоль промерных галсов через 1—2 мили. На планшетах Британского адмиралтейства, охватывающих северо-западную часть Индийского океана, нанесены глубины, измеренные исследовательскими судами «Оуэн» в 1961—1963 гг., «Дарлимпл» в 1963 г., и попутные промеры других судов. На американских планшетах были представлены данные 14 и 16-го рейсов и/с «Вима», касающиеся главным образом срединно-океанических хребтов западной половины Индийского океана и Красного моря, а также рейса и/с «Арго» экспедиции «Муссон» 1960—1961 гг., проходившей в восточной половине океана. Австралийские планшеты покрывали восточную часть океана, прилежащую к западным и северным берегам Австралии. На них были нанесены глубины, измеренные и/с «Диамантина» в 1959—1960 гг.

Кроме того были использованы данные о рельефе дна, полученные шведской кругосветной экспедицией на судне «Альбатрос», представленные в виде списка глубин, обзорных профилей и фотографий характерных участков эхограмм [31]. При изображении в юго-западной части Индийского океана участка Срединно-океанического хребта были использованы небольшие схематические профили [27], которые, однако, до сих пор являются единственным опубликованным источником, дающим наиболее близкое к действительности представление о морфологии этого хребта. При составлении карты

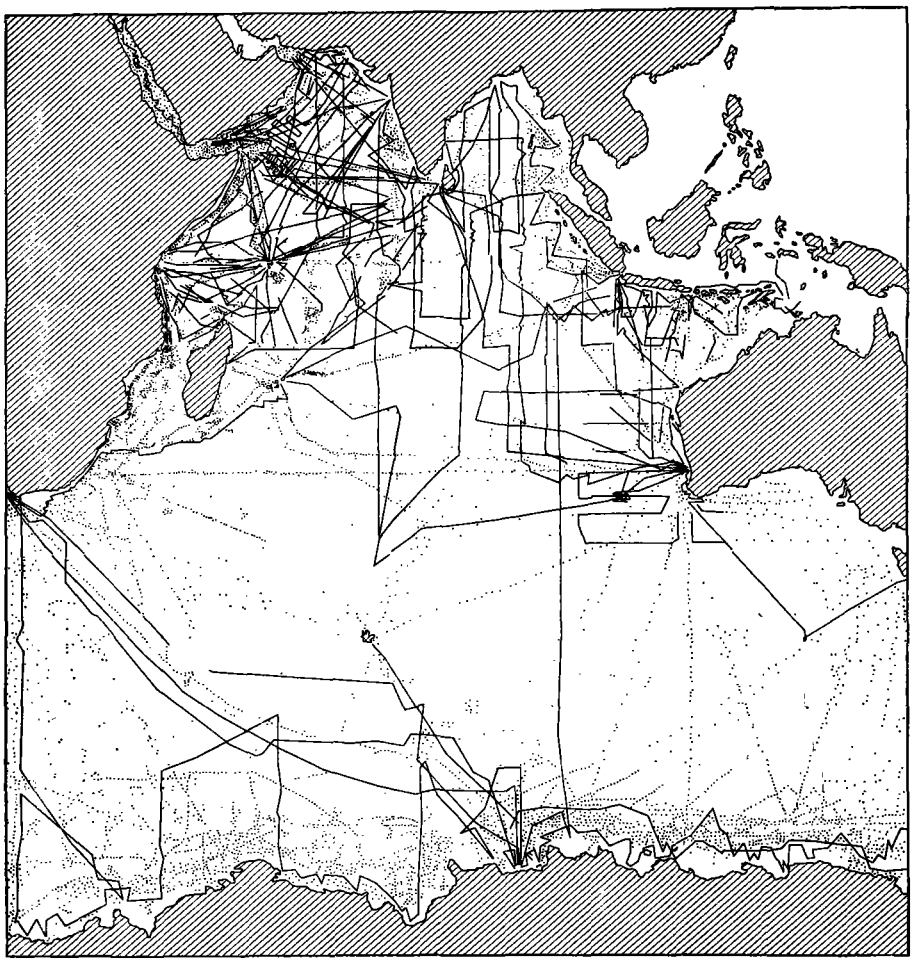

Схема материалов, использованных при составлении карты Индийского океана

Сплошной линией показаны галсы с непрерывным эхолотным промером, точками — места отдельных глубин (более 200 м)

Океанология, № 4 (вклейка к статье В. Ф. Канаева)

также были использованы соответствующие листы Генеральной батиметрической карты океанов [26], а также глубины с морских навигационных карт различных государств.

Использование новых данных позволило составить карту, существенно отличающуюся от ранее изданных. Это относится как к содержанию карты, так и к методике ее составления. При изображении подводного рельефа был использован метод геоморфологической интерполяции [25]. Как известно [15, 19], при помощи изолиний (изогипс и изобат) на картах можно передавать не только плановое распределение различных высот и глубин, но также и морфологические особенности как отдельных форм, так и рельефа в целом. В связи с этим при изображении подводного рельефа рисунок изобат на карте Индийского океана менялся в зависимости от характера подводного рельефа. Для того, чтобы иметь наглядное представление о крутизне склонов, сечение рельефа было принято постоянным и равным 1000 *м*. Рисунок изобат на дне океанических котловин меняется в зависимости от расчлененности дна: в пределах аккумулятивных равнин, расположенных по периферии океанов у подножия материковых склонов, изобаты имеют плавные очертания, а в центральной части океана, где дно сильно расчленено, изобаты делают резкие изгибы. На Срединно-океанических хребтах подчеркивается линейная расчлененность их поверхности и ориентировка этих неровностей вдоль оси хребта, а на дне котловин подчеркивается изометричность положительных форм рельефа, в то время как отрицательные формы рельефа показаны обычно более или менее вытянутыми. На материковых склонах в подавляющем большинстве случаев показано долинное расчленение, кроме тех участков, где склоны ровные.

При составлении карты Индийского океана в связи с появлением сведений о новых крупных формах рельефа и уточнением размеров и очертаний известных ранее форм потребовалось ввести новые или уточнить прежние названия. В тех случаях, когда для одной и той же формы рельефа использовались разные названия, выбиралось наиболее удачное, лучше всего отражающее географическое положение формы: Мозамбикская котловина, Амирантский хребет, желоб Чагос и др. Если же этого нельзя было сделать, то название давалось по наименованию судна, обнаружившего или исследовавшего данную форму (желоб Оби), или в честь выдающихся ученых и исследователей (гора Бардина, гора Афанасия Никитина).

Наиболее существенным изменением в представлениях о рельефе дна Индийского океана явилось изображение на карте огромного Восточно-Индийского хребта длиной более 2700 миль [6, 18]. Следует отметить, что до последнего времени высказывались предположения о существовании в этом районе хребта совершенно иного направления [34]. Восточно-Индийским хребтом огромная Индийско-Австралийская котловина разделена на две части, причем, северное окончание восточной котловины, обособленное валом, протянувшимся от о. Рождества до Кокосовых о-вов, выделено также в качестве самостоятельной котловины. Таким образом, в северо-восточной части Индийского океана сейчас выделяются следующие котловины: Центральная с Бенгальским заливом, Кокосовая, Западно-Австралийская и Северо-Австралийская.

Другим крупным открытием было обнаружение Западно-Индийского хребта [27]. Благодаря этому было доказано, что система Срединных хребтов Мирового океана представляет единое горное сооружение протяженностью около 40 000 миль. Западно-Индийский хребет разделяет большую котловину к юго-востоку от Мадагаскара на две — Мадагаскарскую и Крозе.

Новые данные показали, что вместо предполагавшегося Фэйрбриджем [28] Западно-Австралийского хребта к северо-западу от залива Шарк (Австралия) расположены отдельные крупные горные массивы. В связи с этим название Западно-Австралийский хребет было предложено для массивного поднятия дна, расположенного близ Австралии (вдоль 30° ю. ш.) у южной границы Западно-Австралийской котловины.

На новой карте появилось много небольших желобов-разломов на ложе Индийского океана, которые большей частью протягиваются вдоль подножия хребтов (желоба: Чагос, Обь, Восточно-Индийский, Амирантский и др.). Встречаются желоба и в середине котловин (желоб Диамантина). На карте показано много подводных гор, однако лишь немногие из них были обследованы детально [5, 16, 30, 35].

В. Ф. Канаев

ЛИТЕРАТУРА

1. Атлантический океан (карта). 1963. М-б 1 : 20 000 000. ГУГК ГГК СССР, М.
2. Безруков П. Л. 1961. Исследования Индийского океана в 33-м рейсе э/с «Витязь». Океанология, **I**, вып. 4.
3. Безруков П. Л. 1963. Исследования Индийского океана в 35-м рейсе э/с «Витязь». Океанология, **III**, вып. 3.
4. Безруков П. Л. 1963. Исследования «Витязя» по программе Международной индоокеанской экспедиции. Вестн. АН СССР, № 8.
5. Безруков П. Л., Затонский Л. К., Сергеев И. В. 1961. Гора Афанасия Никитина в Индийском океане. Докл. АН СССР, **139**, № 1.
6. Безруков П. Л., Канаев В. Ф. 1963. Основные черты строения дна северо-восточной части Индийского океана. Докл. АН СССР, **153**, № 4.
7. Белоусов И. М. 1961. 31-й рейс «Витязя». Океанология, **I**, вып. 2.

8. Белоусов И. М., Канаев В. Ф., Марова Н. А. 1964. Геоморфология дна северной части Индийского океана. Докл. АН СССР, **155**, № 5.
9. Данные по рельфу дна, полученные в 33-м рейсе экспедиционного судна Института океанологии АН СССР «Витязь» в 1960—1961 гг. 1963. Изд. Ин-та океанол. АН СССР, М.
10. Данные по рельфу дна, полученные в 1-ом антарктическом рейсе экспедиционного судна «Обь». 1960. Изд. Ин-та океанол. и Ин-та геогр. АН СССР, М.
11. Данные по рельефу дна, полученные во 2-м антарктическом рейсе дизельэлектрохода «Обь». 1960. Изд. Ин-та океанол. и Ин-та географии АН СССР, М.
12. Живаго А. В. 1960. Геоморфология и тектоника дна южной части Индийского океана. В кн. «Морская геология». Междунар. геол. конгр., 21 сессия. Докл. сов. геол., М.
13. Живаго А. В. 1961. Морские геолого-геоморфологические исследования. Тр. Сов. антаркт. экспед., 19.
14. Живаго А. В., Лисицын А. П. 1957. Новые данные о рельефе дна и осадках морей Восточной Антарктики. Изв. АН СССР. Сер. геогр., № 1.
15. Зарудская И. П. 1958. Методы составления рельефа на гипсометрических картах. М.
16. Затонский Л. К. 1964. Новые данные о рельефе дна Индийского океана. Тр. Ин-та океанол. АН СССР, **64**.
17. Индийский океан (карта). 1963. Масштаб 1 : 15 000 000. ГУГК ГГК СССР, М.
18. Канаев В. Ф. 1964. Геоморфология дна северо-восточной части Индийского океана. В кн. «Геология дна океанов и морей». Междунар. геол. конгр., 22 сессия. Докл. сов. геол., М.
19. Леонтьев Н. Ф. 1961. Географические основы картографирования подводного рельефа на гипсометрических картах. Геодезиздат, М.
20. Леонтьев О. К. 1963. Краткий курс морской геологии. Изд. Моск. ун-та.
21. Лисицын А. П., Живаго А. В. 1958. Рельеф дна и осадки южной части Индийского океана. Изв. АН СССР. Сер. геогр., № 2.
22. Материалы океанологических исследований. Рельеф дна. 31-й рейс экспедиционного судна «Витязь», 1962. Изд. Междувед. геофиз. комитета при Президиуме АН СССР, М.
23. Материалы океанологических исследований. Рельеф дна. Экспедиционное судно «Обь» 1957/58 гг. 1964. Изд. Междувед. геофиз. комитета при Президиуме АН СССР М.
24. Тихий океан (карта). 1963. М-б 1 : 25 000 000. ГУГК МГИОН СССР, М.
25. Удинцев Г. Б., Агапова Г. В. и др. 1963. Новая батиметрическая карта Тихого океана. Сб. Океанол. исслед., № 9, X раздел программы МГГ.
26. Carte Generale Bathymetrique des Oceans. 1938—1942. 3-me edition publee par le Bureau Hydrographique International, Monaco.
27. Ewing M., Heezen B. C. 1960. Continuity of Mid-oceanic ridge and rift valey in southwestern Indian ocean confirmed. Science. **131**.
28. Fairbridge R. W. 1955. Some bathymetric and geotectonic features of the eastern part of the Indian ocean. Deep-Sea Res., **2**, No 3.
29. Ocean Indien. Echelle 1 : 10 000 000. Institut Geographique National, Paris.
30. Paisley J. T. K. 1955. Survey of a seapeak in the Mozambique channel. Deep-Sea Res., **3**, No 2.
31. Pettersson H. (Ed.) Reports of the Swedish Deep-Sea Expedition 1947—1948. IV, fasc. II. Göteborg.
32. Stocks Th. 1960. Zur Bodengestalt des Indischen Ozeans. Erdkunde, 14, H. 3.
33. The world. 1960. Scale 1 : 63 360 000. Atlas plate 2. National Geogr. Soc. The National Geogr. Mag.
34. Wilson T. 1963. Hypothesis of earth's behaviour. Nature, **198**, No 4884.
35. Wiseman J., Hall G. 1956. Two recently discovered features on the floor of the Indian ocean: Andrew tablemount and David seaknoll. Deep-Sea Res., **3**, No 4.

Reprinted from *Deep-sea Res.*, vol. II, 1964, p. 921-927.

The crustal structure of the Seychelles Bank

D. DAVIES and T. J. G. FRANCIS
Department of Geodesy and Geophysics, University of Cambridge,
Madingley Rise, Madingley Road, Cambridge.

(*Received* 18 *June* 1964)

Abstract—The Seychelles are anomalous amongst oceanic islands in that Pre-Cambrian granite occurs on them. Seismic investigations are described in which 13 km of granite were found beneath the central group of islands. The depth to the mantle is approximately 33 km, and the crustal structure is continental in character.

THE Seychelles are a group of islands in the Indian Ocean 950 miles east of Kenya. Figure 1 shows the Seychelles Bank, an area of 50,000 square miles, in relation

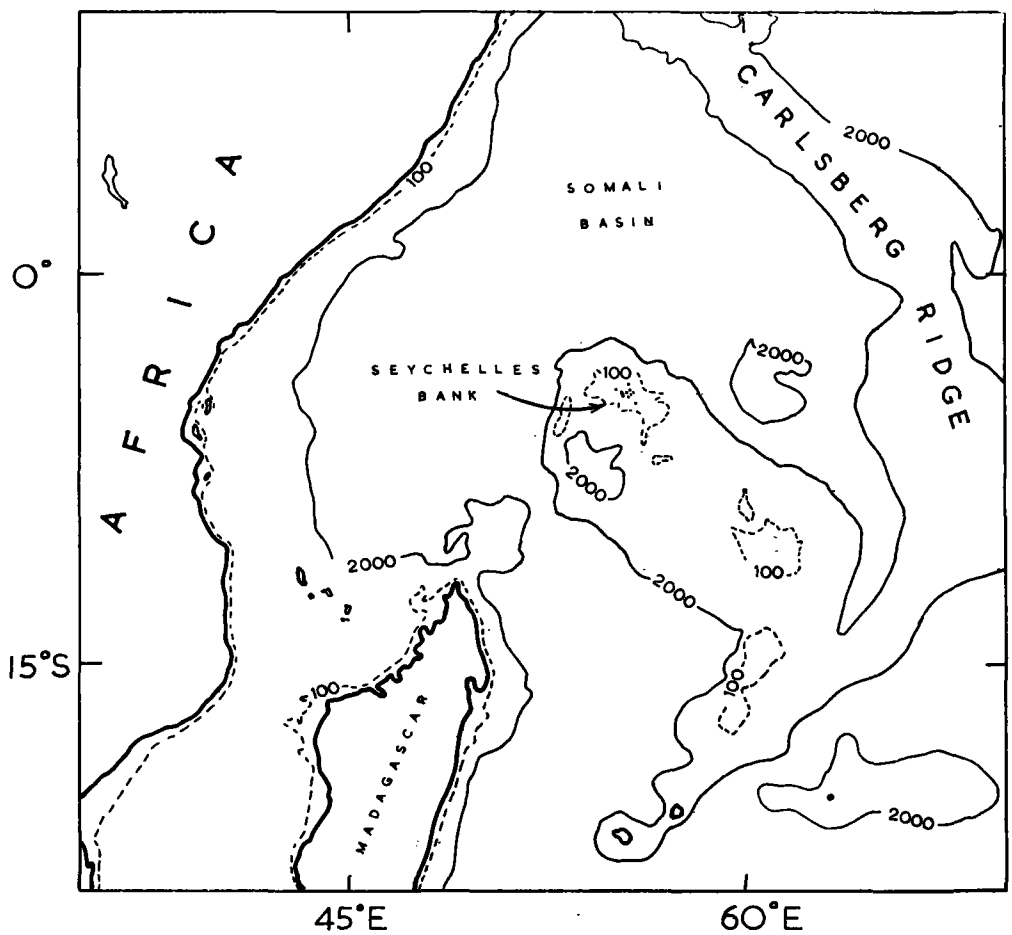

Fig. 1. Topography of the western Indian Ocean. 100 and 2000 fm contours are shown.

to other features in the Western Indian Ocean. The water on the Bank is in most places about 30 fm deep. The central islands of the Bank are Mahé, Praslin and smaller neighbours; they are made of Precambrian granite (BAKER and MILLER, 1963) whilst the fringing islands are coral or sand cays. The geology of all the islands is described in detail by BAKER (1963). Practically all oceanic islands are founded on volcanoes whilst large areas of granite are almost exclusively associated with the continents, and it has often been proposed in the past that the Seychelles may be of continental origin. WEGENER (1922) proposed that the Seychelles had arisen

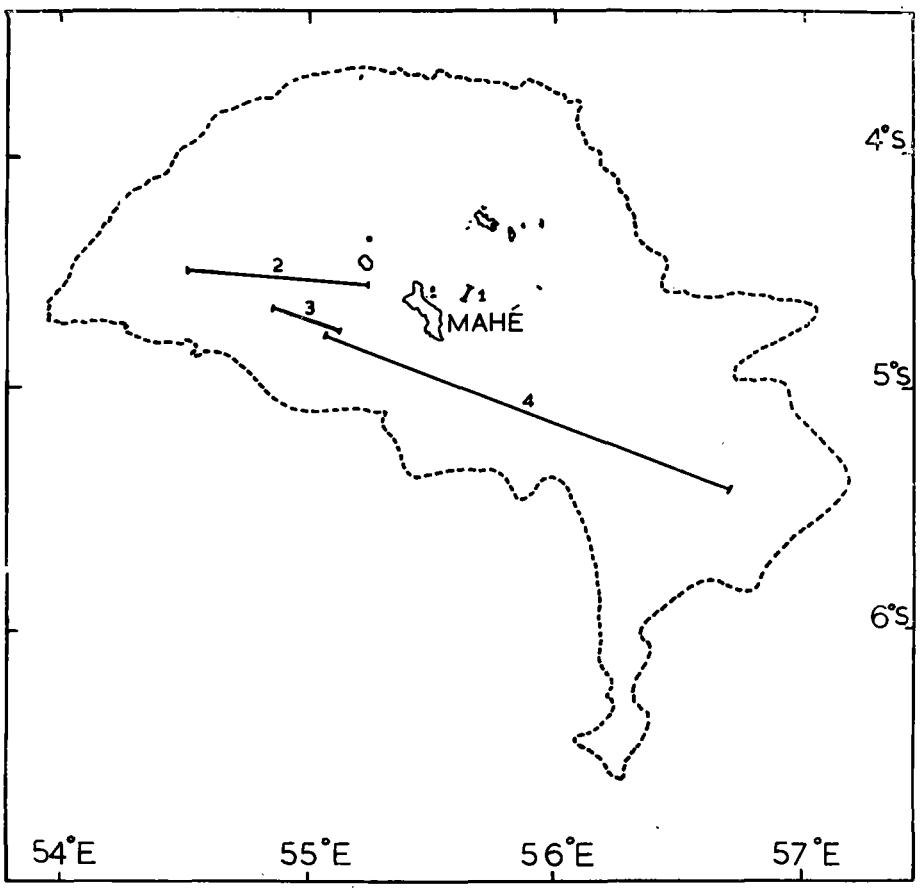

Fig. 2. Seychelles Bank. The 100 fm contour is shown. Positions of the four relevant seismic lines are given.

from beneath the East African coast and been carried towards India. DU TOIT (1937) provided detailed evidence for the displacement of Madagascar from the African coast as part of a large crustal movement in which India separated from Africa leaving the Seychelles behind. Interest in the origin of the crust beneath the Indian Ocean has recently been revived by paleomagnetic and paleoclimatological evidence that India was, 150 million years ago, much further south than it is today (BLACKETT, CLEGG and STUBBS, 1960; BLACKETT, 1961). On the other hand, Baker suggested that large areas off the East African coast might be subsided continental masses and that the African coastline was once much further to the east.

The Department of Geodesy and Geophysics, University of Cambridge, has recently been carrying out seismic investigations in the area as part of its contribution to the International Indian Ocean Expedition. In particular, on the Seychelles Bank, R.R.S. *Discovery* and H.M.S. *Owen* shot 2 seismic lines, shown in Fig. 2, (*Discovery* station 5210), *Discovery* firing short range shots (line 3) and *Owen* firing long range depth charges (line 4). Sonobuoys were used to record the seismic signals (HILL, 1963).

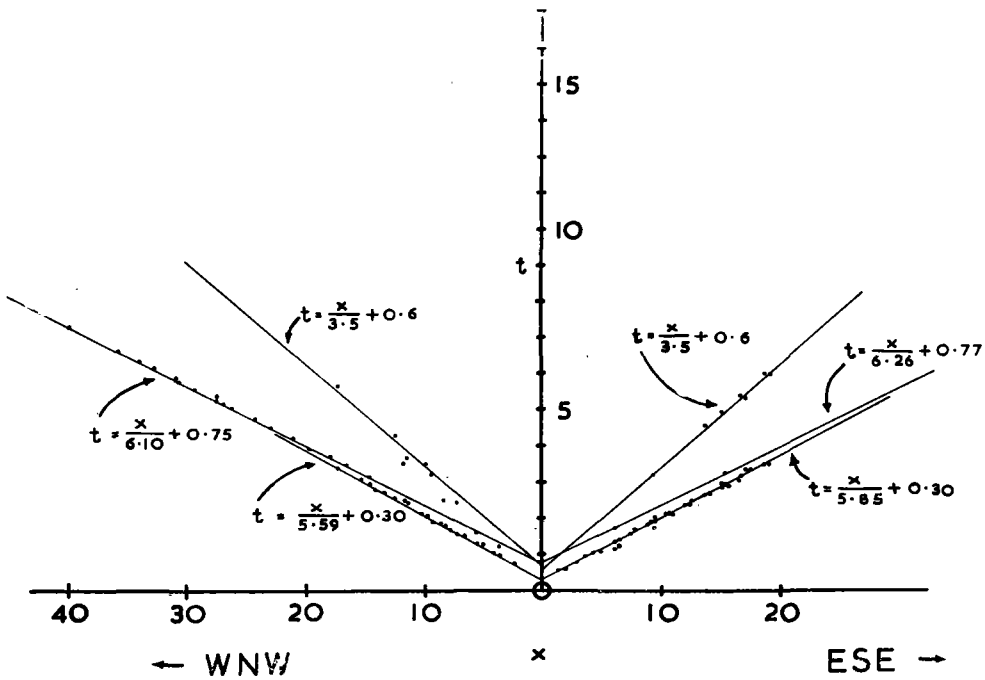

Fig. 3. Travel time curve for *Discovery* shots. The abscissa is kilometres, the ordinate is seconds.

Figure 2 also shows the location of two other relevant lines. Line 1 was fired by H.M.S. *Challenger* (GASKELL, HILL and SWALLOW, 1958) and established granitic velocities under a very thin sedimentary cover. Line 2 was fired by R/Vs *Argo* and *Horizon* (SHOR and POLLARD, 1963) and showed a material, with granitic velocity 6·22 km/s, dipping to the west but remaining present for at least 100 km west of Mahé. Overlying this are two relatively thin layers, probably of sediment and coral. Further work 900 km to the south-east suggested that the Saya de Malha Bank consisted of coral capped volcanic rocks based on a typical oceanic floor. There are no large magnetic anomalies at the edges of the Seychelles Bank such as one would expect at the edge of a basaltic bank.

An important practical problem in seismic work in shallow water is that at distances great compared with the depth of water the high frequency waterborne sound, which is needed to determine shot to receiver range, is gradually lost by destructive interference (PEKERIS, 1948). *Argo* and *Horizon* used a combination of radar and dead-reckoning to obtain range. *Owen* and *Discovery* used taut-wire measuring gear. *Owen* paid out 180 km of taut piano wire while steaming away

and firing charges. Thus it was possible to calculate the range from each shot to each receiving point.

The travel time curve for line 3 is shown in Fig. 3. The abscissa is range from shot to receiver in kilometres. The ordinate is the time after the explosion in seconds at which refracted energy arrives at the receiver.

The following is an interpretation of the results shown in Fig. 3.

On the north-west side all early shots reveal a layer in which the velocity is 5·59 km/s but arrivals from this layer disappear suddenly, revealing arrivals from a layer in which the velocity is 6·10 km/s. There are several possible explanations

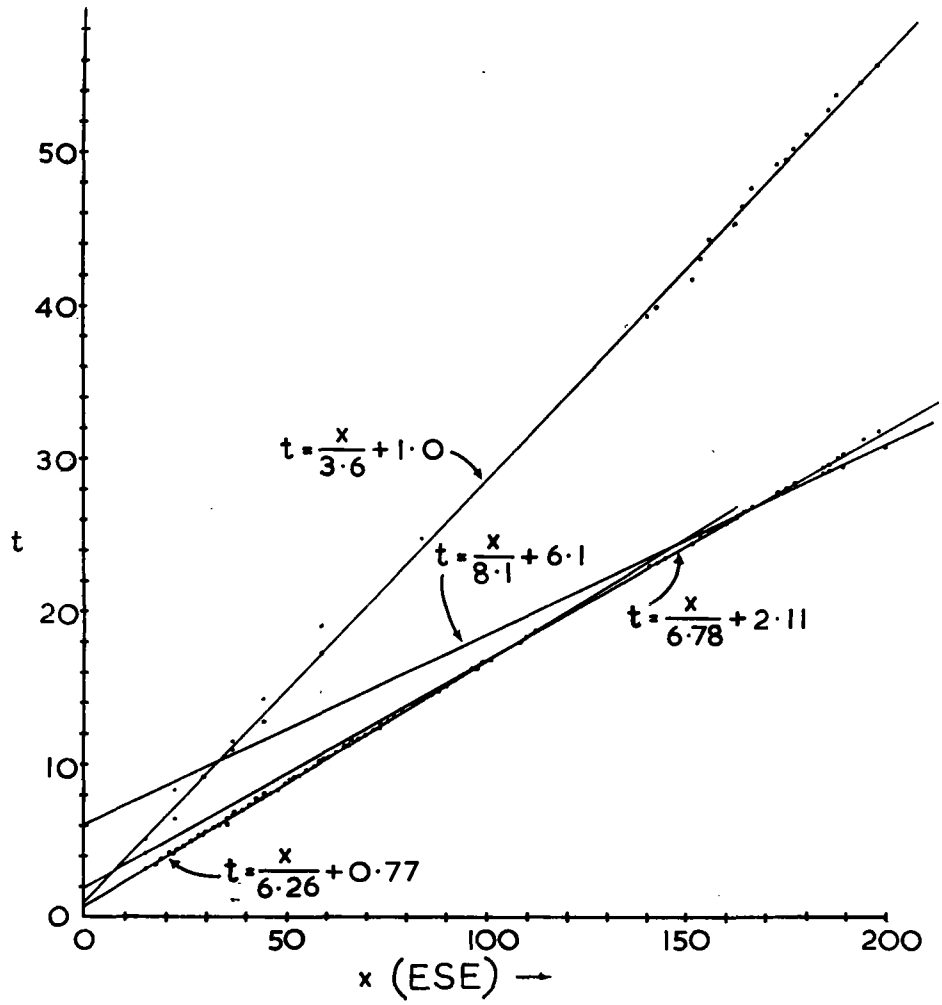

Fig. 4. Travel-time curve for *Owen* shots.

for this sudden loss of signal. The magnetic field in this region shows violent disturbances of short wave-length, presumably associated with dykes, and it is possible that a dyke is acting as a scatterer of seismic energy. On the south-east side only one line was obtained on the travel-time curve; the slope of this line indicated a velocity of 5·85 km/s.

The two velocities of 5·59 km/s and 5·85 km/s were averaged to give a velocity of 5·72 km/s for the first observed layer. This was done in preference to a solution in terms of a dipping interface as the basement topography near Mahé is not likely to persist to any great distance away from the island, and we are really looking for the structure of the Bank as a whole rather than that of the small central part.

The long line, in which the charges were fired by *Owen*, gave the travel-time curve shown in Fig. 4. This is remarkable for its uniformity. A good line of velocity 6·26 km/s and intercept 0·77 sec may be fitted to points out to a range of 110 km. There is some evidence for irregular topography beneath the buoys but otherwise no clear indication of dip. At ranges of 135 km and upwards the points fit on a line of velocity 6·78 km/s and intercept 2·11 sec.

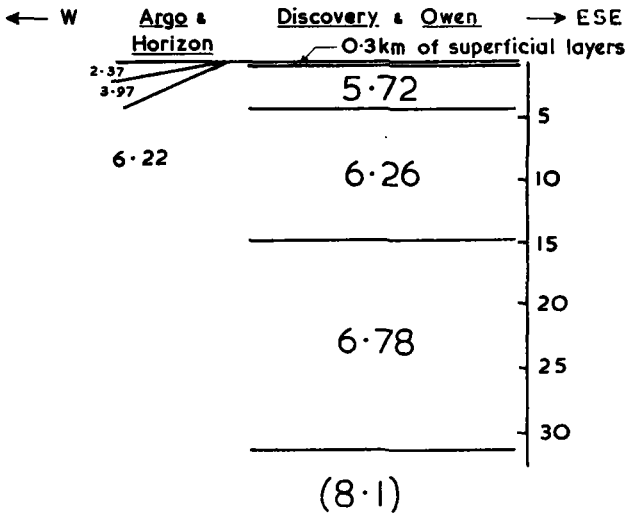

Fig. 5. Calculated structure, including *Argo* and *Horizon* results. Depths in kilometres, seismic velocities in km/s.

At the greatest ranges there are a first and a second arrival on the records. The second arrivals fit well on to the 6·78 km/s line. The first are postulated to be refracted arrivals from the Mohorovičić discontinuity. Only a few points are obtainable for this line since the first arrival is almost lost in the noise. One arrival in particular was much the clearest and in order to get some idea of the thickness of the crust a line representing a velocity of 8·1 km/s was fitted to this one point giving an intercept of 6·1 sec.

Many good late arrivals were seen. Most of these indicated a velocity of approximately 3·5 km/s. This could be due to either a thin layer (e.g. of coral) or a shear wave arrival from the coral–basement interface. Since *Argo* and *Horizon* found a 4·0 km/s layer which gave first arrivals at short ranges, ruling out a shear wave explanation, the thin coral layer explanation is preferred. The 6·26 km/s line of Fig. 4 is shown on Fig. 3 for comparison. If the points from Figs. 3 and 4 were merged there would be some disagreement at 15 km range. This is probably due to the 8 km drift of the buoys in the 10 hours between the shooting of lines 3 and 4. It would be unreasonable to expect that the structure beneath the buoys should be

identical 5 miles apart. Accordingly line 3 has been used for describing the shallow structure, and line 4 for the deep structure.

Figure 5 (which includes *Argo* and *Horizon* results) shows an interpretation of the data on the basis of the above discussion. The interpretation is also given in Table 1. Less than 500 m of sediment and coral cover the first of two layers for which the seismic velocity suggests a granitic material. BIRCH (1960) showed that under a typical

Table 1. *Calculated structure of Discovery Station* 5210. *Velocities bracketed have been assumed.*

Layer	*Seismic velocity* (km/s)	*Thickness* (km)
Water	1·54	·05
1	(2·0) and 3·5	·3
2	5·72	3·3
3	6·26	9·4
4	6·78	18·9
5	(8·1)	—

continent the seismic velocity of granite would increase with depth from 5·3 km/s at the surface to 6·25 km/s at a depth of 10 km. STEINHART and MEYER (1961) demonstrated that a travel-time curve based on Birch's velocity structure might well be interpreted as two layers with velocities 5·57 km/s and 6·18 km/s, the interface being 1·9 km deep. The similarity of these predictions to the results obtained by *Discovery* and *Owen* is striking and so although the structure is interpreted as two granitic-type layers for computational convenience, it is accepted that a velocity gradient could produce an almost identical travel-time curve. That *Argo* and *Horizon* observed just one layer of velocity 6·22 km/s, near Mahé may be due to near surface topographic irregularities which could easily mask an effect which is in any event small.

Table 2. *Seismic profiles in the vicinity of the Seychelles bank with determinations of the seismic velocity and depth of the basaltic layer.*

Source	*Location*	*Velocity of basaltic material*	*Depth below ocean surface*	*Thickness*
AH	300 km ESE of Mahé	6·77 km/s	5 km	?
AH	900 km SE of Mahé	6·81 km/s	8 km	?
D	350 km NE of Mahé	6·86 km/s	6·4 km	4·7 km
D	450 km W of Mahé	No obvious basaltic layer		

AH = *Argo* and *Horizon* station.
D = *Discovery* station – preliminary result.

The 6·78 km/s layer is of considerable interest. Table 2 lists seismic profiles in the vicinity and it is clear that the typically " basaltic " velocity of 6·8 km/s is common to the eastward. The complete lack of a clear 6·8 km/s layer to the west is problematical and will be discussed in greater detail in conjunction with other *Discovery* and *Owen* seismic profiles at a later date. It seems possible that the 6·78 km/s material beneath the Seychelles should be the same as the basaltic layer seen in the eastern vicinity. However, seismic arrivals from a layer with seismic

velocity 6·78 km/s on a continent would be termed P^* and its upper boundary called the Conrad Discontinuity. The velocity of 6·78 km/s and depth of approximately 13 km agree well with continental determinations, of which many are cited in Steinhart and Meyer (*cop. cit.*). Thus it is open to speculation that the sub-oceanic basaltic layer connects directly with a thick sub-continental layer.

Little may be inferred from the depth of 33 km to the Mohorovicic discontinuity as an assumed velocity of 8·1 km/s has been used. A velocity of 7·7 km/s for the material below the Mohorovičić discontinuity would change the depth to 27 km. There is considerable evidence for low mantle velocities to the west, much less to the east. It is clear however that the depth is much nearer to the continental range of values (30–40 km) than the oceanic range (8–15 km).

The results obtained suggest that the Seychelles bank is a continental feature and that the horizontal extent of the " micro-continent " is at least 250 km.

Acknowledgements—We thank the Director of the National Institute of Oceanography for providing the facilities on board R.R.S. *Discovery*, and the Hydrographer of the Navy for the use of H.M.S. *Owen*.

To the Captains, Officers and Crews of H.M.S. *Owen* and R.R.S. *Discovery* we are grateful for their splendid cooperation.

Dr. M. N. HILL, F.R.S., Principal Scientist on R.R.S. *Discovery* suggested the experiments and took an active part in all aspects of the work.

Dr. A. S. LAUGHTON, Mr. E. J. W. JONES and Mr. R. B. WHITMARSH helped in many ways.

This work was supported by O.N.R. Contract No. N62558-3883 and D.S.I.R.

REFERENCES

BAKER, B. H. (1963) Geology and Mineral Resources of the Seychelles Archipelago. *Geol. Surv. Kenya, Memoir* 3.

BAKER B. H. and MILLER J. A. (1963) Geology and Geochronology of the Seychelles Islands. *Nature* **199**, 346–348.

BIRCH F. (1960) Velocity of Compressional Waves in Rocks. *J. Geophys. Res.*, **65**, 1083–1102.

BLACKETT P. M. S. (1961) Comparison of ancient climates with the ancient latitudes deduced from rock magnetic measurements. *Proc. Roy. Soc.* A, **263**, 1–30.

BLACKETT P. M. S., CLEGG J. A. and STUBBS P. H. S. (1960) An analysis of rock magnetic data. *Proc. Roy. Soc.* A, **256**, 291–322.

DU TOIT A. L. (1937) *Our Wandering Continents*. Oliver and Boyd, Edinburgh, 366 pp.

GASKELL T. F., HILL M. N. and SWALLOW J. C. (1958) Seismic investigations made by H.M.S. *Challenger* 1950–53. *Phil. Trans. Roy. Soc.* A, **251**, 23–83.

HILL M. N. (Ed.) (1963) Single-slip seismic refraction shooting. In *The Sea*, Chapt. 3, Vol. 3, 963 pp. Interscience Publishers.

PEKERIS C. L. (1948) Propagation of Explosive Sound in Shallow Water. *Geol. Soc. Amer. Mem.*, 27, 117 pp.

SHOR G. G. JR. and POLLARD D. D. (1963) Seismic Investigations of Seychelles and Saya de Malha Banks, Northwest Indian Ocean, *Science*, **142**, 48–49.

STEINHART J. S. and MEYER R. P. (1961) *Explosion Studies of Continental Structure*, Carnegie Institution of Washington.

WEGENER A. (1922) *The Origin of Continents and Oceans*. Methuen, London, 212 pp.

Reprinted from J. geophys. Res., vol. 71, no. 2, 1966, p. 427-449.

Seismic Refraction Measurements in the Northwest Indian Ocean[1]

TIMOTHY J. G. FRANCIS AND GEORGE G. SHOR, JR.

Marine Physical Laboratory of the Scripps Institution of Oceanography
University of California, San Diego

Abstract. Fifteen seismic refraction profiles in the northwest Indian Ocean are described. The results suggest a connection between the linear Maldive ridge and the Deccan traps of the Indian mainland. No anomalous upper mantle velocities have been found near the crest of the Carlsberg ridge. A great thickness of material with velocity 6.03 km/sec west of the Saya de Malha bank has been interpreted as an extension of the Seychelles granitic block to the south. At two stations between the Chagos archipelago and the Seychelles bank the Mohorovicic discontinuity appears to be less than 8 km below sea level.

INTRODUCTION

In October 1962, the research ships *Argo* and *Horizon* carried out seismic refraction work in the northwest Indian Ocean while on passage between Cochin, India, and Port Louis, Mauritius. This was the second leg of Lusiad Expedition and a contribution of the Scripps Institution of Oceanography to the International Indian Ocean Expedition. Thirty receiving positions were occupied, resulting in 17 reversed profiles and a single unreversed line (Figure 1). The interpretations of 3 of these profiles, over the Seychelles and Saya de Malha banks, have already been published [*Shor and Pollard*, 1963].

GEOGRAPHIC SETTING

The principal topographic feature in the northwest Indian Ocean is the Carlsberg ridge, which runs southeast from the Gulf of Aden towards the Chagos archipelago before turning south at about longitude 68°E. It continues south, as the mid-Indian Ocean ridge, to about 23 or 24°S where it divides, the westerly limb going south of Africa to join the mid-Atlantic ridge and the easterly one extending toward Amsterdam and St. Paul Islands. Although not as spectacular a feature as the mid-Atlantic ridge, the Carlsberg ridge displays all the qualities—rough topography, large magnetic anomalies, association with earthquake epicenters—which characterize mid-ocean ridges [*Wiseman and Sewell*, 1937; *Heezen and Ewing*, 1963; *Admiralty Marine Science Publication*, 1963].

At about 73°E the coral atolls and banks of the Laccadive, Maldive, and Chagos archipelagoes rise from an almost linear north-south ridge which extends from 14°N to 10°S. This ridge appears to be titled down very slightly to the south so that the Chagos banks are the deepest, and many atolls of this group are partly drowned [*Wilson*, 1963].

Between Mauritius and the Seychelles bank lies a large crescent-shaped arc of shallow water, the Mascarene ridge, with coral banks and a few coral islands.

AIMS AND TECHNIQUES

Before Lusiad Expedition the only seismic refraction work in the northwest Indian Ocean was a short buoy line on the Seychelles bank [*Gaskell et al.*, 1958]. *Neprochnov* [1961] has described seismic reflection measurements of sediment thickness in the Arabian basin carried out at the end of 1960. Since then bathymetric, magnetic, and gravity data gathered by many ships during the International Indian Ocean Expedition have provided a clearer picture of the geological setting. The Cochin to Mauritius leg of Lusiad Expedition was therefore planned more as a reconnaissance to get a broad picture of the earth's crust in the area rather than to solve any particular geological problem.

Our techniques were essentially the same as those described by *Raitt* [1956] and *Shor* [1963]. The methods of analysis were also those which have been developed over many years for work in the Atlantic and Pacific Oceans. A major aim of the International Indian Ocean Ex-

[1] Contribution of the Scripps Institution of Oceanography, University of California, San Diego.

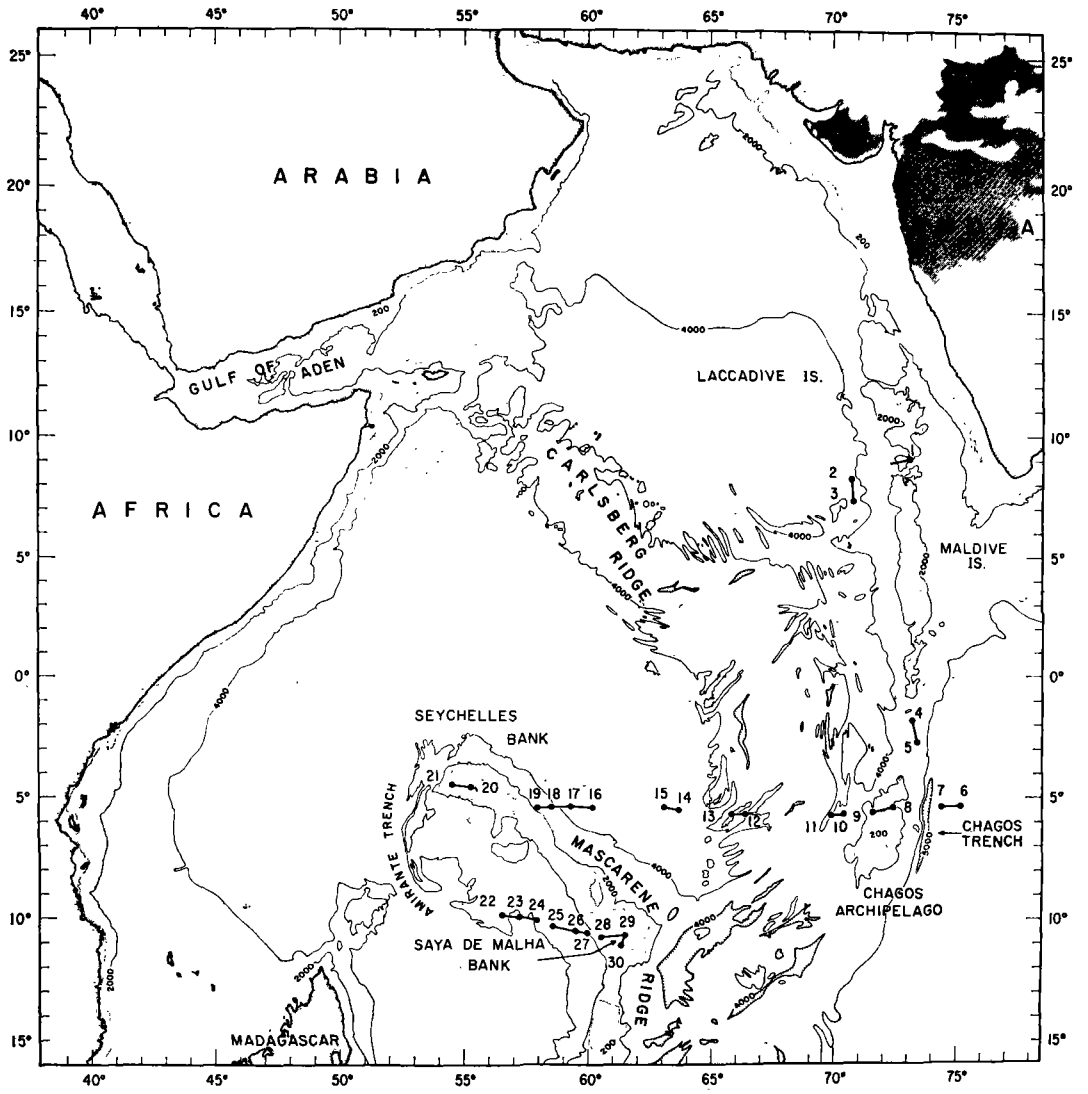

Fig. 1. Station positions; bathymetry was compiled from original unpublished charts of R. L. Fisher, T. C. Hilde, and A. S. Laughton. Contours are not shown if information was unavailable from these sources. The 200-m contour is shown dotted. All depths, in meters, are corrected for velocity of sound in water. Area occupied by the Deccan traps is crosshatched [from *Pepper and Everhart,* 1963].

pedition was to study the area with the well-tried and proved techniques developed elsewhere so as to make up for its previous comparative neglect by oceanographers.

Briefly, range was determined from the travel time of direct sound through the water. Where this was not observed, the range was extrapolated from the times of first and second bottom reflections. A mean velocity for the soft sediment of 2.15 km/sec was used throughout (but see appendix on stations 25, 26, 27). Travel-time plots show the times of first-arrival refracted waves, and later refracted arrivals where these were prominent, with the delay time in the water removed. Least-squares lines and dipping-layer solutions were calculated with computer programs written by Richard Phillips and Helen Kirk. Topographic corrections in addition to removing the water delay time were attempted for stations over rough topography,

TABLE 1. Summary of Velocity and Depth Determinations

Station	Location		Velocity, km/sec				Layer Thickness, km				Thickness of Crust, km	Depth to M, km	Mean Depth to M
			a	b	c	d	Water	a	b	c			
1	9°05′N	73°04′E	(3.85)	(5.00)	(6.84)	(7.97)	1.98	1.87	2.9	10.6	15.4	17.3	
2	8°17′N	70°35′E	2.15*	(5.40)	6.36	8.21	3.89	0.74	0.0	5.5	6.2	10.1	9.6
3	7°22′N	70°40′E					3.94	0.88	1.3	3.1	5.3	9.2	
4	1°41′S	73°06′E	2.15*	6.13	7.11		2.59	1.06	3.9				
5	2°40′S	73°19′E					3.10	1.02	4.9				
6	5°21′S	75°05′E	2.15*	5.0*	6.69	7.78	4.99	0.26	1.3	3.5	5.1	10.0	10.2
7	5°22′S	74°18′E		2.8(S)*			4.69	0.20	0.9	4.6	5.7	10.4	
8	5°23′S	72°25′E	2.15*	3.01	4.76	6.79	0.94	0.23	1.8	5.1			
9	5°36′S	71°32′E					0.88	0.61	0.6	3.3			
10	5°40′S	70°17′E	2.15*	6.31	8.03		3.92	0.66	2.9		3.6	7.5	8.4
11	5°39′S	69°40′E					3.80	0.64	4.8		5.4	9.2	
12	5°52′S	66°36′E	2.15*	6.88	8.36		4.36	0.85	5.9		6.7	11.1	10.2
13	5°54′S	65°58′E					4.25	0.72	4.3		5.0	9.3	
14	5°33′S	63°44′E	2.15*	5.02	6.85	7.81	4.32	0.25	3.2	2.7	6.1	10.5	8.8
15	5°31′S	63°04′E					4.23	0.06	1.6	1.3	3.0	7.2	
16	5°27′S	60°02′E	2.15*	5.79	7.03	8.25	4.09	0.58	1.9	5.3	7.8	11.9	10.9
17-in	5°25′S	59°13′E					4.00	0.75	2.5	2.6	5.8	9.8	
17-out	5°25′S	59°13′E	2.15*	5.41	6.62	8.04	4.00	0.54	1.7	3.2	5.4	9.4	10.3
18-in	5°20′S	58°29′E					3.95	0.35	2.1	4.8	7.2	11.2	
18-out	5°20′S	58°29′E	2.15*	4.48	6.80		3.95	0.73	0.6				
19	5°30′S	57°56′E					2.52	0.51	2.2				
22	9°50′S	56°30′E	2.15*	5.37	6.85	8.01	3.88	0.50	2.9	3.9	7.3	11.2	9.6
23-in	9°58′S	57°07′E					4.03	0.70	1.3	2.1	4.1	8.1	
23-out	9°58′S	57°07′E	2.15*	5.39*	5.95?	8.41	4.03	0.70	2.6	1.8	5.1	9.1	9.6
24	10°05′S	57°53′E					3.93	0.27	0.5	5.4	6.2	10.1	
25	10°20′S	58°30′E	2.15*	5.48	6.03	8.32	3.46	0.41	3.2	9.5	13.1	16.6	17.0
26-in	10°29′S	59°23′E					2.84	0.30	2.4	11.8	14.5	17.3	
26-out	10°29′S	59°23′E	2.15*	5.50	6.03		2.84	0.34	1.9				
27	10°34′S	59°51′E					2.28	0.68	3.1				

* Assumed velocity.
( ) Velocity from a single run.

but did not significantly reduce the residuals of points from their least-squares lines.

The profiles fall conveniently into three groups: (1) those in the region of the Maldive ridge; (2) those along a line between 5 and 6°S from just east of the Chagos archipelago to the Seychelles bank; (3) the group approaching the Saya de Malha bank from the west, culminating in two profiles on the bank itself which have already been reported by *Shor and Pollard* [1963]. Stations 28 and 29 (Figure 1) form one of the Shor and Pollard profiles. Table 1 summarizes station positions, seismic velocities, and layer thicknesses. Detailed descriptions of the individual profiles and travel-time plots are given in the appendix. The equations of the least-squares lines also appear on the travel-time plots, together with the standard errors of the intercepts and apparent velocities. The errors in the real velocities are likely to be greater because of the geological assumptions involved in the dipping-layer solution.

Interpretation

Maldive ridge area. Three of the profiles crossed the axis of this ridge: station 1 midway between the Laccadive and Maldive archipelagoes, stations 4 and 5 in the channel between the Maldive and Chagos archipelagoes, and stations 8 and 9 over the Chagos bank itself. The first profile reveals almost 5 km of volcanic rock (velocities 3.85 and 5.00 km/sec, but see appendix) overlying more than 10 km of crustal material and the Mohorovicic discontinuity at just over 17 km (see Figure 2). This compares closely with the structure in the deep water adjacent to Eniwetok atoll, where layers of similar velocity and thicknesses overlie the Mohorovicic discontinuity at 16 to 17 km [*Raitt*, 1957]. Stations 4 and 5 present what appears at first glance to be a different picture. However, the 6.13-km/sec layer, 4 to 5 km thick, is similar in thickness to the volcanic layers of the first profile. Velocities of this order have been observed in the volcanic material composing the Hawaiian archipelagic apron [*Shor and Pollard*, 1964], whose origin is believed to be lava flows from fissures on the sea floor at the bases of the islands [*Menard*, 1964]. It seems likely, then, that between the Maldive and Chagos groups the ridge is composed of lavas poured out at oceanic depths, but to the north between the Maldive and Laccadive groups the much lower velocities may indicate more broken and vesicular lavas which solidified near the sea surface [see *Menard*, 1964, pp. 57–59]. No mantle arrivals were observed at stations 4 and 5 in spite of a line more than 100 km long; the Mohorovicic discontinuity is unlikely to be shallower than 20 km.

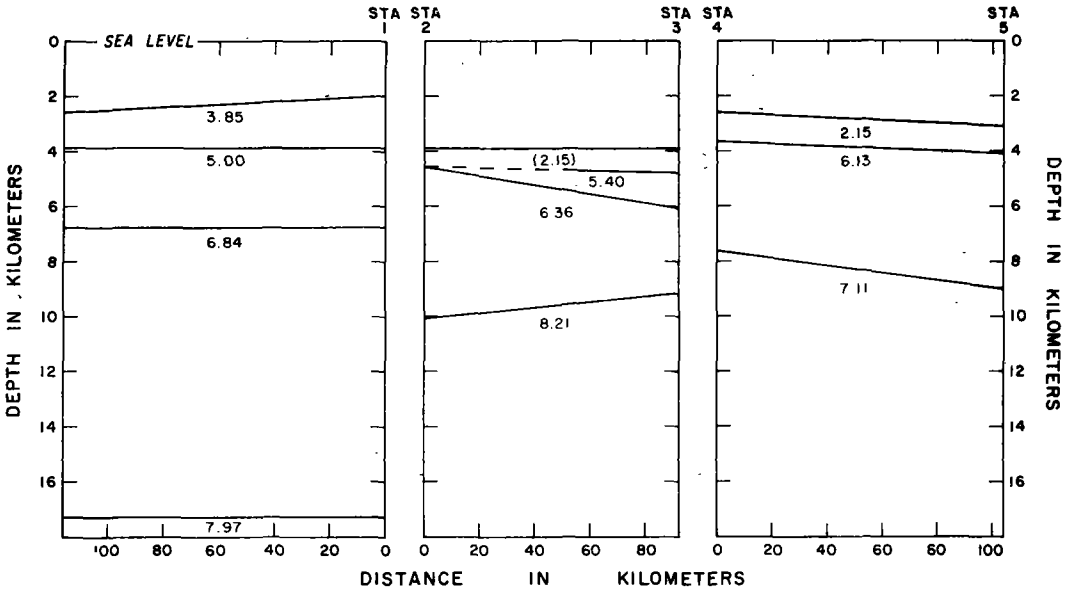

Fig. 2. Computed seismic sections for stations 1, 2 and 3, 4 and 5. Vertical exaggeration 10:1.

The profile over the Chagos bank shows it to have a structure typical of volcanic islands. The velocities 3.01, 4.76, and 6.79 km/sec are typical of coral, volcanic rock, and basic crustal material, respectively [cf. *Raitt*, 1957].

The conclusion, then, is that the Maldive ridge is a continuous feature resulting from a volcanic layer generally between 4 and 5 km thick throughout its length. The Mohorovicic discontinuity appears to be deeper at the southern end of the ridge. *Glennie* [1936] found large negative isostatic gravity anomalies in the Maldive Islands and concluded that the ridge is more likely to consist of a great thickness of coral rock resting on an upwarp in the ocean floor than to be a continental relic as others have proposed [see *Wilson*, 1963]. Further, the large magnetic anomalies more recently observed in the area [*Admiralty Marine Science Publication*, 1963] suggest that the coral has a basalt foundation. The seismic measurements are consistent with these views.

Linear volcanic ridges of the size of the Maldive ridge are well known in the Pacific. The linearity is believed to result from control of the rising magma by faulting, and such archipelagoes are found to develop in one direction only. *Menard* [1964] proposes the following mechanism: (1) A group of volcanoes develops along part of a major fault; (2) the load of the volcanoes produces an encircling moat and arch; (3) New volcanoes tend to develop in the region of tension where the arch intersects the major lineation. If this mechanism has any validity in the case of the Maldive ridge, we can draw the following conclusions:

1. The apparent downtilting of the ridge to the south, with the deepest banks in the Chagos group, shows that the ridge has developed from the Chagos group northward. The fact that the mantle appears to be deeper at the southern end implies that the subsidence which occurs once a large volcanic structure has been built up extends beneath the crust.

2. The absence of an obvious moat and arch may be the result of the proximity of the Carlsberg ridge to the southwest and of India to the northeast. On the other hand, the small trench immediately east of the Chagos bank may owe its existence to subsidence of the Chagos block and be equivalent to the moats observed around Pacific archipelagoes. The dips found in the refracting horizons beneath the Chagos bank (Figure 3) indicate perhaps that the subsidence has been greater on the eastern than on the western side. Precision sounding tracks going due west from the Maldive archipelago between about 2°S and 8°N may yet reveal the presence of a moat and arch structure. The Russian bathymetric chart of the Indian Ocean (1963), the most accurate one yet published for this immediate area, shows patches of shallower water between 200 and 300 km west of the archipelago. This is just the sort of range at which the crest of arches around Pacific archipelagoes have been observed [*Menard*, 1964]. However, two precision sounding tracks of R.V. *Argo* extending west from the Maldive ridge at approximately the equator and 6°N reveal no structure suggestive of subsidence. The abyssal plain bordering the foot of the Maldive ridge extends only 50 to 100 km to the west before being overtaken by the rough flanks of the ridge or abyssal hills. Farther north a moat may be obscured by sediment from the Indus cone [see *Heezen and Tharp*, 1965]. Seismic reflection profiles in this area might be revealing.

3. The abyssal plain reported [*Wilson*, 1963] in the deep channel between the Chagos and Maldive archipelagoes may owe its smoothness to lava flows of a type similar to those which formed the smooth archipelagic aprons of the Pacific [*Menard*, 1964]. This explanation does not preclude the existence of sedimentary cover as well.

Two profiles shot in the deep water immediately west of the ridge (stations 2 and 3 to the north, and stations 10 and 11 to the south) reveal strikingly similar structure. No crustal velocity higher than about 6.3 km/sec is observed. The mantle velocity is normal and its depth rather shallow. The presence of a masked 6.8-km/sec layer in either case can depress the Mohorovicic discontinuity no more than a few hundred meters, and such a layer can be at most 2 km thick. Pressing the comparison with Pacific archipelagoes further, it seems likely that the 6.3-km/sec layer is smooth lava from sea-floor fissure flows, similar to the 6.1-km/sec material found at stations 4 and 5. The shallowness of the mantle is perhaps analogous to the 'high spots' found on the island side of the Hawaiian arch by *Shor and Pollard* [1964].

Large fissure flows of very fluid lava, comparable to those that formed the archipelagic aprons, have also occurred on continents, the Columbia and Snake River basalts of North America and the Deccan traps of India being notable examples. It is striking that the latter occupy just that part of India which is situated at the northward extension of the Maldive ridge, and one is tempted to conclude that the volcanism which produced the Maldive ridge, moving northward from an origin in the Chagos area, continued on into the continent itself to produce the Deccan traps.

Support for this hypothesis comes from laboratory measurements of compressional velocities in Deccan trap material [*Balakrishna*, 1958]. Specimens from two different sites give velocities of 6.25 and 6.4 km/sec. (Presumably these were of a nonvesicular type; the texture of trap rocks varies while their composition remains remarkably uniform [*Wadia*, 1953].) These velocities are effectively identical to the 6.1- and 6.3-km/sec velocities observed beneath the sea. Both stratigraphic (intertrappean beds with fossils) and radioactive age determinations show that the traps range in age from upper Cretaceous to perhaps as late as Oligocene. The bulk of the flows probably occurred in the early Eocene [*Krishnan*, 1960]. The original volcanism in the Chagos area, then, may have commenced in early or middle Cretaceous time.

The seaward extension of the Deccan traps has long been suspected from the great thickness of flows on the coast and the faulted nature of the coast line. As *Krishnan* [1960, p. 77] wrote, 'It would appear that the Traps may

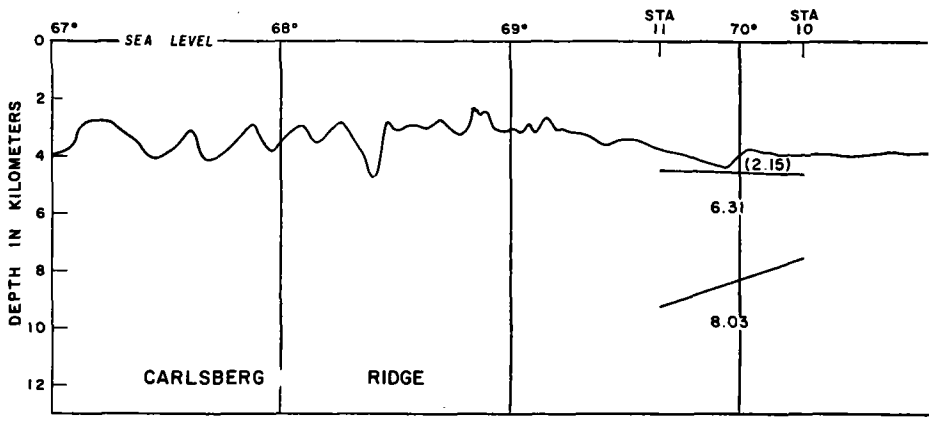

Fig. 3. Topographic and seismic profile between 67 and 75°E along a line between 5

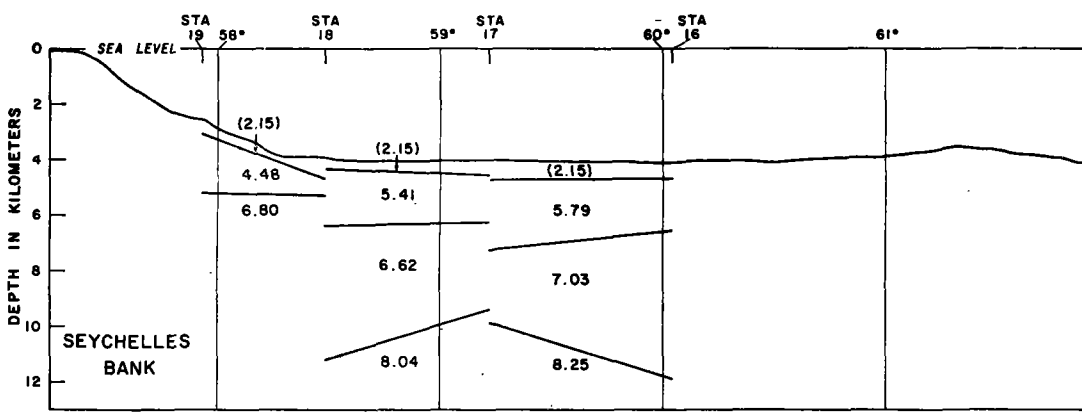

Fig. 4. Topographic and seismic profile between 57 and 67°E along a line between 5 and

have extended formerly for some distance west of Bombay, but that portion has since been faulted down and covered by the sea.' The observed coastal faulting is of Miocene age [*Krishnan*, 1960] and is very probably an expression of subsidence of the Maldive ridge.

Finally, the petrographic analysis of the Deccan traps may reveal a connection with the Maldive ridge volcanism. *Chayes* [1964] has recently shown that TiO_2 content is a remarkably accurate indicator of an 'intraoceanic' and 'circumoceanic' environment among Cenozoic lavas, greater than 1.75% TiO_2 indicating a geographically oceanic environment with less than 1 chance in 14 of error. *Washington* [1922] analyzed samples from many different flows in the Deccan traps and found an average TiO_2 percentage of 1.91. For samples from the lower traps the percentage was 2.34; from the upper traps, it was 0.63 (reported by *Krishnan* [1960]). If Chayes' conclusions can be validly applied to these rocks, they indicate an initially oceanic environment becoming circumoceanic. This is consistent with the movement of volcanic activity northward from the Maldive ridge into the Indian continent. The presence of 'intraoceanic' lava on the continental surface is probably the result of the great size of the magma reservoir and the time required for the continent to change the character of the magma.

East-west section between 5 and 6°S. Eight reversed profiles were shot along an east-west line between 5 and 6°S. The velocity structures deduced from these are shown in Figures 3 and 4, together with the topographic profile. Two profiles (stations 8 and 9, 10 and 11) have al-

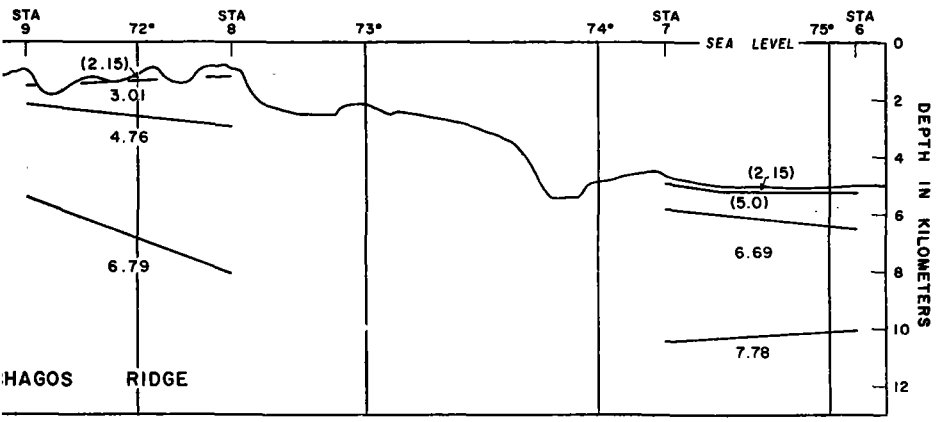

Vertical exaggeration 14:1.

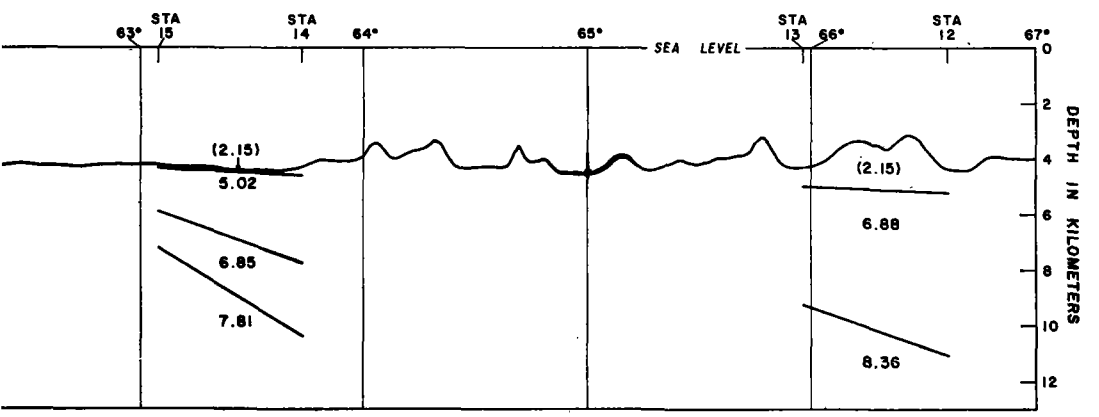

ical exaggeration 14:1.

ready been discussed in the preceding section. Of the remaining six all but one give normal oceanic structures. No low mantle velocities are found in connection with the topographically defined Carlsberg ridge. This result is surprising if, as *Menard* [1964] has proposed, this ridge is at the same stage of development as the mid-Atlantic ridge, since the distance between stations 11 and 12 is only 300 km, and the ridge passes between them. The anomalous mantle region (velocities around 7.3 km/sec) of the mid-Atlantic ridge is between 500 and 1000 km wide [*Ewing and Ewing*, 1959; *Le Pichon et al.*, 1965]. The explanation of this is perhaps simply the smaller scale of the Carlsberg ridge feature. Alternatively, the region of low mantle velocity may be quite narrow, as is the case with the relatively younger [*Menard*, 1964] East Pacific rise. Yet another explanation is indicated by the structure of stations 14 and 15. Here, just west of the flanks of the ridge, it is surprising to find a thick 'layer 2,' a thin crustal layer, and a low mantle velocity—all qualities associated with mid-ocean ridges. This may indicate that the ridge has migrated, possibly as the result of some centering process [*Menard*, 1964, p. 148], but perhaps too much reliance should not be placed on a single profile of rather poor quality. Many more stations need to be shot in the vicinity of the ridge before any definite conclusions about its development can be drawn.

Three stations approach the Seychelles bank from the east. None of these shows the presence of the granitic material which has been found to cover the Seychelles bank to a depth of 13 km [*Davies and Francis*, 1964]. The eastward termination of this block appears to be abrupt. This is in contrast to the situation on the western side of the bank where the presence of a 6.2-km/sec velocity in deep water has been taken to indicate the extension of the granite batholith about 200 km in this direction [*Francis et al.*, 1965]. However, the similarity of the latter structure to that at stations 10 and 11—material with a velocity of about 6.2 km/sec overlying a shallow Mohorovicic discontinuity—may invalidate the grantitic interpretation.

Stations west of the Saya de Malha bank. Figure 5 shows the velocity structures and topographic profiles observed west of the Saya de Malha bank. The structure beneath the bank itself is taken from *Shor and Pollard* [1963]. Two distinct structural changes are apparent. The profile at the western end reveals a typical oceanic structure, that over the bank a structure typical of volcanic islands. Shor and Pollard point out the similarity of the latter structure to that at Eniwetok [*Raitt*, 1957]. The situation between is quite unexpected (stations 25, 26, 27). Beneath the soft sediment, the second layer is 2 to 3 km thick with velocity of 5.5 km/sec. But the well-established 6.03-

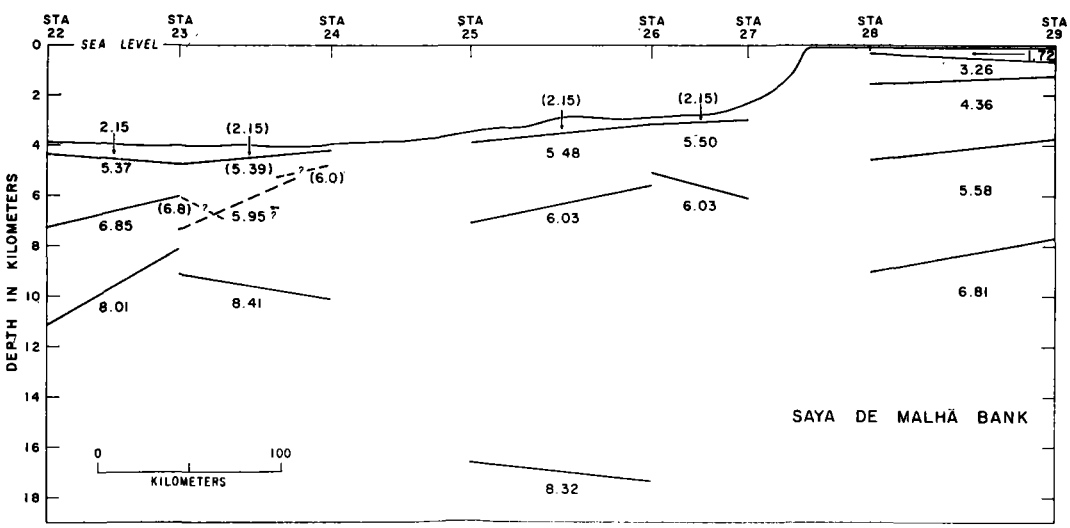

Fig. 5. Topographic and seismic profile to the west of and over the Saya de Malha bank. Vertical exaggeration 14:1.

km/sec velocity is not observed beneath the bank, nor is a 6.8-km/sec crustal velocity observed at stations 25, 26, and 27. If the latter is masked, the crustal layer can be no shallower than 12 km (see appendix). Four possible interpretations are (in order of preference):

1. The 6.03-km/sec velocity represents granitic material like that forming the Seychelles bank. Overlying it is volcanic material similar to that which gives the 4.4- and 5.6-km/sec velocities beneath the Saya de Malha bank.

2. Both the 5.5- and 6.03-km/sec velocities represent granitic material, the two velocities resulting from the effect of pressure on the seismic velocity. The 5.72- and 6.26-km/sec velocities beneath the Seychelles bank were interpreted in this manner [*Davies and Francis,* 1964] following the demonstration by *Steinhart and Meyer* [1961] of the effect of a velocity gradient (deduced from laboratory measurements) on travel-time curves. The rather low velocities for the depths involved make this interpretation less likely in this case. Also, we might expect a closer correlation of dips (i.e., apparent velocities) between the 5.5- and 6.03-km/sec interfaces if both velocities were generated by a single continuous velocity gradient.

3. Since the 6.03-km/sec velocity is quite unlike anything else beneath the bank, it is also possible that the 5.5-km/sec velocity is unassociated with the 4.4- and 5.6-km/sec velocities. If the 6.03-km/sec material is indeed granitic like the Seychelles bank, the 5.5-km/sec velocity may represent a sedimentary formation associated with it, possibly a fairly hard limestone. The magnetic anomaly over the edge of the Saya de Malha bank should indicate whether the volcanic material ends abruptly here.

4. Both the 5.5- and 6.03-km/sec velocities represent basalt, the higher velocity being akin to the high second-layer velocities observed in the Maldive ridge area (stations 2 and 3, 4 and 5, 10 and 11). This interpretation is most unlikely. First, the travel-time plots are in complete contrast, those for stations 25, 26, and 27 yielding a host of second arrivals. Second, the volcanic layer near the Maldive ridge is between 1 and 5 km thick; the 6.03-km/sec layer here is at least 6 km thick, and possibly as thick as 13 km, as is the granitic layer of the Seychelles [*Davies and Francis,* 1964]. Third, where the high second-layer velocities are observed near the Maldive ridge the mantle is quite shallow; here at a similar distance from the shallow water it is 17 km below sea level and perhaps as deep as 19 km (see appendix).

In conclusion, then, granitic material similar to that forming the Seychelles bank appears to exist west of the Saya de Malha bank, in all probability part of the same block. If the westward limit of this material occurs between stations 23 and 24, as seems likely (see appendix), its east-west extent is about 250 km—comparable in dimension to the Seychelles bank. Between these stations and the Seychelles the granitic material is probably confined by the Amirantes trench and the Mascarene ridge; to the south it may well continue as far as the Cargados Carajos shoals. Much of the Mascarene ridge seems to owe its existence to volcanism along the boundary of this continent-type mass. This does not necessarily imply that the eastern part of the continent of Africa once extended as far as the Mascarene ridge, as *Baker and Miller* [1963] have suggested. If the Seychelles bank owes its position as a continental block in mid-ocean to the rupture of India and Africa in the breakup of Gondwanaland [*Du Toit,* 1937], elucidating the exact boundaries of this feature should help to identify its origin. The fact that the granitic material now appears to extend a considerable way south of the Seychelles bank itself makes the possibility of an original connection with northern Madagascar more likely.

Comparison with Other Oceans

Enough seismic refraction work has now been done in the northwest Indian Ocean to make a comparison with the earth's crust beneath other oceans worth while. *Raitt and Shor* [1959] have prepared histograms of velocities and thicknesses for the Pacific Ocean. In Figure 6 some of these are shown, together with similar histograms for the northwest Indian Ocean, the latter being prepared from the results of this paper and of *Francis et al.* [1965]. In the case of the Pacific Ocean, Raitt and Shor were interested in revealing the characteristics of 'typical' or 'average' oceanic structure and neglected the results from islands, trenches, ridges, and seamounts. For the Indian Ocean histograms, the only restriction has been to exclude the results from regions

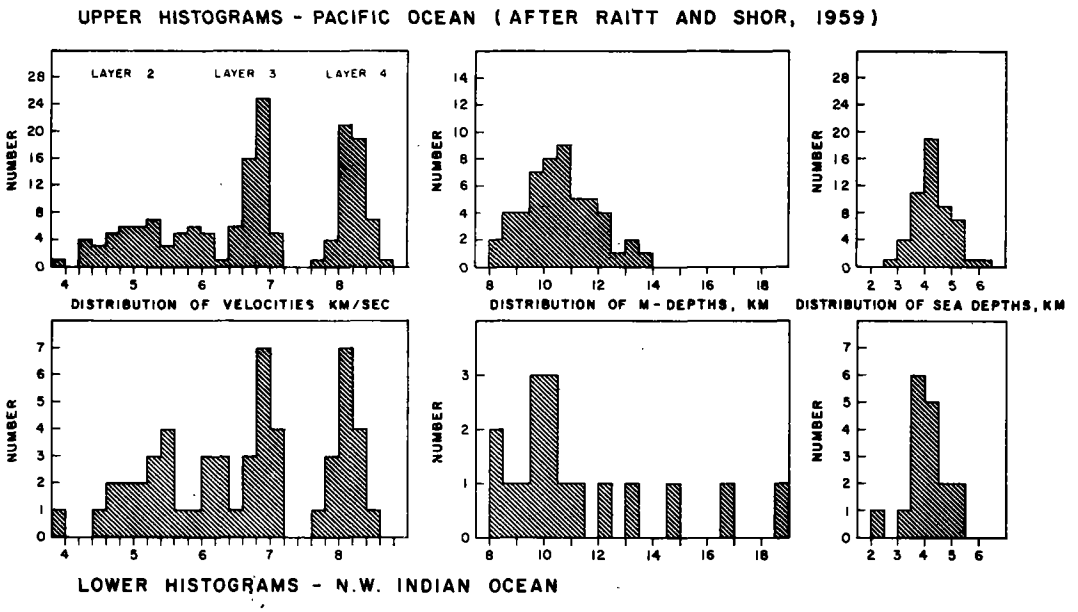

Fig. 6. Histograms of seismic velocity, mantle depth, and sea depth in the Pacific and northwest Indian Oceans

where the water depth is shallower than 2 km. Detailed comparisons of Atlantic and Pacific structure are given by *Raitt* [1963] and *Ewing* [1963].

The most obvious conclusion to be drawn from Figure 6 is, of course, the basic similarity of the two oceans. In both cases layers 3 and 4 are clearly apparent as peaks on the velocity histograms between 6.8 and 7.0 km/sec and 8.0 and 8.2 km/sec, respectively. Layer 2 is not clearly defined. There is a suggestion, however, that the average Indian Ocean crustal velocity is higher than the worldwide (but essentially Atlantic and Pacific Oceans) average of 6.69 km/sec (±0.26 km/sec standard deviation) given by *Raitt* [1963]. The average subcrustal velocity of the northwest Indian Ocean (8.10 km/sec ± 0.19 km/sec standard deviation) may also be significantly less than the Pacific average (8.20 km/sec ± 0.18 km/sec standard deviation for the layer 4 data in the histogram). The t distribution shows with more than 95% confidence that the mantle velocities are different, but the methods of selection of seismic stations may invalidate this as a conclusion for the whole oceans. It might also be concluded that the average depth to the Mohorovicic discontinuity is less in the Indian Ocean proper than in the Pacific Ocean, since all the depths greater than 12 km appearing on the histogram are associated with the unusual continental boundary off Kenya or the granitic material near the Saya de Malha bank. If this is so, the data support the trend of increasing mantle velocity with increasing depth to the Mohorovicic discontinuity which has been reported by *Ewing* [1963].

Appendix

Station 1. The only unreversed line of the group was shot in a direction 251° from a receiving position approximately midway between the Laccadive and Maldive archipelagoes. Water depth increased from just under 2 km at the receiver to just over 2.5 km at the southwest end of the line. The velocities, apart from the first, form a typical oceanic sequence, but the layers are much thicker than usual. The first observed velocity, 3.85 km/sec, appears to crop out at the bottom; any soft sediment overlying it is too thin to be detected. This velocity is not too high for coral; on the other hand, it is high enough to be in the range of volcanic rocks. Since the intercept of this apparent velocity is effectively zero, any dip present would cause the apparent velocity to be less than the

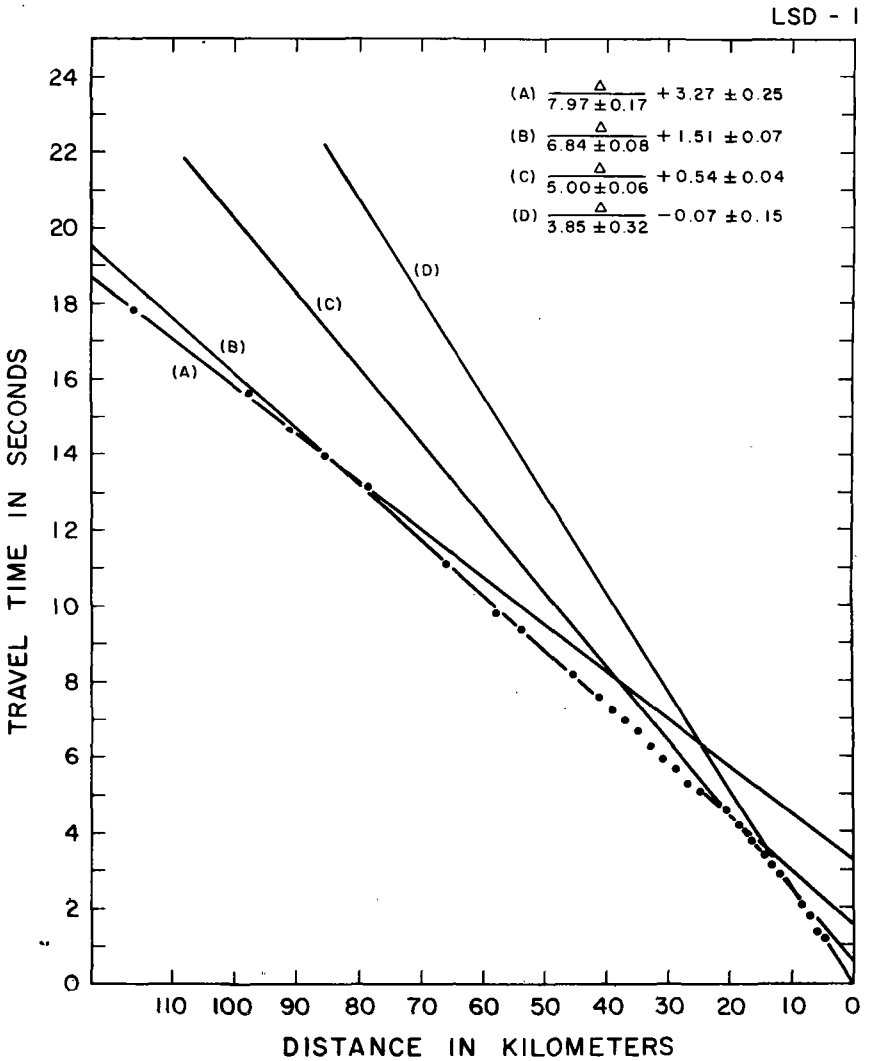

true velocity. A volcanic rock interpretation of this layer is therefore preferred.

Stations 2 and 3 form a profile paralleling the Maldive ridge in just under 4 km of water. The two lowest apparent velocities of station 3—5.40 and 6.31 km/sec—are only poorly established in contrast to the clearcut 6.40 km/sec of station 2. No 6.8-km/sec crustal velocity was observed. The sediment thickness was found to be about 0.8 km. In the same area *Neprochnov* [1961] found about 0.5 km (using a mean velocity of 2.0 km/sec).

Stations 4 and 5 are over the deep-water channel between the Maldive and Chagos archi-

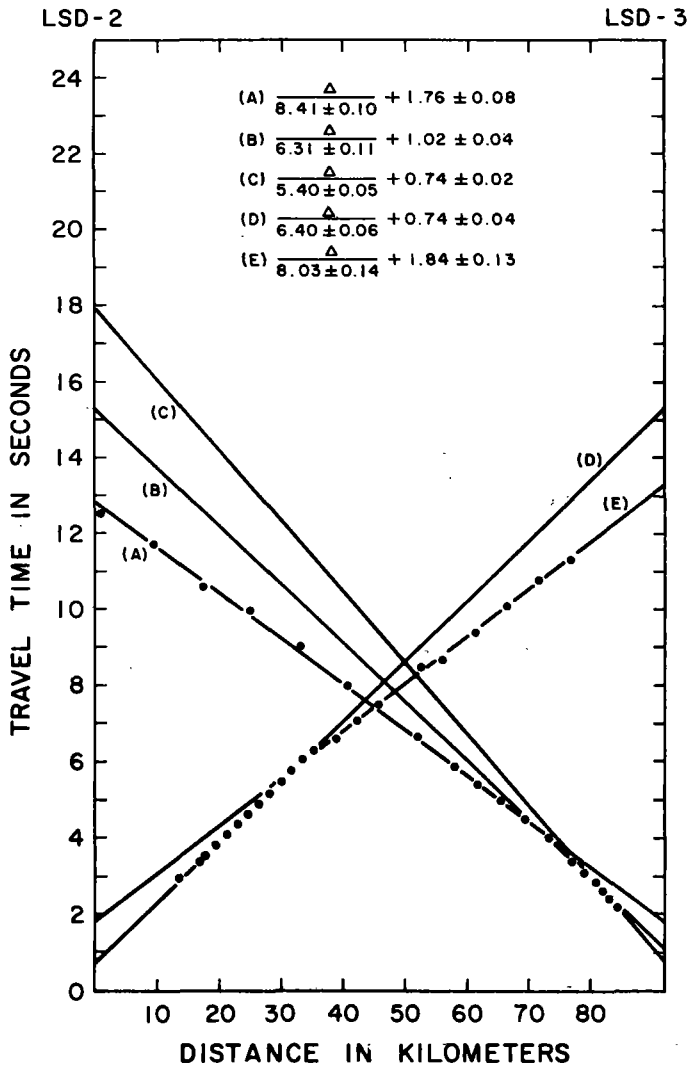
LSD - 2
LSD - 3
(A) Δ / 8.41 ± 0.10 + 1.76 ± 0.08
(B) Δ / 6.31 ± 0.11 + 1.02 ± 0.04
(C) Δ / 5.40 ± 0.05 + 0.74 ± 0.02
(D) Δ / 6.40 ± 0.06 + 0.74 ± 0.04
(E) Δ / 8.03 ± 0.14 + 1.84 ± 0.13
TRAVEL TIME IN SECONDS
DISTANCE IN KILOMETERS
0
2
4
6
8
10
12
14
16
18
20
22
24
10
20
30
40
50
60
70
80

pelagoes. Depths at receiving stations were 2.59 and 3.10 km, respectively; the maximum depth in this channel is about 3.5 km. No mantle velocities were observed, but the 6.13- and 7.11-km/sec velocities are well established. A small seamount close to station 4 prevented the observation of meaningful refracted arrivals out to a range of about 12 km. This feature suggests that lower-velocity volcanic rock may overlie the 6.13-km/sec material and that the soft sediment is thinner than the 1 km calculated.

Stations 6 and 7 are over deep water east of the Chagos archipelago and the diminutive Chagos trench. No apparent compressional wave velocities lower than 6.62 km/sec were observed, but low velocities interpretable as shear waves were observed at both stations. The ratios of compressional to shear velocity were all remarkedly close: 7.77/4.25 = 1.83; 6.75/3.67 = 1.84; 6.62/3.55 = 1.86. Shear waves from the mantle are seldom observed [*Ewing*, 1963]. In this case, the ratio of compressional to shear velocity corresponds to a Poisson ratio of 0.29. A second layer with $V_p = 5.0$ km/sec and $V_s = 2.8$ km/sec is assumed in the interpretation. Assuming further that P to S conversion occurred at the base of the soft sediment, we deduced the first and second layer thicknesses. The structure obtained is very reasonable, and refracted ar-

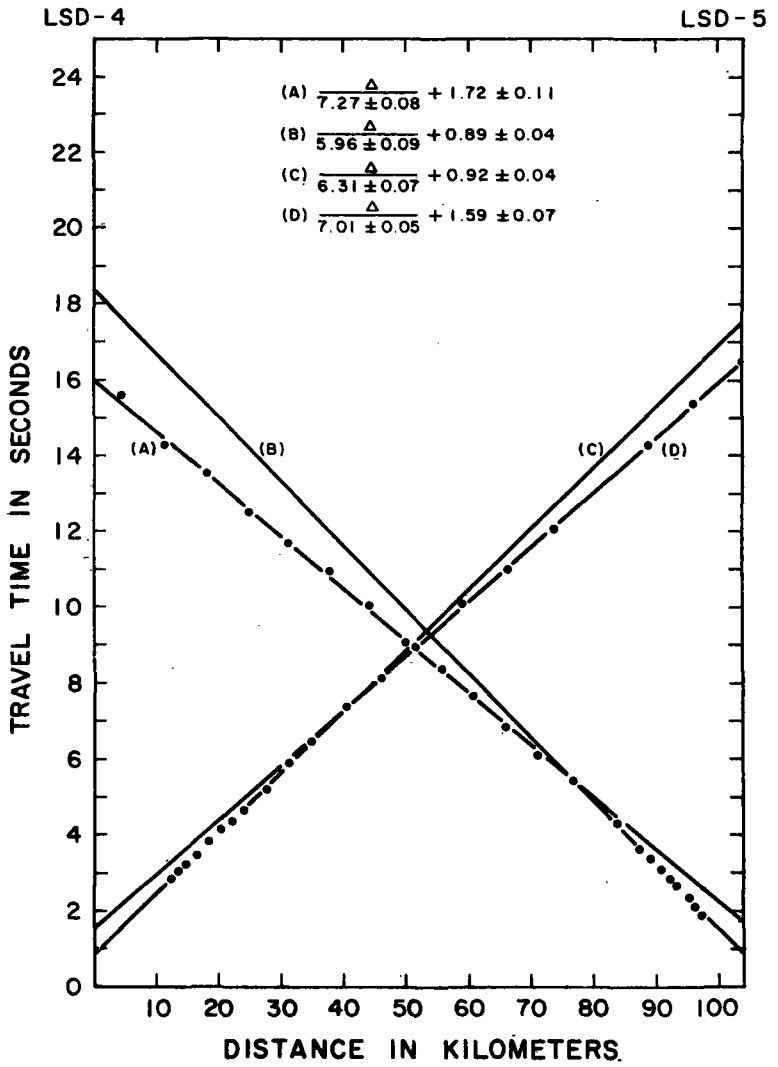

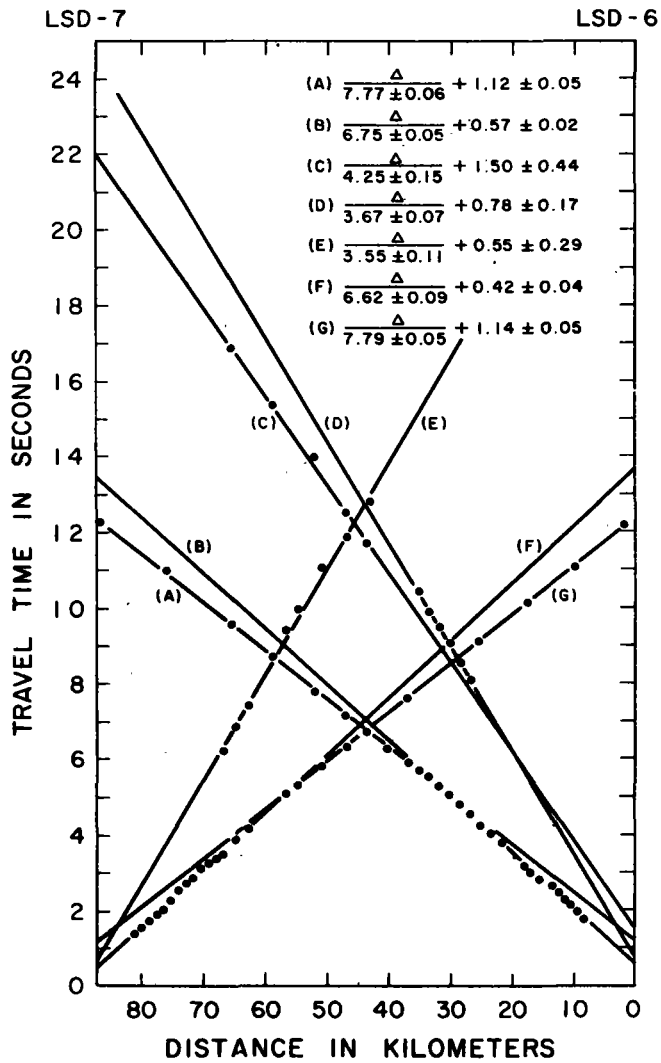
LSD-7
LSD-6
(A) Δ/7.77 ±0.06 + 1.12 ±0.05
(B) Δ/6.75 ±0.05 + 0.57 ±0.02
(C) Δ/4.25 ±0.15 + 1.50 ±0.44
(D) Δ/3.67 ±0.07 + 0.78 ±0.17
(E) Δ/3.55 ±0.11 + 0.55 ±0.29
(F) Δ/6.62 ±0.09 + 0.42 ±0.04
(G) Δ/7.79 ±0.05 + 1.14 ±0.05
TRAVEL TIME IN SECONDS
DISTANCE IN KILOMETERS
0
2
4
6
8
10
12
14
16
18
20
22
24
80 70 60 50 40 30 20 10 0

rivals from the 5.0-km/sec boundary would indeed be masked by arrivals from the deeper crustal layer. The mantle shear velocity observed at station 6 enables us to calculate an alternative thickness for the crustal layer. Assuming plane, horizontal layers, we get a layer thickness of 3.4 km for compressional waves and 2.2 km for shear waves. Finally, since the apparent mantle rock velocities are well determined and little different, the mantle velocity, 7.78 km/sec, in this region (in this direction?) is definitely low.

Stations 8 and 9 are over the Chagos bank. Water depth varied along the line from just under 1 km to almost 2 km. No mantle rock velocities were observed. It is highly improbable that the 3.49- and 2.69-km/sec velocities come from a single plane surface, although this is the convenient formal way of interpreting a refraction profile. For this reason the well-determined 2.69-km/sec velocity of station 8 may represent a truer measurement of the second-layer velocity than 3.01 km/sec, since the latter involves combination with the poorly determined (only three points) 3.49-km/sec velocity. For the same reason the thickness of soft sediment at station 9 may well be closer to the 0.23 km of station 8 than to the 0.61 km determined. The 4.76-km/sec layer would then be thicker at station 9 than 0.6 km.

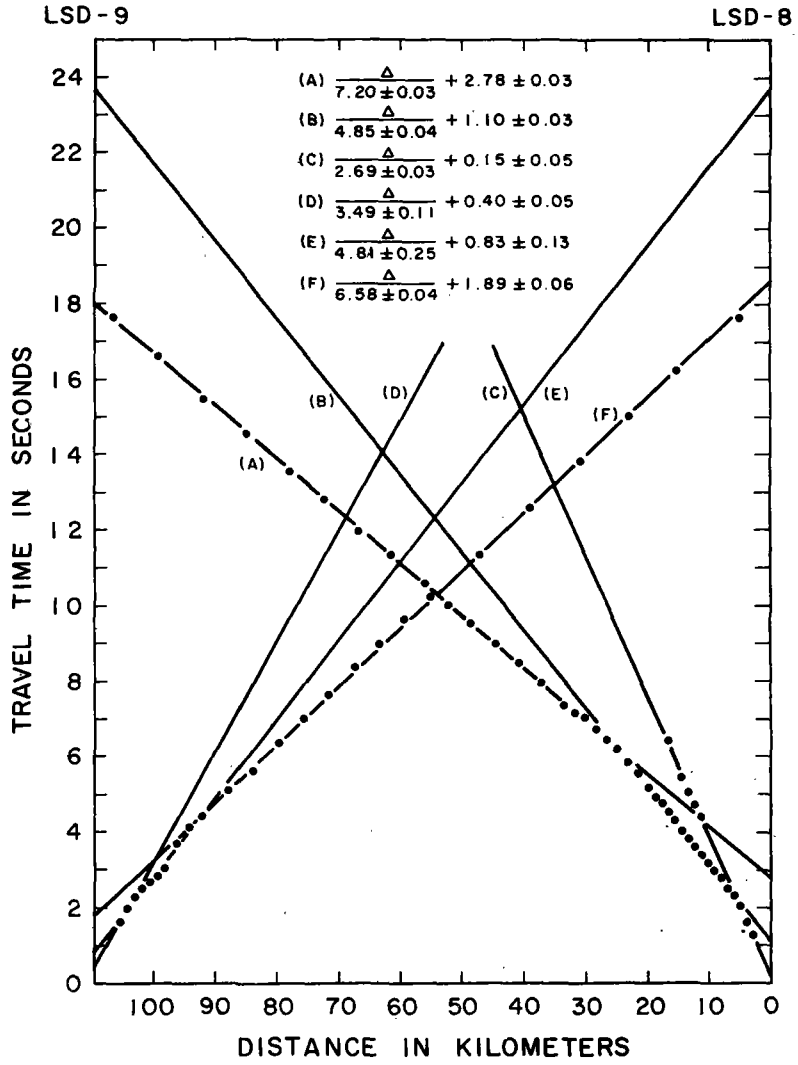

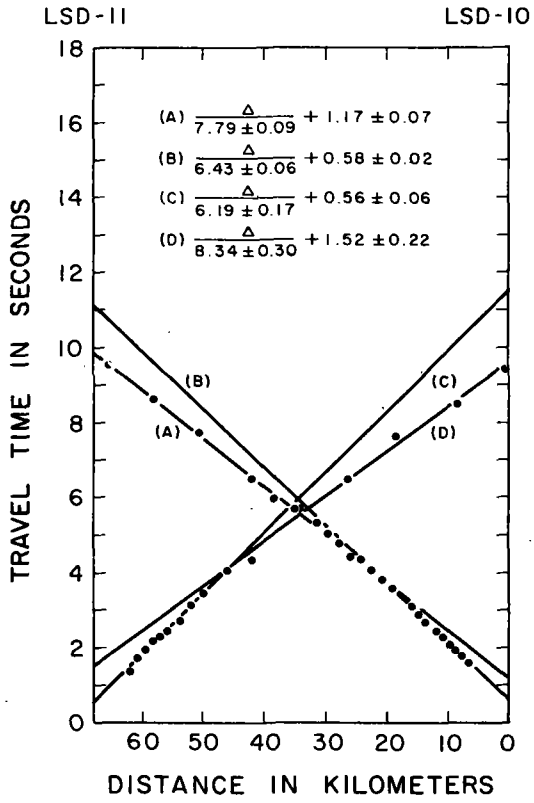

Stations 10 and 11. Only two velocities were determined on this profile: a normal mantle velocity and a lower velocity, 6.31 km/sec, which is higher than usual for the oceanic layer 2 and low for basic crustal material. The soft sediment of 0.6 km seems excessive in view of the step in the bottom topography. If a normal layer 2 with velocity of about 5 km/sec is present, but masked, the 0.6 km of sediment might be replaced by 0.3 km of sediment and about twice that much of layer 2. A further possibility is that a 6.8-km/sec crustal layer is also masked. For station 10, the minimum intercept this velocity could have is 0.75 sec. For plane, horizontal layering at station 10, this means replacing 3.3 km of 6.4-km/sec material with 1.6 km of the same and 2.0 km of 6.8-km/sec material. The conclusion for the station as a whole is that the presence of masked layers is unlikely to depress the Mohorovicic discontinuity by more than 0.6 km. The depth to the mantle at station 10 would then be 8.1 km, which is still anomalously shallow.

Stations 12 and 13 began with a short run to the east of stations 12. The reversed profile itself establishes the crustal and mantle velocities well, but the large thickness of sediment probably indicates a missed layer 2. The two halves of station 12, interpreted as a split profile, indicate the same thickness of sediment and a crustal velocity of 6.64 km/sec. However, assuming no lateral variations of velocity, we find that 6.88 km/sec appears to be the best determination for the crustal layer.

Stations 14 and 15 indicate a fairly normal oceanic sequence of velocities but a surprisingly thin crust. This may in part be a figment of the interpretation. The rather large dips of the crustal layer and Mohorovicic discontinuity depend on the poorly determined velocity, 7.34 km/sec, of station 14. But a lower apparent velocity at 14 would tend to thin the crust at 14 rather than thicken it at 15. The mantle velocity intercept at 15 could be increased slightly by including the last four points on the 6.42-km/sec line, but this is hard to justify. We cannot escape the conclusion that the mantle is unusually shallow at station 15 and that this is the result of an unusually thin crustal layer.

The 3.51-km/sec velocity of station 15 is interpreted as the shear wave from the crustal layer. The ratio is 6.42/3.51 = 1.83 (cf. stations 6 and 7). Assuming a shear velocity in layer 2 of 2.8 km/sec and P to S conversion at the base of the soft sediment, the shear arrivals give the same layer 2 thickness, 1.6 km, as the compressional wave arrivals.

Stations 16, 17, 18, and 19 form a leapfrog sequence approaching the Seychelles bank from the east. The water depth shoaled from 4.1 km at 16 to 2.5 km at 19. The stations have been interpreted as three reversed profiles. The seaward two indicate normal oceanic velocities and thicknesses. No mantle arrivals were detected on the other. The discrepancies in velocity and layer thickness at the stations common to two profiles are not greater than is usual for refraction work and probably reflect geological variations and the simplifying assumptions made in the interpretation rather than errors in the measurements themselves. Low-velocity second arrivals were observed on both sides of station 17. The 2.65-km/sec line probably represents shear arrivals from the second layer, the large ratio, 6.11/2.65 = 2.31, probably being produced by topographic irregularities. The 3.48-km/sec

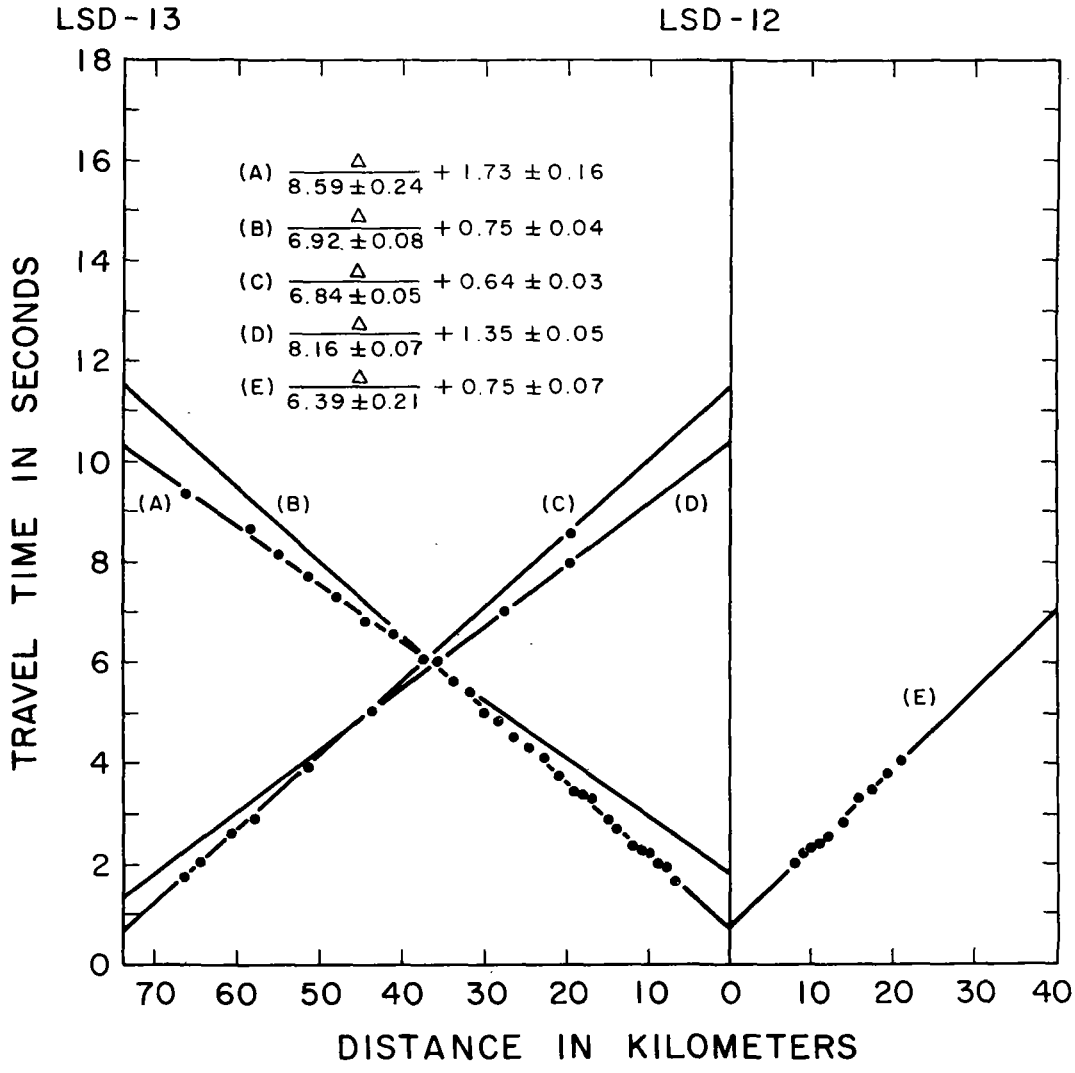
LSD-13
LSD-12
(A) Δ/8.59±0.24 + 1.73 ±0.16
(B) Δ/6.92±0.08 + 0.75 ±0.04
(C) Δ/6.84±0.05 + 0.64 ±0.03
(D) Δ/8.16 ±0.07 + 1.35 ±0.05
(E) Δ/6.39±0.21 + 0.75 ±0.07
(A)
(B)
(C)
(D)
(E)
TRAVEL TIME IN SECONDS
0
2
4
6
8
10
12
14
16
18
70 60 50 40 30 20 10 0 10 20 30 40
DISTANCE IN KILOMETERS

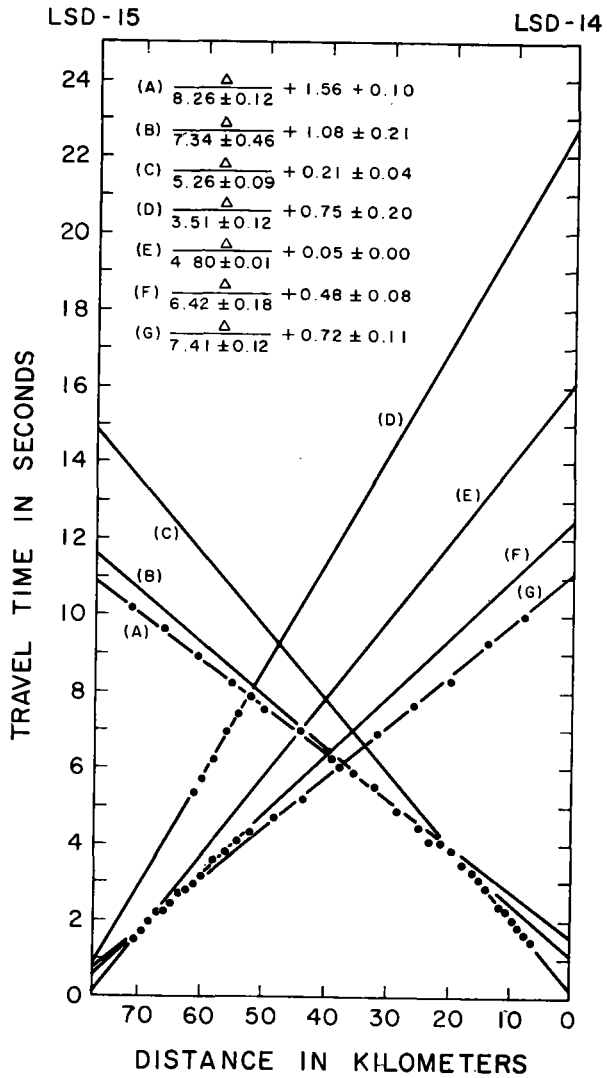
LSD - 15
LSD - 14
(A) Δ / 8.26 ± 0.12 + 1.56 + 0.10
(B) Δ / 7.34 ± 0.46 + 1.08 ± 0.21
(C) Δ / 5.26 ± 0.09 + 0.21 ± 0.04
(D) Δ / 3.51 ± 0.12 + 0.75 ± 0.20
(E) Δ / 4 80 ± 0.01 + 0.05 ± 0.00
(F) Δ / 6.42 ± 0.18 + 0.48 ± 0.08
(G) Δ / 7.41 ± 0.12 + 0.72 ± 0.11
TRAVEL TIME IN SECONDS
DISTANCE IN KILOMETERS
0
2
4
6
8
10
12
14
16
18
20
22
24
70 60 50 40 30 20 10 0

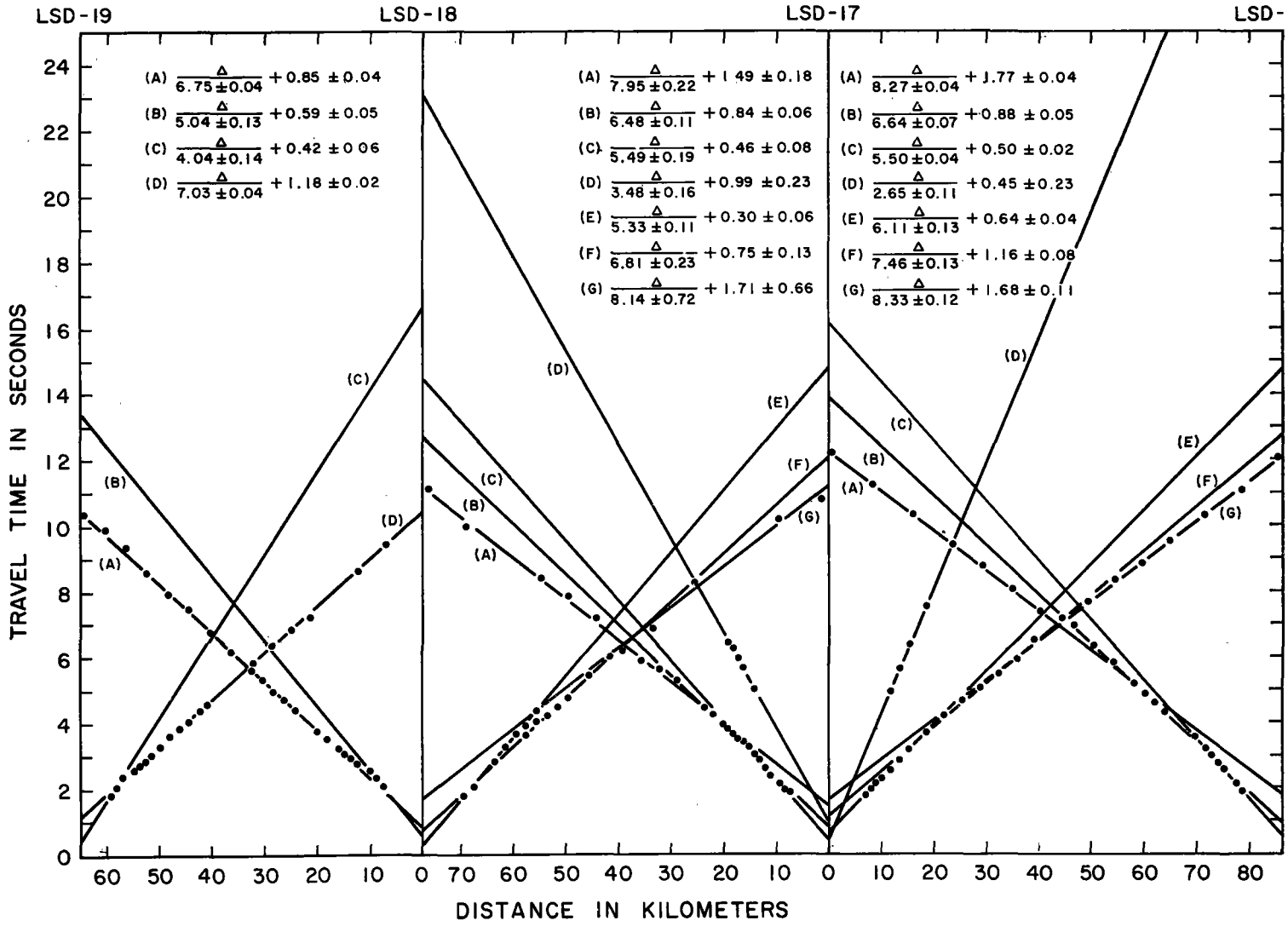
LSD-19
LSD-18
LSD-17
LSD-16.
(A) Δ/6.75±0.04 + 0.85 ±0.04
(B) Δ/5.04±0.13 + 0.59 ±0.05
(C) Δ/4.04±0.14 + 0.42 ±0.06
(D) Δ/7.03±0.04 + 1.18 ±0.02
(A) Δ/7.95±0.22 + 1.49 ±0.18
(B) Δ/6.48±0.11 + 0.84 ±0.06
(C) Δ/5.49±0.19 + 0.46 ±0.08
(D) Δ/3.48±0.16 + 0.99 ±0.23
(E) Δ/5.33±0.11 + 0.30 ±0.06
(F) Δ/6.81±0.23 + 0.75 ±0.13
(G) Δ/8.14±0.72 + 1.71 ±0.66
(A) Δ/8.27±0.04 + 1.77 ±0.04
(B) Δ/6.64±0.07 + 0.88 ±0.05
(C) Δ/5.50±0.04 + 0.50 ±0.02
(D) Δ/2.65±0.11 + 0.45 ±0.23
(E) Δ/6.11±0.13 + 0.64 ±0.04
(F) Δ/7.46±0.13 + 1.16 ±0.08
(G) Δ/8.33±0.12 + 1.68 ±0.11
TRAVEL TIME IN SECONDS
0 2 4 6 8 10 12 14 16 18 20 22 24
60 50 40 30 20 10 0 70 60 50 40 30 20 10 0 10 20 30 40 50 60 70 80
DISTANCE IN KILOMETERS

line is clearly associated with the crustal layer. The ratio 6.48/3.48 = 1.86 is close to that found on other stations (cf. stations 6 and 7, 15).

Stations 22, 23, and 24, in water approximately 4 km deep, have been interpreted as two reversed profiles end to end. Stations 22 and 23-in produce a normal oceanic structure, but 23-out and 24 are anomalous. The two sides appear unrelated. On the other hand, 24 gives a similar sequence of velocities to 25. A marked change in structure between 23 and 24 is indicated. The 3.70-km/sec line of 23-out is interpreted as the result of strictly local structure and for the purposes of the dipping-layer solution is replaced by a line which gives agreement in sediment thickness with 23-in and a similar layer 2 velocity. Nevertheless, the dipping-layer solution appears unrealistic, giving a structure for 23-out quite at odds with that for 23-in. Interpreting 23-in and 23-out as a split profile gives rise to a crustal layer of 6.7 km/sec dipping in the direction of station 24. This suggests a reasonable geological solution to the problem: the crustal layer dips down from 23 to 24 while material represented by the 6.03-km/sec velocities of stations 25, 26, and 27 thins out in the opposite direction. Such a solution implies a masked 6.8-km/sec velocity and hence a greater depth to the mantle at station 24 than that shown in Table 1.

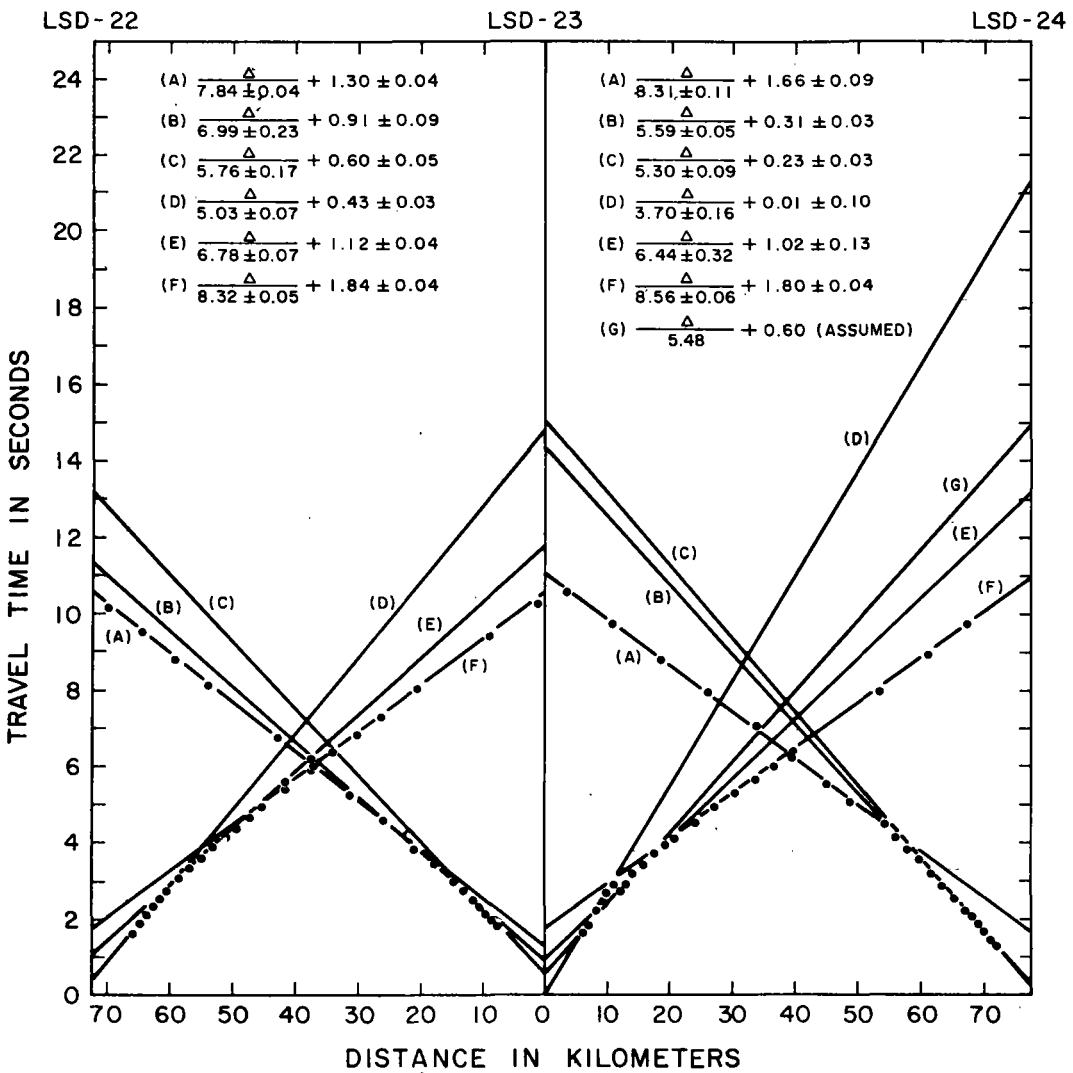

Stations 25, 26, and 27, which are immediately west of the Saya de Malha bank, form two reversed profiles end to end. The host of second arrivals, corresponding to shear and reflected-refracted paths, indicates a structure with uniform layering. This view is supported by the smallness of the residuals of the observed points from their respective lines. The structures deduced for the two profiles agree closely, but only the first profile was long enough to permit us to observe arrivals from beneath the Mohorovicic discontinuity. This is found at a depth of about 17 km, dipping down toward the bank. No 6.8-km/sec crustal velocity is observed. If masked, the smallest intercept such a layer could have at station 25 is 1.76 sec. This would make the 6.03-km/sec layer about 5 km thick and itself be about 7 km thick. Thus the top of a 6.8-

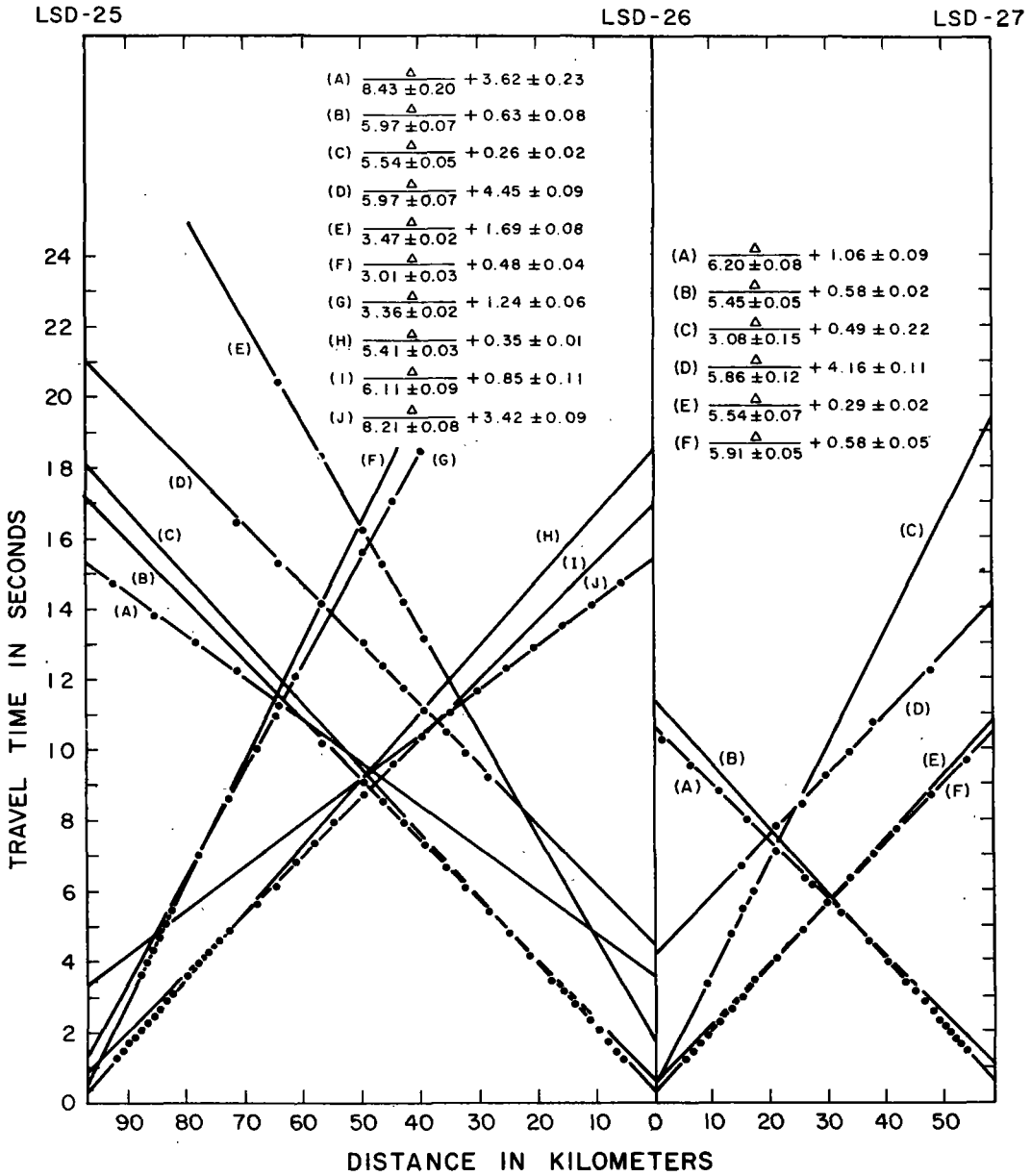

km/sec layer, if present, can be no shallower than 12 km below sea level and the depth to the mantle no more than 19 km.

The 3.01- and 3.36-km/sec velocities observed at station 25 are interpreted as the shear waves associated with the 5.41- and 6.11-km/sec velocities, respectively. The ratios are 5.41/3.01 = 1.80 and 6.11/3.36 = 1.82 (cf. stations 6 and 7, 15). Similarly the 3.47- and 3.08-km/sec velocities of station 26 are from shear waves corresponding to the 5.97- and 5.54-km/sec compressional velocities, respectively. The ratios are 5.97/3.47 = 1.72 and 5.54/3.08 = 1.80. Whereas the P arrivals of station 25 considered alone indicate 0.3 km of sediment overlying 2.8 km of 5.41-km/sec material, the S arrivals show 0.6 km of sediment over 2.4 km of 3.01-km/sec material.

Reflected-refracted arrivals observed on both sides of station 26 suffered reflection at the sea floor in addition to refraction along the 6.03-km/sec layer. The apparent velocities agree closely with those of the simply refracted arrivals.

Variable-angle reflection shots at station 25 produced strong sub-bottom returns which clearly originated from the same horizon as the 5.48-km/sec refracted arrivals. These gave a sediment velocity of 1.70 km/sec, which is considerably less than the 2.15 km/sec which has been assumed throughout this paper. However, since sub-bottom reflections are seldom distinguishable from single shots (and when they are, the reflecting horizon is frequently not the base of the sediment), the assumed velocity has been used throughout. The difference this makes to sediment thickness is small: for station 25, 1.70 km/sec gives 0.31 km of sediment; 2.15 km/sec gives 0.41 km.

Acknowledgments. We thank Captain Marvin Hopkins and the crew of the R.V. *Horizon* and Captain Alan Phinney and the crew of the R.V. *Argo* for their assistance in gathering the data. Alan Jones was responsible for the instrumentation. Dwight Pollard was in charge of seismic operations on *Horizon*. George Hohnhaus handled explosives. Professor Russell Raitt gave advice on methods of analysis. Gloria Slack and Shirley Fisher assisted in data reduction. David Crouch drew the illustrations. Professor H. W. Menard and Dr. R. L. Fisher critically reviewed the manuscript and made helpful suggestions. To all these people we express our thanks.

This work was supported by the National Science Foundation under grant 22255 and by the Office of Naval Research under contract Nonr 2216(05) as part of the International Indian Ocean Expedition.

References

Admiralty Marine Science Publication 4, Bathymetric, magnetic and gravity investigations, H.M.S. OWEN, 1961–1962, London, 1963.

Baker, B. A., and J. A. Miller, Geology and geochronology of the Seychelles Islands, *Nature, 199,* 346–348, 1963.

Balakrishna, S., Velocities of compressional waves in some Indian rocks, *Trans. Am. Geophys. Union, 39,* 711–712, 1958.

Bathymetric Chart of the Indian Ocean, scale 1:15,000,000, published by the Main Administration of Geodesy and Cartography of the Governmental Geological Committee of the U.S.S.R., Moscow, 1963.

Chayes, F., A petrographic distinction between Cenozoic volcanics in and around the open oceans, *J. Geophys. Res., 69,* 1573–1588, 1964.

Davies, D., and T. J. G. Francis, The crustal structure of the Seychelles bank, *Deep-Sea Res., 11,* 921–927, 1964.

Du Toit, A. L., *Our Wandering Continents,* Oliver and Boyd, Edinburgh, 1937.

Ewing, J. I., Elementary theory of seismic refraction and reflection measurements, *The Sea,* vol. 3, pp. 3–19, Interscience Publishers, New York, 1963.

Ewing, J. I., The mantle rocks, *The Sea,* vol. 3, pp. 103–107, Interscience Publishers, New York, 1963.

Ewing, J. I., and M. Ewing, Seismic refraction measurements in the Atlantic Ocean basins, in the Mediterranean Sea, on the mid-Atlantic ridge, and in the Norwegian Sea, *Bull. Geol. Soc. Am., 70,* 291–319, 1959.

Francis, T. J. G., D. Davies, and M. N. Hill, Crustal structure between Kenya and the Seychelles, *Phil. Trans. Roy. Soc. London,* in press, 1965.

Gaskell, T. F., M. N. Hill, and J. C. Swallow, Seismic measurements made by H.M.S. CHALLENGER in the Atlantic, Pacific and Indian Oceans, and in the Mediterranean Sea, 1950–1953, *Phil. Trans. Roy. Soc. London, A, 251,* 23–83, 1958.

Glennie, E. A., Report on the value of gravity in the Maldive and Laccadive Islands, John Murray Expedition, 1933–34, *Sci. Repts. (Brit. Museum Nat. Hist.), 1*(4), 95–107, 1936.

Heezen, B. C., and M. Ewing, The mid-oceanic ridge, *The Sea,* vol. 3, pp. 388–408, Interscience Publishers, New York, 1963.

Heezen, B. C., and M. Tharp, Physiographic Diagram of the Indian Ocean, Geological Society of America, New York, 1965.

Krishnan, M. S., *Geology of India and Burma,* chapter 15, 4th ed., Higginbothams, Madras, 1960.

Le Pichon, X., R. E. Houtz, C. L. Drake, and J. E. Nafe, Crustal structure of the mid-ocean ridges, 1, Seismic refraction measurements, *J. Geophys. Res., 70,* 319–339, 1965.

Menard, H. W., *Marine Geology of the Pacific,* McGraw-Hill Book Company, New York, 1964.

Neprochnov, Iu. P., Sedimentary thickness in the Arabian Sea basin, *Dokl. Akad. Nauk SSR, 139,* 177–179, 1961. (Translated by L. Hutchison, edited by R. L. Fisher, Scripps Institution, 1962.)

Pepper, J. F., and G. M. Everhart, The Indian Ocean—The geology of its bordering lands and the configuration of its floor, Miscellaneous Geologic Investigations Map I-380, U. S. Geological Survey, Washington, D. C., 1963.

Raitt, R. W., Geophysical measurements, *Oceanographic Instrumentation,* Rancho Sante Fe Conference, June 21–23, 1952, *Nat. Acad. Sci.—Natl. Res. Council Publ. 309,* p. 389, 1956.

Raitt, R. W., Seismic refraction studies of Eniwetok atoll, *U. S. Geol. Surv. Profess. Paper 260-S,* 1957.

Raitt, R. W., The crustal rocks, *The Sea,* vol. 3, pp. 85–102, Interscience Publishers, New York, 1963.

Raitt, R. W., and G. G. Shor, Jr., Pacific oceanic crust, *Preprints of Abstracts of Papers,* p. 49, First International Oceanographic Congress, New York, August 31–September 12, 1959.

Shor, G. G., Jr., Refraction and reflection techniques and procedure, *The Sea,* vol. 3, pp. 20–38, Interscience Publishers, New York, 1963.

Shor, G. G., Jr., and D. D. Pollard, Seismic investigations of Seychelles and Saya de Malha banks, northwest Indian Ocean, *Science, 142,* 48–49, 1963.

Shor, G. G., Jr., and D. D. Pollard, Mohole site selection studies north of Maui, *J. Geophys. Res., 69,* 1627–1637, 1964.

Steinhart, J. S., and R. P. Meyer, Explosion studies of continental structure, *Carnegie Inst. Wash. Publ. 622,* 1961.

Wadia, D. N., *Geology of India,* chapter 16, 3rd ed., Macmillan and Company, London, 1953.

Washington, H. W., Deccan traps and other plateau basalts, *Bull. Geol. Soc. Am., 33,* 765–804, 1922.

Wilson, J. T., A resume of the geology of islands in the main ocean basins, vol. 1, Atlantic and Indian Oceans, *Sci. Rept. 4,* Institute of Earth Sciences, University of Toronto, 1963.

Wiseman, J. D. H., and R. B. S. Sewell, The floor of the Arabian Sea, *Geol. Mag., 74,* 219, 1937.

(Manuscript received August 28, 1965; revised October 25, 1965.)

Reprinted from Science, vol. 150, no. 3,696, 1965, p. 605-610.
Copyright 1967 by the American Association for the Advancement of Science.

Igneous Rocks of the Indian Ocean Floor

Celeste G. Engel
Robert L. Fisher
A. E. J. Engel

Abstract. *Four dredge hauls from near the crest and from the eastern flank of the seismically active Mid-Indian Ocean Ridge at 23° to 24°S, at depths of 3700 to 4300 meters, produced only low-potassium tholeiitic basalt similar in chemical and mineralogic composition to basalts characteristic of ridges and rises in the Atlantic and Pacific oceans. A fifth haul, from a depth of 4000 meters on the lower flank of a seamount on the ocean side of the Indonesian Trench, recovered tholeiitic basalt with higher concentrations of K and Ti and slightly lower amounts of Si and Ca than the typical oceanic tholeiite of the ridge. The last sample is vesicular, suggesting depression of the area since the basalt was emplaced. Many of the rocks dredged are variously decomposed and hydrated, but there is no evidence of important chemical modification toward conversion of the lava flows to spilite during extrusion or solidification.*

The complex ridgelike features and extensive intervening basins of the Indian Ocean were first clearly indicated by surveys of the Dana and John Murray expeditions, and by the gravity-measuring traverses of Vening Meinesz (*1*). Recent oceanographic investigations undertaken by the International Indian Ocean Expedition, 1960–1965, have further clarified several major geological features, especially its fascinating patterns of both elongated and bifurcated faulted ridges, the large "plateaus" and irregular deeps, and the texture of the deep-sea floor (*2*). Figure 1 is a simplified map of the Indian Ocean showing one version of the gross patterns of the ridge complex shallower than 4000 m, and the locations of islands and dredge samples discussed in this report.

Early petrologic studies in the Indian Ocean were confined to the volcanic islands which lie along and flank the Indian Ocean ridges (*3*). These islands include Mauritius, Rodriguez, Réunion, New Amsterdam, St. Paul, Crozet, and the Kerguelen Archipelago (Fig. 1). Each consists of one or more variously coalescing, sometimes fragmented, volcanic cones. Continuing studies, ranging over more than a century, have shown that the dominant volcanic rocks capping these islands and the higher submarine volcanoes are alkali basalts, which are commonly accompanied by subordinate, derivative members of the alkali series, especially andesine- and oligoclase-andesites, trachytes, and more rarely phonolites and rhyolites (*4*). Olivine-rich (picritic) basalts are found on some of the islands; tholeiitic basalts with low concentrations of potassium, high concentrations of calcium and silica, and high ratios of calcium to magnesium are extruded, notably on Mauritius and Réunion islands (*5*). Small inclusions of magnesium-rich peridotite and pyroxene amphibolite occur in the alkali basalts and in associated beds of ash, but these inclusions represent less than 0.1 percent of the exposed rock. The alkali-rich basalts comprise over 90 percent of the igneous rocks of most islands.

These relative abundances of rock types from the exposed parts of the volcanic cones along the Indian Ocean ridge systems are similar to those from volcanic islands of the Atlantic and Pacific oceans, where alkali basalts and subordinate members of the alkali series also predominate. In the Atlantic and Pacific, olivine-rich basalts are common but volumetrically subordinate. Tholeiitic basalts occur only rarely, except in the several major oceanic rift-island systems such as Hawaii and Iceland, where they are abundant (*6*).

The alkali basalts which are typical and predominant constituents of the higher oceanic volcanoes are characterized, among the basalts, by relatively high concentrations of K, Na, Ti, and P and a high ratio of Fe^{3+} to Fe^{2+}. They also contain distinctly higher concentrations of Ba, La, Nb, Pb, Rb, Th, U, and Zr, and higher ratios of K to Rb, Sr^{87} to Sr^{86}, and Pb^{206} to Pb^{204} than are found in picritic and tholeiitic basalts of the oceans. Detailed discussions of the chemical characteristics of oceanic basalts, including abundances of minor and trace elements and of the isotopes of strontium and lead, are being published separately (*7*).

The dominance of alkali-rich basalts on readily accessible oceanic islands caused early petrologists to suggest that these rocks were characteristic of the entire oceanic crust (*8*). It was in the light of this petrologic concept that Wiseman (*9*) examined and first described dredge hauls from the more deeply submerged parts of the ridge complex in the northwestern Indian Ocean. The location of Wiseman's samples is shown in Fig. 1 (positior *IM*). Wiseman recognized that the ridge rocks were not typical alkali basalts like those found on the islands of the Indian Ocean. He noted that the dredged basalts were relatively uni-

form in composition and that they contained extremely low concentrations of potassium, relatively high concentrations of sodium and silica, and moderate to low ratios of Fe_2O_3 to FeO, especially in their glassy parts. The differences in composition between the basalts of the submerged ridge and those from the islands naturally perplexed Wiseman. He both suggested and rejected close interrelationships between the island and the submarine basalts (*9*).

Following Wiseman's studies, there ensued three decades during which few rocks were dredged from the deeper parts of the Indian Ocean or other oceans, and none were described and discussed in detail. However, several close students of Hawaiian geology either implied or stated that tholeiitic basalts were common in the central Pacific and that the alkali series of Hawaii appeared to be largely younger than, and probably derivative from, a tholeiitic root of the great Hawaiian Rift (*10*).

Recent studies in the Atlantic and Pacific oceans suggest that a most unique, low-potassium, tholeiitic basalt (oceanic tholeiite) is the dominant igneous rock of the oceans (*11–14*). The alkali basalts so characteristic of the higher volcanoes appear to be derived from oceanic tholeiites, which are the most primitive, least radiogenic basalts yet found in the earth's crust (*7*).

Because of the scarcity of samples of igneous rocks from deeply submerged features of the Indian Ocean, Expedition Dodo of the Scripps Institution of Oceanography undertook in 1964 a series of dredge hauls along a rudely arcuate ENE–WSW profile across the median ridge of the Indian Ocean near latitudes 23° to 24°S (Figs. 1 and 2). Four hauls of bedrock were obtained at depths ranging from 3700 to 4300 m in three portions of the ridge environment. One haul came from near the central, highest portion of the ridge; two from the eastern, irregular "foothills"; and one from generally oceanic depths well off the east side of the ridge (Fig. 2). Later in the expedition a fifth dredge haul, from depths of approximately 3800 to 4300 m, was made on the flank of a seamount on the ocean side of the Indonesian Trench, southwest of Sumatra (Fig. 1, sample D232).

In the mid-ocean region sampled on the expedition, the median ridge is extremely irregular in profile both across and along its northerly trend. Figure 2, prepared from echo-sounding records, shows the topography in an exaggerated fashion. Here the ridge, or more properly the southeast branch of the Mid-Indian Ocean Ridge complex, is 400 to 500 km wide and includes 8 to 12 major peaks and numerous minor pinnacles on each crossing. The depths of a few peaks are 2100 to 2400 m. However, the general range of ridge depths is 3500 to 3900 m, and local depressions or canyons reach 4200 to 4300 m. Such depressions are only 1 to 3 km wide and show only minor evidence of sediment fill. On the flanks of the ridge, pinnacles decrease in height but increase in steepness and number. Steep-walled, fairly linear deeps which may be fault troughs intersect or roughly parallel the ridge. These depressions extend from tens to hundreds of kilometers off the ridge at depths 400 to 500 m greater than the 4000 to 4300 m depth of the sea floor and its abyssal hills.

No obvious central "rift valley" has been traced along this portion of the median ridge. On most profiles the central 200 to 300 km seem to contain larger peaks which are separated by depressions up to 15 km in width; haul D115 was recovered from one such peak. Plots of earthquake epicenters show that in these latitudes the median ridge complex is relatively quiet at present, although earthquakes have occurred in this rifted region. North of 20°S this same median ridge is seismically more active. There is also considerable seismic activity on the NE-trending ridge which presumably intersects the median ridge just west of the area sampled (Fig. 1). The near-absence of sediment-filled depressions in the region makes penetrations with heat-flow equipment difficult. A few measurements from Expedition Monsoon (1960) and Expedition Dodo in the vicinity of the median ridge show values for heat flow somewhat higher than the oceanic average (*15*). These characteristics, as well as the occurrence of only vol-

Table 1. Compositions of basalts from the Mid-Indian Ocean Ridge.

Oxide	Amount present (%)						
	D113 A1*	D113 D1*	D114 A†	D115 B‡	D115 L‡	D143 A§	D 143 B§
SiO_2	50.30	50.20	49.52	49.62	48.77	50.04	49.98
TiO_2	1.38	1.35	1.31	1.13	0.76	1.29	1.37
Al_2O_3	15.88	16.91	18.01	16.48	21.09	16.91	16.70
Fe_2O_3	1.61	1.36	2.12	4.14	2.68	3.08	1.45
FeO	7.88	7.30	5.80	4.53	3.89	4.98	6.64
MnO	0.09	0.15	0.18	0.18	0.10	0.14	0.18
MgO	7.56	7.65	6.83	7.25	5.47	7.38	7.52
CaO	11.43	11.26	11.70	11.35	13.22	10.86	11.10
Na_2O	2.69	2.64	2.81	3.03	2.66	3.51	2.97
K_2O	0.17	0.18	0.19	0.24	0.11	0.25	0.18
H_2O^+	.41	.59	.68	.71	.79	.85	.82
H_2O^-	.27	.24	.54	1.31	.45	.57	.76
P_2O_5	.07	.12	.04	0.07	.11	.10	.10
Total	99.74	99.95	99.73	100.04	100.10	99.96	99.77

* D113 A1 and D113 D1, analyses of the glassy margins of two pillows; interiors of the pillows are porphyritic basalt with phenocrysts of calcic plagioclase, and groundmass is glassy to fine-grained, with abundant plagioclase crystallites; location, 23°20.6'S, 74°56.5'E; depth, 4100 m. † D114 A, porphyritic basalt with phenocrysts of calcic plagioclase (bytownite), groundmass composed largely of labradorite and clinopyroxene, rare small vesicles; location, 24°08.6'S, 72°26.6'E; depth, 4000 m. ‡ D115 B and D115 L, porphyritic basalt with phenocrysts of calcic plagioclase, groundmass largely plagioclase and calcium-rich pyroxene, rare tiny vesicles; location, 24°02'S, 70°14.1'E, depth, 3700 m. § D143 A and D143 B, porphyritic basalt with phenocrysts of labradorite, groundmass composed of plagioclase, clinopyroxene, and olivine; 23°43.7'S, 72°42.6'E, depth, 4300 m.

Table 2. Partial analyses of additional basalts from the Mid-Indian Ocean Ridge. Samples are from the dredge hauls listed in Table 1.

Oxide	Amount present (%)			
	D113 A2*	D113 D2†	D114 B‡	D143 P§
SiO_2	49.61	48.20	49.33	49.62
TiO_2	1.20	1.46	1.39	1.50
Na_2O	2.75	2.82	2.77	3.09
K_2O	0.23	0.19	0.24	0.30
P_2O_5	.08	.04	.12	.14

* D113 A2, porphyritic interior of pillowed basalt (sample D113 A1, Table 1, is the glassy outer margin). † D113 D2, porphyritic, plagioclase-rich interior of pillowed basalt (sample D113 D1, Table 1, is the glassy outer margin). ‡ D114 B, plagioclase-rich basalt from dredge haul D114. § D143 P, porphyritic, labradorite-rich basalt with groundmass of plagioclase, clinopyroxene, and olivine.

canic shards in cores taken nearby by the Monsoon Expedition, and the little-weathered lavas of the dredge collections, indicate abundant recent volcanism.

The compositions of seven basalts from the four dredge hauls made at intervals across the Mid-Indian Ocean Ridge are listed in Table 1. Partial analyses of four more basalts from these localities are listed in Table 2. All of these basalts are similar to the oceanic tholeiites recently recovered from widely separated, submarine segments of both the Atlantic and Pacific ridge and rise systems (*11–14*).

The close compositional similarities of oceanic tholeiites from the oceans, and the contrasting compositions of the average alkali-rich basalts from the islands of the Indian Ocean, are indicated in Table 3. This table contains the compositions of average oceanic tholeiites dredged from the Indian Ocean median ridge in the latitudes 22° to 23°S, the East Pacific Rise, and the Mid-Atlantic Ridge. The average of four basalts described by Wiseman from the Carlsberg Ridge is tabulated in Table 3, column 2 (*9*). A single sample of glassy basalt reported by Korzhinsky (*16*) from the Indian Ocean appears in column 3. Column 6 is an average of 42 published analyses of alkali-rich basalts from islands in the Indian Ocean.

In compiling the averages of oceanic tholeiites from the several oceans we have used only the analyses of essentially unaltered basalts that are not highly porphyritic. This selection of the data indicates the close similarities in composition of the fresh, glassy, and more equigranular oceanic tholeiites which are most likely to represent the compositions of primary magma. The marked departures of individual samples from the average compositions of the submerged ridge basalts that are listed in Table 3 are found in oceanic tholeiites that are (i) highly porphyritic, especially those containing abundant phenocrysts of plagioclase feldspar, (ii) variously altered by sea water, and (iii) recovered from the deeply submerged flanks of large volcanic cones, rather than from extensive submarine flows, fault scarps, or abyssal hills.

Compositional variations induced in primary magmas by growth and redistribution of phenocrysts are well known. Plagioclase is the least dense of the major constituent silicates in basalt, and early formed phenocrysts of labradorite or anorthite may either rise or sink more slowly in the magma than the denser olivine and pyroxene. One of the distinguishing aspects of the oceanic tholeiites is their enrichment in calcic plagioclase relative to the tholeiites which are characteristic of the Hawaiian and Icelandic regions (*6*). This is reflected especially in higher concentrations of alumina and calcium. In the oceanic tholeiites from the Indian Ocean Ridge, Al_2O_3 varies from almost 16 to more than 21 percent by weight, depending upon the amount of calcic plagioclase present as phenocrysts (Table 1); CaO varies from about 10.9 to 13.2 percent (Table 1). Specifically, basalt D113 Al is nonporphyritic and fine-grained to glassy, whereas D143 A is porphyritic. The phenocrysts in D143 A consist almost entirely of labradorite.

Similar variations in calcium and alumina are found in the oceanic tholeiites of the Atlantic and Pacific oceans. The highest concentrations invariably occur in markedly porphyritic

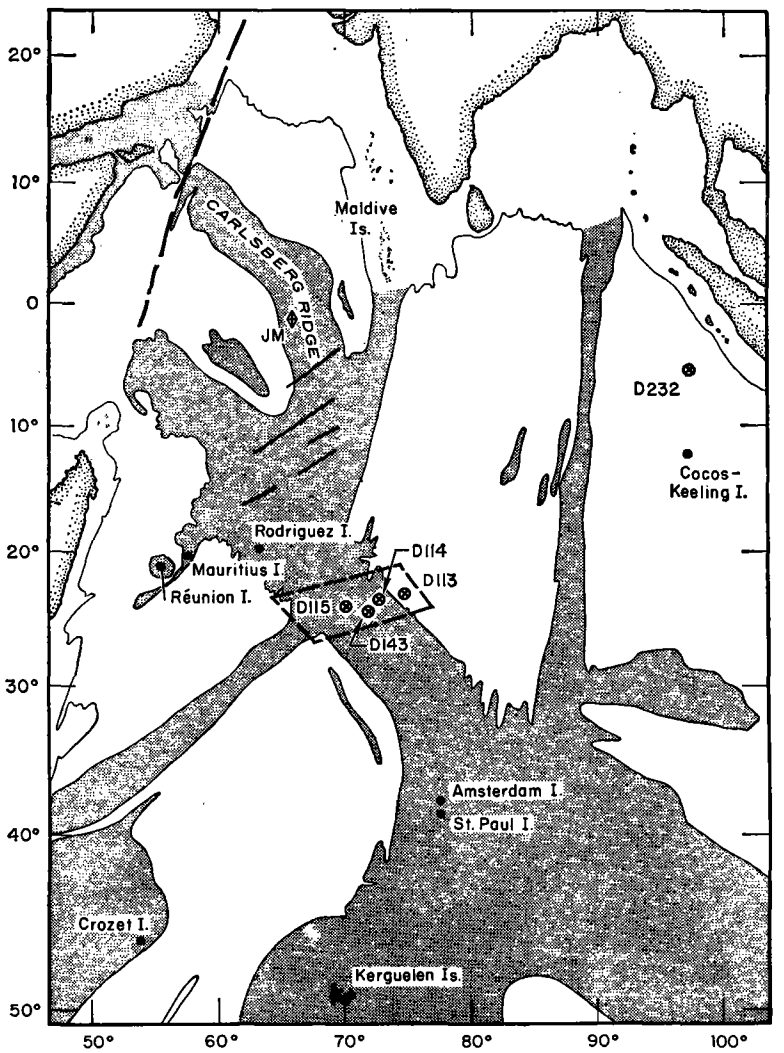

Fig. 1. Index map of the Indian Ocean. Oceanic ridges and associated rises shallower than 4000 m are stippled [after Heezen and Tharp (*2*)]. Islands are represented by black dots. The dashed line approximates the Owen Fracture Zone (*21*) and the heavy solid lines north of Rodriguez Island are inferred cross fractures on the median ridge. The diamond symbol *JM* represents the site of igneous rocks dredged by the John Murray Expedition (*1*). The crossed circles are sites of dredging by Expedition Dodo. The region within the dashed quadrangle is enlarged in Fig. 2.

Table 3. Average compositions of basalts from the Indian, Atlantic, and Pacific Ocean Ridge and Rise systems and of basalts from islands in the Indian Ocean (calculated water-free).

Oxide	Amount present (%)					
	1*	2†	3‡	4§	5‖	6¶
SiO_2	50.65	51.81	51.13	50.25	49.78	47.67
TiO_2	1.36	1.88	0.35	1.56	1.29	2.66
Al_2O_3	17.09	15.56	15.20	16.09	16.92	15.72
Fe_2O_3	1.66	3.56	1.16	2.72	1.94	4.51
FeO	7.00	6.39	7.64	7.20	7.32	7.86
MnO	0.15	0.17	0.18	0.19	0.16	0.30
MgO	7.49	7.10	10.45	7.02	8.18	6.75
CaO	11.52	9.35	11.89	11.81	11.34	9.68
Na_2O	2.82	3.87	1.81	2.81	2.77	3.05
K_2O	0.18	0.11	0.19	0.20	0.16	1.35
P_2O_5	.08	.20	n.d	.15	.14	0.45

* Average of four analyses of oceanic tholeiite from the Mid-Indian Ocean Ridge (Table 1: D113, A1, D113 D1, D114 A, and D115 B). † Average of four analyses of tholeiitic basalt from the Carlsberg Ridge, Indian Ocean (*9*). ‡ Tholeiitic basalt from an abyssal hill, Indian Ocean: 26°18'S, 89°56.5'E; depth, 4900 m (*16*); n.d., not determined. § Average of six analyses of oceanic tholeiite from the East Pacific Rise (*11–12*). ‖ Average of seven analyses of oceanic tholeiite from the Mid-Atlantic Ridge. Detailed analyses are given variously by Engel and Engel (*11*), Nicholls *et al.* (*13*), and Correns (*20*). ¶ Average of 42 published analyses of "alkali" basalt from islands of the Indian Ocean

basalts with calcic plagioclase as the only or predominant phenocryst (*11–14*). The aluminous and calcium-rich tholeiites are either products of partial melting, related to depth of derivation of the primary melt (*17*), or the extrusions of oceanic tholeiites from the upper portions of partially crystallized magma in large chambers in the mantle.

The average of the four basalts from the Carlsberg Ridge, Indian Ocean, that Wiseman analyzed (Table 3, column 2) indicates the low K_2O, high ratios of Na to K, and high silica characteristic of oceanic tholeiites from other localities (Table 3, columns 4 and 5). The high concentrations of Na_2O and the low value for CaO in Wiseman's analyses appear, however, anomalous. For example, the average percentages of Na_2O (3.87) and CaO (9.35) calculated from the four Wiseman analyses seem inconsistent with the remarkably low K_2O (0.11). Very possibly these and other differences in the Wiseman average from the averages in other columns in Table 3 are due to differences in analytical methods.

Variations that are induced in composition of oceanic basalts by submarine alteration are illustrated by the compositions of the three oceanic tholeiites D115 L, D143 A, and D143 B taken from the median ridge (Table 1). The most obvious incipient effects of alteration indicated in these analyses are increases in amounts of water and in the ratio Fe_2O_3 to FeO, which may approach or even exceed 1. Total iron and magnesia frequently decrease slightly, and manganese increases, with increasing alteration, but there is no consistent change in amounts of alkalis or silica. Petrographically the alteration is evidenced by the appearance of palagonite, limonite, hematite, and calcite which replace olivine, pyroxene, magnetite, and small amounts of the constituent plagioclase.

Many samples of pillowed, tholeiitic basalts from the median ridge have glassy to microcrystalline margins which have resisted hydration, oxidation, and other types of weathering far more than have the coarser-grained interior parts of the pillows, many of which are moderately to strongly altered.

Analyses were undertaken to see if there are systematic or important differences in amounts of sodium and potassium in the margins of these pillow lavas, compared with their least altered interior parts. These are illustrated by the pairs D113 A1 and D113 A2 and D113 D1 and D113 D2 (Tables 1 and 2). Samples D113 A1 and D113 D1 (Table 1) are of

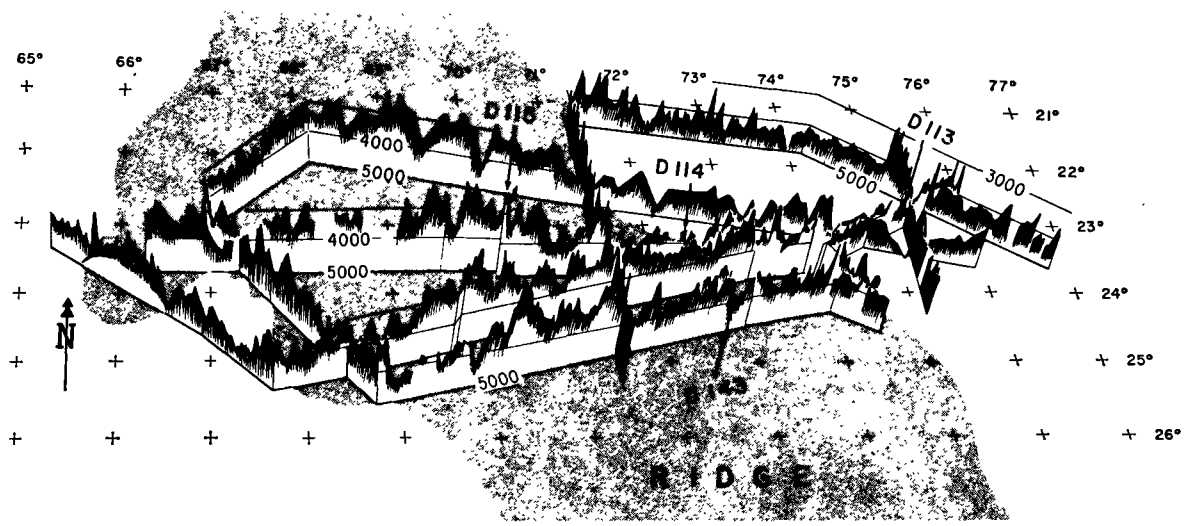

Fig. 2. Intersecting profiles of the Mid-Indian Ocean Ridge in the area of the four dredge localities shown in Fig. 1. The vertical exaggeration is ×50, and the three horizontal lines are respectively the 3000-, 4000-, and 5000-meter isobaths.

Table 4. Composition of vesicular basalt D232 dredged from near the base of a submarine volcano in the eastern Indian Ocean. Sample is porphyritic with phenocrysts of labradorite in a matrix of fine-grained pyroxene, plagioclase, and rare opaque oxide. Vesicles are spherical to slightly flattened and comprise about 20 percent of the rock. A partial analysis of another fragment from the same dredge haul yields: TiO_2, 1.47; Na_2O, 2.93; K_2O, 0.81; P_2O_5, 0.22.

Oxide	Amount present (%)
SiO_2	48.37
TiO_2	1.63
Al_2O_3	16.18
Fe_2O_3	6.07
FeO	2.98
MnO	0.18
MgO	6.20
CaO	10.08
Na_2O	3.04
K_2O	0.85
H_2O^+	1.76
H_2O^-	2.24
P_2O_5	0.30
Total	99.88

the external glassy margins of pillows, and samples D113 A2 and D113 D2 (Table 2) are of crystalline cores some 25 to 30 cm inside the pillows. The glassy margins of the basalt pillows show very slight to negligible enrichment in Na and K and a complementary slight decrease in SiO_2. Other differences are not consistent, and it is clear that the surficial reactions of the basalt flow with sea water do not produce large differences in the composition of the constituent basalt.

The basalt D232 dredged southwest of Sumatra is illustrative of compositional variations in tholeiitic basalts found on the lower flanks of deep submarine volcanoes. These basalts may be designated as oceanic tholeiites with slight alkali affinities. Specifically, silica is slightly lower than it is in the average oceanic tholeiite; potassium and the ratio Fe_2O_3 to FeO are much higher; and titanium, phosphorus, and total alkalis are slightly higher. We have found three somewhat similar basalts on the lower flanks of large submarine volcanoes in the Pacific whose apical parts are largely alkali-rich basalt. Muir and Tilley (*14*) also describe tholeiites with "alkaline affinities" from "lava flows from large volcanoes situated on opposite sides of a valley" in the Mid-Atlantic Ridge, and Engel and Chase (*18*) have studied a typical example from the Cocos Ridge, Pacific Ocean.

We have noted the correlation between composition of basalt and the form, height, and possibly rate of construction of volcanic edifices in the oceans (*7*). Typical alkali basalts and the alkali series appear to be confined largely or entirely to the apical parts of the higher volcanoes. These field relations, coupled with a large amount of supporting chemical data, suggest that the alkali series is derived from a parental oceanic tholeiitic magma within, and not far below, the higher volcanoes. Gravity appears to be the prime factor in differentiation, causing crystal segregation according to relative densities and also the upward transfer of alkalis in aqueous solution. By this hypothesis there should necessarily be melts intermediate between primary tholeiitic magma and derivative alkali basalts, or accidental mixes of the two that may breach lower flanks of the volcanoes and occur there as mantling flows. We suggest that the basalt D232 (Table 4) from the eastern Indian Ocean and the basalts described by Muir and Tilley (*14*) and by Engel and Chase (*18*) from, respectively, the Atlantic and the Pacific oceans are of this type.

Basalt D232, which was dredged from exposures 4000 m deep on the flank of a large volcano, contains about 20 percent vesicles, many almost spherical, with diameters up to 1 mm. Moore has emphasized that in the Hawaiian region there is a fairly systematic decrease in size and abundance of vesicles of basalts with depth of water (*19*). We have also found this to be true for most other regions dredged in the Atlantic and Pacific oceans. Usually basalts extruded at depths of 4000 m or more are devoid of vesicles and have a density of about 3 to 3.1. The low density and abundance of large, round vesicles in the basalt from the eastern Indian Ocean suggest that this region may have sunk at least a kilometer, possibly several kilometers, since the basalt was extruded. While some change in depth would be due to addition of water to the ocean, the position of the seamount may be significant. It lies on the northern edge of the deep Wharton Basin and rises from a discontinuous low swell or rise seaward of the Indonesian Trench. It is very possible that trench-forming processes have caused the entire bordering sea floor to be depressed.

Most submarine basalts dated by radiometric methods show increasing amounts of alteration with age. The extent of the alteration of the basalt D232 of the Indian Ocean suggests the age of extrusion, and hence the date of deep submersion, is not in excess of 30 million years.

CELESTE G. ENGEL
U.S. Geological Survey, La Jolla
ROBERT L. FISHER
Scripps Institution of Oceanography
A. E. J. ENGEL
Department of Earth Sciences, University of California, La Jolla 92038

References and Notes

1. J. Schmidt, *Danas Togh Omkring* (Jorden, Køpenhaven, 1932), p. 255; W. I. Farquharson, *Sci. Repts. John Murray Expedition, Brit. Mus. (Nat. Hist.)* **1** (No. 2), 52 (1936); F. A. Vening Meinesz, *Pub. Neth. Geod. Comm.* **4**, (1948).
2. B. Heezen and M. Tharp, Physiographic Diagram of the Indian Ocean (Geological Society of America, New York, 1965); Bathymetric Map of the Indian Ocean (Bureau Geodesy and Cartography, Geological Commission, U.S.S.R., Moscow, 1963).
3. C. Darwin, *Geological Observations on the Volcanic Islands* (London, 1845); F. Hochstetter, *"Novara"-Reise, Geol. Theil*, vol. 2, No. 1 (1866); S. J. Shand, *Quart. J. Geol. Soc. London* **89**, 1013 (1933); A. Lacroix, *Le Volcan Actif de l'Ile Réunion et ses Produits* (Gauthier and Villars, Paris, 1936). I. B. Balfour and N. S. Maskelyne, *Phil. Trans. Roy. Soc.* **168**, 289 (1879); H. J. Snell and W. H. T. Tams, *Proc. Cambridge Phil. Soc. London* **19**, 6, 283 (1920); A. E. Eaton, *Phil. Trans. Roy. Soc. London* **168**, 1 (1879); A. B. Edwards, *Brit. Australian New Zealand Antarctic Res. Exped. Rept. Ser. A* **2**, pt. 5, 76–86 (1938); G. W. Tyrrell, *Brit. Australian New Zealand Antarctic Res. Exped. Reports* Ser. A **2**, pts. 3 and 4, 29–68 (1937).
4. See references in F. Chayes, *J. Geophys. Res.* **68**, 1519 (1963).
5. F. Walker and L. O. Nicolaysen, *Colonial Geol. Mineral Resources, Gt. Brit.* **4**, 3 (1954); A. Lacroix, *Mineralogie de Madagascar* (Challamel, Paris, 1923), vol. 3, pp. 227–237.
6. G. A. Macdonald and T. Katsura, *J. Petrol.* **5**, 82 (1964); I. S. E. Carmichael, *ibid.*, p. 435; G. P. L. Walker, *Quart. J. Geol. Soc. London* **114**, 367 (1959).
7. A. E. J. Engel, C. G. Engel, R. H. Havens, *Bull. Geol. Soc. Amer.* **76**, 719 (1965); M. Tatsumoto, C. E. Hedge, A. E. J. Engel, *Science*, in press.
8. H. S. Washington, *Ann. Rept. Smithsonian Inst.* **1920**, 307 (1920).
9. J. D. H. Wiseman, "The John Murray Expedition 1933–34," *Publ. Brit. Mus. (Nat. Hist.) Geol. Mineral. Invest.* **3**, 1 (1940).
10. H. T. Stearns and G. A. Macdonald, *Bull. Hawaiian Div. Hydrog.* No. 9, 24 (1946); G. A. Macdonald, *Bull. Geol. Soc. Amer.* **60**, 1541 (1949); H. A. Powers, *Geochim. Cosmochim. Acta* **7**, 77 (1955); G. A. Macdonald and T. Katsura, *J. Petrol.* **5**, (1964).
11. A. E. J. Engel and C. G. Engel, *Science* **144**, 1330 (1964); **146**, 477 (1964).
12. ——— and R. H. Havens, *Bull. Geol. Soc. Amer.* **76**, 719 (1965).
13. G. D. Nicholls, A. J. Nalwalk, E. E. Hays, *Marine Geol.* **1**, 33 (1964).
14. I. D. Muir and C. E. Tilley, *J. Petrol.* **5**, 409 (1964).
15. R. P. Von Herzen and V. Vacquier, in preparation.
16. D. S. Korzhinsky, *Izv. Akad. Nauk SSSR, Ser. Geol.* **12**, No. 9 (1962).
17. Carnegie Inst. Wash. Publ., *Geophys. Lab. Ann. Rept. Director 1963–1964*, pp. 107–120, 147–176.

18. C. G. Engel and T. E. Chase, *U.S. Geol. Survey Profess. Paper* **525-C**, C161 (1965).
19. J. G. Moore, *Amer. J. Sci.* **263**, 40 (1965).
20. C. W. Correns, *Chem. Erde* **5**, 80 (1930).
21. D. H. Matthews, *Nature* **198**, 950 (1963).
22. Laboratory work on this project was supported by the NSF (Gp-2364), the U.S. Geological Survey, and the University of California. Shipboard work was supported by the NSF (G-22255) and by contracts with the Office of Naval Research. William Riedel and Victor Vacquier provided the rock samples; Bonnie Swope and David Crouch prepared the illustrations. Contribution from the Scripps Institution of Oceanography, University of California, San Diego.

20 August 1965

Reprinted from Okeanologia, vol. VI, no. 2, 1966, p. 261-266.

УДК 552.2/333.5(267)

П. Л. БЕЗРУКОВ, А. Я. КРЫЛОВ, В. И. ЧЕРНЫШЕВА

ПЕТРОГРАФИЯ И АБСОЛЮТНЫЙ ВОЗРАСТ БАЗАЛЬТОВ СО ДНА ИНДИЙСКОГО ОКЕАНА

Институт океанологии АН СССР
Радиевый институт

Вопросы состава и времени излияния вулканических пород на дне океанов привлекают к себе все бóльшее внимание. Интерес к этим вопросам вполне закономерен, так как от их освещения во многом зависит дальнейшее развитие представлений о сходстве и различиях в условиях выплавления магмы на материках и в океанах, о связи вулканических пород со структурами дна, о масштабах вулканической деятельности в разные периоды истории Земли.

В настоящее время проблема подводного вулканизма в океанах вступает в новую фазу изучения. Во-первых, в результате работ целого ряда океанографических экспедиций установлено, что вулканические породы обнажаются из-под покрова донных осадков на гораздо более многочисленных и обширных участках дна, чем это представлялось ранее. При этом, с развитием технических средств получение образцов пород с любых глубин океана уже не представляет непреодолимых трудностей. Во-вторых, как показали недавние работы супругов Энгель [9, 10, 11], на дне океанов, по-видимому преобладают не щелочные базальты, характерные для многих океанических островов, *а низкокалиевые толеитовые* базальты. Можно ожидать, что в самом ближайшем будущем наши знания о вулканических породах дна океанов резко расширятся. Пока же данные о их петрографическом и химическом составе и тем более об их возрасте весьма ограничены, и поэтому любые новые материалы по этим вопросам заслуживают внимания.

При работах исследовательского судна «Витязь» Института океанологии АН СССР в 1959—1962 гг. (31, 33 и 35-й рейсы) в центральных частях Индийского океана, в результате изучения подводного рельефа и многочисленных сборов донных проб, было установлено широкое распространение на дне выходов коренных изверженных пород [1, 2, 3]. Особенно обильны они на поверхности и склонах крупных подводных хребтов; кроме того, они часто встречаются на дне глубоких котловин, обладающих расчлененным холмистым рельефом и низкими темпами седиментации. На абиссальных аккумулятивных равнинах, расположенных главным образом в окраинных частях океанов, они отсутствуют.

Сбор проб коренных пород в экспедиции на «Витязе» осуществлялся тралами, дночерпателями, а иногда грунтовыми трубками. На рисунке показано расположение станций, на которых были получены образцы изверженных пород. Здесь же показано место станции (№ 133) в районе Аравийско-Индийского хребта (на иностранных картах хребта Карлсберг), где ранее англо-египетской экспедицией на судне «Мабахис» были добыты с глубины 3385 *м* обломки базальта, исследованные Уайзманом [13].

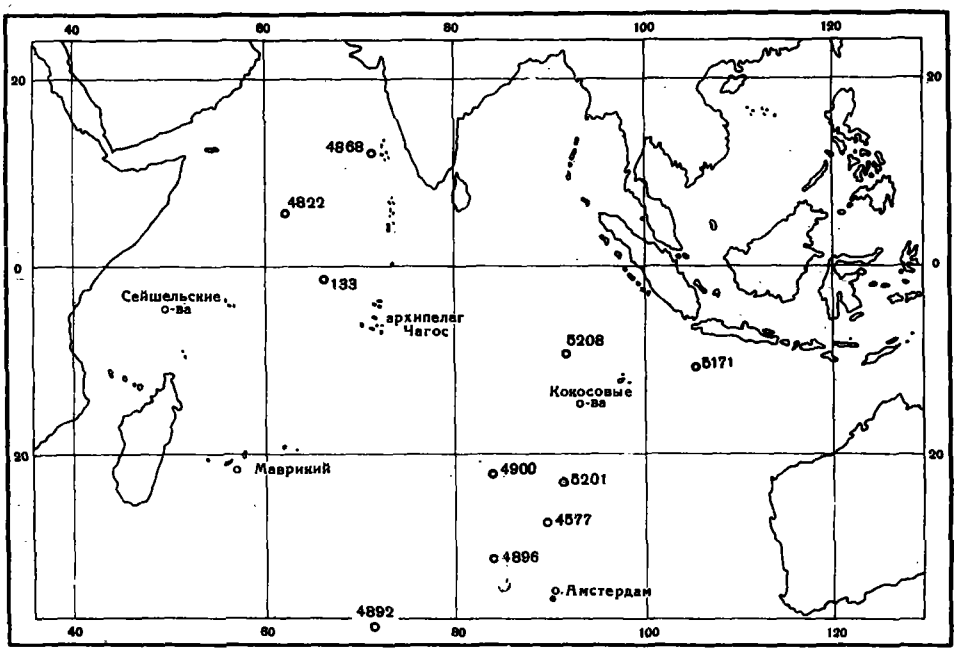

Схема расположения станций, на которых были собраны обломки базальтов

Петрографическое изучение пород проводилось в Институте океанологии, а химические анализы, благодаря любезному содействию Д. С. Коржинского,— в химической лаборатории ИГЕМ АН СССР (аналитики О. А. Алексеева и Е. Н. Шипилина). Три обломка пород было исследовано Д. С. Коржинским; изучение их позволило ему доказать несостоятельность гипотезы трансвапоризации базальтовой магмы на дне океана [4]. Абсолютный возраст пород был определен в Радиевом институте.

Как показало изучение образцов пород, в большинстве случаев они представлены оливиновыми и безоливиновыми базальтами и базальтовыми стеклами (гиалобазальтами). В одном месте, на гребне Аравийско-Индийского хребта (ст. 4822), кроме того, были встречены обломки серпентинитов, описанные в другой статье [8]. Позднее, в 36-м рейсе «Витязя» выходы ультраосновных пород были найдены в Индийском океане в рифтовых зонах срединных хребтов и в нескольких других местах [7].

Перейдем к петрографической характеристике базальтов.

На ст. 4577 (26°19′ ю. ш., 90° 00 в. д., глубина 4808 *м*) при тралении на неровном дне у восточного подножья Восточно-Индийского хребта были извлечены обломки и глыбы базальтов, а также железо-марганцевые конкреции.

Наиболее крупная глыба черного гиалобазальта неправильно округлой формы, до 50 *см* в диаметре, имела стекловатую корку, с поверхности палагонитизированную и имеющую буроватую окраску; глубже вулканическое стекло почти не носит следов вторичных изменений. Показатель преломления его 1,585. Стекло слабо анизотропно из-за наличия мельчайших зерен плагиоклаза, по составу отвечающего лабрадор-битовниту № 70. Встречаются изометрические кристаллы оливина размером до 0,3—0,4 *мм*, а также круглые поры; некоторые из них выполнены халцедоном [4]. Результаты определения абсолютного возраста породы (образец 3) даны ниже в табл. 2.

Другой обломок представляет собой пузырчатый базальт, с поверхности с железо-марганцевой коркой (образец 4). Под микроскопом

Таблица 1

Химический состав базальтов со дна Индийского океана

	№ станций						
	4577 (образец 4)	4822	4892	4896 (образец 1)	133—8 *	133—5 *	133—12 *
SiO_2	31,64	49,40	50,36	48,36	52,24	47,58	49,43
TiO_2	0,33	1,51	1,52	2,58	1,83	2,10	1,94
Al_2O_3	11,53	16,80	16,38	12,97	15,02	15,05	15,04
Fe_2O_3	10,50	2,85	3,54	2,04	2,93	6,74	2,21
FeO	—	6,95	5,32	9,34	6,31	4,42	7,39
MnO	—	0,25	0,24	0,22	0,14	0,14	0,23
MnO_2	17,58	—	—	—	—	—	—
MgO	1,35	7,19	7,09	10,30	6,01	5,71	8,40
CaO	2,34	11,35	12,21	8,78	8,73	10,97	6,69
Na_2O	3,71	2,63	2,55	3,09	4,02	3,19	4,45
K_2O	3,00	0,20	0,40	1,32	0,21	0,04	0,11
H_2O+	6,32	0,60	0,54	0,97	2,25	0,99	3,16
H_2O-	10,26	0,54	0,35	0,16	0,50	2,46	0,86
P_2O_5	—	—	—	—	0,20	0,23	0,19
NiO	0,33	—	—	—	—	—	—
Сумма	98,84	99,97	100,50	100,13	100,39	99,62	100,10

* Станция «Мабахис» [13].

порода имеет пилотакситовую структуру, состоит из ксеноморфных выделений пироксена (авгита), зерен рудных минералов, а также единичных вкрапленников оливина и плагиоклаза в основной стекловатой массе. Пироксен образует вытянутые призматические кристаллы величиной до 0,05 *мм*. В проходящем свете минерал буроватый. Оптические свойства: Ng—Np=0,035; C : Ng=46°, 2V=60°. Лейсты плагиоклаза очень тонкие, расположены беспорядочно и имеют размеры 0,01—0,02 *мм*. Состав плагиоклаза отвечает лабрадор-битовниту. Оливин почти нацело замещен иддингситом зеленовато-бурого цвета с высокой интерференционной окраской и резким плеохроизмом. Встречено только единичное зерно неизмененного оливина. Порода содержит большое количество пор. Проанализирован образец с частью железо-марганцевой корки (см. ниже табл. 1); поэтому результаты анализа не показательны для самой породы.

Третий обломок (образец 5) представляет базальт с порфировой структурой. Основная масса состоит из красно-бурого изотропного вулканического стекла и имеет гиалопилитовую структуру. В ней в виде вкрапленников присутствуют гломеропорфировые выделения и широкотаблитчатые кристаллы плагиоклаза (лабрадор-битовнит № 70), а также единичные зерна моноклинного пироксена. Размеры кристаллов плагиоклаза и моноклинного пироксена — до 0,3 *мм*. Порода также содержит значительное количество пор.

На ст. 4822 (5° 24′ 8 с. ш., 62° 08′ 5 в. д., глубина 1920 *м*) дночерпателем были подняты с гребня Аравийско-Индийского хребта помимо обломков серпентинитов четыре обломка базальта [8]. Под микроскопом порода имеет порфировую структуру и состоит из основной интерсертальной стекловатой массы, в которой содержатся фенокристаллы плагиоклаза (лабрадор № 65), размером до 2—3 *мм*, моноклинного пироксена, единичные зерна оливина и рудного минерала. Оливин почти полностью замещен зеленовато-желтым хлоритоподобным минералом. Абсолютный возраст породы из-за малых размеров обломков определить не удалось.

На ст. 4868 (11° 18′ 2 с. ш., 71° 00′ 1 в. д., глубина 2663 *м*) при тралении близ западного подножья Лаккадивского хребта было поднято несколько обломков базальта, снаружи сильно ожелезненного. Под микроскопом порода имеет порфировую структуру и состоит из фенокристаллов

плагиоклаза, моноклинного пироксена (авгита) и рудного минерала, погруженных в интерсертальную основную массу. Наблюдаются единичные зерна оливина. Плагиоклаз во вкрапленниках представлен широкотаблитчатыми кристаллами размером 1,5—2 *мм*. Состав плагиоклаза отвечает лабрадор-битовниту № 70. Кристаллы авгита имеют размеры до 1 *мм*. Минерал в проходящем свете буроватый. Зерна оливина в проходящем свете — бесцветные, имеют размеры до 1,5 *мм*. Местами оливин замещен хлоритоподобным минералом.

Другие обломки с той же станции представлены пузырчатым гиалобазальтом с порфировой структурой. Основная масса по структуре переходная между кристаллитовой и гиалопилитовой — в вулканическом темно-буром стекле рассеяны беспорядочно ориентированные мельчайшие кристаллы. Во вкрапленниках — лейсты основного плагиоклаза и, реже, моноклинного пироксена. Поры составляют около 30% в поле шлифа.

На ст. 4892 (36° 02′ 0 ю. ш., 71° 17′ 0 в. д., глубина 4740 *м*) дночерпатель принес с холмистого дна котловины Крозе валун оливинового базальта, размером 25×21×18 *см*. С поверхности порода покрыта корочкой окислов Fe и Mn мощностью 1—2 *см*. Структура породы порфировая. Основная масса имеет интерсертальную структуру и состоит из прозрачного коричневато-желтого вулканического стекла с показателем преломления 1,585. Во вкрапленниках — лейсты плагиоклаза (битовнит No 80—84%) длиной до 2—10 *мм* и очень мелкие зерна моноклинного пироксена с показателем преломления Ng = 1,714 и Np = 1,698; 2V = +55°5. В небольшом количестве присутствуют более крупные зерна оливина с 2V = =90°. В отдельных зернах удалось замерить его показатели преломления: Ng = 1,706, Np = 1,677. Оливин частично замещен зеленовато-желтым хлоритоподобным минералом. Встречаются изометрические зерна рудных минералов с размерами 0,1—0,2 *мм*.

На ст. 4896 (29° 56′ 8 ю. ш., 83° 00′ 6 в. д., глубина 3805 *м*) дночерпателем были подняты с холмистого дна Центральной котловины близ западного подножья Восточно-Индийского хребта угловатые обломки сильно пузырчатого гиалобазальта, погруженные в полужидкий ил (по-видимому, результат подводного оползня на склоне). Размеры обломков достигают 10 *см*. Под микроскопом основная масса представлена бурым изотропным вулканическим стеклом, в котором содержатся лейсты плагиоклаза длиной до 0,5 *мм*, соответствующего лабрадор-битовниту. Оливин присутствует в виде вкрапленников с размерами до 0,5 *мм* и выделений с расплывчатыми очертаниями. Встречаются участки двупреломляющего желтовато-коричневого вещества, по оптическим константам близкого к пироксену. Размеры пород достигают 0,5—3 *мм*.

Породы с других станций описываются кратко, так как изучены только петрографически.

На ст. 4900 (21° 28′ 2 ю. ш., 83° 11′ 5 в. д., глубина 4486 *м*) прямоточная грунтовая трубка принесла обломки оливинового базальта, сходного со встреченным на ст. 4892. Проба была взята со склона холма на дне Центральной котловины.

На ст. 5171 (10° 54′ 2 ю. ш., 105° 22′ в. д., глубина 4694 *м*) прямоточной трубкой была взята колонка фораминиферовых илов, длиной около 3 *м*. Почти на всем протяжении колонки в этих илах содержатся угловатые обломки выветрелого пузырчатого базальта, размером до 4 *см*. Место взятия колонки находится близ подножья подводной горы, это позволяет предполагать, что обломки базальта попали в осадки в результате оползня. Наиболее свежий обломок был просмотрен под микроскопом. Порода имеет порфировую структуру. Во вкрапленниках преобладают кристаллы плагиоклаза (лабрадор-битовнит № 70) величиной до 1,5 *мм*; кроме того, присутствуют зерна моноклинного пироксена и рудных минералов. Основная масса породы — гиалопилитовая. Наблюдается большое количество пор размером от 0,01 до 1 *мм*.

На ст. 5201 (22° 21′ 8 ю. ш., 91° 38′ 0 в. д., глубина 5280 *м*) трал принес с неровного дна Западно-Австралийской котловины большое количество обломков сильно выветрелого гиалобазальта и железо-марганцевых конкреций. Размеры обломков гиалобазальта до 20 *см*. Петрографический состав пород близок к составу обломков со ст. 5171.

На ст. 5208 (9° 17′ 2 ю. ш., 91° 22′ 2 в. д., глубина 5165 *м*) прямоточной трубкой было извлечено со дна Кокосовой котловины несколько мелких обломков пузырчатого базальта.

Результаты химических анализов четырех образцов базальтов из сборов «Витязя» даны в табл. 1. Для сравнения здесь же приведены анализы трех образцов базальтов, исследованных Уайзманом [13].

Как видно из таблицы, два проанализированных образца (полученные как с подводного хребта — ст. 4822, так и со дна котловины — ст. 4892) обладают близким химическим составом и, в частности, низким содержанием калия, что характерно для толеитовых базальтов. Сходный химический состав имеют и образцы со ст. 133 «Мабахиса». Наряду с этим, в образце 4 со ст. 4577 и в образце 1 со ст. 4896 содержание калия оказалось высоким. Образец 4 со ст. 4577 отличается также низким содержанием SiO_2, CaO и MgO и повышенным Fe_2O_3, MnO_2, H_2O^+ и H_2O^-, т. е. носит следы резких вторичных изменений. Что же касается образца со ст. 4896, то он, судя по результатам химического анализа (содержание TiO_2, K_2O, N_2O и др.), представляет щелочной базальт.

Таким образом, изложенные данные о составе вулканических пород со дна Индийского океана в общем находятся в соответствии с выводами Энгелей [9, 10] о присутствии на дне океана как толеитовых, так и щелочных базальтов.

Результаты определений абсолютного возраста базальтов калий-аргоновым методом приведены в табл. 2. Следует отметить, что расхождения в содержании калия в образцах со станций 4577 и 4896 в табл. 1 и 2 незначительны.

Как видно из табл. 2, возраст всех проанализированных образцов практически один и тот же. Разброс цифр находится в пределах возможных ошибок, тем более, что сохранность пород различная. Можно считать, что возраст всех базальтов около 60 млн. лет, что соответствует нижнему палеогену (эоцену). Поскольку образцы несколько выветрелы, возможно некоторое занижение возраста — порядка около 10 млн. лет, и тогда их возраст будет соответствовать границе Pg и Cr, т. е. около 70 млн. лет.

Таким образом возраст базальтов со дна Индийского океана оказался близким к возрасту деканских траппов (плато-базальтов) на Индостанском полуострове, излияния которых начались в самом конце верхнего мела, но наибольшую интенсивность имели в эоцене [5, 12]. Пункты,

Таблица 2

Абсолютный возраст базальтов со дна Индийского океана

№ станций	Широта	Долгота	Глубина, *м*	Порода	K, %	$Ar, \frac{см^3}{г} \cdot 10^{-6}$	Возраст, млн. лет
4896	29°56′8 ю. ш.	83°00′6 в. д.	3805	Пузырчатый гиалобазальт (образец 1)	0,99	2,12	55
4577	26°19′ ю. ш.	90°00′ в. д.	4808	Гиалобазальт (образец 3)	1,79	3,48	51
4577	26°19′ ю. ш.	90°00′ в. д.	4808	Пузырчатый измененный гиалобазальт (образец 4)	3,04	7,18	60
4577	26°19′ ю. ш.	90°00′ в. д.	4808	Базальт (образец 5)	0,52	1,28	63

в которых был определен абсолютный возраст базальтов на дне океана, находятся на значительном расстоянии друг от друга и на еще большем удалении от Индостана. Это говорит о том, что нижнетретичная вулканическая деятельность проявилась в бассейне Индийского океана на огромной площади. Для подтверждения этого вывода необходимы дальнейшие исследования абсолютного возраста изверженных пород со дна океана.

Наличие на дне Индийского океана нижнетретичных базальтов не исключает возможности распространения здесь как более молодых, так и более древних вулканических пород. На вероятное проявление в Индийском океане четвертичной подводной вулканической деятельности в литературе имеются указания [6].

ЛИТЕРАТУРА

1. Безруков П. Л. 1961. Исследования Индийского океана в 33 рейсе э/с «Витязь». Океанология, **I**, вып. 4.
2. Безруков П. Л. 1962. О неравномерности распределения глубоководных океанических осадков. Океанология, **II**, вып. 1.
3. Безруков П. Л. 1963. Исследования Индийского океана в 35 рейсе э/с «Витязь». Океанология, **III**, вып. 3.
4. Коржинский Д. С. 1962. Проблема спилитов и гипотеза трансвапоризации в свете новых океанологических и вулканологических данных. Изв. АН СССР, сер. геол., № 9.
5. Кришнан М. С. 1954. Геология Индии и Бирмы. Изд-во иностр. лит., М.
6. Лисицын А. П., Живаго А. В. 1958. Рельеф дна и осадки южной части Индийского океана. Изв. АН СССР, сер. геогр., № 3.
7. Удинцев Г. Б., Чернышева В. И. 1965. Образцы пород мантии из рифтовой зоны Индийского океана. Докл. АН СССР, **165**, 5.
8. Чернышева В. И., Безруков П. Л. 1966. Серпентиниты с гребня Аравийско-Индийского подводного хребта. Докл. АН СССР, **166**, № 4.
9. Engel A. E. J., Engel C. G. 1963. Basalts dredgad from the Northeastern Pacific ocean. Science, **140**, No 3573.
10. Engel A. E. J., Engel C. G., 1964. Composition of basalts from the Mid-Atlantic Ridge. Science, **14**, No 3624.
11. Engel A. E. J., Engel C. G. and Havens R. G. 1965. Chemical characteristic of oceanic basalts and the upper mantle. Bull. Geol. Soc. Amer., **76**, No 7.
12. Prakash U. 1960. A survey of the Deccan intertrappean flora of India. J. Paleontol., **34**, No 5.
13. Wiseman J. D. H. 1937. Basalts from the Carlsberg ridge, Indian ocean. British museum. The J. Murray expedition 1933—1934. Scient. Rep., **3**, No 1

Поступила в редакцию
12.I.1966

P. L. BEZRUKOV, A. Ya. KRYLOV, V. I. CHERNYSHEVA

PETROGRAPHY AND THE ASBOLUTE AGE OF THE INDIAN OCEAN FLOOR BASALTS

Summary

Volcanic rock from the Indian Ocean bottom was sampled during the R/V «Vityaz» 1959—62 cruise operations. The petrographic study of the samples has shown that in most cases the rocks are represented by olivine and nonolivine basalts and basalt glass (hyalobasalts). The chemical analysis has indicated that part of the samples belongs to low kalium tholeitic while another part to alkaline basalts. The K-argon method has been used to determine the absolute age of four rock samples from two stations in the southern part of the ocean. Their age has appeared to be about 60 million years corresponding to Lower Paleogene (Eocene).

Reprinted from Okeanologia, vol. VI, no. 2, 1966, p. 267-275.

УДК 551.352

З. Н. ГОРБУНОВА

РАСПРЕДЕЛЕНИЕ ГЛИНИСТЫХ МИНЕРАЛОВ В ОСАДКАХ ИНДИЙСКОГО ОКЕАНА

Институт океанологии АН СССР

До последнего времени глинистые минералы в осадках Индийского океана были очень мало изучены. В литературе можно найти только некоторые сведения о качественном их составе.

Кьюнен [14] исследовал рентгеновским методом осадки морей Малайского архипелага и прилегающей части Индийского океана, собранные в экспедиции на «Снеллиусе», и нашел во всех образцах мусковит (вероятно, иллит), каолинит и монтмориллонит.

Горбуновой [5] изучался состав глинистых минералов в 30 пробах осадков, собранных в рейсах «Оби» по разрезу, пересекающему Индийский океан от Антарктиды до Бенгальского залива. Состав глинистых минералов меняется в направлении с юга на север: в приантарктической области преобладают гидрослюды, севернее возрастает содержание каолинита.

Эл Вэкил и Рилей [11], изучив 12 образцов, сделали вывод о качественном сходстве состава глинистых минералов в Атлантическом, Тихом и Индийском океанах.

Бискай [7] изучил количественный и качественный состав глинистых минералов в 50 пробах осадков, взятых по меридиональному разрезу в западной части Индийского океана.

Материалом для исследования глинистых минералов в поверхностном слое осадков послужили пробы, собранные сотрудниками отдела морской геологии Института океанологии АН СССР во время 31, 33 и 35-го рейсов судна «Витязь» [1—3]. Всего было изучено 70 проб, преимущественно из северной и восточной частей океана (см. рис. 3).

Основными методами изучения глинистых минералов были рентгенографический и дифрактометрический. Съемка образцов производилась на отечественных аппаратах УРС-55а с железным анодом и дифрактометре УРС-50 ИМ с медным анодом.

Отдельные образцы перед съемкой на дифрактометре были обработаны по методу Мира и Джексона [15] для удаления гидратов окислов железа и алюминия, а также аморфного кремнезема. Это позволило получить на рентгенограммах и дифрактограммах четкие рефлексы.

В изученных осадках были найдены минералы монтмориллонитовой, иллитовой, каолинитовой, хлоритовой и палыгорскитовой групп.

Определение минералов монтмориллонитовой группы производилось по рефлексу 17 Å после насыщения образца глицерином.

Наиболее простым является определение минералов иллитовой (гидрослюдистой) группы. Иллит характеризуется серией базальных отражений: 10 Å (001), 5,0 Å (002), 3,3 Å (003) и т. д., которые не изменяются при насыщении образца глицерином и при нагревании до 400—550°.

Большие трудности возникают при определении минералов хлоритовой и каолинитовой групп. Хлориты характеризуются серией базальных отражений: 14 Å (001), 7 Å (002), 4,7 Å (003), 3,5 Å (004), причем отражения 14 Å и 4,7 Å железистых хлоритов очень слабы, а отражения 7 Å и 3,5 Å совпадают с каолинитовыми.

Бискай [7] предлагает отличать эти минералы по присутствию двойных отражений 7,08 Å/7,16 Å (хлорит, каолинит) и 3,54 Å/3,58 Å (хлорит, каолинит). К сожалению, эти двойные отражения в большинстве случаев плохо различаются, поэтому приходится пользоваться рекомендациями Броуна [9]. Для выявления хлорита перед рентгеносъемкой образцы нагревались до 550 и 400°, так как устойчивость хлоритов к термической обработке неодинакова. При таких обработках появлялся четкий рефлекс хлорита 14 Å, а рефлекс 7 Å обычно исчезает или ослабевает. Кроме того, образцы обрабатывались 10%-ной соляной кислотой, после чего отражение хлорита 7 Å сильно ослабевало, а каолинита сохранялось. Хотя эта методика не совершенна, так как свойства хлоритов (термическая устойчивость и растворение в кислоте) сильно варьируют, но другой пока не существует.

В настоящей работе интенсивность базальных отражений глинистых минералов или площади дифракционных эффектов представлены в виде весовых процентов, как это сделано у Биская [7]. Следует подчеркнуть, что точность этого метода не велика и в литературе имеются и другие рекомендации [24].

Необходимо также учитывать, что по рентгенограммам можно определить только интенсивность рефлексов, а не площади. Это существенно сказывается при определении содержания монтмориллонита. При сравнении с дифрактометрическими данными содержание монтмориллонита снижается примерно в 1,5 раза.

Сравнение наших данных и материалов Биская [7] по району Мадагаскара, показало, что данные весового содержания монтмориллонита, приводимые Бискаем, сильно завышены. По-видимому, это связано с тем, что площадь эффекта 17 Å трудно измерить точно из-за плохой записи в области малых углов.

Учитывая недостатки принятого метода определения весового содержания минералов, следует рассматривать наши данные как полуколичественные.

В водосборном бассейне Индийского океана выделяется несколько климатических поясов, каждый из которых характеризуется определенными типами почв и преобладающими в них глинистыми минералами.

В средней части Африканского побережья по западному и восточному побережьям Индостана, в Бирме, на Малаккеком п-ве, в юго-восточной Азии, на о-вах Малайского архипелага и в северной части Австралии развиты различные почвы гумидного тропического и субтропического пояса. К северу и к югу от этой зоны на Африканском материке, в северной части Индии, на значительной площади Австралии почвы влажного пояса постепенно сменяются почвами полупустынь и пустынь.

Данные о составе глинистых минералов в почвах Малайского архипелага, Мадагаскара и западного побережья Индии приводятся в монографии Мора и Барена [20]. На основании изучения большого фактического материала эти авторы пришли к заключению, что состав глинистых минералов в пределах гумидного тропического пояса определяется в основном условиями дренажа. На одних и тех же вулканических горах они находили разные минералы. В верхней части гор, где вымывание было наибольшим, образуются каолиниты, гибситы, гидроокислы железа, в нижней части — монтмориллониты. На Суматре почвы настолько сильно промываются, что кристаллические глинистые минералы здесь не образуются вообще.

Довольно подробно изучены глинистые минералы в почвах южной Африки [16—18]. Здесь были выделены три основные группы почв: почвы пустынных и полупустынных районов, латеритовые и связанные с ними почвы, субтропические черные и связанные с ними почвы. Каждая из этих групп характеризуется определенным комплексом глинистых минералов. В первых преобладает иллит, иногда с небольшой примесью монтмориллонита или смешаннослоистого иллит-монтмориллонита. В латеритах при сочетании большого количества осадков и хорошего дренажа накапливаются коллоиды, состоящие из каолинита, гиббсита и окислов железа. В условиях плохого дренажа в местах распространения интразональных черных почв (третья группа) преобладают монтмориллониты.

На значительной территории центральной и южной Индии распространены две разновидности почв (черные и красные), которые характеризуются определенным составом глинистых минералов. В тонкой фракции черных почв преобладают минералы монтмориллонитовой группы, а в красных — каолинитовой [21—23]. Изучены также некоторые почвы в западной Бенгалии и в бассейне р. Ганг, которые содержат монтмориллонит, иллит, каолинит в разных количественных соотношениях [10, 6].

Крупнейшие реки Индии — Ганг и Брамапутра несут в составе взвеси иллит, хлорит, небольшое количество монтмориллонита и каолинита. Реки Годавари и Висакапатнам также выносят в основном иллит и немного каолинита [22].

В почвах северо-западных районов Индии (Пенджаб) преобладают иллиты и хлориты [12, 13, 19]. В этом же районе найдены древние отложения монтмориллонитов [8].

В северной части Африки, на Аравийском п-ве и в западной Австралии глинистые минералы в почвах мало изучены. В этих районах преобладают почвы пустынные и полупустынные, выветривание которых идет чрезвычайно медленно. Из глинистых минералов в таких почвах преобладают обычно гидрослюды.

Максимальное количество глинистых минералов выносится, очевидно, крупнейшими реками Индии — Индом и Гангом, которые в своем верхнем течении в основном дренируют почвы, содержащие иллит и хлорит.

В северной части Африки, с Аравийского п-ва и западного побережья Австралии тонкодисперсный материал поступает в океан главным образом в результате ветровой денудации.

Тропические гумидные районы Африки, Индии, о-вов Малайского архипелага и северной части Австралии дренируются более мелкими реками. Здесь коры выветривания содержат каолинит и монтмориллониты. В северной Австралии глинистые минералы представлены в основном плохо окристаллизованными каолинитами [25].

Обратимся к экспериментальным данным о составе и количественном содержании глинистых минералов в поверхностном слое осадков Индийского океана.

Иллиты широко распространены в пределах изученного района (рис. 1). Максимальное их содержание наблюдается в осадках Аравийского моря. Дифрактометрические эффекты этих минералов чрезвычайно четко выражены (рис. 2, ст. 4808). Для них характерно также очень высокое содержание K_2O (до 5—6%), которое не отмечалось нигде в Тихом океане [4]. Небольшой максимум выделяется также у северной половины Суматры. Высокое содержание иллитов (до 40—60%) сохраняется в осадках примерно до зоны Южного пассатного течения, а к югу постепенно уменьшается. Полоса минимального содержания иллитов доходит до 30° ю. ш., а южнее количество иллитов снова возрастает. Увеличение содержания этих минералов отмечено также у северо-западного побережья Австралии.

Хлориты в северной половине Индийского океана в большом количестве встречены только в осадках Аравийского моря (рис. 3). Район максимального содержания хлоритов почти совпадает с районом максимального содержания иллита.

Небольшое содержание хлоритов отмечено в осадках Бенгальского залива. В остальных районах океана вплоть до 30° ю. ш. хлориты в сколько-либо заметных количествах не обнаружены. Хлориты в осадках Индийского океана термически мало устоичивы; при температуре 550° они уже разлагаются. Этим свойством они существенно отличаются от

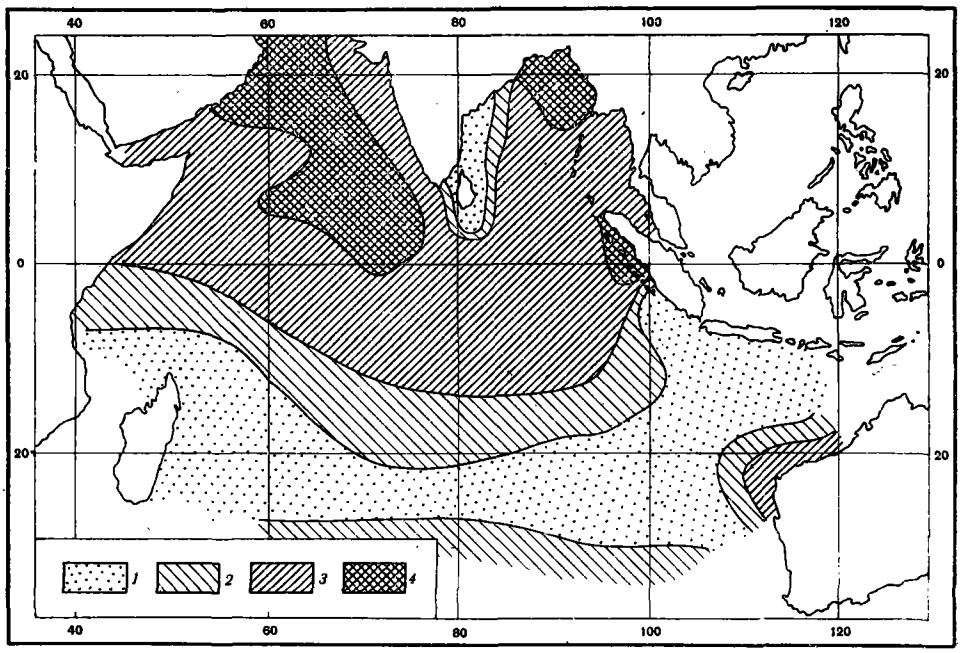

Рис. 1. Содержание иллитов во фракции <0,001 *мм* (в процентах от общего количества глинистых минералов):
1 — <20; *2* — 20—40; *3* — 40—60; *4* — 60—80

термически более устойчивых хлоритов осадков высоких широт. Хлориты засушливых районов относятся, очевидно, к типу железистых, что видно на дифрактограммах (отражения нечетных порядков слабее четных, см. рис. 2, ст. 4808).

Каолиниты дают два максимума распределения в осадках: близ Мадагаскара и в полосе, протягивающейся от Явы на юго-запад (рис. 4). Высокое содержание каолинитов отмечено в осадках южнее Южного пассатного течения. Этот район совпадает с районом невысокого содержания иллитов. Минимально содержание каолинитов в осадках Аравийского моря и западной части Бенгальского залива, где выделяется область высокого содержания хлоритов.

Каолиниты в исследованной части Индийского океана плохо окристаллизованы и дают слабые эффекты на дифрактограммах, несмотря на то, что аморфные вещества были из них удалены.

Монтмориллониты широко распространены в пределах изученной части Индийского океана (рис. 5). Высокое их содержание (20—40%) отмечено в осадках, взятых южнее Южного пассатного течения. Севернее содержание монтмориллонитов постепенно падает и в западной части Аравийского моря является минимальным.

В пределах Красного моря и у восточного побережья Индии намечаются два максимума с содержанием монтмориллонитов от 60 до 90%.

Определение происхождения этих минералов показало, что они образовались при разложении вулканогенного материала.

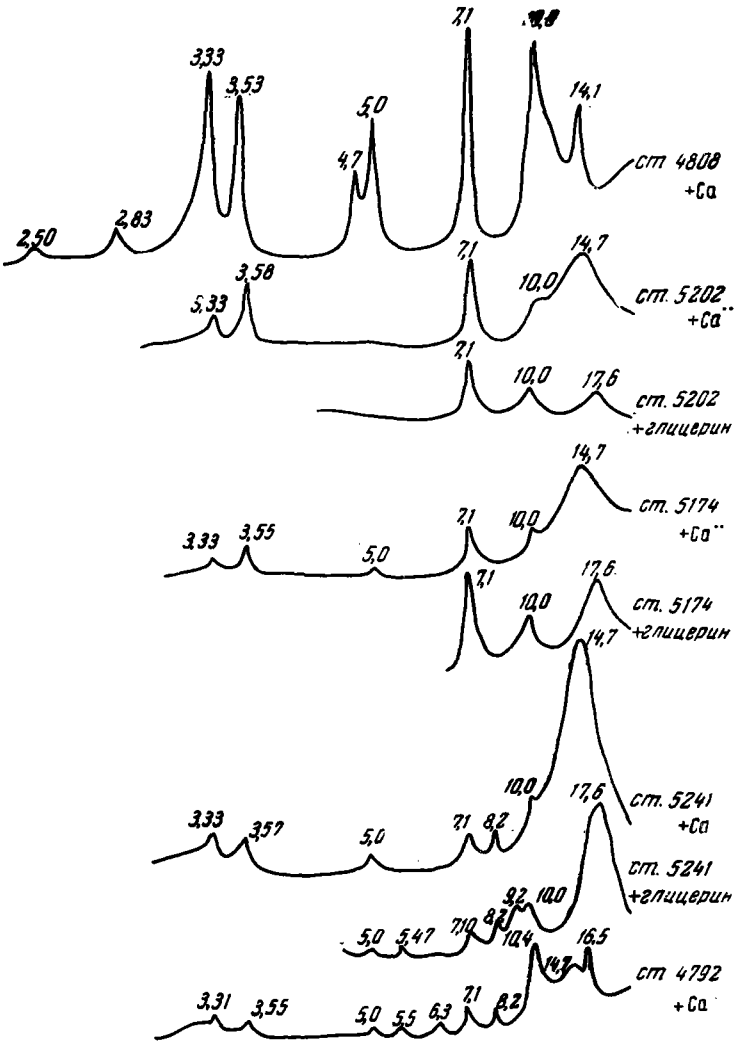

Рис. 2. Дифрактограммы фракций < 0,001 *мм*, выделенных из осадков Индийского океана

Минералы палыгорскитовой группы впервые обнаружены в современных океанских осадках в больших количествах. Эти глинистые минералы имеют цепочечную структуру и относятся к магниевым алюмосиликатам. Их дифрактометрическая картина весьма своеобразна (см. рис. 2, ст. 4792). К сожалению, наиболее интенсивное отражение палыгорскитов около 10,4 Å совпадает с отражением иллитов, поэтому определение их количественного содержания затруднено. Палыгорскиты образуют своеобразные кристаллы в виде тонких палочек, которые хорошо выделяются на электронномикроскопических снимках. Максимальное

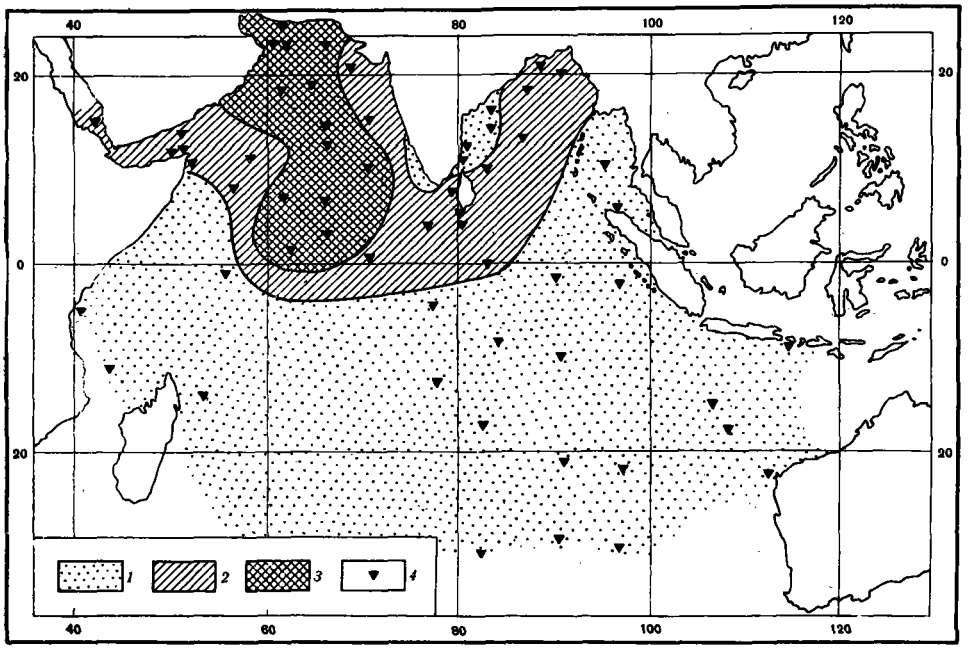

Рис. 3. Содержание хлоритов во фракции <0,001 *мм* (в процентах от общего количества глинистых минералов):

1 — <5; *2* — 5—20; *3* — >20; *4* — станции

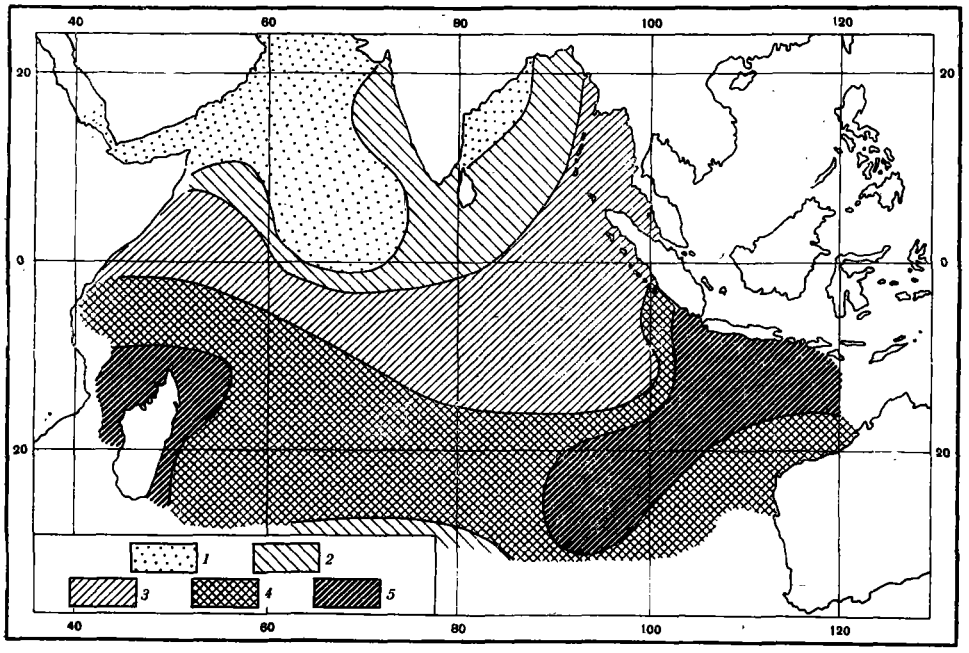

Рис. 4. Содержание каолинитов во фракции <0,001 *мм* (в процентах от общего количества глинистых минералов):

1 — <10; *2* — 10—20; *3* — 20—40; *4* — 40—50; *5* — >50

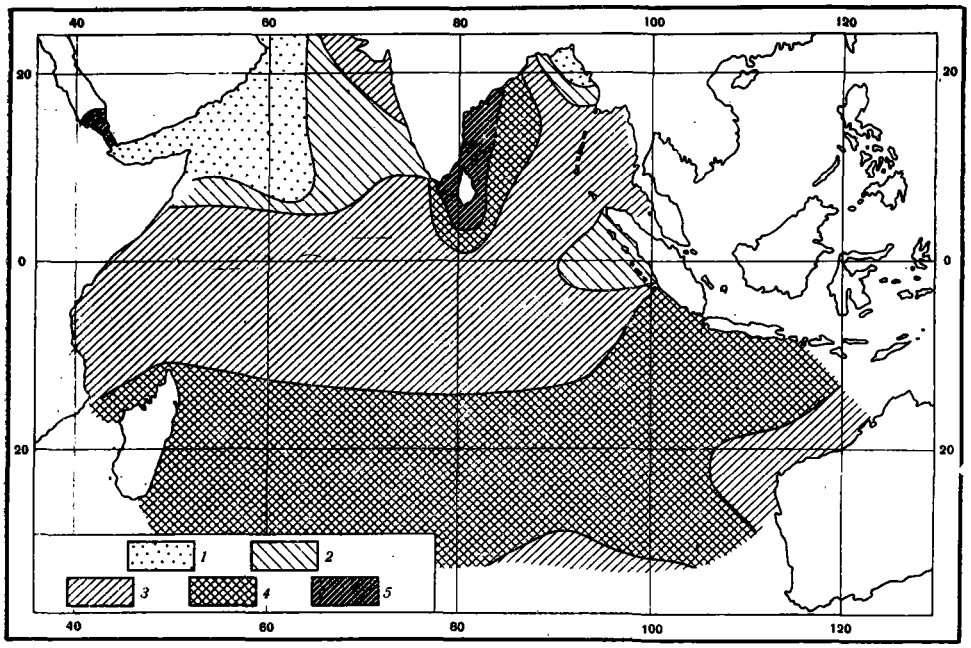

Рис. 5. Содержание монтмориллонитов во фракции <0,001 *мм* (в процентах от общего количества глинистых минералов):

1 — <5; *2* — 5—10; *3* — 10—20; *4* — >40

содержание палыгорскитов приурочено к осадкам Аденского залива. В сторону Аравийского моря их количество постепенно падает. В пределах Красного моря палыгорскиты не найдены. Таким образом, Баб-эль-Мандебский пролив разделяет районы с разным составом глинистых минералов.

ЗАКЛЮЧЕНИЕ

Распределение глинистых минералов в поверхностном слое осадков Индийского океана определяется климатической зональностью процессов выветривания и почвообразования на суше.

Высокодисперсная часть осадков Бенгальского залива и Аравийского моря состоит в основном из минералов иллитовой и хлоритовой групп. Это обусловлено тем, что на прилегающих территориях развиты пустынные и полупустынные почвы, в которых преобладающими глинистыми минералами являются иллиты и хлориты. Палыгорскитовые минералы также характерны для кор выветривания аридного климата. Они выносятся с Аравийского п-ова.

Минералы каолинитовой группы преобладают в осадках тропического гумидного пояса, что связано с их высоким содержанием в латеритных почвах Центральной Африки, о-вов Малайского архипелага и Северной Австралии. К северу и к югу от этого пояса содержание каолинита как в осадках, так и в почвах постепенно падает, а количество иллитов соответственно увеличивается.

Минералы монтмориллонитовой группы труднее связать с широтной зональностью. Их содержание в осадках высокое по всей площади дна северной и центральной частей Индийского океана, за исключением Аравийского моря. Черные почвы тропического пояса, содержащие монт-

мориллониты в качестве преобладающих глинистых минералов, могут быть источником их поступления в океан.

Возможно, что часть монтмориллонита образуется на дне океана из вулканогенного материала. Этот материал широко распространен в осадках Бенгальского залива, близ о-вов Малайского архипелага и Мадагаскара. Как наиболее высокодисперсные минералы, монтмориллониты могут переноситься на огромные расстояния.

ЛИТЕРАТУРА

1. Безруков П. Л. 1961. Исследования Индийского океана в 33-м рейсе э/с «Витязь». Океанология, **1**, вып. 4.
2. Безруков П. Л. 1961. Исследование донных осадков северной части Индийского океана. МГГ. Океанологические исследования. Сб. статей, № 9.
3. Безруков П. Л. 1963. Исследования Индийского океана в 35-м рейсе э/с «Витязь». Океанология, **III**, вып. 3.
4. Горбунова З. Н. 1963. Глинистые минералы в осадках Тихого океана. Литология и полезные ископаемые, № 1.
5. Горбунова З. Н. 1960. Высокодисперсные минералы в осадках Индийского океана. Докл. АН СССР, 134, № 4.
6. Adhikari M. 1957. Physico-chemical properties of some west Bengal clays. Indian Soc. of Soil Sci., **5**, No 4.
7. Biscaye P. E. 1964. Mineralogy and sedimentation of the deep-sea sediment fine fraction in the Atlantic ocean and adjacent seas and oceans. Geochemistry technical report, 8.
8. Bose A. K., Sengupta P. 1954. X-ray and differential thermal studies of some Indian montmorillonites. Nature, **174**, No 4418.
9. Brown G. and oth. 1961. The X-ray identification and crystal strectures of clay minerals. London.
10. Chatterjee B. 1955. Properties of some soils of west Bengal clay mineralogy in relation to chemical, electrochemical and physical properties. Proceedings of the symposium on recent trends in soil research, part 2. Alleahabad.
11. El. Wakeel S. K., Riley J. P. 1961. Chemical and mineralogical studies of deep-sea sediments. Geochim. et cosmochim. acta, **25**, No 2.
12. Kanwar I. S. 1959. Two dominant clay minerals in Penjab Soils. Indian Soc. of Soil Sci., **7**, No 4.
13. Kanwar I. S. 1961. Clay minerals in saline alkali soils of the Punjab. Indian Soc. of Soil Sci., **9**, No 1.
14. Kuenen P. H. 1942. The «Snellius» expedition in the eastern part of the Netherland east Indies, **5**, pt. 3, section 1, Leiden.
15. Mehra O. P. Jackson M. L. 1960. Iron oxide removal from soils and clays system buffered with sodium bicarbonate by dithionite-citrate. Clays and clay minerals, **5**.
16. Merwe C. R. van der, Heystek H. 1952. Clay minerals of south African soil groups: I. Laterites and related soils. Soil Sci., **74**, No 5.
17. Merwe C. R. van der, Heystek H. 1955. Clay minerals of south African soil groups: IV. Subtropical black clays and related soils. Soil Sci., **79**, No 2.
18. Merwe C. R. van der Heystek H. 1955. Clay minerals of South African soil groups: III Soils of the desert and adjoning semiarid region. Soil Sci., **80**, N 6.
19. Mitra R. P. 1954. Some resent developments in the field of fundamental clay research. Indian Soc. of Soil Sci., **7**, N 4.
20. Mohr E. C. I., Baren F. A. V. 1954. Tropical soils. Intersciens pub.
21. Nagelschmidt O., Desal A. D., Muir A. 1940. The minerals in clay fractions of a black cotton soil and a red earth from Hyderabad, Deccan state, India. Agricultural Sci., **30**, part 4.
22. Rao M. S. 1963. Clay mineral composition of shelf sediments of the east coast India. Indian Acad. Sci. Proc., Sec. A, **58**.
23. Raychaudhuri S. P., Sulaiman M., Bhuiyan A. B. 1943. Physico-chemical and mineralogical studies of black and red soil profiles near Coimbater. Ind. J. Agricultural Sci., **XIII**, part III.
24. Schultz L. G. 1960. Quantitative evaluation of the kaolinite and illite in underclays. Clays and clay minerals, **5**.
25. Simonett D. S., Bauleke M. P., 1963. Mineralogy of soils on basalt in North Queensland. Soil Sci Soc. America Proc., **27**, N 2.

Поступила в редакцию
3.VI.1965

Z. N. GORBUNOVA

DISTRIBUTION OF CLAY MINERALS IN THE SEDIMENTS OF THE INDIAN OCEAN

Summary

Clay minerals were identified in 70 samples of recent marine sediments from the Indian Ocean north of the latitude 30° S, X-ray diffraction, DTA, electron microscopy, chemical and semi-quantitative analyses having been applied. Illites, chlorites, kaolinites, montmorillonites and palygorskits were shown to be dominant. For the former four minerals the map of their distribution in sediments is presented.

Clay minerals are formed in the crusts of weathering and soils, then carried away by streams and deposited in the ocean. High concentrations of illites and chlorites in sediments of the Arabian Sea can be explained by the fact that they are swept away from desert and semi-desert lands. Kaolinites are carried away from red soils and latosols and deposited in marine sediments of the tropic humid zone. Some peculiarities in the distribution of montmorillonites can be explained by their formation in the oceans and soils due to the decomposition of volcanic ash.

UNESCO ARCHIVES

Reprinted from J. geophys. Res., vol. 71, no. 2, 1966, p. 583-586.

Heat-Flow Measurements in the Atlantic Ocean, Indian Ocean, Mediterranean Sea, and Red Sea[1]

F. S. Birch[2] and A. J. Halunen, Jr.[2]

Woods Hole Oceanographic Institution
Woods Hole, Massachusetts

Abstract. Eight heat-flow stations in the Atlantic Ocean southeast of Bermuda and on the outer ridge of the Puerto Rico trench have a mean of 1.01 μcal/cm^2 sec. A single station on the mid-Atlantic ridge gave a value of 0.90μcal/cm^2 sec. The results of four stations north of the Seychelles in the Indian Ocean range from 0.87 to 1.35 μcal/cm^2 sec. Four stations east and west of the Seychelles-Mauritius ridge vary from 0.86 to greater than 1.97 μcal/cm^2 sec. In the Mediterranean Sea one station southeast of Sicily gave a result of 0.64 μcal/cm^2 sec. One on the flank of the active volcano Stromboli gave a result of 0.42 to 1.83 μcal/cm^2 sec. A station in the northern end of the Red Sea gave a result of higher than 2.29 μcal/cm^2 sec.

Introduction

Heat-flow measurements were made during geophysical surveys on several cruises of R.V. *Chain*. Because these measurements were taken to extend world coverage of heat-flow stations, the distance between stations was usually large. No detailed analysis of the results was made for this reason and also because regional variations of heat flow have been discussed already [*Lee and Uyeda*, 1965].

Method of Measurement

Temperature gradients were measured with the equipment and method developed and described by *Reitzel* [1963]. Two thermistors, mounted in small probes about 2 m apart on a gravity or piston corer, measured temperature differences in the bottom sediment. The upper thermistor also measured temperature of the upper probe so that depth of upper probe penetration could be estimated by dividing the temperature increase of the upper thermistor by the temperature gradient, which was assumed constant with depth. On occasion, it was necessary to rely on the length of the core and external mud marks to determine the extent of upper probe penetration. Penetration was judged complete if the length of the undisturbed section of core was greater than the distance of the upper thermistor from the end of the core barrel. Mud smears on the outside of the core barrel were not relied on; they are particularly suspect in sandy or silty sediments. A good criterion of penetration was sediment firmly packed around the thermistor probes or under the plastic tape securing the thermistor cables to the core barrel.

Thermal resistivities were determined from the cores by the water content method of *Bullard and Day* [1961]. Their corrections for pressure (water depth) and temperature were applied. For most cores, the resistivities of about ten equally spaced samples were determined and averaged. In some cases it was necessary to estimate resistivities. The resistivities may be systematically high by 5 to 10% if recent studies by A. H. Lachenbruch (personal communication) are applicable.

Results

The heat-flow results are listed in Table 1. When upper and lower limits of heat flow are given, upper probe penetration is questionable. The lower limit corresponds to possible penetration by both thermistors, the upper to partial penetration corresponding to the length of the core.

The estimated experimental standard deviation of the temperature gradients is calculated from the scatter of the temperature difference readings in the water and in the sediment. The estimated experimental standard deviation of the resistivities is calculated from the differences of the computed resistivities of the samples in

[1] Contribution 1708 from the Woods Hole Oceanographic Institution.

[2] Now at Hawaii Institute of Geophysics, University of Hawaii, Honolulu.

TABLE 1. Heat-Flow Stations

Heat-Probe Station		Latitude	Longitude	Water Depth Corrected, meters	Thermal Resistivity,* cm sec°C / cal	Heat Flow, μcal / cm² sec	Experimental Standard Deviation, %
Chain–36	1	21°08′N	65°03′W	5696	543	1.00	4
	3	19°25′N	61°30′W	5468	525	1.03	5
Chain–39	1	29°00′N	59°11′W	5811	509	0.95	6
	2	25°18′N	55°44′W	5932	530	1.19†	6
	3	24°04′N	55°15′W	5984	550	0.61	7
	5	28°30′N	57°59′W	5800	605	0.79	5
	6	29°56′N	60°33′W	5715	544	1.32	5
	7	29°47′N	62°12′W	4865	547	1.20	9
Chain–43	4	00°55′N	51°38′E	5110	589	1.08	8
	5	00°22′S	54°33′E	4863	580	1.35	8
	6	01°38′S	53°20′E	4780	588	0.87	7
	8	02°55′S	55°43′E	3690	(590)	0.89	5‡
	11	17°26′S	58°06′E	4034	497	0.87–2.61	7‡
	13	14°14′S	62°51′E	3811	520	1.97–5.16	11‡
	14	11°30′S	58°24′E	4104	(500)	0.86	16‡
	16	18°04′S	57°40′E	3873	472	1.15	24
	24	25°24′N	36°10′E	2205	(500)	≥2.29	§
	25	35°47′N	17°29′E	4036	(500)	0.64	3‡
	27	38°47′N	15°04′E	2013	(500)	0.42–1.83	6‡
	33	42°37′N	28°47′W	2565	499	0.90	8

* These values may be systematically high by 5 to 10%.

† This result may be as much as 30% too low because one of the thermistor probes slipped on the core barrel.

‡ These estimates of experimental standard deviation do not include error in assuming a resistivity or error of partial penetration.

§ No upper limit can be assigned because recorder went off scale.

each core and the inaccuracy of the empirical resistivity formula. The estimated experimental standard deviation of the heat flow is the square root of the sum of the squares of the standard deviations of gradient and resistivity.

Discussion

Atlantic Ocean. The *Chain*-39 heat probes are in the abyssal hills region southeast of Bermuda; the *Chain*-36 heat probes are on the outer ridge of the Puerto Rico trench (Figure 1). The mean of these stations is 1.01 μcal/cm² sec ±0.20 μcal/cm² sec standard deviation (for brevity, the units of heat flow will hereafter be omitted). The mean for the basins of the Atlantic Ocean is 1.13 ±0.24 [*Lee and Uyeda,* 1965]. The mean for the stations to the west on the thermal plain of *Reitzel* [1963] is 1.14 ±0.06. Thus, these *Chain* stations may perhaps indicate a region of slightly low heat flow.

Heat-probe station 33 of *Chain*-43 is in a flat-floored valley about 30 km east of the median valley of the mid-Atlantic ridge. The result, 0.90, is below the 25 percentile line for stations within 100 km of the crest of the mid-Atlantic ridge [*Lee and Uyeda,* 1965].

Indian Ocean. The stations in the Indian Ocean are too far apart to be treated as a group (Figure 2).

Heat-probe station 4 of *Chain*-43 is in the Somali abyssal plain. The result, 1.08, is not significantly different from the other results there [*Sclater,* 1966].

Heat-probe stations 6, 8, and 5 of *Chain*-43 are in a region of rough topography north of the Seychelles Islands. The results for the first two, 0.87 and 0.89, are low compared with the last, 1.35, and with several values reported by *Von Herzen and Langseth* [1965].

Heat-probe station 13 of *Chain*-43 is east of the Seychelles-Mauritius ridge; the result, 1.97 to 5.16, agrees with two other values [*Von*

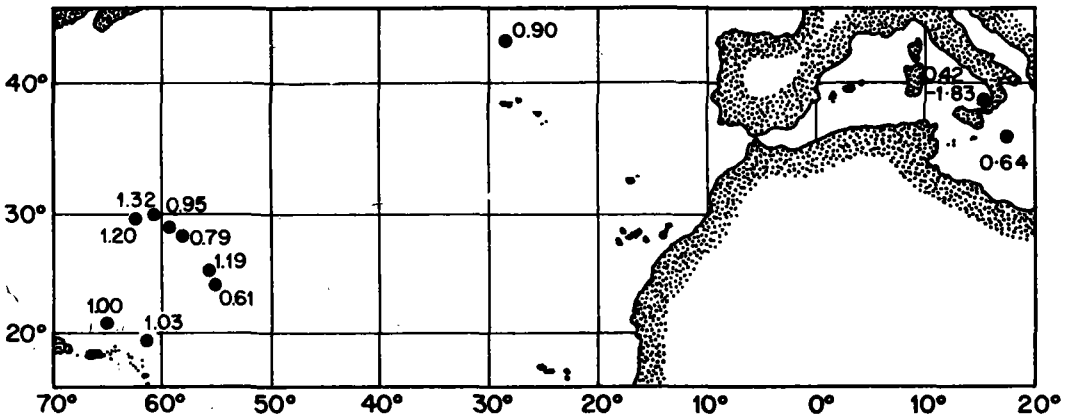

Fig. 1. Heat-flow values, μcal/cm^2 sec, in the Atlantic Ocean and Mediterranean Sea.

Herzen and Langseth, 1965] and suggests that this may be an area of high heat flow.

Heat-probe stations 11 and 16 of *Chain*-43 are at the western base of Cargados Carajos shoals. The results, 0.87 to 2.61 and 1.15, are in general agreement with a result, 1.32, at an intermediate station [*Von Herzen and Langseth,* 1965].

Heat-probe station 14 of *Chain*-43 is on the slope at the western base of Saya de Malha bank. The result, 0.86, agrees well with four others from the same region [*Von Herzen and Langseth,* 1965]. The results of these five stations range from 0.86 to 1.44 and the corresponding depths from 4104 to 2315 meters. The heat flow decreases linearly at a rate of 0.33 μcal/cm^2 sec per kilometer of depth. The correlation coefficient for this linear relationship between heat flow and water depth is -0.96 with a 95% confidence interval of -0.51 to -1.00 (to two decimal places). The former value is very sensitive to the small number of stations. In contrast to this apparent regularity, stations to the northwest in rugged terrain off the smooth slope of the Saya de Malha bank have widely scattered heat flow. Possible physical explanations for the correlation of heat flow with depth are high sedimentation rates and greater sediment thickness at the base of the slope or radioactive heat generation in the possibly granitic rock under Saya de Malha bank.

Red Sea. Heat-probe station 34 of *Chain*-43, in the northern Red Sea, gives a result of ≥ 2.29. This result and several others suggest that the Gulf of Aden and the Red Sea have heat flow two or three times the world average [*Von Herzen,* 1963; *Sclater,* 1966].

Mediterranean Sea. Heat-probe station 25 of *Chain*-43, on the western end of the abyssal plain southeast of Sicily, gives a result of 0.64. There are no nearby stations with which to compare this low value.

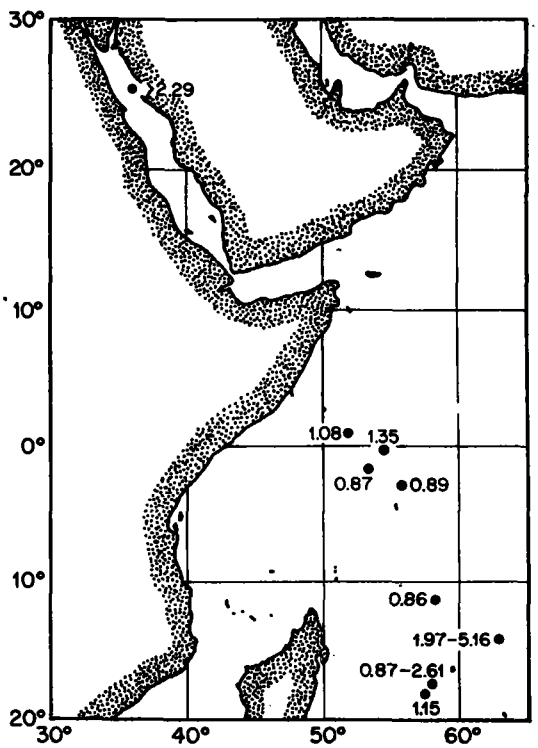

Fig. 2. Heat-flow values, μcal/cm^2 sec, in the Indian Ocean and Red Sea.

Heat-probe station 27 of *Chain*-43 is on the northwest flank of Stromboli about 12 km from the center of the island. The heat flow is 0.42 to 1.83. This result can be compared to a result of 1.46 obtained about 30 km from the erupting volcano Miyake-Jima southeast of Japan [*Yasui et al.*, 1963].

Acknowledgments. We wish to thank Miss Elizabeth T. Bunce, Dr. J. B. Hersey, Dr. C. O. Bowin, and Dr. R. L. Chase, chief scientists on the *Chain* cruises, for the opportunity to make these measurements, and also the officers and crew of the R.V. *Chain*.

This work was supported by the Office of Naval Research under contract Nonr-4029(00) and the National Science Foundation under grants GP-2370 and GP-1123 to the Woods Hole Oceanographic Institution.

References

Bullard, E. C., and A. Day. The flow of heat through the floor of the Atlantic Ocean, *Geophys. J.*, *4*, 282–292, 1961.

Lee, W. H. K., and S. Uyeda, Review of heat-flow data, *Terrestrial Heat Flow*, chapter 6, *Geophys. Monograph 8*, American Geophysical Union, Washington, D. C., 1965.

Reitzel, J. S., A region of uniform heat flow in the North Atlantic, *J. Geophys. Res.*, *68*, 5191–5196, 1963.

Sclater, J. G., Heat flow in the north west Indian Ocean and Red Sea, *Phil. Trans. Roy. Soc. London*, *297A*, 1966.

Von Herzen, R. P., Geothermal heat flow in the Gulfs of California and Aden, *Science*, *140*, 1207–1208, 1963.

Von Herzen, R. P., and M. G. Langseth, Present status of oceanic heat-flow measurements, *Phys. Chem. Earth*, *6*, 365–407, 1965.

Yasui, M., K. Horai, S. Uyeda, and H. Akamatsu, Heat flow measurements in the western Pacific during the JEDS-5 and other cruises in 1962 aboard M/S RYOFU-MARU, *Oceanog. Mag., Japan Meteorol. Agency*, *14*, 147–156, 1963.

(Manuscript received September 4, 1965; revised October 15, 1965.)

Reprinted from J. geophys. Res., vol. 71, no. 10, 1966, p. 2625-2630.

Magnetic Lineation between Carlsberg Ridge and Seychelles Bank, Indian Ocean[1]

CARL O. BOWIN

Department of Geophysics, Woods Hole Oceanographic Institution
Woods Hole, Massachusetts

PETER R. VOGT

Geophysical and Polar Research Center, Department of Geology
University of Wisconsin, Madison

The azimuths of isoanomaly lines of strong magnetic anomalies of total intensity, discovered during a cruise of H.M.S. *Owen* in 1962 in the eastern Somali basin, Indian Ocean, were investigated on a cruise of R.V. *Chain* in 1964. Forty-eight azimuths were determined, having an average bearing of 295°. Compilation of this result with magnetic information from studies from H.M.S. *Owen* and R.R.S. *Discovery* indicate that a magnetic lineation (305° to 295°) occurs over a broad region (at least 600,000 km²) of the western Indian Ocean. This lineation may become an important key in determining the structure and geologic history of the western Indian Ocean.

INTRODUCTION

Magnetic anomalies with amplitudes of several hundred gammas were first observed over the eastern Somali abyssal basin between the Carlsberg ridge and Seychelles bank by scientists on H.M.S. *Owen* [*Hydrographer*, 1963; *Loncarevic*, 1964]. The R.V. *Chain* of the Woods Hole Oceanographic Institution also visited this region in May 1964 while participating in the Indian Ocean Expedition. At this time the local azimuths of the isoanomaly lines forming these strong anomalies were determined.

METHOD

The method used to determine the local azimuth of isoanomaly lines follows that described by *Raff* [1962]. The sensing head of a Varian nuclear precession magnetometer was towed 150 m astern of the ship, and the total intensity F of the earth's magnetic field was recorded on a graphic strip chart recorder (Varian model G14). The procedure was to allow the magnetic observer to call a 90° course change whenever it appeared that the steepest slope on the flank of a pronounced anomaly had been reached, that is, a place showing nearly linear change of F with displacement along the ship's track. The new course was held for several miles, long enough to determine the gradient in this direction, whereupon the original heading was resumed and often held for 15 to 30 km. A second pair of right-angle turns was effected over the opposite slope of the anomaly in such a manner as to return the vessel to its original base track.

ANALYSIS OF DATA

The data were analyzed directly on the analog chart, each course change yielding a local azimuth for the isoanomaly lines. In Figure 1, S_1 and S_2 represent reciprocals of directional gradients, in arbitrary units. The azimuth of the isoanomaly lines (γ_1 to γ_5) equals $\alpha + \tan^{-1} S_2/S_1$, where α is the acute angle between the initial course and the meridian. A large turning radius is thus no problem. S_1 and S_2 were determined from the chart, in convenient units, and a regional slope correction was applied to each, using the polynomial fitted field represented in Figure 6 of *Hydrographer* [1963]. The regional pattern of total intensity in the locality of the measurements shows a general rise toward the east, but the

[1] Contribution 1728 of the Woods Hole Oceanographic Institution.

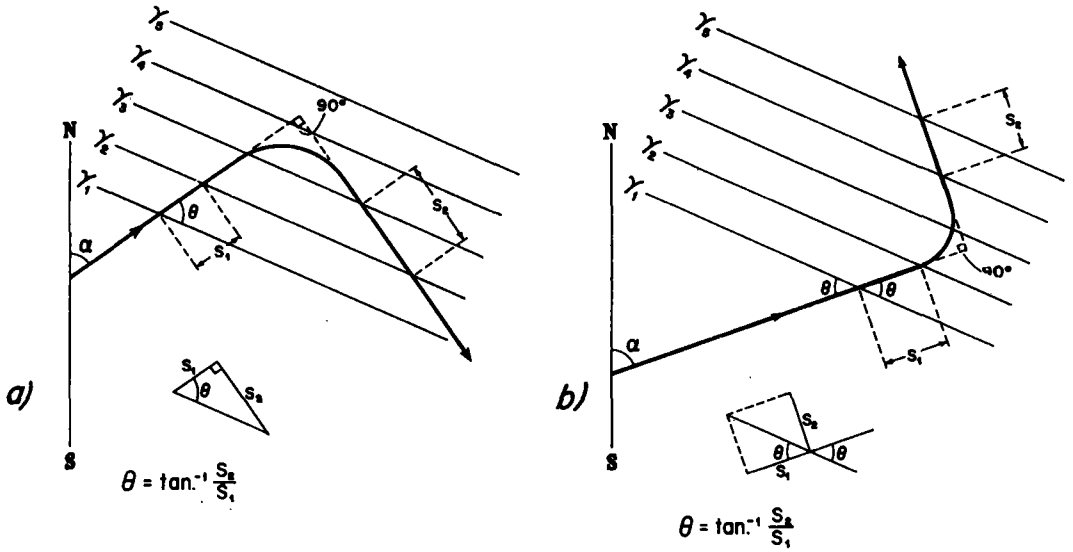

Fig. 1. Calculation of azimuth of isoanomaly lines from jog in ship's track: (*a*) turn to starboard, (*b*) turn to port. The γ lines are isoanomaly lines of the magnetic total intensity. For the purpose of determining the azimuth, it does not matter whether the isoanomaly lines are numbered in the direction of increasing or decreasing total intensity.

slope is only about 1.5 gammas per km, so these corrections are small enough to be of little effect relative to the anomalies encountered. Where the course changes differed from 90°, azimuths were constructed graphically. However, most of the azimuths were computed from right-angle turns by trigonometry. Because of the high sampling rate (6 sec), there was no problem in distinguishing gradient reversals resulting from change of direction on the same flank of the anomaly from those due to crossing to the other flank of the anomaly. From Figure 1 it is clear that azimuths can be determined from either port or starboard turns of the ship. The major problem is that the isoanomaly lines are not always uniform, as shown in Figure 1, but may commonly be irregular or curved. Since determination of values for S_1 and S_2 will always allow an azimuth to be calculated, little significance can be attached to any single azimuth value. It is only from the results of many such determinations that conclusions can have validity. *Raff* [1962] discusses the use of real and model histograms to aid in the interpretation of azimuth determinations.

Forty-eight azimuths were determined in the period May 26 to May 28, 1964, along a course between a point lying immediately northeast of the Seychelles bank and a point on the equator at 62°E, northeast of which the magnetic anomalies have lower amplitudes and shorter wavelengths (Figures 2 and 3), as shown by profiles obtained on H.M.S. *Owen* in 1962.

The azimuth frequency in bearing intervals of 10° is shown in the rose diagram of Figure 2. Seventy-five per cent of all the azimuths fall between N30°W and N80°W, with a mean at N65°W. Out of 20 pairs of azimuths obtained from adjacent corners of the short right-angle legs, only 4 pairs have azimuths which differ by more than 10° from each other. These pairs were generally those obtained when the ship turned too late, that is, after the region of maximum slope had been traversed.

Geologic Setting and Compiled Magnetic Data

The general nature of the sea bottom is suggested by the bathymetric profile of Figure 3. Fairly level terrain ranging in depth from 4000 m to nearly 4600 m (2200–2500 fathoms), not corrected for variation in sound velocity with depth, is interrupted by scattered abyssal hills. These hills are commonly tens of meters, and

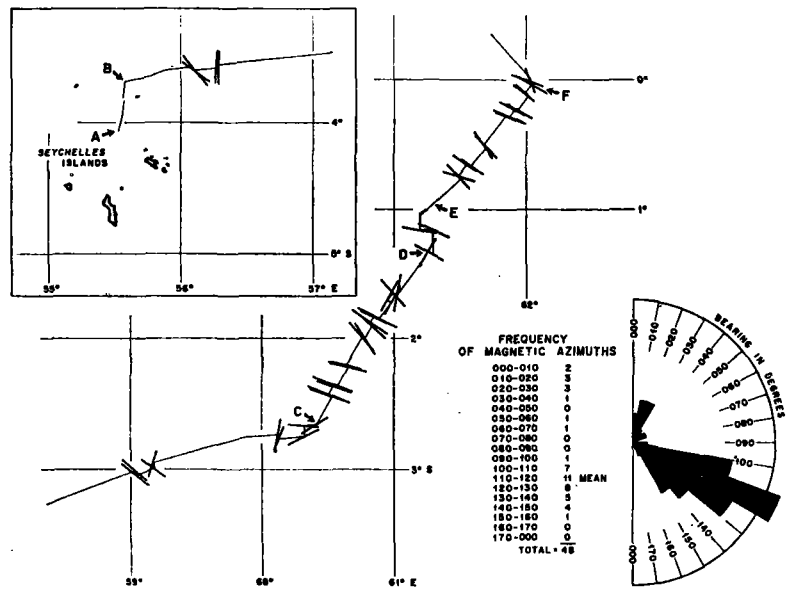

Fig. 2. Track of R.V. *Chain* and location of azimuth determinations. Letters are for reference to profile shown in Figure 3. Rose diagram shows distribution of azimuth of isoanomaly lines.

more rarely several hundreds of meters, high, the highest rising to about 3100 m. Several plains occur along the ship's track; these are generally not horizontal but have gentle uniform dip or dip away in both directions from a central high area.

The seismic reflection profiling records reveal acoustic reflectors below the flatter parts of the sea bottom (Figure 3). The deepest reflectors lie about 0.25 to 0.65 sec (two-way travel time) below the sea bottom. Gaps in the record are mostly due to technical difficulties. In several places the sub-bottom reflectors rise close to the sea bottom, and they appear to form at least some of the abyssal hills. The seismic reflection profiles reveal no pronounced structural differences between the area of large magnetic anomalies and the area of smaller anomalies to the west.

The strong magnetic anomalies discussed above occur as a distinctive group. A similar distinctive group of anomalies was observed by *Owen* about 700 km to the northwest [*Hydrographer*, 1963]. The heavy dashed lines in Figure 4 indicate the limits of a belt of strong magnetic anomalies inferred from the two magnetic profiles from the 1962 cruise of *Owen*. Also shown are trends of anomalies obtained by correlating information from profiles *A-A'*, and *B-B'*, and from *C-C'* and *D-D'*. Figure 5 reproduces the profiles obtained during cruises of *Owen*, 1962–1963 [*Anonymous*, 1964*a*] and *Discovery* 1963 [*Anonymous*, 1964*b*]. The magnetic azimuth lines given in Figure 2 are repeated in Figure 4. A magnetic survey (90 × 75 km) over the central part of the Carlsberg ridge (H.M.S. *Owen* in November 1962 [*Vine and Matthews*, 1963; *Matthews et al.*, 1965]) is indicated by ruled lines. Matthews et al. report that the topography and magnetic anomalies there are generally elongated parallel to the trend of the Carlsberg ridge (N45°W). The southern part of their magnetic map [*Matthews et al.*, 1965, Figure 4] shows the magnetic anomalies to trend about N45° to 60°W.

Discussion

The data presented in Figures 2 and 4 strongly suggest that a magnetic lineation trending between N55°W and N65°W exists between the Carlsberg ridge and the Seychelles bank over an area of at least 600,000 km². The trends of the Carlsberg and the Seychelles–Saya de Malha ridges, which border the line-

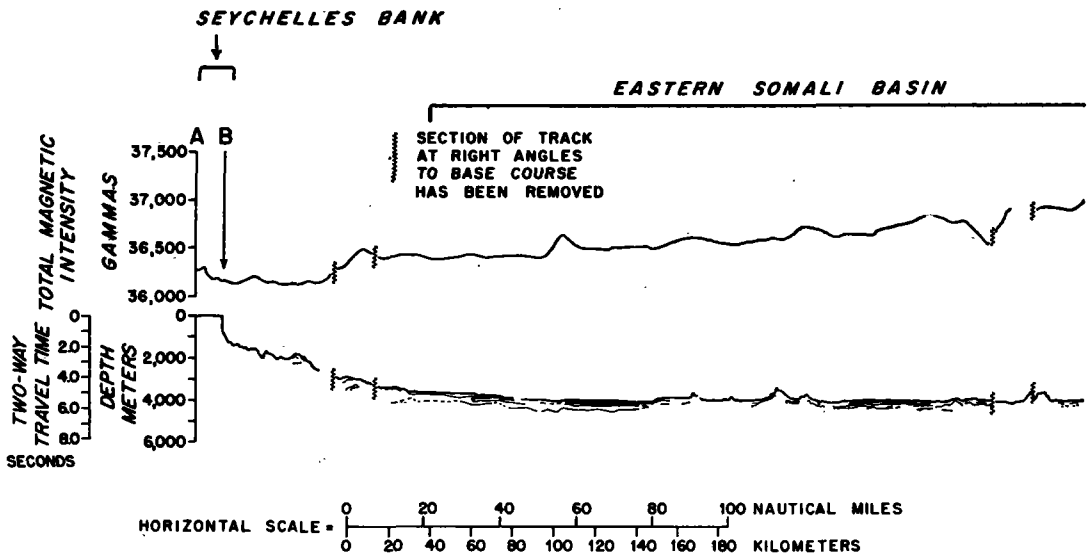

ated area, are close to N45°W according to the Physiographic Diagram of the Indian Ocean of *Heezen and Tharp* [1964].

There appears to be a distinct difference between the regional trends of the topography of the two bordering ridges and that of the magnetic anomalies, although the trends are similar. The significance of this difference in trend, if real, is unknown, as is the nature and origin of the source of the magnetic anomalies. There is a possibility that, if the magnetization (either induced or remanent) of the source is parallel to the current geomagnetic vector and of appropriate dimensions, the source might trend near N45°W but the isoanomaly lines would trend closer to N55° to 65°W (Figures A30 and A36 of *Vacquier et al.* [1951] help to illustrate this possibility). *Vine and Matthews* [1963] postulate that the strong magnetic anomalies result from alternating normally and reversely magnetized strips of the crust (usually about 20 km wide). Such strips would have large apparent susceptibility contrasts and would explain the anomalies without the necessity of assuming unusual magnetic properties of the crustal rocks. In the central part of the Carlsberg ridge, Vine and Matthews found that topographic features were at least partly responsible for the magnetic anomalies. They assumed a thickness of 8 km for the magnetic crustal material in their computer models which reproduced the major anomaly pattern for the Carlsberg ridge.

Southwest of the Carlsberg ridge in the relatively smooth topography of the eastern Somali basin (Figure 3) there is little correspondence between bathymetry and the large magnetic anomalies. The magnetic susceptibility of sedimentary rocks is very small compared with common values for basic igneous, acidic igneous, and metamorphic rocks [*Dobrin*, 1960 p. 270], and therefore the bottom sediments are not believed to be the magnetic source. Since there is no obvious correlation between the anomalies and the deepest sub-bottom reflector observed on the continuous seismic profile (Figure 3), no clue is given by these records as to whether the material immediately below these reflection surfaces is the magnetic source. *Loncarevic* [1964, p. 45] concluded that the source of the magnetic anomalies is about 25 km deep, and therefore it is in the upper mantle below the base of the crust, assuming that the depth to the magnetic material is roughly equal to the half-width of the anomaly.

The discovery of a large area having a magnetic lineation in the western Indian Ocean stirs hope that an important key to the structure and geologic history of this region has been found. It is important to ascertain what happens to this lineation to the east, where the Carlsberg ridge trends nearly due south. Does

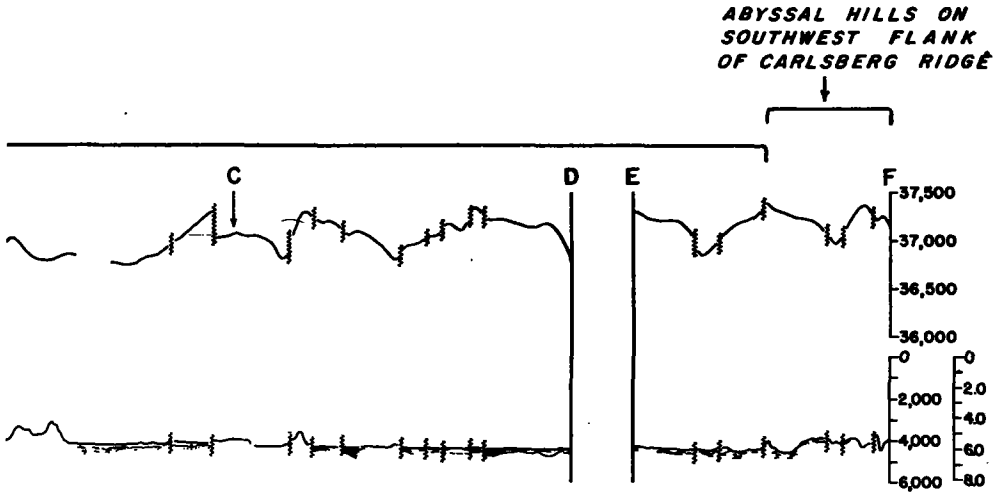

Fig. 3. Profile of total magnetic intensity, bathymetry, and sub-bottom reflections along track of R.V. *Chain*. Location of profile given in Figure 2.

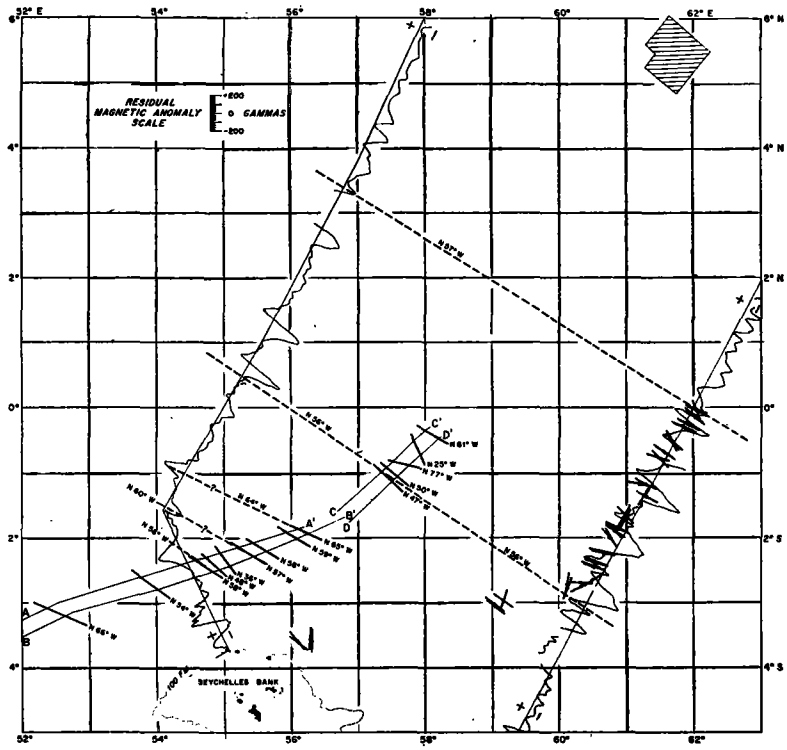

Fig. 4. Magnetic lineations between Carlsberg ridge and Seychelles bank. Area investigated by *Vine and Matthews* [1963] and *Matthews et al.* [1965] indicated by ruled lines. Lettered magnetic profiles are shown in Figure 5. Discussion in text.

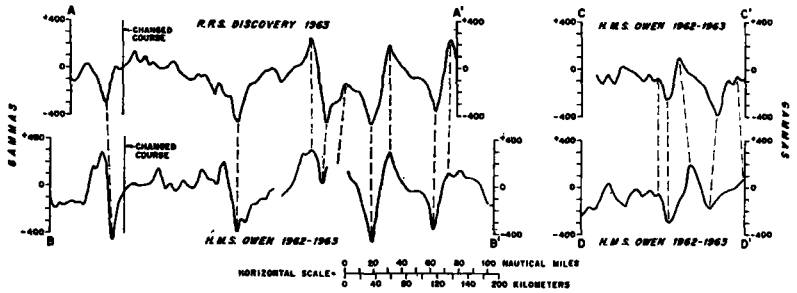

Fig. 5. Magnetic profiles determined aboard R.R.S. *Discovery* and H.M.S. *Owen*. Location of profiles given in Figure 4.

the magnetic lineament cross the ridge, disappear, change direction, or maybe even appear on the opposite side of the ridge? To the west the lineament pattern may be helpful in determining displacement on the Owen fracture zone [*Heezen and Tharp*, 1964] and its possible continuation southward. The magnetic trends shown in Figure 4 suggest that the lineation may also occur on the western side of the Seychelles bank and thereby furnish clues concerning the setting of this Precambrian granitic platform.

Acknowledgments. The assistance of G. N. Ruppert and Miss E. T. Bunce in preparing the record of sub-bottom reflection (Figure 3) is appreciated. We thank Miss Bunce and Dr. R. L. Chase for critically reading this manuscript.

Support for this work has been provided by the National Science Foundation, grant NSF GP-2370, and by the Office of Naval Research, contract Nonr-4029(00) NR 260-101.

References

Anonymous, Bathymetric and magnetic investigations, H.M.S. *Owen* 1962–1963, Provisional results, Department of Geodesy and Geophysics, Cambridge University, 1964*a*.

Anonymous, R.R.S. *Discovery* Cruise 2: Bathymetric and magnetic results obtained on passage 1963, Department of Geodesy and Geophysics, Cambridge University, 1964*b*.

Dobrin, M. B., *Introduction to Geophysical Prospecting*, 2nd ed., 446 pp., McGraw-Hill Book Company, New York, 1960.

Heezen, B. C., and M. Tharp, Physiographic Diagram of the Indian Ocean, The Geological Society of America, New York, 1964.

Hydrographer, Bathymetric, magnetic and gravity investigations, H.M.S. *Owen* 1961–1962, *Admiralty Marine Sci. Publ. 4*, parts 1 and 2, London, 1963.

Loncarevic, B. D., Geophysical studies in the Indian Ocean, *Endeavor, 23*(88), 43–47, 1964.

Matthews, D. H., F. J. Vine, and J. R. Cann, Geology of an area of the Carlsberg ridge, Indian Ocean, *Bull. Geol. Soc. Am., 76*, 675–682, 1965.

Raff, A. D., A time saving method for determining the characteristic shape and strike of oceanic magnetic anomalies, *Marine Physical Lab. Tech. Mem. 127*, Scripps Institution of Oceanography, San Diego, Calif., 1962.

Vacquier, V., N. C. Steenland, R. G. Henderson, and Isidore Zietz, Interpretation of aeromagnetic maps, *Geol. Soc. Am. Mem. 47*, 1951.

Vine, F. J., and D. H. Matthews, Magnetic anomalies over ocean ridges, *Nature*, 199(4897), 947–949, 1963.

(Manuscript received November 13, 1965; revised January 25, 1966.)

Reprinted from *Erdöl und Kohle-Erdgas-Petrochemie*, 18 Jahrgang, Nr. 12, 1965, S. 945-950.

Über rezente Sedimentation im Indischen Ozean, ihre Bedeutung für die Entstehung kohlenwasserstoffhaltiger Sedimente

Erster Überblick*)

(Vorausbericht aus den „Meteor"-Forschungsberichten, Expedition 1964/1965 in den Indischen Ozean)

*Von Wolfgang Schott und Ulrich von Stackelberg***)

Vorgetragen von W. Schott auf der 17. Jahrestagung der Deutschen Gesellschaft für Mineralölwissenschaft und Kohlechemie in Hannover, am 7. Oktober 1965

Zusammenfassung: Der Stand der Kenntnis über Auftreten von Kohlenwasserstoffen in rezenten Sedimenten wird in einem Überblick beschrieben. Es zeigt sich, daß die Kohlenwasserstoffe in rezenten Sedimenten und im Erdöl fossiler Sedimente in ihrer Zusammensetzung voneinander abweichen.

Ziel der meeresgeologischen Arbeiten während der Expedition des deutschen Forschungsschiffes „Meteor" in den Indischen Ozean (1964/1965) war es, u. a. die Bedingungen der Ablagerung, Erhaltung und Umwandlung der organischen Substanz im marinen Sediment zu untersuchen. Als erster vorläufiger Überblick werden 2 Karten über die Sedimentverteilung auf dem Meeresboden vor der ostafrikanischen und der indisch-pakistanischen Küste vorgelegt und diskutiert. Beide Gebiete weisen eine ähnliche Sedimentverteilung mit einer deutlichen Abhängigkeit der Fazies von der Meerestiefe auf. Von besonderem Interesse ist ein biogener Kalksand, der den größten Teil des Schelfes beider Bereiche bedeckt. Es handelt sich hierbei wohl z. T. um pleistozäne Ablagerungen.

Recent sedimentation in the Indian Ocean, its significance for the origin of hydrocarbonaceous sediments: The state of knowledge on the occurence of hydrocarbons in recent sediments is described briefly. It is shown that the composition of the hydrocarbons in recent sediments and in the petroleum of fossil sediments differ from each other.

The object of the marine geological work during the expedition of the German research ship „Meteor" in the Indian Ocean in 1964/65 was, amongst other things, to investigate the conditions of deposition, preservation, and transformation of the organic matter in the marine sediment. As a first preliminary summary, two maps showing the distribution of sediments of the sea floor off the East African and Indian-Pakistan coast are displayed and dicussed. Both areas show a similar distribution of sediments with a clear dependence of the facies on the water depth. A biogenic calcareous sand which covers the main part of the shelf of both areas is of special interest. Part of this sand is supposed to be a pleistocene deposit.

Einleitung

Erdöllagerstätten sind vorwiegend in marinen, brackischen und limnischen fossilen Sedimenten vorhanden. Dabei finden sich die meisten Vorkommen in marinen Ablagerungen. Von der organischen Substanz dieser fossilen Sedimente wird im allgemeinen das Erdöl abgeleitet. Erdölähnliche Kohlenwasserstoffgemische sind nämlich, wenn auch in geringen diffusen Spuren, in Sedimentgesteinen als Mikronaphtha weit verbreitet[1,2,3]).

Diese Erkenntnisse haben in den letzten Jahren zu einer intensiven Untersuchung des organischen Inhaltes rezenter Sedimente geführt. Man hofft, auf diese Weise weitere Anhaltspunkte über die Bildung von Öl und Gas und über ihre Anreicherung zu Lagerstätten in der Lithosphäre während der geologischen Vergangenheit erhalten zu können.

Smith[4,5]) hat flüssige Paraffine, Naphthene und verschiedene aromatische Kohlenwasserstoffe in rezenten marinen, brackischen und limnischen Sedimenten nachgewiesen. Das Material, das *Smith* untersuchte, stammte vorwiegend aus dem Golf von Mexico, den Lagunen und Küstengebieten von Texas und Louisiana, dem Mississippi- und Orinoco-Delta sowie von dem californischen Schelf westlich von Los Angeles. Die Zusammensetzung dieser Kohlenwasserstoffansammlungen in rezenten Sedimenten stimmt nicht mit der des Erdöls überein. So konnte *Hunt*[6]) in rezenten Ablagerungen keine C_3- bis C_8-Kohlenwasserstoffe feststellen, während sie in fossilen Sedimenten vorhanden sind (l. c., S. 406). Nach *Stevens, Bray* u. *Evans*[7]) enthalten ferner die Kohlenwasserstoffe rezenter Ablagerungen eine relativ einfache Mischung aromatischer Komponenten im Vergleich zu der komplizierten Zusammensetzung im Erdöl.

Nach *Hedberg*[8]) können daher wegen dieser Unterschiede die flüssigen Kohlenwasserstoffe heutiger Sedimente noch nicht zur Gruppe der Erdöle gerechnet werden (l. c., S. 1762). Weitere Veränderungen und Umwandlungen der organischen Substanz und der beobachteten Kohlenwasserstoffe rezenter Ablagerungen werden im Laufe der Zeit erfolgt sein müssen, bis daraus Erdöl entstanden ist, so wie es in fossilen Gesteinen vorkommt.

Viele zusätzliche Arbeiten werden somit noch erforderlich sein, um ein lückenloses Bild der Entwicklungsreihe von den Organismen im Wasserraum über die organische Substanz in rezenten Sedimenten bis zum Erdöl zu erhalten. Die Untersuchungen heutiger Ablagerungen, die im Rahmen der intensiven ozeanographischen Tätigkeit in allen Meeren während der letzten Jahre verstärkt eingesetzt haben, werden dabei zweifellos wertvolle Anhaltspunkte über Herkunft und Ansammlung von Erdöl in fossilen Ablagerungen erbringen können. So dürften sich für das große erdölreiche Tertiärbecken von Los Angeles wichtige Erkenntnisse aus der eingehenden Bearbeitung des angrenzenden californischen Schelfes durch *Emery*[9]) ergeben haben, der hier ein Gebiet heutiger Erdölbildung sieht. Infrarotspektren der Paraffin-/Naphthen- und der aromatischen Fraktion aus den rezenten Sedimenten des dortigen Schelfgebietes sind nämlich den entsprechenden Spektren eines pliozänen Erdöls aus dem Los Angeles-Becken sehr ähnlich.

*) Eine kürzere Fassung dieser Ausarbeitung ist in englischer Sprache unter dem Titel „Recent sedimentation in the Indian Ocean, its significance for the origin of hydrocarbonaceous sediments (First review)" auf dem Third Symposium on the Development of Petroleum Resources of Asia and the Far East, November 1965, in Tokio (Japan) vorgelegt worden und wird später von den Vereinten Nationen in den Proceedings dieses Symposiums veröffentlicht werden.

**) Anschrift: Professor Dr. W. Schott, Dr. U. von Stackelberg, Bundesanstalt für Bodenforschung, Hannover-Buchholz, Alfred-Bentz-Haus.

[1]) *K. Krejci-Graf*, Diagnostik der Herkunft des Erdöls. Erdöl u. Kohle **12**, 706/12, 805/15 [1959].

[2]) — —, Mikronaphtha und Entstehung des Erdöls. Mitt. geol. Ges. Wien, Bd. 53, S. 133/76. Wien 1960.

[3]) *N. B. Wassojewitsch*, Probleme der Erdölgenese. Z. angew. Geologie **4**, 512/15 [1958].

[4]) *P. V. Smith*, Preliminary note on origin of petroleum. Bull. Amer. Assoc. Petroleum Geologists **36**, 411/13 [1952].

[5]) — —, Studies on origin of petroleum: Occurences of hydrocarbons in recent sediments. Bull. Amer. Assoc. Petroleum Geologists **38**, 377/404 [1954].

[6]) *J. M. Hunt*, Geochemical data on organic matter in sediments. Wiss. Tagung für Erdölbergbau. Vorträge der III. Internationalen Wissenschaftlichen Konferenz für Geochemie, Mikrobiologie und Erdölchemie, Bd. I, Geochemie und Mikrobiologie, S. 394/412. Budapest 1963.

[7]) *U. P. Stevens, E. E. Bray* u. *E. D. Evans*, Hydrocarbons in sediments of Gulf of Mexico. Bull. Amer. Assoc. Petroleum Geologists **40**, 975/83 [1956].

[8]) *H. D. Hedberg*, Geologic aspects of origin of petroleum. Bull. Amer. Assoc. Petroleum Geologists **48**, 1757/1803 [1964].

[9]) *K. O. Emery*, The Sea off Southern California. A modern habitat of petroleum. 366 Seiten. New York–London 1960.

Sedimentation im Indischen Ozean

Die letzte, neu bearbeitete Übersichtskarte über die Sedimentverteilung im gesamten Indischen Ozean ist vor 30 Jahren veröffentlicht worden[10,11]). Hierbei wurden vor allem Verbreitung, Ausbildung und Entstehung der Tiefsee-Sedimente besprochen, die den größten Teil des Meeresbodens im Indischen Ozean bedecken[12]).

Der Indische Ozean, der ein Siebentel der Erdoberfläche einnimmt, ist von allen Weltmeeren bisher am wenigsten erforscht. Deshalb wird z. Z. eine intensive ozeanographische und damit auch meeresgeologische Bearbeitung dieses Ozeans im Rahmen der Internationalen Indischen-Ozean-Expedition, die von September 1959 bis Ende 1965 dauert, durchgeführt. 40 Forschungsschiffe mit Wissenschaftlern aus mehr als 20 Ländern sind an dieser Zusammenarbeit beteiligt. Die Bundesrepublik Deutschland hat für diesen Zweck vom 29. Oktober 1964 bis 18. Mai 1965 das neue deutsche Forschungsschiff „Meteor" in den Indischen Ozean entsandt[13]). Hauptzweck der Reise war neben Arbeiten im Roten Meer, im Golf von Aden und im Persischen Golf eine intensive Untersuchung der Meeresregionen vor der ostafrikanischen Küste zwischen Kap Guardafui und Mombasa sowie vor der indisch-pakistanischen Küste zwischen Cochin und Karachi. Auf 13 Profilen, die von der Küste bis in die Tiefsee des Somali-Beckens bzw. des Arabischen Beckens hinabreichten, wurden Sedimentproben vom Meeresboden entnommen. Im Anschluß an die Fahrten der „Meteor" im Arabischen Meer erfolgte im Rahmen einer deutsch-pakistanischen Zusammenarbeit noch eine spezielle Bearbeitung der Sedimente im Bereich der Indus-Mündung. Für die Untersuchung stehen Sedimentproben von 150 Stationen aus dem Arabischen Meer zur Verfügung; sie wurden mit dem Kolbenlot, Schwerelot, van Veen-Greifer, Kastengreifer oder mit dem Kuttertrawl gewonnen.

Ziel der meeresgeologischen Arbeiten im Arabischen Meer ist es, einen Überblick über den Fazieswechsel der Sedimente von der Küste bis in die Tiefsee zu erhalten und die dort herrschenden Sedimentationsbedingungen zu erfassen. Ferner sollen die diagenetischen Veränderungen der organischen und anorganischen Komponenten der Ablagerungen in den bis zu 5 m langen Sedimentkernen untersucht werden. Außerdem soll versucht werden zu klären, wo vor allem die feinste Trübe des Induswassers auf dem Meeresboden des Arabischen Beckens sedimentiert wird.

Diese Ziele können erst nach einer detaillierten Untersuchung des gewonnenen Sedimentmaterials erreicht werden. Gegenwärtig kann nur eine erste allgemeine Übersicht über die Sedimentverteilung auf dem heutigen Meeresboden beider Küstenregionen gegeben werden.

Sedimente vor der ostafrikanischen Küste

In den Ablagerungen vor der ostafrikanischen Küste lassen sich 5 Faziesbereiche unterscheiden, die sich etwa parallel zur Küste anordnen. Von der Tiefsee in Richtung zur Küste sind folgende Sedimente beobachtet worden (s. *Abb. 1*):

Tiefseeton

In größeren Tiefen des Somalibeckens ist ein rotbrauner Ton mit wechselndem Gehalt an pelagischen Foraminiferen vorhanden. Er wurde in Tiefen zwischen 4130 und 5050 m gefunden.

Globigerinenschlamm

Anschließend an den Tiefseeton ist in Tiefen zwischen 1670 und 4610 m bis an den Fuß des Kontinentalabhanges Globigerinenschlamm beobachtet worden.

Foraminiferensand

Östlich von Mombasa und Obbia sowie südlich der Insel Sokotra treten am Kontinentalabhang zwischen 700 und 1710 m olivgraue Foraminiferensande auf. Pelagische Foraminiferen der Familie **Globigerinidae** herrschen darin vor.

Olivgrauer Schlick

Der obere Teil des Kontinentalabhanges wird zwischen 540 und 980 m vorwiegend von olivgrauem Schlick mit unterschiedlichem Gehalt an pelagischen Foraminiferen eingenommen; stellenweise geht der Schlick seitlich aus dem Foraminiferensand hervor.

Biogener Kalksand

Riffschutt bildet den wesentlichen Anteil eines hellbraunen bis olivbraunen Kalksandes, der vorwiegend den schmalen Schelf vor der ostafrikanischen Küste zu bedecken scheint, aber auch am Kontinentalabhang in 650 m Tiefe gefunden wurde. Die flachste Station, die Kalksand lieferte, lag bei 30 m Wassertiefe. In einigen Proben ist ein Teil der Kalkpartikeln leicht abgerollt und von einer Glasur überzogen. Quarz, Glimmer und Glaukonit treten oft in wechselnder Menge auf. Mit dem Kuttertrawl wurden an einigen Stellen im Bereich der biogenen Kalksandfazies große verfestigte Riffkalkbrocken gewonnen.

Sedimente vor der indisch-pakistanischen Küste

7 Faziesbereiche, deren Grenzen — wie in der ostafrikanischen Region — mehr oder weniger der Küste parallel verlaufen, sind in den Sedimenten von der Tiefsee in Richtung zur Küste festgestellt worden (s. *Abb. 2*):

Globigerinenschlamm

Gelblichbrauner Globigerinenschlamm bedeckt in einem Tiefenbereich von 1730 bis 3670 m den küstenfernen Meeresboden.

Grauer Schlick

Der untere Teil des Kontinentalabhanges zwischen 1920 und 2980 m wird von einem grauen Schlick eingenommen, der zu den hemipelagischen Sedimenten gehört und im Vergleich zum Globigerinenschlamm mengenmäßig weniger pelagische Foraminiferen enthält. Auf der Höhe von Bombay, wo der Kontinentalabhang verhältnismäßig steil ist, konnte dieser graue Schlick nicht nachgewiesen werden. Hier scheint Globigerinenschlamm direkt an die nächste Fazieszone zu grenzen.

Olivgrauer Schlick

Den oberen Teil des Kontinentalabhanges bedeckt ein olivgrauer Schlick, in dem, ähnlich wie beim grauen Schlick, nur relativ wenige pelagische Foraminiferen vorhanden sind. Er fand sich in Tiefen zwischen 220 und 2070 m.

Foraminiferensand

Westlich von Cochin tritt am Schelfrand in 210 m Tiefe ein von dunkelolivbraunem Schlick durchsetzter Foraminiferen-

[10]) *W. Schott*, Die Bodenbedeckung des Indischen und Stillen Ozeans. In: *G. Schott*, Geographie des Indischen und Stillen Ozeans, S. 109/22. Hamburg 1935.

[11]) — —, Deep-sea sediments of the Indian Ocean. In: Recent Marine Sediments, a Symposium, edited by *P. D. Trask*, S. 396/408. Published by Amer. Assoc. Petroleum Geologists, Tulsa 1939; reprinted by Soc. econ. Paleontologists Mineralogists, spec. Publ. Nr. 4, Tulsa 1955.

[12]) — —, Rezente Tiefseesedimente in ihrer Abhängigkeit vom Ozeanwasser. Festschrift zum 60. Geburtstag von Hans Stille, S. 428/37. Stuttgart 1936.

[13]) *G. Dietrich*, Die Internationale Indische Ozean-Expedition. — Die Erde **96**, Nr. 1, 5/20 [1965]. — Die Organisation und Durchführung dieses deutschen Beitrages zu der Internationalen Indischen-Ozean-Expedition lag in den Händen der Deutschen Forschungsgemeinschaft.

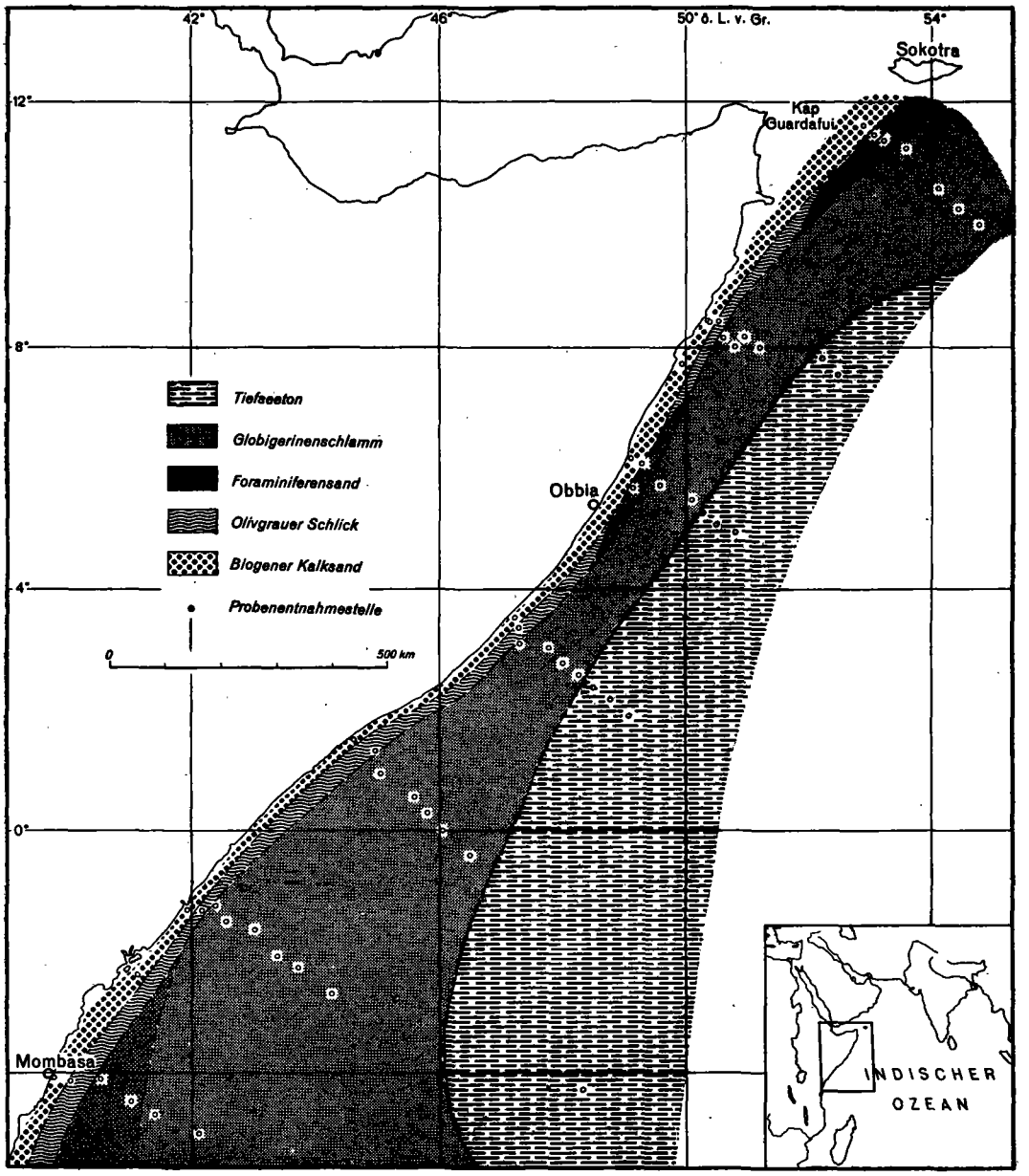

Abb. 1. Sedimentverteilung auf dem Meeresboden vor der ostafrikanischen Küste

sand auf. Er besteht vorwiegend aus pelagischen Foraminiferen der Familie Globigerinidae.

Biogener Kalksand

Im Tiefenbereich von 70 bis 200 m ist ein Kalksand, vermischt mit einer geringen Menge olivgrauen Schlickes, beobachtet worden. Der Kalksand läßt sich in zwei deutlich unterscheidbare Komponenten aufteilen. Die eine setzt sich vorwiegend aus einer guterhaltenen pelagischen Foraminiferenfauna zusammen. Die andere besteht aus abgerollten Bruchstücken dickschaliger Schnecken und Muscheln sowie benthonischer Foraminiferen. Die Bruchstücke sind häufig von einer Glasur überzogen. Charakteristisch für diese Komponente ist außerdem ein oft erheblicher Anteil kugeliger bzw. länglicher Kalkkörper, die mindestens zu einem Teil Koprolithen sein werden. Die Kalkkörper zeigen verschiedentlich eine mehrschichtige Glasur. Ob es sich hierbei um beginnende Ooïdbildung handelt, muß erst noch untersucht werden. Stets ist im Kalksand ein gewisser Prozentsatz an Quarzkörnern vorhanden, in zahlreichen Sedimentproben findet sich auch Glaukonit.

Grauer bis olivbrauner Schlick

An die biogene Kalksandzone schließt sich küstenwärts grauer bis olivbrauner Schlick an. Er tritt in Tiefen zwischen 30 und 90 m auf. Hierin finden sich auf Grund erster Untersuchungen häufig Flachwasserforaminiferen der Gattung Ammonia sowie

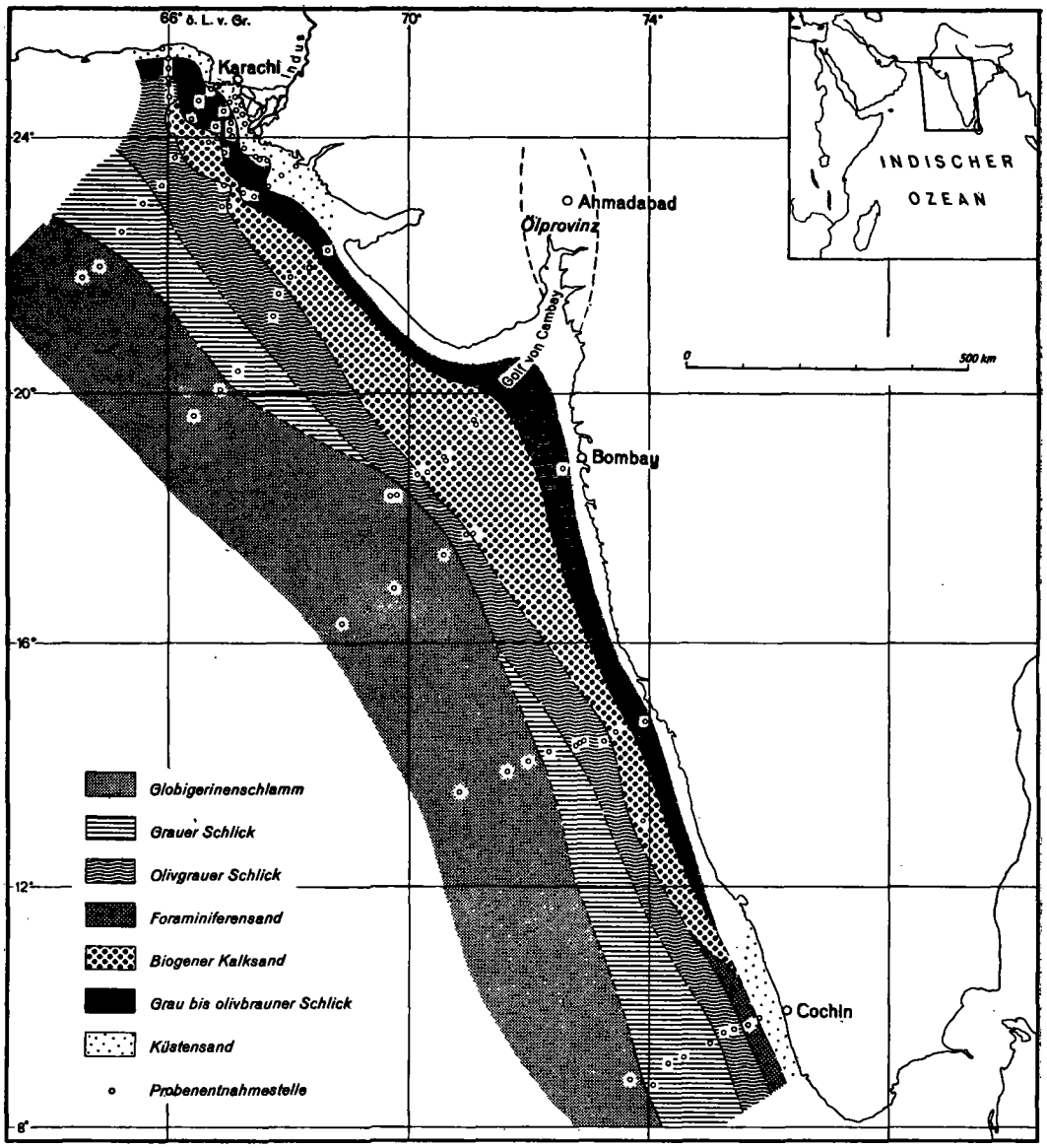

Abb. 2. Sedimentverteilung auf dem Meeresboden vor der indisch-pakistanischen Küste

Diatomeen und eingeschwemmte Reste von Landpflanzen. Pelagische Foraminiferen sind selten.

Küstensand

Über die Faziesausbildung in Strandnähe können Angaben nur aus dem genauer untersuchten pakistanischen Küstengebiet gemacht werden. Entlang der Küste sind hier bis zu einer Tiefe von etwa 30 m graue, z. T. sehr glimmerreiche Quarzfeinsande vorhanden. Glimmerreiche Quarzsande, vermengt mit biogenem Material, wurden außerdem westlich von Cochin in 50 m Wassertiefe angetroffen.

Vergleich der Sedimente beider Meeresregionen

Die Sedimente der beiden Meeresregionen zeigen im großen und ganzen recht ähnliche Faziesverhältnisse. Die Sedimenttypen sind mehr oder weniger an bestimmte Meerestiefen gebunden.

Tiefseeton, wie er im tieferen Teil des Somali-Beckens angetroffen wurde, fehlt in den Profilen der indisch-pakistanischen Region. Die Meerestiefen sind hier zu gering. Globigerinenschlamm reicht in beiden Gebieten etwa bis an den Fuß des Kontinentalabhanges. Foraminiferensande finden sich an mehreren Stellen des ostafrikanischen Kontinentalabhanges in einem Tiefenbereich von 700 bis 1710 m. Ein ähnliches Sediment wurde in der indisch-pakistanischen Küstenregion nur westlich von Cochin am Schelfrand bei 210 m, also in geringeren Meerestiefen, beobachtet. Ob das häufigere Auftreten von Foraminiferensand im Bereich des ostafrikanischen Kontinentalabhanges etwa dadurch verursacht worden ist, daß ein stärkerer Bodenstrom die Ablagerung der feinen tonigen Trübe verhindert, muß noch näher untersucht werden. Der obere Teil des Kontinentalabhanges wird in beiden Regionen meist von olivgrauem Schlick eingenommen. Da der

ostafrikanische Kontinentalabhang i. allg. steiler ist als der indisch-pakistanische, ist der olivgraue Schlick vor Ostafrika nur auf einen sehr schmalen Streifen beschränkt, während er vor Indien und Pakistan einen wesentlich breiteren Raum einnimmt.

Große Unterschiede in ihrer Zusammensetzung und Verbreitung zeigen die biogenen Kalksande beider Regionen. Auf der ostafrikanischen Seite zieht sich ein schmaler Streifen dieses biogenen Sandes, der überwiegend aus Riffschutt besteht, entlang der Küste, der an einigen Stellen Riffe vorgelagert sind. Diese Kalksandzone scheint bis dicht unter die Küste zu reichen. Ihre Breite ist gering, da bereits wenige Seemeilen östlich der Küste der Meeresboden zur Tiefsee abfällt. Auf der indisch-pakistanischen Seite ist der Schelf dagegen wesentlich breiter; der biogene Kalksand nimmt deshalb bei Meerestiefen von 70 bis 200 m eine größere Fläche ein. Das starke Auftreten von abgerollten Bruchstücken biogenen Materials, von Koprolithen sowie fraglichen Ooiden ist für ihn charakteristisch. In Richtung zur Küste geht der biogene Kalksand in einen Flachwasserschlick über. Äquivalente dieses Schlickes konnten auf dem ostafrikanischen Schelf nicht gefunden werden.

Die biogenen Kalksande werfen hinsichtlich ihres Alters und ihrer Entstehung eine Reihe interessanter Fragen auf, die jedoch vorerst offen bleiben müssen, da die Untersuchung des Probenmaterials erst im Anfang steht. Die im Kalksand gefundenen abgerollten Bruchstücke biogenen Materials auf dem indisch-pakistanischen Schelf und die großen verfestigten Riffkalkbrocken vor der ostafrikanischen Küste sind höchstwahrscheinlich nicht rezent, sondern haben pleistozänes Alter.

Subba Rao[14]) erwähnt von der indischen Schelfregion des Golfes von Bengalen „calcareous oolitic sands", die den biogenen Kalksanden, besonders der indisch-pakistanischen Region, in Zusammensetzung und geographischer Position stark ähneln. Er nimmt an, daß es sich hierbei um strandnahe pleistozäne Sedimente handelt, die durch die Meeresspiegelhebung nach der Eiszeit versenkt wurden. Das Fehlen einer Bedeckung mit rezenten Sedimenten erklärt er durch küstenparallele Meeresströmungen.

Stetson[15]) hat schon 1938 das Auftreten von gröberem Material in küstenferneren Sedimenten am Schelfrand vor der Ostküste der Vereinigten Staaten in derselben Weise wie *Subba Rao* gedeutet.

Nach der ersten Durchsicht der Sedimentproben liegen somit auf dem ostafrikanischen und indisch-pakistanischen Schelf ähnliche Verhältnisse vor wie im Golf von Bengalen vor der Ostküste Indiens bzw. in den südlichen Teilen des nordamerikanischen atlantischen Schelfes.

Schlußbemerkungen

Vor allem Beobachtungen in rezenten Flachwassergebieten können Beiträge zur Lösung mancher erdölgeologischer Probleme in fossilen Sedimenten liefern. Die Verteilung des organischen Materials im Wasser und im Sediment spielt dabei eine besonders wichtige Rolle.

Phytoplankton, vorwiegend Diatomeen, sind die Hauptproduzenten der organischen Materie im Oberflächenwasser der heutigen Ozeane. In verschiedenen Meeresräumen, u. a. in der indisch-pakistanischen Küstenregion des Arabischen Meeres, beobachtet man eine starke Verbreitung des pflanzlichen Planktons[16]). Dabei zeigen Gebiete mit aufquellendem kaltem Tiefenwasser eine besonders intensive Entwicklung des Phythoplanktons, da das aufquellende Wasser viele Nährstoffe, wie Phosphate, Nitrate und Silicate, enthält.

Das organische Material, das nach dem Absterben der Organismen auf den Meeresboden absinkt, kann dort nur bei einer gleichzeitigen verhältnismäßig schnellen Sedimentation von anorganischem Material bzw. bei Anwesenheit von O_2-armem oder -freiem Bodenwasser erhalten bleiben. Solche Verhältnisse können an tieferen Teilen des Kontinentalabhanges und in Spezialrinnen und -senken innerhalb des Schelfes auftreten[9]).

Für die Frage einer etwaigen Bildung von Kohlenwasserstoffen aus dem organischen Material ist daher die Bearbeitung der Sedimente am Kontinentalabhang und auf dem Schelf vor allem wichtig. Günstig liegen in dieser Beziehung die Verhältnisse auf der indisch-pakistanischen Seite, da hier der Schelf verhältnismäßig breit ist (stellenweise über 300 km) und der Indus erhebliche Sedimentmassen ins Meer verfrachtet. Westlich von Bombay wurden am Kontinentalabhang bei Tiefen von 480 und 895 m in einem grauen Schlick Gase von unangenehmem fauligem Geruch beobachtet. Diese Gasbildung ist wahrscheinlich auf die Zersetzung von organischem Material zurückzuführen. Ob unter den Zersetzungsprodukten auch gasförmige Kohlenwasserstoffe sind, wie sie z. B. *Weber* u. *Turkeljtaub*[17]) in rezenten Lagunen-Sedimenten des Asowschen Meeres sowie in Ablagerungen des Schwarzen und Kaspischen Meeres gefunden haben, muß noch untersucht werden.

Die Sedimente im Gebiet nordwestlich von Bombay unter dem 20. Grad nördlicher Breite sind von besonderem Interesse, wenn man in die jüngere geologische Vergangenheit des Indischen Ozeans zurückgeht. Nach den großen basaltischen Ergüssen des Dekhantrapps (Kreide—Paläozän) ist während des Eozäns das Meer aus diesem Raum im Zuge der großen Transgressionen gegen das indische Gondwanaland über den heutigen Golf von Cambay nach Norden bis weit über die Stadt Ahmadabad vorgestoßen. Dieser Transgression des tertiären Indischen Ozeans ist die Entstehung der dortigen Erdölprovinz zu verdanken (*Abb. 2*). Mehr als 2000 m tertiäre Sedimente marinen und brackischen bis lagunären Ursprungs bzw. von Deltaschüttungen sind in dieser Erdölprovinz abgelagert worden[18,19,20]). Der Fund von Asphalt in Hohlräumen des Dekhanbasaltes bei Bombay zeigt, daß Erdölbildung in der Küstenregion des tertiären Indischen Ozeans am Rande des Indischen Kontinents nicht nur auf diese Erdölprovinz von Cambay beschränkt war[21]). Im Offshoregebiet des Golfes von Cambay werden daher seit 1963 von der Oil and Natural

[14]) *M. Subba Rao*, Some aspects of Continental Shelf sediments off the East coast of India. Marine Geology 1, Nr. 1, 59/67 [1964].

[15]) *H. C. Stetson*, The sediments of the Continental Shelf off the Eastern coast of the United States. Papers in Physical Oceanography and Meteorology, published by Massachusetts Institute of Technology and Woods Hole Oceanographic Institution, Vol. V, Nr. 4, S. 1/48. Cambridge und Woods Hole 1938.

[16]) *K. O. Emery*, Oceanographic factors in accumulation of petroleum. Proc. 6th Wld. Petroleum Congr., Sect. I, S. 483/91 (Fig. 2). Hamburg 1964.

[17]) *W. W. Weber* u. *N. M. Turkeljtaub*, Die Bildung gasförmiger Kohlenwasserstoffe in rezenten marinen Sedimenten. Wopr. Sediment **1960**, 9/16 (russ.).

[18]) *L. P. Mathur* u. *G. Kohli*, Exploration and development for oil in India. Proc. 6th Wld. Petroleum Congr., Sect. I, S. 633/58. Hamburg 1964.

[19]) *M. C. Poddar*, Geology and oil possibilities of the Tertiary rocks of Western India. Proc. 2nd Symposium on the Development of Petroleum Resources of Asia and the Far East, Mineral Resources Development Series, Nr. 18, Vol. I, S. 226/30. New York 1963.

[20]) *J. F. Pepper*, Prospective contributions of the International Indian Ocean Expedition to Indian Ocean continental shelf geology. Ibid., S. 250/55.

[21]) *C. S. Fox*, The occurrence of bitumen in Bombay Island. Records of the Geological Survey of India, Vol. 54, S. 117/28. Calcutta 1923.

Gas Commission geophysikalische Untersuchungen durchgeführt.

Die Sedimentverteilung vor der pakistanischen Küste im Gebiet des Indus-Deltas näher kennenzulernen, ist gleichfalls für die Erklärung mancher Sedimentationsverhältnisse in fossilen erdölführenden Ablagerungen wichtig. Werden doch z. B. die ölführenden Schichten des Miozän-Pliozän der Halbinsel Apscheron im Kaspischen Meer als Deltabildungen der jungtertiären Flüsse Kura und Wolga angesehen[22]).

Dieser kurze erste Überblick über die heutige Sedimentation in der ostafrikanischen und indisch-pakistanischen Meeresregion des Indischen Ozeans hat somit bereits einige Anhaltspunkte über die Entstehung kohlenwasserstoffhaltiger fossiler Sedimente erbracht. Die detaillierte Ausarbeitung wird sicherlich weitere Hinweise liefern.

Die systematische Sammlung des Sedimentmaterials vor der ostafrikanischen Küste wurde durch die Herren Dr. *H. E. Reineck* und Dr. *W. F. Gutmann* von der Forschungsanstalt für Meeresgeologie und Meeresbiologie „Senckenberg", Wilhelmshaven, und durch den zuerst genannten Verf. dieses Berichtes vorgenommen, vor der indisch-pakistanischen Küste und im Gebiet des Indus-Deltas von den beiden Verfassern. Im Mündungsgebiet des Indus war außerdem der Geologe Herr *R. Islam* von der Geological Survey of Pakistan daran beteiligt. Die deutsch-pakistanische Gemeinschaftsarbeit vor der Indus-Mündung wurde von der Deutschen Forschungsgemeinschaft unterstützt.

[22]) *H. G. Kugler*, A visit to Russian oil districts. J. Inst. Petroleum **25**, 68/88 [1939].

Reprinted from *Erdöl und Kohle-Erdgas-Petrochemie*, 19 Jahrgang, Nr. 4, 1966, S. 237-243.

Seismische Untersuchungen im nördlichen Teil des Arabischen Meeres (Golf von Oman)

*Von Herwald Bungenstock, Hans Closs und Karl Hinz**)

Vorgetragen von H. Closs auf der 17. Jahrestagung der Deutschen Gesellschaft für Mineralölwissenschaft und Kohlechemie in Hannover, am 8. Oktober 1965

Zusammenfassung: Mit der im Jahre 1964 erfolgten Indienststellung des neuen Forschungsschiffes „Meteor" wurde es der Bundesrepublik Deutschland ermöglicht, die seit langem geplante Beteiligung an einer internationalen Gemeinschaftsarbeit zur Untersuchung des Indischen Ozeans (International Indian Ocean Expedition) zu verwirklichen. Im Rahmen des deutschen Beitrags wurden u. a. seismische Untersuchungen im zentralen Teil des Golfes von Oman ausgeführt, über die berichtet wird. Registriert wurde auf „Meteor" und mittels eines Hubschraubers, der zur Expeditionsausrüstung gehörte. Die Schießarbeiten wurden von einem Beiboot der „Meteor" ausgeführt. Es ergaben sich unter rd. 3000 m Wasserbedeckung eine Sedimentschicht von mehr als 4000 m Mächtigkeit und Geschwindigkeiten von weniger als 2000 m/s bis zu mehr als 4000 m/s.

Seismic tests in the northern part of the Arabian Gulf: After taking over, in 1964, the new research ship „Meteor", the Federal Republic could realise the long standing plan to participate in the international investigation program for the Indian Ocean (International Indian Ocean Expedition). The German contribution consisted, amongst other matters, in seismic tests in the central part of the Gulf of Oman. Seismic data were recorded aboard the „Meteor" and by a helicopter which was a part of the expedition's equipment. The shooting was carried out from a tender belonging to the „Meteor". Layers of sediments with a thickness of more than 4000 m and wave travelling speeds of less than 2000 m/sec up to more than 4000 m/sec were found in a water depth of abt. 3000 m.

1. Einleitung

Mit der Indienststellung des neuen Forschungsschiffes „Meteor" im Jahre 1964 wurde nunmehr auch eine deutsche Beteiligung an dem Programm der Internationalen Indischen-Ozean-Expedition möglich. Diese Beteiligung an dem Forschungsunternehmen wurde durch Bereitstellung von Mitteln der Bundesregierung und der Deutschen Forschungsgemeinschaft finanziert.

Marine Seismik ist innerhalb des vielseitigen Forschungsprogramms der „Meteor" auf einigen Profilen im Golf von Cambay, im Golf von Kutch und im nördlichen Teil des Arabischen Meeres durchgeführt worden. Soweit Untersuchungen in der Tiefsee durchgeführt worden sind, handelt es sich um die ersten deutschen Arbeiten dieser Art. Über die Forschungen im Golf von Oman soll hier berichtet werden**).

2. Lage des Untersuchungsgebietes

Der Golf von Oman (*Abb. 1*) ist der nordwestliche Teil des Arabischen Meeres, an den sich nach NW der Persische Golf anschließt. Der Golf von Oman stellt eine etwa dreieckförmige abyssische Ebene mit maximalen Wassertiefen über 3000 m dar. Im SE wird der Golf von Oman durch den Murray-Ridge, einen etwa NE—SW verlaufenden untermeerischen Rücken, der an einigen Stellen von über 3000 m Tiefe bis zu 500 m unter NN aufsteigt, von dem übrigen Arabischen Meer abgetrennt.

3. Zur Meßmethodik

Die Profile waren als refraktionsseismische Messungen angelegt. Die Entfernungsbestimmung wurde nach Möglichkeit mit dem an Bord der „Meteor" installierten Wind-Wetter-Radar vorgenommen. Für die seismischen Arbeiten im Arabischen Meer war das Forschungsschiff u. a. mit einem Hubschrauber ausgerüstet. Es seien nachfolgend die verschiedenen Einsatzmöglichkeiten eines Hubschraubers, der seismische Registrierungen im Schwebeflug vornimmt, aufgeführt (*Abb. 2, 3*). Von Erdölgesellschaften sind für die übliche marine Reflexionsseismik vor allem große Hubschrauber schon mehrfach eingesetzt worden.

Bei der zurückliegenden Meteorreise sind nicht alle hier beschriebenen Möglichkeiten angewandt worden, aber die bei den Einsätzen gesammelten Erfahrungen werden hier mit benutzt. Bei der Arbeitsweise a liegt der Schußpunkt fest. Der Hubschrauber fliegt auf dem Profil zum Registrieren von einem Beobachtungspunkt zum anderen, wobei Abstände von etwa 1000 m eingehalten werden. Nachteile dieser Arbeitsweise liegen darin, daß ein größeres Schiff schon bei geringen Windstärken vertriftet. Da der Abstand Schiff—Sprengladung bei größeren Ladungen mehrere 100 m betragen muß, sind zeitraubende Schiffsmanöver notwendig. Wenn das Schießboot ankern kann und starke Strömung herrscht, die das Auslegen der Ladung erleichtert, hat dieses Verfahren Vorzüge, also z. B. bei seismischen Aufnahmen von Schelfgebieten mit starken Gezeitenströmen. Zur Aufnahme eines vollständig hin- und rückgeschossenen Profils muß das Schiff einmal seine Position ändern, was bei einer Marschgeschwindigkeit von 10 Knoten etwa 2,5 Stunden in Anspruch nimmt. Die unter a) gezeichnete Aufnahme ist weniger vollständig, doch ist die bearbeitete Länge des Profils etwas größer. Diese Art der Aufnahme von Richtung und Gegenrichtung ist in tektonisch ruhigen Gebieten zu verantworten.

Das Ausschießen des Profils mit Hin- und Rückschüssen in Abständen von 1 km würde 23 Einsatzstunden erfordern, vorausgesetzt, daß sich der Hubschrauber 2 Stunden ohne Unterbrechung in der Luft halten kann und seine Geschwindigkeit bei 100 km/h liegt. Dazu kommen noch 2,5 Stunden für den Positionswechsel, der mit der Aufnahme eines Echolotprofils verbunden werden muß. Da nur bei Tag geschossen werden kann, benötigt also ein so ausgeschossenes Profil zwei volle Arbeitstage.

Die Arbeitsweise b ist i. allg. vorteilhafter, vor allem auf dem offenen Ozean. Durch Setzen einer Markierung, z. B. Abwerfen von Farbstoff, wird eine Beobachtungsstelle für den Hubschrauber markiert. Das Schiff bewegt sich — wobei sich eine Fahrtgeschwindigkeit von 4 kn bei 1000 m Schußpunktabstand bewährt hat — in Profilrichtung auf den Hubschrauber zu, der immer an derselben Stelle registriert. Entweder wird das Profil wie unter b gezeichnet ausgeschossen, oder das Schießboot hat das gleiche Profilstück zweimal zu durchfahren, während der Hubschrauber zunächst an einem und dann am anderen Profilende registriert. Vorteile dieses Verfahrens sind, daß eine auf der Meeresoberfläche markierte Stelle unter Windeinfluß nur wenig vertriftet, die Peilung zum Hubschrauber gleich bleibt, während der Arbeitsfahrt das Bodenprofil ausgelotet wird und die Beobachtungs- bzw. Schußintervalle gut eingehalten werden können. Die Sprengladungen lassen sich leicht ausbringen. Die Einsatzzeit für das vollständige Hin- und Rückschußprofil beträgt insgesamt etwa 18 Stunden. Da auch eine spezielle Fahrt für die Echolotung entfällt, können etwa 7 Arbeitsstunden eingespart werden, und das seismische Gesamtergebnis ist meist besser. Zwar ist die Arbeitszeit — wie man sieht — kürzer geworden, doch erfordert das Profil immer noch zwei Arbeitstage.

Bei der Arbeitsweise c beobachtet der Hubschrauber jeweils abwechselnd an zwei Punkten, die 5 oder 6 km Abstand in der Profillinie haben, während sich das Schießboot von einem

*) Anschriften: Dipl.-Geophys. H. Bungenstock, Niedersächsisches Landesamt für Bodenforschung, 3 Hannover-Buchholz, Alfred-Bentz-Haus. — Ltd. Direktor und Professor Dr. H. Closs, Bundesanstalt für Bodenforschung, 3 Hannover-Buchholz, Alfred-Bentz-Haus. — Dr. K. Hinz, Bundesanstalt für Bodenforschung, 3 Hannover-Buchholz, Alfred-Bentz-Haus.

**) Vorausbericht aus den „Meteor-Forschungsberichten" der Expedition 1964/65 in den Indischen Ozean.

Endpunkt des Profils beginnend kontinuierlich fortbewegt und ebenso wie bei den anderen Arbeitsweisen nur dann stoppt, wenn der Hubschrauber zur Versorgung auf das Mutterschiff zurückkehren muß. Man kann die Schußfolge zumindest in gewissen Bereichen der Laufzeitkurve etwas dichter wählen, um die von den Beobachtungspunkten I und II ausgehenden Linien ausreichend mit Registrierpunkten zu besetzen. Das Ergebnis sind zwei voneinander unabhängige Laufzeitkurven, aufgenommen für die gleiche Beobachtungsrichtung. Aus dem Vergleich dieser beiden Kurven ist bekanntlich abzuleiten, ob und in welcher Richtung eine Schichtneigung vorliegt, sofern ebene Schichtgrenzen im Untergrund angenommen werden dürfen. Mit anderen Worten, es ergibt sich unter gewissen Annahmen vor allem dann, wenn spätere Einsätze sicher korreliert werden können, die Möglichkeit der Konstruktion eines hypothetischen Gegenschusses, für dessen Laufzeitkurve für jeden Geschwindigkeitsast allerdings nur zwei Konstruktionspunkte gegeben sind. Wenn man sich mit dieser Information begnügen kann, wird gegenüber a und b ein vollerArbeitstag eingespart, da die erforderliche Gesamtarbeitszeit nur 9 Stunden beträgt.

Auch für die Arbeitsweise a ist eine sehr ähnliche Variante möglich. Das Schießboot läuft während des Schießens auf einer Kreisbahn, die einen Umfang von bspw. 2000 m hat. Jedesmal, wenn das Boot die Profillinie überfährt, wird eine Ladung gezündet. Es entsteht dann ebenfalls ein Laufzeitkurvenpaar, das von zwei Schußpunkten herrührt, die in unserem Beispiel einen Abstand in Profilrichtung von rd. 650 m haben. Zur Neigungskontrolle mit Hilfe eines konstruierten Gegenschusses könnte dieser Abstand gerade noch ausreichen. Bei dieser Arbeitsweise könnte das Profil a in der einen Richtung in 9 Stunden Arbeitszeit plus 2,5 Fahrtstunden für die Echolotung aufgenommen werden. Auch wenn man die Beobachtungsfolge etwas dichter als 1 km anlegt, um beide Kurvenäste ausreichend zu besetzen, könnte somit das Profil an einem Tag seismischer Arbeit erledigt werden. Das Abloten könnte in die Nachtstunden verlegt werden. Arbeitstechnisch schwierig ist es nur, dem Hubschrauber durch geeignete Radarmessung vom Schiff aus seine Position so durchzugeben, daß das Profil gleichmäßig und wie gewünscht mit Beobachtungspunkten besetzt wird.

Eine wesentliche Änderung tritt ein, wenn außer dem Hubschrauber zusätzlich ein Schießboot S 2 zur Verfügung steht. Von der „Meteor" aus wurde bei guten Wetterlagen ein Verkehrsboot mit 8 t Wasserverdrängung als Schießboot eingesetzt. Als Erweiterung der Arbeitsweise c ergibt sich dann eine Kombination d, bei der das Schiff S 1 als Registrier- und Hubschraubermutterschiff seine Position beibehält und der Hubschrauber in Entfernungen von 10 bis 15 km vom Schiff S 1 wechselweise registriert. Es würde in unserem Beispiel genügen, das Profil, auf welchem die Sprengpunkte liegen, etwa auf 34 km oder noch etwas mehr zu reduzieren. Wenn dann in Abständen von 1 km gesprengt würde, ergäbe sich eine Arbeitszeit von 7 Stunden und für den Hubschrauber eine Flugzeit von etwa 6 Stunden. Für die Konstruktion des Gegenschusses stehen für jeden Geschwindigkeitsast 3 Punkte zur Verfügung. Der Sprengstoffverbrauch beträgt bei 40 kg Einheitsladung und 1 km Schußpunktabstand jetzt 1,4 t gegenüber 3,3 t im Fall a oder b. Zur Aufnahme des Reliefs des Meeresbodens muß weiterhin die Gesamtprofilstrecke abgelotet werden, was in unserem Fall einer Fahrtstrecke von 64 km, also etwa 3,5 Stunden Fahrtzeit, entsprechen würde. Auch in diesem Fall ist nur ein Tag für die seismische Aufnahme des Profils erforderlich.

Im Fall e verbleiben sowohl das Hubschraubermutterschiff S 1 als auch der Hubschrauber an einem Ende des Profils. Es ergibt sich dann durch die Fahrt des Schießbootes S 2 ein Profil, das seismisch vollständig aufgenommen ist. Die Arbeits-

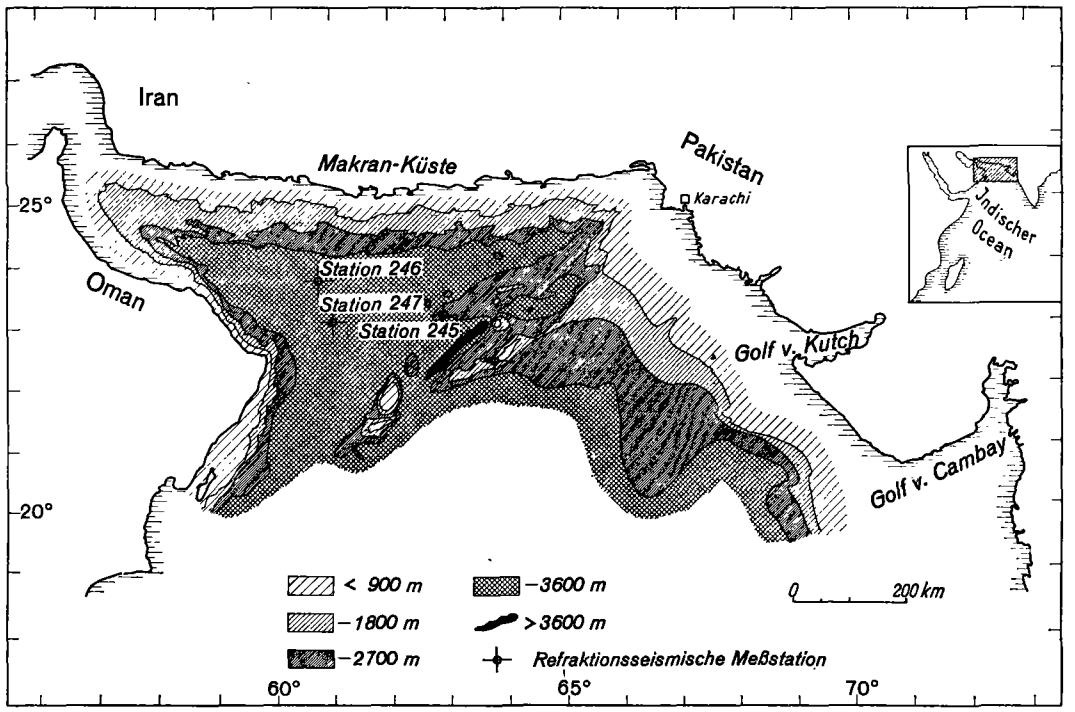

Abb. 1. Lageplan der refraktionsseismischen Meßstationen mit bathymetrischer Übersichtskarte „Arabisches Meer"

zeit beträgt etwa 9 Stunden, hinzu kommen 2,5 Stunden für das Abloten des Profils. Wenn das Schießboot auch Mutterschiff des Hubschraubers ist und somit gleichzeitig eine große Echolotanlage führt, das Beiboot dagegen für die Registrierung am Profilende benutzt wird, kann die gesamte Arbeitszeit um das Ablaufen des Profils für Lotungszwecke, also 2,5 Stunden, verkürzt werden.

Die größte Profillänge, die bisher bei der Entwicklung dieses Meßverfahrens mit dem Hubschrauber beflogen worden ist, war 80 km.

Bis jetzt war nur von Refraktionsaufnahmen die Rede. Es scheint jedoch möglich zu sein, auch Reflexionen auf größere Entfernungen hin zu verfolgen. Dafür ist es notwendig, Teile von Profilen mit geringeren Schußpunktabständen zu belegen, z. B. im Fall d die Strecke zwischen S 1 und Hubschrauber Position I. Wenn es gelingt, Hyperbel-Äste von Reflexionen — bzw. angenäherte Hyperbeln bei mehrschichtigem Aufbau — über 10 km Entfernung zu verfolgen, dann kann über den Aufbau des Untergrundes gerade jener Bereiche sehr viel ausgesagt werden, die häufig mit Refraktion nicht oder nur sehr summarisch beurteilt werden können. Zumindest kann die Kombination von Reflexion und Refraktion recht wertvolle Aufschlüsse geben.

In unserem Fall sind in den Tiefseebereichen häufig außer einigen normalen Reflexionen auch eine erste multiple Serie und eine zweite multiple Serie beobachtet worden, wobei Wasseroberfläche und Meeresboden oder eine Schicht nahe am Meeresboden als Refraktoren dafür dienen. Es hängt also von der Wassertiefe ab, welche Zeitspanne für einfache Reflexionen zur Verfügung steht, bevor die erste multiple Reflexionsserie beginnt, das Reflexionsbild überdeckt und dieses einer weiteren Analyse entzieht. Da bei den multiplen Serien die Zeitabstände zweier aufeinanderfolgender Reflexionen entsprechend vergrößert werden, kann man dies in günstigen Fällen als eine Erweiterung des Auflösungsvermögens speziell für die allerobersten Reflexionshorizonte ausnutzen. Im Grundsatz müßte es möglich sein, dadurch Anhaltspunkte über die Geschwindigkeitsverhältnisse innerhalb dieser Schichten zu gewinnen.

Für die Messungen standen zwei Hall-Sears-Apparaturen, Modell HS-300, zur Verfügung; Filterabfall 18 db/octave.

Die refraktierten Einsätze zeichneten sich durch Frequenzen um 20 Hz aus, wohingegen die Bodenreflexion ähnlich der direkten Welle mehr hochfrequente Anteile aufweist.

4. Zur Auswertung

Die Laufzeit-Weg-Diagramme der Stationen im Golf von Oman zeigen hyperbolische Reflexionskurven und refraktierte Laufzeitäste. Es ist auffällig, daß in allen diesen Laufzeit-Weg-Diagrammen bisher kein tangential zur Bodenreflexion verlaufender Laufzeitast gefunden wurde. Dies kann davon herrühren, daß die Geschwindigkeit im oberen Sediment etwa gleich der Ausbreitungsgeschwindigkeit longitudinaler Wellen im Wasser ist. Das Vorhandensein reflektierter Einsätze vom Meeresboden macht dagegen deutlich, daß Unterschiede in der Schallhärte vorliegen müssen. Da auch für noch etwas spätere Reflexionen die korrespondierenden refraktierten Laufzeitäste

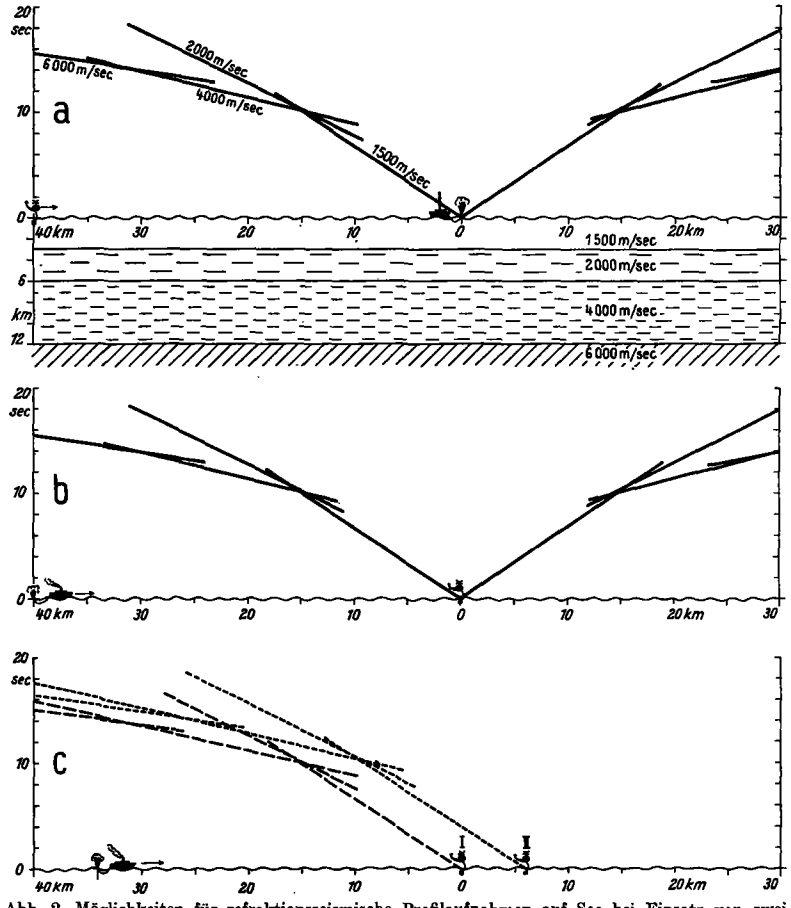

Abb. 2. Möglichkeiten für refraktionsseismische Profilaufnahmen auf See bei Einsatz von zwei Arbeitsgruppen: a) Das Schießboot operiert stationär, während der Meßhubschrauber die Profilstrecke abfliegt. — b) Die Registriereinheit arbeitet stationär; das Schießboot läuft die Profilstrecke ab. — c) Das Schießboot läuft die Profilstrecke ab; der Meßhubschrauber bedient abwechselnd zwei etwa 5 bis 6 km auseinanderliegende Registrierpositionen

zu fehlen scheinen, kann angenommen werden, daß die entsprechenden reflektierenden Horizonte entweder sehr dünn sind, oder daß nur Unterschiede in der Schallhärte vorliegen. Es liegt nahe, in einem solchen Fall eine weitgehend kontinuierliche Zunahme der Geschwindigkeit mit der Tiefe anzunehmen.

Bei einer linearen Zunahme der Geschwindigkeit mit der Tiefe im Sediment sind die Wellenstrahlen bekanntlich Kreisbögen (*Abb. 4*).

Für eine bestimmte Wassertiefe und einen bestimmten Wert für die Ausbreitungsgeschwindigkeit longitudinaler Wellen gibt

es eine kritische Mindestentfernung, bei der ein von der Meeresoberfläche ausgehender und ins Sediment laufender Wellenstrahl zur Oberfläche zurückkommen kann. In Bereichen, die größer als die kritische Entfernung sind, werden 2 Einsätze beobachtet. Der eine, hier mit R_D bezeichnet, entspricht einem

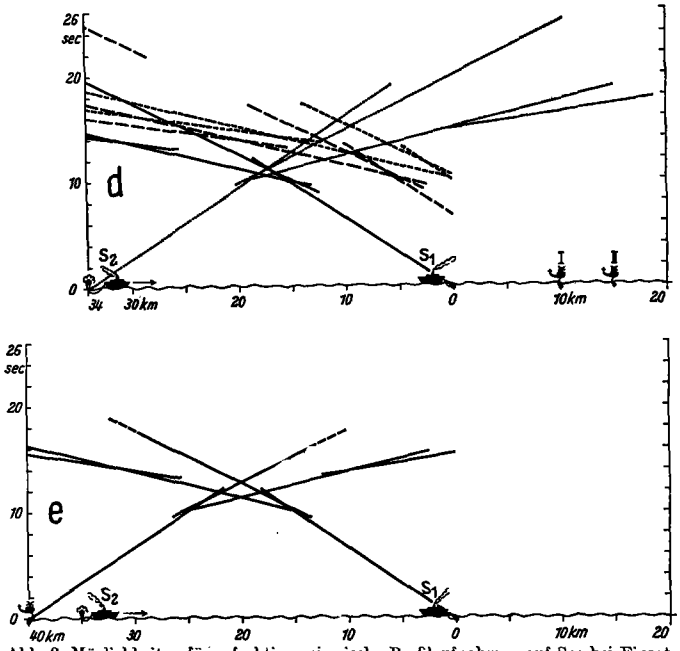

Abb. 3. Möglichkeiten für refraktionsseismische Profilaufnahmen auf See bei Einsatz von drei Arbeitsgruppen: d) Das Hubschrauberträgerschiff wird als stationäre Registriereinheit eingesetzt; der Meßhubschrauber bedient abwechselnd zwei etwa 5 bis 6 km auseinanderliegende Registrierpositionen; das Schießboot läuft die Profilstrecke ab. — e) Das Hubschrauberträgerschiff steht stationär als Registriereinheit am Anfang des Profiles; der Meßhubschrauber besetzt das Profilende, während das Schießboot die Profilstrecke abläuft

tief ins Sediment eintauchenden Strahl, wohingegen der andere, hier mit R_S bezeichnet, von einem nur wenig ins Sediment eintauchenden Strahl herrührt. Der tiefer eintauchende Wellenstrahl kommt früher an, da er den größten Teil des Weges durch ein Medium mit höherer

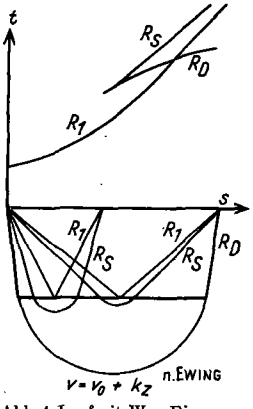

Abb. 4. Laufzeit-Weg-Diagramm am Meeresboden reflektierter Wellen nach *Ewing*

Geschwindigkeit läuft. Eine so beschaffene Schicht liefert also zwei verschiedene Laufzeitäste zusätzlich zur Bodenreflexion.

Mit Hilfe eines Rechenprogramms wurden für bestimmte Wassertiefen und bei verschiedenen Ausbreitungsgeschwindigkeiten im oberen Sediment die Laufzeiten in Abhängigkeit von der Entfernung berechnet und zu Laufzeitdiagrammen zusammengestellt (*Abb. 5*). Bei Annahme einer linearen Zunahme der Geschwindigkeit mit der Tiefe läßt sich durch Vergleich der theoretischen Kurven mit den gemessenen Kurven die Geschwindigkeitsfunktion im oberen Sediment näherungsweise bestimmen.

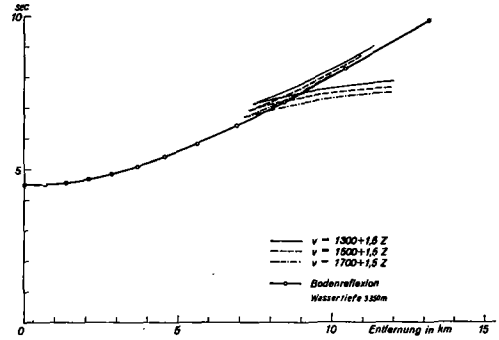

Abb. 5. Laufzeit-Weg-Diagramm für drei berechnete Geschwindigkeitsfunktionen nach *Hinz* u. *Stein*

Für die Stationen im Golf von Oman kann auf diese Weise die Geschwindigkeitsfunktion für die oberen Sedimente etwa mit $V = 1300 + 1{,}5\ Z$ angegeben werden. Diese Anfangsgeschwindigkeit erscheint jedoch gering, zumal Testmessungen an Sedimentproben aus dem Golf von Oman, die Herr Professor Dr. *E. Seibold*, Kiel, uns freundlicherweise zur Verfügung stellte und die von Herrn Dr. *W. Giesel* untersucht worden sind, Werte um 1500 m/s ergaben. Deshalb wurden zusätzlich alle korrelierbaren Reflexionseinsätze zur Bestimmung der Geschwindigkeiten im oberen Sedimentpaket benutzt. Dabei erfolgte eine erste Auswahl dahingehend, daß spätere Reflexionen mit starker Hyperbelkrümmung, also offensichtlich multiple, nicht berücksichtigt wurden. Mit Hilfe eines Rechenprogramms wurden zunächst unter Vernachlässigung der Brechung und mit Anwendung der Methode der kleinsten Quadrate Durchschnittsgeschwindigkeiten nach der $T(x)^2$-x^2-Methode ermittelt und dann die wahren Schichtgeschwindigkeiten nach *Dürbaum**) bestimmt. Das so erhaltene stufenförmige Geschwindigkeitstiefendiagramm (*Abb. 6*) wurde durch eine lineare Geschwindigkeitsfunktion angenähert. Eine noch engere Anlage der Meßpunkte, zumindest im ersten Teil des Profils, würde die Auswertung der Reflexionen wesentlich erleichtert haben.

Die Geschwindigkeitsfunktion für die oberen Sedimente im Bereich der Stationen 245, 246 und 247 läßt sich unter der Annahme einer linearen Zunahme der Geschwindigkeit mit der Tiefe durch Kombination der vorherbeschriebenen Verfahren näherungsweise mit $V = 1400 + 1{,}5\ Z$ angeben.

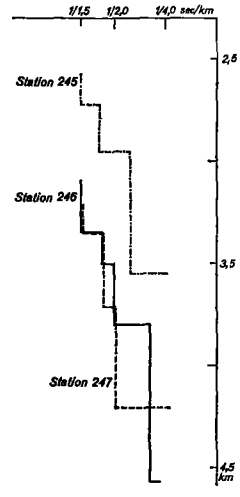

Abb. 6. Geschwindigkeits-Tiefen-Diagramm nach *Closs* u. *Hinz*

*) Literaturverzeichnis am Schluß der vorliegenden Arbeit.

5. Meßergebnisse

a) Die Station 247 liegt im zentralen Teil des Golfs von Oman bei einer Wassertiefe von über 3000 m (*Abb. 8*). Das Laufzeit-Weg-Diagramm zeigt Laufzeitäste von reflektierten und refraktierten Wellen. Ein tangential zur Bodenreflexion verlaufender Laufzeitast wurde nicht gefunden (s. o.).

Unter der 3350 m mächtigen Wasserschicht scheint eine etwa 1,0 km dicke Sedimentschicht mit $V = 1400 + 1{,}5\ Z$ zu liegen. Darunter folgt eine 1,7 km dicke Schicht mit einer Geschwindigkeit von 3,2 km/s, die von einer 2,7 km mächtigen Schichtserie mit einer Geschwindigkeit von 4,0 km/s unterlagert wird.

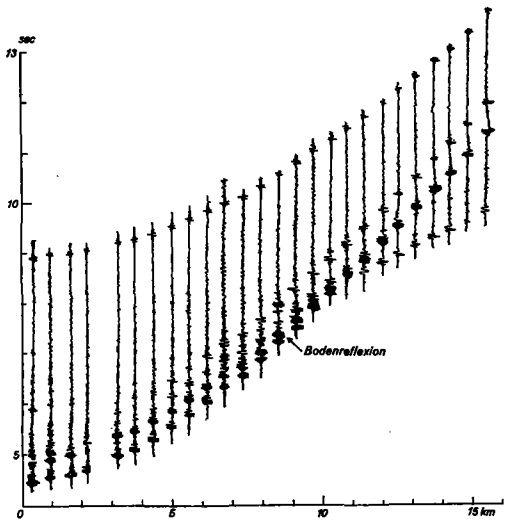

Abb. 7. Laufzeitdiagrammzusammenstellung „Station 247 Golf von Oman"

Das Liegende bildet Material mit $V = 6{,}0$ km/s, das als Kristallin angesehen werden kann.

b) Die Station 246 liegt ebenfalls im zentralen Teil des Golfs von Oman. Wie bei der vorhergehenden Station, ergeben sich wiederum (*Abb. 9*) mehrere Reflexionslaufzeitkurven ohne die entsprechenden refraktierten Laufzeitäste.

Die Mächtigkeit der ersten Sedimentschicht beträgt 1,4 km. Darunter folgt ein 1,5 km dickes Schichtpaket mit einer Geschwindigkeit von 3,5 km/s und weiter eine 5,3 km dicke Schicht mit einer Geschwindigkeit von 4,25 km/s. Das Liegende bilden wahrscheinlich kristalline oder metamorphe Gesteine mit einer Geschwindigkeit von 6,3 km/s. Im NE-Teil des Profils findet sich eine Versetzung im Laufzeitdiagramm, die nur durch eine größere Verwerfung, d. h. durch eine Absenkung nach NE, erklärbar ist.

c) Die Station 245 liegt an den nordwestlichen Ausläufern des Murray-Ridge. Die Wassertiefe beträgt 2750 m. Die Mächtigkeit der oberen Sedimentschicht wurde mit 1,0 km bestimmt. Es folgt eine 1,8 km dicke Schichtserie mit einer Geschwindigkeit von 2,95 km/s und eine 2,45 km mächtige Schicht mit einer Geschwindigkeit von 4,6 km/s.

Das Liegende bildet ein Gesteinskomplex mit $V = 6{,}9$ km/s (*Abb. 10*). Die Annahme, daß es sich hier um basisches Kristallin handelt, scheint berechtigt.

Soweit die Tatsachen (vgl. *Zahlentafel 1*). Sie sind spärlich genug für ein Areal der Größenordnung von 100 000 km². Da sich aber Sedimentmächtigkeiten ergeben haben, die untypisch für Ozeanböden unter mehr als 3000 m Wasserbedeckung sind, kommt man an einer grundsätzlichen geologischen Diskussion dieses geophysikalischen Befundes nicht vorbei, so spekulativ sie auch sein mag.

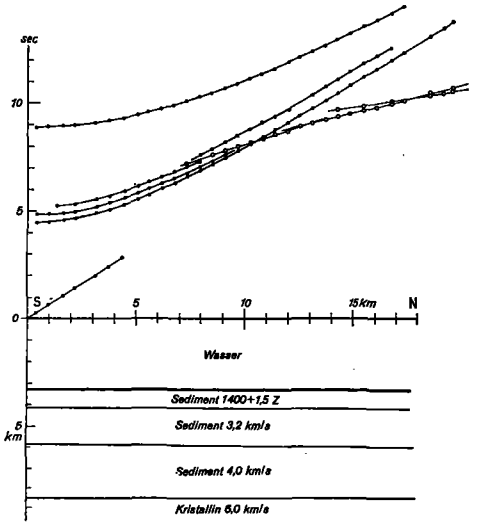

Abb. 8. Laufzeit-Weg-Diagramm „Station 247 Golf von Oman" nach *Closs* u. *Hinz*

6. Versuch einer geologischen Deutung

Der Golf von Oman findet (s. o.) seinen Abschluß mit dem NE streichenden Murray-Ridge, der sich mit einiger Wahrscheinlichkeit in das nördlich Karachi verlaufende Kirthar-Gebirge (auch „Axial Belt" genannt) fortsetzt (*Abb. 11*). Innerhalb des „Axial Belt" ist an zahlreichen Stellen basisches Kristallin (Ophiolithe) nachgewiesen worden (im übrigen auch im Oman-Gebirge). Die Bildung des „Axial Belt", der als geantiklinalartiges Element (*Zuberi, Rahmann*) angesehen wird, setzte wohl in der Jurazeit ein und dauerte im Tertiär an. Der „Axial Belt" teilte das ehemalige einheitliche Sedimen-

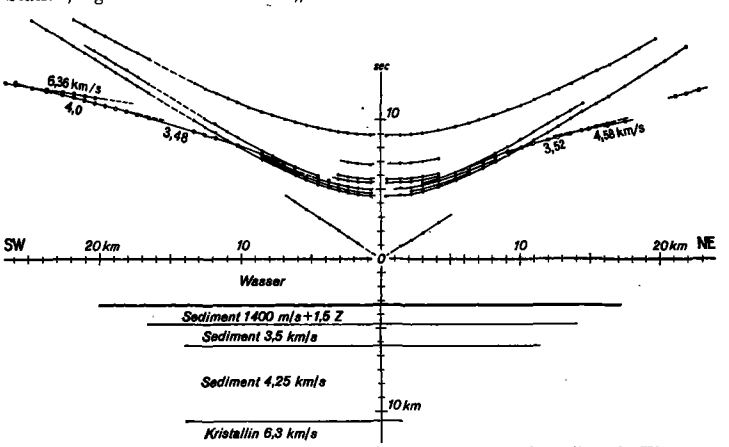

Abb. 9. Laufzeit-Weg-Diagramm „Station 246 Golf von Oman" nach *Hinz*

tationsgebiet Westpakistans in das Indus-Becken im E und das Baluchistan-Becken im W.

In *Abb. 11* wurden die Meßergebnisse zu Profilschnitten zusammengestellt. Allen Stationen ist folgender Schichtenaufbau gemeinsam: Unter einer Deckschicht mit niedriger Geschwindigkeit folgt eine Schichtserie mit einer Geschwindigkeit von 2,95 bis 3,5 km/s, die von einem Schichtpaket mit einer Geschwindigkeit von 4,0 bis 4,6 km/s unterlagert wird. Das Liegende bildet in allen Fällen ein Gesteinsverband mit $V < 6{,}0$ km/s.

Die starke Mächtigkeitsreduktion des Schichtpaketes mit einer Geschwindigkeit von etwa 4 km/s zwischen den Stationen 246 und 247 deutet auf Hebung des Bereiches östlich der Station 246 hin (*Abb. 11*, A). Auch die Korrelation des tiefsten nachgewiesenen Gesteinsverbandes mit $V = 6$ km/s ist zwischen den Stationen 246 und 247 nur bei Annahme einer größeren Verwerfung möglich, die etwa z. Z. der Ablagerung der Sedimente mit $V \approx 4{,}0$ km/s angelegt worden sein könnte.

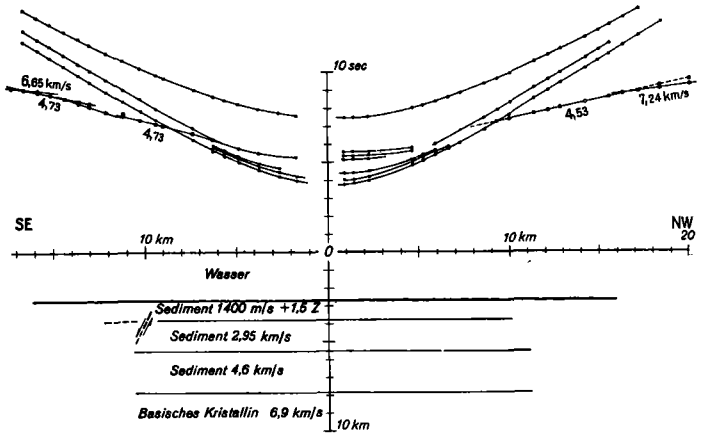

Abb. 10. Laufzeit-Weg-Diagramm „Station 245 Golf von Oman" nach *Hinz*

Aufschlüsse innerhalb der Makran-Küste in Westpakistan werden als Hinweise für die stratigraphische Zuordnung der refraktionsseismisch ermittelten Gesteinsverbände benutzt. Die ältesten Gesteine, die im Gebiet der Makran-Küste bekannt geworden sind (*Rahmann*), sind kretazische (Parh) Mergel (*Abb. 11*, B), die von paleozänen Konglomeraten (Isphikan-Konglomerat) überlagert werden. Darüber folgen eozäne Kalke (der Wakai-Serie). Mit dem Oligozän wurden vorwiegend flyschartige Sedimente (Pungjur- und Parkini-Serie) abgelagert. Im Miozän und Pliozän wurde vorwiegend klastisches Material sedimentiert.

Beim gegenwärtigen Stand der Überlegungen möchte man das Ende der kalkigen Sedimentation (d. h. Top der Wakai-Serie) mit dem Top der Schichtserie gleichsetzen, die durch eine Geschwindigkeit von etwa 4 km/s charakterisiert ist. Der Schichtverband mit einer Geschwindigkeit von etwa 3,3 km/s könnte der Oligozän-Serie entsprechen, wohingegen die oberste seismisch nachgewiesene Sedimentschicht mit klastischen miozänen und pliozänen Ablagerungen identifiziert werden könnte.

Unter dieser Voraussetzung ist eine Korrelation der im Makranbereich nachgewiesenen stratigraphischen Einheiten mit den refraktionsseismisch ermittelten Schichtverbänden nur unter Annahme bedeutender Verwerfungen im Schelfbereich bzw. Kontinentalabfall der Makranküste möglich.

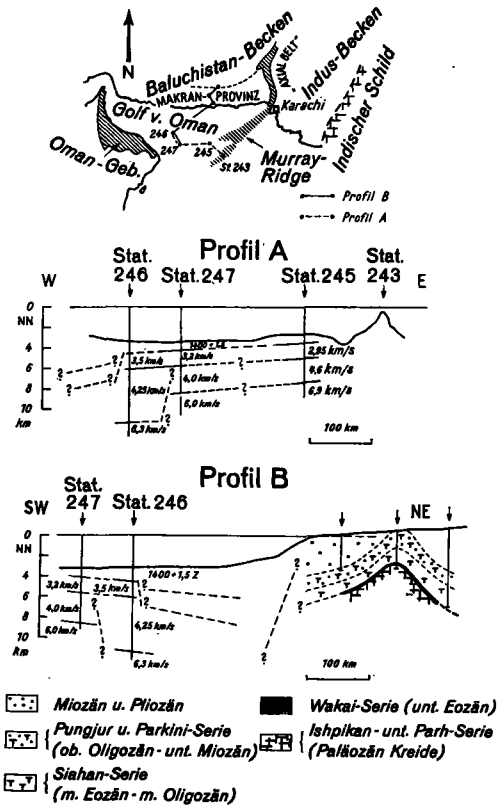

Abb. 11. A: Schematischer Profilschnitt W—E (Golf von Oman) nach *Hinz*. — B: Schematischer Profilschnitt SW—NE (Golf von Oman) nach *Hinz*

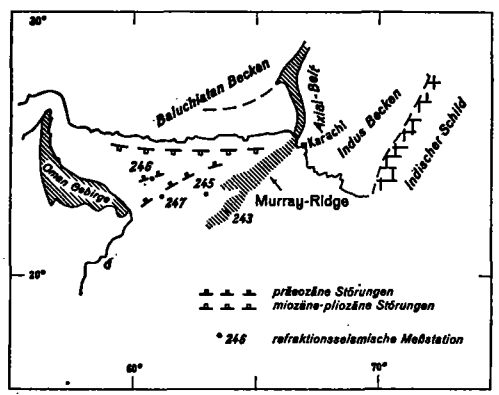

Abb. 12. Strukturskizze (Nordteil des Arabischen Meeres) nach *Hinz*

In Analogie zum Axial-Belt könnte jurassisches bzw. kretazisches Alter für den Murray-Ridge angenommen werden. Im Zusammenhang mit der Hebung dürften in der Nähe des Murray-Ridge größere Verwerfungen angelegt worden sein. Im Laufe des Tertiärs vertiefte sich das heutige Gebiet des Golfs von Oman ständig. Mit einiger Wahrscheinlichkeit ist anzu-

Zahlentafel 1. Zusammenstellung der Meßergebnisse

	Station 245	Station 246	Station 247
Geograph. Koordinaten	23°11,8′N 62°55′E	23°42,6′N 60°43′E	23°03,5′N 60°59′E
Wassertiefe	2725 m	3350 m	3345 m
	1. Schicht		
Geschwindigkeit	1400 m/s +1,5 Z	1400 m/s +1,5 Z	1400 m/s +1,5 Z
Mächtigkeit	1,0 km	1,4 km	1,0 km
	2. Schicht		
Geschwindigkeit	a) 2,95 km/s b) 4,6 km/s	a) 3,5 km/s b) 4,25 km/s	a) 3,2 km/s b) 4,0 km/s
Mächtigkeit	a) 1,8 km b) 2,45 km	a) 1,5 km b) 5,3 km	a) 1,7 km b) 2,7 km
	3. Schicht		
Geschwindigkeit	6,9 km/s	6,3 km/s	6,0 km/s

nehmen, daß sich im Zusammenhang mit der Vertiefung schließlich größere Verwerfungen am heutigen Schelf bzw. am Kontinentalabfall vor der Makranküste in miozäner oder pliozäner und pleistozäner Zeit bildeten.

7. Schlußbemerkung

Es gibt nach vorstehenden Überlegungen Gründe dafür, das heutige Gebiet des Golf von Oman nach den bisher vorliegenden spärlichen Ergebnissen als seewärtige Fortsetzung des Baluchistan-Beckens anzusehen. Mit dem Aufstieg des Murray-Ridge könnte der anschließende Bereich des Golfs von Oman als Folge von Ausgleichsbewegungen eine Absenkung erfahren haben.

Mit zunehmender Vertiefung bei entsprechender Sedimentation könnte es in miozäner oder pliozäner Zeit zur Bildung großer Verwerfungssysteme gekommen sein, die im Schelf oder am Kontinentalabfall vor der Makranküste zu vermuten sind. Man möchte demnach beim gegenwärtigen Kenntnisstand den Golf von Oman als eine spitzwinklig zulaufende, staffelförmige Einbruchszone mit bemerkenswerten Sedimentmächtigkeiten ansehen, also nicht als ein Stück ozeanischer Kruste, sondern als einen in junger und jüngster Zeit abgesunkenen Schelf.

Ihren Kollegen, den Herren Dr. *A. Stein* und Dr. *E. Mundry*, verdanken die Verff. die Erstellung von Rechenprogrammen und mancherlei Anregungen. Sie sind ferner dem Präsidenten der Bundesanstalt für Bodenforschung, Herrn Professor Dr. *H. J. Martini*, dem Koordinator des deutschen Beitrages zur Internationalen Indischen-Ozean-Expedition, Herrn Professor Dr. *G. Dietrich*, dem Fahrtleiter während des Expeditionsabschnittes Golf von Oman, Herrn Professor Dr. *E. Seibold*, und Herrn Dr. *Meyl* von der Deutschen Forschungsgemeinschaft zu Dank verpflichtet.

Literaturverzeichnis

Barker, P. F., A reconnaissance survey of the Murray Ridge. Univ. Bericht Geophysics Department, Imperial College London, im Druck.

Crookshank, H., A note on the western margin of Gondwana Land. 19th International Geol. Congr., Sympos. sur les séries de Gondwana, S. 175/79. Algier 1952.

Dietrich, G., Die Internationale Indische-Ozean-Expedition und die deutsche Beteiligung mit dem neuen Forschungsschiff „Meteor". Die Erde **1965**, Nr. 1, 5/20.

Dietz, R. S., Collapsing continental rises: An actualistic concept of geosynclines an mountain building. J. Geol. **71**, Nr. 3, 314/33 [1963].

Dürbaum, H., Zur Bestimmung von Wellengeschwindigkeiten. Geophysical Prospecting **2**, Nr. 2 [1954].

Ewing, J. J., u. *J. E. Nafe*, The unconsolidate sediments. The Sea, Vol. 3, S. 73/82. New York 1963.

Ewing, M., u. *J. L. Worzel*, Long-range sound transmission. Geol. Soc. America, Memoir 27. New York 1948.

Gansser, A., Außeralpine Ophiolitprobleme. Eclog. Geol. Helv. **52**, 659/80 [1959].

Ghosh, A. M. N., Possible oil-bearing regions of India. Proc. 5th Wld. Petroleum Congr., Sect. I, 1023/35. New York 1959.

Giesel, W., Elastische Anisotropie in tektonisch verformten Sedimentgesteinen. Geophysical Prospecting **11**, Nr. 4, 423/58 [1963].

Hagedorn, J. G., A process of seismic reflection interpretation. Geophysical Prospecting **2**, Nr. 2, 85/128 [1954].

Hamilton, E. L., Thickness and consolidation of deep-sea sediments. Bull. geol. Soc. America **70**, 1399/1424 [1959].

Hamilton, E. L., Sound speed and related physical properties of sediments from experimental Mohole. Geophysics **21**, 257/61 [1965].

Hunting Survey Corp. Ltd., Reconnaissance geology of part of West-Pakistan. Report, Government of Canada for the Government of Pakistan. Ottawa 1960.

International Indian Ocean Expedition, bathymetric, magnetic and gravity investigations by *H. M. S. Owen*, 1961—62. Admiralty Marine Science Publ. Nr. 4. London 1963.

Katz, S., u. *M. Ewing*, Seismic-refraction measurements in the Atlantic Ocean. Bull. geol. Soc. America **67**, 475/510 [1956].

Krishnan, M. S., Geology of India and Burma. Madras 1960.

Laughton, A. S., Sound propagation in Ocean sediments. Geophysics **22**, Nr. 2, 233/60 [1957].

Matthews, D. H., A major fault scarp under the Arabian Sea displacing the Carlsberg Ridge near Socotra. Nature [London] **198**, 950/52 [1963].

Meinicke, S., Die digitale Berechnung von seismischen Geschwindigkeiten aus Reflexionen. Prakla-Seismos Mitteilungsbl. Nr. 5. Hannover 1965.

Morton, D. M., The geology of Oman. Proc. 5th Wld. Petroleum Congr., Sect. I, 299/94. New York 1959.

Nafe, J. E., u. *C. L. Drake*, Variation with depth in shallow and deep water marine sediments. Geophysics **22**, 523/52 [1957].

Officer, C. B., Sound Transmission. New York 1958.

Pepper, J. F., The Indian Ocean. The Geology of its Bordering Lands and the Configuration of its Floor. Washington 1963.

Rahmann, H., Geology of petroleum in Pakistan. Proc. 6th Wld. Petroleum Congr., Sect. I, S. 659/83. Hamburg 1964.

Raitt, R. W., The crustal rocks. The Sea, Vol. 3, S. 85/101. New York 1963.

Stöcklin, J., New data on the Lower Paleozoic and Precambrium of North Iran. Geol. Survey of Iran, Rep. Nr. 1. Teheran 1964.

Wisemann, I. D. H., u. *R. B. Seymour Sewell*, The floor of the Arabian Sea. Geol. Mag. **1937**, 219/30.

Zuberi, W. A., u. *E. P. Dubois*, Basin architecture West Pakistan. Symposium on Development of Petroleum Resources of Asia and Far East (Pak-Stanvac Petroleum Project). Teheran 1962.

Part V

Papers presented by title or an abstract only

STATE OF ISRAEL

PRIME MINISTER'S OFFICE
NATIONAL COUNCIL FOR
RESEARCH AND DEVELOPMENT

MINISTRY OF AGRICULTURE
DEPARTMENT OF FISHERIES
SEA FISHERIES RESEARCH STATION

BULLETIN No. 35

ISRAEL SOUTH RED SEA EXPEDITION, 1962, REPORTS

Nos. 1—4

HYDROGRAPHY OF DAHLAK ARCHIPELAGO (RED SEA)
by O. H. OREN
Sea Fisheries Research Station, Haifa

ON THE PREDATION OF CORAL BY THE SPINY STARFISH ACANTHASTER PLANCI (L.) IN THE SOUTHERN RED SEA
by T. GOREAU
Department of Physiology, University of West Indies

REPORT ON THE PYCNOGONIDA OF THE ISRAEL SOUTH RED SEA EXPEDITION
by J. H. STOCK
Zoölogisch Museum, Amsterdam, The Netherlands

A COLLECTION OF REPTILES FROM THE DAHLAK ARCHIPELAGO
by J. H. HOOFIEN *and* Z. YARON
Tel-Aviv University

HAIFA, ISRAEL
January, 1964

STATE OF ISRAEL

PRIME MINISTER'S OFFICE
NATIONAL COUNCIL FOR
RESEARCH AND DEVELOPMENT

MINISTRY OF AGRICULTURE
DEPARTMENT OF FISHERIES
SEA FISHERIES RESEARCH STATION

BULLETIN No. 38

ISRAEL SOUTH RED SEA EXPEDITION, 1962, REPORTS

Nos. 5—12

HAIFA, ISRAEL
March, 1965

STATE OF ISRAEL

PRIME MINISTER'S OFFICE
NATIONAL COUNCIL FOR
RESEARCH AND DEVELOPMENT

MINISTRY OF AGRICULTURE
DEPARTMENT OF FISHERIES
SEA FISHERIES RESEARCH STATION

BULLETIN No. 40

ISRAEL SOUTH RED SEA EXPEDITION, 1962, REPORTS

Nos. 13—17

HAIFA, ISRAEL
NOVEMBER, 1965

Volume 8, No. 2
New Series

February 1966

RECORDS OF OCEANOGRAPHIC WORKS IN JAPAN

General Report of the Participation of Japan in the International Indian Ocean Expedition

The National Committee for IIOE,
The Science Council of Japan,
March, 1965

CONTENTS

Published by
Science Council of Japan

Reprinted from *Phil. Trans. Roy. Soc.*, series A, vol. 259, no. 1,099, 1966.

International Indian Ocean Expedition

A Discussion concerning the floor of the Northwest Indian Ocean

Organized by M. N. Hill, F.R.S.*

(*Discussion held* 12 *November* 1964—*MSS received* 12 *May* 1965)

[Plates 2 to 5]

CONTENTS

* As these pages were being passed for press it was learnt with sorrow of the death of Dr Hill on 11 January 1966.

A DISCUSSION CONCERNING THE FLOOR OF THE NORTHWEST INDIAN OCEAN

Organized for the Royal Society

by

M. N. HILL, F.R.S.

PREFACE

Some years ago at the first and preliminary meeting of the Scientific Committee on Oceanic Research (S.C.O.R.) of the International Council of Scientific Unions (I.C.S.U.), one of the prime tasks was to seek some major international sea-going undertaking which the Committee could initiate and subsequently sponsor. This undertaking would have to interest many nations and embrace many oceanographical disciplines.

The meeting took place at the Woods Hole Oceanographic Institution and it was therefore appropriate (although not improbable!) that Dr C. H. O'D. Iselin should be first to suggest that an international research programme in the Indian Ocean fulfilled both these objects. He emphasized that many nations bordered it and that there were interests in this comparatively unknown ocean for any scientist concerned with meteorology, biology (above or below sea level), the physics and chemistry of the ocean waters, or the Earth beneath the sea. He also made clear that the monsoons made the Indian Ocean unique as regards oceanic and atmospheric circulation.

The meeting, after lengthy discussion, endorsed Dr Iselin's proposal and the end results of the tremendous international effort which thereby was created are now coming in. Some of these results were delivered at a Discussion Meeting held in the rooms of the Royal Society on 12 November 1964.

The papers given at this meeting, and which are published below were restricted to geological and geophysical aspects of the northwest Indian Ocean (except for the first paper concerning the physiography of the *whole* of the Indian Ocean). This collection of papers represents, by no means, the last word on these aspects of this area. Indeed there is much more work to be published on experimental work already completed, and for many of us the work already accomplished has produced many new problems which require further experimental work in the area.

The contributors to this Discussion Meeting were from the U.S.A. and the U.K.; regrettably, there were none from the U.S.S.R. The results published by the U.S.S.R. National Academy of Sciences have, however, been extensively used.

Research of the kind discussed below can be divided into various diffuse and interlinked categories; one is concerned with new concepts and with undiscovered features of the floor of the Ocean and what lies below, the second is less spectacular in that it confirms

predictions based on work elsewhere and the third is of an essential but routine nature without which the other investigations would be valueless and which provides the basic information for work already completed but not included here, or for work to be undertaken in the future.

The main topics described here are:

(i) the description of the physiography of the Indian Ocean, based largely on bathymetry;

(ii) the geological history and present structural and geophysical features of the Gulf of Aden, which, with the Red Sea, seems to be an area of high stresses and movement in the mantle and crust of the Earth;

(iii) the major fracture crossing the northern end of the Carlsberg Ridge represented by the Owen Fracture Zone and the Murray Ridge, and the consequent displacement of the axis of the Ridge;

(iv) the mineralogy and petrology of rocks collected from a small but well surveyed and fractured area of the Carlsberg Ridge lying some hundreds of miles to the southeast of the Owen Fracture Zone;

(v) the sediments of the Seychelles Bank and a description of the late Glacial and post-Glacial platforms on which they are distributed;

(vi) the age, the deep structure and the origin of the Seychelles Bank;

(vii) the preliminary results concerning the structural changes which exist along the length of the Seychelles to Mauritius Ridge;

(viii) the deep structure, obtained by seismic refraction shooting methods, of the section between the Seychelles and the Kenya coast, and its relation to the structures found at each end, and to the structure of the deep ocean between the Seychelles and the Carlsberg Ridge.

(ix) the relation between the gravity and magnetic field anomalies and the many structural features of the northwest Indian Ocean;

(x) the heat flow results in the Red Sea, the Gulf of Aden and over the Carlsberg Ridge and its flanks;

(xi) the recent sediments in the Persian Gulf which represents an exceptional and almost totally enclosed shallow sea.

We are indebted to the Royal Society for the opportunity of holding this Discussion Meeting and I should like to express my gratitude for the cooperation and hard work from the participants, from the men and organizations ashore and at sea, which resulted in the Meeting being a success.

M. N. HILL

The Report of this Discussion which has been published in *Philosophical Transactions of the Royal Society*, Series A, Volume 259, is available for general sale as a separate paper and can be obtained either through any bookseller or direct from the Royal Society at £3. 6*s*. (U.S. $9.90) as part number 1099.

Physiography of the Indian Ocean

By B. C. Heezen and Marie Tharp

Department of Geology and Lamont Geological Observatory, Columbia University, New York, N.Y.

As a result of the International Indian Ocean Expedition, the bottom of the Indian Ocean is now one of the best known areas of the ocean floor.

The Mid-Indian Ocean Ridge, a rugged mountain range, lies in the centre of the Indian Ocean. North-northeast trending fractures offset the axis of the ridge. In the Arabian Sea these fractures are right lateral; in the southwest Indian Ocean they are left lateral. Displacements range from a few miles* to over 200 miles.

The northeast Arabian Sea and the Bay of Bengal are occupied by huge abyssal cones built by sediments discharged from the Indo-Gangetic plain. Extensive abyssal plains lie seaward of the abyssal cones.

In low latitudes smooth topography is characteristic of the continental rise, the abyssal cones, and the oceanic rises. However, near the polar front smooth 'swale' topography laps over the normally rugged Mid-Oceanic Ridge. This 'swale' smoothing appears the result of the higher organic productivity of the Antarctic seas.

Microcontinents, mostly linear meridional ridges, are unique features of the Indian Ocean. These massive but smooth-surfaced blocks contrast markedly with the broad rugged Mid-Oceanic Ridge.

The Gulf of Aden

By A. S. Laughton

The National Institute of Oceanography, Wormley, Godalming, Surrey

The details of topography outlined in a new contour chart of the sea floor are related to the geophysical studies made in the Gulf of Aden during the last decade. These studies include magnetic and gravity field, seismic refraction, heat flow and earthquake epicentre measurements. The Gulf is interpreted as a tensional feature involving the separation of the continental blocks of Arabia and Africa and the formation of new oceanic crust in between. The central rough zone is compared with mid-ocean ridges. The matching of pre-Miocene continental geology on either side is discussed in the light of this theory.

The Owen fracture zone and the northern end of the Carlsberg Ridge

By D. H. Matthews

Department of Geodesy and Geophysics, University of Cambridge

Examination of the shape of the earthquake epicentre belt near Socotra led to the suggestion that a major fracture displaces the axis of the mid-ocean ridge in that area (Matthews 1963). Subsequent surveys have confirmed the existence of a fracture zone which extends 1500 miles from the coast near Karachi southwestwards to the middle of the Somali Basin. Linear ridges and troughs in the zone are associated with negative gravity anomalies but not with magnetic anomalies. Where the fracture zone crosses the line of the Carlsberg Ridge a sinuous trough is developed: south of this feature a characteristic pattern of magnetic anomalies is associated with the volcanic structures of the mid-ocean ridge, north of it a line of large non-magnetic seamounts has been found. It is concluded that the structure underlying the Owen fracture zone is a system of parallel transcurrent faults affecting the ocean floor only, at which the axis of the mid-ocean ridge suffers a net right lateral displacement of 170 mi.

A reconnaissance survey of the Murray Ridge

By P. F. Barker

Department of Geophysics, University of Birmingham

Bathymetric and magnetic measurements at a 10-mile line spacing across the mouth of the Gulf of Oman have made a substantial contribution to knowledge of the area. A northeast–southwest alinement of bathymetric features, the presence of many fault scarps and the occurrence of elongated weakly magnetized seamounts similar to others farther south suggest that the Murray Ridge is continuous with the Owen fracture zone and support the idea that both are loci of strike-slip movement.

AN AREA ON THE CREST OF THE CARLSBERG RIDGE: PETROLOGY AND MAGNETIC SURVEY

By J. R. CANN
Department of Mineralogy and Petrology, University of Cambridge
AND F. J. VINE*
Department of Geodesy and Geophysics, University of Cambridge

Rocks collected in the vicinity of a transcurrent fault cutting the crest of the Ridge have been affected by brecciation and, in some cases, metamorphism and hydrothermal action. These processes have led to the formation of spilites from crystalline basalts, and ultramafic rocks from basalt glasses. Further hydrothermal action has taken the form of replacement of some ultramafic rocks by quartz, ending in a nearly pure quartzite. The mineralogy is characteristic of greenschist facies metamorphism.

Fresh basalts were collected from a nearby hill, which seems to be a recent volcano post-dating the faulting and metamorphism.

The magnetic survey reveals a marked parallelism between the anomalies and the trend of the ridge, regardless of bathymetry. Computations confirm that uniform magnetization of the material represented by the bathymetry can in no way simulate the observed anomalies. Application of a vector fitting technique suggests that the remanent magnetization of this material is often reversed and from this a very crude and simple model is developed to account for the observed anomalies. The model is consistent with an ocean floor spreading hypothesis and periodic reversals in the earth's magnetic field. If substantiated it would have important implications in deducing the history of the ocean basins. Above all it provides a plausible explanation to account for the magnetic gradients and amplitudes observed over ridges without implying improbable magnetic contrasts, structures, or changes in petrology.

PRELIMINARY RESULTS OF THE 1964 CRUISE OF R.V. *CHAIN* TO THE INDIAN OCEAN*

BY ELIZABETH T. BUNCE, C. O. BOWIN AND R. L. CHASE
Woods Hole Oceanographic Institution, Woods Hole, Massachusetts

Geophysical investigations of the northern Somali Basin and the Seychelles–Mauritius Ridge conducted aboard R.V. *Chain* of the Woods Hole Oceanographic Institution are described and some results presented. Gravitational and total magnetic fields and bathymetry were measured continuously, and continuous seismic reflexion profiles were recorded over a major portion of the track. Cores, dredge samples, heat flow measurements, and underwater photographs were also obtained.

It is considered that the northern portion of the Somali Basin is a deep sedimentary basin partially enclosed to the east by a submarine ridge from which alkaline gabbro has been dredged and to the south by partially buried abyssal hills.

On the evidence from seven crossings of the Seychelles–Mauritius Ridge, it is proposed that the Ridge comprises two sections. The northern section, composed of nearly horizontally stratified rocks, extends from near the northern part of Saya de Malha Bank to the Seychelles Platform. The southern section is a linear, probably volcanic ridge that extends from north of Mauritius through Saya de Malha Bank, and may continue as a subsurface feature to the northeast. The two sections abut near Saya de Malha Bank, forming a continuous topographic feature.

Geophysical studies of the Seychelles Bank

By D. H. Matthews and D. Davies

Department of Geodesy and Geophysics, University of Cambridge

Geological studies of the islands on the Seychelles Bank, and the results of seismic refraction experiments made on the bank, are reviewed. They show that the crust is of continental type under the centre of the bank. Gravity measurements confirm that the thick crust extends to the northern edge of the bank and show that the Mohorovičić discontinuity slopes upward at an angle of about 19° under the peripheral cliff. Large narrow magnetic anomalies occurring in the central area of the bank are ascribed to minor intrusions of dolerite found in the Precambrian granites, and it is suggested that the edge of this area may mark the limit of the granite mass. Magnetic anomaly profiles of the Mascarene Ridge are similar to those over the Seychelles Bank and could result from a similar structure.

Crustal structure between Kenya and the Seychelles

By T. J. G. Francis, D. Davies and M. N. Hill, F.R.S.

Department of Geodesy and Geophysics, University of Cambridge

A series of seismic refraction profiles has been shot between Kenya and the Seychelles Bank and in the neighbourhood of the Bank itself. Thick sediments have been observed for 300 to 400 km from the African coast. Near Kenya, great thicknesses of material of about 4·8 km/s velocity match closely the 9 to 10 km of Karroo beds expected on the coast at Lamu. The Mohorovičić discontinuity has been traced from 100 km off the African coast to the Seychelles Bank. West of the Bank the mantle is unusually shallow, rising to only 8·5 km below the surface, and the 6·8 km/s crustal layer unusually thin or absent. The absence of a gravity anomaly associated with this very shallow mantle raises a problem which has yet to be resolved.

Heat flow and magnetic profiles on the Mid-Indian Ocean Ridge*

By R. P. von Herzen† and V. Vacquier

Marine Physical Laboratory of the Scripps Institution of Oceanography, University of California, San Diego

Sixty heat flow values were measured along nine profiles across the Mid-Indian Ocean Ridge. The results were roughly of the same character as the ones previously reported for the South Atlantic Ridge. The correlation of high heat flow with the centre of the ridge was less pronounced. The scatter of heat flow values when plotted as a function of distance from the ridge was even greater. The average of all values is 1·35 μcal cm^{-2} s^{-1}, indicating that over the surveyed area the heat flow is normal. The cause for the low values on the flanks of the ridge remains unknown. A right lateral displacement of about 200 km across the Vema Trench was measured from the offset of the magnetic anomaly on the ridge crest.

Heat flow in the northwest Indian Ocean and Red Sea

By J. G. Sclater

Department of Geodesy and Geophysics, University of Cambridge

Twenty-four measurements of the heat flow through the ocean floor were made in the Indian Ocean and three in the Red Sea. A critical analysis of the effects of fluctuations of bottom-water temperature on the geothermal gradient in the Red Sea shows that these fluctuations do not invalidate the measurements of heat flow. The mean value for the Gulf of Aden (this includes five previous measurements) is 3·89 ± 0·49 μcal cm^{-2} s^{-1}. This high value, combined with the shape of a profile across the Gulf, suggests a region of unusually high temperature at a depth of less than 10 km below the bottom. The seventeen heat flow measurements made by R.R.S. *Discovery* and R.V. *Vema* between the African coast and the Seychelles show little variation about a mean value of 1·17 μcal cm^{-2} s^{-1}. The comparison of these observations and the deep structure, as determined by a series of seismic lines, shows a constant heat flow across the continental margin.

The author is indebted to Mr R. Belderson of the National Institute of Oceanography for a brief description of the cores taken on the cruise.

Marine sediments and bottom communities of the Seychelles

By M. S. Lewis and J. D. Taylor

Department of Geology, University of London, King's College

The shoal water region of the Seychelles Bank, covering about 31 000 km², is floored by relatively thin detrital carbonate sediments. Around the granitic and coral islands at least four submarine platforms can be recognized and are tentatively related to Late-glacial and Postglacial sea levels. A shallow discontinuous rim is developed around the margin of the Bank.

The sediments and bottom communities of the open Bank and of the reef flats are described in terms of nine principal environments. Sedimentary facies are distinguished by the proportions of different organic constituents, by variations in grain size and by presence or absence of quartz. Syngenetic pyrite and collophane occur locally as minor constituents. Away from the reef flats the Bank supports a fairly uniform bottom community, the main elements being mollusca and foraminifera.

The reefs may be considered as large intertidal pools with many microenvironments and with a complex zonation of communities showing rapid lateral changes in composition. There is a close relation between the sedimentary facies of the reefs and the distribution of the bottom communities.

The recent sedimentary facies of the Persian Gulf region

By G. Evans

Imperial College, London

The Persian Gulf, which is a shallow marginal sea of the Indian Ocean, is an excellent model for the study of some ancient troughs.

It is bordered on the west by the Arabian Precambrian shield and on the east by the Persian Tertiary fold mountains.

Persia is an area of extensive continental deposition. It is bordered by a narrow submarine shelf. The deeper trough of the Persian Gulf lying along the Persian Coast seaward of the shelf is floored by marly sediments. East of this, the Arabian shelf is covered with skeletal calcarenites and calcilutites. To the northwest is the Mesopotamian alluvial plain and deltaic lobe.

Arabia is bordered on the Persian Gulf littoral by a coastal complex of carbonate environments. Barrier islands, tidal deltas (the site of oolitic calcarenite formation) and reefs protect lagoons where calcilutites, pelletal-calcarenites and calcilutites and skeletal calcarenites and calcilutites are forming. There are Mangrove swamps, extensive algal flats and broad intertidal flats bordering the lagoons and landward sides of the islands. A wide coastal plain, the sabkha, borders the mainland. Here evaporation and reactions between the saline waters percolating from the lagoons, and calcium carbonate deposited during a seaward regression, leads to the production of evaporitic minerals including anhydrite, celestite, dolomite, gypsum and halite. Inland, wide dune sand areas pass into the outwash plains skirting the mountain rim of Arabia.

Reprinted from Excerpta Medica International Congress Series No. 91
containing abstracts of papers read at the
SECOND INTERNATIONAL CONFERENCE ON PROTOZOOLOGY
London, August 1965

255. Infraciliary morphology of a little-known echinophilous hymenostome ciliate from the Indo-West Pacific

BERGER, J., *Department of Zoology, University of Toronto, Toronto 5, Canada*

Silver-impregnated specimens of the echinophilous inquilinic ciliate, *Cryptochilidium polynucleatum* Nie, 1934, were obtained during surveys of Indo-West Pacific sea urchins. They do not exhibit a cryptochilid infraciliary morphology.

Superficially, *C. polynucleatum* displays the laterally-compressed appearance of its presumed congeners. However, its buccal and somatic infraciliature differ significantly from true cryptochilids. The infraciliature of the 14 sigmoid kineties of the concave right surface is dimorphic. The two kineties adjacent to the naked oral region consist entirely of contiguous kinetosomes. The posterior 10% of the next 5-6 kineties is of a similar granular density. These dense areas presumably act as a thigmotactic field. The remainder of the dextral kineties are provided with ⅓ as many kinetosomes. All dextral kineties extend for *ca.* ¾ the somatic length leaving an agranular posterior zone continuous with the oral region. The convex left surface has 10-12 straight kineties of a non-thigmotactic kinetosomal density. All somatic cilia are of equal length except the caudal tuft which arises from 3-4 polar-basal granules.

The infraciliary buccal apparatus consists of two subequatorial parallel rows of 1-3 kinetosomes' width. They extend for *ca.* ⅓ the somatic length along the *right* margin of the naked inter-kinetal ventral area. The left membranellar base is longer and less curved than its dextral counterpart. Both end at the cytostome. They resemble pseudocohnilembid oral membranes and the composite AZM of hemispeirid thigmotrichs. As no stomatogenic individuals were observed among the 300+ specimens examined, speculation concerning the phylogenetic implications of these organelles is premature.

The cytoproct is immediately caudad of the cytostome. A single contractile vacuole pore lies behind the thigmotactic dextral kineties.

Elevation of *C. polynucleatum* to a distinct generic status within the HYMENOSTOMATIDA seems justified as does the placing of *Cryptochilidium ozakii* Yagiu, 1935, into junior synonomy with it.

Reprinted from Excerpta Medica International Congress Series No. 91
containing abstracts of papers read at the
SECOND INTERNATIONAL CONFERENCE ON PROTOZOOLOGY
London, August 1965

272. A preliminary report on the Tintinnida of the Indian Ocean from the collections of Cruise 2 of the "Anton Bruun", June to August, 1963

McDOWELL, S., *Dept. of Biology, Montclair State College, Upper Montclair, N. J., U.S.A.*

Samples were taken from over 40 stations in a north-south transect from Bombay due south on the 70° parallel to south latitude 38° and due north on the 80° parallel to Ceylon and Bombay. Collections were made by surface tows, 200 meter to surface tows, and volume samples from several depths concentrated by millipore filters. The last method revealed few forms except minute ones that tend to escape from the usual nets.

The overall species complex resembled that of the eastern tropical Pacific Ocean. Common oceanic forms proved to be such genera as *Codonella, Cyttarocylis, Rhabdonella, Rhabdonellopsis, Parundella, Xystonella, Xystonellopsis, Proplectella, Undella, Amplectella, Dictyocysta, Amphorella, Eutintinnus* and *Salpingella.* The paper will be illustrated by photographs using conventional light as well as phase contrast and polarization optics were made of living specimens and loricas alone.

A more complete account will appear later including collections from other cruises. (Supported by the NSF as a part of the U.S. Program in Biology, International Indian Ocean Expedition.)